I. Hybrid Androgen Receptor Antagonist – Histone Deacetylase Inhibitors

and

II. Development of an oxy-Cope / Michael Cascade Reaction

Ryan R. G. Barrett

Department of Chemistry, McGill University

Montréal, QC, Canada

January 2022

A thesis submitted to McGill University in partial fulfillment of the requirements of the degree of Doctor of Philosophy

© Ryan Barrett 2022

CONTENTS

Abstract....4

Résumé....5

Acknowledgements....6

Contribution of authors....8

List of Figures....9

List of Schemes....11

List of Tables....14

Abbreviations....15

Part I. Hybrid Androgen Receptor Antagonist – Histone Deacetylase Inhibitors

Chapter 1. Introduction

1.1.1. Prostate Cancer: Statistics and Significance....22

1.1.2. Prostate Cancer: Disease Origins and General Biology....23

1.1.3. Prostate Cancer: Treatment Options and Androgen Deprivation therapy....26

1.2.1. Nuclear Receptors: an Overview....30

1.2.2. Androgen Receptor: Molecular Biology....32

1.2.3. Androgen Receptor: Structure....37

1.2.4. Androgen Receptor: Agonists and SARMs....39

1.2.5. Androgen Receptor: Antagonists....40

1.3.1. Histone Deacetylases: Global and Molecular Biology....44

1.3.2. Histone Deacetylases: Structure and Mechanism....47

1.3.3. Histone Deacetylases: Inhibitors....49

1.4.1. Hybrid Inhibitors: General Design Principles and Hybrids in Each Class....54

1.4.2. Hybrid Inhibitors: AA-HDACi Hybrids....56

Chapter 2. Development of Novel Hybrid AA-HDACi

2.1.1. Design of an Expanded 1st Generation of AA-HDACi....60

2.1.2. Synthesis of RU59063-Inspired Hydroxamic Acid Hybrids....63

2.1.3. Synthesis of Enzalutamide-Inspired Hybrids.....64
2.1.4. Synthesis of Flutamide-Inspired Benzamide Hybrids.....65
2.2.1. AR and HDAC Inhibition Activity of 1st Generation Hybrids.....67
2.2.2. Cell Viability Assays of 1st Generation Hybrids.....72
2.3.1. Design of 2nd Generation Hybrids.....73
2.3.2. Synthesis of Enzalutamide or Apalutamide-Inspired Benzamide Hybrids.....76
2.3.3. Synthesis of Enzalutamide-Inspired Hybrids with Alternative Linkers.....79
2.3.4. Synthesis of a Darolutamide-Inspired Benzamide Hybrid.....82
2.4.1. AR and HDAC Activity of 2nd Generation Hybrids.....82
2.4.2. Activity of Select Hybrids in Cells.....91
2.5.1. Conclusions and Outlook.....94
2.5.2. References for Part I.....96
Part II. Development of an oxy-Cope / Michael Cascade Reaction
Chapter 3. Introduction
3.1.1. Cope Rearrangements and Related Sigmatropic Shifts.....117
3.1.2. Anionic oxy-Cope (AOC) rearrangements.....120
3.1.3. Cascades Incorporating oxy-Cope Rearrangements.....124
3.2.1. The aza-Cope / Mannich Reaction.....129
3.2.2. The Prins-Pinacol Reaction.....131
3.2.3. Overman's Mechanism Tests.....132
3.3.1. Catalysis of (oxy-)Cope Rearrangements.....134
3.3.2. Iminium and Carboxyhydrazonium Catalysis, *esp.* of Pericyclic Reactions.....135
Chapter 4. Development of an oxy-Cope / Michael Reaction
4.1.1. Designing an oxy-Cope / Michael Reaction Cascade.....141
4.1.2. Synthesis of Cyclic oxy-Cope / Michael Substrates.....142
4.1.3. Development of the Cyclic oxy-Cope / Michael Reaction.....149
4.1.4. The Roles of Acid and Solvent in the Cyclic oxy-Cope / Michael Reaction.....152
4.1.5. Scope of the Cyclic oxy-Cope / Michael Reaction.....154

4.1.6. The Cyclic Methyl Ether oxy-Cope / Michael Reaction.....161

4.2.1. Designing an oxy-Cope / Michael Mechanism Test.....161

4.2.2. Synthesis of Acyclic oxy-Cope / Michael Alcohol Substrates.....163

4.2.3. Synthesis of Racemic Acyclic Methyl Ether Substrates.....164

4.2.4. Synthesis of Enantio-Enriched Acyclic Methyl Ether Substrates.....166

4.2.5. Development of the Acyclic oxy-Cope / Michael Reaction.....169

4.2.6. Mechanism of the oxy-Cope / Michael Reaction.....172

4.3.1. Conclusions and Outlook.....177

4.3.2. References for Part II.....179

Contributions to original knowledge 188

Experimental Procedures and Characterization Data

Chapter 5. Experimental

5.1. General procedures.....189

5.2. Synthetic Procedures for Part I.....191

5.3. Synthetic Procedures for Part II.....258

5.4. Biological Assay Methods.....378

5.5. References for Chapter 5.....382

Chapter 6. Appendix.....386

Abstract

Part I

Prostate cancer treatment options have improved in recent years, but the disease remains prevalent in the elderly Canadian male population. Existing treatments for castration-resistant prostate cancer are inadequate and this necessitates innovation in treatment by drug co-administration or drug design. This century, and especially in the past decade, the concept of hybrid drug design has taken root in the literature. A series of hybrid compounds which combine key structural features of both androgen receptor antagonists and histone deacetylase inhibitors have been designed using the structure-activity relationship data available for each. Certain molecules are shown to inhibit the desired targets both *in vitro* and in cell assays. Furthermore, select hybrids were more effective in antiproliferation assays with prostate cancer cell lines than second-generation antiandrogen prostate cancer drug enzalutamide. Those hybrids also demonstrated less general cytotoxicity than known histone deacetylase inhibitors such as entinostat.

Part II

Since the discovery of massive rate enhancements with anionic conditions, the oxy-Cope reaction has proven immensely popular and useful in synthetic efforts. However, few methods have been developed for catalyzing the oxy-Cope reaction. Our group previously communicated the use of iminium catalysis in the Cope rearrangement of 1,5-hexadienes bearing 2-carboxaldehydes using diazepane hydrazide ammonium salts. This methodology has now been extended to the oxy-Cope rearrangement, resulting in catalysis not only of the sigmatropic shift, but also a subsequent Michael addition. The result is an oxy-Cope / Michael cascade reaction. We demonstrate ring expansions using 5 to 7-membered divinylcycloalkanes to access fused hydrindane, hydrazulene, and 8/5 bicycles in excellent yield with very high diastereoselectivity. We have also extended this to acyclic substrates which allow the synthesis of substituted cyclopentanes from linear hexadiene precursors. This has allowed us to study the reaction of enantioenriched linear substrates and confirm the mechanism of the transformation.

Résumé

Première Partie

Les traitements du cancer de la prostate se sont améliorés au cours des dernières années, mais la maladie demeure répandue chez les hommes âgés au Canada. Les traitements existants pour le cancer de la prostate résistant à la castration sont inadéquats et pourraient être améliorés par la co-administration de médicaments ou la conception de nouvelles molécules thérapeutiques. Au cours de la dernière décennie, le concept de médicaments hybrides s'est enracinée dans la littérature. Une série de composés hybrides ont été conçus en utilisant les données de relation structure-activité disponibles sur les antagonistes des récepteurs aux androgènes et les inhibiteurs de l'histone désacétylase. Certaines de ces molécules se sont montrées capables d'inhiber les cibles désirées dans des tests *in vitro* et in cellulo. De plus, dans le cas de tests de prolifération de cellule cancereuse, certains hybrides ont démontré être plus efficaces que l'enzalutamide, un médicament anti-androgène contre le cancer de la prostate de deuxième génération. Ces hybrides ont également démontré une cytotoxicité réduit à celle des inhibiteurs d'histone désacétylase connus tels que l'entinostat.

Deuxième Partie

En raison de sa grande vitesse réactionnelle en condition anionique, le populaire réarrangement oxy-Cope s'est avérée fortement utile en synthèse organique. Cependant, il existe très peu de méthodes servant à catalyser la réaction oxy-Cope. Notre groupe a précédemment communiqué l'utilisation de la catalyse à l'iminium dans le réarrangement Cope de 1,5-hexadiènes portant des 2-carboxaldéhydes à l'aide de sels d'ammonium diazépane hydrazide. Nous avons étendu cette méthodologie au réarrangement oxy-Cope, résultant non seulement en une catalyse du déplacement sigmatropique, mais également à une addition de Michael. Le résultat est une réaction en cascade oxy-Cope / Michael. Nous avons démontré des expansions de cycle à l'aide de divinylcycloalcanes à 5 à 7 chaînons pour accéder à l'hydrindane fusionné, à l'hydrazulène et aux bicycles 8/5 avec un excellent rendement et une diastéréosélectivité très élevée. Nous avons également déployé cette approche sur des substrats acycliques pour la synthèse de cyclopentanes substitués à partir de précurseurs d'hexadiène linéaire. Cela nous a permis d'étudier la réaction de substrats linéaires énantioenrichis et de démontrer le mécanisme réactionnel.

Acknowledgements

Academically speaking, I must first acknowledge my supervisor, Dr. Jim Gleason, for providing general insight, guidance, and expertise in both synthetic and medicinal chemistry, and for advice in preparing this document. (That sentence probably should have been two.) Beyond the nuts and bolts of the projects, the example which was set to constantly learn new areas of chemistry, combined with excellent all-around mentorship, fostered a terrific environment to grow and develop in. The teaching I've received in this department has been outstanding, and I would like to thank the following professors (listed in no particular order): Drs. Jim Gleason, Bruce Arndtsen, C. J. Li, Jean-Philip Lumb, Nicolas Moitessier, and Youla Tsantrizos. I would also like to thank my undergraduate research supervisor, Dr. Harry Brumer, for introducing me to research and biochemical experience which has been invaluable in the course of further studies.

I have been fortunate to work with numerous highly skilled colleagues in our group, elsewhere in the department, and in collaboration with external groups, whose passion for knowledge both inspired and challenged me constantly. I had the opportunity to work with several outstanding scientists on the antiandrogen project. I should thank Christopher Doyle specifically for starting this project and for establishing synthetic routes to several hybrid inhibitors. Of course, our main collaborators in Dr. Sylvie Mader's group, Marine Diennet and David Cotnoir-White, must be mentioned for their important biochemical assay work. Also, Dr. Claire Nash and Dr. Axel Thomson provided the penultimate prostate cancer antiproliferation assays and general prostate cancer expertise. I thank Dr. Dainis Kaldre for training me for our in-house HDAC assays, as well as for valuable discussions in the areas of both medicinal chemistry and organocatalysis. Dr. Jonathan Hughes deserves credit for generously contributing enough of a [1.1.1]propellane derivative to synthesize hybrid RB-433. Both he and David Scarlata contributed general advice and expertise in the preparation, handling, and usage of [1.1.1]propellane (in addition to countless valuable discussions in general). Dr. Gerardo Martin Torres and Arndtsen lab deserve credit for assistance with reactions using carbon monoxide gas and for helpful discussions regarding necessary pressure optimization. I wish to thank also Dr. Cyrus Lacbay, and Yuting Feng for assistance with their Tsantrizos group's preparatory HPLC (as well as being excellent friends).

With respect to the oxy-Cope / Michael project, I must first recognize Donald Campbell for his outstanding work developing the extremely challenging 7 to 8 ring expansion and for extending

the reaction to the cyclic methyl ether substrates. Without his persistence, this project would be a mere shadow of its present state. In addition to him, I have had countless invaluable discussions with all members of the group involved in organocatalysis, but I would especially like to acknowledge Dr. Dainis Kaldre, Dr. Nicklas Häggman, Dr. Samuel Plamondon, Josephine Warnica, HyunJune Jun, and Anthony Izzotti in this regard. I would additionally like to acknowledge the financial support of the McGill-CIHR Drug Development Training Program, NSERC, and McGill University.

I was also lucky enough to have worked with plenty of talented chemists not yet specifically mentioned, all of whom have been an absolute pleasure and inspiration to work with: Dr. Florent Larnaud, Shuo Xing, Anthony Palermo, Dr. Adam Elmehriki, Adamo Sulpizi, Ali Mansour, Yufei Wang, Zhizhong Gao, Angela Novakovic, and Amelia Caza. I would like to add several individuals in other groups who have impacted me, such as the various members of Tsantrizos group, especially Ifenna for hilarious conversations. Also, members of Lumb group with whom we have had plenty of shared group meetings, especially Dr. Wenbo Xu, Dr. Naresh Vemula, Dr. Ana Albertson, Dr. Kenneth Esguerra, Haiyan, and Matt for intellectual stimulation, friendship, and encouragement. There are too many others in the department to name, but I would especially like to thank the people I've played intramural sports with over the years, especially members of the Black Shuck Chemistry hockey team – you folks made grad school fun.

Several other McGill Chemistry personnel have provided various assistance and made my time here truly special. Of course, I would like to acknowledge the facilities managers Drs. Fred Morin, Robin Stein, Nadim Saadé, and Alex Wahba for their expertise over the years, and for many friendly conversations. The teaching staff I've come to know have also been an absolute pleasure to know and work with. I would like to offer a special thanks to the administrative staff, both in the office and at stores, for always ensuring things run smoothly. I would like to especially thank Sandra for assistance on a few occasions, Chantal for her wonderful demeanor and support, and Jean-Marc, who seems to make sure the entire building doesn't fall apart.

On a personal level, I would like to extend my most sincere and profound thanks to my close friends and family, who supported me unfailingly throughout this program and this trying COVID-19 pandemic. I would especially like to dedicate this thesis to my wonderful sister Emily, of whom I am so very proud.

Contribution of authors

In Part I of this thesis, collaborative research work is presented and discussed which has been published and will be referenced therein, and the contribution of collaborators will be clearly delineated in the text. Assays involving androgen receptor antagonism and HDAC Western blots were conducted by Dr. Sylvie Mader's group. Cell proliferation assays were conducted by Dr. Axel Thomson's lab. All of the synthetic work discussed was performed by the author, although some of it was based heavily on previous efforts by Christopher Doyle, who had previously prepared some compounds which are clearly noted in the text.

The oxy-Cope / Michael reaction discussed in Part II was developed in conjunction with Donald Campbell. However, the substrates explored by him are not included, except for a general example. All DFT calculations were performed by Dr. Gleason. Dr. Dainis Kaldre also first prepared and employed the diazepane carboxylate catalyst used throughout this project.

The French translation of the abstract was performed by Dr. Julie Ducharme with some helpful contributions by Anthony Izzotti.

List of Figures

Figure 1.1. Structure of (dihydro)testosterone.....25
Figure 1.2. Non-steroidal antiandrogens.....29
Figure 1.3. Lipophilic hormone ligands and the NRs they interact with.....31
Figure 1.4. Normal androgen receptor (AR) function.....33
Figure 1.5. Normal androgen receptor (AR) function...Resistance mechanisms.....35
Figure 1.6. Examples of small molecule drug candidates targeting androgen receptor.....37
Figure 1.7. AR-LBD crystal structure (PDB ID 2AMA) with bound DHT.....38
Figure 1.8. AR W741L LBD crystal structure (PDB ID 1Z95) with bound CDX.....39
Figure 1.9. Examples of SNuRM structures and drug candidates.....40
Figure 1.10. Steroidal AR ligands. Non-steroidal first-generation AR antagonists.....41
Figure 1.11. Non-steroidal second-generation AR antagonists.....43
Figure 1.12. Experimental AR antagonists. 43
Figure 1.13. HDAC deacetylation mechanism at the enzyme active site.....48
Figure 1.14. HDAC2 catalytic domain crystal structure (PDB ID 4LY1).....49
Figure 1.15. Examples of carboxylic and hydroxamic acid HDACi.....50
Figure 1.16. Structural variety of pan-HDACi and Macrocyclic HDACi.....52
Figure 1.17. (**A**) Examples of HDAC6i. (**B**) Examples of Class I-selective HDACi.....53
Figure 1.18. Examples of hybrid compounds.....55
Figure 1.19. Other published AA-HDACi hybrid structures and summarized data.....59
Figure 2.1. CDX-inspired hybrids previously prepared by the Gleason group.....61
Figure 2.2. RU59063-inspired hybrids previously prepared by the Gleason group.....62
Figure 2.3. Proposed extension of this 1st generation of AA-HDACi hybrids.....63
Figure 2.4. Known AR effectors, HDACi, and all 1st generation hybrid compounds.....68
Figure 2.5. Single-concentration inhibition of AR activity by CDX or hybrids.....68
Figure 2.6. Antiandrogenic activity of AA-HDACi hybrids.....69
Figure 2.7. Antiproliferative activity of select 1st generation hybrids in LNCaP cells.....72
Figure 2.8. Various alternative components of 2nd generation hybrid AR-HDACi.....74
Figure 2.9. Chosen targets for 2nd generation hybrid AR-HDAC inhibitors.....75
Figure 2.10. Single-point inhibition of AR activity by BRET assay with HEK293T cells.....83

Figure 2.11. Summary of all hybrid structures. 84
Figure 2.12. Biochemical data summary for 1st generation hybrids.....85
Figure 2.13. Biochemical data summary for 2nd generation hybrids based on ENZ and APL.....86
Figure 2.14. Biochemical data for 2nd generation hybrids with pyridyl linkers.....87
Figure 2.15. Biochemical data for 2nd generation hybrids with methylene spacers.....88
Figure 2.16. Antiandrogenic activity of 2nd generation AA-HDACi hybrids.....88
Figure 2.17. Summary of all biochemical data for 1st and 2nd generation hybrids.....90
Figure 2.18. HDACi activity in LNCaP cells.....91
Figure 2.19. Antiproliferative activity of second-generation hybrids in LNCaP cells.....92
Figure 2.20. Antiproliferative activity of second-generation hybrids in 4 cell lines.....92
Figure 3.1. Variants of Cope and hetero-Cope [3,3] rearrangements.....119
Figure 3.2. Charged Variants of Cope and hetero-Cope [3,3] rearrangements.....120
Figure 3.3. Composite schematic of various oxy-Cope cascade reactions.....125
Figure 3.4. Qualitative π-orbital energy diagrams showing...LUMO-lowering effects.....136
Figure 4.1. Complex natural products...mapping onto...oxy-Cope / Michael reaction products..142
Figure 4.2. Association equilibrium between HX conjugate base and an iminium.....153
Figure 4.3. Scope of the cyclic oCM reaction.....155
Figure 4.4. Unsuccessful alcohol oCM substrates.....157
Figure 4.5. (**A**) Isomerization between hydroazulene diastereomers. (**B**) DFT energies of isomeric hydrazulenes.....158
Figure 4.6. NOESY correlations for oCM hydrazulene products.....159
Figure 4.7. Conformations leading to oCM bicyclic products from *cis* and *trans* substrates.....159
Figure 4.8. Unsuccessful alcohol oCM substrates due to alternative oxa-Michael reactivity.....160
Figure 4.9. Possible mechanisms for the oCM reaction.....162
Figure 4.10. DFT calculations on the mechanism of the oCM reaction.....173
Figure 4.11. Mechanism of the linear oCM reaction.....174
Figure 4.12. Transition states and DFT energies of the key oCM transition states (R=Me).....177

List of Schemes

Scheme 2.1. Synthesis of RU59063-inspired hydroxamic acid hybrids.....64
Scheme 2.2. Synthesis of enzalutamide-inspired hydroxamic acid hybrids.....65
Scheme 2.3. Synthesis of flutamide-inspired HDACi hybrids with "inverted" amides.....66
Scheme 2.4. Synthesis of flutamide-inspired HDACi hybrids with "normal" amides.....66
Scheme 2.5. Preparation of α-cyanoanilines.....76
Scheme 2.6. Synthesis of hybrids related to RB-250.....78
Scheme 2.7. Synthesis of A-ring and linker pyridyl hybrids based on RB-250.....78
Scheme 2.8. Synthesis of enzalutamide-inspired hybrids with methylene spacers.....80
Scheme 2.9. Attempted routes to compact BCP linkers.....81
Scheme 2.10. Synthesis of a darolutamide-inspired hybrid.....82
Scheme 3.1. Examples of sigmatropic shifts.....117
Scheme 3.2. (**A**) Cope's reaction. (**B**) Orbital depiction and transition state for a Cope shift.....118
Scheme 3.3. (**A**) Urion's divinylglycol pyrolysis. (**B**) Berson's thermal oxy-Cope.....119
Scheme 3.4. The Evans group's thermal and AOC reactions.....121
Scheme 3.5. The Evans group's proof of stereochemical transfer in the AOC.....121
Scheme 3.6. (**A**) Boekman's approach to pleuromutilin by 6 to 8 ring expansion. (**B**) Allyl transposition in Guerrero's synthesis of Mulinane 1.....122
Scheme 3.7. (A) Saito's Di-AOC rearrangement from chiral diols with no apparent loss of *e.e.* **(B)** Generic scheme of Paquette's bis-additions to squarate esters and di-AOC / aldol sequence.....123
Scheme 3.8. Sarpong's magnesium alkoxide formal [1,3] shift.....124
Scheme 3.9. (**A**) Greeve's tandem alkylation, Wittig / AOC cascade. (**B**) Leighton's Ireland-Claisen / oxy-Cope approach to the cyclocintrinol core. (**C**) Rajagopalan's oxy-Cope / transannular ene reaction. (**D**) Barriault's oxy-Cope/Claisen/ene cascade. (**E**) Jacobi's approach to gnididione.....126
Scheme 3.10. (**A**) Sworin's hydrazulene synthesis. (**B**) Paquette's pentannulation. (**C**) Vanderwal's approach to the pseudopterosins.....128
Scheme 3.11. Model substrate for Leighton's approach to the phomoidrides.....128
Scheme 3.12. Mechanism of the aza-Cope / Mannich reaction.....129
Scheme 3.13. Aza-Cope / Mannich reaction by the Overman group toward strychnine.....130

Scheme 3.14. (**A**) Mechanism of the prins-pinacol reaction. (**B**) Overman's approach to the ophiobolin core by stepwise double-ring expansion using prins-pinacol reactions.....131
Scheme 3.15. The two possible pathways for the aza-Cope / Mannich and Prins-pinacol.....132
Scheme 3.16. Overman's mechanism test of the aza-Cope / Mannich and Prins-pinacol.....133
Scheme 3.17. Gangé's Au-catalyzed asymmetric formal Cope rearrangement.....134
Scheme 3.18. MacMillan's iminium-catalyzed Diels-Alder cycloaddition.....136
Scheme 3.19. Tomkinson's hydrazide-catalyzed Diels-Alder cycloaddition.....137
Scheme 3.20. (**A**) Hydrazide catalysts explored by our group (**B**) Our group's organocatalytic Cope rearrangement.....138
Scheme 3.21. Our group's organocatalytic transformations. These include (**A**) Diels-Alder reaction, (**B**) Michael addition, and (**C**) polyene cyclization.....140
Scheme 4.1. (**A**) Organocatalytic Cope mechanism. (**B**) Conceptual extension to proposed oxy-Cope / Michael rearrangement.....141
Scheme 4.2. Retrosynthesis of cyclic oxy-Cope / Michael substrates.....143
Scheme 4.3. Synthesis of the key intermediate ketone.....143
Scheme 4.4. Synthesis of a divinyl cyclohexane-based oCM substrate.....144
Scheme 4.5. Synthesis of cyclohexane-based oxy-Cope / Michael substrates with 5,6-vinyl hexadiene substitution.....144
Scheme 4.6. Synthesis of cyclohexane-based oxy-Cope / Michael substrates with alkynes and the corresponding alkenes.....145
Scheme 4.7. Efforts toward substrates bearing ethyl vinyl ether or vinylsulfone groups.....146
Scheme 4.8. Synthesis of cyclic oxy-Cope / Michael substrates with 3-Me substitution.....147
Scheme 4.9. Synthesis of cyclic oxy-Cope / Michael substrates with β-enal substitution.....147
Scheme 4.10. Synthesis of cyclopentane-based oxy-Cope / Michael substrates.....148
Scheme 4.11. Synthesis of cyclopentane-based oxy-Cope / Michael substrates.....149
Scheme 4.12. Donald Campbell's cyclic methyl ether oCM reaction.....161
Scheme 4.13. Initial attempts toward a benzyl-tagged linear alcohol vinyl substrate.....163
Scheme 4.14. Initial synthesis of benzyl-tagged linear alcohol vinyl substrate.....164
Scheme 4.15. Preparation of linear methyl ether substrates.....165
Scheme 4.16. Olefination strategy toward an enantioselective epoxidation substrate.....166
Scheme 4.17. Final route to an enantio-enriched epoxide.....168

Scheme 4.18. Final route to enantio-enriched linear methyl ether substrates.....169
Scheme 4.19. Conversion of linear oCM products to methyl esters for HPLC analysis.....172
Scheme 5.1. Initial synthesis of ketone **4.89**.....316
Scheme 5.2. Attempted organometallic additions to ketone intermediates.....318
Scheme 5.3. Synthesis of cyclohexyl-tagged acyclic alcohol oCM substrates.....323
Scheme 5.4. Synthesis of a cyclohexyl-tagged acyclic methyl ether oCM substrate.....333

List of Tables

Table 2.1. Biochemical summary of 1st generation hybrids.....70
Table 4.1. Optimization of the oCM reaction for the canonical cyclic substrate.....150
Table 4.2. Optimization of water content in the cyclic oCM reaction.....152
Table 4.3. (Within Scheme **4.17**) S.A.E. conditions.....168
Table 4.4. Development of the linear oCM reaction.....170

Abbreviations

‡	transition state
°C	degrees Celsius
Å	angstrom
δ	chemical shift (ppm)
σ*	antibonding sigma orbital
AA	androgen receptor antagonist / antiandrogen
AAWS	antiandrogen withdrawal syndrome
ABC	ATP binding cassette
ADT	androgen deprivation therapy
AF	activation function
AMC	7-amino-4-methylcoumarin
AOC	anionic oxy-Cope
APL	apalutamide (ARN509)
AR	androgen receptor
ARE	androgen response element
AR-V7	androgen receptor, splice variant 7
ATP	adenosine triphosphate
BCP	bicyclo[1.1.1]pentane
BHPrS	benign human prostate stroma
Boc	*tert*-butoxycarbonyl
BPH	benign prostatic hyperplasia
BRET	bioluminescence resonance energy transfer
C	Celsius, cholesterol
CAF	cancer-associated fibroblast
CD	catalytic domain
CDX	casodex (bicalutamide)
CHD	chromatin helicase
CRPC	castration-resistant prostate cancer
cryoEM	cryoelectron microscopy

CS	corticosteroids
CSS	charcoal-stripped serum
CTD	*C*-terminal domain
CYP17A1	Cytochrome P450 17A1
D	dihydrotestosterone, deuterium
DAR	darolutamide (ODM-201)
DBD	DNA-binding domain
D-box	dimerization box
DCC	*N,N'*-dicyclohexylcarbodiimide
DCM	dichloromethane
DHT	dihydrotestosterone
DIAD	diisopropyl azodicarboxylate
DIBAL	diisobutylaluminum hydride
DMAP	4-(dimethylamino)pyridine
DMF	*N,N*-dimethylformamide
DMSO	dimethylsulfoxide
DNA	deoxyribonucleic acid
DPPF	1,1'-Bis(diphenylphosphino)ferrocene
DPPP	1,3-Bis(diphenylphosphino)propane
d.r.	diastereomeric ratio
DuCAP	Dura mater Cancer of the Prostate
E	estrogen
E+	electrophile
E_a	activation energy
EDC	1-ethyl-3-(3-dimethylaminopropyl)carbodiimide
e.e.	enantiomeric excess
ent	enantiomer
ENZ	enzalutamide (MDV3100)
ENT	entinostat (MS-275)
epi-	epimer
equiv	equivalent

ER	estrogen receptor
ERG	ETS-related gene
ESI	electrospray ionization
ETOP	etoposide
ETS	erythroblast transformation-specific
ETV	ETS Variant Transcription Factor
FBS	fetal bovine serum
FGFR	Fibroblast growth factor receptor
FRET	fluorescence resonance energy transfer
FZ	frizzled receptor
GnRH	gonadotropin-releasing hormone
GPCR	G protein-coupled receptor
GR	glucocorticoid receptor
H	helix
HA	hydroxamic acid
HAT	histone acyltransferase
HDAC	histone deacetylase
HDACi	histone deacetylase inhibitor
HDLP	histone deacetylase-like protein
HER	human epidermal growth factor receptor
HMBC	heteronuclear multiple-bond correlation
HMDS	hexamethyldisilazide
HMPT	hexamethylphosphoramide
HOAt	1-hydroxy-7-azabenzotriazole
HOMO	highest occupied molecular orbital
HPLC	high-performance liquid chromatography
HRMS	high-resolution mass spectroscopy
HSP	heat shock protein
HSQC	heteronuclear single quantum correlation
imid.	imidazole
IC_{50}	half maximum inhibitory concentration

IL	interleukin
IR	infrared
J	coupling constant
kcal	kilocalorie
KDAC	lysine deacetylase
KHMDS	potassium hexamethyldisilazide
KIE	kinetic isotope effect
L_n	ligand
LBD	ligand-binding domain
LHMDS	lithium hexamethyldisilazide
LHRH	luteinizing hormone releasing hormone
LDA	lithium diisopropylamide
LNCaP	Lymph Node Carcinoma of the prostate
LUMO	lowest unoccupied molecular orbital
m/z	mass to charge ratio
m	meta
m-CPBA	*meta*-chloroperoxybenzoic acid
MDSC	Myeloid-derived suppressor cell
mPCa	metastatic prostate cancer
MR	mineralocorticoid receptor
MRI	magnetic resonance imaging
NAD	nicotinamide adenine dinucleotide
NCoR	nuclear receptor corepressor
NE	neuroendocrine
NLS	nuclear localization sequence
NMR	nuclear magnetic resonance
nOe	nuclear Overhauser effect
NOESY	nuclear Oherhauser effect spectroscopy
NR	nuclear receptor
NTD	*N*-terminal domain
o	ortho

OAP	organic anion transporter
oCM	oxy-Cope / Michael
OCT	organic cation transporter
OATP	organic anion transporting polypeptide
P	progesterone
p	para
PCa	prostate cancer
PDB	Protein Data Bank
PDC	pyridinium dichromate
PI3K	phosphatidylinositol 3-kinase
ppm	parts per million
PR	progesterone receptor
PROTAC	proteolysis-targeting chimera
PSA	prostate-specific antigen
PTEN	phosphatase and tensin homologue
pyr	pyridine
R	generic group (typically carbon-based)
R	rectus
R_f	retention factor
RAF	Rapidly Accelerated Fibrosarcoma
RAR	retinoic acid receptor
RAS	Rat sarcoma virus
recryst.	recrystallization
RNF	ring-finger protein
rsm	recovered starting material
rt	room temperature
S	sinister
S_N	nucleophilic substitution
SAHA	Vorinostat / suberoylhydroxyanilide
SARD	Selective androgen receptor degrader
SARM	Selective androgen receptor modulator

SERM	Selective estrogen receptor modulator
Sirtuins	yeast SIR2, silent information regulators II
SLCO	solute carrier of organic transporters
SMRT	silencing mediator of retinoic acid and thyroid hormone receptor
SNP	single-nucleotide polymorphism
SNuRM	selective nuclear receptor modulator
SOMO	singly occupied molecular orbital
SPINK	serine protease inhibitor
SPOP	Speckle Type BTB/POZ Protein
SRC	steroid receptor coactivator
SRD5A2	steroid 5α-reductase type 2
SUMO	Small Ubiquitin-like Modifier
SWI/SNF	SWItch/Sucrose Non-Fermentable
T	testosterone
TBAF	tetra-*n*-butylammonium fluoride
TBDPS	*tert*-butyldiphenylsilyl
TBS	*tert*-butyldimethylsilyl
Tf	trifluoromethansulfonyl
TFA	trifluoroacetic acid
THF	tetrahydrofuran
THP	tetrahydropyran
TIPS	triisopropylsilyl
TLC	thin layer chromatography
TMPRSS2	trans-membrane protease, serine 2
TMS	trimethylsilyl
TR	thyroid hormone receptor
TSA	trichostatin A
WNT	Wingless / Int-1 protein
WT	wild type
VCaP	Vertebral Cancer of the Prostate
VDR	Vitamin D receptor

X	generic group (typically a heteroatom or halogen)
YFP	yellow fluorescent protein
ZBG	zinc binding group

Part I. Hybrid Androgen Receptor Antagonist – Histone Deacetylase Inhibitors

Chapter 1. Introduction

1.1.1. *Prostate Cancer: Statistics and Significance*

Prostate cancer (PCa) is by far the most prevalent cancer in Canadian men, with 12% population lifetime probability and 3.5% lifetime mortality. PCa currently accounts for 14% of all male cancer deaths, although it affects older men, predominantly those over 60 years of age.[1] In the United States, PCa is the second-leading cause of cancer death after lung cancer despite representing only 10% of total cancer cases, and the 98% overall five-year survival rate belies the poor 30% five-year survival of metastatic PCa (mPCa) patients.[2] Also obscured by the high survival rate is the lack of cure and poor quality of life for mPCa patients or those with resistant forms of the disease, in which setting modern treatment can only slightly prolong patient lifespan. Historically, the PCa mortality rate peaked in the 1990's, but advances in radiation and hormonal therapies since then have witnessed a steady increase in life expectancy post-diagnosis.[1] Increased screening of elevated prostate-specific antigen (PSA) in middle-aged men has provided a useful early indicator of PCa and has certainly facilitated earlier intervention and/or monitoring. PSA blood levels at 50-70 years of age can predict lifetime susceptibility to more aggressive PCa, but broad population screening has been met with concerns about overdiagnosis and possibly needless surgical intervention.[3] Given the exclusive onset in elderly populations and slow progression, PCa treatment options which simply stave off disease progression and maintain quality of life as long as possible are readily adopted.

The following two sections of this introduction will provide an overview of PCa biology and common modern treatments framed within the context of small molecule intervention to provide context for the work described in Chapter 2. After describing the treatments using androgen receptor antagonists already in use, the biology of that receptor will be summarized to rationalize the motivation for new compounds. The biology of histone deacetylases and common pharmacophores used in targeting this family of enzymes will then be discussed. Lastly, the principles of hybrid drug design, known hybrid drugs, and previous examples of antiandrogen-histone deacetylase inhibitors will be outlined. Chapter 1 will therefore lay the groundwork for understanding our approach to hybrid design using the desired classes of compounds.

1.1.2. *Prostate Cancer: Disease Origins and General Biology*

Prostate cancer (PCa) has been the focus of much dedicated genetic and biological research, so consequently much is known about the development and progression of the disease. In addition, the molecular biological mechanisms and resulting phenotypic variants of the disease are uniquely well-documented and understood. Since excellent reviews exist on the many diverse aspects of PCa, each delving into particular topics well beyond the scope of this thesis, only key points will be summarized here to enhance the understanding of the reader and build a digestible argument for the construction of novel hybrid androgen receptor antagonists and histone deacetylase inhibitors. This section will introduce the biological origins of PCa, progression of the illness, and key aspects of androgen hormone signaling in the body, but only aspects which inform the treatment options discussed in the next section or this project will be included.

A significant amount of research has been done to elucidate the biological origins of prostate cancer, some of which are distinct from other cancers due to the cell types involved. Certain causative factors have been implicated in PCa concerning environment, lifestyle, and diet due to its greater prevalence among men in "Western" societies, but race, age, and family history are the only concrete risk factors established for the disease.[3-5] Cancer typically arises in the epithelial cells of the prostate with 90% known as acinar adenocarcinomas which arise in glands and 5-10% non-acinar adenocarcinomas which imply ductal, basal cell, and neuroendocrine tumours. Many tumours are non-threatening and may not require immediate treatment, while others require immediate intervention. Genome-wide associated studies have identified 77 single-nucleotide polymorphisms and mutations of genes involved in DNA repair which are associated with PCa. One early mechanism of dysfunction involves activated androgen receptor (AR), a key transcription factor in the prostate tissue, damaging DNA during the transcription process to generate gene fusions of AR-controlled genes with members of the erythroblast transformation-specific (ETS) family of transcription factors (ETS+ PCa).[3] By doing so, the fused transcription factor is essentially brought under AR control and is thereby upregulated. Critically, cancers with these fusions are both clonal and AR-driven, which implies that the phenotype is a consistent, meaningful description and that AR-targeted treatments are appropriate. Other genomic issues are required to cause cancer, such as growth dysregulation by loss of phosphatase and tensin homologue (PTEN).[6] Therefore, classic cancer-causing genomic mechanisms such as double-stranded DNA breaks and loss of cell growth control play a clear role in cancer formation.

Prostate cancer can be classified according to molecular subtypes such as ETS+, which is functionally useful since the biological features of each subtype may determine the success of a given therapy and may one day allow development of personalized treatment regimens. It is important to understand the empirical nature of such analyses, which facilitate classification of the cancer according to specific biological markers. Cancers typified by this ETS+ feature account for 50-60% of PSA-screened PCa in (white) patients and the most common fusion components are described by the well-known trans-membrane protease, serine 2 – ETS-related gene (TMPRSS2-ERG) fused combination. The ETS+ subtype stands in contrast to the less common ETS– variants. SPOP mutation, a protein which involves ubiquitination and transcriptional regulation, characterize 5-10% of samples and these are always ETS–. Mutations or deletions in chromatin helicase (CHD1) account for 5-15% and these cancers are always ETS–. Gene fusions of RAF-RAS-FGFR proteins occur rarely in about 1-2% of samples but these tumours are always ETS–. Tumours with overexpressed serine protease inhibitor (SPINK1) are always ETS– and represent about 5-10% of samples. The remaining ~5-35% of tumors not accounted for are either unknown or possess highly unique subtypes. It is not yet determined how disease progression leads to resistance, whether by selection pressure on a tumour heterogeneous in cell phenotype or by compensation mechanisms of tumor cells which lead to proliferation (or both), but these subtypes may be of clinical use in determining treatment course and assessing the potential for development of resistance to treatment. First, a brief description of androgen signaling in the body is needed to understand those treatment options.

Androgens are critical steroid hormones required in both men and women for normal development but are especially important to male physiology since they contribute to development of muscle mass, bone density, male genitalia, and the prostate gland.[7] The prostate's normal function is to provide seminal fluid for reproduction, but the gland commonly becomes enlarged later in life resulting in discomfort or other symptoms in a condition known as benign prostatic hyperplasia (BPH). A common treatment of both BPH and PCa involves suppression of androgen synthesis and signaling, essentially starving the prostate tissues of androgens. Key circulating androgen testosterone **1.1** (Figure **1.1**) is synthesized primarily from cholesterol in the Leydig cells of the testes, although the adrenal cortex secretes ~10% of total bodily content,[8] while in women both the liver and ovary also contribute to secretion. Oddly, it has recently been demonstrated that under castrate conditions, androgen contributions from gut microbiota may become important.[9]

Testosterone circulates in the blood, ca. 98% plasma-bound with sex hormone-binding globulin or albumin, but radiolabeled androgens have been shown to accumulate in prostate and other target tissues where they are required.[10] Once inside prostate cells, testosterone is reduced by 5α-reductase to dihydrotestosterone (DHT) **1.1a**, which is a far better ligand for the androgen receptor, and through this receptor activates general transcription factors to promote cell growth.[11]

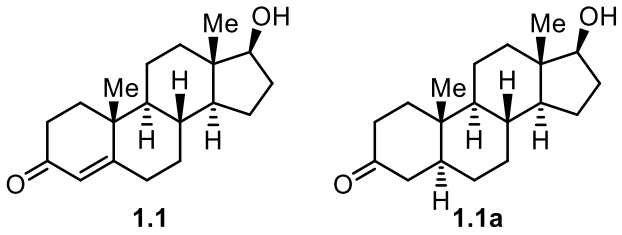


Figure 1.1. Structure of (dihydro)testosterone.

Despite the common perception that steroid hormones achieve their function by simple passive diffusion across cell membranes, which is certainly possible, the notion does not address the ability of PCa cells to maintain testosterone levels 15-50 times that of the surrounding medium.[12] A subset of the solute carrier of organic transporters (SLCO) superfamily has been implicated in PCa and may play a significant role in androgen localization, especially in castrate scenarios.[13, 14] The SLCO transporter family consists of organic anion transporting polypeptides (OATPs), organic anion transporters (OAPs), and organic cation transporters (OCTs), individual members of which are expressed in essentially every bodily epithelium and which are primarily involved in influx of compounds to the cell.[15] Such membrane proteins were known to be involved in bile acid and steroid hormone transport in other tissues including kidney or liver for some time, performing functions such as the elimination of toxic compounds or even drug metabolites,[16] but it has only recently become apparent that these are also expressed in prostate and other cancer-prone tissues. For example, OATP1B3 is clearly upregulated in PCa and clearly increases testosterone uptake, perhaps explaining both the excessive localization of testosterone in the prostate and ability to maintain growth under castrate conditions.[17] SLCOs have also been identified as detrimental to breast cancers by transporting estrone sulfate, while upregulation of certain SLCOs has been observed in resistant PCa and single-nucleotide polymorphism (SNP) analysis supports SLCO involvement.[18, 19] Furthermore, suggestive evidence exists from SNP analysis that certain members of the ATP binding cassette (ABC) transporter superfamily, which generally perform efflux

functions counter to SLCO action, may help to facilitate DHT exit from prostate cells and thereby improve overall patient survival.[20] The role of organic transporters is a research topic in urgent need of study, and may become incredibly important in engineering novel anti-cancer treatments. Unfortunately, even a firm understanding of androgen signaling and the biological origins of prostate cancer does not impart a complete grasp of the complex nature of PCa tumours, since cells do not exist in isolation and are liable to influences from neighbouring cells.

The last point hints at the tumour microenvironment as an important aspect of PCa biology, which has been elucidated in recent years, and the importance of which is fast becoming recognized in other cancers. The prostate stroma, which interacts with and can influence cancerous epithelial cells, is heterogeneous connective tissue primarily composed of smooth muscle cells, fibroblasts, vascular cells, nerve cells, and infiltrating immune cells.[21-23] Such epithelial:stromal interactions are obviously complex and not well understood to date, but it is known for example that stromal cells lacking AR stimulate PCa while stromal cells expressing AR suppress PCa growth *in vitro* and *in vivo*. Cancer-associated fibroblasts (CAFs), stromal cells which secrete collagen for extra-cellular matrix formation and play roles in wound healing or crosstalk with immune cells, have been acknowledged in recent years as generally involved in cancer and PCa tumorigenesis.[24-26] Androgen receptor signaling in CAFs also has a different profile than in epithelial cells since AR normally activates a signaling network that suppresses inflammatory cytokine release, and androgen depletion therefore derepresses tumour-stimulating cytokine secretions.[26] It has also been recently shown that neural progenitor cells released by the brain can infiltrate PCa tumours and initiate new nerve-cell formation, or neurogenesis, and such nerve cells are able to cause further malignancy and metastasis.[27, 28] Myeloid-derived suppressor cells (MDSCs), a population of heterogeneous activated monocytes and granulocytes, are capable of secreting IL-23 and thereby activating signal transduction pathways supporting AR expression and PCa growth or resistance to treatment.[29] Surely the examples included here just scratch the surface of the complex intercellular interactions in the tumour microenvironment, but they do highlight the complex biological and therapeutic context in which various PCa treatments are administered.

1.1.3. *Prostate Cancer: Treatment Options and Androgen Deprivation therapy*

Most PCa cases present with no symptoms but are detected due to increased prostate-specific antigen (PSA) screening and are diagnosed by PSA levels, examination, biopsy, and magnetic

resonance imaging (MRI) or other medical imaging options.[30-32] Once identified, the cancer is graded according to Gleason score, which considers the aggressiveness and prognosis of the disease based on microscopic appearance of glandular architecture. A treatment course is then selected accounting for the grade, localization, and patient's wishes, but for the majority of cases the prognosis is quite good. Active surveillance is increasingly used since it is now established that in many cases PCa will not progress significantly over the (elderly) patient's lifespan, and prostatectomy or radiotherapy offer up to a 90% 10-year survival rate for localized PCa. Locally advanced PCa requires radiotherapy and hormonal treatment for 2-3 years, typically giving a 58% 10-year survival rate. For metastatic PCa (mPCa), the median survival is just 5-6 years, with 80% of metastases occurring in bone. Most cancers at diagnosis are localized and responsive to hormonal therapy, termed castration-sensitive, but eventually progress to castration-resistant PCa (CRPC) following hormonal treatment. Contrary to long-held belief, CRPC growth in many cases does still rely on androgens and does respond to newer therapies, so CRPC as a term has largely replaced the misnomers "androgen-independent" or "hormone refractory" PCa. Despite this, there are certain extremely resistant forms of PCa which hormone therapy cannot successfully treat and for which reliance on androgens and AR is minimal to nonexistent. Neuroendocrine (NE) PCa is an especially deadly form of tumour which is rare at the time of PCa diagnosis (<1%), but NE differentiation can be induced by treatment and patients with this subtype typically do not survive more than two years.[33-36] Treatment-induced double-negative PCa, which describes AR-negative cancer also lacking NE differentiation,[37-39] is likewise coming to be better understood but neither these nor the similarly resistant and rare small-cell PCa[40, 41] (<1% occurrence at time of diagnosis) will be discussed further since the treatment strategies described here are inappropriate. Hormonal therapy is indicated in many instances such as neoadjuvant use to improve response from radiotherapy or adjuvant use post-radiotherapy. It can also be used in palliative care for mPCa and CRPC, since nearly all patients respond initially and for a median of 12 months, but both of these states ultimately remain incurable. A critical option for PCa hormonal treatment, and the focus of this section, involves androgen deprivation therapy.

Besides surgery and radiation treatments, which can cure and treat localized disease, androgen deprivation therapy (ADT) remains a highly relevant and frequently used treatment option for advanced, metastatic, or resistant PCa today.[2, 31, 42-48] Chemical castration is preferred today over surgical castration, which remains an effective but stigmatizing approach that was more common

decades ago. ADT aims to reduce levels of circulating testosterone in the body to the lowest possible level, where a castrate serum level is defined as < 50 ng/dL (1.7 nM) in order and to directly inhibit androgen receptor stimulation. Reducing androgen levels even below this castrate level to < 20 ng/dL (0.7 nM) is thought to be additionally helpful,[47, 49] underscored by the observation that in primary prostate tumors a decrease in DHT levels by 97% to just 1.25 nM still results in AR activation.[50] Chemical castration employs gonadotropin-releasing hormone (GnRH), also known as luteinizing hormone releasing hormone (LHRH), agonists such as polypeptides goserelin, histrelin, leuprolide, and triptorelin or antagonist polypeptide degarelix to dramatically decrease testosterone production in the Leydig cells of the testes within 3-4 weeks. Abiraterone acetate (Zytiga) inhibits p450 enzyme CYP17A1, which is primarily operative in the adrenal gland, and thereby reduces synthesis of testosterone.[51] Current treatment strategies then frequently use either abiraterone acetate, an androgen receptor (AR) antagonist, or a combination of the two in order to combat PCa on two fronts.[52-54]

Direct inhibition of the key androgen-binding transcription factor AR is achieved with antagonists bicalutamide **1.2** (brand name Casodex), enzalutamide **1.3** (Xtandi), apalutamide **1.4** (Erleada), or darolutamide **1.5** (Nubeqa) (Figure **1.2**). As a terminological aside, the term antiandrogen is sometimes used to refer loosely to any compounds which counteract the effects of androgens, encompassing various compounds affecting AR or other targets. However, it is common in the PCa literature to implicitly equate antiandrogens with AR antagonists. To avoid confusion, the more specific term AR antagonist will frequently be used where appropriate in this thesis, although all AR antagonists are by definition antiandrogens. Although slightly older, the "first generation" AR antagonist bicalutamide remains commonly prescribed earlier in treatment due to the tolerability of side effects and ability to use large doses.[55] The so-called "second-generation" AR antagonists enzalutamide, apalutamide, and darolutamide are all approved for use in non-metastatic CRPC. Despite the effectiveness of second-generation AR antagonists, they inevitably lose effectiveness due to a variety of known resistance mechanisms which will be discussed in Section **1.2.2**, while antiandrogen structures and development will be described in Section **1.2.5**. The predictable induction of resistance has led to a clinical phenomenon known as antiandrogen withdrawal syndrome (AAWS), known since the first nonsteroidal AR antagonist flutamide came into use, which describes an improvement in clinical biomarkers such as PSA levels following AR antagonist removal from the treatment regimen.[56-58] One factor contributing

to AAWS involves point mutations in AR allowing it to bind these antagonists in an agonist mode.[48, 59, 60] Regardless of its lack of curative power, ADT remains a powerful tool to buy time for cancer patients and remains the gold standard of care for advanced PCa.

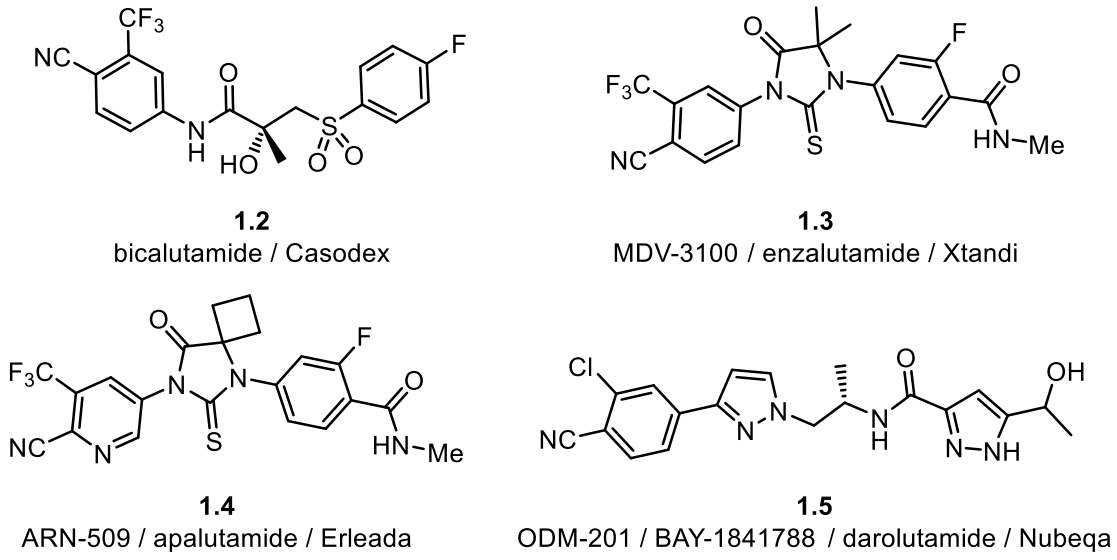


Figure 1.2. Non-steroidal antiandrogens.

Advances in medications have been accompanied by different perspectives on treatment strategies.[61] Combinations of surgical or chemical castration with antiandrogens in a combined / maximal androgen blockade have been effective at dropping testosterone production. Intermittent alternatives to continuous therapy have also had some success recently, such as adaptive treatment cycles,[62] which seek to delay resistance development by starting and stopping treatment to allow tumour recovery and reduce selection pressure. Bipolar androgen therapy (BAT) exploits the fact that supraphysiological levels of testosterone can cause apoptosis in CRPC by injection of intramuscular testosterone cypionate every 28 days while receiving continuous treatment of an LHRH agonist or antagonist, rapidly cycling between very high and castrate levels of testosterone. Remarkably, in some trial cases BAT has re-sensitized patients to treatment with enzalutamide.[63, 64] Despite these and other novel approaches to treating CRPC,[65] the fact that AR signalling is now confirmed relevant even in many CRPC cases validates new approaches targeting this receptor in unique ways. The following section will outline general aspects of nuclear receptor function to provide a basis for understanding androgen receptor function, PCa resistance mechanisms, and to place certain strategies of targeting AR in context.

1.2.1. *Nuclear Receptors: an Overview*

Nuclear receptors (NRs) constitute a family of structurally related, ligand regulated transcription factors which typically bind steroid hormones and other lipid-soluble, membrane-permeable signaling molecules to influence cell processes such as development, metabolism, proliferation, and reproduction.[66-69] Due to their ability to respond to lipophilic hormones capable of both cell permeation and bodily circulation, evolution has utilized the 48 human NRs as the primary mediators of organ physiology. Scientific elucidation of the myriad functions of these proteins accelerated in the 1980's and has since blossomed into many stratified fields concerning each individual receptor or related groups of NRs. This buildup of knowledge concerning NR structure and function has resulted in an understanding of NR roles in various diseases, which has been applied to the development of numerous clinical drugs and drug candidates.[70, 71]

The general NR structure consists of a variable *N*-terminal domain (NTD), conserved DNA-binding domain (DBD), short flexible hinge region, large ligand-binding domain (LBD), and in some cases short variable *C*-terminal domain (CTD). Each region contains subsections critical to proper overall function. The NTD often contains an activation function 1 region (AF-1), which contains binding sites for transcriptional coregulators. The DBD contains two highly conserved zinc fingers and recognizes DNA sequences known as hormone response elements, binding to which allows NR transcription factor function. The hinge region contains a nuclear localization sequence (NLS) allowing import to the cell nucleus, although additional NLSs may be present elsewhere in NRs. The LBD contains an AF-2 quaternary structural domain which acts in concert with the AF-1 region to interact with coregulators of gene transcription, and over 100 such coregulators common to various NRs have been identified. Biologically active conformations of both AF regions are encouraged by NR-specific binding of endogenous ligands.

Despite the structural similarity shared by this class of transcription factors, the ligands recognized by each are diverse in structure (Figure **1.3**). A subset of NRs recognize steroids such as testosterone **1.1** or dihydrotestosterone (androgen receptor / AR), estrogen or estradiol **1.6** (estrogen receptor / ER), cortisol **1.7** (glucocorticoid receptor / GR), aldosterone **1.8** (mineralocorticoid receptor / MR), and progesterone **1.9** (progesterone receptor / PR). Others recognize diverse molecules such as retinoic acid **1.10** (retinoic acid receptor / RAR), 1,25-dihydroxyvitamin D_3 **1.11** (Vitamin D_3 receptor / VDR), and triiodothyronine **1.12** (thyroid

hormone receptor / TR).[66-68, 72] Although typically necessary for function, ligand binding is not the only method of NR biological regulation.

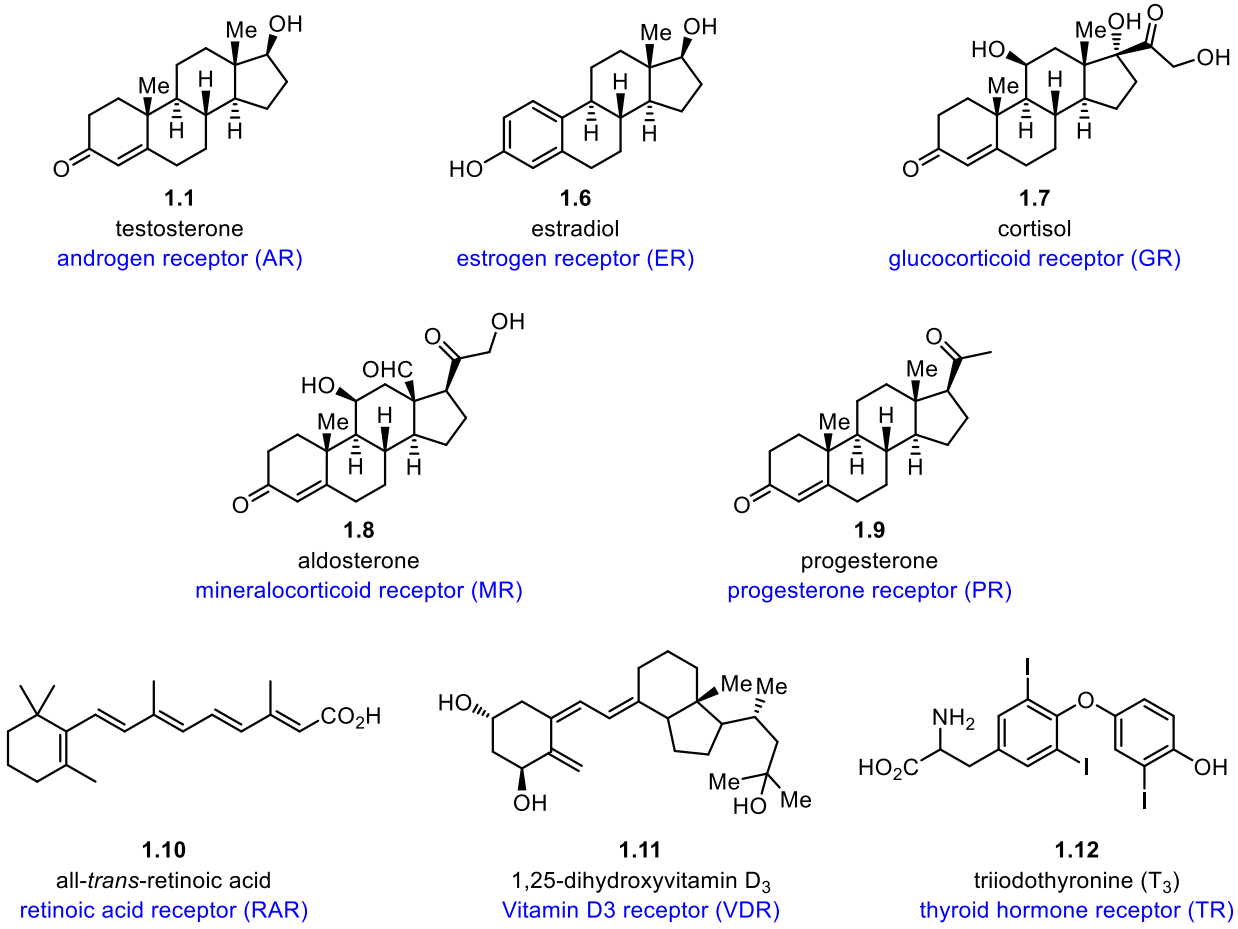


Figure 1.3. Lipophilic hormone ligands and the NRs they interact with.

Ligand binding in fact represents only one of several mechanisms regulating NR function. Phosphorylation, ubiquitination, and SUMOlyation can also serve to respectively activate, terminate, and repress activity of some NRs at multiple locations on each NR. A more fundamental physiological control describes the capacity for certain NRs to display differential gene regulation according to tissue type, which has been suggested to result from differences in accessible chromatin and in co-activator/co-repressor expression.[66, 68] The variety of control mechanisms and ligands bound reflects the variety of purposes and corresponding molecular signaling pathways for each NR, which remain beyond the scope of this thesis. Out of the NRs, this Chapter will focus solely on the structure, function, and ligands of the androgen receptor.

1.2.2. *Androgen Receptor: Molecular Biology*

Androgen receptor (AR) is one of the most well-studied NRs, especially with respect to its critical role in prostate cancer growth and the clinical promise of numerous compounds targeting it.[73-81] This section concentrates on the canonical AR pathway of ligand-dependent transcription factor activity, starting from unliganded AR which has been visualized multiple times using fluorescent tags as primarily located in the cytoplasm. Cytoplasmic AR binds a ligand such as dihydrotestosterone (DHT or D), undergoes a conformational change allowing nuclear translocation, interacts with coactivators and androgen response elements (AREs), then induces target gene transcription (Figure **1.4**). One important gene under control of AR is prostate-specific antigen (PSA), which explains its therapeutic use in the clinical setting. It should not be overlooked that steroid receptors ER, GR, and AR can also act in alternative non-genomic signaling pathways. These pathways are commonly mediated by NR palmitoylation, cell membrane localization / association, signal transduction using kinases, and crosstalk with G protein-coupled receptors (GPCRs) which provoke more rapid downstream cellular effects independent of NR transcription factor activity.[82-84] Methods targeting canonical AR function should affect non-genomic signaling and this section will limit itself to describing the better understood classical genomic signaling. Following this, some documented mechanisms of resistance and key therapeutic methods targeting the entire pathway will be addressed.

Ligand-dependent activation of AR has been reviewed extensively,[4, 85] and only critical details are included here for brevity. Like other steroid receptors GR and PR,[69] unliganded AR resides in the cytoplasm, stabilized with chaperones or other affiliated proteins such as heat shock protein (HSP) 70, HSP90, p23, and other members of the foldosome. AR is maintained in a conformation that potentiates high-affinity binding, but regulatory proteasomal degradation occurs if AR is unable to successfully activate. Endogenous ligands DHT or testosterone (T) bind inside a cleft in the AR LBD, triggering a conformational change which displaces the foldosome and elicits formation of the AF-2 region containing a hydrophobic binding groove (Figure **1.4**). The hydrophobic AF-2 groove accommodates the FXXLF motif present in the NTD region, which results in an intramolecular NTD to *C*-terminal LBD (N-C) interaction.[86-88] Such interactions are absent or weak in other NRs, perhaps due to the uniquely long AR-NTD of 110 kDa. This interaction slows ligand dissociation and prolongs AR half-life.[89, 90] After the N-C interaction forms, nuclear translocation occurs via dynein transport along the microtubule network and

through the nuclear pore complex with the aid of importin proteins.[91, 92] This whole process grants AR access to the nuclear DNA.

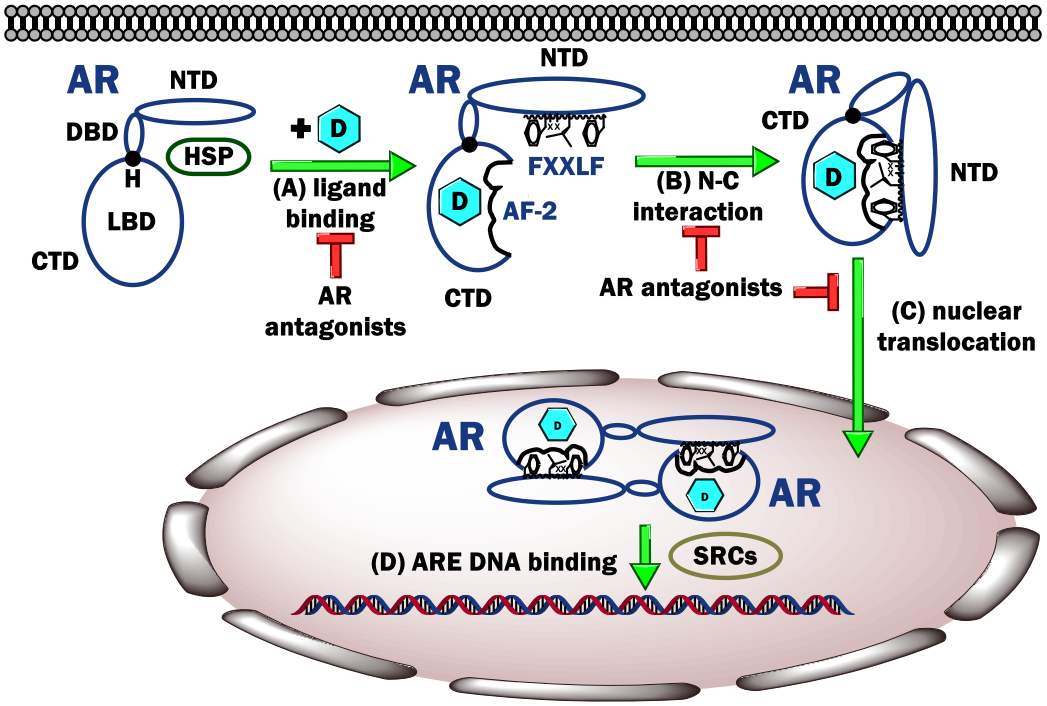


Figure 1.4. Normal androgen receptor (AR) function (green arrows): (**A**) dihydrotestosterone D binding at the ligand binding domain (LBD) in the cellular cytoplasm, (**B**) N-C interaction, (**C**) nuclear translocation, AR dimerization, coactivator association, and (**D**) DNA binding. AR antagonism blocks D binding, N-C interaction, and translocation.

Following nuclear translocation, AR carries out its complex role as a transcription factor. AR homodimerization can occur and AR monomers exhibit differing capacity to activate genes under the control of AREs than dimers, in an ARE-dependent manner. This has been shown using fluorescence resonance energy transfer (FRET) experiments, with which it has also been shown that dimerization occurs post-translocation and is critically mediated through three hydrogen bonds in the dimerization box (D-box) on the second zinc finger of the AR DBD. To allow for intermolecular N-C interactions, this homodimer was originally proposed to be antiparallel as depicted here (Figure **1.4**).[93] However, the full AR homodimer structure has recently been elucidated using cryoelectron microscopy (cryoEM),[94] with and without complexed DNA, as an unsymmetrical head-to-head and tail-to-tail dimer involving all domains but centrally featuring the DBD and LBD.[85, 95] Activated AR was shown by cryoEM to interact with steroid receptor coactivator (SRC) 3, mediated through the AR-NTD rather than AF-2 binding of LXXLL amino acid sequences on SRC-3, which matches the known affinity preference of the AF-2 pocket for the

FXXLF motif present in the NTD.[96, 97] This new structural knowledge seemingly unifies earlier confusion about this homodimer and prior observations that AF-1 function is a stronger mediator of transcription activity than AF-2. Transcription assemblies are in truth both large and complex, and in total over 200 co-activators and co-repressors have been identified for the entire AR pathway, which is far too many to encapsulate in this thesis.[98-100] This entire pathway may also be impacted by various strategies discussed below regarding targeting of AR.

As previously discussed, androgen deprivation therapy (ADT) seeks to reduce AR activity by reducing circulating blood testosterone and by direct small molecule AR inhibition, respectively decreasing and inhibiting ligand activation of AR. Hormone therapy has already been addressed in Section **1.1.3** and AR antagonists will be examined further in Section **1.2.5**. Antagonists competitively bind AR at the same LBD site as endogenous ligands and thereby inhibit normal N-C transactivation, nuclear translocation, and transcription functions. These points will be discussed in greater detail in conjunction with AR structure, but it will suffice to be aware that competitive inhibition critically relies on good binding of AR antagonists in a manner specifically disruptive to function.

AR antagonist binding modes are counteracted by many well-documented mutations in AR which confer eventual resistance to antagonist treatment. These mutations have been compiled in the AR gene mutations database overseen by the Lady Davis Institute at the Jewish General Hospital and McGill University here in Montréal.[101] Many types of mutations affecting clinical outcomes are known along the length of AR and represent just one manner of AR sequence modulation affecting treatment resistance.[102] Several mutations occur in the LBD and confer partial or strong agonist activity for antiandrogens with mutated AR, a phenomenon which has been proposed as one basis for antiandrogen withdrawal syndrome. Point mutations are thought to occur in 20-30% of CRPC cases[103] and are a recurring theme over the years despite advancement in AR antagonist design, but these still constitute just one resistance mechanism.

Many other mechanisms of resistance are known which compensate for androgen deprivation and maintain growth signaling, some of which will be addressed here (Figure **1.5**, **2-9**).[4, 73, 77, 104, 105] AR overexpression is a common early form of resistance to treatment and LNCaP cells bearing this feature are commonly employed in assessing novel therapeutics.[106-109] AR upregulation acts in concert with changes to coregulator expression to potentiate cellular response to limited

androgens and low AR levels.[110-112] To counter low steroid levels, prostate cells adopt *de novo* steroidogenesis, also referred to as intracrinology, which describes the ability to take up and reduce circulating testosterone to DHT with steroid 5α-reductase type 2 (SRD5A2) or convert other steroidal precursors, such that prostatic CYP17A enzymes are thought to play a critical role in PCa progression. AR mutation can also overcome low androgen supply by enhancing its promiscuous binding of alternative steroids such as estrogen, progesterone, and corticosteroids. Certain splice variants of AR such as AR-V7 lack a LBD and exhibit constitutive activity impervious to classical treatments. Splice variants have been identified in advanced CRPC and have come to be a subject

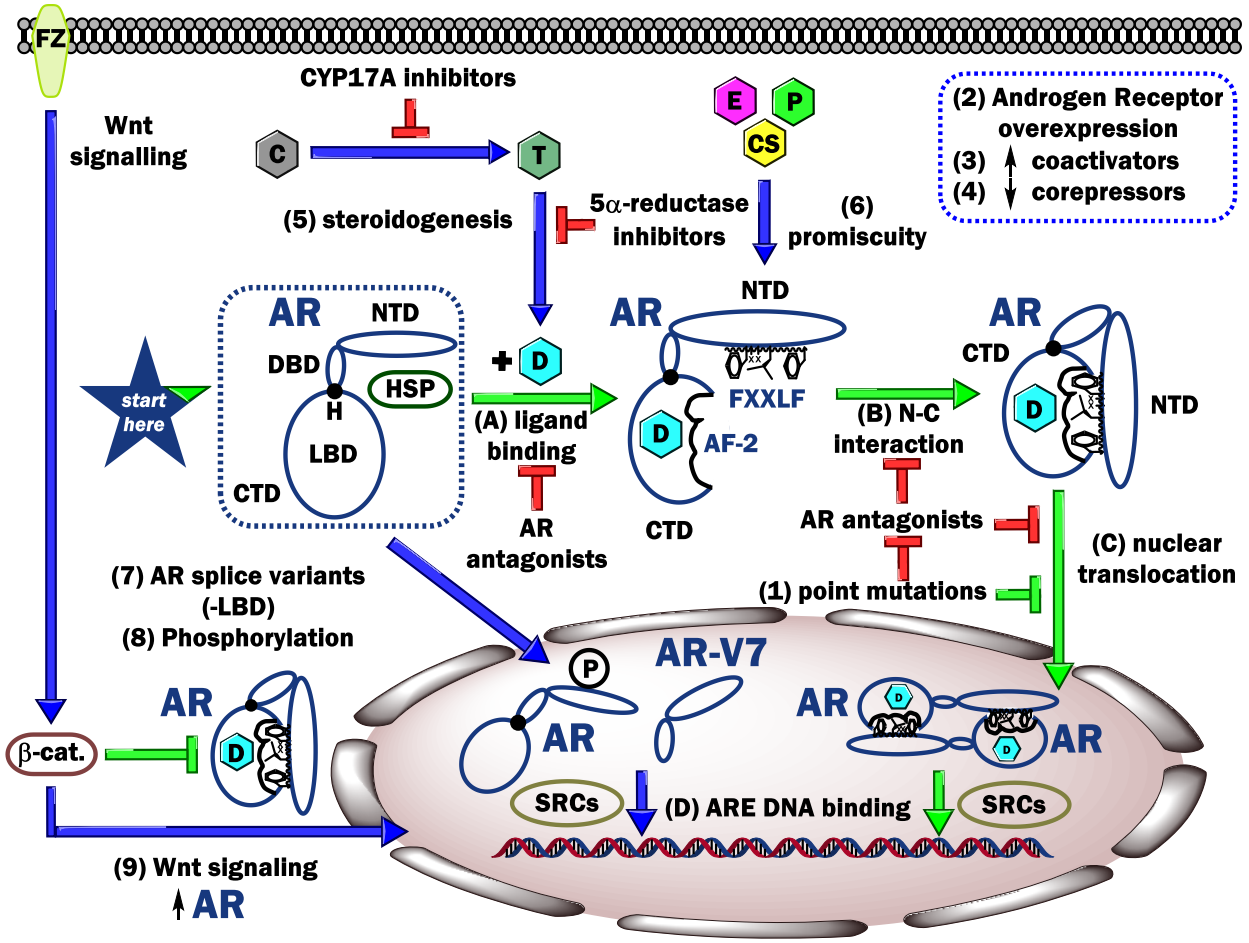


Figure 1.5. Normal androgen receptor (AR) function (green arrows): (**A**) dihydrotestosterone *D* binding at the ligand binding domain (LBD) in the cellular cytoplasm, (**B**) N-C interaction, (**C**) nuclear translocation, AR dimerization, coactivator association, and (**D**) DNA binding. AR antagonism blocks D binding, N-C interaction, and translocation. Resistance mechanisms (blue arrows): (**1**) AR LBD point mutation, (**2**) AR overexpression, (**3**) coactivator upregulation, (**4**) corepressor downregulation, (**5**) steroidogenesis, (**6**) promiscuous binding of steroids, (**7**) constitutive activity of AR splice variants, (**8**) phosphorylation-induced AR activation, and (**9**) WNT-signaling pathways. Other steroids: cholesterol *C*, testosterone *T*, estrogen *E*, progesterone *P*, and corticosteroids *CS*.

of particular concern in recent years, especially since certain variants may be capable of activating gene sets associated with mitotic and anti-apoptotic pathways.[102, 113-119] Various kinases play a role in normal AR function, however certain kinases are thought to directly activate AR in some cases and bypass requirement for ligand binding.[120-123] Lastly, Wnt/β-catenin signalling is thought to be a major driving force behind neuroendocrine and mCRPC.[4, 77] Extracellular Wnt protein can interact with transmembrane Frizzled (FZ) receptors, which activate β-catenin via signal transduction and allow it to bind DHT-complexed AR as a coactivator. In an androgen-deprived environment, β-catenin is left free to promote upregulation of target genes such as AR itself. These and yet other unmentioned mechanisms of PCa resistance remain an area of vigorous research,[124] but both the activity of AR signaling in PCa and the viability of AR as a target has been established and re-established over the decades.

Small molecule drug candidates have therefore been developed against various AR-associated targets to counteract the aforementioned resistance mechanisms, and select strategies will be presented here.[2, 4, 50, 63, 73, 75, 78, 79, 81, 125-127] As previously mentioned, the drug abiraterone acetate **1.13** (Figure **1.6**) is frequently incorporated into ADT treatment regimens alongside AR antagonists since abiraterone inhibits cytochrome P450 17A (CYP17A), a key enzyme in the production of DHT in the adrenal glands, prostate, and tumour cells.[63, 128] Inhibitors of 5α-reductase finasteride **1.14** and duasteride **1.15** have been used for treatment of benign prostatic hyperplasia (BPH), but both compounds caused selective formation of high-grade tumours when used in PCa trials. HSP inhibitors have been explored due their role as stabilizing chaperone proteins for AR, although promising candidates such as the ansamycin geldanamycin **1.16** proved too toxic in clinical trials.[129-133] In contrast to the popular class of "-lutamide" AR antagonists, agents have been developed to target the AR-NTD such as ralaniten (EPI-002) **1.17**, which irreversibly binds the AF-1 region to weaken association with general transcription factors and coactivators.[134, 135] NTD targeting remains a rare and possibly underutilized strategy due to the poorly understood, inherently disordered tertiary structure of the NTD. EPI-002 is currently in a Phase I trial (NCT04421222), while related analogs also appear promising against AR LBD and splice variants in highly resistant PCa models. One final approach worth mentioning concerns attempts to induce AR degradation using compounds such as proteolysis-targeting chimeras (PROTACs),[136-142] which is a new method gaining popularity in medicinal chemistry. PROTAC hybrids are bifunctional molecules which bind a target protein as well as E3 ligase and bring about

the target protein's degradation, which is made particularly effective because the PROTAC is not destroyed and is therefore essentially a catalytic inducer of degradation. Selective AR degraders (SARDs) follow a similar principle and can interact with either the AR-NTD or LBD. Having described the general biology and methods for targeting AR in this section, the following sections will present more detailed knowledge of AR structure and interaction with antagonists.

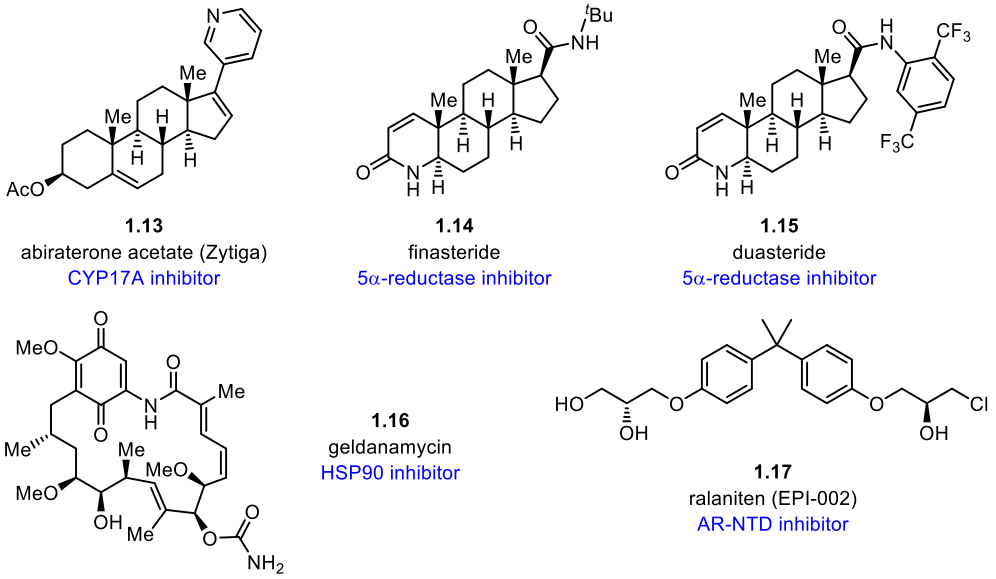


Figure 1.6. Examples of small molecule drug candidates targeting androgen receptor signaling.

1.2.3. *Androgen Receptor: Structure*

The AR ligand-binding domain (LBD) has been analyzed by X-ray crystallography over 90 times, all with compounds bound in an agonist conformation.[143] The AR-LBD bound with DHT **1.1a** (PDB ID 2AMA, Figure **1.7**)[144] consists of just 11 α-helices and two pairs of β-hairpin motifs, since helix H2 is "missing" by comparison to other steroid NR LBDs. The steroid ligand binding site is buried in the core of this large, flexible LBD which resembles a tri-layered antiparallel α-helical sandwich. On binding agonists, H12 repositions to properly form the AF-2 FXXLF hydrophobic binding groove between H3, 4, and 12 (shaded green) and prevents dissociation of bound ligand. Crystal structures are also available showing coactivator peptides bound to AR LBD at the AF-2 site (for example, PDB ID 1T7R).[145] Disruption of the H12 interaction to form the AF-2 region is thought to be generally antagonistic to NRs including RAR, AR, VDR,[146] and ER, where clear crystal structure evidence for H12 displacement has been observed for pure ER antiestrogen binding.[147, 148] Furthermore, molecular dynamics simulations of the *apo*-AR LBD or the LBD bound to DHT and various AR ligands confirm application of the disruption hypothesis

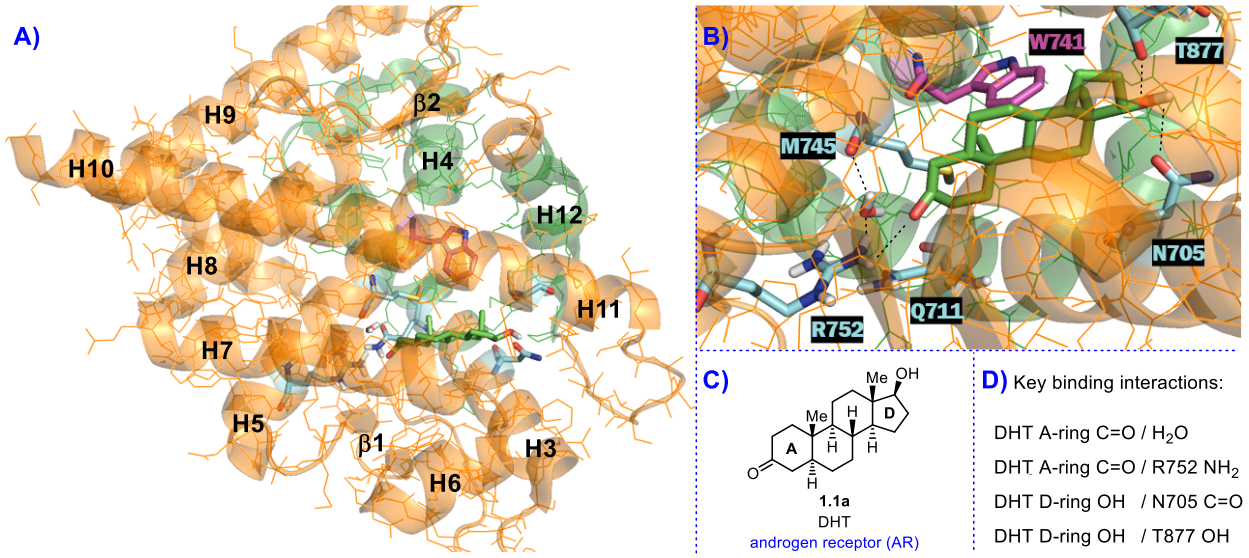


Figure 1.7. (**A**) Full view of AR-LBD crystal structure (PDB ID 2AMA) with bound DHT. The bulk domain is shaded orange, but part of helices H3, 4, and 12 are shaded green to indicate the AF-2 binding groove. Key amino acids are shown with colour using a ball-and-stick model. DHT is shown in green. (**B**) Expansion view showing key binding interactions of AR-DHT. (**C**) Structure of DHT. (**D**) Key hydrogen bonding interactions in AR-DHT.

to AR, since antagonists enzalutamide, apalutamide, and bicalutamide all caused interruption of the H11/H12 interactions key for AF-2 shape except in point mutated models where they would act as agonists.[149-151] The interior of the ligand binding cavity contains many hydrophobic amino acids complemented by polar functionality, which must be precisely positioned to afford binding selectivity between various steroidal compounds and to interact with both ends of natural ligands (dihydro)testosterone. In the heart of the LBD, a hydrogen bonding network forms between Arg752 guanidine, Met745 carbonyl, Gln711 primary amide, DHT carbonyl, and a bound water molecule (dotted lines). The other end of DHT forms another hydrogen bonding network between the DHT hydroxyl, Asn705 carbonyl on H3, and Thr877 hydroxyl on H11. The T877 interaction is key since the more promiscuous T877A variant is known to bind androgens, antiandrogens, progesterone, and estrogen as agonists. Despite its size, Trp741 is known to adopt alternative orientations to accommodate steroidal methyl substitution tetrahydrogestrinone. Trp741 bears special mention since the AR point mutation W741L is established to bind bicalutamide in an agonist rather than antagonist mode.

To date, the only crystal structures of AR complexed with antiandrogens have been solved with ligand bound in an agonist mode with mutated AR such as AR T877A-hydroxyflutamide[152] and AR W741L-bicalutamide (PDB ID 1Z95, Figure **1.8**).[153] The latter produces much the same

overall LBD structure as WT AR-DHT, but still provides some insight into positive binding determinants and ability to subvert antagonism. The A-ring of bicalutamide (CDX) **1.2** mimics that of DHT, with a similar hydrogen bonding network established between the CDX aryl nitrile, Arg752 guanidine, Met745 carbonyl, Gln711 primary amide, and a bound water molecule. A second H-bonding network involves the CDX aryl amide N-H, CDX OH, and Leu704 carbonyl. The degree of hydrogen bonding observed with the alcohol is likely responsible for the fact that (*R*)-bicalutamide has roughly 30 times the binding affinity for AR over the enantiomer. CDX also tends to form an intramolecular OH-SO_2 H-bond, which may reinforce the bent shape observe in this mutant lacking the bulky Trp741. In fact, the smaller Leu741 is thought to directly allow CDX to adopt an agonist conformation and allow H12 to fold correctly to form the AF-2 pocket. Nevertheless, the direct observation of A-ring and adjacent interactions informs AR ligand design, which will be the focus of the following two sections.

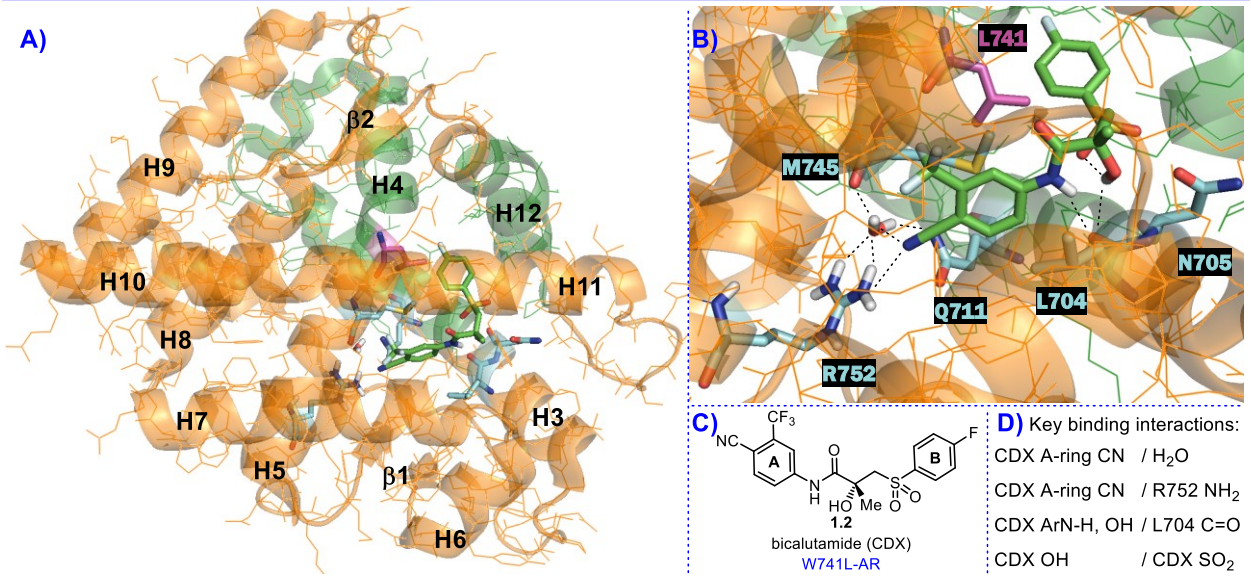
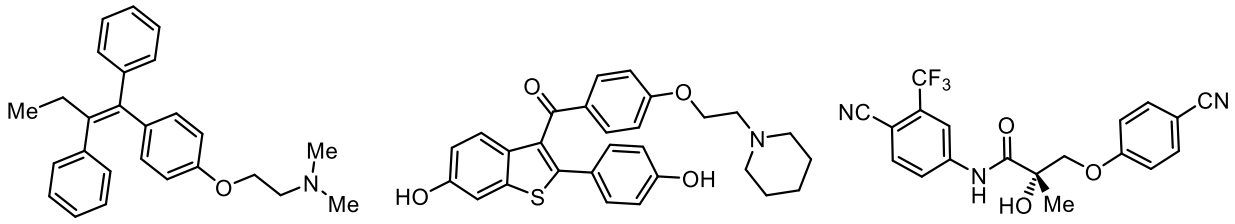


Figure 1.8. (**A**) Full view of AR W741L LBD crystal structure (PDB ID 1Z95) with bound CDX. The bulk domain is shaded orange, but part of helices H3, 4, and 12 are shaded green to indicate the AF-2 binding groove. Key amino acids are shown with colour using a ball-and-stick model. CDX is shown in green. (**B**) Expansion view showing key binding interactions of AR-CDX. (**C**) Structure of CDX. (**D**) Key hydrogen bonding interactions in AR-CDX.

1.2.4. *Androgen Receptor: Agonists and SARMs*

Although the focus of this Chapter is undoubtedly AR antagonism, an introduction to the topic would be remiss to ignore the ill-understood balance between AR modulator agonism, antagonism, and tissue-specific effects or even mixed biological activity. The goal in AR targeting is either to inhibit growth in the prostate tissue or promote growth signaling in other tissues, and the corollaries

of each effect are not desirable though they are frequently encountered as side effects. It must be stressed that AR ligands which accomplish either intended biological purpose while minimizing undesired effects in other tissues are extremely desirable. Tissue-specific effects are actually a general concept with nuclear receptor ligands, possibly reflecting tissue-specific roles of the NRs themselves, and compounds capable of such profiles are generally known as selective nuclear receptor modulators (SNuRMs).[68] The most famous and original examples of such compounds are the selective estrogen receptor modulators (SERMs) tamoxifen **1.18** and raloxifene **1.19** (Figure **1.9**), which act as ER antagonists in breast tissue but agonists in uterus and bone. AR ligands which display tissue-specific effects are therefore known as selective androgen receptor modulators (SARMs).[7, 70, 154-160] The groundwork for nonsteroidal SARM structure was laid out by James Dalton's group, where systematic modification of the bicalutamide structure yielded compounds which displayed anabolic effects, resulting in the discovery of enobosarm **1.20** (also known as ostarine).[161-166] Despite longstanding knowledge of the mixed biological activity of AR ligands, decoupling the differential effects observed between bodily tissues has always complicated identifying new ligands targeting this protein. Antiandrogens are concerned with the inhibition of AR and prostate growth and will be discussed in the following section.



1.18
tamoxifen / Nolvadex
ICI Pharm.
SERM

1.19
raloxifene / Evista
Eli Lilly
SERM

1.20
enobosarm / ostarine
GTx, Inc.
SARM

Figure 1.9. Examples of SNuRM structures and drug candidates.

1.2.5. *Androgen Receptor: Antagonists*

This section will summarize the advances made in the field of antiandrogen drug discovery, with a particular focus on key structural aspects and crucial pharmacological details for the drugs or drug candidates, starting with steroidal antiandrogens.[71, 143, 167, 168] The original synthetic antiandrogens were steroid derivatives such as megestrol acetate **1.21** and cyproterone acetate **1.22** (Figure **1.10A**), which are structurally related to natural steroid progesterone **1.9**. Galeterone **1.23**

and abiraterone acetate **1.13** also act as AR antagonists in addition to their activity as CYP17 inhibitors, perhaps unsurprising given their structure reminiscent of steroidal AR ligands. Although numerous attempts have been made to prepare steroidal antiandrogens or use steroids as a basis for hybrid drug discovery, such compounds will not be discussed. Steroidal antiandrogens elicited numerous undesirable side effects such as hepatotoxicity or virilizing effects, and so numerous non-steroidal AR antagonists have been developed and studied over the past 40 years.

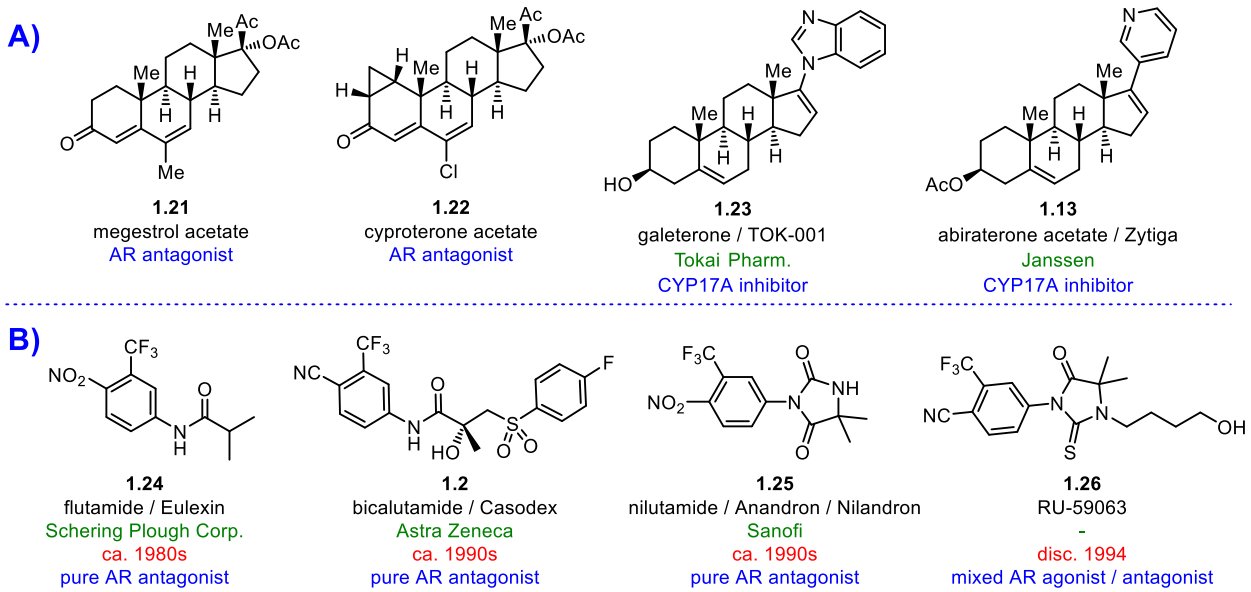
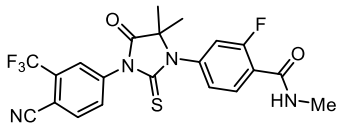


Figure 1.10. (**A**) Steroidal AR ligands. (**B**) Non-steroidal first-generation AR antagonists.

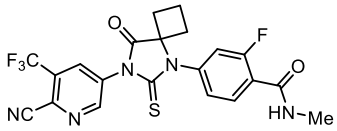
The structures of nonsteroidal antiandrogens have been refined over the decades since their discovery (Figure **1.10B**), originating with *N*-aryl amides flutamide **1.24** (Eulexin, ca. 1980s) and bicalutamide **1.2** (CDX / Casodex, ca. 1990s). Flutamide itself possess low affinity for AR but the carbonyl α-proton is rapidly oxidized to form the active metabolite hydroxyflutamide. CDX possesses much higher AR binding affinity, has fewer side effects, and a longer half-life, which is why CDX is still very commonly prescribed even today. The absolute configuration of the chiral center in CDX greatly impacts its efficacy: *(R)*-bicalutamide displays 30x higher binding affinity and is 100x more metabolically stable than the *(S)* enantiomer. Intriguingly, CDX is known to promote nuclear AR translocation, albeit less strongly than androgens, and a crucial component to its antiandrogen action is thought to be disruption of N-C interaction, SRC recruitment, and transcription activity in the nucleus itself.[169] Furthermore, it is known that CDX typically promotes recruitment of co-repressor NCoR (nuclear receptor corepressor) - SMRT (silencing mediator of retinoic acid and thyroid hormone receptor) complex, but can still allow some coactivator AF-2

association through LXXLL or FXXLF peptide motifs which renders this antiandrogen prone to subverting its own effectiveness.[170] The CDX scaffold has been extensively modified to probe structural features granting AA or SARM activity, but no tangible advances in antiandrogens appear to have arisen.[171-175] In an interesting departure from conventional thought, it was proposed that incorporation of a pyridine A-ring into CDX was able to induce covalent binding to the A-ring nitrile from attack of the C784 thiol. This proposition would seem relevant in the context of second-generation compound apalutamide were it not for the questionable distance (>10 Å) between that C784 and the CDX-CN in the 1Z95 X-ray structure. The authors argued that the more flexible CDX may be able to adopt alternative binding conformations.[176] Hydantoin nilutamide **1.25** (Anandron / Nilandron, ca. 1990s) displays lesser AR affinity than CDX but has milder side effects than flutamide. It was from this core hydantoin structure that thiohydantoin RU59063 **1.26** was discovered. RU59063 binds rat AR with a very high affinity similar to R1881, thrice that of testosterone, greater than DHT, and 20 to 100-fold greater than other first-generation antiandrogens, but possess mixed biological and partial agonist activity *in vitro* and *in vivo*.[177, 178] That compound was therefore never developed into a drug, but the thiohydantoin core was used as a basis by the Jung group for the SAR investigations leading to the discovery of enzalutamide, which heralded a new era of antiandrogen drug development, and has retrospectively been classified as the first of the so-called second-generation antiandrogens.

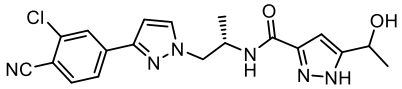
The second-generation antiandrogens have collectively reaffirmed AR targeting in ADT as viable in the face of CRPC, and have significantly extended the lifespan of patients with advanced and resistant PCa.[71] Enzalutamide **1.27** (ENZ / MDV3100 / Xtandi, Figure **1.11**) binds AR about 5-8 times better than CDX, about the same as testosterone, and only 2-3 times less than DHT, while maintaining the same binding specificity for AR over other steroid receptors as observed with RU59063.[170, 179] Additionally, ENZ prevents AR nuclear translocation to a much greater extent than CDX while still inhibiting DNA association, and also inhibited a W741C AR mutant which binds CDX as an agonist similar to W741L. As a drug, ENZ is long-acting and requires days to clear the body, mostly via the urine as the carboxylic acid which forms after metabolic demethylation of the primary amide, which is also a bioactive compound. ENZ is generally very well tolerated and capable of extending CRPC patient lifespan by several months, or up to several years in mPCa, which has dramatically altered PCa management strategies.[180, 181] Nevertheless, point mutation F877L is capable of binding ENZ as a weak agonist and the combination of F877L/



1.27
MDV-3100 / enzalutamide / Xtandi
Astellas / Pfizer
ca. 2012
pure AR antagonist



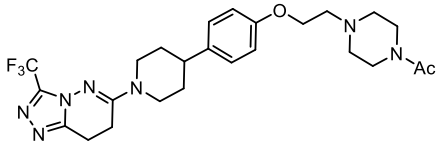
1.28
ARN-509 / apalutamide / Erleada
Aragon Pharm. / Janssen
ca. 2018
pure AR antagonist



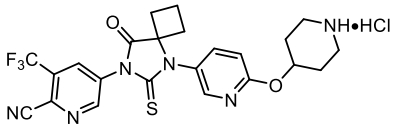
1.29
ODM-201 / BAY-1841788 / darolutamide / Nubeqa
Orion Corp. / Bayer
ca. 2019
pure AR antagonist

Figure 1.11. Non-steroidal second-generation AR antagonists.

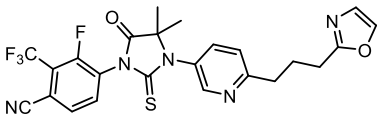
T878A point mutations work in concert to render ENZ a strong AR agonist.[182] Apalutamide **1.28** (APL / ARN-509 / Erleada), a pyridine derivative of ENZ, has similar potency, mode of action, and effectiveness in cell models reliant on AR signaling but possesses certain advantageous pharmacological features.[183-185] APL is metabolized faster as compared to ENZ, primarily by the same *N*-demethylation, with a half-life of about 3 days. Unfortunately, the structural similarity to ENZ has rendered APL susceptible to similar mechanisms of resistance such as the F877L point mutation, which in one study was identified as occurring in 10% of patients.[186] Darolutamide **1.29** (DAR / ODM-201 / Nubeqa), the newest AR antagonist to come to market,[187] is about 7 times more potent than ENZ against AR and in tumors.[188] Note the alcohol stereocenter is not defined since the two diastereomeric compounds interconvert *in vivo* via the oxidized ketone, and all three compounds possess similarly potent activity against AR. DAR has been shown effective against all previous AR LBD point mutations allowing antiandrogen binding in an agonist mode, continuing the trend of newer compounds being successfully tested against the Achilles heel of previous antiandrogens.[187, 189, 190] While no AR point mutations binding DAR as an agonist have been identified, it may simply be a matter of time until similar resistance mechanisms are found. Nevertheless, the potency of DAR and performance in the clinical setting has again re-affirmed novel antiandrogen research.



1.30
AZD3514
Astra Zeneca
currently in Phase 1/2A clinical trials
pure AR antagonist / SARD



1.31
TRC-253 / JNJ-63576253
TRACON / Janssen
currently in Phase 1/2A clinical trials
AR antagonist



1.32
proxalutamide / GT0918
Kintor Pharm.
currently in Phase 1/2 clinical trials
pure AR antagonist / SARD

Figure 1.12. Experimental AR antagonists.

Newer antiandrogens have continued the trend of exhibiting multiple modes of action on AR. Galeterone **1.23**, in addition to CYP17 inhibitor activity as an AR antagonist 10-fold more potent than bicalutamide, additionally induces proteasomal AR degradation. Galeterone is thus considered one member of the class of selective androgen receptor degraders (SARDs), which induce AR degradation or down-regulation by direct interaction with the AR LBD. Diverse molecular scaffolds have been utilized as SARDs,[191-193] but Astra Zeneca's AR antagonist AZD3514 **1.30** (Figure **1.12**) proved quite effective in preclinical studies as it potently binds AR, inhibits AR nuclear translocation, affects AR transcriptional activity, and causes AR levels to drop sharply over a few days. Unfortunately, the compound proved intolerable in clinical trials despite its promise in resistant preclinical cancer models.[194, 195] New AR antagonists are constantly being developed by various pharmaceutical companies. TRACON pharmaceuticals currently has TRC-253 **1.31** in Phase 1/2 clinical trials in a partnership with Janssen Pharmaceuticals, which is 10-fold better at binding AR than ENZ and outperformed ENZ in an antiproliferation assay using LNCaP cells with the F877L AR mutant.[196] Proxalutamide **1.32** has also been reported as a more effective AR antagonist than ENZ, and is reported effective in AR-reliant cell lines LNCaP and C4-2, but success in PCa clinical trials remains to be seen.[197-199] Hopefully this section has emphasized that the discovery of novel antiandrogens is still very much an active field of global research and development.

1.3.1. *Histone Deacetylases: Global and Molecular Biology*

The histone deacetylase (HDAC) family of enzymes cleave acetyl groups from the amino acid side chain of lysine residues on many types of proteins, and thus they are perhaps more properly referred to as general lysine deacetylases (KDACs).[200-205] This unmasking of primary amino groups results in charged lysine ammoniums at physiological pH. Through their action, HDACs alter the surface charge properties of a given target protein substrate and therefore its affinity for various other interactions. HDAC activity is offset by histone acyltransferase (HAT) enzymes such as p300, which catalyze the reverse process using acetyl-CoA. Together these HDAC/HAT enzymes establish a critical equilibrium of lysine acylation which, similar to processes such as methylation, ubiquitination, SUMOylation, and phosphorylation, serves as one major type of protein modification and regulates various cell processes. Importantly, irregular HDAC activity profiles have been identified in several disease states, including various types of cancer. The implication is that inhibition of HDACs could produce sweeping beneficial effects for the cells in

diseased tissue by ameliorating the HDAC/HAT activity imbalance, especially as relating to the transcriptome. In a field where only 100 publications existed prior to 1996, acetylation sites on over 1700 proteins had already been identified over a dozen years ago.[206] Despite intense research, the myriad biological functions of HATs[207] and HDACs remain unelucidated, although a few major cellular roles such as epigenetic regulation are now well understood.

In the cell nucleus, the HDAC/HAT equilibrium carries out the important task of histone modification, for which role the enzymes are named.[208-213] Histone proteins bind the DNA backbone rather than base pairs and can thus bind any DNA regardless of sequence. HDACs modulate histone positive surface charge via lysine deacetylation to increase histone affinity for the negatively charged phosphate-containing DNA backbone. This brief description is likely an oversimplification, and it is now thought that finer control over deacetylation at specific sites may also create binding sites for transcriptional repressors of specific genes while providing little change in histone electrostatic charge. Histone proteins are involved in DNA packing at multiple levels, with the DNA strand being wound in a left-handed superhelix 1.6 times (146 bp) around an octameric nucleosome core containing two copies each of histones H2A, H2B, H3, and H4 at regular base intervals along the DNA sequence in the so-called “beads on a string” model. H1 binds the DNA spacer between nucleosomes and allows additional packing to achieve the 30 nM chromatin fiber structure, which is then further condensed in stages to achieve the tightly packed chromosome structure colloquially associated with DNA. The packing of DNA directly controls access to genes available to the cell transcription machinery and provides a very high-level physical control over transcription, such as allowing tissue-type specific gene expression. In fact, HDAC/HAT proteins can be recruited directly by transcription complexes to regulate local DNA access. Many transcriptional activators possess HAT activity, while repressors recruit HDACs such as the NCoR/SMRT complex which associates with AR and activates HDAC3.[112] Paradoxically, HDACs can also elicit transcriptional increase by causing down-regulation of transcriptional repressors or direct deacetylation of proteins involved in transcription. Histone lysine acetylation is truly a dynamic equilibrium, with a half-life of as short as minutes in transcriptionally active chromatin regions or much longer in silent regions. Massive increases in transcription are observed with less than 50% of maximum histone surface lysine acetylation, which indicates potentiation by some mechanism such as other protein modifications working in concert with acetylation status. The interested reader should note that other chromatin remodeling

mechanisms like ATP-dependent SWI/SNF complex operate concurrently. Furthermore, the HDAC/HAT equilibrium is merely one type of epigenetic regulation among other offsetting enzymes such as the histone methyltransferases and demethylases.

Out of the protein families which regulate epigenetics, HDACs have been the most successfully and prolifically targeted. Explanations for the biological impact of HDAC inhibition are wide-ranging: induction of apoptosis, cell cycle arrest, influence on DNA repair mechanisms, oxidative autophagy pathways, and others.[214] As an example, overactive HDACs may cause repression of cell mechanisms which prevent DNA damage detection or cancer proliferation, and HDAC inhibition can therefore reactivate apoptotic pathways. Unfortunately, the global, multifaceted roles of HDAC enzymes in the cell preclude simplistic analysis of their contribution to a disease such as cancer, or the effect of inhibitors on a diseased state. Isoform-specific mouse HDAC knockdown studies have confirmed the major influences of each, but the fact that not all phenotypes are lethal confirms some functional overlap or ability to compensate and hardly imparts a concrete understanding.[214] A rudimentary yet common way of understanding the various HDAC roles involves classification of the constituent isozymes by structure and function.

The 18 human HDACs are grouped into 4 classes based on phylogenetic analysis of sequence homology, but are numbered rather by their order of discovery.[215] Each HDAC number is commonly referred to as a particular "isoform" or "isozyme" as will be the case in this thesis, but each in fact represents a collection of literal biological isoforms. Class I (HDAC1-3, 8), Class II (HDAC4-7, 9, 10), and Class IV (HDAC11) are all metalloenzymes dependent on bound metal ions such as Zn (II) or Fe (II) for catalytic activity. The 7 Sirtuins (yeast SIR2, silent information regulators II) which constitute Class III use a distinct mechanism involving nicotinamide adenine dinucleotide (NAD^+) to perform deacetylation,[216] rendering them valid yet distinct drug targets in their own right.[217] It is fast being understood by the scientific community that, despite some capability for redundant function, each of the isozymes HDAC1-11 play distinct roles.

The Class I enzymes are heavily involved in histone regulation, although they are commonly mischaracterized as nucleus-associated due to their NLS, and some members do perform other extra-nuclear tasks in organelles or the cytoplasm. Complicating our understanding of discrete functions, Class I HDACs typically operate as part of protein complexes, which may regulate their activity or site of reactivity such as with the HDAC3-NCoR/SMRT complex recently mentioned,

although HDAC8 can operate alone.[218] The need for coregulators has historically led to frustrations in assaying certain inhibitors against HDACs such as 3, and one method of circumnavigating this issue has been to assay compounds using cell extracts, which contain the necessary components for natural HDAC activity. Furthermore, it is thought that HDAC3 expression is tissue-specific, and this may be the case for other isoforms too.

The larger Class II HDACs all show at least partial cytoplasmic localization, implying roles in general protein regulation throughout the cell. ClassIIb (HDAC6, 10) are distinct from Class IIa (HDAC4, 5, 7, 9) or other HDAC isoforms since they possess two non-identical deacetylase domains and, while the much smaller secondary domain in HDAC10 is bereft of residues for metal binding and catalysis, both are catalytically functional in HDAC6.[219] HDAC6 has been particularly well-studied and is known to predominantly localize to the cytoplasm due to its nuclear export signal, where it carries out functions such as regulating cytoskeleton microtubule dynamics by deacylating α-tubulin through its catalytic domain 2 (CD2) subunit.[220-222] By contrast, structure-function studies on HDAC10 only recently revealed it to be a polyamine deacetylase.[223-225]

In truth, HDACs are also capable of cleaving longer acyl groups such as malonyl, succinyl, and crotonyl substrates with varying efficiency. Class IV HDAC11 actually possesses weak lysine deacetylase activity and is rather a long-chain fatty acid lysine deacylase with distinct structure, substrate, and inhibitor requirements.[226-228] As such, the following sections will focus on describing with structure and inhibition of Class I and II HDAC enzymes.

1.3.2. *Histone Deacetylases: Structure and Mechanism*

Understanding of HDAC structure and inhibition has evolved substantially in recent years, and crystal structures are now available on the Protein Data Bank (https://www.rcsb.org) for most human HDAC isoforms with various inhibitors, as part of around 200 structures of human, zebrafish, parasite, plant, and bacterial HDACs or closely related proteins. Just 10 years ago, many models were still based on zebrafish (*Danio rerio*) HDAC or HDAC-like protein (HDLP)[229] since the only human HDACs characterized by X-ray spectroscopy were 2, 4, 7, and 8. Mechanistic studies with HDAC8 have unraveled the somewhat intuitive mechanism likely shared by other HDACs.[204] The mechanism is depicted (Figure **1.13**) using the inconsequential HDAC2 amino acid numbering since a crystal structure of that isoform will be examined below. The acetyl-lysine on a protein substrate is able to span a hydrophobic channel leading to the enzyme active site,

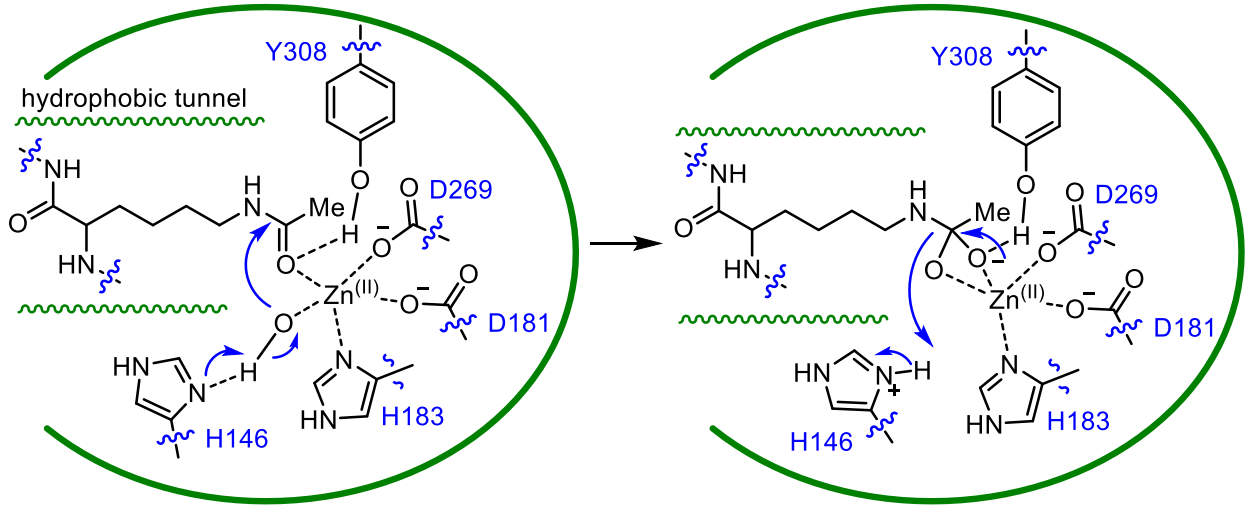


Figure 1.13. HDAC deacetylation mechanism at the enzyme active site.

where the amide carbonyl coordinates to the bound Zn(II) ion. The d^{10} Zn (II) coordination geometry is trigonal bipyramidal and the metal is otherwise bound by water, Asp269, Asp181, and His183. Y308 is a critical residue for deacetylation, since substitution with a histidine as seen in Class IIa HDAC is sufficient to produce markedly lower deacetylase activity that can be restored by mutation to tyrosine. The Y308 shown acts as a hydrogen bond donor to bind the amide carbonyl along with carbonyl-Zn coordination, both of which facilitate attack by a Zn-associated water molecule. Zn coordination lowers the pKa of this water molecule and facilitates deprotonation by H146. Prior displacement of H145 (not shown) on Zn by water allows this residue to remain protonated throughout the entire cycle and generally act as an electrostatic catalyst. H145 also donates a hydrogen bond to the incipient water nucleophile to orient it for optimal attack on the amide carbonyl. Following water addition, H146 acts as an acidic proton source for the departing amine upon collapse of the tetrahedral intermediate. In HDAC8, the acetate exits through an acetate release channel, a feature which may also facilitate weak deacylase activity for longer acyl groups. HDACi borrow many of the same binding interactions.

One of the most relevant crystal structures to this thesis is HDAC2 co-crystallized with model inhibitor **1.33** (Figure **1.14**) bearing a large benzamide ZBG (PDB ID 4LY1).[230] Although there are differences in the shape of the tunnels and clefts wherein the active sites are embedded, the HDAC2 active site presents a typical model and will be especially relevant to the rest of this introduction. Almost the entire structure of **1.33** fits inside the enzyme, with only an acetamide left

exposed to solution, and bidentate Zn (II) coordination is observed through both the aniline and amide carbonyl. The inhibitor participates in hydrogen bonding to Tyr308 through the benzoic carbonyl, with Gly154 through the internal amide N-H (not shown), and with the His145 / 146 pair through the aniline N-H. The thiophene ring of **1.33** buries deep into a 14 Å cavity "foot pocket" and makes additional hydrophobic contacts. This pocket, found in HDAC1-2 and HDLP, appears to be a truncation of the acetate release channel in HDAC8.[229, 231] Benzamides substituted similarly therefore display selectivity against HDAC1-2, a factor which will be further discussed at the end of the next Section. The zinc-binding here mimics that in an HDAC2-SAHA crystal structure (PDB ID 4LXZ) and parallels the normal binding of natural acetyl-lysine substrate. Having discussed the mechanism of deacetylation and outlined the key binding determinants of a model inhibitor, the following section will examine HDAC inhibition.

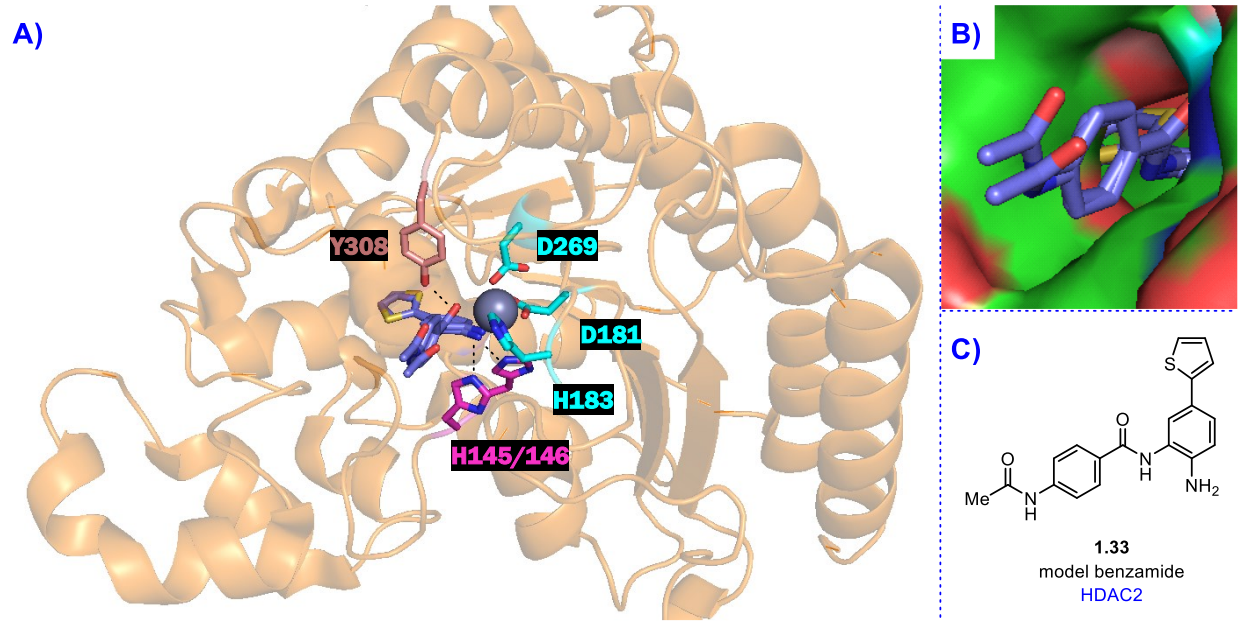


Figure 1.14. (**A**) HDAC2 catalytic domain crystal structure (PDB ID 4LY1) with a bound benzamide. The bulk domain is shaded orange, and the inner surface of the "foot pocket" is shown with partial surface rendering. Key amino acids are shown in colour using a ball-and-stick model. The benzamide compound is shown in blue/grey, with its hydrogen bonding interactions indicated by dashed lines. (**B**) HDAC2 surface rendering showing the tunnel and inner foot pocket. (**C**) Structure of the model benzamide **1.39** used in this complex.

1.3.3. *Histone Deacetylases: Inhibitors*

This section will provide an overview of clinically approved HDACi with certain very conserved structural features as well as more advanced designs which bestow isoform selectivity.[200, 201, 232-235] Natural bodily compounds such as small biological carboxylic acid butyric

acid **1.34** (Figure **1.15**) act as natural HDACi, since carboxylates are capable of binding enzymatic metal sites with weak affinity. Valproic acid **1.35**, a simple alkyl carboxylic acid marketed as a drug for epilepsy, migraines, bipolar disorder, or seizure disorders, has also been shown to have weak millimolar HDACi activity. More potent HDACi are readily identified by rational design and this, coupled to the plethora of conditions displaying dysregulated HDAC activity, has driven the search for more effective inhibitors over the decades.

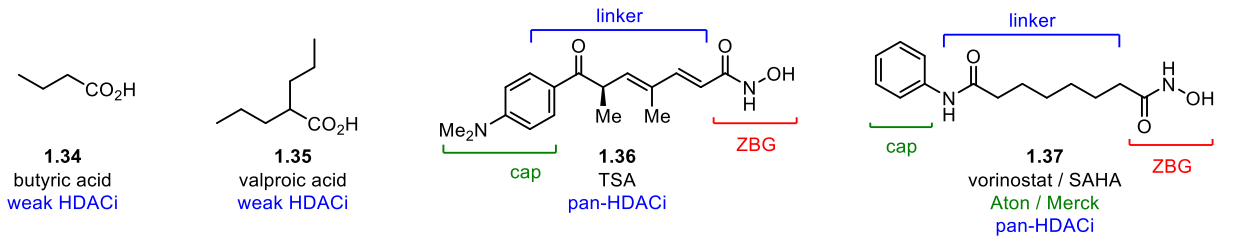


Figure 1.15. Examples of carboxylic and hydroxamic acid HDACi.

All of the compounds discussed in this section share certain structural features which are established in HDACi design, which will be described with two well-known examples (Figure **1.15**). In 1990, hydroxamic acid natural product and antifungal antibiotic trichostatin A (TSA) **1.36** was isolated from *Streptomyces* and found to possess low nanomolar *in vitro* IC_{50} activity against multiple HDACs. The ability to inhibit several HDAC isoforms is a property commonly observed with hydroxamic acid HDACi, leading to the term "pan-HDACi" to describe the promiscuity, although that term is misleading due to some selectivity in a proper biological setting.[218] Unfortunately, its toxicity has precluded its use as a drug to date but closely related hydroxamic acids have been approved as drugs. Vorinostat / suberoylhydroxyanilide (SAHA) **1.37**,[236] the structure of which replaces the stereocenter and branched unsaturated hydrocarbon chain in TSA with aliphatic alkane of equal length, possesses similar potency and lack of isoform selectivity as TSA. The critical structural component in both cases is a metal chelating functional group often referred to as a zinc-binding group (ZBG). ZBG's commonly terminate the inhibitor and are connected to a long hydrophobic moiety necessary to reach through the 11 Å hydrophobic HDAC tunnel between the enzyme surface and active site. Inhibitors then incorporate an aromatic or macrocyclic "cap" group on the other end, which associates with the lip of the HDAC tunnel. Hydroxamic acids are common ZBGs but other more exotic groups have been infrequently used including mercaptoacetamides,[237] trifluoromethyl-oxadiazoles, hydroxy-pyridones, and sulfamides.[238, 239] The ZBGs are a major component of binding potency, while the linker is merely

necessary and is readily optimized. Correspondingly, there is little variety in the ZBGs and linkers commonly used in novel HDACi, while cap groups are a consistent point of differentiation since that position tolerates a staggering array of chemical diversity. The cap group can provide significant potency while being much harder to design due to the number of potential interactions available. The other compounds discussed here should give the reader a further sense of the diversity of chemical subunits incorporated for each HDACi segment.

To give the reader an indication of the types of successful linkers and cap groups commonly featured in drug candidates, the structures of several pan-HDACi are shown (Figure **1.16**). Belinostat **1.38**, panobinostat **1.39**, pracinostat **1.40**, abexinostat **1.41**, resminostat **1.42**, quisinostat **1.43**, and givinostat **1.44** incorporate diverse hydrophobic aromatic / alkyl linkers and both electron-rich and poor aromatic and heteroaromatic cap groups. Several macrocyclic HDACi are also known, where the macrocycle cap group acts as a mimic for an HDAC substrate protein surface. Romidepsin **1.45**, another natural product, is not a hydroxamic acid but rather a disulfide which *in vivo* reduction reveals as the corresponding thiol (or thiolate) ZBG. Romidepsin and similarly masked thiol macrocycle largazole are the most potent HDACi known, and HDAC8 has been shown to undergo significant conformational change to interact with the macrocyclic cap which likely contributes substantially to their potency.[240, 241] Trapoxin **1.46** represents an example of the epoxy ketone macrocycles, which binds the Zn in HDAC8 as the geminal diol or diolate derivative of the ketone and acts as essentially an irreversible inhibitor of Class I HDAC.[242] Note that although the cap groups are quite different, the linkers in both cases are hydrocarbon chains, in keeping with the same overarching design as the hydroxamic acids discussed here.

These HDACi discussed so far have been selected because several of them are under development in clinical trials for various conditions. Vorinostat (2006), romidepsin (2009), belinostat (2014), and panobinostat (2015) have been approved by the US FDA for treating T cell lymphomas, while pracinostat (2014-2017)[243, 244] has been granted orphan drug status for treating both that condition and acute myelocytic leukemia. Most HDACi drugs approved to date are hydroxamic acids, but their use has been limited to rare blood cancers by both poor bioavailability in solid tumours and general toxicity as related to poorly tolerated side effects. Despite their drawbacks, hydroxamic acids remain by far the most common ZBG in new publications due to their potency, and certain characteristics therefore deserve further discussion.

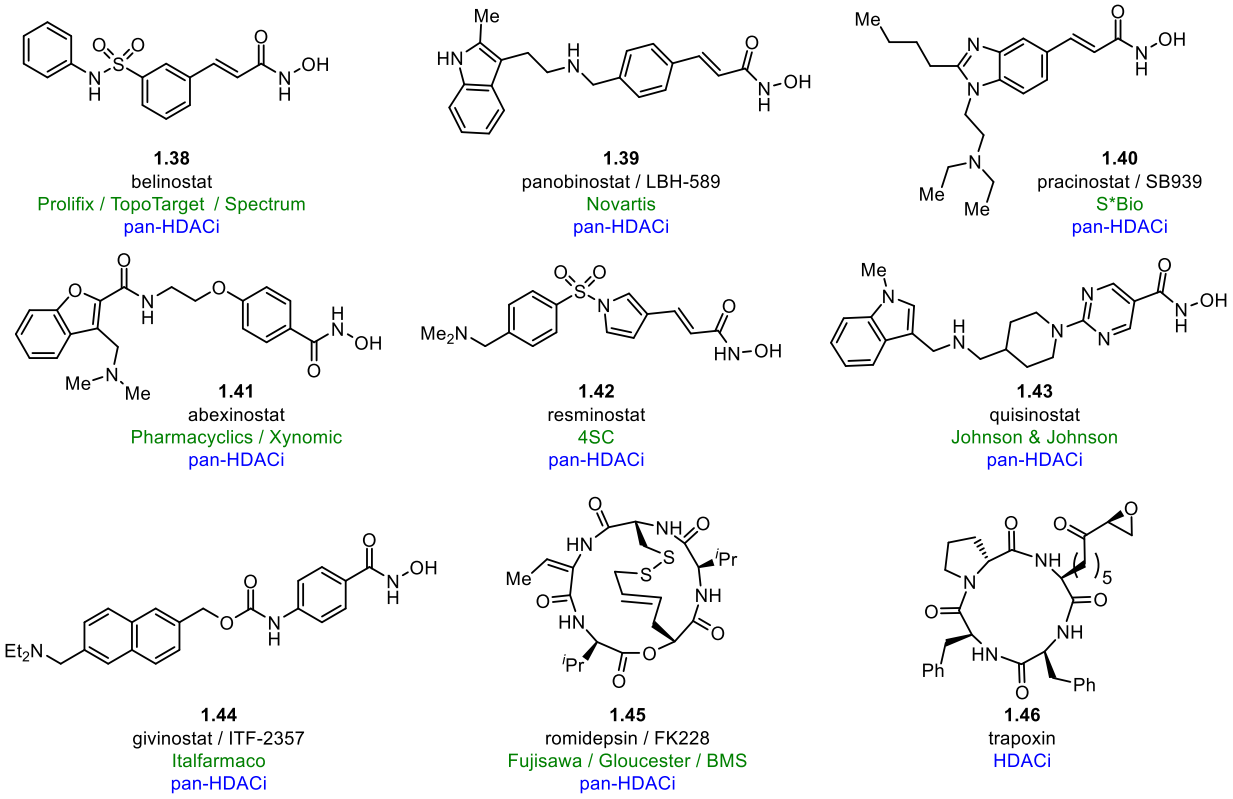


Figure 1.16. Structural variety of pan-HDACi and Macrocyclic HDACi.

Hydroxamic acids (HAs) are well-known metal binding agents used in both organometallic catalysis and nature due to their advantageous unique chemical properties.[245] Typically, HAs are designed such that the carbonyl, nitrogen, and *N*-hydroxyl form a terminus of an inhibitor, and these can coordinate metal ions in either monodentate fashion using the hydroxyl or bidentate fashion through both the hydroxyl and carbonyl. In HAs with both NH and OH protons, aqueous pKa is typically around 8.8-9.3 and represents OH deprotonation, although the pKa increases slightly as expected in organic solvent such as 1,4-dioxane mimicking a likely increase in the organic-lined enzyme active site.[246] In pure DMSO the opposite extreme is reached such that NH deprotonation becomes dominant,[247] and in organic solvent rotational restriction about the C-N bond can become important such that the iminol tautomer which bears two acidic OH groups can dominate.[245, 248] In fact, a relationship might exist between protonation state and the monodentate or bidentate HDACi HA enzymatic chelation modes because in crystal structures hydroxamate anions are found as bidentate ligands while neutral hydroxamic acids are found as monodentate ligands. Alternatively, it has been suggested that water molecules in the hydrophobic tunnel influence denticity.[249] HAs are therefore quite versatile in binding HDACs.

Their versatility might be one reason HAs often display little to modest isoform selectivity within a family of metalloenzymes, and that isozyme binding promiscuity doubtless contributes to their general toxicity. Although it might be thought that toxicity due to general metal chelation is a risk with metalloenzyme binding agents, that assumption is apparently invalid at relevant biological concentrations.[250] HAs do suffer from poor bioavailability outside the blood due to polarity and are readily conjugated through glucuronidation. HAs are also established mutagenic functional groups by way of O-acylation and Lossen rearrangement to produce isocyanates, although such mutagenicity is compound-specific and Vorinostat is admittedly weakly mutagenic.[251] Isoform selectivity is thought to be one way to avoid broad cytotoxic effects of HAs, and selective HAs which have been developed constitute just one subset of selective HDACi.

Isoform selectivity among HDACs has been achieved in certain cases by exploiting subtle differences in HDAC structure, providing notable yet distinct design principles.[214, 252, 253] Such selectivity is desirable to avoid broad, global effects on the cell and hopefully lessen the toxicity of HDACi medications. Numerous selective HDAC6i have been designed which tend to exploit a wider basin at the mouth of the tunnel leading to the HDAC6 active site.[254-263] HDAC6i therefore tend to feature Y-shaped cap-group branching, following rather short linker chains in some cases, for exclusion from other HDACs.[239, 264] HPB **1.47**, compound **1.48**, and bavarostat **1.49** all incorporate Y-branching with tertiary amines or amides (Figure **1.17A**). Compounds selective for the Class I isoforms over the Class IIa enzymes have also been very well studied and are more relevant to this thesis.

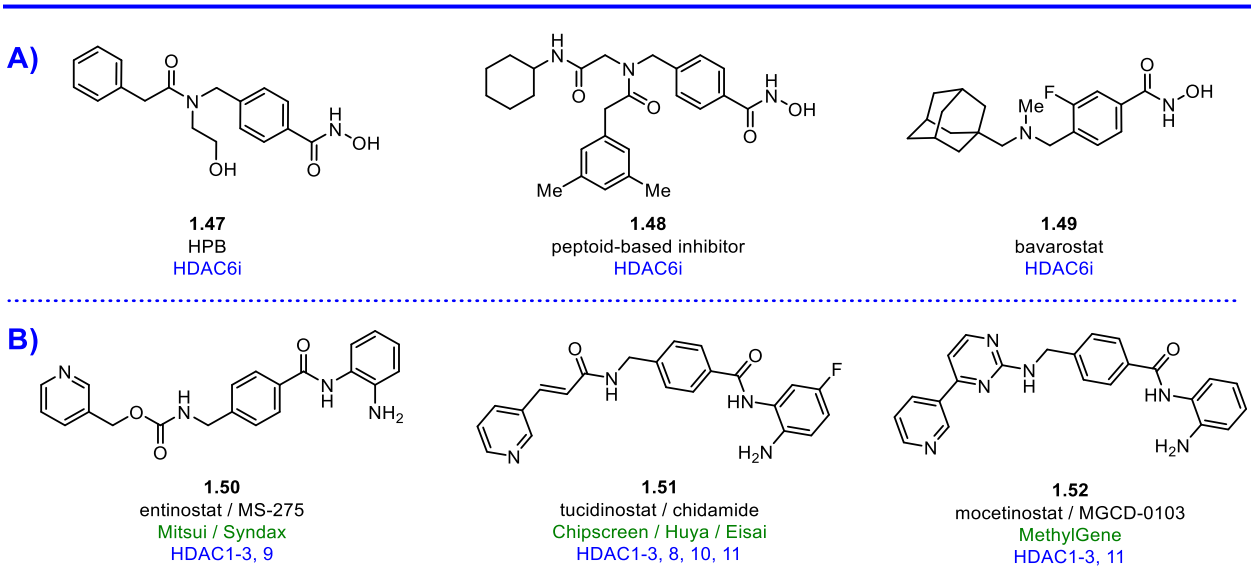


Figure 1.17. (**A**) Examples of HDAC6i. (**B**) Examples of Class I-selective HDACi.

Class I HDACi are unique in structure and commonly feature *o*-aminoanilide ZBGs, commonly referred to simply as benzamides. The three best-known benzamide HDACi are entinostat (ENT) **1.50**, chidamide **1.51**, and mocetinostat **1.52** (Figure **1.17B**). The SAR for benzamide ZBGs include combinations of arene-substituted or unsubstituted *o*-aminoanilides or *o*-hydroxyanilides, variation of the linkers by pyridyl or alkyl spacer incorporation, and numerous cap groups.[265-270] The 14 Å foot-pocket in HDAC1-2 has been exploited to design HDAC1-2 selective benzamides with arene substitution *para* to the aniline.[271] Such substituted benzamides display unusual slow-association / dissociation kinetics but are tight-binding. A mismatch between longer dissociation times as compared to association leads to pseudo-irreversible kinetics, where residence times (k_{off}^{-1}) of 2-38 hours were obtained with HDAC1-2 and substituted benzamides proved particularly slow.[230] New HDACi are being designed and tested in clinical trials all the time and their design is an active area of global drug research.

1.4.1. *Hybrid Inhibitors: General Design Principles and Hybrids in Each Class*

Polypharmacy refers to the administration of two or more medicinal compounds. Drug combinations are commonly employed in treatment since development of resistance against two agents with two distinct modes of action is widely believed to be more difficult than resistance to a single medication alone. The androgen deprivation therapy methods outlined in Section **1.1.3** provide two perfect examples of polypharmacy: first, the combined androgen blockage strategy using LHRH agonists and AR antagonists; second, the co-administration of abiraterone acetate with AR antagonists. The idea of a single compound impacting multiple biological targets is instead referred to as polypharmacology. The concept of hybrid drugs, agents which combine multiple pharmacophores to impact multiple biological targets, stems rather from this latter idea.

Several key advantages are touted for hybrid compounds. First, there can be potentiation of activity by proximity in cases where target proteins associate or are similarly localized. The pharmacology is simplified by administration of one compound rather than two with respect to bioavailability, dosing, and eliminating drug-drug interactions. Third, hybrid drugs are supposed to shift the risk earlier in the drug development process where costs are lesser. Hybrid drugs are especially desirable in the context of complex diseases such as cancer, which adapt and develop resistant biological states to overcome single treatments.[272-276]

Designing one molecular compound capable of interaction with multiple biological targets has been an aspiration of medicinal chemists for decades. In the past 10-12 years, this field of hybrid compounds, or dual inhibitors / agents or designed multiple ligands (other terms abound), has truly exploded in the medicinal chemistry literature. Early this century, many dual inhibitors were discovered through serendipity and most targeted multiple proteins which were either similar or literal isoforms of each other.[277, 278] Slowly, the concept of rational hybrid drug design has taken hold based on screening or knowledge-based approaches, the latter of which is most pertinent here.[279] Design of a compound with two distinct pharmacophores has been achieved using various degrees of scaffold hybridization, from simply conjugating the two with a generic chemical linker, or overlapping common structural features of both pharmacophores, to highly integrated hybrid compounds which fully merge the pharmacophores. The main challenges in hybrid drug design involve increases in molecular weight, increased lipophilicity, incompatibility between hydrophobic / hydrophilic pharmacophores, and balancing bioactivity against multiple targets. Philosophically, activity against each target need be tuned such that it remains effective against each *in vivo*. Obviously, certain pharmacophore classes are more chemically and structurally reasonable to combine than others, and biological motivation for the selection is critical. The design issues can therefore be mitigated by designing more highly merged hybrids, choosing targets where lipophilicity is not problematic such as antiandrogens, selection of matched pharmacophores, and balancing lead compound activity in the cheaper early stages of drug development. This section will first outline a few examples of hybrid drugs in other fields, then examples of hybrid agents which have been formed from each HDACi and antiandrogens.

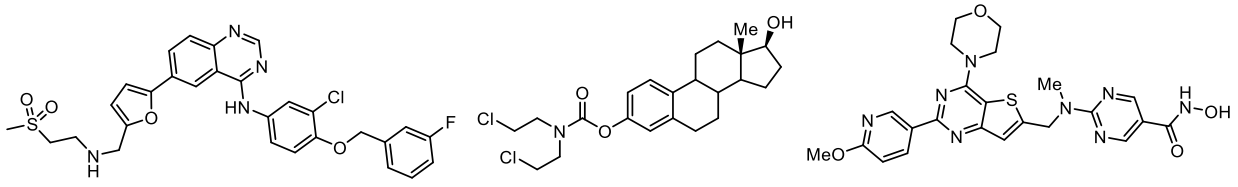


Figure 1.18. Examples of hybrid compounds.

Despite the desire to create hybridized drugs, few designed hybrid drugs exist on the market. Most affect very similar targets such as breast cancer drug lapatinib **1.53** (Figure **1.18**), which acts on the two kinases human epidermal growth factor receptor (EGFR or HER1) and human

epidermal growth factor receptor 2 (HER2). The first drug marketed combining action against truly distinct targets was estramustine **1.54** phosphate, which is both a nitrogen mustard ester and a precursor to estradiol, which is used to treat certain types of PCa.[272]

There are many specific examples of hybrid compounds containing HDACi motifs.[280, 281] The tolerance of HDACi to cap group substitution has been repeatedly exploited and often requires simple fine-tuning of linker length.[274-276] Dual inhibition of HDACi and other targets in many cases leads to synergism, or HDACi can sensitize cells toward an anticancer compound by upregulating the latter's intended target. A handful of HDACi-bearing hybrids have demonstrated promise in early clinical trials for hematological cancers, such as PI3K-HDACi hybrid fimepinostat / CUDC-907 **1.55** (Figure **1.18**).[280] Despite the early success, no hybrids containing HDACi activity have yet been marketed. The literature is replete with specific niche examples of hybrid compounds containing HDACi function, but certain classes of drugs are particularly popular to hybridize such as those targeting kinases,[282, 283] hormone receptors,[284, 285] topoisomerases,[286-288] and PROTACs.[239, 289-291] Creating novel hybrids with both hormone receptor binding and HDACi activity has been a major focus of our group for over 10 years. Aside from the work in this thesis, our group has published several instances to date of NR-HDACi hybrids including VDR agonists[292-296] and ER antagonists.[297, 298] The following section will outline work from other groups in AR-HDACi hybrid compounds.

1.4.2. *Hybrid inhibitors: AA-HDACi hybrids*

It has been shown that when SAHA and bicalutamide are used in combination, they dramatically increase apoptosis in androgen-responsive LNCaP cells at concentrations where either compound alone has minimal effect.[299] Significantly, apoptosis was reduced upon adding DHT to the medium. The lack of a similar effect in PC-3 cells, which do not rely on AR growth, indicates the combination truly impacts AR signaling. Another example of similar synergy causing increased cell death was noted in AR+/ERG+ VCaP cells treated with flutamide in combination with each of the HDACi entinostat, SAHA, and TSA.[300] Intriguingly, this study stemmed from the finding that HDAC1 is upregulated in ERG+ cell lines, while the genes affected by HDAC1 are downregulated, and showed that HDAC1 represses the ERG gene expression signature. Cell lines VCap, and the similarly AR+/ERG+ DuCAP, were both more sensitive to induced apoptosis and caspase induction by combination treatment than any of the ERG– LNCaP, PC-3, or DU-145 cells.

LNCaP cells, which express the TMPRSS2-ETS fusion ETV1 rather than ERG, were somewhat more sensitive to combination treatments than the other two ETS– lines. It was surmised that the effectiveness in AR+ cells might stem from the increased HDACi effectiveness observed in androgen depleted media. The pan-HDACi TSA and SAHA suppressed AR levels, which may relate to inhibiting HDAC6 acetylation of HSP90, while entinostat and SAHA both interfered with AR nuclear transport. HDACi activity also led to suppression of WNT signaling and activated apoptosis pathways. A third report indicated synergy between bicalutamide and TSA to reduce cell viability and cause apoptosis in a novel cell line DuCaP-N. That line had been generated by converting CRPC model DuCaP cells to a hormone therapy naïve line by treatment with synthetic steroidal androgen metribolone (R1881) until resistance developed.[301] A large portion of the motivation for hybrids combining AR antagonist and HDACi functionality is therefore based on the demonstrated synergy with co-administering compounds from each class in PCa cell models.

Although the possible mechanisms for HDACi effectiveness in PCa remain unclear, the sheer versatility of these enzymes complicates the issue. HDACi are expected to have wide-ranging effects on the cell but are undeniably effective regardless of the inability to pinpoint the exact targets or the critical actions of those targets which are inhibited. Class 1 HDAC1-3 upregulation in PCa correlates with higher Gleason scores, greater cellular proliferation, and lower probability of disease-free survival. Specific mechanisms of HDACi in PCa include acetylation of AR-associated HSP90 leading to AR degradation, de-repression of tumour-suppressor transcription factor p53 which is activated through acylation by HAT p300, or affecting activity of signal transduction signaling pathways.[302] AR itself can be acetylated by p300 and Tip60, an event which aids in DHT-dependent AR activation. Certain AR functions also appear to be downregulated by HDAC1, which is capable of forming a trimeric complex with AR and Tip60.[303, 304] Although this would seem to present an argument against HDAC inhibition, that finding is included to underscore the complexity of HDAC regulation and this AR-HDAC1 interaction may ultimately prove inconsequential, poorly understood, or even beneficial. Importantly, HDACi are known to suppress AR expression in LNCaP cells[108] and have been used in PCa trials.[305, 306] Multiple phase II PCa clinical trials have examined various hydroxamic acid-equipped HDACi alone or in combination with bicalutamide. Unfortunately, these agents have not proved effective against solid tumours and have produced many side effects.[302] Nevertheless, the potency of such compounds *in vitro* and the success of benzamide HDACi entinostat in breast cancer treatment warrants further

understanding of HDAC as a target in PCa. As discussed in the preceding section, hybrid agents offer the ability to affect multiple cellular targets while simplifying pharmacology relative to separate compounds, and hybrids may therefore provide a more potent alternative to the co-administration of antiandrogens and HDACi.

Examples of androgen receptor antagonist hybrids with HDACi function have been published prior to or in the course of the work contained in this thesis (Figure **1.19**). The Oyelere group has developed a series of very long hydantoin-based conjugated pharmacophores such as compound **1.56**, which was one of the most potent compounds assayed for HDAC (IC_{50} ca. 20 nM), AR (IC_{50} 690 nM), and LNCaP cell growth inhibition. Their compounds were shown to exhibit a Trojan-horse effect provided by the antiandrogen pharmacophore, which allowed nuclear import by AR translocation as observed by fluourescence microscopy. Surprisingly, potent AR binding was found to be necessary but not sufficient for AR nuclear localization, while increased HDACi potency was actually found to correlate with increased AR nuclear translocation.[307, 308] Further testing of the hybrids in mouse tumours showed moderate activity indistinguishable from treatment with ENZ or ENZ+SAHA.[309] A follow-up patent disclosed a series of similar hydantoins bearing methylene-linked fluorinated arene cinnamyl hydroxamates.[310]

The Qin group developed slightly more compact bis-aryl thiohydantoin hybrids but only published two compounds, with the more potent **1.57** bearing a long-chain alkyl hydroxamate, and the other a simple cinnamyl hydroxamate from the same fluorobenzene unit. Hybrid **1.57** displayed less potent HDAC6 inhibition than SAHA at 2 μM, and also showed micromolar HDACi activity against nuclear cell extract enriched in HDAC1-2, but was not assessed for AR inhibition *in vitro*. The hybrids induced degradation of AR and HSP90 unlike ENZ, and induced both HSP90 and α-tubulin acetylation similar to SAHA, which strongly suggests these compounds are active primarily in the cytosol against HDAC6. The hybrids also reduced the cell viability of androgen overexpressing, TMPRSS2-fusion positive C4-2 cells but not AR insensitive PC-3 cells.[311, 312]

The last set consists of a series of hybrids bearing 14 distinct linker/ZBG combinations, with many unique examples of each component. The best of the more relevant hydroxamic acid and benzamide compounds are shown. The hydroxamic acids **1.58**-**1.59** each displayed ca. 3 μM inhibition of HDAC1 but far better HDAC6 inhibition and very potent AR inhibition near the assay limit. Benzamide **1.60** instead displayed the expected Class 1 HDAC isoform selectivity,

particularly against HDAC1 and 3 (IC_{50} 5-6 μM for each), while proving to be a very weak HDAC6i but a reasonable AR binding agent (IC_{50} 330 nM).[238] Some unorthodox ZBGs were incorporated such as trifluoromethylketone, sulfamide, hydroxypyridone, and its thiocarbonyl equivalent, but these were generally weak HDACi.

Other new reports of AA-HDACi bearing long linkers and hydroxamic acids have been disclosed solely in the patent literature.[313] Although many of these investigations were reported in the course of the work described in this thesis, these studies collectively validate the motivation for novel hybrid inhibitors of androgen receptor and the histone deacetylases. Efforts to prepare and assess novel hybrids of this type will be described in Chapter 2 of this thesis.

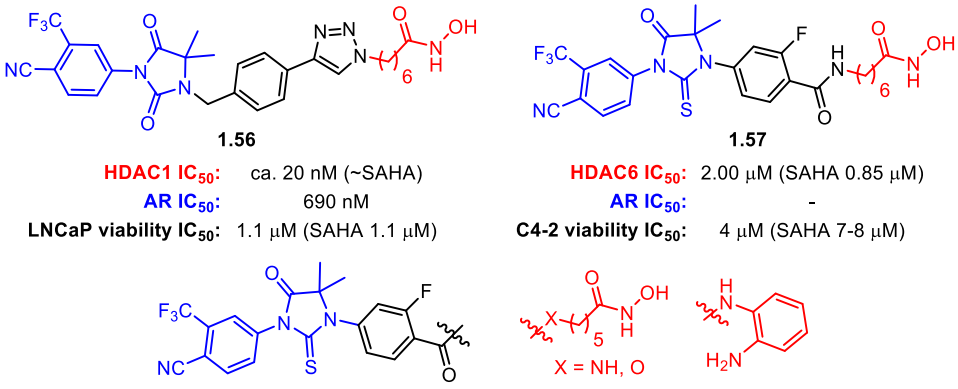


Figure 1.19. Other published AA-HDACi hybrid structures and summarized biological data.

Chapter 2. Development of Novel Hybrid AA-HDACi

2.1.1. *Design of an Expanded 1st Generation of AA-HDACi*

This chapter describes the development of novel AR antagonist-HDAC inhibitor (AA-HDACi) hybrid compounds as potential future therapies for prostate cancer. The proof-of-concept work for the project was done by Christopher Doyle, who developed a series of hybrids that incorporated hydroxamic acids into the structures of either bicalutamide or RU59063.[314] The new contributions include further exploration of hydroxamic acid-bearing hybrids and the development of novel hybrids bearing benzamide zinc-binding groups. Most of the work has been published in the literature, and some figures will be used directly or with slight modification based on that article.[315]

As described in Chapter 1, clinical use of antiandrogens in prostate cancer treatment leads to the development of resistance. Clinical resistance has led to the exploration of related treatment regimens such as the co-administration of additional drugs, such as abiraterone acetate, in combination with AR antagonists. As discussed in Section **1.4.2**, co-administration of either antiandrogen flutamide or bicalutamide with one of the HDAC inhibitors entinostat, SAHA, and TSA led to synergistic reductions in cell viability in AR-expressing prostate cancer cell models. Given the synergy, a clinical trial examining the combination treatment of enzalutamide and entinostat (NCT03829930) was launched in 2019.[316] Also based on that synergy, multiple research groups, including the Gleason group, initiated hybrid drug discovery projects aimed at combining antiandrogen and HDACi pharmacophores.

Within our group, the initial studies were conducted by Christopher Doyle, an M.Sc. student. Due to a lack of good structural data on antagonist conformations of AR, it was initially desired to explore the incorporation of hydroxamic acid zing-binding groups (ZBGs), such as seen in HDACi drug vorinostat **1.37**, to either end of the structure of antiandrogen bicalutamide **1.2** (Figure **2.1**). Our design strategy resulted in highly merged hybrids which in the case of **2.1a-b** sought to use the hydroxamic acid on the A-ring as a nitrile / carbonyl replacement in the AR binding pocket while the bicalutamide structure would need to act as a linker spanning the HDAC hydrophobic tunnel. Hybrid **2.2** would rely instead on canonical antiandrogen A-ring interactions but aim to disrupt H12 folding with the hydroxamic acid. As shown, **2.1a-b** were capable of inhibiting HDAC6, while **2.2** was a much weaker inhibitor, but neither of **2.1a-b** retained AR antagonist

activity. The poor results obtained from the bicalutamide-based hybrids may be attributed to the lower AR affinity of the parent compound, which cannot tolerate further loss of potency due to hydroxamic acid incorporation. Structurally, the hydroxamic acid would probably need to displace the water in the hydrogen bonding network at the A-ring of (anti)androgens, and the group may not adequately replace those same interactions or be physically accommodated.

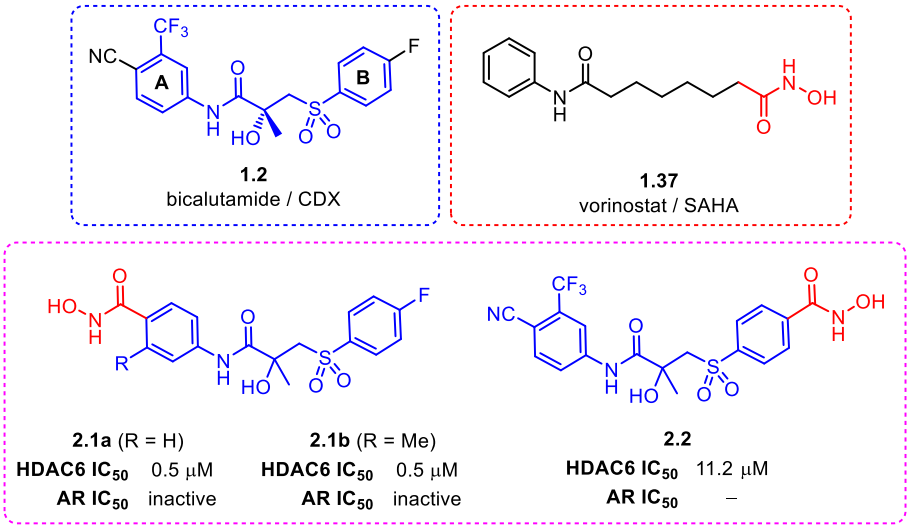


Figure 2.1. CDX-inspired hybrids previously prepared by the Gleason group.

It was desired to then use a more potent antiandrogen scaffold, either RU-59063 **1.26** or enzalutamide (ENZ) **1.27**, and retain the shared A-ring and thiohydantoin core to maintain effective AR binding. The potency of antiandrogens is highly sensitive to the aniline A-ring and is thought to require a compound to maintain a conformation which disrupts AR H12 folding. Unfortunately, the lack of good structural data for WT-AR bound with antagonists hampers efforts to predict how subtle changes in antagonist structure will affect inhibition, which has frustrated computational drug discovery modelling efforts for some time.[149, 317, 318] The rigidity of antiandrogen conformation is also thought to be helpful, since intramolecular hydrogen bonding has been proposed in both hydroxyflutamide[167] and bicalutamide,[153] and the rigid planar structure of biaryl thiohandantoins possessing two preferred conformations is thought to contribute to their disruption of H12 folding.[149] Although the gem-dimethyl on the thiohydantoin ring is very amenable to substitution by hydrocarbon rings, the added size may present issues with HDAC binding.[319] Lastly, it was never clear whether the aryl fluoride in ENZ was necessary for binding potency, but was rather assumed to be incorporated for metabolism, and was not included to simplify hybrid structure. The selected hybrids therefore replaced the RU-59063 alkyl alcohol with

alkyl tethers terminating in hydroxamic acids (**2.3a**,**c**, Figure **2.2**) or substituted the methyl acetamide on enzalutamide for a hydroxamic acid moiety (**2.4**-**2.5**) to deviate as little as possible from the successful scaffolds. Hybrids **2.3c** and **2.5** which bear longer hexyl and cinnamyl linkers were found to be more effective HDACi, with respective IC_{50} values of 2.5 μM and 1.5 μM, than **2.3a** (58 μM) and **2.4** (17 μM). All compounds in the set were found to be active AR antagonists, but the most potent compounds against this target were rather the shortest butyl hybrid **2.3a** (IC_{50} = 60 nM) and longest cinnamyl hybrid **2.5** (IC_{50} = 63 nM). The initial results provided a valuable proof-of-concept for hybrids based on the ENZ scaffold.

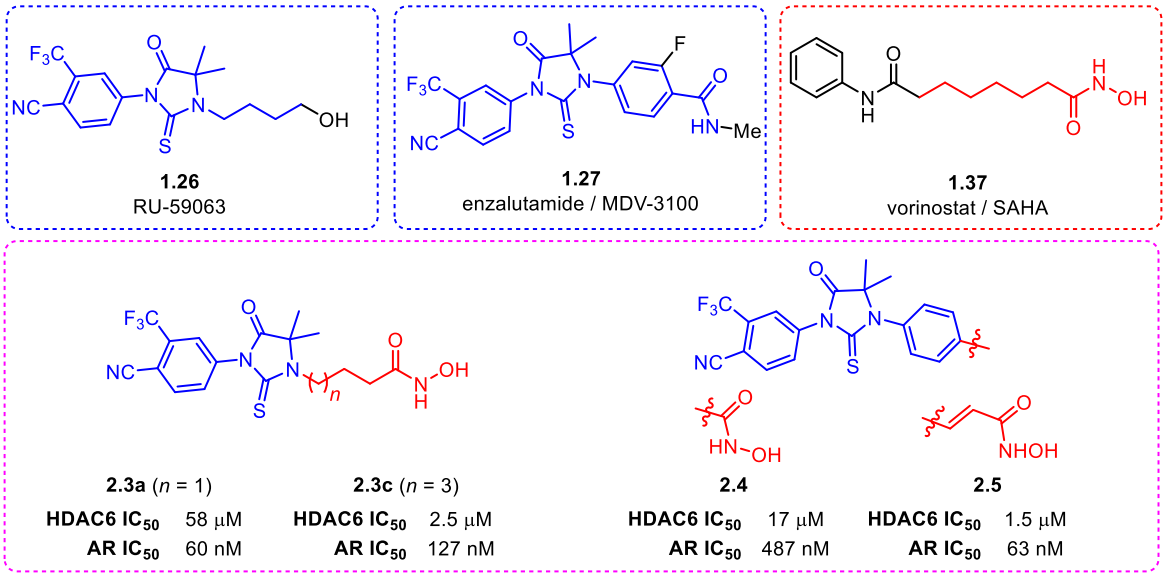


Figure 2.2. RU59063-inspired hybrids previously prepared by the Gleason group.

To build on the initial work, it was desired to expand the 1st generation set of hybrids while synthesizing additional novel compounds. Again, our hybrids needed to be based on the known antiandrogen SAR data rather than attempting novel structure based on molecular modelling. To fully examine linker lengths, it was decided to complete the set of alkyl hydroxamates (**2.3b**,**d**, Figure **2.3**). Hybrids bearing benzamide ZBGs were also desired due to the issues of toxicity and bioavailability associated with hydroxamic acids generally, which were outlined in Section **1.3.3**. To avoid those issues, benzamide ZBGs were incorporated onto the structures of ENZ **1.27** (**2.6a**-**b**) or flutamide **1.24** (**2.7**-**2.8**) in place of alkyl amides in each case, with both unsubstituted and phenyl-substituted benzamides. As before, the antiandrogen features were conserved and relied on to span the hydrophobic channel leading to the HDAC active site, and any leftover portion would hopefully find favourable surface interactions. Small hybrids **2.7**-**2.8** would probably fully reside

in the enzyme much like tool compound **1.33** in the HDAC2 crystal structure depicted in Section **1.3.2**. These HDACi ZBGs would serve a second purpose in the AR binding cleft, where they would be required to make contacts or disrupt H12 folding, since they would be on the "tail" pointing toward the AF-2 region, which models describe as the source of AR antagonism.

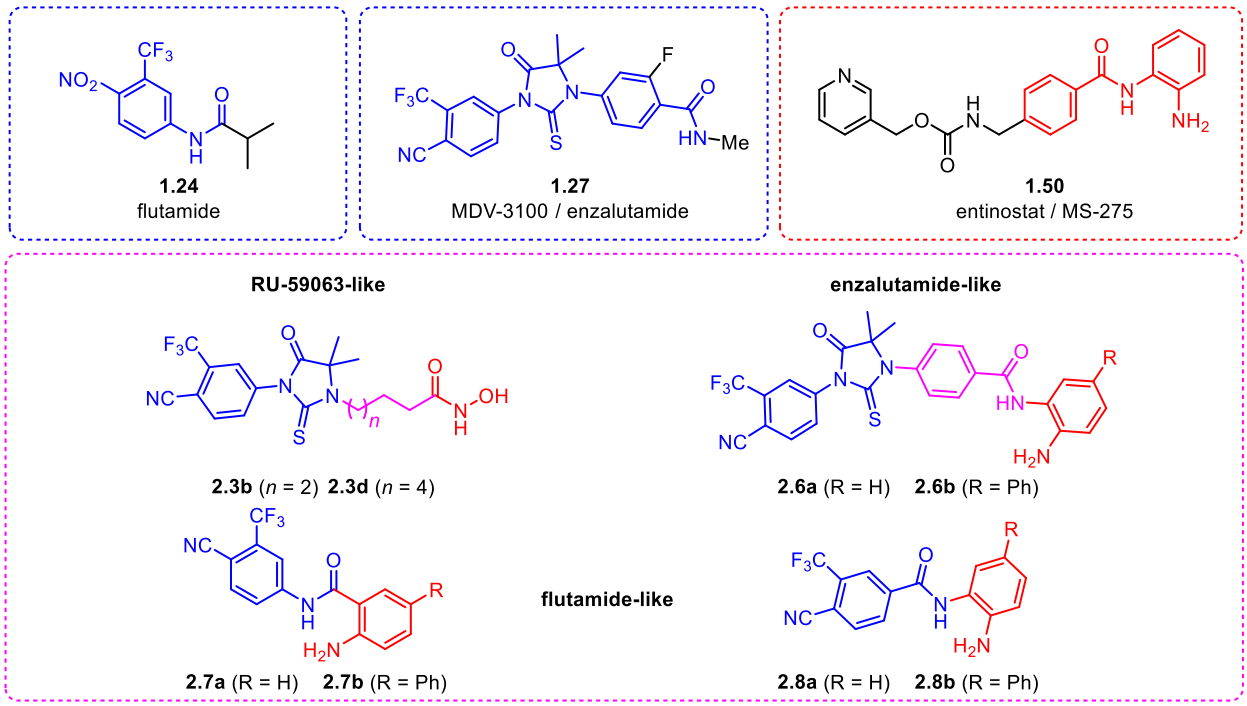


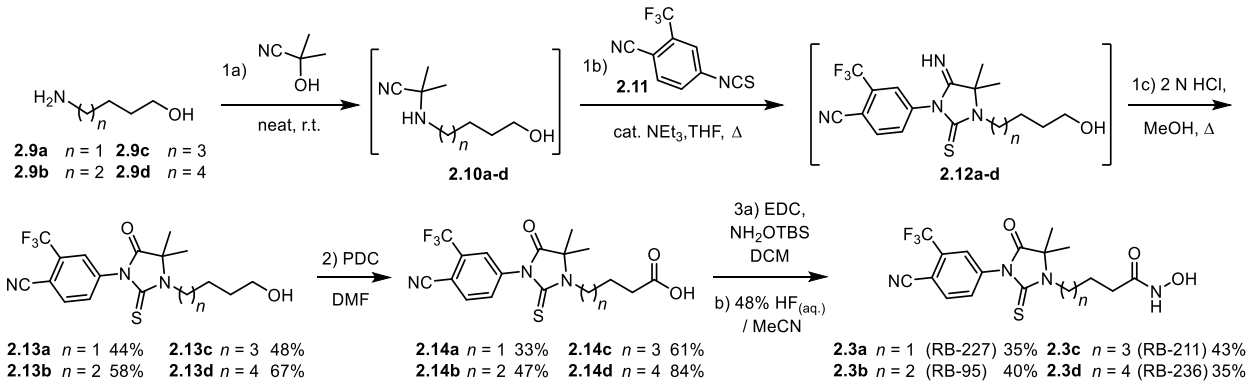
Figure 2.3. Proposed extension of the 1st generation of AA-HDACi hybrids.

This Chapter will first outline the preparation of the expanded set of 1st generation AA-HDACi hybrids, then their biological evaluation against each target and in cell antiproliferation assays. The design, synthesis, and evaluation of a 2nd generation of hybrids, based on a lead compound from the 1st generation, will then be described. The SAR information gleaned from both generations will be assessed to guide any future efforts in similar hybrid inhibitor design.

2.1.2. *Synthesis of RU59063-Inspired Hydroxamic Acid Hybrids*

Hydroxamic acid hybrids **2.3a-d**, featuring alkyl linkers of various lengths, were synthesized as previously reported by Christopher Doyle using standard methods for thiohydantoin synthesis.[178, 314] Briefly, condensation of simple amino alcohols **2.9a-d** with commercially available acetone cyanohydrin, often in the presence of drying agents such as $MgSO_4$, provided α-cyanoamines **2.10a-d** which were used directly in the following step (Scheme **2.1**). The cyanoamines could be reacted with known aryl isothiocyanate **2.11**[179] in the presence of catalytic triethylamine in refluxing THF to provide iminothiohydantoin intermediates **2.12a- d**. The imines

were hydrolyzed with HCl in refluxing water / methanol to thiohydantoins **2.13a-d** in 44-67% yield over 3 steps. Oxidation of the primary alcohols was previously observed to be complicated by sulfur oxidation. However, direct oxidation to carboxylic acids **2.14a-d** with PDC in DMF was found to selectively oxidize the alcohols in 33-84% yield. The yield was impacted in some cases by chromium sequestration, but vigorous ethereal trituration was found to greatly increase the yield for **2.14d**. Acids **2.14a-d** were then subjected to EDC-mediated peptide coupling with NH_2OTBS followed by HF-mediated silyl deprotection to furnish target hydroxamic acids **2.3a-d** (RB-227, 95, 211, and 236) in 35-43% yield.

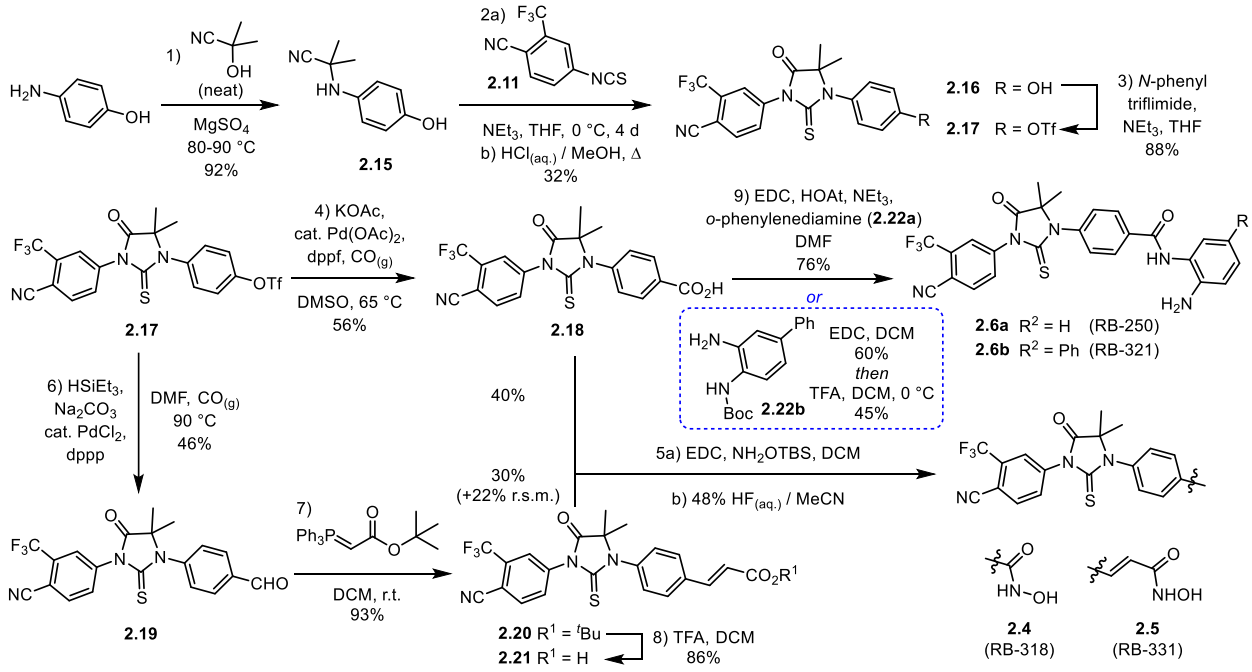


Scheme 2.1. Synthesis of RU59063-inspired hydroxamic acid hybrids RB-227, 95, 211, and 236.

2.1.3. *Synthesis of Enzalutamide-Inspired Hybrids*

Hydroxamic acid hybrids **2.4** (RB-318) and **2.5** (RB-331) have been previously prepared by Christopher Doyle and were remade based on those reported procedures.[314] The early portion of the synthesis involves thermal condensation of *p*-aminophenol with acetone cyanohydrin over $MgSO_4$ to provide cyanoaniline **2.15** in 92% yield (Scheme **2.2**). The subsequent thiohydantoin synthesis combining **2.15** with isothiocyanate **2.11**, affording a mediocre 32% yield of **2.16** by simple stirring in THF in the presence of catalytic triethylamine for days at 0 °C, has also been reported in nearly identical yield by Jung as part of the initial SAR toward discovery of ENZ.[179] Triflation of phenol **2.16** with *N*-phenyltriflimide and triethylamine in THF gave aryl triflate **2.17** in 88% yield and provided a point of synthetic divergence. Palladium-catalyzed carboxylation of **2.17** under a carbon monoxide atmosphere gave acid **2.18** in 56% yield, which was smoothly converted to hydroxamic acid **2.4** (RB-318) by EDC-mediated peptide coupling with NH_2OTBS followed by HF-mediated silyl deprotection in 40% yield. Alternatively, the aryl triflate **2.17** was successfully carbonylated to aldehyde **2.19** in 46% yield. Aldehyde **2.19** was transformed by

Wittig olefination with (*tert*-butoxycarbonyl-methylene)triphenylphosphorane to enoate **2.20** in 93% yield followed by trifluoroacetic acid (TFA) *t*-butyl ester cleavage to acid **2.21** in 86% yield. Acid **2.21** was then converted to hydroxamic acid **2.5** (RB-331) in 30% yield with the same EDC coupling as used for **2.4**.



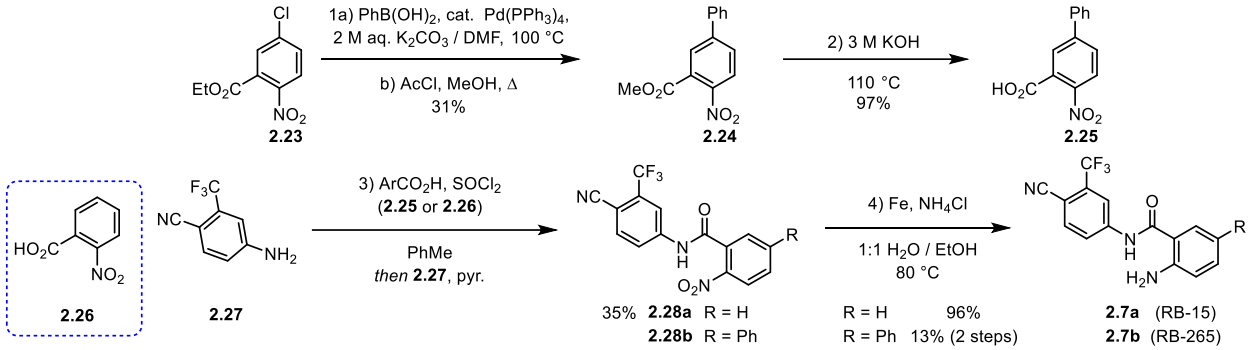
Scheme 2.2. Synthesis of enzalutamide-inspired hydroxamic acid hybrids RB-318 and RB-331.

Benzoic acid **2.18** prepared above was also initially employed to synthesize two benzamide hybrids bearing either a simple *o*-aniline (**2.6a**, RB-250) or a phenyl substituted variant (**2.6b**, RB-321). The former was obtained by EDC-mediated peptide coupling with *o*-phenylenediamine **2.22a** followed by recrystallization in 54% overall yield. EDC-mediated peptide coupling of benzoic acid **2.18** with protected aniline **2.22b** proceeded in 60% yield, followed by TFA-mediated Boc deprotection of the intermediate to provide a 45% yield of RB-321 **2.6b**.

2.1.4. *Synthesis of Flutamide-Inspired Benzamide Hybrids*

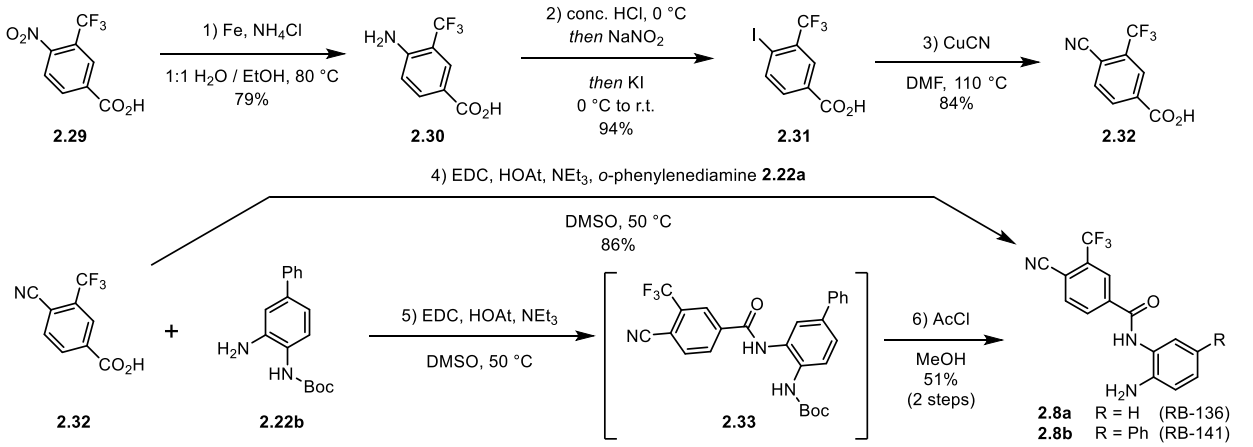
The flutamide-based hybrids with "inverted" amides were synthesized by simple functional group manipulations and amide bond formations involving aniline **2.27** (Scheme **2.3**). First, aryl chloride **2.23** was converted into desired biphenyl peptide coupling partner **2.25** by Pd-catalyzed Suzuki cross-coupling, followed by re-esterification of the saponified intermediate to allow purification of the mixture, providing methyl ester **2.24** in 31% yield over 2 steps. Subsequent

saponification of the methyl ester gave 97% yield of the Ph-substituted amide coupling partner carboxylic acid **2.25**. To access the unsubstituted benzamide, aniline **2.27** was used in DCC coupling with commercially available benzoic acid **2.26** to afford a sufficient 35% yield of **2.28a**, which was reduced with activated iron powder to **2.7a** (RB-15) in 96% yield. Toward the Ph-substituted hybrid, carboxylic acid **2.25** was treated with thionyl chloride followed by pyridine and aniline **2.27**, and the resulting amide **2.28b** was similarly reduced with activated iron powder to afford **2.7b** (RB-265) in 13% yield over 2 steps.



Scheme 2.3. Synthesis of flutamide-inspired HDACi hybrids with "inverted" amides.

The other flutamide-inspired hybrids, possessing "normal" amide connectivity, required a lengthier synthesis to prepare the appropriate A-ring coupling partner (Scheme **2.4**). Reduction of commercially available nitro aryl **2.29** with activated iron gave a 79% yield of aniline **2.30**. Diazotization and decomposition of aniline **2.30** in the presence of KI furnished aryl iodide **2.31** in 94% yield. Iodide **2.31** was converted via a Cu(I) coupling to afford benzonitrile-acid **2.32** in 84% yield. Benzoic acid **2.32** was used in EDC-mediated peptide coupling with *o*-phenylene-



Scheme 2.4. Synthesis of flutamide-inspired HDACi hybrids with "normal" amides.

diamine **2.22a** in warm DMSO to furnish benzamide **2.8a** (RB-136) in 86% yield. Benzoic acid **2.32** was also used in EDC-mediated peptide coupling with Ph-substituted Boc-aniline **2.22b** to prepare intermediate **2.33** and provide a 51% yield of **2.8b** (RB-141) over two steps after deprotection with TFA.

2.2.1. *AR and HDAC Inhibition Activity of 1st Generation Hybrids*

The initial set of hybrid compounds were screened for AR inhibition through collaboration with the Mader lab at the University of Montreal, using a reporter assay for nuclear receptors similar to that previously established in collaborative work with their group on the estrogen receptor.[297, 298] The assay measures bioluminescence resonance energy transfer (BRET) signal from association of yellow fluorescent protein (YFP) tagged FXXLF motif-bearing peptide with LucII-tagged AR. That peptide, which is derived from the AR coactivator ring-finger protein (YFP-RNF14), binds at the hydrophobic AF-2 pocket formed by androgen-induced AR-LBD conformational change.[320] Compounds which disrupt coactivator binding are likely preventing AF-2 formation and should thereby inhibit AR N/C interaction, translocation, dimerization, and transcription signaling activity. On the other hand, an increase in BRET signal would be diagnostic of agonist activity. The BRET assay therefore simultaneously provides a measurement of compound potency and indicates the type of activity, whether agonist or antagonist.

The assay was validated by including known AR inhibitor bicalutamide (Casodex® / CDX) in an assessment of the first batch of inhibitors (Figure **2.4**) at a single concentration of 5 μM (Figure **2.5**), with and without 1 nM of AR ligand DHT. In the presence of DHT, CDX reduced BRET signal to approximately one fifth of that seen with the vehicle, while CDX displayed no agonism in the absence of DHT, as expected. By comparison, only hydroxamic acid hybrids RB-227, 211, 236, and 331, along with benzamide RB-250, produced comparable results with and without DHT, decreasing BRET signals to less than about 20% that of the vehicle with DHT. Hydroxamic acids RB-95 and 318, as well as Ph-substituted enzalutamide-based benzamide RB-321 and flutamide-based benzamide RB-265, did not reduce BRET signal by more than 50% in the presence of DHT. Other flutamide-based benzamides RB-136 and 141 displayed extremely poor activity and are not shown here. Benzamide RB-15 uniquely showed higher BRET activity in the absence of DHT and may therefore be a weak competitive agonist of AR since it exhibited comparable activity with

and without DHT. Due to poor collective activity, the flutamide-based hybrids were not assessed further against AR.

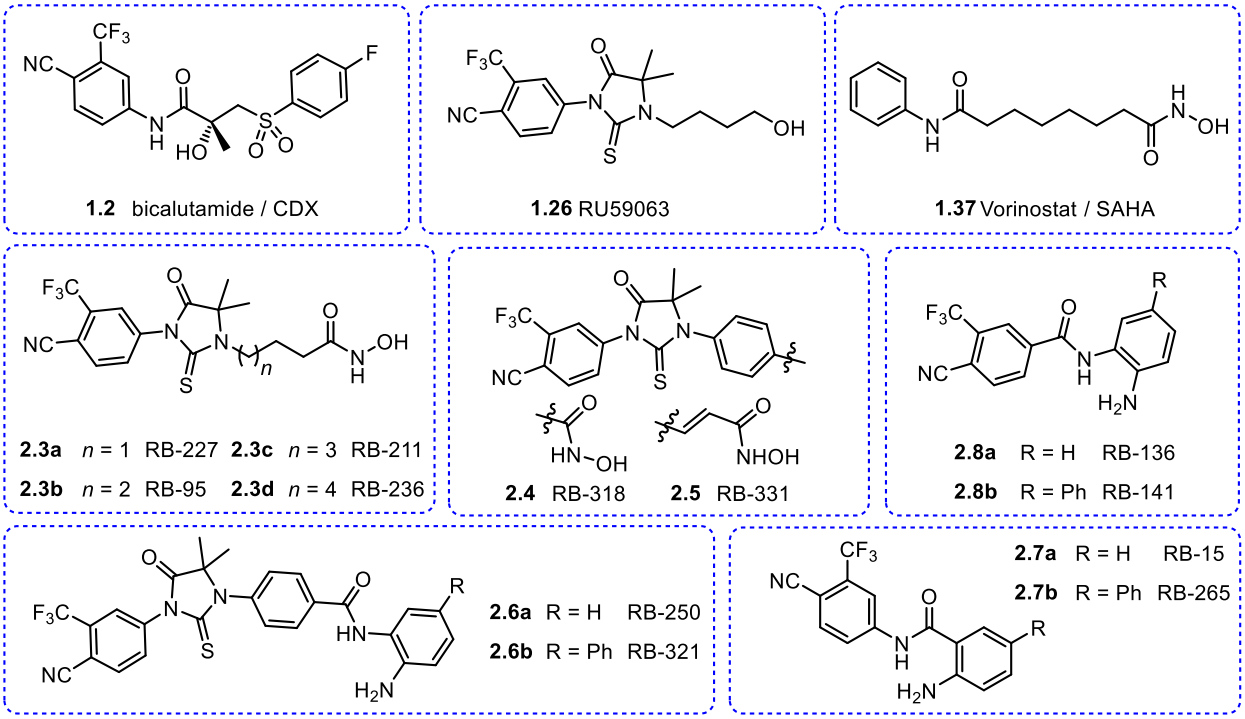


Figure 2.4. Known AR effectors, HDACi, and all 1st generation hybrid compounds.

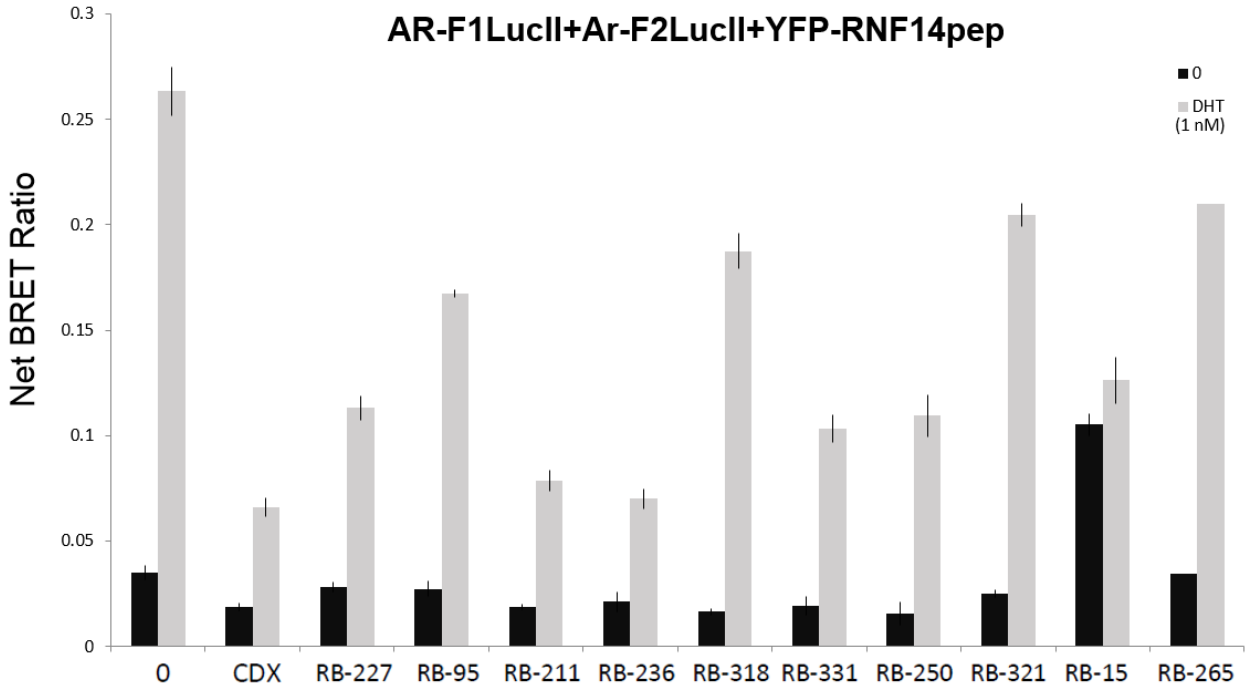


Figure 2.5. Single-concentration inhibition of AR activity by CDX or hybrid compounds (5 μM) using BRET assay in HEK293 cells.

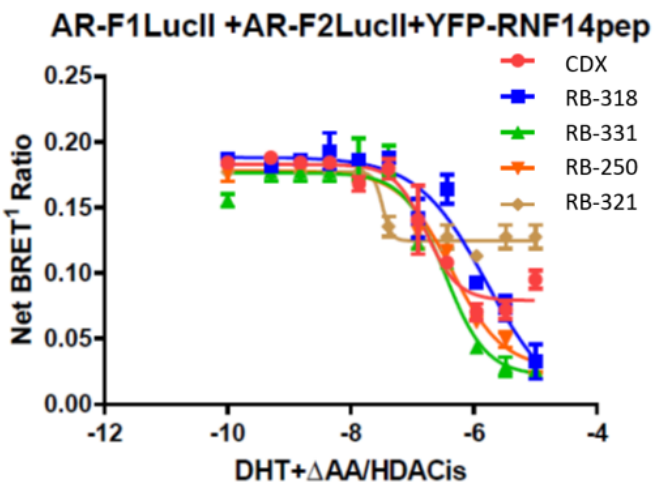


Figure 2.6. Antiandrogenic activity of AA-HDACi hybrids in the presence of DHT in PCA-BRET assay. Dose response curves were performed in HEK293T cells cultured in estrogen depleted media and co-transfected with AR-F1RLucII, ARF2RLucII and the YFP-RNF14 peptide. After 48 h, cells were treated for 1 h with 2 nM DHT and increasing concentrations of CDX, ENZ, or hybrids. BRET was then measured between AR-F1/F2RLucII and YFP-RNF14. Graphs represent the mean ± SD of data from 3 independent biological replicates.

All hybrids, except the flutamide-based compounds, were examined further to obtain dose-dependent inhibition curves. Examination of the IC_{50} values measured against AR (Table **2.1**) show that potent binding is generally maintained in the hybrids and many display similar activity to CDX, for which an IC_{50} of 0.14-0.33 μM was measured. For those compounds previously synthesized and tested, the new values were very comparable to those previously attained, which are provided in parentheses.[314] Hydroxamic acids RB-227 (0.16 μM), 211 (0.19 μM), 236 (0.15 μM), and 331 (0.34 μM) all gave low IC_{50} values, while RB-95 (0.69 μM) and 318 (1.63 μM) displayed reduced inhibition potency by comparison, which may indicate helpful interactions at both shorter and longer lengths to prevent an active AR conformation. Benzamide RB-250 (0.43 μM) also displayed activity roughly on par with the better alkyl hydroxamates. RB-321, however, showed dismal activity, attributed to visible aqueous buffer insolubility, with less than 50% reduction in assay signal (Figure **2.6**) providing a deceptively low IC_{50}.

Although all IC_{50} values were significantly higher than RU59063 (0.007 μM), that compound is known to be an exceptional binder of AR with mixed biological activity. Only 50% reduction in BRET signal was previously observed for that compound, which implies incomplete AR inhibition, unlike the hybrids which display more complete suppression of BRET signal at high concentration.[314] One other critical takeaway was that all hybrids assayed except RB-321 displayed ca. 40% greater maximum inhibition as compared to CDX (Figure **2.6**), which indicates not only more complete AR inhibition by the hybrids, but impacts the meaning of the IC_{50} value for CDX, RU59063, and RB-321 for which incomplete inhibition was observed. The inhibition curve

inflection point is artificially shifted to lower concentrations since maximum inhibition is also reached at lower concentration. Many 1st generation hybrids were therefore at least as effective as CDX against AR in this BRET assay, despite higher IC_{50} values.

Table 2.1. Biochemical summary of 1st generation hybrids.

Compound	AR-BRET IC_{50} (μM)	HDAC1 IC_{50} (μM)	HDAC6 IC_{50} (μM)[a]
Bicalutamide	0.14-0.33	-	-
RU59063	(0.007)[b]	-	-
SAHA	-	0.023	-
2.3a (RB-227)	0.16 (0.13)	44.9	58
2.3b (RB-95)	0.69	3.09	-
2.3c (RB-211)	0.19 (0.76)	1.33	2.5
2.3d (RB-236)	0.15	0.993	-
2.4 (RB-318)	1.63 (1.47)	13.1	17
2.5 (RB-331)	0.34 (0.26)	0.911	1.5
2.6a (RB-250)	0.43	1.36	-
2.6b (RB-321)	0.033[d]	5.96[c]	-
2.7a (RB-15)	n.i.	n.i.	-
2.7b (RB-265)	n.i.	n.i.	-
2.8a (RB-136)	n.i.	n.i.	-
2.8b (RB-141)	n.i.	15.7	-

[a]Results for HDAC6 were previously reported for certain compounds. [b]Values in brackets were previously obtained with slightly different assay conditions (5 nM DHT). [c]Pre-incubation for 18 h with HDAC enzyme was necessary to observed activity. [d]Less that 50% overall reduction in signal was observed. n.i. = no detectable inhibition of HDAC or not quantified against AR due to poor results on initial screening. Results not obtained are indicated by a hyphen.

All hybrids were assessed for HDAC inhibition in our lab against HDAC1, chosen for its nucleus-associated activity. Using 96-well plates, a standard HDAC two-stage biochemical fluorogenic assay was employed.[321, 322] Stage one involves the incubation of HDAC enzyme with known modified acylated coumarin peptide Ac-Leu-Gly-Lys(Ac)-AMC,[323] which is a good substrate for several isoforms of HDAC including both 1 and 2. Substrate which is deacetylated in stage one is susceptible to cleavage by the excess trypsin added at stage two, to release free coumarin which is measured by fluorescence spectroscopy. HDACi therefore ultimately reduce the coumarin released during the assay, providing a dose-dependent response. In our HDACi assay, the shortest hydroxamic acid RB-227 (44.9 μM) was easily the weakest inhibitor bearing

that ZBG (Table **2.1**). A trend of increasing potency is then observed in the alkyl series from longer RB-95 (3.09 μM), then RB-211 (1.33 μM), to longest compound RB-236 (0.993 μM). The results clearly suggest that linker chain length correlates with potency. Benzoic hydroxamic acid RB-318 (13.1 μM) displayed inhibition between that of RB-227 and RB-95, while cinnamyl hydroxamic acid RB-331 (0.911 μM) displayed intermediate potency on par with the longest alkyl chain. The results continue to indicate a clear correlation between linker length and HDACi potency irrespective of whether alkyl or aryl linkers are used. The fact that short linkers dramatically raise the obtained IC_{50} values may indicate that the thiohydantoin core does not readily enter the hydrophobic tunnel spanning the surface to the catalytic site, either due to size exclusion or favourable interactions at the surface.

In addition to the hydroxamic acid hybrids, benzamide RB-250 also appeared quite promising. It displayed reasonable potency compared to the hydroxamic acids, belying perhaps greater overall efficacy considering the known slow binding kinetics of benzamides. However, RB-321 was a very poor inhibitor with no measurable activity until it was incubated in the fridge with HDAC1 enzyme for 18 h, resulting in a measured IC_{50} value of 5.96 μM. Finally, the flutamide-derived hybrids were uniformly awful in this assay as well. Even 24 h incubation with HDAC gave no measurable activity except for RB-141 which produced a high IC_{50} of 15.7 μM. The "inverted" amides RB-15 and RB-265 were, however, found to be quite fluorescent, giving much higher than the normalized output at high compound concentration (>1 mM). Fluorescence was actually found to be a common problem encountered generally with the benzamides, which capped the highest concentrations usable in the assay, although the small benzamides were particularly bad.

Considering both targets together, the hybrids which retained good activity against each were the longer hydroxamic acids RB-211, RB-236, and RB-331 as well as benzamide RB-250. The latter was especially promising for further work since it was desired to move away from hydroxamic acids due to the pharmacological issues, mentioned in Section **1.3.3**, which have plagued the compounds in the clinic. The antiproliferative activity of the hybrids needed to be examined, however, to ensure both that the compounds retained enough activity against each target to be biologically meaningful, and to validate the use of benzamide hybrids, since all known AA-HDACi inhibitors at the time employed hydroxamic acid ZBGs.

2.2.2. *Cell Viability Assays of 1st Generation Hybrids*

All 1st generation hybrids were evaluated by Dr. Claire Nash for their ability to inhibit LNCaP cell growth in a cell viability endpoint assay. The cell assay employed a standard CellTiter-Glo® kit, which measures ATP as a surrogate for metabolically active cells, in a 96-well plate format (Figure **2.7**). Representing one positive HDACi control, SAHA showed some activity at high concentrations, while entinostat (ENT) appeared more potent at even 10 μM which may simply indicate strong cytotoxicity. However, enzalutamide (ENZ) was quite inactive even at very high concentration, establishing a clear baseline for improvement. In the hydroxamic acid series, the potency correlated quite well with HDACi activity, where RB-227, RB-95, and RB-318 were all similarly ineffective while RB-211, RB-236, and RB-331 all showed reasonable to excellent potency at high concentrations. In fact, RB-236 and RB-331 both appeared comparable to SAHA at 100 μM, while a modest impact was observed for RB-331 even at 10 μM.

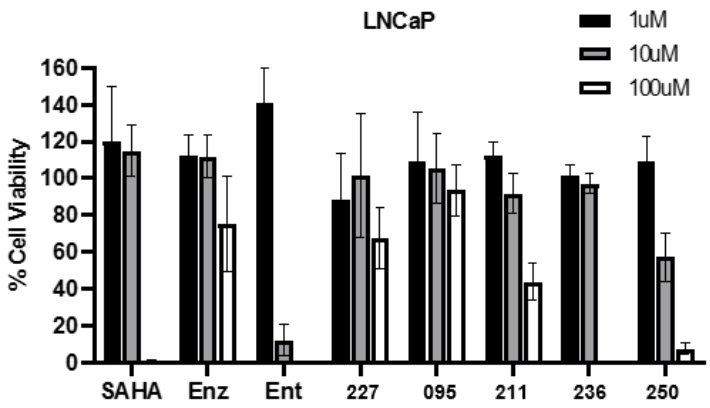


Figure 2.7. Antiproliferative activity of select 1st generation hybrids in LNCaP cells. LNCaP cells were exposed to a panel of hybrid compounds as well as a series of control compounds (SAHA, Enzalutamide and Entinostat) at the indicated concentrations for 5 days and assayed for cell viability. Data is presented as % cell viability after 5 days versus vehicle (DMSO) and is the average of a minimum of 2 independent biological replicate experiments each with 4 technical replicates. Error bars denote standard deviation. *(Reproduced with permission.)*[315]

Hybrid RB-250, however, provided the best inhibition at 10 μM of any hybrids surveyed, bucking the correlation of cell potency with lower HDAC1 IC_{50} and defying interpretation based solely on the AR BRET assay results. As previously outlined, benzamides have been shown to display unusual binding kinetics, which may explain their greater-than-expected efficacy based on IC_{50} data acquired over short assay time periods. The discrepancy of efficacy also hearkens to a philosophy, mentioned during discussion of hybrid drugs in Section **1.4.1**, that hybrids should display balanced activity against both targets to remain effective compounds overall. The other benzamides, however, did not impress in this assay. Although "inverted" flutamide benzamides RB-15 and RB-265 (not shown) showed 50% reduction in cell viability at 1 μM, this did not

increase with concentration. Combined with their lack of demonstrated activity against either biochemical target, the growth assay result defies SAR interpretation and is likely due to some other effect. As for the rest, neither RB-136 nor RB-141 showed activity until 100 μM, and RB-321 showed little activity even at that concentration, matching their poor AR and HDACi activity.

Two factors which influence interpretation of the results deserve comment. First, the choice of fetal bovine serum (FBS) in the growth assays, rather than charcoal-stripped serum (CSS), is critical since FBS contains the endogenous AR ligands which are otherwise removed by charcoal treatment. The assay is therefore far more challenging for antiandrogens than many published in the literature, although comparisons are always difficult due to this and differences in resistant cell lines used. Under the assay conditions, it is not surprising that enzalutamide has little to moderate impact on cell viability. In fact, as of its publication, 1 or 10 μM ENZ was considered excellent for halting cell growth of VCaP cells in FBS media relative to the vehicle.[170] Again, comparison of models is difficult, but the data clearly suggest that RB-250 at least is more effective than ENZ by head-to-head comparison in a stringent assay using LNCaP cells, and RB-250 was therefore identified as a lead compound for further work.

2.3.1. *Design of 2nd Generation Hybrids*

Based on the success of benzamide hybrid RB-250, a 2nd generation series was planned using SAR information available in the literature which has been previously discussed in Section **1.3.3**. This generation was intended to explore some variation in all components of the hybrid structure: the benzonitrile A-ring, thiohydantoin core, aryl linker, and aniline ZBG group (Figure **2.8**). First, the antiandrogen A/B "half" was considered. Since apalutamide (APL) displays slightly better affinity for AR, a series of compounds were included which incorporate the APL A-ring pyridine, a feature which may also lend itself to aqueous solubility. Darolutamide (ODM-201), was used as a rationale for swapping the thiohydantoin for a pyrazole ring. It was thought that the switch could favourably impact the overall pharmacokinetics of a hybrid inhibitor since darolutamide is ten times less effective at crossing the blood-brain-barrier than ENZ, although this core switch alters the angle of branching slightly. Chronologically, the imidazole hybrid was designed after some data for RB-405 (*vide infra*) was known, and so imidazole hybrid uses the benzyl linker from RB-405.

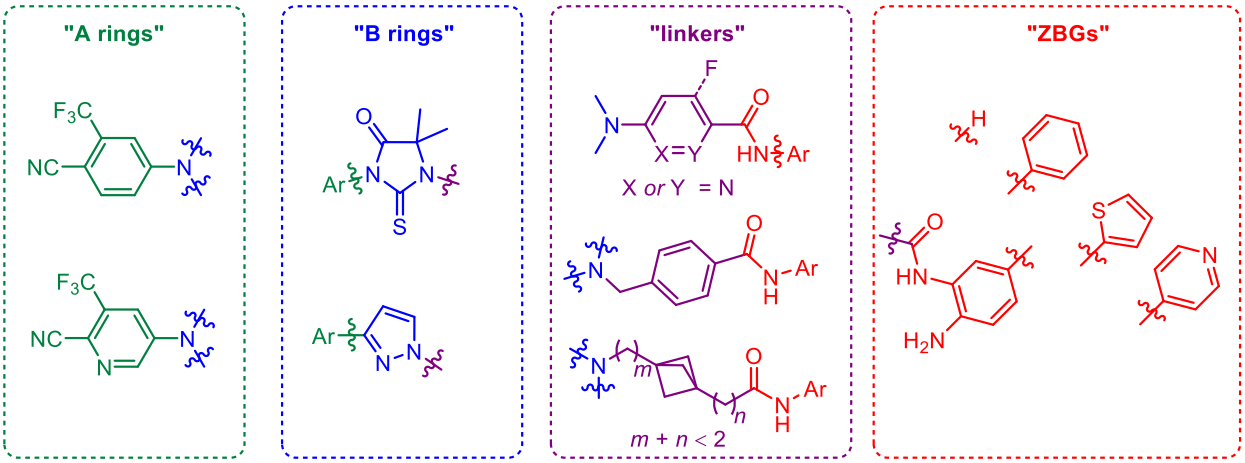
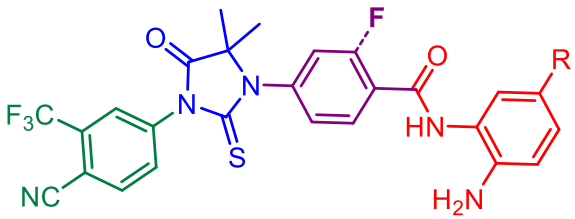


Figure 2.8. Various alternative components of 2nd generation hybrid AR-HDAC inhibitors.

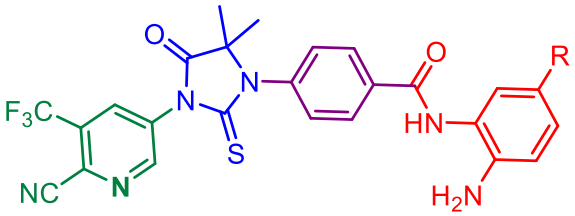
Secondly, options for the HDACi linker portion were weighed. Eight distinct linkers were identified for exploration: the original *p*-disubstituted benzoic acid, a fluoro derivative reminiscent of ENZ, both 2- and 3-pyridyl isosteric replacements, a thiohydantoin-methylene homologue, and three types of [1.1.1]propellane linkers bearing one methylene at either end or none at all. The ability to incorporate pyridines into HDACi linkers is established.[324, 325] The propellane segments arose from our recent work in the area,[326] which was ongoing at the time and from which we desired to identify novel bioisosteric HDACi linkers. Note that the linkers are all aromatic or pseudo-aromatic substitutes for the C-ring of ENZ which should help retain AR antagonist activity.

Finally, four different benzamide ZBGs were chosen, again based on HDACi SAR publications: the simple *o*-aniline, along with three different substituents *para* to the aniline including phenyl, 2-thienyl, and 4-pyridyl groups. The groups were chosen for their effectiveness in other publications and were intended to delve into the so-called "foot pocket" of HDACs 1 and 2, although it was noted that increased size may be problematic as in RB-321. On the other hand, it was thought that the poor solubility of RB-321 might be ameliorated by incorporation of up to three pyridyl rings. Given the hydrophobic drug behavior of ENZ, the overall goal was also to explore opportunities for hydrogen bonding at various points, with one or multiple pyridyls or a pyrazole, and explore the biochemical and biological potency.

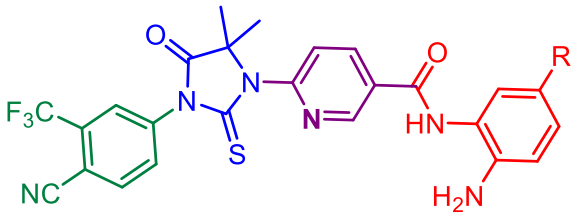
All 128 potential combinations of the various options were not prepared, and some judgement was used in deciding how to proceed. Given the solubility issues of RB-321, only the pyridyl and not thienyl biarylaniline was chosen for combination with the same A-ring and linker. Since the



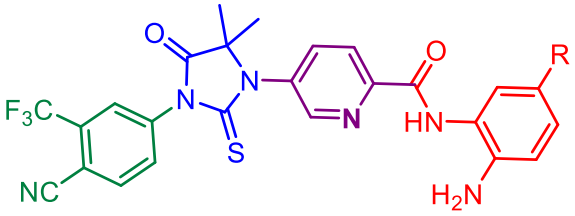
2.6a	R = H	RB-250
2.6b	R = Ph	RB-321
2.6d	R = 4-pyridinyl	RB-416
2.34	F, R = H	RB-391



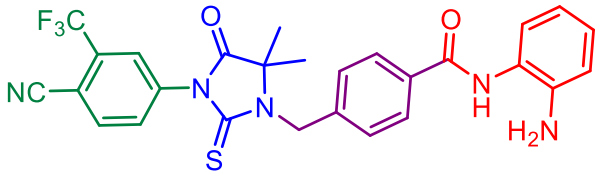
2.35a	R = H	RB-445
2.35b	R = Ph	RB-446
2.35c	R = 2-thienyl	RB-447
2.35d	R = 4-pyridinyl	RB-448



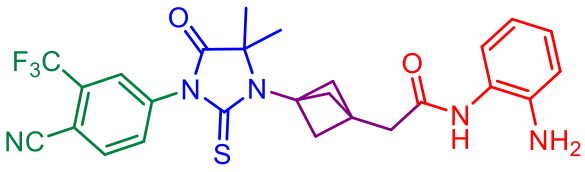
2.36a	R = H	RB-398
2.36b	R = Ph	RB-412
2.36c	R = 2-thienyl	RB-400
2.36d	R = 4-pyridinyl	RB-440



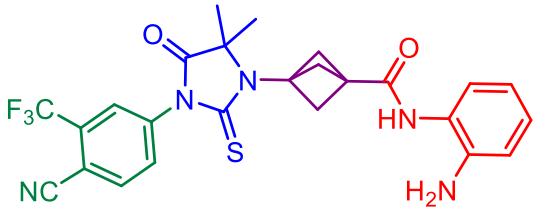
2.37a	R = H	RB-422
2.37b	R = Ph	RB-442
2.37c	R = 2-thienyl	RB-443
2.37d	R = 4-pyridinyl	RB-439



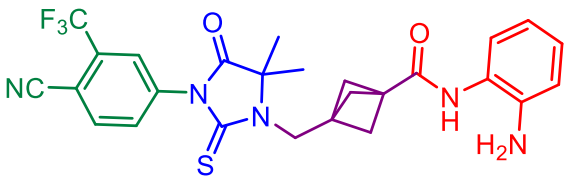
2.38 RB-405



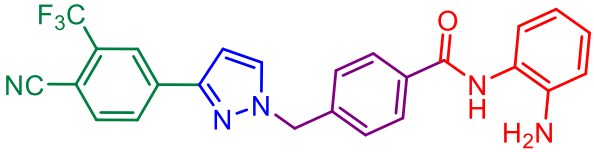
2.39 RB-433



2.40



2.41



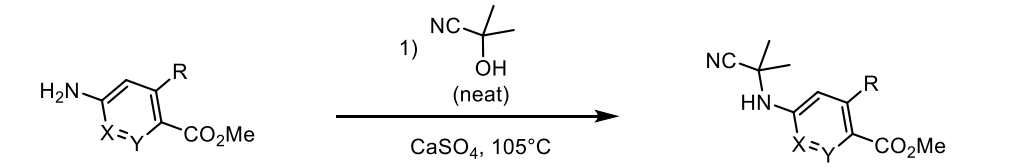
2.42 RB-461

Figure 2.9. Chosen targets for 2nd generation hybrid AR-HDAC inhibitors.

fluoro substituent in ENZ should primarily be for metabolism, it was thought to compare a direct fluoro analogue of RB-250 to verify its HDACi potency. Only the unsubstituted aniline ZBG and canonical A-ring were paired with the more highly experimental combinations such as B-ring pyrazole, benzyl linker, or any of the [1.1.1]propellane linkers. For ease of synthesis, the only pyrazole hybrid used the benzyl linker and simple benzamide. However, all four ZBGs were chosen for combination with the APL A-ring / *p*-disubstituted benzoic acid linker and with ENZ A-ring / both pyridyl linkers. The 21 new proposed hybrid inhibitors are shown (Figure **2.9**) colour-coded according to the design philosophy with the antiandrogen A-ring shaded green, B-ring blue, shared C-ring linker structural overlap in purple, and HDACi ZBG in red.

2.3.2. *Synthesis of Enzalutamide or Apalutamide-Inspired Benzamide Hybrids*

For the 2nd generation benzamide hybrids, it was desired to re-examine the synthetic approach to the bis-aryl thiohydantoin core. The prior synthesis of RB-250, starting from *p*-aminophenol, had needed multiple days to form the iminothiohydantoin in disappointing yield, and then still required subsequent triflation and carboxylation with pressurized carbon monoxide to reach a peptide coupling precursor to the benzamide hybrid. To this end, α-cyanoanilines **2.44a-d**, which already contain a carboxylic ester at the desired position, were all readily prepared by heating anilines **2.43a-d** with neat acetone cyanohydrin over drying agent (Scheme **2.5**), providing them in 34-92% yield.



2.43a R = H **2.43c** X = N
2.43b R = F **2.43d** Y = N

2.44a R = H 92% **2.44c** X = N 34%
2.44b R = F 77% **2.44d** Y = N 79%

Scheme 2.5. Preparation of α-cyanoanilines.

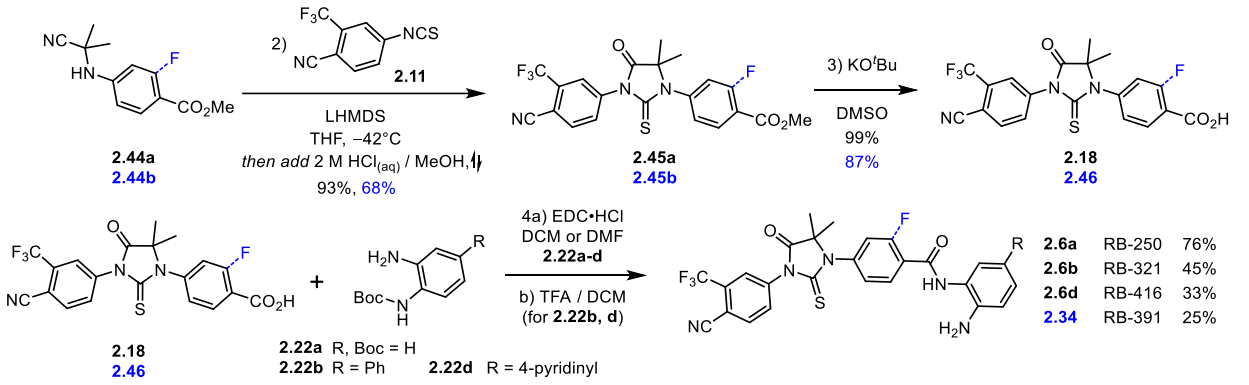
Next, it was necessary to couple the cyanoanilines with isothiocyanates **2.11** and **2.47** to generate the thiohydantoin cores of the hybrids. Consideration of the approximate pKa of these α-cyano-*p*-aminobenzoate methyl esters, approximately 26 in DMSO,[327] relative to various bases led to the conclusion that HMDS bases might be sufficient to enable fast and potentially irreversible deprotonation. It was reasoned that rapid deprotonation might allow for a faster, higher-yielding reaction with isothiocyanate **2.11** when compared to the prior use of weak base triethylamine.

Fortuitously, it was found that addition of a slight excess of LHMDS to a premixed solution of the cyanoanilines and aryl isothiocyanates induced their coupling in very short timespans at –42 °C. Simple subsequent addition of aqueous HCl, along with enough methanol to combine the phases, successfully hydrolyzed the iminothiohydantoin at reflux without any complications. The initial reaction was extremely rapid, sometimes being complete after a few minutes according to TLC analysis. The reaction yield and amount of byproduct formation was noticeably impacted both by deviation of reactant stoichiometry from an optimal 1:1 ratio and by slower addition of LHMDS. In fact, the main reason reduced temperature was chosen for conducting the reaction was to compensate for heat of proton transfer upon the necessarily fast addition of base. For most substrates, the reaction consistently proved an extremely clean and high yielding method for accessing such biaryl thiohydantoins (*vide infra*).

Using this modified thiohydantoin synthesis, bis-aryl thiohydantoin esters **2.45a-b** were prepared rapidly from isothiocyanate **2.11** and cyanoanilines **2.44a-b** in 93% yield or 68% yield in the case of the aryl fluoride (Scheme **2.6**). The slightly lower yield obtained for fluoride **2.45b** reflects greater byproduct formation observed in the course of this reaction, which may be explained by reduced nucleophilicity of the deprotonated aniline **2.44b** relative to **2.44a**. Cleavage of the benzoic methyl esters **2.45a-b** was not trivial due to facile saponification of the thiohydantoin itself, which occurs even with bicarbonate in aqueous media. Chang and Wood had reported conditions for dealkylating esters, which is another known strategy for their cleavage, using potassium *t*-butoxide in DMSO.[328] Using this method, carboxylic acids **2.18** and **2.46** were attained in mostly high to excellent 99% and 87% yield, respectively. Fast reaction times of under an hour were observed with as little as 5 equivalents of butoxide, although dropping the loading led to longer reaction times of a few hours, some of which may be due to a significant exotherm upon butoxide addition.

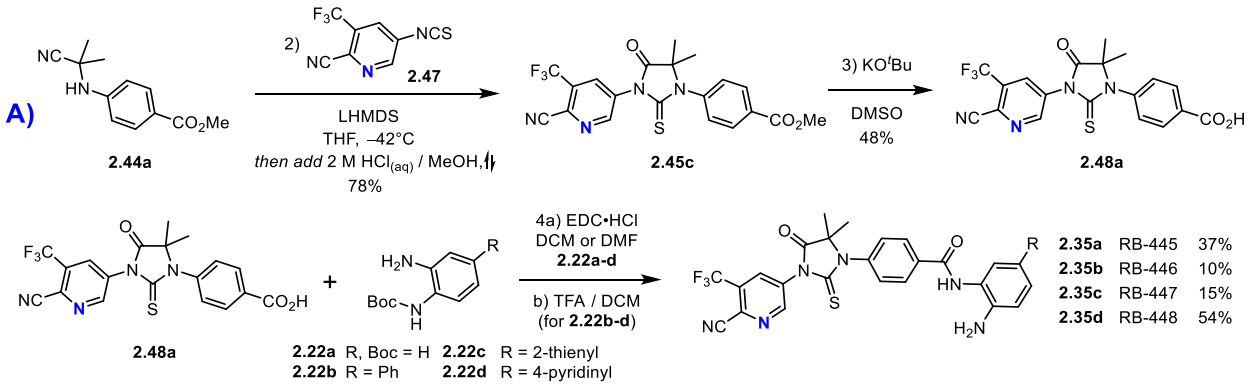
The acids were then used in EDC-mediated peptide coupling reactions with *o*-phenylenediamine **2.22a** or Boc-protected biaryl anilines **2.22b** or **d**. The latter compounds were readily prepared in a few steps centrally featuring palladium-catalyzed Suzuki cross-coupling.[329] Deprotection of the Boc-protected aniline intermediates was performed with TFA in DCM, which unfortunately caused significant visible decomposition to brightly coloured precipitates and this impacted the yields substantially in some cases. Further mass balance was sacrificed during

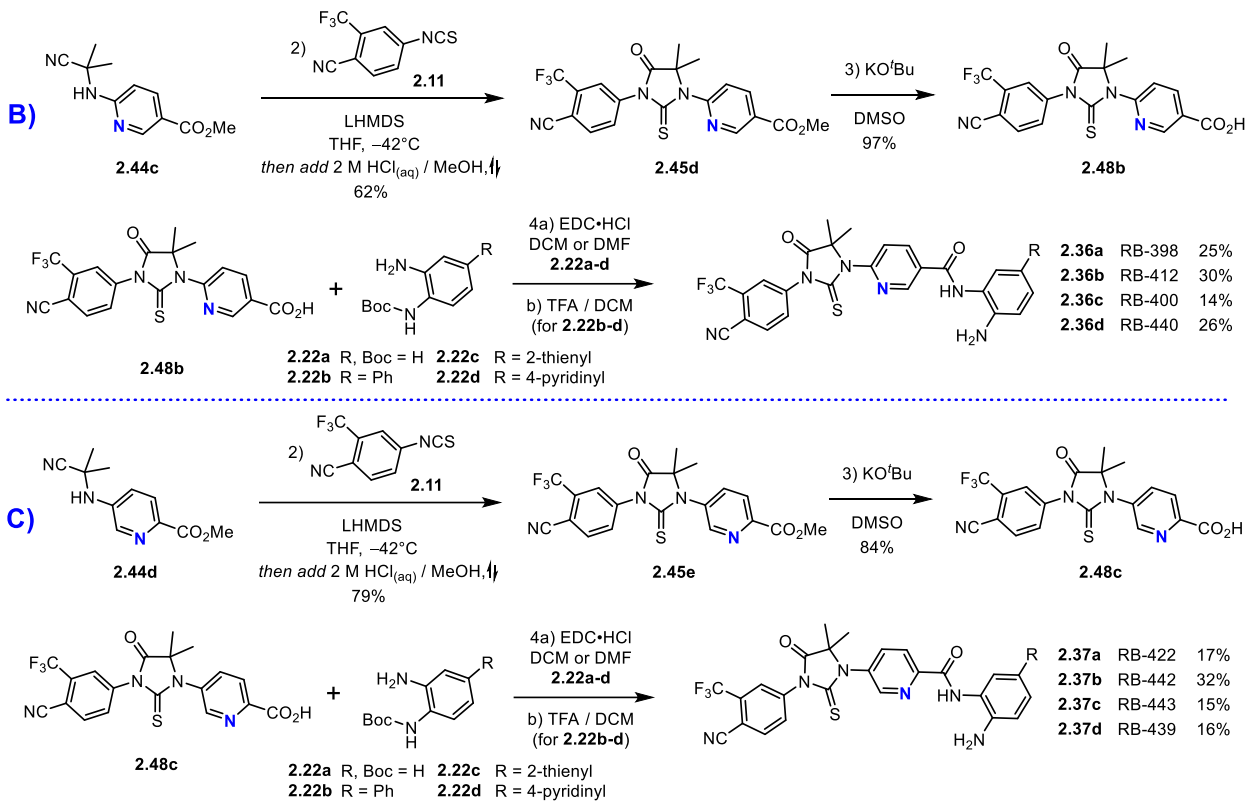
recrystallization or chromatography for the sake of purity, but all 4 desired hybrids in the set **2.6abd** and **2.45** were successfully obtained in 25-76% yield, which was sufficient for biological assessment. By this sequence, the synthesis of RB-250 was scaled up to produce up over 200 mg.



Scheme 2.6. Synthesis of hybrids related to RB-250.

The same synthetic sequence was used to prepare the rest of the bis-aryl thiohydantoin hybrids in the 2nd generation (Scheme **2.7A-C**). Thiohydantoin esters **2.45c-e** were prepared from corresponding cyanoanilines **2.40acd**, the latter compounds featuring aryl pyridine linkers, and pyridine isothiocyanate **2.47** or aryl isothiocyanate **2.11** in 62-79% yield. As with the fluoride, the slightly lower 62% yield obtained for pyridine **2.45d** reflects byproduct formation and may again be explained by reduced nucleophilicity of the deprotonated aniline relative to the rest of the set. As before, the esters were converted to the carboxylic acids **2.48a-c** in 48-97% yield and all 12 benzamides **2.35a-d** through **2.37a-d** in 10-54% yield, after TFA deprotection where required.



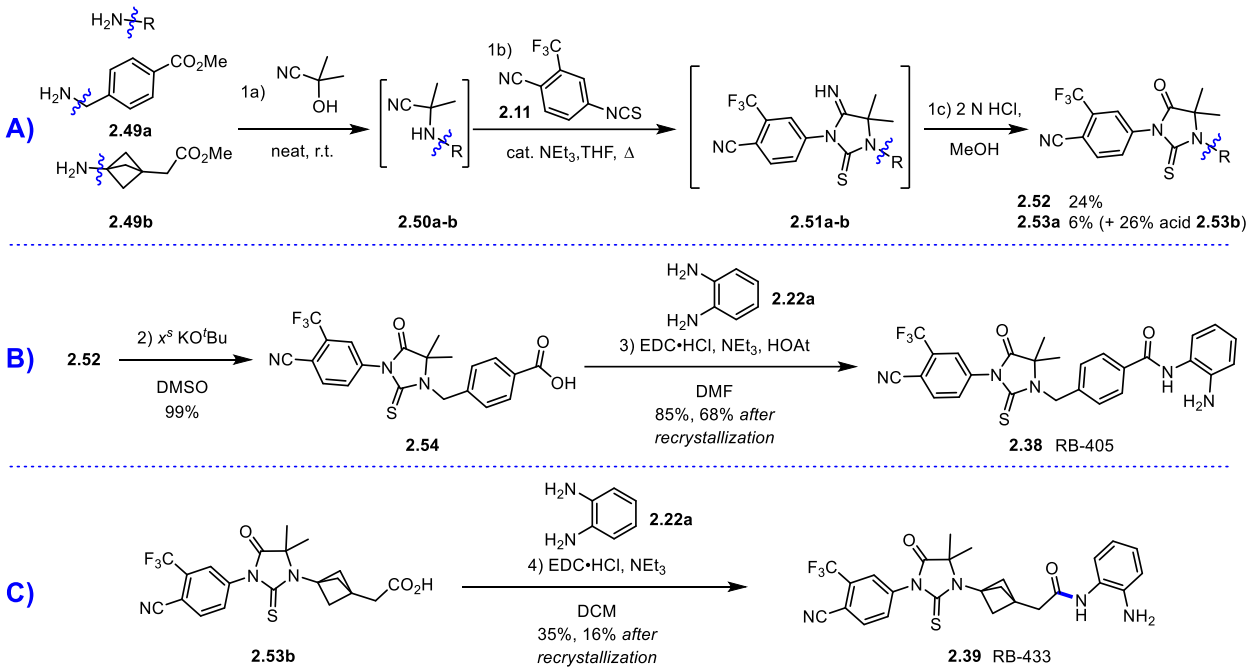


Scheme 2.7. Synthesis of A-ring and linker pyridyl hybrids based on RB-250.

2.3.3. Synthesis of Enzalutamide-Inspired Hybrids with Alternative Linkers

Hybrids with both the benzyl and bicylo[1.1.1]pentane-methylene linkers were made using the same chemistry as for the *N*-alkyl thiohydantoins (Scheme **2.8A**). Amino-bicylo[1.1.1]pentane (BCP) **2.49b** was obtained as previously reported by our group[326] from the dibenzylamine methyl ester using material kindly donated by Dr. Jonathan Hughes. Thus, BCP amine **2.49b** and benzylamine **2.49a** were each condensed with acetone cyanohydrin, then the resulting α-cyanoamines **2.50a-b** were combined with isothiocyanate **2.11** in refluxing THF with catalytic triethylamine. The corresponding iminothiohydantoins **2.51a-b** were directly hydrolyzed without isolation, using HCl in methanol / water to afford benzyl thiohydantoin methyl ester **2.52** in 24% yield and BCP thiohydantoin methyl ester **2.53a** in 6% yield along with the carboxylic acid **2.53b** in 26% yield. The recovery of BCP thiohydantoin as its carboxylic acid rather than methyl ester was fortunate because butoxide dealkylation of failed on ester **2.53a** with even 15 equivalents of KO^{t}Bu. Dealkylation of **2.52** readily occurred in 99% yield (Scheme **2.8B**) and carboxylic acid **2.54** was converted to benzamide **2.38** (RB-405), in 68% after recrystallization, by EDC coupling with *o*-phenylenediamine **2.22a**. Similarly, EDC coupling between BCP acid **2.53b** and **2.22a**

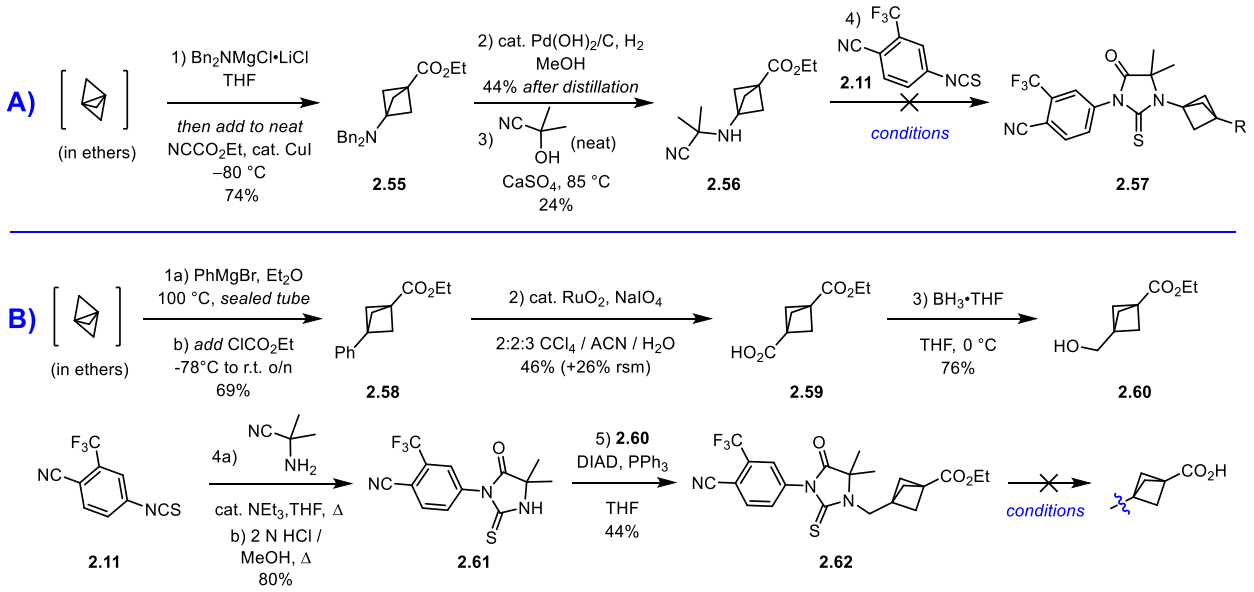
(Scheme **2.8C**) gave 16% of **2.39** (RB-433) after recrystallization. Interestingly, RB-433 was found to exist as a set of rotational conformers in $CDCl_3$, with a coalescence temperature of between 40 and 52 °C, but not in d_6-DMSO. The signals involved arise from the amino protons, α-protons of the amide, and diamino-arene protons and indicates the data likely reflects restricted rotation about the emboldened amide C-N bond in blue. Perhaps amide bond rotation is slowed due to internal aniline-carbonyl hydrogen bonding, which is replaced by intermolecular hydrogen bonding in DMSO.



Scheme 2.8. Synthesis of enzalutamide-inspired hybrids with methylene spacers. (**A**) Thiohydantoin core preparation. (**B**) Preparation of RB-405 featuring a benzyl linker. (**C**) Preparation of RB-433 featuring a [1.1.1]propellane-methylene linker.

The other compounds related to RB-433, incorporating BCP and methylene-BCP linkers, resisted efforts towards their preparation (Scheme **2.9**). Di-functionalization of [1.1.1]propellane with dibenzylamine turbo amide and ethyl cyanoformate, analogous to that previously reported by our group, proceeded smoothly to afford amine **2.55** in 74% yield (Scheme **2.9A**). Subsequent dibenzylamine hydrogenolysis over $Pd(OH)_2/C$ afforded the corresponding primary amine intermediate in 44% yield after distillation. However, cyanohydrin formation did not proceed except when heated with $CaSO_4$ in just 24% yield, reminiscent of the conditions used for aniline condensation. The lack of reactivity perhaps indicates some inductive electronic effects across the propellane framework reducing the amine nucleophilicity, since a steric effect can likely be ruled

out by comparison to the successful preparation of RB-433. Further evidence of reduced amine nucleophilicity is ascertained from the failure of cyanoamine **2.56** to react with isothiocyanate **2.11**, as thermal conditions using catalytic triethylamine resulted only in isolation of the corresponding thiourea through isobutyronitrile loss. Furthermore, application of stronger LHMDS conditions only gave complex mixtures, indicating the unique nature of this amine. Significant future work would be required to access the intended hybrid.

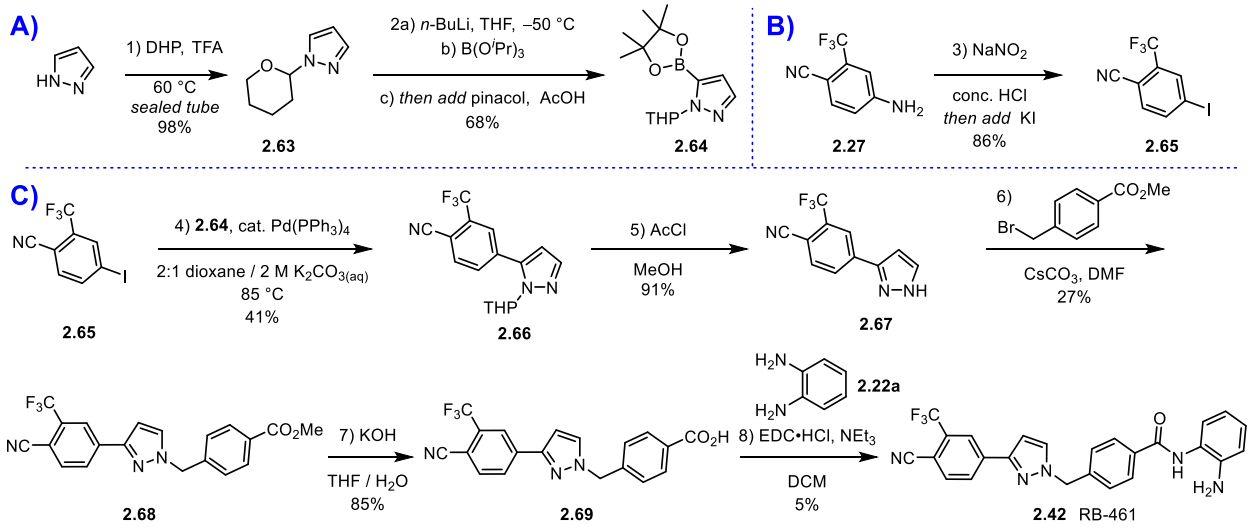


Scheme 2.9. Attempted routes to compact BCP linkers.

The final BCP variant, with a methylene-BCP linker structurally similar to RB-405, presented different and as-yet unsolved challenges (Scheme **2.9B**). Knochel's method of reacting propellane with phenylmagnesium bromide and trapping with ethyl chloroformate[330] was used to access aryl propellane **2.58** in 69% yield. Oxidative degradation with ruthenium tetraoxide[331] provided carboxylic acid **2.59** in 46% yield, along with 26% yield of recovered **2.58**. Subsequent borane reduction of the acid afforded alcohol **2.60** in 76% yield. That alcohol was successfully displaced by thiohydantoin **2.61**, itself readily prepared in 80% yield from isothiocyanate **2.11** and 2-cyanoisopropylamine. The displacement utilized Mitsonobu conditions with diisopropyl azodicarboxylate and triphenylphosphine and occurred in 44% yield, however thiohydantoin-methylene-propellane **2.62** was difficult to isolate. Furthermore, all attempts at cleaving the ester with acid or dealkylation resulted in decomposition, appearing to occur even on silica gel. Future work and an alternative strategy may be similarly required to acquire this linker.

2.3.4. *Synthesis of a Darolutamide-Inspired Benzamide Hybrid*

The synthetic strategy for the B-ring imidazole hybrid RB-461 involved simple alkylation of advanced pyrazole intermediate **2.67** and an appropriate benzyl bromide (Scheme **2.10**). Following literature precedent,[332-334] pyrazole was protected as a THP derivative in 98% yield by heating with dihydropyran and TFA in a sealed tube. THP-directed *o*-lithiation of **2.63** and interception with triisopropoxyborane followed by acid-catalyzed pinacol transesterification provided desired boronic ester **2.64** in 68% yield. Suzuki coupling partner aryl iodide **2.65** was prepared by iodide treatment of the diazonium salt made from aniline **2.27** in 86% yield. The pinacol boronic ester **2.64** and aryl iodide **2.65** were then combined by palladium-catalyzed Suzuki cross-coupling in 41% yield of **2.66**. The THP was removed in acidic methanol to afford a 91% yield of key pyrazole intermediate **2.67**. Pyrazole **2.67** was alkylated with methyl 4-(bromomethyl)benzoate to give 27% yield of methyl ester **2.68**, which was saponified to acid **2.69** in 85% yield. Carboxylic acid **2.42** was subsequently coupled to *o*-phenylenediamine using EDC to provide 5% yield of benzamide RB-461. In this case, much material was sacrificed for the sake of purity, but a quantity sufficient for biochemical analysis was obtained.



Scheme 2.10. Synthesis of a darolutamide-inspired hybrid. (**A**) Preparation of pyrazole boronic ester coupling partner. (**B**) Diazotization of aniline **2.27**. (**C**) Suzuki coupling of key pieces and completion of RB-461.

2.4.1. *AR and HDAC Activity of 2nd Generation Hybrids*

As before, compounds from this new set were evaluated at single concentrations (10 μM) in the AR BRET assay (Figure **2.10**), with older compounds re-assayed for direct comparison (see

Figure **2.11** for structures). In the presence of DHT, all hybrids showed more activity than the blank and negative controls of SAHA and ENT, which clearly are not competitive AR ligands. Several compounds appeared about as effective as ENZ in this first-pass test, but many others were clearly not as effective as CDX and many of the new variations in hybrid structure were not met with improved outcomes. The flutamide benzamides were again simply poor. The A-ring pyridyl apalutamide-inspired hybrids RB445-448, although somewhat effective at countering DHT in the single-point screen, still displayed higher BRET activity and therefore weaker antagonism than many other hybrids. As a direct comparison, RB445 is obviously less effective than non-pyridyl analogue RB-250. Unfortunately, the large benzamides with foot pocket-binding arenes do not appear to be well-tolerated generally by AR and consequently none of these compounds were assayed further. Due to timing, hybrids RB-440, 416 and 461 were not available for assay, and may warrant future investigation. However, several 2nd generation hybrids bearing unsubstituted benzamides were quite active against AR, and these were assessed further at multiple concentrations to obtain dose-response curves. The 2nd generation hybrids were also assessed for HDAC inhibition against HDAC1 and in some cases HDAC2. The results from both assays will be presented together for each set of structurally related compounds and the implications for SAR discussed within each set. Note that does not imply that the sets were necessarily assayed in the same batch, although most 2nd generation results were obtained within a short period of time for each protein assayed.

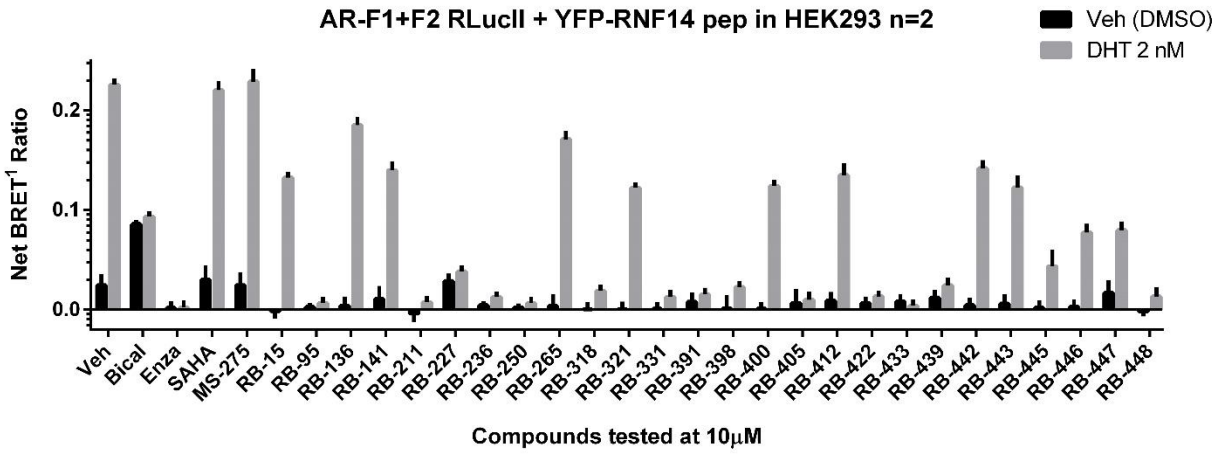


Figure 2.10. Single-point inhibition of AR activity by BRET assay with HEK293T cells.

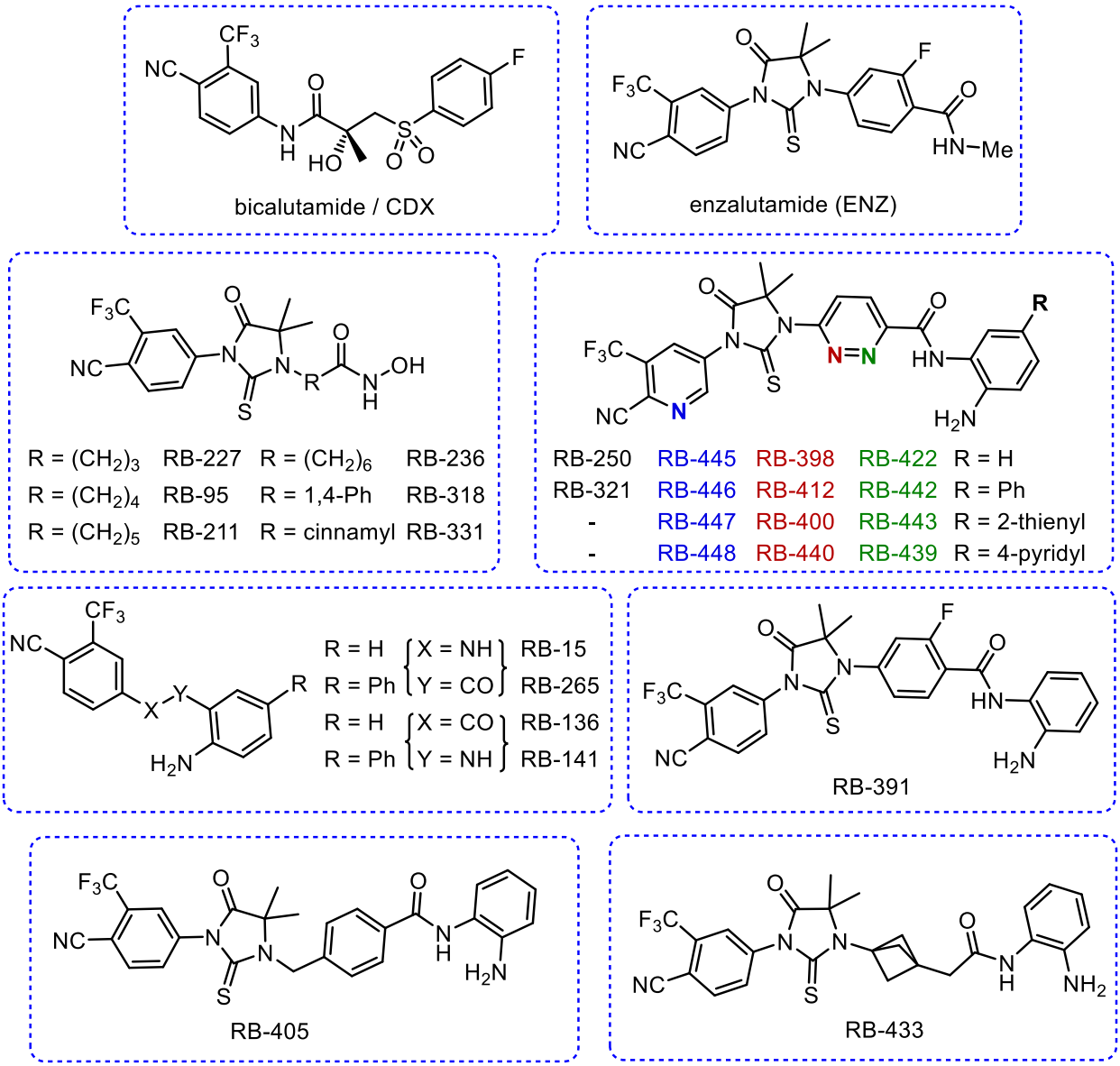


Figure 2.11. Summary of all hybrid structures. For the bis-aryl thiohydantoins, the colours indicate which compounds have substitution of a carbon for a nitrogen atom at the indicated position, while the rows correspond to R substituents.

To provide positive controls and points of comparison, new dose-response curves were obtained alongside the 2nd generation hybrids for HDACi vorinostat **1.37** and entinostat **1.50** as well as AR antagonist enzalutamide **1.27**. Very similar data was obtained for each HDACi against both HDAC isoforms 1 and 2, with IC_{50} values of ca. 20 nM for SAHA and ca. 300 nM for ENT (Figure **2.12A**). ENZ gave an IC_{50} against AR of 450 nM, which should be noted is higher than was obtained for CDX (140-330 nM) alongside the 1st generation results despite ENZ being known as a better AR ligand. ENZ was also used as a negative control in the HDAC1 assay.

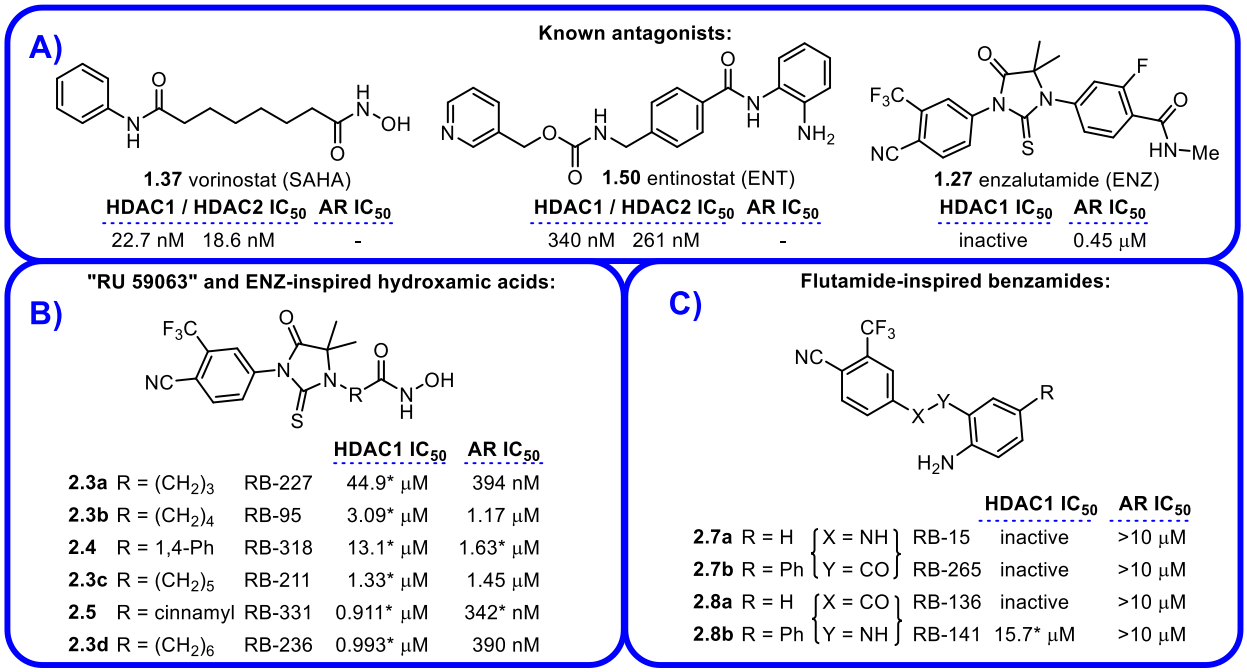
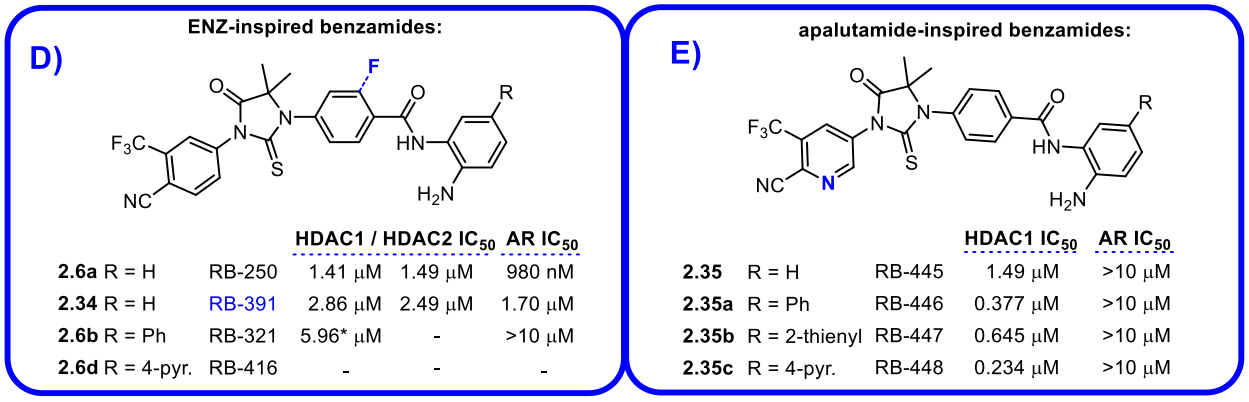


Figure 2.12. Biochemical data summary for 1st generation hydroxamic acid and flutamide -like hybrids. *Previously obtained assay values. Compounds not assayed are indicated by a hyphen.

Reassessment of the hydroxamic acid hybrids **2.3a-d** revealed similar, though slightly elevated, IC_{50} values compared to prior assay results. Again RB-227 and RB-236 were the best antagonists with respective IC_{50} values just slightly lower than ENZ at 394 nM and 390 nM, respectively (Figure **2.12B**). The other hydroxamic acids were not analyzed further since they did not outperform the others in the single-point assay. Clearly, interactions are possible at both shorter and longer lengths within AR to prevent proper active conformation. Consideration of the trend with longer linkers producing better HDAC inhibition leads to the obvious conclusion that compounds RB-211, 332, and 236 are the most effective hybrid AA-HDACi in this set. Small benzamides **2.7-8** were not re-assayed nor effective and are included here only for completeness.

As before, RB-250 was observed to have good activity against AR (980 nM), although the value is approximately twice that previously obtained, and the potency against HDAC1 (1.41 μM) almost perfectly matches the previous result which demonstrates the reproducibility of this assay (Figure **2.13D**). It was also desired to test the best 2nd generation hybrids against HDAC2, and RB-250 proved similarly effective against this isoform (1.49 μM). As the lead compound, RB-250 provides a point of comparison for all other benzamides in this 2nd generation. Fluoride analog RB-391 was less potent against HDAC1 (2.86 μM), HDAC2 (2.49 μM), and AR (1695 nM). These

results indicate that the fluoride is detrimental to HDAC inhibition effect and does in fact affect AR binding to some extent, the latter of which was unexpected given the fluoride at the same position in ENZ and APL. As already discussed, RB-321 was ineffective, likely for reasons concerning solubility. Due to the timing of its preparation, RB-416 was first tested in a LNCaP cell antiproliferation assay and was not assayed further due to poor performance there, but given the assay results obtained from other foot pocket-binding benzamides there is no reason to expect any AR activity. The A-ring pyridines **2.35** were uniformly ineffective at AR inhibition (Figure **2.13E**), which was especially surprising for RB-445 since it is a direct pyridine analog of RB-250. Intriguingly, this series demonstrated improved potency against HDAC1 with substituted benzamides 4-pyridyl RB-448 (234 nM), phenyl RB-446 (377 nM), and thienyl RB-447 (645 nM) as compared to the unsubstituted aniline RB-445 (1.49 μM). The increased effectiveness of RB-446 relative to RB-321 is attributed to increased solubility of the compound, since A-ring pyridine RB-445 showed identical effectiveness as RB-250. However, these points of deviation from the RB-250 structure clearly did not produce better hybrid compounds.



		HDAC1 / HDAC2 IC_{50}		AR IC_{50}
2.6a R = H	RB-250	1.41 μM	1.49 μM	980 nM
2.34 R = H	RB-391	2.86 μM	2.49 μM	1.70 μM
2.6b R = Ph	RB-321	5.96* μM	-	>10 μM
2.6d R = 4-pyr.	RB-416	-	-	-

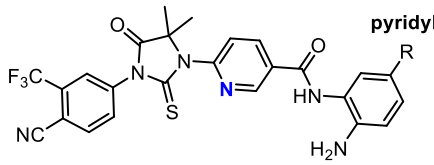
			HDAC1 IC_{50}	AR IC_{50}
2.35	R = H	RB-445	1.49 μM	>10 μM
2.35a	R = Ph	RB-446	0.377 μM	>10 μM
2.35b	R = 2-thienyl	RB-447	0.645 μM	>10 μM
2.35c	R = 4-pyr.	RB-448	0.234 μM	>10 μM

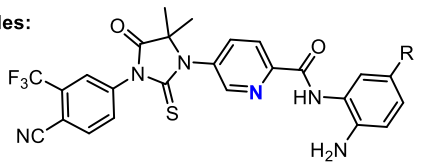
Figure 2.13. Biochemical data summary for 2nd generation hybrids based on ENZ and APL. *Previously obtained assay values. Compounds not assayed are indicated by a hyphen.

The hybrids employing pyridyl linkers were also less effective than RB-250 (Figure **2.14**). Direct pyridyl analog RB-398 had high but measurable HDAC1 (6.51 μM) and AR (2339 nM) activity, whereas isomer RB-422 was slightly better at inhibiting AR than RB-250 (748 nM) but did not fully inhibit HDAC1. None of the substituted anilines measurably impacted AR activity, and phenyl substituted compounds RB-412 / 442 did not fully inhibit HDAC. The HDAC1 IC_{50} values for thienyl compounds RB-400 / 443 afforded measurable but high results of 11.1 μM and 3.67 μM, respectively. Like RB-416, 4-pyridyl hybrid RB-440 was first tested in a LNCaP cell

antiproliferation assay and was not assayed further due to poor performance. RB-439 was effective against HDAC1 with an IC_{50} of 1.51 μM, which is reminiscent of the trend in the A-ring pyridine series where RB-448 performed best, but in this case an activity merely approximating that of RB-250 is achieved. Obviously, these sets of pyridyl compounds do not produce hybrids more effective than RB-250 either.

F)





			HDAC1 IC_{50}	AR IC_{50}				HDAC1 IC_{50}	AR IC_{50}
2.36	R = H	RB-398	6.51 μM	2.34 μM	**2.37**	R = H	RB-422	5.58** μM	748 nM
2.36a	R = Ph	RB-412	2.39** μM	>10 μM	**2.37a**	R = Ph	RB-442	>1 mM	>10 μM
2.36b	R = 2-thienyl	RB-400	11.1 μM	>10 μM	**2.37b**	R = 2-thienyl	RB-443	3.67 μM	>10 μM
2.36c	R = 4-pyr.	RB-440	-	-	**2.37c**	R = 4-pyr.	RB-439	1.51 μM	>10 μM

Figure 2.14. Biochemical data for 2nd generation hybrids with pyridyl linkers. **Less than 50% reduction in signal was observed. Compounds not assayed are indicated by a hyphen.

The remaining compounds will be discussed together despite their structural diversity, although they do all incorporate methylene spacers at one end of the linker arene or pseudo-arene unit. Thiohydantoin-methylene homologue RB-405 was about twice as potent against AR as ENZ (280 nM), and about four times more potent than RB-250 (Figure **2.15**). RB-405 was also a slightly better HDACi than RB-250, though not as effective as ENT, and produced a slightly lower IC_{50} for HDAC1 (1.04 μM) than for HDAC2 (1.57 μM). Propellane hybrid RB-433 surprisingly showed the strongest AR antagonism of all compounds screened in this batch (186 nM), four times more potent than ENZ, which may be due to its unique shape imparted by the methylene position further from the thiohydantoin. However, RB-433 was not an inhibitor of HDAC1, possibly due to the bend in the linker induced by the methylene position which may not be accommodated in the HDAC hydrophobic tunnel. B-ring imidazole RB-461 was not available at the time of AR assay, but this compound was a slightly better HDACi than RB-250 / 405 with an IC_{50} of 913 nM so clearly the methylene at the internal end of the linker is generally helpful for potency. Gratifyingly, RB-405 was a slightly more effective hybrid AA-HDACi against both targets than RB-250, and was furthermore the only member of the 2nd generation hybrids to achieve this distinction.

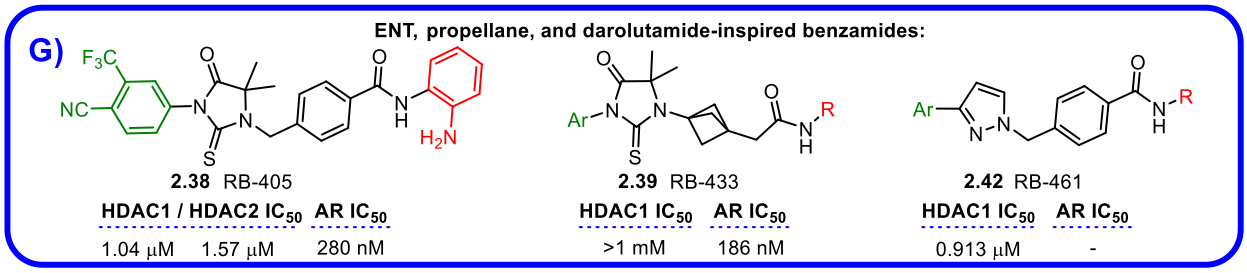


Figure 2.15. Biochemical data for 2nd generation hybrids with methylene spacers. The compound not assayed is indicated by a hyphen.

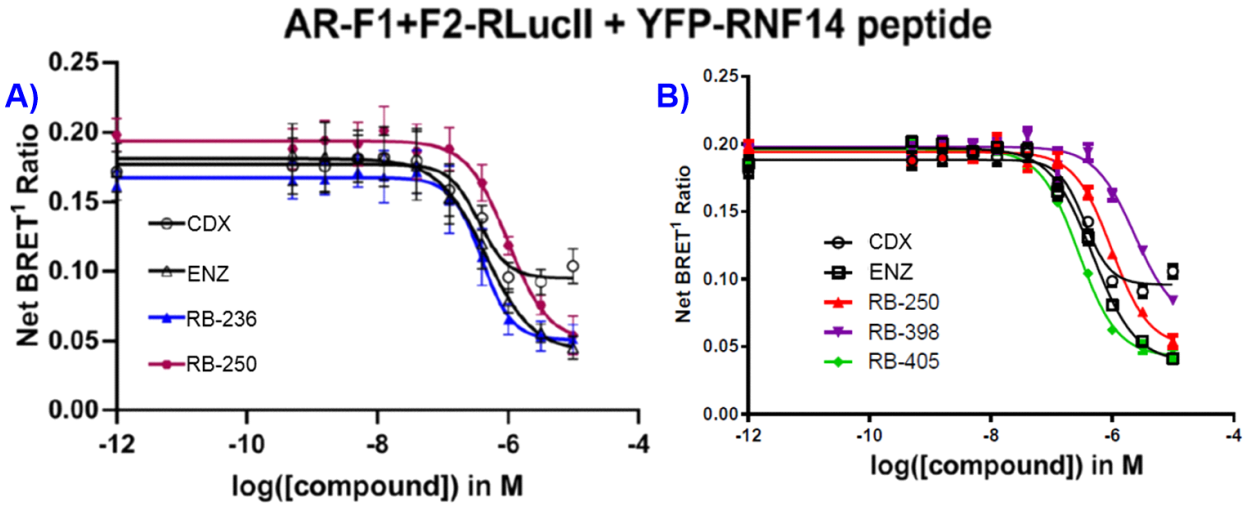


Figure 2.16. Antiandrogenic activity of 2nd generation AA-HDACi hybrids in the presence of DHT in PCA-BRET assay. Dose response curves were performed in HEK293T cells cultured in estrogen depleted media and co-transfected with AR-F1RLucII, ARF2RLucII and the YFP-RNF14 peptide. After 48 h, cells were treated with 2 nM DHT and increasing concentrations of Bicalutamide or Enzalutamide or AA/HDACi hybrids for 1 h. Transfer of energy between AR-F1/F2RLucII and YFP-RNF14 peptide was measured in a BRET1 assay. Graphs represent the mean ± SD of data from 3 independent biological replicates. (**A**) Curves for hydroxamate RB-236 and benzamide RB-250 are shown for comparison with CDX and ENZ. (**B**) Curves for RB-398 and 405 are displayed with RB-250 and CDX / ENZ. *(**A** reproduced with permission.)*[315]

Prior to a final discussion of SAR, a couple of details deserve comment. Once again, a distinction must be made between the completeness of AR antagonism in the BRET assay. As previously seen in the 1st generation assay results, bicalutamide was incapable of achieving the same level of maximum inhibition as ENZ regardless of the IC_{50} values measured (Figure **2.16**). Like 1st generation hydroxamic acid RB-236, 2nd generation benzamides RB-250 and the thiohydantoin-methylene variant RB-405 were able to inhibit AR at the same maximal level as ENZ. The titration curve for pyridyl linker hybrid RB-398 potentially truncates too early to be informative, but similarly low levels of AR inhibition were seen for other 2nd generation

benzamides. Secondly, the results outlined here indicate that the single-point BRET analysis correlates quite well with assay results. Compounds which looked promising by that analysis produced measurable IC_{50} values, while phenyl foot-pocket binding benzamide RB-321 provides one example of the corollary. This first-pass BRET assay therefore provides an excellent qualitative tool of inclusion or exclusion.

Some comparison between the various sets of benzamide hybrids is warranted (see data summary Figure **2.17**). The compact flutamide-like benzamides (Figure **2.17C**) were not effective against either target, which may indicate the A-ring is both insufficient for AR binding and not accommodated in the HDACi hydrophobic tunnel. In the closely related ENZ / APL / pyridyl linker sets (Figure **2.17D-F**), hybrid effectiveness appears easily compromised by deviation from the RB-250 scaffold since incorporation of nitrogen at any of the three sites in RB-445, 398, and 422 removed one activity or the other and even fluoride RB-391 was slightly weakened in efficacy.

Arene-substitution *para* to the benzamide aniline was simply deleterious to AR activity and was surprisingly unhelpful for HDACi potency except in the APL series. These APL-based hybrids demonstrate that the incorporation of large ZBGs, especially the 4-pyridyl, can be beneficial at least with respect to HDAC inhibition. It was surprising that the same trend was not observed in all three series, for example given the reports describing a boost in potency observed with these types of compounds. It is possible that the binding kinetics are simply slower than the assay time allowed for, but the lack of AR activity renders testing this hypothesis meaningless.

The ineffectiveness of all pyridyl linkers, bearing in mind that such linkers are known in HDACi reports, tempts the conclusion that the thiourea may need to be somewhat electron-rich to participate in an interaction such as hydrogen bonding near the mouth of the hydrophobic channel. This may provide an alternative explanation for fluoride RB-391's reduced effectiveness, as well. In any case, incorporation of linker pyridines was not helpful and they should be altogether avoided in the future. Incorporation of methylenes into the linker produced differential effects since RB-405 was slightly more potent than RB-250 in both AR and HDAC. Likewise, the similar methylene position in imidazole RB-461 imparted better HDAC1i activity compared to RB-250. BCP-methylene RB-433 was very potent against AR but totally ineffective against HDAC1 (Figure **2.17G**). The latter results indicate that either the propellane core is not tolerated by HDAC or that the methylene position induces a bend in a position not accommodated by the enzyme.

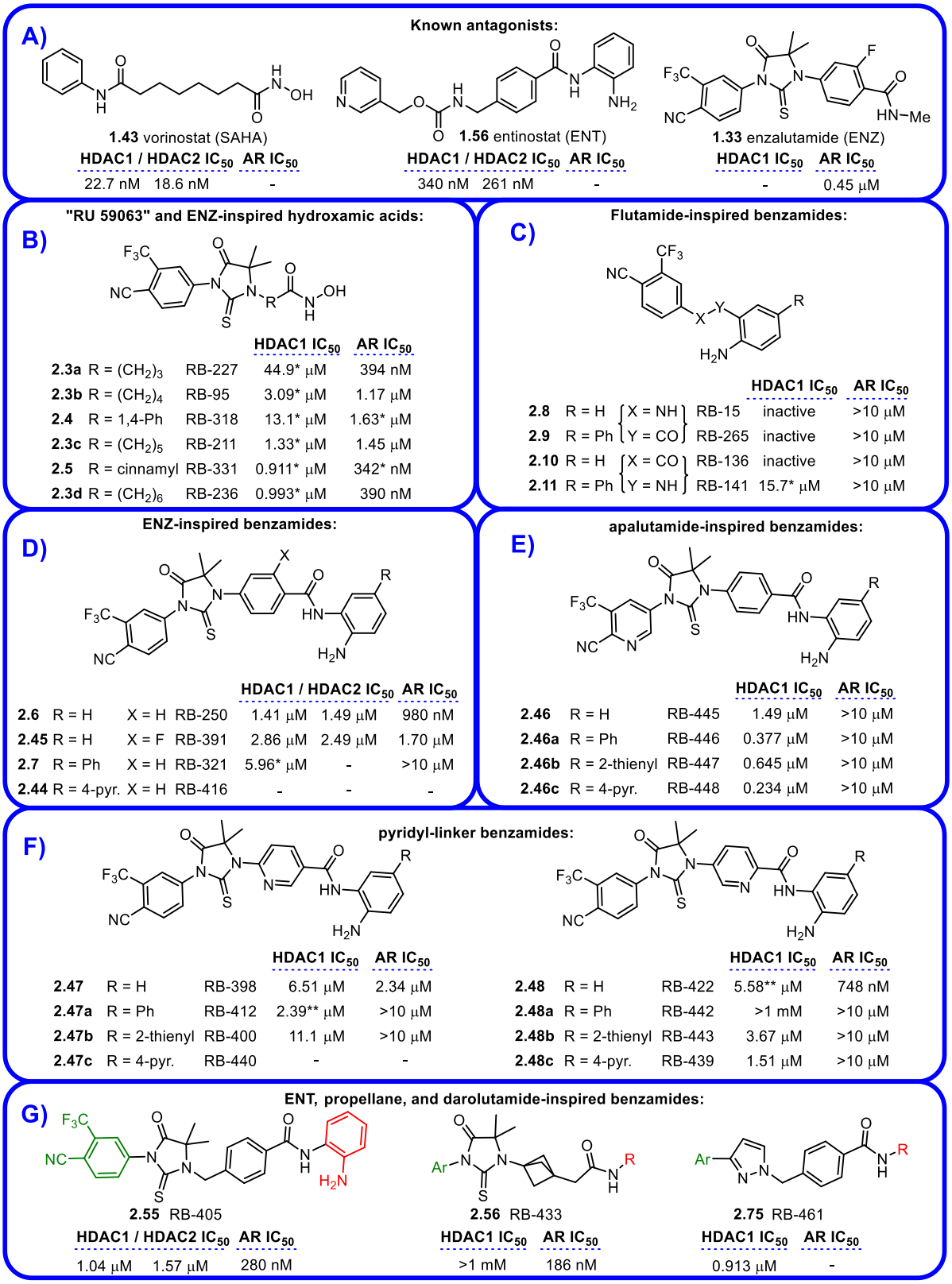


Figure 2.17. Summary of all biochemical data for 1st and 2nd generation hybrids. *Previously obtained assay values. **Less than 50% reduction in signal was observed. Compounds not assayed are indicated by a hyphen.

Unfortunately, the former hypothesis cannot be ruled out at this time since the syntheses of other propellane hybrids failed. Taken together, these last compounds demonstrate that benzamide hybrids can be more effective against AR than hydroxamic acid hybrids and that molecular shape is likely critical. This concludes analysis of the *in vitro* results obtained for these hybrids, and the cell activity of the 2nd generation compounds will be described next.

2.4.2. *Activity of Select Hybrids in Cells*

Having demonstrated respective *in vitro* and cell-based activity of the 2nd generation hybrids against HDAC and AR, it was desirable to show cell-based activity against HDAC by observing protein acetylation with a Western blot. Like the BRET assays, these experiments were conducted by the Mader group. At 10 μM concentration (Figure **2.18**), clear bands of Ac-tubulin α are seen with both hydroxamic acids SAHA and RB-236. This result is expected from direct HDAC6 inhibition since the cytoplasmic Class IIb HDAC deacetylates tubulin α. All bands for RB-227 are weak or nonexistent, which agrees with its poorer *in vitro* activity. Taken together with the controls, the antiandrogen "half" of the hybrids clearly has no HDACi effect biologically. Bands for Ac-H3 and Ac-H4 were observed for all hybrids except weak inhibitor RB-227. The profile indicates desirable nuclear HDAC inhibition, which is expected from both pan-HDACi hydroxamic acids and Class I selective benzamides. The fact that the benzamides selectively inhibit histone deacetylation and mimic the known ENT profile suggests that the same isoform selectivity is operating as is known for ENT.

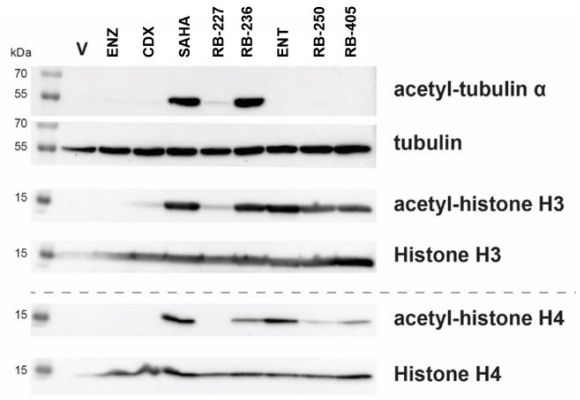


Figure 2.18. HDACi activity in LNCaP cells. LNCap cells cultured in full media were treated for 8 h with vehicle (V) or 10 μM of test compound. Acetylation of α-tubulin and histones H3 and H4 was analyzed by Western blotting with antibodies against each protein. Identical samples were loaded on two different gels (separated here by the dashed line) for probing with different antibodies. Similar results were obtained in 2 independent experiments, one representative result is shown. *(Reproduced with permission)*[315]

Most 2nd generation compounds (excluding RB439, 440, 448, and 461) were screened in a LNCaP antiproliferation assay, as previously done for the 1st generation of hybrids (Figures **2.19**, **2.20A** top). The assay time was shortened from 5 to 3 days to avoid changing the growth media,

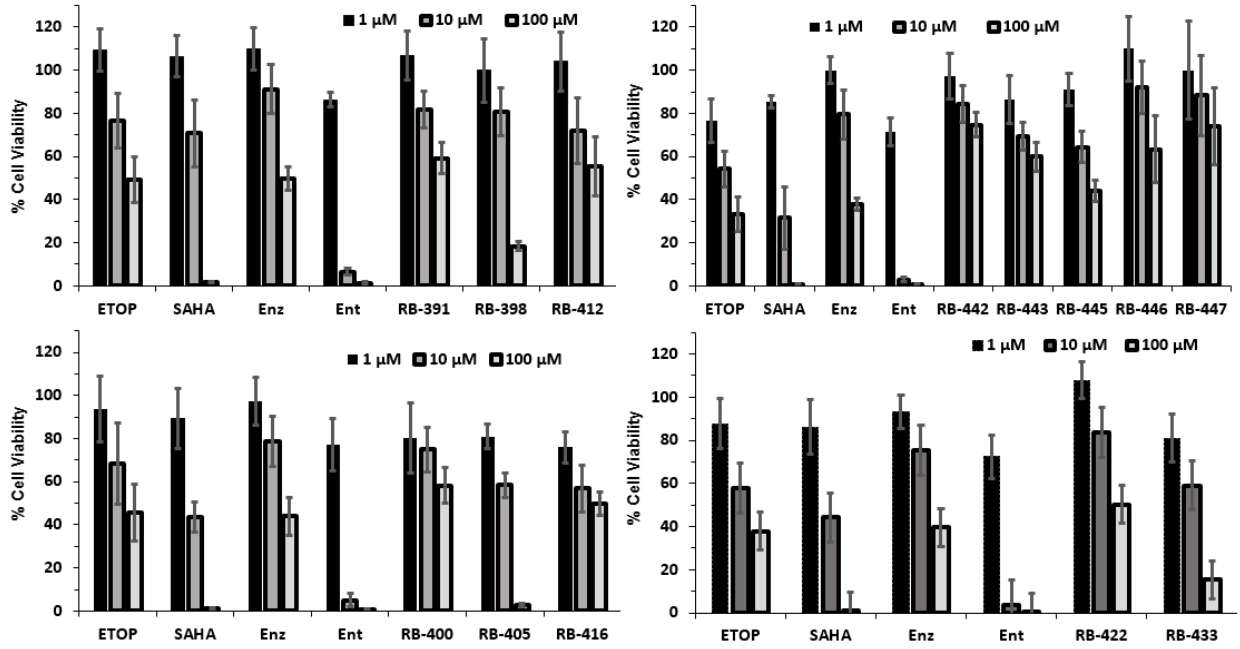


Figure 2.19. Antiproliferative activity of second-generation hybrids in LNCaP cells. These were exposed to select hybrid compounds or one of four control compounds (ETOP, SAHA, ENZ, and ENT) at the indicated concentrations for 72 h and assayed for cell viability. Data is presented as % cell viability after 72 h versus a DMSO vehicle control and is the average of 3 independent biological replicate experiments (n = 3). Error bars denote standard deviation.

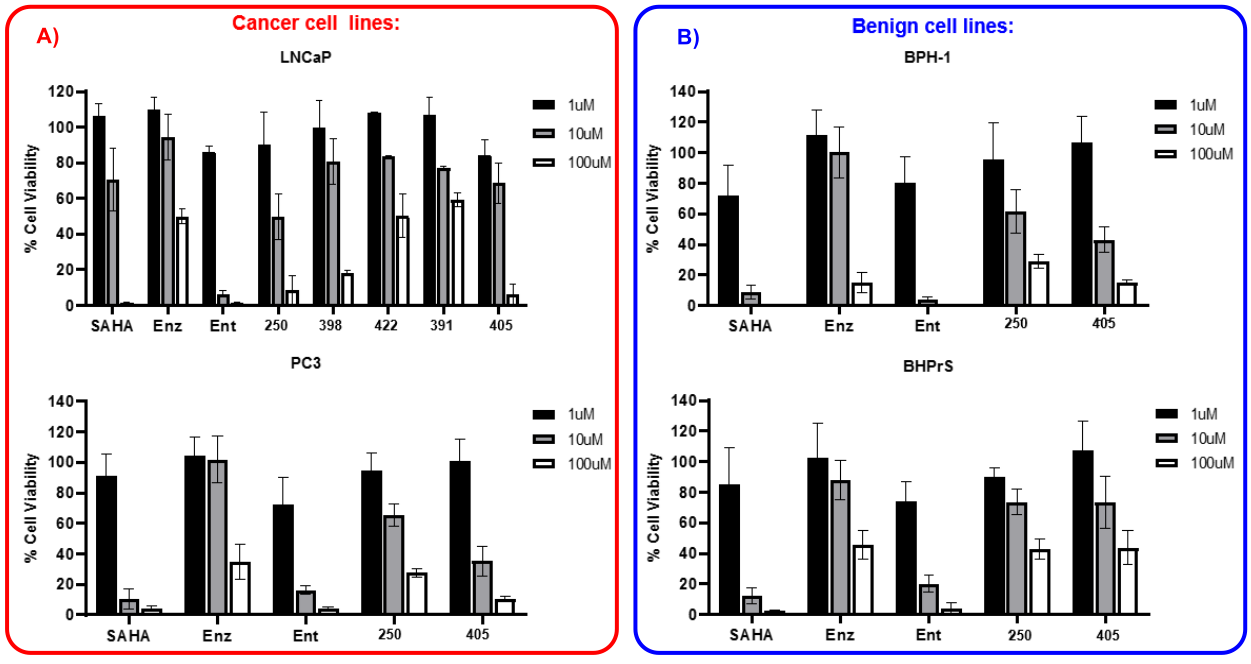


Figure 2.20. Antiproliferative activity of second-generation hybrids in (**A**) LNCaP and PC3 (**B**) BPH-1 and BHPrS. Cell lines were exposed to select hybrid compounds or one of three control compounds (SAHA, ENZ, and ENT) at the indicated concentrations for 72 h and assayed for cell viability. Data is presented as % cell viability after 72 h versus a DMSO vehicle control and is the average of 3 independent biological replicate experiments (n = 3). Error bars denote standard deviation. *(Reproduced with permission.)*[315]

during which process cells could be lost. The compounds were again assayed at 1, 10, and 100 μM concentration using chemotherapy drug etoposide (ETOP), SAHA, ENZ, and ENT as positive controls. Many hybrid compounds had little effect and did not reduce LNCaP cell viability by half even at the highest 100 μM concentration assayed. Fluoride RB-391, A-ring pyridyl RB-445 and linker pyridyls RB-422 and RB-412 (Ph benzamide) reduced viability by approximately half at that concentration, which closely mimicked the activity of ENZ. Only RB-250, linker pyridyl RB-398, BCP-methylene RB-433 and thiohydantoin-methylene RB-405 outperformed ENZ in LNCaP cells, and all four compounds produced at least 75% reduction in LNCaP cell viability. Notably, the hybrids were also more effective than ETOP, but none decreased cell viability as dramatically as ENT or SAHA, which may indicate less overall cytotoxicity (*vide infra*).

Hybrids RB-250, 398, and 405 were then tested in three other cell lines. The PC3 cell line (Figure **2.20A**), isolated from a bone metastasis, is essentially androgen-independent since growth is not driven by AR. Two benign cell lines were also selected to allow certain comparisons (Figure **2.20B**). Benign prostatic hyperplasia (BPH-1) lacks AR expression and is consequently androgen-insensitive, while benign human prostate stroma (BHPrS) was chosen to provide an androgen-sensitive immortalized cell line. As expected, SAHA and ENT were quite toxic in each line, cancerous or otherwise. RB-250 and 405 both affected proliferation similarly in each benign cell culture, with dose-dependent relationships and maximal potency very similar to ENZ at around 40% cell viability. ENZ had little effect on PC3 cells except at very high concentration. Perhaps surprisingly, RB-250 and 405 were both effective and outperformed ENZ in PC3 cells, even at 10 μM concentration. In contrast, RB-398 was ineffective except at very high concentration. Additionally, RB-250 was similar to, and RB-405 more effective than, ETOP in these cells. Although both compounds were also antiproliferative in the non-cancerous cells, they were far less cytotoxic than the known HDACi.

A few comparisons and hypothetical conclusions can be drawn from the above information. First, reinforcing general design philosophy, balanced activity against both targets does in fact appear requisite but not sufficient to affect cell proliferation. Generally, compounds which did not retain activity against one target had little to no effect in cell culture. HDACi activity seems especially helpful in PC3 cells from the performance of RB-250 and 405, which may indicate this is their primary mode of action in this AR-insensitive line. Furthermore, these hybrids showed

very similar potency in AR– non-cancerous BPH-1 cells, which may indicate good general activity in the epithelial cells where cancer typically forms. The combination of activity in epithelial cells, resistant cancerous cell lines, and reduced apparent effect on non-cancerous AR+ stromal cells may represent desirable selective toxicity to epithelial and/or cancerous cells and a therapeutic window. Alternatively, since stromal cells are known to be involved in complex interactions with cancerous tumors in the tumor microenvironment, and appear to provide a supportive role once cancer has matured,[26] the activity in stromal cells which roughly parallels ENZ may be desirable.

2.5.1. *Conclusions and Outlook*

Two successive generations of hybrid androgen receptor antagonists / histone deacetylase inhibitors were designed based on available SAR information for each respective class of compounds. The 1st generation described comprised 6 hydroxamic acid compounds, most previously prepared within our group, 4 novel flutamide-based benzamides, and 2 novel biaryl thiohydantoin benzamides. This set of compounds was directly compared for activity against either target in AR-BRET and HDAC biological assays, as well as for overall effectiveness in antiproliferative assays using LNCaP cells. All 4 flutamide-based benzamides, along with enzalutamide-based biphenyl benzamide RB-321, were essentially inactive. RB-227 was not an effective HDACi but retained good AR antagonism, while RB-95 and 318 exhibited relatively poor activity against both targets. RB-211, 236, 331, and 250 demonstrated approximately micromolar HDAC inhibition and sub-micromolar potency in the AR BRET assay. Compounds RB-211 and 250, which displayed good activity against both targets, were also found to be the most antiproliferative against LNCaP cells. RB-250, which outperformed all other 1st generation compounds in the LNCaP assay, was then used as a basis for a 2nd generation of hybrids.

Several 2nd generation benzamide hybrids were designed based on RB-250 and literature SAR knowledge. A general synthetic route was established to a variety of alternative biaryl thiohydantoin compounds, incorporating the use of a novel method of bis-aryl thiohydantoin synthesis with LHMDS, allowing the preparation of fifteen hybrid compounds. This set of compounds explored combinations of 4 different benzamides (unsubstituted, 2-thienyl, 4-pyridyl, and phenyl) with A-ring and linker pyridines as well as a fluorobenzene linker (RB-391). Simple *o*-diamino benzamides were also prepared for alternative benzyl (RB-405) and BCP-methylene

linkers, but other [1.1.1]propellane and methylene-propellane linkers eluded synthetic efforts. Lastly, a darolutamide-inspired *o*-diamino benzamide was also prepared.

Inhibition curves were obtained for the hybrids against up to two HDAC isoforms in addition to AR-BRET assay curves. Inhibitors RB-250, 391, 398, and 405 were found to retain activity against both AR and type I HDAC enzymes, while substitution *para* to the aniline on the benzamide ring was found to be unanimously deleterious to AR activity and frequently harmful to HDAC inhibition. A-ring pyridyl substitution gave a series of compounds (RB445-448) which were potent HDACi but poor AR antagonists. Pyridyl linkers gave compounds which were less effective in all cases than parent compound RB-250. The BCP-methylene linker in RB-433 was also deleterious to HDAC activity.

Activity against both targets was found to be crucial in antiproliferative cell assays with two different resistant prostate cancer cell line LNCaP and PC-3 models. RB-250 and 405 were found to be the most effective in both cell lines, and both caused greater antiproliferation than ENZ while demonstrating lesser cytotoxicity than HDACi SAHA and ENT. The activity observed in cells whose growth is not driven by AR, especially in PC-3 epithelial cells, indicates probable HDACi activity and is promising in light of the need for treatments of advanced resistant and metastatic prostate cancer. The combination of antiproliferative activity observed in LNCaP and PC-3 cells, and the weaker activity in non-cancerous cells, may indicate a therapeutic treatment window. The SAR information may be used to feed back into the design of additional generations of hybrids.

Future work stemming from this project could include animal studies to examine whether RB-250 and RB-405 have any effect on tumours *in vivo*, which could include pharmacological assessment and examination of pharmacokinetics or metabolism of these compounds. Alternatively, the scaffolds could be reoptimized to try to achieve better activity against HDAC enzymes and androgen receptor or identify compounds which are more strongly antiproliferative. These could likely include linkers similar to RB-250 or RB-405 and explore alternative substitution on the aniline ring. Certainly, the hybrids which were not successfully prepared could be synthesized and assessed for biological activity, while the compounds not fully assessed could be assayed.

2.5.2. *References for Part I*

1. Canadian Cancer Statistics Advisory Committee in collaboration with the Canadian Cancer Society, Statistics Canada and the Public Health Agency of Canada. *Canadian Cancer Statistics 2021.* Toronto, ON: Canadian Cancer Society; 2021.
2. Desai, K.; McManus, J. M.; Sharifi, N., *Endocr. Rev.* **2021**, *42*, 354-373.
3. Attard, G.; Parker, C.; Eeles, R. A.; Schröder, F.; Tomlins, S. A.; Tannock, I.; Drake, C. G.; de Bono, J. S., *The Lancet* **2016**, *387*, 70-82.
4. Dehm, S. M.; Tindall, D. J. *Prostate Cancer,* 2nd ed.; Springer, 2019.
5. Coleman, W. B., Molecular Pathogenesis of Prostate Cancer. In *Molecular Pathology*, 2018; pp 555-568.
6. Berger, M. F.; Lawrence, M. S.; Demichelis, F.; Drier, Y.; Cibulskis, K.; Sivachenko, A. Y.; Sboner, A.; Esgueva, R.; Pflueger, D.; Sougnez, C.; Onofrio, R.; Carter, S. L.; Park, K.; Habegger, L.; Ambrogio, L.; Fennell, T.; Parkin, M.; Saksena, G.; Voet, D.; Ramos, A. H.; Pugh, T. J.; Wilkinson, J.; Fisher, S.; Winckler, W.; Mahan, S.; Ardlie, K.; Baldwin, J.; Simons, J. W.; Kitabayashi, N.; MacDonald, T. Y.; Kantoff, P. W.; Chin, L.; Gabriel, S. B.; Gerstein, M. B.; Golub, T. R.; Meyerson, M.; Tewari, A.; Lander, E. S.; Getz, G.; Rubin, M. A.; Garraway, L. A., *Nature* **2011**, *470*, 214-20.
7. Mohler, M. L.; Bohl, C. E.; Jones, A.; Coss, C. C.; Narayanan, R.; He, Y.; Hwang, D. J.; Dalton, J. T.; Miller, D. D., *J. Med. Chem.* **2009**, *52*, 3597-617.
8. Vis, A. N.; Schroder, F. H., *BJU Int.* **2009**, *104*, 438-48.
9. Pernigoni, N.; Zagato, E.; Calcinotto, A.; Troiani, M.; Mestre, R. P.; Cali, B.; Attanasio, G.; Troisi, J.; Minini, M.; Mosole, S.; Revandkar, A.; Pasquini, E.; Elia, A. R.; Bossi, D.; Rinaldi, A.; Rescigno, P.; Flohr, P.; Hunt, J.; Neeb, A.; Buroni, L.; Guo, C.; Welti, J.; Ferrari, M.; Grioni, M.; Gauthier, J.; Gharaibeh, R. Z.; Palmisano, A.; Lucchini, G. M.; D'Antonio, E.; Merler, S.; Bolis, M.; Grassi, F.; Esposito, A.; Bellone, M.; Briganti, A.; Rescigno, M.; Theurillat, J. P.; Jobin, C.; Gillessen, S.; de Bono, J.; Alimonti, A., *Science* **2021**, *374*, 216-224.
10. Carlson, K. E.; Katzenellenbogen, J. A., *J. Steroid Biochem.* **1990**, *36*, 549-561.
11. Vis, A. N.; Schroder, F. H., *BJU Int.* **2009**, *104*, 1191-7.
12. Wu, Y.; Godoy, A.; Azzouni, F.; Wilton, J. H.; Ip, C.; Mohler, J. L., *Prostate* **2013**, *73*, 1470-82.

13. Yang, M.; Xie, W.; Mostaghel, E.; Nakabayashi, M.; Werner, L.; Sun, T.; Pomerantz, M.; Freedman, M.; Ross, R.; Regan, M.; Sharifi, N.; Figg, W. D.; Balk, S.; Brown, M.; Taplin, M. E.; Oh, W. K.; Lee, G. S.; Kantoff, P. W., *J Clin Oncol* **2011**, *29*, 2565-73.
14. Sharifi, N.; Hamada, A.; Sissung, T.; Danesi, R.; Venzon, D.; Baum, C.; Gulley, J. L.; Price, D. K.; Dahut, W. L.; Figg, W. D., *BJU Int.* **2008**, *102*, 617-21.
15. Roth, M.; Obaidat, A.; Hagenbuch, B., *Br. J. Pharmacol.* **2012**, *165*, 1260-87.
16. Sekine, T.; Miyazaki, H.; Endou, H., *Am. J. Physiol. Renal. Physiol.* **2006**, *290*, F251-61.
17. Hamada, A.; Sissung, T.; Price, D. K.; Danesi, R.; Chau, C. H.; Sharifi, N.; Venzon, D.; Maeda, K.; Nagao, K.; Sparreboom, A.; Mitsuya, H.; Dahut, W. L.; Figg, W. D., *Clin. Cancer Res.* **2008**, *14*, 3312-8.
18. Wright, J. L.; Kwon, E. M.; Ostrander, E. A.; Montgomery, R. B.; Lin, D. W.; Vessella, R.; Stanford, J. L.; Mostaghel, E. A., *Cancer Epidemiol. Biomarkers Prev.* **2011**, *20*, 619-27.
19. Alsinnawi, M.; Zhang, A.; Bianchi-Frias, D.; Burns, J.; Cho, E.; Zhang, X.; Sowalsky, A.; Ye, H.; Slee, A. E.; True, L.; Porter, C.; Taplin, M. E.; Balk, S.; Nelson, P. S.; Montgomery, R. B.; Mostaghel, E. A., *Prostate Cancer Prostatic Dis.* **2019**, *22*, 560-568.
20. Cho, E.; Montgomery, R. B.; Mostaghel, E. A., *Endocrinology* **2014**, *155*, 4124-32.
21. Kruslin, B.; Ulamec, M.; Tomas, D., *Bosn. J. Basic Med. Sci.* **2015**, *15*, 1-8.
22. McAllister, M. J.; Underwood, M. A.; Leung, H. Y.; Edwards, J., *Transl. Res.* **2019**, *206*, 91-106.
23. Franco, O. E.; Hayward, S. W., *Adv. Pharmacol.* **2012**, *65*, 267-313.
24. Sahai, E.; Astsaturov, I.; Cukierman, E.; DeNardo, D. G.; Egeblad, M.; Evans, R. M.; Fearon, D.; Greten, F. R.; Hingorani, S. R.; Hunter, T.; Hynes, R. O.; Jain, R. K.; Janowitz, T.; Jorgensen, C.; Kimmelman, A. C.; Kolonin, M. G.; Maki, R. G.; Powers, R. S.; Pure, E.; Ramirez, D. C.; Scherz-Shouval, R.; Sherman, M. H.; Stewart, S.; Tlsty, T. D.; Tuveson, D. A.; Watt, F. M.; Weaver, V.; Weeraratna, A. T.; Werb, Z., *Nat. Rev. Cancer* **2020**, *20*, 174-186.
25. Nash, C.; Boufaied, N.; Mills, I. G.; Franco, O. E.; Hayward, S. W.; Thomson, A. A., *Mol. Cell Endocrinol.* **2018**, *471*, 1-14.
26. Bonollo, F.; Thalmann, G. N.; Kruithof-de Julio, M.; Karkampouna, S., *Cancers (Basel)* **2020**, *12*.
27. Schafer, S. T.; Gage, F. H., *Nature* **2019**, *569*, 637-638.

28. Mauffrey, P.; Tchitchek, N.; Barroca, V.; Bemelmans, A. P.; Firlej, V.; Allory, Y.; Romeo, P. H.; Magnon, C., *Nature* **2019**, *569*, 672-678.
29. Calcinotto, A.; Spataro, C.; Zagato, E.; Di Mitri, D.; Gil, V.; Crespo, M.; De Bernardis, G.; Losa, M.; Mirenda, M.; Pasquini, E.; Rinaldi, A.; Sumanasuriya, S.; Lambros, M. B.; Neeb, A.; Luciano, R.; Bravi, C. A.; Nava-Rodrigues, D.; Dolling, D.; Prayer-Galetti, T.; Ferreira, A.; Briganti, A.; Esposito, A.; Barry, S.; Yuan, W.; Sharp, A.; de Bono, J.; Alimonti, A., *Nature* **2018**, *559*, 363-369.
30. Waldron, N.; Chowdhury, S., *Medicine* **2020**, *48*, 119-122.
31. Brown, M.; Cato, L.; Jeselsohn, R., Hormone-Responsive Cancers. In *Yen and Jaffe's Reproductive Endocrinology*, 2019; pp 717-741.e8.
32. Abraham, J.; Staffurth, J., *Medicine* **2020**, *48*, 103-107.
33. Epstein, J. I.; Amin, M. B.; Beltran, H.; Lotan, T. L.; Mosquera, J. M.; Reuter, V. E.; Robinson, B. D.; Troncoso, P.; Rubin, M. A., *Am. J. Surg. Pathol.* **2014**, *38*, 756-67.
34. Aggarwal, R.; Zhang, T.; Small, E. J.; Armstrong, A. J., *J. Natl. Compr. Canc. Netw.* **2014**, *12*, 719-26.
35. Wang, H. T.; Yao, Y. H.; Li, B. G.; Tang, Y.; Chang, J. W.; Zhang, J., *J. Clin. Oncol.* **2014**, *32*, 3383-90.
36. Beltran, H.; Prandi, D.; Mosquera, J. M.; Benelli, M.; Puca, L.; Cyrta, J.; Marotz, C.; Giannopoulou, E.; Chakravarthi, B. V.; Varambally, S.; Tomlins, S. A.; Nanus, D. M.; Tagawa, S. T.; Van Allen, E. M.; Elemento, O.; Sboner, A.; Garraway, L. A.; Rubin, M. A.; Demichelis, F., *Nat. Med.* **2016**, *22*, 298-305.
37. Shen, M. M., *Cancer Cell* **2019**, *36*, 117-119.
38. Su, W.; Han, H. H.; Wang, Y.; Zhang, B.; Zhou, B.; Cheng, Y.; Rumandla, A.; Gurrapu, S.; Chakraborty, G.; Su, J.; Yang, G.; Liang, X.; Wang, G.; Rosen, N.; Scher, H. I.; Ouerfelli, O.; Giancotti, F. G., *Cancer Cell* **2019**, *36*, 139-155 e10.
39. Bluemn, E. G.; Coleman, I. M.; Lucas, J. M.; Coleman, R. T.; Hernandez-Lopez, S.; Tharakan, R.; Bianchi-Frias, D.; Dumpit, R. F.; Kaipainen, A.; Corella, A. N.; Yang, Y. C.; Nyquist, M. D.; Mostaghel, E.; Hsieh, A. C.; Zhang, X.; Corey, E.; Brown, L. G.; Nguyen, H. M.; Pienta, K.; Ittmann, M.; Schweizer, M.; True, L. D.; Wise, D.; Rennie, P. S.; Vessella, R. L.; Morrissey, C.; Nelson, P. S., *Cancer Cell* **2017**, *32*, 474-489 e6.

40. Yao, J. L.; Madeb, R.; Bourne, P.; Lei, J.; Yang, X.; Tickoo, S.; Liu, Z.; Tan, D.; Cheng, L.; Hatem, F.; Huang, J.; Anthony di Sant'Agnese, P., *Am. J. Surg. Pathol.* **2006**, *30*, 705-12.
41. Tzelepi, V.; Zhang, J.; Lu, J. F.; Kleb, B.; Wu, G.; Wan, X.; Hoang, A.; Efstathiou, E.; Sircar, K.; Navone, N. M.; Troncoso, P.; Liang, S.; Logothetis, C. J.; Maity, S. N.; Aparicio, A. M., *Clin. Cancer Res.* **2012**, *18*, 666-77.
42. Moeller, A.; Cookson, M.; Patel, S. G., *Physician Assistant Clinics* **2018**, *3*, 11-21.
43. Lowrance, W. T.; Murad, M. H.; Oh, W. K.; Jarrard, D. F.; Resnick, M. J.; Cookson, M. S., *J. Urol.* **2018**, *200*, 1264-1272.
44. Etheridge, T.; Damodaran, S.; Schultz, A.; Richards, K. A.; Gawdzik, J.; Yang, B.; Cryns, V.; Jarrard, D. F., *Asian J. Urol.* **2019**, *6*, 57-64.
45. Stein, M. N.; Jang, T. L., *J. Clin. Oncol.* **2016**, *34*, 2075-8.
46. Gamat, M.; McNeel, D. G., *Endocr. Relat. Cancer* **2017**, *24*, T297-T310.
47. Shore, N. D.; Morgans, A. K.; Ryan, C. J., *Clin. Genitourin. Cancer* **2021**, *19*, 199-207.
48. Pelekanou, V.; Castanas, E., *J. Cell Biochem.* **2016**, *117*, 2224-34.
49. Sharifi, N.; Dahut, W. L.; Figg, W. D., *BJU Int.* **2008**, *101*, 271-4.
50. Scher, H. I.; Sawyers, C. L., *J. Clin. Oncol.* **2005**, *23*, 8253-61.
51. Han, C. S.; Patel, R.; Kim, I. Y., *Expert Opin. Drug Metab. Toxicol.* **2015**, *11*, 967-75.
52. Pereira-Salgado, A.; Kwan, E. M.; Tran, B.; Gibbs, P.; De Bono, J.; M, I. J., *Eur. Urol. Focus* **2021**, *7*, 752-763.
53. Emamekhoo, H.; Barata, P. C.; Edwin, N. C.; Woo, K. M.; Grivas, P.; Garcia, J. A., *Clin. Genitourin. Cancer* **2018**, *16*, 429-436.
54. Dhawan, M.; Ryan, C. J., *Urol. Oncol.* **2016**, *34*, 340-7.
55. Ricci, F.; Buzzatti, G.; Rubagotti, A.; Boccardo, F., *Expert Opin. Drug Saf.* **2014**, *13*, 1483-99.
56. Small, E. J.; Halabi, S.; Dawson, N. A.; Stadler, W. M.; Rini, B. I.; Picus, J.; Gable, P.; Torti, F. M.; Kaplan, E.; Vogelzang, N. J., *J. Clin. Oncol.* **2004**, *22*, 1025-33.
57. Huan, S. D.; Gerridzen, R. G.; Yau, J. C.; Stewart, D. J., *Urology* **1997**, *49*, 632-634.
58. Leone, G.; Tucci, M.; Buttigliero, C.; Zichi, C.; Pignataro, D.; Bironzo, P.; Vignani, F.; Scagliotti, G. V.; Di Maio, M., *Endocr. Relat. Cancer* **2018**, *25*, R1-R9.

59. Soo, A.; O'Callaghan, M. E.; Kopsaftis, T.; Vatandoust, S.; Moretti, K.; Kichenadasse, G., *Prostate Cancer Prostatic Dis.* **2021**, *24*, 826-836.
60. Li, Q.; Deng, Q.; Chao, H. P.; Liu, X.; Lu, Y.; Lin, K.; Liu, B.; Tang, G. W.; Zhang, D.; Tracz, A.; Jeter, C.; Rycaj, K.; Calhoun-Davis, T.; Huang, J.; Rubin, M. A.; Beltran, H.; Shen, J.; Chatta, G.; Puzanov, I.; Mohler, J. L.; Wang, J.; Zhao, R.; Kirk, J.; Chen, X.; Tang, D. G., *Nat. Commun.* **2018**, *9*, 3600.
61. Saad, F.; Fizazi, K., *Urology* **2015**, *86*, 852-61.
62. Zhang, J.; Cunningham, J. J.; Brown, J. S.; Gatenby, R. A., *Nat. Commun.* **2017**, *8*, 1816.
63. Dellis, A.; Papatsoris, A. G., *Expert Opin. Investig. Drugs* **2016**, *25*, 697-707.
64. Sena, L. A.; Wang, H.; Lim Sc, M. S.; Rifkind, I.; Ngomba, N.; Isaacs, J. T.; Luo, J.; Pratz, C.; Sinibaldi, V.; Carducci, M. A.; Paller, C. J.; Eisenberger, M. A.; Markowski, M. C.; Antonarakis, E. S.; Denmeade, S. R., *Eur. J. Cancer* **2021**, *144*, 302-309.
65. Miyahira, A. K.; Cheng, H. H.; Abida, W.; Ellis, L.; Harshman, L. C.; Spratt, D. E.; Simons, J. W.; Pienta, K. J.; Soule, H. R., *Prostate* **2017**, *77*, 1478-1488.
66. Sever, R.; Glass, C. K., *Cold Spring Harb. Perspect. Biol.* **2013**, *5*, a016709.
67. Mangelsdorf, D. J.; Thummel, C.; Beato, M.; Herrlich, P.; Schütz, G.; Umesono, K.; Blumberg, B.; Kastner, P.; Mark, M.; Chambon, P.; Evans, R. M., *Cell* **1995**, *83*, 835-839.
68. Gronemeyer, H.; Gustafsson, J. A.; Laudet, V., *Nat. Rev. Drug Discov.* **2004**, *3*, 950-64.
69. Frigo, D. E.; Bondesson, M.; Williams, C., *Essays Biochem.* **2021**, *65*, 847-856.
70. Chen, T., *Curr. Opin. Chem. Biol.* **2008**, *12*, 418-26.
71. Zhao, L.; Zhou, S.; Gustafsson, J. A., *Endocr. Rev.* **2019**, *40*, 1207-1249.
72. Reau, M.; Lagarde, N.; Zagury, J. F.; Montes, M., *J. Med. Chem.* **2019**, *62*, 2894-2904.
73. Anantharaman, A.; Friedlander, T. W., *Urol. Oncol.* **2016**, *34*, 356-67.
74. Chen, Y.; Sawyers, C. L.; Scher, H. I., *Curr. Opin. Pharmacol.* **2008**, *8*, 440-8.
75. Friedlander, T. W.; Ryan, C. J., *Urol. Clin. North Am.* **2012**, *39*, 453-64.
76. Reichert, Z. R.; Hussain, M., *Cancer J.* **2016**, *22*, 326-329.
77. Katzenwadel, A.; Wolf, P., *Cancer Lett.* **2015**, *367*, 12-7.
78. Narayanan, R., *Asian J. Urol.* **2020**, *7*, 271-283.
79. Quero, L.; Rozet, F.; Beuzeboc, P.; Hennequin, C., *Cancer Radiother.* **2015**, *19*, 220-7.
80. Shafi, A. A.; Yen, A. E.; Weigel, N. L., *Pharmacol. Ther.* **2013**, *140*, 223-38.
81. Taplin, M. E., *Nat. Clin. Pract. Oncol.* **2007**, *4*, 236-44.

82. Wilkenfeld, S. R.; Lin, C.; Frigo, D. E., *Steroids* **2018**, *133*, 2-7.
83. Li, J.; Fu, X.; Cao, S.; Li, J.; Xing, S.; Li, D.; Dong, Y.; Cardin, D.; Park, H. W.; Mauvais-Jarvis, F.; Zhang, H., *J. Biol. Chem.* **2018**, *293*, 12719-12729.
84. Bajpai, P.; Koc, E.; Sonpavde, G.; Singh, R.; Singh, K. K., *J. Biol. Chem.* **2019**, *294*, 6621-6634.
85. Yi, P.; Yu, X.; Wang, Z.; O'Malley, B. W., *Essays Biochem.* **2021**, *65*, 857-866.
86. He, B.; Kemppainen, J. A.; Wilson, E. M., *J. Biol. Chem.* **2000**, *275*, 22986-94.
87. He, B.; Wilson, E. M., *Mol. Cell. Biol.* **2003**, *23*, 2135-50.
88. He, B.; Kemppainen, J. A.; Voegel, J. J.; Gronemeyer, H.; Wilson, E. M., *J. Biol. Chem.* **1999**, *274*, 37219-25.
89. Langley, E.; Kemppainen, J. A.; Wilson, E. M., *J. Biol. Chem.* **1998**, *273*, 92-101.
90. Zhou, Z. X.; Lane, M. V.; Kemppainen, J. A.; French, F. S.; Wilson, E. M., *Mol. Endocrinol.* **1995**, *9*, 208-18.
91. Cutress, M. L.; Whitaker, H. C.; Mills, I. G.; Stewart, M.; Neal, D. E., *J. Cell. Sci.* **2008**, *121*, 957-68.
92. Kaku, N.; Matsuda, K.; Tsujimura, A.; Kawata, M., *Endocrinology* **2008**, *149*, 3960-9.
93. van Royen, M. E.; van Cappellen, W. A.; de Vos, C.; Houtsmuller, A. B.; Trapman, J., *J. Cell. Sci.* **2012**, *125*, 1970-9.
94. Callaway, E., *Nature* **2020**, *578*, 201.
95. Yu, X.; Yi, P.; Hamilton, R. A.; Shen, H.; Chen, M.; Foulds, C. E.; Mancini, M. A.; Ludtke, S. J.; Wang, Z.; O'Malley, B. W., *Mol. Cell.* **2020**, *79*, 812-823 e4.
96. Estebanez-Perpina, E.; Moore, J. M.; Mar, E.; Delgado-Rodrigues, E.; Nguyen, P.; Baxter, J. D.; Buehrer, B. M.; Webb, P.; Fletterick, R. J.; Guy, R. K., *J. Biol. Chem.* **2005**, *280*, 8060-8.
97. He, B.; Bowen, N. T.; Minges, J. T.; Wilson, E. M., *J. Biol. Chem.* **2001**, *276*, 42293-301.
98. Heemers, H. V.; Tindall, D. J., *Cancer Cell.* **2009**, *15*, 245-7.
99. Cano, L. Q.; Lavery, D. N.; Bevan, C. L., *Mol. Cell. Endocrinol.* **2013**, *369*, 52-62.
100. Hsu, C. L.; Liu, J. S.; Wu, P. L.; Guan, H. H.; Chen, Y. L.; Lin, A. C.; Ting, H. J.; Pang, S. T.; Yeh, S. D.; Ma, W. L.; Chen, C. J.; Wu, W. G.; Chang, C., *Mol. Oncol.* **2014**, *8*, 1575-87.

101. Gottlieb, B.; Beitel, L. K.; Nadarajah, A.; Paliouras, M.; Trifiro, M., *Hum. Mutat.* **2012**, *33*, 887-94.
102. McCrea, E.; Sissung, T. M.; Price, D. K.; Chau, C. H.; Figg, W. D., *Pharmacol. Res.* **2016**, *114*, 152-162.
103. Taplin, M. E.; Rajeshkumar, B.; Halabi, S.; Werner, C. P.; Woda, B. A.; Picus, J.; Stadler, W.; Hayes, D. F.; Kantoff, P. W.; Vogelzang, N. J.; Small, E. J.; Cancer; Leukemia Group, B. S., *J. Clin. Oncol.* **2003**, *21*, 2673-8.
104. Mostaghel, E. A.; Plymate, S., *Endocrinol. Metab. Clin. North Am.* **2011**, *40*, 625-42.
105. Obinata, D.; Lawrence, M. G.; Takayama, K.; Choo, N.; Risbridger, G. P.; Takahashi, S.; Inoue, S., *Front. Oncol.* **2020**, *10*, 581515.
106. Wang, J.; Zou, J. X.; Xue, X.; Cai, D.; Zhang, Y.; Duan, Z.; Xiang, Q.; Yang, J. C.; Louie, M. C.; Borowsky, A. D.; Gao, A. C.; Evans, C. P.; Lam, K. S.; Xu, J.; Kung, H. J.; Evans, R. M.; Xu, Y.; Chen, H. W., *Nat. Med.* **2016**, *22*, 488-96.
107. Koivisto, P.; Kononen, J.; Palmberg, C.; Tammela, T.; Hyytinen, E.; Isola, J.; Trapman, J.; Cleutjens, K.; Noordzij, A.; Visakorpi, T.; Kallioniemi, O. P., *Cancer Res.* **1997**, *57*, 314-9.
108. Shiota, M.; Yokomizo, A.; Naito, S., *J. Mol. Endocrinol.* **2011**, *47*, R25-41.
109. Cotter, K. A.; Rubin, M. A., *Nature* **2018**, *560*, 557-559.
110. Belikov, S.; Oberg, C.; Jaaskelainen, T.; Rahkama, V.; Palvimo, J. J.; Wrange, O., *Mol. Cell Endocrinol.* **2013**, *365*, 95-107.
111. Liu, X.; Gomez-Pinillos, A.; Liu, X.; Johnson, E. M.; Ferrari, A. C., *Prostate* **2010**, *70*, 179-89.
112. Burd, C. J.; Morey, L. M.; Knudsen, K. E., *Endocr Relat Cancer* **2006**, *13*, 979-94.
113. Cao, B.; Qi, Y.; Zhang, G.; Xu, D.; Zhan, Y.; Alvarez, X.; Guo, Z.; Fu, X.; Plymate, S. R.; Sartor, O.; Zhang, H.; Dong, Y., *Oncotarget.* **2014**, *5*, 1646-56.
114. Antonarakis, E. S.; Lu, C.; Wang, H.; Luber, B.; Nakazawa, M.; Roeser, J. C.; Chen, Y.; Mohammad, T. A.; Chen, Y.; Fedor, H. L.; Lotan, T. L.; Zheng, Q.; De Marzo, A. M.; Isaacs, J. T.; Isaacs, W. B.; Nadal, R.; Paller, C. J.; Denmeade, S. R.; Carducci, M. A.; Eisenberger, M. A.; Luo, J., *N. Engl. J. Med.* **2014**, *371*, 1028-38.
115. Hu, R.; Dunn, T. A.; Wei, S.; Isharwal, S.; Veltri, R. W.; Humphreys, E.; Han, M.; Partin, A. W.; Vessella, R. L.; Isaacs, W. B.; Bova, G. S.; Luo, J., *Cancer Res.* **2009**, *69*, 16-22.

116. Rana, M.; Dong, J.; Robertson, M. J.; Basil, P.; Coarfa, C.; Weigel, N. L., *Sci. Rep.* **2021**, *11*, 1393.
117. Zhan, Y.; Zhang, G.; Wang, X.; Qi, Y.; Bai, S.; Li, D.; Ma, T.; Sartor, O.; Flemington, E. K.; Zhang, H.; Lee, P.; Dong, Y., *Mol. Cancer Res.* **2017**, *15*, 59-68.
118. Li, Q.; Wang, Z.; Yi, J.; Shen, H.; Yang, Z.; Yan, L.; Xie, L., *Transl. Oncol.* **2021**, *14*, 101145.
119. Sprenger, C. C.; Plymate, S. R., *Horm. Cancer* **2014**, *5*, 207-17.
120. Dagar, M.; Singh, J. P.; Dagar, G.; Tyagi, R. K.; Bagchi, G., *J. Biol. Chem.* **2019**, *294*, 8699-8710.
121. Gioeli, D.; Ficarro, S. B.; Kwiek, J. J.; Aaronson, D.; Hancock, M.; Catling, A. D.; White, F. M.; Christian, R. E.; Settlage, R. E.; Shabanowitz, J.; Hunt, D. F.; Weber, M. J., *J. Biol. Chem.* **2002**, *277*, 29304-14.
122. Guo, Z.; Dai, B.; Jiang, T.; Xu, K.; Xie, Y.; Kim, O.; Nesheiwat, I.; Kong, X.; Melamed, J.; Handratta, V. D.; Njar, V. C.; Brodie, A. M.; Yu, L. R.; Veenstra, T. D.; Chen, H.; Qiu, Y., *Cancer Cell* **2006**, *10*, 309-19.
123. Koryakina, Y.; Ta, H. Q.; Gioeli, D., *Endocr. Relat. Cancer* **2014**, *21*, T131-45.
124. Howard, N.; Clementino, M.; Kim, D.; Wang, L.; Verma, A.; Shi, X.; Zhang, Z.; DiPaola, R. S., *Semin. Cancer Biol.* **2019**, *57*, 111-116.
125. Bambury, R. M.; Rathkopf, D. E., *Urol. Oncol.* **2016**, *34*, 348-55.
126. Monaghan, A. E.; McEwan, I. J., *Asian J. Androl.* **2016**, *18*, 687-94.
127. Maylin, Z. R.; Nicolescu, R. C.; Pandha, H.; Asim, M., *Transl. Oncol.* **2021**, *14*, 101115.
128. Richards, J.; Lim, A. C.; Hay, C. W.; Taylor, A. E.; Wingate, A.; Nowakowska, K.; Pezaro, C.; Carreira, S.; Goodall, J.; Arlt, W.; McEwan, I. J.; de Bono, J. S.; Attard, G., *Cancer Res.* **2012**, *72*, 2176-82.
129. Georget, V.; Terouanne, B.; Nicolas, J. C.; Sultan, C., *Biochemistry* **2002**, *41*, 11824-31.
130. Centenera, M. M.; Carter, S. L.; Gillis, J. L.; Marrocco-Tallarigo, D. L.; Grose, R. H.; Tilley, W. D.; Butler, L. M., *Endocr. Relat. Cancer* **2015**, *22*, 805-18.
131. Centenera, M. M.; Gillis, J. L.; Hanson, A. R.; Jindal, S.; Taylor, R. A.; Risbridger, G. P.; Sutherland, P. D.; Scher, H. I.; Raj, G. V.; Knudsen, K. E.; Yeadon, T.; Australian Prostate Cancer, B.; Tilley, W. D.; Butler, L. M., *Clin. Cancer Res.* **2012**, *18*, 3562-70.
132. Li, L.; Wang, L.; You, Q. D.; Xu, X. L., *J. Med. Chem.* **2020**, *63*, 1798-1822.

133. Liu, C.; Lou, W.; Yang, J. C.; Liu, L.; Armstrong, C. M.; Lombard, A. P.; Zhao, R.; Noel, O. D. V.; Tepper, C. G.; Chen, H. W.; Dall'Era, M.; Evans, C. P.; Gao, A. C., *Nat. Commun.* **2018**, *9*, 4700.
134. De Mol, E.; Fenwick, R. B.; Phang, C. T.; Buzon, V.; Szulc, E.; de la Fuente, A.; Escobedo, A.; Garcia, J.; Bertoncini, C. W.; Estebanez-Perpina, E.; McEwan, I. J.; Riera, A.; Salvatella, X., *ACS Chem. Biol.* **2016**, *11*, 2499-505.
135. Banuelos, C. A.; Ito, Y.; Obst, J. K.; Mawji, N. R.; Wang, J.; Hirayama, Y.; Leung, J. K.; Tam, T.; Tien, A. H.; Andersen, R. J.; Sadar, M. D., *Cancers (Basel)* **2020**, *12*.
136. Han, X.; Wang, C.; Qin, C.; Xiang, W.; Fernandez-Salas, E.; Yang, C. Y.; Wang, M.; Zhao, L.; Xu, T.; Chinnaswamy, K.; Delproposto, J.; Stuckey, J.; Wang, S., *J. Med. Chem.* **2019**, *62*, 941-964.
137. Han, X.; Zhao, L.; Xiang, W.; Qin, C.; Miao, B.; Xu, T.; Wang, M.; Yang, C. Y.; Chinnaswamy, K.; Stuckey, J.; Wang, S., *J. Med. Chem.* **2019**, *62*, 11218-11231.
138. Salami, J.; Alabi, S.; Willard, R. R.; Vitale, N. J.; Wang, J.; Dong, H.; Jin, M.; McDonnell, D. P.; Crew, A. P.; Neklesa, T. K.; Crews, C. M., *Commun. Biol.* **2018**, *1*, 100.
139. Kargbo, R. B., *ACS Med. Chem. Lett.* **2021**, *12*, 518-520.
140. Petrylak, D. P.; Gao, X.; Vogelzang, N. J.; Garfield, M. H.; Taylor, I.; Dougan Moore, M.; Peck, R. A.; Burris, H. A., *J. Clin. Oncol.* **2020**, *38*, 3500-3500.
141. Snyder, L. B.; Neklesa, T. K.; Chen, X.; Dong, H.; Ferraro, C.; Gordon, D. A.; Macaluso, J.; Pizzano, J.; Wang, J.; Willard, R. R.; Vitale, N.; Peck, R.; Moore, M. D.; Crews, C. M.; Houston, J.; Crew, A. P.; Taylor, I., Abstract 43: Discovery of ARV-110, a first in class androgen receptor degrading PROTAC for the treatment of men with metastatic castration resistant prostate cancer. In *Experimental and Molecular Therapeutics*, 2021; pp 43-43.
142. Kregel, S.; Wang, C.; Han, X.; Xiao, L.; Fernandez-Salas, E.; Bawa, P.; McCollum, B. L.; Wilder-Romans, K.; Apel, I. J.; Cao, X.; Speers, C.; Wang, S.; Chinnaiyan, A. M., *Neoplasia* **2020**, *22*, 111-119.
143. Gao, W.; Bohl, C. E.; Dalton, J. T., *Chem. Rev.* **2005**, *105*, 3352-70.
144. Pereira de Jesus-Tran, K.; Cote, P. L.; Cantin, L.; Blanchet, J.; Labrie, F.; Breton, R., *Protein Sci.* **2006**, *15*, 987-99.
145. Hur, E.; Pfaff, S. J.; Payne, E. S.; Gron, H.; Buehrer, B. M.; Fletterick, R. J., *PLoS Biol.* **2004**, *2*, E274.

146. Hosoda, S.; Hashimoto, Y., *Pure Appl. Chem.* **2007**, *79*, 615-626.
147. Pike, A. C. W.; Brzozowski, A. M.; Walton, J.; Hubbard, R. E.; Thorsell, A.-G.; Li, Y.-L.; Gustafsson, J.-Å.; Carlquist, M., *Structure* **2001**, *9*, 145-153.
148. Brzozowski, A. M.; Pike, A. C.; Dauter, Z.; Hubbard, R. E.; Bonn, T.; Engstrom, O.; Ohman, L.; Greene, G. L.; Gustafsson, J. A.; Carlquist, M., *Nature* **1997**, *389*, 753-8.
149. Gim, H. J.; Park, J.; Jung, M. E.; Houk, K. N., *Sci. Rep.* **2021**, *11*, 15887.
150. Osguthorpe, D. J.; Hagler, A. T., *Biochem.* **2011**, *50*, 4105-13.
151. Liu, H.; Wang, L.; Tian, J.; Li, J.; Liu, H., *J. Cell. Biochem.* **2017**, *118*, 2792-2801.
152. Bohl, C. E.; Miller, D. D.; Chen, J.; Bell, C. E.; Dalton, J. T., *J. Biol. Chem.* **2005**, *280*, 37747-54.
153. Bohl, C. E.; Gao, W.; Miller, D. D.; Bell, C. E.; Dalton, J. T., *Proc. Natl. Acad. Sci. U S A* **2005**, *102*, 6201-6.
154. Bhasin, S., *J. Frailty Aging* **2015**, *4*, 121-2.
155. Chen, J.; Kim, J.; Dalton, J. T., *Mol. Interv.* **2005**, *5*, 173-88.
156. Dalton, J. T., *Br. J. Clin. Pharmacol.* **2017**, *83*, 2131-2133.
157. Gao, W.; Dalton, J. T., *Drug Discov. Today* **2007**, *12*, 241-8.
158. Narayanan, R.; Coss, C. C.; Dalton, J. T., *Mol. Cell Endocrinol.* **2018**, *465*, 134-142.
159. Segal, S.; Narayanan, R.; Dalton, J. T., *Expert Opin. Investig. Drugs* **2006**, *15*, 377-87.
160. Cadilla, R.; Turnbull, P., *Curr. Top. Med. Chem.* **2006**, *6*, 245-70.
161. Marhefka, C. A.; Gao, W.; Chung, K.; Kim, J.; He, Y.; Yin, D.; Bohl, C.; Dalton, J. T.; Miller, D. D., *J. Med. Chem.* **2004**, *47*, 993-8.
162. Bohl, C. E.; Wu, Z.; Chen, J.; Mohler, M. L.; Yang, J.; Hwang, D. J.; Mustafa, S.; Miller, D. D.; Bell, C. E.; Dalton, J. T., *Bioorg. Med. Chem. Lett.* **2008**, *18*, 5567-70.
163. Chen, J.; Hwang, D. J.; Bohl, C. E.; Miller, D. D.; Dalton, J. T., *J. Pharmacol. Exp. Ther.* **2005**, *312*, 546-53.
164. Chen, J.; Hwang, D. J.; Chung, K.; Bohl, C. E.; Fisher, S. J.; Miller, D. D.; Dalton, J. T., *Endocrinology* **2005**, *146*, 5444-54.
165. Gao, W.; Reiser, P. J.; Coss, C. C.; Phelps, M. A.; Kearbey, J. D.; Miller, D. D.; Dalton, J. T., *Endocrinology* **2005**, *146*, 4887-97.
166. Kim, J.; Wu, D.; Hwang, D. J.; Miller, D. D.; Dalton, J. T., *J. Pharmacol. Exp. Ther.* **2005**, *315*, 230-9.

167. Singh, S. M.; Gauthier, S.; Labrie, F., *Curr. Med. Chem.* **2000**, *7*, 211-47.
168. Haendler, B.; Cleve, A., *Mol. Cell. Endocrinol.* **2012**, *352*, 79-91.
169. Masiello, D.; Cheng, S.; Bubley, G. J.; Lu, M. L.; Balk, S. P., *J. Biol. Chem.* **2002**, *277*, 26321-6.
170. Tran, C.; Ouk, S.; Clegg, N. J.; Chen, Y.; Watson, P. A.; Arora, V.; Wongvipat, J.; Smith-Jones, P. M.; Yoo, D.; Kwon, A.; Wasielewska, T.; Welsbie, D.; Chen, C. D.; Higano, C. S.; Beer, T. M.; Hung, D. T.; Scher, H. I.; Jung, M. E.; Sawyers, C. L., *Science* **2009**, *324*, 787-90.
171. Kandil, S.; Lee, K. Y.; Davies, L.; Rizzo, S. A.; Dart, D. A.; Westwell, A. D., *Eur. J. Med. Chem.* **2019**, *167*, 49-60.
172. Duke, C. B.; Jones, A.; Bohl, C. E.; Dalton, J. T.; Miller, D. D., *J. Med. Chem.* **2011**, *54*, 3973-6.
173. Yin, D.; He, Y.; Perera, M. A.; Hong, S. S.; Marhefka, C.; Stourman, N.; Kirkovsky, L.; Miller, D. D.; Dalton, J. T., *Mol. Pharmacol.* **2003**, *63*, 211-23.
174. Bohl, C. E.; Chang, C.; Mohler, M. L.; Chen, J.; Miller, D. D.; Swaan, P. W.; Dalton, J. T., *J. Med. Chem.* **2004**, *47*, 3765-76.
175. Hwang, D. J.; Yang, J.; Xu, H.; Rakov, I. M.; Mohler, M. L.; Dalton, J. T.; Miller, D. D., *Bioorg. Med. Chem.* **2006**, *14*, 6525-38.
176. de Jesus Cortez, F.; Nguyen, P.; Truillet, C.; Tian, B.; Kuchenbecker, K. M.; Evans, M. J.; Webb, P.; Jacobson, M. P.; Fletterick, R. J.; England, P. M., *ACS Chem. Biol.* **2017**, *12*, 2934-2939.
177. Karvonen, U.; Kallio, P. J.; Janne, O. A.; Palvimo, J. J., *J Biol Chem* **1997**, *272*, 15973-9.
178. Teutsch, G.; Goubet, F.; Battmann, T.; Bonfils, A.; Bouchoux, F.; Cerede, E.; Gofflo, D.; Gaillard-Kelly, M.; Philibert, D., *J. Steroid Biochem. Mol. Biol.* **1994**, *48*, 111-119.
179. Jung, M. E.; Ouk, S.; Yoo, D.; Sawyers, C. L.; Chen, C.; Tran, C.; Wongvipat, J., *J. Med. Chem.* **2010**, *53*, 2779-96.
180. Dumas, L.; Payne, H.; Chowdhury, S., *Expert Rev. Anticancer. Ther.* **2012**, *12*, 131-3.
181. Alcaraz, A., *Eur. Urol.* **2020**, *77*, 286-287.
182. Prekovic, S.; van Royen, M. E.; Voet, A. R.; Geverts, B.; Houtman, R.; Melchers, D.; Zhang, K. Y.; Van den Broeck, T.; Smeets, E.; Spans, L.; Houtsmuller, A. B.; Joniau, S.; Claessens, F.; Helsen, C., *Mol. Cancer Ther.* **2016**, *15*, 1702-12.

183. Jung, M. E.; Sawyers, C. L.; Ouk, S.; Tran, C.; Wongvipat, J. US 8445507 B2, May 21, 2013.
184. Alkhudair, N. A., *Saudi Pharm. J.* **2019**, *27*, 368-372.
185. Clegg, N. J.; Wongvipat, J.; Joseph, J. D.; Tran, C.; Ouk, S.; Dilhas, A.; Chen, Y.; Grillot, K.; Bischoff, E. D.; Cai, L.; Aparicio, A.; Dorow, S.; Arora, V.; Shao, G.; Qian, J.; Zhao, H.; Yang, G.; Cao, C.; Sensintaffar, J.; Wasielewska, T.; Herbert, M. R.; Bonnefous, C.; Darimont, B.; Scher, H. I.; Smith-Jones, P.; Klang, M.; Smith, N. D.; De Stanchina, E.; Wu, N.; Ouerfelli, O.; Rix, P. J.; Heyman, R. A.; Jung, M. E.; Sawyers, C. L.; Hager, J. H., *Cancer Res.* **2012**, *72*, 1494-503.
186. Claessens, F.; Helsen, C.; Prekovic, S.; Van den Broeck, T.; Spans, L.; Van Poppel, H.; Joniau, S., *Nat. Rev. Urol.* **2014**, *11*, 712-6.
187. Moilanen, A. M.; Riikonen, R.; Oksala, R.; Ravanti, L.; Aho, E.; Wohlfahrt, G.; Nykanen, P. S.; Tormakangas, O. P.; Palvimo, J. J.; Kallio, P. J., *Sci. Rep.* **2015**, *5*, 12007.
188. Zurth, C.; Sandmann, S.; Trummel, D.; Seidel, D.; Gieschen, H., *J. Clin. Oncol.* **2018**, *36*, 345-345.
189. Lallous, N.; Snow, O.; Sanchez, C.; Parra Nunez, A. K.; Sun, B.; Hussain, A.; Lee, J.; Morin, H.; Leblanc, E.; Gleave, M. E.; Cherkasov, A., *Cancers (Basel)* **2021**, *13*.
190. Sugawara, T.; Baumgart, S. J.; Nevedomskaya, E.; Reichert, K.; Steuber, H.; Lejeune, P.; Mumberg, D.; Haendler, B., *Int. J. Cancer* **2019**, *145*, 1382-1394.
191. Hwang, D. J.; He, Y.; Ponnusamy, S.; Mohler, M. L.; Thiyagarajan, T.; McEwan, I. J.; Narayanan, R.; Miller, D. D., *J. Med. Chem.* **2019**, *62*, 491-511.
192. Ponnusamy, S.; Coss, C. C.; Thiyagarajan, T.; Watts, K.; Hwang, D. J.; He, Y.; Selth, L. A.; McEwan, I. J.; Duke, C. B.; Pagadala, J.; Singh, G.; Wake, R. W.; Ledbetter, C.; Tilley, W. D.; Moldoveanu, T.; Dalton, J. T.; Miller, D. D.; Narayanan, R., *Cancer Res.* **2017**, *77*, 6282-6298.
193. Dalal, K.; Morin, H.; Ban, F.; Shepherd, A.; Fernandez, M.; Tam, K. J.; Li, H.; LeBlanc, E.; Lack, N.; Prinz, H.; Rennie, P. S.; Cherkasov, A., *Eur. J. Med. Chem.* **2018**, *157*, 1164-1173.
194. Loddick, S. A.; Ross, S. J.; Thomason, A. G.; Robinson, D. M.; Walker, G. E.; Dunkley, T. P.; Brave, S. R.; Broadbent, N.; Stratton, N. C.; Trueman, D.; Mouchet, E.; Shaheen, F. S.; Jacobs, V. N.; Cumberbatch, M.; Wilson, J.; Jones, R. D.; Bradbury, R. H.; Rabow,

A.; Gaughan, L.; Womack, C.; Barry, S. T.; Robson, C. N.; Critchlow, S. E.; Wedge, S. R.; Brooks, A. N., *Mol. Cancer Ther.* **2013**, *12*, 1715-27.

195. Omlin, A.; Jones, R. J.; van der Noll, R.; Satoh, T.; Niwakawa, M.; Smith, S. A.; Graham, J.; Ong, M.; Finkelman, R. D.; Schellens, J. H.; Zivi, A.; Crespo, M.; Riisnaes, R.; Nava-Rodrigues, D.; Malone, M. D.; Dive, C.; Sloane, R.; Moore, D.; Alumkal, J. J.; Dymond, A.; Dickinson, P. A.; Ranson, M.; Clack, G.; de Bono, J.; Elliott, T., *Invest. New Drugs* **2015**, *33*, 679-90.
196. Branch, J. R.; Bush, T. L.; Pande, V.; Connolly, P. J.; Zhang, Z.; Hickson, I.; Ondrus, J.; Jaensch, S.; Bischoff, J. R.; Habineza, G.; Van Hecke, G.; Meerpoel, L.; Packman, K.; Parrett, C. J.; Chong, Y. T.; Gottardis, M. M.; Bignan, G., *Mol. Cancer Ther.* **2021**, *20*, 763-774.
197. Tong, Y.; Chen, C.; Wu, J.; Yang, J.; Zhang, H.; Wu, X.; Duan, Y.; Gao, W.; Qian, W.; Niu, X.; Mi, L.; Guo, C., Abstract 614: Proxalutamide (GT0918), a potent androgen receptor pathway inhibitor. In *Endocrinology*, 2014; pp 614-614.
198. Tong, Y.; Chen, C.; Wu, J.; Zhang, H.; Wu, X.; Duan, Y.; Gao, W.; Niu, X.; Ma, L.; Guo, C., Abstract 2460: Discovery of potent androgen receptor antagonists for treating CRPC and AR+ breast cancer. In *Cancer Chemistry*, 2013; pp 2460-2460.
199. Yang, M.; He, S.; Fan, Y.; Wang, Y.; Ge, Z.; Shan, L.; Gong, W.; Huang, X.; Tong, Y.; Gao, C., *Int. J. Pharm.* **2014**, *475*, 97-109.
200. Seto, E.; Yoshida, M., *Cold Spring Harb. Perspect Biol.* **2014**, *6*, a018713.
201. Ganesan, A., HDAC inhibitors in cancer therapy. In *Histone Modifications in Therapy*, 2020; pp 19-49.
202. Lombardi, P. M.; Cole, K. E.; Dowling, D. P.; Christianson, D. W., *Curr. Opin. Struct. Biol.* **2011**, *21*, 735-43.
203. Minucci, S.; Pelicci, P. G., *Nat. Rev. Cancer* **2006**, *6*, 38-51.
204. Porter, N. J.; Christianson, D. W., *Curr. Opin. Struct. Biol.* **2019**, *59*, 9-18.
205. de Ruijter, A. J.; van Gennip, A. H.; Caron, H. N.; Kemp, S.; van Kuilenburg, A. B., *Biochem. J.* **2003**, *370*, 737-49.
206. Choudhary, C.; Kumar, C.; Gnad, F.; Nielsen, M. L.; Rehman, M.; Walther, T. C.; Olsen, J. V.; Mann, M., *Science* **2009**, *325*, 834-40.
207. He, M.; Han, Z.; Liu, L.; Zheng, Y. G., *Angew. Chem. Int. Ed. Engl.* **2018**, *57*, 1162-1184.

208. Wolffe, A. P.; Guschin, D., *J. Struct. Biol.* **2000**, *129*, 102-22.

209. Kallin, E.; Zhang, Y. Chromatin Remodeling. In *Encyclopedia of Biological Chemistry*; Elsevier, 2004; pp 456-463.

210. Wu, J., *Trends in Biochemical Sciences* **2000**, *25*, 619-623.

211. Kornberg, R. D.; Lorch, Y., *Cell* **1999**, *98*, 285-294.

212. Stillman, B., *Cell* **2018**, *175*, 6-9.

213. Alberts, B. *Essential Cell Biology;* Garland Science, Taylor & Francis Group, LLC, 2010.

214. Balasubramanian, S.; Verner, E.; Buggy, J. J., *Cancer Lett.* **2009**, *280*, 211-21.

215. Gregoretti, I. V.; Lee, Y. M.; Goodson, H. V., *J. Mol. Biol.* **2004**, *338*, 17-31.

216. Sauve, A. A., *Biochim. Biophys. Acta.* **2010**, *1804*, 1591-603.

217. Wang, Y.; He, J.; Liao, M.; Hu, M.; Li, W.; Ouyang, H.; Wang, X.; Ye, T.; Zhang, Y.; Ouyang, L., *Eur. J. Med. Chem.* **2019**, *161*, 48-77.

218. Bantscheff, M.; Hopf, C.; Savitski, M. M.; Dittmann, A.; Grandi, P.; Michon, A. M.; Schlegl, J.; Abraham, Y.; Becher, I.; Bergamini, G.; Boesche, M.; Delling, M.; Dumpelfeld, B.; Eberhard, D.; Huthmacher, C.; Mathieson, T.; Poeckel, D.; Reader, V.; Strunk, K.; Sweetman, G.; Kruse, U.; Neubauer, G.; Ramsden, N. G.; Drewes, G., *Nat. Biotechnol.* **2011**, *29*, 255-65.

219. Osko, J. D.; Christianson, D. W., *Biochem.* **2019**, *58*, 4912-4924.

220. Ustinova, K.; Novakova, Z.; Saito, M.; Meleshin, M.; Mikesova, J.; Kutil, Z.; Baranova, P.; Havlinova, B.; Schutkowski, M.; Matthias, P.; Barinka, C., *J. Biol. Chem.* **2020**, *295*, 2614-2628.

221. Balmik, A. A.; Chidambaram, H.; Dangi, A.; Marelli, U. K.; Chinnathambi, S., *Biochem.* **2020**, *59*, 4546-4562.

222. Hai, Y.; Christianson, D. W., *Nat. Chem. Biol.* **2016**, *12*, 741-7.

223. Hai, Y.; Shinsky, S. A.; Porter, N. J.; Christianson, D. W., *Nat. Commun.* **2017**, *8*, 15368.

224. Herbst-Gervasoni, C. J.; Christianson, D. W., *Biochem.* **2021**, *60*, 303-313.

225. Shinsky, S. A.; Christianson, D. W., *Biochem.* **2018**, *57*, 3105-3114.

226. Son, S. I.; Su, D.; Ho, T. T.; Lin, H., *ACS Chem. Biol.* **2020**, *15*, 2866-2871.

227. Kutil, Z.; Novakova, Z.; Meleshin, M.; Mikesova, J.; Schutkowski, M.; Barinka, C., *ACS Chem. Biol.* **2018**, *13*, 685-693.

228. Liu, S. S.; Wu, F.; Jin, Y. M.; Chang, W. Q.; Xu, T. M., *Biomed. Pharmacother.* **2020**, *131*, 110607.
229. Wang, D. F.; Wiest, O.; Helquist, P.; Lan-Hargest, H. Y.; Wiech, N. L., *J. Med. Chem.* **2004**, *47*, 3409-17.
230. Lauffer, B. E.; Mintzer, R.; Fong, R.; Mukund, S.; Tam, C.; Zilberleyb, I.; Flicke, B.; Ritscher, A.; Fedorowicz, G.; Vallero, R.; Ortwine, D. F.; Gunzner, J.; Modrusan, Z.; Neumann, L.; Koth, C. M.; Lupardus, P. J.; Kaminker, J. S.; Heise, C. E.; Steiner, P., *J. Biol. Chem.* **2013**, *288*, 26926-43.
231. Wang, D. F.; Helquist, P.; Wiech, N. L.; Wiest, O., *J. Med. Chem.* **2005**, *48*, 6936-47.
232. Bertrand, P., *Eur. J. Med. Chem.* **2010**, *45*, 2095-116.
233. Paris, M.; Porcelloni, M.; Binaschi, M.; Fattori, D., *J. Med. Chem.* **2008**, *51*, 1505-29.
234. Sangwan, R.; Rajan, R.; Mandal, P. K., *Eur. J. Med. Chem.* **2018**, *158*, 620-706.
235. Manal, M.; Chandrasekar, M. J.; Gomathi Priya, J.; Nanjan, M. J., *Bioorg. Chem.* **2016**, *67*, 18-42.
236. Marks, P. A.; Breslow, R., *Nat. Biotechnol.* **2007**, *25*, 84-90.
237. Tavares, M. T.; Kozikowski, A. P.; Shen, S., *Eur. J. Med. Chem.* **2021**, *209*, 112887.
238. Jadhavar, P. S.; Ramachandran, S. A.; Riquelme, E.; Gupta, A.; Quinn, K. P.; Shivakumar, D.; Ray, S.; Zende, D.; Nayak, A. K.; Miglani, S. K.; Sathe, B. D.; Raja, M.; Farias, O.; Alfaro, I.; Belmar, S.; Guerrero, J.; Bernales, S.; Chakravarty, S.; Hung, D. T.; Lindquist, J. N.; Rai, R., *Bioorg. Med. Chem. Lett.* **2016**, *26*, 5222-5228.
239. Zhang, X. H.; Qin, M.; Wu, H. P.; Khamis, M. Y.; Li, Y. H.; Ma, L. Y.; Liu, H. M., *J. Med. Chem.* **2021**, *64*, 1362-1391.
240. Cole, K. E.; Dowling, D. P.; Boone, M. A.; Phillips, A. J.; Christianson, D. W., *J. Am. Chem. Soc.* **2011**, *133*, 12474-7.
241. Decroos, C.; Clausen, D. J.; Haines, B. E.; Wiest, O.; Williams, R. M.; Christianson, D. W., *Biochem.* **2015**, *54*, 2126-35.
242. Porter, N. J.; Christianson, D. W., *ACS Chem. Biol.* **2017**, *12*, 2281-2286.
243. Novotny-Diermayr, V.; Sangthongpitag, K.; Hu, C. Y.; Wu, X.; Sausgruber, N.; Yeo, P.; Greicius, G.; Pettersson, S.; Liang, A. L.; Loh, Y. K.; Bonday, Z.; Goh, K. C.; Hentze, H.; Hart, S.; Wang, H.; Ethirajulu, K.; Wood, J. M., *Mol. Cancer Ther.* **2010**, *9*, 642-52.
244. Chen, J.; Li, N.; Liu, B.; Ling, J.; Yang, W.; Pang, X.; Li, T., *Life Sci.* **2020**, *248*, 117469.

245. Kurzak, B.; Kozłowski, H.; Farkas, E., *Coord. Chem. Rev.* **1992**, *114*, 169-200.
246. Fazary, A. E., *J. Chem. Eng. Data* **2005**, *50*, 888-895.
247. Bordwell, F. G.; Fried, H. E.; Hughes, D. L.; Lynch, T. Y.; Satish, A. V.; Whang, Y. E., *J. Org. Chem.* **2002**, *55*, 3330-3336.
248. Brown, D. A.; Glass, W. K.; Mageswaran, R.; Girmay, B., *Magn. Reson. Chem.* **1988**, *26*, 970-973.
249. Wu, R.; Lu, Z.; Cao, Z.; Zhang, Y., *J. Am. Chem. Soc.* **2011**, *133*, 6110-3.
250. Cohen, S. M., *Acc. Chem. Res.* **2017**, *50*, 2007-2016.
251. Smith, G. F., *Prog. Med. Chem.* **2011**, *50*, 1-47.
252. Yang, F.; Zhao, N.; Ge, D.; Chen, Y., *RSC Adv.* **2019**, *9*, 19571-19583.
253. Maolanon, A. R.; Madsen, A. S.; Olsen, C. A., *Cell Chem. Biol.* **2016**, *23*, 759-768.
254. Wang, X. N.; Wang, K. Y.; Zhang, X. S.; Yang, C.; Li, X. Y., *Biochem. Biophys. Res. Commun.* **2018**, *504*, 812-819.
255. Vogerl, K.; Ong, N.; Senger, J.; Herp, D.; Schmidtkunz, K.; Marek, M.; Muller, M.; Bartel, K.; Shaik, T. B.; Porter, N. J.; Robaa, D.; Christianson, D. W.; Romier, C.; Sippl, W.; Jung, M.; Bracher, F., *J. Med. Chem.* **2019**, *62*, 1138-1166.
256. Ferreira de Freitas, R.; Harding, R. J.; Franzoni, I.; Ravichandran, M.; Mann, M. K.; Ouyang, H.; Lautens, M.; Santhakumar, V.; Arrowsmith, C. H.; Schapira, M., *J. Med. Chem.* **2018**, *61*, 4517-4527.
257. Lee, H. Y.; Nepali, K.; Huang, F. I.; Chang, C. Y.; Lai, M. J.; Li, Y. H.; Huang, H. L.; Yang, C. R.; Liou, J. P., *J. Med. Chem.* **2018**, *61*, 905-917.
258. Saraswati, A. P.; Relitti, N.; Brindisi, M.; Osko, J. D.; Chemi, G.; Federico, S.; Grillo, A.; Brogi, S.; McCabe, N. H.; Turkington, R. C.; Ibrahim, O.; O'Sullivan, J.; Lamponi, S.; Ghanim, M.; Kelly, V. P.; Zisterer, D.; Amet, R.; Hannon Barroeta, P.; Vanni, F.; Ulivieri, C.; Herp, D.; Sarno, F.; Di Costanzo, A.; Saccoccia, F.; Ruberti, G.; Jung, M.; Altucci, L.; Gemma, S.; Butini, S.; Christianson, D. W.; Campiani, G., *ACS Med. Chem. Lett.* **2020**, *11*, 2268-2276.
259. Yu, C. W.; Hung, P. Y.; Yang, H. T.; Ho, Y. H.; Lai, H. Y.; Cheng, Y. S.; Chern, J. W., *J. Med. Chem.* **2019**, *62*, 857-874.
260. Porter, N. J.; Shen, S.; Barinka, C.; Kozikowski, A. P.; Christianson, D. W., *ACS Med. Chem. Lett.* **2018**, *9*, 1301-1305.

261. Burli, R. W.; Luckhurst, C. A.; Aziz, O.; Matthews, K. L.; Yates, D.; Lyons, K. A.; Beconi, M.; McAllister, G.; Breccia, P.; Stott, A. J.; Penrose, S. D.; Wall, M.; Lamers, M.; Leonard, P.; Muller, I.; Richardson, C. M.; Jarvis, R.; Stones, L.; Hughes, S.; Wishart, G.; Haughan, A. F.; O'Connell, C.; Mead, T.; McNeil, H.; Vann, J.; Mangette, J.; Maillard, M.; Beaumont, V.; Munoz-Sanjuan, I.; Dominguez, C., *J. Med. Chem.* **2013**, *56*, 9934-54.

262. Luckhurst, C. A.; Breccia, P.; Stott, A. J.; Aziz, O.; Birch, H. L.; Burli, R. W.; Hughes, S. J.; Jarvis, R. E.; Lamers, M.; Leonard, P. M.; Matthews, K. L.; McAllister, G.; Pollack, S.; Saville-Stones, E.; Wishart, G.; Yates, D.; Dominguez, C., *ACS Med. Chem. Lett.* **2016**, *7*, 34-9.

263. Blackburn, C.; Barrett, C.; Chin, J.; Garcia, K.; Gigstad, K.; Gould, A.; Gutierrez, J.; Harrison, S.; Hoar, K.; Lynch, C.; Rowland, R. S.; Tsu, C.; Ringeling, J.; Xu, H., *J. Med. Chem.* **2013**, *56*, 7201-11.

264. Brindisi, M.; Saraswati, A. P.; Brogi, S.; Gemma, S.; Butini, S.; Campiani, G., *J. Med. Chem.* **2020**, *63*, 23-39.

265. Raeppel, S.; Zhou, N.; Gaudette, F.; Leit, S.; Paquin, I.; Larouche, G.; Moradei, O.; Frechette, S.; Isakovic, L.; Delorme, D.; Fournel, M.; Kalita, A.; Lu, A.; Trachy-Bourget, M. C.; Yan, P. T.; Liu, J.; Rahil, J.; Wang, J.; Besterman, J. M.; Murakami, K.; Li, Z.; Vaisburg, A., *Bioorg. Med. Chem. Lett.* **2009**, *19*, 644-9.

266. Hamblett, C. L.; Methot, J. L.; Mampreian, D. M.; Sloman, D. L.; Stanton, M. G.; Kral, A. M.; Fleming, J. C.; Cruz, J. C.; Chenard, M.; Ozerova, N.; Hitz, A. M.; Wang, H.; Deshmukh, S. V.; Nazef, N.; Harsch, A.; Hughes, B.; Dahlberg, W. K.; Szewczak, A. A.; Middleton, R. E.; Mosley, R. T.; Secrist, J. P.; Miller, T. A., *Bioorg. Med. Chem. Lett.* **2007**, *17*, 5300-9.

267. Methot, J. L.; Chakravarty, P. K.; Chenard, M.; Close, J.; Cruz, J. C.; Dahlberg, W. K.; Fleming, J.; Hamblett, C. L.; Hamill, J. E.; Harrington, P.; Harsch, A.; Heidebrecht, R.; Hughes, B.; Jung, J.; Kenific, C. M.; Kral, A. M.; Meinke, P. T.; Middleton, R. E.; Ozerova, N.; Sloman, D. L.; Stanton, M. G.; Szewczak, A. A.; Tyagarajan, S.; Witter, D. J.; Secrist, J. P.; Miller, T. A., *Bioorg. Med. Chem. Lett.* **2008**, *18*, 973-8.

268. Methot, J. L.; Hamblett, C. L.; Mampreian, D. M.; Jung, J.; Harsch, A.; Szewczak, A. A.; Dahlberg, W. K.; Middleton, R. E.; Hughes, B.; Fleming, J. C.; Wang, H.; Kral, A. M.;

Ozerova, N.; Cruz, J. C.; Haines, B.; Chenard, M.; Kenific, C. M.; Secrist, J. P.; Miller, T. A., *Bioorg. Med. Chem. Lett.* **2008**, *18*, 6104-9.

269. Witter, D. J.; Harrington, P.; Wilson, K. J.; Chenard, M.; Fleming, J. C.; Haines, B.; Kral, A. M.; Secrist, J. P.; Miller, T. A., *Bioorg. Med. Chem. Lett.* **2008**, *18*, 726-31.
270. Bressi, J. C.; Jennings, A. J.; Skene, R.; Wu, Y.; Melkus, R.; De Jong, R.; O'Connell, S.; Grimshaw, C. E.; Navre, M.; Gangloff, A. R., *Bioorg. Med. Chem. Lett.* **2010**, *20*, 3142-5.
271. Moradei, O. M.; Mallais, T. C.; Frechette, S.; Paquin, I.; Tessier, P. E.; Leit, S. M.; Fournel, M.; Bonfils, C.; Trachy-Bourget, M. C.; Liu, J.; Yan, T. P.; Lu, A. H.; Rahil, J.; Wang, J.; Lefebvre, S.; Li, Z.; Vaisburg, A. F.; Besterman, J. M., *J. Med. Chem.* **2007**, *50*, 5543-6.
272. Gediya, L. K.; Njar, V. C., *Expert Opin. Drug. Discov.* **2009**, *4*, 1099-111.
273. Kabir, A.; Muth, A., *Pharmacol. Res.* **2022**, *176*, 106055.
274. Fu, R. G.; Sun, Y.; Sheng, W. B.; Liao, D. F., *Eur. J. Med. Chem.* **2017**, *136*, 195-211.
275. Fortin, S.; Berube, G., *Expert Opin. Drug. Discov.* **2013**, *8*, 1029-47.
276. Raghavendra, N. M.; Pingili, D.; Kadasi, S.; Mettu, A.; Prasad, S., *Eur. J. Med. Chem.* **2018**, *143*, 1277-1300.
277. Morphy, R.; Kay, C.; Rankovic, Z., *Drug Discov. Today* **2004**, *9*, 641-651.
278. Morphy, R.; Rankovic, Z., *J. Med. Chem.* **2005**, *48*, 6523-43.
279. Morphy, R.; Rankovic, Z., *Curr. Pharm. Des.* **2009**, *15*, 587-600.
280. Gao, Y.; Zhang, H.; Lirussi, F.; Garrido, C.; Ye, X. Y.; Xie, T., *Biochem. Pharmacol.* **2020**, *182*, 114224.
281. Vaidya, G. N.; Rana, P.; Venkatesh, A.; Chatterjee, D. R.; Contractor, D.; Satpute, D. P.; Nagpure, M.; Jain, A.; Kumar, D., *Eur. J. Med. Chem.* **2021**, *209*.
282. Luan, Y.; Li, J.; Bernatchez, J. A.; Li, R., *J. Med. Chem.* **2019**, *62*, 3171-3183.
283. Ling, Y.; Liu, J.; Qian, J.; Meng, C.; Guo, J.; Gao, W.; Xiong, B.; Ling, C.; Zhang, Y., *Curr. Med. Chem.* **2020**, *27*, 7264-7288.
284. Gryder, B. E.; Rood, M. K.; Johnson, K. A.; Patil, V.; Raftery, E. D.; Yao, L. P.; Rice, M.; Azizi, B.; Doyle, D. F.; Oyelere, A. K., *J. Med. Chem.* **2013**, *56*, 5782-96.
285. Patel, H. K.; Siklos, M. I.; Abdelkarim, H.; Mendonca, E. L.; Vaidya, A.; Petukhov, P. A.; Thatcher, G. R., *ChemMedChem* **2014**, *9*, 602-13.
286. Guerrant, W.; Patil, V.; Canzoneri, J. C.; Oyelere, A. K., *J. Med. Chem.* **2012**, *55*, 1465-77.

287. Guerrant, W.; Patil, V.; Canzoneri, J. C.; Yao, L. P.; Hood, R.; Oyelere, A. K., *Bioorg. Med. Chem. Lett.* **2013**, *23*, 3283-7.
288. Zhang, X.; Bao, B.; Yu, X.; Tong, L.; Luo, Y.; Huang, Q.; Su, M.; Sheng, L.; Li, J.; Zhu, H.; Yang, B.; Zhang, X.; Chen, Y.; Lu, W., *Bioorg. Med. Chem.* **2013**, *21*, 6981-95.
289. An, Z.; Lv, W.; Su, S.; Wu, W.; Rao, Y., *Protein Cell* **2019**, *10*, 606-609.
290. Smalley, J. P.; Adams, G. E.; Millard, C. J.; Song, Y.; Norris, J. K. S.; Schwabe, J. W. R.; Cowley, S. M.; Hodgkinson, J. T., *Chem. Commun. (Camb.)* **2020**, *56*, 4476-4479.
291. Yang, K.; Song, Y.; Xie, H.; Wu, H.; Wu, Y. T.; Leisten, E. D.; Tang, W., *Bioorg. Med. Chem. Lett.* **2018**, *28*, 2493-2497.
292. Bijian, K.; Kaldre, D.; Wang, T. T.; Su, J.; Bouttier, M.; Boucher, A.; Alaoui-Jamali, M.; White, J. H.; Gleason, J. L., *J. Steroid Biochem. Mol. Biol.* **2018**, *177*, 135-139.
293. Fischer, J.; Wang, T. T.; Kaldre, D.; Rochel, N.; Moras, D.; White, J. H.; Gleason, J. L., *Chem. Biol.* **2012**, *19*, 963-71.
294. Kaldre, D.; Wang, T. T.; Fischer, J.; White, J. H.; Gleason, J. L., *Bioorg. Med. Chem.* **2015**, *23*, 5035-5049.
295. Tavera-Mendoza, L. E.; Quach, T. D.; Dabbas, B.; Hudon, J.; Liao, X.; Palijan, A.; Gleason, J. L.; White, J. H., *Proc. Natl. Acad. Sci. U.S.A.* **2008**, *105*, 8250-5.
296. Barbier, C.; Mansour, A.; Ismailova, A.; Sarmadi, F.; Scarlata, D. A.; Bouttier, M.; Zeitouni, C.; Wang, C.; Gleason, J. L.; White, J. H., *Sci. Rep.* **2022**, *12*, 6745.
297. Mendoza-Sanchez, R.; Cotnoir-White, D.; Kulpa, J.; Jutras, I.; Pottel, J.; Moitessier, N.; Mader, S.; Gleason, J. L., *Bioorg. Med. Chem.* **2015**, *23*, 7597-606.
298. Palermo, A. F.; Diennet, M.; El Ezzy, M.; Williams, B. M.; Cotnoir-White, D.; Mader, S.; Gleason, J. L., *Bioorg. Med. Chem.* **2018**, *26*, 4428-4440.
299. Marrocco, D. L.; Tilley, W. D.; Bianco-Miotto, T.; Evdokiou, A.; Scher, H. I.; Rifkind, R. A.; Marks, P. A.; Richon, V. M.; Butler, L. M., *Mol. Cancer Ther.* **2007**, *6*, 51-60.
300. Bjorkman, M.; Iljin, K.; Halonen, P.; Sara, H.; Kaivanto, E.; Nees, M.; Kallioniemi, O. P., *Int. J. Cancer* **2008**, *123*, 2774-81.
301. Pfeiffer, M. J.; Mulders, P. F.; Schalken, J. A., *The Prostate* **2010**, *70*, 1524-1532.
302. Kaushik, D.; Vashistha, V.; Isharwal, S.; Sediqe, S. A.; Lin, M. F., *Ther. Adv. Urol.* **2015**, *7*, 388-95.

303. Fu, M.; Wang, C.; Reutens, A. T.; Wang, J.; Angeletti, R. H.; Siconolfi-Baez, L.; Ogryzko, V.; Avantaggiati, M. L.; Pestell, R. G., *J. Biol. Chem.* **2000**, *275*, 20853-60.

304. Gaughan, L.; Logan, I. R.; Cook, S.; Neal, D. E.; Robson, C. N., *J. Biol. Chem.* **2002**, *277*, 25904-13.

305. Rana, Z.; Diermeier, S.; Walsh, F. P.; Hanif, M.; Hartinger, C. G.; Rosengren, R. J., *Pharmaceuticals (Basel)* **2021**, *14*.

306. Rana, Z.; Diermeier, S.; Hanif, M.; Rosengren, R. J., *Biomedicines* **2020**, *8*.

307. Gryder, B. E.; Akbashev, M. J.; Rood, M. K.; Raftery, E. D.; Meyers, W. M.; Dillard, P.; Khan, S.; Oyelere, A. K., *ACS Chem. Biol.* **2013**, *8*, 2550-60.

308. Oyelere, A.; Gryder, B. WO 2012/050858 A1, April 19, 2012.

309. Sun, C.; Arnold, R.; Gaul, D.; Tapadar, S.; Gryder, B.; Oyelere, A.; Petros, J., *J. Urol.* **2016**, *195*.

310. Oyelere, A.; Tapadar, S.; Gaul, D. WO 2017/120328 A1, July 13, 2017.

311. Qin, Z.; Ratnam, M. US 2017/0217903 A1, August 3, 2017.

312. Rosati, R.; Chen, B.; Patki, M.; McFall, T.; Ou, S.; Heath, E.; Ratnam, M.; Qin, Z., *Mol. Pharmacol.* **2016**, *90*, 225-37.

313. CN 109796437 A, May 24, 2019.

314. Doyle, C. M.Sc. Dissertation, McGill University, Montréal, QC, 2014.

315. Barrett, R. R. G.; Nash, C.; Diennet, M.; Cotnoir-White, D.; Doyle, C.; Mader, S.; Thomson, A. A.; Gleason, J. L., *Bioorg. Med. Chem. Lett.* **2022**, *55*, 128441.

316. Connolly, R. M.; Zhao, F.; Miller, K. D.; Lee, M. J.; Piekarz, R. L.; Smith, K. L.; Brown-Glaberman, U. A.; Winn, J. S.; Faller, B. A.; Onitilo, A. A.; Burkard, M. E.; Budd, G. T.; Levine, E. G.; Royce, M. E.; Kaufman, P. A.; Thomas, A.; Trepel, J. B.; Wolff, A. C.; Sparano, J. A., *J. Clin. Oncol.* **2021**, *39*, 3171-3181.

317. Nyronen, T. H.; Soderholm, A. A., *Expert Opin. Drug. Discov.* **2010**, *5*, 5-20.

318. Wahl, J.; Smiesko, M., *Int. J. Mol. Sci.* **2018**, *19*.

319. Balbas, M. D.; Evans, M. J.; Hosfield, D. J.; Wongvipat, J.; Arora, V. K.; Watson, P. A.; Chen, Y.; Greene, G. L.; Shen, Y.; Sawyers, C. L., *Elife* **2013**, *2*, e00499.

320. He, B.; Minges, J. T.; Lee, L. W.; Wilson, E. M., *J. Biol. Chem.* **2002**, *277*, 10226-35.

321. Villadsen, J. S.; Stephansen, H. M.; Maolanon, A. R.; Harris, P.; Olsen, C. A., *J. Med. Chem.* **2013**, *56*, 6512-20.

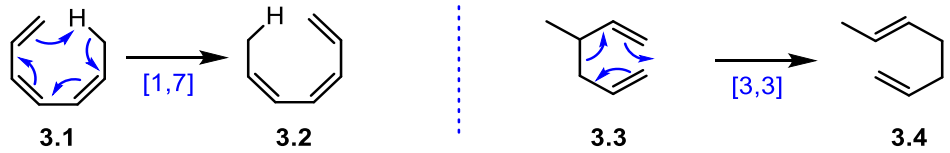
322. Adams, M. K.; Banks, C. A. S.; Miah, S.; Killer, M.; Washburn, M. P., *Methods Enzymol.* **2019**, *626*, 23-40.
323. Bradner, J. E.; West, N.; Grachan, M. L.; Greenberg, E. F.; Haggarty, S. J.; Warnow, T.; Mazitschek, R., *Nat. Chem. Biol.* **2010**, *6*, 238-243.
324. Sugawara, T.; Lejeune, P.; Kohr, S.; Neuhaus, R.; Faus, H.; Gelato, K. A.; Busemann, M.; Cleve, A.; Lucking, U.; von Nussbaum, F.; Brands, M.; Mumberg, D.; Jung, K.; Stephan, C.; Haendler, B., *Oncotarget.* **2016**, *7*, 6015-28.
325. Kawata, H.; Arai, S.; Nakagawa, T.; Ishikura, N.; Nishimoto, A.; Yoshino, H.; Shiraishi, T.; Tachibana, K.; Nakamura, R.; Sato, H., *Prostate* **2011**, *71*, 1344-56.
326. Hughes, J. M. E.; Scarlata, D. A.; Chen, A. C. Y.; Burch, J. D.; Gleason, J. L., *Org. Lett.* **2019**, *21*, 6800-6804.
327. Bordwell, F. G.; Algrim, D. J., *J. Am. Chem. Soc.* **2002**, *110*, 2964-2968.
328. Chang, F. C.; Wood, N. F., *Tetrahedron Lett.***1964**, *5*, 2969-2973.
329. Stolfa, D. A.; Stefanachi, A.; Gajer, J. M.; Nebbioso, A.; Altucci, L.; Cellamare, S.; Jung, M.; Carotti, A., *ChemMedChem* **2012**, *7*, 1256-66.
330. Makarov, I. S.; Brocklehurst, C. E.; Karaghiosoff, K.; Koch, G.; Knochel, P., *Angew. Chem. Int. Ed. Engl.* **2017**, *56*, 12774-12777.
331. Carlsen, P. H. J.; Katsuki, T.; Martin, V. S.; Sharpless, K. B., *J. Org. Chem.* **2002**, *46*, 3936-3938.
332. Mistico, L.; Querolle, O.; Meerpoel, L.; Angibaud, P.; Durandetti, M.; Maddaluno, J., *Chem. Eur. J.* **2016**, *22*, 9687-92.
333. McLaughlin, M.; Marcantonio, K.; Chen, C. Y.; Davies, I. W., *J. Org. Chem.* **2008**, *73*, 4309-12.
334. Ahmed, B. M.; Mezei, G., *RSC Adv.* **2015**, *5*, 24081-24093.

Part II. Development of an oxy-Cope / Michael Cascade Reaction

Chapter 3. Introduction

3.1.1 *Cope Rearrangements and Related Sigmatropic Shifts*

Sigmatropic rearrangements are a specific type of pericyclic reaction, which can be defined as the migration of a sigma bond across a π system. Unlike cycloadditions and electrocyclic reactions, sigmatropic rearrangements produce no net change in the types of valence bonds involved. Sigmatropic shifts include simple [1,*n*] shifts (*n* > 1) such as the [1,7] hydrogen shift between structures **3.1** and **3.2** and more complex migrations across multiple π systems such as the [3,3] shift going interconverting **3.3** and **3.4** (Scheme **3.1**). The reactions exhibit key stereospecific features regarding their transformation, dictated by orbital symmetry, as laid out by Woodward and Hoffman.[1] An in-depth understanding of reaction mechanism is not typically required to successfully predict and utilize sigmatropic rearrangements, since modern understanding of the reactions can usually be reduced to simplistic back-of-the-envelope sketches and rationalizations. As with many reactions in organic chemistry, six-membered transition states are commonly featured in the many varieties of [3,3] rearrangements discovered to date, which can be visualized as σ bond migration across two separate three-atom allyl systems. Excellent theoretical and conceptual treatments of general sigmatropic rearrangements exist, and the interested reader is directed there for further insight.[2] This Chapter will focus on the specific type of [3,3] shift involved in converting **3.3.** to **3.4**, known as the Cope rearrangement, along with closely related variants of that reaction.

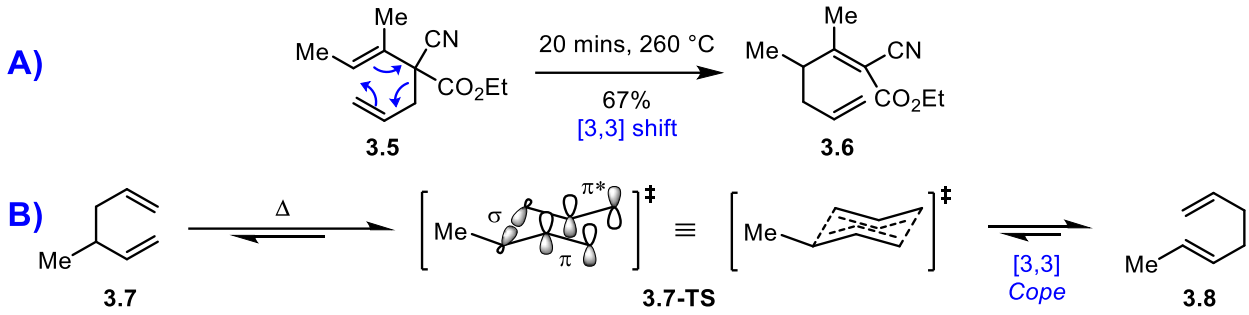


3.1 **3.2** **3.3** **3.4**

Scheme 3.1. Examples of sigmatropic shifts.

The Cope rearrangement (Scheme **3.2A**) has been very popular with theoretical and computational chemists since it describes the prototypical all-carbon [3,3] rearrangement.[3] It was discovered in 1940, when Arthur Cope and Elizabeth Hardy released their seminal publication on the thermally induced migration of allyl groups in compounds such as **3.5**, which was found to

rearrange to provide 67% yield of isomer **3.6** at 260 °C.[4] Cope rearrangements of simple 1,5-hexadienes such as **3.7** produce an equilibrating mixture of reactant and product **3.8** since the reaction is approximately if not fully thermoneutral (Scheme **3.2B**).[5] A quick conceptual rationalization involves considering that the products and starting materials contain roughly the same types of carbon-carbon bonds. Cope rearrangements are stereoselective, and the outcome can be usually predicted by consideration of steric interactions or constraints in various chair or boat-like transition states such as **3.7-TS** available to the substrate. Fundamentally, the stereoselectivity also relies on symmetry requirements, where migration must be suprafacial with respect to each allyl system. The suprafacial requirement can be visualized by a rudimentary orbital overlap diagram depicted for a typical chair-like transition state as in **3.7-TS**. The transition state itself is in most cases relatively late with a large amount of bond formation between the terminal atoms. As with other pericyclic reactions, concerted Cope reactions do not have observable intermediates. A typical activation energy for the reactions is ca. 34 kcal/mol, although substitution in the saturated portion encourages reactivity, as does strain-release from a 3 or 4-membered ring. As will be seen, Cope-like rearrangements have been incorporated in numerous syntheses.



Scheme 3.2. (**A**) Cope's reaction. (**B**) Orbital depiction and transition state for a Cope shift.

The thermoneutral profile of the Cope rearrangement stands in contrast to known rearrangements incorporating heteroatoms at certain points along the hexadiene. The Claisen rearrangement, for example of allyl vinyl ether **3.9** to ketone **3.10**, generates a carbonyl directly from isomerization which provides an immediate enthalpic sink for the reaction (Figure **3.1**).[6] A similar driving force is found in the oxy-Cope reaction. After [3,3] shift from alcohol **3.11** to enol **3.12**, final tautomerization forms the more stable 4,5-unsaturated carbonyl **3.13**. It is worth noting that the nitrogen analogs of both reactions are known. The aza-Claisen (or 3-aza-Cope) described the reaction from allylamine **3.14** to imine **3.15**. The amino-Cope reaction, which describes the

conversion of amine **3.16** to **3.17**, was discovered at about the same time as the oxy-Cope reaction (*vide infra*) but has been infrequently studied and used.[7] Both aza-rearrangement products imine **3.15** and enamine **3.17** can be hydrolyzed to the corresponding ketones **3.10** and **3.13**.

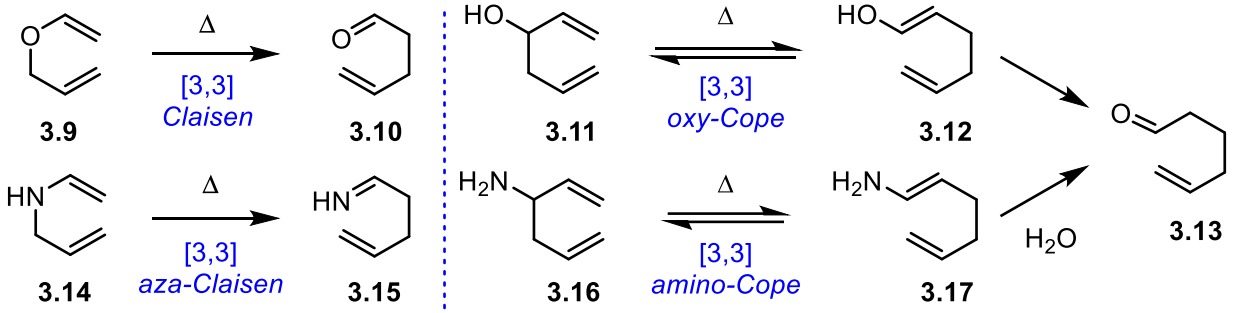
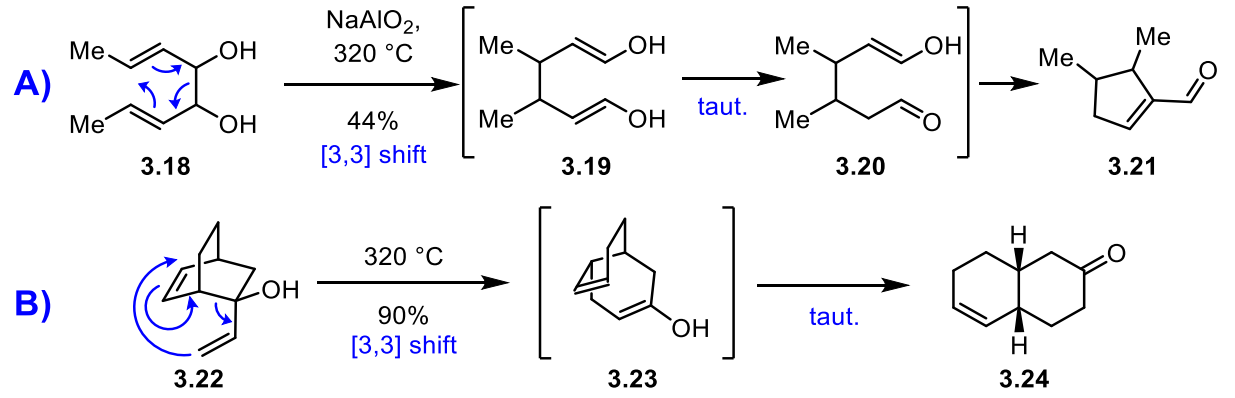


Figure 3.1. Variants of Cope and hetero-Cope [3,3] rearrangements

To the best of this author's knowledge, the first records of the transformation which has come to be known as the oxy-Cope rearrangement were in fact reported by Urion in 1930 and 1934 as studies on the pyrolysis of divinylglycols. As one example, diol **3.18** was heated at 320 °C over alumina to provide a 44% yield of cyclopentene **3.21** after distillation, formed from tautomerization and aldol condensation of Cope product **3.19** (Scheme **3.3A**).[8] As Urion's work took place over 30 years before even the description of the famous Woodward-Hoffmann (W-H) rules, the discussion of the reaction was understandably empirical. In 1964, 24 years after Cope's discovery and just one year before the W-H rules were released, Jerome Berson and Maitland Jones published a pair of articles describing the oxy-Cope variant of Cope's isomerization (Scheme **3.3B**).[9] Bicycle **3.22** was heated at 320 °C to provide ketone **3.24** in 90% yield, and the reaction was determined to likely proceed by a biradical mechanism.



Scheme 3.3. (**A**) Urion's divinylglycol pyrolysis. (**B**) Berson's oxy-Cope.

In contrast to neutral rearrangements, which require high temperatures as in the examples shown thus far, charged rearrangements are extremely facile. Compared to those without charge, they dramatically lower the typical activation energy for rearrangement from over 30 kcal/mol[5a] to allow reaction at or near ambient temperature. Incorporation of an oxygen as in **3.25** (Figure **3.2**) should in theory allow ready oxonia-Cope rearrangement to isomer **3.26** but, as will be seen in Section **3.2.2**, the oxocarbeniums are prone rather to Prins reaction and fragmentation. In fact, the first oxonia-Cope, reported by Mousset in 1969, was in truth a Prins-pinacol reaction.[10] The 2-aza-Cope, usually performed from *N*-alkyl or protonated ammoniums such as **3.27**, is one good example of charge acceleration since azonium shifts typically occur reversibly at or near room temperature. The cationic 2-azonia-Cope, first reported by Geissman in 1950,[11] has been used in cascades featuring subsequent addition to trap isomerized iminium **3.28** as cyclized product **3.29**. An example will be seen in a discussion of the aza-Cope / Mannich reaction in Section **3.2.1**. Both cationic rearrangements are directly applicable to the cationic iminium-catalyzed oxy-Cope / Michael reaction which will be described in Chapter 4. Another example of charge acceleration will be seen in the following section concerning the anionic oxy-Cope (AOC) reaction with the corresponding alkoxides of the neutral substrates. The next section will describe the discovery of the anionic oxy-Cope reaction and its use in synthesis.

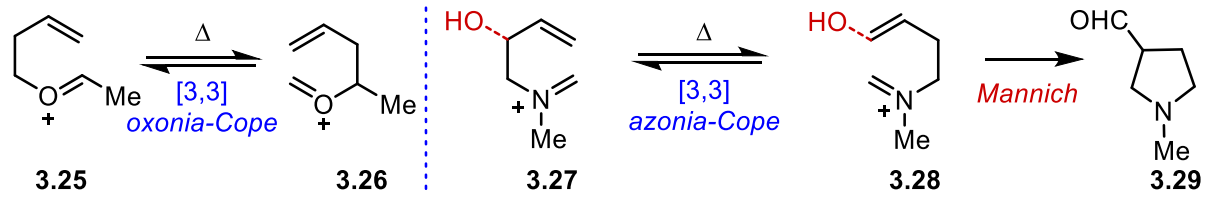
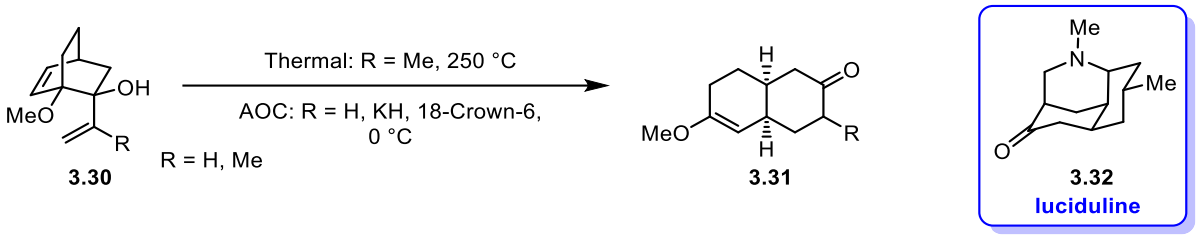


Figure 3.2. Charged variants of Cope and hetero-Cope [3,3] rearrangements.

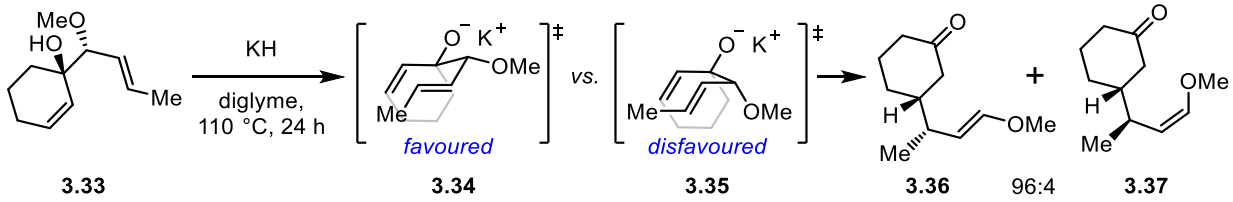
3.1.2. Anionic oxy-Cope (AOC) rearrangements

In 1975, the Evans group made the discovery of dramatic rate enhancements on the order of 10^{10}-10^{17} in oxy-Cope rearrangement by treatment with potassium hydride, especially when the potassium cation was dissociated by coordination by 18-Crown-6.[12a-f] Their group had been applying a thermal oxy-Cope rearrangement in the racemic synthesis of luciduline **3.32**, a small *Lycopodium* alkaloid. They generated *cis*-decalins **3.31** from simple [2,2,2]-bicyclic ketone isopropenylmagnesium bromide adducts **3.30** (Scheme **3.4**).[12a,b] Neat bicyclic dienes **3.30** were found to undergo [3,3] shift in a day at 195 °C, or in 4 h at 250 °C.



Scheme 3.4. The Evans group's thermal and AOC reactions.

In their first experiments, they used a similar substrate to that used for luciduline except bearing a simple vinyl group, which was found to have a very similar activation energy (E_a) for rearrangement as Berson's initial substrate **3.22** (35.9 vs. 41.8 kcal/mol). Lithium, magnesium, and sodium alkoxides were increasingly more reactive although still requiring highly elevated temperatures. However, potassium hydride brought about rearrangement at only 66 °C in THF in just minutes. An E_a of just 19.4 kcal/mol was calculated, a parameter which dropped further to 18.2 kcal/mol when run in the presence of crown ethers and allowed fast reaction at 0 °C. They then applied the novel anionic conditions to a variety of oxy-Cope substrates, rearranging at 85 °C in reasonable timeframes with KH. They also demonstrated that substrate **3.33** produced the expected transfer of (relative) stereochemistry to form predominantly ketone **3.36** in a 96:4 ratio over **3.37**. The oxy-Cope shift must occur by a concerted chair-like transition state **3.34**, preferred over boat-like transition state **3.35** (Scheme **3.5**).[12d] AOC reactions are now established as extremely predictable with regard to the transfer of stereochemistry.

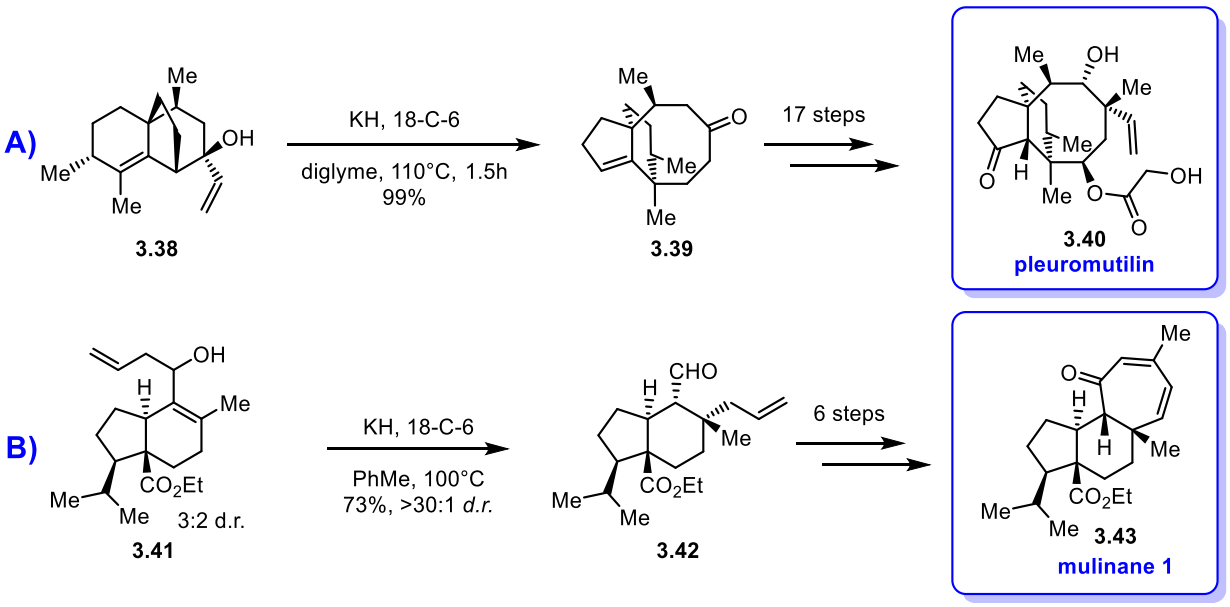


Scheme 3.5. The Evans group's proof of stereochemical transfer in the AOC.

It is worth delving into the physical chemistry behind such a remarkable improvement in reactivity.[12g-l] Oxygen lone-pair donation into geminal $\sigma_{C\text{-}C}$*, reminiscent of bond lengthening observed in the anomeric effect with electronegative geminal substituents, can aid in geminal bond cleavage. An oxyanion, especially one dissociated from its counter-cation and more fully bearing its charge, provides a much stronger donation and assistance for bond cleavage. Evans showed that the increase in reaction rate was indeed due to crown ether chelation-driven ion pair dissociation

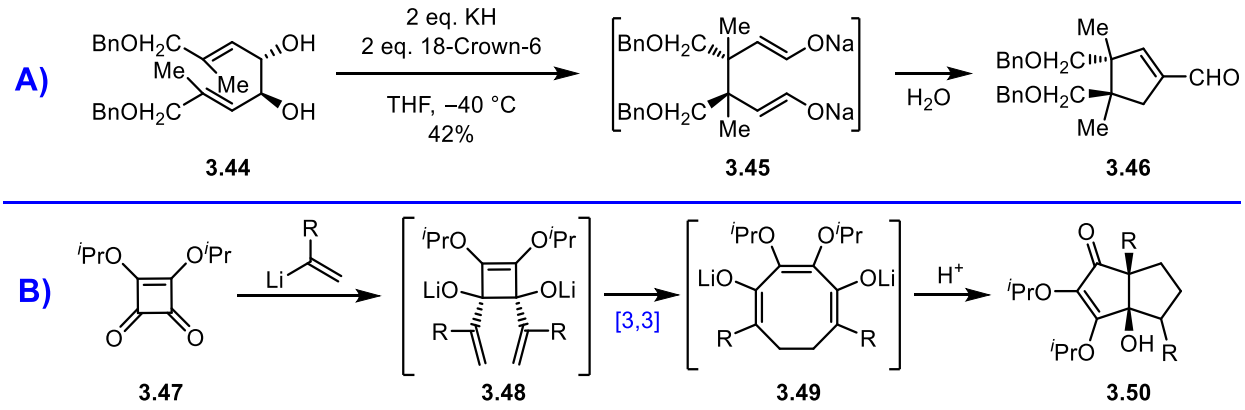
rather than solvent dielectric constant. Thus, there was no additional benefit observed from the use of very polar HMPT and a detrimental effect was observed using sodium-specific 15-Crown-5 with the potassium salt in an intentional mis-match.[12c]

The facility of the AOC reaction, combined with its predictable stereochemical outcome, have enabled its strategic incorporation in a wide range of synthetic applications, two of which will be shown here (additional examples are cited in the references). Similar to the thermal rection, it is readily incorporated into cascade sequences which will be discussed in Section **3.1.3**, but one of the strengths of oxy-Cope rearrangements is in ring expansions. Boeckman's key step toward pleuromutilin **3.40** (Scheme **3.6A**) provides an example of ring expansion from a 6 to 8-memebered ring transforming alcohol **3.38** into ketone **3.39**, in near-quantitative yield albeit at elevated temperatures.[13] Another common synthetic use of the oxy-Cope involves allyl transposition, such as from homoallylic alcohol **3.41** to aldehyde **3.42** in the course of Guerrero's synthesis of mulinane 1 **3.43** (Scheme **3.6B**).[14] As with the previous example, moderately vigorous heating is required due to terminal di-substitution, but the transposition proceeds in high 73% yield and essentially perfect *d.r.* to provide a synthetic handle for cycloheptanone ring installation. Such ring interconversions,[15] transpositions,[16] and cascade reactions (*vide infra*) represent the main uses of the oxy-Cope reaction in synthesis.



Scheme 3.6. (**A**) Boekman's approach to pleuromutilin by 6 to 8 ring expansion. (**B**) Allyl transposition in Guerrero's synthesis of Mulinane 1.

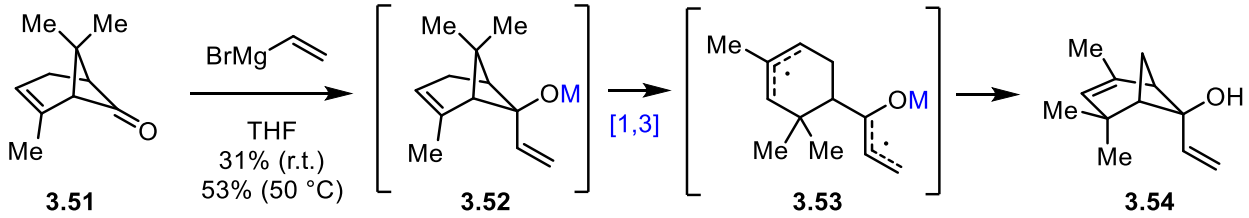
A natural but rarely used extension of the AOC, the di-anionic rearrangement, is a double alkoxide equivalent of a divinylglycol rearrangement.[17] Simple examples of divinylglycol di-AOC are known, and the Butenschön group has published extensively on expansion of divinyl or diaryl adducts from benzocyclobutenediones.[18] A common feature of such reactions, similar to Urion's original results, is a tandem aldol reaction or condensation depending on substrate and conditions.[19] Stereochemical transfer can still be observed in di-anionic shifts, which has been used in conjunction with aldol reactivity of the products to form enantioenriched substituted cyclopentene carboxaldehydes (Scheme **3.7A**). In one example, diol **3.44** underwent oxy-Cope rearrangement with 2 equivalents of base to bis-enolate **3.45** and subsequently cyclized in an aldol condensation to produce **3.46**, bearing adjacent quaternary carbons.[20] In another example, Paquette employed a di-AOC expansion from *cis*-divinyl adducts **3.48**, produced *in situ* from squarate esters such as **3.47** (Scheme **3.7B**).[21] Rearrangement then leads to cyclooctatriene **3.49** and bicycle **3.50** following a transannular aldol condensation.



Scheme 3.7. (A) Saito's Di-AOC rearrangement from chiral diols with no apparent *e.e.* loss. **(B)** Generic scheme of Paquette's bis-additions to squarate esters and di-AOC / aldol sequence.

Non-concerted homolytic cleavage has been proposed to occur under weakly ionizing anionic conditions, such as in the serendipitous identification by the Sarpong group of spontaneous [1,3] shifts occurring from Mg alkoxide Grignard adducts such as **3.52** of chrysanthenone ketones such as **3.51** (Scheme **3.8**).[22] Calculations showed that homolytic cleavage passing through biradical intermediate **3.53** was favoured over heterolytic cleavage, itself only slightly disfavoured over the desired concerted [3,3] shift. The [1,3] shift producing alcohol **3.54** in 53% yield occurred selectively with vinyl Grignards, which was rationalized on the effects on stability of the radical

borne by the alkoxide carbon. Homolytic cleavage represents just one mode of fragmentation which can occur in the alkoxides of oxy-Cope substrates.



Scheme 3.8. Sarpong's magnesium alkoxide formal [1,3] shift.

Heterolytic cleavage can also occur from alkoxides in certain systems to result in unconcerted reactions and [1,3] shifts. Heterolytic cleavage is exacerbated in the related anionic amino-Cope systems which exhibit dramatically lowered energies for heterolytic cleavage, resulting in many cases in stepwise fragmentation-recombination and inability to transfer chirality even when recombination is successful.[23] Naturally, heterolytic cleavage pathways are encouraged by additional stabilizing groups on the carbon receiving the charge, or by strain relief, which can also lead to the ill-studied but necessarily stepwise anionic [1,3]-oxy-Cope.[24a] The use of strain-release has been exploited in cyclobutanone ring expansions,[24b] and aromatic or bis-allylic stabilization of putative carbanion fragments seems helpful.[24] Taken together, the various modes of reactivity of 3-alkoxy-1,5-hexadienes indicates the concerted AOC reaction may be viewed as striking a balance between heterolytic fragmentation and neutral biradical homolytic cleavage. Regardless, the AOC reaction has proven to be extremely useful in organic synthesis.

3.1.3. *Cascades Incorporating oxy-Cope Rearrangements*

Since its inception, many beautiful, effective cascade reactions or tandem sequences have been developed based around the oxy-Cope transformation.[25] Some examples of different modes of oxy-Cope cascade reactions are shown from **3.55** (Figure **3.3**), where enol Cope product **3.56** is depicted as participating optionally in cyclization by S_N' allylic rearrangement, aldol addition to a tautomerized ketone produced from divinylglycol rearrangement, or functionalization by an electrophile (E^+). Alternatively, cyclization can also occur from full oxy-Cope product **3.57** via transannular ene reaction, and thermal oxy-Cope reactions have been paired with such ene reactions in numerous instances. The cascade reactions incorporating oxy-Cope rearrangement will be grouped for discussion here according to a simple system as follows: oxy-Cope cascades

with other pericyclic reactions, oxy-Cope followed by enol addition reactions, and organometallic functionalization followed by oxy-Cope reactions. Examples of each will be presented to provide a comprehensive yet strategic overview of the oxy-Cope reaction in synthesis.

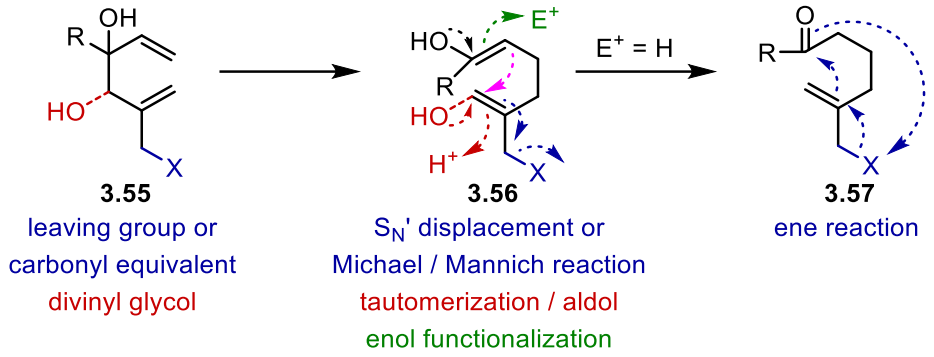
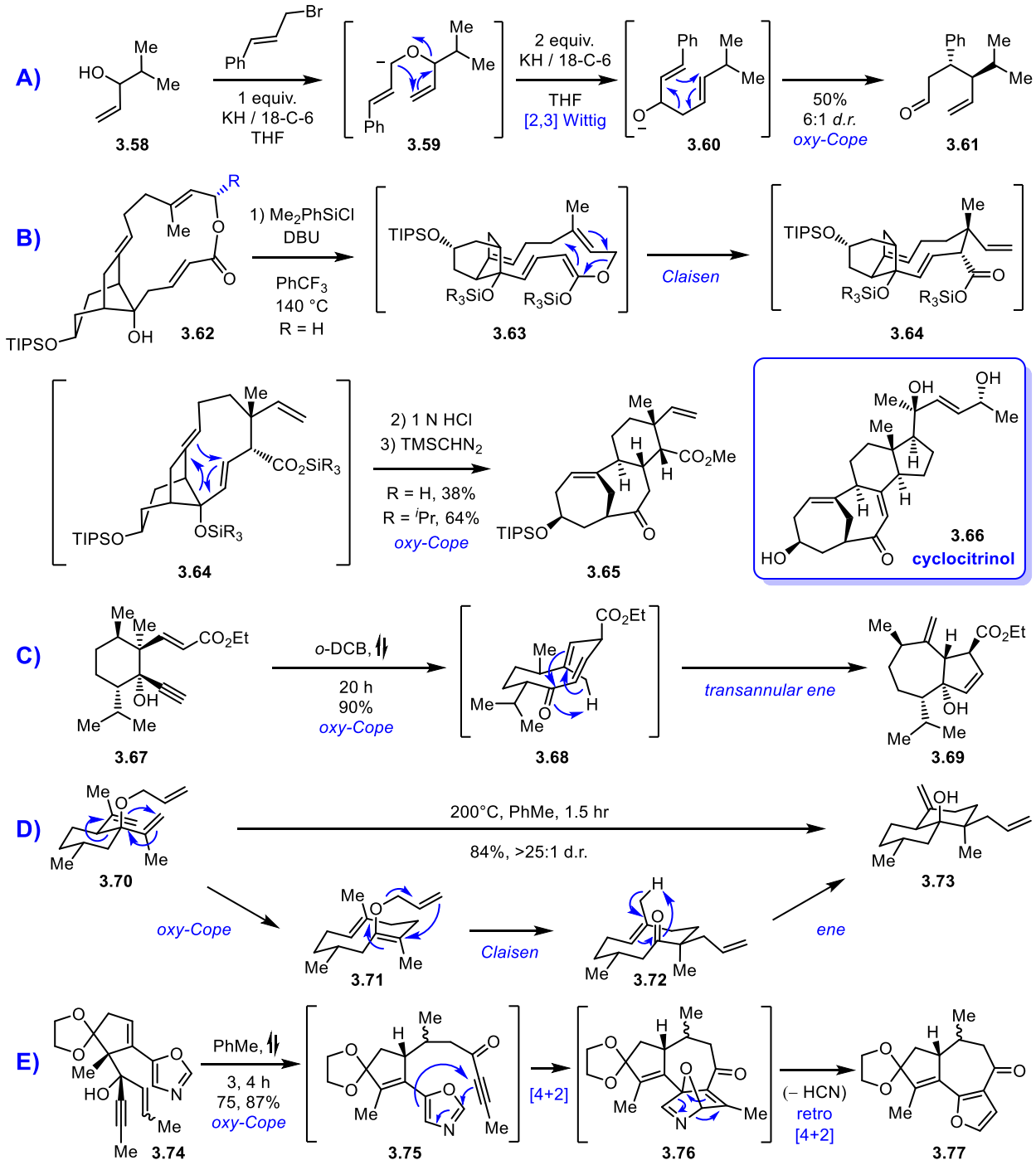


Figure 3.3. Composite schematic of various oxy-Cope cascade reactions.

The oxy-Cope reaction has been built into cascades requiring other pericyclic reactions including Wittig, Claisen, ene, and cycloaddition reactions. A number of [2,3] Wittig / AOC cascades have been reported, mostly by the Greeves group (Scheme **3.9A**). They also developed tandem conditions to generate bis-allyl etherate **3.59** *in situ* from alcohols such as **3.58**. Additional KH then induces the cascading [2,3] / [3,3] shifts through intermediate **3.60** to give aldehyde **3.61** in 50% yield and 6:1 *d.r.* upon isolation.[26] One powerful example incorporating a different [3,3] shift is found in Leighton's synthetic study toward cyclocitrinol **3.66**, which employs an Ireland-Claisen / oxy-Cope cascade (Scheme **3.9B**) starting from macrolactone **3.62**. Silyl ketene acetal formation as in **3.63** triggers the first [3,3] Claisen reaction to silyl ester **3.64**. Subsequent strain-driven thermal (sil)oxy-Cope follows to form **3.65** under moderately vigorous thermal conditions (140 °C) in 38% yield, or 64% yield with an isopropyl substituent.[27] Sigmatropic rearrangements are not the only pericyclic reactions paired with oxy-Cope shifts in cascades. Rajagopalan reported probably the first examples of oxy-Cope / ene cascades from substrates such as **3.67** (Scheme **3.9C**). This cascade gave hydrazulene **3.69**, after passing through **3.68**, in 90% yield after 20 h in refluxing *o*-dichlorobenzene.[28-30] Such cascades have been explored by the Barriault group to prolific extent, and even extended to longer oxy-Cope / Claisen / ene transformations such as that shown from ether **3.70**. This substrate was smoothly converted though oxy-Cope to **3.71**, Claisen to **3.72**, then ene reaction to afford nearly a single isomer of decalin **3.73** in 84% yield at 200 °C under microwave irradiation (Scheme **3.9D**).[31] The last major class of pericyclic reactions,

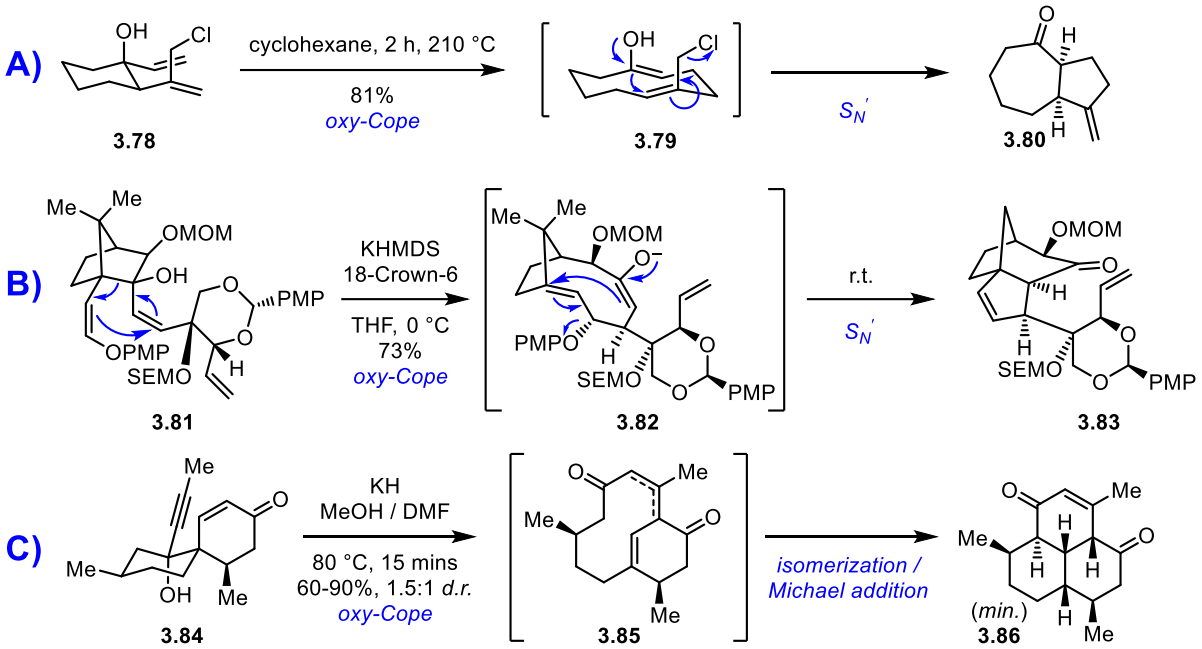
cycloadditions, was successfully paired with an oxy-Cope transposition in Jacobi's synthesis of gnididione from olefin isomers **3.74** (Scheme **3.9E**). Each isomer underwent the oxy-Cope /



Scheme 3.9. (**A**) Greeve's tandem alkylation, Wittig / AOC cascade. (**B**) Leighton's Ireland-Claisen / oxy-Cope approach to the cyclocintrinol core. (**C**) Rajagopalan's oxy-Cope / transannular ene reaction. (**D**) Barriault's oxy-Cope/Claisen/ene cascade. (**E**) Jacobi's approach to gnididione.

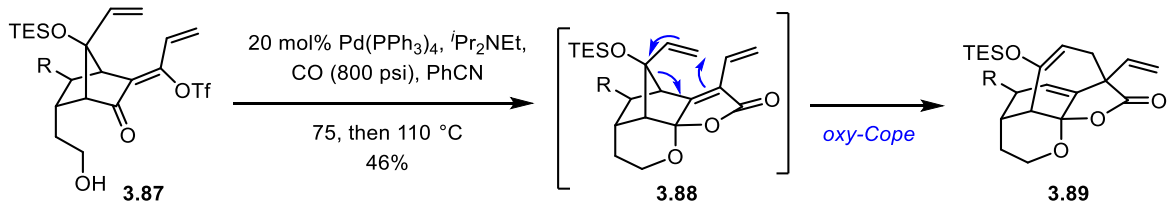
cycloaddition / retro-cycloaddition cascade through intermediates **3.75-3.76** to ketone **3.77** in 75-87% yield and 3-4 h.[32] The examples just mentioned demonstrate that all major classes of pericyclic reactions have been used in cascades featuring oxy-Cope rearrangement.

The enol generated from the [3,3] shift of oxy-Cope substrates has been used in various ways in cascade reactions. One good example is the aza-Cope / Mannich reaction which will be thoroughly discussed in later sections. Another common example is the tendency of divinylglycols and di-AOC substrates to undergo aldol reaction following tautomerization of one enol, as seen in several examples discussed above. In a related instance, AOC has been followed by Claisen condensation toward CP-263,114.[33] A less common example which has nonetheless experienced use in synthesis is the oxy-Cope / S_N' cascade. The pairing with S_N' reactivity was utilized by the Sworin group to access hydrazulene ketones from substrates such as alkyl chloride **3.78**, where enol intermediate **3.79** undergoes transannular allylic rearrangement to ketone **3.80** in 81% yield over 2 h (Scheme **3.10A**).[34] The Paquette group published examples of this type of cascade such as from alcohol **3.81**, where warming the reaction to room temperature caused cyclization of [3,3] product **3.82** to form ketone **3.83** in 73% yield (Scheme **3.10B**).[35] A final example of post-rearrangement addition cascades concerns oxy-Cope / Michael reactions developed first by Rajagopalan.[30] The Vanderwal group then used the same cascade manifold to access a known precursor **3.86** to the pseudopterosin aglycones, starting from propargylic alcohol **3.84** (Scheme **3.10C**). The 1,5-enyne could be rearranged either in stepwise tandem reactions or one pot through intermediate **3.85** to form **3.86** in poor *d.r.* but high yield.[36] The dashed lines indicate isomerization that is known *in situ* since the oxy-Cope product would have the skipped diene while exclusion of methanol from the conditions gives the conjugated diene. Regardless, at least one alkene must isomerize to allow the transannular Michael addition, although mixtures of stereoisomers were obtained. Other notable tandem conditions have also been used to trap oxy-Cope enols / enolates, since these are amenable to electrophilic attack. Methyl iodide is a popular chemical, frequently used by Paquette,[37] which exemplifies the ability to readily alkylate oxy-Cope reaction products. The above examples collectively demonstrate the synthetic utility of the oxy-Cope enol to rapidly generate additional molecular complexity.



Scheme 3.10. (**A**) Sworin's hydrazulene synthesis. (**B**) Paquette's pentannulation. (**C**) Vanderwal's approach to the pseudopterosins.

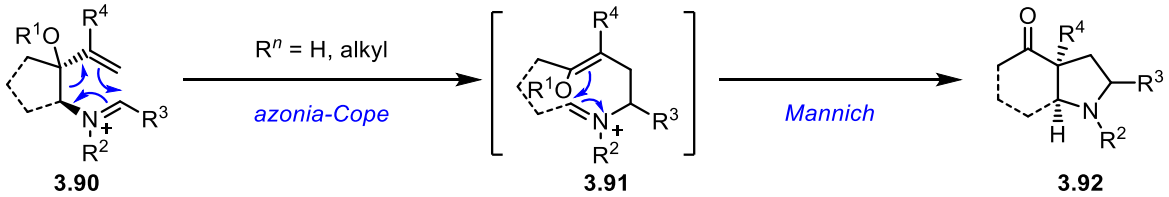
The final category of cascade concerns organometallic functionalization followed by oxy-Cope reaction. The Leighton group used a palladium-catalyzed carbonylation of vinyl triflate **3.87** to induce sequential acetal then ester formation, followed by *in situ* siloxy-Cope rearrangement of **3.88** to access the phomoidride core **3.89** in 46% yield (Scheme **3.11**).[38] The authors note both the incompatibility of the carbonylation with anionic conditions and the remarkable ease of the strain-release transformation, given the known difficulty Clive reported in inducing a similar [3,3] anionic shift.[39] The example demonstrates the opportunity for pairing organometallic transformations with subsequent thermal (sil)oxy-Cope reaction,[40] and conclude this section on various cascade reactions.[41] As previously alluded to, the following sections will deal more specifically with two particular well-known cascades developed by the Overman group known as the aza-Cope / Mannich and Prins-pinacol reactions.



Scheme 3.11. Model substrate for Leighton's approach to the phomoidrides.

3.2.1. *The aza-Cope / Mannich Reaction*

Through the 1980's and 90's, the Overman group developed two conceptually similar cascade transformations known as the aza-Cope / Mannich and Prins-pinacol reactions, each of which spawned numerous natural product synthetic efforts by their group and others.[42] The aza-Cope / Mannich[43] was initially designed as an exothermic means of trapping the less stable isomer of the cationic Brønsted acid-catalyzed 2-azonia-[3,3]-sigmatropic shifts.[43a] Operationally, the aza-Cope / Mannich reaction initially relied on the use of preformed ammonium salts or strong Brønsted acids to elicit decomposition of preformed oxazolines to iminiums. Once formed, the iminiums **3.90** undergo facile aza-Cope sigmatropic shift to generate the isomeric iminium and enol ether in **3.91**, which recombine in a Mannich reaction to bicycle **3.92** (Scheme **3.12**). Other variants of this reaction involve heating the amine with an aldehyde such as paraformaldehyde in the presence of sodium sulfate, or decomposing α-cyanomethylamines, known to protect amines from oxidation chemistry,[43l,y] with silver or copper salts. In a philosophical sense, this transformation combines elements of both aza-Cope and oxy-Cope rearrangements and couples the facility of the charged cationic shift to the twin thermodynamic driving forces of subsequent carbonyl generation and Mannich cyclization.

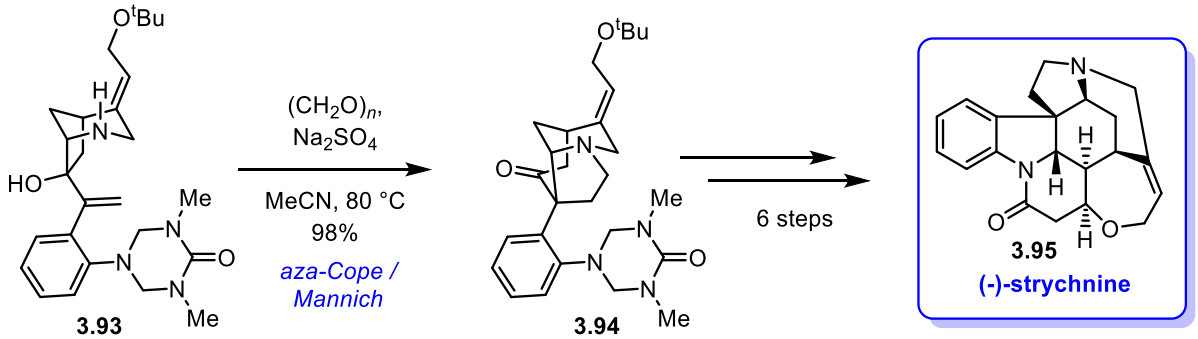


Scheme 3.12. Mechanism of the aza-Cope / Mannich reaction.

In the case of linear substrates, the aza-Cope / Mannich is a reliable substituted pyrrolidine synthesis with good, predictable stereocontrol. The substrate geometry is transferred stereospecifically to the products through chair-like transition states, where substituents exhibit the usual preference for pseudo-equatorial orientation, such that the carbonyl forms *cis* to branching adjacent to the amine (shown by a dotted line). The distal stereocenter bearing R^3 is set according to the preferred iminium geometry. Small R^2 groups like hydrogen or methyl favour a *cis* relationship to R^3 in the transition state, producing a *cis* relationship between R^3 and acetyl. Large R^2 benzyl substituents favour a *trans* iminium transition state orientation relative to R^2 and invert the stereocenter formed. For substrates bound on a cyclic backbone, typically cyclopentane

although both cyclobutanes and cyclohexanes have been used, the aza-Cope / Mannich results in a one-carbon ring expansion and allows access to a range of bicyclic amino ketones. Notably, the alkene geometry is again transferred to the products[43w] and *cis*-fused rings are formed *kinetically* from either relative amino alcohol orientation (or equivalent masked functional groups), although this can be modulated to a minor extent by solvent choice for *N*-benzyl substrates.[43e,g,h,l,m] The *N*-alkyl substituent R^2 size also determines the relative orientation of the distal stereocenter formed on these bicycles with higher aldehydes: *cis* to groups at the ring fusion for benzyl R^2 and *trans* for small hydrogen and methyl.[44] These stereochemical features have made this an attractive methodology for total synthesis, which the Overman group has prolifically exploited.

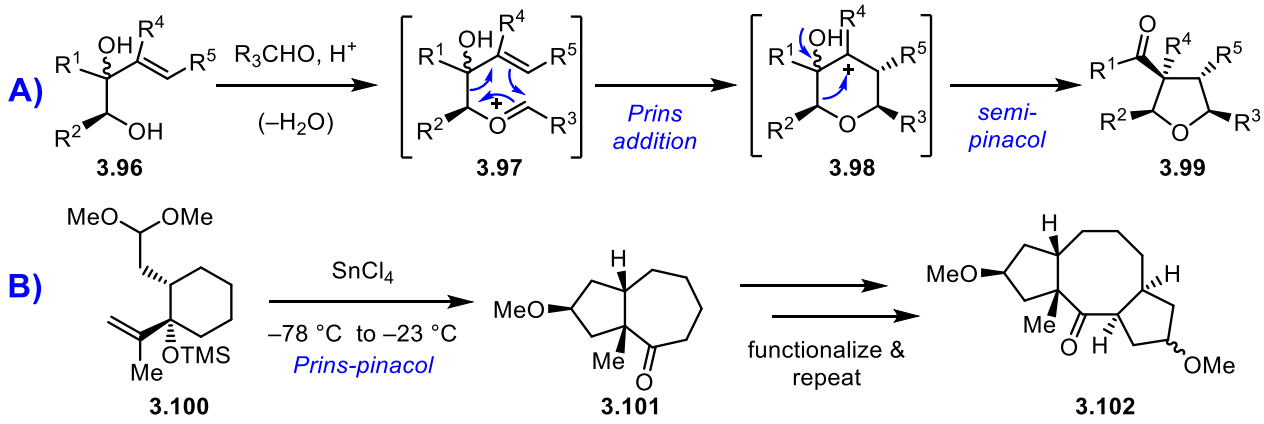
Although not present in the natural products themselves, the bicyclic hydroindolone motif proved a useful platform for the successful synthesis of several *Aspidosperma*, *Amarylidacae*, *Melodinus*, and *Strychnos* alkaloids, one example of each (in order) being 16-methoxytabersonine,[43j,u] pancracine,[43n,w,y] meloscine,[43t,u] akuammicine,[43x] and the ever-popular target strychnine,[43z,ab] as well as actinophyllic acid.[45] As one well-known example, Overman's synthesis of the famous alkaloid strychnine **3.95** incorporates a key aza-Cope / Mannich reaction to forge the caged core in a powerful complexity-generating transformation (Scheme **3.13**). Secondary amino-alcohol **3.93** required just moderate heat in the presence of drying agent and paraformaldehyde to undergo condensation, rearrangement, and cyclization in near-quantitative yield to **3.94**. This inspiring example represents just one among many syntheses using the aza-Cope / Mannich reaction, much like its conceptual counterpart the Prins-pinacol reaction, which will be discussed next.



Scheme 3.13. Aza-Cope / Mannich reaction by the Overman group toward strychnine.

3.2.2. *The Prins-Pinacol Reaction*

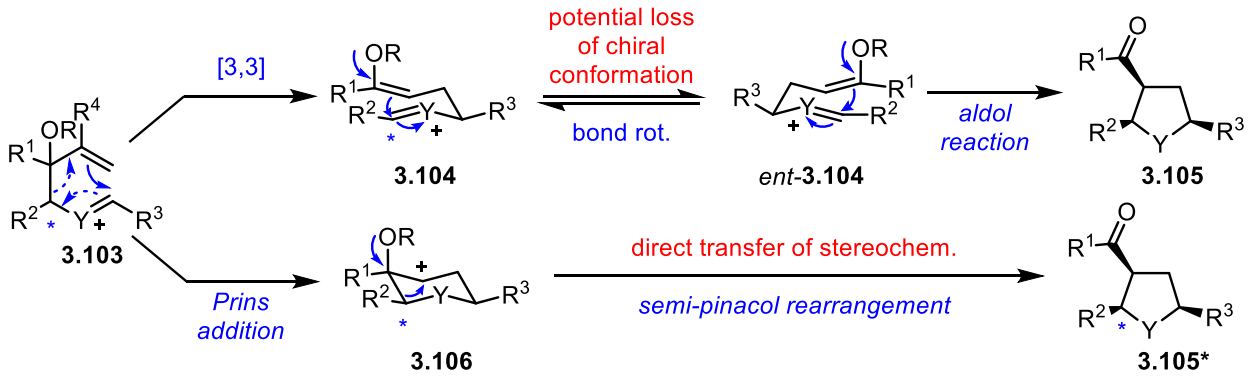
The Prins-pinacol tetrahydrofuran synthesis[46a] was developed after, and conceptually designed based on, its counterpart the aza-Cope / Mannich. The Prins-pinacol involves the use of strong Lewis acid additives to decompose an acetal or promote intermolecular condensation of a substrate such as **3.96** with a carbonyl, thereby initiating Prins addition of a pendant olefin as shown for **3.97** to the cationic oxocarbenium and setting the stage for semipinacol [1,2] alkyl shift as shown in **3.98** to generate carbonyl **3.99** (Scheme **3.14A**). Briefly, the stereochemical features of the transformation are that substituents described by R^2 and R^3 are produced with a *cis* relationship across tetrahydrofuran **3.99**, both to each other and the resulting carbonyl-R^1 group. Additionally, the reaction preserves the relative relationship between olefin substituents R^4 and R^5 and ablates the initial allylic alcohol stereocenter. That stereocenter is also typically inconsequential since either alcohol orientation can fragment through the same chair-like transition state and transfer the adjacent alkyl group with stereo-fidelity.[42b] The reaction has experienced repeated use in natural product synthesis,[46] such as in the synthesis of polysubstituted tetrahydrofurans, fused or spirocyclic THF-containing ring systems, and complex natural products such as the eunicellin family of diterpenoids. Another application saw allylic silyl ethers used in combination with dimethyl acetals in one-carbon ring expansions analogous to the cyclic aza-Cope / Mannich examples. The technique culminated in the stepwise dual ring expansions of cyclohexane **3.100** outward first to 7/5 **3.101** and then to the 5-8-5 ophiobolin ring system in **3.102** (Scheme **3.14B**).[46b] Sadly, the Prins-pinacol was never realized in a complete synthesis of any ophiobolins, fusicoccins, or other related members of fused 5-8-5 tricyclic natural products.



Scheme 3.14. (**A**) Mechanism of the prins-pinacol reaction. (**B**) Overman's approach to the ophiobolin core by stepwise double-ring expansion using prins-pinacol reactions.

3.2.3. *Overman's Mechanism Tests*

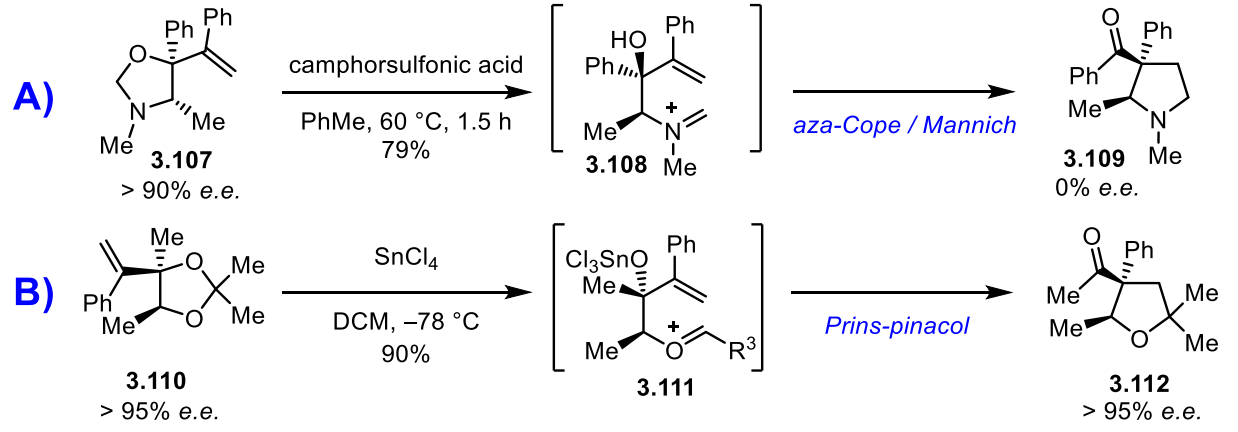
The mechanisms of the aza-Cope / Mannich and Prins-pinacol reactions were of critical interest to their use in synthesis and are directly relevant to the oxy-Cope / Michael project which will be described in Chapter 4. Determining the exact mechanisms of the Prins-pinacol and aza-Cope / Mannich reactions required some careful experiments in each case. Both reactions could conceivably occur by either a concerted [3,3] shift followed by enol addition or by cyclization to a cationic intermediate followed by semi-pinacol rearrangement (Scheme **3.15**). These two pathways would exhibit a similar relative stereochemical result due to a shared preference for similar chair-like transition states. In the case of the aza-Cope / Mannich, some support for the upper pathway was derived from the fact that a substituent as R^4 could be electron-donating or withdrawing. The mechanism test used in each case was the same and used enantioenriched starting materials represented by **3.103** to observe retention or erosion of *e.e.* in the reaction products **3.105**. A pathway involving [3,3] sigmatropic rearrangement, whether concerted or stepwise, passes through achiral intermediate **3.104**, where relatively facile bond rotation would be expected to scramble the stereochemical information before cyclization can occur (Scheme **3.15**, upper mechanism). However, a [1,2] semipinacol shift, induced by olefin Prins addition to the carbenium and formation of hypothetical intermediate **3.106**, would faithfully transfer the stereochemical information to **3.105** (Scheme **3.15**, lower mechanism). Thus, the sigmatropic reaction / cyclization path would lead to substantial or complete racemization of the input material while the cyclization / semi-pinacol path would lead to retention of enrichment. Note that a [3,3] shift only raises the possibility of *e.e.* erosion if bond rotation is faster than bond formation. This does not hold true if the chiral conformation is sufficiently constrained within a medium-size ring



Scheme 3.15. The two possible pathways for the aza-Cope / Mannich and Prins-pinacol reaction.

connecting R^1 and R^2. This assumption also fails if a stereocenter formed with substituent R^3 is influenced by, retains, and transfers back the original stereochemical information.

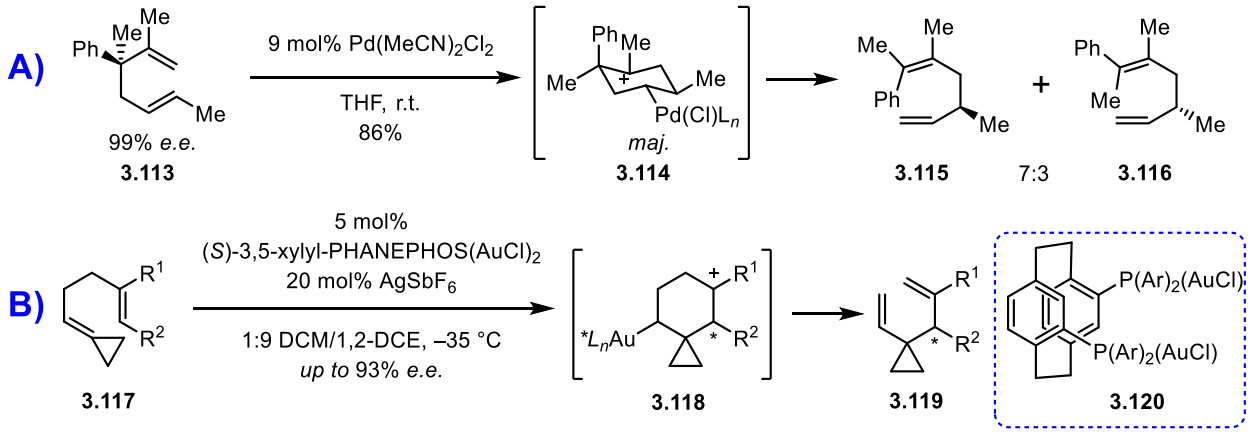
For the aza-Cope / Mannich, the key experiment utilized an enantioenriched methylene oxazolidine **3.107**. This compound, prepared in at least 90% *e.e.*, was heated at 60 °C in toluene with one equivalent of camphorsulphonic acid to induce fragmentation to iminium **3.108** and produce racemic pyrrolidine **3.109** (Scheme **3.16A**). This evidence is strongly indicative of a [3,3] shift, double bond rotation, and Mannich reaction. Importantly, it was established that neither enantioenriched starting material nor resolved enantioenriched product were racemizing to a significant extent under the reaction conditions, with excess acid, or during *rapid* silica gel column chromatography. This distinction is critical, since a similar test on an optically active cyclopentane amino alcohol led to formation of enantiopure ring expanded hydroindolone due to constrained bond rotation in the medium-ring intermediate.[43r] Furthermore, it was later demonstrated with a linear amino alcohol in decanal that optically active products were obtained,[43aa] which demonstrates the second exception for retention of stereochemistry from [3,3] shift cascades discussed above. It was shown that the product enantiomers could be interconverted with Et_2AlCl through retro-Mannich fragmentation and re-addition, which may explain the requirement for rapid chromatography. In the case of the Prins-pinacol reaction, it was readily shown that dimethyl ketal **3.110**, readily obtained from ethyl *L*-lactate, showed no erosion of enantiomeric purity during the transformation to tetrahydrofuran **3.112**.[46a] The evidence of retention is strongly indicative of the pinacol shift occurring from intermediate **3.111** (Scheme **3.16B**).



Scheme 3.16. Overman's mechanism test of the (**A**) aza-Cope / Mannich and (**B**) Prins-pinacol.

3.3.1. *Catalysis of (oxy-)Cope Rearrangements*

Methods for catalysis of Cope rearrangements have been developed, but only two enantioselective processes have been reported. Alkoxide base catalysis of formal oxy-Cope rearrangements was discussed in the previous AOC section but is rarely used. Dauben used both Brønsted and Lewis acid catalysis in Cope rearrangements of cyclohexane-based exocyclic enone methylenes.[47] Other examples of acid, alumina, and iodine catalysis of Cope shifts are also known.[10b,48] Palladium and other transition metals have been shown to catalyze the Cope and oxy-Cope rearrangement, with several contributions again by the Overman group.[10b,48,49] In one notable example, they showed that Pd(II) chloride catalyzed shift from enantiopure hexadiene **3.113** afforded an 86% yield and 7:3 ratio of isomers **3.115** and **3.116**, which proves a preference for similar chair-like transition states as in thermal rearrangement (Scheme **3.17A**).[50] Regarding the mechanism of the Pd-catalyzed reaction, it was tentatively proposed that olefin engagement of the metal is followed by addition of the distal olefin to create alkyl carbocation **3.114** and subsequent fragmentation affords the products. Just ten years ago, the first asymmetric Cope rearrangement was reported by the Gangé group, employing Au catalysis (Scheme **3.17B**). A unique type of strain-driven shift from cyclopropyl alkenes such as **3.117** was used to drive Cope isomerization to products **3.119** in high *e.e.* using cyclophane bis-phosphine ligand **3.120**. The calculated reaction pathway, constructed in collaboration with Tantillo, showed that same stepwise mechanism was operative, involving cationic intermediate **3.118**.[51]



Scheme 3.17. Gangé's Au-catalyzed asymmetric formal Cope rearrangement.

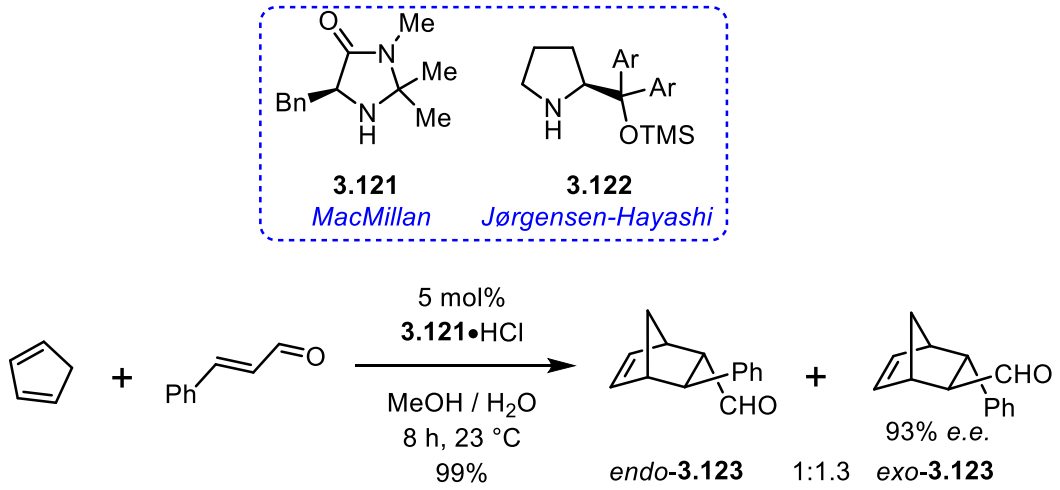
Other niche catalytic methods have also been developed, such as antibodies trained on a cyclohexanol mimic which bind and facilitate rearrangement of 2,5-diphenyl-1,5-hexadiene

through a diyl intermediate in stepwise fashion.[52] Enantioselective N-oxide mediated allylboration of β,γ-unsaturated α-ketoesters has also been used in conjunction with $Ni(OTf)_2$ to effect a net allyl conjugate addition reaction by subsequent Lewis-acid assisted neutral oxy-Cope rearrangement at just 35 °C.[53] The cascade may be viewed as an organometallic functionalization / oxy-Cope cascade reaction, but is included here because the Ni(II) was shown to promote the oxy-Cope rearrangement itself. Finally, the Jacobsen group applied their urea catalysts and was able to observe some enantioselectivity (< 50% *e.e.*) in the oxy-Cope rearrangement of achiral tertiary di-cinnamyl allyl alcohols with hydrogen bonding and cation-binding catalysis.[54] In summary, the development of novel catalytic methods for oxy-Cope rearrangements, especially those with opportunity for asymmetric reaction development, is sorely needed and would likely be rapidly adopted by the synthetic community.

3.3.2. *Iminium and Carboxyhydrazonium Catalysis, esp. of Pericyclic Reactions*

The 21st century has witnessed an explosion of research in the field of organocatalysis, originating largely with the exploration of amine and ammonium catalysis.[55] In fact, amine organocatalysis has spawned three distinct fields known as LUMO, HOMO, and SOMO catalysis, and has been applied to numerous types of reactions with excellent yields and stereoselectivity possible.[56] Aside from the commonly employed amino acids and short polypeptides, the most famous secondary amine catalysts are the amino acid-derived MacMillan **3.121** and Jørgensen-Hayashi **3.122** classes of catalysts (Scheme **3.18**), which have been widely employed in various reactions including Diels-Alder cycloadditions. A famous example by the MacMillan group employed imidazolidinone **3.121** in the Diels-Alder reaction between cinnamaldehyde and cyclopentadiene, giving a near-equal mixture of *endo* and *exo* bicyclic adducts **1.123** in 99% yield, and also providing the *exo* product in 93% *e.e.*[57] This catalyst also provided a range of cyclohexene adducts in high yields and high to excellent enantioselectivity from simple dienes and aldehydes.

As the only class of pericyclic reaction currently catalyzed by such amine catalysts, these iminium cycloadditions are instructive in a qualitative theoretical sense. In cycloadditions, the catalytic iminium intermediate accelerates the reaction by providing a dienophile with a lower energy LUMO than the aldehyde, a strategy commonly referred to as LUMO-lowering catalysis, which has been more traditionally achieved with various Lewis Acids. In fact, LUMO-lowering catalysis is simply an extension of the ability of electron-withdrawing groups such as carbonyls to



Scheme 3.18. MacMillan's iminium-catalyzed Diels-Alder cycloaddition.

enhance the reactivity of olefins toward dienes by providing significantly lower-lying LUMO π-type olefin orbitals. A back-of-the-envelope conceptualization involves qualitatively mixing the energy levels of naïve π bonds of isolated olefin and carbonyl systems, such as shown for ethylene and formaldehyde (Figure **3.4**). serving to decrease the HOMO-LUMO gap between a diene and the dienophile (or other nucleophile) and reduce the activation energy required for cycloaddition (or other addition).

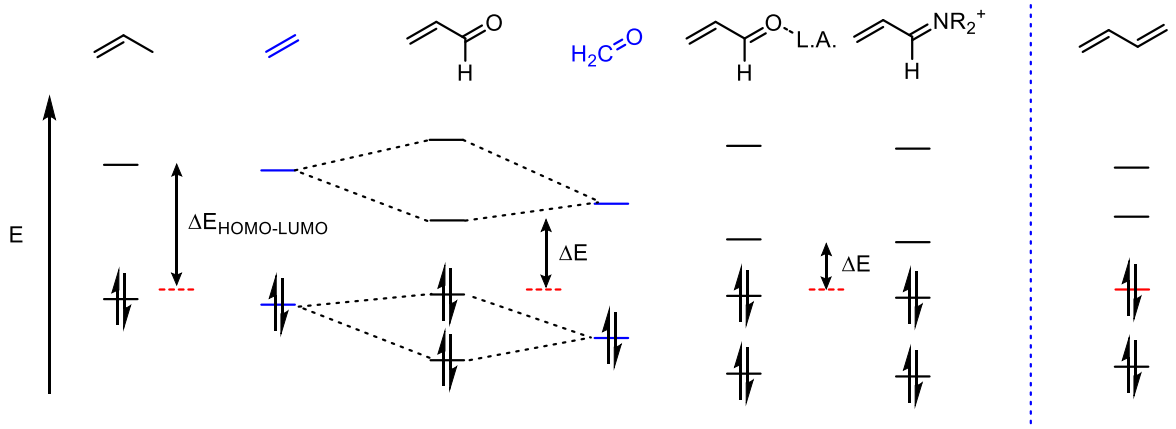
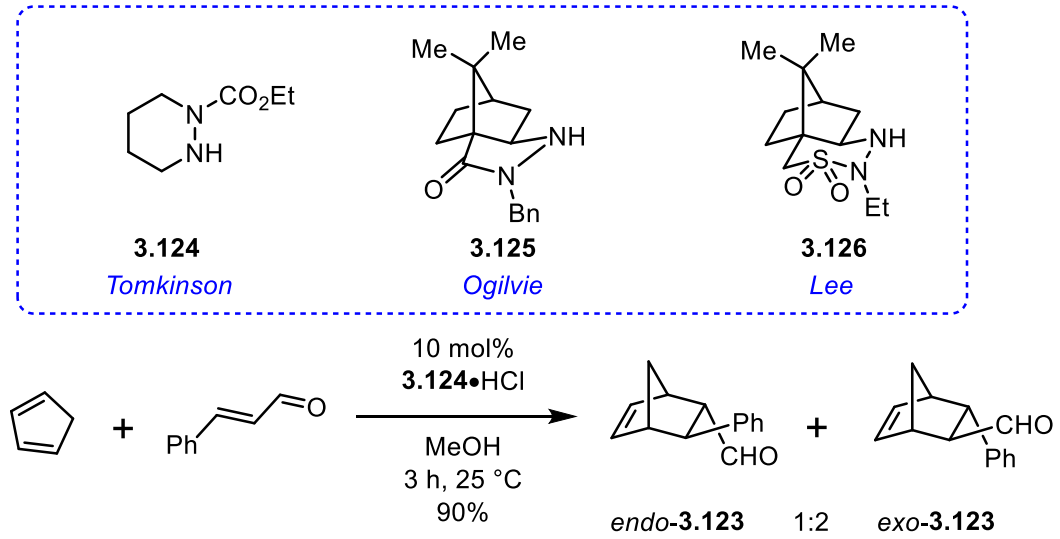


Figure 3.4. Qualitative π-orbital energy diagrams showing orbital combination of carbonyl and olefin orbitals and the LUMO-lowering effects of electron-poor substituents. Qualitative comparisons to a butadiene reaction partner are shown, depicting the HOMO-LUMO gap decrease (HOMO orbital in red)

The Tomkinson, Ogilvie, Lee, and Suzuki groups[58-59] have explored hydrazide-based catalysts **3.124-3.126** in [4+2] cycloadditions and found beneficial rate enhancements (Scheme **3.19**). Rather than the other camphor-derived scaffolds, Tomkinson group arrived at a different cyclic

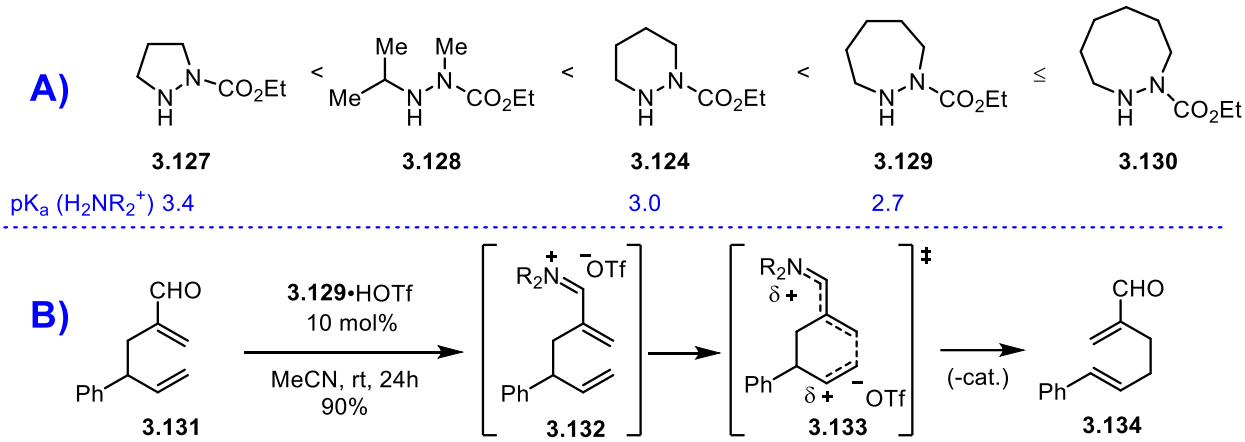
hydrazide catalyst structure through careful optimization from simple 1,2-dimethylhydrazine. Cyclic 5 and 6-membered hydrazides such as **3.124** showed particularly enhanced reactivity over secondary amines or linear alkyl hydrazides in cycloadditions. As one example, 10 mol% of the HCl salt of **3.124** catalyzed the Diels-Alder reaction between cyclopentadiene and cinnamaldehyde, providing cycloadducts **3.123** in 90% yield in just 3 h. The main rationale provided for increased catalytic activity with all such catalysts centered on increased nucleophilicity due to the α-heteroatom effect, resulting in faster iminium ion formation as observed by NMR, which was thought to be rate-limiting in amine catalysis. Tomkinson further rationalized the effectiveness of the pyridazine carboxylate over the analogous amines and pyrazolidine carboxylate, respectively, with calculated catalyst ammonium proton affinity and iminium LUMO energy values. Cyclic hydrazides had not been applied to pericyclic reactions other than cycloadditions prior to our group's interest in such catalysts.



Scheme 3.19. Tomkinson's hydrazide-catalyzed Diels-Alder cycloaddition.

Years ago, our group sought to extend iminium catalysis from cycloadditions to sigmatropic shifts such as the Cope rearrangement. It was envisioned that hexadiene-2-carboxaldehydes such as **3.131** could be used as substrates for iminium catalysis since catalyst condensation forms α,β-unsaturated iminium **3.132** and should increase the electrophilicity of this system relative to the aldehyde (Scheme **3.20**). Several amine catalysts were examined, but only hydrazide catalysts similar to those designed by Tomkinson showed any useful activity.[60a] Acyclic alkyl hydrazides were shown inferior to cyclic hydrazides of six-membered rings or larger, and the yields from cyclic catalysts were found to positively correlate both with ring size and acid co-catalyst

strength.[60b] A ceiling to this trend was found since very little improvement in yield was observed between diazepane **3.129** and 8-membered hydrazide **3.130**. Since the former catalyst was easier to make due to a higher yield obtained from alkylation of simple carboxyhydrazides with 1,5-dibromopentane, its use was popularized in our group for subsequent work. In the organocatalytic Cope rearrangement, 10 mol% of the triflic acid salt of diazepane carboxylate **3.129** allowed conversion of aldehyde **3.131** to product aldehyde **3.134** in 90% yield over 24 h using acetonitrile as solvent. The base transformation was then extended to several other examples.



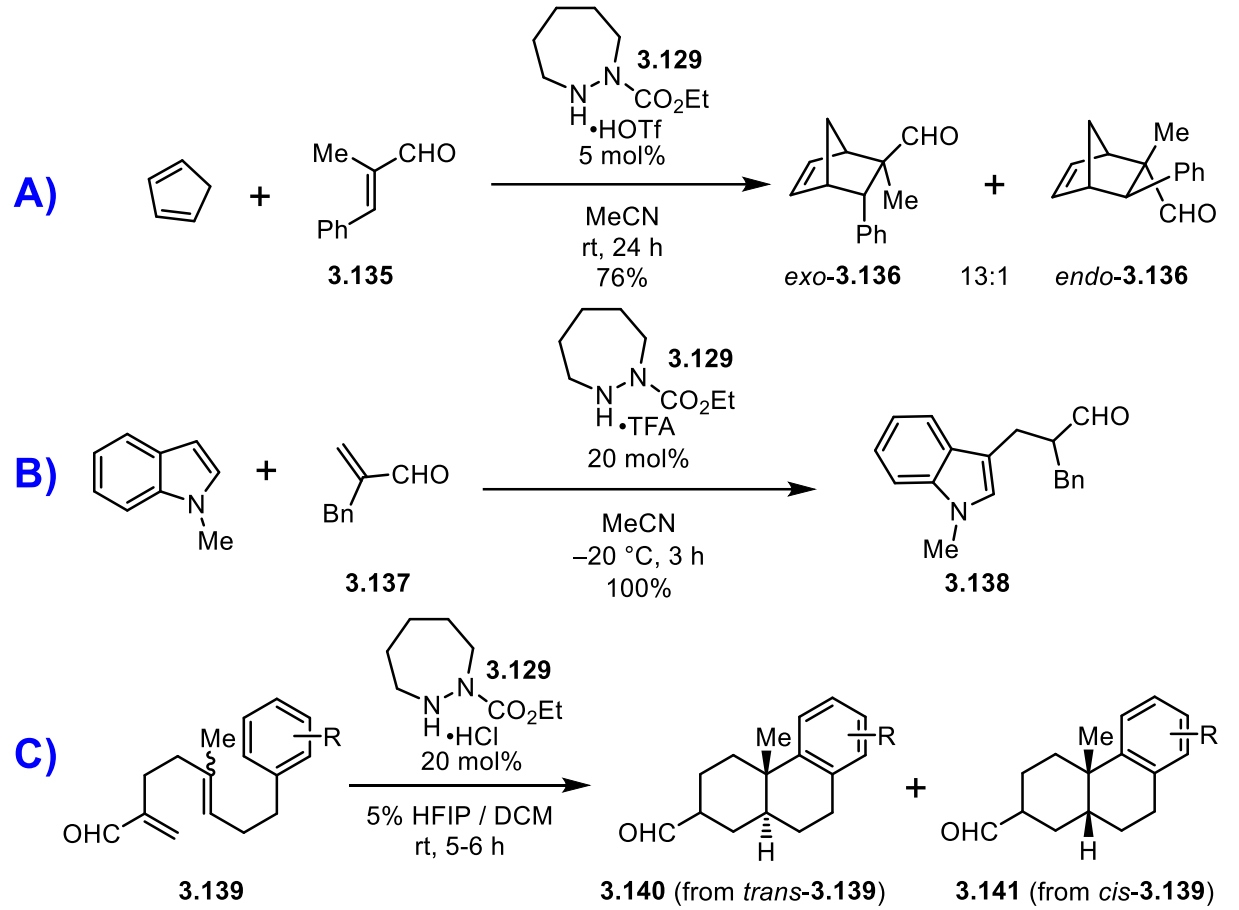
Scheme 3.20. (**A**) Hydrazide catalysts explored by our group, with experimentally determined conjugate acid pKa values listed below. (**B**) Our group's organocatalytic Cope rearrangement.

The factors contributing to the greater reactivity of hydrazide catalysts appear complex. Importantly, the protonated hydrazide ammoniums are far more acidic than the amine equivalents, and their acidity correlates with their observed reactivity for cyclic hydrazides since diazepane **3.129** has a pK_a of 2.7 while 5-membered **3.127** has a pK_a of 3.4.[60e] Another way of quantifying the trend is by the proton affinity of the ammoniums, where much of the same trend is observed and weaker affinity correlates with increased activity.[60a] Compared to the amines, the hydrazide reactivity was thought to reflect a better ability to initiate aldehyde condensation via carbonyl protonation, which for amines is thought to be rate-limiting due to the A-1,3 strain. Similar A-1,3 strain exists in what might be appropriately called a carboxyhydrazonium intermediate (hydrazide iminium equivalent). Combined with a total lack of iminium-like intermediate formation as observed by NMR in our group's collective experiments, the notable strain might tempt the simplistic hypotheses that either catalyst acidity or flexibility explain the reactivity trend regarding catalyst ring size.

However, computational insight in collaboration with the Houk group, in combination with ^{13}C kinetic isotope effects (KIE) determination, has revealed that Cope rearrangement is indeed rate-limiting since the largest KIE were observed and calculated on the terminal carbons of the hexadiene rather than the iminium carbon.[60c] The elucidated computational pathway additionally suggests associative conjugate addition character in the transition state, with the potential for a shallow-energy cationic intermediate close in energy to the transition state of the concerted pathway, the existence of which was sensitive to hexadiene substitution. Examination of LUMO-lowering effects on the iminium system indicated that although the energy decreases as expected from 5-7 member hydrazide rings (from –1.69 to –1.91 eV), the changes were small compared to the $HOMO_{alkene}$–$LUMO_{iminium}$ gap of >7 eV. The catalyst trend was rather attributed to the larger ring size permitting greater twisting about the N-N hydrazide bond to minimize lone pair repulsion in the transition state, since the conjugate character would place electron density on the iminium nitrogen. Thus, while the increased acidity of the hydrazide ammoniums might explain enhanced reactivity with respect to amine catalysts, the ability of the catalyst to twist is critical to their ultimate catalytic activity in the rate-determining sigmatropic shift.

The hydrazide catalysts have proven generally applicable across a range of conceptually linked transformations. The Gleason group has reported a Diels-Alder reaction with cyclic hydrazide **3.129** which work on methyl α-substituted enals such as **3.135**, which is a challenging substrate for cycloaddition reactions. It was found that 5 mol% of the triflic acid salt of **3.129** provided a 76% yield and 13:1 *exo*:*endo* ratio of Diels-Alder adducts **3.136** in 24 h in MeCN (Figure **3.21A**).[60e] Our group has also demonstrated conjugate additions using indoles, such as methylindole addition to unsaturated aldehyde **3.137**, which afforded **3.138** in 100% yield in just 3 h at –20 °C in MeCN using 20 mol% of the trifluoroacetic (TFA) acid salt of **3.129** (Figure **3.21B**).[60d] Finally, the intermediacy of cationic character on C-5 of the hexadiene scaffold led to the successful catalysis of polyene cyclizations (Figure **3.21C**). For example, when employing 20 mol% of the HCl salt of **3.129**, polyene cyclizations proceeded from either alkene isomer of **3.139** to provide high yields of either *trans*-decalin **3.140** (from *cis*-**3.139**) or *cis*-decalin **3.141** (from *trans*-**3.139**) with a variety of electron-donating aryl substituents. The polyene reaction was then extended to enantioselective variants and used in a total synthesis by our group.[60f-h] Exploring catalysis of the oxy-Cope rearrangement presented a natural extension of the total methodology manifold. If possible, and oxy-Cope rearrangement would also provide a more synthetically

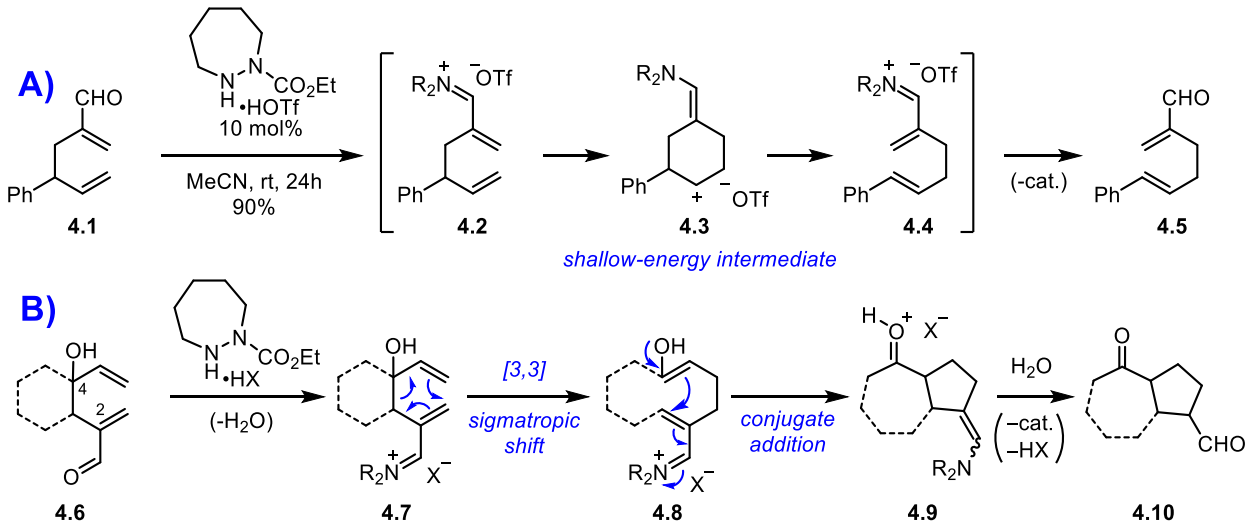
valuable catalyzed transformation than the Cope rearrangement, and may be useful in further total synthesis efforts.



Scheme 3.21. Our group's organocatalytic transformations. These include (**A**) Diels-Alder reaction, (**B**) Michael addition, and (**C**) polyene cyclization.

4.1.1. *Designing an oxy-Cope / Michael Reaction Cascade*

As mentioned in Chapter 3, our group's successful catalysis of the Cope rearrangement (Scheme **4.1A**) provided critical proof-of-concept in sigmatropic shift catalysis. However, the poor general synthetic utility of simple Cope rearrangements, combined with its inherent lack of enthalpic potential, meant that extending our carboxyhydrazonium catalysis to the synthetically powerful oxy-Cope reaction would be desirable. Furthermore, consideration of a potential alcohol position at C4 on hexadiene scaffold **4.6** relative to the aldehyde at C2 (Scheme **4.1B**) led to the realization that the Cope product **4.8** might be inclined to react in a cascade sequence. This would result in Michael addition of the *in situ*-generated enol **4.8** with the new α,β-unsaturated iminium in that structure, both generated from [3,3] rearrangement (Scheme **4.1B**). If successful, this would result in an oxy-Cope / Michael (oCM) cascade reaction. Both steps appeared entirely possible based on the established hydrazide iminium catalysis in the Cope rearrangement, in conjunction with our established catalysis of arene Michael additions to activated enals. Such a mildly acidic reaction would complement the harsh basic AOC conditions, while the cascade reaction potential could rapidly generate molecular complexity.



Scheme 4.1. (**A**) Organocatalytic Cope mechanism. (**B**) Conceptual extension to proposed oxy-Cope / Michael rearrangement.

For hexadiene substrates bound with a cyclic backbone, the proposed cascade sequence would result in synthetically desirable fused bicycles, passing through medium-sized diene rings in **4.8**

as intermediates which would restrict or eliminate rotation and encourage ring closure. The feasibility of the aza-Cope / Mannich and Prins-pinacol reactions, which proceed via analogous cyclizations, suggest our intended cascade should be physically possible. Other cationic Mannich[61] and enolate-oxonium closures are also known.[62] It was therefore of interest to base substrates off cyclohexane backbones to facilitate stereocontrolled substrate synthesis and potentially produce desirable 7/5 fused bicycles represented by **4.10**. These fused bicycles are commonly featured in natural product scaffolds including daphnane diterpenoids such as englerin A **4.11** and guaianolide sesquiterpenoids **4.12** (Figure **4.1**). Ideally, the methodology could be extended to produce the ubiquitous hydrindane bicycle as well as 8/5 rings such as those possessed by the challenging synthetic targets ophiobolin A **4.13** and fusicoccin A **4.14**. The development of a linear variant of the reaction was also desired from the outset in order to access decorated cyclopentanes.

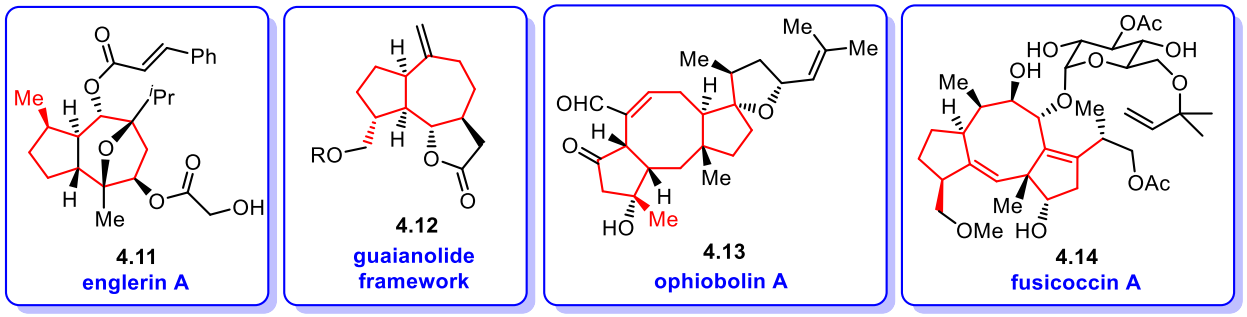
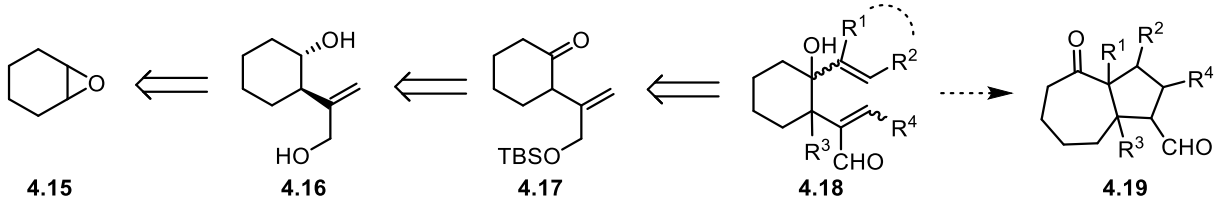


Figure 4.1. Complex natural products with carbon frameworks in red mapping onto our proposed oxy-Cope / Michael reaction products.

4.1.2. *Synthesis of Cyclic oxy-Cope / Michael Substrates*

A range of substituted cyclohexane-based substrates represented by structure **4.18** (Scheme **4.2**) were initially conceived to test our reaction hypothesis, although other ring sizes were also desired and will be discussed later in this section. Various points of cyclohexane diversification were considered, primarily regarding olefin substitution as represented by generic groups R^1 and R^2. From the outset, it seemed that substitution at R^1 might influence the reaction since cationic character is expected at this position according to our group's knowledge of the asynchronous or stepwise organocatalytic Cope mechanism. Additionally, substituents R^1 and R^3 would allow production of quaternary stereocenters, which are particularly valuable in syntheses due to challenge in their preparation, at the fusion of the hydrazulene ring in oxy-Cope / Michael (oCM) products **4.19**. Testing terminal substitution at R^2 and R^4 would also be desirable since substitution

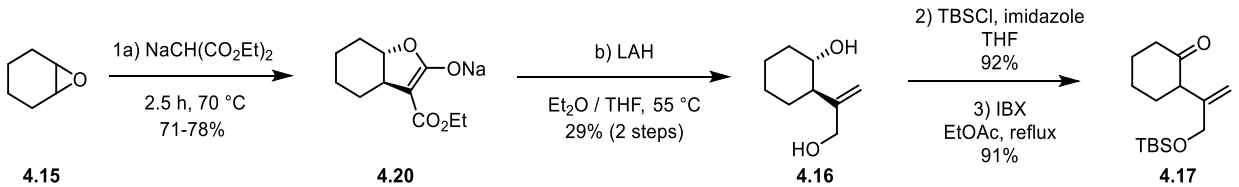
is known to raise the energy of sigmatropic reactions. Furthermore, one example of amine catalysis is known to tolerate β,β-dimethyl substitution in polyene cyclizations.[63]



Scheme 4.2. Retrosynthesis of cyclic oxy-Cope / Michael substrates.

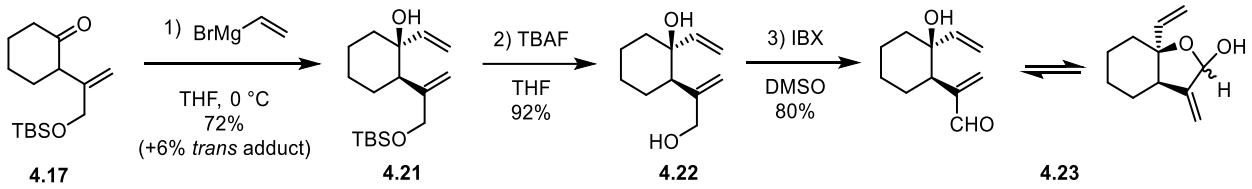
As will be seen, the oCM reaction turned out to be successful and warranted the development of the full range of substrate scope we envisioned. In the course of this work, it also quickly became obvious that both diastereomers of substrates were needed to evaluate differences in their reactivity under catalytic conditions. In the interest of providing an organized discussion, the synthesis of the entire scope of cyclic substrates will be described prior to the cyclic reaction development, beginning with the simplest divinylcyclohexane substrates. It was determined early in the project that advanced ketone intermediate **4.17** would allow preparation of a range of substrates **4.18** with a variety of substituents simply through addition of vinyl organometallic species. This potential intermediate was readily traced back to diol **4.16** and cyclohexene oxide **4.15** using well-established and scalable chemistry.

Ketone **4.17** was readily prepared in decagram quantities (Scheme **4.3**) starting from inexpensive cyclohexene oxide **4.15**. A well-established sequence for opening cyclohexene oxide with sodiated diethyl malonate, affording sodiated lactone **4.20** after thermal lactonization and filtration, then reduction-elimination with lithium aluminum hydride provided known up to 9-10 g of diol **4.16** in 29% yield over three steps.[64] Protection of the primary alcohol with TBSCl and oxidation of the secondary alcohol with IBX proceeded in 92% and 91% yield, respectively, to readily prepare batches of key intermediate ketone **4.17**.



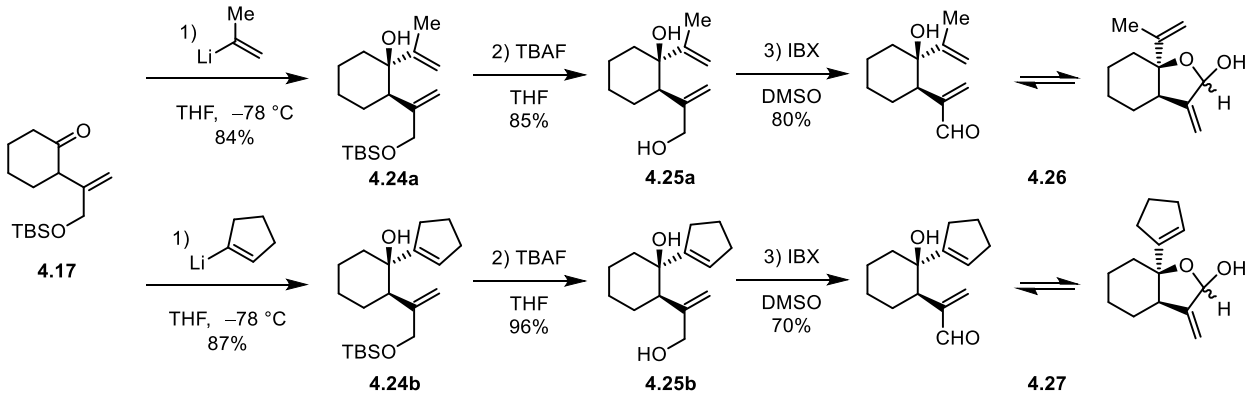
Scheme 4.3. Synthesis of the key intermediate ketone.

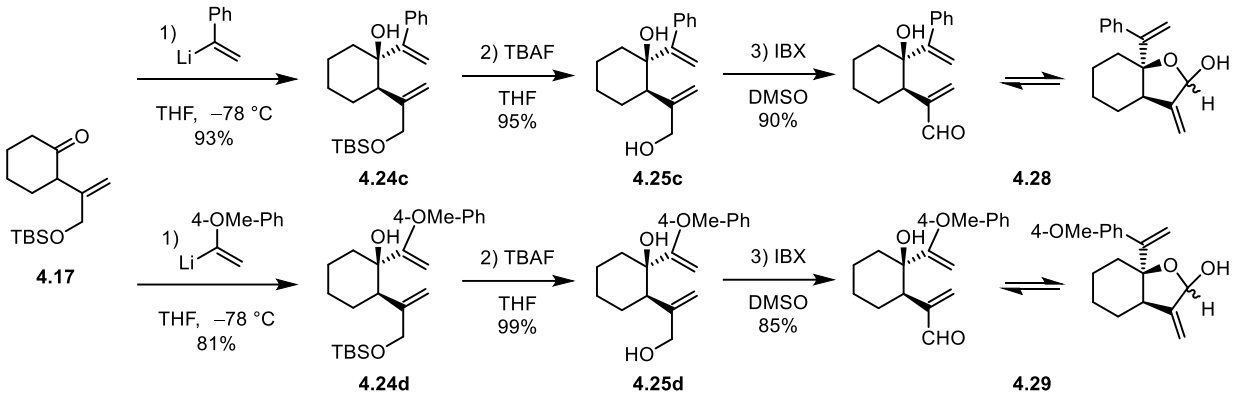
Attempts to react ketone **4.17** with vinylmagnesium bromide, along with organo-zinc and -cerium reagents prepared from it, were initially stymied by poor yields. Fortunately, it was found that inverse addition of ketone to the Grignard reagent provided a robust 72% yield of tertiary alcohol **4.21**. The silyl ether was deprotected with TBAF to provide a 92% yield of diol **4.22**, and subsequently oxidized with just less than one equivalent of IBX in DMSO to provide catalytic substrate **4.23** in 80% yield, which was found to exist as a mixture of aldehyde and hemiacetals.



Scheme 4.4. Synthesis of a divinyl cyclohexane-based oCM substrate.

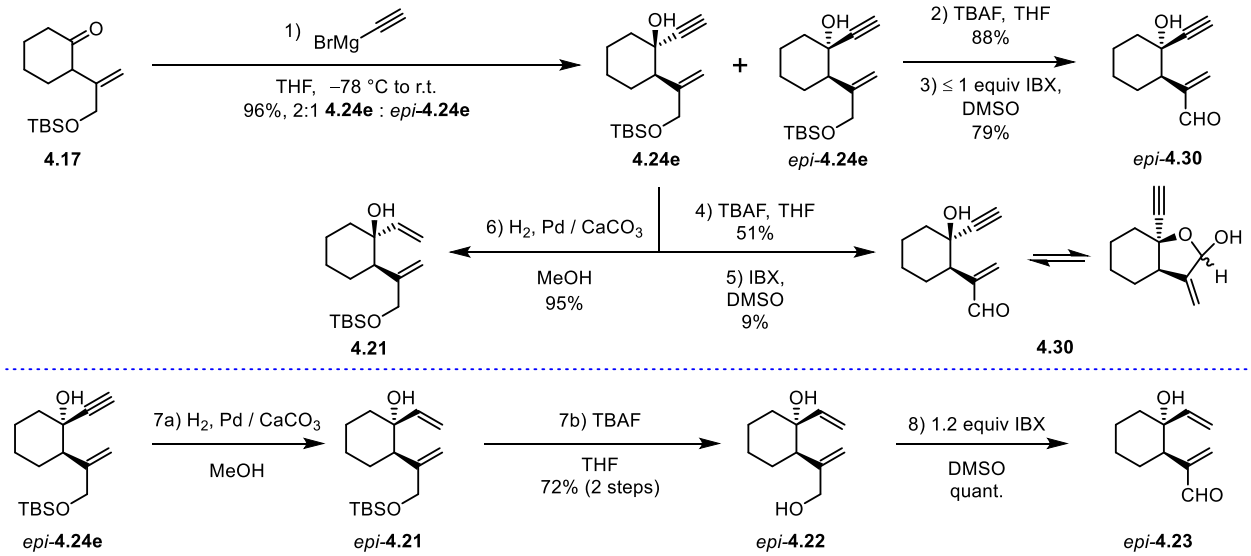
The substituted substrates were prepared in very similar fashion. As before, ketone **4.17** resisted reaction with isopropenylmagnesium bromide, proceeding in at most 48% yield. However, vinyllithium reagents prepared via lithium-halogen exchange proved quite successful in adding to ketone **4.17** and allowed the preparation of a range of adducts. The tertiary alcohols **4.24a-d** were prepared from 2-bromopropene in 84% yield, 1-bromocyclopentene in 87% yield, α-bromostyrene in 93% yield, and *p*-methoxy-α-bromostyrene in 81% yield (Scheme **4.5**). The entire series of silyl ethers **4.24a-d** was then elaborated by TBAF deprotection to provide diols **4.25a-d** in 85-99% yield followed by IBX oxidation to provide aldehyde substrates **4.26-4.29** in 70-90% yield. This strategy furnished the *cis* isomers of substrates containing isopropenyl, cyclopentenyl, styrenyl, and 4-OMe-styrenyl groups. As with divinyl substrate **4.23**, the substituted substrates were found to exist as mixtures of aldehydes and hemiacetals.





Scheme 4.5. Synthesis of cyclohexane-based oxy-Cope / Michael substrates with 5,6-vinyl hexadiene substitution.

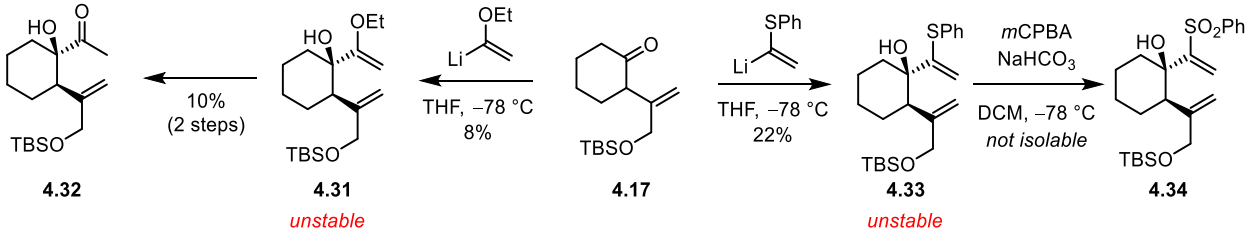
In contrast to vinylic Grignard reagents, ethynylmagnesium bromide readily added to ketone **4.17** in 96% yield of isolated material and 2:1 *d.r.* favouring the *cis*-adduct **4.24e** over *epi*-**4.24e** (Scheme **4.6**). The silyl ethers were elaborated to the corresponding alkyne substrates as follows. TBAF deprotection afforded the corresponding diols in 51% and 88% yield, respectively, and subsequent IBX oxidation provided aldehyde substrates **4.30** and *epi*-**4.30** in 9% and 79% yield, respectively. Each alkyne adduct could also be utilized in synthesis of divinyl substrates. To this end, Lindlar hydrogenation of **4.24e** in MeOH over 10 mol% Pd/$CaCO_3$ poisoned with pyridine gave **4.21** in 95% yield. Similar semihydrogenation of *epi*-**4.24e** and subsequent TBAF deprotection in THF produced the corresponding diol intermediate *epi*-**4.22** in 72% yield over two



Scheme 4.6. Synthesis of cyclohexane-based oxy-Cope / Michael substrates with alkynes and the corresponding alkenes.

steps. Oxidation of the diol with IBX then afforded *trans* divinyl substrate *epi*-**4.23** in quantitative yield.

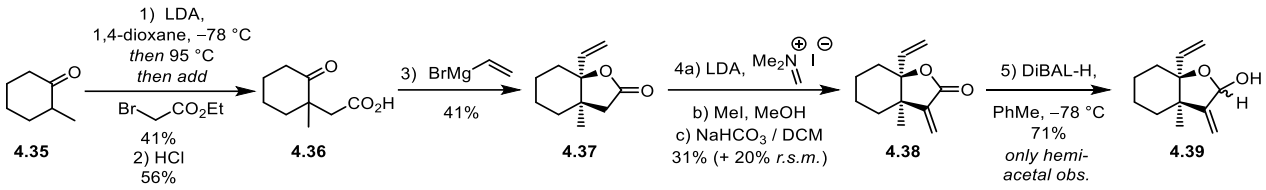
Unfortunately, not all desired substrates were successfully prepared. The initial plan to produce a family of substrates with both very electron rich and poor olefins was frustrated by either the stability of synthetic intermediates or intermediates to reaction conditions. Unfortunately, lithium-halogen exchange of *p*-nitro-α-bromostyrene failed to produce anything but brightly coloured solutions, likely resulting from alternative reduction of the nitro group, precluding preparation of a nitroarene-bearing substrate by this method. Addition of deprotonated ethyl vinyl ether and phenylvinylsulfide to ketone **4.17** also afforded <10 and 22% respective yields of the adducts (Scheme **4.7**). Although the addition product of ethyl vinyl ether **4.31** could be isolated in 8% yield, it proved unstable due to hydrolysis, resulting in isolation of ketone **4.32** in 10% yield over 2 steps. Subsequent attempts to oxidize the unstable vinyl sulfide **4.33** to desired sulfone **4.34** with *m*CPBA led to complex mixtures wherein the presence of both sulfoxide and sulfone were observed by mass spectrometry. The syntheses of the ether and sulfone substrates were therefore abandoned since a sufficient range of substrates exploring olefin substitution had been prepared, and other points of interest were examined.



Scheme 4.7. Efforts toward substrates bearing ethyl vinyl ether or vinylsulfone groups.

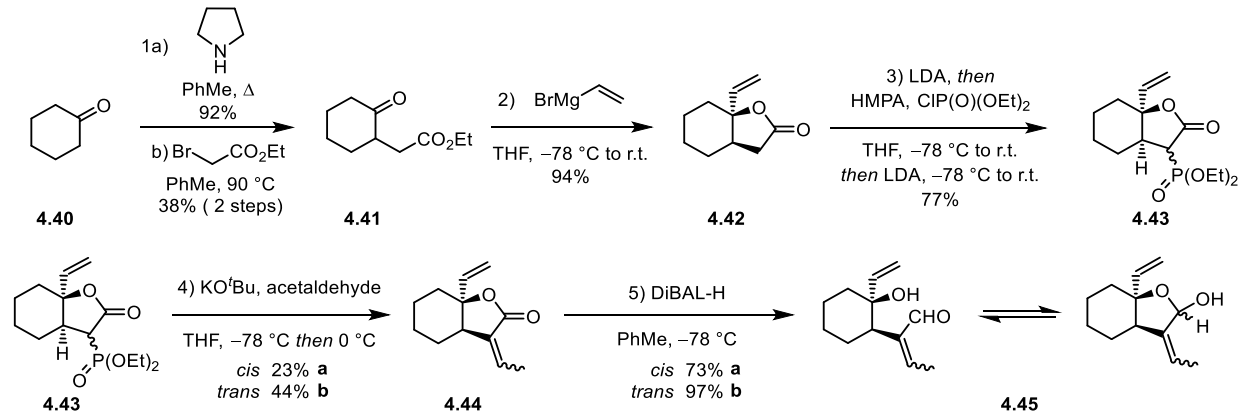
To explore 3-Me substitution, substrate **4.39** was needed (Scheme **4.8**). A short synthesis of substrate **4.39** was designed from 2-methylcyclohexanone **4.35**. First, LDA deprotonation and alkylation of the themodynamic enolate with ethyl bromoacetate was performed, followed by hydrolysis of the ester intermediate to keto-acid **4.36** in 23% yield over two steps. Hydrolysis was necessary since attempted Grignard addition to the esters resulted in intractable mixtures. Subsequent addition of vinylmagnesium bromide to the ketone of **4.36** and subsequent lactonization allowed isolation of *cis*-lactone **4.37** in 41% yield. Methylenation employing Eschenmoser's salt provided enoate **4.38** in 31% yield along with 20% recovered **4.37**. Partial

reduction of the lactone with DIBAL furnished a 71% yield of lactol **4.39**, which contained no detectable aldehyde content.



Scheme 4.8. Synthesis of cyclic oxy-Cope / Michael substrates with 3-Me substitution.

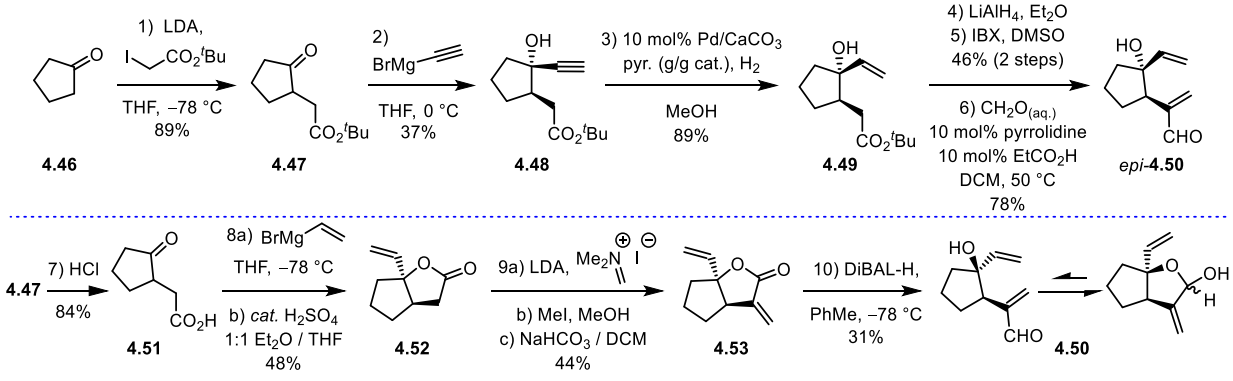
To explore β-enal substitution, either or both isomers of substrate **4.45** was desired (Scheme **4.9**). It was decided that Horner-Wadsworth-Emmons olefination from intermediate **4.43** would give the easiest entry to the substrates, although it was likely to be unselective with regard to olefin geometry. A short synthesis was devised starting from cyclohexanone, which was condensed with pyrrolidine to form the corresponding enamine in 92% yield. The enamine was alkylated with ethyl bromoacetate at 90 °C to form **4.41** in 38% yield over two steps. The keto-ester **4.41** was treated with vinylmagnesium bromide to produce 94% yield of *cis*-lactone **4.42**, with ca. 3% of the *trans* adduct observed in the crude mixture. To convert the lactone into an HWE reactant, the lithium enolate of **4.42**, resulting from LDA deprotonation, was treated with diethyl chlorophosphate. The chlorophosphate is known to functionalize an enolate at oxygen and undergo a vinyl phosphate-phosphonate rearrangement via [1,3] shift to the carbonyl α-carbon upon warming.[65] Use of the reaction provided **4.43** in 77% yield as an inconsequential 88:12 mixture of epimers. This mixture of phosphonate epimers **4.43** was subsequently used in HWE olefination with acetaldehyde to give 23% yield of *cis* enoate **4.44a** and 44% yield of *trans* enoate **4.44b**,



Scheme 4.9. Synthesis of cyclic oxy-Cope / Michael substrates with β-enal substitution.

respectively. Each was reduced with DIBAL to the aldehyde/lactol mixtures **4.45a-b**, affording respective 73% and 97% yields for the *cis* and *trans* enal isomers.

To explore the ring size of the backbone, it was desired to prepare both *cis* and *trans* diastereomers of simple the divinyl cyclopentane **4.50** (Scheme **4.10**). This seemed feasible using a similar promiscuous ethynylmagnesium bromide addition as done with the cyclohexane substrates. Alkylation of cyclopentanone was carried out by sequential treatment with LDA followed by *t*-butyl iodoacetate, giving an 89% yield of keto-ester **4.47**. The *t*-butyl ester was selected because it proved more resilient than either ethyl or benzyl esters to Grignard over-addition in the next step. Unfortunately, ethynylmagnesium bromide addition only gave a 37% yield of *trans* ester **4.48**, while attempts to purify the diastereomer or its lactone proved unsuccessful. However, the yield for Grignard addition was deemed satisfactory for this isomer since it was expected to be the minor product from this addition given the 1:2 *d.r.* observed with the cyclohexane analogue. Lindlar hydrogenation of the alkyne **4.48** in MeOH over 10 mol% $Pd/CaCO_3$ poisoned with pyridine provided an 89% yield of alkene **4.49**. Unfortunately, methylenation with Eschenmoser's salt failed on ester **4.49**, which is unsurprising since few examples of the methylenation with free alcohols are known. A workaround, featuring Pihko's organocatalytic methylenation[66] of the aliphatic aldehyde, was then employed to install the enal methylene. Ester **4.49** was reduced with $LiAlH_4$ to the primary alcohol and re-oxidized with IBX to the corresponding aliphatic aldehyde in 46% yield over 2 steps. Finally, catalytic pyrrolidine methylenation was employed with propionic acid in warm DCM to access *trans* substrate *epi*-**4.50** in 78% yield. It's worth nothing that *epi*-**4.50** displayed no hemiacetal content, similar to the *trans* divinyl-cyclohexane analogue. Unfortunately, the route did not provide access to *cis* divinyl

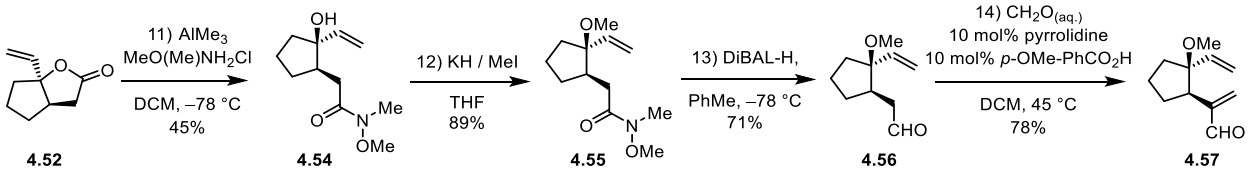


Scheme 4.10. Synthesis of cyclopentane-based oxy-Cope / Michael substrates.

cyclopentane **4.50** since neither the corresponding diastereomer of ethynylmagnesium bromide adduct **4.48** nor its lactone was successfully isolated from the crude mixture of Grignard addition.

Although the strategy of mixed ethynylmagnesium bromide addition did not provide access to the epimer of **4.50**, it was expected to be the major product of vinylmagnesium bromide addition. Once again, attempted addition of the Grignard to keto-esters produced complex mixtures. To overcome the issue, ester **4.47** was hydrolyzed in concentrated HCl to give an 84% yield of acid **4.51**. Vinylmagnesium bromide addition to the free carboxylic acid rather than the ester selectively produced *cis*-adduct **4.52** in 48% yield after subsequent lactonization with a catalytic amount of sulfuric acid. Methylenation with Eschenmoser's salt proceeded in a 44% yield of enoate **4.53** and subsequent partial ester reduction with DIBAL afforded a 31% yield of *cis* substrate **4.50**. In contrast to *epi*-**4.50**, **4.50** displayed high lactol content and only about 5% of the aldehyde ring-chain tautomer.

It appeared possible that the dominating hemiacetal content of **4.50** might negatively impact iminium catalysis, so a methyl ether protected equivalent **4.57** was sought to prevent cyclization to the lactol (Scheme **4.11**). Introduction of a Weinreb amide, by opening lactone **4.52** through transamidation, would facilitate methylation by leaving the hydroxyl free for protection and allowing easy conversion to an aliphatic aldehyde. The latter step was effected using trimethylaluminum-facilitated amidation with *N,O*-dimethyl hydroxylamine hydrochloride to produce free alcohol **4.54** in 45% yield. Methylation of the alcohol with KH and MeI afforded methyl ether **4.55** in 89% yield. Reduction of the Weinreb amide with DIBAL then produced aldehyde **4.56** in 71% yield. Finally, catalytic pyrrolidine methylenation provided desired protected *cis* cyclopentane substrate **4.57** in 78% yield.

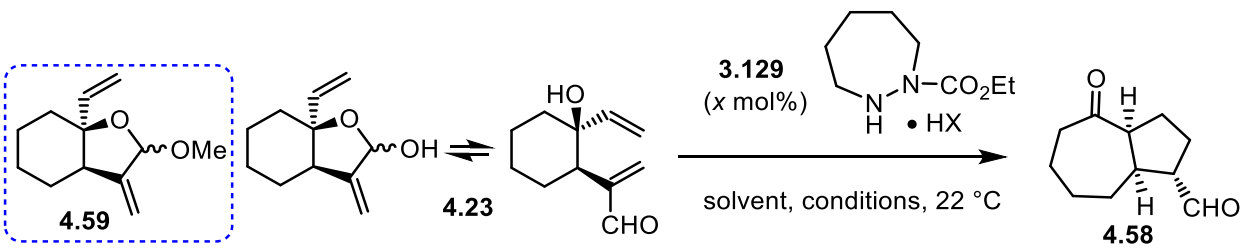


Scheme 4.11. Synthesis of cyclopentane-based oxy-Cope / Michael substrates.

4.1.3. *Development of the Cyclic oxy-Cope / Michael Reaction*

To establish baseline reactivity, model substrate **4.23** was first exposed to thermal conditions in DMSO (Table **4.1**, entry **1**). However, a complex mixture resulted which precluded isolation,

having produced a streak by thin-layer chromatography. It is worth noting that both isomers of perhydrazulene **4.58**, isolated from subsequent catalytic reactions, were observed by ^{1}H NMR spectroscopy in the reaction mixture, but the number of signals present made yield estimation impossible. The first few catalytic conditions explored resembled those employed during development of the organocatalytic Cope reaction. However, treating **4.23** with the hydrochloric acid salt of the cyclic diazepane carboxylate hydrazide catalyst **3.129** in MeCN (entry **2**) provided only a trace of product after a week. The same catalyst in methanol instantly produced methyl acetal **4.59** as a mixture of diastereomers (entry **3**), which proved inert to further reaction, and the use of alcohol solvents were precluded from further screening. Acetal formation highlights a complex solvent- and concentration-dependent dynamic ring-chain tautomeric equilibrium of the open enal and two diastereomeric hemiacetals which exists for all *cis* cyclic substrates. Fortunately, use of the stronger perchloric acid salt of the catalyst (entry **4**) afforded a reasonable 44% yield, based on ^{1}H NMR analysis, of the desired perhydroazulene product as essentially one diastereomer in just 48 h. Counterion effects on reactivity were next explored. It was found that HBF_4 was clearly inferior to other strong acids due to byproducts visible in the reaction mixture



Entry	Solvent[a]	*x* mol%	HX	Time (h)	% Yield[b]
1	DMSO[c]	0	*none*	72	n/a[d]
2	MeCN	15	HCl	180	tr.
3	MeOH	15	HCl	84	0
4	MeCN	15	$HClO_4$	48	44
5	$CHCl_3$	15	$HClO_4$	48	11[d]
6	DMSO	15	$HClO_4$	72	3
7	MeCN	15	HOTf	48	54
8	MeCN	15	$HNTf_2$	48	53
9	$MeNO_2$	15	$HClO_4$	48	55
10	$MeNO_2$	10	$HNTf_2$	48	55

In all cases, 0.1 mmol of substrate was used. [a]Substrate concentration was 0.2 M. Perdeuterated solvent was used for all reactions except $MeNO_2$. [b]Yields were determined by ^{1}H NMR spectroscopy using mesitylene as an internal standard. Parentheses indicate yield after chromatography. [c]Run at 90 instead of 22 °C. [d]Many products observed.

Table 4.1. Optimization of the oCM reaction for the canonical cyclic substrate.

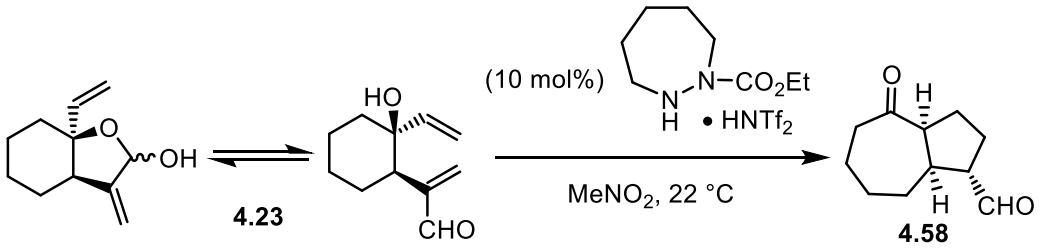
by NMR. The use of the triflic acid catalyst salt in MeCN, which had been the optimal conditions for the organocatalytic Cope reaction, provided a 54% NMR yield in 48 h (entry **7**). The use of a triflimide salt provided a similar result (entry **8**). However, in both cases byproducts complicated product isolation.

The next point of optimization concerned solvent choice, which was found to be critical for the desired reaction. With the perchlorate salt of the catalyst, the use of chloroform (Table **4.1**, entry **5**) resulted in extensive decomposition and dimethyl sulfoxide essentially inhibited catalytic reactivity (entry **6**). With the triflic acid salt of the catalyst, known to provide robust reactivity in MeCN, the reaction was examined in other common solvents such as Et_2O, THF, 1,4-dioxane, EtOAc and DMF but little to no product formation was observed by ^1H NMR analysis of the reaction mixtures. The yields as assessed by ^1H NMR were generally low in toluene with any of the strong acid catalyst salts mentioned, although reactions did proceed somewhat. Use of 15 mol% of the perchloric or 10 mol% of the triflimide acid salts in nitromethane (entries **9** and **10**) provided fewer byproducts as observed by NMR, and each gave 55% yield in 48 h. The fewer byproducts observed by ^1H NMR in $MeNO_2$, combined with the relative ease of handling of crystalline triflimide, made it an attractive catalytic combination. Unfortunately, attempts to scale up the reaction under these conditions led to decreases in the yield.

Extensive follow-up experimentation with **4.23** and other cyclohexane-based substrates, which proved far more reactive even in initial experiments, led to some helpful conclusions. For concision, the factors which were determined to contribute to successful catalysis of the oCM reaction will simply be summarized here rather than presenting a lot of experimentation across various substrates. First, catalyst quality was found to be important. Originally, crystalline salts of the diazepane catalyst were made with each acid co-catalyst, but it was found that they led to unpredictable reaction times which may relate to the hygroscopic nature of the salts. Therefore, it became regular practice to prepare fresh solutions of catalyst salts on the day of use by mixing nitromethane solutions of neutral diazepane catalyst and triflimide. However, even with freshly prepared catalyst, difficulties persisted in scaling the reaction. The alcohol oCM substrates are quite sensitive to acid, and addition of strong acid to a premixed solution of substrate and catalyst results only in instant substrate decomposition. However, exposure of the substrate to the triflic acid salt of an N-Me catalyst analogue did not cause appreciable decomposition, so the substrates

are stable to acids of approximately the same strength of our catalyst. In instances where hundreds of milligrams of substrates were employed, visible sludge was noted to accumulate in the reactions, which indicates a decomposition of substrate and/or catalyst. After isolation by filtration, the material appeared to be polymeric in nature due to the NMR spectrum obtained.

After establishing the critical contributions of solvent choice and catalyst quality in the oxy-Cope / Michael reaction, the quality of the solvent was next considered. It seemed logical to exclude water from the reaction to avoid potential oxa-Michael reaction, which was an issue encountered in the organocatalytic Cope rearrangement when methanol was used as solvent. A surprisingly poor 38% yield resulted from use of dry nitromethane (Table **4.2**, entry **2**), so the corollary of that empirical finding was explored. Increasing the amount of water to 250 mol%, then $MeNO_2$ saturated with water, and finally biphasic 9:1 $MeNO_2$ / H_2O resulted in increased yields, from 55% to 65% to 68% in sequence (entries **3-5**). The conditions presumably provide protection from degradation somehow, which is likely occurring via polymerization pathways initiated by Michael addition or oxocarbenium ion formation. With the optimal conditions established, this section will attempt to rationalize the trends in observed reactivity.



Entry	Water Content[a]	mmol sub.	Time (h)	% Yield[b]
1	-	0.1	48	55
2	anhydrous	1.1	48	31
3	2.5 equiv H_2O	1.1	48	55
4	H_2O-saturated	1.0	60	65 (65)
5	10% H_2O / $MeNO_2$	**1.1**	**60**	**68 (68)**

[a]Substrate concentration was 0.2 M. [b]Yields were determined by ^1H NMR spectroscopy using mesitylene as an internal standard. Parentheses indicate yield after chromatography.

Table 4.2. Optimization of water content in the cyclic oCM reaction.

4.1.4. *The Roles of Acid and Solvent in the Cyclic oxy-Cope / Michael Reaction*

Certain factors affecting the success of the oxy-Cope / Michael reaction have been clarified such as acid strength. Stronger acid "co-catalysts" which provide weakly associated counterions

outperform HCl salts, which may be rationalized as providing a more dissociated cationic iminium-like species. Counterion coordination may be viewed as a continuum between complete dissociation (**4.60**) and addition to the iminium species (**4.61**, Figure **4.2**). For this reason, weaker conjugate bases would be expected to be more dissociated stemming from their reduced nucleophilicity. The degree of dissociation might be expected to correlate with a consequent increase in the electrophilicity and reactivity of oxy-Cope / Michael (oCM) substrates. Regardless of acidity, the structure of the counterion may be important since HBF_4 produced numerous byproducts despite being a strong acid like HOTf, $HClO_4$, and $HNTf_2$. The latter provided a convenient anhydrous, crystalline source of strong acid and consistently afforded cleaner reaction profiles in test reactions as well as the ability to conduct reactions on millimole scale. Less clear is the reason why $MeNO_2$ supersaturated with water proved so invaluable for high yields upon scaling the reaction.

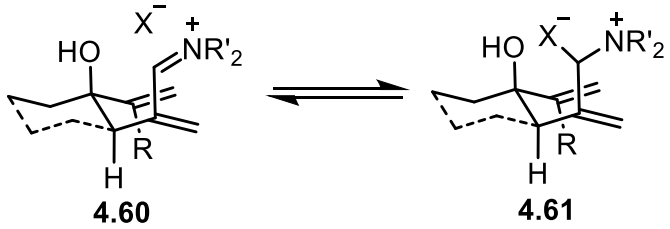


Figure 4.2. Association equilibrium between HX conjugate base and an iminium intermediate.

It is clear from the results presented above that polar solvents facilitate the oCM reaction, especially MeCN and $MeNO_2$, but polarity cannot be the only property affecting reactivity. Solvent polarity is expected to stabilize cationic transition states and intermediates, and solvent polarity has been quantified using the empirical parameter of solvent polarity (E_T^N).[67] It is true that little to no reaction was observed in less polar solvents such as ethyl ether ($E_T^N = 0.117$), THF ($E_T^N = 0.207$), $CHCl_3$ ($E_T^N = 0.259$), and EtOAc ($E_T^N = 0.228$) while very polar MeCN ($E_T^N = 0.460$) and $MeNO_2$ ($E_T^N = 0.481$) allowed good oCM reactivity. However, the fact that there was no reaction in any of DMF ($E_T^N = 0.386$), DMSO ($E_T^N = 0.444$), or MeOH ($E_T^N = 0.762$), combined with the moderate catalyst activity observed in non-polar PhMe ($E_T^N = 0.099$), counters the polarity argument. Inhibition by alcohol solvent is readily explained on the basis of acetal formation, but also raises the general question of whether particular solvents might interact in a detrimental fashion with either substrate or catalyst. Examination of the dielectric constants of DMSO ($\varepsilon_r = 46.45$) and DMF

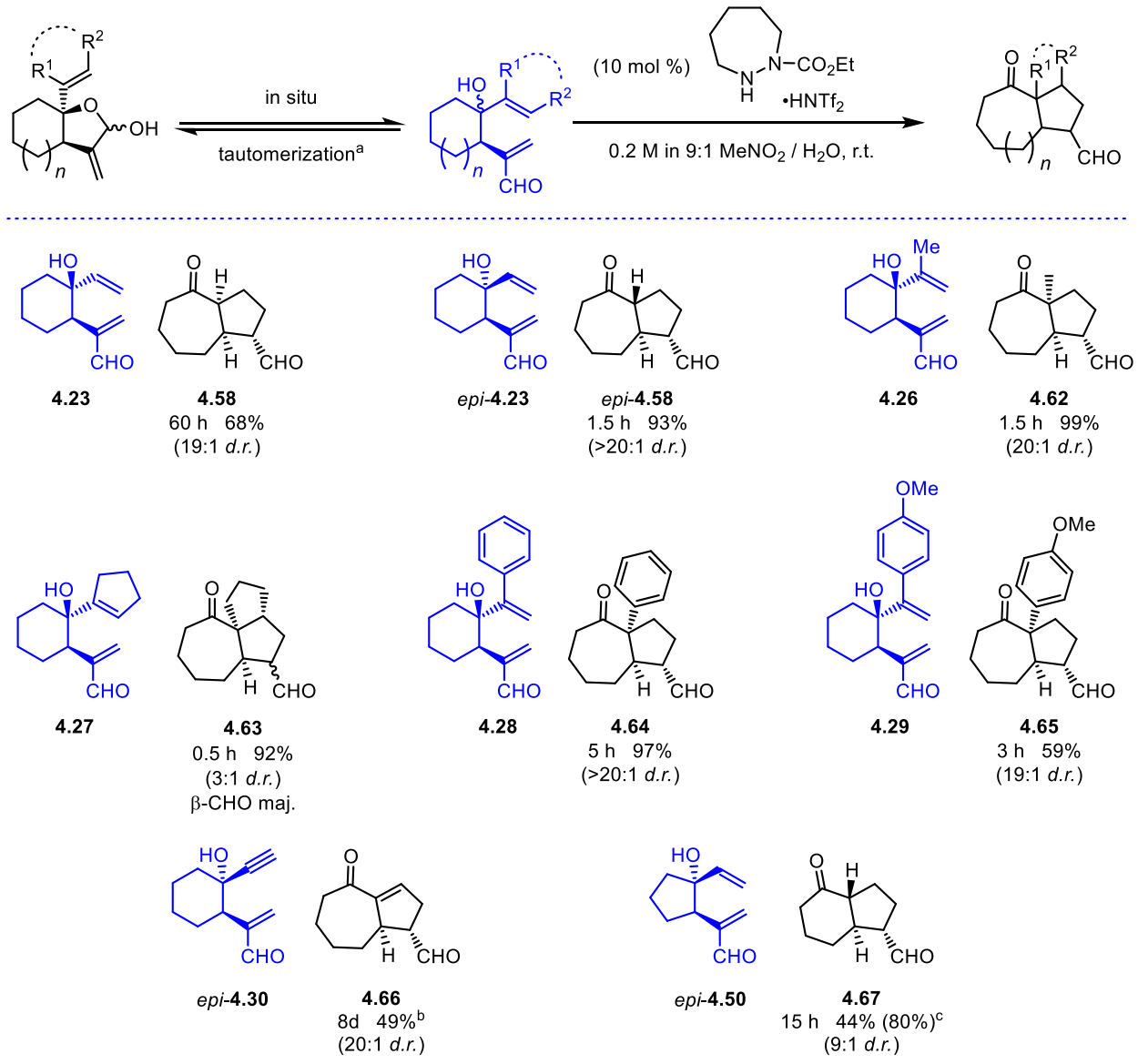
(ε_r = 36.71) as compared to PhMe (ε_r = 2.38), MeCN (ε_r = 35.94), or $MeNO_2$ (ε_r = 35.87) also does not provide a satisfying rationale for reactivity trends. The phenomenon that added water dramatically improves oCM yields further complicates an understanding of how solvent properties affect the oCM reaction at this time. Water is a unique solvent which possess high polarity (E_T^N = 1.000), high dielectric constant (ε_r = 78.36), and excellent hydrogen bonding capability. The only conclusions which can be drawn at this time is that a polar solvent is helpful for the reaction, but the chemical structure of the solvent and its possible interactions with substrate or catalyst likely influence the reaction to a greater extent. Therefore, the greater nucleophilicity of DMSO or DMF may explain their inhibition of the reaction. If solvent chemical interactions are accepted a dominating characteristic, the question then arises of how exactly water stabilizes the substrate to prevent decomposition and increase the oCM yield.

The improved yield with added water suggests it may be preventing loss due to decomposition, possibly by polymerization as indicated by the sludge observed in some reactions. One likely decomposition pathway involves ionization of the tertiary allylic alcohol. Another involves conjugate addition of a nucleophile such as an alcohol to the substrate enal, triggering the enol to add in conjugate fashion to a second substrate molecule and propagating polymerization. A third pathway involves ionization from the hemiacetal to an allylic oxocarbenium and further reactions stemming from addition of another substrate molecule adding to the stabilized cationic species. Of the pathways oulined, it seems most likely that water would act preventatively on the last, since a vast excess of water may conceptually trap that cation and prevent unproductive decomposition.

4.1.5. *Scope of the Cyclic oxy-Cope / Michael Reaction*

Having established conditions for conducting the oxy-Cope / Michael reaction in high yield and on scale, we turned our attention to exploring the scope of the reaction (Figure **4.3**). When the optimal conditions of biphasic 9:1 $MeNO_2$ / H_2O with 10 mol% of triflimide diazepane catalyst salt were employed with *epi*-**4.23**, the *trans* diastereomer of the model divinylcyclohexane, *trans* hydrazulene product *epi*-**4.58** was isolated in 93% yield. Only 1.5 h of reaction was required for *epi*-**4.23**, which contains no hemiacetal content, as compared to the 60 h needed for *cis* cyclohexane **4.23** which suggests a strong influence of this equilibrium on catalytic activity in the oCM reaction. Isopropenyl substrate **4.26** afforded corresponding hydrazulene **4.62** in a remarkable 99% yield, also occurring in just 1.5 h. Cyclopentenyl substrate **4.27** demonstrates the

tolerance of terminal substitution and exhibited outstanding reactivity, providing hydrazulene **4.63** in 92% yield while requiring just 30 mins. Styryl substrate **4.28** provided oCM product **4.64** in 97% yield but required 5 h, while 4-methoxystyryl substrate **4.29** afforded only a 59% yield of **4.65** although that reaction only took 3 h to complete. Alkyne substrate *epi*-**4.30** was tolerated, but only in the absence of water, and 50 mol% of triflimide catalyst salt was required to achieve enone **4.66** in a modest 49% yield over 8 d. Lastly, divinyl cyclopentane *epi*-**4.50** afforded the corresponding hydrindane oCM product **4.67** in a robust 80% yield as assessed by NMR, but due



[a]A dynamic equilibrium involving two diastereomeric hemiacetals was observed for alcohols *cis* to the aldehyde. [b]50 mol% of catalyst was employed and no water was added. [c]NMR yield indicated in parentheses.

Figure 4.3. Scope of the cyclic oCM reaction.

to some decomposition during workup only afforded a 44% yield of isolated material. That reaction required 15 h to consume the substrate, which indicates this is substantially less reactive than the corresponding divinylcyclohexane, despite also not having any hemiacetal content. Taken together, the substrates just described allow access to both isomers of parent hydrazulene **4.58**, hydrazulenes bearing persubstituted carbons **4.62-4.65**, unsaturated enone **4.66**, and the synthetically ubiquitous hydrindane motif in **4.67**.

As just described, the yields for the cyclic oxy-Cope / Michael reaction range from good to essentially quantitative, depending on substrate reactivity, but the diastereoselectivity was also high. The oCM products were all isolated in >19:1 *d.r.* except for the for **4.63 (**3:1 *d.r.*) and **4.67 (**9:1 *d.r.*), where the minor products in all cases correspond to aldehyde stereochemistry, and not that of the ring fusion. The stereochemistry of the ring junction appears to be the kinetic reaction product since diastereomers **4.23** and *epi*-**4.23** gave different products. Also, no isomerization between **4.58** and *epi*-**4.58** was ever observed for either reaction product, even after prolonged reaction times, which further indicates that the reaction conditions are not likely to induce ketone enolization. The stereochemistry adjacent to the aldehyde carbon depends on thermodynamic preference for the aldehyde to occupy the face opposite adjacent ring branching. The preference is perturbed with tricycle **4.63**, likely from destabilization due to steric repulsion by the third ring, and variations in the *d.r.* throughout its reaction and isolation indicate thermodynamic control.

Certain trends are visible within the scope which dictate future considerations in applying the oCM reaction. First, comparison of both reaction time and yield for the diastereomeric pair of vinyl cyclohexanes **4.23** demonstrates the dramatic increase in reactivity for substrates which do not feature the indicated hemiacetal equilibrium. *Epi*-**4.23**, for which no hemiacetal has ever been observed by NMR spectroscopy (in $CDCl_3$, *d*$_6$-DMSO, or CD_3NO_2), reacted in just 1.5 h while canonical substrate **4.23** required days. Two extreme cases reinforce the importance of the hemiacetal equilibrium. Substrates **4.39** and **4.50** (Figure **4.4**) were both entirely unreactive and both displayed little to no aldehyde content by NMR. Olefin substitution also provided a remarkable boost in reactivity despite hemiacetal content, and isopropene **4.26** performed similarly to *epi*-**4.23**. Evidently olefin nucleophilicity improves reactivity, since cyclopentenyl substrate **4.27** was consistently faster than all others. The arenes rearranged slower than alkyl substituted substrates, which may indicate that steric factors impact reactivity. Between the aryl substrates, an

electronic effect is still observed since electron-rich 4-methoxy **4.29** required shorter reaction time than simple phenyl **4.28**. Alkynes are normally excellent functional groups for sigmatropic shifts, but are less reactive in cationic rearrangements. *Epi*-**4.30** was tolerated under more vigorous catalytic conditions, but its *cis* isomer **4.30** was unreactive despite containing plenty of aldehyde content. Only the *trans* isomer of cyclopentane *epi*-**4.50** was tolerated, but took ten times as long as the analogous cyclohexane substrate. In fact, the methyl ether of **4.50**, aldehyde **4.57**, gave only ca. 40-50% yield by NMR over 21 h using the HNO_3 diazepane catalyst salt (known to be good conditions for the cyclic oCM methyl ether reaction – *vide infra*). The latter comparison may indicate increased strain in the medium-size ring intermediate during the reaction. The results clearly indicate the increased reactivity of substrates which do not have hemiacetal content.

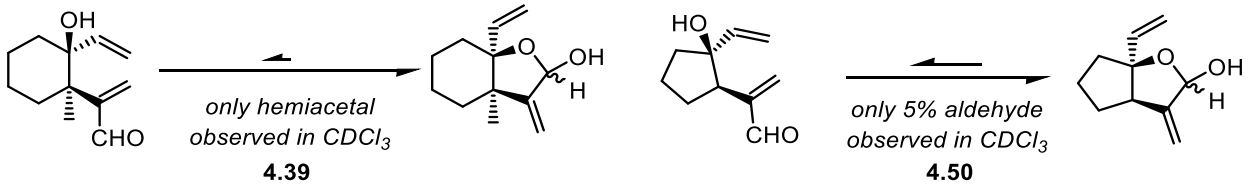


Figure 4.4. Unsuccessful alcohol oCM substrates.

The stereochemistry of the products was primarily determined by NOE correlations, although isomerization experiments were initially used assign hydrazulene products (Figure **4.5**). The production of a unique isomeric perhydrazulene from each epimer of canonical vinyl cyclohexane **4.23** was highly suggestive as to their stereochemical identity. However, the aldehyde stereocenter complicated matters somewhat. Selective ^1H-^1H NMR spectroscopy decoupling was used to identify the coupling constant across the ring fusion in each isomeric product (Figure **4.5A**), but they were remarkably close at 10.7 (*cis*) and 10.5 Hz (*trans*). The chemical shift was actually more informative, based on literature precedent, which suggested that the higher chemical shift of H_a at 3.15 ppm should belong to the *cis* isomer, while the upfield shift of H_e at 2.96 ppm should belong to the *trans* isomer.[68] When isomerically pure hydrazulene **4.58** was treated with aqueous hydroxide in THF, partial isomerization was observed over 6 d from the putative *cis* to *trans* hydrazulene *epi*-**4.58**. The result matches similar experiments in the literature, where similar hydrazulene ketones are known to be close in energy and exhibit only a slight thermodynamic preference in some cases for the *trans* isomer.[68] In fact, it has been shown that the parent hydrocarbon favours the *cis* by 0.7 kcal/mol due to lessened steric and torsional strain.[69] DFT

calculations (Figure **4.5B**), performed by Dr. Gleason, reinforced the idea of a slight 1.2 kcal/mol thermodynamic preference for the *trans* isomer and provided insight into the aldehyde configurational preferences. For each hydrazulene isomer, structures with the aldehyde oriented opposite the adjacent ring branching were lower in energy than their epimers by very similar 1.8-2.0 kcal/mol energies. Efforts to acquire direct evidence for stereochemistry were frustrated due to lack of signal in 2D NOESY experiments.

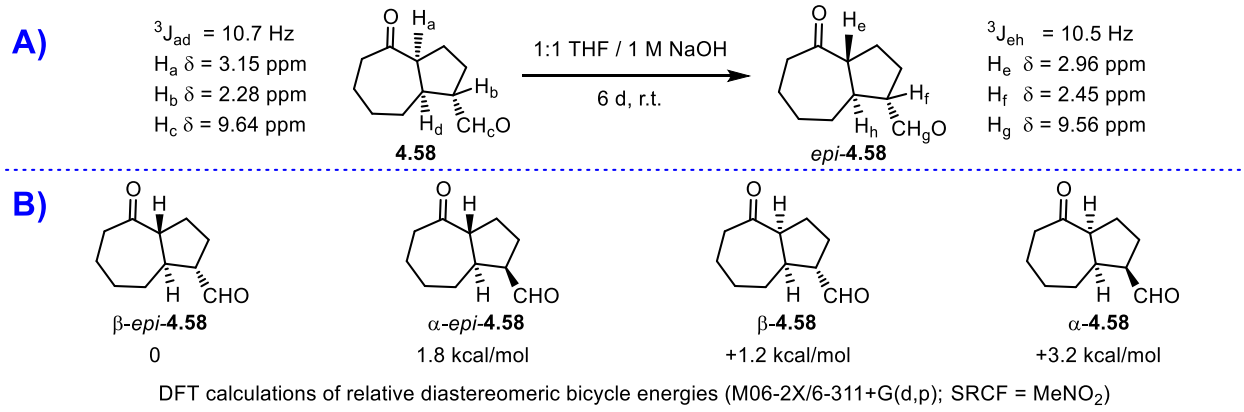


Figure 4.5. (**A**) Isomerization between hydroazulene diastereomers. (**B**) DFT energies of isomeric hydrazulenes.

Eventually, one-dimensional selective nOe experiments were able to clearly confirm the expected stereochemical relationships for most oCM products (Figure **4.6**). *Cis* hydrazulene **4.58** displayed correlations between the aldehyde proton and those at the ring fusion, while the *trans* isomer *epi*-**4.58** possessed a correlation between the ketone and aldehyde α-protons. The nOe data confirm the chemical shift predictions for **4.58** / *epi*-**4.58**. It was found that substituted hydrazulenes **4.62**, **4.64**, and the major product of **4.65** all possessed key NOE correlations from substituent protons to the aldehydes and, critically, to the proton at the ring fusion. An NMR sample enriched in the minor isomer of **4.65** was used to demonstrate correlations not to the aldehyde proton, but rather to the ring fusion proton and the aldehyde α-proton, providing evidence that the minor isomers are in fact the aldehyde epimers. Both epimers of **4.63** were also isolated, which was especially critical for this tricycle due to the low 3:1 *d.r.* obtained and additional stereocenter. As shown, various correlations about the structure confirm that the major isomer possess the same relative aldehyde orientation as the other products. Finally, enone product **4.66** also appears to maintain the same aldehyde orientation relative to the cycloheptane, as determined by a correlation between the aldehyde and ring fusion proton.

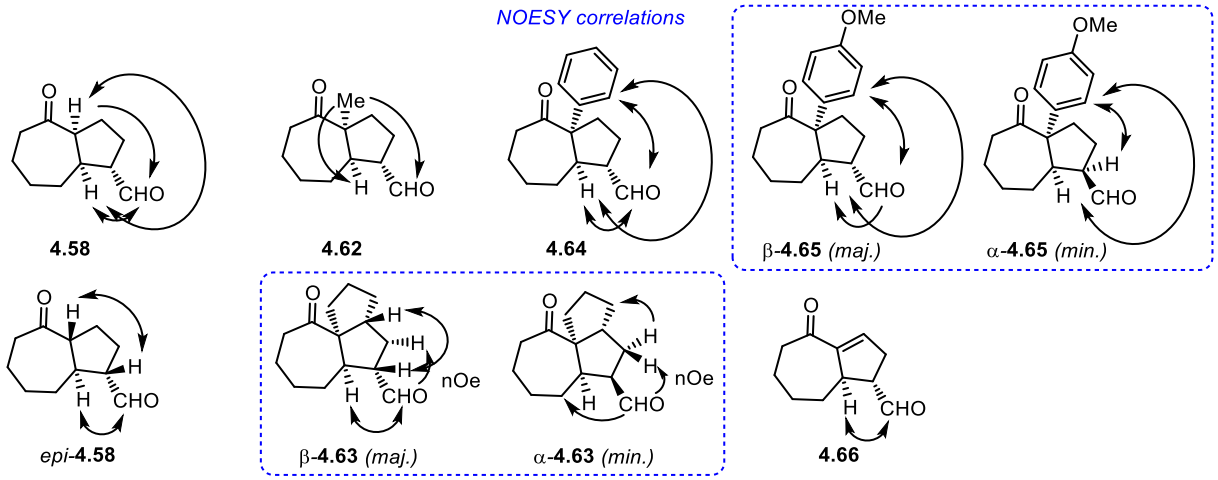


Figure 4.6. NOESY correlations for oCM hydrazulene products.

The oCM products in all cases are consistent with chair-like transition states, shown in Figure **4.7**. Following condensation, the iminium formed from substrate **4.23** can exist in one of two possible conformations, **4.68** or **4.69**, but only the latter conformation would be productive in the oCM reaction. A *trans*-decalin transition state arising from intermediate **4.69** would provide *cis*-hydrazulene **4.70** provided no bond rotation occurs in a putative Cope intermediate. That bond rotation in that hypothetical medium ring is known to be very energetically demanding, and the lack of rotation observed with cyclic aza-Cope / Mannich reactions provides further support that this scenario in the oCM is unlikely.[70] The iminium formed from *epi*-**4.23** could exist in conformations **4.71** or **4.72**, but a reaction proceeding from **4.71** would give rise to the same product as substrate **4.27**, which was not observed. Therefore, conformation **4.72**, which orients two substituents in an equatorial position rather than two axial, must be the reactive conformation.

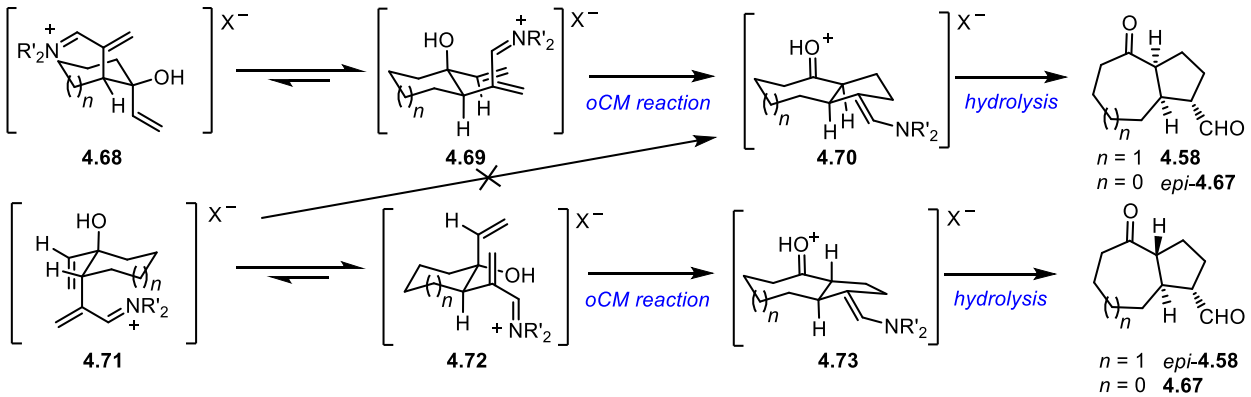


Figure 4.7. Conformations leading to oCM bicyclic products from *cis* (top) and *trans* (bottom) substrates.

Conformer **4.72** would give rise to *trans* intermediate **4.73** and subsequently *trans*-**4.58**. The stereochemistry for the hydrindane oCM product **4.67** is based off that model, since NOESY determination failed in that case. Based on the data, the stereochemistry of cyclic oCM products appears predictable from the known relative substrate geometry.

With *cis* and *trans* enals **4.45**, for which substantial aldehyde content was observed, attempted oCM reaction led primarily to tetrahydrofuran products **4.74** and **4.75** via oxa-Michael addition (Figure **4.8**). Intriguingly, both olefin isomers gave rise to initial mixtures dominated by product isomer αMe-**4.74** (87:13 and 55:45 respectively from *cis*- and *trans*-**4.45**), which slowly isomerized to βMe-**4.75** in 71% yield from *cis*-**4.45** or 42% yield from *trans*-**4.45**, as determined by NMR. The stereochemistry of the oxa-Michael products was determined using coupling constants. The two large coupling constants of 9.1 and 10.1 Hz displayed by H^b in αMe-**4.74** clearly indicate *pseudo*-trans-diaxial relationships with adjacent protons H^a and H^c. Proton H^a is clearly equatorial, since it possesses no other large coupling constant, only two smaller 5-6 Hz couplings, while H^x in βMe-**4.75** does possesses a second large coupling constant and is clearly axial. The only structure befitting the large 9.3 Hz and intermediate 5.9 Hz coupling constants is inverted with respect to the relative methyl geometry. Minor epimers for each product were not observed, likely due to reinforced aldehyde facial preference by methyl steric interactions.

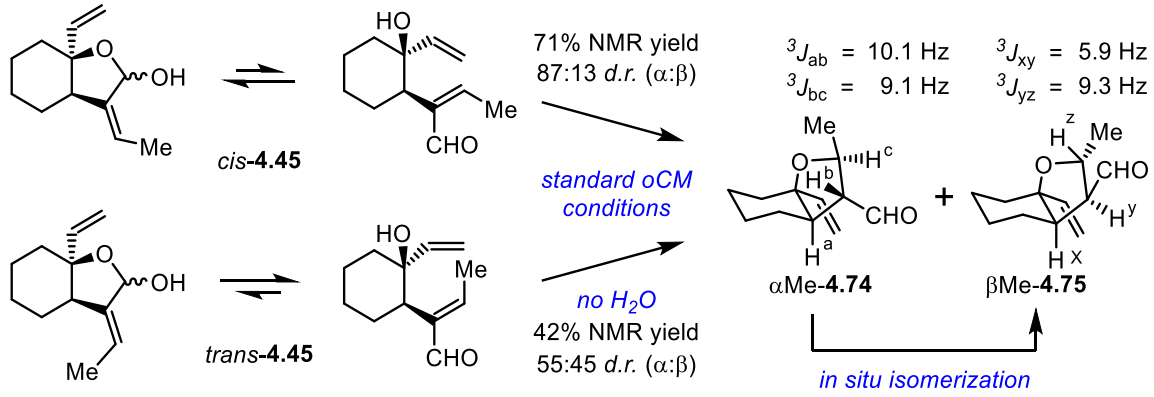


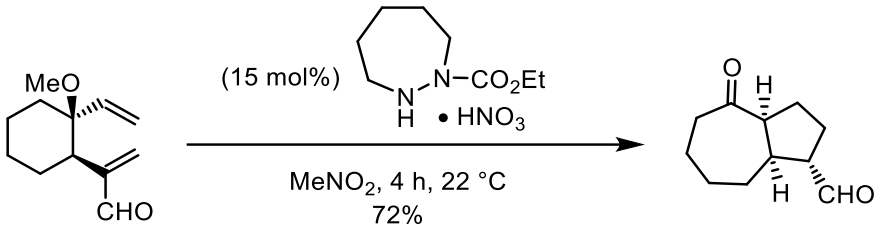
Figure 4.8. Unsuccessful alcohol oCM substrates due to alternative oxa-Michael reactivity.

Oxa-Michael products were not observed with the other substrates described here, but were identified as problematic in the organocatalytic Cope screening and precluded the use of alcohol solvents in that reaction.[60b] Oxa-addition was thought to be reversible, as evidenced by the *in situ* conversion of αMe-**4.74** to βMe-**4.75**. Oxa-Michael reaction may be an unobserved off-cycle

equilibrium in all oCM reactions which simply becomes favourable with 1-Me substrates. The stable and isolable products suggest that oxa-Michael addition is not the mode of decomposition observed on scaling the oCM reaction. Furthermore, the apparent convergence of product isomers to favour αMe-**4.74** clearly implies enal isomerization which, in combination with reversibility of the oxa-Michael, may indicate future use for direct use of mixtures of isomers in similar reactions.

4.1.6. *The Cyclic Methyl Ether oxy-Cope / Michael Reaction*

Donald Campbell of our group worked on developing a methyl ether variant of the cyclic oCM reaction in parallel to the work described in this Chapter. Re-optimization of conditions in that reaction identified the nitric acid salt of the catalyst in $MeNO_2$ as providing short reaction times and high yields. As one example, the methyl ether of substrate **4.23** rearranged in just 4 h to hydrazulene **4.58** in 72% yield (Scheme **4.12**). The current substrate scope of the ether reaction largely resembles that described in the preceding section, although methyl protection of the alcohol allowed the use of certain substrates which were dominated by lactol content for the alcohols. Two examples are a cycloheptane OMe analogue of **4.23** and the OMe analogue of 3-Me substrate **4.39**, both of which displayed no free aldehyde content as the corresponding alcohols. Importantly, the ether reaction was known to us when setting out to test the mechanism of the oCM reaction using linear substrates, a point which will become relevant in later sections.



OMe-**4.23** **4.58**

Scheme 4.12. Donald Campbell's cyclic methyl ether oCM reaction.

4.2.1. *Designing an oxy-Cope / Michael Mechanism Test*

The possible mechanisms for the oCM reaction mimic those discussed for the aza-Cope / Mannich and Prins-pinacol reactions. It was briefly mentioned during the reaction development that the isoprenyl cyclohexane substrate was subjected to the triflic acid salt of an N-Me variant of the catalyst to test for stability to the catalyst acidity. Having shown the impressive reactivity of the isoprenyl substrate in the oCM reaction, the fact that no reaction occurred with the N-Me catalyst salt provides a good control reaction, since lack of reaction indicates that general acid

catalysis is not occurring and clearly suggests rather that hydrazide iminium catalysis is operational. After hydrazide catalyst condensation to structure **4.76**, two main pathways are possible (Figure **4.9**). Cope sigmatropic shift could occur, either in asynchronous concerted or stepwise fashion, to give the enol and isomeric unsaturated hydrazide iminium in **4.77** which may then react by conjugate addition. Alternatively, distal olefin 1,4-addition could lead to cationic intermediate **4.78**, especially if positive charge is stabilized by substitution (eg. R = alkyl / aryl), which might rearrange in a semi-pinacol [1,2]-alkyl shift to **4.79** rather than complete the Cope process to **4.77**. Both pathways lead to the same product **4.79**, and in the case of cyclic examples would give the same *cis* geometry of the bicycle generated.

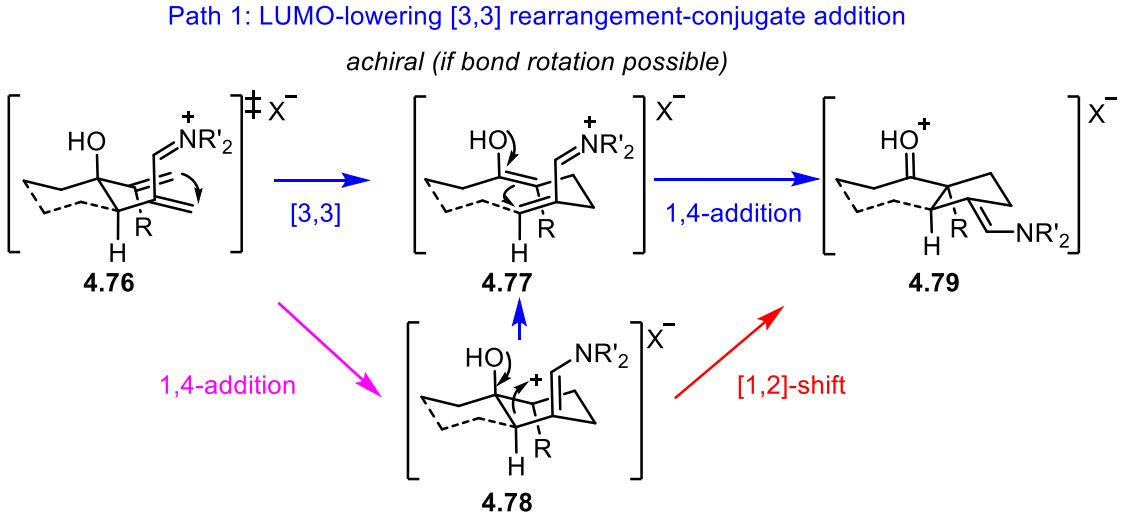


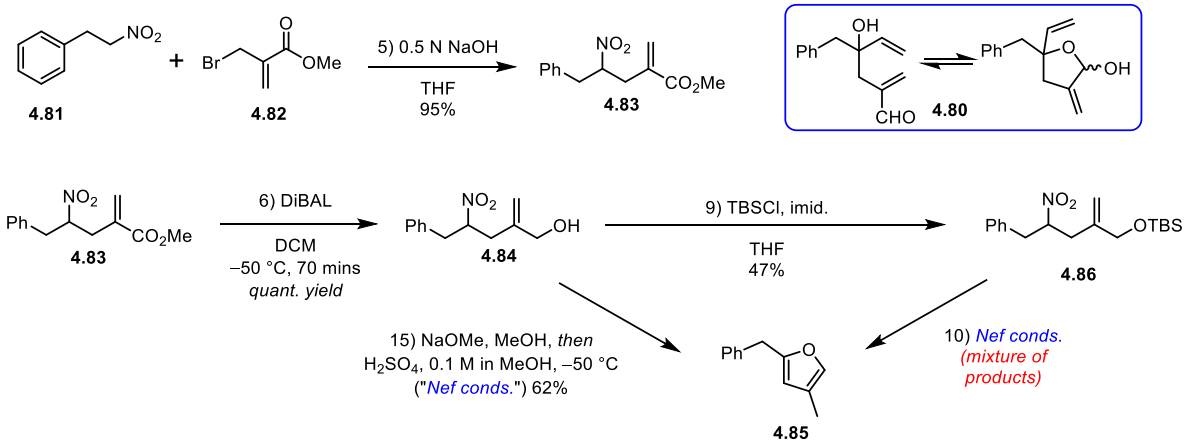
Figure 4.9. Possible mechanisms for the oCM reaction.

The two pathways could conceivably be differentiated by the loss of stereochemical information in intermediate **4.77**. In theory, enantio-enriched starting material could produce racemic oCM product via double bond rotation since the structure of **4.77** is not itself chiral. In contrast, a semi-pinacol mechanism would retain the stereochemical information. As mentioned above for cyclohexane substrates, the loss of chiral conformation in **4.77** by rotation through the ring for cyclic structures may be difficult at ambient temperature without tautomerization, and some unsaturated medium rings are known to maintain chiral conformation.[70] Therefore, enantioenriched substrates not bound on a cyclic ring were required to distinguish these pathways, similar to the tests used by the Overman group. An acyclic Cope intermediate **4.77** could lose its

chiral conformation by simple double bond rotation and thereby erode any *e.e.* input, provided that subsequent bond formation is a slower process. Alternatively, the stereospecific semipinacol rearrangement from **4.78** would preserve *e.e.* through the reaction.

4.2.2. *Synthesis of Acyclic oxy-Cope / Michael Alcohol Substrates*

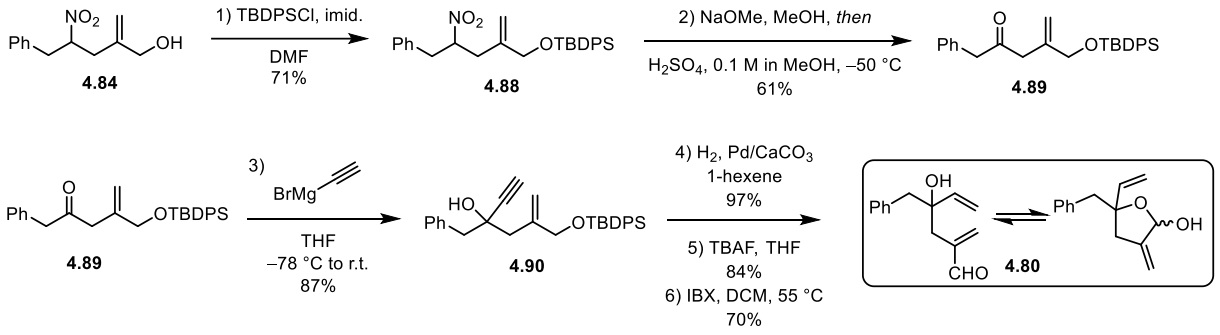
As alluded to, linear substrates were desired to not only expand the scope of the oxy-Cope / Michael reaction, but also to test the mechanism of the novel cascade reaction sequence. Hexadiene **4.80** was designed bearing an aldehyde at the 2-position for catalysis, and a simple 4-benzyl tag to provide a ketone rather than a new aldehyde after oCM reaction. To this end, a straightforward, albeit lengthy, synthesis of substrate **4.80** was developed (Scheme **4.13**) which was intended to access an advanced intermediate ketone for scope diversification as done with the cyclohexane-based family of cyclic substrates. This sequence began with coupling known compounds nitroethylbenzene **4.81** and allyl bromide **4.82** in the presence of sodium hydroxide to afford nitroalkane ester **4.83** in 95% yield.[71] Nitro-ester **4.83** was then reduced with DIBAL to provide nitro-alcohol **4.84** in quantitative yield, but a subsequent Nef reaction surprisingly afforded solely methylfuran **4.85** in 62% yield. The TBS-protected silyl ether **4.85** was prepared in 47% yield from the alcohol using TBSCl and imidazole. However, Nef reaction with **4.86** afforded an unhelpful 33:13:53 mixture of TBS-protected and deprotected ketones along with furan **4.85** again. Clearly a protecting group more stable to acid was required.



Scheme 4.13. Initial attempts toward a benzyl-tagged linear alcohol vinyl substrate.

TBDPS silyl ether **4.88** was therefore prepared from alcohol **4.84** with TBDPSCl in DMF in 71% yield, and this silyl ether survived the acidic Nef reaction conditions to afford ketone **4.89** in

61% yield. Only metalated alkynes could be added to ketone **4.89**, and ethynylmagnesium bromide addition provided propargylic alcohol **4.90** in 87% yield. With alcohol **4.90** in hand, conditions were explored to effect controlled Lindlar semihydrogenation of the alkyne. Use of 1-hexene, a cheap sacrificial alkene, as a solvent[72] gave consistent clean semi-hydrogenation to the corresponding olefin in an excellent 97% yield. Following hydrogenation, TBAF deprotection afforded the diol in 87% yield and IBX oxidation in refluxing DCM provided a robust 70% yield of substrate **4.80**, which existed in equilibrium with its hemiacetals.



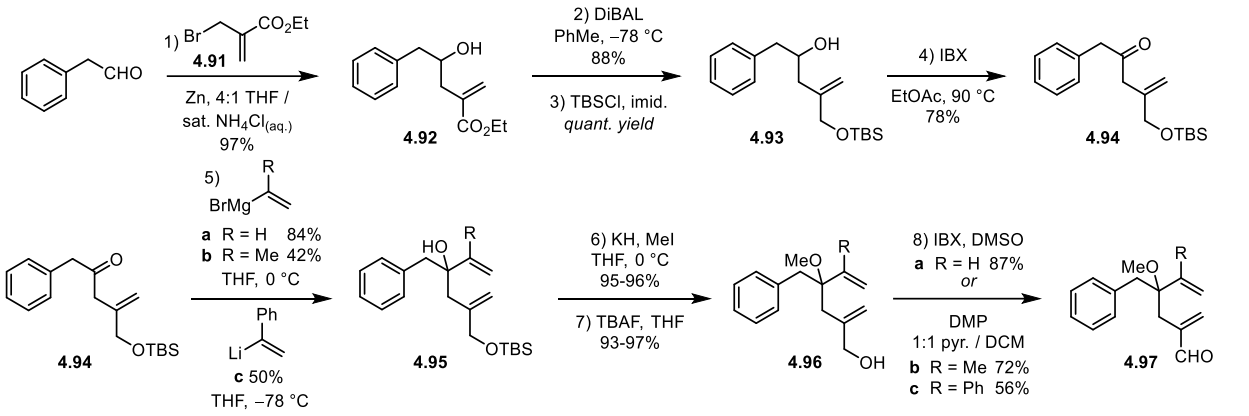
Scheme 4.14. Initial synthesis of benzyl-tagged linear alcohol vinyl substrate.

Unfortunately, early efforts to effect the catalytic oCM with substrate **4.80** were frustrated by facile acid-mediated decomposition. We hypothesized that, since decomposition rather than lack of reactivity was observed, re-engineering the substrate may be advantageous. The idea was to avert any potential for π-cation stabilization of transition states or intermediates which might facilitate other reaction pathways. We thus prepared substrates bearing a methylcyclohexane tag in place of the 4-benzyl substituent, maintaining ketone reaction products and removing the neighbouring π functionality. For concision, the synthesis of these substrates is not discussed here (see Chapter **5** for their preparation), since the compounds were similarly unstable to oCM conditions as Ph substrate **4.80**, suggesting that the aromatic tag was not problematic.

4.2.3. *Synthesis of Racemic Acyclic Methyl Ether Substrates*

Given Donald Campbell's success using methyl or benzyl ethers to successfully effect oCM rearrangement using substrates based on cyclohexane and -heptanes, the synthesis of acyclic methyl ether substrates was undertaken. The dramatic increase in cyclic substrate reactivity with C5 alkene substitution indicated that acyclic substrates bearing substitutents might be more reactive. A revised synthesis was therefore devised to access substrates **4.97a-c** (Scheme **4.15**).

Reminiscent of the strategy for cyclic substrates, the methyl ether linear substrates were intended to diverge from common ketone intermediate **4.94**. Ketone **4.94** was prepared on multi-gram scale in 4 steps from phenylacetaldehyde, starting with zinc-promoted Barbier reaction with allyl bromide **4.91** to furnish secondary alcohol **4.92** in 97% yield. Ester **4.92** was then reduced with DIBAL in 88% yield. The resulting primary alcohol was protected with TBSCl, and IBX oxidation was conducted to provide desired ketone intermediate **4.94** in 78% yield. As before, inverse addition of Grignard reagents vinyl- and isopropenylmagnesium bromide was more effective, and gave a high 84% yield of alcohol **4.95a** along with a useful 42% yield of **4.95b**, along with 34% recovered ketone **4.94**. Notably, even α-lithiated styrene only afforded a modest 50% yield of **4.95c**, which reflected the estimated conversion since a 1:1 product / ketone ratio was observed in the crude mixture. The similarly troublesome reactivity of ketone **4.94** as compared to cyclohexanone **4.17** and TBDPS ether **4.89** indicates either moderate steric encumbrance by the allyl $OSiR_3$ moiety or that deprotonation is competing with addition. The fact that vinylcerium reagents did not facilitate addition in other cases suggests that steric congestion is a major factor, especially considering the unanimous success of the smaller acetylide additions.



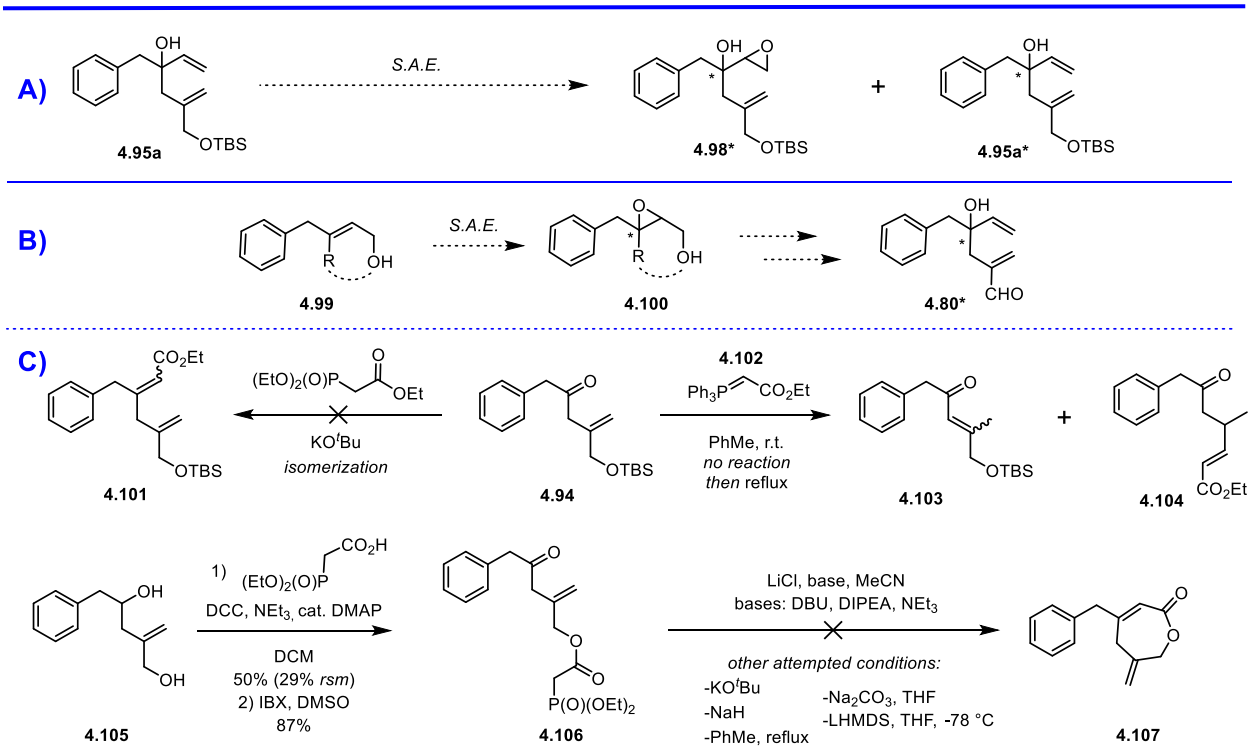
Scheme 4.15. Preparation of linear methyl ether substrates.

Nevertheless, the useful synthetic quantities of alcohols **4.95a-c** thus obtained were all smoothly methylated in 95-96% yield and deprotected with TBAF in 93-97% yield. Oxidation of divinyl alcohol **4.96a** with IBX in DMSO provided an 87% yield of methyl ether divinyl substrate **4.97a**. The conditions employed for final oxidation of **4.96b** and **4.96c** were more particular, since both IBX in DMSO and PCC in DCM caused a significant amount of Cope rearrangement to the corresponding enol ethers. Facile thermal Cope shift provided an additional challenge in isolating and using the substrates. Use of DMP in 1:1 pyridine / DCM allowed oxidation without any Cope

products observed in the reaction mixture, then the use of NEt_3-neutralized silica gel was useful to prevent further rearrangement during chromatography, and heat was strictly avoided when removing solvents. Careful handling afforded 72% yield of isopropenyl **4.97b** and 56% yield of styryl **4.97c**, which were used within hours of their isolation in the oCM reaction. It should be noted that no such issues were encountered with the simple vinyl substrate, which could be stored in the freezer for months and did not rearrange at room temperature or with routine mild heating. The use of the linear substrates in the oCM reaction will be discussed in Section **4.2.5**.

4.2.4. *Synthesis of Enantio-Enriched Acyclic Methyl Ether Substrates*

In order to conduct a mechanism test reminiscent of Overman's aza-Cope / Mannich reaction, enantio-enriched substrates were required. Sharpless asymmetric epoxidation (SAE), which could potentially provide kinetic resolution to enrich substrates such as **4.95a** (Scheme **4.16A**) by selectively producing one enantiomer of chiral epoxide **4.98***, failed on this substrate. In each case the reaction only occurred to a minor extent on the less encumbered 1,1-disubstituted olefin, and only after at least one week at –20 °C for the epoxidation or at room temperature for the dihydroxylation, which was also attempted. The failure to epoxidize was not unexpected since SAE is known to be incompatible with tertiary alcohols.



Scheme 4.16. Olefination strategy toward an enantioselective epoxidation substrate.

Direct asymmetric synthesis of an enriched substrate was then contemplated, conceptually based around an asymmetric epoxidation on a 1,1',2-trisubstituted olefin adjacent to a primary allylic alcohol or cyclized lactone represented by **4.99** (Scheme **4.16B**). Early attempts to achieve the stereoselective synthesis of the trisubstituted olefin employed Horner-Wadsworth-Emmons (HWE) or Wittig olefinations (Scheme **4.16C**), either in an inter– or intramolecular fashion. HWE reaction with triethylphosphonoacetate gave rise only to olefin isomerization and failed to produce any desired enoate **4.101**. Stabilized Wittig reaction of ethyl (triphenylphosphoranylidene)acetate **4.102** with ketone **4.94** gave rise only to alkene isomerization to **4.103** upon heating, including aldehyde formation and subsequent olefination at the newly formed carbonyl to produce enoate **4.104**. An intramolecular sequence was next explored starting from diol **4.105**, via DCC coupling with diethylphosphonoacetic acid in 50% yield and IBX oxidation to provide phosphonate ester **4.106** in 87% yield. However, exposure of **4.106** to a variety of bases led only to decomposition and isomerization products rather than lactone **4.107**.

An alternative strategy toward a SAE allyl alcohol such as **4.112** was then considered, relying on net alkyne hydroalkylation of **4.109** (Scheme **4.17**). Protection of alkynyl alcohol **4.108** as a TBDPS silyl ether and subsequent treatment of the protected alkynyllithium, generated from treatment with *n*-BuLi, with paraformaldehyde provided propargyl alcohol **4.109** in 82% yield over 2 steps. A recently reported modification[73a] of Hoveyda's hydrocupration-borylation reaction[73b-c] was then employed in a tandem sequence incorporating palladium-catalyzed cross-coupling with benzyl bromide. This sequence afforded desired allylic alcohol **4.111** in good 65% yield after separation from regioisomer *iso*-**4.111**, which was isolated in 14% yield. Allylic alcohol **4.111** was treated with *m*CPBA in DCM to obtain a racemic standard of epoxide **4.112** in 60% yield. Conditions were then explored to provide acceptable level of enantioselectivity in the Sharpless asymmetric epoxidation[74] of allylic alcohol **4.111** (Scheme **4.17**, Table **4.3**). Exposure of 1 g of **4.111** to 5 mol% Ti(IV) and 15 mol% *L*-DIPT at –20 °C afforded epoxide **4.112*** in just 66% *e.e.* and 85% yield. A drop in *e.e.* from 66% to 55% was observed when 4 g of **4.111** was instead used. Increasing the Ti(IV) loading to 15 mol% and *L*-DIPT loading to 18 mol%, while decreasing the temperature slightly to –30 °C, resulted in an improved 72% *e.e.* with 3 g of **4.111**. Extrapolating from this trend, the loadings were further increased to 50 mol% in Ti(IV) and 60 mol% of *L*-DIPT, while the temperature decreased to –40 °C, but the *e.e.* stayed roughly the same at 74% using 5 g of substrate. The end purpose of the substrates, a simple mechanism test for

faithful transfer of stereochemistry or erosion in the oCM reaction, obviated the need for higher enantioselectivity. It should be noted that the entire sequence until **4.112*** was readily conducted on multi-gram scale, with as much as 7 g being used in the hydroboration reaction.

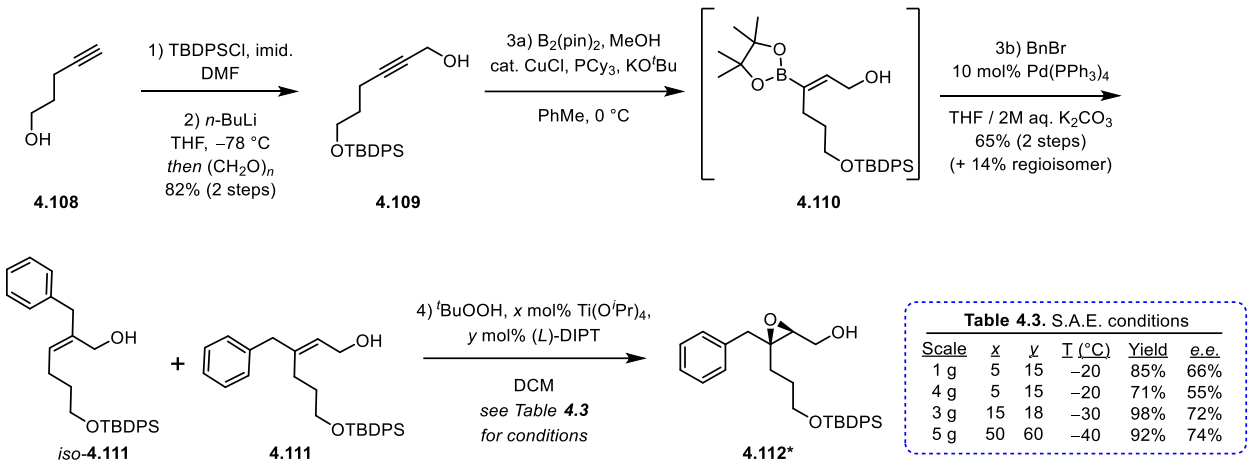
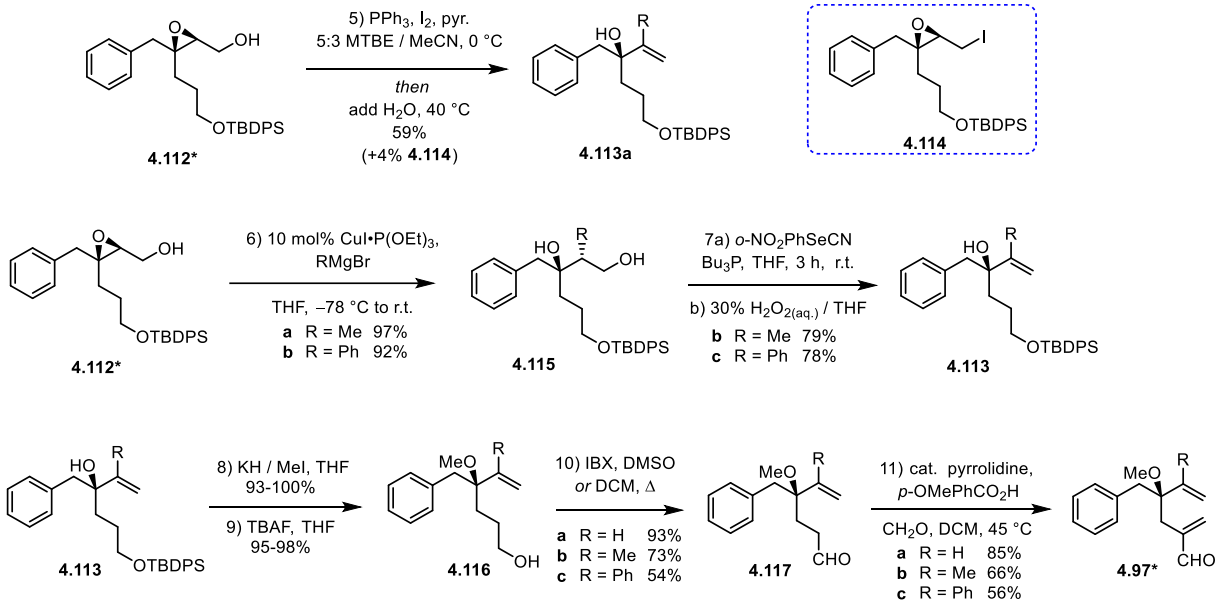


Table 4.3. S.A.E. conditions

Scale	*x*	*y*	T (°C)	Yield	*e.e.*
1 g	5	15	–20	85%	66%
4 g	5	15	–20	71%	55%
3 g	15	18	–30	98%	72%
5 g	50	60	–40	92%	74%

Scheme 4.17. Final route to an enantio-enriched epoxide.

Reductive opening of epoxy alcohols such as **4.112** have been studied and applied in previous total syntheses, frequently via conversion to the primary iodide.[75] A variety of conditions were first attempted to reduce Appel reaction product iodide **4.114** (Scheme **4.18**), including $HSnBu_3$ / AIBN in refluxing toluene, NaI in refluxing acetone, Mg or Zn in THF, and Zn in THF / sat. NH_4Cl, but they elicited either unproductive decomposition or excessive byproduct formation. Although some alkene was always formed when preparing the iodide, especially upon concentration after washing out imidazole and presumably due to an iodide source such as triphenylphosphine diiodide, the mixtures became complex and recovered yields were always poor. A similarly complex result was obtained from treating the iodide with additional PPh_3 / I_2 after washing out imidazole or treating with iodine in MeCN. However, a reported two-step, one-pot protocol employing triphenylphosphine, iodine, then water in a critical second step,[75e] furnished tertiary alcohol **4.113a** in 59% yield along with a 4% yield of the iodide. Grignard reagents methylmagnesium bromide and phenylmagnesium bromide could also be used to open epoxide **4.112***, with catalytic quantities of Nishizawa's purified copper iodide - triphenylphosphite complex,[76] and the primary alcohols **4.115** thereby obtained in respective 97 and 92% yields were subjected to Greico's elimination[77] to provide tertiary alcohols **4.113b-c** in 78-79% yield.



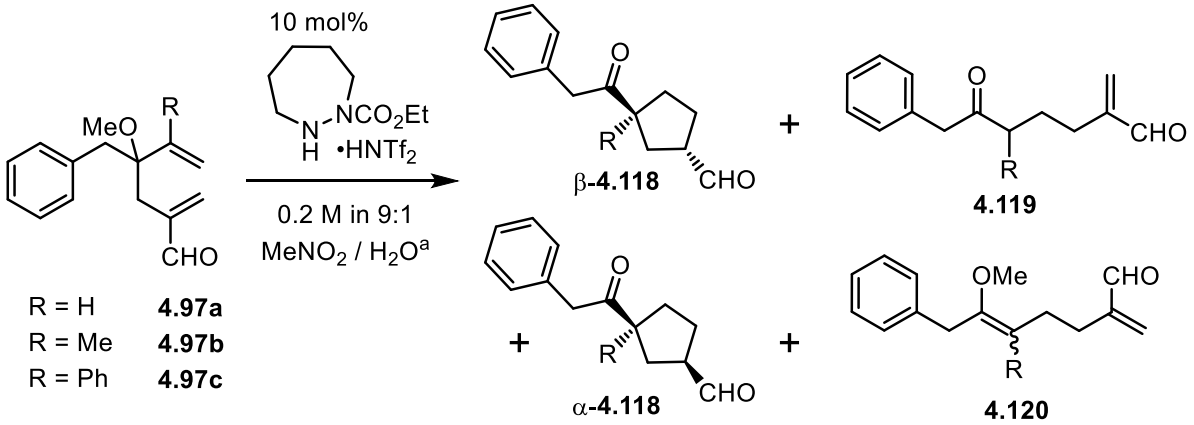
Scheme 4.18. Final route to enantio-enriched linear methyl ether substrates.

Alcohols **4.113a-c** were rapidly elaborated to substrates **4.97a-c***, starting with tertiary alcohol methylation in >93% yield, followed by silyl ether TBAF deprotection to afford primary alcohols **4.116a-c** in 95-98% yield, and subsequent primary alcohol IBX oxidation to provide aldehydes **4.117a-c** in 54-93% yield. Finally, Pihko organocatalytic methylenation was employed to afford 56-85% yield of the desired substrates. The one caveat to the sequence was the aforementioned ease of Cope shift for **4.97b-c***, since enol ether Cope products were observed in the methylenation reaction mixture itself. The mixtures were still competent in the oxy-Cope / Michael reaction, and were still suitable for the mechanism test as will be discussed in the following section.

4.2.5. *Development of the Acyclic oxy-Cope / Michael Reaction*

The linear substrates were far more challenging to use in the oCM reaction and the free alcohols proved in many cases unstable to the reaction conditions. The first substrates tested, benzyl tagged alcohol **4.80** and the corresponding cyclohexyl-tagged substrates, experienced near-total decomposition under all conditions, affording at most ca. 5% yield as assessed by NMR. Various salts of the hydrazide catalyst, including HCl, HBF_4, HOTf, $HClO_4$, and $HNTf_2$, were screened in combination with several solvents including MeCN, $MeNO_2$, $CHCl_3$, THF, 1,4-dioxane, Et_2O, EtOAc, PhMe, and DMF. Thermal rearrangement was possible in PhMe, but the reactions gave mixtures of oxy-Cope and oxy-Cope / aldol addition products in all cases.

The acyclic benzyl-tagged methyl ether vinyl substrate **4.97a** was found to require days to rearrange under optimized catalytic conditions from the cyclic reactions. Both HNO_3 and $HNTf_2$ catalyst salt systems in $MeNO_2$ were initially employed with substrate **4.97a**. Unfortunately, they afforded only low yields over several days while increasing the catalyst loading at room temperature led to byproducts such as oxy-Cope / aldol products dominating the reaction. However, warming the reactions slightly to 55-60 °C in $MeNO_2$ in the presence of 10 mol% of the triflimide catalyst salt induced conversion of **4.97a** to oCM cyclopentane products **4.118** in < 24 h



Entry	Substrate[b]	% e.e.	Temp. (°C)	Time (h)	% Yield[c] 4.118	4.119	4.120	α 4.118 % e.e.[d]	β 4.118 % e.e.[d]
1	**4.97a**	0	55	24	(60)	(7)	0	1	0
2	**4.97a***	73	59	20	63	7 (7)	0	13	14
3	**4.97b**	0	22	1.5	61 (80)	0	0	2	2
4	**4.97b***	74	22	1.5	(78)	0	0	1	3
5	**4.97c**	0	22	2	71 (85)	0	0	1	3
6	**4.97c***	74	22	1	73[e] (81)	0	0	2	1
7	**4.97a**[f]	-	55	24	0	(7)	(27:7)	-	-
				96	0	(40)	(21:11)		
				192	0	(64)	(2:6)		
8	**4.97a**[g]	-	55	96	0	(34)	0	-	-
9	**4.97b**[f,h]	-	22	144	0	0	(62:38)	-	-

[a]These standard conditions were used unless otherwise noted. Scale was 0.25-0.55 mmol in substrate except test reactions which used 24 mg. [b]Me and Ph substituted substrates were used as mixtures with up to 20% already rearranged to enol ethers **4.120**. Yields are based on total input material. [c]Yields of isolated material. Parentheses indicate yield assessed by ^1H NMR spectroscopy using mesitylene as an internal standard. The aldehyde epimer ratio in the cyclopentanes was always ~1:1. [d]Yields of *cis*/*trans* olefins. [d]Product *e.e.* was assessed following conversion to the methyl esters as shown in Scheme **4.19**. [e]Yield taken after air oxidation of pure aldehyde to carboxylic acid. [f]No catalyst or acid used. [g]N-Me catalyst used. [h]In $CDCl_3$.

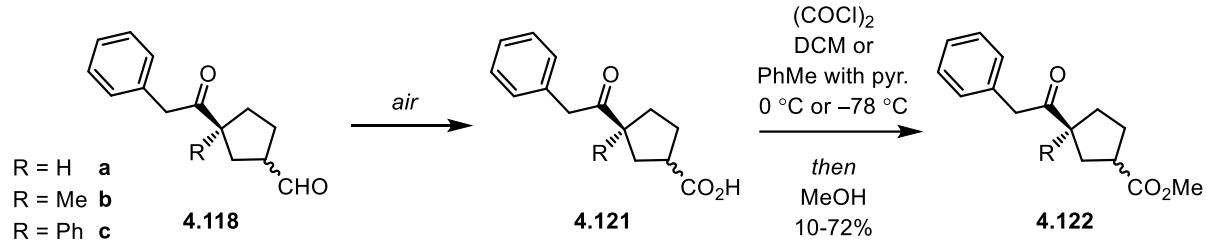
Table 4.4. Development of the linear oCM reaction.

(Table **4.4**, entries **1**-**2**). Identical yields were observed by NMR on 30 or 100 mg scale, 60% oCM product **4.118** along with 7% oxy-Cope product **4.119**, and a 70% combined yield of products was isolated. A control reaction using the same conditions without catalyst or acid produced 39% conversion in 24 h to a mixture of oxy-Cope products consisting of the intermediate enol ethers **4.120** and ketone **4.119** in a 27:7:7 NMR ratio. The mixture evolved over 8 days to a mixture with minimal Cope enol ethers, 64% NMR yield of oxy-Cope ketone **4.119** (entry **7**). A second control reaction using N-Me catalyst (entry **8**) slowly produced a low yield of oxy-Cope product over days, but no oCM or enol ethers were observed in the reaction mixture, indicating enol ether cleavage is fast at this temperature and under these acidic conditions.

Substituted olefin methyl ethers **4.97b-c** were much more reactive, as already mentioned, and they were in fact almost too reactive to prepare or handle. Although very little Cope rearrangement occurred during DMP oxidation for the racemic compounds, 8-9% of each was found to have shifted upon oCM reaction setup within hours, and rearrangement was 10% higher in the enantioenriched material. These partly rearranged mixtures proved fully competent in the reaction (Table **4.4**, entries **3**-**6**) and all elicited very similar 78-85% NMR yields of aldehydes **4.118** as ~1:1 mixtures of epimers in just 1-2 h under standard triflimide oCM conditions. The lower temperatures required and shortened reaction time of <2 h for **4.97b-c**, as compared to >20 h with **4.97a**, mimics the difference in reactivity witnessed with the cyclic substrate series. Trace Cope / oxy-Cope products were observed in the final reaction mixtures, but these were observed throughout the reaction, indicating they may be competent intermediates. Isopropenyl enal **4.97b** was found to rearrange uncatalyzed at room temperature, producing inseparable mixtures of enol ethers and starting material. Cope shift occurred both on standing neat and at room temperature in $CDCl_3$ over 6 d in 95% conversion (entry **9**). In contrast, styrenyl enal **4.97c** did not completely convert on standing, even after weeks, but this preemptive reactivity remained a nuisance.

An important caveat to the linear oCM reaction concerns the aldehyde product stabilities. In some cases, oxidation of the aldehyde to carboxylic acid was sufficiently rapid at room temperature, even in solution, to hinder HPLC analysis. In one case with styryl oCM product, oxidation precluded an accurate calculation of yield until it was fully oxidized (Table **4.4**, entry **6**). Therefore, purified samples of each oCM product from both racemic and enriched substrates were allowed to passively oxidize on the benchtop exposed to air to provide carboxylic acids **4.121a-c** (Scheme **4.19**). Samples of the acids were then esterified by treatment with $(COCl)_2$ in

DCM over ice or pyridine / PhMe at –78 °C and subsequent addition of MeOH to provide methyl esters **4.122a-c** in 10-72% yield.



Scheme 4.19. Conversion of linear oCM products to methyl esters for HPLC analysis.

Methyl esters **4.122a-c** from both racemic and enantio-enriched starting materials were then assessed by analytical chiral HPLC. The enantioenriched substrates all lost substantial *e.e.* during oCM reaction. Substituted substrates **4.97b-c*** were both reduced from 74% *e.e.* to racemic product, while vinyl substrate **4.97a*** *e.e.* was substantially reduced from 73% to 13-14% *e.e.* The results from **4.97b-c*** are unsurprising due to their facile thermal Cope rearrangement and apparent competence of Cope intermediates in converting to oCM products. More surprising is the incomplete erosion of *e.e.* in **4.97a***, the significance of which will be discussed later.

4.2.6. *Mechanism of the oxy-Cope / Michael Reaction*

To gain insight into the energetics of each pathway, DFT calculations were performed by Dr. James Gleason using simple ammonia as a catalyst surrogate. No conjugate addition-pinacol pathways were identified, and only the stepwise Cope reaction / Michael addition was found with the isopropenyl substrate (Figure **4.10**). An associative transition state **4.124**, 14 kcal/mol higher in energy than iminium **4.123**, is predicted similar to the simple organocatalytic Cope reaction. Transition state **4.124** collapses to shallow-energy cationic intermediate **4.125**, 3.5 kcal/mol below the transition state. The methyl-stabilized cationic intermediate is only 0.4 kcal/mol below the energy of the transition state for completing the [3,3] shift **4.126**. The corresponding vinyl substrate would likely produce a less stable cationic intermediate and might be expected to proceed via a concerted [3,3] shift. Once the Cope shift is complete, giving intermediate **4.127** 13.9 kcal/mol below second transition state, the 9.4 kcal/mol barrier for Michael addition shown by transition state **4.128** is predicted to be comparably low. The calculation predicts that the Cope shift should remain the rate-determining step in the oxy-Cope / Michael. Finally, though not shown, catalyst hydrolysis would give the dicarbonyl oCM product far lower in energy than Michael adduct **4.129**.

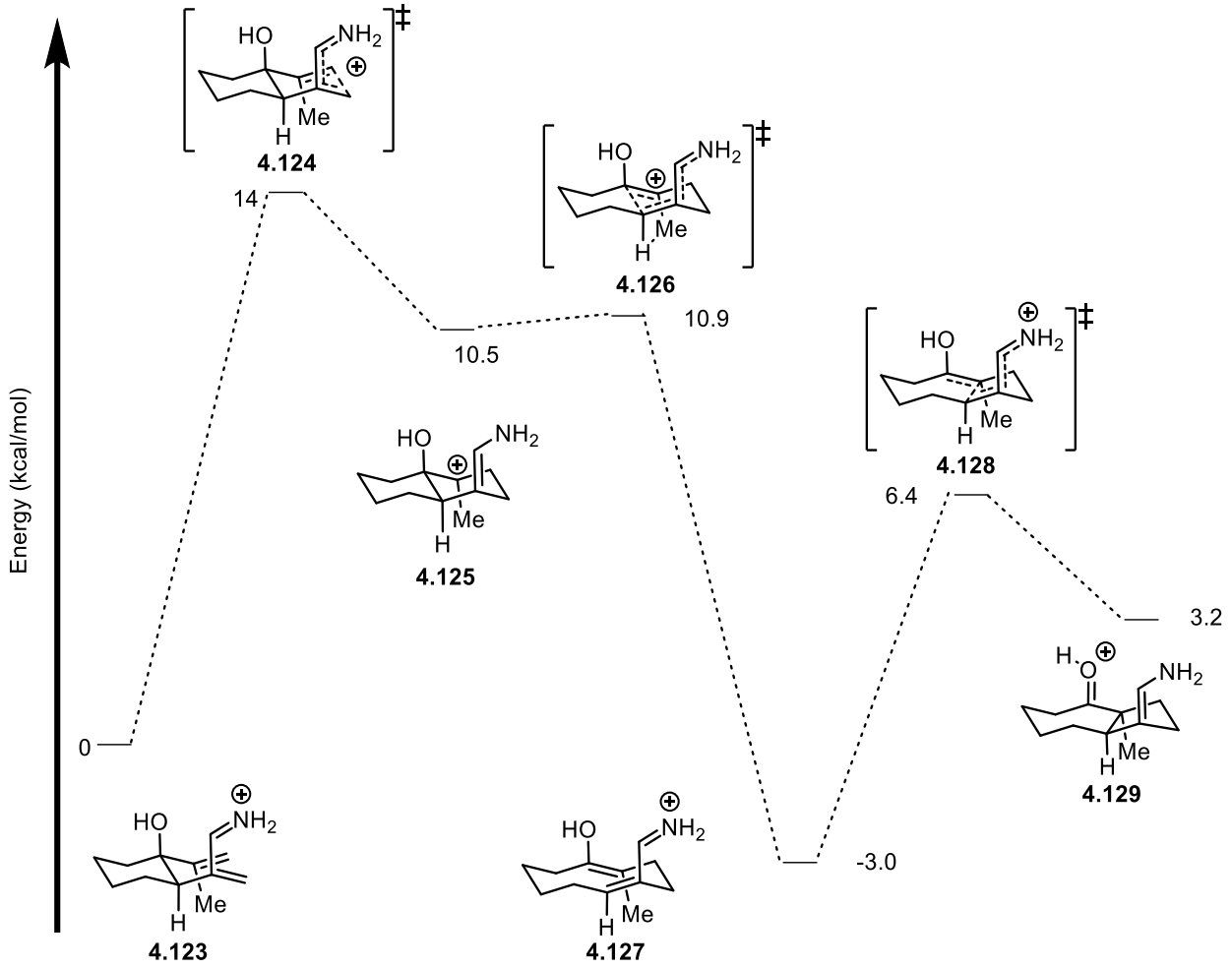


Figure 4.10. DFT calculations on the mechanism of the oCM reaction (M06-2X/6-311+G(d,p); SCRF = $MeNO_2$).

The dramatic lowering of *e.e.* observed with enantioenriched acyclic substrates **4.97a-c** in the oCM reaction provides the critical evidence needed to discuss the possible mechanisms of the reaction. The two possible mechanisms, oxy-Cope / Michael and conjugate addition / semipinacol shift, are shown from either of two possible chair-like conformer iminiums **4.130** and **4.131** for the acyclic substrates (Figure **4.11**). Each substrate conformer could undergo concerted [3,3] shift to the corresponding enol ether iminiums **4.132** (from **4.130**) or **4.135** (from **4.131**), each of which could cyclize by Michael addition to the corresponding cyclopentane iminiums **4.134** (from **4.132**) or **4.137** (from **4.135**). Note that the significant possibility exists for bond rotation in the enol ethers, where subsequent Michael addition would allow **4.132** to also access **4.137** with inverted stereochemistry relative to **4.134**, and similarly **4.135** could give rise to **4.134** after bond rotation. Since bond rotation is typically a low energy process, each enol ether would be expected to give

rise to both quaternary carbon configurations and therefore each starting conformer (**4.130** and **4.131**) would be expected to give rise to both ketone epimers of oCM products **4.118** following catalyst hydrolysis. Alternatively, conjugate addition of the distal olefin to the unsaturated iminium would give hypothetical cationic intermediate **4.133** (from **4.130**) or **4.136** (from **4.131**), each of which could complete an asynchronous Cope rearrangement to enol ethers **4.132** and **4.135** or instead undergo semipinacol [1,2] alkyl shift to **4.134** and **4.137** directly. This dichotomy of scenarios is, of course, the basis for the mechanism test with enantioenriched starting material.

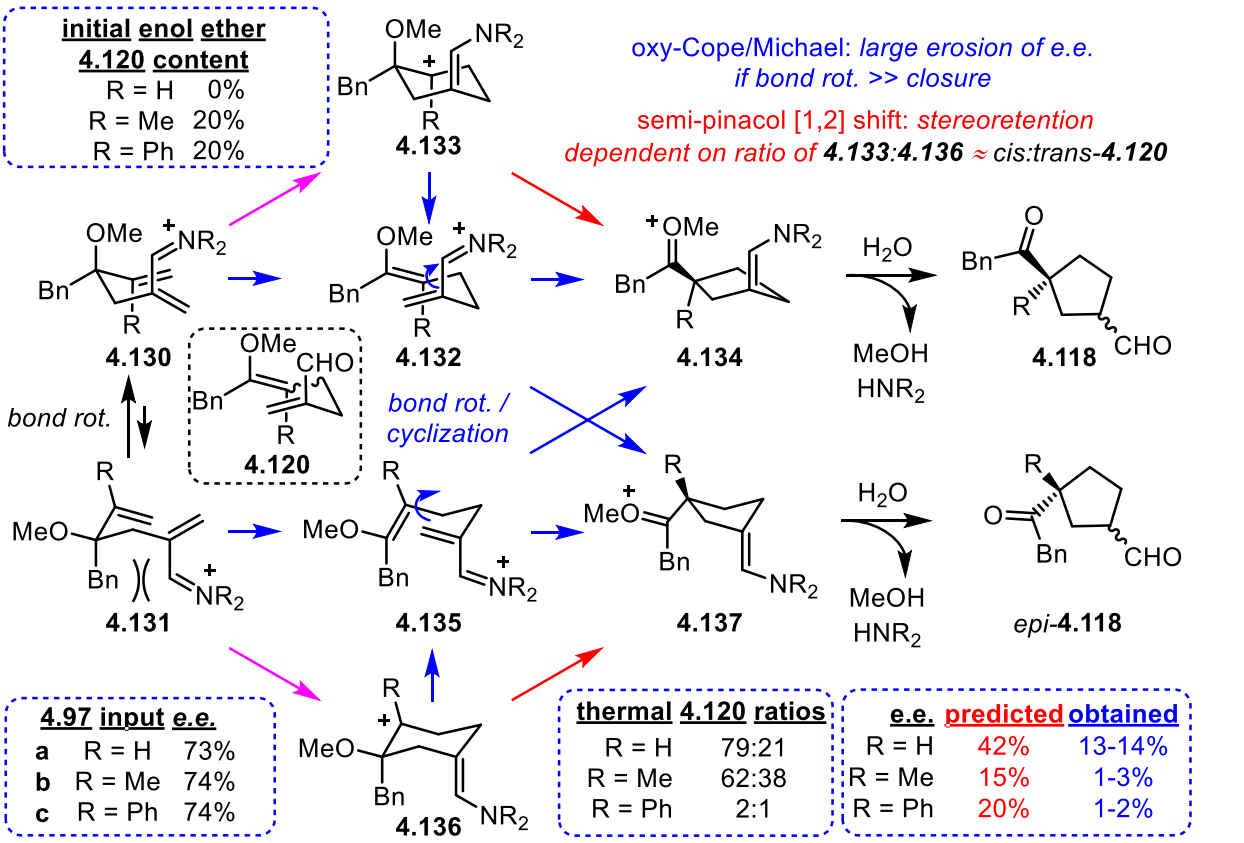


Figure 4.11. Mechanism of the linear oCM reaction. The isomeric ratios of enol ethers observed from thermal Cope reaction for each substrate are used to calculate estimates of the apparent loss of *e.e.* due to stereoretentive semipinacol reaction from either conformation **4.130** or **4.131**. The discrepancy with experimental *e.e.* values obtained after derivatization of oCM product aldehydes to their esters supports the oxy-Cope / Michael pathway, where *e.e.* is eroded both by starting conformation and bond rotation from enol ethers **4.132** and **4.135**.

Starting from enantioenriched substrate, either a concerted or asynchronous Cope reaction followed by Michael addition would afford the opportunity for significant racemization *en route* to the oCM products whereas an addition / semipinacol mechanism would be expected to maintain

some stereochemical information from the starting material. Technically, the product enantiomeric ratio following an oxy-Cope / Michael mechanism would depend on three factors: the input *e.e.*, conformational bias in the Cope rearrangement, and rates of bond rotation versus ring closure. A racemate would result irrespective of the other factors if bond rotation is faster than the rate of cyclization, which is a likely scenario *a priori*. If a conjugate addition / semipinacol mechanism is operative, each conformer of the starting material **4.130** and **4.131** would give rise stereo-specifically to one enantiomer of product since the stereochemistry cannot be scrambled. The overall enantiomeric ratio in the product would therefore depend on only two factors: the input *e.e.* and the conformational bias in the formation of an intermediate competent in a semipinacol shift. Importantly, since an associative, asynchronous Cope mechanism is likely, the transition states leading to each cationic intermediate **4.133** and **4.136** would be similar between the two pathways.

The difference between the E_a for the transition states leading to cationic intermediates **4.133** and **4.136** would determine the ratio of the hypothetical cationic intermediates. Following a pinacol pathway from that point, the ratio of cationic intermediates **4.133** and **4.136** would determine the enantiomeric ratio in oCM product **4.118** with respect to the ketone-bearing stereocenter. If a Cope pathway is followed, that E_a difference would determine the ratio of iminium enol ethers **4.132** and **4.135**, but these were never observed in the reactions.

Although transition state energies might be calculated to predict the difference in energy between the two cationic pathways, an experimentally observed surrogate is available from the ratio of enol ethers **4.120** formed from the uncatalyzed thermal reaction. It is expected that the uncatalyzed Cope would have similar steric and stereoelectronic requirements as the catalyzed reaction. These enol ether ratios were listed in Table **4.4** and are included in Figure **4.11** for each substrate. Using the ratios of **4.120**, the decrease in *e.e.* which would be expected from a conjugate addition / semipinacol pathway can be calculated for comparison with the obtained values. The thermal control reaction with **4.97a** had provided an initial enol ether ratio of 79:21 at 24 h. Given the 73% *e.e.* of the enantioenriched starting material **4.97a***, that enol ether ratio was used to predict an output *e.e.* value of 42% if a pinacol mechanism is followed. Isomerization of **4.97b** in $CDCl_3$ at room temperature had provided an enol ether ratio of 62:38. Accounting for the 20% thermal isomerization which had occurred for enantioenriched substrate **4.97b*** upon oCM reaction setup, which is both assumed to be competent and contribute only racemic product,

catalysis of the remainder by a pinacol mechanism should give an *e.e.* of 15%. A similar calculation for enriched substrate **4.97c***, using the 2:1 ratio of enol ethers observed from pre-isomerization, affords a predicted *e.e.* of 20%.

A comparison of the obtained versus calculated *e.e.* values answers the penultimate question of mechanism. The complete erosion of enantio-enrichment from 74% to at most 3% *e.e.* for substituted substrates **4.97b-c**, combined with their facile thermal Cope reaction and the apparent competence of Cope products as reaction intermediates, strongly indicates that the oxy-Cope / Michael pathway is operative. The incomplete erosion of enantio-enrichment from 73% to 13-14% *e.e.* for simple divinyl substrate **4.97a***, well below the predicted value of 42% *e.e.*, still suggests an oxy-Cope / Michael pathway is operative. A switch in mechanism favouring pinacol shift would not be expected for substrate **4.97a** in any case, since the intermediate cation is less stabilized, but the residual 13-14% *e.e.* remains nevertheless intriguing. It should be noted that great care was taken to ensure that no epimerization of oxidized derivatives of **4.97a*** occurred, and no epimerization of oCM aldehyde was observed on re-subjecting unequal mixtures of epimers to silica gel chromatography. The uneroded 13-14% *e.e.* therefore reflects a process occurring under the reaction conditions and may simply indicate that Michael addition competes with bond rotation specifically for the substrate at 55 °C. The scenario may be explained by structural variation between the substrates, since unsubstituted **4.97a** (R=H) may undergo faster Michael addition than substituted **4.97b-c** (R=Me, Ph).

Note that the above analysis only provides a rough estimate of output *e.e.*, since the mechanism of the thermal reaction with the less electrophilic enal functional group may be different and the catalyst itself would be expected to impact the conformational bias. In fact, the calculation likely overestimates the decrease in *e.e.* since the catalyst likely introduces more costly steric interactions with the benzyl substituent (shown for **4.131**), in addition to favourable electrostatic interactions between the methoxy and iminium, to reinforce conformational preference for **4.130** and any transition state arising from that structure. The claim that the discussion has underestimated output *e.e.* is reinforced by the computed energy difference of 2.9 kcal/mol between the transition states arising from **4.130** and **4.131**, performed by Dr. Gleason and shown in Figure **4.12**. However, even these very generous overestimations of the expected decrease in *e.e.* remain much larger than the experimentally obtained values of the oCM products.

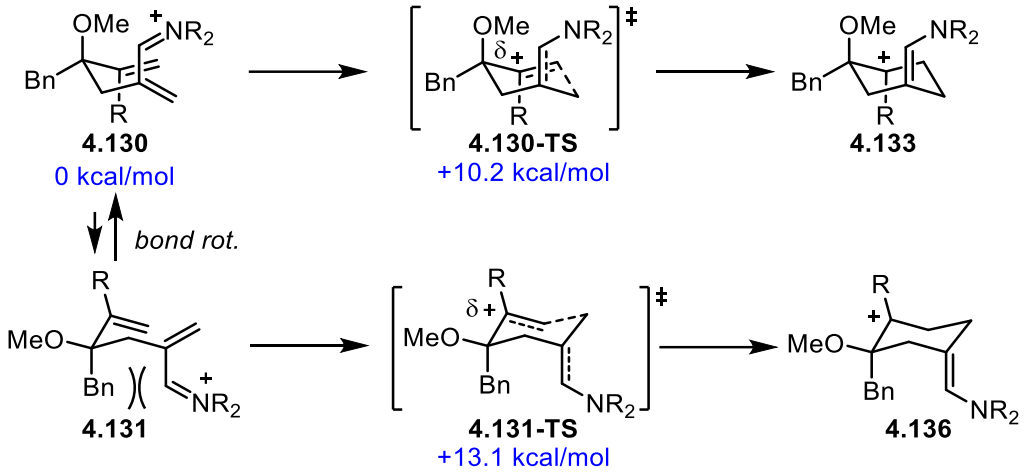


Figure 4.12. Transition states and DFT energies of the key oCM transition states (R=Me). M06-2X/6-311+G(d); SCRF = $MeNO_2$.

The evidence that Michael addition is close in energy to bond rotation allows the extrapolation of some additional conclusions about the oCM reaction mechanism. Since thermal reaction of **4.97a** with N-Me catalyst produced only oxy-Cope ketone **4.119**, without visible enol ether content like in the thermal control experiment, enol ether cleavage must be fast under the reaction conditions at 55 °C. The small quantity of oxy-Cope ketone **4.119** produced is therefore likely due to uncatalyzed thermal reaction. If enol Michael addition competes with bond rotation, then cyclization likely occurs before ether cleavage by water. Furthermore, the competition signifies that the Michael addition kinetic barrier is low, certainly lesser than the barrier to Cope shift, which fits the DFT calculations (Figure **4.10**). Since the kinetics of hydrazide condensation are unlikely to be affected in the oCM reaction, as in our organocatalytic Cope rearrangement, it can be concluded that the [3,3] sigmatropic shift should remain rate-determining in the oCM reaction.

4.3.1. *Conclusions and Outlook*

An organocatalytic oxy-Cope / Michael cascade reaction was developed, in both cyclic and acyclic variants, which relies on iminium-like catalysis by a diazepane carboxylate hydrazide. The cyclic and acyclic classes of reaction required separate optimization of conditions by exploring factors such as catalyst salt, solvent, and temperature. Embedded within the project was the exploration of synthetic routes to these various substrates and their successful preparation in sufficient quantity to sustain test reactions, in some cases with hundreds of milligrams of substrates to overcome challenges in scaling the reaction.

For substrates bound on cyclic backbones, the optimal conditions employed 10 mol% of each diazepane carboxylate catalyst and triflimide in a 10% by volume mixture of water and nitromethane at a substrate concentration of 0.2 M. The conditions were then applied to various substrates to establish the reaction scope, and a variety of ring expanded bi- and tricyclic dicarbonyls were produced in very high *d.r.* and good to excellent yield. The reaction was showed to tolerate alkene substitution at both C5 and C6 of the oxy-Cope hexadiene substrates. Products containing up to 4 stereocenters were obtained, demonstrating the complexity-generating transformation possible with this oxy-Cope / Michael reaction.

Issues of ring-chain tautomerization were identified and overcome where necessary by methyl ether protection of the alcohols, which allowed the exploration of an acyclic variant of this oxy-Cope / Michael reaction. The same optimized catalytic conditions as just described allowed the preparation of three novel cyclopentane dicarbonyls in good yield, although simplest divinyl substrates needed slightly warmer conditions. The mechanism was also probed by the transformation of enantioenriched linear substrates into racemic or nearly racemic products. The results support the intermediacy of an achiral intermediate and support an oxy-Cope / Michael pathway rather than a conjugate addition / semi-pinacol shift mechanism.

Future work stemming from the oxy-Cope/Michael reaction could include enantioselective variations, relying on the demonstrated intermediacy of Cope products prior to a selective Michael addition, performed using chiral hydrazide catalysts such as demonstrated previously for the organocatalytic Cope reaction. Unfortunately, this may be limited to olefin-substituted acyclic substrates, which were tougher compounds to work with, since the cyclic substrates appear to retain relative stereochemistry. Another obvious application of the oxy-Cope/Michael methodology would be in the area of natural product synthesis, as alluded to in the introduction to Chapter 4. Finally, the oxy-Cope/Michael reaction could be incorporated into more complex cascade sequences.

4.3.2. *References for Part II*

1. Woodward, R. B.; Hoffmann, R. *J. Am. Chem. Soc.* **1965**, *87,* 2511.
2. (a) Fleming, I. Thermal Pericyclic Reactions. In *Molecular Orbitals and Organic Chemical Reactions;* John Wiley and Sons, 2010; pp 253-368. (b) Armstrong, S. K. Molecular Rearrangements: Part 1. In *Organic Reaction Mechanisms;* John Wiley and Sons, 2007; pp 469-498.
3. (a) Jiao, H.; Schleyer, P. R. *Angew. Chem., Int. Ed. Engl.* **1995**, *34,* 334. (b) Hrovat, D. A.; Beno, B. R.; Lange, H.; Yoo, H.-Y.; Houk, K. N.; Borden, W. T. *J. Am. Chem. Soc.* **1999**, *121,* 10529.
4. Cope, A. C.; Hardy, E. M. *J. Am. Chem. Soc.* **1940**, *62,* 441.
5. (a) Doering, W. E; Toscano, V. G.; Beasley, G. H. *Tetrahedron* **1971**, *27,* 5299. *For reviews of Cope rearrangements, see:* (b) Hill, R. K. Cope, Oxy-Cope and Anionic Oxy-Cope Rearrangements. In *Comprehensive Organic Synthesis;* Elsevier Science Ltd., 1991; pp 786-826. (c) Schneider, C.; Weise, C. F. Cope, Oxy-Cope and Anionic Oxy-Cope Rearrangements. In *Comprehensive Organic Synthesis;* Elsevier Science Ltd., 2014; pp 867-909.
6. (a) Claisen, L. *Chem. Ber.* **1912**, *45,* 3157. *For reviews of Claisen rearrangements, see:* (b) Wipf, P. Claisen Rearrangements. In *Comprehensive Organic Synthesis;* Elsevier Science Ltd., 1991; pp 827-873. (c) Martin-Castro, A. M.; Tortosa, M. Claisen Rearrangements. In *Comprehensive Organic Synthesis;* Elsevier Science Ltd., 2014; pp 913-977. (d) Ziegler, F. E. *Chem. Rev.* **1988**, *88,* 1423. (e) Martin-Castro, A. M. *Chem. Rev.* **2004**, *104,* 2939.
7. Stogryn, E. L.; Brois, S. J. *J. Org. Chem.* **1965**, *30,* 88.
8. Urion, M. *Compt. Rend.* **1930**, *190,* 1512; *Ann. Chimie.* **1934**, *1,* 5.
9. (a) Berson, J. A.; Jones, M. *J. Am. Chem. Soc.* **1964**, *86,* 5017. (b) Berson, J. A.; Jones, M. *J. Am. Chem. Soc.* **1964**, *86,* 5019. (c) Berson, J. A.; Walsh, E. J. *J. Am. Chem. Soc.* **1968**, *90,* 4729. (d) Berson, J. A.; Walsh, E. J. *J. Am. Chem. Soc.* **1968**, *90,* 4730. (e) (d) Berson, J. A.; Walsh, E. J. *J. Am. Chem. Soc.* **1968**, *90,* 4732.
10. Martinet, P.; Mousset, G.; Michel, M. *C. R. Acad. Sci. Paris, Ser. C* **1969**, *268,* 1303.
11. Horowitz. R. M.; Geissman, T. A. *J. Am. Chem. Soc.* **1950**, *72,* 1518.
12. (a) Evans, D. A.; Scott, W. L.; Truesdale, L. K. *Tetrahedron Lett.* **1972**, 137. (b) Scott, W. L.; Evans, D. A. *J. Am. Chem. Soc.* **1972**, *94,* 4779. (c) Evans, D. A.; Golob, A. M. *J. Am. Chem.*

Soc. **1975**, *97,* 4765. (d) Evans, D. A.; Baillargeon, D. J.; *Tetrahedron Lett.* **1978**, 3315; 3319. (e) Evans, D. A.; Baillargeon, D. J.; Nelson, J. V. *J. Am. Chem. Soc.* **1978**, *100,* 2242. (f) Steigerwald, M. L.; Goddard, W. A.; Evans, D. A. *J. Am. Chem. Soc.* **1979**, *101,* 1994. *For additional insight into the AOC mechanism, see:* (g) Haeffner, F.; Houk, K. N.; Reddy, R.; Paquette, L. A. *J. Am. Chem. Soc.* **1999**, *121,* 11880. (h) Rozeboom, M. D.; Kiplinger, J. P.; Bartmess, J. E. *J. Am. Chem. Soc.* **1984**, *106,* 1025. (i) Gajewski, J. J.; Gee, K. R. *J. Am. Chem. Soc.* **1991**, *113,* 967. (j) Yoo, H. Y.; Houk, K. N.; Lee, J. K.; Scialdone, M. A.; Meyers, A.I. *J. Am. Chem. Soc.* **1998**, *120,* 205. (k) Schulze, S. M.; Santella, N.; Grabowski, J. J.; Lee, J. K. *J. Org. Chem.* **2001**, *66,* 7247. (l) Baumann, H.; Chen, P. *Helv. Chim. Acta* **2001**, *84,* 124.

13. Reber, K. P.; Xu, J.; Guerrero, C. A. *J. Org. Chem.* **2015**, *80,* 2397.
14. Boeckman, R. K.; Springer, D. M.; Alessi, T. R. *J. Am. Chem. Soc.* **1989**, *111,* 8284.
15. *Additional examples of ring interconversions. 5 to 6:* (a) Jung, M. E.; Hudspeth, J. P. *J. Am. Chem. Soc.* **1978**, *100,* 4309. *Spinosyn A:* (b) Paquette, L. A.; Gao, Z.; Ni, Z.; Smith, G. F. *J. Am. Chem. Soc.* **1998**, *120,* 2543. *6 to 8:* (c) Gentric, L.; Hanna, I.; Huboux, A.; Zaghdoudi, R. *Org. Lett.* **2003**, *5,* 3631. *Ceroplastins:* (d) Paquette, L. A.; Liang, S.; Galatsis, P. *Synlett* **1990**, 663. (e) Paquette, L. A.; Liang, S.; Wang, H.-L. *J. Org. Chem.* **1996**, *61,* 3268. *6 to 10:* (f) Clive, D. L. J.; Russell, C. G.; Suri, S. C. *J. Org. Chem.* **1982**, *47,* 1632. (g) Schreiber, S. L.; Satini, C. *J. Am. Chem. Soc.* **1984**, *106,* 4038. (h) Paquette, L. A.; DeRussey, D. T.; Gallucci, J. C. *J. Org. Chem.* **1989**, *54,* 2278. *6 to 14:* (i) Wender, P. A.; Sieburth, S. *Tetrahedron Lett.* **1981**, *22,* 2471. *Review of other miscellaneous ring expansions:* (j) Durairaj, K. *Curr. Sci.* **1994**, *66,* 917. *Ring interconversion to clerodanes:* (k) Liu, W.-C.; Liao, C.-C. *Synlett* **1998**, 912. *Ring contraction, 9 to 5 for prostaglandins:* (l) Paquette, L. A.; Crouse, G. D.; Sharma, A. K. *J. Am. Chem. Soc.* **1980**, *102,* 3972. (m) Paquette, L. A.; Crouse, G. D. *Tetrahedron* **1981**, *37,* 281. (n) Paquette, L. A.; Crouse, G. D.; Sharma, A. K. *J. Am. Chem. Soc.* **1982**, *104,* 4411.
16. *For additional examples of allyl transpositions in total synthesis. Indoxamicin B:* (a) Jeker, O. F.; Carreira, E. M. *Angew. Chem. Int. Ed.* **2012**, *51,* 3474. *Hasubanonine:* (b) Jones, S. B.; He, L.; Castle, S. L. *Org. Lett.* **2006**, *8,* 3757. *Talpinine and talcarpine:* (c) Yu, P.; Cook, J. M. *J. Org. Chem.* **1998**, *63,* 9160. *Suaveoline and raumacline:* (d) Fu, X.; Cook, J. M. *J. Org. Chem.* **1993**, *58,* 661.

17. (a) Brown, E; Leriverend, P.; Conia, J.-M. *Tetrahedron Lett.* **1966**, 6115. (b) Leriverend, P.; Conia, J.-M. *Tetrahedron Lett.* **1969**, 2681.
18. Abdelhamid, I. A.; Abdelmoniem, A. M.; Fohrer, J.; Bardenhorst, I.; Wartchow, R.; Butenschön, H. *Eur. J. Org. Chem.* **2017**, 6951 *(and references therein)*.
19. Geetha, P.; Huq, C. A. M. A.; Rajagopalan, K.; Swaminathan, S. *Tetrahedron Lett.* **1982**, *23,* 569.
20. Saito, S.; Yamamoto, T.; Matsuoka, M.; Moriwake, T. *Synlett* **1992**, 239.
21. Paquette, L. A. *Eur. J. Org. Chem.* **1998**, 1709 *(and references therein)*.
22. Jones, K. E.; Park, B.; Doering, N. A.; Baik, M.-H.; Sarpong, R. *J. Am. Chem. Soc.* **2021**, *143,* 20482.
23. (a) Allin, S. M.; Button, M. A. C. *Tetrahedron Lett.* **1998**, 3345. (b) Dobson, H. K.; LeBlanc, R.; Perrier, H.; Stephenson, C.; Welch, T. R.; Macdonald, D. *Tetrahedron Lett.* **1999**, 3119. (c) Allin, S. M.; Button, M. A. C. *Tetrahedron Lett.* **1999**, 3801. (d) Chogii, I.; Das, P.; Fell, J. S.; Scott, K. A.; Crawford, M. N.; Houk, K. N.; Njardarson, J. T., *J. Am. Chem. Soc.* **2017**, *139*, 13141-13146.
24. (a) Wilson, S. R.; Mao, D. T. *Tetrahedron Lett.* **1977**, 2559. (b) Danheiser, R. L.; Martinez-Davila, C.; Sard, H. *Tetrahedron* **1981**, *37,* 3943. (c) Franzus, B.; Scheinbaum, M. L.; Waters, D. L.; Bowlin, H. B. *J. Am. Chem. Soc.* **1976**, *98,* 1241. (d) Miyashi, T.; Hazato, A.; Mukai, T. *J. Am. Chem. Soc.* **1978**, *100,* 1008. (e) Thies, R. W.; Seitz, E. P. *J. Org. Chem.* **1978**, *43,* 1050. (f) Snider, B. B.; Niwa, M. *Tetrahedron Lett.* **1988**, *29,* 3175. (g) Jung, M. E.; Kaas, S. M. *Tetrahedron Lett.* **1989**, *30,* 641. (h) Shing, T. K. M.; Zhu, X. Y.; Yeung, Y. Y. *Chem. Eur. J.* **2003**, *9,* 5489. *Related anionic [1,3]-shift with nitrogen:* (i) Krow, G. R.; Reilly, J. *J. Am. Chem. Soc.* **1975**, *97,* 3837.
25. *For reviews of oxy-Cope in cascades, see:* (a) Paquette, L. A. *Angew. Chem. Int. Ed. Engl.* **1990**, *29,* 609. (b) Paquette, L. A. *Synthesis* **1990**, 67. (c) Wilson, S. R. *Org. React.* **1993**, *43,* pp 93-250. (d) Paquette, L. A. *Tetrahedron* **1997**, *53,* 13971. (e) Arns, S.; Barriault, L. *Chem. Commun.* **2007**, 2211. (f) Poulin, J.; Grisé-Bard, C. M.; Barriault, L. *Chem. Soc. Rev.* **2009**, *38,* 3092. (g) Jones, A. C.; May, J. A.; Sarpong, R.; Stoltz, B. M. *Angew. Chem. Int. Ed.* **2014**, *53,* 2556. (h) Rhoads, S. J.; Raulins, N. R. *Org. React.* **1975**, pp 1-252. (i) Paquette, L. A. *Chem. Soc. Rev.* **1995**, *24,* 9. (j) Neuschütz, K.; Velker, J.; Neier, R. *Synthesis* **2008**, 227. (k) Ilardi, E. A.; Stivala, C. E.; Zakarian, A. *Chem. Soc. Rev.* **2009**, *38,* 3133.

26. Greeves, N.; Lee, W.-M.; Barkley, J. V. *Tetrahedron Lett.* **1997**, *38,* 6453.
27. Plummer, C. W.; Wei, C. S.; Yozwiak, C. E.; Soheili, A.; Smithback, S. O.; Leighton, J. L. *J. Am. Chem. Soc.* **2014**, *136,* 9878.
28. (a) Janardhanam, S.; Rajagopalan, K. *J. Chem. Soc. Perkin Trans. 1* **1992**, 2727. (b) Janardhanam, S.; Devan, B.; Rajagopalan, K. *Tetrahedron Lett.* **1993**, *34,* 6761. (c) Srinivasan, R.; Rajagopalan, K. *Tetrahedron Lett.* **1998**, *39,* 4133.
29. A family of bicyclic ring expansions were explored by Swaminathan and Rajagopalan (see ref. 30) through the 60's into the 90's, where it was eventually conceded that a stepwise mechanism was operative, although a concerted AOC was proposed using dissociative conditions.
30. (a) Swaminathan, S.; John, J. P.; Ramachandran, S. *Tetrahedron Lett.* **1962**, 729. (b) John, J. P.; Srinivasan, K. G.; Venkataramani, P. S.; Swaminathan, S. *Tetrahedron* **1969**, *25,* 2661. (c) Swaminathan, S.; Srinivasan, K. G.; Venkataramani, P. S. *Tetrahedron* **1970**, *26,* 1453. (c) Chandrasekara, S.; Venkataramani, P. S.; Srinivasan, K. G.; Swaminathan, S. *Tetrahedron Lett.* **1973**, 991. (c) Geetha, K. Y.; Rajagopalan, K.; Swaminathan, S. *Tetrahedron* **1978**, *34,* 2201. (c) Raju, N.; Rajagopalan, K.; Swaminathan, S. *Tetrahedron Lett.* **1980**, *21,* 1577. (d) Kalyanasundaram, M.; Rajagopalan, K.; Swaminathan, S. *Tetrahedron Lett.* **1980**, *21,* 4391. (e) Rao, C. S. S.; Kumar, G.; Rajagopalan, K.; Swaminathan, S. *Tetrahedron* **1982**, *38,* 2195. (f) Uma, R.; Swaminathan, S.; Rajagopalan, K. *Tetrahedron Lett.* **1984**, *25,* 5825. (g) Uma, R.; Rajagopalan, K.; Swaminathan, S. *Tetrahedron* **1986**, *42,* 2757. (h) Sathyamoorthi, G.; Thangaraj, K.; Srinivasan, P. C.; Swaminathan, S. *Tetrahedron* **1990**, *46,* 3559. (i) Balakumar, A.; Janardhanam, S.; Rajagopalan, K. *J. Org. Chem.* **1993**, *58,* 5482.
31. (a) Barriault, L.; Deon, D. H. *Org. Lett.* **2001**, *3,* 1925. (b) Barriault, L.; Denissova, I. *Org. Lett.* **2002**, *4,* 1371. (c) Sauer, E. L. O.; Barriault, L. *J. Am. Chem. Soc.* **2004**, *126,* 8569. (d) Gauvreau, D.; Barriault, L. *J. Org. Chem.* **2005**, *70,* 1382. (e) Warrington, J. M.; Barriault, L. *Org. Lett.* **2005**, *7,* 4589. (f) Arns, S.; Barriault, L. *J. Org. Chem.* **2006**, *71,* 1809. (g) Clément, R.; Grisé, C. M.; Barriault, L. *Chem. Commun.* **2008**, 3004. (h) Hooper, J.; Sauer, E. L. O.; Arns, S.; Woo, T. K.; Barriault, L. *Chem. Eur. J.* **2010**, *16,* 14124. (i) Barriault, L.; Denissova, I.; Goulet, N. *Synthesis* **2012**, *44,* 1833.
32. Jacobi, P. A.; Selnick, H. G. *J. Org. Chem.* **1990**, *55,* 202.
33. Chen, C.; Layton, M. E.; Sheehan, S. M.; Shair, M. D., *J. Am. Chem. Soc.* **2000**, *122*, 7424.

34. (a) Sworin, M.; Lin, K.-C. *J. Org. Chem.* **1987**, *52,* 5640. (b) Sworin, M.; Lin, K.-C. *J. Am. Chem. Soc.* **1989**, *111,* 1815.
35. Johnston, J. N.; Long, Y. O.; Paquette, L. A. *Synth. Commun.* **1998**, *28,* 1509.
36. (a) Roosen, P. C.; Vanderwal, C. D. *Org. Lett.* **2014**, *16,* 4368. (b) Ramella, V.; Roosen, P. C.; Vanderwal, C. D. *Org. Lett.* **2020**, *22,* 2883.
37. (a) Paquette, L. A.; Andrews, D. R.; Springer, J. P. *J. Org. Chem.* **1983**, *48,* 1147. (b) Paquette, L. A.; Colapret, J. A.; Andrews, D. R. *J. Org. Chem.* **1985**, *50,* 201.
38. Bio, M. M.; Leighton, J. L. *J. Org. Chem.* **2003**, *68,* 1693.
39. Sgarbi, P. W. M.; Clive, D. L. J. *Chem. Commun.* **1997**, 2157.
40. *The siloxy-Cope reaction is a valuable variant of the thermal oxy-Cope reaction. For its development, see:* (a) Thies, R. W.; Wills, M. T. *Tetrahedron Lett.* **1970**, 513. (b) Thies, R. W. *Chem. Commun.* **1971**, 237. (c) Thies, R. W. *J. Am. Chem. Soc.* **1972**, *94,* 7074. (d) Thies, R. W.; Wills, M. T.; Chin, A. W.; Schick, L. E.; Walton, E. S. *J. Am. Chem. Soc.* **1973**, *95,* 5281. (e) Thies, R. W.; Billigmeir, J. E. *J. Am. Chem. Soc.* **1974**, *96,* 200.
41. *Additional examples of cascade reactions involving oxy-Cope rearrangements in total synthesis. Organometallic addition-Brook rearrangement-cyclization-AOC:* (a) Takeda, K.; Nakane, D.; Takeda, M. *Org. Lett.* **2000**, *2,* 1903. *Organometallic addition-AOC-deprotection-aldol for polyquinanes:* (b) Santora, V. J.; Moore, H. W. *J. Am. Chem. Soc.* **1995**, *117,* 8486. (c) MacDougall, J. M.; Santora, V. J.; Verma, S. K.; Turnbull, P.; Hernandez, C. R.; Moore, H. *J. Org. Chem.* **1998**, *63,* 6905. *Retro-aldol-AOC-Michael addition:* (d) Tice, C. M.; Heathcock, C. H. *J. Org. Chem.* **1981**, *46,* 9.
42. *For reviews of the aza-Cope Mannich and Prins-pinacol reactions, see:* (a) Overman, L. E. *Acc. Chem. Res.* **1992**, *25,* 352. (b) Overman, L. E. *Aldrichim. Acta* **1995**, *28,* 107. (c) Overman, L. E.; Humphreys, P. G. *Org. React.* **2011**, *75,* 747.
43. *For the first 28 reports of the aza-Cope Mannich reaction development and synthetic applications, see:* (a) Overman, L. E.; Kakimoto, M. *J. Am. Chem. Soc.* **1979**, *101,* 1310. (b) Overman, L. E.; Kakimoto, M.; Okawara, M. *Tetrahedron Lett.* **1979**, 4041. (c) Overman, L. E.; Fukaya, C. *J. Am. Chem. Soc.* **1980**, *102,* 1454. (d) Overman, L. E.; Yokomatsu, T. *J. Org. Chem.* **1980**, *45,* 5229. (e) Overman, L. E.; Mendelson, L. T. *J. Am. Chem. Soc.* **1981**, *103,* 5579. (f) Overman, L. E.; Sworin, M. *Tetrahedron* **1981**, *37,* 4041. (g) Overman, L. E.; Mendelson, L. T.; Flippin, L. A. *Tetrahedron Lett.* **1982**, *23,* 2733. (h) Overman, L. E.;

Jacobsen, E. J. *Tetrahedron Lett.* **1982**, *23,* 2737. (i) Overman, L. E.; Jacobsen, E. J. *Tetrahedron Lett.* **1982**, *23,* 2741. (j) Overman, L. E.; Sworin, M.; Burk, R. M. *J. Org. Chem.* **1983**, *48,* 2685. (k) Overman, L. E.; Kakimoto, M.; Okazaki, M. E.; Meier, G. P. *J. Am. Chem. Soc.* **1983**, *105,* 6622. (l) Overman, L. E.; Mendelson, L. T.; Jacobsen, E. J. *J. Am. Chem. Soc.* **1983**, *105,* 6629. (m) Overman, L. E.; Jacobsen, E. J.; Doedens, R. J. *J. Org. Chem.* **1983**, *48,* 3393. (n) Overman, L. E.; Sugai, S. *Helv. Chim. Acta.* **1985**, *68,* 745. (o) Overman, L. E.; Angle, S. R. *J. Org. Chem.* **1985**, *50,* 4021. (p) Overman, L. E.; Okazaki, M. E.; Jacobsen, E. J. *J. Org. Chem.* **1985**, *50,* 2403. (q) Doedens, R. J.; Meier, G. P.; Overman, L. E. *J. Org. Chem.* **1988**, *53,* 685. (r) Jacobsen, E. J.; Levin, J.; Overman, L. E. *J. Am. Chem. Soc.* **1988**, *110,* 4329. (s) Overman, L. E.; Wild, H. *Tetrahedron Lett.* **1989**, *30,* 647. (t) Overman, L. E.; Robertson, G. M.; Robichaud, A. J. *J. Org. Chem.* **1989**, *54,* 1236. (u) Overman, L. E.; Robertson, G. M.; Robichaud, A. J. *J. Am. Chem. Soc.* **1991**, *113,* 2598. (v) Fevig, J. M.; Marquis, R. W.; Overman, L. E. *J. Am. Chem. Soc.* **1991**, *113,* 5085. (w) Overman, L. E.; Shim, J. *J. Org. Chem.* **1991**, *56,* 5005. (x) Angle, S. R.; Fevig, J. M.; Knight, S. D.; Marquis, R. W.; Overman, L. E. *J. Am. Chem. Soc.* **1993**, *115,* 3966. (y) Overman, L. E.; Shim, J. *J. Org. Chem.* **1993**, *58,* 4662. (z) Knight, S. D.; Overman, L. E.; Pairaudeau, G. *J. Am. Chem. Soc.* **1993**, *115,* 9293. (aa) Deng, W.; Overman, L. E. *J. Am. Chem. Soc.* **1994**, *116,* 11241. (ab) Knight, S. D.; Overman, L. E.; Pairaudeau, G. *J. Am. Chem. Soc.* **1995**, *117,* 5776.

44. Overman, L. E.; Trenkle, W. C. *Isr. J. Chem.* **1997**, *37,* 23.
45. Martin, C. L.; Overman, L. E.; Rohde, J. M. *J. Am. Chem. Soc.* **2010**, *132,* 4894.
46. (a) Hopkins, M. H.; Overman, L. E. *J. Am. Chem. Soc.* **1987**, *109,* 4748. (b) Hirst, G. C.; Howard, P. N.; Overman, L. E. *J. Am. Chem. Soc.* **1989**, *111,* 1514. (c) Hopkins, M. H.; Overman, L. E.; Rishton, G. M. *J. Am. Chem. Soc.* **1991**, *113,* 5354. (d) Brown, M. J.; Harrison, T.; Herrinton, P. M.; Hopkins, M. H.; Hutchinson, K. D.; Mishra, P.; Overman, L. E. *J. Am. Chem. Soc.* **1991**, *113,* 5365. (e) Overman, L. E.; Rishton, G. M. *Org. Synth.* **1993**, *71,* 63. (f) Lolkema, L. D. M.; Hiemstra, H.; Semeyn, C.; Speckamp, W. N. *Tetrahedron* **1994**, *50,* 7115. (g) Lolkema, L. D. M.; Semeyn, C.; Ashek, L.; Hiemstra, H.; Speckamp, W. N. *Tetrahedron* **1994**, *50,* 7129. (h) Ando, S.; Minor, K. P. Overman, L. E. *J. Org. Chem.* **1997**, *62,* 6379. (i) Cohen, F.; MacMillan, D. W. C.; Overman, L. E.; Romero, A. *Org. Lett.* **2001**, *3,* 1225. (j) Gahman, T. C.; Overman, L. E. *Tetrahedron* **2002**, *58,* 6473. (k) Overman, L. E.; Wolfe, J. P. *J. Org. Chem.* **2002**, *67,* 6421. (l) Overman, L. E.; Velthuisen, E. J.; *Org. Lett.*

2004, *6,* 3853. (m) Overman, L. E.; Velthuisen, E. J.; *J. Org. Chem.* **2006**, *71,* 1581. (n) Overman, L. E.; Tanis, P. S. *J. Org. Chem.* **2010**, *75,* 455.

47. Dauben, W. G.; Chollet, A. *Tetrahedron Lett.* **1981**, *22,* 1583.
48. Lutz, R. P. *Chem. Rev.* **1984**, *84,* 205.
49. Overman, L. E. *Angew. Chem. lnt. Ed. Engl.* **1984**, *23,* 579.
50. Overman, L. E.; Jacobsen, E. J. *J. Am. Chem. Soc.* **1982**, *104,* 7225.
51. Felix, R. J.; Weber, D.; Gutierrez, O.; Tantillo, D. J.; Gagné, M. R. *Nat. Chem.* **2012**, *4,* 405.
52. (a) Braisted, A. C.; Schultz, P. G. *J. Am. Chem. Soc.* **1994**, *116,* 2211. (b) Black, K. A.; Leach, A. G.; Kalani, M. Y. S.; Houk, K. N. *J. Am. Chem. Soc.* **2004**, *126,* 9695.
53. Tang, Q.; Fu, K.; Ruan, P.; Dong, S.; Su, Z.; Liu, X.; Feng, X. *Angew. Chem. Int. Ed.* **2019**, *58,* 11846.
54. Kennedy, C. R.; Choi, B. Y.; Reeves, M.-G. R.; Jacobsen, E. N. *Isr. J. Chem.* **2020**, *60,* 461.
55. MacMillan, D. W. C. *Nature* **2008**, *455,* 304.
56. Erkkilä, A.; Majander, I.; Pihko, P. M. *Chem. Rev.* **2007**, *107,* 5416.
57. Ahrendt, K. A.; Borths, C. J.; MacMillan, D. W. C. *J. Am. Chem. Soc.* **2000**, *122,* 4243.
58. (a) Cavill, J. L.; Peters, J.-U.; Tomkinson, N. C. O. *Chem. Commun.* **2003**, 728. (b) Cavill, J. L.; Elliott, R. L.; Evan, G.; Jones, I. L.; Platts, J. A.; Ruda, A. N.; Tomkinson, N. C. O. *Tetrahedron* **2006**, *62,* 410. (c) Brazier, J. B.; Cavill, J. L.; Elliott, R. L.; Evan, G.; Gibbs, T. J. K.; Jones, I. L.; Platts, J. A.; Tomkinson, N. C. O. *Tetrahedron* **2009**, *65,* 9961.
59. (a) Lemay, M.; Ogilvie, W. W. *Org. Lett.* **2005**, *7,* 4141. (b) Lemay, M.; Ogilvie, W. W. *J. Org. Chem.* **2006**, *71,* 4663. (c) Lemay, M.; Aumand, L; Ogilvie, W. W. *Adv. Synth. Catal.* **2007**, *349,* 441. (d) He, H.; Pei, B.-J.; Chou, H.-H.; Tian, T.; Chan, W.-H.; Lee, A. W. M. *Org. Lett.* **2008**, *10,* 2421. (e) Li, Q.; Wong, W.-Y.; Chan, W.-H.; Lee, A. W. M. *Adv. Synth. Catal.* **2010**, *352,* 2142. (f) Suzuki, I.; Ando, M.; Shimabara, R.; Hirata, A.; Takeda, K. *Org. Biomol. Chem.* **2011**, *9,* 3033.
60. *Cope catalysis:* (a) Kaldre, D. Ph.D. Thesis, McGill University, Montreal, Canada, 2015. (b) Kaldre, D.; Gleason, J. L. *Angew. Chem. Int. Ed.* **2016**, *55,* 11557. (c) Sanders, J. N.; Jun, H.; Yu, R. A.; Gleason J. L.; Houk, K. N. *J. Am. Chem. Soc.* **2020**, *142,* 16877. *Michael addition catalysis:* (d) Larnaud, F.; Sulpizi, A.; Häggman, N. O.; Hughes, J. M. E.; Dewez, D. F.; Gleason, J. L. *Eur. J. Org. Chem.* **2017**, 2637. *Diels-Alder catalysis:* (e) Häggman, N. O.; Zank, B.; Jun, H.; Kaldre, D.; Gleason, J. L. *Eur. J. Org. Chem.* **2018**, 5412. *Polyene*

cyclizations: (f) Plamondon, S. J.; Warnica, J. M.; Kaldre, D.; Gleason, J. L. *Angew. Chem. Int. Ed.* **2020**, *59,* 253. (g) Warnica, J. M.; Gleason, J. L. *Can. J. Chem.* **2022**, *100,* 212. (h) Plamondon, S. J.; Gleason, J. L. *Org. Lett.* **2022**, *24,* 2305.

61. Marti, C.; Carreira, E. M. *J. Am. Chem. Soc.* **2005**, *127,* 11505.
62. Petasis, N. A.; Lu, S.-P. *J. Am. Chem. Soc.* **1995**, *117,* 6394.
63. Di Scienze, F. Aminocatalyzed biomimetic cyclization for the synthesis of terpenes and sesquiterpenes like systems. M.Sc. Dissertation, Università degli Studi di Pavia, Pavia, Italy, 2016.
64. (a) Coffey, S. *Rec. Trav. Chim.* **1923**, *42,* 387. (b) Newman, M. S.; VanderWerf, C. A. *J. Am. Chem. Soc.* **1945**, *67,* 233. (c) Parent, J.-F.; Bertrand, X.; Deslongchamps, G.; Deslongchamps, P. *J. Org. Chem.* **2020**, *85,* 758.
65. Jackson, J. A.; Hammond, G. B.; Wiemer, D. F. *J. Org. Chem.* **1989**, *54,* 4750.
66. (a) Erkkilä, A.; Pihko, P. *J. Org. Chem.* **2006**, *71,* 2538. (b) Erkkilä, A.; Pihko, P. M. *Eur. J. Org. Chem.* **2007**, 4205.
67. (a) E_T^N values are described in the following reference as derived from "the transition energy at 25 °C of the long-wavelength visible absorption of a standard pyridinium *N*-phenolate betaine dye." (b) Welton, T. Appendix. In *Solvents and Solvent Effects in Organic Chemistry;* WILEY-VCH Verlag GmbH & Co. KGaA, 2011; pp 570-573.
68. House, H. O.; Gaa, P. C.; Lee, J. H. C.; VanDerveer, D. *J. Org. Chem.* **1983**, *48,* 1670.
69. Saito, F.; Becker, J.; Schreiner, P. R. *J. Org. Chem.* **2020**, *85,* 4441.
70. Ring inversions (a) Sauer, E. L. O.; Hooper, J.; Woo, T.; Barriault, L. *J. Am. Chem. Soc.* **2007**, *129,* 2112. (b) Barriault, L.; Deon, D. H. *Org. Lett.* **2001**, *3,* 1925. (c) Gauvreau, D.; Barriault, L. *J. Org. Chem.* **2005**, *70,* 1382. (d) Jacobsen, E. J.; Levin, J.; Overman, L. E. *J. Am. Chem. Soc.* **1988**, *110,* 4329.
71. Ballini, R.; Bosica, G.; Livi, D. *Synthesis* **2001**, 1519.
72. Ho, T.-L.; Liu, S.-H. *Synth. Commun.* **1987**, *17,* 969.
73. (a) Moure, A. L.; Arrayás, R. G.; Cárdenas, D. J.; Alonso, I.; Carretero, J. C. *J. Am. Chem. Soc.* **2012**, *134,* 7219. (b) Jang, H.; Zhugralin, A. R.; Lee, Y.; Hoveyda, A. H. *J. Am. Chem. Soc.* **2011**, *133,* 7859. (c) Lee, Y.; Jang, H.; Hoveyda, A. H. *J. Am. Chem. Soc.* **2009**, *131,* 18234.
74. Gao, Y.; Hanson, R. M.; Klunder, J. M.; Ko, S. Y.; Masamune, H.; Sharpless, K. B. *J. Am. Chem. Soc.* **1987**, *109,* 5765.

75. (a) Mori, K.; Ueda, H. *Tetrahedron* **1981**, *37,* 2581. (b) Burke, S. D.; Buchanan, J. L.; Rovin, J. D. *Tetrahedron Lett.* **1991**, *32,* 3961. (c) Myers, A. G.; Hammond, M.; Wu, Y.; Xiang, J.-N.; Harrington, P. M.; Kuo, E. Y. *J. Am. Chem. Soc.* **1996**, *118,* 10006. (d) Dorta, R. L.; Rodriguez, M. S.; Salazar, J. A.; Suarez, E. *Tetrahedron Lett.* **1997**, *38,* 4675. (e) Zhang, F.; Zeng, J.; Gao, M.; Wang, L.; Chen, G-Q.; Lu, Y.; Zhang, X. *Nat. Chem.* **2021**, *13,* 692.
76. (a) Langille, N. F.; Jamison, T. F. *Org. Lett.* **2006**, *8,* 3761. (b) Nishizawa, Y. *Bull. Chem. Soc. Jpn.* **1961**, *34,* 1170.
77. Greico, P. A.; Gilman, S.; Nishizawa, M. *J. Org. Chem.* **1976**, *41,* 1485.

Contributions to original knowledge

1. Part I of this thesis describes how several novel hybrid antiandrogen-histone deacetylase inhibitors were prepared and were found to possess reasonable potency against both androgen receptor function and HDAC during biological evaluation.

2. Based on the identification of RB-250 as a desirable lead compound, a second series of hybrid compounds were designed based on available SAR data and synthesized. To facilitate their preparation, a novel method of preparing bis-aryl thiohydantoin compounds was discovered and employed for many of the 2nd set of hybrids. Valuable new SAR data was thereby acquired regarding the retention of activity against either target based on structural modification.

3. Certain compounds were shown to be active against both androgen receptor and HDAC, and some were found to be highly effective in cell viability assays with established resistant prostate cancer cell lines, outperforming known anticancer compounds. The lower activity observed in epithelial cells may additionally be useful in the overall activity of the compounds, or it may in fact indicate a therapeutic window and selective action in cancerous cells.

4. In Part II, the development of the first organocatalytic oxy-Cope rearrangement was described, paired in a cascade reaction with subsequent Michael addition. The reaction represents a new complexity-generating transformation with direct application to the synthesis of complex natural products frameworks.

5. The scope of the reaction was evaluated, and remarkably increased reaction rates were observed with more electron-rich olefins distal to the 2-carboxaldehyde on the 1,5-hexadiene scaffold. Several 7/5 fused bicycles were prepared and the stereochemistry was determined by NMR techniques.

6. The mechanism of the novel organocatalytic oxy-Cope / Michael reaction was investigated and discussed with respect to DFT calculations. The erosion of *e.e.* observed and facile uncatalyzed rearrangement of substrates with substituted olefins strongly indicates that the reaction proceeds as named.

Experimental Procedures and Characterization Data

Chapter 5. Experimental

5.1. *General Procedures*

All air sensitive reactions were performed under an inert argon atmosphere. All moisture-sensitive reactions were conducted using flame or oven-dried flasks, thrice evacuated and backfilled under argon. The following solvents were dried as described here before use in reactions in all cases, unless stated otherwise. Tetrahydrofuran (THF) and diethyl ether (Et_2O) were distilled from sodium/benzophenone under a nitrogen atmosphere. Dichloromethane (DCM) and toluene (PhMe) were distilled from calcium hydride (CaH_2) under a drying tube. Triethylamine (NEt_3) and diisopropylamine (HN^iPr_2) were distilled from CaH_2 under a nitrogen atmosphere. Dry dimethylformamide (DMF), 1,4-dioxane, dimethyl sulfoxide (DMSO) and acetonitrile (MeCN) were obtained by storing over 4 Å molecular sieves under argon. Dry MeOH was obtained by storing over 3 Å molecular sieves under argon for at least 3 days. When used as a reagent, DMSO was purified by fractional distillation, the steady boiling middle fraction being collected, and stored over 4 Å molecular sieves under argon. For use in Barbier reactions, Zn dust was typically activated by brief treatment with sat. aq. NH_4Cl, recovered by filtration, rinsed with water followed by ethyl ether, and dried briefly with suction followed by vacuum drying. All other reagents and solvents, including nitromethane, were used as purchased from standard suppliers and without further purification unless otherwise noted. Suberoylanilide hydroxamic acid (SAHA) was previously synthesized by Dr. Dainis Kaldre, and MS-275 was prepared as previously described.[1] Enzalutamide was purchased from 1Click Chemistry and bicalutamide was purchased from TCI. Unless otherwise noted, all reactions were performed at room temperature, typically 21-23 °C. Reactions performed at –78 °C were conducted in a bath of either acetone or isopropyl alcohol saturated with dry ice. Reactions performed at –42 °C were conducted in a bath of MeCN saturated with dry ice. Where necessary, alkyllithiums were titrated using 2,2'-bipyridine.

Thin-layer chromatography (TLC) was performed using glass plates, manufactured by Merck, coated with a 250 μm layer of F_{254} fluorescence indicator-impregnated silica gel of 10-12 μm particle size and 60 Å pore size. TLC plates were visualized with ultraviolet light and/or heating

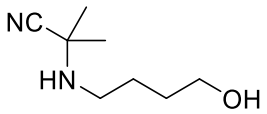
with common stains including $KMnO_4$, *p*-anisaldehyde, and phosphomolybdic acid. Hydroxamic acids were stained with a solution of 2% $FeCl_3$ in 1% aq. HCl. Silica gel flash column chromatography was performed with 40-64 μm (230-400 mesh) irregular silica gel purchased from Silicycle and was conducted either in a glass column with compressed air or on a Combiflash R_f separation instrument. Reverse-phase chromatography was performed on a Combiflash R_f separation instrument with 20-40 μm 100 Å C_{18}-silica gel purchased from Teledyne Isco.

Preparative reverse-phase high-pressure liquid chromatography (HPLC) was performed using a Waters Atlantis C18 T3 OBD Prep Column (100Å, 5 μm, 19 mm X 150 mm) equipped with a guard column. All batches of compounds assessed in biological assays were first analyzed for >95% sample purity by nuclear magnetic resonance spectroscopy (NMR) and homogeneity by liquid chromatography-mass spectrometry (LC-MS). LC-MS was done with a Waters Atlantis C18 T3 OBD, 5 μm, 4.6 mm × 100 mm column. A linear gradient from 95:5 to 5:95 H_2O:MeCN (0.1% formic acid) in 13 min, followed by 100% MeCN for 2 min, at a flow rate of 1 mL/min was employed. Electrospray ionization (ESI) mass spectra were acquired in both + and – modes with a Waters 3100 single-quadrupole mass detector. High-pressure liquid chromatography (HPLC) was performed using an Agilent 1260 Infinity instrument and columns purchased from Daicel Corporation.

Infrared spectroscopy was performed using a Bruker Alpha ATR-IR instrument, either with neat substances or as thin films. and select absorptions are reported by frequency (cm^{-1}). Proton (^1H) and carbon (^{13}C) nuclear magnetic resonance (NMR) spectroscopy was performed using Varian Mercury 300 MHz, Varian Mercury 400 MHz, Varian VNMRS 500 MHz, Varian Inova 500 MHz, Bruker AVIIIHD 400 MHz, Bruker AVIIIHD 500 MHz, and Bruker AVIIIHD 800 MHz spectrometers. Proton chemical shifts are expressed as parts per million (ppm, δ scale) ands are referenced to the appropriate deuterated solvent. Data is reported as follows: chemical shift, multiplicity (s = singlet, bs = broad singlet, d = doublet, dd = double of doublets, dt = doublet of triplets, q = quartet, m = multiplet), coupling constant *J* in Hertz (Hz), and integration. High-resolution mass spectrometry (HRMS) was conducted by Dr. Alexander Wahba or Dr. Nadim Saadé in the Mass Spectrometry Facility in the Department of Chemistry, McGill University.

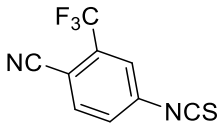
5.2. *Synthetic Procedures for Part I*

2-((4-hydroxybutyl)amino)-2-methylpropanenitrile 2.10a



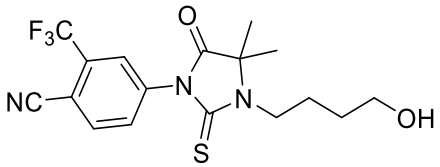
To a stirred solution of neat, commercially available, 4-aminobutanol **2.9a** (0.2156 g, 2.408 mmol, 1 equiv) in acetone cyanohydrin (0.230 mL, 2.52 mmol, 1.05 equiv) was added $MgSO_4$ (0.294 g, 2.44 mmol, 1.01 equiv) over an ice bath. The cooling bath was removed, and the reaction stirred 4 h until complete conversion was observed by NMR. The suspension was filtered on cotton using minimal DCM, concentrated, and used without further purification. **IR** ν_{max} (cm^{-1}): 3600-3300 (broad), 3286, 3260, 2928, 2873, 2235, 1755, 1677, 1504, 1484, 1315, 1178, 1138. **^{1}H NMR** (400 MHz, $CDCl_3$) δ 3.65 (t, J = 5.7 Hz, 2H), 2.79 (t, J = 6.2 Hz, 2H), 1.74 – 1.58 (m, 4H), 1.48 (s, 6H).

4-isothiocyanato-2-(trifluoromethyl)benzonitrile 2.11



This compound was prepared as described by Jung.[2,3] The characterization data are in agreement with that reference.[2] **IR** ν_{max} (ground solid, cm^{-1}): 3118, 3080, 3050, 2228, 2027 (very broad), 1604, 1493, 1431, 1320, 1144, 1123. **^{1}H NMR** (300 MHz, $CDCl_3$) δ 7.88 – 7.80 (m, 1H), 7.59 (dd, *J* = 1.4, 0.6 Hz, 1H), 7.48 (dd, *J* = 8.3, 2.1 Hz, 1H).

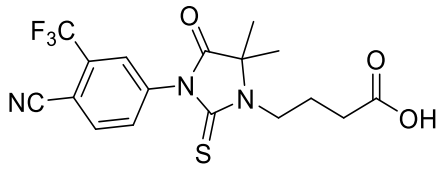
4-(3-(4-hydroxybutyl)-4,4-dimethyl-5-oxo-2-thioxoimidazolidin-1-yl)-2-(trifluoromethyl)benzonitrile 2.13a



To a solution of aryl isothiocyanate **2.11** (0.5467 g, 2.396 mmol, 0.99 equiv) and triethylamine (46.0 μL, 0.330 mmol, 0.14 equiv) in 4.0 mL dry THF was added *α*-cyanoamine **2.10a** (1 equiv) in 0.8 mL dry THF. The solution was rapidly heated to reflux for 30 mins, then cooled to room

temperature and concentrated. The dark residue was purified by silica gel flash chromatography with 15-40% acetone / DCM (R_f 0.13, 20% acetone / DCM) to afford 0.4830 g or 52% yield of the iminothiohydantoin. To a solution of the iminothiohydantoin (0.472 g, 1.23 mmol, 1 equiv) in 7.0 mL MeOH was added 1.0 mL of 2 M aq. HCl. The solution was refluxed 2.5 h then cooled to room temperature, diluted with water, and concentrated to remove MeOH. The concentrate was extracted with 3x10 mL EtOAc and the combined organic layers were washed with 5 mL brine, then dried over anhydrous Na_2SO_4. Concentration of the crude material afforded 0.4085 g or 44% yield of pure thiohydantoin **2.13a** (R_f 0.41, 20% acetone / DCM) from the isothiocyanate. The ^{1}H NMR data in $CDCl_3$ agrees with the literature.[4] **IR** ν_{max} (cm^{-1}): 3419, 2233, 1751, 1127. **^{1}H NMR** (500 MHz, $CDCl_3$) δ 7.95 (d, J = 8.3 Hz, 1H), 7.89 (d, J = 2.0 Hz, 1H), 7.77 (dd, J = 8.3, 2.1 Hz, 1H), 3.78 – 3.71 (m, 4H), 1.95 (tt, J = 8.0, 6.4 Hz, 2H), 1.67 (ddd, J = 13.6, 7.4, 6.2 Hz, 2H), 1.60-1.56 (bs, 1H) 1.59 (s, 6H). **^{13}C NMR** (126 MHz, $CDCl_3$) δ 178.49, 175.37, 137.23, 135.26, 133.64 (q, J = 33.4 Hz), 132.21, 127.16 (q, J = 4.8 Hz), 122.02 (q, J = 274.3 Hz), 114.97, 110.16 (q, J = 2.2 Hz), 65.25, 62.12, 44.04, 29.77, 24.87, 23.35.

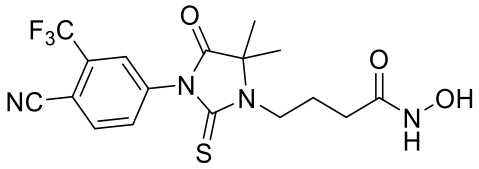
4-(3-(4-cyano-3-(trifluoromethyl)phenyl)-5,5-dimethyl-4-oxo-2-thioxoimidazolidin-1-yl)butanoic acid 2.14a



To a solution of thiohydantoin alcohol **2.13a** (0.3961 g, 1.03 mmol, 1 equiv) in 4.1 mL DMF was added C18 celite (1.35 g) and pyridinium dichromate (1.35 g, 3.59 mmol, 3.48 equiv). This was stirred 4 d, then additional PDC (0.614 g, 1.63 mmol, 1.58 equiv) and C18 celite (0.61 g) were added. The mixture was stirred one additional day, then filtered on celite and rinsed with 80 mL of diethyl ether. The filtrate was diluted with 40 mL of water, 1 M aq. HCl was added to achieve a pH < 2, the layers were separated, and the aqueous layer extracted once more with 40 mL EtOAc. The organic layers were washed separately with 40 mL each water and brine, combined, dried over $MgSO_4$, and concentrated. The crude extract was triturated thoroughly in ether and filtered again on celite, then purified by silica gel flash chromatography with 75-100% EtOAc / hexanes (R_f 0.32, 5% MeOH / 20% acetone / 75% DCM) to afford 0.134 g or 33% yield of **2.14a**. The ^{1}H NMR data in $CDCl_3$ agrees with the literature.[5] **IR** ν_{max} (cm^{-1}): 3400 – 3100 (broad), 2931, 2235, 1754,

1711, 1504, 1484, 1433, 1420, 1377, 1311, 1279, 1177, 1138. **^{1}H NMR** (400 MHz, $CDCl_3$) δ 9.09 – 8.02 (bs, 1H), 7.95 (d, J = 8.3 Hz, 1H), 7.89 (d, J = 2.0 Hz, 1H), 7.76 (dd, J = 8.3, 2.1 Hz, 1H), 3.81 – 3.72 (m, 2H), 2.51 (t, J = 6.9 Hz, 2H), 2.22 – 2.10 (m, 2H), 1.60 (s, 6H). **HRMS** (ESI) *m/z* calcd for $C_{17}H_{15}O_3N_3F_3S$ [$(M–H)^-$]: 398.07917, measured: 398.07930.

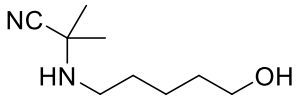
4-(3-(4-cyano-3-(trifluoromethyl)phenyl)-5,5-dimethyl-4-oxo-2-thioxoimidazolidin-1-yl)-N-hydroxybutanamide (RB-227) 2.3a



To a solution of carboxylic acid **2.14a** (96.2 mg, 0.241 mmol, 1 equiv) and NH_2OTBS (72.3 mg, 0.491 mmol, 2.04 equiv) in 2.0 mL dry DCM was added HOAt (36.1 mg, 0.265 mmol, 1.1 equiv), followed by EDC hydrochloride (56.1 mg, 0.293 mmol, 1.21 equiv). The reaction was stirred 28 h, then diluted with 5 mL water and 8 mL DCM, and separated. The aqueous layer pH was adjusted to 4 with a few drops of 1 M HCl, then extracted with 2x15 mL EtOAc. The DCM and EtOAc extracts were each washed separately with 3 mL of brine, combined, dried over $MgSO_4$, and concentrated for 0.1482 g of crude TBS-protected hydroxamic acid. To this extract in 2.5 mL of MeCN in a 15 mL conical falcon tube was added dropwise 0.6 mL of 48 wt.% $HF_{(aq.)}$. The resulting mixture was stirred 7 h at room temperature, then quenched with sat. $NaHCO_3$ dropwise until bubbling ceased. The MeCN was removed by rotary evaporation, then the aqueous layer was diluted with 5 mL water and extracted with 3x12 mL EtOAc. The combined organic layers were washed with 5 mL of brine, dried over anhydrous Na_2SO_4, filtered, and concentrated. The concentrate was purified by C18 silica gel flash chromatography with 10-90% MeCN / H_2O (R_f 0.2, 20% acetone / DCM by normal phase TLC) to afford 25.8 mg or 27% yield of recovered carboxylic acid **2.14a** in addition to 35.3 mg or 35% yield of hydroxamic acid **2.3a** (RB-227) as a white powder, pure by NMR. Purification by preparatory HPLC with MeCN / water furnished compound, which was pure by NMR and 97% homogeneous by LC-MS analysis, for use in biological assays. **IR** ν_{max} (cm^{-1}): 2283, 1753, 1643, 1614, 1482, 1310, 1275, 1126. **^{1}H NMR** (500 MHz, CD_3CN) δ 9.52 – 8.20 (bs, 1H), 8.09 (d, J = 8.2 Hz, 1H), 8.02 (d, J = 2.0 Hz, 1H), 7.87 (dd, J = 8.2, 2.1 Hz, 1H), 7.74 – 6.70 (bs, 1H), 3.76 – 3.69 (m, 2H), 2.17 (t, J = 7.2 Hz, 2H), 2.13 – 2.03 (m, 2H), 1.55 (s, 6H). **^{13}C NMR** (126 MHz, CD_3CN) δ 179.89, 176.55, 170.62, 139.00, 136.70,

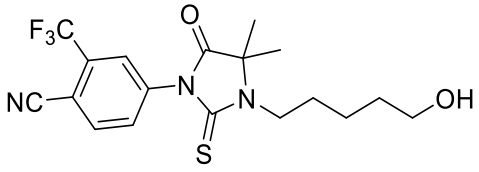
134.01, 133.01 (q, J = 33.0 Hz), 128.42 (q, J = 4.9 Hz), 123.32 (q, J = 273.1 Hz), 116.05, 110.23 (m), 66.41, 44.10, 30.41, 24.55, 22.91. **HRMS** (ESI) *m/z* calcd for $C_{17}H_{16}O_3N_4F_3S$ [$(M–H)^-$]: 413.09007, measured: 413.08913, *m/z* calcd for $C_{17}H_{18}O_3N_4F_3S$ [$(M+H)^+$]: 415.10462, measured: 415.10404.

2-((5-hydroxypentyl)amino)-2-methylpropanenitrile 2.10b



To neat, commercially available, 5-aminopentanol **2.9b** (0.4900 g, 4.75 mmol, 1 equiv) in a flame-dried flask was added acetone cyanohydrin (0.455 mL, 4.98 mmol, 1.05 equiv). The flask was swirled to dissolve the amine then left overnight without stirring, after which quantitative conversion was observed by NMR. The α-cyanoamine **2.10b** was used directly and without further purification in the following step. **^{1}H NMR** (500 MHz, $CDCl_3$) δ 3.66 (t, J = 6.5 Hz, 2H), 2.74 (t, J = 7.0 Hz, 2H), 1.64 – 1.57 (m, 3H), 1.57 – 1.51 (m, 3H), 1.49-1.42 (m, 2H), 1.46 (s, 6H).

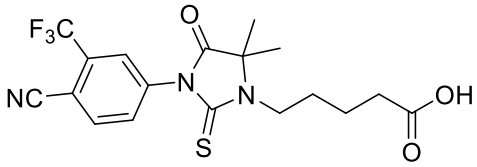
4-(3-(5-hydroxypentyl)-4,4-dimethyl-5-oxo-2-thioxoimidazolidin-1-yl)-2-(trifluoromethyl)benzonitrile 2.13b



To a solution of aryl isothiocyanate **2.11** (1.08 g, 4.73 mmol, 1.0 equiv) and triethylamine (86.0 μL, 0.617 mmol, 0.13 equiv) in 8.1 mL dry THF was added *α*-cyanoamine **2.10b** (1 equiv) in 1.0 mL dry THF by cannula. The solution was heated to reflux for 35 mins, cooled, and concentrated by rotary evaporation. Silica gel flash chromatography with 0-40% acetone / DCM (R_f 0.18, 20% acetone / DCM) afforded partially purified iminothiohydantoin product which was hydrolyzed and isolated as done for **2.13a**. Silica gel flash chromatography of the resulting crude mixture with 20% acetone / DCM (R_f 0.48, 25% acetone / DCM) afforded 1.09 g or 58% yield of thiohydantoin **2.13b**. **IR** ν_{max} (cm^{-1}): 3455 (broad), 2937, 2862, 2233, 1754, 1613, 1503, 1311, 1176, 1137. **^{1}H NMR** (500 MHz, $CDCl_3$) δ 7.94 (d, J = 8.2 Hz, 1H), 7.89 (d, J = 2.0 Hz, 1H), 7.77 (dd, J = 8.2, 2.1 Hz, 1H), 3.72 – 3.65 (m, 4H), 1.92 – 1.82 (m, 2H), 1.65 (dq, J = 8.3, 6.4 Hz, 2H), 1.58 (s, 6H),

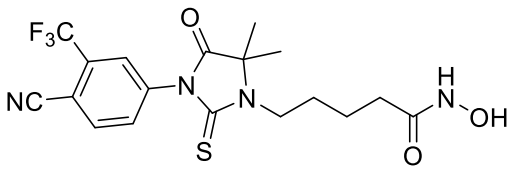
1.49 (qd, *J* = 9.6, 8.8, 6.2 Hz, 2H), 1.41 (bs, 1H). **^{13}C NMR** (126 MHz, $CDCl_3$) δ 178.40, 175.40, 137.26, 135.24, 133.58 (q, *J* = 33.4 Hz), 132.23, 127.16 (q, *J* = 4.8 Hz), 122.01 (q, *J* = 274.2 Hz), 114.97, 110.09 (q, *J* = 2.0 Hz), 65.24, 62.64, 44.39, 32.15, 28.00, 23.48, 23.33. **HRMS** (ESI) *m/z* calcd for $C_{18}H_{20}F_3N_3NaO_2S$ [$(M+Na)^+$]: 422.1121, measured: 422.1109.

5-(3-(4-cyano-3-(trifluoromethyl)phenyl)-5,5-dimethyl-4-oxo-2-thioxoimidazolidin-1-yl)pentanoic acid 2.14b



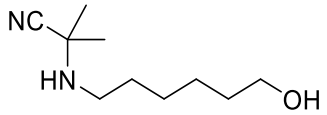
To a solution of thiohydantoin alcohol **2.13b** (1.09 g, 2.73 mmol, 1 equiv) in 9.3 mL DMF was added 4.1 g celite, then pyridinium dichromate (4.13 g, 11.0 mmol, 4.02 equiv) in portions over 2 h. The mixture was stirred 30 h, then poured into 300 mL of diethyl ether to precipitate the chromium species, filtered on celite with 100 mL of ether premixed with 2.0 mL AcOH. The ethereal filtrate was washed successively with 2x100 mL 0.5 M HCl, 20 mL water, and 20 mL brine, then dried over $MgSO_4$. Silica gel flash chromatography with 1% AcOH / 25% acetone / 74% DCM (R_f 0.29, 25% acetone / DCM) afforded 0.533 g or 47% yield of the carboxylic acid **2.14b**. The ^{1}H NMR data in $CDCl_3$ agrees with the literature.[5] **IR** ν_{max} (cm^{-1}): 2238, 1753, 1698, 1134. **^{1}H NMR** (500 MHz, $CDCl_3$) δ 9.61 – 9.10 (bs, 1H), 7.95 (d, *J* = 8.3 Hz, 1H), 7.89 (d, *J* = 2.0 Hz, 1H), 7.77 (dd, *J* = 8.3, 2.1 Hz, 1H), 3.75 – 3.68 (m, 2H), 2.48 (t, *J* = 7.2 Hz, 2H), 1.96 – 1.86 (m, 2H), 1.75 (p, *J* = 7.4 Hz, 2H), 1.59 (s, 6H). **^{13}C NMR** (126 MHz, $CDCl_3$) δ 179.20, 178.52, 175.32, 137.21, 135.25, 133.52 (q, *J* = 33.4 Hz), 132.21, 127.12 (q, *J* = 4.8 Hz), 121.99 (q, *J* = 274.2 Hz), 114.94, 110.07 (q, *J* = 2.2 Hz), 65.21, 43.89, 33.40, 27.59, 23.27, 22.10.

5-(3-(4-cyano-3-(trifluoromethyl)phenyl)-5,5-dimethyl-4-oxo-2-thioxoimidazolidin-1-yl)-N-hydroxypentanamide (RB-95) 2.3b



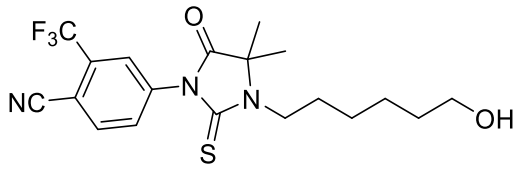
Carboxylic acid **2.14b** (0.2630 g, 0.6362 mmol, 1 equiv) was added to a pre-mixed solution of EDC•HCl (0.1287 g, 0.6714 mmol, 1.06 equiv) and NH_2OTBS (0.0995 g, 0.676 mmol, 1.06 equiv) in 3.0 mL dry DCM. The reaction was stirred for 22 h, then diluted with 5 mL DCM and separated from 3 mL 0.1 N HCl. The aqueous layer was extracted with 3x5 mL DCM, then the combined organic layers were washed with 5 mL brine, dried over anhydrous Na_2SO_4, filtered, and concentrated. A solution of the crude residue in 6.0 mL of 10% HF/MeCN (prepared from 48 wt.% $HF_{(aq)}$) in a plastic conical centrifuge tube was stirred for 48 h, then sat. $NaHCO_3$ was added to fully quench the acid. The aqueous solution was filtered and extracted with 3x10 mL DCM. The combined organic layers were washed sequentially with 5 mL each water and brine, dried over anhydrous Na_2SO_4, filtered, and concentrated. The residue was purified by C18 silica gel flash chromatography with 35-50% MeCN / H_2O and afforded 110 mg or 40% yield of hydroxamic acid **2.3b** (RB-95) as a white powder which was pure by NMR. Purification by preparatory HPLC with MeCN / water gave compound which was pure by NMR and 98.7% homogeneous by LC-MS analysis for use in biological assays. **IR** ν_{max} (cm^{-1}): 3541, 2234, 1753, 1612, 1503, 1130. **^{1}H NMR** (500 MHz, $CDCl_3$) δ 8.36 (s, 2H), 7.95 (d, *J* = 8.2 Hz, 1H), 7.88 (d, *J* = 1.9 Hz, 1H), 7.76 (dd, *J* = 8.1, 2.0 Hz, 1H), 3.74 – 3.67 (m, 2H), 2.25 (t, *J* = 7.2 Hz, 2H), 1.91 – 1.82 (m, 2H), 1.79 – 1.73 (m, 2H), 1.58 (s, 6H). **^{13}C NMR** (126 MHz, $CDCl_3$) δ 178.65, 175.26, 170.74, 137.17, 135.33, 133.64 (q, *J* = 33.6 Hz), 132.24, 127.17 (q, *J* = 4.8 Hz), 122.01 (q, *J* = 274.2 Hz), 114.95, 110.22 (q, *J* = 2.0 Hz), 65.31, 43.75, 32.10, 27.56, 23.34, 22.66. **HRMS** (ESI) *m/z* calcd for $C_{18}H_{18}O_3N_4F_3S$ $[(M–H)^–]$: 427.10572, measured: 427.10460.

2-((6-hydroxyhexyl)amino)-2-methylpropanenitrile 2.10c



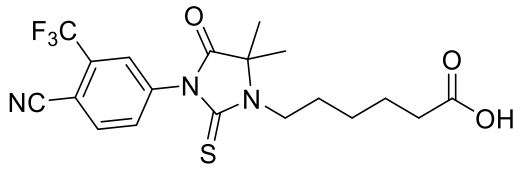
To neat, commercially available, 6-aminohexanol **2.9c** (0.5248 g, 4.48 mmol, 1 equiv) in a flame-dried flask was added acetone cyanohydrin (0.429 mL, 4.70 mmol, 1.05 equiv). The flask was swirled to dissolve the amine then left overnight for 12 h without stirring, after which quantitative conversion was observed by NMR. The α-cyanoamine **2.10c** was used directly and without further purification. **^{1}H NMR** (500 MHz, $CDCl_3$) δ 3.67 (t, *J* = 6.6 Hz, 2H), 2.75 (t, *J* = 7.2 Hz, 2H), 1.66 (s, 1H), 1.64 – 1.50 (m, 4H), 1.48 (s, 6H), 1.42 (p, *J* = 3.5 Hz, 5H).

4-(3-(6-hydroxyhexyl)-4,4-dimethyl-5-oxo-2-thioxoimidazolidin-1-yl)-2-(trifluoromethyl)benzonitrile 2.13c



To a solution of aryl isothiocyanate **2.11** (1.02 g, 4.38 mmol, 0.98 equiv) and triethylamine (81.0 μL, 0.581 mmol, 0.13 equiv) in 4.6 mL dry THF was added *α*-cyanoamine **2.10c** (1 equiv) in 4.0 mL dry THF by cannula. The solution was refluxed 30 mins, then cooled and concentrated by rotary evaporation. Silica gel flash chromatography with 0-40% acetone / DCM (R_f 0.29, 20% acetone / DCM) afforded partially purified iminothiohydantoin intermediate, which was subsequently hydrolyzed as done for **2.13a**. Silica gel flash chromatography with 20% acetone / DCM afforded 0.862 g or 48% yield of the thiohydantoin **2.13c**. **IR** ν_{max} (cm^{-1}): 3425 (broad), 2933, 2860, 2234, 1754, 1613. **^{1}H NMR** (500 MHz, $CDCl_3$) δ 7.93 (d, *J* = 8.3 Hz, 1H), 7.88 (d, *J* = 2.0 Hz, 1H), 7.76 (dd, *J* = 8.2, 2.1 Hz, 1H), 3.70 – 3.64 (m, 2H), 3.62 (t, *J* = 6.5 Hz, 2H), 2.15 – 1.90 (bs, 1H), 1.87 – 1.77 (m, 2H), 1.62 – 1.52 (m, 2H), 1.56 (s, 6H), 1.47 – 1.35 (m, 4H). **^{13}C NMR** (126 MHz, $CDCl_3$) δ 178.22, 175.37, 137.25, 135.17, 133.38 (q, *J* = 33.4 Hz), 132.22, 127.10 (q, *J* = 4.8 Hz), 121.96 (q, *J* = 274.2 Hz), 114.94, 109.87 (q, *J* = 2.1 Hz), 65.19, 62.64, 44.33, 32.53, 28.08, 26.88, 25.33, 23.21. **HRMS** (ESI) *m/z* calcd for $C_{19}H_{22}F_3N_3NaO_2S$ [$(M+Na)^+$]: 436.1277, measured: 436.1291.

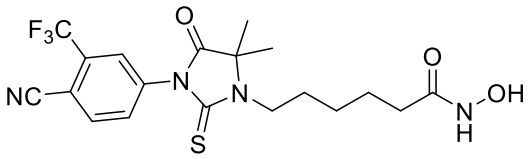
6-(3-(4-cyano-3-(trifluoromethyl)phenyl)-5,5-dimethyl-4-oxo-2-thioxoimidazolidin-1-yl)hexanoic acid 2.14c



To a solution of thiohydantoin alcohol **2.13c** (0.862 g, 2.09 mmol, 1 equiv) in 6.3 mL DMF was added 3.1 g celite, then pyridinium dichromate (3.144 g, 8.37 mmol, 4.01 equiv) in portions over 2 h. The mixture was stirred 30 h, then poured into 200 mL of diethyl ether to precipitate the chromium species, filtered on celite, and rinsed with 50 mL of ether followed by 100 mL diethyl

ether premixed with 1.0 mL AcOH. The ethereal filtrate was washed successively with 2x50 mL 0.5 M HCl, 10 mL water, and 10 mL brine then dried over $MgSO_4$. Silica gel flash chromatography with 1% AcOH / 20% acetone / 79% DCM (R_f 0.22, 20% acetone / DCM) afforded 0.546 g or 61% yield of the carboxylic acid **2.14c**. The ^{1}H NMR data in $CDCl_3$ agrees with the literature.[5] **IR** ν_{max} (cm^{-1}): 3051 (broad), 2235, 1755, 1698, 1139. **^{1}H NMR** (500 MHz, $CDCl_3$) δ 9.95 (bs, 1H), 7.96 (d, *J* = 8.2 Hz, 1H), 7.91 (d, *J* = 2.0 Hz, 1H), 7.79 (dd, *J* = 8.3, 2.1 Hz, 1H), 3.74 – 3.66 (m, 2H), 2.40 (t, *J* = 7.4 Hz, 2H), 1.86 (p, *J* = 7.8 Hz, 2H), 1.72 (p, *J* = 7.4 Hz, 2H), 1.58 (s, 6H), 1.46 (p, *J* = 7.6 Hz, 2H).

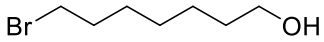
6-(3-(4-cyano-3-(trifluoromethyl)phenyl)-5,5-dimethyl-4-oxo-2-thioxoimidazolidin-1-yl)-N-hydroxyhexanamide (RB-211) 2.3c



Carboxylic acid **2.14c** (0.1647 g, 0.3583 mmol, 1 equiv) was added to a pre-mixed solution of EDC•HCl (0.2222 g, 1.159 mmol, 3.0 equiv) and NH_2OTBS (0.1704 g, 1.158 mmol, 3.2 equiv) in 5.5 mL dry DCM. The reaction was stirred 26 h, then passed through a 2" thick plug of silica gel and eluted with 60 mL of 10% acetone / DCM to obtain 0.1371 g of partially purified TBS-protected hydroxamic acid intermediate. To a solution of this residue in 2.5 mL MeCN in a plastic conical centrifuge tube was added 0.25 mL of 48 wt.% $HF_{(aq)}$ dropwise. This reaction was stirred 2 h, then carefully added to 10 mL sat. aq. $NaHCO_3$ and 10 mL H_2O was added. MeCN was removed *in vacuo* and the aqueous solution extracted with 3x15 mL EtOAc. The combined organic layers were washed sequentially with 5 mL each water and brine, dried over anhydrous Na_2SO_4, filtered, and concentrated. The residue was purified by C18 silica gel flash chromatography with 30-50% MeCN / H_2O and afforded 7.7 mg or 5% yield of **2.3c** (RB-211), pure by NMR and 97.9% homogeneous by LC-MS analysis. This had been recovered as a fluffy white powder directly by filtration after organic solvent removal by rotary evaporation from the recovered fractions. Concentration and lyophilization of the remainder gave a further crop of 65.3 mg or 41% yield of hydroxamic acid **2.3c** as a faint yellow film, also pure by NMR, for a combined 43% yield over two steps. **IR** ν_{max} (cm^{-1}): 3216 (broad), 2938, 2863, 2234, 2162, 1752, 1651, 1614. **^{1}H NMR** (400 MHz, $CDCl_3$) δ 8.95 (bs, 2H), 7.94 (d, *J* = 8.11 Hz, 1H), 7.89 (s, 1H), 7.76 (d, *J* = 8.12 Hz, 1H),

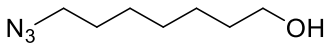
3.65 (t, J = 8.0 Hz, 2H), 2.17 (m, 2H), 1.83 (m, 2H), 1.68 (m, 2H), 1.55 (s, 6H), 1.40 (m, 2H). **^{13}C NMR** (101 MHz, $CDCl_3$) δ 178.40, 175.34, 171.49, 137.23, 135.31, 133.43 (q, J = 33.3 Hz), 132.30, 127.17 (q, J = 4.4 Hz), 122.00 (q, J = 274.2 Hz), 114.97, 109.98 (m, J = 2.3 Hz), 65.32, 44.10, 32.63, 27.63, 26.33, 24.78, 23.21. **HRMS** (ESI) *m/z* calcd for $C_{19}H_{21}F_3N_4NaO_3S$ [$(M+Na)^+$]: 465.1179, measured: 465.1178.

7-bromoheptan-1-ol



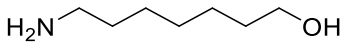
Roughly following Chong's procedure,[6] to a solution of 1,7-heptanediol (1.0 g, 7.6 mmol, 1 equiv) in 30 mL dry PhMe was added 48% HBr (1.0 mL, 8.9 mmol, 1.2 equiv) dropwise, then the resulting solution refluxed at 120 °C for 41 h until TLC indicated consumption of the diol. The reaction was cooled and poured into 45 mL sat. $NaHCO_3$, then extracted with 3x100 mL diethyl ether. The combined organic layers were washed with 10 mL brine, dried over anhydrous $MgSO_4$, filtered, and concentrated to afford 1.5 g or quantitative yield of 7-bromoheptanol. This used without further purification, and the characterization data matched the literature.[7]

7-azidoheptan-1-ol



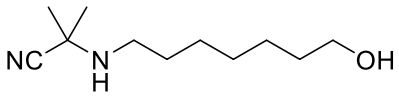
To a solution of 7-bromoheptanol (0.4946 g, 2.538 mmol, 1 equiv) in 8.3 mL dry DMF was added sodium azide (0.3374 g, 5.190 mmol, 2.0 equiv) and the mixture was stirred for 48 h. The reaction was poured into 80 mL 0.5 N HCl then extracted with 3x30 mL EtOAc. The combined organic layers were washed sequentially with 10 mL 0.5 N HCl, water, and brine, dried over anhydrous Na_2SO_4, filtered, and concentrated. The concentrate was taken up into 1:1 Et_2O / water and washed sequentially with water and brine, dried over anhydrous $MgSO_4$, filtered, and concentrated to afford 0.3669 g or 92% yield of 7-azidoheptanol. This used without further purification, and the characterization data matched the literature.[7]

7-aminoheptan-1-ol 2.9d



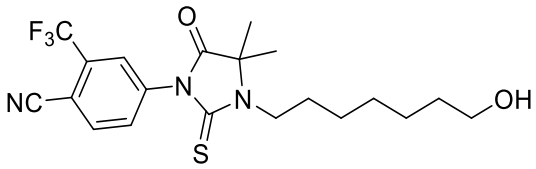
To a solution of 7-azidoheptanol (0.4307 g, 2.739 mmol, 1 equiv) in 10 mL EtOH and 1 mL aq. NaOH was added PPh_3 (2.18 g, 8.31 mmol, 3.0 equiv) and the solution stirred for 3 d. Ethanol was removed by rotary distillation, the reaction diluted with water, and 1 M NaOH was added to achieve a pH of 14 and 20 mL total aqueous volume. This was extracted with 7x50 mL $CHCl_3$, then the combined organic layers were washed with 50 mL brine, dried over anhydrous Na_2SO_4, filtered and concentrated to afford 0.2528 g or 70% yield of 7-aminoheptanol **2.9d**. This used without further purification, and the characterization data matched the literature.[7]

2-((7-hydroxyheptyl)amino)-2-methylpropanenitrile 2.10d



To neat 7-aminoheptanol **2.9d** (0.333 g, 2.54 mmol, 1 equiv) was added neat acetone cyanohydrin (0.275 mL, 3.05 mmol, 1.2 equiv). The solution was stirred overnight, after which time quantitative conversion was observed by NMR. Cyanoamine **2.10d** was used directly and without further purification.

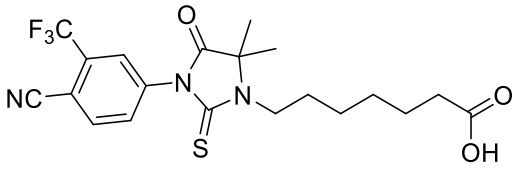
4-(3-(7-hydroxyheptyl)-4,4-dimethyl-5-oxo-2-thioxoimidazolidin-1-yl)-2-(trifluoromethyl)benzonitrile 2.13d



A solution of α-cyanoamine **2.10d** (1 equiv) in 5.0 mL dry THF was added to the aryl isothiocyanate **2.11** (0.5856 g, 2.57 mmol, 1.01 equiv). Triethylamine (46.0 µL, 0.330 mmol, 0.13 equiv) was added and the solution was heated to reflux for 35 mins, then cooled over a water bath and concentrated onto silica gel by rotary evaporation. Silica gel flash chromatography with 5-20% acetone / DCM (R_f 0.23, 20% acetone / DCM) afforded partially purified iminothiohydantoin product which was hydrolyzed akin to thiohydantoin **2.13a**. Silica gel flash chromatography with 0-10% acetone / DCM (R_f 0.38, 10% acetone / DCM) afforded 0.724 g or 67% yield of thiohydantoin **2.13d**. **IR** ν_{max} (cm^{-1}): 3461 (broad), 2931, 2857, 2234, 1752, 1613. **^{1}H NMR** (500 MHz, $CDCl_3$) δ 7.93 (d, J = 8.2 Hz, 1H), 7.88 (d, J = 2.1 Hz, 1H), 7.76 (dd, J = 8.3, 2.1 Hz, 1H),

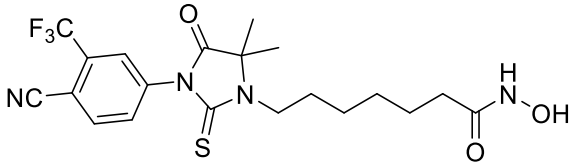
3.68 – 3.62 (m, 2H), 3.59 (t, J = 6.6 Hz, 2H), 1.85-1.77 (m, 2H), 1.71 (s, 1H), 1.55 (s, 6H), 1.57-1.50 (m, 2H), 1.37 (m, 6H). **^{13}C NMR** (126 MHz, $CDCl_3$) δ 178.13, 175.35, 137.23, 135.14, 133.30 (q, J = 33.4 Hz), 132.20, 127.07 (q, J = 4.8 Hz), 121.93 (q, J = 274.2 Hz), 114.91, 109.80 (q, J = 2.2 Hz), 65.16, 62.73, 44.36, 32.57, 28.88, 28.01, 27.00, 25.61, 23.16. **HRMS** (ESI) *m/z* calcd for $C_{20}H_{25}F_3N_3O_2S$ [$(M+H)^+$]: 428.16141, measured: 428.16175, *m/z* calcd for $C_{20}H_{24}F_3N_3O_2SNa$ [$(M+Na)^+$]: 450.14335, measured: 450.14341.

7-(3-(4-cyano-3-(trifluoromethyl)phenyl)-5,5-dimethyl-4-oxo-2-thioxoimidazolidin-1-yl)heptanoic acid 2.14d



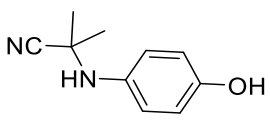
To a solution of thiohydantoin alcohol **2.13d** (0.580 g, 1.36 mmol, 1 equiv) in 6.0 mL DMF was added 2.0 g celite, followed by pyridinium dichromate (2.03 g, 5.53 mmol, 4.07 equiv) and a few drops of water, which was found to prevent dimeric esters from forming. The mixture was stirred 22 h, then poured into 150 mL diethyl ether to precipitate the chromium species. The resulting suspension was filtered on celite and rinsed thoroughly with additional ether to give a tan solution. The ethereal filtrate was washed with 100 mL 0.5 M HCl, which was subsequently extracted with 2x200 mL ether. The combined organic layers were washed twice with each 50 mL 1 M HCl and 50 mL water, then with 50 mL brine. The combined aqueous was then extracted with 2x80 mL ether further, and these combined organic layers were then washed with 20 mL each water and brine. The total combined organic layers were dried over $MgSO_4$ and concentrated to afford 0.505 g or 84% yield of pure carboxylic acid **2.14d** (R_f 0.19, 10% acetone / DCM). The ^{1}H NMR data in $CDCl_3$ agrees with the literature.[5] **IR** ν_{max} (cm^{-1}): 2236, 1758, 1725, 1693, 1126. **^{1}H NMR** (500 MHz, DMSO-d_6) δ 11.97 (s, 1H), 8.31 (d, J = 8.2 Hz, 1H), 8.22 (d, J = 1.9 Hz, 1H), 8.00 (dd, J = 8.2, 2.0 Hz, 1H), 3.71 – 3.64 (m, 2H), 2.21 (t, J = 7.3 Hz, 2H), 1.76 (td, J = 10.9, 9.3, 5.4 Hz, 2H), 1.59 – 1.48 (m, 8H), 1.38 – 1.29 (m, 4H).

7-(3-(4-cyano-3-(trifluoromethyl)phenyl)-5,5-dimethyl-4-oxo-2-thioxoimidazolidin-1-yl)-N-hydroxyheptanamide (RB-236) 2.3d



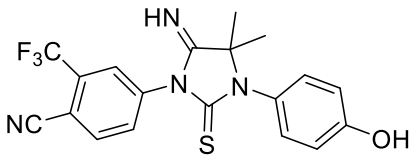
Carboxylic acid **2.14d** (75.0 mg, 0.170 mmol, 1 equiv), NH_2OTBS (49.8 mg, 0.338 mmol, 2.0 equiv), HOAt (26.4 mg, 0.194 mmol, 1.1 equiv), and EDC hydrochloride (39.7 mg, 0.207 mmol, 1.2 equiv) were dissolved in 1.5 mL dry DCM and stirred 17 h. Additional EDC (16.0 mg) and NH_2OTBS (18.9 mg) were added and the reaction stirred 7 h longer. The reaction was diluted with 10 mL each DCM and water, then the aqueous layer was extracted with 2x5 mL EtOAc. The combined organic layers were washed with 2 mL brine, dried over Na_2SO_4, and concentrated. To the crude residue, dissolved in 2.5 mL of MeCN in a plastic conical tube, was added 0.6 mL of 48 wt.% $HF_{(aq)}$ dropwise and the solution stirred 10 h. The HF was quenched with 100 mL sat. aq. $NaHCO_3$ and extracted with 3x100 mL EtOAc. The combined organic layers were washed with 10 mL water and brine, concentrated, and purified by C18 silica gel flash chromatography with 10-90% MeCN / H_2O to afford 27.0 mg or 35% yield of **2.3d** (RB-236) as a colourless oil. This was further purified by preparatory HPLC with MeCN / water and gave RB-236 as a white powder, totally pure by NMR and 98.9% homogeneous by LC-MS analysis, for use in biological assays. **IR** ν_{max} (cm^{-1}): 1753, 1645, 1613, 1134. **^{1}H NMR** (500 MHz, DMSO-d_6) δ 10.32 (s, 1H), 8.64 (s, 1H), 8.34 (d, J = 8.2 Hz, 1H), 8.23 (d, J = 1.9 Hz, 1H), 8.01 (dd, J = 8.2, 2.0 Hz, 1H), 3.68 – 3.64 (m, 2H), 1.95 (t, J = 7.4 Hz, 2H), 1.75 (p, J = 7.9 Hz, 2H), 1.58 – 1.44 (m, 8H), 1.38 – 1.23 (m, 4H). **^{13}C NMR** (126 MHz, $CDCl_3$) δ 178.35, 175.38, 171.27, 137.18, 135.29, 133.58 (q, J = 33.5 Hz), 132.25, 127.17 (q, J = 4.8 Hz), 121.99 (q, J = 274.2 Hz), 114.99, 110.11 (q, J = 2.3 Hz), 65.27, 44.31, 32.81, 28.58, 27.95, 26.75, 25.11, 23.34. **HRMS** (ESI) *m/z* calcd for $C_{20}H_{23}F_3N_4O_3SNa$ [$(M+Na)^+$]: 479.13461, measured: 479.13427.

Cyanoamine phenol 2.15



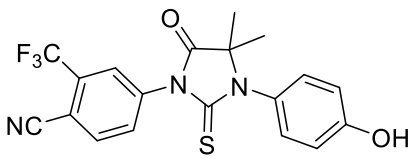
To *p*-aminophenol (0.3947 g, 3.62 mmol, 1 equiv) in a dry flask under argon was added 0.517 g $MgSO_4$ and acetone cyanohydrin (1.15 mL, 12.6 mmol, 3.5 equiv), then the suspension heated at 80-90 °C for 6 h. The reaction was cooled, 2 mL water was added, and the mixture vigorously agitated then filtered with vacuum. The recovered solid was concentrated from dry PhMe until dry and afforded 0.5868 g or 92% yield of cyanoamine **2.15**. The spectroscopic data in $CDCl_3$ are in agreement with the literature[3] and that previously described by our group.[8] **^{1}H NMR** (500 MHz, $CDCl_3$) δ 6.96 – 6.90 (m, 2H), 6.77 (d, *J* = 8.5 Hz, 2H), 1.59 (s, 6H). **^{1}H NMR** (500 MHz, DMSO-d_6) δ 8.88 (bs, 1H), 6.80 – 6.76 (m, 2H), 6.66 – 6.62 (m, 2H), 5.20 (s, 1H), 1.52 (s, 6H). **HRMS** (ESI) *m/z* calcd for $C_{10}H_{11}ON_2$ [$(M–H)^–$]: 175.0877, measured: 175.0869.

Iminothiohydantoin 2.16a



To a solution of cyanoamine **2.15** (0.7031 g, 3.990 mmol, 1 equiv) and isothiocyanate **2.11** (0.9225 g, 4.043 mmol, 1.0 equiv) in 10 mL dry THF at 0 °C over an ice bath was added NEt_3 (0.278 mL, 1.99 mmol, 0.5 equiv) and the reaction stirred 4 d. The THF was removed by rotary evaporation and the dark residue purified by silica gel flash chromatography in EtOAc / hexanes. Silica gel flash chromatography with 5-15% acetone / DCM (R_f 0.81, 20% acetone / DCM) afforded 0.5395 g or 33% yield of iminothiohydantoin **2.16a**. **^{1}H NMR** (400 MHz, DMSO-d_6) δ 9.78 (s, 1H), 9.06 (s, 1H), 8.31 (d, *J* = 8.3 Hz, 1H), 8.19 (d, *J* = 1.8 Hz, 1H), 8.01 (dd, *J* = 8.3, 1.7 Hz, 1H), 7.11 (d, *J* = 8.7 Hz, 2H), 6.85 (d, *J* = 8.8 Hz, 2H), 1.46 (s, 6H). **HRMS** (ESI) *m/z* calcd for $C_{19}H_{14}ON_4F_3S$ [$(M–H)^–$]: 403.08459, measured: 403.08452.

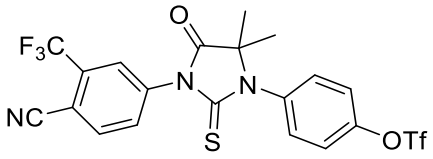
Thiohydantoin phenol 2.16



To iminothiohydantoin **2.16a** in 12.5 mL MeOH was added 5 mL 2 N HCl dropwise over an ice bath, and the solution refluxed at 84 °C for 4 h, at which time TLC analysis indicated complete

hydrolysis. The reaction was cooled, diluted with water, and MeOH removed by rotary evaporation, then the aqueous extracted with 3x15 mL EtOAc. The combined organic layers were washed sequentially with 5 mL each water and brine, then dried over anhydrous Na_2SO_4, filtered, and concentrated to afford 0.5227 g or 32% yield over 2 steps of phenol **2.16** as a brown crystalline material. The spectroscopic data in $CDCl_3$ are in agreement with the literature[3] and that previously described by our group.[8] **IR** ν_{max} (ground solid, cm^{-1}): 3406, 3089, 2975, 2930, 2855, 2235, 1723, 1641, 1615, 1598, 1516, 1504, 1440, 1388, 1365, 1343, 1304, 1272, 1218, 1189, 1175, 1164, 1136, 1104, 1054, 1007, 970, 956. **^{1}H NMR** (500 MHz, $CDCl_3$) δ 7.90 – 7.84 (m, 2H), 7.74 (dd, *J* = 8.2, 2.1 Hz, 1H), 7.08 – 7.04 (m, 2H), 6.88 – 6.84 (m, 2H), 5.08 (bs, 1H), 1.48 (s, 6H). **^{1}H NMR** (500 MHz, DMSO-d_6) δ 9.87 (d, *J* = 1.8 Hz, 1H), 8.35 (d, *J* = 8.2 Hz, 1H), 8.29 (s, 1H), 8.07 (d, *J* = 8.2 Hz, 1H), 7.19 – 7.11 (m, 2H), 6.95 – 6.85 (m, 2H), 1.48 (s, 6H). **^{13}C NMR** (126 MHz, DMSO-d_6) δ 180.01, 175.11, 157.98, 138.22, 136.05, 133.97, 131.07 (q, *J* = 32.5 Hz), 130.76, 128.06 (q, *J* = 4.7 Hz), 126.18, 122.24 (q, *J* = 273.8 Hz), 115.96, 115.05, 108.52 (q, *J* = 1.9 Hz), 66.11, 22.87. **HRMS** (ESI) *m/z* calcd for $C_{19}H_{13}O_2N_3F_3S$ [$(M–H)^–$]: 404.06861, measured: 404.06830, *m/z* calcd for $C_{19}H_{14}O_2N_3F_3SNa$ [$(M+Na)^+$]: 428.0651, measured: 428.0650.

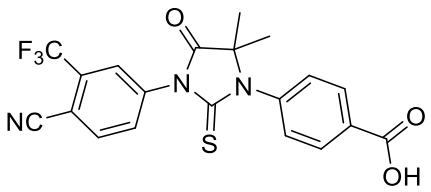
Triflate 2.17



To a solution of phenol **2.16** (0.2968 g, 0.732 mmol, 1 equiv) and N-Phenyl-bis(trifluoro-methanesulfonimide) (0.3927 g, 1.10 mmol, 1.5 equiv) in 7 mL dry THF was added NEt_3 (200 µL, 1.43 mmol, 2.0 equiv) and the solution was stirred 18 h, then concentrated to a very dark syrup. Silica gel flash chromatography with 0-30% EtOAc / hexanes (R_f 0.68, 50% EtOAc / hexanes) afforded 345 mg or 88% yield of aryl triflate **2.17** as off-white crystals. The spectroscopic data are in agreement with that previously described by our group.[8] **IR** ν_{max} (thin film, cm^{-1}): 3081, 2990, 2926, 2233, 1760, 1614, 1501, 1421, 1370, 1309, 1250, 1213, 1192, 1178, 1135, 1056,1020, 1010, 958. **^{1}H NMR** (500 MHz, $CDCl_3$) δ 8.00 – 7.95 (m, 2H), 7.84 (dd, *J* = 8.2, 2.0 Hz, 1H), 7.50 – 7.44 (m, 2H), 7.46 – 7.40 (m, 2H), 1.61 (s, 6H). **^{13}C NMR** (101 MHz, $CDCl_3$) δ 180.13, 174.64, 149.79, 137.06, 135.39, 135.28, 133.65 (q, *J* = 33.5 Hz), 132.28, 131.95, 127.16 (q, *J* = 4.7 Hz), 123.08, 121.95 (q, *J* = 274.3 Hz), 118.78 (q, *J* = 320.8 Hz), 114.87, 110.34 (q, *J* = 1.8 Hz), 66.60,

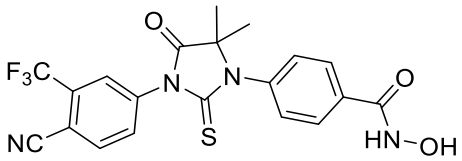
23.83. **HRMS** (ESI) *m/z* calcd for $C_{20}H_{13}O_4N_3F_6S_2Na$ [$(M+Na)^+$]: 560.0144, measured: 560.0149, *m/z* calcd for $C_{20}H_{13}O_4N_3F_6S_2K$ [$(M+K)^+$]: 575.9883, measured: 575.9857.

Benzoic acid 2.18



To a dry 25 mL Shlenck tube charged with triflate **2.17** (99.5 mg, 0.185 mmol, 1 equiv), $Pd(OAc)_2$ (2.9 mg, 0.013 mmol, 0.07 equiv), 1,1'-Bis(diphenylphosphino)ferrocene (dppf; 20.9 mg, 0.038 mmol, 0.2 equiv), and KOAc (72.2 mg, 0.736 mmol, 4.0 equiv), then purged under argon, was added 2 mL dry DMSO. The tube was evacuated and backfilled with 4 atm $CO_{(g)}$, then heated at 65 °C for 20 h. The vessel was cooled, then the contents were diluted with 50 mL EtOAc and filtered on celite into 110 mL 1 N HCl. The layers were separated, then the aqueous was extracted again with 50 mL EtOAc. The combined organic layers were washed with 3x15 mL 1 N HCl, then 15 mL brine. Silica gel flash chromatography with EtOAc / hexanes, then 1% AcOH / EtOAc afforded 45.2 mg or 56% yield of acid **2.18** as off-white crystals. Our group has reported this compound, and the spectroscopic data from this method are in agreement with that reported.[8,9] The data match that of **2.18** prepared by reaction with LHMDS and aniline **2.44a** (*vide infra*).

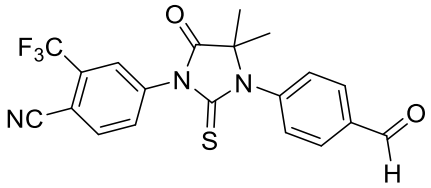
Hydroxamic acid (RB-318) 2.4



This compound was prepared from acid **2.18** (41.8 mg, 0.0964 mmol) by a similar procedure as that used for RB-331 (*vide infra*). Reverse-phase C18 gel flash chromatography with 20-60% MeCN / H_2O afforded 17.2 mg or 40% yield of hydroxamic acid **2.4** as a white powder, which precipitated upon selective rotary evaporation of the organic solvent, pure by NMR and 98.2% homogeneous by LC-MS analysis. The spectroscopic data are in agreement with that previously described by our group.[8] **IR** ν_{max} (cm^{-1}): 3304, 3132 (broad), 2874, 2235, 1758, 1611, 1497, 1437, 1427, 1303, 1149. **^{1}H NMR** (400 MHz, CD_3OD) δ 8.21 – 8.13 (m, 2H), 8.00 (dd, *J* = 8.3, 1.8 Hz,

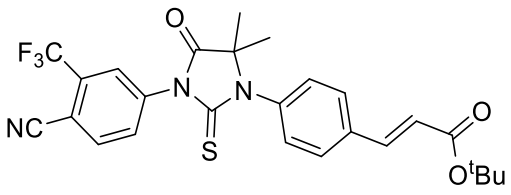
1H), 7.92 (d, J = 8.5 Hz, 2H), 7.52 (d, J = 8.6 Hz, 2H), 1.58 (s, 6H). **^{1}H NMR** (500 MHz, CD_3CN) δ 10.52 – 6.14 (bs, 2H), 8.13 (d, J = 8.3 Hz, 1H), 8.11 (d, J = 1.5 Hz, 1H), 7.96 (dd, J = 8.2, 1.7 Hz, 1H), 7.90 (d, J = 8.5 Hz, 2H), 7.47 (d, J = 8.5 Hz, 2H), 1.55 (s, 6H). **^{13}C NMR** (126 MHz, CD_3CN) δ 181.53, 176.10, 165.27, 139.61, 138.92, 136.89, 134.10, 133.71, 133.17 (q, J = 32.9 Hz), 131.20, 129.25, 128.50 (q, J = 4.9 Hz), 123.33 (q, J = 273.1 Hz), 116.03, 110.53 (q, J = 2.3 Hz), 67.73, 23.64. **HRMS** (ESI) *m/z* calcd for $C_{20}H_{14}O_3N_4F_3S$ [$(M–H)^-$]: 447.07442, measured: 447.07424.

Aldehyde **2.19**



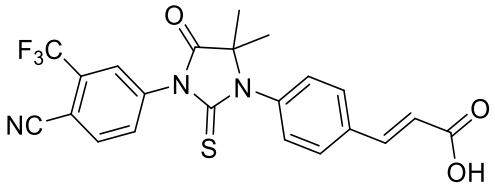
A 25 mL Schlenck tube was charged with triflate **2.17** (0.2515 g, 0.4680 mmol, 1 equiv), Na_2CO_3 (49.5 mg, 0.467 mmol, 1.0 equiv), $PdCl_2$ (2.6 mg, 0.015 mmol, 3.0 mol%),1,3-Bis(diphenyl-phosphino)propane (5.0 mg, 0.012 mmol, 2.6 mol%), 0.65 mL dry DMF, and triethylsilane (150.0 μL, 0.939 mmol, 2.0 equiv), then the mixture was frozen, evacuated, and backfilled with carbon monoxide gas to 45 psi. The reaction was stirred at 90 °C for 24 h, then filtered on celite into 15 mL 0.5 N HCl using 30 mL DCM, then the layers were separated. The aqueous was extracted with 2x30 mL DCM further. The combined organic layers were washed sequentially with 5 mL each water and brine, then dried over anhydrous Na_2SO_4, filtered and concentrated. Silica gel flash chromatography with EtOAc / hexanes (R_f 0.57, 75% EtOAc / hexanes) afforded 89.4 mg or 46% yield of aldehyde **2.19**. The spectroscopic data are in agreement with that previously described by our group.[8] **IR** ν_{max} (ground solid, cm^{-1}): 3048, 2923, 2853, 2233, 1754, 1723, 1612, 1503, 1433, 1385, 1308, 1285, 1175, 1129, 1054, 1007, 947. **^{1}H NMR** (400 MHz, $CDCl_3$) δ 10.09 (s, 1H), 8.06 (d, J = 8.3 Hz, 2H), 8.01 – 7.95 (m, 2H), 7.85 (dd, J = 8.4, 1.7 Hz, 1H), 7.51 (d, J = 8.3 Hz, 2H), 1.62 (s, 6H). **^{13}C NMR** (101 MHz, $CDCl_3$) δ 190.86, 179.89, 174.70, 140.57, 137.00, 135.42, 133.80 (q, J = 33.3 Hz), 132.27, 131.13, 130.67, 128.66, 127.20 (q, J = 4.7 Hz), 121.97 (q, J = 274.2 Hz), 114.86, 110.52 (q, J = 2.0 Hz), 66.76, 24.03.

Enoate 2.20



A solution of aldehyde **2.19** (89.4 mg, 0.214 mmol, 1 equiv) and (tert-Butoxycarbonyl-methylene)triphenylphosphorane (89.4 mg, 0.237 mmol, 1.1 equiv) in 8 mL dry DCM was stirred 7 h, then concentrated under reduced pressure. Silica gel flash chromatography with EtOAc / hexanes (R_f 0.71, 75% EtOAc / hexanes) afforded 103 mg or 93% yield of crystalline compound **2.20** as pale yellow needles. The spectroscopic data are in agreement with that previously described by our group.[8] **IR** ν_{max} (thin film, cm^{-1}): 2925, 2855, 2235, 2024, 1760, 1706, 1638, 1613, 1504, 1440, 1424, 1368, 1312, 1260, 1193, 1176, 1145. **^{1}H NMR** (400 MHz, $CDCl_3$) δ 7.97 (s, 2H), 7.85 (dd, *J* = 8.2, 2.0 Hz, 1H), 7.65 (d, *J* = 8.1 Hz, 2H), 7.60 (d, *J* = 16.0 Hz, 1H), 7.32 (d, *J* = 8.1 Hz, 2H), 6.42 (d, *J* = 16.0 Hz, 1H), 1.59 (s, 6H), 1.54 (s, 9H). **^{13}C NMR** (126 MHz, $CDCl_3$) δ 179.79, 174.83, 165.80, 141.63, 137.01, 136.22, 136.14, 135.24, 133.62 (q, *J* = 33.4 Hz), 132.18, 130.02, 129.22, 127.11 (q, *J* = 4.8 Hz), 122.43, 121.86 (q, *J* = 274.2 Hz), 114.78, 110.27 (q, *J* = 2.2 Hz), 81.02, 66.54, 28.19, 23.80. **HRMS** (ESI) *m/z* calcd for $C_{26}H_{24}O_3N_3F_3SNa$ [$(M+Na)^+$]: 538.1383, measured: 538.1379.

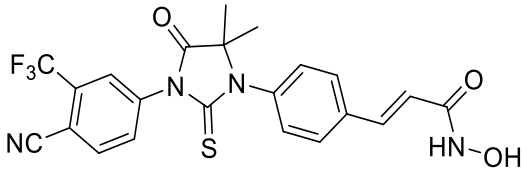
Carboxylic acid 2.21



To a solution of ester **2.20** (103 mg, 0.200 mmol, 1 equiv) in 4 mL dry DCM was added 0.45 mL trifluoroacetic acid (TFA) dropwise, with the reaction turning bright yellow upon starting the addition. After 18 h, the reaction was concentrated under reduced pressure to afford a bright yellow residue. Silica gel flash chromatography with EtOAc / hexanes (R_f 0.13, 40% acetone / DCM) afforded 79.4 mg or 86% yield of carboxylic acid **2.21**. This compound has been previously described by our group.[8] **IR** ν_{max} (ground solid, cm^{-1}): 3400-2500 (very broad), 2988, 2932, 2233, 1767, 1695, 1634, 1613, 1504, 1439, 1421, 1370, 1309, 1284, 1219, 1176, 1109, 1054. **^{1}H NMR**

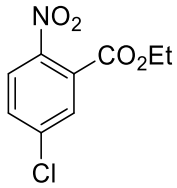
(500 MHz, Acetone-d_6) δ 10.89 (bs, 1H), 8.27 (d, J = 8.3 Hz, 1H), 8.22 (d, J = 2.0 Hz, 1H), 8.08 (dd, J = 8.3, 2.1 Hz, 1H), 7.87 (d, J = 8.2 Hz, 2H), 7.75 (d, J = 16.0 Hz, 1H), 7.50 (d, J = 8.1 Hz, 2H), 6.63 (d, J = 16.0 Hz, 1H), 1.64 (s, 6H). **^{13}C NMR** (126 MHz, Acetone-d_6) δ 181.23, 175.84, 167.57, 144.12, 139.13, 138.28, 136.59, 136.33, 134.30, 132.82 (q, J = 32.9 Hz), 131.38, 130.01, 128.54 (q, J = 4.9 Hz), 123.31 (q, J = 273.3 Hz), 120.85, 115.66, 110.17 (q, J = 2.0 Hz), 67.44, 23.70. **HRMS** (ESI) *m/z* calcd for $C_{22}H_{15}O_3N_3F_3S$ [(M–H)$^-$]: 458.07917, measured: 458.07886.

Hydroxamic acid (RB-331) 2.5



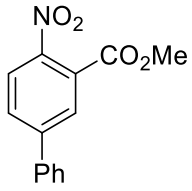
A solution of acid **2.21** (79.4 mg, 0.173 mmol. 1 equiv), H_2NOTBS (26.8 mg, 0.182 mmol, 1.05 equiv), and EDC•HCl (34.3 mg, 0.179 mmol, 1.03 equiv) in 0.9 mL dry DCM was stirred 24 h, then extracted with 3x10 mL DCM from added NaH_2PO_4 buffer. The combined organic layers were washed sequentially with 5 mL each NaH_2PO_4 buffer, water, and brine, then concentrated. To a solution of the residue in 2 mL MeCN was added 0.30 mL 48% HF in a 15 mL plastic Falcon tube and the reaction stirred 4 h, then sat. aq. $NaHCO_3$ was added until bubbling ceased. Reverse-phase C18 gel flash chromatography with 25-90% MeCN / H_2O (elutes at ~50%) afforded 24.8 mg or 30% yield of hydroxamic acid **2.5** as a clear film, pure by NMR and 100% homogeneous by LC-MS analysis, along with 17.2 mg or 22% recovery of acid **2.21**. This compound has been previously described by our group.[8] **IR** ν_{max} (thin film, cm^{-1}): 3299, 2924, 2853, 2245, 2233, 1759, 1702, 1612, 1504, 1440, 1312, 1194, 1177, 1140, 1090, 1056, 1007. **^{1}H NMR** (500 MHz, DMSO-d_6) δ 10.87 (bs, 1H), 9.13 (bs, 1H), 8.39 (d, J = 8.2 Hz, 1H), 8.31 (s, 1H), 8.09 (d, J = 8.2 Hz, 1H), 7.75 (d, J = 8.3 Hz, 2H), 7.52 (d, J = 16.1 Hz, 1H), 7.42 (d, J = 8.3 Hz, 2H), 6.54 (d, J = 15.8 Hz, 1H), 1.52 (s, 6H). **HRMS** (ESI) *m/z* calcd for $C_{22}H_{16}O_3N_4F_3S$ [(M–H)$^-$]: 473.09007, measured: 473.09033.

Aryl chloride 2.23



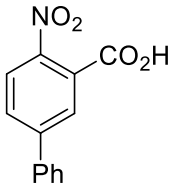
This was prepared from commercially available 5-chloro-2-nitrobenzoic acid (200.0 mg, 0.928 mol, 1 equiv) by Fisher esterification with 70 µL H_2SO_4 in 1.5 mL of ethanol at reflux for 45 h in 69% yield. The spectroscopic data are in agreement with the literature.[10] **^{1}H NMR** (500 MHz, $CDCl_3$) δ 7.87 (d, J = 8.68 Hz, 1H), 7.65 (d, J = 2.32 Hz, 1H), 7.55 (dd, J = 8.69, 2.29 Hz, 1H), 4.37 (q, J = 7.13 Hz, 2H), 1.33 (t, J = 7.15 Hz, 3H). **^{13}C NMR** (101 MHz, $CDCl_3$) δ 164.24, 146.19, 139.60, 131.53, 129.81, 129.69, 125.48, 62.95, 13.79.

Biphenyl 2.24



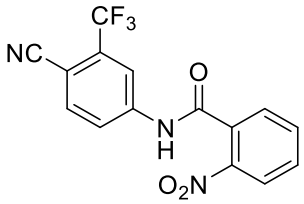
To a solution of ethyl 5-chloro-2-nitrobenzoate **2.23** (0.4936 g, 2.150 mmol, 1 equiv) and phenylboronic acid (0.3160 g, 2.592 mmol, 1.2 equiv) in 3.3 mL DMF was added 4.3 mL of 2 M K_2CO_3. To this was added by cannula the concentrated residue from a solution of $Pd(OAc)_2$ (24.3 mg, 0.108 mmol, 0.05 equiv) and PPh_3 (143.1 mg, 0.546 mmol, 0.25 equiv), which had been premixed for 1.5 h in dry DCM until bright yellow, followed by rotary evaporation and dissolution in 1.0 mL DMF. The reaction was heated at 100 °C for 24 h, then DMF was removed *in vacuo*. Silica gel flash chromatography with EtOAc / hexanes, followed by 1% AcOH / EtOAc afforded impure carboxylic acid, which was treated with AcCl in refluxing MeOH for 24 h. Silica gel flash chromatography with DCM / hexanes afforded 172.9 mg or 31% yield of methyl benzoate **2.24**. The spectroscopic data are in agreement with the literature.[11] **^{1}H NMR** (500 MHz, $CDCl_3$) δ 8.04 (d, *J* = 8.5 Hz, 1H), 7.90 (d, *J* = 2.0 Hz, 1H), 7.81 (dd, *J* = 8.4, 2.0 Hz, 1H), 7.65 – 7.58 (m, 2H), 7.54 – 7.42 (m, 3H), 3.96 (s, 3H). **^{13}C NMR** (126 MHz, $CDCl_3$) δ 166.36, 146.67, 146.60, 137.95, 129.83, 129.41, 129.39, 128.79, 128.32, 127.48, 124.87, 53.53.

Benzoic acid 2.25



A solution of ethyl 5-chloro-2-nitrobenzoate (172.9 mg, 0.672 mmol) in 2 mL of 3 M KOH was heated at 110 °C for 30 mins, at which time TLC analysis indicated complete saponification. The mixture was cooled, acidified with 2 M HCl to pH<1, extracted with 3x15 mL EtOAc, dried over Na_2SO_4, and concentrated to afford 158.5 mg or 97% yield of carboxylic acid **2.25** as a tan solid. The spectroscopic data are in agreement with the literature.[11] **^{1}H NMR** (500 MHz, DMSO-d_6) δ 13.95 (s, 1H), 8.09 (d, J = 8.3 Hz, 1H), 8.08 – 8.01 (m, 2H), 7.83 – 7.78 (m, 2H), 7.58 – 7.50 (m, 2H), 7.52 – 7.45 (m, 1H). **^{13}C NMR** (126 MHz, DMSO-d_6) δ 166.11, 146.73, 144.80, 137.17, 129.78, 129.26, 129.15, 128.96, 127.48, 127.31, 124.67. **HRMS** (APCI) *m/z* calcd for $C_{13}H_8O_4N$ $[(M–H)^–]$: 242.04588, measured: 242.04612.

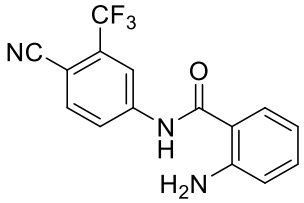
N-(4-cyano-3-(trifluoromethyl)phenyl)-2-nitrobenzamide 2.28a



To a solution of *o*-nitrobenzoic acid **2.26** (0.5927 g, 3.55 mmol, 1 equiv) dissolved in 3.0 mL of dry toluene in an argon-purged flask was added DMF (0.04 mL, 0.517 mmol, 0.15 equiv). The resulting solution was warmed to 40 °C, thionyl chloride was added dropwise (260 µL, 3.58 mmol, 1.0 equiv), and the reaction was stirred overnight. An additional 260 µL of thionyl chloride was added and the reaction was stirred an additional 4 h, at which time aniline **2.27** (0.660 g, 3.55 mmol, 1.0 equiv) and pyridine (0.570 mL, 7.05 mmol, 1.99 equiv) were added in sequence. The reaction was monitored by TLC until completion within 3 h, then diluted with water and extracted thrice with EtOAc. The combined organic layers were washed successively with sat. $NaHCO_3$, water which was brought to pH 3 by addition of 1 M HCl, water, and brine, then dried over anhydrous Na_2SO_4. Silica gel flash chromatography with 0-50% EtOAc / hexanes (R_f 0.5, Et_2O)

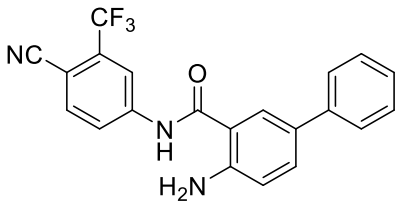
to afford 0.4115 g or 35% yield of benzamide **2.28a** as a yellow solid. **IR** ν_{max} (solid sample, cm^{-1}): 3359, 3328, 2234, 1690, 1613, 1589, 1530, 1322. **^{1}H NMR** (300 MHz, DMSO-d_6) δ 11.46 (s, 1H), 8.32 (d, J = 2.0 Hz, 1H), 8.22 (dd, J = 8.1, 1.2 Hz, 1H), 8.18 (d, J = 8.5 Hz, 1H), 8.07 (dd, J = 8.5, 2.1 Hz, 1H), 7.94 (td, J = 7.4, 1.1 Hz, 1H), 7.90 – 7.76 (m, 2H). **^{13}C NMR** (126 MHz, DMSO-d_6) δ 165.21, 146.19, 143.29, 136.69, 134.42, 131.91 (q, J = 31.89 Hz), 131.64, 131.61, 129.32, 124.49, 122.47, 122.40 (q, J = 273.66 Hz), 116.86 (q, J = 5.10 Hz), 115.68, 102.49 (q, J = 2.06 Hz). **HRMS** (ESI) *m/z* calcd for $C_{15}H_7O_3N_3F_3$ [$(M–H)^–$]: 334.04450, measured: 334.04455.

Benzamide aniline (RB-15) 2.7a



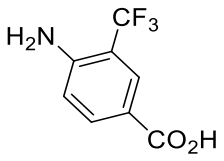
Reduction of nitro arene **2.28a** (300.8 mg) with iron powder was carried out as described in the literature,[12] requiring 45 min at reflux. The reaction was basified with 1 M NaOH to pH 8, filtered, and extracted thrice with chloroform. The combined organic layers were washed twice with brine, dried over Na_2SO_4, and concentrated to afford 264 mg or 96% yield of benzamide **2.7a** as tan crystals, pure by NMR and 96% homogeneous by LC-MS analysis. **IR** ν_{max} (thin film, cm^{-1}): 3480, 3363, 2958, 2926, 2860, 2230, 1668, 1614, 1584, 1558, 1521, 1504, 1452, 1424, 1325, 1302, 1276, 1238, 1205, 1179, 1134, 1095, 1065, 1050, 1023, 950. **^{1}H NMR** (500 MHz, $CDCl_3$) δ 8.15 (s, 1H), 8.10 (d, J = 2.0 Hz, 1H), 7.96 (dd, J = 8.5, 2.1 Hz, 1H), 7.81 (d, J = 8.5 Hz, 1H), 7.48 (d, J = 7.9 Hz, 1H), 7.31 (ddd, J = 8.4, 7.0, 1.3 Hz, 1H), 6.78 – 6.71 (m, 2H), 5.58 (bs, 2H). **^{1}H NMR** (300 MHz, CD_3CN) δ 9.03 (s, 1H), 8.30 (d, J = 2.1 Hz, 1H), 8.05 (ddd, J = 8.6, 2.1, 0.6 Hz, 1H), 7.91 (d, J = 8.6 Hz, 1H), 7.62 (dd, J = 8.0, 1.4 Hz, 1H), 7.28 (ddd, J = 8.5, 7.1, 1.5 Hz, 1H), 6.78 (dd, J = 8.3, 0.8 Hz, 1H), 6.69 (ddd, J = 8.2, 7.1, 1.2 Hz, 1H), 5.87 (bs, 2H). **^{1}H NMR** (400 MHz, Acetone-d_6) δ 9.92 (s, 1H), 8.48 (d, J = 2.0 Hz, 1H), 8.29 (dd, J = 8.5, 1.8 Hz, 1H), 8.02 (dd, J = 8.6, 0.8 Hz, 1H), 7.72 (dd, J = 8.0, 1.5 Hz, 1H), 7.25 (ddd, J = 8.5, 7.1, 1.5 Hz, 1H), 6.85 (dd, J = 8.3, 1.1 Hz, 1H), 6.61 (ddd, J = 8.2, 7.1, 1.2 Hz, 1H), 6.32 (bs, 2H). **^{13}C NMR** (126 MHz, $CDCl_3$) δ 167.61, 149.70, 142.53, 135.97, 134.18 (q, J = 32.5 Hz), 134.01, 127.25, 122.32 (q, J = 274.3 Hz), 122.24, 118.17, 117.74 (q, J = 4.9 Hz), 117.22, 115.77, 114.43, 104.30 (q, J = 2.3 Hz). **HRMS** (ESI) *m/z* calcd for $C_{15}H_9ON_3F_3$ [$(M–H)^–$]: 304.07032, measured: 304.07010.

Benzamide aniline (RB-265) 2.7b



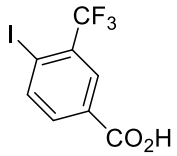
To 4-phenyl-2-nitrobenzoic acid **2.25** (0.1537 g, 0.632 mmol, 1 equiv) in 0.65 mL dry PhMe was added DMF (150 µL, 1.94 mmol, 3 equiv), then thionyl chloride (53.0 µL, 0.727 mmol, 1.15 equiv) while heating at 40 °C. After 2 h, additional thionyl chloride (50.0 µL, 0.685 mmol, 1.08 equiv) was added. After 4 h, solvent was removed by distillation *in vacuo* and more PhMe was added before repeating distillation. The dark syrup was combined with pyridine (250 µL, 3.09 mmol, 4.9 equiv) and aniline **2.27** (0.115 g, 0.618 mmol, 0.98 equiv), then suspended in 0.5 mL dry THF and monitored by TLC. After concentration, silica gel flash chromatography with EtOAc / hexanes afforded 134 mg of an inseparable 1:2 mixture of the desired product and aniline starting material. This was then treated with iron powder in a similar fashion to the procedure used for reduction of benzamide **2.28a**.[12] Silica gel flash chromatography with 0-50% EtOAc / hexanes (R_f 0.51, 50% EtOAc / hexanes) afforded 31.9 mg or 13 % (2 steps) of benzamide **2.7b** as a yellow solid, pure by NMR and 98% homogeneous by LC-MS analysis. **IR** ν_{max} (ground solid, cm^{-1}): 3471, 3364, 2225, 1739, 1666, 1612, 1520, 1419, 1230, 1174, 1124, 1049. **^{1}H NMR** (400 MHz, Acetone-d_6) δ 9.99 (s, 1H), 8.35 (d, J = 1.6 Hz, 1H), 8.16 (dd, J = 8.6, 1.8 Hz, 1H), 7.90 (d, J = 8.6 Hz, 1H), 7.85 (d, J = 2.0 Hz, 1H), 7.51 – 7.44 (m, 3H), 7.28 (t, J = 7.7 Hz, 2H), 7.15 (t, J = 7.4 Hz, 1H), 6.83 (d, J = 8.6 Hz, 1H), 6.29 (s, 2H). **^{13}C NMR** (101 MHz, Acetone-d_6) δ 169.40, 151.04, 145.02, 141.25, 136.90, 133.38 (q, J = 32.0 Hz), 132.64, 129.65, 129.09, 127.53, 127.24, 126.85, 123.73 (q, J = 273.0 Hz), 123.69, 118.59 (q, J = 5.2 Hz), 118.52, 116.48, 115.12, 103.65 (q, J = 2.0 Hz). **HRMS** (ESI) *m/z* calcd for $C_{21}H_{13}ON_3F_3$ $[(M–H)^–]$: 380.10162, measured: 380.10164, calcd for $C_{21}H_{15}ON_3F_3$ $[(M+H)^+]$: 382.11617, measured: 382.11591.

Aniline 2.30



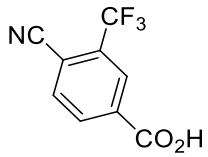
Reduction of commercially available nitro arene **2.29** (119.0 mg) with iron powder was carried out as described in the literature,[12] requiring 35 min at reflux. The reaction was basified with 15% NaOH, filtered, and ethanol removed *in vacuo*. After acidification to pH 3-4 with 2 M HCl, and extraction thrice with EtOAc, the combined organic layers were washed with water, brine, dried over Na_2SO_4, and concentrated to afford 81.6 mg or 79% yield of carboxylic acid **2.30**. **^{1}H NMR** (500 MHz, DMSO-d_6) δ 12.50 (s, 1H), 7.90 (s, 1H), 7.80 (d, J = 8.6 Hz, 1H), 6.89 (d, J = 8.7 Hz, 1H), 6.39 (s, 2H). **^{13}C NMR** (126 MHz, DMSO-d_6) δ 166.67, 150.05, 134.12, 128.43 (q, J = 5.3 Hz), 124.74 (q, J = 271.8 Hz), 116.90, 116.33, 109.73 (q, J = 30.1 Hz). **HRMS** (ESI) *m/z* calcd for $C_8H_6O_2NNaF_3$ [$(M+Na)^+$]: 228.0243, measured: 228.0241.

Aryl iodide 2.31



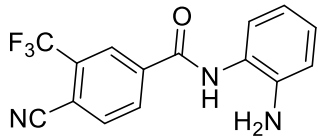
To amino acid **2.30** (69.7 mg, 0.340 mmol, 1 equiv), suspended in 1.1 mL conc. HCl and cooled with an ice bath to 0 °C, was added dropwise a solution of $NaNO_2$ (29.0 mg, 0.420 mmol, 1.25 equiv) in 0.58 mL water. After the resulting yellow mixture was stirred for 30 mins, KI (93.7 mg, 0.564 mmol, 1.66 eq) was added dropwise as a solution in 0.16 mL water. After stirring this orange mixture for 80 mins further, the reaction was extracted with 3x10 mL EtOAc. The combined organic layers were washed with 5 mL brine, dried over Na_2SO_4, filtered, and concentrated to afford 100.8 mg or 94% of aryl iodide **2.31**. This is a known procedure for the preparation of this compound.[13] **^{1}H NMR** (400 MHz, $CDCl_3$) δ 8.14 (d, J = 1.6 Hz, 1H), 8.06 (dd, J = 8.1, 1.6 Hz, 1H), 7.53 (d, J = 8.1 Hz, 1H). **^{1}H NMR** (400 MHz, CD_3CN) δ 8.21 (d, J = 7.9 Hz, 1H), 8.21 (d, J = 1.9 Hz, 1H), 7.83 (dd, J = 8.2, 1.6 Hz, 1H), 7.46–4.38 (bs, 1H).

Benzonitrile 2.32



To a solution of aryl iodide **2.31** (112.8 mg, 0.357 mmol, 1 equiv) in 3.5 mL dry DMF was added CuCN (48.1 mg, 0.537 mmol, 1.5 equiv), and the resulting mixture was heated at 120 °C for 30 h. The reaction was filtered on celite and extracted from 35 mL of 1 N HCl with 3x15 mL EtOAc. The combined organic layers were washed with 5 mL of 1 M HCl, 5 mL brine, and dried over $MgSO_4$. Silica gel flash chromatography with 1:1 DCM / hexanes, followed by 5% AcOH / DCM afforded 64.3 mg or 84% of known benzonitrile **2.32**.[14] **IR** ν_{max} (ground solid, cm^{-1}): 3200-2500 (very broad), 3064, 2918, 2849, 2236, 1703, 1618, 1446, 1434. **^{1}H NMR** (300 MHz, $CDCl_3$) δ 12.02 (bs, 1H), 8.39 (d, *J* = 1.3 Hz, 1H), 8.30 (dd, *J* = 7.9, 1.5 Hz, 1H), 7.90 (d, *J* = 7.9 Hz, 1H). **HRMS** (ESI) *m/z* calcd for $C_9H_3O_2NF_3$ $[(M–H)^–]$: 214.01214, measured: 214.01149.

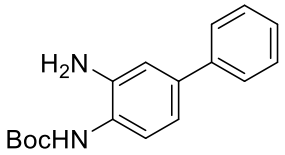
Benzamide aniline (RB-136) 2.8a



Triethylamine (28 µL, 0.20 mmol, 2.0 equiv) was added to a solution of carboxylic acid **2.32** (21.5 mg, 0.100 mmol, 1 equiv), *o*-phenylenediamine (22.4 mg, 0.207 mmol, 2.1 equiv), HOAt (13.9 mg, 0.102 mmol, 1.0 equiv), and N-(3-Dimethylaminopropyl)-N′-ethylcarbodiimide hydrochloride (EDC•HCl; 23.1 mg, 0.121 mmol, 2.0 equiv) in 1.0 mL dry DMSO under argon. After heating at 50 °C for 10 h, the reaction was poured into 10 mL pH 7 sodium phosphate buffer and extracted with 3x10 mL EtOAc. The combined organic layers were washed sequentially with 5 mL each water and brine, then dried over anhydrous Na_2SO_4, filtered and concentrated. Silica gel flash chromatography with 0-100% EtOAc / hexanes (R_f 0.63, EtOAc) afforded 26.2 mg or 86% yield of yellow solid. This was purified by C18 silica gel flash chromatography with 35-65% MeCN / H_2O to afford benzamide **2.8a** as a yellow powder, pure by NMR and 100% homogeneous by LC-MS analysis. **IR** ν_{max} (ground solid, cm^{-1}): 3425, 3354 3261, 3082, 3048, 2968, 2926, 2233, 1739, 1638, 1594, 1570, 1520, 1498, 1484, 1460, 1409, 1321, 1301, 1284, 1272, 1252, 1221, 1184, 1160, 1126, 1053, 1036, 948. **^{1}H NMR** (400 MHz, Acetone-d_6) δ 9.50 (s, 1H), 8.56 (s, 1H), 8.51 (dd, *J* = 8.1, 1.8 Hz, 1H), 8.26 (d, *J* = 8.0 Hz, 1H), 7.28 (dd, *J* = 7.9, 1.6 Hz, 1H), 7.04 (td, *J* = 7.7, 1.5 Hz, 1H), 6.87 (dd, *J* = 8.1, 1.5 Hz, 1H), 6.68 (td, *J* = 7.6, 1.4 Hz, 1H), 4.70 (s, 2H). **^{13}C NMR** (101 MHz, Acetone-d_6) δ 162.68, 143.25, 139.54, 135.55, 132.10, 131.89 (q, *J* = 33.2 Hz), 127.30,

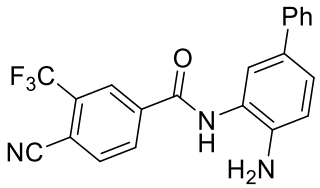
126.49, 126.05 (q, J = 4.7 Hz), 123.05, 122.66 (q, J = 273.0 Hz), 117.11, 116.71, 114.89, 111.72 (m). **HRMS** (ESI) *m/z* calcd for $C_{15}H_9ON_3F_3$ [$(M–H)^-$]: 304.07032, measured: 304.07080.

tert-butyl (3-amino-[1,1'-biphenyl]-4-yl)carbamate 2.22b



Aniline **2.22b** was prepared as described in the literature, essentially as described for the pyridyl compound **2.22d** (*vide infra*), and the spectroscopic data matched that previously reported.[15]

Benzamide aniline (RB-141) 2.8b

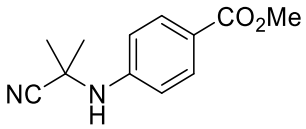


To a solution of benzoic acid **2.32** (27.0 mg, 0.126 mmol, 1 equiv), Boc-aniline **2.22b** (42.7 mg, 0.150 mmol, 1.2 equiv), EDC•HCl (31.6 mg, 0.165 mmol, 1.3 equiv), and HOAt (18.5 mg, 0.136 mmol, 1.1 equiv) in 1.1 mL dry DMSO was added NEt_3 (35.0 µL, 0.251 mmol, 2.0 equiv) and the reaction stirred at 50 °C for 12 h, at which time additional HOAt (12.2 mg) and EDC•HCl (14.0 mg) were added. The reaction was then stirred at 70 °C for 25 h, then cooled, diluted with NaH_2PO_4 buffer, and extracted thrice with EtOAc. The combined organic layers were washed sequentially with buffer, water, and brine, then dried over anhydrous Na_2SO_4, filtered, and concentrated. Silica gel flash chromatography with 0-20 % EtOAc / hexanes afforded the coupled Boc-protected aniline **2.33**, which was used directly without further purification.

To a solution of the Boc-aniline intermediate in 1 mL MeOH was added 40 µL AcCl over an ice bath, followed by 1 mL DCM to dissolve the precipitates, then the reaction followed by TLC. The organic solvents were removed by rotary evaporation and 2 mL 5% $NaHCO_3$ was added, then the aqueous extracted with 3x5 mL EtOAc. The combined organic layers were washed sequentially with 2 mL each water and brine, then dried over anhydrous Na_2SO_4, filtered, and concentrated. Silica gel flash chromatography with 0-40 % EtOAc / hexanes afforded 24.7 mg or 51% yield over two steps of benzamide **2.8b** as a yellow powder, pure by NMR and 100% homogeneous by LC-

MS analysis. **IR** ν_{max} (ground solid, cm^{-1}): 3473, 3391, 3228, 3029, 2927, 2855, 2240, 1739, 1637, 1613, 1588, 1573, 1548, 1513, 1487, 1418, 1330, 1314, 1280, 1248, 1202, 1174, 1132, 1054, 929. **^{1}H NMR** (400 MHz, Acetone-d_6) δ 9.61 (s, 1H), 8.60 (s, 1H), 8.55 (dd, J = 8.1, 1.7 Hz, 1H), 8.27 (d, J = 8.0 Hz, 1H), 7.65 (d, J = 2.2 Hz, 1H), 7.61 – 7.54 (m, 2H), 7.44 – 7.33 (m, 3H), 7.30 – 7.21 (m, 1H), 6.97 (d, J = 8.4 Hz, 1H), 4.87 (s, 2H). **^{13}C NMR** (101 MHz, DMSO-d_6) δ 162.96, 143.39, 140.02, 139.38, 135.69, 132.57, 130.76 (q, J = 32.3 Hz), 128.80, 127.73, 126.22 (q, J = 4.9 Hz), 126.01, 125.42, 125.30, 122.48 (q, J = 273.4 Hz), 122.21, 116.14, 115.24, 110.58 (m). **HRMS** (ESI) *m/z* calcd for $C_{21}H_{13}ON_3F_3$ $[(M–H)^–]$: 380.10162, measured: 380.10052.

Methyl 4-((2-cyanopropan-2-yl)amino)benzoate 2.44a



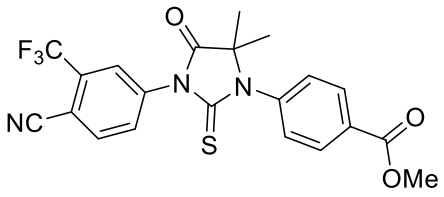
Methyl 4-aminobenzoate **2.43a** (1.0554 g, 0.007304 mol, 1 equiv), prepared by Fischer esterification of the benzoic acid, anhydrous ground $CaSO_4$ (Drierite ®, 6.5 g, 0.048 mol, 6.5 equiv) and acetone cyanohydrin (2.67 mL, 0.0292 mol, 4 equiv) were combined and heated at 105-110 °C for 12 h under argon. Upon completion, as observed by ^{1}H NMR, the solid mixture was combined with silica gel and purified by silica gel flash chromatography with 10-50% EtOAc / hexanes (R_f 0.47, 50% EtOAc / hexanes) to afford 1.4752 g or 93% yield of **2.44a** as colourless crystals. **IR** ν_{max} (cm^{-1}): 3388, 3020, 2939, 2231, 1695, 1605, 1523, 1271, 1175, 1113. **^{1}H NMR** (500 MHz, $CDCl_3$) δ 7.93 (d, J = 8.6 Hz, 2H), 6.84 (d, J = 8.4 Hz, 2H), 4.20 (s, 1H), 3.87 (s, 3H), 1.76 (s, 6H). **^{13}C NMR** (126 MHz, $CDCl_3$) δ 167.06, 147.89, 131.52, 121.28, 121.22, 114.54, 51.89, 48.10, 28.29. **HRMS** (ESI) *m/z* calcd for $C_{12}H_{14}N_2NaO_2$ $[(M+Na)^+]$: 241.0947, measured: 241.0942.

General Procedure A for bis-aryl thiohydantoin synthesis:

To an anhydrous, vigorously stirred, 0.1 M THF solution of *α*-cyanoamine and aryl isothiocyanate under argon at –42 °C (dry ice / acetonitrile) was added a 1.0 M solution in THF of lithium hexamethyldisilazide (LHMDS) by a single fast injection. It should be noted that more complex mixtures resulted from slower LHMDS addition, less pure reactant material, or unequal reactant ratios. The stoichiometry and quality of the LHMDS itself, however, appeared unimportant provided it was used in slight excess. The reaction was followed closely by TLC at this temperature

and was typically complete in 15-45 mins. The dark red solution was poured into 2 N aq. HCl and the vessel rinsed with sufficient MeOH to provide a clear monophasic solution, which was subsequently refluxed for 1-3 h at 85 °C and followed by TLC.

Methyl 4-(3-(4-cyano-3-(trifluoromethyl)phenyl)-5,5-dimethyl-4-oxo-2-thioxoimidazolidin-1-yl)benzoate 2.45a



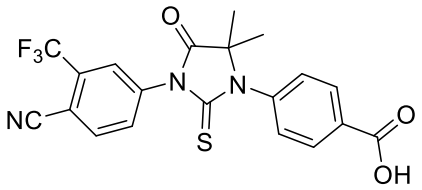
General procedure **A** was employed with *α*-cyanoamine **2.44a** (0.3631 g, 1.664 mmol, 1 equiv), aryl isothiocyanate **2.11** (0.4193 g, 1.838 mmol, 1.10 equiv) and 2.5 mL LHMDS (2.5 mmol, 1.5 equiv), taking 17 mins, followed by 20 mL of 2 N HCl in stage two for 1 h. The solution was cooled, solvent was removed *in vacuo*, and the aqueous concentrate extracted with 2x30 mL EtOAc. The combined organic layers were washed sequentially with 10 mL each water and brine, dried over anhydrous Na_2SO_4, filtered, and concentrated. Silica gel flash chromatography with EtOAc / hexanes (R_f 0.26, 30% EtOAc / hexanes) afforded 0.6890 g or 93% yield of carboxylic ester **2.45a**, the characterization of which matches the literature.[3] **IR** ν_{max} (cm^{-1}): 3106, 2976, 2957, 2232, 1759, 1716, 1178, 1116. **^{1}H NMR** (400 MHz, $CDCl_3$) δ 8.26 – 8.19 (m, 2H), 7.99 (d, *J* = 8.3 Hz, 1H), 7.96 (d, *J* = 2.0 Hz, 1H), 7.84 (dd, *J* = 8.3, 2.1 Hz, 1H), 7.44 – 7.37 (m, 2H), 3.96 (s, 3H), 1.61 (s, 6H). **HRMS** (ESI) *m/z* calcd for $C_{21}H_{16}O_3N_3ClF_3S$ $[(M+Cl)^-]$: 482.05585, measured: 482.05609.

General Procedure B carboxylic ester deprotection:

This procedure was adapted from that of Chang and Wood.[16] To a 0.1 M solution of the ester (1 equiv) in dry DMSO (1 vol equiv) was added potassium *tert*-butoxide (5-15 equiv) in one portion. Although an exotherm was noted, no instance resulted in uncontrolled heating, and this could be controlled with an ice bath on larger scale or with more equivalents of butoxide. The suspension was stirred at room temperature and followed by TLC. When complete, this was poured into 10 vol equiv of aqueous HCl, with a concentration sufficient to produce a 0.5 N solution in HCl after base consumption, and extracted with 3x3 vol equiv EtOAc. The combined organic layers were

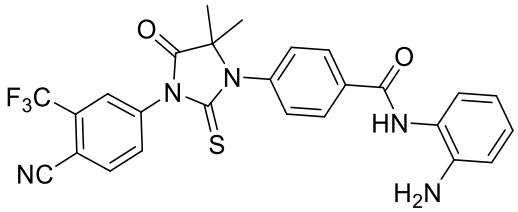
washed with 5 vol equiv each of water and brine, dried over anhydrous Na_2SO_4, filtered, and concentrated.

4-(3-(4-cyano-3-(trifluoromethyl)phenyl)-5,5-dimethyl-4-oxo-2-thioxoimidazolidin-1-yl)benzoic acid 2.18



General procedure **B** was employed with carboxylic ester **2.45a** (0.5141 g, 1.149 mmol, 1 equiv) and KO^{t}Bu (1.2629 g, 11.255 mmol, 10.1 equiv) for 1.5 h. The crude extract was triturated with Et_2O, then filtered. The filtrate was recovered to afford 0.1806 g or 36% yield of carboxylic acid **2.18** as a light yellow crystalline solid. The white undissolved solid was also recovered for 0.3169 g or 64% yield of carboxylic acid **2.18**. Both crops were pure enough for characterization and were used without further purification. **IR** ν_{max} (cm^{-1}): 2838 (broad), 2234, 1753, 1737, 1688, 1141, 833. **^{1}H NMR** (500 MHz, $CDCl_3$) δ 11.68 (bs, 1H), 8.31 (d, J = 8.6 Hz, 2H), 7.99 (d, J = 8.3 Hz, 1H), 7.98 (d, J = 2.0 Hz, 1H), 7.85 (dd, J = 8.3, 2.1 Hz, 1H), 7.46 (d, J = 8.5 Hz, 2H), 1.63 (s, 6H). **^{13}C NMR** (126 MHz, $CDCl_3$) δ 179.90, 174.80, 170.59, 140.26, 137.06, 135.42, 133.82 (q, J = 33.4 Hz), 132.29, 131.98, 130.62, 130.09, 127.23 (q, J = 4.7 Hz), 121.99 (q, J = 274.2 Hz), 114.87, 110.51 (q, J = 2.1 Hz), 66.76, 24.02. **HRMS** (ESI) *m/z* calcd for $C_{20}H_{13}O_3N_3F_3S$ [$(M–H)^–$]: 432.06352, measured: 432.06359.

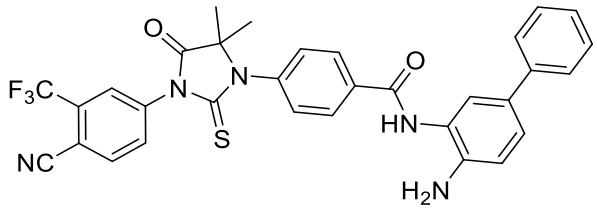
N-(2-aminophenyl)-4-(3-(4-cyano-3-(trifluoromethyl)phenyl)-5,5-dimethyl-4-oxo-2-thioxoimidazolidin-1-yl)benzamide (RB-250) 2.6a



To a solution of *o*-phenylenediamine (0.4059 g, 3.7535 mmol, 5.0 equiv), HOAt (0.1093 g, 0.8030 mmol, 1.06 equiv), and EDC•HCl (0.4334 g, 2.261 mmol, 3.0 equiv) in 5.5 mL dry DMF was added NEt_3 (0.315 mL, 2.258 mmol, 3.0 equiv), followed by carboxylic acid **2.18** (0.3269 g,

0.7543 mmol, 1 equiv) as a solution in 2.0 mL dry DMF. The reaction was stirred 21 h, then concentrated *in vacuo* and suspended in minimal DCM. Silica gel flash chromatography with 60-75% EtOAc / hexanes (R_f 0.45, 75% EtOAc / hexanes) afforded 0.3007 g (76%) of **2.6a** (RB-250) as a hetereogeneous yellow and white solid. This was recrystallized from $CHCl_3$-hexanes to afford 0.2133 g of off-white flakes (71% recovery, 54% overall yield), pure by NMR and 98.6% homogeneous by LC-MS analysis, for use in biological assays. **IR** ν_{max} (cm^{-1}): 3370, 3260, 2236, 1759, 1636, 1428, 1148, 747. **^{1}H NMR** (500 MHz, DMSO-d_6) δ 9.80 (s, 1H), 8.41 (d, J = 8.2 Hz, 1H), 8.33 (s, 1H), 8.16 (d, J = 8.1 Hz, 2H), 8.11 (dd, J = 8.3, 1.9 Hz, 1H), 7.55 (d, J = 8.6 Hz, 2H), 7.19 (dd, J = 7.8, 1.6 Hz, 1H), 6.99 (ddd, J = 8.7, 7.4, 1.6 Hz, 1H), 6.79 (dd, J = 8.0, 1.5 Hz, 1H), 6.61 (td, J = 7.5, 1.4 Hz, 1H), 4.96 (s, 2H), 1.56 (s, 6H). **^{13}C NMR** (201 MHz, DMSO-d_6) δ 179.91, 174.86, 164.58, 143.27, 138.03, 138.02, 136.19, 135.34, 134.01, 131.08 (q, J = 32.7 Hz), 129.71, 129.08, 128.06 (q, J = 5.0 Hz), 126.79, 126.65, 122.97, 122.22 (q, J = 273.7 Hz), 116.13, 116.01, 115.02, 108.64, 66.47, 23.03. **HRMS** (ESI) *m/z* calcd for $C_{26}H_{21}F_3N_5O_2S$ [$(M+H)^+$]: 524.1363, measured: 524.1356, calcd for $C_{26}H_{20}F_3N_5NaO_2S$ [$(M+Na)^+$]: 546.1182, measured: 546.1175.

N-(4-amino-[1,1'-biphenyl]-3-yl)-4-(3-(4-cyano-3-(trifluoromethyl)phenyl)-5,5-dimethyl-4-oxo-2-thioxoimidazolidin-1-yl)benzamide (RB-321) 2.6b

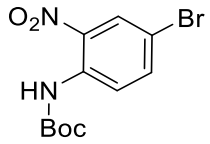


Carboxylic acid **2.18** (110.5 mg, 0.2550 mmol, 1 equiv), EDC•HCl (53.6 mg, 0.280 mmol, 1.1 equiv), and aniline **2.22b** (32.7 mg, 0.115 mmol, 0.45 equiv) were dissolved in 2.5 mL dry DCM and stirred at r.t. 16 h. This was poured into 15 mL of K_2HPO_4 buffer and extracted with 3x25 mL DCM. The combined organic layers were washed sequentially with 5 mL each water and brine, dried over anhydrous $MgSO_4$, filtered, and concentrated. Silica gel flash chromatography with EtOAc / hexanes (R_f 0.65, Et_2O) afforded 48.2 mg or 60% yield of the Boc-protected aniline intermediate.

To this Boc-protected aniline intermediate (48.2 mg, 0.0689 mmol, 1 equiv), dissolved in 2.0 mL dry DCM, was added TFA (0.4 mL, 5 mmol) dropwise at 0 °C over an ice bath. The bath was

allowed to warm over 5 h, then concentrated and the residue obtained was purified by C18 silica gel flash chromatography with 45-80% MeCN / H_2O (R_f 0.09, Et_2O) to afford 18.6 mg or 45% yield of the benzamide. This was recrystallized from $CHCl_3$-hexanes and gave biphenyl benzamide **2.6b** as off-white crystals, pure by NMR and 98.7% homogeneous by LC-MS analysis, for use in biological assays. **IR** ν_{max} (cm^{-1}): 3487, 3387, 3267, 3034, 2986, 2939, 2235, 1752, 1646, 1627, 1495, 1440, 1421, 1133. **^{1}H NMR** (500 MHz, $CDCl_3$) δ 8.08 (m, 3H), 8.00 – 7.96 (m, 2H), 7.84 (dd, *J* = 8.2, 2.1 Hz, 1H), 7.60 (s, 1H), 7.54 (d, *J* = 7.7 Hz, 2H), 7.45 – 7.36 (m, 5H), 7.33 – 7.27 (m, 1H), 6.93 (d, *J* = 8.3 Hz, 1H), 3.95 (s, 2H), 1.60 (s, 6H). **^{13}C NMR** (126 MHz, $CDCl_3$) δ 179.97, 174.77, 164.82, 140.42, 140.09, 138.44, 137.02, 135.64, 135.44, 133.79 (q, *J* = 33.5 Hz), 133.28, 132.28, 130.26, 129.16, 128.91, 127.21 (q, *J* = 4.8 Hz), 126.92, 126.67, 126.35, 124.62, 123.87, 121.97 (q, *J* = 274.3 Hz), 119.10, 114.88, 110.50 (m), 66.71, 23.97. **HRMS** (ESI) *m/z* calcd for $C_{32}H_{24}F_3N_5NaO_2S$ [$(M+Na)^+$]: 622.1495, measured: 622.1489, calcd for $C_{32}H_{24}F_3N_5KO_2S$ [$(M+K)^+$]: 638.1234, measured: 638.1225.

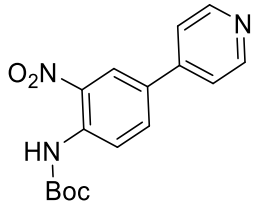
Boc-aniline 5.1



To a solution of commercially available 4-bromo-2-nitroaniline (2.1058 g, 9.703 mmol, 1 equiv) in 30 mL dry THF was added NEt_3 (4.0 mL, 29 mmol, 3.0 equiv), 4-dimethylaminopyridine (DMAP; 0.0555 g, 0.454 mmol, 0.05 equiv), and finally Boc_2O (6.3808 g, 29.2 mmol, 3.0 equiv), then the light orange solution was refluxed for 7 h and cooled. After addition of 13.0 mL of 15% aq. NaOH, the reaction was again refluxed at 85 °C for 20 h. A pellet of solid NaOH was then added and the dark orange solution refluxed an additional 2 h until selective saponification was complete by ^{1}H NMR. The solution was then poured into slightly acidified NaH_2PO_4 buffer, which was adjusted to pH 1 with HCl, and extracted with 3x30 mL Et_2O. The combined organic layers were washed sequentially with 10 mL each water and brine, then dried over anhydrous $MgSO_4$, filtered, and concentrated. Silica gel flash chromatography with 0-30% Et_2O / hexanes (R_f 0.28, 33% Et_2O / hexanes) afforded 3.0211 g or 98% yield of bright yellow crystalline **5.1**. The characterization data are in agreement with the literature.[15] **IR** ν_{max} (ground solid, cm^{-1}): 3361, 3121, 3105, 3076, 2996, 2973, 2937, 1732, 1694, 1606, 1569, 1542, 1495, 1475, 1460, 427, 1393,

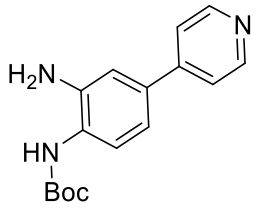
1366, 1332, 1294, 1260, 1241, 1216, 1159, 1143, 1079, 1048, 1023, 983. **^{1}H NMR** (400 MHz, $CDCl_3$) δ 9.61 (s, 1H), 8.51 (d, *J* = 9.2 Hz, 1H), 8.33 (d, *J* = 2.4 Hz, 1H), 7.69 (dd, *J* = 9.2, 2.4 Hz, 1H), 1.54 (s, 9H). The di-Boc aniline could alternatively be isolated in 78% yield by simple concentration of the initial mixture and direct silica gel flash chromatography with 0-30% Et_2O / hexanes (R_f 0.63, 33% Et_2O / hexanes) or the residue. **^{1}H NMR** (400 MHz, $CDCl_3$) δ 8.19 (d, *J* = 2.3 Hz, 1H), 7.75 (dd, *J* = 8.4, 2.3 Hz, 1H), 7.20 (d, *J* = 8.4 Hz, 1H), 1.40 (s, 22H).

Aryl nitro 5.2



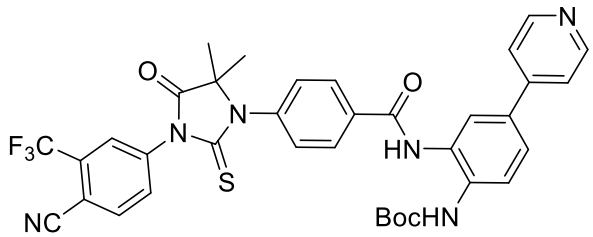
A solution of $Pd(OAc)_2$ (0.1011 g, 0.450 mmol, 0.1 equiv) and PPh_3 (0.6624 g, 2.53 mmol, 0.55 equiv) in 5 mL dry DCM was stirred 1 h until bright yellow then concentrated. Bromide **5.1** (1.4576 g, 4.596 mmol, 1 equiv) and 4-pyridinylboronic acid (0.7128 g, 5.06 mmol, 1.1 equiv) were added, followed by 9.2 mL of dry 1,4-dioxane and 4.6 mL 2 M aq. K_2CO_3. The resulting biphasic solution was refluxed 20 h, then cooled and filtered on celite with additional EtOAc. The organic solvent was removed by rotary evaporation and the aqueous diluted with 5 mL water, then extracted with 2x30 mL EtOAc. The combined organic layers were washed sequentially with 10 mL each water and brine, then dried over anhydrous Na_2SO_4, filtered, and concentrated. Silica gel flash chromatography with 30-100% EtOAc / hexanes (R_f 0.37, EtOAc) afforded 0.2632 g or 53% yield of **5.2** as a yellow solid. **IR** ν_{max} (ground solid, cm^{-1}): 3361, 2980, 2933, 1738, 1624, 1602, 1577, 1552, 1523, 1494, 1438, 1418, 1393, 1367, 1345, 1294, 1248, 1213, 1141, 1087, 1046, 1023, 993, 961, 902. **^{1}H NMR** (400 MHz, $CDCl_3$) δ 9.74 (s, 1H), 8.73 (d, *J* = 8.9 Hz, 1H), 8.73 – 8.67 (m, 2H), 8.50 (d, *J* = 2.2 Hz, 1H), 7.89 (dd, *J* = 8.9, 2.1 Hz, 1H), 7.56 – 7.46 (m, 2H), 1.56 (s, 9H). **^{13}C NMR** (101 MHz, $CDCl_3$) δ 152.17, 150.79, 145.42, 136.63, 136.26, 133.92, 131.86, 124.16, 121.59, 121.12, 82.48, 28.33. **HRMS** (ESI) *m/z* calcd for $C_{16}H_{18}O_4N_3$ [$(M+H)^+$]: 316.12918, measured: 316.12936.

Aniline 2.22d



To a solution of nitro arene **5.2** (0.7742 g, 2.45 mmol) in 25 mL of 3:2 EtOAc / MeOH under argon was added 0.2632 g of 5% Pd/C, then hydrogen gas was bubbled through from a double-skinned balloon for 3 h. The suspension was filtered on celite with EtOAc and shaken with aq. Na_2CO_3, then extracted with EtOAc, dried over anhydrous Na_2SO_4, and concentrated. Silica gel flash chromatography with 0-10% ^{i}PrOH / DCM (R_f 0.15, EtOAc) afforded 0.5474 g or 78% yield of aniline **2.22d** as peach flakes. **IR** ν_{max} (ground solid, cm^{-1}): 3374, 3221, 3058, 2977, 2933, 1683, 1593, 1547, 1525, 1499, 1431, 1408, 1393, 1364, 1323, 1303, 1247, 1211, 1157, 1056, 1041, 1026. **^{1}H NMR** (500 MHz, DMSO-d_6) δ 8.57 (d, J = 5.3 Hz, 2H), 8.43 (s, 1H), 7.58 – 7.53 (m, 2H), 7.42 (d, J = 8.2 Hz, 1H), 7.11 (d, J = 2.1 Hz, 1H), 6.98 (dd, J = 8.3, 2.1 Hz, 1H), 5.08 (s, 2H), 1.48 (s, 9H). **^{13}C NMR** (126 MHz, DMSO-d_6) δ 153.39, 150.07, 147.23, 141.03, 133.10, 125.13, 124.09, 120.65, 114.78, 113.48, 79.00, 28.14. **HRMS** (ESI) *m/z* calcd for $C_{16}H_{20}O_2N_3$ [$(M+H)^+$]: 286.15500, measured: 286.15493.

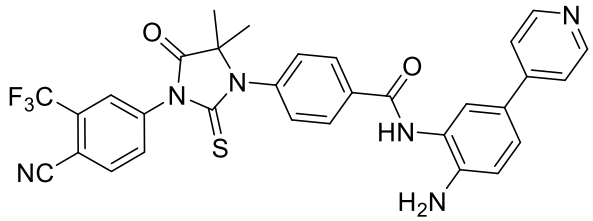
Boc-protected biaryl benzamide 5.3



To a solution of acid **2.18** (0.2372 g, 0.5473 mmol, 1 equiv), HOAt (74.5 mg, 0.547 mmol, 1.0 equiv), and EDC•HCl (0.1165 g, 0.6078 mmol, 1.1 equiv) in 5.5 mL dry DMF was added NEt_3 (0.230 mL, 1.65 mmol, 3.0 equiv) and aniline **2.22d** (0.1771 g, 0.6206 mmol, 1.1 equiv), then the reaction stirred 46 h before the solvent was removed under reduced pressure. The dark yellow residue was partitioned between 20 mL 5% aq. Na_2CO_3 and 30 mL EtOAc, then the aqueous layer

acidified to pH 9, and the layers were separated. The aqueous was further extracted with 2x10 mL EtOAc and the combined organic layers were washed sequentially with 10 mL each water and brine, then dried over anhydrous Na_2SO_4, filtered, and concentrated. Silica gel flash chromatography with 1-3% MeOH / DCM (R_f 0.65, 10% MeOH / DCM) afforded 0.2255 g or 59 % yield of yellow crystalline intermediate **5.3**, along with 0.1206 g of a 1:1 mixture of **5.3** and aniline **2.22d**. **^{1}H NMR** (500 MHz, DMSO-d_6) δ 10.08 (s, 1H), 8.91 (s, 1H), 8.63 (d, J = 5.0 Hz, 2H), 8.41 (d, J = 8.2 Hz, 1H), 8.33 (s, 1H), 8.18 (d, J = 8.2 Hz, 2H), 8.11 (d, J = 8.3 Hz, 1H), 7.97 (s, 1H), 7.84 (d, J = 8.6 Hz, 1H), 7.73 – 7.66 (m, 3H), 7.60 (d, J = 8.3 Hz, 2H), 1.57 (s, 6H), 1.48 (s, 9H). **^{13}C NMR** (126 MHz, DMSO-d_6) δ 179.97, 174.85, 165.03, 153.13, 150.28, 146.03, 138.43, 138.03, 136.22, 135.01, 134.02, 133.59, 132.10, 131.09 (q, J = 32.7 Hz), 129.91, 129.34, 129.11, 128.07 (q, J = 4.3 Hz), 124.84, 124.26, 123.43, 122.23 (q, J = 273.6 Hz), 120.72, 115.02, 108.67 (q, J = 2.3 Hz), 79.90, 66.49, 28.03, 23.04.

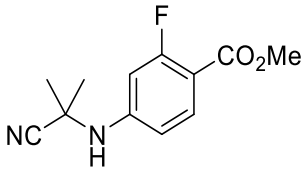
***o*-amino biaryl benzamide (RB-416) 2.6d**



To a solution of intermediate **5.3** (205.9 mg, 0.2938 mmol) in 3 mL dry DCM was added 0.3 mL TFA and the reaction stirred 24 h, then 15 mL DCM was added followed by 15 mL sat. aq. $NaHCO_3$ dropwise and 5 mL water. The layers were separated and the aqueous was extracted with 2x15 mL DCM further. The combined organic layers were washed sequentially with 5 mL each water and brine, then dried over anhydrous Na_2SO_4, filtered, and concentrated. Silica gel flash chromatography with 0-2% MeOH / DCM (R_f 0.47, 10% MeOH / DCM), followed by C18 silica gel flash chromatography with 30-90% MeOH / H_2O (elutes at ~70%) afforded 59.0 mg or 33% yield of RB-416 as a bright yellow powder, pure by NMR and 98.8% homogeneous by LC-MS analysis. **IR** ν_{max} (ground solid, cm^{-1}): 3347, 2234, 1753, 1660, 1596, 1367, 1285, 1130. **^{1}H NMR** (500 MHz, DMSO-d_6) δ 9.91 (s, 1H), 8.52 (d, J = 4.8 Hz, 2H), 8.41 (d, J = 8.2 Hz, 1H), 8.33 (d, J = 1.6 Hz, 1H), 8.20 (d, J = 8.4 Hz, 2H), 8.11 (dd, J = 8.2, 1.7 Hz, 1H), 7.70 (d, J = 1.8 Hz, 1H), 7.63 – 7.49 (m, 5H), 6.90 (d, J = 8.4 Hz, 1H), 5.46 (s, 2H), 1.56 (s, 6H). **^{13}C NMR** (126 MHz, DMSO-d_6) δ 179.95, 174.88, 164.92, 150.03, 146.73, 145.02, 138.11, 138.05, 136.23, 135.29,

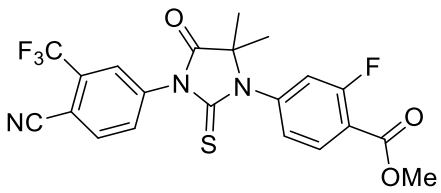
134.03, 131.09 (q, J = 32.7 Hz), 129.72, 129.19, 128.09 (q, J = 4.8 Hz), 125.37, 125.19, 123.98, 123.06, 122.24 (q, J = 273.8 Hz), 119.61, 116.12, 115.04, 108.66 (q, J = 2.3 Hz), 66.48, 23.05. **HRMS** (ESI) *m/z* calcd for $C_{31}H_{22}O_2N_6F_3S$ [(M–H)$^-$]: 599.14825, measured: 599.14867, calcd for $C_{31}H_{24}O_2N_6F_3S$ [(M+H)$^+$]: 601.16281, measured: 601.16301.

Methyl 4-((2-cyanopropan-2-yl)amino)-2-fluorobenzoate 2.44b



Methyl 4-amino-2-fluorobenzoate (0.1905 g, 1.126 mmol, 1 equiv), prepared by Fischer esterification of the benzoic acid, anhydrous ground $CaSO_4$ (Drierite ®, 1.5842 g, 0.01164 mol, 10.3 equiv) which was dried overnight at 180 °C under vacuum in the reaction vessel, and acetone cyanohydrin (1.05 mL, 0.0115 mol, 10 equiv) were heated at 105 °C for 21 h with a venting needle. Upon completion, observed by ^{1}H NMR, the solid mixture was combined with silica gel and purified by silica gel flash chromatography with 5-60% EtOAc / hexanes (R_f 0.38, 50% EtOAc / hexanes) to afford 0.2043 g or 77% yield of cyanoamine **2.44b** as peach crystals. **IR** ν_{max} (cm^{-1}): 3421, 3354, 1689, 1610, 1279. **^{1}H NMR** (400 MHz, $CDCl_3$) δ 7.87 (t, J = 8.4 Hz, 1H), 6.71 – 6.52 (m, 2H), 4.27 (s, 1H), 3.91 (s, 3H), 1.79 (s, 6H). **^{13}C NMR** (101 MHz, $CDCl_3$) δ 164.92, 163.61 (d, J = 255.0 Hz), 149.40 (d, J = 11.4 Hz), 133.79 (d, J = 2.9 Hz), 120.80, 110.59 (d, J = 2.8 Hz), 109.21 (d, J = 10.1 Hz), 102.49 (d, J = 27.4 Hz), 52.07, 48.08, 28.23. **HRMS** (ESI) *m/z* calcd for $C_{12}H_{13}FN_2NaO_2$ [(M+Na)$^+$]: 259.0853, measured: 259.0843.

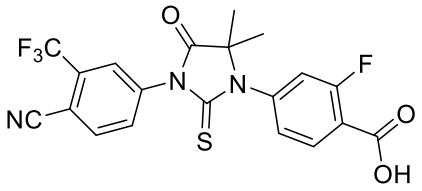
methyl 4-(3-(4-cyano-3-(trifluoromethyl)phenyl)-5,5-dimethyl-4-oxo-2-thioxoimidazolidin-1-yl)-2-fluorobenzoate 2.45b



General procedure **A** was employed with *α*-cyanoamine **2.44b** (198.3 mg, 0.8394 mmol, 1 equiv), aryl isothiocyanate **2.11** (191.9 mg, 0.8410 mmol, 1.0 equiv) and 1.25 mL LHMDS (0.125 mmol, 1.5 equiv), taking 40 mins, followed by 10 mL 2N HCl in stage two for 1 h. The solution was

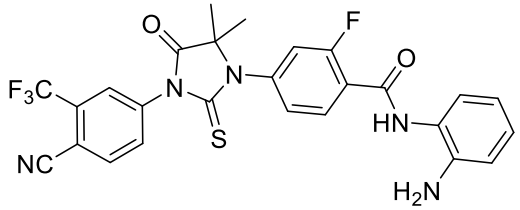
cooled, solvent was removed *in vacuo*, and the aqueous concentrate extracted with 50 mL, then 2x10 mL EtOAc. The combined organic layers were washed sequentially with 10 mL each water and brine, then dried over anhydrous Na_2SO_4, filtered, and concentrated. Silica gel flash chromatography with 0-5% ^{i}PrOH / DCM (R_f 0.45, 50% EtOAc / hexanes) afforded 265.3 mg or 68% yield of thiohydantoin **2.45b** as a faintly yellow crystalline solid. The ^{1}H NMR data in DMSO-d_6 agrees with the literature,[17] but a characterization in $CDCl_3$ is provided here. **IR** ν_{max} (cm^{-1}): 2986, 2959, 2235, 1757, 1725, 1619, 1435, 1410, 1133. **^{1}H NMR** (500 MHz, $CDCl_3$) δ 8.12 (t, *J* = 8.0 Hz, 1H), 7.99 (d, *J* = 8.3 Hz, 1H), 7.95 (d, *J* = 2.0 Hz, 1H), 7.83 (dd, *J* = 8.3, 2.0 Hz, 1H), 7.21 (dd, *J* = 8.1, 1.9 Hz, 1H), 7.16 (dd, *J* = 10.5, 2.0 Hz, 1H), 3.98 (s, 3H), 1.62 (s, 6H). **^{13}C NMR** (101 MHz, $CDCl_3$) δ 179.65, 174.39, 163.79 (d, *J* = 4.0 Hz), 162.02 (d, *J* = 263.7 Hz), 140.27 (d, *J* = 10.0 Hz), 136.80, 135.30, 133.71 (q, *J* = 33.7 Hz), 133.39 (d, *J* = 2.0 Hz), 132.11, 127.05 (q, *J* = 4.8 Hz), 125.46 (d, *J* = 4.0 Hz), 121.82 (q, *J* = 274.4 Hz), 120.12 (d, *J* = 10.2 Hz), 118.83 (d, *J* = 24.1 Hz), 114.70, 110.45 (q, *J* = 2.2 Hz), 66.63, 52.76, 23.89. **HRMS** (ESI) *m/z* calcd for $C_{21}H_{15}F_4N_3NaO_3S$ [$(M+Na)^+$]: 488.0662, measured: 488.0663.

4-(3-(4-cyano-3-(trifluoromethyl)phenyl)-5,5-dimethyl-4-oxo-2-thioxoimidazolidin-1-yl)-2-fluorobenzoic acid 2.46



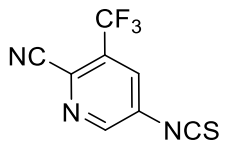
Carboxylic ester **2.45b** (0.2297 g, 0.4935 mmol, 1 equiv) was treated with KO^{t}Bu (0.8306 g, 7.402 mmol, 15.0 equiv) according to General Procedure **B** for 3.5 h, and afforded 0.1926 g or 86% yield of carboxylic acid **2.46** as a faintly yellow crystalline solid. The ^{1}H NMR data in $CDCl_3$ agrees with the literature.[18] **IR** ν_{max} (cm^{-1}): 3500-2500 (broad), 3059, 2988, 2971, 2237, 1753, 1724, 1618, 1580. **^{1}H NMR** (400 MHz, $CDCl_3$) δ 8.19 (t, *J* = 8.1 Hz, 1H), 8.00 (d, *J* = 8.3 Hz, 1H), 7.95 (d, *J* = 2.0 Hz, 1H), 7.83 (dd, *J* = 8.3, 2.1 Hz, 1H), 7.22 (dd, *J* = 8.3, 2.0 Hz, 1H), 7.18 (dd, *J* = 10.4, 2.0 Hz, 1H), 1.62 (s, 6H). **HRMS** (ESI) *m/z* calcd for $C_{20}H_{13}F_4N_3NaO_3S$ [$(M+Na)^+$]: 474.0506, measured: 474.0517.

N-(2-aminophenyl)-2-fluoro-4-(3-(4-isocyano-3-(trifluoromethyl)phenyl)-5,5-dimethyl-4-oxo-2-thioxoimidazolidin-1-yl)benzamide (RB-391) 2.34



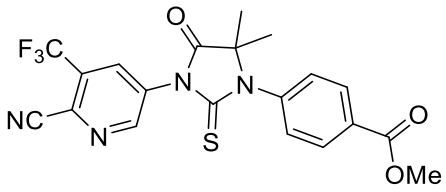
To a solution of carboxylic acid **2.46** (0.1797 g, 0.3981 mmol, 1 equiv), EDC•HCl (101.8 mg, 0.5310 mmol, 1.3 equiv), and *o*-phenylenediamine (127.0 mg, 1.174 mmol, 3.0 equiv) in 4.0 mL dry DCM was added NEt_3 (83 µL, 0.60 mmol, 1.5 equiv). The reaction was stirred 8 h, then extracted from 40 mL 5% aq. $NaHCO_3$ with 3x40 mL EtOAc. The combined organic layers were washed sequentially with 20 mL each water and brine, then dried over anhydrous Na_2SO_4, filtered, and concentrated. Silica gel flash chromatography with 25-50% EtOAc / PhMe (R_f 0.39, 50% EtOAc / PhMe), followed by C18 silica gel flash chromatography with 5-95% MeCN / H_2O afforded 53.1 mg or 25% yield of off-white benzamide **2.34** (RB-391), pure by NMR and 100% homogeneous by LC-MS analysis. The ^{1}H NMR data in DMSO-d_6 agrees with the literature.[19] **IR** ν_{max} (cm^{-1}): 3382, 2240, 1758, 1651, 1147. **^{1}H NMR** (500 MHz, DMSO-d_6) δ 9.73 (s, 1H), 8.41 (d, J = 8.2 Hz, 1H), 8.31 (d, J = 1.9 Hz, 1H), 8.10 (dd, J = 8.2, 1.9 Hz, 1H), 7.94 (t, J = 8.0 Hz, 1H), 7.50 (dd, J = 10.5, 1.9 Hz, 1H), 7.39 (dd, J = 8.1, 1.9 Hz, 1H), 7.31 (dd, J = 7.9, 1.5 Hz, 1H), 6.98 (ddd, J = 8.7, 7.3, 1.6 Hz, 1H), 6.78 (dd, J = 8.0, 1.5 Hz, 1H), 6.61 (td, J = 7.5, 1.4 Hz, 1H), 4.97 (s, 2H), 1.57 (s, 6H). **^{13}C NMR** (126 MHz, $CDCl_3$) δ 179.93, 174.52, 160.53 (d, J = 250.4 Hz), 160.47 (d, J = 4.1 Hz), 140.60, 139.74 (d, J = 10.9 Hz), 136.92, 135.47, 133.91 (d, J = 3.3 Hz), 133.88 (d, J = 33.5 Hz), 132.25, 127.78, 127.20 (q, J = 4.8 Hz), 126.62 (d, J = 3.2 Hz), 125.42, 124.12, 122.72 (d, J = 12.0 Hz), 121.96 (d, J = 274.4 Hz), 120.00, 118.47, 118.28 (d, J = 26.4 Hz), 114.83, 110.64 (q, J = 2.0 Hz), 66.80, 24.05. **HRMS** (ESI) *m/z* calcd for $C_{26}H_{20}O_2N_5F_4S$ [$(M+H)^+$]: 542.12683, measured: 542.12745.

5-isothiocyanato-3-(trifluoromethyl)picolinonitrile 2.47



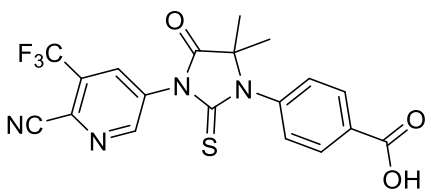
This compound was prepared as described by Jung.[2] The characterization data are in agreement with that reference. **^{1}H NMR** (500 MHz, $CDCl_3$) δ 8.73 (d, *J* = 2.3 Hz, 1H), 7.85 (d, *J* = 2.2 Hz, 1H). **^{13}C NMR** (126 MHz, $CDCl_3$) δ 150.39, 145.00, 133.66, 131.64 (q, *J* = 34.4 Hz), 130.44 (q, *J* = 4.3 Hz), 127.66, 121.17 (q, *J* = 274.4 Hz), 113.71.

Benzoic ester 2.45c



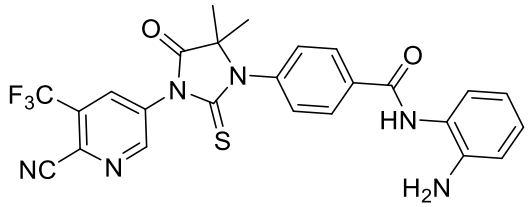
General Procedure **A** was employed with *α*-cyanoamine **2.44a** (400.8 mg, 1.836 mmol, 1 equiv), pyridyl isothiocyanate **2.47** (421.4 mg, 1.839 mmol, 1.0 equiv) and 2.75 mL LHMDS (2.75 mmol, 1.5 equiv) for 1 h, then 5.5 mL 2N HCl was used to hydrolyze for 40 mins. After cooling, organic solvent was removed *in vacuo* and the residue taken up in EtOAc / water. Sat. $NaHCO_3$ was added to achieve a pH of 7 in the aqueous layer, which was extracted with 3x20 mL EtOAc total. The combined organic layers were washed sequentially with 5 mL each water and brine, then dried over anhydrous Na_2SO_4, filtered, and concentrated. Silica gel flash chromatography with 0-10% acetone / DCM (R_f 0.54, 50% EtOAc / hexanes) afforded 644.9 mg or 78% yield of ester **2.45c** as fine white crystals. **IR** ν_{max} (ground solid, cm^{-1}): 3081, 2987, 2952, 2163, 1763, 1718, 1460, 1433, 1418, 1278. **^{1}H NMR** (500 MHz, $CDCl_3$) δ 9.09 (d, *J* = 2.2 Hz, 1H), 8.36 (d, *J* = 2.2 Hz, 1H), 8.25 – 8.21 (m, 2H), 7.42 – 7.37 (m, 2H), 3.97 (s, 3H), 1.63 (s, 6H). **^{13}C NMR** (126 MHz, $CDCl_3$) δ 179.10, 174.60, 165.94, 152.39, 139.02, 134.22 (q, *J* = 4.4 Hz), 132.39, 131.79, 131.42, 130.65 (q, *J* = 34.7 Hz), 130.29 (q, *J* = 2.0 Hz), 129.79, 121.41 (q, *J* = 274.6 Hz), 113.83, 66.91, 52.72, 24.02. **HRMS** (ESI) *m/z* calcd for $C_{20}H_{15}O_3N_4F_3SNa$ $[(M+Na)^+]$: 471.0709, measured: 471.0715, calcd for $C_{20}H_{15}O_3N_4F_3SK$ $[(M+K)^+]$: 487.0449, measured: 487.0446.

Benzoic acid 2.48a



Carboxylic ester **2.45c** (0.6449 g, 1.438 mmol, 1 equiv) was treated with KO^{t}Bu (2.4230 g, 21.66 mmol, 15.1 equiv) according to General Procedure **B** for 14 h. Silica gel flash chromatography with 1% AcOH in 30-100% EtOAc / hexanes (R_f 0.42, 1% AcOH / EtOAc) afforded 0.2986 g or 48% yield of carboxylic acid **2.48a**. **IR** ν_{max} (thin film, cm^{-1}): 3400-2500 (very broad), 3445, 3232, 2985, 2917, 2620, 2496, 1765, 1707, 1662, 1604, 1569, 1512, 1472, 1434, 1417, 1367, 1311, 1292, 1247, 1196, 1144, 1120, 1054. **^{1}H NMR** (500 MHz, DMSO-d_6) δ 13.39 (bs, 1H), 9.26 (d, J = 2.0 Hz, 1H), 8.84 (d, J = 2.1 Hz, 1H), 8.15 – 8.08 (m, 2H), 7.50 (d, J = 8.4 Hz, 2H), 1.55 (s, 6H). **^{13}C NMR** (126 MHz, DMSO-d_6) δ 179.85, 175.07, 167.18, 154.24, 139.19, 136.40 (q, J = 4.8, 4.2 Hz), 133.72, 131.00, 130.31, 129.50 (q, J = 2.4 Hz), 129.25 (q, J = 33.9 Hz), 128.67, 122.05 (q, J = 274.2 Hz), 114.73, 67.24, 23.46. **HRMS** (ESI) *m/z* calcd for $C_{19}H_{13}O_3N_4F_3SNa$ [(M+Na)$^+$]: 457.0553, measured: 467.0558.

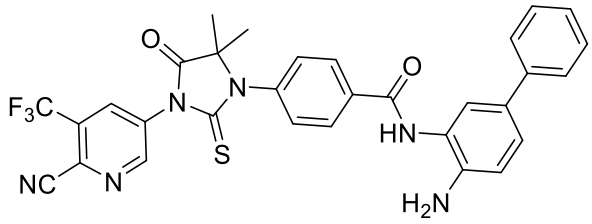
***o*-amino benzamide (RB-445) 2.35a**



To a solution of carboxylic acid **2.48a** (0.0524 g, 0.121 mmol, 1 equiv), EDC•HCl (34.1 mg, 0.178 mmol, 1.5 equiv), and *o*-phenylenediamine (38.6 mg, 0.357 mmol, 3.0 equiv) in 1.2 mL dry DCM was added NEt_3 (25.0 μL, 0.179 mmol, 1.5 equiv). The reaction was stirred for 25 h, then additional EDC•HCl (24.1 mg) was added, and the reaction stirred 24 h further. The DCM was removed by rotary evaporation, then the residue partitioned between EtOAc and 5 mL 5% aq. $NaHCO_3$, and the aqueous extracted with 3x10 mL EtOAc. The combined organic layers were washed sequentially with 5 mL each water and brine, then dried over anhydrous Na_2SO_4, filtered, and concentrated. Silica gel flash chromatography with 20-100% EtOAc / hexanes (R_f 0.51, EtOAc), then C18 silica gel flash chromatography with 30-95% MeCN / H_2O (eluting at ca. 65%) afforded 23.2 mg or 37% yield of benzamide **2.35a** as a yellow powder, pure by NMR and 95.3% homogeneous by LC-MS analysis. **IR** ν_{max} (ground solid, cm^{-1}): 3492, 3396, 3191, 2971, 2163, 1772, 1460, 1431, 1287, 1129. **^{1}H NMR** (400 MHz, DMSO-d_6) δ 9.80 (s, 1H), 9.27 (d, J = 2.1 Hz, 1H), 8.85 (d, J = 2.1 Hz, 1H), 8.17 (d, J = 8.2 Hz, 2H), 7.54 (d, J = 8.5 Hz, 2H), 7.18 (d, J = 7.8 Hz, 1H), 6.99 (td, J = 7.6, 1.4 Hz, 1H), 6.79 (dd, J = 8.0, 1.4 Hz, 1H), 6.61 (td, J = 7.5, 1.4 Hz,

1H), 4.96 (s, 2H), 1.57 (s, 6H). **^{13}C NMR** (126 MHz, DMSO-d_6) δ 179.47, 174.61, 164.55, 153.75, 143.29, 137.78, 135.92 (m), 135.48, 133.27, 129.62, 129.17, 129.03 (m), 128.77 (q, J = 33.6 Hz), 126.80, 126.67, 122.94, 121.58 (q, J = 274.4 Hz), 116.12, 115.99, 114.26, 66.73, 23.03. **HRMS** (ESI) *m/z* calcd for $C_{25}H_{19}O_2N_6F_3SNa$ [$(M+Na)^+$]: 547.1135, measured: 547.1149.

***o*-amino biphenyl benzamide (RB-446) 2.35b**

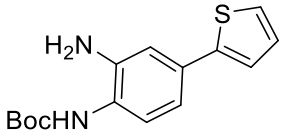


To solid carboxylic acid **2.48a** (0.0827 g, 0.190 mmol, 1 equiv), EDC•HCl (41.2 mg, 0.215 mmol, 1.1 equiv), and Boc-aniline **2.22b** (51.4 mg, 0.181 mmol, 0.95 equiv) was added 1.9 mL dry DCM, then the reaction stirred 24 h. Additional EDC•HCl (24.7 mg) was added, the reaction stirred 2 d further, then additional aniline (35.2 mg) was added. After stirring 24 h longer, EDC•HCl (31.1 mg), NEt_3 (40.0 μL, 0.287 mmol, 1.5 equiv), and HOBt (32.6 mg, 0.213 mmol, 1.1 equiv) were added. After a further 24 h, the reaction was diluted with 20 mL DCM, poured into pH 3 phosphate buffer prepared from 1 N H_3PO_4, the layers were separated, and the aqueous extracted with 2x20 mL $CHCl_3$. The combined organic layers were washed sequentially with 15 mL each sat. aq. $NaHCO_3$, water, and brine, then dried over anhydrous Na_2SO_4, filtered, and concentrated.

To a solution of the crude Boc-protected aniline intermediate in 1.9 mL dry DCM was added 0.2 mL TFA and the solution stirred for 20 h. This was poured into 10 mL 5% aq. Na_2CO_3, then extracted with 3x8 mL DCM. The combined organic layers were washed sequentially with 3 mL each water and brine, dried over anhydrous Na_2SO_4, filtered, and concentrated. Reverse-phase C18 silica gel flash chromatography with MeCN / H_2O, followed by silica gel flash chromatography with 10-60% EtOAc / hexanes (R_f 0.70, 10% MeOH / DCM), afforded 11.5 mg or 10% yield over 2 steps of benzamide **2.35b**, pure by NMR and 100.0% homogeneous by LC-MS analysis. **IR** ν_{max} (ground solid, cm^{-1}): 3306 (broad), 2987, 2162, 1764, 1461, 1416, 1278, 1139, 1053. **^{1}H NMR** (500 MHz, DMSO-d_6) δ 9.89 (s, 1H), 9.28 (d, J = 1.8 Hz, 1H), 8.85 (d, J = 1.8 Hz, 1H), 8.20 (d, J = 8.3 Hz, 2H), 7.59 – 7.52 (m, 5H), 7.40 (t, J = 7.7 Hz, 2H), 7.35 (dd, J = 8.3, 2.0 Hz, 1H), 7.25 (t, J = 7.3 Hz, 1H), 6.88 (d, J = 8.4 Hz, 1H), 5.16 (s, 2H), 1.58 (s, 6H). **^{13}C NMR** (126 MHz,

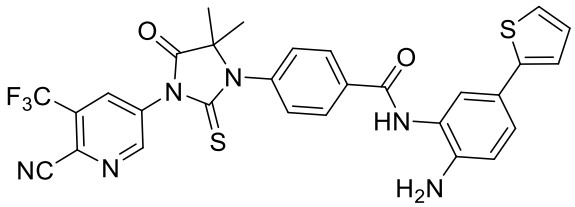
DMSO-d_6) δ 179.49, 174.62, 164.74, 153.76, 142.95, 140.17, 137.84, 135.93 (q, J = 4.4 Hz), 135.48, 133.28, 129.63, 129.22, 129.03 (q, J = 2.3 Hz), 128.80, 128.79 (q, J = 33.8 Hz), 128.02, 126.01, 125.47, 124.90, 123.23, 121.58 (q, J = 274.1 Hz), 116.40, 114.26, 66.73, 23.04. **HRMS** (ESI) *m/z* calcd for $C_{31}H_{22}O_2N_6F_3S$ [$(M–H)^-$]: 599.14825, measured: 599.14798, calcd for $C_{31}H_{23}O_2N_6ClF_3S$ [$(M+Cl)^-$]: 635.12493, measured: 635.12501.

tert-butyl (2-amino-4-(thiophen-2-yl)phenyl)carbamate 2.22c



Aniline **2.22c** was prepared as described in the literature, essentially as done for **2.22d** (*vide supra*), and the spectroscopic data matched that previously reported.[15]

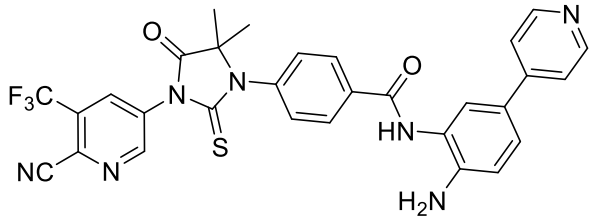
***o*-amino biaryl benzamide (RB-447) 2.35c**



Acid **2.48a** (78.3 mg, 0.180 mmol) was reacted with thienyl aniline **2.22c** and deprotected with TFA as just described for RB-446. Reverse-phase C18 silica gel flash chromatography with 30-95% MeCN / H_2O (eluting at ~75%), followed by silica gel flash chromatography with 0-10% acetone / DCM (R_f 0.78, 10% MeOH / DCM), then recrystallization from $CHCl_3$ / hexanes afforded 16.3 mg or 15% yield of benzamide **2.35c** as golden yellow crystals, pure by NMR and 98.7% homogeneous by LC-MS analysis. **IR** ν_{max} (thin film, cm^{-1}): 3337 (broad), 3233 (broad), 3073, 2924, 2852, 2254, 1764, 1662, 1629, 1608, 1573, 1527, 1504, 1462, 1435, 1419, 1297, 1256, 1196, 1173, 1147, 1057, 1025, 1008. **^{1}H NMR** (400 MHz, DMSO-d_6) δ 9.89 (s, 1H), 9.28 (d, J = 1.9 Hz, 1H), 8.85 (d, J = 2.0 Hz, 1H), 8.20 (d, J = 8.4 Hz, 2H), 7.56 (d, J = 8.4 Hz, 2H), 7.49 (d, J = 1.8 Hz, 1H), 7.36 (dd, J = 5.1, 0.9 Hz, 1H), 7.32 (dd, J = 8.3, 2.1 Hz, 1H), 7.25 (d, J = 2.7 Hz, 1H), 7.06 (dd, J = 5.0, 3.6 Hz, 1H), 6.82 (d, J = 8.4 Hz, 1H), 5.23 (s, 2H), 1.58 (s, 6H). **^{13}C NMR** (101 MHz, DMSO-d_6) δ 179.48, 174.62, 164.75, 153.76, 144.21, 143.21, 137.87, 135.94 (q, J = 4.2 Hz), 135.36, 133.28, 129.63, 129.25, 129.03 (q, J = 2.1 Hz), 128.79 (q, J = 33.9 Hz), 128.21,

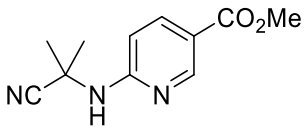
124.16, 124.09, 123.22, 123.02, 122.14, 121.58 (q, J = 274.4 Hz), 120.99, 116.25, 114.26, 66.73, 23.04. **HRMS** (ESI) *m/z* calcd for $C_{29}H_{20}O_2N_6F_3S_2$ [(M–H)$^-$]: 605.10467, measured: 605.10363, calcd for $C_{29}H_{21}O_2N_6ClF_3S_2$ [(M+Cl)$^-$]: 641.08135, measured: 641.08162.

***o*-amino biaryl benzamide (RB-448) 2.35d**



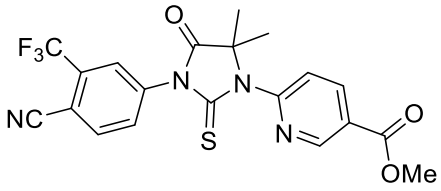
Acid **2.48a** (65.7 mg, 0.151 mmol) was reacted with pyridinyl aniline **2.22d** as described for RB-446, except that DMF was employed as solvent and DCM for extraction. Rapid silica gel chromatography with 1% NEt_3 / EtOAc was also performed after amide coupling to provide a mixture of unreacted aniline and coupled intermediate, which was treated with TFA as for RB-446. Extraction after deprotection was accomplished with EtOAc, which aided in solubilizing brightly coloured neon orange-pink precipitate. Silica gel flash chromatography with 0-10% MeOH / DCM (R_f 0.52, 10% MeOH / DCM), followed by C18 silica gel flash chromatography with 30-90% MeCN / H_2O (eluting at ~70%) afforded 49.3 mg or 54% yield of benzamide **2.35d** as a white-yellow solid. Recrystallization of this material from $CHCl_3$ / hexanes afforded 25.2 mg or 51% recovery of benzamide **2.35d** as a light yellow powder, pure by NMR and 100.0% homogeneous by LC-MS analysis. **IR** ν_{max} (ground solid, cm^{-1}): 3333, 1760, 1651, 1597, 1312, 1290, 1141. **^{1}H NMR (**500 MHz, DMSO-d_6) δ 9.89 (s, 1H), 9.28 (d, J = 2.1 Hz, 1H), 8.85 (d, J = 2.1 Hz, 1H), 8.52 (s, 2H), 8.20 (d, J = 8.4 Hz, 2H), 7.70 (d, J = 2.2 Hz, 1H), 7.63 – 7.49 (m, 5H), 6.90 (d, J = 8.4 Hz, 1H), 5.45 (s, 2H), 1.58 (s, 6H). **^{13}C NMR** (126 MHz, DMSO-d_6) δ 179.49, 174.62, 164.89, 153.76, 150.01, 146.75, 145.02, 137.87, 135.93 (q, J = 3.9 Hz), 135.41, 133.28, 129.62, 129.27, 129.03 (q, J = 2.1 Hz), 128.79 (q, J = 33.8 Hz), 125.37, 125.21, 123.98, 123.03, 121.59 (q, J = 274.2 Hz), 119.60, 116.12, 114.26, 66.73, 23.05. **HRMS** (ESI) *m/z* calcd for $C_{30}H_{21}O_2N_7F_3S$ [(M–H)$^-$]: 600.14350, measured: 600.14404.

Methyl 6-((2-cyanopropan-2-yl)amino)nicotinate 2.44c



Methyl 6-aminonicotinate (2.0333 g, 0.01336 mol, 1 equiv), prepared by Fischer esterification of the benzoic acid, anhydrous ground $CaSO_4$ (Drierite ®, 7.4 g, 0.05436 mol, 4.1 equiv), and acetone cyanohydrin (12.0 mL, 0.131 mol, 9.8 equiv) were heated at 85-90 °C for 3.5 d and followed by ^{1}H NMR. The mixture was filtered on celite with DCM and purified by silica gel flash chromatography with 0-10% acetone / DCM (R_f 0.51, 10% acetone / DCM), then recrystallized from hot DCM / hexanes to afford an initial crop of 0.6795 g or 23% yield of colourless needles. A second crop of 0.6119 g or 21% yield was obtained as a white powder for 44% overall yield of **2.44c**. **IR** ν_{max} (cm^{-1}): 3347, 2237, 1709, 1608, 1509, 1288. **^{1}H NMR** (500 MHz, DMSO-d_6) δ 8.67 (dd, J = 2.4, 0.7 Hz, 1H), 7.94 (dd, J = 8.8, 2.4 Hz, 1H), 7.83 (s, 1H), 6.67 (dd, J = 8.7, 0.8 Hz, 1H), 3.80 (s, 3H), 1.72 (s, 6H). **^{13}C NMR** (126 MHz, DMSO-d_6) δ 165.56, 159.11, 149.73, 137.34, 122.17, 115.02, 109.43, 51.65, 46.69, 27.01. **HRMS** (ESI) *m/z* calcd for $C_{11}H_{13}N_3NaO_2$ [$(M+Na)^+$]: 242.0900, measured: 242.0896.

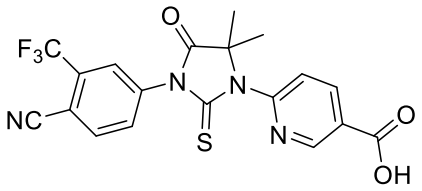
methyl 6-(3-(4-cyano-3-(trifluoromethyl)phenyl)-5,5-dimethyl-4-oxo-2-thioxoimidazolidin-1-yl)nicotinate 2.45d



General procedure **A** was employed with α-cyanoamine **2.44c** (60.6 mg, 0.276 mmol, 1 equiv), aryl isothiocyanate **2.11** (69.9 mg, 0.306 mmol, 1.1 equiv) and 0.360 mL LHMDS (0.360 mmol, 1.3 equiv), taking 40 mins, and 5 mL 2N HCl in stage two for 1.5 h. The solution was then cooled, solid $NaHCO_3$ was added, the organic solvent was removed *in vacuo*, and the pH was adjusted above 8 with 1N aq. NaOH. This solution was extracted with 3x40 mL EtOAc. The combined organic layers were washed sequentially with 10 mL water and brine, dried over anhydrous Na_2SO_4, filtered, and concentrated. Silica gel flash chromatography with 0-10% ^{i}PrOH / DCM (R_f 0.56, 50% EtOAc / hexanes) afforded 76.4 mg or 62% yield of **2.45d** as a yellow crystalline solid.

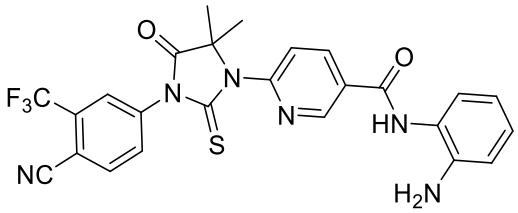
IR ν_{max} (cm^{-1}): 2234, 1758, 1722, 1595, 1116. **^{1}H NMR** (500 MHz, $CDCl_3$) δ 9.16 (dd, *J* = 2.4, 0.8 Hz, 1H), 8.40 (dd, *J* = 8.5, 2.3 Hz, 1H), 8.12 (dd, *J* = 8.5, 0.8 Hz, 1H), 7.99 (d, *J* = 8.2 Hz, 1H), 7.92 (d, *J* = 2.0 Hz, 1H), 7.80 (dd, *J* = 8.2, 2.0 Hz, 1H), 3.98 (s, 3H), 1.81 (s, 6H). **^{13}C NMR** (126 MHz, $CDCl_3$) δ 178.84, 174.98, 164.95, 153.24, 150.42, 138.99, 137.05, 135.46, 133.81 (q, *J* = 33.5 Hz), 132.56, 127.46 (q, *J* = 4.7 Hz), 125.17, 122.03, 121.94 (q, *J* = 274.2 Hz), 114.84, 110.62 (q, *J* = 2.1 Hz), 67.84, 52.76, 24.49. **HRMS** (ESI) *m/z* calcd for $C_{20}H_{15}F_3N_4NaO_3S$ [$(M+Na)^+$]: 471.0709, measured: 471.0701.

6-(3-(4-cyano-3-(trifluoromethyl)phenyl)-5,5-dimethyl-4-oxo-2-thioxoimidazolidin-1-yl)nicotinic acid 2.48b



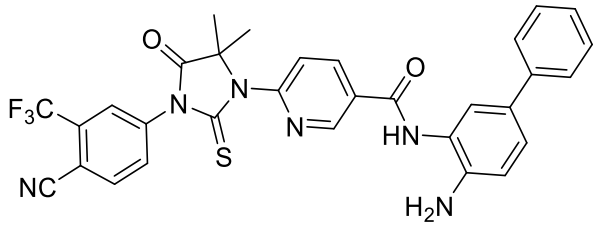
General procedure **B** was employed with carboxylic ester **2.45d** (0.3619 g, 0.8071 mmol, 1 equiv) and KO^{t}Bu (1.3606 g, 12.125 mmol, 15.0 equiv) for 2.6 h. The crude extract was triturated with Et_2O, and the gummy residue discarded, to afford 0.3255 g or 93% yield of carboxylic acid **2.48b** as a light yellow crystalline solid. **IR** ν_{max} (cm^{-1}): 2232, 1756, 1703, 1594, 1121. **^{1}H NMR** (500 MHz, DMSO-d_6) δ 13.56 (s, 1H), 9.08 (d, *J* = 1.8 Hz, 1H), 8.46 (dd, *J* = 8.4, 2.3 Hz, 1H), 8.41 (d, *J* = 8.2 Hz, 1H), 8.36 (d, *J* = 1.3 Hz, 1H), 8.13 (dd, *J* = 8.2, 1.4 Hz, 1H), 8.01 (d, *J* = 8.4 Hz, 1H), 1.68 (s, 6H). **^{13}C NMR** (126 MHz, DMSO-d_6) δ 179.58, 174.74, 165.55, 152.82, 149.93, 139.16, 137.94, 136.29, 134.25, 131.21 (q, *J* = 32.6 Hz), 128.27 (q, *J* = 4.8 Hz), 126.10, 123.58, 122.21 (q, *J* = 273.8 Hz), 115.00, 108.88 (q, *J* = 2.1 Hz), 67.20, 23.48. **HRMS** (ESI) *m/z* calcd for $C_{19}H_{12}F_3N_4O_3S$ [$(M-H)^-$]: 433.0588, measured: 433.0604.

N-(2-aminophenyl)-6-(3-(4-cyano-3-(trifluoromethyl)phenyl)-5,5-dimethyl-4-oxo-2-thioxoimidazolidin-1-yl)nicotinamide (RB-398) 2.36a



To a solution of carboxylic acid **2.48b** (0.1089 g, 0.2507 mmol, 1 equiv) in 2.5 mL dry DCM were added EDC•HCl (62.4 mg, 0.326 mmol, 1.3 equiv), NEt_3 (52 µL, 0.37 mmol, 1.5 equiv), and *o*-phenylenediamine (81.0 mg, 0.749 mmol, 3.0 equiv). This was stirred 21 h, then additional EDC•HCl (20.0 mg, 0.104 mmol, 0.4 equiv) was added for another 3 h of reaction time. The reaction was partitioned between 10 mL DCM and 10 mL 5% aq. $NaHCO_3$, then extracted with 2x20 mL EtOAc. The combined EtOAc organic layers and DCM layer were separately washed sequentially with 5 mL each water and brine. The combined organic layers were dried over anhydrous Na_2SO_4, filtered, concentrated, taken up into 15 mL EtOAc, and washed again with 5 mL each 2 M K_2CO_3, water and brine. Purification by C18 silica gel flash chromatography with 10-95% MeCN / H_2O, followed by NEt_3-neutralized silica gel flash chromatography with 0-100% EtOAc / hexanes afforded 33.3 mg or 25 % yield of benzamide **2.36a** (RB-398). This was recrystallized from EtOAc-hexanes to afford 28.2 mg or 85% recovery of faintly yellow crystals of benzamide **2.36a**, pure by NMR and 98.0% homogeneous by LC-MS analysis. **IR** ν_{max} (cm^{-1}): 3388, 3358, 3264, 2235, 1763, 1658, 1624, 1590, 1532, 1501. **^{1}H NMR** (400 MHz, DMSO-d_6) δ 9.90 (s, 1H), 9.16 (d, J = 2.5 Hz, 1H), 8.52 (dd, J = 8.4, 2.4 Hz, 1H), 8.42 (d, J = 8.2 Hz, 1H), 8.38 (d, J = 1.9 Hz, 1H), 8.14 (dd, J = 8.3, 1.9 Hz, 1H), 7.96 (d, J = 8.4 Hz, 1H), 7.18 (dd, J = 7.9, 1.5 Hz, 1H), 7.00 (td, J = 7.6, 1.6 Hz, 1H), 6.78 (dd, J = 8.0, 1.4 Hz, 1H), 6.60 (td, J = 7.6, 1.4 Hz, 1H), 5.04 (s, 2H), 1.69 (s, 6H). **^{13}C NMR** (101 MHz, DMSO-d_6) δ 179.62, 174.78, 163.19, 151.51, 148.60, 143.48, 137.97, 137.95, 136.29, 134.24, 131.18 (q, J = 32.5 Hz), 130.00, 128.29 (q, J = 4.7 Hz), 126.99, 126.92, 123.46, 122.35, 122.23 (q, J = 273.9 Hz), 115.95, 115.81, 115.02, 108.84 (q, J = 2.3 Hz), 67.03, 23.48. **HRMS** (ESI) *m/z* calcd for $C_{25}H_{18}F_3N_6O_2S$ [$(M–H)^-$]: 523.1170, measured: 523.1192.

N-(4-amino-[1,1'-biphenyl]-3-yl)-6-(3-(4-cyano-3-(trifluoromethyl)phenyl)-5,5-dimethyl-4-oxo-2-thioxoimidazolidin-1-yl)nicotinamide (RB-412) 2.36b

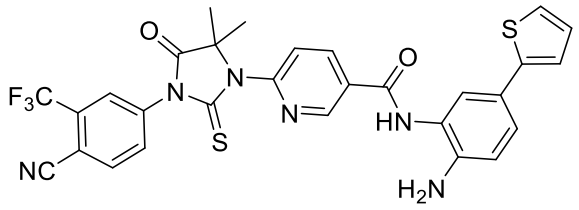


To a solution of carboxylic acid **2.48b** (0.1304 g, 0.3002 mmol, 1 equiv), aniline **2.22b** (0.0863 g, 0.304 mmol, 1.01 equiv), EDC•HCl (0.0686 g, 0.358 mmol, 1.19 equiv), and HOAt (0.0416 g,

0.306 mmol, 1.02 equiv) in 3.0 mL dry DMF was added NEt_3 (125 µL, 0.896 mmol, 2.99 equiv) and the solution was stirred for 42 h. This was poured into 30 mL 5% $NaHCO_3$ and extracted with 3x15 mL EtOAc. The combined organic layers were washed sequentially with 5 mL water and brine, then dried over anhydrous Na_2SO_4, filtered, and concentrated. Silica gel flash chromatography with 0-50% EtOAc / hexanes (R_f 0.88, 10% MeOH / DCM) afforded 0.1483 g or 70% yield of light yellow crystalline solid.

To a solution of the Boc-protected aniline intermediate (0.1423 g, 0.2031 mmol, 1 equiv) in 2.0 mL dry DCM was added TFA (0.4 mL, 5 mmol) and the solution stirred for 14 h. This was poured into 5 mL sat. aq. $NaHCO_3$, and additional 5% aq. $NaHCO_3$ was added until the acid was fully quenched. The resulting aqueous solution was then extracted with 3x15 mL DCM. The combined organic layers were washed sequentially with 3 mL water and brine, dried over anhydrous Na_2SO_4, filtered, and concentrated. The residue was purified by silica gel flash chromatography with 10-80% EtOAc / hexanes (R_f 0.10, 50% EtOAc / hexanes), then recrystallized from $CHCl_3$ to afford 36.6 mg or 30% yield of benzamide **2.36b** as yellow flakes, pure by NMR and 100% homogeneous by LC-MS. **IR** ν_{max} (cm^{-1}): 3349, 3241, 2925, 2234, 1760, 1664, 1438, 1411, 1313, 1139. **^{1}H NMR** (500 MHz, DMSO-d_6) δ 9.99 (s, 1H), 9.20 (d, J = 2.4 Hz, 1H), 8.56 (dd, J = 8.4, 2.4 Hz, 1H), 8.42 (d, J = 8.2 Hz, 1H), 8.38 (d, J = 2.0 Hz, 1H), 8.15 (dd, J = 8.2, 2.0 Hz, 1H), 7.99 (d, J = 8.4 Hz, 1H), 7.59 – 7.54 (m, 3H), 7.40 (t, J = 7.6 Hz, 2H), 7.37 (dd, J = 8.5, 2.2 Hz, 1H), 7.24 (t, J = 7.3 Hz, 1H), 6.88 (d, J = 8.3 Hz, 1H), 5.25 (s, 2H), 1.70 (s, 6H). **^{13}C NMR** (126 MHz, DMSO-d_6) δ 179.63, 174.79, 163.39, 151.56, 148.67, 143.15, 140.12, 137.99, 137.97, 136.28, 134.23, 131.20 (q, J = 32.5 Hz), 130.00, 128.80, 128.29 (q, J = 4.9 Hz), 127.86, 126.01, 125.45, 125.15, 125.10, 123.46, 122.65, 122.23 (q, J = 273.7 Hz), 116.22, 115.02, 108.85 (q, J = 2.1 Hz), 67.05, 23.50. **HRMS** (ESI) *m/z* calcd for $C_{31}H_{24}F_3N_6O_2S$ [$(M+H)^+$]: 601.1628, measured: 601.1651.

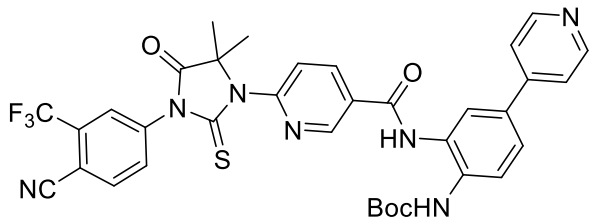
N-(2-amino-5-(thiophen-2-yl)phenyl)-6-(3-(4-cyano-3-(trifluoromethyl)phenyl)-5,5-dimethyl-4-oxo-2-thioxoimidazolidin-1-yl)nicotinamide (RB-400) 2.36c



A solution of carboxylic acid **2.48b** (0.1093 g, 0.2516 mmol, 1 equiv), aniline **2.22c** (0.0813 g, 0.280 mmol, 1.11 equiv), and EDC•HCl (0.0647 g, 0.338 mmol, 1.34 equiv) was stirred in 2.5 mL dry DCM for 28 h, then poured into 5 mL 5% aq. $NaHCO_3$ and extracted with 3x10 mL DCM. The combined organic layers were washed sequentially with 5 mL each water and brine, dried over anhydrous Na_2SO_4, filtered, and concentrated. Silica gel flash chromatography with 0-100% EtOAc / hexanes (R_f 0.20, 10% MeOH / DCM) afforded an inseparable mixture of coupled Boc-protected benzamide intermediate and aniline starting material.

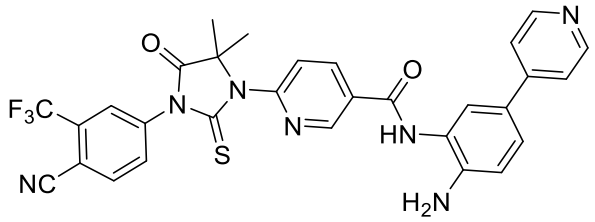
To a solution of that mixture in 2.0 mL dry DCM was added TFA (0.4 mL, 5 mmol) and the solution stirred for 5 h. This was poured into 10 mL 5% aq. $NaHCO_3$ and extracted with 3x10 mL DCM. The combined organic layers were washed sequentially with 3 mL each water and brine, then dried over anhydrous Na_2SO_4, filtered, and concentrated. The residue was purified by C18 silica gel flash chromatography with 10-95% MeCN / H_2O, then by silica gel flash chromatography with EtOAc / hexanes, and finally by treatment with charcoal to afford 20.7 mg or 14% yield of the title benzamide. This was recrystallized from DCM and afforded 8.2 mg or 5% overall yield of benzamide **2.36c** as a yellow powder, pure by NMR and 97.5% homogeneous by LC-MS analysis. **IR** ν_{max} (cm^{-1}): 3401, 3356, 3071, 2921, 2850, 2234, 1755, 1656, 1629, 1595. **^{1}H NMR** (400 MHz, DMSO-d_6) δ 9.97 (s, 1H), 9.18 (d, J = 2.4 Hz, 1H), 8.54 (dd, J = 8.4, 2.5 Hz, 1H), 8.42 (d, J = 8.2 Hz, 1H), 8.38 (d, J = 1.9 Hz, 1H), 8.14 (dd, J = 8.2, 1.9 Hz, 1H), 7.97 (d, J = 8.4 Hz, 1H), 7.48 (d, J = 2.2 Hz, 1H), 7.36 (dd, J = 5.1, 1.1 Hz, 1H), 7.33 (dd, J = 8.4, 2.2 Hz, 1H), 7.24 (dd, J = 3.6, 1.2 Hz, 1H), 7.06 (dd, J = 5.1, 3.6 Hz, 1H), 6.81 (d, J = 8.4 Hz, 1H), 5.31 (s, 2H), 1.69 (s, 6H). **^{13}C NMR** (101 MHz, DMSO-d_6) δ 180.11, 175.26, 163.86, 152.04, 149.16, 144.66, 143.88, 138.50, 138.45, 136.78, 134.73, 131.66 (d, J = 32.7 Hz), 130.38, 128.77 (q, J = 5.0 Hz), 128.70, 124.89, 124.75, 123.93, 123.68, 122.89, 122.71 (q, J = 274.7 Hz), 122.44, 121.45,116.53, 115.50, 109.32 (q, J = 2.2 Hz), 67.52, 23.98. **HRMS** (ESI) *m/z* calcd for $C_{29}H_{22}F_3N_6O_2S_2$ [$(M+H)^+$]: 607.1192, measured: 607.1188, calcd for $C_{29}H_{21}F_3N_6O_2S_2Na$ [$(M+Na)^+$]: 629.1012, measured: 629.1024.

Boc-protected benzamide 5.4



This intermediate could be prepared as described below from 0.1304 g of acid **2.48b** to afford 0.1392 g or 66% isolated yield after silica gel flash chromatography with 0-10% MeOH / DCM (R_f 0.64, 10% MeOH / DCM). **^{1}H NMR** (500 MHz, DMSO-d_6) δ 10.16 (s, 1H), 9.17 (s, 1H), 8.95 (s, 1H), 8.62 (d, J = 5.2 Hz, 2H), 8.53 (d, J = 8.3 Hz, 1H), 8.41 (d, J = 8.2 Hz, 1H), 8.37 (s, 1H), 8.13 (d, J = 8.4 Hz, 1H), 8.00 (d, J = 8.3 Hz, 1H), 7.95 (s, 1H), 7.87 (d, J = 8.6 Hz, 1H), 7.71 (dd, J = 8.4, 1.8 Hz, 2H), 7.67 (d, J = 5.4 Hz, 2H), 1.69 (s, 6H), 1.47 (s, 9H).

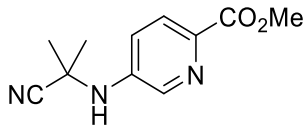
***o*-amino biaryl benzamide (RB-440) 2.36d**



A solution of carboxylic acid **2.48b** (0.1433 g, 0.3299 mmol, 1 equiv), aniline **2.22d** (0.1253 g, 0.4391 mmol, 1.3 equiv), EDC•HCl (0.0704 g, 0.367 mmol, 1.1 equiv), and HOBt (0.0270 g, 0.176 mmol, 0.5 equiv) in 3.3 mL dry DMF was stirred for 12 h. The bright orange solution was poured into 40 mL 5% Na_2CO_3 and extracted with 4x30 mL EtOAc. The combined organic layers were washed sequentially with 2x20 mL each sat. aq. Na_2CO_3, water and brine, then dried over anhydrous Na_2SO_4, filtered, and concentrated. To a solution of the residue in 3.3 mL dry DCM was added 0.25 mL TFA and the blood orange solution stirred for 20 h, at which time an additional 0.3 mL TFA was added for an additional 6 h. The bright orange solution was poured into 50 mL 5% Na_2CO_3 and extracted with 3x50 mL EtOAc. The combined organic layers were washed sequentially with 10 mL each water and brine, then dried over anhydrous Na_2SO_4, filtered, and concentrated. Silica gel flash chromatography with 0-10% MeOH / DCM (R_f 0.29, EtOAc) provided a mixture of unreacted aniline **2.22d** and **2.36d**, which was further purified by C18 silica

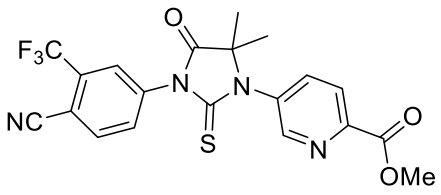
gel flash chromatography with 30-90% MeCN / H_2O to afford 51.2 mg or 26% yield of solid pale orange **2.36d**. This was recrystallized from MeOH / hexanes to afford 36.9 mg of **2.36d** as bright yellow crystals, pure by NMR and 100% homogeneous by LC-MS analysis. **IR** ν_{max} (ground solid, cm^{-1}): 3349, 3085, 2237, 1766, 1659, 1595, 1311. **^{1}H NMR** (400 MHz, DMSO-d_6) δ 9.99 (s, 1H), 9.19 (d, J = 2.2 Hz, 1H), 8.59 – 8.48 (m, 3H), 8.43 (d, J = 8.2 Hz, 1H), 8.38 (d, J = 1.6 Hz, 1H), 8.14 (dd, J = 8.2, 1.7 Hz, 1H), 7.98 (d, J = 8.3 Hz, 1H), 7.70 (d, J = 2.1 Hz, 1H), 7.59 (d, J = 6.1 Hz, 2H), 7.54 (dd, J = 8.5, 2.2 Hz, 1H), 6.89 (d, J = 8.5 Hz, 1H), 5.54 (s, 2H), 1.70 (s, 6H). **^{13}C NMR** (126 MHz, DMSO-d_6) δ 179.63, 174.77, 163.51, 151.56, 150.03, 148.69, 146.67, 145.22, 138.02, 137.96, 136.30, 134.24, 131.18 (q, J = 32.6 Hz), 129.94, 128.29 (q, J = 4.8 Hz), 125.56, 125.44, 123.79, 123.45, 122.42, 122.23 (q, J = 273.8 Hz), 119.56, 115.92, 115.02, 108.84, 67.03, 23.50. **HRMS** (ESI) *m/z* calcd for $C_{30}H_{21}O_2N_7F_3S$ $[(M–H)^–]$: 600.14350, measured: 600.14418.

Methyl 5-((2-cyanopropan-2-yl)amino)picolinate 2.44d



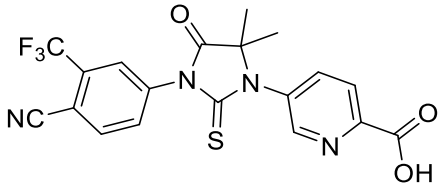
Methyl 5-aminopicolinate (0.4471 g, 0.002939 mol, 1 equiv), prepared by Fischer esterification of the benzoic acid, anhydrous ground $CaSO_4$ (Drierite ®, 2.4 g, 0.018 mol, 6.0 equiv), and acetone cyanohydrin (2.7 mL, 0.030 mol, 10 equiv) were heated at 100 °C for 13 h and followed by ^{1}H NMR. Silica gel flash chromatography with 2:18:80 NEt_3 / EtOAc / hexanes to 5:85:10 NEt_3 / EtOAc / MeOH (R_f 0.52, 10% MeOH / DCM) afforded 0.5120 g or 79% yield of cyanoamine **2.44d** as a pale yellow solid. **IR** ν_{max} (cm^{-1}): 3233, 3160, 3088, 3073, 2232, 1722, 1583. **^{1}H NMR** (500 MHz, DMSO-d_6) δ 8.67 (dd, J = 2.4, 0.7 Hz, 1H), 7.94 (dd, J = 8.8, 2.4 Hz, 1H), 7.83 (s, 1H), 6.67 (dd, J = 8.7, 0.8 Hz, 1H), 1.72 (s, 6H). **^{13}C NMR** (101 MHz, $CDCl_3$) δ 165.72, 143.03, 138.56, 138.37, 126.40, 120.59, 119.68, 52.67, 48.08, 28.01. **HRMS** (ESI) *m/z* calcd for $C_{11}H_{13}N_3NaO_2$ $[(M+Na)^+]$: 242.0900, measured: 242.0904.

methyl 5-(3-(4-cyano-3-(trifluoromethyl)phenyl)-5,5-dimethyl-4-oxo-2-thioxoimidazolidin-1-yl)picolinate 2.45e



General procedure **A** was employed with α-cyanoamine **2.44d** (0.2842 g, 1.296 mmol, 1 equiv), aryl isothiocyanate **2.11** (0.2945 g, 1.291 mmol, 1.00 equiv) and 1.95 mL LHMDS (1.95 mmol, 1.5 equiv), taking 10 mins, followed by 10 mL of 2N HCl in stage two for 2 h. The solution was cooled, organic solvent was removed in vacuo, and the aqueous concentrate poured into 20 mL each EtOAc and water. Sat. aq. $NaHCO_3$ was added to achieve a pH of 7-8, then the biphasic solution was separated and the aqueous layer was further extracted with 2x20 mL EtOAc. The combined organic layers were washed sequentially with 5 mL each water and brine, dried over anhydrous Na_2SO_4, filtered, and concentrated. Silica gel flash chromatography with EtOAc / hexanes (R_f 0.81, EtOAc) afforded 0.4114 g or 71% yield of carboxylic ester **2.45e**. **IR** ν_{max} (cm^{-1}): 2232, 1748, 1238, 1117. **^{1}H NMR** (500 MHz, $CDCl_3$) δ 8.72 (dd, *J* = 2.5, 0.7 Hz, 1H), 8.33 (dd, *J* = 8.3, 0.7 Hz, 1H), 8.00 (d, *J* = 8.3 Hz, 1H), 7.96 (d, *J* = 2.0 Hz, 1H), 7.85 (dd, *J* = 8.3, 2.4 Hz, 1H), 7.84 (dd, *J* = 8.1, 2.2 Hz, 1H), 4.06 (s, 3H), 1.63 (s, 6H). **^{13}C NMR** (126 MHz, $CDCl_3$) δ 180.35, 174.38, 164.73, 150.64, 148.47, 138.68, 136.82, 135.48, 135.30, 133.90 (q, *J* = 33.6 Hz), 132.20, 127.12 (q, *J* = 4.7 Hz), 126.06, 121.93 (q, *J* = 274.2 Hz), 114.79, 110.68 (q, *J* = 2.1 Hz), 66.71, 53.48, 24.10. **HRMS** (ESI) *m/z* calcd for $C_{20}H_{15}F_3N_4NaO_3S$ [$(M+Na)^+$]: 471.0709, measured: 471.0725.

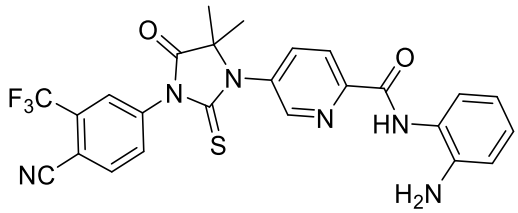
5-(3-(4-cyano-3-(trifluoromethyl)phenyl)-5,5-dimethyl-4-oxo-2-thioxoimidazolidin-1-yl)picolinic acid 2.48c



General procedure **B** was employed with carboxylic ester **2.45e** (0.4114 g, 0.9174 mmol, 1 equiv) and KO^{t}Bu (1.5299 g, 13.634 mmol, 14.9 equiv) for 15 h, but the workup was modified as follows.

The solution was poured into 75 mL 1 N H_3PO_4 and solid $NaHCO_3$ was added to achieve a pH of 3, then this was extracted with 3x35 mL EtOAc. The combined organic layers were washed sequentially with 10 mL each water and brine, then dried over anhydrous Na_2SO_4, filtered, and concentrated. The concentrate was then taken into 10 mL EtOAc, washed with 50 mL of 1 N pH 3 phosphate buffer (H_3PO_4 / NaH_2PO_4), 2x40 mL brine, then dried over anhydrous $MgSO_4$, filtered, and concentrated for 0.3345 g or 84% yield of carboxylic acid **2.48c**, which was used without further purification. **IR** ν_{max} (cm^{-1}): 22387, 1752, 1308, 1125. **^{1}H NMR** (500 MHz, DMSO-d_6) δ 13.49 (s, 1H), 8.74 (dd, J = 2.4, 0.8 Hz, 1H), 8.41 (d, J = 8.2 Hz, 1H), 8.32 (d, J = 1.9 Hz, 1H), 8.25 (dd, J = 8.3, 0.7 Hz, 1H), 8.11 (dd, J = 8.3, 1.9 Hz, 1H), 8.06 (dd, J = 8.3, 2.4 Hz, 1H), 1.57 (s, 6H). **^{13}C NMR** (126 MHz, DMSO-d_6) δ 180.60, 174.70, 165.47, 150.42, 148.50, 138.80, 137.86, 136.30, 135.11, 133.97, 131.15 (q, J = 32.7 Hz), 127.97 (q, J = 4.7 Hz), 125.55, 122.19 (q, J = 273.8 Hz), 114.98, 108.80 (q, J = 2.0 Hz), 66.70, 22.89. **HRMS** (ESI) *m/z* calcd for $C_{19}H_{14}F_3N_4O_3S$ [$(M+H)^+$]: 435.0733, measured: 435.0723.

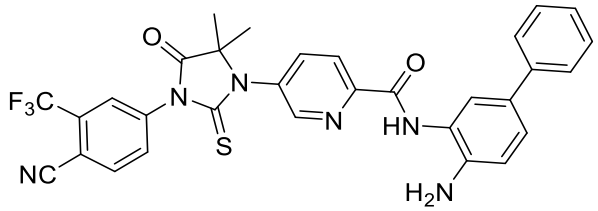
N-(2-aminophenyl)-5-(3-(4-cyano-3-(trifluoromethyl)phenyl)-5,5-dimethyl-4-oxo-2-thioxoimidazolidin-1-yl)picolinamide (RB-422) 2.37a



To a solution of carboxylic acid **2.48c** (0.0795 g, 0.183 mmol, 1 equiv), EDC•HCl (71.2 mg, 0.371 mmol, 2.0 equiv), and *o*-phenylenediamine (59.6 mg, 0.551 mmol, 3.0 equiv) in 1.8 mL dry DCM was added NEt_3 (38.0 µL, 0.272 mmol, 1.5 equiv). The reaction was stirred for 6 h, then diluted with 5 mL of water and extracted with 3x7 mL DCM. The combined organic layers were washed sequentially with 2 mL each water and brine, dried over anhydrous Na_2SO_4, filtered, and concentrated. The concentrate was purified by C18 silica gel flash chromatography with 50-95% MeOH / H_2O, then recrystallized from DCM-hexanes, and afforded 16.5 mg or 17% yield of faintly yellow crystals of benzamide **2.37a**, pure by NMR and 100.0% homogeneous by LC-MS analysis. **IR** ν_{max} (cm^{-1}): 3355, 2921, 2234, 1762, 1678, 1313, 1138. **^{1}H NMR** (500 MHz, DMSO-d_6) δ 10.11 (s, 1H), 8.76 (d, J = 1.9 Hz, 1H), 8.42 (d, J = 8.3 Hz, 1H), 8.35 (d, J = 8.4 Hz, 1H), 8.33 (d, J = 1.7 Hz, 1H), 8.14 – 8.11 (m, 2H), 7.46 (dd, J = 7.9, 1.2 Hz, 1H), 6.98 (td, J = 8.0, 1.4 Hz, 1H),

6.83 (dd, *J* = 8.0, 1.3 Hz, 1H), 6.66 (td, *J* = 7.7, 1.3 Hz, 1H), 4.96 (s, 2H), 1.60 (s, 6H). **^{13}C NMR** (126 MHz, DMSO-d_6) δ 180.67, 174.74, 161.54, 150.15, 149.44, 142.13, 139.29, 137.87, 136.33, 134.91, 133.97, 131.16 (q, *J* = 32.5 Hz), 127.97 (q, *J* = 5.1, 4.4 Hz), 126.20, 124.94, 123.58, 123.25, 122.21 (q, *J* = 273.9 Hz), 116.84, 116.62, 115.00, 108.80 (q, *J* = 1.7 Hz), 66.70, 22.92. **HRMS** (ESI) *m/z* calcd for $C_{25}H_{20}F_3N_6O_2S$ $[(M+H)^+]$: 525.1315, measured: 525.1320, calcd for $C_{25}H_{19}F_3N_6NaO_2S$ $[(M+Na)^+]$: 547.1135, measured: 547.1140, calcd for $C_{25}H_{19}F_3N_6KO_2S$ $[(M+K)^+]$: 563.0874, measured: 563.0878.

N-(4-amino-[1,1'-biphenyl]-3-yl)-5-(3-(4-cyano-3-(trifluoromethyl)phenyl)-5,5-dimethyl-4-oxo-2-thioxoimidazolidin-1-yl)picolinamide (RB-442) 2.37b

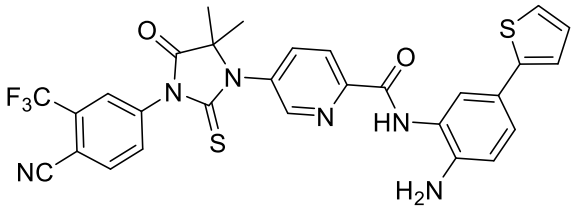


A solution of carboxylic acid **2.48c** (0.0814 g, 0.187 mmol, 1 equiv) and NEt_3 (78.0 µL, 0.559 mmol, 2.9 equiv) in 1.8 mL dry DMF was added to EDC•HCl (46.9 mg, 0.245 mmol, 1.3 equiv), HOAt (25.3 mg, 0.186 mmol, 1.0 equiv), and aniline **2.22b** (50.4 mg, 0.177 mmol, 0.95 equiv). The reaction was stirred for 20 h then poured into 20 mL 5% aq. Na_2CO_3 and extracted with 3x10 mL EtOAc. The combined organic layers were washed sequentially with 10 mL each Na_2HPO_4 buffer, water, and brine, then dried over anhydrous Na_2SO_4, filtered, and concentrated.

The residue was taken up into 2.0 mL dry DCM, TFA (0.20 mL, 2.6 mmol) was added, and the solution stirred for 19 h. This was poured into 15 mL 5% aq. Na_2CO_3 and extracted with 3x10 mL DCM. The combined organic layers were washed sequentially with 5 mL each water and brine, then dried over anhydrous Na_2SO_4, filtered, and concentrated. The residue was purified by C18 silica gel flash chromatography with MeOH / H_2O, then MeCN / H_2O, and afforded 33.9 mg or 32% yield of benzamide **2.37b** as a yellow powder, found to be pure by NMR and 100.0% homogeneous by LC-MS analysis. **IR** ν_{max} (cm^{-1}): 3377, 3321, 3062, 3033, 2239, 1764, 1661, 1627, 1604, 1515, 1422, 1310, 1150. **^{1}H NMR** (500 MHz, DMSO-d_6) δ 10.21 (s, 1H), 8.78 (d, *J* = 2.2 Hz, 1H), 8.43 (d, *J* = 8.2 Hz, 1H), 8.37 (d, *J* = 8.3 Hz, 1H), 8.33 (s, 1H), 8.17 – 8.09 (m, 2H), 7.80 (d, *J* = 1.9 Hz, 1H), 7.57 (d, *J* = 7.8 Hz, 2H), 7.41 (t, *J* = 7.6 Hz, 2H), 7.34 (dd, *J* = 8.3, 1.8

Hz, 1H), 7.26 (t, *J* = 7.1 Hz, 1H), 6.92 (d, *J* = 8.3 Hz, 1H), 5.15 (s, 2H), 1.60 (s, 6H). **^{13}C NMR** (126 MHz, DMSO-d_6) δ 181.14, 175.19, 162.18, 150.57, 149.93, 142.38, 140.71, 139.74, 138.34, 136.78, 135.41, 134.43, 131.62 (d, *J* = 32.6 Hz), 129.27, 129.16, 128.42 (q, *J* = 4.5 Hz), 126.58, 126.07, 124.98, 124.22, 123.75, 122.7 (q, *J* = 274.2 Hz), 117.41, 115.46, 109.27 (q, *J* = 1.8 Hz), 67.16, 23.39. **HRMS** (ESI) *m/z* calcd for $C_{31}H_{22}O_2N_6F_3S$ [$(M–H)^–$]: 599.14825, measured: 599.14735, calcd for $C_{31}H_{23}O_2N_6F_3SCl$ [$(M+Cl)^-$]: 635.12493, measured: 635.12539.

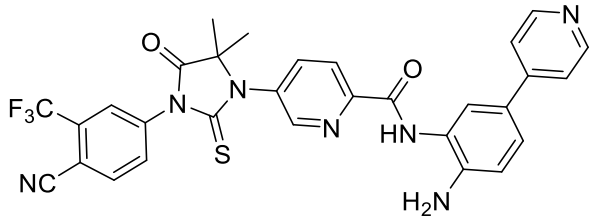
N-(2-amino-5-(thiophen-2-yl)phenyl)-5-(3-(4-cyano-3-(trifluoromethyl)phenyl)-5,5-dimethyl-4-oxo-2-thioxoimidazolidin-1-yl)picolinamide (RB-443) 2.37c



A solution of carboxylic acid **2.48c** (0.0814 g, 0.187 mmol, 1 equiv) and NEt_3 (78.0 µL, 0.559 mmol, 2.9 equiv) in 1.8 mL dry DMF was added to EDC•HCl (47.9 mg, 0.250 mmol, 1.3 equiv), HOAt (25.9 mg, 0.190 mmol, 1.0 equiv), and aniline **2.22c** (51.9 mg, 0.179 mmol, 0.95 equiv). The reaction was stirred for 21 h, then poured into 20 mL 5% aq. Na_2CO_3 and extracted with 3x10 mL EtOAc. The combined organic layers were washed sequentially with 10 mL each aq. Na_2HPO_4 buffer, water, and brine, then dried over anhydrous Na_2SO_4, filtered, and concentrated. The residue was taken up into 2.0 mL dry DCM, TFA (0.20 mL, 2.6 mmol) was added, and the solution stirred for 19 h. This was poured into 15 mL 5% aq. Na_2CO_3 and extracted with 3x10 mL DCM. The combined organic layers were washed sequentially with 5 mL each water and brine, then dried over anhydrous Na_2SO_4, filtered, and concentrated. The residue was purified by C18 silica gel flash chromatography with MeCN / H_2O and afforded 16.2 mg or 15% yield of benzamide **2.37c** as a yellow powder, which was found to be pure by NMR and 98.7% homogeneous by LC-MS analysis. **IR** ν_{max} (cm^{-1}): 3387, 3309, 2238, 1763, 1661, 1419, 1309, 1138. **^{1}H NMR** (400 MHz, DMSO-d_6) δ 10.20 (s, 1H), 8.77 (d, *J* = 2.1 Hz, 1H), 8.43 (d, *J* = 8.3 Hz, 1H), 8.36 (d, *J* = 8.3 Hz, 1H), 8.33 (d, *J* = 1.6 Hz, 1H), 8.13 (td, *J* = 7.4, 6.4, 2.0 Hz, 2H), 7.74 (d, *J* = 2.1 Hz, 1H), 7.38 (dd, *J* = 5.1, 1.0 Hz, 1H), 7.31 (dd, *J* = 8.3, 2.2 Hz, 1H), 7.25 (dd, *J* = 3.6, 1.1 Hz, 1H), 7.06 (dd, *J* = 5.1, 3.6 Hz, 1H), 6.86 (d, *J* = 8.3 Hz, 1H), 5.21 (s, 2H), 1.60 (s, 6H). **^{13}C NMR** (101 MHz, DMSO-d_6) δ 180.68, 174.73, 161.81, 150.04, 149.46, 144.22, 142.21, 139.25, 137.87, 136.32, 134.96,

133.97, 131.15 (q, J = 32.7 Hz), 128.22, 127.97 (q, J = 4.6 Hz), 123.75, 123.54, 123.40, 123.31, 122.72, 122.49, 122.21 (q, J = 274.0 Hz), 121.18, 116.78, 115.00, 108.80, 66.70, 22.93. **HRMS** (ESI) *m/z* calcd for $C_{29}H_{20}F_3N_6O_2S_2$ [$(M–H)^–$]: 605.10467, measured: 605.10464, calcd for $C_{29}H_{21}F_3N_6O_2S_2Cl$ [$(M+Cl)^-$]: 641.08135, measured: 641.08162.

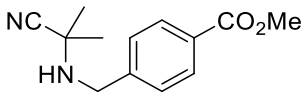
***o*-amino biaryl benzamide (RB-439) 2.37d**



To a solution of carboxylic acid **2.48c** (0.0768 g, 0.177 mmol, 1 equiv), EDC•HCl (44.0 mg, 0.230 mmol, 1.3 equiv), HOAt (24.5 mg, 0.180 mmol, 1.0 equiv), and aniline **2.22d** (47.5 mg, 0.166 mmol, 0.94 equiv) in 1.8 mL dry DCM was added NEt_3 (74.0 µL, 0.531 mmol, 3.0 equiv). After stirring at room temperature for 4.5 h, the reaction was diluted with 10 mL of water and extracted with 3x6 mL DCM. The combined organic layers were washed sequentially with 2 mL each water and brine, dried over anhydrous Na_2SO_4, filtered, and concentrated. Silica gel flash chromatography with 50-100% EtOAc / hexanes (R_f 0.17, EtOAc) afforded 95.6 mg of Boc-protected benzamide intermediate contaminated with aniline starting material. The mixture was taken up into 2.0 mL dry DCM, TFA (0.20 mL, 2.6 mmol) was added, and the solution stirred for 12 h. This was poured into 10 mL sat. Na_2CO_3, and 1 M NaOH was added to adjust the pH to 10. The resulting aqueous solution was then extracted with 3x20 mL EtOAc. The combined organic layers were washed sequentially with 5 mL water and brine, dried over anhydrous Na_2SO_4, filtered, and concentrated. Purification by C18 silica gel flash chromatography with MeOH / H_2O afforded 16.9 mg or 16% yield of faintly orange crystals of benzamide **2.37d**, pure by NMR and 100.0% homogeneous by LC-MS analysis. **IR** ν_{max} (ground solid, cm^{-1}): 3345, 2925, 2854, 2234, 1762, 1737, 1414, 1311, 1178, 1141, 906. **^{1}H NMR** (500 MHz, DMSO-d_6) δ 10.22 (s, 1H), 8.78 (dd, J = 2.4, 0.8 Hz, 1H), 8.56 – 8.50 (m, 2H), 8.43 (d, J = 8.2 Hz, 1H), 8.36 (d, J = 8.4 Hz, 1H), 8.33 (d, J = 1.7 Hz, 1H), 8.17 – 8.10 (m, 2H), 7.89 (d, J = 2.2 Hz, 1H), 7.61 – 7.57 (m, 2H), 7.52 (dd, J = 8.4, 2.2 Hz, 1H), 6.93 (d, J = 8.4 Hz, 1H), 5.43 (s, 2H), 1.60 (s, 6H). **^{13}C NMR** (126 MHz, DMSO-d_6) δ 180.69, 174.74, 161.98, 150.08, 150.05, 149.48, 146.81, 144.24, 139.24, 137.88, 136.34, 134.97, 133.98, 131.16 (q, J = 32.6 Hz), 127.97 (q, J = 4.9 Hz), 124.95, 124.58, 124.05, 123.35,

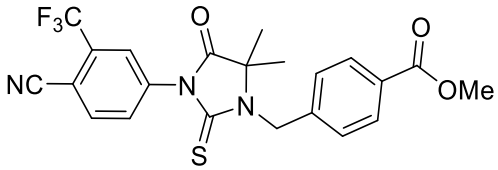
122.22 (q, J = 273.9 Hz), 119.74, 116.59, 115.01, 108.82, 66.70, 22.95. **HRMS** (ESI) *m/z* calcd for $C_{30}H_{23}F_3N_7O_2S$ [$(M+H)^+$]: 602.1581, measured: 602.1587.

Methyl 4-(((2-cyanopropan-2-yl)amino)methyl)benzoate 2.50a



Methyl 4-(aminomethyl)benzoate (1.1692 g, 7.078 mmol, 1 equiv), prepared by Fischer esterification of the benzoic acid, was treated with acetone cyanohydrin (0.65 mL, 7.12 mmol, 1.01 equiv) in 30 mL dry DCM at r.t. for 3.5 h. Solvent was removed *in vacuo*, followed by brief stirring of the concentrate. A crystalline solid rapidly formed, which was determined to be the desired product with ca. 10% remaining starting material. Additional acetone cyanohydrin (0.1 equiv) was then added along with 2 mL DCM. After briefly stirring for 15 mins, solvent and leftover cyanohydrin were removed *in vacuo* to give cyanoamine **2.50a** as a yellow solid, pure by NMR, which was used in the next step without further purification. **IR** ν_{max} (cm^{-1}): 3314, 2218, 1698, 1282. **^{1}H NMR** (500 MHz, $CDCl_3$) δ 8.01 (d, J = 8.3 Hz, 2H), 7.44 (d, J = 8.1 Hz, 2H), 3.96 (s, 2H), 3.91 (s, 3H), 1.60 (s, 1H), 1.52 (s, 6H). **^{13}C NMR** (126 MHz, $CDCl_3$) δ 166.01, 143.52, 129.01, 128.47, 127.28, 121.74, 51.24, 50.94, 48.31, 26.61. **HRMS** (ESI) *m/z* calcd for $C_{13}H_{16}NaN_2O_2$ [$(M+Na)^+$]: 255.1104, measured: 255.1098, calcd for $C_{13}H_{16}KN_2O_2$ [$(M+K)^+$]: 271.0843, measured: 271.0836.

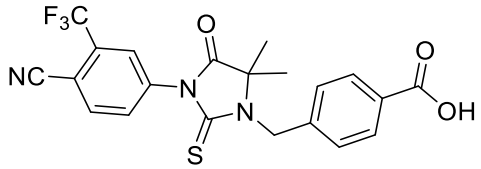
methyl 4-((3-(4-cyano-3-(trifluoromethyl)phenyl)-5,5-dimethyl-4-oxo-2-thioxoimidazolidin-1-yl)methyl)benzoate 2.52



To a solution of cyanoamine **2.50a** (1 equiv) in 15.5 mL dry THF was added NEt_3 (0.14 mL, 1.0 mmol, 0.14 equiv) followed by aryl isothiocyanate **2.11** (1.6071 g, 7.043 mmol, 1.0 equiv). The solution was placed in an 85 °C oil bath and refluxed for 1 h. Silica gel was then added to the dark viscous mixture and solvent removed to dryness *in vacuo*, followed by silica gel flash chromatography with 10-40% acetone / DCM (R_f 0.40, 10% acetone / DCM), to elute the desired

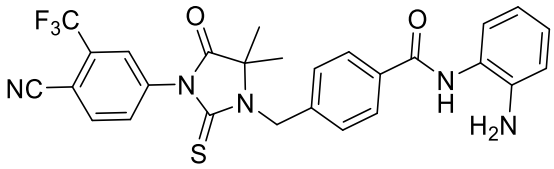
iminothiohydantoin intermediate in a green band. A solution of this material in 35 mL MeOH was treated with 5.3 mL 2N HCl and refluxed 40 mins. The solution was cooled, MeOH was removed *in vacuo*, and the aqueous concentrate extracted with 3x60 mL EtOAc. The combined organic layers were washed sequentially with 20 mL each water and brine, then dried over anhydrous Na_2SO_4. Silica gel flash chromatography with 0-50% EtOAc / hexanes (R_f 0.22, 33% EtOAc / hexanes) afforded 0.7821 g or 24% of desired carboxylic ester **2.52**. **IR** ν_{max} (cm^{-1}): 2989, 2950, 2236, 1765, 1713, 1613, 1502, 1311, 1286, 1138. **^{1}H NMR** (400 MHz, $CDCl_3$) δ 8.11 – 8.00 (m, 2H), 7.98 (d, *J* = 8.3 Hz, 1H), 7.94 (d, *J* = 2.0 Hz, 1H), 7.83 (dd, *J* = 8.2, 2.0 Hz, 1H), 7.49 (d, *J* = 8.5 Hz, 2H), 5.17 (s, 2H), 3.92 (s, 3H), 1.46 (s, 6H).**^{13}C NMR** (126 MHz, $CDCl_3$) δ 180.26, 175.30, 166.65, 141.29, 137.34, 135.33, 133.72 (q, *J* = 33.5 Hz), 132.25, 130.32, 130.27, 127.71, 127.16 (q, *J* = 4.7 Hz), 122.00 (q, *J* = 273.6 Hz), 114.92, 110.35 (q, *J* = 1.8 Hz), 65.47, 52.40, 47.30, 23.76. **HRMS** (ESI) *m/z* calcd for $C_{22}H_{18}F_3NaN_3O_3S$ [$(M+Na)^+$]: 484.0913, measured: 484.0915.

4-((3-(4-cyano-3-(trifluoromethyl)phenyl)-5,5-dimethyl-4-oxo-2-thioxoimidazolidin-1-yl)methyl)benzoic acid 2.54



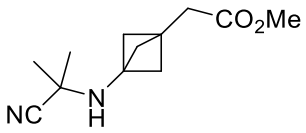
Carboxylic ester **2.52** (0.7589 g, 1.645 mmol, 1 equiv) was treated with KO^{t}Bu (0.9250 g, 8.243 mmol, 5.0 equiv) according to General Procedure **B** for 2.75 h. Brief trituration of the residue with EtOAc afforded an initial crop of carboxylic acid **2.54** as off-white solids (0.4211 g or 57%). Blowing air over the solution cooled it sufficiently to afford a second crop as a yellow gummy solid (0.3108 g or 42%), for 99% combined yield. **IR** ν_{max} (cm^{-1}): 2235, 1753, 1685, 1124. **^{1}H NMR** (500 MHz, DMSO-d_6) δ 12.91 (s, 1H), 8.38 (d, *J* = 8.2 Hz, 1H), 8.33 (s, 1H), 8.11 (d, *J* = 8.1 Hz, 1H), 7.92 (d, *J* = 8.2 Hz, 2H), 7.59 (d, *J* = 8.1 Hz, 2H), 5.17 (s, 2H), 1.47 (s, 6H). **^{13}C NMR** (126 MHz, DMSO-d_6) δ 180.01, 175.31, 167.10, 141.78, 138.26, 136.04, 134.14, 131.02 (q, *J* = 32.5 Hz), 129.72, 129.25, 128.11 (q, *J* = 4.7 Hz), 127.30, 122.26 (q, *J* = 273.8 Hz), 115.07, 108.52 (q, *J* = 2.1 Hz), 65.49, 46.03, 22.44. **HRMS** (ESI) *m/z* calcd for $C_{21}H_{16}F_3KN_3O_3S$ [$(M+K)^+$]: 486.0496, measured: 486.0489.

N-(2-aminophenyl)-4-((3-(4-isocyano-3-(trifluoromethyl)phenyl)-5,5-dimethyl-4-oxo-2-thioxoimidazolidin-1-yl)methyl)benzamide (RB-405) 2.38



To a solution of *o*-phenylenediamine (0.5084 g, 4.701 mmol, 5.0 equiv), HoAt (0.1281 g, 0.9412 mmol, 1.0 equiv), and EDC•HCl (0.5429 g, 2.832 mmol, 3.0 equiv) in 7.0 mL dry DMF was added NEt_3 (0.394 mL, 2.825 mmol, 3.0 equiv), followed by carboxylic acid **2.54** (0.4211 g, 0.9412 mmol, 1 equiv) as a solution in 2.5 mL dry DMF. The reaction was stirred 20 h, then concentrated and purified by silica gel flash chromatography with 65-75% EtOAc / hexanes (R_f 0.35, 75% EtOAc / hexanes) to afford 0.4319 g or 85% yield of a tan solid. This was recrystallized from $CHCl_3$-hexanes for 0.3430 g of **2.38** (RB-405) as tan flakes (79% recovery, 68% overall yield), pure by NMR and 100% homogeneous by LC-MS analysis, for use in biological assays. **IR** ν_{max} (cm^{-1}): 3451, 3366, 2232, 1746, 1644, 1283, 1128. **^{1}H NMR** (800 MHz, DMSO-d_6) δ 9.65 (s, 1H), 8.39 (d, *J* = 8.2 Hz, 1H), 8.34 (d, *J* = 1.9 Hz, 1H), 8.12 (dd, *J* = 8.2, 2.0 Hz, 1H), 7.96 (d, *J* = 7.9 Hz, 2H), 7.59 (d, *J* = 8.0 Hz, 2H), 7.16 (d, *J* = 8.2 Hz, 1H), 6.97 (td, *J* = 7.6, 1.6 Hz, 1H), 6.78 (dd, *J* = 8.0, 1.4 Hz, 1H), 6.60 (td, *J* = 7.5, 1.5 Hz, 1H), 5.18 (s, 2H), 4.89 (s, 2H), 1.49 (s, 6H). **^{13}C NMR** (201 MHz, DMSO-d_6) δ 179.97, 175.35, 164.99, 143.20, 140.12, 138.29, 136.06, 134.16, 133.50, 130.99 (q, *J* = 32.6 Hz), 128.15 (q, *J* = 5.0 Hz), 127.74, 126.97, 126.74, 126.52, 123.26, 122.27 (q, *J* = 273.7 Hz), 116.22, 116.09, 115.08, 108.50, 65.51, 45.99, 22.48. **HRMS** (ESI) *m/z* calcd for $C_{27}H_{23}F_3N_5O_2S$ [$(M+H)^+$]: 538.1519, measured: 538.1529.

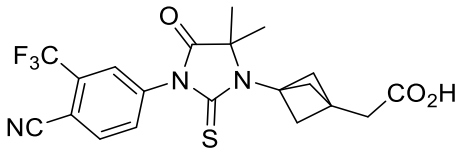
Methyl 2-(3-((2-cyanopropan-2-yl)amino)bicyclo[1.1.1]pentan-1-yl)acetate 2.50b



Methyl 2-(3-aminobicyclo[1.1.1]pentan-1-yl)acetate, previously reported by our group as the ammonium chloride salt,[20] was obtained without HCl treatment, by filtration through celite using $CHCl_3$. The amine thus obtained (0.1113 g, 0.7171 mmol, 1 equiv), essentially pure as a yellow oil, was treated directly with acetone cyanohydrin (65.5 µL, 0.717 mmol, 1.0 equiv) in 1 mL dry

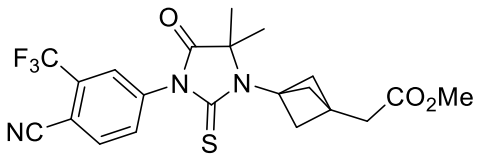
DCM. This was stirred for 5 d while following by ^{1}H NMR, during which time additional cyanohydrin (20 μL, 0.219 mmol, 0.3 equiv) was to achieve complete consumption of starting material. The DCM was removed *in vacuo* and the product **2.50b** was used in the next step without further purification. **IR** ν_{max} (cm^{-1}): 3432, 3304, 2971, 2870, 2252, 1737, 1366, 1229, 1216, 1205, 1053, 1027, 1007, 823, 761. **^{1}H NMR** (400 MHz, $CDCl_3$) δ 3.69-3.65 (3H), 2.60-2.55 (2H), 2.00 (s, 6H), 1.85 (s, 1H), 1.48 (s, 6H). Note that due to rotational isomerism, the first two peaks are each observed as two singlets. **HRMS** (ESI) *m/z* calcd for $C_{12}H_{18}O_2N_2Na$ [$(M+Na)^+$]: 245.12605, measured: 245.12628.

2-(3-(3-(4-cyano-3-(trifluoromethyl)phenyl)-5,5-dimethyl-4-oxo-2-thioxoimidazolidin-1-yl)bicyclo[1.1.1]pentan-1-yl)acetic acid 2.53b



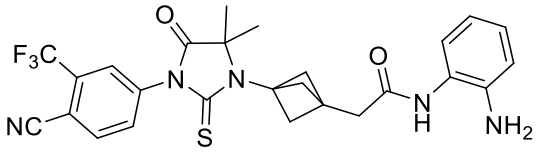
To *α*-cyanoamine **2.50b** (1 equiv) in 1.4 mL dry THF under argon was added NEt_3 (15 μL, 0.11 mmol, 0.15 equiv) then isothiocyanate **7** (0.1788 g, 0.7836 mmol, 1.09 equiv), and the solution was refluxed at 85 °C for 30 mins. The solvent was removed *in vacuo* and the residue partitioned between 20 mL each EtOAc and 0.1 N HCl, which was extracted further with 2x20 mL EtOAc. The combined organic layers were washed with 10 mL each water and brine, then dried over anhydrous Na_2SO_4, filtered, and concentrated. Silica gel flash chromatography with 0-10% acetone / DCM gave two fractions containing the imine intermediate. These fractions were separately stirred in 1:1 THF / 2 N aq. HCl overnight at room temperature, extracted with EtOAc, and independently purified by silica gel flash chromatography with 0-20% acetone / DCM to give a combined three-step yield of 81.5 mg or 26% of carboxylic acid **2.53b** as a yellow crystalline solid. An additional 17.7 mg or 6% yield of ester **2.53a** was also obtained as a yellow crystalline solid. **IR** ν_{max} (cm^{-1}): 2236, 1749, 1708, 1423, 1311, 1275, 1129. **^{1}H NMR** (500 MHz, $CDCl_3$) δ 7.94 (d, J = 8.2 Hz, 1H), 7.83 (d, J = 2.0 Hz, 1H), 7.70 (dd, J = 8.3, 2.1 Hz, 1H), 2.72 (s, 2H), 2.58 (s, 6H), 1.67 (s, 6H). **^{13}C NMR** (126 MHz, $CDCl_3$) δ 178.18, 175.40, 174.72, 137.02, 135.29, 133.70 (q, J = 33.7 Hz), 132.56, 127.56 (q, J = 4.8 Hz), 122.02 (q, J = 274.2 Hz), 114.95, 110.35 (q, J = 2.0 Hz), 66.52, 55.15, 50.29, 34.98, 34.63, 24.43. **HRMS** (ESI) *m/z* calcd for $C_{20}H_{18}F_3KN_3O_3S$ [$(M+K)^+$]: 476.0653, measured: 476.0642.

[1.1.1]propellane methyl ester 2.53a



^{1}H NMR (500 MHz, $CDCl_3$) δ 7.94 (d, *J* = 8.2 Hz, 1H), 7.85 – 7.81 (m, 1H), 7.70 (dd, *J* = 8.3, 2.0 Hz, 1H), 3.70 (s, 3H), 2.66 (s, 2H), 2.55 (s, 6H), 1.66 (s, 6H). **^{13}C NMR** (126 MHz, $CDCl_3$) δ 178.10, 175.43, 171.46, 137.03, 135.26, 133.64 (q, *J* = 33.5 Hz), 132.56, 127.55 (q, *J* = 4.6 Hz), 122.00 (q, *J* = 274.4 Hz), 114.96, 110.28 (q, *J* = 2.3 Hz), 66.52, 55.11, 51.84, 50.25, 35.29, 34.97, 24.40. **HRMS** (ESI) *m/z* calcd for $C_{21}H_{20}O_3F_3N_3NaS$ [$(M+Na)^+$]: 474.1070, measured: 474.1061.

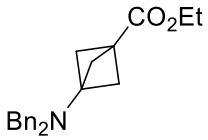
N-(2-aminophenyl)-2-(3-(3-(4-cyano-3-(trifluoromethyl)phenyl)-5,5-dimethyl-4-oxo-2-thioxoimidazolidin-1-yl)bicyclo[1.1.1]pentan-1-yl)acetamide (RB-433) 2.39



To a solution of carboxylic acid **2.53b** (0.0762 g, 0.174 mmol, 1 equiv), *o*-phenylenediamine (0.0568 g, 0.525 mmol, 3.0 equiv), and EDC•HCl (0.0432 g, 0.225 mmol, 1.3 equiv) in 1.7 mL dry DCM was added NEt_3 (0.0360 mL, 0.258 mmol, 1.5 equiv). The reaction was stirred 57 h at room temperature, poured into 3 mL H_2O, and extracted with 3x5 mL DCM. The combined organic layers were washed with 2 mL each water and brine, then dried over anhydrous Na_2SO_4, filtered, and concentrated. Silica gel flash chromatography with 50-100% EtOAc / hexanes (R_f 0.38, EtOAc), followed by C18 silica gel flash chromatography with 30-95% MeOH / H_2O, then silica gel flash chromatography with 20% MeCN / DCM afforded 32.3 mg or 35% yield of the benzamide **2.39** (RB-433) as a white solid. This material was recrystallized from DCM-hexanes to afford 15.0 mg of off-white crystals (46% recovery, 16% overall yield), pure by NMR and 100.0% homogeneous by LC-MS analysis. **IR** ν_{max} (cm^{-1}): 3460, 3384, 3362, 3314, 3064, 3036, 2232, 1761, 1661, 1642, 1625, 1592, 1419, 1306, 1129. **^{1}H NMR** (400 MHz, DMSO-d_6) δ 9.16 (s, 1H), 8.34 (d, *J* = 8.2 Hz, 1H), 8.23 (d, *J* = 1.9 Hz, 1H), 7.99 (dd, *J* = 8.2, 1.9 Hz, 1H), 7.16 (dd, *J* = 7.9, 1.5 Hz, 1H), 6.90 (td, *J* = 7.6, 1.5 Hz, 1H), 6.72 (dd, *J* = 8.0, 1.4 Hz, 1H), 6.55 (td, *J* = 7.5,

1.4 Hz, 1H), 4.81 (s, 2H), 2.63 (s, 2H), 2.48 (s, 6H), 1.61 (s, 6H). It should be noted that conformational isomers were observed by ^{1}H NMR in $CDCl_3$, and a coalescence temperature between 40 and 52 °C was estimated in that solvent. **^{13}C NMR** (101 MHz, DMSO-d_6) δ 178.04, 175.17, 168.38, 141.88, 137.93, 136.04, 134.38, δ 131.01 (q, J = 32.5 Hz), 128.47 (q, J = 4.8 Hz), 125.86, 125.34, 123.35, 122.22 (q, J = 273.8 Hz), 116.21, 115.93, 115.03, 108.55 (q, J = 2.4 Hz), 66.34, 54.61, 49.45, 36.78, 35.83, 23.47. **HRMS** (ESI) *m/z* calcd for $C_{26}H_{24}F_3NaN_5O_2S$ [$(M+Na)^+$]: 550.1495, measured: 550.1496, calcd for $C_{26}H_{24}F_3KN_5O_2S$ [$(M+K)^+$]: 566.1234, measured: 566.1233.

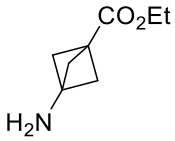
Dibenzylamine 2.55



The following procedure is based on previous work reported by our group, and the characterization data are in agreement with that reference.[20] To a solution of dibenzylamine (3.74 mL, 19.5 mmol, 2.0 equiv), freshly distilled from CaH_2 under argon, and 9.7 mL dry THF in a 100 mL Shlenck flask under argon was added ^{i}PrMgCl•LiCl (1.31 M in THF, 16.3 mL, 2.2 equiv) dropwise. The resulting solution was stirred 2 h during which it deepened in colour from pink to dark red, then a solution of [1.1.1]propellane (0.81 M in ethers, 11.8 mL, 9.56 mmol, 1 equiv) was added dropwise and the vessel sealed with parafilm with stirring for 16 h. The solution, now peach in colour, was cooled over a EtOAc / liquid nitrogen bath, then cannulated under reduced pressure into a similarly cooled 250 mL Shlenck bomb round bottom flask, which had been flame-dried while charged with CuI (0.1846 g, 0.969 mmol, 0.10 equiv) and had received neat ethyl cyanoformate (4.72 mL, 47.8 mmol, 5.0 equiv) once cooled in the bath. The combined solution was stirred 2.5 h in the cooling bath, at which time 5 mL sat. aq. NH_4Cl was added and the bath removed. The mixture was diluted with 100 mL EtOAc and water, then conc. NH_4OH and 15 % aq. NaOH were added as needed to simplify emulsions. The layers were separated, and the aqueous extracted with 2x100 mL further with EtOAc. The combined organic layers were washed sequentially with water and brine, then dried over anhydrous Na_2SO_4, filtered, and concentrated. Silica gel flash chromatography with DCM, followed by chromatography with 5% Et_2O / DCM (R_f 0.58, 25% EtOAc / hexanes) afforded 2.3673 g or 74% yield of ester **2.55** as a bright yellow liquid. **^{1}H NMR** (500 MHz, $CDCl_3$)

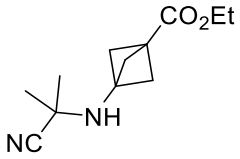
δ 7.37 (d, *J* = 7.3 Hz, 4H), 7.31 – 7.25 (m, 4H), 7.20 (t, *J* = 7.3 Hz, 2H), 4.07 (q, *J* = 7.1 Hz, 2H), 3.65 (s, 4H), 1.93 (s, 6H), 1.21 (t, *J* = 7.1 Hz, 3H). **^{13}C NMR** (126 MHz, $CDCl_3$) δ 170.80, 140.20, 128.47, 128.28, 126.96, 60.57, 57.58, 55.19, 51.60, 34.60, 14.31. **HRMS** (ESI) *m/z* calcd for $C_{22}H_{26}NO_2$ [$(M+H)^+$]: 336.1958, measured: 336.1944.

Amine 5.5



The following procedure is adapted from previous work reported by our group.[20] To a solution of dibenzylamine **2.55** (2.3673 g, 7.057 mmol) in 60 mL EtOH under argon was added 0.375 g of 20% $Pd(OH)_2$/C, and hydrogen gas was bubbled through solution until ^{1}H NMR analysis indicated deprotection. The suspension was filtered on celite with additional EtOH, then solvent was removed by rotary evaporation and the liquid concentrated repeatedly from Et_2O. Simple distillation of the liquid under reduced pressure afforded **5.5** in 0.4794 g or 44% yield of colourless, remarkably sweet-smelling liquid (d = 1.024 g/mL). A sample allowed to stand in the freezer (–16 °C) solidified into large, soft, pale yellow crystals. **IR** ν_{max} (ground sample, cm^{-1}): 2892, 2813, 2731, 2671, 2577, 2495, 2021, 1731, 1519, 1502, 1477, 1452, 1373, 1331, 1279, 1252, 1199, 1140, 1114, 1085, 1061. **^{1}H NMR** (500 MHz, $CDCl_3$) δ 4.12 (q, *J* = 7.1 Hz, 2H), 2.07 (s, 6H), 1.70 (s, 2H), 1.25 (t, *J* = 7.1 Hz, 3H). **^{13}C NMR** (126 MHz, $CDCl_3$) δ 170.63, 60.65, 55.01, 49.21, 33.41, 14.34. **HRMS** (ESI) *m/z* calcd for $C_8H_{14}NO_2$ [$(M+H)^+$]: 156.1019, measured: 156.1018.

Cyanoamine 2.56



To amine **5.5** (50 µL, 0.33 mmol, 1 equiv) in 0.5 mL dry THF was added acetone cyanohydrin (30 µL, 0.33 mmol, 1.0 equiv) and the solution refluxed at 85 °C overnight. Partial completion was observed by ^{1}H NMR, so a scoop of ground $CaSO_4$ was added, and heating continued a further 9 h until completion was observed by NMR. Dry silica was added to the reaction and the mixture combined thoroughly before direct silica gel flash chromatography with 5% ^{i}PrOH / DCM (R_f

0.67, 10% ^{i}PrOH / DCM), which afforded 17.9 mg or 24% yield of cyanoamine **2.56**. **^{1}H NMR** (500 MHz, $CDCl_3$) δ 4.12 (q, *J* = 7.1 Hz, 2H), 2.27 (s, 6H), 2.02 (bs, 1H), 1.49 (s, 6H), 1.25 (t, *J* = 7.1 Hz, 3H). **^{13}C NMR** (126 MHz, $CDCl_3$) δ 169.91, 123.83, 60.78, 54.68, 50.73, 49.43, 35.36, 28.49, 14.30. **HRMS** (ESI) *m/z* calcd for $C_{12}H_{19}N_2O_2$ [$(M+H)^+$]: 223.1441, measured: 223.1447.

Aryl propellane 2.58



Prepared by Knochel's method from phenylmagnesium bromide, and [1.1.1]propellane (0.725 M in ethers, 11.96 mmol) in Et_2O at 100 °C in a sealed Shlenck tube for 3 h, then reacting with ethyl chloroformate. After workup, excess ethyl benzoate was removed by partial distillation under vacuum before chromatography, affording 1.7839 g or 69% yield of aryl propellane **2.58** as a clear colourless liquid. The characterization data are in agreement with the literature.[21] **IR** ν_{max} (neat liquid, cm^{-1}): 3060, 3028, 2979, 2916, 2877, 1726, 1544, 1493, 1446, 1371, 1352, 1296,1198, 1110, 1071, 1039, 1015. **^{1}H NMR** (500 MHz, $CDCl_3$) δ 7.34 – 7.29 (m, 2H), 7.25 – 7.20 (m, 3H), 4.17 (q, *J* = 7.1 Hz, 2H), 2.32 (s, 6H), 1.29 (t, *J* = 7.2 Hz, 3H). **^{13}C NMR** (126 MHz, $CDCl_3$) δ 170.56, 139.90, 128.40, 127.03, 126.20, 60.68, 53.44, 41.82, 37.24, 14.39.

Carboxylic acid propellane 2.59



Arene **2.58** was oxidized with RuO_2 and $NaIO_4$, which is a known transformation of the equivalent methyl ester,[22] adapted from Sharpless's procedure.[23] To a solution of arene **2.58** (0.7071 g, 3.269 mmol, 1 equiv) in 26 mL of 1:1 CCl_4 / MeCN and 19 mL water was added RuO_2 hydrate (18.6 mg, 2.2 mol%) then $NaIO_4$ (6.9928 g, 10 equiv). The biphasic mixture was stirred 28 h, then filtered on celite using 100 mL EtOAc and 20 mL water to rinse the pad. The filtrate layers were separated and the aqueous extracted with 2x100 mL EtOAc further. The combined organic layers were washed sequentially with water and brine, then dried over anhydrous Na_2SO_4, filtered, and concentrated to a red-purple liquid. Silica gel flash chromatography with 1% AcOH in EtOAc / hexanes (R_f 0.06, 1% AcOH in 50% EtOAc / hexanes) afforded 0.2763 g or 46% yield of acid **2.59** as a colourless solid, 18 mg of which was surprisingly recovered from the evaporation trap after concentrating thrice from PhMe, along with 0.1867 g or 26% yield of recovered starting material

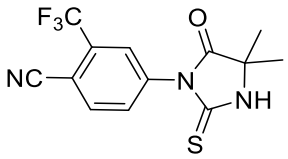
as a red liquid. **IR** ν_{max} (ground solid, cm^{-1}): 3500-2400 (very broad), 2982, 2925, 2610, 1762, 1728, 1692, 1543, 1518, 1500, 1475, 1427, 1371, 1334, 1290, 1219,1180, 1138, 1042, 1005. **^{1}H NMR** (500 MHz, $CDCl_3$) δ 4.15 (q, *J* = 7.1 Hz, 2H), 2.35 (s, 6H), 1.28 (t, *J* = 7.1 Hz, 3H). **^{13}C NMR (**126 MHz, $CDCl_3$) δ 174.91, 169.35, 61.02, 52.91, 37.88, 37.49, 14.29. **HRMS** (ESI) *m/z* calcd for $C_9H_{11}O_4$ [$(M–H)^–$]: 183.06628, measured: 183.06540.

Propellane alcohol 2.60



To a solution of the acid **2.59** (0.2683 g, 1.457 mmol, 1 equiv) in 10 mL dry THF cooled over ice and under argon was added BH_3 (1.0 M in THF, 1.8 mL, 1.25 equiv) dropwise. The solution was allowed to warm in the bath for 1 h, then solvent was removed by rotary evaporation. The residue was extracted from 0.1 N HCl with 3x20 mL Et_2O. The combined organic layers were washed sequentially with water and brine, then dried over anhydrous $MgSO_4$, filtered, and concentrated. Silica gel flash chromatography with 80% Et_2O / pentane (R_f 0.25, 1% AcOH in 50% EtOAc / hexanes) afforded 0.1879 g or of pure alcohol **2.60** as a colourless liquid. This transformation has been reported with $NaBH_4$ by way of an acid chloride intermediate, and the characterization data here are in agreement with the literature.[24] **IR** ν_{max} (neat liquid, cm^{-1}): 3436 (broad), 2981, 2917, 2879, 1730, 1449, 1371, 1334, 1279, 1191, 1143, 1096, 1070, 1041, 1020. **^{1}H NMR** (500 MHz, $CDCl_3$) δ 4.13 (q, *J* = 7.1 Hz, 2H), 3.63 (s, 2H), 1.99 (s, 6H), 1.26 (t, *J* = 7.1 Hz, 3H), 1.23 (bs, 1H). **^{13}C NMR** (126 MHz, $CDCl_3$) δ 170.28, 62.90, 60.64, 50.27, 40.15, 38.36, 14.35.

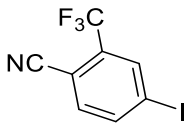
Thiohydantoin 2.61



To a solution of 2-amino-2-methylpropanenitrile (0.5383 g, 6.40 mmol, 1.05 equiv) and triethylamine (0.18 mL, 0.2 equiv) in 30 mL dry THF was added isothiocyanate **2.11** (1.387 g, 6.078 mmol, 1 equiv) and the resulting solution refluxed at 82 °C for 1.6 h. Then, 3.5 mL of 2 N HCl was added and the biphasic solution refluxed at 82 °C for a further 1.3 h. The reaction was cooled, the THF removed under reduced pressure, and the aqueous layer extracted thrice with

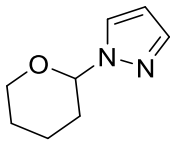
diethyl ether. The combined organic layers were dried over $MgSO_4$, filtered, and concentrated. Silica gel flash chromatography with EtOAc / hexanes (R_f 0.38, 50% EtOAc / hexanes) afforded 0.1.52 g or 80% yield of thiohydantoin **2.61** as a yellow solid. **IR** ν_{max} (ground solid, cm^{-1}): 3345, 2922, 2853, 2241, 1758, 1670, 1612, 1578, 1500, 1455, 1435, 1400, 1377, 1327, 1298, 1263, 1202, 1169, 1124, 1053, 1008. **^{1}H NMR** (500 MHz, DMSO-d_6) δ 10.88 (s, 1H), 8.34 (d, J = 8.2 Hz, 1H), 8.22 (d, J = 1.7 Hz, 1H), 8.00 (dd, J = 8.2, 1.8 Hz, 1H), 1.47 (s, 6H). **^{13}C NMR** (126 MHz, DMSO-d_6) δ 178.96, 176.24, 137.93, 135.97, 133.89, 130.93 (q, J = 32.4 Hz), 127.97 (q, J = 4.9 Hz), 122.24 (q, J = 273.7 Hz), 115.08, 108.27, 61.28, 23.68. **HRMS** (ESI) *m/z* calcd for $C_{13}H_9N_3F_3OS$ $[(M–H)^–]$: 312.0424, measured: 312.0432.

Aryl iodide 2.65



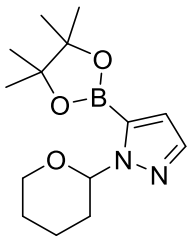
To a solution of 4-amino-2-(trifluoromethyl)benzonitrile **2.27** (0.5123 g, 2.752 mmol, 1 equiv) in 2.5 mL conc. HCl over a brine ice bath maintained between –5 and 0 °C was added $NaNO_2$ (0.2395 g, 3.47 mmol, 1.26 equiv) dropwise as a solution in 4.65 mL water. The reaction was stirred 30 mins, then KI (0.7611 g, 4.56 mmol, 1.67 equiv) was added dropwise as a solution in 1.5 mL water. The bath was removed, and the reaction stirred 1 h, then diluted with 5 mL water and extracted with 3x15 mL DCM. The combined organic layers were washed sequentially with 10 mL each sat. aq. NaS_2O_3, water (twice), and brine, then dried over anhydrous $MgSO_4$, filtered, and concentrated. Silica gel flash chromatography with 10-20% DCM / hexanes (R_f 0.47, 50% DCM / hexanes) afforded 0.7061 g or 86% yield of iodide **2.65** as white crystals. The ^{1}H NMR data are in agreement with the literature.[25] **IR** ν_{max} (ground solid, cm^{-1}): 3102, 3071, 3033, 2234, 1807, 1587, 1558, 1480, 1400, 1379, 1303, 1268, 1201, 1189, 1175, 1126, 1077, 1055. **^{1}H NMR** (500 MHz, $CDCl_3$) δ 8.14 (d, J = 1.6 Hz, 1H), 8.06 (dd, J = 8.2, 1.6 Hz, 1H), 7.60 – 7.48 (m, 1H). **^{13}C NMR** (126 MHz, $CDCl_3$) δ 141.70, 136.04 (q, J = 4.9 Hz), 135.48, 133.83 (q, J = 33.1 Hz), 121.39 (q, J = 274.7 Hz), 115.09, 109.64 (q, J = 2.3 Hz), 99.90. **HRMS** (APCI) *m/z* calcd for $C_8H_4F_3NI$ $[(M+H)^+]$: 297.9335, measured: 297.9338.

Pyrazole 2.63



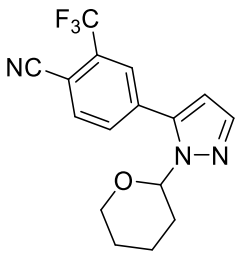
This was prepared by a known procedure,[26a] and characterization data are in agreement with the literature.[26] **^{1}H NMR** (500 MHz, $CDCl_3$) δ 7.66 – 7.60 (m, 1H), 7.58 (d, *J* = 1.9 Hz, 1H), 6.32 (t, *J* = 2.1 Hz, 1H), 5.42 (dd, *J* = 9.5, 2.7 Hz, 1H), 4.11 – 4.02 (m, 1H), 3.71 (td, *J* = 11.2, 2.8 Hz, 1H), 2.19 – 1.98 (m, 3H), 1.76 – 1.57 (m, 3H). **^{13}C NMR** (126 MHz, $CDCl_3$) δ 139.66, 127.80, 106.23, 87.68, 67.98, 30.73, 25.11, 22.63. **HRMS** (ESI) *m/z* calcd for $C_8H_{12}ON_2Na$ $[(M+Na)^+]$: 175.0842, measured: 175.0843.

Pyrazole boronic ester 2.64



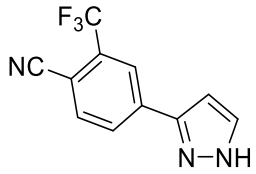
This was prepared from pyrazole **2.63** by a known procedure,[27] and characterization data are in agreement with that reference. **NMR** (500 MHz, $CDCl_3$) δ 7.58 (d, *J* = 1.7 Hz, 1H), 6.75 (d, *J* = 1.8 Hz, 1H), 5.86 (dd, *J* = 10.2, 2.4 Hz, 1H), 4.11 – 3.99 (m, 1H), 3.67 (td, *J* = 11.4, 2.6 Hz, 1H), 2.54 – 2.40 (m, 1H), 2.14 – 2.03 (m, 1H), 2.01 – 1.93 (m, 1H), 1.79 – 1.64 (m, 2H), 1.63 – 1.52 (m, 1H), 1.34 (s, 12H). **^{13}C NMR** (126 MHz, $CDCl_3$) δ 139.40, 116.42, 86.44, 84.25, 68.09, 29.90, 25.22, 25.09, 24.81, 23.14. **HRMS** (ESI) *m/z* calcd for $C_{14}H_{23}O_3BN_2Na$ $[(M+Na)^+]$: 301.1694, measured: 301.1696.

Pyrazole 2.66



Aryl iodide **2.65** (0.6488 g, 2.18 mmol) was reacted with boronic ester **2.64** as done with biarene **5.2**. After 20 h at reflux, the reaction was cooled, diluted with 30 mL water, and extracted with 3x30 mL EtOAc. The combined organic layers were washed sequentially with 10 mL each water and brine, then dried over anhydrous Na_2SO_4, filtered, and concentrated. Silica gel flash chromatography with 50-100% DCM / hexanes (R_f 0.11, DCM) afforded 0.2889 g or 41% yield of solid pyrazole **2.66**. **IR** ν_{max} (ground solid, cm^{-1}): 3117, 2966, 2945, 2868, 2855, 2234, 1615, 1568, 1502, 1453, 1425, 1403, 1357, 1340, 1320, 1309, 1292, 1257, 1209, 1173, 1143, 1123, 1104, 1078, 1056, 1036, 989, 938, 927, 913. **^{1}H NMR** (500 MHz, $CDCl_3$) δ 8.11 (d, *J* = 1.6 Hz, 1H), 7.94 (d, *J* = 8.0 Hz, 1H), 7.87 (dd, *J* = 8.1, 1.6 Hz, 1H), 7.65 (d, *J* = 1.8 Hz, 1H), 6.49 (d, *J* = 1.8 Hz, 1H), 5.11 (dd, *J* = 10.1, 2.5 Hz, 1H), 4.20 – 4.10 (m, 1H), 3.61 (td, *J* = 11.6, 2.4 Hz, 1H), 2.59 (tdd, *J* = 13.6, 10.0, 4.2 Hz, 1H), 2.15 – 2.06 (m, 1H), 1.93 – 1.85 (m, 1H), 1.82 – 1.70 (m, 1H), 1.65 – 1.54 (m, 2H). **^{13}C NMR** (126 MHz, $CDCl_3$) δ 141.13, 139.84, 135.48, 135.19, 133.51 (q, *J* = 32.7 Hz), 132.29, 127.20 (q, *J* = 5.0 Hz), 122.33 (q, *J* = 274.2 Hz), 115.32, 109.83 (q, *J* = 2.0 Hz), 108.38, 84.94, 67.75, 29.52, 24.84, 22.95. **HRMS** (ESI) *m/z* calcd for $C_{16}H_{14}ON_3F_3Na$ $[(M+Na)^+]$: 344.0981, measured: 344.0971.

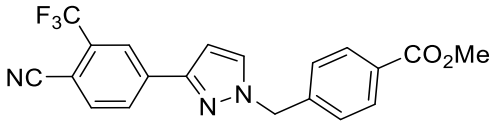
Pyrazole 2.67



To a solution of THF-pyrazole **2.66** (0.2782 g, 0.8659 mmol) in 5 mL MeOH was added 0.62 mL AcCl dropwise, then the reaction stirred 18 h. Sat. aq. $NaHCO_3$ was then carefully added until bubbling ceased, MeOH was removed by rotary evaporation, and the aqueous concentrate was diluted with 10 mL water and extracted with 3x15 mL EtOAc. The combined organic layers were washed sequentially with 5 mL each water and brine, then dried over anhydrous Na_2SO_4, filtered, and concentrated. Silica gel flash chromatography with 25-50% EtOAc / hexanes (R_f 0.24, 50% EtOAc / hexanes) afforded 0.1808 g or 91% yield of pyrazole **2.67** as a white powder. **IR** ν_{max} (thin film, cm^{-1}): 2984, 2931, 2255, 2232, 1730, 1617, 1374, 1321, 1246, 1180, 1144, 1046, 905. **^{1}H NMR** (500 MHz, DMSO-d_6) δ 13.33 (s, 1H), 8.36 (d, *J* = 1.6 Hz, 1H), 8.31 (d, *J* = 8.2 Hz, 1H), 8.19 (d, *J* = 8.1 Hz, 1H), 7.91 (s, 1H), 7.08 (d, *J* = 2.4 Hz, 1H). **^{13}C NMR** (126 MHz, DMSO-d_6)

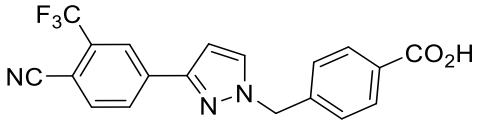
δ 147.31, 138.94, 136.02, 131.34 (q, J = 31.2 Hz), 130.92, 128.99, 122.77 – 122.61 (m), 122.60 (q, J = 273.4 Hz), 115.79, 106.26 (m), 103.70. **HRMS** (ESI) *m/z* calcd for $C_{11}H_6N_3F_3Na$ [$(M+Na)^+$]: 260.0406, measured: 260.0409.

Benzoic ester 2.68



To a solid mixture of pyrazole **2.67** (0.5897 g, 2.486 mmol, 1 equiv), methyl 4-(bromomethyl)benzoate (0.5494 g, 2.40 mmol, 0.96 equiv), and Cs_2CO_3 (4.0593 g, 12.5 mmol, 5.0 equiv) was added 12.4 mL dry DMF. The reaction was stirred 4.5 h then poured into 120 mL water and extracted thrice with ethyl acetate. The combined organic layers were washed sequentially with water and brine, then dried over anhydrous Na_2SO_4, filtered, and concentrated. Silica gel flash chromatography with 30-60% EtOAc / hexanes (R_f 0.71, EtOAc) afforded 0.2561 g or 27% yield of ester **2.68** as a white powder. **IR** ν_{max} (thin film, cm^{-1}): 2924, 2850, 2231, 1721, 1615, 1572, 1499, 1434, 1353, 1311, 1281, 1228, 1178, 1136, 1110, 1054. **^{1}H NMR** (500 MHz, $CDCl_3$) δ 8.24 (s, 1H), 8.07 (dd, J = 8.1, 1.3 Hz, 1H), 8.03 (d, J = 8.3 Hz, 2H), 7.84 (d, J = 8.1 Hz, 1H), 7.49 (d, J = 2.4 Hz, 1H), 7.30 (d, J = 8.2 Hz, 2H), 6.71 (d, J = 2.4 Hz, 1H), 5.43 (s, 2H), 3.91 (s, 3H). **^{13}C NMR** (126 MHz, $CDCl_3$) δ 166.68, 148.83, 140.99, 138.36, 135.22, 133.43 (q, J = 32.9 Hz), 131.86, 130.39, 130.36, 128.62, 127.61, 123.72 (q, J = 4.3 Hz), 122.59 (q, J = 274.2 Hz), 115.93, 108.31 (q, J = 2.1 Hz), 104.81, 56.23, 52.40. **HRMS** (ESI) *m/z* calcd for $C_{20}H_{14}N_3F_3NaO_2$ [$(M+Na)^+$]: 408.0930, measured: 408.0945.

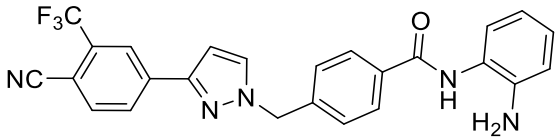
Benzoic acid 2.69



To a solution of ester **2.68** (0.2561 g, 0.665 mmol) in 10 mL THF was added 1 mL 3 M aq. KOH and the reaction stirred 18 h, then refluxed 4 h further. Sat. aq. NH_4Cl and 1 M HCl were added to achieve pH 1, then the aqueous extracted with 3x60 mL EtOAc. The combined organic layers were washed sequentially with water and brine, then dried over anhydrous Na_2SO_4, filtered, and concentrated. This afforded 0.2087 g or 85% yield of acid **2.69** as a white powder. **IR** ν_{max} (thin

film, cm^{-1}): 3500-2500 (very broad), 2922, 2850, 2227, 1698, 1614, 1580, 1495, 1448, 1427, 1351, 1311, 1286, 1222, 1175, 1137, 1115, 1055, 1024. **^{1}H NMR** (500 MHz, DMSO-d_6) δ 12.93 (bs, 1H), 8.30 (s, 1H), 8.27 (d, J = 8.3 Hz, 1H), 8.18 (d, J = 8.1 Hz, 1H), 8.05 (d, J = 2.3 Hz, 1H), 7.92 (d, J = 8.2 Hz, 2H), 7.36 (d, J = 8.2 Hz, 2H), 7.13 (d, J = 2.3 Hz, 1H), 5.54 (s, 2H). **^{13}C NMR** (126 MHz, DMSO-d_6) δ 166.97, 147.75, 141.98, 138.28, 136.07, 133.42, 131.43 (q, J = 31.6 Hz), 130.21, 129.68, 129.02, 127.51, 122.63 (q, J = 4.8 Hz), 122.57 (q, J = 273.7 Hz), 115.74, 106.50 (q, J = 2.1 Hz), 105.07, 54.83. **HRMS** (ESI) *m/z* calcd for $C_{19}H_{12}N_3F_3NaO_2$ [$(M+Na)^+$]: 394.0774, measured: 394.0771.

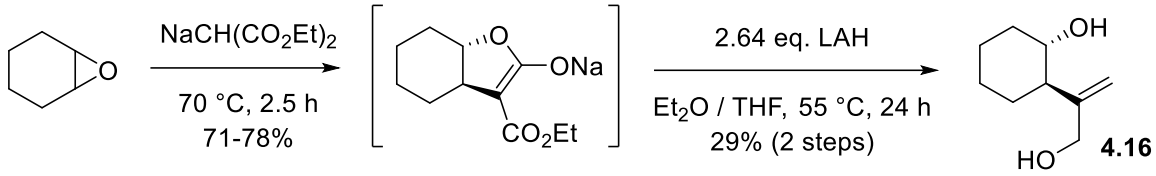
Pyrazole-Benzamide (RB-461) 2.42



To a solution of acid **2.69** (0.2466 g, 0.664 mmol, 1 equiv), *o*-phenylenediamine (0.2556 g, 2.36 mmol, 3.6 equiv), and EDC•HCl (0.1962 g, 1.5 equiv) in 8 mL dry DCM was added 165 μL NEt_3 and the reaction stirred 12 h then concentrated. The residue was extracted from 10 mL 1 N aq. HCl with 3x25 mL EtOAc. The combined organic layers were washed sequentially with water and brine, then dried over anhydrous Na_2SO_4, filtered, and concentrated. Silica gel flash chromatography with 70-100% EtOAc / hexanes (R_f 0.45, EtOAc), followed by C18 silica gel flash chromatography with 30-95% MeCN / H_2O (eluting at ~65%) afforded 14.3 mg or 5% yield of off-white crystals of benzamide **2.42**, pure by NMR and 97% homogeneous by LC-MS analysis. **IR** ν_{max} (thin film, cm^{-1}): 3349, 2962, 2924, 2853, 2229, 1657, 1615, 1582, 1526, 1503, 1453, 1426, 1310, 1282, 1228, 1178, 1138, 1053. **^{1}H NMR** (500 MHz, DMSO-d_6) δ 9.62 (s, 1H), 8.31 (s, 1H), 8.28 (d, J = 8.3 Hz, 1H), 8.19 (d, J = 8.1 Hz, 1H), 8.07 (d, J = 2.3 Hz, 1H), 7.95 (d, J = 8.1 Hz, 2H), 7.40 (d, J = 8.2 Hz, 2H), 7.17 – 7.11 (m, 2H), 6.96 (t, J = 7.6 Hz, 1H), 6.77 (d, J = 8.1 Hz, 1H), 6.58 (t, J = 7.6 Hz, 1H), 5.53 (s, 2H), 4.88 (s, 2H). **^{13}C NMR** (126 MHz, DMSO-d_6) δ 164.9 (*observed by HMBC*), 147.70, 143.11, 140.32, 138.31, 136.08, 134.13, 133.30, 131.43 (q, J = 31.9 Hz), 128.99, 128.12, 127.41, 126.65, 126.49, 123.15, 122.60 (q, J = 3.7 Hz), 124.5 (m, J = ca. 280 Hz, *observed by HMBC*), 116.18, 116.04, 115.74, 106.46 (m), 105.02, 54.88. **HRMS** (ESI) *m/z* calcd for $C_{20}H_{14}N_3F_3NaO_2$ [$(M–H)^–$]: 460.13907, measured: 460.13943.

5.3. *Synthetic Procedures for Part II.*

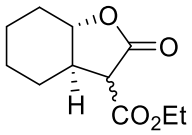
Diol 4.16



Adapting from known procedures,[28-30] sodium (5.18 g, 0.225 mol, 1.02 equiv) was added in portions to 195 mL absolute ethanol under argon over an ice bath, then warmed to room temperature, needing about 4-5 h to be consumed. Diethyl malonate (35.3 mL, 0.231 mol, 1.05 equiv) was then added via syringe as a gentle stream over a water bath cooled at 16-18 °C, the reaction stirred 30 minutes, cyclohexene oxide (22.3 mL, 0.220 mol, 1 equiv) was added as a gentle stream, then the bath was warmed to 70 °C over 30 mins. The thick slurry which formed was heated 2-2.5 h longer, then cooled to room temperature and the sodium enolate intermediate **4.20** was recovered by vacuum filtration on a fritted glass funnel using ca. 300 mL hexanes to transfer and wash the soft white solid. This was dried overnight under vacuum to afford typically 36.87 - 40.29 g or 71-78% yield of soft, white, sweet-smelling solids.

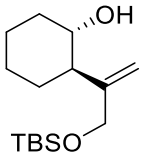
To a suspension of sodiated lactone (18.65 g, 79.6 mmol) in 550 mL dry Et_2O and 400 mL dry THF in a condenser-equipped 2 L 3-neck flask under argon was added lithium aluminum hydride (8.01 g) in portions, and the reaction warmed to 55 °C. After refluxing 24 h, Fieser's workup was conducted and the resulting suspension was filtered on celite, then the pad was washed thoroughly with THF. A second portion of enolate (18.42 g) was treated similarly, and the crude mixtures combined for silica gel flash chromatography with 60-75% EtOAc / hexanes (R_f 0.11, 50% EtOAc / hexanes) afforded 10.11 g of diol **4.16** as colourless crystals or 29% yield over two steps. The characterization data for the diol are in agreement with the literature.[30] **IR** ν_{max} (thin film, cm^{-1}): 3318 (broad), 2926, 2856, 1649, 1448, 1062. **^{1}H NMR** (500 MHz, $CDCl_3$) δ 5.20 (d, J = 1.2 Hz, 1H), 5.05 (s, 1H), 4.15 (d, J = 12.9 Hz, 1H), 4.09 (d, J = 12.9 Hz, 1H), 3.51 (td, J = 9.9, 4.0 Hz, 1H), 2.28 (bs, 2H), 2.09 – 1.95 (m, 2H), 1.84 – 1.64 (m, 3H), 1.39 – 1.15 (m, 4H). **^{13}C NMR (**126 MHz, $CDCl_3$) δ 151.03, 112.66, 73.68, 65.86, 50.72, 35.09, 31.98, 25.97, 25.05.

Lactone ester 4.20′



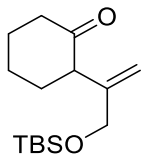
The characterization data are in agreement with the literature.[30] **^{1}H NMR** (500 MHz, $CDCl_3$) δ 4.36 – 4.21 (m, 2.35H), 3.84 (dd, *J* = 11.1, 3.5 Hz, 1H), 3.51 (dd, *J* = 8.3, 3.0 Hz, 0.18H), 3.27 (dd, *J* = 13.0, 1.3 Hz, 0.94H), 2.44 – 2.24 (m, 2.13H), 2.08 – 1.89 (m, 2.53H), 1.89 – 1.74 (m, 1.29H), 1.67 – 1.56 (m, 1.18H), 1.48 – 1.24 (m, 7.35H). **^{13}C NMR** (126 MHz, $CDCl_3$) δ 171.60, 167.67, 83.33, 83.16, 62.05, 61.92, 53.13, 51.67, 48.25, 47.84, 30.62, 30.14, 27.63, 25.60, 25.39, 25.13, 24.04, 23.92, 14.40, 14.29. **HRMS** (ESI) *m/z* calcd for $C_{11}H_{16}NaO_4$ [$(M+Na)^+$]: 235.09408, measured: 235.09329.

Silyl ether alcohol 4.16′



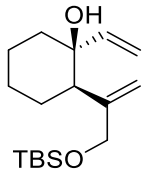
A solution of *tert*-butyldimethylsilyl chloride (12.30 g, 0.08161 mol, 1.01 equiv) in 50 mL THF was added dropwise via addition funnel to a solution of diol **4.16** (12.62 g, 0.08078 mol, 1 equiv) and imidazole (8.81 g, 0.129 mol, 1.60 equiv) in 200 mL THF over an ice bath. After 1 h, the ice bath was removed and the reaction stirred an additional 6 h at room temperature, then filtered on celite. The filter cake was washed with 3x100 mL of THF, and the filtrate concentrated under reduced pressure. Silica gel flash chromatography with 2-15% EtOAc / hexanes (R_f 0.45, 20% EtOAc / hexanes) afforded 20.05 g or 92% yield of silyl ether **4.16′** as a clear colourless liquid. **IR** ν_{max} (thin film, cm^{-1}): 3439 (broad), 2928, 2856, 1650, 1254, 1120, 1067. **NMR** (500 MHz, $CDCl_3$) δ 5.19 (q, *J* = 1.5 Hz, 1H), 5.02 (dd, *J* = 1.7, 0.8 Hz, 1H), 4.13 (dt, *J* = 12.9, 1.0 Hz, 1H), 4.07 (dt, *J* = 12.9, 1.2 Hz, 1H), 3.48 (tdd, *J* = 10.1, 4.2, 2.2 Hz, 1H), 2.76 (d, *J* = 2.3 Hz, 1H), 2.09 – 2.03 (m, 1H), 1.96 – 1.88 (m, 1H), 1.81 – 1.74 (m, 1H), 1.74 – 1.64 (m, 2H), 1.37 – 1.15 (m, 4H), 0.92 (s, 9H), 0.10 (s, 6H). **^{13}C NMR** (126 MHz, $CDCl_3$) δ 150.33, 112.38, 73.14, 65.94, 51.09, 34.59, 32.01, 26.12, 26.06, 25.06, 18.51, -5.26. **HRMS** (ESI) *m/z* calcd for $C_{15}H_{30}NaO_2Si$ [$(M+Na)^+$]: 293.19073, measured: 293.19077.

Ketone 4.17



A solution of alcohol **4.16′** (19.98 g, 0.07387 mol, 1 equiv) and IBX (22.70 g, 0.08107 mol, 1.10 equiv) in 740 mL EtOAc was heated at 80-88 °C for 12 h, at which time ^{1}H NMR spectroscopy indicated full conversion. The suspension was cooled to room temperature and filtered. Silica gel flash chromatography with 5-20% Et_2O / pentane (R_f 0.55, 20% EtOAc / hexanes) afforded 18.17 g or 91% yield of ketone **4.17** as a clear, colourless, non-viscous liquid. **IR** ν_{max} (neat liquid, cm^{-1}): 2930, 2857, 1711, 1652, 1252, 900, 774. **^{1}H NMR** (400 MHz, $CDCl_3$) δ 5.25 (s, 1H), 4.88 (s, 1H), 4.13 (s, 2H), 3.13 (dd, *J* = 11.8, 5.0 Hz, 1H), 2.50 – 2.26 (m, 2H), 2.16 – 2.01 (m, 2H), 2.01 – 1.63 (m, 4H), 0.90 (s, 9H), 0.06 (s, 6H). **^{13}C NMR** (101 MHz, $CDCl_3$) δ 210.79, 146.65, 111.13, 65.71, 53.88, 42.41, 32.51, 28.04, 26.08, 25.37, 18.50, -5.21, -5.26. **HRMS** (APCI) *m/z* calcd for $C_{15}H_{29}O_2Si$ [$(M+H)^+$]: 269.19313, measured: 269.19353.

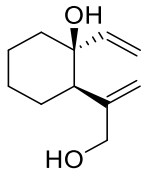
Alcohol 4.21



A solution of ketone **4.17** (2.84 mL, 2.68 g, 0.00999 mol, 1 equiv) in 20 mL THF was added dropwise by cannula over 5 mins to a solution of vinylmagensium bromide (1.0 M, 25.0 mL, 2.5 equiv) in 80 mL THF, after cooling both solutions over ice baths, and the resulting combined reaction mixture was allowed to warm to room temperature. After 12 h, the reaction was again cooled over an ice bath, 20 mL of sat. aq. NH_4Cl was added, the THF was removed *in vacuo*, and the aqueous concentrate was extracted with 3x60 mL EtOAc. The combined organic layers were washed sequentially with 20 mL each water and brine, then dried over anhydrous Na_2SO_4, filtered, and concentrated. Silica gel flash chromatography with 3-5% EtOAc / hexanes (R_f 0.49, 10% EtOAc / hexanes) afforded 2.12 g or 72% yield of allylic alcohol **4.21**, along with 0.192 g or 6% yield of the diastereomer allylic alcohol *epi*-**4.21**, both pale yellow liquids. **IR** ν_{max} (thin film, cm^{-}

[1]): 3439 (broad), 2930, 2884, 2857, 1638, 1463, 1255, 1096, 1050. **^{1}H NMR** (500 MHz, $CDCl_3$) δ 5.84 (dd, *J* = 17.2, 10.7 Hz, 1H), 5.19 (dd, *J* = 17.2, 1.6 Hz, 1H), 5.08 (q, *J* = 1.4 Hz, 1H), 4.97 (dd, *J* = 10.7, 1.7 Hz, 1H), 4.89 (d, *J* = 1.9 Hz, 1H), 4.10 (dd, *J* = 12.7, 1.4 Hz, 1H), 3.98 (dt, *J* = 12.7, 0.9 Hz, 1H), 3.40 (d, *J* = 2.2 Hz, 1H), 2.18 (dd, *J* = 12.9, 3.4 Hz, 1H), 1.87 (qd, *J* = 12.9, 3.6 Hz, 1H), 1.82 – 1.63 (m, 3H), 1.59 – 1.49 (m, 1H), 1.47 – 1.38 (m, 2H), 1.33 – 1.21 (m, 1H), 0.92 (s, 9H), 0.09 (s, 3H), 0.08 (s, 3H). **^{13}C NMR** (126 MHz, $CDCl_3$) δ 149.07, 146.49, 114.79, 111.22, 72.55, 66.02, 51.41, 38.20, 27.06, 26.39, 26.10, 21.39, 18.59, -5.15, -5.28. **HRMS** (ESI) *m/z* calcd for $C_{17}H_{32}NaO_2Si$ [$(M+Na)^+$]: 319.20638, measured: 319.20606.

Diol 4.22

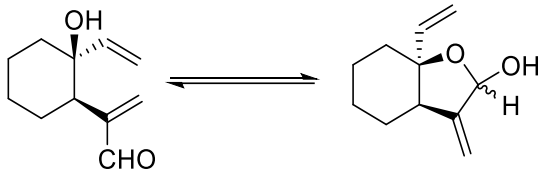


To a solution of silyl ether **4.21** (2.1187 g, 7.1450 mmol, 1 equiv) in 71 mL THF was added tetrabutylammonium fluoride (TBAF; 2.1913 g, 8.3806 mmol, 1.17 equiv), and the solution stirred 3 h. Then, 15 mL each of sat. aq. NH_4Cl and water were added, then the mixture extracted with 3x50 mL EtOAc. The combined organic layers were washed sequentially with 10 mL each water and brine, then dried over anhydrous Na_2SO_4, filtered, and concentrated. Silica gel flash chromatography with 10-60% EtOAc / hexanes (R_f 0.14, 20% EtOAc / hexanes) afforded 1.1930 g or 92% yield of diol **4.22** as white crystals. The characterization data are in agreement with the literature.[31-33] **IR** ν_{max} (thin film, cm^{-1}): 3261, 3086, 2928, 2855, 1703, 1638, 1446, 1409, 1261. **^{1}H NMR** (500 MHz, $CDCl_3$) δ 5.88 (dd, *J* = 17.3, 10.7 Hz, 1H), 5.19 (dd, *J* = 17.3, 1.4 Hz, 1H), 5.12 – 5.08 (m, 1H), 5.01 (dd, *J* = 10.7, 1.4 Hz, 1H), 4.94 (d, *J* = 1.6 Hz, 1H), 4.08 (d, *J* = 12.7 Hz, 1H), 3.99 (d, *J* = 12.7 Hz, 1H), 2.93 (bs, 1H), 2.25 (dd, *J* = 12.9, 3.4 Hz, 1H), 2.04 (bs, 1H), 1.90 (qd, *J* = 12.9, 3.7 Hz, 1H), 1.84 – 1.77 (m, 1H), 1.77 – 1.61 (m, 2H), 1.61 – 1.41 (m, 3H), 1.30 (qt, *J* = 13.2, 3.8 Hz, 1H). **^{13}C NMR** (126 MHz, $CDCl_3$) δ 149.67, 146.34, 116.06, 111.43, 73.04, 65.46, 51.76, 38.56, 27.25, 26.24, 21.33. **HRMS** (ESI) *m/z* calcd for $C_{11}H_{18}NaO_2$ [$(M+Na)^+$]: 205.11990, measured: 205.12014.

General Procedure C for IBX oxidations of alcohols in DMSO:

To a 0.35 M solution of the diol in DMSO was added IBX (0.95-0.99 equiv for the preparation of compounds with lactol content), then the reaction was stirred at room temperature and monitored by ^{1}H NMR spectroscopy for consumption of the starting material. Once the starting material was nearly consumed, 10 volumetric equivalents of water was added, and the benzoic acids were allowed to fully precipitate. The resulting suspension was filtered on a celite pad, which was washed with a minimal quantity of the solvent used for subsequent extraction.

Vinyl alcohol aldehyde / hemiacetal 4.23

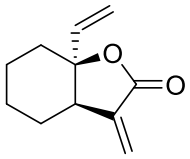


Diol **4.22** (0.5226 g, 2.867 mmol, 1 equiv) was oxidized with IBX (0.7891 g, 2.818 mmol, 0.98 equiv) according to General Procedure **C** for 1.5 h. The aqueous filtrate was extracted with 3x40 mL EtOAc, then the combined organic layers were washed sequentially with 20 mL each water and brine, dried over anhydrous Na_2SO_4, filtered, and concentrated. The concentrate was filtered repeatedly through a cotton plug using minimal diethyl ether until no further precipitates formed. Silica gel flash chromatography with 40% Et_2O / pentane (R_f 0.32, 25% EtOAc / hexanes) afforded 0.4109 g or 80% yield of aldehyde **4.23** as a pale yellow liquid. The characterization data are in agreement with the partial characterization in the literature.[31,32] **IR** ν_{max} (neat liquid, cm^{-1}): 3414 (broad), 2931, 2860, 1686, 1642. *All integrals of signals clearly arising from the aldehyde tautomer are reported as integers, but integrals from signals partly or fully arising from either hemiacetal are reported to two decimal places.* **^{1}H NMR** (400 MHz, $CDCl_3$) δ 9.39 (s, 1H), 6.43 (s, 1H), 6.07 (s, 1H), 6.01 (dd, *J* = 17.4, 10.9 Hz, 0.38H), 5.96 (dd, *J* = 17.4, 10.8 Hz, 0.43H), 5.76 (dd, *J* = 17.2, 10.7 Hz, 1H), 5.73 (s, 0.33H), 5.65 (dd, *J* = 9.4, 1.3 Hz, 0.36H), 5.38 (dd, *J* = 17.4, 1.3 Hz, 0.39H), 5.35 (dd, *J* = 17.4, 1.2 Hz, 0.48H), 5.35 (dd, *J* = 2.6, 1.7 Hz, 0.50H), 5.25 (t, *J* = 1.5 Hz, 0.42H), 5.16 (dd, *J* = 10.8, 1.2 Hz, 0.46H), 5.12 (dd, *J* = 10.8, 1.2 Hz, 0.44H), 5.10 (dd, *J* = 4.1, 2.1 Hz, 0.93H), 5.05 (dd, *J* = 17.2, 1.3 Hz, 1H), 4.90 (dd, *J* = 10.7, 1.3 Hz, 1H), 2.85 – 2.74 (m, 1.39H), 2.66 – 2.52 (m, 1.28H), 1.98 – 1.22 (m, 18.28H). **^{13}C NMR** (126 MHz, $CDCl_3$) *Only peaks arising from the aldehyde tautomer are reported, assigned by HSQC analysis (provided).* δ

195.20, 151.49, 145.56, 137.19, 111.41, 73.08, 43.28, 38.57, 27.03, 26.01, 21.23. **^{1}H NMR** (500 MHz, DMSO-d_6) δ 9.35 (s, 1H), 6.53 (d, J = 1.4 Hz, 1H), 6.46 (d, J = 6.1 Hz, 0.71H), 6.28 (d, J = 7.3 Hz, 0.56H), 6.13 (d, J = 1.4 Hz, 1H), 6.02 (dd, J = 17.4, 10.9 Hz, 0.58H), 5.96 (dd, J = 17.3, 10.8 Hz, 0.81H), 5.62 (dd, J = 17.2, 10.7 Hz, 1H), 5.54 (dd, J = 6.1, 1.9 Hz, 0.73H), 5.47 (dq, J = 7.3, 1.4 Hz, 0.59H), 5.32 (dd, J = 17.4, 1.8 Hz, 0.62H), 5.24 (dd, J = 17.4, 1.7 Hz, 0.80H), 5.16 – 5.10 (m, 1.30H), 5.09 – 5.04 (m, 1.28H), 5.01 (dd, J = 17.2, 2.1 Hz, 1H), 5.02 – 4.97 (m, 0.76H), 4.95 (t, J = 2.0 Hz, 0.56H), 4.78 (dd, J = 10.6, 2.1 Hz, 1H), 4.31 (d, J = 1.0 Hz, 1H), 2.63 – 2.56 (m, 1.61H), 2.46 (s, 0.98H), 1.90 – 1.82 (m, 0.89H), 1.78 – 1.65 (m, 4.12H), 1.64 – 1.53 (m, 2.94H), 1.53 – 1.40 (m, 4.42H), 1.38 – 1.19 (m, 6.69H). **^{13}C NMR** (126 MHz, DMSO-d_6) δ 195.14, 152.84, 152.69, 150.51, 145.84, 142.50, 141.94, 137.51, 113.29, 113.13, 111.08, 107.41, 106.92, 96.60, 96.57, 81.54, 81.42, 72.00, 46.08, 44.97, 40.56, 38.17, 34.05, 33.44, 27.16, 25.65, 24.38, 24.35, 22.43, 21.81, 20.65, 20.63, 20.61. **HRMS** (ESI) *m/z* calcd for $C_{11}H_{16}NaO_2$ $[(M+Na)^+]$: 203.10425, measured: 203.10383. **HRMS** (APCI) *m/z* calcd for $C_{11}H_{17}O_2$ $[(M+H)^+]$: 181.12231, measured: 181.12190, *m/z* calcd for $C_{11}H_{15}O_2$ $[(M–H)^+]$: 179.10775, measured: 179.10668.

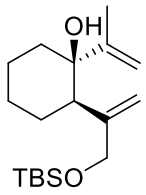
Note: Other oxidations proved problematic for this transformation and led to unacceptable amounts of dehydration, decomposition, or over-oxidation to lactone **4.23′**.

Lactone 4.23′



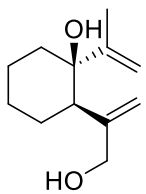
This lactone was isolated from several conditions, such as with excess IBX in refluxing DCM, as an over-oxidation byproduct during the oxidation of diol **4.22**, and the characterization data are in agreement with the literature.[31,32] **^{1}H NMR** (500 MHz, $CDCl_3$) δ 6.22 (d, J = 2.8 Hz, 1H), 5.97 (dd, J = 17.3, 10.9 Hz, 1H), 5.48 (d, J = 2.6 Hz, 1H), 5.39 (dd, J = 17.3, 0.5 Hz, 1H), 5.23 (dd, J = 10.9, 0.6 Hz, 1H), 2.89 (tt, J = 5.3, 2.5 Hz, 1H), 1.91 (ddd, J = 12.3, 6.2, 2.0 Hz, 1H), 1.86 – 1.75 (m, 2H), 1.67 – 1.53 (m, 2H), 1.51 – 1.33 (m, 3H). **^{13}C NMR** (126 MHz, $CDCl_3$) δ 170.15, 139.75, 138.69, 119.83, 115.47, 83.90, 44.42, 34.04, 25.55, 21.27, 20.45.

Isopropenyl Alcohol 4.24a



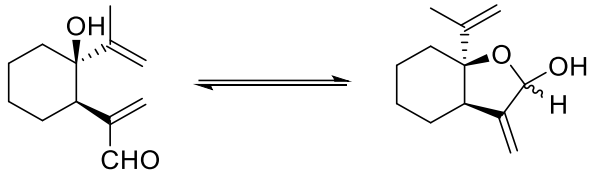
To a solution of commercially available isopropenyl bromide (0.8725 g, 7.212 mmol, 2.50 equiv), which had been passed through basic alumina, in 43 mL THF at –78 °C was added a solution of 1.7 M ^{t}BuLi in pentane (4.16 mL, 7.07 mmol, 2.46 equiv) dropwise and the resulting mixture stirred 1.5 h. A solution of ketone **4.17** (0.82 mL, 0.77 g, 2.87 mmol, 1 equiv) in 15 mL THF at –42 °C was then added dropwise by cannula over 20 mins, stirring was continued 1 h further, then 5 mL sat. aq. NH_4Cl and 5 mL water were added and the bath was removed. The reaction mixture was warmed to room temperature, the THF was removed *in vacuo*, 5 mL 0.1 N HCl was added, and the aqueous mixture extracted with 3x20 mL EtOAc. The combined organic layers were washed sequentially with 5 mL each water and brine, then dried over anhydrous Na_2SO_4, filtered, and concentrated. Silica gel flash chromatography with 10% EtOAc / hexanes (R_f 0.82, 50% EtOAc / hexanes) afforded 0.75 g or 84% yield of allylic alcohol **4.24a** as a pale yellow oil. **IR** ν_{max} (neat liquid, cm^{-1}): 3411, 2928, 2856, 1640. **^{1}H NMR** (500 MHz, $CDCl_3$) δ 5.07 – 5.02 (m, 1H), 5.00 – 4.96 (m, 1H), 4.92 – 4.87 (m, 1H), 4.81 – 4.76 (m, 1H), 4.09 (d, *J* = 12.9 Hz, 1H), 3.98 (d, *J* = 12.9 Hz, 1H), 3.47 (d, *J* = 1.8 Hz, 1H), 2.46 (dd, *J* = 12.8, 3.5 Hz, 1H), 1.88 (qd, *J* = 12.9, 3.5 Hz, 1H), 1.81 – 1.60 (m, 6H), 1.59 – 1.41 (m, 3H), 1.27 (qt, *J* = 13.8, 4.3 Hz, 1H), 0.91 (s, 9H), 0.08 (s, 3H), 0.07 (s, 3H). **^{13}C NMR** (126 MHz, $CDCl_3$) δ 151.32, 149.48, 114.04, 109.97, 75.31, 65.95, 48.79, 36.95, 27.72, 26.45, 26.09, 21.49, 20.09, 18.58, -5.19, -5.32. **HRMS** (ESI) *m/z* calcd for $C_{18}H_{35}SiO_2$ $[(M+H)^+]$: 311.24008, measured: 311.23981, *m/z* calcd for $C_{18}H_{34}NaSiO_2$ $[(M+Na)^+]$: 333.22203, measured: 333.22175.

Isopropenyl diol 4.25a



To a solution of silyl ether **4.24a** (0.7423 g, 2.390 mmol, 1 equiv) in 24 mL THF was added TBAF (0.6922 g, 2.647 mmol, 1.1 equiv) and the solution stirred 90 mins, after which 5 mL sat. aq. NH_4Cl was added and THF removed *in vacuo*. After diluting with 10 mL water, the aqueous was extracted with 3x20 mL EtOAc. The combined organic layers were washed sequentially with 10 mL each water and brine, then dried over anhydrous Na_2SO_4, filtered, and concentrated. Silica gel flash chromatography with 10-30% EtOAc / hexanes (R_f 0.49, 50% EtOAc / hexanes) afforded 0.3979 g or 85% yield of diol **4.25a** as pale yellow crystals. **IR** ν_{max} (solid sample, cm^{-1}): 3158 (broad), 2926, 2851, 1642. **^{1}H NMR** (500 MHz, $CDCl_3$) δ 5.04 (s, 1H), 5.02 – 4.98 (m, 1H), 4.94 (d, *J* = 1.7 Hz, 1H), 4.82 – 4.78 (m, 1H), 4.07 (dd, *J* = 12.6, 5.2 Hz, 1H), 3.97 (d, *J* = 12.4 Hz, 1H), 3.34 (s, 1H), 2.52 (dd, *J* = 12.7, 3.5 Hz, 1H), 2.43 (bs, 1H), 1.93 (qd, *J* = 12.9, 3.6 Hz, 1H), 1.82 – 1.76 (m, 4H), 1.76 – 1.66 (m, 2H), 1.60 – 1.48 (m, 2H), 1.47 – 1.40 (m, 1H), 1.30 (qt, *J* = 13.0, 3.8 Hz, 1H). **^{13}C NMR** (126 MHz, $CDCl_3$) δ 151.46, 149.93, 115.96, 109.90, 75.82, 65.10, 49.53, 37.25, 27.84, 26.28, 21.43, 19.94. **HRMS** (ESI) *m/z* calcd for $C_{12}H_{20}NaO_2$ [$(M+Na)^+$]: 219.1356, measured: 219.1359.

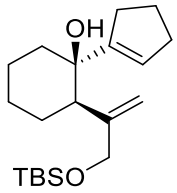
Isopropenyl alcohol enal / hemiacetal 4.26



Diol **4.25a** (0.4070 g, 2.073 mmol, 1 equiv) was oxidized with IBX (0.5695 g, 2.034 mmol, 0.98 equiv) according to General Procedure **C**, taking 1 h. The aqueous filtrate was extracted with 3x40 mL EtOAc, then the combined organic layers were washed with 10 mL brine, dried over anhydrous Na_2SO_4, filtered, and concentrated. The concentrate was filtered through a cotton plug using minimal DCM. Silica gel flash chromatography with 40% ethyl ether / pentane (R_f 0.37, 25% EtOAc / hexanes) afforded 0.3717 g or 92% yield of pure aldehyde **4.26** as a clear colourless oil, in addition to 19.6 mg or 5% yield of less pure aldehyde. **IR** ν_{max} (neat liquid, cm^{-1}): 3399 (broad), 3090, 2933, 2860, 1683, 1643, 1447. *All integrals of signals clearly arising from the aldehyde tautomer are reported as integers, but integrals from signals partly or fully arising from either hemiacetal are reported to two decimal places.* **^{1}H NMR** (500 MHz, $CDCl_3$) δ 9.36 (s, 1H), 6.49 (s, 1H), 6.03 – 6.01 (m, 1H), 5.67 – 5.61 (m, 0.75H), 5.31 – 5.28 (m, 0.33H), 5.19 (t, *J* = 1.4 Hz,

0.48H), 5.18 – 5.15 (m, 0.47H), 5.10 (t, J = 2.1 Hz, 0.35H), 5.09 (t, J = 1.6 Hz, 0.45H), 5.05 – 5.03 (m, 0.35H), 4.96 – 4.94 (m, 0.32H), 4.91 – 4.89 (m, 0.48H), 4.89 – 4.87 (m, 1H), 4.72 – 4.69 (m, 1H), 2.91 (dd, J = 12.8, 3.6 Hz, 1H), 2.88 – 2.79 (m, 1.13H), 2.57 (d, J = 10.1 Hz, 0.46H), 2.43 (s, 1H), 1.90 – 1.70 (m, 9.38H), 1.70 – 1.67 (m, 3H), 1.63 – 1.40 (m, 6.77H), 1.39 – 1.28 (m, 1.85H), 1.27 – 1.18 (m, 0.61H). **^{13}C NMR** (126 MHz, $CDCl_3$) δ 195.44, 155.26, 153.59, 151.62, 150.65, 150.54, 147.06, 137.72, 112.29, 112.03, 110.17, 108.67, 108.56, 98.00, 97.43, 85.37, 85.33, 75.44, 44.26, 44.23, 42.42, 37.12, 33.45, 32.91, 28.33, 27.86, 26.71, 26.16, 22.86, 22.60, 21.87, 21.62, 21.29, 19.67, 19.40, 19.14. **HRMS** (ESI) *m/z* calcd for $C_{12}H_{18}NaO_2$ [$(M+Na)^+$]: 217.11990, measured: 217.11965.

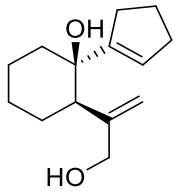
Cyclopentenyl alcohol 4.24b



To a solution of cyclopentenyl bromide[34] (2.2334 g, 15.19 mmol, 2.50 equiv), which had been passed through neutral alumina and distilled immediately prior to use, in 70 mL THF at –78 °C was added a solution of 1.7 M ^{t}BuLi in pentane (9.30 mL, 15.8 mmol, 2.60 equiv) dropwise and the resulting mixture stirred 45 mins. A solution of ketone **4.17** (1.69 mL, 1.63 g, 6.08 mmol, 1 equiv) in 20 mL THF at –78 °C was then added dropwise by cannula over 15 mins, stirring was continued 1 h, the cooling bath was removed, and the mixture allowed to warm for 1 h longer. At this time, 5 mL sat. aq. NH_4Cl and 5 mL water were added, and the reaction mixture was warmed to room temperature. The THF was removed *in vacuo*, 5 mL 0.1 N HCl was added, the emulsions were filtered on celite, and the aqueous mixture extracted with 3x75 mL EtOAc. The combined organic layers were washed sequentially with 10 mL each sat. aq. $NaHCO_3$, water, and brine, then dried over anhydrous Na_2SO_4, filtered, and concentrated. Silica gel flash chromatography with 5% EtOAc / hexanes (R_f 0.68, 20% EtOAc / hexanes) afforded 1.78 g or 87% yield of allylic alcohol **4.24b** as a pale yellow oil. **IR** ν_{max} (thin film, cm^{-1}): 3425 (broad), 2929, 2854, 1641, 1471, 1463, 1446, 1254, 1110, 1091, 1047. **^{1}H NMR** (400 MHz, $CDCl_3$) δ 5.52 – 5.47 (m, 1H), 5.07 (d, J = 1.7 Hz, 1H), 4.89 (d, J = 1.8 Hz, 1H), 4.06 (d, J = 13.2 Hz, 1H), 3.95 (d, J = 13.1 Hz, 1H), 3.27 (d, J = 1.8 Hz, 1H), 2.38 – 2.24 (m, 5H), 1.93 – 1.56 (m, 7H), 1.54 – 1.39 (m, 2H), 1.26 (dt, J =

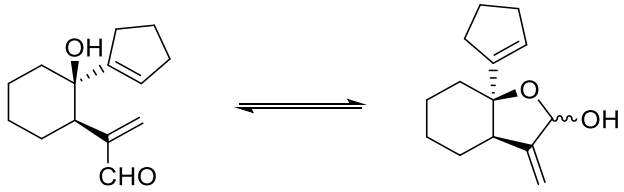
13.1, 3.6 Hz, 1H), 0.92 (s, 9H), 0.08 (s, 3H), 0.07 (s, 3H). **^{13}C NMR** (126 MHz, $CDCl_3$) δ 151.66, 150.00, 123.55, 113.21, 73.23, 65.99, 49.21, 37.35, 32.73, 32.32, 27.58, 26.43, 26.09, 24.04, 21.30, 18.59, -5.19, -5.30. **HRMS** (ESI) *m/z* calcd for $C_{20}H_{36}NaO_2Si$ [$(M+Na)^+$]: 359.2377, measured: 359.2371.

Cyclopentenyl diol 4.25b



To a solution of silyl ether **4.24b** (1.4566 g, 4.328 mmol, 1 equiv) in 40 mL THF was added solid TBAF (1.4116 g, 5.399 mmol, 1.25 equiv) the solution stirred 40 mins, after which 5 mL sat. aq. NH_4Cl and 20 mL water were added. The THF was removed *in vacuo*, then the aqueous was extracted with 3x50 mL EtOAc. The combined organic layers were washed sequentially with 10 mL each water and brine, then dried over anhydrous Na_2SO_4, filtered, and concentrated. Silica gel flash chromatography with 35-50% EtOAc / hexanes (R_f 0.16, 25% EtOAc / hexanes) afforded 0.9227 g or 96% yield of diol **4.25b** as white crystals. **IR** ν_{max} (solid sample, cm^{-1}): 3254 (broad), 2930, 2851, 1636, 1445. **^{1}H NMR** (500 MHz, $CDCl_3$) δ 5.52 (p, *J* = 1.9 Hz, 1H), 5.03 (d, *J* = 1.6 Hz, 1H), 4.91 (d, *J* = 1.8 Hz, 1H), 4.04 (d, *J* = 12.6 Hz, 1H), 3.93 (d, *J* = 12.6 Hz, 1H), 3.30 – 3.00 (bs, 1H), 2.74 – 2.48 (bs, 1H), 2.42 (dd, *J* = 12.9, 3.6 Hz, 1H), 2.35 – 2.23 (m, 4H), 1.97 – 1.49 (m, 8H), 1.46 – 1.39 (m, 1H), 1.29 (qt, *J* = 12.5, 3.6 Hz, 1H). **^{13}C NMR** (126 MHz, $CDCl_3$) δ 151.56, 150.21, 123.65, 115.38, 73.93, 65.18, 50.16, 37.72, 32.67, 32.26, 27.56, 26.27, 24.11, 21.23. **HRMS** (ESI) *m/z* calcd for $C_{14}H_{22}NaO_2$ [$(M+Na)^+$]: 245.1512, measured: 245.1509.

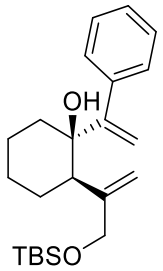
Cyclopentenyl alcohol enal / hemiacetal 4.27



Diol **4.25b** (0.9227 g, 4.150 mmol, 1 equiv) was oxidized with IBX (1.1506 g, 4.1090 mmol, 0.99 equiv), then additional IBX (0.2320 g, 0.8285 mmol, 0.20 equiv) after 70 mins, according to

General Procedure **C**, taking 5 h in total. The aqueous filtrate was extracted with 3x30 mL EtOAc, then the combined organic layers were washed sequentially with 10 mL each water and brine, dried over anhydrous Na_2SO_4, filtered, and concentrated. Silica gel flash chromatography with 40% ethyl ether / pentane (R_f 0.35, 20% EtOAc / hexanes) afforded 0.6415 g or 70% yield of aldehyde **4.27** as a clear colourless oil. It was found to be stable at –20 °C for at least two months but eventually degraded rapidly after several months. **IR** ν_{max} (thin film, cm^{-1}): 3425 (broad), 3056, 2930, 2853, 1690, 1446, 1258, 1007. *All integrals of signals clearly arising from the aldehyde tautomer are reported as integers, but integrals from signals partly or fully arising from either hemiacetal are reported to two decimal places.* **^{1}H NMR** (500 MHz, $CDCl_3$) δ 9.35 (s, 1H), 6.46 (s, 1H), 6.00 (s, 1H), 5.74 – 5.67 (m, 1.32H), 5.60 (dd, *J* = 9.6, 1.5 Hz, 0.47H), 5.39 (t, *J* = 2.1 Hz, 1H), 5.36 – 5.32 (m, 0.43H), 5.23 (t, *J* = 1.6 Hz, 0.50H), 5.09 (d, *J* = 7.3 Hz, 0.92H), 2.93 – 2.81 (m, 2.12H), 2.53 – 2.11 (m, 9.81H), 1.98 – 1.18 (m, 21.42H). **^{13}C NMR** (126 MHz, $CDCl_3$) δ 194.95, 155.05, 153.03, 151.90, 151.01, 149.40, 146.08, 136.78, 127.26, 126.18, 123.94, 108.54, 108.52, 97.97, 97.64, 83.02, 82.92, 73.49, 45.14, 44.62, 42.17, 37.60, 34.25, 33.12, 32.82, 32.73, 32.41, 32.24, 31.82, 31.72, 27.54, 27.31, 26.10, 25.10, 23.95, 23.67, 23.55, 23.28, 22.38, 21.93, 21.13, 21.10. **HRMS** (APCI) *m/z* calcd for $C_{14}H_{20}NaO_2$ [$(M+Na)^+$]: 243.13555, measured: 243.13553.

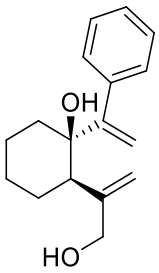
Styrenyl alcohol 4.24c



To a solution of α-bromostyrene[35] (1.13 mL, 1.59 g, 8.70 mmol, 2.42 equiv), freshly distilled from basic alumina, in 40 mL THF at –78 °C was added a solution of 1.7 M ^{t}BuLi in pentane (5.35 mL, 9.10 mmol, 2.53 equiv) dropwise over 10 mins and the resulting mixture then stirred 30 mins. A solution of ketone **4.17** (1.00 mL, 0.965 g, 3.60 mmol, 1 equiv) in 10 mL THF at –78 °C was then added dropwise by cannula over 20 mins, stirring was continued 1.25 h, the cooling bath was removed, and the mixture allowed to warm for 1 h longer. At this time, 5 mL sat. aq. NH_4Cl and 5 mL water were added, and the reaction mixture was warmed to room temperature. The THF was

removed *in vacuo* and the aqueous mixture extracted with 3x50 mL EtOAc. The combined organic layers were washed sequentially with 10 mL each sat. aq. $NaHCO_3$, water, and brine, then dried over anhydrous Na_2SO_4, filtered, and concentrated. Silica gel flash chromatography with 5% EtOAc / pentane (R_f 0.37, 50% EtOAc / hexanes) afforded 1.25 g or 93% yield of allylic alcohol **4.24c** as a pale yellow oil. **IR** ν_{max} (thin film, cm^{-1}): 3402 (broad), 3075, 3027, 2929, 2856, 1723, 1636, 1600, 1447, 1255, 1101. **^{1}H NMR** (500 MHz, acetone-d_6) δ 7.32 – 7.21 (m, 5H), 5.49 (d, *J* = 2.1 Hz, 1H), 5.18 – 5.13 (m, 1H), 5.01 (s, 1H), 4.92 (d, *J* = 2.1 Hz, 1H), 4.29 (dt, *J* = 14.4, 1.7 Hz, 1H), 4.11 (dt, *J* = 14.5, 1.5 Hz, 1H), 3.60 (d, *J* = 0.9 Hz, 1H), 2.46 (dd, *J* = 12.6, 3.5 Hz, 1H), 1.94 (qd, *J* = 13.0, 3.6 Hz, 1H), 1.84 – 1.62 (m, 4H), 1.53 – 1.42 (m, 2H), 1.24 (qt, *J* = 13.2, 3.8 Hz, 1H), 0.92 (s, 9H), 0.07 (s, 3H), 0.05 (s, 3H). **^{13}C NMR** (126 MHz, acetone-d_6) δ 158.71, 151.40, 143.33, 129.77, 128.25, 127.44, 114.55, 112.59, 76.53, 66.08, 50.10, 40.66, 27.03, 26.33, 22.14, 18.94, -5.13, -5.17. **HRMS** (ESI) *m/z* calcd for $C_{23}H_{36}NaO_2Si$ [$(M+Na)^+$]: 395.23768, measured: 395.23789.

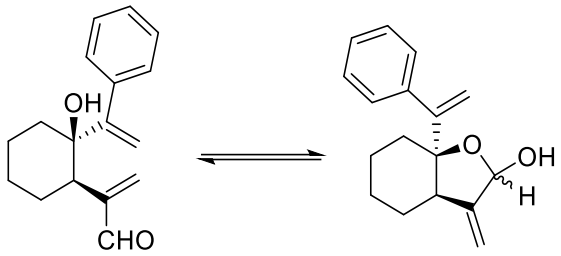
Styrenyl Diol 4.25c



To a solution of silyl ether **4.24c** (0.9554 g, 2.564 mmol, 1 equiv) in 25 mL THF was added TBAF (1.0 M in THF, 3.1 mL, 1.2 equiv) and the solution stirred 90 mins, after which 1 mL sat. aq. NH_4Cl was added and the THF was removed *in vacuo*. After diluting with 10 mL water, the aqueous was extracted with 3x30 mL EtOAc. The combined organic layers were washed sequentially with 10 mL each sat. aq. $NaHCO_3$, water, and brine, then dried over anhydrous Na_2SO_4, filtered, and concentrated. Silica gel flash chromatography with 10-25% EtOAc / hexanes (R_f 0.20, 20% EtOAc / hexanes) afforded 0.6298 g or 95% yield of diol **4.25c** as off-white crystals. **IR** ν_{max} (solid sample, cm^{-1}): 3372, 2933, 2863, 1685, 1448. **^{1}H NMR** (500 MHz, acetone-d_6) δ 7.32 – 7.20 (m, 5H), 5.47 (d, *J* = 2.1 Hz, 1H), 5.08 (dt, *J* = 2.5, 1.3 Hz, 1H), 4.91 (d, *J* = 2.0 Hz, 1H), 4.90 – 4.87 (m, 1H), 4.21 (s, 1H), 4.16 – 4.08 (m, 2H), 4.05 – 3.99 (m, 1H), 2.53 (dd, *J* = 12.6, 3.5 Hz, 1H), 1.98 (qd, *J* = 12.9, 3.7 Hz, 1H), 1.85 – 1.66 (m, 4H), 1.51 – 1.40 (m, 2H), 1.26

(qt, J = 13.1, 3.7 Hz, 1H). **^{13}C NMR** (126 MHz, acetone-d_6) δ 158.74, 151.96, 143.43, 129.85, 128.18, 127.38, 114.69, 114.43, 76.34, 65.07, 51.03, 40.69, 29.84, 27.02, 22.20. **^{1}H NMR** (500 MHz, DMSO-d_6) δ 7.31 – 7.18 (m, 5H), 5.41 (d, J = 2.3 Hz, 1H), 5.05 – 5.00 (m, 1H), 4.97 – 4.92 (m, 1H), 4.84 (d, J = 2.3 Hz, 1H), 4.78 (bs, 1H), 4.61 (s, 1H), 3.97 (d, J = 14.9 Hz, 1H), 3.80 (d, J = 14.9 Hz, 1H), 2.25 (dd, J = 12.5, 3.3 Hz, 1H), 1.82 (qd, J = 12.9, 3.3 Hz, 1H), 1.72 – 1.47 (m, 4H), 1.42 – 1.34 (m, 2H), 1.13 (tdd, J = 16.7, 11.0, 3.6 Hz, 1H). **^{13}C NMR** (126 MHz, DMSO-d_6) δ 157.12, 151.39, 142.31, 128.57, 127.38, 126.45, 114.06, 111.09, 75.12, 63.09, 48.74, 38.87, 28.62, 25.87, 20.94. **HRMS** (ESI) *m/z* calcd for $C_{17}H_{22}NaO_2$ [$(M+Na)^+$]: 281.15120, measured: 281.15141.

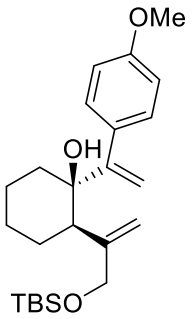
Styrenyl alcohol aldehyde / hemiacetal 4.28



Diol **4.25c** (0.2682 g, 1.038 mmol, 1 equiv) was oxidized with IBX (0.2887 g, 1.031 mmol, 0.99 equiv) according to General Procedure **C**, taking 2 h. The aqueous filtrate was extracted with 3x20 mL EtOAc, then the combined organic layers were washed sequentially with 20 mL brine, dried over anhydrous Na_2SO_4 and $MgSO_4$, filtered, and concentrated. Silica gel flash chromatography with 15% EtOAc / hexanes (R_f 0.43, 25% EtOAc / hexanes) afforded 0.2390 g or 90% yield of aldehyde **4.28** as a clear colourless oil. **IR** ν_{max} (neat liquid, cm^{-1}): 3398 (broad), 3082, 3053, 3019, 2931, 2860, 1689, 1628, 1598, 1573, 1491, 1444. *All integrals of signals clearly arising from the aldehyde tautomer are reported as integers, but integrals from signals partly or fully arising from either hemiacetal are reported to two decimal places.* **^{1}H NMR** (500 MHz, DMSO-d_6) δ 9.37 (s, 1H), 7.49 – 7.43 (m, 3.60H), 7.41 – 7.35 (m, 6.16H), 7.35 – 7.20 (m, 18.26H), 7.07 – 7.02 (m, 1.96H), 6.92 (d, J = 1.5 Hz, 1H), 6.55 (d, J = 6.2 Hz, 2.85H), 6.40 (d, J = 7.1 Hz, 1.70H), 6.21 (d, J = 1.8 Hz, 1H), 5.56 (dd, J = 6.2, 2.0 Hz, 3.04H), 5.55 – 5.52 (m, 1.78H), 5.52 (d, J = 0.9 Hz, 1.98H), 5.45 (d, J = 0.8 Hz, 3.13H), 5.36 (d, J = 2.4 Hz, 1H), 5.19 (d, J = 0.9 Hz, 5.04H), 5.15 (q, J = 2.4, 2.0 Hz, 5.06H), 5.00 (t, J = 2.2 Hz, 3.05H), 4.98 (t, J = 2.1 Hz, 1.96H), 4.78 (d, J = 2.4 Hz, 1H), 4.73 (d, J = 1.4 Hz, 1H), 2.97 (s, 1.90H), 2.75 (s, 3.15H), 2.69 (dd, J = 11.5, 2.5 Hz, 1H),

1.87 – 1.46 (m, 25.45H), 1.47 – 1.06 (m, 28.89H). **^{13}C NMR** (126 MHz, DMSO-d_6) δ 195.48, 156.42, 152.63, 152.58, 151.16, 150.93, 150.86, 141.61, 141.36, 141.27, 138.30, 128.70, 128.47, 128.29, 127.76, 127.64, 127.45, 127.02, 126.95, 126.55, 116.66, 116.51, 114.57, 107.20, 106.87, 96.61, 96.50, 83.44, 83.36, 74.56, 44.12, 42.67, 38.23, 33.19, 32.78, 32.77, 28.74, 25.65, 24.41, 24.24, 22.49, 21.81, 20.81, 20.77, 20.66. **HRMS** (ESI) *m/z* calcd for $C_{17}H_{20}NaO_2$ [$(M+Na)^+$]: 279.1356, measured: 279.1351.

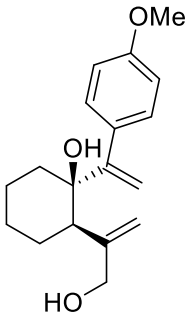
Alcohol 4.24d



To a solution of the freshly chromatographed 4-OMe-α-bromostyrene[34] (3.0066 g, 14.11 mmol, 2.45 equiv) in 65 mL THF at –78 °C was added a solution of 1.7 M ^{t}BuLi in pentane (8.13 mL, 13.8 mmol, 2.40 equiv) dropwise and the resulting mixture then stirred 2 h. A solution of ketone **4.17** (1.64 mL, 1.54 g, 5.75 mmol, 1 equiv) in 50 mL THF at –42 °C was then added dropwise by cannula over 45 mins, then stirring was continued 5 h. At this time, 10 mL sat. aq. NH_4Cl and 10 mL water were added, and the reaction mixture was warmed to room temperature. The THF was removed *in vacuo*, 10 mL 0.1 N HCl added, and the aqueous mixture extracted with 3x50 mL EtOAc. The combined organic layers were washed sequentially with 10 mL each water and brine, then dried over anhydrous Na_2SO_4, filtered, and concentrated. Silica gel flash chromatography with sequential gradients of 80-100% DCM / hexanes followed by 0-1% acetone / DCM (R_f 0.40, 5% EtOAc / hexanes) afforded 1.87 g or 81% yield of allylic alcohol **4.24d** as a pale yellow oil. **IR** ν_{max} (thin film, cm^{-1}): 3360 (broad), 3083, 2991, 2933, 2856, 1650, 1446, 1245. **^{1}H NMR** (500 MHz, $CDCl_3$) δ 7.20 (d, *J* = 8.7 Hz, 2H), 6.80 (d, *J* = 8.8 Hz, 2H), 5.35 (d, *J* = 1.7 Hz, 1H), 5.07 (d, *J* = 1.8 Hz, 1H), 5.01 (d, *J* = 1.7 Hz, 1H), 4.83 (d, *J* = 1.5 Hz, 1H), 4.16 (dd, *J* = 12.8, 1.3 Hz, 1H), 4.09 – 4.02 (m, 1H), 3.80 (s, 3H), 3.60 (d, *J* = 1.7 Hz, 1H), 2.56 (dd, *J* = 12.7, 3.6 Hz, 1H), 1.90 (qd, *J* = 13.0, 3.5 Hz, 1H), 1.84 – 1.65 (m, 4H), 1.55 – 1.42 (m, 2H), 1.32 – 1.21 (m, 1H), 0.91 (s, 9H), 0.07 (s, 3H), 0.05 (s, 3H). **^{13}C NMR** (126 MHz, $CDCl_3$) δ 158.59, 157.07, 149.30,

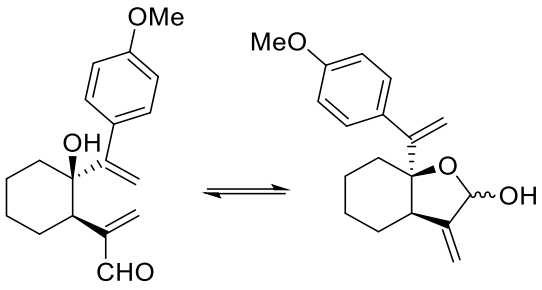
134.65, 130.18, 115.62, 114.29, 113.02, 75.55, 66.25, 55.36, 50.32, 40.10, 28.76, 26.38, 26.09, 21.73, 18.57, -5.24, -5.29. **HRMS** (ESI) *m/z* calcd for $C_{14}H_{22}NaO_2$ [$(M+Na)^+$]: 425.24824, measured: 425.24826.

Diol 4.25d



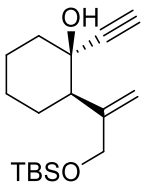
To a solution of silyl ether **4.24d** (2.0053 g, 4.980 mmol, 1 equiv) in 50 mL THF was added TBAF (1.0 M in THF, 5.5 mL, 1.1 equiv) and the solution stirred 90 mins, after which 3 mL sat. aq. NH_4Cl and 5 mL water were added. The THF was removed *in vacuo*, then the aqueous was diluted with 25 mL water and extracted with 3x50 mL EtOAc. The combined organic layers were washed sequentially with 20 mL each water and brine, then dried over anhydrous Na_2SO_4, filtered, and concentrated. Silica gel flash chromatography with 20-50% EtOAc / hexanes (R_f 0.43, 50% EtOAc / hexanes) afforded 1.4262 g or 99% yield of diol **4.25d** as white crystals. **IR** ν_{max} (solid sample, cm^{-1}): 3332 (broad), 3082, 2931, 2857, 1607, 1508, 1242. **^{1}H NMR** (500 MHz, $CDCl_3$) δ 7.20 (d, *J* = 8.7 Hz, 2H), 6.82 (d, *J* = 8.8 Hz, 2H), 5.36 (d, *J* = 1.5 Hz, 1H), 5.08 (dt, *J* = 2.0, 1.1 Hz, 1H), 5.03 (d, *J* = 1.5 Hz, 1H), 4.89 (d, *J* = 1.9 Hz, 1H), 4.11 (d, *J* = 12.9 Hz, 1H), 4.05 (dd, *J* = 12.8, 1.0 Hz, 1H), 3.80 (s, 3H), 3.10 (bs, 1H), 2.57 (dd, *J* = 12.7, 3.6 Hz, 1H), 2.11 (bs, 1H), 1.94 (qd, *J* = 13.0, 3.6 Hz, 1H), 1.87 – 1.66 (m, 4H), 1.61 – 1.51 (m, 1H), 1.51 – 1.42 (m, 1H), 1.29 (dt, *J* = 13.1, 3.9 Hz, 1H). **^{13}C NMR** (126 MHz, $CDCl_3$) δ 158.79, 156.72, 149.95, 133.99, 130.30, 117.01, 114.31, 113.18, 75.94, 65.58, 55.36, 51.06, 40.30, 28.96, 26.26, 21.68. **HRMS** (ESI) *m/z* calcd for $C_{18}H_{24}NaO_3$ [$(M+Na)^+$]: 311.1618, measured: 311.1608.

Aldehyde-lactol 4.29



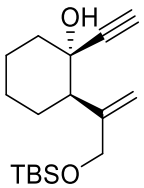
Diol **4.25d** (0.6038 g, 1.997 mmol, 1 equiv) was oxidized with IBX (0.5462 g, 1.951 mmol, 0.98 equiv) according to General Procedure **C**, taking 1 h. The aqueous filtrate was extracted with 3x30 mL EtOAc, then the combined organic layers were washed with 50 mL brine, dried over anhydrous Na_2SO_4 and $MgSO_4$, filtered, and concentrated. The concentrate was filtered through a cotton plug using minimal ethyl ether. Silica gel flash chromatography with 15-20% EtOAc / hexanes (R_f 0.37, 25% EtOAc / hexanes) afforded 0.4835 g or 85% yield of aldehyde **4.29** as a clear colourless oil. **IR** ν_{max} (neat liquid, cm^{-1}): 3397 (broad), 3092, 2932, 2860, 1688, 1607, 1572, 1445, 1242. *All integrals of signals clearly arising from the aldehyde tautomer are reported as integers, but integrals from signals partly or fully arising from either hemiacetal are reported to two decimal places.* **^{1}H NMR** (400 MHz, $CDCl_3$) δ 9.41 (s, 1H), 7.33 (d, *J* = 8.6 Hz, 11.29H), 7.07 (d, *J* = 8.7 Hz, 2H), 6.88 – 6.78 (m, 13.71H), 6.63 (s, 1H), 6.10 (s, 1H), 5.72 (d, *J* = 7.0 Hz, 3.30H), 5.68 (d, *J* = 10.1 Hz, 2.11H), 5.56 – 5.51 (m, 2.35H), 5.45 (d, *J* = 1.0 Hz, 3.66H), 5.34 – 5.32 (m, 3.64H), 5.31 (d, *J* = 1.6 Hz, 1H), 5.28 – 5.24 (m, 2.42H), 5.24 (d, *J* = 1.3 Hz, 3.63H), 5.16 (d, *J* = 1.4 Hz, 2.30H), 5.10 – 5.05 (m, 5.96H), 4.90 (d, *J* = 1.4 Hz, 1H), 3.83 – 3.78 (m, 21.30H), 3.00 – 2.91 (m, 1H), 2.89 – 2.79 (m, 5.82H), 2.73 (d, *J* = 7.3 Hz, 3.36H), 2.63 (s, 1H), 2.46 (d, *J* = 10.5 Hz, 2.09H), 2.07 – 1.99 (m, 3.83H), 1.86 – 1.62 (m, 24.90H), 1.60 – 1.38 (m, 16.46H), 1.38 – 1.23 (m, 11.03H). **^{13}C NMR** (126 MHz, $CDCl_3$) δ 195.97, 159.00, 158.93, 158.83, 155.77, 154.82, 154.27, 152.87, 152.20, 150.66, 139.33, 133.90, 133.87, 133.71, 130.15, 130.13, 130.07, 116.75, 116.17, 114.75, 113.35, 113.32, 113.26, 108.66, 108.53, 98.39, 97.69, 85.17, 85.14, 75.70, 55.36, 55.36, 44.84, 44.54, 43.67, 43.66, 39.97, 34.18, 33.88, 29.08, 27.47, 26.07, 25.43, 23.19, 22.41, 22.05, 21.45, 21.39. **HRMS** (ESI) *m/z* calcd for $C_{18}H_{22}NaO_3$ [$(M+Na)^+$]: 309.14612, measured: 309.14600.

Alkyne 4.24e



To a solution of ketone **4.17** (2.498 g, 9.305 mmol, 1 equiv) in 60 mL dry THF at –78 °C was added ethynylmagnesium bromide (0.37 M, 38.0 mL, 1.5 equiv), fast dropwise or as a gentle stream. The bath was removed after 3 h and the reaction allowed to warm to room temperature, then stirred 16 h further. At this time, 10 mL of sat. aq. NH_4Cl and 130 mL H_2O were added and THF was removed *in vacuo*. The aqueous layer was diluted with 10 mL 1 N HCl and extracted with 3x200 mL Et_2O, then the combined organic layers were washed sequentially with 50 mL each water and brine, dried over anhydrous $MgSO_4$, filtered, and concentrated. Silica gel flash chromatography with 8-10% Et_2O / hexanes afforded 1.8074 g or 66% yield of *cis*-cyclohexyl alcohol **4.24e** (R_f 0.25, 8% Et_2O / hexanes) along with 0.8341 g or 30% yield of *trans*-cyclohexyl alcohol *epi*-**4.24e** (R_f 0.17, 8% Et_2O / hexanes), both as pale yellow oils. **IR** ν_{max} (thin film, cm^{-1}): 3363 (broad), 3309, 2930, 2884, 2857, 1707, 1656, 1608, 1471, 1463, 1447, 1254, 1089, 1068. **^{1}H NMR** (400 MHz, $CDCl_3$) δ 5.18 (d, *J* = 1.6 Hz, 1H), 5.07 (d, *J* = 1.7 Hz, 1H), 4.32 (d, *J* = 1.9 Hz, 1H), 4.18 (s, 2H), 2.38 (s, 1H), 2.36 – 2.28 (m, 1H), 2.21 – 2.13 (m, 1H), 1.89 – 1.58 (m, 4H), 1.54 – 1.39 (m, 2H), 1.35 – 1.22 (m, 1H), 0.93 (s, 9H), 0.12 (s, 6H). **^{13}C NMR** (101 MHz, $CDCl_3$) δ 148.31, 116.45, 89.03, 71.30, 67.57, 65.84, 52.40, 39.71, 26.19, 26.06, 26.01, 20.66, 18.54, -5.04, -5.22. **HRMS** (APCI) *m/z* calcd for $C_{17}H_{31}O_2Si$ [$(M+H)^+$]: 295.2088, measured: 295.2090.

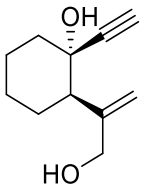
Alkyne *epi*-4.24e



IR ν_{max} (thin film, cm^{-1}): 3407 (broad), 3309, 3085, 2930, 2857, 1639, 1556, 1463, 1449, 1410, 1390, 1362, 1329, 1255, 1159, 1136, 1093, 1003. **^{1}H NMR** (400 MHz, $CDCl_3$) δ 5.27 (d, *J* = 1.3 Hz, 1H), 5.24 (s, 1H), 4.51 (s, 1H), 4.22 (d, *J* = 12.2 Hz, 1H), 4.09 (dd, *J* = 12.2, 1.1 Hz, 1H), 2.47 (s, 1H), 2.20 – 2.08 (m, 2H), 1.78 – 1.58 (m, 5H), 1.52 (dd, *J* = 12.8, 3.9 Hz, 1H), 1.28 – 1.16 (m,

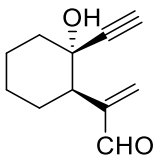
1H), 0.92 (s, 9H), 0.11 (s, 6H). **^{13}C NMR** (101 MHz, $CDCl_3$) δ 147.70, 115.94, 86.03, 74.19, 71.62, 68.20, 52.31, 41.36, 30.40, 26.06, 26.05, 23.88, 18.50, -5.15, -5.23. **HRMS** (ESI) *m/z* calcd for $C_{17}H_{30}O_2SiNa$ [$(M+Na)^+$]: 317.1907, measured: 317.1894.

Alkyne *epi*-4.24e′



To a solution of silyl ether *epi*-**4.24e** (0.2104 g, 0.7144 mmol, 1 equiv) was added TBAF (1.0 M in THF, 0.86 mL, 1.2 equiv) and the reaction stirred 24 h. Then, 5 mL each sat. aq. NH_4Cl and H_2O along with 15 mL EtOAc were added, the layers separated, and the aqueous layer further extracted with 2x10 mL EtOAc. The combined organic layers were washed with 10 mL brine, dried over anhydrous Na_2SO_4, filtered, and concentrated. Silica gel flash chromatography with 10-30% EtOAc / hexanes (R_f 0.16, 33% EtOAc / hexanes) afforded 0.1135 g or 88% yield of diol *epi*-**4.24e′** as white crystals. The characterization data are in agreement with the literature.[36] **IR** ν_{max} (thin film, cm^{-1}): 3289 (broad), 2932, 2858, 1643, 1446, 1328, 1262, 1130, 1061, 999. **^{1}H NMR** (400 MHz, $CDCl_3$) δ 5.30 – 5.25 (m, 1H), 5.21 (s, 1H), 4.46 – 3.92 (bs, 1H), 4.21 (d, *J* = 12.5 Hz, 1H), 4.06 (d, *J* = 12.5 Hz, 1H), 3.05 (bs, 1H), 2.51 (s, 1H), 2.22 – 2.14 (m, 1H), 2.16 – 2.08 (m, 1H), 1.80 – 1.49 (m, 6H), 1.24 (ddt, *J* = 11.8, 8.0, 4.4 Hz, 1H). **^{13}C NMR** (126 MHz, $CDCl_3$) δ 148.41, 116.12, 85.42, 74.84, 72.18, 67.53, 51.92, 41.48, 30.19, 25.86, 23.91. **HRMS** (ESI) *m/z* calcd for $C_{11}H_{16}NaO_2$ [$(M+Na)^+$]: 203.1043, measured: 203.1049.

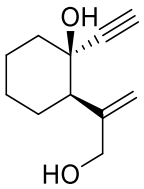
Enal alkyne *epi*-4.30



Diol *epi*-**4.24e′** (42.6 mg, 0.236 mmol, 1 equiv) was oxidized with IBX (66.6 mg, 0.238 mmol, 1.0 equiv) according to General Procedure **C**, taking 30 mins. The reaction was poured into 10 mL 0.5 N HCl and extracted with 20 mL of 1:1 Et_2O / EtOAc, then 2x10 mL Et_2O. The combined organic layers were washed sequentially with 5 mL each 5% aq. $Na_2S_2O_5$, sat. aq. Na_2CO_3, water, and

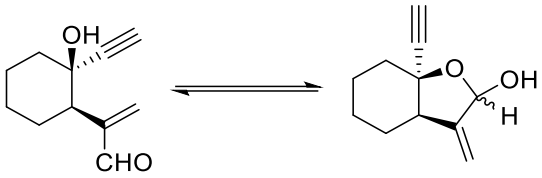
brine, then dried over anhydrous $MgSO_4$, filtered, and concentrated. Silica gel flash chromatography with 50% Et_2O / pentane (R_f 0.18, 40% Et_2O / hexanes) afforded 33.2 mg or 79% yield of aldehyde *epi*-**4.30** as colourless crystals after subsequent concentration from Et_2O. **IR** ν_{max} (thin film, cm^{-1}): 3442 (broad), 3281 (broad), 2933, 2859, 1683, 1624, 1446, 1133, 1064. **^{1}H NMR** (500 MHz, $CDCl_3$) δ 9.57 (s, 1H), 6.59 (s, 1H), 6.24 (s, 1H), 2.81 (dd, *J* = 13.1, 3.0 Hz, 1H), 2.62 (s, 1H), 2.52 (s, 1H), 2.18 (dt, *J* = 9.2, 1.5 Hz, 1H), 1.82 – 1.54 (m, 6H), 1.35 – 1.24 (m, 1H). **^{13}C NMR** (126 MHz, $CDCl_3$) δ 196.37, 150.14, 137.49, 84.09, 75.11, 73.35, 44.47, 42.23, 29.54, 25.59, 24.05. **HRMS** (ESI) *m/z* calcd for $C_{11}H_{14}NaO_2$ [$(M+Na)^+$]: 201.08860, measured: 201.08836.

Alkyne 4.24e′



To a solution of silyl ether **4.24e** (0.2114 g, 0.7178 mmol, 1 equiv) was added TBAF (1.0 M in THF, 0.86 mL, 1.2 equiv) and the reaction stirred 22 h. The solvent was removed *in vacuo*, then 5 mL 0.1 N HCl was added, and the mixture extracted with 3x20 mL Et_2O. The combined organic layers were washed with 5 mL brine, dried over anhydrous $MgSO_4$, filtered, and concentrated. Silica gel flash chromatography with 5-25% EtOAc / hexanes (R_f 0.28, 33% EtOAc / hexanes) afforded 65.7 mg or 51% yield of diol **4.24e′** as white crystals. The characterization data in $CDCl_3$ are in agreement with the literature, but a characterization in DMSO is provided here.[36] **IR** ν_{max} (thin film, cm^{-1}): 3289 (broad), 2933, 2857, 1638, 1446, 1144, 1092, 1069, 1018, 973. **^{1}H NMR** (300 MHz, $CDCl_3$) δ 5.22 (s, 1H), 5.11 (s, 1H), 4.19 (d, *J* = 4.9 Hz, 2H), 3.99 (s, 1H), 2.47 – 2.41 (m, 1H), 2.38 (dd, *J* = 12.9, 3.4 Hz, 1H), 2.20 – 2.11 (m, 1H), 1.99 (s, 1H), 1.92 – 1.64 (m, 4H), 1.64 – 1.40 (m, 2H), 1.40 – 1.21 (m, 1H). **^{1}H NMR** (500 MHz, DMSO) δ 5.17 (s, 1H), 5.06 (q, *J* = 1.6 Hz, 2H), 4.97 (d, *J* = 2.3 Hz, 2H), 4.92 (t, *J* = 5.4 Hz, 1H), 4.00 (dd, *J* = 14.5, 5.7 Hz, 2H), 3.94 (dd, *J* = 14.5, 5.2 Hz, 2H), 3.16 (s, 1H), 2.08 (dd, *J* = 12.7, 3.2 Hz, 1H), 1.97 – 1.87 (m, 1H), 1.73 – 1.59 (m, 2H), 1.58 – 1.48 (m, 3H), 1.44 – 1.30 (m, 3H), 1.28 – 1.16 (m, 1H). **^{13}C NMR** (126 MHz, DMSO-d_6) δ 150.06, 111.65, 89.47, 72.96, 66.79, 63.59, 50.53, 40.39, 26.52, 25.47, 20.20. **HRMS** (ESI) *m/z* calcd for $C_{11}H_{16}NaO_2$ [$(M+Na)^+$]: 203.1043, measured: 203.1043.

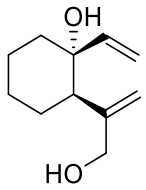
Aldehyde alkyne 4.30



Diol **4.24e′** (63.5 mg, 0.352 mmol, 1 equiv) was oxidized with IBX (93.1 mg, 0.332 mmol, 0.94 equiv) at a concentration of 0.35 M in DMSO at room temperature for 3 h, with additional IBX (8.5 mg, 0.030 mmol, 0.09 equiv) added after 1 h. The reaction was poured into 10 mL 0.5 N HCl and extracted with 2x20 mL EtOAc. The combined organic layers were washed sequentially with 5 mL each 5% aq. $Na_2S_2O_5$, sat. aq. Na_2CO_3, water, and brine, then dried over anhydrous $MgSO_4$, filtered, and concentrated. Silica gel flash chromatography with 30% Et_2O / pentane (R_f 0.25, 40% Et_2O / hexanes) afforded 5.9 mg or 9% yield of aldehyde **4.30** as a colourless oil. **IR** ν_{max} (thin film, cm^{-1}): 3419 (broad), 3291, 2933, 2859, 2701, 1688, 1553, 1447, 1368, 1256, 1068, 1007, 970. *All integrals of signals clearly arising from the aldehyde tautomer are reported as integers, but integrals from signals partly or fully arising from either hemiacetal are reported to two decimal places.* **^{1}H NMR** (500 MHz, DMSO-d_6) δ 9.47 (s, 1H), 6.67 (d, J = 6.4 Hz, 0.80H), 6.66 (d, J = 0.9 Hz, 1H), 6.48 (d, J = 7.6 Hz, 0.49H), 6.24 (d, J = 1.3 Hz, 1H), 5.59 (d, J = 6.3 Hz, 0.79H), 5.43 (dd, J = 7.6, 1.2 Hz, 0.51H), 5.23 (d, J = 1.1 Hz, 1H), 5.18 (dd, J = 2.9, 1.5 Hz, 0.77H), 5.17 (dd, J = 2.7, 1.2 Hz, 0.52H), 5.05 (t, J = 2.2 Hz, 0.80H), 5.01 (t, J = 2.0 Hz, 0.52H), 3.43 (s, 0.61H), 3.42 (s, 0.45H), 3.08 (s, 1H), 2.87 (s, 0.52H), 2.73 (dd, J = 12.2, 3.1 Hz, 1.81H), 1.97 – 1.85 (m, 1.90H), 1.82 – 1.20 (m, 18.34H). **^{1}H NMR** (400 MHz, $CDCl_3$) δ 9.53 (s, 1H), 6.56 (s, 1H), 6.19 (s, 1H), 5.82 (dtd, J = 6.5, 2.0, 0.8 Hz, 0.26H), 5.66 (dq, J = 10.5, 1.6 Hz, 0.44H), 5.38 (dd, J = 2.8, 1.7 Hz, 0.27H), 5.33 (t, J = 1.4 Hz, 0.46H), 5.21 (t, J = 1.6 Hz, 0.46H), 5.13 (dd, J = 2.6, 2.0 Hz, 0.27H), 3.00 – 2.88 (m, 2.94H), 2.79 (d, J = 12.3 Hz, 1.40H), 2.50 (s, 0.24H), 2.50 (s, 0.42H), 2.34 (s, 1H), 2.13 – 1.60 (m, 8.39H), 1.56 – 1.23 (m, 6.29H). **^{13}C NMR** (101 MHz, $CDCl_3$) δ 195.31, 154.17, 151.04, 150.10, 138.08, 110.28, 109.75, 98.59, 98.11, 88.24, 87.72, 85.41, 77.36, 76.17, 72.52, 72.39, 71.94, 67.60, 49.31, 48.33, 45.54, 39.87, 36.62, 34.62, 27.72, 26.50, 25.68, 24.10, 23.10, 22.71, 20.90, 20.61, 20.48. **HRMS** (ESI) *m/z* calcd for $C_{11}H_{14}NaO_2$ [$(M+Na)^+$]: 201.0886, measured: 201.0881.

Note: This compound was poorly reactive under optimized reaction conditions but afforded the same reaction product as its more reactive diastereomer *epi*-**4.30**.

Diol *epi*-4.22

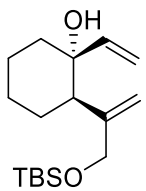


To a solution of alkyne *epi*-**4.24e** (0.5044 g, 1.713 mmol, 1 equiv) in 17 mL MeOH and 0.371 mL pyridine under argon was added Pd/$CaCO_3$ (5 wt.%, 0.3657 g, 0.1 equiv, poisoned with Pb), then a balloon of hydrogen was added to bubble through the solution. The reaction was followed closely by ^{1}H NMR for 1 h, whereupon it was filtered on celite using 50 mL MeOH and concentrated.

To a solution of the resulting residue in 20 mL THF was added TBAF (1.0 M in THF, 1.88 mL, 1.1 equiv) and the reaction stirred 24 h, then concentrated. The residue was taken up into 20 mL water and 2 mL sat. aq. NH_4Cl, then extracted with 3x20 mL EtOAc. The combined organic layers were washed sequentially with 5 mL each water and brine, dried over anhydrous Na_2SO_4, filtered, and concentrated. Silica gel flash chromatography with 30% EtOAc / hexanes (R_f 0.21, 30% EtOAc / hexanes) afforded 0.2238 g or 72% yield of diol *epi*-**4.22** as white crystals.

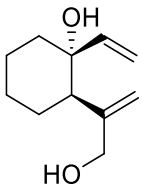
Note: Failure to add pyridine during the hydrogenation of *epi*-**4.24e** (338 mg) by a similar procedure, and after subsequent TBAF deprotection of the mixture, resulted in a 1:1 mixture of alkane *epi*-**4.22′** and desired alkene diol *epi*-**4.22**. These products were separated using $AgNO_3$ adsorbed onto silica gel (0.25g/g) to afford 65.5 mg or 31% and 62.7 mg or 30% yield of each compound as white crystals, respectively. A similar issue of over-hydrogenation was encountered when *cis* diol alkyne **4.24e** was not carefully followed by ^{1}H NMR, even with pyridine, providing a sample of **4.22′**.

Silyl ether *epi*-4.21



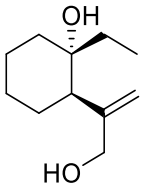
An analytical sample was obtained after hydrogenation by silica gel flash chromatography with 0-10% Et_2O / pentane (R_f 0.67, 30% EtOAc / hexanes) to afford silyl ether *epi*-**4.21** as a pale yellow oil. **IR** ν_{max} (thin film, cm^{-1}): 3419 (broad), 3087, 2929, 2857, 1639, 1556, 1471, 1463, 1450, 1409, 1390, 1362, 1330, 1254, 1091, 1048. **^{1}H NMR** (400 MHz, $CDCl_3$) δ 6.25 (dd, *J* = 17.2, 10.8 Hz, 1H), 5.31 (dd, *J* = 17.2, 2.0 Hz, 1H), 5.18 (d, *J* = 1.2 Hz, 1H), 5.12 (dd, *J* = 10.8, 1.9 Hz, 1H), 4.88 (s, 1H), 4.07 (s, 2H), 3.77 (s, 1H), 2.23 (dd, *J* = 12.8, 3.5 Hz, 1H), 1.94 – 1.86 (m, 1H), 1.84 – 1.76 (m, 1H), 1.73 – 1.61 (m, 2H), 1.61 – 1.51 (m, 2H), 1.51 – 1.37 (m, 1H), 1.31 (qt, *J* = 12.7, 3.7 Hz, 1H), 0.92 (s, 9H), 0.09 (s, 3H), 0.08 (s, 3H). **^{13}C NMR** (101 MHz, $CDCl_3$) δ 148.46, 140.14, 114.94, 113.87, 73.81, 68.31, 52.94, 41.35, 29.78, 26.56, 26.08, 23.73, 18.54, -5.16, -5.21. **HRMS** (ESI) *m/z* calcd for $C_{17}H_{32}NaO_2Si$ [$(M+Na)^+$]: 319.2064, measured: 319.2061.

Diol *epi*-4.22



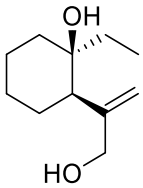
Obtained as white crystals. The characterization data are in agreement with the literature.[31-33] **IR** ν_{max} (solid sample, cm^{-1}): 3300 (broad), 3104, 3087, 3022, 2935, 2920, 2862, 1655, 1157, 1133, 1099, 1087, 1058, 985. **^{1}H NMR** (500 MHz, $CDCl_3$) δ 6.25 (dd, *J* = 17.3, 10.9 Hz, 1H), 5.29 (dd, *J* = 17.3, 1.5 Hz, 1H), 5.19 (d, *J* = 1.0 Hz, 1H), 5.17 (dd, *J* = 10.9, 1.4 Hz, 1H), 4.88 (s, 1H), 4.12 (d, *J* = 12.5 Hz, 1H), 4.04 (d, *J* = 12.5 Hz, 1H), 2.67 (bs, 2H), 2.33 (dd, *J* = 12.9, 3.3 Hz, 1H), 1.93 – 1.87 (m, 1H), 1.87 – 1.78 (m, 1H), 1.75 – 1.66 (m, 2H), 1.66 – 1.40 (m, 3H), 1.33 (qt, *J* = 13.2, 3.9 Hz, 1H). **^{13}C NMR** (126 MHz, $CDCl_3$) δ 149.32, 139.68, 115.02, 114.27, 74.76, 68.06, 51.94, 41.50, 29.49, 26.36, 23.84. **^{1}H NMR** (500 MHz, DMSO-d_6) δ 6.18 (dd, *J* = 17.2, 10.9 Hz, 1H), 5.17 (dd, *J* = 17.2, 2.5 Hz, 1H), 5.03 (q, *J* = 1.7 Hz, 1H), 5.01 (dd, *J* = 10.9, 2.5 Hz, 1H), 4.76 (t, *J* = 5.5 Hz, 1H), 4.69 – 4.65 (m, 1H), 4.62 (s, 1H), 3.99 (dd, *J* = 14.4, 5.6 Hz, 1H), 3.80 (dd, *J* = 14.4, 5.4 Hz, 1H), 2.00 (dd, *J* = 9.1, 7.0 Hz, 1H), 1.71 (tt, *J* = 12.3, 3.2 Hz, 2H), 1.58 (dt, *J* = 12.8, 3.4 Hz, 1H), 1.51 (td, *J* = 9.4, 8.9, 3.2 Hz, 2H), 1.45 (dd, *J* = 12.5, 3.7 Hz, 1H), 1.36 (qt, *J* = 13.0, 3.4 Hz, 1H), 1.29 – 1.17 (m, 1H). **^{13}C NMR** (126 MHz, DMSO-d_6) δ 151.26, 140.32, 112.99, 109.56, 73.53, 65.76, 50.56, 41.54, 28.99, 25.89, 23.21.

Diol *epi*-4.22′



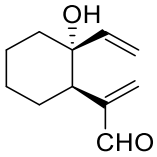
IR ν_{max} (thin film, cm^{-1}): 3262 (broad), 3058, 2930, 2859, 1638, 1453, 1151, 1134, 1102, 1018, 972. **^{1}H NMR** (500 MHz, DMSO-d_6) δ 5.13 (q, J = 1.7 Hz, 1H), 4.79 (t, J = 5.6 Hz, 1H), 4.72 (dq, J = 2.4, 1.2 Hz, 1H), 4.22 (d, J = 0.4 Hz, 1H), 4.07 (dd, J = 14.4, 5.6 Hz, 1H), 3.80 (dd, J = 14.4, 5.6 Hz, 1H), 2.01 – 1.92 (m, 1H), 1.84 – 1.76 (m, 1H), 1.68 – 1.58 (m, 1H), 1.56 – 1.42 (m, 4H), 1.28 (dq, J = 14.8, 7.5 Hz, 1H), 1.22 – 1.08 (m, 3H), 0.74 (t, J = 7.5 Hz, 3H). **^{13}C NMR** (126 MHz, DMSO-d_6) δ 151.84, 109.68, 72.38, 66.27, 51.04, 36.58, 28.90, 25.69, 23.59, 22.95, 6.85. **HRMS** (ESI) *m/z* calcd for $C_{11}H_{20}NaO_2$ [$(M+Na)^+$]: 207.1356, measured: 207.1361.

Diol 4.22′



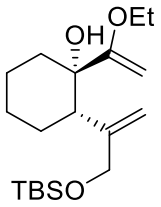
IR ν_{max} (thin film, cm^{-1}): 3250 (broad), 2932, 2856, 1722, 1634, 1460, 1446, 1378, 1353, 1334, 1309, 1260, 1201, 1156, 1133, 1092, 1012. **^{1}H NMR** (500 MHz, DMSO-d_6) δ 5.02 – 4.97 (m, 1H), 4.94 (t, J = 5.4 Hz, 1H), 4.89 (d, J = 2.8 Hz, 1H), 4.14 (s, 1H), 3.99 (dd, J = 14.4, 5.5 Hz, 1H), 3.79 (dd, J = 14.4, 5.4 Hz, 1H), 2.00 (dd, J = 12.7, 3.2 Hz, 1H), 1.77 (qd, J = 12.8, 3.4 Hz, 1H), 1.68 – 1.56 (m, 2H), 1.52 (d, J = 12.9 Hz, 1H), 1.44 – 1.30 (m, 3H), 1.30 – 1.24 (m, 1H), 1.24 – 1.10 (m, 2H), 0.78 (t, J = 7.5 Hz, 3H). **^{13}C NMR** (126 MHz, DMSO-d_6) δ 151.08, 111.58, 71.08, 62.80, 50.58, 35.34, 33.50, 27.68, 26.12, 21.05, 7.87. **HRMS** (ESI) *m/z* calcd for $C_{11}H_{20}NaO_2$ [$(M+Na)^+$]: 207.1356, measured: 207.1349.

Allylic Alcohol Enal *epi*-4.23



Diol *epi*-**4.22** (0.1171 g, 0.6425 mmol, 1 equiv) was oxidized with IBX (0.2197 g, 0.7846 mmol, 1.22 equiv) according to General Procedure **C** for 3 h, at which time additional IBX (49.4 mg, 0.27 equiv) was added, and the reaction left one hour further. The aqueous filtrate was extracted with 3x20 mL EtOAc, then the combined organic layers were washed sequentially with 5 mL water and brine, dried over anhydrous Na_2SO_4, filtered, and concentrated. The concentrate was filtered twice through a cotton plug using minimal diethyl ether. Silica gel flash chromatography with 40-50% ethyl ether / pentane (R_f 0.38, 33% EtOAc / hexanes) afforded 0.1159 g or quantitative yield of aldehyde *epi*-**4.23** as a clear colourless liquid. **IR** ν_{max} (thin film, cm^{-1}): 3489, 3093, 2932, 2862, 1684, 1621, 1449, 1161. *It should be noted that no hemiacetals were ever observed by ^1H NMR spectroscopy in any solvent.* **^{1}H NMR** (500 MHz, $CDCl_3$) δ 9.50 (s, 1H), 6.17 (s, 1H), 6.14 (s, 1H), 6.09 (dd, *J* = 17.1, 10.9 Hz, 1H), 5.23 (dd, *J* = 17.1, 1.9 Hz, 1H), 5.15 (dd, *J* = 10.9, 1.9 Hz, 1H), 2.89 – 2.80 (m, 1H), 2.37 (s, 1H), 1.96 (dtd, *J* = 12.6, 3.4, 1.5 Hz, 1H), 1.87 – 1.78 (m, 1H), 1.74 (dt, *J* = 13.4, 3.4 Hz, 1H), 1.67 – 1.55 (m, 3H), 1.49 (qt, *J* = 13.1, 3.6 Hz, 1H), 1.43 – 1.32 (m, 1H). **^{1}H NMR** (500 MHz, CD_3NO_2) δ 9.44 (s, 1H), 6.30 – 6.23 (m, 2H), 6.19 (s, 1H), 5.16 (dd, *J* = 17.1, 2.2 Hz, 1H), 5.11 (dd, *J* = 10.9, 2.2 Hz, 1H), 2.82 (dd, *J* = 12.9, 3.5 Hz, 1H), 2.38 (bs, 1H), 1.88 – 1.77 (m, 2H), 1.77 – 1.47 (m, 5H), 1.40 (qt, *J* = 12.6, 3.9 Hz, 1H). **^{13}C NMR** (126 MHz, $CDCl_3$) δ 196.66, 150.60, 137.34, 137.14, 115.37, 74.71, 45.75, 41.94, 28.91, 26.08, 23.75. **HRMS** (ESI) *m/z* calcd for $C_{11}H_{16}NaO_2$ [$(M+Na)^+$]: 203.10425, measured: 203.10397.

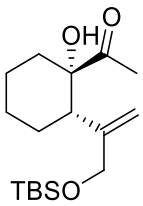
Ethyl enol ether 4.31



Adapted from known procedures,[37] to a solution of ethyl vinyl ether (400 µL, 4.18 mmol, 3.5 equiv) at –78 °C in 2 mL dry THF under argon was added dropwise a solution of *t*-butyllithium (1.7 M in pentane, 0.80 mL, 1.1 equiv) over 10 mins. After addition, the solution was stirred 45 mins at –21 °C, then cooled again to –78 °C and added dropwise by syringe to a solution of ketone **4.17** (0.322 g, 1.20 mmol, 1 equiv) at –78 °C in 2 mL dry THF. The reaction was allowed to warm in the bath and stirred for 18 h, then quenched with sat. aq. NH_4Cl and extracted thrice with EtOAc. The combined organic layers were washed sequentially with water and brine, then dried over

anhydrous Na_2SO_4, filtered, and concentrated. Silica gel flash chromatography with EtOAc / hexanes (R_f 0.45, 10% Et_2O / hexanes) afforded 11.1 mg or 8% yield of enol ether **4.31** as a clear oil and 128.8 mg or 35% yield of recovered ketone starting material. **^{1}H NMR** (400 MHz, acetone-d_6) δ 5.07 (s, 1H), 4.89 (s, 1H), 4.29 (d, J = 1.4 Hz, 1H), 4.12 (d, J = 14.2 Hz, 1H), 3.96 (d, J = 14.2 Hz, 1H), 3.89 – 3.85 (m, 1H), 3.76 – 3.57 (m, 2H), 3.51 (s, 1H), 2.55 (dd, J = 13.1, 3.4 Hz, 1H), 1.92 – 1.78 (m, 2H), 1.78 – 1.63 (m, 2H), 1.55 – 1.39 (m, 3H), 1.34 – 1.24 (m, 1H), 1.30 (t, J = 7.0 Hz, 3H), 0.92 (s, 9H), 0.07 (s, 3H), 0.07 (s, 3H). **^{13}C NMR** (101 MHz, acetone-d_6) δ 168.80, 150.49, 111.86, 79.80, 74.63, 66.09, 63.29, 47.79, 37.55, 27.97, 26.96, 26.28, 21.91, 18.92, 14.91, -5.11, -5.23. **HRMS** (ESI) *m/z* calcd for $C_{19}H_{36}NaO_3Si$ [$(M+Na)^+$]: 363.23259, measured: 363.23285.

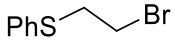
Ketone 4.32



To a solution of ethyl vinyl ether (1.38 mL, 14.4 mmol, 4.13 equiv) at –78 °C in 6 mL dry THF under argon was added a solution of *t*-butyllithium (1.7 M in pentane, 2.4 mL, 1.2 equiv) dropwise over 10 mins. After addition, the solution was stirred at –78 °C 2 h, in which time a white precipitate formed, then 45 mins at –21 °C. The reaction was cooled again to –78 °C and added dropwise by cannula over 20 mins to a solution of ketone **4.17** (0.9368 g, 3.49 mmol, 1 equiv) at –78 °C in 12 mL dry THF. The reaction was stirred at –78 °C 1.5 h, warmed to 0 °C, quenched with 5 mL sat. aq. NH_4Cl, then THF was removed by rotary evaporation. The concentrate was extracted with 3x20 mL EtOAc. The combined organic layers were washed sequentially with sat. aq. $NaHCO_3$, water, and brine, then dried over anhydrous Na_2SO_4, filtered, and concentrated. Dehydrated silica gel flash chromatography with 2-6% EtOAc / hexanes afforded an otherwise clean preparation of enol ether which had partly hydrolyzed to ketone **4.32**. Filtration and chromatography on neutral alumina did not halt hydrolysis or afford separation. On standing, the sample fully hydrolyzed to provide 0.1079 g or 10% yield of ketone **4.32** as a colourless oil. **IR** ν_{max} (thin film, cm^{-1}): 3376 (broad), 2929, 2856, 1704, 1463, 1446, 1414, 1390, 1361, 1310, 1255, 1223, 1194, 1127, 1095, 1048, 1005. **^{1}H NMR** (500 MHz, $CDCl_3$) δ 5.02 (q, J = 1.3 Hz, 1H), 4.94

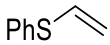
(d, J = 2.2 Hz, 1H), 4.75 (s, 1H), 4.10 (d, J = 12.6 Hz, 1H), 3.94 (d, J = 12.7 Hz, 1H), 2.72 (dd, J = 12.7, 3.6 Hz, 1H), 2.19 (s, 3H), 1.85 – 1.77 (m, 2H), 1.73 – 1.64 (m, 2H), 1.64 – 1.50 (m, 2H), 1.42 – 1.31 (m, 2H), 0.94 (s, 9H), 0.11 (s, 3H), 0.11 (s, 3H). **^{13}C NMR** (126 MHz, $CDCl_3$) δ 215.18, 147.51, 116.27, 81.14, 65.28, 48.47, 35.19, 26.55, 26.11, 26.07, 26.05, 20.75, 18.56, -5.29, -5.37. **HRMS** (ESI) *m/z* calcd for $C_{17}H_{32}NaO_3Si$ [$(M+Na)^+$]: 335.20129, measured: 335.20080.

Alkyl bromide 5.6



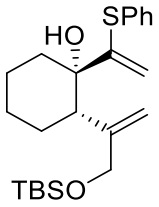
This compound was prepared as described[38] from 20.0 mL thiophenol and 1,2-dibromoethane. The characterization are in agreement with the literature. **^{1}H NMR** (400 MHz, $CDCl_3$) δ 7.42 – 7.22 (m, 5H), 3.50 – 3.42 (m, 2H), 3.34 – 3.24 (m, 2H). **^{13}C NMR** (101 MHz, $CDCl_3$) δ 134.22, 130.74, 129.39, 127.31, 36.26, 29.97. **HRMS** (APCI) *m/z* calcd for $C_8H_{10}BrS$ [$(M+H)^+$]: 216.96811, measured: 216.96806.

Phenylvinylsulfane 5.7



This compound was prepared as described[38] from 27 g of bromide **5.6**. The characterization are in agreement with the literature. **^{1}H NMR** (400 MHz, $CDCl_3$) δ 7.43 – 7.23 (m, 5H), 6.55 (dd, J = 16.6, 9.6 Hz, 1H), 5.36 (d, J = 9.6 Hz, 1H), 5.35 (d, J = 16.6 Hz, 1H). **^{13}C NMR** (101 MHz, $CDCl_3$) δ 134.41, 132.03, 130.67, 129.28, 127.27, 115.64. **HRMS** (APCI) *m/z* calcd for C_8H_9S [$(M+H)^+$]: 137.04195, measured: 137.04179.

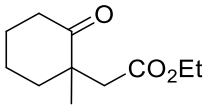
Vinyl sulfide 4.33



To a solution of *n*-butyllithium (2.40 M in hexanes, 1.0 mL, 1.05 equiv) at –78 °C in 7.5 mL dry THF under argon was added dropwise a solution of phenyl vinyl sulfide (0.310 mL, 2.33 mmol, 1.02 equiv) in 7.5 mL dry THF. After addition, the solution was stirred 1.5 h at –78 °C then added dropwise by cannula over 20 mins to a solution of ketone **4.17** (0.614 g, 2.29 mmol, 1 equiv) at –

78 °C in 10.5 mL dry THF. The reaction was stirred at –78 °C for 2.5 h, the bath was removed, and the reaction allowed to warm to 0 °C. Following this, 5 mL sat. aq. NH_4Cl was added, THF was removed by rotary evaporation, and the concentrate was extracted thrice with EtOAc. The combined organic layers were washed sequentially with water and brine, then dried over anhydrous Na_2SO_4, filtered, and concentrated. Silica gel flash chromatography with 40% DCM / hexanes (R_f 0.57, 10% EtOAc / hexanes) afforded 0.2056 g or 22% yield of vinyl sulfide **4.33** as a yellow oil. **IR** ν_{max} (thin film, cm^{-1}): 3377 (broad), 3059, 2930, 2856, 1704, 1651, 1582, 1554, 1472, 1440, 1374, 1330, 1285, 1254, 1192, 1113, 1075, 1055, 1024. **^{1}H NMR** (400 MHz, $CDCl_3$) δ 7.45 (d, *J* = 7.0 Hz, 2H), 7.36 – 7.24 (m, 3H), 5.52 (s, 1H), 5.16 (s, 1H), 5.13 (s, 1H), 4.72 (s, 1H), 4.46 (d, *J* = 2.0 Hz, 1H), 4.18 (d, *J* = 12.5 Hz, 1H), 4.06 (d, *J* = 12.4 Hz, 1H), 2.82 (dd, *J* = 12.7, 3.4 Hz, 1H), 2.00 – 1.84 (m, 2H), 1.84 – 1.69 (m, 3H), 1.62 – 1.46 (m, 2H), 1.40 – 1.27 (m, 1H), 0.94 (s, 9H), 0.13 (s, 3H), 0.11 (s, 3H). **^{13}C NMR** (101 MHz, $CDCl_3$) δ 153.66, 147.95, 134.41, 133.43, 129.26, 127.79, 116.38, 111.64, 76.52, 65.98, 50.04, 37.90, 27.41, 26.18, 26.12, 21.60, 18.63, -5.16, -5.31. **HRMS** (ESI) *m/z* calcd for $C_{23}H_{37}SO_2Si$ [$(M+H)^+$]: 405.22780, measured: 405.22723.

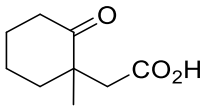
Keto-ester 5.8



To a solution of diisopropylamine (0.668 mL, 4.73 mmol, 1.15 equiv) in 4.6 mL dry 1,4-dioxane at –78 °C was added *n*-BuLi (2.55 M in hexane, 1.77 mL, 1.10 equiv) dropwise via syringe, then the solution was stirred 10 mins. A solution of 2-methylcyclohexanone **4.35** (0.500 mL, 4.119 mmol, 1 equiv), in 2.3 mL dry dioxane was then added dropwise by cannula and the mixture was heated at 95 °C for 3 h, then cooled to room temperature. Ethyl bromoacetate (0.548 mL, 4.94 mmol, 1.2 equiv), which had been passed through basic alumina, was then added dropwise and the reaction stirred 2 h longer. The reaction was cooled over an ice bath, 20 mL 0.5 N HCl was added, and extraction performed with 3x30 mL EtOAc. The combined organic layers were washed sequentially with 10 mL each 1 N HCl, water, and brine, then dried over anhydrous Na_2SO_4, filtered, and concentrated. Silica gel flash chromatography with 0-20% EtOAc / DCM (R_f 0.48, 33% EtOAc / hexanes) afforded 0.3324 g or 41% yield of ester **5.8** as a yellow liquid. The characterization data are in agreement with the literature.[39] **^{1}H NMR** (500 MHz, $CDCl_3$) δ 4.10 (q,

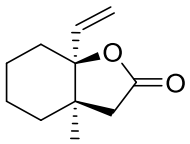
J = 7.1 Hz, 2H), 2.61 (d, J = 15.5 Hz, 1H), 2.48 (d, J = 15.5 Hz, 1H), 2.46 – 2.42 (m, 2H), 2.02 – 1.88 (m, 2H), 1.88 – 1.79 (m, 1H), 1.79 – 1.66 (m, 3H), 1.24 (t, J = 7.2 Hz, 3H), 1.21 (s, 3H). **^{13}C NMR** (126 MHz, $CDCl_3$) δ 213.98, 171.79, 60.43, 47.32, 42.84, 38.55, 38.53, 26.98, 23.66, 21.38, 14.33.

Keto-ester 4.36



To a solution of ethyl ester **5.8** (2.586 g, 13.04 mmol, 1 equiv) in 13 mL MeOH was added 1.25 mL 50% aq. NaOH and the resulting solution refluxed 1 h, then cooled and the MeOH removed by rotary evaporation. The aqueous was diluted with 5 mL water and poured into 18 mL 1 N HCl, then extracted with 3x25 mL EtOAc. The combined organic layers were washed sequentially with 5 mL each water and brine, then dried over anhydrous Na_2SO_4, filtered, and concentrated. Silica gel flash chromatography with 1% AcOH in 10-40% ^{i}PrOH / hexanes (R_f 0.44, EtOAc) afforded 1.2454 g or 56% yield of known carboxylic acid **4.36**[40] as a white solid.

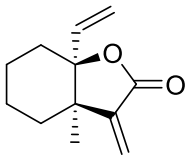
Lactone 4.37



To a solution of carboxylic acid **4.36** (1.2454 g, 7.317 mmol, 1 equiv) in 70 mL dry THF at –78 °C was added vinylmagnesium bromide (1.0 M THF, 18.3 mL, 2.5 equiv) fast dropwise, after which the reaction was allowed to warm to room temperature in the bath. After stirring for a total of 12 h, 25 mL of 1 M aq. HCl was added over an ice bath and the mixture stirred 3 h further to encourage lactone formation. The THF was then removed *in vacuo*, then the aqueous was diluted with 35 mL water and extracted with 3x60 mL EtOAc. The combined organic layers were washed sequentially with 15 mL each water and brine, then dried over anhydrous Na_2SO_4, filtered, and concentrated. The crude residue was taken up in 70 mL THF and stirred with cat. *p*TSA overnight to complete lactonization of the desired isomer, after which it was quenched by addition of solid $NaHCO_3$ until bubbling ceased, then dried over anhydrous Na_2SO_4, filtered, and concentrated. Silica gel flash chromatography with 10-100% EtOAc / hexanes (R_f 0.43, 25% EtOAc / hexanes)

afforded 0.1447 g of lactone **4.37** as a clear colourless liquid, along with 0.3972 g of the same compound as a red syrup for 41% combined yield. Despite the colour, only trace impurities were visible by ^{1}H NMR in the red sample. **IR** ν_{max} (neat liquid, cm^{-1}): 2935, 2862, 1764, 1642, 1450, 1419, 1384, 1355, 1280, 1260, 1225, 1194, 1163, 1137, 1105, 1082, 1059, 1044, 1028, 992, 977, 953, 929. **^{1}H NMR** (500 MHz, $CDCl_3$) δ 5.86 (dd, *J* = 17.2, 11.0 Hz, 1H), 5.33 (d, *J* = 17.1 Hz, 1H), 5.18 (d, *J* = 11.0 Hz, 1H), 2.38 (d, *J* = 16.5 Hz, 1H), 2.24 (d, *J* = 16.6 Hz, 1H), 1.73 – 1.64 (m, 1H), 1.69 (ddd, *J* = 14.8, 8.7, 6.1 Hz, 1H), 1.61 – 1.48 (m, 5H), 1.47 – 1.39 (m, 1H), 1.11 (s, 3H). **^{13}C NMR** (126 MHz, $CDCl_3$) δ 176.67, 137.63, 114.76, 88.24, 43.59, 40.97, 35.69, 31.95, 21.36, 21.34, 21.10. **HRMS** (ESI) *m/z* calcd for $C_{11}H_{16}O_2Na$ [$(M+Na)^+$]: 203.10425, measured: 203.10430.

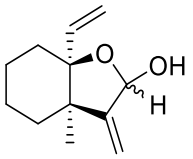
Methylene lactone 4.38



To a solution of diisopropylamine (0.364 mL, 2.60 mmol, 1.2 equiv) in 11 mL dry THF at –78 °C was added *n*-BuLi (2.60 M in hexane, 0.917 mL, 1.1 equiv) dropwise, then the solution stirred 5 mins. A solution of lactone **4.37** (0.3906 g, 2.167 mmol, 1 equiv) in 11 mL dry THF was then added dropwise by cannula, and the mixture stirred 30 mins. Solid *N,N*-dimethyl-methyleneiminium iodide (Eschenmoser's salt; 1.2008 g, 3.0 equiv) was then added in one portion and the suspension allowed to warm to room temperature overnight. The reaction was concentrated and the residue taken up in 15 mL MeOH, then 5 mL MeI was added and the solution stirred 24 h. This solution was concentrated to a dark syrup, which was then taken up in 50 mL of 1:1 DCM / 5% aq. $NaHCO_3$ and stirred 3 h. The layers were separated and the aqueous extracted further with 3x25 mL DCM. The combined organic layers were washed sequentially with 25 mL each water and brine, then dried over anhydrous Na_2SO_4, filtered, and concentrated. Silica gel flash chromatography with 20-25% Et_2O / hexanes (R_f 0.50, 25% EtOAc / hexanes) afforded 0.1292 g or 31% of methylene lactone **4.38** as a yellow liquid and 77.4 mg or 20% yield of recovered lactone **4.37**. **IR** ν_{max} (thin film, cm^{-1}): 2936, 2862, 1765, 1666, 1645, 1449, 1414, 1266, 1208, 1197. **^{1}H NMR** (500 MHz, $CDCl_3$) δ 6.12 (s, 1H), 5.85 (dd, *J* = 17.2, 11.1 Hz, 1H), 5.34 (s, 1H), 5.33 (dd, *J* = 17.2, 1.0 Hz, 1H), 5.17 (dd, *J* = 11.1, 0.9 Hz, 1H), 1.86 – 1.79 (m, 1H), 1.78 – 1.68 (m, 2H),

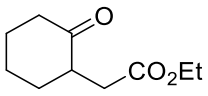
1.62 – 1.56 (m, 1H), 1.54 – 1.39 (m, 4H), 1.12 (s, 3H). **^{13}C NMR** (126 MHz, $CDCl_3$) δ 170.73, 146.06, 136.86, 118.11, 115.30, 86.68, 45.53, 35.32, 33.37, 22.02, 21.57, 21.24. **HRMS** (ESI) *m/z* calcd for $C_{12}H_{16}O_2Na$ [$(M+Na)^+$]: 215.10425, measured: 215.10331.

Lactol 4.39



To a solution of methylene lactone **4.38** (0.1395 g, 0.7256 mmol, 1 equiv) in 7.0 mL dry PhMe at –78 °C was added DiBAL-H (25% in PhMe, 0.537 mL, 1.1 equiv) dropwise and the solution stirred 2 h. Fieser's workup was conducted, and the resulting suspension filtered on celite then concentrated. Silica gel flash chromatography with 40% Et_2O / pentane (R_f 0.35, 25% EtOAc / hexanes) afforded 99.8 mg or 71% of lactols **4.39** as a clear yellow liquid. **IR** ν_{max} (thin film, cm^{-1}): 3402 (broad), 3088, 3016, 2930, 2861, 1776 (weak), 1761 (weak), 1672, 1641, 1449, 1415, 1376, 1340, 1263, 1206, 1174, 1159, 1121, 1091, 1062, 1039, 991, 959. **^{1}H NMR** (500 MHz, $CDCl_3$) δ 5.95 (dd, *J* = 17.2, 11.0 Hz, 0.68H), 5.91 (dd, *J* = 17.2, 11.0 Hz, 0.46H), 5.80 (q, *J* = 1.8 Hz, 0.49H), 5.81 – 5.77 (m, 0.50H), 5.43 (dd, *J* = 17.2, 1.8 Hz, 0.64H), 5.33 (dd, *J* = 17.2, 1.9 Hz, 0.51H), 5.27 (d, *J* = 1.6 Hz, 0.42H), 5.20 (d, *J* = 1.6 Hz, 0.61H), 5.11 (dd, *J* = 11.1, 1.9 Hz, 0.48H), 5.08 (dd, *J* = 11.0, 1.8 Hz, 0.67H), 4.99 (d, *J* = 1.9 Hz, 0.45H), 4.96 (d, *J* = 2.0 Hz, 0.61H), 2.91 (d, *J* = 6.7 Hz, 0.43H), 2.65 (d, *J* = 9.4 Hz, 0.59H), 1.96 – 1.88 (m, 0.53H), 1.77 – 1.71 (m, 1.56H), 1.68 – 1.59 (m, 0.96H), 1.59 – 1.24 (m, 8.73H), 1.10 (s, 1.89H), 0.97 (s, 1.53 H). **^{13}C NMR** (126 MHz, $CDCl_3$) δ 159.83, 157.61, 142.36, 138.29, 114.30, 113.84, 107.63, 107.09, 97.84, 97.48, 86.13, 85.83, 46.96, 46.57, 36.78, 35.75, 34.43, 31.72, 24.13, 23.12, 21.79, 21.75, 21.61, 19.62. **HRMS** (ESI) *m/z* calcd for $C_{12}H_{18}O_2Na$ [$(M+Na)^+$]: 217.11990, measured: 217.11978.

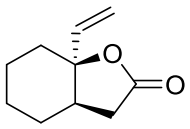
Keto-ester 4.41



This known compound was prepared according to a modification of standard procedures for Dean-Stark condensation with pyrrolidine and subsequent alkylation.[41a-c] To a solution of cyclohexanone (10.0 mL, 96.5 mmol, 1 equiv) in 50 mL dry PhMe over 4 Å molecular sieves, contained in a 100

mL 3-neck flask topped with a Dean-Stark apparatus, was added dry pyrrolidine (15.0 mL, 180 mmol, 1.86 equiv) and the mixture heated at 120-150 °C for 24 h. The suspension was filtered on celite and concentrated by rotary evaporation to provide 13.3953 g or 92 % yield of enamine intermediate as a yellow / orange syrup which rapidly darkened on standing. This was combined with 73 mL dry PhMe at warmed to 90 °C, then a solution of ethyl bromoacetate (11.8 mL, 1.1 equiv) in 35 mL dry PhMe was added as a stream via syringe. The precipitate which formed immediately was suspended by addition of 60 mL dry PhMe and manual agitation by spatula, then the mixture refluxed 3 h. The reaction cooled to room temperature, 35 mL water was added, and the mixture extracted with 3x50 mL EtOAc. The combined organic layers were washed sequentially with 20 mL each water and brine, then dried over anhydrous Na_2SO_4, filtered, and concentrated. Silica gel flash chromatography with 15-20% EtOAc / hexanes (R_f 0.40, 33% EtOAc / hexanes), followed by distillation under reduced pressure, afforded 6.6743 g or 38% yield of ketone **4.41** as a pale yellow oil. The characterization data are in agreement with the literature.[41d] **^{1}H NMR** (500 MHz, $CDCl_3$) δ 4.17 – 4.09 (m, 2H), 2.86 (dq, *J* = 12.4, 6.1 Hz, 1H), 2.76 (dd, *J* = 16.4, 7.1 Hz, 1H), 2.46 – 2.31 (m, 2H), 2.17 – 2.07 (m, 3H), 1.92 – 1.83 (m, 1H), 1.80 – 1.57 (m, 2H), 1.41 (qd, *J* = 12.9, 3.7 Hz, 1H), 1.25 (t, *J* = 7.1 Hz, 3H).

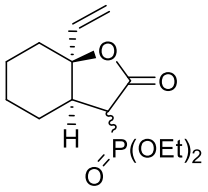
Lactone 4.42



To solution of ketone **4.41** (2.4631 g, 13.37 mmol, 1 equiv) in 115 mL dry THF at –78 °C was added vinyl-magnesium bromide (16.0 mL, 1.0 M in THF, 1.2 equiv) fast dropwise. The reaction was warmed in the bath to room temperature and stirred for 18 h total, then cooled over ice again before 3 mL sat. aq. NH_4Cl was added. The THF was removed by rotary evaporation and the aqueous layer diluted with 20 mL each water and 0.1 N HCl, then extracted with 3x50 mL EtOAc. The combined organic layers were washed sequentially with 10 mL each water and brine, then dried over anhydrous Na_2SO_4, filtered, and concentrated. Silica gel flash chromatography with 20% EtOAc / hexanes (R_f 0.40, 33% EtOAc / hexanes) afforded 2.092 g or 94% yield of lactone **4.42** as a pale yellow oil. The characterization data are in agreement with the literature.[42] **^{1}H NMR** (500 MHz, $CDCl_3$) δ 5.84 (dd, *J* = 17.2, 10.9 Hz, 1H), 5.33 (dd, *J* = 17.2, 0.6 Hz, 1H), 5.17 (dd, *J*

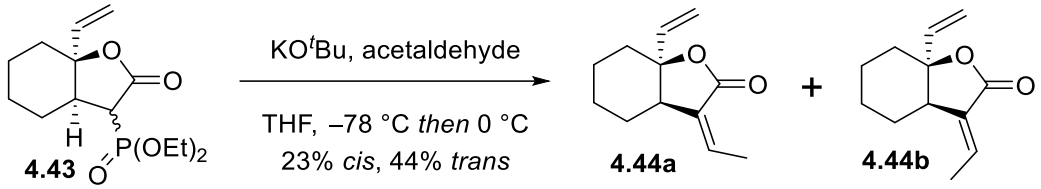
= 10.9, 0.6 Hz, 1H), 2.65 (dd, *J* = 16.8, 6.9 Hz, 1H), 2.31 – 2.22 (m, 1H), 2.18 (dd, *J* = 16.7, 3.6 Hz, 1H), 1.93 (dt, *J* = 14.1, 4.2 Hz, 1H), 1.79 (dt, *J* = 12.8, 6.5 Hz, 1H), 1.70 – 1.56 (m, 2H), 1.55 – 1.45 (m, 2H), 1.36 – 1.27 (m, 2H).

Ketophosphonate 4.43



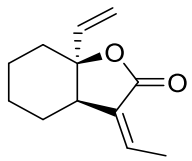
Adapted from Weimer's procedure,[43] to a solution of diisopropylamine (0.97 mL, 6.9 mmol, 1.2 equiv) in 60 mL dry THF at –78 °C was added *n*-BuLi (2.5 M in hexane, 1.65 mL, 1.1 equiv) dropwise, then the solution stirred 10 mins. A solution of lactone **4.42** (1.002 g, 6.028 mmol, 1 equiv) in 5 mL dry THF was then added dropwise by cannula, and the mixture stirred 30 mins. At this time, hexamethylphosphoramide (1.26 mL, 7.24 mmol, 1.2 equiv), which had been heated at 90-95 °C with then distilled from CaH_2 under argon, then diethyl chlorophosphate (1.05 mL, 7.27 mmol, 1.2 equiv), were each added neat and the reaction was allowed to come to room temperature within the bath over 1 h. After cooling again to –78 °C, lithium diisopropylamide (5.30 mL *n*-BuLi, 13.6 mmol, 2.2 equiv), prepared as described above in 18 mL dry THF, was added dropwise by cannula. The pale orange reaction was allowed to warm again to room temperature in the bath, turning first blood orange then brown. The reaction was cooled over ice and quenched by careful addition of a solution of 1 M AcOH (1.5 mL, 26.2 mmol, 4.4 equiv) in Et_2O, then filtered on a pad of magnesium silicate, which was then rinsed with 150 mL THF. Silica gel flash chromatography of the concentrate with 50% EtOAc / hexanes then 50% EtOAc / MeCN (R_f 0.55, 10% MeCN / EtOAc) afforded 1.4048 g or 77% of a mixture of epimers of lactone phosphonate **4.43** as a pale yellow oil. **IR** ν_{max} (neat liquid, cm^{-1}): 3464 (broad), 2982, 2936, 2866, 1764, 1645, 1452, 1417, 1392, 1369, 1237, 1165, 1122, 1096, 1047, 1019, 952. *All integrals of signals clearly arising from the major epimer are reported as integers, but integrals from signals partly or fully arising from them minor are reported to two decimal places. For simplicity, only carbon signals arising from the major isomer are listed here.* **^{1}H NMR** (500 MHz, $CDCl_3$) δ 6.04 (dd, *J* = 17.4, 11.0 Hz, 1H), 5.76 (dd, *J* = 17.2, 10.8 Hz, 0.14H), 5.46 (dd, *J* = 17.4, 0.7 Hz, 1H), 5.35 (d, *J* = 17.1 Hz, 0.17H), 5.30 (dd, *J* = 11.0, 0.7 Hz, 1H), 5.19 (d, *J* = 11.1 Hz, 0.15H), 4.35 – 4.15 (m, 4.86H), 3.38 (dd, *J*

= 24.3, 5.9 Hz, 0.19H), 3.12 (dd, *J* = 23.0, 12.6 Hz, 1H), 2.86 – 2.75 (m, 1H), 2.47 (dt, *J* = 12.0, 6.0 Hz, 0.15H), 2.11 (dd, *J* = 23.5, 13.3 Hz, 2.58H), 1.75 – 1.68 (m, 1H), 1.67 – 1.58 (m, 2.74H), 1.47 (td, *J* = 13.4, 4.0 Hz, 1H), 1.39 – 1.26 (m, 9.97H). **^{13}C NMR** (126 MHz, $CDCl_3$) δ 170.76 (d, *J* = 1.3 Hz), 137.08, 116.56, 85.02 (d, *J* = 13.9 Hz), 63.73 (d, *J* = 6.6 Hz), 62.76 (d, *J* = 6.7 Hz), 42.57 (d, *J* = 151.5 Hz), 42.34 (d, *J* = 1.9 Hz), 33.71, 24.16, 22.08, 19.54, 16.58 (d, *J* = 5.9 Hz), 16.53 (d, *J* = 5.7 Hz). **HRMS** (ESI) *m/z* calcd for $C_{14}H_{23}NaO_5P$ [$(M+Na)^+$]: 325.11753, measured: 325.11757.



To a solution of phosphonate **4.43** (0.3964 g, 1.311 mmol, 1 equiv) in 13 mL dry THF at 0 °C was added 0.37 mL acetaldehyde, freshly distilled, then KO^{t}Bu (0.1762 g, 1.57 mmol, 1.2 equiv) and the reaction allowed to warm overnight. Additional KO^{t}Bu (0.0986 g, 0326 mmol, 0.25 equiv) and 1.0 mL acetaldehyde, freshly distilled from *p*TSA, were added the following day, then the reaction stirred 2 h further. The THF was removed by rotary evaporation and the residue partitioned between 25 mL EtOAc, 10 mL water, and 10 mL 2N HCl. The layers were separated, and the aqueous extracted with 2x25 mL EtOAc further, then the combined organic layers were washed sequentially with 10 mL each water and brine, then dried over Na_2SO_4, filtered, and concentrated. Silica gel flash chromatography with 10-15% EtOAc / hexanes afforded 57.8 mg of *cis*-**4.44a** (R_f 0.53, 25% EtOAc / hexanes) and 111.1 mg of *trans*-**4.44b** (R_f 0.46, 20% EtOAc / hexanes), both lime green liquids, for a combined 67% yield.

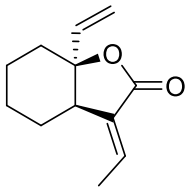
***cis*-Alkene lactone 4.44a**



IR ν_{max} (neat liquid, cm^{-1}): 2935, 2861, 1747, 1676, 1448, 1416, 1377, 1348, 1311, 1247, 1230, 1202, 1156, 1123, 1079. **^{1}H NMR** (500 MHz, $CDCl_3$) δ 6.09 (qd, *J* = 7.3, 2.2 Hz, 1H), 5.94 (dd, *J* = 17.3, 10.9 Hz, 1H), 5.37 (d, *J* = 17.3 Hz, 1H), 5.19 (d, *J* = 10.9 Hz, 1H), 2.77 (dp, *J* = 5.9, 2.5

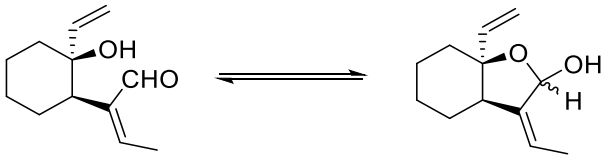
Hz, 1H), 2.17 (dd, *J* = 7.3, 2.2 Hz, 3H), 1.82 (ddd, *J* = 13.7, 7.9, 3.6 Hz, 1H), 1.78 – 1.64 (m, 3H), 1.60 – 1.51 (m, 1H), 1.49 – 1.35 (m, 3H). **^{13}C NMR** (126 MHz, $CDCl_3$) δ 170.08, 139.60, 136.40, 130.63, 115.19, 83.17, 45.40, 33.83, 26.25, 21.40, 20.79, 14.03. **HRMS** (ESI) *m/z* calcd for $C_{12}H_{16}NaO_2$ [$(M+Na)^+$]: 215.1043, measured: 215.1034.

***trans*-Alkene lactone 4.44b**



IR ν_{max} (neat liquid, cm^{-1}): 2986, 2935, 2860, 1750, 1684, 1443, 1412, 1380, 1333, 1304, 1281, 1232, 1194, 1129, 1075, 1053. **^{1}H NMR** (500 MHz, $CDCl_3$) δ 6.65 (qd, *J* = 7.1, 1.5 Hz, 1H), 5.75 (dd, *J* = 17.2, 10.8 Hz, 1H), 5.23 (d, *J* = 17.1 Hz, 1H), 5.06 (d, *J* = 10.8 Hz, 1H), 2.82 (t, *J* = 7.9 Hz, 1H), 2.10 – 2.01 (m, 1H), 1.95 – 1.87 (m, 1H), 1.83 (d, *J* = 7.2 Hz, 3H), 1.70 – 1.56 (m, 3H), 1.54 – 1.44 (m, 1H), 1.30 – 1.24 (m, 2H). **^{13}C NMR** (126 MHz, $CDCl_3$) δ 171.29, 141.85, 134.54, 134.05, 114.15, 83.12, 41.60, 32.54, 27.78, 22.25, 20.30, 14.97. **HRMS** (ESI) *m/z* calcd for $C_{12}H_{16}NaO_2$ [$(M+Na)^+$]: 215.1043, measured: 215.1044.

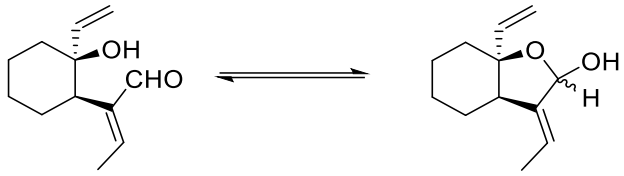
***cis*-Alkene enal / hemiacetal 4.45a**



To a solution of *cis*-lactone **4.44a** (0.0536 g, 0.2788 mmol, 1 equiv) in 2.5 mL dry PhMe at –78 °C was added DiBAL-H (25% in PhMe, 0.240 mL, 1.25 equiv) dropwise and the solution stirred 3 h. Fieser's workup was conducted, and the resulting suspension stirred overnight then filtered on celite and concentrated. Silica gel flash chromatography with 40-50% Et_2O / pentane (R_f 0.30, 25% EtOAc / hexanes) afforded 39.7 mg or 73% of **4.45a** as a clear colourless liquid. **IR** ν_{max} (neat liquid, cm^{-1}): 3399, 3088, 2930, 2859, 1671, 1642, 1448, 1415, 1380, 1327, 1265, 1188, 1134, 1071, 1043, 990, 961, 936, 916. *All integrals of signals clearly arising from the aldehyde tautomer are reported as integers, but integrals from signals partly or fully arising from either hemiacetal are reported to two decimal places.* **^{1}H NMR** (500 MHz, $CDCl_3$) δ 10.04 (s, 1H), 6.70 (q, *J* = 7.6

Hz, 1H), 6.07 (dd, *J* = 17.5, 10.9 Hz, 2.83H), 5.86 – 5.68 (m, 9.13H), 5.53 – 5.41 (m, 5.78H), 5.36 (dd, *J* = 17.5, 1.2 Hz, 3.09H), 5.26 (dd, *J* = 17.3, 1.4 Hz, 2.86H), 5.14 (dd, *J* = 10.9, 1.2 Hz, 2.89H), 5.09 – 5.02 (m, 3.64H), 4.87 (dd, *J* = 10.7, 1.4 Hz, 1H), 3.10 (d, *J* = 6.3 Hz, 2.68H), 2.80 (d, *J* = 8.4 Hz, 2.73H), 2.68 (dd, *J* = 13.1, 3.1 Hz, 1H), 2.64 (s, 2.97H), 2.48 (bs, 1H), 2.39 (t, *J* = 6.5 Hz, 2.79H), 2.12 (d, *J* = 7.6 Hz, 2.77H), 1.93 – 1.85 (m, 3.74H), 1.78 – 1.74 (m, 19.37H), 1.73 – 1.46 (m, 38.43H), 1.44 – 1.22 (m, 20.90H). **^{13}C NMR** (126 MHz, $CDCl_3$) δ 191.69, 147.11, 146.06, 144.01, 143.88, 143.27, 142.58, 142.17, 120.30, 119.96, 114.01, 113.35, 111.11, 96.49, 96.10, 83.19, 83.12, 73.46, 47.04, 45.21, 38.72, 38.72, 34.25, 33.99, 27.78, 27.02, 26.35, 26.16, 22.39, 22.36, 22.21, 21.35, 21.27, 14.16, 14.04, 13.36. **HRMS** (ESI) *m/z* calcd for $C_{12}H_{18}NaO_2$ [$(M+Na)^+$]: 217.11990, measured: 217.11950.

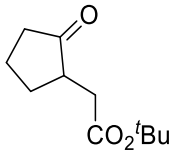
***trans*-Alkene enal / hemiacetal 4.45b**



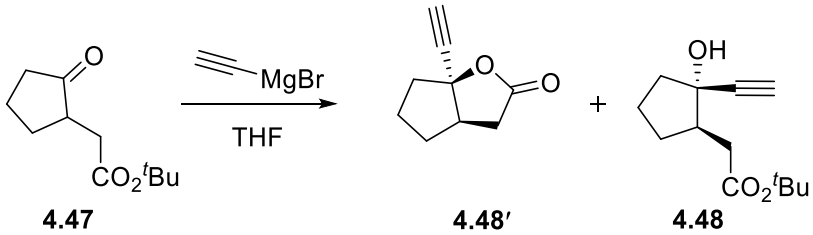
To a solution of *cis*-lactone **4.44b** (0.0389 g, 0.2023 mmol, 1 equiv) in 2.5 mL dry PhMe at –78 °C was added DiBAL-H (25% in PhMe, 0.170 mL, 1.25 equiv) dropwise and the solution stirred 6 h. Fieser's workup was conducted, and the resulting suspension filtered on celite and concentrated. Silica gel flash chromatography with 10% EtOAc / hexanes (R_f 0.20, 20% EtOAc / hexanes) afforded 38.0 mg or 97% of **4.45b** as a clear colourless liquid. **IR** ν_{max} (thin film, cm^{-1}): 3384 (broad), 3081, 3058, 2930, 2856, 2736, 1668, 1624, 1446, 1411, 1381, 1267, 1234, 1196, 1172, 1158, 1132, 1094, 1075. *All integrals of signals clearly arising from the aldehyde tautomer are reported as integers, but integrals from signals partly or fully arising from either hemiacetal are reported to two decimal places.* **^{1}H NMR (**500 MHz, $CDCl_3$) δ 9.20 (d, *J* = 1.4 Hz, 1H), 6.70 (q, *J* = 7.0 Hz, 1H), 5.93 (dd, *J* = 17.4, 10.9 Hz, 0.23H), 5.70 – 5.57 (m, 1.65H), 5.50 (d, *J* = 7.5 Hz, 0.17H), 5.29 (dd, *J* = 17.4, 1.3 Hz, 0.27H), 5.24 – 5.14 (m, 1.95H), 5.01 (dd, *J* = 10.9, 1.4 Hz, 0.23H), 4.95 (dd, *J* = 10.6, 1.4 Hz, 0.17H), 4.88 (dd, *J* = 10.6, 1.8 Hz, 1H), 2.93 (d, *J* = 7.6 Hz, 0.14H), 2.69 (dd, *J* = 10.7, 6.6 Hz, 0.27H), 2.66 – 2.56 (m, 1.15H), 2.50 (dd, *J* = 11.3, 6.6 Hz, 0.18H), 2.12 (qd, *J* = 12.7, 3.5 Hz, 1H), 2.04 – 1.74 (m, 6.23H), 1.71 – 1.62 (m, 2.86H), 1.59 – 1.05 (m, 6.87H). **^{13}C NMR** (126 MHz, $CDCl_3$) δ 198.88, 156.01, 148.04, 146.86, 146.70, 146.22,

145.06, 144.17, 120.17, 119.42, 113.11, 112.40, 111.83, 98.50, 98.46, 83.09, 82.49, 73.20, 45.94, 43.02, 42.52, 38.66, 34.00, 33.98, 28.94, 28.16, 26.68, 25.79, 24.10, 23.94, 21.18, 21.16, 21.10, 15.44, 14.64, 14.54. **HRMS** (ESI) *m/z* calcd for $C_{12}H_{18}NaO_2$ [$(M+Na)^+$]: 217.11990, measured: 217.11934.

Keto-ester 4.47



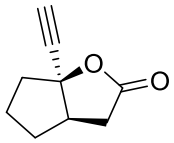
To a solution of diisopropylamine (2.57 mL, 18.3 mmol, 1.2 equiv) in 50 mL dry THF at –78 °C was added *n*-BuLi (2.754 M in hexane, 6.10 mL, 1.1 equiv) dropwise via syringe, then the solution was stirred 2 mins. A solution of cyclopentanone (1.35 mL, 15.26 mmol, 1 equiv), freshly distilled from $MgSO_4$ under argon, in 20 mL dry THF was then added dropwise by cannula over 5 mins, and the mixture stirred 1 h. A solution of *t*-butyl 2-iodoacetate (3.20 mL, 4.76 g, 19.7 mmol, 1.3 equiv), which had been passed through basic alumina, in 20 mL dry THF was then added dropwise by cannula over 5-10 mins and the reaction stirred 1 h longer. At this time, 6 mL each sat. aq. NH_4Cl and water were added, the bath was removed, and the reaction allowed to warm to room temperature. The THF was removed *in vacuo*, after which the aqueous was diluted with 20 mL water and 5 mL 1 M HCl then extracted with 3x50 mL EtOAc. The combined organic layers were washed sequentially with 10 mL each water and brine, then dried over anhydrous Na_2SO_4, filtered, and concentrated. Silica gel flash chromatography with 10-15% EtOAc / hexanes (R_f 0.52, 33% EtOAc / hexanes) afforded 2.6786 g or 89% yield of ester **4.47** as a pale yellow liquid. The characterization data are in agreement with the literature.[44] **^{1}H NMR** (400 MHz, $CDCl_3$) δ 2.65 (dd, *J* = 15.9, 3.7 Hz, 1H), 2.45 – 2.24 (m, 4H), 2.23 – 2.11 (m, 1H), 2.09 – 1.99 (m, 1H), 1.87 – 1.72 (m, 1H), 1.62 (qd, *J* = 11.7, 6.7 Hz, 1H), 1.44 (s, 9H).



4.47 **4.48′** **4.48**

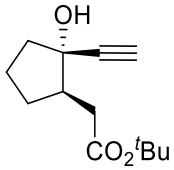
To a solution of ketone **4.47** (1.00 mL, 0.992 g/mL, 5.004 mmol, 1 equiv) in 50 mL dry THF at 0 °C was added ethynylmagnesium bromide (0.5 M in THF, 10.0 mL, 1.0 equiv) dropwise over 15 mins. The reaction was followed by ^{1}H NMR spectroscopy, taking 1.5 h for consumption of the ketone and 4 h total for lactonization of the *cis* adduct, at which time 10 mL sat. aq. NH_4Cl was added while still over an ice bath then THF was removed *in vacuo*. The aqueous was diluted with 5 mL 1 N HCl and extracted with 3x60 mL EtOAc. The combined organic layers were washed sequentially with 10 mL each sat. aq. $NaHCO_3$, water, and brine, then dried over anhydrous Na_2SO_4, filtered, and concentrated. Silica gel flash chromatography with 10-20% EtOAc / hexanes afforded 0.417 g or 37% yield of desired *t*-butyl ester **4.48** as a clear colourless liquid (R_f 0.41, 20% EtOAc / hexanes) along with 0.102 g or 14% yield of lactone **4.48′** (R_f 0.31, 20% EtOAc / hexanes), which crystallized on standing at –16 °C in the freezer.

Alkynyl lactone 4.48′



IR ν_{max} (neat liquid, cm^{-1}): 3271, 2967, 2877, 2116 (weak), 1770, 1469, 1453, 1438, 1417, 1324, 1302, 1254, 1206, 1180, 1148, 1084, 1046, 965, 908. **^{1}H NMR** (500 MHz, $CDCl_3$) δ 3.04 – 2.92 (m, 2H), 2.66 (s, 1H), 2.40 – 2.29 (m, 2H), 2.15 – 1.96 (m, 2H), 1.87 – 1.68 (m, 2H), 1.59 – 1.50 (m, 1H). **^{13}C NMR** (126 MHz, $CDCl_3$) δ 176.22, 87.38, 82.75, 74.97, 46.65, 40.99, 36.14, 33.57, 24.43. **HRMS** (ESI) *m/z* calcd for $C_9H_{20}NaO_2$ [$(M+Na)^+$]: 173.0573, measured: 173.0567.

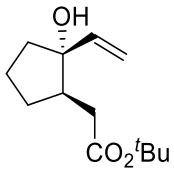
Alkynyl ester 4.48



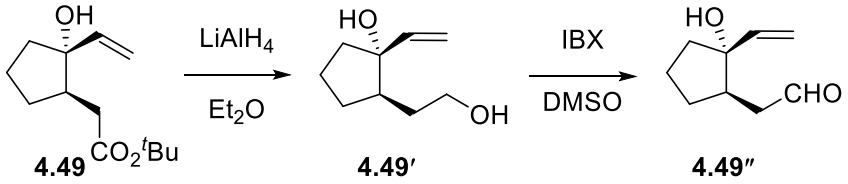
IR ν_{max} (thin film, cm^{-1}): 3415 (very broad), 3306 (broad), 2974, 2874, 1723, 1453, 1393, 1330, 1300, 1255, 1222, 1146, 1099. **^{1}H NMR** (500 MHz, $CDCl_3$) δ 4.57 (s, 1H), 2.69 (dd, *J* = 17.2, 10.1 Hz, 1H), 2.53 (s, 1H), 2.46 (dd, *J* = 17.2, 4.7 Hz, 1H), 2.28 (tdd, *J* = 10.3, 8.0, 4.7 Hz, 1H), 2.20 (ddd, *J* = 13.3, 8.0, 5.7 Hz, 1H), 2.01 (dt, *J* = 13.0, 8.5 Hz, 1H), 1.92 (dtd, *J* = 12.7, 7.9, 4.7

Hz, 1H), 1.79 – 1.66 (m, 2H), 1.46 (s, 9H), 1.35 (ddt, J = 12.9, 10.5, 8.2 Hz, 1H). **^{13}C NMR** (126 MHz, $CDCl_3$) δ 174.44, 85.75, 81.43, 74.06, 47.31, 42.05, 37.88, 30.70, 28.22, 21.26. **HRMS** (ESI) *m/z* calcd for $C_{13}H_{20}NaO_3$ [$(M+Na)^+$]: 247.13047, measured: 247.13073.

Ester 4.49



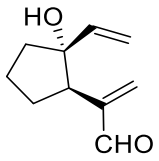
To a solution of alkyne ester **4.48** (0.4055 g, 1.808 mmol, 1 equiv) in 18 mL MeOH and 0.39 mL pyridine under argon was added $Pd/CaCO_3$ (5 wt.%, 0.3865 g, 0.1 equiv, poisoned with Pb) and H_2 gas was bubbled through the solution from a double-skinned balloon for 1.5 h, at which time the reaction was determined complete by ^{1}H NMR spectroscopy. The black suspension was filtered on celite using EtOAc and concentrated. Silica gel flash chromatography with 25% EtOAc / hexanes (R_f 0.35, 25% EtOAc / hexanes) afforded 0.3629 g or 89% yield of olefin **4.49** as a clear colourless oil. Due to contamination with inseparable saturated compound, the material was used directly in the next step.



4.49 **4.49′** **4.49″**

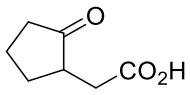
To a solution of ester **4.49** (0.2607 g, 1.152 mmol, 1 equiv) in 10 mL dry Et_2O was added $LiAlH_4$ (47.5 mg, 1.25 mmol, 1.1 equiv) in portions, then the reaction stirred 1 h. Fieser's workup was conducted, and the resulting suspension filtered on celite, then concentrated to a white residue of diol **4.49′**, the data for which are in agreement with the literature.[45] The residue was treated according to General Procedure **C**, then extracted with 3x20 mL Et_2O. The combined organic layers were washed with 10 mL brine, dried over anhydrous $MgSO_4$, filtered, and concentrated. Silica gel flash chromatography with 20% EtOAc / hexanes (R_f 0.25, 33% EtOAc / hexanes) afforded 81.1 mg or 46% yield of aldehyde **4.49″** over two steps as a clear colourless liquid. This was used directly in the following step without further purification.

Aldehyde *epi*-4.50



To a solution of aldehyde **4.49″**(75.0 mg, 0.486 mmol, 1 equiv) in 0.490 mL DCM was added pyrrolidine (4.0 µL, 0.048 mmol, 0.1 equiv), aq. formaldehyde (37 wt.%, 36 µL, 0.48 mmol, 1.0 equiv), then propionic acid (3.5 µL, 0.047 mmol, 0.1 equiv) and the solution was immersed in a 50 °C oil bath for 1 h.[46] The reaction was diluted with 10 mL DCM and washed sequentially with 2 mL each 0.1 N HCl and brine. The aqueous layers were combined and extracted with 2x2 mL DCM. The combined organic layers were dried over anhydrous $MgSO_4$, filtered, and concentrated. Silica gel flash chromatography with 40% Et_2O / pentane (R_f 0.33, 25% EtOAc / hexanes) afforded 62.9 mg or 78% yield of enal *epi*-**4.50** as a clear colourless liquid. **IR** ν_{max} (neat liquid, cm^{-1}): 3459, 3088, 2957, 2874, 2706, 1676, 1639, 1623, 1450, 1367, 1293, 1257, 1202, 1105, 1057, 985, 948, 917. **^{1}H NMR** (500 MHz, $CDCl_3$) δ 9.42 (s, 1H), 6.27 (d, *J* = 1.7 Hz, 1H), 6.09 (d, *J* = 1.0 Hz, 1H), 5.58 (dd, *J* = 17.1, 10.6 Hz, 1H), 5.11 (dd, *J* = 17.1, 1.6 Hz, 1H), 4.86 (dd, *J* = 10.6, 1.6 Hz, 1H), 4.06 (s, 1H), 2.96 (dd, *J* = 11.3, 6.3 Hz, 1H), 2.01 – 1.64 (m, 6H). **^{13}C NMR** (126 MHz, $CDCl_3$) δ 197.36, 150.24, 141.94, 135.69, 111.10, 81.84, 52.51, 40.68, 29.46, 23.20. **HRMS** (ESI) *m/z* calcd for $C_{10}H_{14}NaO_2$ [$(M+Na)^+$]: 189.0886, measured: 189.0880.

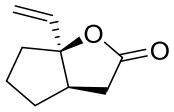
Keto-acid 4.51



To *t*-butyl ester **4.47** (1.3517 g, 6.818 mmol) was added 6.8 mL conc. HCl and the biphasic mixture stirred 15 mins until homogeneous, at which time it had also darkened in colour. The reaction was extracted with 3x20 mL EtOAc followed by 3x20 mL of 3:1 $CHCl_3$ / ^{i}PrOH. The EtOAc layers were washed sequentially with 3 mL water and brine, while the $CHCl_3$ layers were washed with 10 mL brine. The combined organic layers were dried over anhydrous Na_2SO_4 and $MgSO_4$, filtered, and concentrated. Silica gel flash chromatography with 60% EtOAc / hexanes (R_f 0.13, 33% EtOAc / hexanes) afforded 0.8172 g or 84% yield of carboxylic acid **4.51** as an off-white solid. The characterization data are in agreement with the literature.[47] **IR** ν_{max} (neat substance, cm^{-}

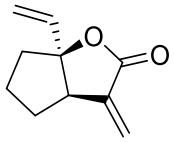
[1]): 3550 – 2500 (very broad), 2965, 2881, 1706, 1454, 1402, 1323, 1269, 1238, 1183, 1158, 1117, 1029. **^{1}H NMR** (500 MHz, $CDCl_3$) δ 10.18 (bs, 1H), 2.84 – 2.74 (m, 1H), 2.53 – 2.42 (m, 2H), 2.43 – 2.29 (m, 2H), 2.24 – 2.13 (m, 1H), 2.13 – 2.03 (m, 1H), 1.90 – 1.76 (m, 1H), 1.64 (qd, *J* = 11.7, 6.6 Hz, 1H). **^{13}C NMR** (126 MHz, $CDCl_3$) δ 219.44, 176.27, 45.62, 37.51, 33.71, 29.50, 20.76.

Vinyl lactone 4.52



To a solution of carboxylic acid **4.51** (0.7600 g, 5.346 mmol, 1 equiv) in 50 mL dry THF at –78 °C was added vinylmagnesium bromide (1.0 M THF, 11.8 mL, 2.2 equiv) fast dropwise, after which the reaction was allowed to warm to room temperature in the bath. After stirring for a total of 18 h, 10 mL of sat. aq. NH_4Cl and 20 mL water were added over an ice bath and the THF was removed *in vacuo*, then the aqueous was extracted with 3x30 mL EtOAc. The combined organic layers were washed sequentially with 10 mL each water and brine, then dried over anhydrous Na_2SO_4, filtered, and concentrated. The crude residue was taken up in 20 mL of 1:1 Et_2O / THF and a drop of conc. H_2SO_4 was added, then the reaction stirred overnight to complete lactonization of the desired isomer, after which it was quenched by addition of 5 mL sat. aq. $NaHCO_3$ and concentrated. The aqueous was diluted with water and extracted with 3x20 mL EtOAc. The combined organic layers were washed with 5 mL brine then dried over anhydrous Na_2SO_4, filtered, and concentrated. Silica gel flash chromatography with 25% EtOAc / hexanes (R_f 0.49, 50% EtOAc / hexanes) afforded 0.3637 g or 48% yield of lactone **4.52** as a clear colourless liquid. The characterization data are in agreement with the literature.[42] **IR** ν_{max} (neat liquid, cm^{-1}): 3091, 2960, 2875, 1765, 1643, 1416, 1207, 1187, 1154, 1107, 1049, 966. **^{1}H NMR** (500 MHz, $CDCl_3$) δ 5.92 (dd, *J* = 17.2, 10.8 Hz, 1H), 5.32 (dt, *J* = 17.2, 0.8 Hz, 1H), 5.13 (dd, *J* = 10.8, 0.9 Hz, 1H), 2.80 (dd, *J* = 18.2, 9.5 Hz, 1H), 2.61 (tdd, *J* = 9.5, 4.1, 1.9 Hz, 1H), 2.30 (dd, *J* = 18.1, 1.9 Hz, 1H), 2.17 – 2.07 (m, 1H), 2.07 – 1.97 (m, 1H), 1.86 – 1.72 (m, 3H), 1.63 – 1.52 (m, 1H). **^{13}C NMR** (126 MHz, $CDCl_3$) δ 177.28, 138.89, 113.63, 96.43, 43.74, 38.89, 36.00, 33.97, 24.54. **HRMS** (ESI) *m/z* calcd for $C_9H_{13}O_2$ $[(M+H)^+]$: 153.09101, measured: 153.09075, *m/z* calcd for $C_9H_{12}NaO_2$ $[(M+Na)^+]$: 175.07295, measured: 175.07270.

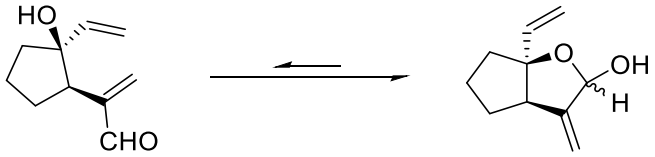
Lactone 4.53



To a solution of diisopropylamine (0.54 mL, 3.7 mmol, 1.2 equiv) in 10 mL dry THF at –78 °C was added *n*-BuLi (2.75 M in hexane, 1.28 mL, 1.1 equiv) dropwise, then the solution stirred 2 mins. A solution of lactone **4.52** (1.051 g/mL, 0.465 mL, 3.21 mmol, 1 equiv) in 7.8 mL dry THF was then added dropwise by cannula, and the mixture stirred 30 mins. A suspension of *N,N*-dimethylmethyleneiminium iodide (Eschenmoser's salt; 1.1915 g, 2.0 equiv) was then added in ca. 40 mL THF and the suspension allowed to warm to room temperature overnight. The reaction was concentrated, the residue taken up in 10 mL MeOH, 2.5 mL MeI was added, and the solution stirred 28 h. This solution was concentrated to a dark syrup, which was then taken up in 150 mL of 1:2 DCM / 5% aq. $NaHCO_3$ and stirred 15 mins. The layers were separated and the aqueous extracted further with 4x50 mL DCM. The combined organic layers were washed with 10 mL brine, then dried over anhydrous Na_2SO_4, filtered, and concentrated. Further extraction with 3x80 mL EtOAc was conducted after acidifying the aqueous layer to pH < 1 with 2 M HCl. These combined organic layers were washed sequentially with 10 mL each water and brine, then dried over anhydrous Na_2SO_4, filtered, and concentrated. Silica gel flash chromatography of the combined crude extracts with 10-20% EtOAc / hexanes (R_f 0.53, 33% EtOAc / hexanes) afforded 0.2336 g or 44% of methylene lactone **4.53** as a yellow liquid. **IR** ν_{max} (neat liquid, cm^{-1}): 3096, 2961, 2872, 1754, 1662, 1643, 1436, 1274, 1182, 1108, 1081, 1061. **^{1}H NMR** (400 MHz, $CDCl_3$) δ 6.25 (d, *J* = 2.3 Hz, 1H), 5.93 (dd, *J* = 17.2, 10.8 Hz, 1H), 5.63 (d, *J* = 2.0 Hz, 1H), 5.34 (dd, *J* = 17.2, 0.8 Hz, 1H), 5.13 (dd, *J* = 10.8, 0.8 Hz, 1H), 3.16 (dd, *J* = 9.2, 2.0 Hz, 1H), 2.16 – 2.03 (m, 2H), 1.83 – 1.62 (m, 4H). **^{13}C NMR** (126 MHz, $CDCl_3$) δ 170.62, 140.74, 139.09, 123.28, 113.95, 93.28, 49.23, 38.98, 36.29, 24.50. **HRMS** (ESI) *m/z* calcd for $C_{10}H_{12}NaO_2$ [$(M+Na)^+$]: 187.0730, measured: 187.0722.

Note: Simple heating of lactone **4.52** with 1.1 equiv each paraformaldehyde and K_2CO_3 in DMF produced only 13-14% yield of the desired methylene lactone.

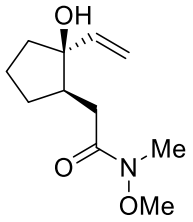
Aldehyde – hemiacetal 4.50



To a solution of methylene lactone **4.53** (60.8 mg, 0.370 mmol, 1 equiv) in 3.7 mL dry PhMe at –78 °C was added DiBAL-H (25% in PhMe, 0.275 mL, 1.1 equiv) dropwise and the solution allowed to warm in the bath for 13 h. Fieser's workup was conducted, and the resulting suspension filtered on celite then concentrated. Silica gel flash chromatography with 10-15% EtOAc / pentane (R_f 0.40, 33% EtOAc / hexanes) afforded 22.8 mg or 31% of lactol **4.50** as a colourless liquid. **IR** ν_{max} (thin film, cm^{-1}): 3407 (broad), 3085, 2955, 2868, 1692, 1640, 1448, 1434, 1408, 1336, 1318, 1279, 1252, 1153, 1098, 1057, 992, 966. *All integrals of signals clearly arising from the aldehyde tautomer are reported as integers, but integrals from signals partly or fully arising from either hemiacetal are reported to two decimal places.* **^{1}H NMR** (500 MHz, $CDCl_3$) δ 9.47 (s, 1H), 6.48 (s, 1H), 6.16 (s, 1H), 6.10 (dd, *J* = 17.2, 10.7 Hz, 10.65H), 5.88 (dd, *J* = 17.2, 10.7 Hz, 1H), 5.85 (dd, *J* = 17.1, 10.6 Hz, 6.49H), 5.72 (dq, *J* = 7.2, 1.6 Hz, 10.78H), 5.64 (dt, *J* = 7.8, 1.8 Hz, 6.74H), 5.36 (dd, *J* = 17.2, 1.5 Hz, 11.52H), 5.28 (dd, *J* = 17.1, 1.5 Hz, 7.30H), 5.23 (dd, *J* = 2.0, 1.3 Hz, 11.57H), 5.22 (t, *J* = 2.0 Hz, 7.38H), 5.12 (dd, *J* = 17.2, 1.2 Hz, 1H), 5.09 (t, *J* = 1.7 Hz, 11.59H), 5.08 (t, *J* = 1.9 Hz, 7.48), 5.03 (dd, *J* = 10.7, 1.5 Hz, 11.22H), 5.00 (dd, *J* = 10.6, 1.5 Hz, 7.44H), 4.97 (dd, *J* = 10.7, 1.3 Hz, 1H), 3.34 (d, *J* = 7.8 Hz, 6.84H), 3.11 – 3.05 (m, 1H), 3.05 (d, *J* = 7.3 Hz, 11.17H), 3.00 (dt, *J* = 9.3, 1.8 Hz, 11.05H), 2.86 (dq, *J* = 9.3, 2.5 Hz, 6.84H), 2.01 – 1.83 (m, 55.49H), 1.76 (s, 9.66H), 1.70 – 1.56 (m, 66.28H). **^{13}C NMR** (126 MHz, $CDCl_3$) δ 194.95, 155.37 (broad, *HMBC correlations from both lactols*), 148.05, 143.23, 143.18, 141.73, 137.08, 112.44, 112.26, 111.81, 109.79, 109.48, 100.30, 99.23, 95.59, 93.28, 82.02, 51.87, 51.30, 46.88, 40.31, 40.21, 40.01, 35.21, 35.15, 29.09, 24.79, 24.66, 21.47. **HRMS** (ESI) *m/z* calcd for $C_{10}H_{14}NaO_2$ [$(M+Na)^+$]: 189.08860, measured: 189.08783.

Note: This decomposed slowly over 14 h when subjected to the standard catalytic conditions according to General Procedure **E** (*vide infra*). Standard conditions at 50 °C in a sealed 1 dr. vial caused decomposition within just 3 h.

***N*-methoxy-*N*-methyl amide alcohol 4.54**



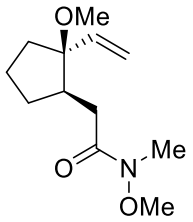
To a suspension of *N,O*-dimethylhydroxylamine hydrochloride (0.3233 g, 3.314 mmol, 3.0 equiv) in 1.8 mL dry DCM at –78 °C was added trimethylaluminum (2 M PhMe, 1.66 mL, 3.0 equiv) dropwise, then the bath was removed and the reaction stirred overnight. A solution of lactone **4.52** (0.1684 g, 1.107 mmol, 1 equiv) in 1.5 mL dry DCM was then added dropwise over an ice bath, then the bath was removed and the mixture stirred 2.5 h further. The reaction was again cooled over ice and 2.5 mL sat. aq. sodium potassium tartrate was carefully added dropwise, then the suspension stirred briefly and filtered on celite. The filtrate was diluted with 35 mL water and extracted with 3x30 mL EtOAc. The combined organic layers were washed sequentially with 20 mL each water and brine, then dried over anhydrous Na_2SO_4, filtered, and concentrated. Silica gel flash chromatography with 50% EtOAc / hexanes (R_f 0.22) afforded 0.1057 g or 45% of amide **4.54** as a nearly colourless clear liquid. **IR** ν_{max} (neat liquid, cm^{-1}): 3443 (broad), 3088, 2940, 2872, 2824, 1638, 1461, 1441, 1414, 1385, 1300, 1277, 1174, 1108, 993, 914. **^{1}H NMR** (500 MHz, $CDCl_3$) δ 5.87 (dd, *J* = 17.2, 10.7 Hz, 1H), 5.28 (d, *J* = 17.2 Hz, 1H), 5.08 (d, *J* = 10.7 Hz, 1H), 3.69 (s, 3H), 3.14 (s, 3H), 2.56 (dd, *J* = 15.0, 6.4 Hz, 1H), 2.42 (dd, *J* = 14.8, 7.1 Hz, 1H), 2.35 (bs, 1H), 2.22 (dq, *J* = 10.8, 7.3 Hz, 1H), 1.99 (dtd, *J* = 12.0, 8.2, 3.5 Hz, 1H), 1.90 – 1.77 (m, 2H), 1.76 – 1.63 (m, 2H), 1.62 – 1.50 (m, 1H). **^{13}C NMR** (126 MHz, $CDCl_3$) δ 174.63 (*observed by HMBC*), 144.11, 112.23, 82.41, 61.55, 45.63, 40.98, 32.34 (broad), 31.16 (broad), 30.49, 21.86. **HRMS** (ESI) *m/z* calcd for $C_{11}H_{19}NNaO_3$ [$(M+Na)^+$]: 236.1257, measured: 236.1255.

General Procedure D for methylation of alcohols with KH:

To a 0.1 M solution of the tertiary alcohol in dry THF, cooled over an ice bath, was added 3 equiv KH (oil-free basis), followed by 5 equiv MeI, and the reaction followed by TLC while being allowed to warm in the bath. Once the alcohol was fully consumed, sat. aq. NH_4Cl and H_2O were added over a fresh ice bath, and this was stirred briefly prior to extraction until a clear biphasic solution was achieved.

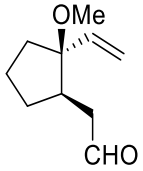
Note: The KH was often freed from oil before use by washing with pentane or hexanes and collected by filtration, but this was not necessary. The wt. % of the oil dispersion was determined by this method for direct use.

_N_-methoxy-_N_-methyl amide methyl ether 4.55



General Procedure **D** was followed using alcohol **4.54** (97.3 mg, 0.456 mmol, 1 equiv), taking 12 h. To quench, 2 mL each sat. aq. NH_4Cl and water were added, THF removed *in vacuo*, and the aqueous layer extracted with 3x10 mL EtOAc. The combined organic layers were washed sequentially with 3 mL each water and brine, then dried over anhydrous Na_2SO_4, filtered, and concentrated. Silica gel flash chromatography with 25-30% EtOAc / hexanes (R_f 0.20, 25% EtOAc / hexanes) afforded 71.9 mg or 69% yield of ether **4.55** as a clear colourless liquid. **IR** ν_{max} (neat liquid, cm^{-1}): 3080, 2959, 2939, 2873, 2824, 1662, 1461, 1445, 1411, 1382, 1348, 1303, 1177, 1106, 1065, 998, 921. **^{1}H NMR** (500 MHz, $CDCl_3$) δ 5.71 (dd, *J* = 17.4, 11.1 Hz, 1H), 5.18 (dd, *J* = 11.0, 1.6 Hz, 1H), 5.17 (dd, *J* = 17.4, 1.6 Hz, 1H), 3.68 (s, 3H), 3.16 (s, 3H), 3.13 (s, 3H), 2.58 (d, *J* = 15.1 Hz, 1H), 2.41 (dd, *J* = 15.8, 10.0 Hz, 1H), 2.20 (qd, *J* = 9.9, 3.5 Hz, 1H), 2.10 – 1.95 (m, 2H), 1.72 – 1.57 (m, 3H), 1.48 (dq, *J* = 12.5, 8.9, 8.3 Hz, 1H). **^{13}C NMR** (126 MHz, $CDCl_3$) δ 174.92 (*observed by HMBC*), 139.52, 115.12, 87.27, 61.33, 50.63, 45.56, 32.36, 31.90, 30.78, 29.85, 21.22. **HRMS** (ESI) *m/z* calcd for $C_{12}H_{21}NNaO_3$ [$(M+Na)^+$]: 250.1414, measured: 250.1415.

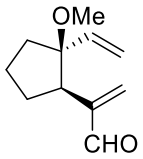
Aldehyde 4.56



To a solution of amide **4.55** (66.0 mg, 0.2904 mmol, 1 equiv) in 3.0 mL dry PhMe at –78 °C was added DiBAL-H (25% in PhMe, 0.215 mL, 1.1 equiv) dropwise and the solution was stirred 2 h.

Fieser's workup was conducted, and the resulting suspension filtered on celite then concentrated. Silica gel flash chromatography with 10-20% Et_2O / hexanes (R_f 0.52, 25% EtOAc / hexanes) afforded 32.5 mg or 67% of aldehyde **4.56** as a clear colourless oil. **IR** ν_{max} (thin film, cm^{-1}): 3087, 2946, 2875, 2825, 2715, 1721, 1638, 1449, 1407, 1389, 1364, 1307, 1213, 1184, 1120, 1067, 997. **^{1}H NMR** (500 MHz, $CDCl_3$) δ 9.77 (t, *J* = 2.0 Hz, 1H), 5.68 (dd, *J* = 17.5, 10.9 Hz, 1H), 5.22 – 5.13 (m, 2H), 3.10 (s, 3H), 2.60 (dd, *J* = 17.2, 4.2 Hz, 1H), 2.40 (ddd, *J* = 17.2, 8.9, 1.8 Hz, 1H), 2.14 (qd, *J* = 9.0, 4.4 Hz, 1H), 2.09 – 2.01 (m, 1H), 2.03 – 1.92 (m, 1H), 1.75 – 1.55 (m, 3H), 1.54 – 1.45 (m, 1H). **^{13}C NMR** (126 MHz, $CDCl_3$) δ 203.21, 139.35, 115.56, 86.96, 50.60, 44.42, 43.24, 31.63, 29.50, 21.43. **HRMS** (ESI) *m/z* calcd for $C_{10}H_{16}NaO_2$ [$(M+Na)^+$]: 191.1043, measured: 191.1034.

Enal 4.57



To neat aldehyde **4.56** (30.5 mg, 0.181 mmol, 1 equiv) was added 450 µL of a pyrrolidine solution (0.040 M in DCM), followed by *p*-methoxybenzoic acid (2.7 mg, 0.0018 mmol, 0.1 equiv), then aq. formaldehyde (37 wt.%, 15 µL, 0.20 mmol, 1.1 equiv). The solution was immersed in a 45 °C oil bath for 1.5 h,[46] then cooled and chromatographed directly. Silica gel flash chromatography with 10% Et_2O / pentane (R_f 0.48, 33% EtOAc / hexanes) afforded 26.4 mg or 81% yield of enal **4.57** as a clear colourless liquid. **IR** ν_{max} (thin film, cm^{-1}): 2956, 2922, 2853, 1729, 1695, 1462, 1377, 1260, 1157, 1098, 1072, 1025. **^{1}H NMR** (500 MHz, $CDCl_3$) δ 9.48 (s, 1H), 6.60 (s, 1H), 6.13 (d, *J* = 1.0 Hz, 1H), 5.62 (dd, *J* = 17.5, 11.0 Hz, 1H), 5.10 (dd, *J* = 10.9, 1.4 Hz, 1H), 5.08 (dd, *J* = 17.5, 1.4 Hz, 1H), 3.10 (s, 3H), 2.98 (dd, *J* = 10.3, 8.7 Hz, 1H), 2.15 – 2.06 (m, 1H), 1.99 – 1.89 (m, 1H), 1.86 – 1.67 (m, 4H). **^{13}C NMR** (126 MHz, $CDCl_3$) δ 195.18, 148.24, 138.98, 137.40, 115.24, 86.73, 50.61, 46.06, 31.65, 30.08, 21.10. **HRMS** (ESI) *m/z* calcd for $C_{11}H_{16}NaO_2$ [$(M+Na)^+$]: 203.10425, measured: 203.10383.

General Procedure E for the catalytic oxy-Cope / Michael reaction:

From a solution of the substrate and the internal standard mesitylene (1 equiv) in $MeNO_2$ was taken an aliquot for ^{1}H NMR analysis, then water was added followed by a solution of 0.04-0.07

M preformed catalyst salt solution in $MeNO_2$ dropwise at room temperature, to give a final reaction solution with a catalyst loading of 10 mol% and a substrate concentration of 0.2 M in 9:1 $MeNO_2$ / water. The reaction was monitored by ^1H NMR analysis of aliquots until full consumption of the starting material was observed. The reaction was diluted with 5 mL EtOAc and poured into 5-10 mL each of water and 0.1 N HCl, depending on scale. This was extracted with 3x15-30 mL EtOAc and the combined organic layers were sequentially washed with 2-5 mL each sat. $NaHCO_3$, water, and brine, then dried over anhydrous Na_2SO_4, filtered, and concentrated.

Note 1: The catalyst solution was routinely prepared fresh on the day of use by adding a $MeNO_2$ solution of $HNTf_2$ to an equal volume of $MeNO_2$ solution of diazepane carboxylate catalyst. A variety of acid salts of these hydrazide catalysts were alternatively prepared by addition of aqueous acid to the neutral hydrazide in MeCN, then concentrated and dried with PhMe azeotropic distillation and recovered in solid crystalline form. However, despite appearing only slightly hygroscopic, it was found in the course of this work that catalyst salts which had been stored in solid crystalline form were inferior to those which had been freshly prepared in $MeNO_2$ solution directly from the desired acid and neutral diazepane carboxylate. This proved true despite subsequent efforts to remove water absorbed by the crystals through further azeotropic distillation with PhMe and drying under reduced pressure.

Note 2: Since the quality of the $HNTf_2$, purchased from TCI America, appeared critical for optimal performance, it was refrigerated in a desiccator jar under argon and was only handled with glass implements.

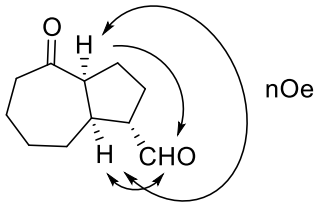
Note 3: At least two different bottles of $MeNO_2$ were used for catalytic reactions in the course of this work, with no apparent difference whatsoever. The biphasic conditions employed negate any issues stemming from variability in water content.

Note 4: All diastereomeric ratios (*d.r.*) reported are based on integration of the product aldehyde doublet signals in ^1H NMR spectra. In a few cases, both epimers formed were characterized and reported, but in other cases the minor product is simply assumed to be the minor epimer defined by the aldehyde α-carbon.

Note 5: As explained in the optimization of the reaction, excess acid is deleterious to the stability of the alcohol substrates, and therefore the hydrazide salts should be pre-formed rather than adding

strong acid to the other components. Additionally, care must be taken to always ensure a slight excess of hydrazide relative to acid.

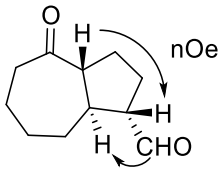
Ketone 4.58



General Procedure **E** was followed using aldehyde **4.23** (0.1935 g, 1.074 mmol) and the reaction was complete in 60 h in 68% yield as determined by ^{1}H NMR analysis, as a 95:5 mixture of isomers. Silica gel flash chromatography with 10-40% Et_2O / pentane (R_f 0.30, 40% Et_2O / hexanes), followed by filtering through cotton, afforded 0.1309 g or 68% yield of ketone **4.58** as a clear colourless liquid and a single stereoisomer. **IR** ν_{max} (thin film, cm^{-1}): 2932, 2865, 1720, 1700, 1449, 1166. **^{1}H NMR** (500 MHz, $CDCl_3$) δ 9.61 (d, *J* = 2.5 Hz, 1H), 3.20 (dt, *J* = 10.4, 8.2 Hz, 1H), 2.60 (tdd, *J* = 10.5, 7.7, 2.4 Hz, 1H), 2.49 (ddd, *J* = 13.5, 9.7, 3.6 Hz, 1H), 2.41 – 2.30 (m, 2H), 2.11 (dtd, *J* = 12.2, 10.1, 9.6, 7.6 Hz, 1H), 2.00 – 1.89 (m, 2H), 1.81 – 1.61 (m, 4H), 1.59 – 1.48 (m, 2H), 1.22 – 1.10 (m, 1H). **^{13}C NMR** (126 MHz, $CDCl_3$) δ 212.55, 202.72, 59.94, 54.59, 43.23, 40.32, 31.92, 27.65, 26.67, 25.64, 24.45. **HRMS** (ESI) *m/z* calcd for $C_{11}H_{16}NaO_2$ [$(M+Na)^+$]: 203.1043, measured: 203.1039.

Note: This compound was subsequently treated with 1 M NaOH (vol/vol with THF) at room temperature for 6 d and followed by ^{1}H NMR, then the layers were separated. The crude mixture obtained from the concentrate indicated a 23:77 ratio of this ketone to the diastereomeric ketone product *epi*-**4.58** obtained from diastereomeric enal *epi*-**4.23**. This supports the stated assignments of each as the *cis* and *trans* hydroazulenes since the *trans* is expected to be slightly thermodynamically favoured in such scaffolds, and closely matches ratios obtained by base isomerization.[48,49]

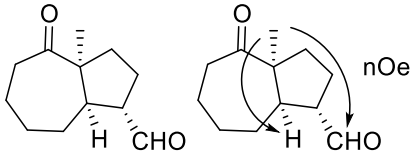
Ketone *epi*-4.58



General Procedure **E** was followed using aldehyde *epi*-**4.23** (0.3383 g, 1.877 mmol) and the reaction complete in 90 mins, in 96% yield with a 4:1 mixture of stereoisomers, as determined by ^{1}H NMR analysis. It should be noted that extraction was performed with 3x25 mL Et_2O rather than EtOAc, and this was dried over anhydrous $MgSO_4$. A 9:1 *d.r.* was observed for the products in the crude material. Silica gel flash chromatography with 50-60% Et_2O / pentane (R_f 0.20, 20% EtOAc / hexanes), followed by filtering through cotton, afforded 0.3140 g or 93% yield of ketone *epi*-**4.58** in >20:1 *d.r.* as a clear, pale yellow liquid. **IR** ν_{max} (thin film, cm^{-1}): 2924, 2855, 2715, 1717, 1695, 1449, 1359, 1197. **^{1}H NMR** (500 MHz, $CDCl_3$) δ 9.53 (d, *J* = 3.1 Hz, 1H), 2.91 (dt, *J* = 10.9, 8.4 Hz, 1H), 2.56 (dt, *J* = 18.6, 3.5 Hz, 1H), 2.47 – 2.33 (m, 2H), 2.22 – 2.11 (m, 1H), 2.11 – 2.03 (m, 1H), 2.03 – 1.96 (m, 1H), 1.96 – 1.62 (m, 6H), 1.45 – 1.20 (m, 2H). **^{13}C NMR** (126 MHz, $CDCl_3$) δ 212.35, 202.66, 59.69, 57.20, 45.03, 43.69, 35.64, 28.85, 25.59, 25.26, 23.25. **HRMS** (ESI) *m/z* calcd for $C_{11}H_{16}NaO_2$ [$(M+Na)^+$]: 203.1043, measured: 203.1042.

Note: The changing *d.r.* reflects the labile stereocentre adjacent to the aldehyde, indicating that isomerization at this position is possible under the reaction conditions, on workup, and during silica gel chromatography. No isomerization was observed at the hydrazulene ring fusion.

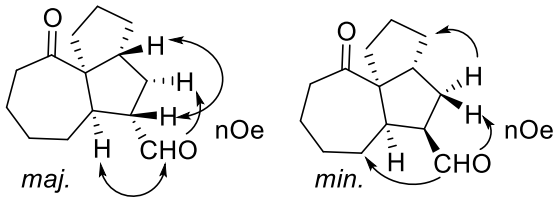
Ketone 4.62



General Procedure **E** was followed using aldehyde **4.26** (0.1599 g, 0.8231 mmol) and the reaction was complete in 60 mins in 98% yield as determined by ^{1}H NMR analysis, with a 20:1 ratio of stereoisomers. Silica gel flash chromatography 30-40% ethyl ether / pentane (R_f 0.21, 20% EtOAc / hexanes), followed by filtering through cotton, afforded 0.1343 g or 84% yield of ketone **4.62** as a colourless liquid and single isomer, along with a 23.8 mg quantity of ketone **4.62** as a mixture of

epimers, for a combined 99% yield. **IR** ν_{max} (thin film, cm^{-1}): 2932, 2866, 1720, 1699, 1459, 1447. **^{1}H NMR** (500 MHz, $CDCl_3$) δ 9.68 (d, *J* = 2.1 Hz, 1H), 2.74 (td, *J* = 11.6, 3.2 Hz, 1H), 2.50 (dddd, *J* = 10.2, 8.2, 5.7, 2.1 Hz, 1H), 2.35 (dddd, *J* = 11.1, 6.9, 2.6, 1.3 Hz, 1H), 2.18 – 2.06 (m, 2H), 1.96 (dddd, *J* = 13.0, 8.9, 7.4, 1.7 Hz, 1H), 1.89 – 1.75 (m, 3H), 1.65 (ddd, *J* = 14.7, 6.5, 1.8 Hz, 1H), 1.56 – 1.40 (m, 3H), 1.27 (dtd, *J* = 14.6, 11.2, 1.7 Hz, 1H), 1.16 (s, 3H). **^{13}C NMR** (126 MHz, $CDCl_3$) δ 215.19, 202.49, 60.55, 59.20, 47.77, 40.48, 35.26, 33.47, 28.99, 27.05, 25.30, 24.24. **HRMS** (ESI) *m/z* calcd for $C_{12}H_{18}NaO_2$ [$(M+Na)^+$]: 217.1199, measured: 217.1194.

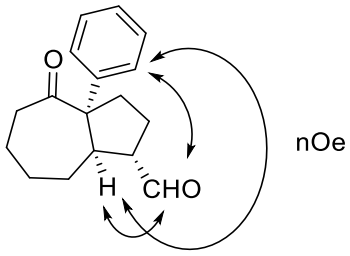
Ketone 4.63



General Procedure **E** was followed using aldehyde **4.27** (0.1502 g, 0.6818 mmol) and the reaction was complete in 30 mins in quantitative yield as determined by ^{1}H NMR analysis. Silica gel flash chromatography with 20-40% EtOAc / hexanes (R_f 0.24 and 0.28 (major isomer), 20% EtOAc / hexanes), followed by filtering twice through cotton, afforded 0.1375 g or 92% yield of ketone **4.63** as a colourless liquid and a 3:1 mixture of diastereomers, as determined by ^{1}H NMR. Further chromatography with 20% EtOAc / hexanes yielded analytically pure samples of each epimer, with the major isomer eluting first. *Major isomer:* **IR** ν_{max} (thin film, cm^{-1}): 2930, 2862, 2709, 1719, 1690, 1447, 1336, 1315, 1229, 1155, 1098, 1060, 1039. **^{1}H NMR** (500 MHz, $CDCl_3$) δ 9.60 (d, *J* = 2.7 Hz, 1H), 3.00 (q, *J* = 7.9 Hz, 1H), 2.71 (ddd, *J* = 12.6, 9.8, 3.9 Hz, 1H), 2.57 (dtd, *J* = 10.3, 7.4, 2.7 Hz, 1H), 2.38 (ddd, *J* = 12.4, 8.2, 3.1 Hz, 1H), 2.26 (td, *J* = 9.4, 2.4 Hz, 1H), 2.11 (dt, *J* = 12.7, 7.7 Hz, 1H), 2.03 (dt, *J* = 12.3, 7.5 Hz, 1H), 1.84 – 1.43 (m, 11H), 1.36 (qd, *J* = 10.3, 4.6 Hz, 1H). **^{13}C NMR** (126 MHz, $CDCl_3$) δ 213.21, 203.05, 70.52, 59.51, 48.82, 45.31, 40.46, 37.78, 33.19, 31.84, 31.64, 25.90, 25.59, 24.49. **HRMS** (ESI) *m/z* calcd for $C_{14}H_{20}NaO_2$ [$(M+Na)^+$]: 243.1356, measured: 243.1358. *Minor isomer:* **IR** ν_{max} (thin film, cm^{-1}): 2930, 2860, 2708, 1717, 1696, 1447, 1346, 1333, 1316, 1261, 1220, 1166, 1117, 1089, 1044. **^{1}H NMR** (800 MHz, $CDCl_3$) δ 9.85 (d, *J* = 0.9 Hz, 1H), 3.09 (q, *J* = 8.2 Hz, 1H), 2.98 (dtd, *J* = 12.6, 6.6, 1.1 Hz, 1H), 2.73 (ddd, *J* = 12.8, 11.0, 2.9 Hz, 1H), 2.48 – 2.43 (m, 2H), 2.12 – 2.05 (m, 1H), 2.05 (td, *J* = 12.8, 9.4 Hz, 1H), 2.01 – 1.97 (m, 1H), 1.96 – 1.88 (m, 2H), 1.64 – 1.57 (m, 3H), 1.51 (dd, *J* =

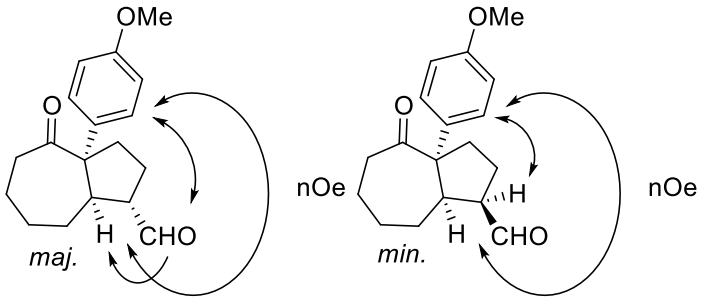
13.1, 6.6 Hz, 1H), 1.48 – 1.39 (m, 2H), 1.35 – 1.28 (m, 1H), 1.21 (ddt, *J* = 13.1, 10.6, 6.6 Hz, 1H), 1.08 – 1.01 (m, 1H). **^{13}C NMR** (201 MHz, $CDCl_3$) δ 213.02, 204.30, 72.41, 54.86, 49.35, 41.94, 39.73, 39.28, 35.83, 30.81, 30.24, 29.06, 27.56, 25.92. **HRMS** (ESI) *m/z* calcd for $C_{14}H_{20}NaO_2$ [$(M+Na)^+$]: 243.1356, measured: 243.1351.

Ketone 4.64



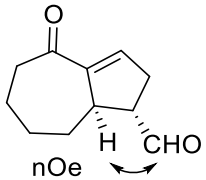
General procedure **E** was followed using aldehyde **4.28** (0.1517 g, 0.5918 mmol) and the reaction was complete in 5 h in 99% yield as determined by ^{1}H NMR analysis. A trace quantity of the epimer was observed in the reaction and crude mixtures. Silica gel flash chromatography with 20-40% EtOAc / hexanes (R_f 0.28, 20% EtOAc / hexanes) afforded 0.1476 g or 97% yield of ketone **4.64** as a pale yellow liquid and essentially one stereoisomer. **IR** ν_{max} (neat liquid, cm^{-1}): 2931, 2860, 1718, 1699, 1495, 1445. **^{1}H NMR** (500 MHz, acetone-d_6) δ 9.80 (d, *J* = 1.4 Hz, 1H), 7.40 – 7.33 (m, 2H), 7.34 – 7.28 (m, 2H), 7.30 – 7.23 (m, 1H), 3.28 (dd, *J* = 10.59, 5.8 Hz, 1H), 2.68 – 2.59 (m, 1H), 2.42 (td, *J* = 12.9, 6.3 Hz, 1H), 2.35 (td, *J* = 12.0, 3.3 Hz, 1H), 2.12 – 2.02 (m, 1H), 1.91 – 1.78 (m, 4H), 1.78 – 1.69 (m, 1H), 1.64 – 1.51 (m, 1H), 1.50 – 1.32 (m, 3H). **^{13}C NMR** (101 MHz, acetone-d_6) δ 210.91, 202.47, 143.27, 129.65, 127.80, 127.48, 69.09, 61.51, 41.95, 41.90, 36.75, 36.10, 29.66, 26.98, 24.39. **HRMS** (ESI) *m/z* calcd for $C_{17}H_{20}NaO_2$ [$(M+Na)^+$]: 279.1356, measured: 279.1345.

Ketone 4.65



General procedure **E** was followed using aldehyde **4.29** (0.4609 g, 1.609 mmol) and the reaction was complete in 2 h in 78% yield as determined by ^{1}H NMR analysis, as a 95:5 mixture of epimers at the aldehyde-bearing carbon. Silica gel flash chromatography with 20-30% EtOAc / hexanes (R_f 0.19, 20% EtOAc / hexanes) afforded 0.2695 g or 58% yield of ketone **4.65** as a clear colourless oil, along with 4.2 mg or 1% yield of a 83:17 mixture favouring the minor epimer as a colourless film. *Major isomer:* **IR** ν_{max} (thin film, cm^{-1}): 2930, 2860, 2715, 1718, 1698, 1607, 1579, 1510, 1445, 1250, 1184, 1031. **^{1}H NMR** (500 MHz, $CDCl_3$) δ 9.75 (d, *J* = 1.4 Hz, 1H), 7.18 (d, *J* = 8.9 Hz, 2H), 6.87 (d, *J* = 8.9 Hz, 2H), 3.79 (s, 3H), 3.17 (dd, *J* = 10.5, 5.4 Hz, 1H), 2.61 – 2.51 (m, 1H), 2.44 – 2.33 (m, 2H), 2.17 (ddd, *J* = 11.1, 6.6, 2.4 Hz, 1H), 1.97 – 1.71 (m, 5H), 1.58 – 1.37 (m, 4H). **^{13}C NMR** (126 MHz, $CDCl_3$) δ 212.08, 202.25, 158.76, 133.70, 127.97, 114.39, 67.87, 61.21, 55.37, 41.54, 41.46, 35.97, 35.75, 29.41, 26.54, 24.20. **HRMS** (APCI) *m/z* calcd for $C_{18}H_{23}O_3$ [(M+H)$^+$]: 287.16417, measured: 287.16402. *Minor isomer:* **IR** ν_{max} (thin film, cm^{-1}): 2931, 2857, 2720, 1717, 1699, 1607, 1510, 1445, 1429, 1252, 1184, 1111, 1032. *By comparison to the data from the epimer, peaks arising from that isomer are not picked, integrated, or reported here.* **^{1}H NMR** (500 MHz, $CDCl_3$) δ 9.84 (d, *J* = 1.9 Hz, 1H), 7.32 (d, *J* = 8.9 Hz, 2H), 6.89 (d, *J* = 8.9 Hz, 2H), 3.80 (s, 3H), 3.27 (dd, *J* = 10.8, 7.1 Hz, 1H), 3.08 (dt, *J* = 8.8, 7.0 Hz, 1H), 2.68 (ddd, *J* = 14.1, 10.5, 7.2 Hz, 1H), 2.54 – 2.46 (m, 1H), 2.43 – 2.30 (m, 1H), 2.20 – 1.62 (m, 12H), 1.58 – 1.44 (m, 5H). **^{13}C NMR** (126 MHz, $CDCl_3$) δ 211.69, 203.80, 158.88, 133.08, 127.81, 114.60, 68.74, 55.45, 54.98, 45.42, 41.26, 33.58, 30.56, 28.74, 27.52, 21.91. **HRMS** (ESI) *m/z* calcd for $C_{18}H_{22}NaO_3$ [(M+Na)$^+$]: 309.1461, measured: 309.1464.

Ketone 4.66

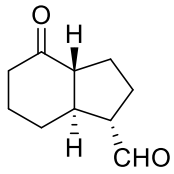


General Procedure **E** was followed using aldehyde *epi*-**4.30** (0.1336 g, 0.7496 mmol), except that no water was added and 50 mol% of catalyst was used. The reaction was complete in 8 d in 51% yield as determined by ^{1}H NMR analysis, with no other stereoisomers being observed in the reaction mixture. It should be noted that extraction was performed with 15 mL 0.1 N aq. HCl and 3x30 mL Et_2O rather than EtOAc, and the combined organic layers were washed sequentially with

1 mL each water and brine, then dried over anhydrous $MgSO_4$. An epimer ratio of 20:1 was observed in the crude mixture. Silica gel flash chromatography with 40-60% Et_2O / pentane (R_f 0.18, 40% Et_2O / hexanes), followed by chromatography with 0-2% Et_2O / DCM, afforded 64.8 mg or 49% yield of ketone **4.66** as a pale yellow oil and a 20:1 mixture of isomers. **IR** ν_{max} (thin film, cm^{-1}): 2921, 2852, 2719, 1721, 1677, 1607, 1485. **^{1}H NMR** (500 MHz, $CDCl_3$) δ 9.73 (d, *J* = 1.8 Hz, 1H), 6.69 (q, *J* = 2.5 Hz, 1H), 3.22 (dtd, *J* = 11.8, 4.2, 2.1 Hz, 1H), 2.84 (dtd, *J* = 9.5, 6.0, 1.8 Hz, 1H), 2.79 – 2.66 (m, 2H), 2.59 (dd, *J* = 13.4, 7.0 Hz, 1H), 2.51 (td, *J* = 13.1, 2.0 Hz, 1H), 2.08 – 1.95 (m, 3H), 1.68 – 1.54 (m, 1H), 1.46 (dtd, *J* = 22.3, 12.5, 1.6 Hz, 2H). **^{13}C NMR** (101 MHz, $CDCl_3$) δ 201.39, 199.86, 146.66, 139.47, 58.44, 45.92, 44.99, 37.29, 31.64, 30.67, 25.07. **HRMS** (ESI) *m/z* calcd for $C_{11}H_{13}O_2$ [$(M–H)^-$]: 177.09210, measured: 177.09175.

Note: Water was deleterious to catalytic rearrangement of alkyne substrate *epi*-**4.30**. In one experiment where the reaction had progressed, the reaction halted upon addition of water.

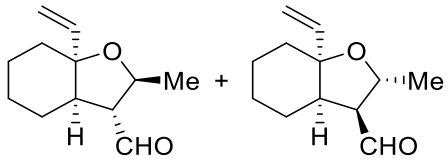
Ketone 4.67



General procedure **E** was followed using aldehyde *epi*-**4.50** (57.9 mg, 0.348 mmol) and the reaction was complete in 15 h in 80% yield as determined by ^{1}H NMR analysis, as a 10:1 mixture of epimers at the aldehyde-bearing carbon. It should be noted that extraction was performed with 2 mL 0.1 N aq. HCl and 3x8 mL Et_2O rather than EtOAc, and the combined organic layers were washed sequentially with 2 mL each water and brine, then dried over anhydrous $MgSO_4$. The crude isomer ratio reflected that observed in the reaction. Silica gel flash chromatography with 50% Et_2O / pentane (R_f 0.12, 20% EtOAc / hexanes) afforded 25.7 mg or 44% yield of aldehyde **4.67** as a clear colourless liquid. Some isomerization had occurred on silica, giving a final 71:10:9 ratio of isomers. **IR** ν_{max} (neat liquid, cm^{-1}): 2940, 2867, 2719, 1707, 1447, 1427, 1370, 1321, 1304, 1258, 1215, 1157, 1111, 1076, 1051. **^{1}H NMR** (500 MHz, $CDCl_3$) δ 9.59 (d, *J* = 3.3 Hz, 1H), 2.55 (dddd, *J* = 11.0, 9.9, 7.7, 3.3 Hz, 1H), 2.44 – 2.34 (m, 2H), 2.27 (tdd, *J* = 13.8, 6.6, 1.4 Hz, 1H), 2.18 – 2.11 (m, 1H), 2.10 – 2.04 (m, 1H), 1.98 – 1.76 (m, 5H), 1.68 (qt, *J* = 13.6, 13.1, 4.8 Hz, 1H), 1.49 (tdd, *J* = 12.9, 11.5, 3.9 Hz, 1H). **^{13}C NMR** (126 MHz, $CDCl_3$) *Signals arising from major isomer:*

δ 210.06, 202.68, 57.64, 57.13, 49.51, 41.35, 29.59, 27.40, 23.27, 22.52. *Signals arising from minor isomers:* δ 212.14, 210.18, 204.11, 202.58, 55.76, 55.35, 53.10, 52.71, 51.04, 49.52, 43.41, 40.13, 27.91, 27.29, 26.45, 25.78, 24.54, 23.35, 22.95, 22.16. **HRMS** (ESI) *m/z* calcd for $C_{10}H_{14}NaO_2$ [$(M+Na)^+$]: 189.0886, measured: 189.0877.

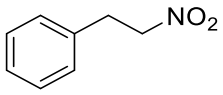
Tetrahydrofurans 4.74 and 4.75



General Procedure **E** was followed using aldehyde **4.45a** (35.5 mg, 0.183 mmol) and the reaction was complete in 10 h in 89% yield as determined by ^{1}H NMR analysis, as an 86:14 mixture of isomers. Silica gel flash chromatography with Et_2O / pentane afforded 9.1 mg or 26% yield of aldehydes **4.74** and **4.75** in 1:3 *d.r.* as a clear colourless liquid. **IR** ν_{max} (thin film, cm^{-1}): 3090, 2974, 2931, 2860, 2723, 1717, 1639, 1449, 1430, 1399, 1380, 1339, 1299, 1256, 1235, 1205, 1153, 1087, 1039, 994, 963, 925. *All integrals of signals clearly arising from the minor isomer are reported as integers, but integrals from signals partly or fully arising from the major isomer are reported to two decimal places.* **^{1}H NMR** (500 MHz, $CDCl_3$) δ 9.80 (d, *J* = 1.4 Hz, 2.74H), 9.71 (d, *J* = 3.7 Hz, 1H), 6.02 (dd, *J* = 17.4, 10.9 Hz, 1H), 5.86 (dd, *J* = 17.2, 10.7 Hz, 3.20H), 5.39 (dd, *J* = 17.5, 1.3 Hz, 1H), 5.35 (dd, *J* = 17.3, 1.5 Hz, 3.07H), 5.18 (dd, *J* = 10.9, 1.3 Hz, 1H), 5.08 (dd, *J* = 10.7, 1.4 Hz, 3.14H), 4.63 (dq, *J* = 9.3, 6.2 Hz, 3.02H), 4.55 (dq, *J* = 9.1, 6.6 Hz, 1H), 3.12 (ddd, *J* = 10.3, 9.1, 3.7 Hz, 1H), 2.94 (ddd, *J* = 9.3, 5.9, 1.3 Hz, 2.99H), 2.53 (dt, *J* = 10.1, 5.0, 4.1 Hz, 1H), 2.45 (dt, *J* = 11.7, 6.0 Hz, 3.34H), 1.81 – 1.75 (m, 3.29H), 1.75 – 1.56 (m, 13.65H), 1.56 – 1.47 (m, 5.97H), 1.47 – 1.38 (m, 6.22H), 1.33 (d, *J* = 6.2 Hz, 11.59H), 1.30 (d, *J* = 6.6 Hz, 4.83H), 1.22 – 1.12 (m, 3.53H). **^{13}C NMR** (126 MHz, $CDCl_3$) δ 202.67, 201.66, 145.95, 141.07, 114.41, 113.59, 84.25, 82.79, 72.89, 72.86, 62.49, 57.36, 44.14, 43.75, 35.03, 32.23, 25.04, 24.48, 24.11, 22.79, 21.67, 21.19, 20.54, 18.96. **HRMS** (ESI) *m/z* calcd for $C_{12}H_{18}NaO_2$ [$(M+Na)^+$]: 217.11990, measured: 217.11986.

Note: The major isomer of product observed in the reaction became the minor product during isolation.

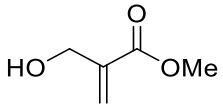
(2-nitroethyl)benzene 4.81



To a solution of benzaldehyde (10.0 mL, 0.0984 mol, 1 equiv) and nitromethane (5.86 mL, 0.108 mol, 1.1 equiv) in 33 mL MeOH at 0 °C was added aq. NaOH (10.0 M, 12.3 mL, 1.25 equiv) dropwise via an addition funnel over 20 mins at a rate of approximately 6 drops per 10 secs. A white precipitate formed immediately and the reaction became thick and foamy in 1 h, at which time 30 mL water was added and the reaction poured onto 100 mL crushed ice in a beaker also containing 20 mL conc. HCl. After the ice had melted, the mixture was extracted with 2x200 mL Et_2O. The combined organic layers were washed sequentially with 40 mL each water and brine, then dried over anhydrous $MgSO_4$, filtered, and concentrated. A 64:36 mixture of nitro-aldol and condensation products was observed.

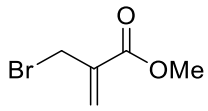
To a solution of the residue in 100 mL dry DCM was added 4-(Dimethylamino)pyridine (0.60 g, 4.9 mmol, 0.05 equiv), then acetic anhydride (5.6 mL, 0.059 mol, 0.60 equiv) carefully dropwise. The ratio of nitro-aldol to condensation product decreased to 32:68 in 8 h, at which time additional Ac_2O (3.0 mL, 0.032 mol, 0.32 equiv) was added carefully dropwise and the reaction stirred a further 18 h. The DCM was removed by rotary evaporation, then 65 mL DMSO and 17 mL AcOH were added. The solution was cooled over an ice bath and 6 g $NaBH_4$ was added in portions. The bath was removed after addition was complete and the reaction stirred 2 h. The reaction was diluted with 900 mL water and 200 mL 1 N HCl, then extracted with 2x250 mL EtOAc. Each organic layer was washed separately with 50 mL each sat. aq. $NaHCO_3$, water, and brine, then dried over Na_2SO_4, filtered, and concentrated. The crude afforded 12.66 g or 85% yield of reasonably clean compound, however further distillation afforded 8.8727 g or 60% yield of pure nitroethylbenzene **4.81** as a clear colourless liquid. The characterization data are in agreement with the literature.[50]
^{1}H NMR (400 MHz, $CDCl_3$) δ 7.41 – 7.27 (m, 3H), 7.26 – 7.21 (m, 2H), 4.64 (t, J = 7.4 Hz, 2H), 3.35 (t, J = 7.4 Hz, 2H).

Alcohol 5.9



Based on a known procedure,[51] methyl acrylate (20.0 mL, 0.222 mol, 1 equiv), paraformaldehyde (8.87 g, 0.295 mol, 1.33 equiv), and DABCO (33.35 g, 0.297 mol, 1.34 equiv) were stirred in 90 mL of 1:1 DMF / water for 19 h. The reaction was poured into 150 mL of 2 N HCl and extracted with 3x300 mL EtOAc, then 3x250 mL EtOAc further. The combined organic layers were washed sequentially with 40 mL water and 140 mL brine, then dried over anhydrous Na_2SO_4, filtered, and concentrated. EtOAc and DMF were removed under reduced pressure and the desired product collected by distillation to provide 9.79 g or 38% yield of alcohol **5.9** as a clear colourless liquid. The characterization data are in agreement with the literature.[52] **^{1}H NMR** (500 MHz, $CDCl_3$) δ 6.26 (dt, *J* = 2.2, 1.1 Hz, 1H), 5.84 (p, *J* = 1.4 Hz, 1H), 4.33 (s, 2H), 3.79 – 3.78 (m, 3H). **^{13}C NMR** (126 MHz, $CDCl_3$) δ 166.91, 139.39, 126.05, 62.68, 52.08.

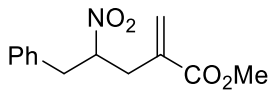
Bromide 4.82



To a solution of pure distilled allylic alcohol **5.9** (12.3527 g, 0.1064 mol, 1 equiv) in 120 mL dry Et_2O, cooled over an ice bath, was added PBr_3 (4.00 mL, 0.0426 mol, 0.4 equiv) dropwise under argon. The bath was removed and the reaction allowed to passively warm for 1.25 h, then the reaction was quenched over ice with 60 mL water and the layers separated. The aqueous was extracted with 2x50 mL Et_2O, then the combined organic layers were washed sequentially with 10 mL each water and brine. This was dried over anhydrous $MgSO_4$, filtered, and concentrated to afford 17.4587 g or 92% yield of pure bromide **4.82** as a pale yellow liquid. The characterization data are in agreement with the literature.[53] **^{1}H NMR** (400 MHz, $CDCl_3$) δ 6.34 (d, *J* = 0.8 Hz, 1H), 5.96 (d, *J* = 0.9 Hz, 1H), 4.18 (d, *J* = 0.9 Hz, 2H), 3.82 (s, 3H). **^{13}C NMR** (126 MHz, $CDCl_3$) δ 165.48, 137.41, 129.42, 52.48, 29.44.

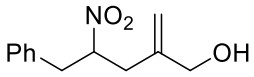
Note: This bromide is a severe lachrymator.

Ester 4.83



To a solution of nitroethylbenzene **4.81** (0.7591 g, 5.021 mmol, 1 equiv) and allyl bromide methyl ester **4.82** (0.8988 g, 5.021 mmol, 1.0 equiv) in 25 mL THF was added aq. NaOH (0.5 N, 10.0 mL, 1.0 equiv) slowly dropwise via addition funnel over an ice bath. After 2 h, ^{1}H NMR revealed near-completion, which was achieved by adding a few drops of aq. 1 N NaOH and following by NMR. THF was removed *in vacuo* without heat, and the aqueous layer extracted with 3x25 mL Et_2O. The combined organic layers were washed sequentially with 10 mL each water and brine, then dried over anhydrous $MgSO_4$, filtered, and concentrated. Silica gel flash chromatography with 20-30% Et_2O / pentane (R_f 0.29, 15% EtOAc / hexanes) afforded 1.1863 g or 95% yield of nitroalkane **4.83** as a yellow liquid. **IR** ν_{max} (neat liquid, cm^{-1}): 3032, 2954, 1717, 1632, 1549, 1497, 1439, 1371, 1312, 1258, 1197, 1144, 1083, 1031. **^{1}H NMR** (500 MHz, $CDCl_3$) δ 7.35 – 7.28 (m, 2H), 7.30 – 7.24 (m, 1H), 7.21 – 7.15 (m, 2H), 6.26 (d, *J* = 0.9 Hz, 1H), 5.68 (q, *J* = 1.1 Hz, 1H), 5.04 (dddd, *J* = 9.9, 9.0, 5.6, 4.4 Hz, 1H), 3.76 (s, 3H), 3.29 (dd, *J* = 14.3, 8.9 Hz, 1H), 3.09 (dd, *J* = 14.2, 5.5 Hz, 1H), 2.89 (ddd, *J* = 14.4, 4.4, 1.3 Hz, 1H), 2.84 (ddd, *J* = 14.4, 9.9, 0.8 Hz, 1H). **^{13}C NMR** (126 MHz, $CDCl_3$) δ 166.48, 135.21, 134.47, 129.69, 128.99, 128.98, 127.67, 88.80, 52.36, 40.11, 36.75. **HRMS** (ESI) *m/z* calcd for $C_{13}H_{15}NNaO_4$ [$(M+Na)^+$]: 272.0893, measured: 272.0884.

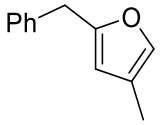
Alcohol 4.84



To a solution of methyl ester **4.83** (2.767 g, 11.10 mmol, 1 equiv) in 20 mL dry DCM at –50 °C was added DiBAL-H (1.0 M in DCM, 23 mL, 2.1 equiv), then the solution was allowed to warm to –20 °C over 1 h. Excess acetone was added over an ice bath, followed by sat. aq. sodium potassium tartrate. The DCM was removed by rotary evaporation and EtOAc added and the cloudy mixture stirred vigorously until clear. This was diluted further with water, EtOAc, and sat. aq. sodium potassium tartrate to provide 100 mL of aqueous layer in total, which was extracted with 3x350 mL EtOAc. The combined organic layers were washed sequentially with 50 mL each water and brine, then dried over anhydrous Na_2SO_4, filtered, and concentrated to afford 2.53 g or quantitative yield of essentially pure allylic alcohol **4.84**. Although this was typically used without further purification, in a separate instance silica gel flash chromatography with 25-40% EtOAc / hexanes (R_f 0.31, 40% EtOAc / hexanes) afforded **4.84** as a clear colourless oil. **IR** ν_{max} (thin film, cm^{-1}): 3366 (broad), 3086, 3066, 3032, 2921, 2872, 1656, 1605, 1549, 1496, 1455, 1439, 1371, 1331, 1210, 1029. **^{1}H NMR** (500 MHz, $CDCl_3$) δ 7.35 – 7.24 (m, 3H), 7.17 (d, *J* = 7.0 Hz, 2H),

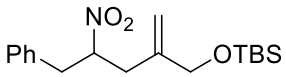
5.15 (s, 1H), 5.06 – 4.96 (m, 2H), 4.12 (t, J = 5.8 Hz, 2H), 3.28 (dd, J = 14.2, 8.8 Hz, 1H), 3.08 (dd, J = 14.2, 5.5 Hz, 1H), 2.79 (dd, J = 14.9, 10.2 Hz, 1H), 2.61 (dd, J = 14.8, 4.4 Hz, 1H), 1.43 (t, J = 6.0 Hz, 1H). **^{13}C NMR** (126 MHz, $CDCl_3$) δ 142.88, 135.45, 129.05, 129.00, 127.69, 115.30, 88.74, 65.99, 40.26, 37.54. **HRMS** (ESI) *m/z* calcd for $C_{12}H_{15}NNaO_3$ [$(M+Na)^+$]: 244.0944, measured: 244.0934.

Furan 4.85



Nitroalkane alcohol **4.84** (1.244 g, 5.622 mmol) was treated according to the procedure used for ketone **4.89**, except that the crude material was passed through a 2" plug of silica gel with 200 mL of 30% DCM / pentane to remove a strongly coloured dark residue. This afforded 0.5975 g or 62% yield of furan **4.85** as a yellow oil. The characterization data are in agreement with the literature.[54] **^{1}H NMR** (500 MHz, $CDCl_3$) δ 7.34 – 7.27 (m, 2H), 7.23 (d, J = 7.5 Hz, 3H), 7.09 (p, J = 1.2 Hz, 1H), 5.86 (s, 1H), 3.92 (s, 2H), 1.98 (d, J = 1.2 Hz, 3H). **^{13}C NMR** (126 MHz, $CDCl_3$) δ 154.75, 138.40, 138.18, 128.84, 128.62, 126.58, 120.74, 109.16, 34.76, 9.94.

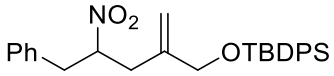
Silyl ether 4.86



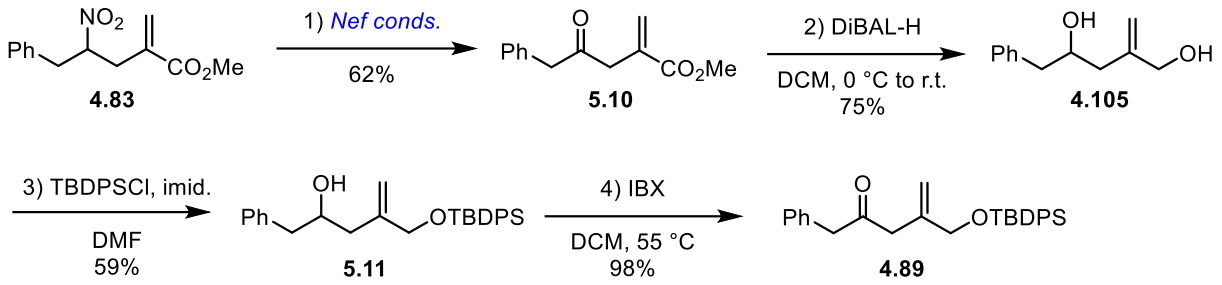
To a suspension of *tert*-butyldimethylsilyl chloride (1.7761 g, 11.784 mmol, 1.06 equiv) and imidazole (1.2947 g, 19.017 mmol, 1.7 equiv) in 10 mL THF was added crude alcohol **4.84** (2.53 g, 11 mmol, 1 equiv) as a solution in 20 mL THF. The reaction was stirred 12 h, then the THF was removed by rotary evaporation, and the residue taken up into 70 mL of 1:1 Et_2O / EtOAc and shaken with 30 mL 0.3 N HCl. The layers were separated and the aqueous extracted further with 2x20 mL Et_2O. The combined organic layers were washed sequentially with 20 mL each water and brine, then dried over anhydrous $MgSO_4$, filtered, and concentrated. Silica gel flash chromatography with 0-5% EtOAc / hexanes (R_f 0.59, 25% EtOAc / hexanes) afforded 1.7507 g of silyl ether **4.86** as a clear colourless oil. **IR** ν_{max} (thin film, cm^{-1}): 3084, 3066, 3032, 2954, 2929, 2895, 2885, 2856, 1551, 1497, 1471, 1462, 1438, 1369, 1332, 1311, 1253, 1112, 1080, 1006. **^{1}H NMR** (500 MHz, $CDCl_3$) δ 7.33 – 7.28 (m, 2H), 7.28 – 7.23 (m, 1H), 7.18 – 7.14 (m, 2H), 5.10

(d, J = 1.4 Hz, 1H), 4.96 (dddd, J = 9.7, 8.7, 5.6, 4.7 Hz, 1H), 4.91 (p, J = 1.2 Hz, 1H), 4.13 (dt, J = 13.4, 1.4 Hz, 1H), 4.07 (dt, J = 13.4, 1.4 Hz, 1H), 3.26 (dd, J = 14.2, 8.7 Hz, 1H), 3.07 (dd, J = 14.2, 5.6 Hz, 1H), 2.73 (ddd, J = 14.8, 9.8, 0.9 Hz, 1H), 2.59 (ddd, J = 14.7, 4.7, 1.1 Hz, 1H), 0.89 (s, 9H), 0.05 (s, 3H), 0.05 (s, 3H). **^{13}C NMR** (126 MHz, $CDCl_3$) δ 142.83, 135.58, 129.00 (broad), 127.61, 113.89, 88.57, 65.77, 40.26, 37.19, 26.01, 18.43, -5.29, -5.31. **HRMS** (ESI) *m/z* calcd for $C_{18}H_{29}NNaO_3Si$ [$(M+Na)^+$]: 358.18089, measured: 358.18003.

Silyl ether 4.88

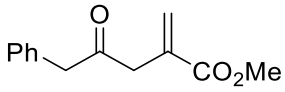


To a solution of alcohol **4.84** (8.9112 g, 0.04027 mol, 1 equiv) in 18.0 mL dry DMF was added imidazole (6.8572 g, 0.1007 mol, 2.5 equiv), followed by TBDPSCl (11.5 mL, 0.0442 mol, 1.1 equiv) fast dropwise over an ice bath. The reaction was allowed to warm for 14 h in the bath, then poured into 300 mL 0.5 N HCl and extracted with 3x150 mL Et_2O. The combined organic layers were washed sequentially with 180 mL each water and brine, then dried over anhydrous $MgSO_4$, filtered, and concentrated. Silica gel flash chromatography with 20-30% DCM / hexanes (R_f 0.15, 20% DCM / hexanes, R_f 0.65, 33% EtOAc / hexanes) afforded 10.4972 g or 57% yield of pure silyl ether **4.88** as a pale yellow liquid, along with another 2.5978 g or 14% of slightly lesser purity, for a total 71% yield. **IR** ν_{max} (thin film, cm^{-1}): 3070, 3030, 2957, 2930, 2893, 2857, 1719, 1552, 1496, 1472, 1456, 1428, 1390, 1370, 1331, 1111, 1083. **^{1}H NMR** (500 MHz, $CDCl_3$) δ 7.64 (ddd, J = 8.0, 3.8, 1.5 Hz, 4H), 7.46 – 7.35 (m, 6H), 7.31 – 7.23 (m, 3H), 7.12 – 7.07 (m, 2H), 5.16 (q, J = 1.5 Hz, 1H), 4.97 – 4.89 (m, 2H), 4.15 (dt, J = 13.4, 1.4 Hz, 1H), 4.10 (dt, J = 13.5, 1.3 Hz, 1H), 3.23 (dd, J = 14.2, 8.9 Hz, 1H), 3.02 (dd, J = 14.2, 5.5 Hz, 1H), 2.76 (dd, J = 14.7, 9.6 Hz, 1H), 2.58 (dd, J = 14.8, 4.8 Hz, 1H), 1.04 (s, 9H). **^{13}C NMR** (126 MHz, $CDCl_3$) δ 142.24, 135.65, 135.64, 135.49, 133.30, 133.27, 129.98, 129.96, 129.00, 128.98, 127.94, 127.92, 127.59, 114.13, 88.48, 66.36, 40.19, 37.24, 26.94, 19.37. **HRMS** (ESI) *m/z* calcd for $C_{28}H_{33}NNaO_3Si$ [$(M+Na)^+$]: 482.2122, measured: 482.2108.



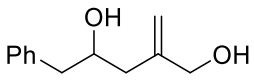
Scheme 5.1. Initial synthesis of ketone **4.89**.

Ketone 5.10



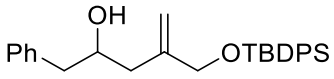
To a solution of nitroalkane **4.83** (2.4255 g, 9.730 mmol, 1 equiv) cooled over an ice bath in 12 mL dry MeOH was added a solution of freshly prepared NaOMe (0.269 g sodium metal, 11.7 mmol, 1.2 equiv) in 14 mL dry MeOH. The bath was removed and the reaction stirred 1 h, then this was added to a solution of conc. H_2SO_4 (5.40 mL, 10 equiv) in 200 mL MeOH at –50 °C by a 16 G cannula at a rate of 4-5 drops/s over 10 mins. The solution was stirred for 1.5 h at –50 °C, then 5 mL sat. aq. $NaHCO_3$ was added and the bath was replaced with a room temperature water bath. Once at room temperature, the MeOH was removed by rotary evaporation and the concentrate dilute with 150 mL EtOAc and 80 mL water. The layers were separated and the aqueous extracted further with 2x150 mL EtOAc. The combined organic layers were washed sequentially with 50 mL each water and brine, then dried over anhydrous Na_2SO_4, filtered, and concentrated. Silica gel flash chromatography with EtOAc / hexanes (R_f 0.41, 33% EtOAc / hexanes) afforded 1.408 g or 66% yield of diol **5.10** as a pale yellow oil. This was used without further purification. **^{1}H NMR** (400 MHz, $CDCl_3$) δ 7.38 – 7.20 (m, 5H), 6.32 (d, J = 1.0 Hz, 1H), 5.60 (q, J = 1.2 Hz, 1H), 3.78 (s, 2H), 3.71 (s, 3H), 3.42 (d, J = 1.0 Hz, 2H). **HRMS** (ESI) *m/z* calcd for $C_{13}H_{14}NaO_3$ [$(M+Na)^+$]: 241.0835, measured: 241.0830.

Diol 4.105



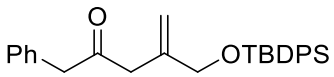
To a solution of keto-ester **5.10** (0.9201 g, 4.216 mmol, 1 equiv) in 29 mL dry DCM at 0 °C was added DiBAL-H (1.0 M in DCM, 13.0 mL, 3.1 equiv). The solution was allowed to warm in the bath for 6 h, at which time excess acetone was added and solvent removed by rotary distillation. Sat. aq. sodium potassium tartrate and water were added as necessary to clarify emulsions in 150 mL EtOAc, giving an aqueous volume of 220 mL. The layers were separated and the aqueous extracted further with 2x150 mL EtOAc. The combined organic layers were washed sequentially with 40 mL each water and brine, then dried over anhydrous Na_2SO_4, filtered, and concentrated. Silica gel flash chromatography with EtOAc / hexanes (R_f 0.17, 50% EtOAc / hexanes) afforded 0.6109 g or 75% yield of diol **4.105** as a pale yellow oil. **IR** ν_{max} (neat liquid, cm^{-1}): 3320 (very broad), 3086, 3027, 2916, 2858, 1753, 1649, 1602, 1495, 1453, 1031. **^{1}H NMR** (500 MHz, $CDCl_3$) δ 7.32 (t, *J* = 7.3 Hz, 2H), 7.27 – 7.20 (m, 3H), 5.14 (d, *J* = 1.3 Hz, 1H), 4.98 (s, 1H), 4.10 (s, 2H), 3.99 (dp, *J* = 8.3, 4.4 Hz, 1H), 2.83 (dd, *J* = 13.6, 4.7 Hz, 1H), 2.75 (dd, *J* = 13.6, 8.3 Hz, 1H), 2.50 (bs, 1H), 2.44 (dd, *J* = 14.3, 2.7 Hz, 1H), 2.35 (bs, 1H), 2.26 (dd, *J* = 13.9, 8.8 Hz, 1H). **^{13}C NMR** (126 MHz, $CDCl_3$) δ 146.06, 138.35, 129.55, 128.77, 126.75, 114.54, 71.97, 66.64, 43.95, 41.52. **HRMS** (ESI) *m/z* calcd for $C_{12}H_{16}NaO_2$ [$(M+Na)^+$]: 215.10425, measured: 215.10420.

TBDPS ether 5.11



Silyl ether protection of 0.6109 g of diol **4.105** was conducted as for **4.88**. Silica gel flash chromatography with EtOAc / hexanes (R_f 0.67, 50% EtOAc / hexanes) afforded 0.8054 g or 59% yield of silyl ether **5.11**, which was used without further purification.

Ketone 4.89

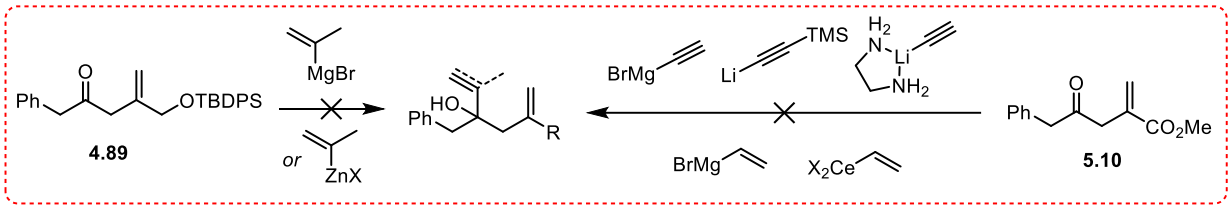


A solution of alcohol **5.11** (0.8054 g, 1.870 mmol, 1 equiv) and IBX (7.4573 g, 26.63 mmol, 14 equiv) in 20 mL DCM was refluxed for 20 h. The suspension was cooled to room temperature and filtered into 50 mL of 1:1 sat. aq. $Na_2S_2O_3$ and 5% $NaHCO_3$, then the layers were separated and the aqueous extracted further with 2x50 mL DCM. The combined organic layers were washed sequentially with 30 mL each water and brine, then dried over anhydrous Na_2SO_4, filtered, and

concentrated to afford 0.7875 g or 98% yield of ketone **4.89**. **IR** ν_{max} (thin film, cm^{-1}): 3070, 3028, 2957, 2930, 2891, 2856, 1716, 1652, 1428, 1110 (broad). **^{1}H NMR** (500 MHz, $CDCl_3$) δ 7.69 – 7.65 (m, 4H), 7.44 (d, *J* = 7.2 Hz, 2H), 7.43 – 7.38 (m, 4H), 7.34 – 7.30 (m, 2H), 7.26 (d, *J* = 7.3 Hz, 1H), 7.19 – 7.14 (m, 2H), 5.35 (d, *J* = 1.7 Hz, 1H), 4.98 (d, *J* = 1.3 Hz, 1H), 4.13 (d, *J* = 1.5 Hz, 2H), 3.71 (s, 2H), 3.19 (s, 2H), 1.08 (s, 9H). **^{13}C NMR** (126 MHz, $CDCl_3$) δ 205.78, 141.64, 135.65, 134.22, 133.50, 129.86, 129.63, 128.83, 127.85, 127.15, 113.96, 66.45, 49.33, 46.46, 26.96, 19.41. **HRMS** (ESI) *m/z* calcd for $C_{28}H_{32}NaO_2Si$ [$(M+Na)^+$]: 451.2064, measured: 451.2065.

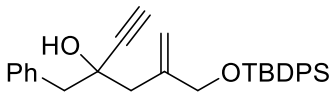
Note 1: This compound was also prepared from nitroalkane TBDPS ether **4.88** (5.0514 g, 10.99 mmol) by a similar procedure as used for ketone **5.10**. Silica gel chromatography with 5-10% Et_2O / hexanes (R_f 0.38, 10% Et_2O / hexanes) afforded 1.5855 g of pure and 1.2949 g of slightly less pure ketone **4.89** as a pale yellow oil and in 61% combined yield.

Note 2: As stated in the text, ketones **4.89** and **5.10** proved recalcitrant to additions by several vinyl and alkynyl organometallic reagents as shown in Scheme **5.2**.



Scheme 5.2. Attempted organometallic additions to ketone intermediates.

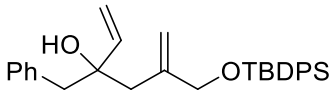
Propargylic alcohol 4.90



To a solution of ketone **4.89** (2.0533 g, 4.790 mmol, 1 equiv) in 12 mL dry THF at –78 °C was added ethynylmagnesium bromide (0.33 M, 36.0 mL, 2.5 equiv) fast dropwise. The reaction was allowed to warm to room temperature in the bath and stirred 16 h. At this time, 5 mL of sat. aq. NH_4Cl was added and the THF was removed *in vacuo*. The aqueous layer was diluted with 10 mL 1 N HCl and 115 mL water, then extracted with 3x150 mL EtOAc. The combined organic layers were washed sequentially with 100 mL each water and brine, dried over anhydrous Na_2SO_4, filtered, and concentrated. Silica gel flash chromatography with 10% EtOAc / hexanes (R_f 0.28,

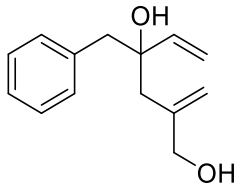
10% EtOAc / hexanes) afforded 1.8794 g or 87% yield of propargylic alcohol **4.90** as soft, white to yellow crystals. **IR** ν_{max} (thin film, cm^{-1}): 3380 (broad), 3299, 3070, 3029, 2957, 2930, 2893, 2857, 1554, 1428, 1111 (broad). **^{1}H NMR** (500 MHz, $CDCl_3$) δ 7.72 – 7.65 (m, 4H), 7.46 – 7.40 (m, 2H), 7.40 – 7.35 (m, 4H), 7.33 – 7.23 (m, 5H), 5.33 (q, *J* = 1.6 Hz, 1H), 5.11 (s, 1H), 4.30 (d, *J* = 13.8 Hz, 1H), 4.18 (d, *J* = 13.8 Hz, 1H), 3.42 (s, 1H), 2.99 (d, *J* = 1.9 Hz, 2H), 2.47 (d, *J* = 13.8 Hz, 1H), 2.43 (d, *J* = 13.8 Hz, 1H), 2.34 (s, 1H), 1.06 (s, 9H). **^{13}C NMR** (126 MHz, $CDCl_3$) δ 143.04, 136.24, 135.82, 135.73, 133.30, 133.24, 131.10, 129.91, 129.89, 128.10, 127.86, 127.83, 127.00, 116.31, 86.44, 74.05, 69.92, 67.81, 48.53, 45.85, 26.93, 19.34. **HRMS** (ESI) *m/z* calcd for $C_{30}H_{34}NaO_2Si$ [$(M+Na)^+$]: 477.2220, measured: 477.2230.

Allylic alcohol 5.12



To a solution of alkyne ester **4.90** (0.4564 g, 1.004 mmol, 1 equiv) and 2.5 µL quinoline in 4.5 mL 1-hexene under argon was added $Pd/CaCO_3$ (5 wt.%, 47.6 mg, 0.025 equiv, poisoned with Pb), and H_2 gas was bubbled through the solution from a balloon for 8 h, at which time 47.4 mg of additional $Pd/CaCO_3$ was added. After 24 h total, the reaction was determined complete by ^{1}H NMR. The black suspension was filtered on celite using DCM and concentrated to afford 0.4429 g or 97% yield of olefin **5.12** as a clear colourless oil (R_f 0.71, 33% EtOAc / hexanes). **IR** ν_{max} (neat liquid, cm^{-1}): 3419 (broad), 3070, 3028, 2956, 2930, 2857, 1726, 1644, 1589, 1495, 1472, 1455, 1427, 1266, 1110, 1031. **^{1}H NMR** (500 MHz, $CDCl_3$) δ 7.71 – 7.65 (m, 4H), 7.45 (t, *J* = 7.3 Hz, 2H), 7.39 (td, *J* = 7.2, 2.6 Hz, 4H), 7.31 – 7.18 (m, 5H), 5.80 (dd, *J* = 17.1, 10.7 Hz, 1H), 5.27 (q, *J* = 1.8 Hz, 1H), 5.11 (dd, *J* = 17.2, 1.5 Hz, 1H), 4.99 (dd, *J* = 10.7, 1.5 Hz, 1H), 4.95 (dt, *J* = 2.2, 1.1 Hz, 1H), 4.17 (dt, *J* = 13.9, 1.5 Hz, 1H), 4.09 (dt, *J* = 13.8, 1.4 Hz, 1H), 2.84 (s, 2H), 2.71 (s, 1H), 2.37 (s, 2H), 1.07 (s, 9H). **^{13}C NMR** (126 MHz, $CDCl_3$) δ 143.99, 143.51, 137.08, 135.71, 133.34, 130.99, 129.86, 128.01, 127.83, 126.54, 114.99, 113.19, 74.63, 67.75, 48.25, 44.79, 26.94, 19.36. **HRMS** (ESI) *m/z* calcd for $C_{30}H_{36}NaO_2Si$ [$(M+Na)^+$]: 479.23768, measured: 479.23748.

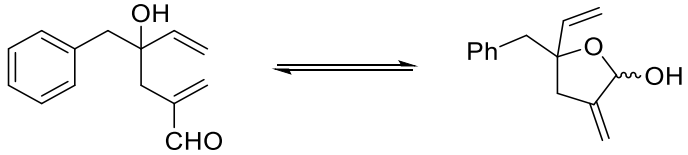
Diol 5.13



To TBDPS ether **5.12** (0.2179 g, 0.4771 mmol, 1 equiv) in 5 mL THF was added TBAF (0.1567 g, 1.25 equiv). After 2.5 h, 2 mL sat. aq. NH_4Cl and 2 mL H_2O were added, THF removed *in vacuo*, and the aqueous concentrate was extracted with 3x20 mL EtOAc. The combined organic layers were washed with 5 mL each water then brine and dried over anhydrous Na_2SO_4, filtered, and concentrated. Silica gel flash chromatography with 25% EtOAc / hexanes (R_f 0.15, 20% EtOAc / hexanes) afforded 87.4 mg or 84% yield of alcohol **5.13** as a pale yellow oil. **IR** ν_{max} (neat oil, cm^{-1}): 3317 (broad), 3085, 3028, 2983, 2918, 2855, 1642, 1603, 1495, 1453, 1411, 1339. **^{1}H NMR** (500 MHz, $CDCl_3$) δ 7.33 – 7.20 (m, 3H), 7.22 – 7.16 (m, 2H), 5.89 (dd, *J* = 17.2, 10.8 Hz, 1H), 5.14 (q, *J* = 1.4 Hz, 1H), 5.11 – 5.02 (m, 2H), 4.93 – 4.88 (m, 1H), 4.10 (q, *J* = 13.1 Hz, 2H), 2.91 (d, *J* = 13.3 Hz, 1H), 2.84 (d, *J* = 13.3 Hz, 1H), 2.71 (bs, 1H), 2.53 (bs, 1H), 2.48 (s, 2H). **^{13}C NMR** (126 MHz, $CDCl_3$) δ 144.81, 143.20, 136.34, 130.94, 128.25, 126.89, 116.63, 113.55, 75.23, 67.19, 47.82, 45.93. **HRMS** (ESI) *m/z* calcd for $C_{14}H_{18}NaO_2$ [$(M+Na)^+$]: 241.11990, measured: 241.12017.

This compound was also prepared from TBAF deprotection of TBS silyl ether **4.95a** by a similar procedure in 99% yield.

Enal alcohol-hemiacetal 4.80



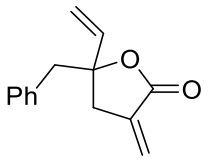
To a solution of diol **5.13** (0.2474 g, 1.133 mmol, 1 equiv) in 10 mL dry DCM was added IBX (0.2851 g, 1.018 mmol, 0.90 equiv) and the suspension was heated at 55 °C for 17 h. The reaction was then cooled to room temperature and filtered on celite using minimal DCM until free of precipitate. Silica gel flash chromatography with 15-20% EtOAc / hexanes (R_f 0.23, 20% EtOAc / hexanes) afforded 0.2012 g or 82% of a mixture of aldehyde-lactols **4.80** as a clear colourless

liquid. **IR** ν_{max} (thin film, cm^{-1}): 3565 (broad), 3441, 3087, 3062, 3029, 2919, 2848, 2700, 1684, 1642, 1625, 1604, 1495, 1454, 1436, 1411, 1335, 1121, 1000. *All integrals of signals clearly arising from the aldehyde tautomer are reported as integers, but integrals from signals partly or fully arising from either hemiacetal are reported to two decimal places.* **^{1}H NMR** (500 MHz, $CDCl_3$) δ 9.47 (s, 1H), 7.31 – 7.18 (m, 7.48H), 6.39 – 6.33 (m, 1H), 6.14 (d, *J* = 0.8 Hz, 1H), 5.99 (dd, *J* = 17.3, 10.8 Hz, 0.22H), 5.83 (dd, *J* = 17.1, 10.7 Hz, 0.24H), 5.79 (dd, *J* = 17.1, 10.8 Hz, 1H), 5.61 – 5.55 (m, 0.46H), 5.30 (dd, *J* = 17.3, 1.3 Hz, 0.23H), 5.19 – 5.17 (m, 0.48H), 5.18 (dd, *J* = 17.1, 1.4 Hz, 0.25H), 5.11 (dd, *J* = 10.8, 1.3 Hz, 0.22H), 5.08 – 5.03 (m, 0.77H), 5.04 (dd, *J* = 9.4, 1.4 Hz, 1H), 5.01 (q, *J* = 1.4 Hz, 1H), 3.00 (d, *J* = 13.6 Hz, 0.26H), 2.96 (d, *J* = 13.5 Hz, 0.26H), 2.94 (d, *J* = 13.6 Hz, 0.23H), 2.89 (d, *J* = 13.4 Hz, 1H), 2.85 (d, *J* = 13.6 Hz, 0.28H), 2.85 (d, *J* = 13.3 Hz, 1H), 2.78 – 2.73 (m, 0.24H), 2.73 (d, *J* = 9.1 Hz, 0.26H), 2.65 – 2.61 (m, 0.73H), 2.61 (d, *J* = 14.0 Hz, 1H), 2.54 (d, *J* = 13.8 Hz, 1H), 2.46 (dt, *J* = 15.5, 1.9 Hz, 0.29H), 2.45 (s, 1H), 1.68 (s, 0.30H). **^{13}C NMR** (126 MHz, $CDCl_3$) δ 195.84, 149.65, 148.68, 145.81, 143.44, 142.30, 141.69, 138.92, 136.95, 136.75, 136.55, 130.95, 130.88, 130.82, 128.15, 128.07, 128.04, 126.75, 126.71, 126.60, 114.01, 113.69, 113.18, 110.18, 110.11, 98.82, 98.65, 85.27, 85.26, 74.94, 48.28, 46.72, 46.39, 40.12, 39.91, 38.83. **HRMS** (ESI) *m/z* calcd for $C_{14}H_{16}NaO_2$ $[(M+Na)^+]$: 239.10425, measured: 239.10445.

Note 1: All attempts to use this substrate in the oCM reaction failed, producing at most trace quantities of the desired product. Conditions screened included HCl, HBF_4, HOTf, $HClO_4$, and $HNTf_2$ salts of the catalyst in various combinations with solvents MeCN, $MeNO_2$, $CHCl_3$, THF, 1,4-dioxane, ethyl ether, EtOAc, PhMe, and DMF. Either the HCl or HOTf salts in DMSO were almost totally unreactive, and the HOTf salt in methanol again formed the methyl acetals, where no reaction occurred even after addition of water. Very dilute conditions in MeCN and $MeNO_2$ also elicited decomposition, as did reactions in MeCN which were cooled to just above –42 °C, where no reaction occurred, and allowed to warm slowly to room temperature.

Note 2: Thermal rearrangement was conducted by heating 0.1 mmol of substrate at 170 °C in d_8-toluene in a sealed vial for 16 h, but afforded only a mixture of oxy-Cope product and intramolecular aldol addition products arising from that compound.

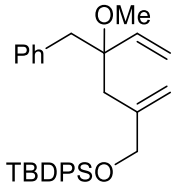
Lactone 4.80′



Use of excess IBX equivalents in the preparation of substrate **4.80** resulted in formation of this lactone as a byproduct. An authentic sample was prepared with excess IBX in DMSO. **IR** ν_{max} (thin film, cm^{-1}): 3028, 2924, 2855, 1763, 1496, 1455, 1438, 1412, 1265, 1146, 1082, 1032. **^{1}H NMR** (500 MHz, $CDCl_3$) δ 7.33 – 7.21 (m, 5H), 6.08 (t, *J* = 2.8 Hz, 1H), 5.94 (dd, *J* = 17.2, 10.9 Hz, 1H), 5.46 (t, *J* = 2.4 Hz, 1H), 5.30 (d, *J* = 17.2 Hz, 1H), 5.19 (d, *J* = 10.9 Hz, 1H), 3.12 (d, *J* = 14.0 Hz, 1H), 2.98 (d, *J* = 13.9 Hz, 1H), 2.94 (dd, *J* = 16.7, 2.8 Hz, 1H), 2.80 (dt, *J* = 16.7, 2.5 Hz, 1H). **^{13}C NMR** (126 MHz, $CDCl_3$) δ 169.79, 139.45, 134.59, 134.54, 130.82, 128.34, 127.12, 121.90, 114.68, 84.14, 45.86, 37.31. **HRMS** (ESI) *m/z* calcd for $C_{14}H_{14}NaO_2$ $[(M+Na)^+]$: 237.08860, measured: 237.08844.

The following compound was originally used to access methyl ether substrate **4.97a**, but the sequence described in Scheme **4.15** was used subsequently.

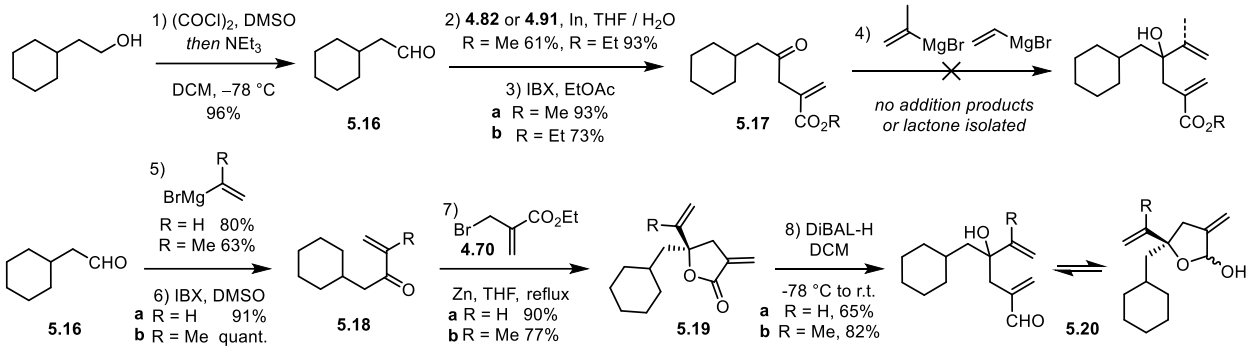
Methyl ether 5.14



To a solution of alcohol **5.12** (0.3853 g, 0.8437 mmol, 1 equiv) in 8.5 mL dry THF at 0 °C was added first oil-free KH (0.1411 g, 3.518 mmol, 4.2 equiv), then MeI (0.53 mL, 8.513 mmol, 10.1 equiv) 3 mins later. After 3.5 h, TLC analysis indicated completion, and 2 mL each sat. aq. NH_4Cl and water were added, then the biphasic solution was extracted with 3x15 mL EtOAc. The combined organic layers were washed sequentially with 5 mL each water and brine, then dried over anhydrous Na_2SO_4, filtered, and concentrated. Silica gel flash chromatography with 2.5% EtOAc / hexanes (R_f 0.44, 10% EtOAc / hexanes) afforded 0.3696 g or 93% yield of ether **5.14** as a translucent colourless oil. **IR** ν_{max} (neat liquid, cm^{-1}): 3071, 3028, 2930, 2856, 2826, 1728, 1648, 1589, 1495, 1471, 1461, 1105, 1080. **^{1}H NMR** (500 MHz, $CDCl_3$) δ 7.68 (d, *J* = 7.3 Hz, 4H), 7.45

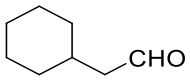
– 7.33 (m, 6H), 7.24 – 7.11 (m, 5H), 5.61 (dd, *J* = 17.7, 11.1 Hz, 1H), 5.42 (d, *J* = 1.7 Hz, 1H), 5.14 (d, *J* = 11.2 Hz, 1H), 5.07 (d, *J* = 1.0 Hz, 1H), 5.05 (d, *J* = 17.9 Hz, 1H), 4.12 (s, 2H), 3.14 (s, 3H), 2.91 (d, *J* = 13.9 Hz, 1H), 2.82 (d, *J* = 13.9 Hz, 1H), 2.28 (d, *J* = 15.2 Hz, 1H), 2.17 (d, *J* = 15.1 Hz, 1H), 1.06 (s, 9H). **^{13}C NMR** (126 MHz, $CDCl_3$) δ 144.06, 141.56, 137.53, 135.68, 133.95, 133.93, 130.88, 129.72, 127.87, 127.76, 126.21, 115.49, 112.72, 79.50, 67.29, 50.14, 42.16, 38.04, 27.01, 19.45. **HRMS** (ESI) *m/z* calcd for $C_{31}H_{38}NaO_2Si$ [$(M+Na)^+$]: 493.25333, measured: 493.25314.

The cyclohexyl-tagged alcohol substrates were prepared as follows:



Scheme 5.3. Synthesis of cyclohexyl-tagged acyclic alcohol oCM substrates.

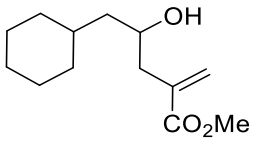
2-cyclohexyl ethanal 5.16



Commercially available cyclohexyl ethanol (2.00 mL, 14.3 mmol) was oxidized according to Swern's procedure[55] then purified by silica gel flash chromatography with 40-50% DCM / pentane (R_f 0.16, 25% DCM / hexanes) to afford 1.74 g or 96% yield of aldehyde **5.16** as a faintly yellow liquid. The characterization data are in agreement with the literature.[56] **^{1}H NMR** (500 MHz, $CDCl_3$) δ 9.75 (t, *J* = 2.4 Hz, 1H), 2.29 (dd, *J* = 6.8, 2.3 Hz, 2H), 1.89 (dtp, *J* = 14.2, 6.8, 3.3 Hz, 1H), 1.76 – 1.62 (m, 5H), 1.29 (dddd, *J* = 15.0, 12.1, 7.8, 3.2 Hz, 2H), 1.21 – 1.11 (m, 1H), 1.00 (qd, *J* = 14.1, 13.1, 3.5 Hz, 2H). **^{13}C NMR** (126 MHz, $CDCl_3$) δ 203.11, 51.53, 33.37, 32.83, 26.21, 26.19.

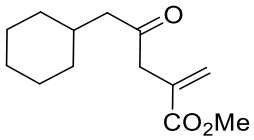
Note: This compound readily trimerizes on standing or in subsequent Grignard additions. The compound was distilled immediately prior to use.

Alcohol methyl ester 5.17a′



To a solution of allyl bromide methyl ester **4.82** (2.4578 g, 13.73 mmol, 1.0 equiv) and cyclohexylethanal (1.7331 g, 13.73 mmol, 1 equiv) in 35 mL of 3:2 THF / water was added indium powder (1.5744 g, 13.71 mmol, 1.0 equiv) and the suspension stirred vigorously for 14 h. The reaction was filtered on celite and the THF removed by rotary evaporation. The aqueous was diluted with 36 mL water and 60 mL EtOAc, filtered again on celite, the layers were separated, then the aqueous further extracted with 3x60 mL EtOAc. The combined organic layers were washed sequentially with 20 mL of water and brine, dried over anhydrous Na_2SO_4, filtered, and concentrated. Silica gel flash chromatography with 20% EtOAc / hexanes (R_f 0.22, 20% EtOAc / hexanes) afforded 1.885 g or 61% yield of nearly pure alcohol **5.17a′** as a clear colourless liquid. **^{1}H NMR** (500 MHz, $CDCl_3$) δ 6.25 (d, *J* = 1.5 Hz, 1H), 5.66 (d, *J* = 1.1 Hz, 1H), 3.90 – 3.82 (m, 1H), 3.77 (s, 3H), 2.57 (ddd, *J* = 14.0, 3.5, 1.0 Hz, 1H), 2.30 (ddd, *J* = 13.9, 8.4, 0.9 Hz, 1H), 1.97 (bs, 1H), 1.82 – 1.75 (m, 1H), 1.74 – 1.60 (m, 4H), 1.53 – 1.43 (m, 1H), 1.40 (ddd, *J* = 14.0, 8.6, 5.4 Hz, 1H), 1.32 – 1.09 (m, 4H), 0.99 – 0.81 (m, 2H). **^{13}C NMR** (126 MHz, $CDCl_3$) δ 168.28, 137.67, 127.91, 68.10, 52.22, 45.23, 41.09, 34.29, 34.22, 33.08, 26.75, 26.51, 26.35.

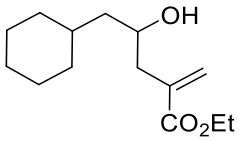
Ketone methyl ester 5.17a



To alcohol **5.17a′** (1.8765 g, 8.291 mmol, 1 equiv) in 40 mL EtOAc was added IBX (3.0218 g, 10.79 mmol, 1.3 equiv) and the suspension refluxed 28 h until complete as assessed by TLC. The reaction was cooled, filtered on celite, and concentrated. Silica gel flash chromatography with 10% EtOAc / hexanes (R_f 0.43, 20% EtOAc / hexanes) afforded 1.73 g or 93% yield of ketone **5.17a** as a clear colourless liquid. **IR** ν_{max} (neat liquid, cm^{-1}): 2921, 2850, 1713, 1637, 1438, 1404, 1375, 1338, 1305, 1199, 1167, 1146, 1102, 1084, 1059. **^{1}H NMR** (500 MHz, $CDCl_3$) δ 6.33 (d, *J* = 1.0 Hz, 1H), 5.62 (d, *J* = 1.0 Hz, 1H), 3.74 (s, 3H), 3.38 (s, 2H), 2.35 (d, *J* = 6.9 Hz, 2zH), 1.85 (dddq,

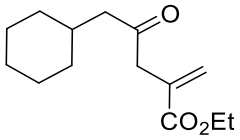
J = 14.4, 10.3, 6.8, 3.3 Hz, 1H), 1.73 – 1.60 (m, 5H), 1.33 – 1.21 (m, 2H), 1.13 (dtd, *J* = 12.8, 9.5, 9.1, 2.9 Hz, 1H), 1.00 – 0.85 (m, 2H). **^{13}C NMR** (126 MHz, $CDCl_3$) δ 207.14, 166.98, 134.42, 128.72, 52.21, 50.45, 46.50, 33.95, 33.29, 26.35, 26.23. **HRMS** (ESI) *m/z* calcd for $C_{13}H_{20}NaO_3$ [$(M+Na)^+$]: 247.13047, measured: 247.13008.

Alcohol ethyl ester 5.17b′



Cyclohexylethanal (0.5022 g, 3.979 mmol) was reacted with ethyl ester **4.91**[57] as described for the methyl ester. After 17 h, 3 mL sat. aq. NH_4Cl and 3 mL H_2O were added and the solution was extracted with 3x15 mL EtOAc. The combined organic layers were washed sequentially with 5 mL of water and brine, then dried over anhydrous Na_2SO_4, filtered, and concentrated. Silica gel flash chromatography with 20% EtOAc / pet. ether (R_f 0.21, 20% EtOAc / hexanes) afforded 0.8879 g or 93% yield of alcohol **5.17b′** as a clear colourless liquid. **IR** ν_{max} (neat liquid, cm^{-1}): 3424 (broad), 2981, 2920, 2850, 1712, 1629, 1447, 1410, 1369, 1324, 1305, 1285, 1198, 1177, 1145, 1094, 1069, 1026. **^{1}H NMR** (500 MHz, $CDCl_3$) δ 6.24 – 6.20 (m, 1H), 5.62 (s, 1H), 4.26 – 4.13 (m, 2H), 3.84 (tt, *J* = 8.2, 4.0 Hz, 1H), 2.54 (dd, *J* = 14.0, 3.4 Hz, 1H), 2.28 (dd, *J* = 14.0, 8.4 Hz, 1H), 2.14 (bs, 1H), 1.76 (d, *J* = 12.7 Hz, 1H), 1.72 – 1.57 (m, 4H), 1.50 – 1.41 (m, 1H), 1.37 (ddd, *J* = 13.9, 8.5, 5.5 Hz, 1H), 1.31 – 1.06 (m, 7H), 0.97 – 0.77 (m, 2H). **^{13}C NMR** (126 MHz, $CDCl_3$) δ 167.77, 137.91, 127.58, 68.02, 61.04, 45.17, 41.02, 34.21, 34.14, 33.02, 26.69, 26.45, 26.29, 14.24. **HRMS** (ESI) *m/z* calcd for $C_{14}H_{24}NaO_3$ [$(M+Na)^+$]: 263.16177, measured: 263.16106.

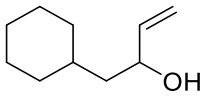
Ketone ethyl ester 5.17b



To a solution of alcohol **5.17b′** (0.8879 g, 3.694 mmol, 1 equiv) in 11 mL dry DMSO was added IBX (1.2410 g, 4.432 mmol, 1.2 equiv), and the suspension stirred overnight, then addition IBX (0.5336 g, 1.906 mmol, 0.5 equiv) was added. After 24 h in total, the reaction was filtered on celite

using minimal Et_2O into 100 mL 1:1 5% $NaHCO_3$ and sat. aq. $Na_2S_2O_3$, then the aqueous was extracted with 3x30 mL Et_2O. The combined organic layers were washed sequentially with 30 mL each 0.5 N HCl, water, and brine, then dried over anhydrous $MgSO_4$, filtered, and concentrated. Silica gel flash chromatography with 15% EtOAc / pet. ether (R_f 0.50, 25% EtOAc / hexanes) afforded 0.6441 g or 73% yield of alcohol **5.17b** as a clear colourless liquid which solidified on standing in a freezer. **IR** ν_{max} (neat liquid, cm^{-1}): 2983, 2922, 2851, 1711, 1636, 1448, 1404, 1369, 1331, 1303, 1196, 1175, 1146, 1117, 1097, 1059, 1026. **^{1}H NMR** (500 MHz, $CDCl_3$) δ 6.32 (d, *J* = 1.1 Hz, 1H), 5.62 – 5.57 (m, 1H), 4.19 (q, *J* = 7.1 Hz, 2H), 3.37 (s, 2H), 2.34 (d, *J* = 6.9 Hz, 2H), 1.84 (dtp, *J* = 14.4, 6.8, 3.3 Hz, 1H), 1.72 – 1.58 (m, 5H), 1.33 – 1.20 (m, 5H), 1.13 (dtt, *J* = 12.7, 9.5, 4.9 Hz, 1H), 0.98 – 0.85 (m, 2H). **^{13}C NMR** (126 MHz, $CDCl_3$) δ 207.17, 166.50, 134.72, 128.42, 61.10, 50.42, 46.50, 33.93, 33.29, 26.33, 26.21, 14.26. **HRMS** (ESI) *m/z* calcd for $C_{14}H_{22}NaO_3$ $[(M+Na)^+]$: 261.14612, measured: 261.14576.

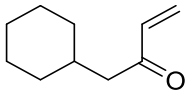
Allyl alcohol 5.18′



To a solution of freshly distilled 2-cyclohexyl ethanal (1.25 mL, 9.91 mmol, 1 equiv) in 100 mL dry THF at –78 °C was add vinylmagnesium bromide (1.0 M in THF, 15.0 mL, 1.5 equiv) and the solution allowed to warm 11 h in the bath. The reaction was cooled over ice, then 5 mL sat. aq. NH_4Cl and 10 mL water were added, then the THF was removed *in vacuo*. The concentrate was diluted with 5 mL 0.1 N HCl and extracted with 3x40 mL EtOAc. The combined organic layers were washed sequentially with 10 mL of water and brine, dried over anhydrous Na_2SO_4, filtered, and concentrated. Silica gel flash chromatography with 20% EtOAc / pet. ether (R_f 0.38, 20% EtOAc / hexanes) afforded 1.22 g or 80% yield of alcohol **5.18a′** as a clear colourless liquid. The characterization data are in agreement with the literature.[58] **IR** ν_{max} (neat liquid, cm^{-1}): 3350 (broad), 3078, 2920, 2850, 1708, 1645, 1617, 1448, 1424, 989. **^{1}H NMR** (500 MHz, $CDCl_3$) δ 5.87 (ddd, *J* = 16.9, 10.4, 6.3 Hz, 1H), 5.22 (dt, *J* = 17.1, 1.5 Hz, 1H), 5.09 (dt, *J* = 10.4, 1.3 Hz, 1H), 4.21 (p, *J* = 6.2 Hz, 1H), 1.79 (d, *J* = 12.8 Hz, 1H), 1.73 – 1.61 (m, 4H), 1.49 – 1.41 (m, 2H), 1.40 (d, *J* = 4.3 Hz, 1H), 1.38 – 1.30 (m, 1H), 1.29 – 1.09 (m, 3H), 1.01 – 0.84 (m, 2H). **^{13}C NMR** (126 MHz, $CDCl_3$) δ 141.92, 114.43, 71.02, 45.04, 34.12, 34.02, 33.24, 26.73, 26.46, 26.36.

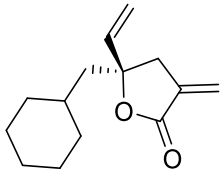
HRMS (APCI) *m/z* calcd for $C_{10}H_{19}O$ [$(M+H)^+$]: 155.14304, measured: 155.14268, *m/z* calcd for $C_{10}H_{17}O$ [$(M–H)^–$]: 153.12739, measured: 153.12712.

Enone 5.18a



To a solution of alcohol **5.18a′** (0.991 g, 6.42 mmol, 1 equiv) in 18.4 mL dry DMSO was added IBX (2.15 g, 7.69 mmol, 1.2 equiv) and the suspension stirred 40 mins, then filtered on celite into 30 mL of equal parts sat. aq. $Na_2S_2O_3$, sat. aq. Na_2CO_3 and water. This was diluted further with 160 mL 5% aq. $NaHCO_3$ and 30 mL Et_2O, then the layers were separated. The organic phase was washed sequentially with 40 mL water and brine then dried over anhydrous $MgSO_4$, filtered, and concentrated. Purification by silica gel flash chromatography with 10% EtOAc / pentane (R_f 0.53, 20% EtOAc / hexanes) afforded 0.887 g or 91% yield of ketone **5.18a** as a pale yellow liquid. The characterization data are in agreement with the literature.[59] **^{1}H NMR** (500 MHz, $CDCl_3$) δ 6.35 (dd, *J* = 17.6, 10.6 Hz, 1H), 6.19 (d, *J* = 17.6 Hz, 1H), 5.80 (d, *J* = 10.6 Hz, 1H), 2.44 (d, *J* = 6.9 Hz, 2H), 1.85 (dtq, *J* = 14.4, 6.8, 3.3 Hz, 1H), 1.72 – 1.64 (m, 5H), 1.32 – 1.21 (m, 2H), 1.17 – 1.07 (m, 1H), 1.00 – 0.87 (m, 2H). **^{13}C NMR** (126 MHz, $CDCl_3$) δ 200.98, 137.20, 128.03, 47.45, 34.41, 33.45, 26.36, 26.26. **HRMS** (APCI) *m/z* calcd for $C_{10}H_{17}O$ [$(M+H)^+$]: 153.12739, measured: 153.12740.

Lactone 5.19a

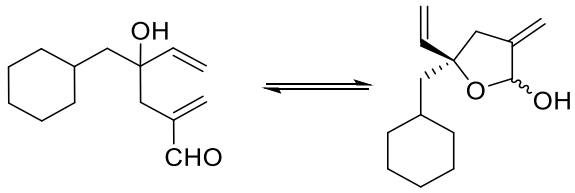


To a solution of ketone **5.18a** (0.8840 g, 5.807 mmol, 1 equiv) and allyl bromide ethyl ester **4.91**[57] (0.88 mL, 1.23 g, 6.38 mmol, 1.1 equiv) in 60 mL dry THF was added Zn dust (0.5992 g, 8.763 mmol, 1.5 equiv) and the suspension was refluxed under a condenser for 1.5 h. The reaction was then checked by ^{1}H NMR for completion, cooled to room temperature, filtered on celite with EtOAc and concentrated. Silica gel chromatography with 5% EtOAc / hexanes (R_f 0.32, 10% EtOAc / hexanes) afforded 1.1499 g or 90% yield of lactone **5.19a** as a clear colourless liquid. **IR**

ν_{max} (thin film, cm^{-1}): 2920, 2850, 1763, 1716, 1666, 1448, 1411, 1374, 1273, 1162, 1098. **^{1}H NMR** (500 MHz, $CDCl_3$) δ 6.20 (t, *J* = 2.7 Hz, 1H), 5.83 (dd, *J* = 17.2, 10.9 Hz, 1H), 5.58 (t, *J* = 2.4 Hz, 1H), 5.25 (d, *J* = 16.7 Hz, 1H), 5.14 (d, *J* = 10.9 Hz, 1H), 2.84 (dt, *J* = 16.6, 2.3 Hz, 1H), 2.77 (dt, *J* = 16.6, 2.8 Hz, 1H), 1.85 – 1.78 (m, 1H), 1.72 – 1.55 (m, 6H), 1.46 (tdq, *J* = 11.4, 5.9, 2.9, 2.3 Hz, 1H), 1.26 – 1.05 (m, 3H), 0.95 (dddd, *J* = 19.9, 15.8, 9.4, 6.1 Hz, 2H). **^{13}C NMR** (126 MHz, $CDCl_3$) δ 170.10, 139.66, 134.86, 122.27, 114.18, 85.24, 47.95, 40.25, 34.71, 34.39, 33.72, 26.36, 26.27, 26.24. **HRMS** (APCI) *m/z* calcd for $C_{14}H_{21}O_2$ [$(M+H)^+$]: 221.15361, measured: 221.15371.

Note: This methylene lactone was found to frequently polymerize on standing as a neat substance, in one instance providing gram quantities of a soft, clear gel. In certain instances, this complicated purification as significant polymerization had occurred prior to or during chromatography. Careful neutralization, additional filtration on celite, and treatment with charcoal to remove possible metal impurities were uniformly unsuccessful at preventing this process. Whenever possible it was used when freshly prepared or stored as a solution in a freezer.

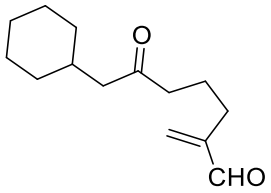
Aldehyde-hemiacetals 5.20a



To a solution of DiBAL-H (25% in PhMe, 1.28 mL, 1.05 equiv) in 22 mL dry THF at –78 °C was added neat lactone **5.19a** (0.400 g, 1.816 mmol, 1 equiv) dropwise via syringe and the solution stirred 4 h. Fieser's workup was conducted, the resulting suspension filtered on celite, then concentrated. Silica gel chromatography with 30% Et_2O / pentane (R_f 0.30, 33% EtOAc / hexanes) afforded 0.2641 g or 65% yield of aldehyde-lactol mixture **5.20a** as a clear colourless liquid. **IR** ν_{max} (thin film, cm^{-1}): 3427 (broad), 3086, 2919, 2849, 2694, 1681, 1642, 1626, 1447, 1410, 1331, 1260, 994. **^{1}H NMR (**500 MHz, $CDCl_3$) *All integrals of signals clearly arising from the aldehyde tautomer are reported as integers, but integrals from signals partly or fully arising from either hemiacetal are reported to two decimal places.* δ 9.48 (s, 1H), 6.34 (s, 1H), 6.14 (s, 1H), 5.97 (dd, *J* = 17.4, 10.8 Hz, 0.29H), 5.79 (dd, *J* = 17.2, 10.7 Hz, 0.32H), 5.73 (dd, *J* = 17.2, 10.7 Hz, 1H), 5.63 – 5.57 (m, 0.55H), 5.32 (dd, *J* = 17.4, 1.3 Hz, 0.31H), 5.24 (dt, *J* = 3.1, 1.6 Hz, 0.31H), 5.23

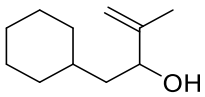
– 5.22 (m, 0.33H), 5.19 (dd, *J* = 17.1, 1.5 Hz, 0.39H), 5.16 – 5.09 (m, 1.96H), 5.05 (dd, *J* = 10.7, 1.5 Hz, 0.37H), 5.04 (dd, *J* = 10.7, 1.5 Hz, 1H), 2.73 (dq, *J* = 15.5, 1.7 Hz, 0.31H), 2.68 – 2.60 (m, 0.34H), 2.57 – 2.47 (m, 3.30H), 2.38 (s, 1H), 1.85 – 1.75 (m, 1.85H), 1.74 – 1.56 (m, 8.16H), 1.54 – 1.37 (m, 4.72H), 1.28 – 1.16 (m, 3.93H), 1.16 – 1.09 (m, 1.73H), 0.99 – 0.87 (m, 3.74H). **^{13}C NMR** (126 MHz, $CDCl_3$) δ 196.04, 150.46, 149.14, 146.03, 143.93, 143.19, 141.94, 138.64, 113.61, 112.77, 112.75, 110.22, 110.06, 98.68, 98.50, 85.44, 83.78, 75.47, 49.00, 48.96, 48.22, 42.56, 42.40, 40.76, 35.25, 35.20, 34.85, 34.83, 34.79, 34.75, 34.10, 33.91, 33.52, 26.52, 26.52, 26.47, 26.45, 26.44. **HRMS** (ESI) *m/z* calcd for $C_{14}H_{22}NaO_2$ $[(M+Na)^+]$: 245.1512, measured: 245.1511.

Keto-enal 5.21



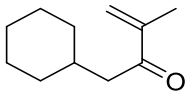
To a solution of substrate **5.20a** (32.9 mg, 0.148 mmol, 1 equiv) in 740 μL *d*$_6$-DMSO in an NMR tube was added 20.6 μL mesitylene and 6.6 mg of crystalline $HNTf_2$•diazepane catalyst **3.129**, then the solution was stirred at 45 °C and followed by ^{1}H NMR. After stirring for 10 d, the mixture was poured into 8 mL 0.1 N HCl and extracted with 3x5 mL Et_2O. The combined organic layers were washed with 1 mL each water and brine, then dried over $MgSO_4$, filtered, and concentrated. Silica gel chromatography with 20% Et_2O / hexanes (R_f 0.34, 33% Et_2O / hexanes) afforded 3.8 mg or 12% yield of oxy-Cope ketone **5.21**. It should be noted that this was by far the major product observed in the reaction by NMR analysis. **IR** ν_{max} (thin film, cm^{-1}): 2921, 2851, 2698, 1692, 1628, 1448, 1408, 1365, 1282, 1261, 1208, 1178, 1149,1088, 1021, 951. **^{1}H NMR (**500 MHz, $CDCl_3$) δ 9.54 (s, 1H), 6.28 (s, 1H), 6.02 (s, 1H), 2.40 (t, *J* = 7.3 Hz, 2H), 2.28 – 2.20 (m, 4H), 1.81 (ddt, *J* = 14.4, 7.0, 3.5 Hz, 1H), 1.73 (p, *J* = 7.5 Hz, 2H), 1.71 – 1.60 (m, 5H), 1.32 – 1.19 (m, 2H), 1.19 – 1.07 (m, 1H), 0.91 (qd, *J* = 12.5, 11.5, 3.6 Hz, 2H). **^{13}C NMR** (126 MHz, $CDCl_3$) δ 210.57, 194.72, 149.82, 134.57, 50.77, 42.87, 34.10, 33.39, 27.29, 26.35, 26.23, 21.94. **HRMS** (ESI) *m/z* calcd for $C_{14}H_{22}NaO_2$ $[(M+Na)^+]$: 245.15120, measured: 245.15111.

Allyl alcohol 5.18b′



To a solution of cyclohexylethanal (1.40 mL, 1.19 g, 9.46 mmol, 1 equiv) in 100 mL dry THF at –78 °C was added isopropenylmagnesium bromide (0.5 M in THF, 24.0 mL, 1.26 equiv) over 10 mins. After 3 h at this temperature, the bath was removed and the solution briefly allowed to warm, then 5 mL each sat. aq. NH_4Cl and water were added. After being allowed to warm to room temperature, the THF was removed by rotary evaporation, then 40 mL water and 5 mL 0.1 N HCl were added and the aqueous extracted with 3x40 mL Et_2O. The combined organic layers were washed sequentially with 10 mL each 5% aq. $NaHCO_3$, water, and brine, then dried over anhydrous $MgSO_4$, filtered, and concentrated. Silica gel flash chromatography with 15-20% Et_2O / pentane (R_f 0.20, 10% Et_2O / hexanes) afforded 1.01 g or 63% yield of alcohol **5.18b′** as a clear colourless liquid. The characterization data are in agreement with the literature.[60] **IR** ν_{max} (neat liquid, cm^{-1}): 3352, 3072, 2920, 2851, 1707, 1650, 1447, 1372, 1345, 1320, 1294, 1262,1240, 1199, 1171, 1129, 1083, 1063, 1048, 1002, 965. **^{1}H NMR** (500 MHz, $CDCl_3$) δ 4.94 (dt, *J* = 2.0, 1.1 Hz, 1H), 4.81 (p, *J* = 1.7 Hz, 1H), 4.17 (dt, *J* = 7.8, 4.1 Hz, 1H), 1.80 (d, *J* = 12.8 Hz, 1H), 1.72 (t, *J* = 1.3 Hz, 3H), 1.71 – 1.60 (m, 4H), 1.47 – 1.35 (m, 4H), 1.31 – 1.08 (m, 3H), 1.02 – 0.84 (m, 2H). **^{13}C NMR** (126 MHz, $CDCl_3$) δ 148.39, 110.85, 73.72, 43.13, 34.33, 34.13, 33.16, 26.74, 26.48, 26.36, 17.61. **HRMS** (ESI) *m/z* calcd for $C_{11}H_{20}ONa$ $[(M+Na)^+]$: 191.14064, measured: 191.14024. **HRMS** (APCI) *m/z* calcd for $C_{11}H_{21}O$ $[(M+H)^+]$: 169.15869, measured: 169.15831, *m/z* calcd for $C_{11}H_{19}O$ $[(M–H)^–]$: 167.14304, measured: 167.14272.

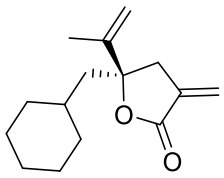
Enone 5.18b



To a solution of alcohol **5.18b′** (0.3016 g, 1.792 mmol, 1 equiv) in 5 mL dry DMSO was added IBX (0.6030 g, 2.153 mmol, 1.2 equiv) and the suspension stirred 2 h, then poured into 50 mL 0.5 N HCl and extracted with 3x30 mL EtOAc. The combined organic layers were washed sequentially with 5 mL each 5% aq. $NaHCO_3$, sat. aq. $Na_2S_2O_3$, water (twice), and brine. The extract was dried over anhydrous $MgSO_4$, filtered, and concentrated to provide a quantitative yield of essentially pure ketone **5.18b**, which was used without further purification. In other instances, silica gel flash

chromatography with 10% Et_2O / pentane (R_f 0.60, 10% EtOAc / hexanes) afforded ketone **5.18b** as a pale yellow liquid in 82% yield from 1.3 g of alcohol by essentially the same procedure. The characterization data are in agreement with the literature.[60] **IR** ν_{max} (neat liquid, cm^{-1}): 2921, 2851, 1673, 1448, 1060. **^{1}H NMR** (500 MHz, $CDCl_3$) δ 5.93 (s, 1H), 5.75 (s, 1H), 2.53 (d, *J* = 6.9 Hz, 2H), 1.86 (s, 3H), 1.85 – 1.78 (m, 1H), 1.74 – 1.60 (m, 5H), 1.32 – 1.20 (m, 2H), 1.18 – 1.06 (m, 1H), 1.01 – 0.85 (m, 2H).

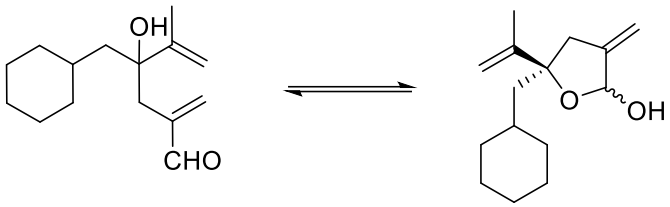
Lactone 5.19b



To a solution of ketone **5.18b** (0.767 g, 4.61 mmol, 1 equiv) and allyl bromide ethyl ester **4.91**[57] (0.70 mL, 0.98 g, 5.08 mmol, 1.1 equiv) in 125 mL dry THF was added Zn dust (0.5225 g, 7.641 mmol, 1.66 equiv) and the suspension was heated at 95 °C under a condenser for 4 h. The reaction was then cooled to room temperature, checked by ^{1}H NMR for completion, filtered on celite and concentrated to afford 0.8645 g or 73% yield of lactone **5.19b** as a colourless liquid, pure by NMR and this could be used directly in the next step without further purification. In other instances, silica gel chromatography was conducted with 10% EtOAc / hexanes (R_f 0.48, 33% EtOAc / hexanes). **IR** ν_{max} (thin film, cm^{-1}): 2922, 2852, 1764, 1448, 1397, 1290, 1264, 1163, 999. **^{1}H NMR** (500 MHz, $CDCl_3$) δ 6.20 (q, *J* = 2.5 Hz, 1H), 5.58 (dt, *J* = 3.5, 1.7 Hz, 1H), 5.07 (d, *J* = 1.8 Hz, 1H), 4.90 (q, *J* = 1.5 Hz, 1H), 2.89 (dtd, *J* = 16.7, 2.7, 1.2 Hz, 1H), 2.73 (dtd, *J* = 16.7, 2.6, 1.1 Hz, 1H), 1.92 – 1.83 (m, 1H), 1.77 – 1.68 (m, 4H), 1.68 – 1.52 (m, 5H), 1.44 – 1.33 (m, 1H), 1.28 – 1.03 (m, 3H), 1.01 – 0.86 (m, 2H). **^{13}C NMR** (126 MHz, $CDCl_3$) δ 169.96, 144.71, 135.12, 122.09, 112.02, 87.58, 46.21, 39.86, 34.68, 34.42, 33.83, 26.48, 26.32, 26.29, 19.25. **HRMS** (APCI) *m/z* calcd for $C_{15}H_{23}O_2$ [$(M+H)^+$]: 235.16926, measured: 235.17019.

Note: This methylene lactone was found to frequently polymerize on standing as a neat substance, so whenever possible it should be used when freshly prepared or stored as a solution in a freezer.

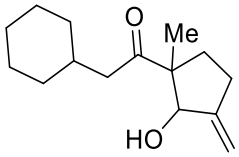
Aldehyde-hemiacetals 5.20b



To a solution of lactone **5.19b** (0.8645 g, 3.689 mmol, 1 equiv) in 50 mL dry DCM at – 78 °C was added DIBAL (1.0 M in DCM, 5.5 mL, 5.53 mmol, 1.5 equiv) dropwise via syringe, and the solution stirred 5 h. Fieser's workup was conducted, the resulting suspension filtered on celite then concentrated. Silica gel chromatography with Et_2O / pentane (R_f 0.36, 33% Et_2O / hexanes) afforded 0.7144 g or 82% yield of aldehyde-lactol mixture **5.20b** as a clear colourless liquid. *All integrals of signals clearly arising from the aldehyde tautomer are reported as integers, but integrals from signals partly or fully arising from either hemiacetal are reported to two decimal places.* **^{1}H NMR** (500 MHz, $CDCl_3$) δ 9.47 (s, 1H), 6.33 (d, *J* = 0.9 Hz, 1H), 6.12 (d, *J* = 0.8 Hz, 1H), 5.60 (d, *J* = 6.5 Hz, 0.31H), 5.57 (d, *J* = 9.5 Hz, 0.36H), 5.22 (dt, *J* = 3.8, 2.3 Hz, 0.72H), 5.16 – 5.12 (m, 0.42H), 5.12 (q, *J* = 1.9 Hz, 0.38H), 5.10 (q, *J* = 1.9 Hz, 0.35H), 5.02 – 4.98 (m, 0.46H), 4.99 – 4.95 (m, 1H), 4.89 – 4.85 (m, 0.40H), 4.85 – 4.81 (m, 1H), 4.84 – 4.79 (m, 0.39H), 2.73 (s, 1H), 2.56 (s, 3H), 1.90 – 1.80 (m, 2.11H), 1.75 – 1.46 (m, 16.89H), 1.44 – 1.35 (m, 2.34H), 1.27 – 1.03 (m, 7.23H), 0.98 – 0.82 (m, 4.67H). **^{13}C NMR** (126 MHz, $CDCl_3$) δ 196.19, 150.21, 149.37, 148.58, 147.77, 146.82, 146.09, 138.46, 111.73, 111.41, 110.57, 109.77, 109.71, 98.46, 98.21, 88.00, 87.84, 77.72, 46.64, 46.46, 45.85, 42.29, 41.78, 39.92, 35.08, 34.84, 34.65, 34.59, 34.54, 34.47, 33.99, 33.81, 33.55, 26.49, 26.43, 26.39, 26.36, 26.33, 20.04, 19.78, 19.54. **HRMS** (ESI) *m/z* calcd for $C_{15}H_{24}NaO_2$ $[(M+Na)^+]$: 259.16685, measured: 259.16644.

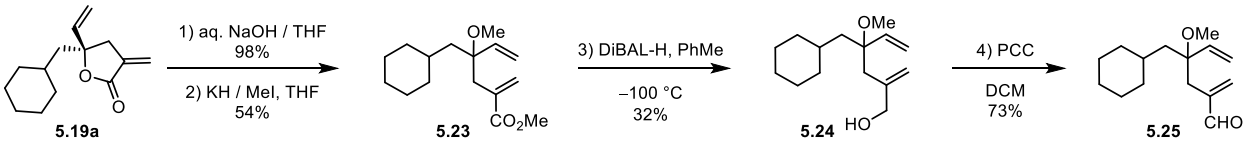
Note: This compound was stored in solution and kept cold to avoid the following reaction.

Ketone 5.22



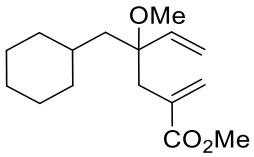
Neat substrate **5.20b** was observed to spontaneously rearrange to the diastereomers of ketone **5.22** at room temperature, occurring to a significant extent in mere hours. Silica gel chromatography

with 66% DCM / hexanes afforded a pure analytical sample of ketone **5.22**. **IR** ν_{max} (thin film, cm^{-1}): 3464 (broad), 2921, 2851, 2253, 1779, 1696, 1448, 1404, 1373, 1354, 1287, 1211, 1138, 1073, 1029, 961. **^{1}H NMR** (500 MHz, $CDCl_3$) δ 5.21 – 5.16 (m, 1H), 5.11 (q, *J* = 2.3 Hz, 0.71H), 5.01 – 4.93 (m, 1.71H), 4.54 (s, 0.67H), 4.06 (d, *J* = 5.3 Hz, 1H), 3.03 (d, *J* = 6.3 Hz, 1H), 2.46 (q, *J* = 4.3 Hz, 1H), 2.43 – 2.27 (m, 7.37H), 2.18 (ddd, *J* = 13.1, 9.5, 6.4 Hz, 1H), 1.89 – 1.70 (m, 3.35H), 1.69 – 1.56 (m, 12.13H), 1.53 (ddd, *J* = 13.2, 8.6, 6.4 Hz, 1H), 1.30 – 1.17 (m, 5.28H), 1.14 (s, 3H), 1.14 – 1.03 (m, 2.55H), 1.01 (s, 2.36H), 0.91 – 0.78 (m, 4.58H). **^{13}C NMR** (126 MHz, $CDCl_3$) δ 215.78, 215.18, 151.75, 150.22, 109.64, 107.62, 82.03, 77.06, 58.14, 56.69, 46.34, 45.74, 33.34, 33.27, 33.25, 33.23, 33.14, 33.02, 31.15, 29.79, 27.15, 26.31, 26.19, 25.60, 21.07, 15.30. **HRMS** (ESI) *m/z* calcd for $C_{15}H_{24}NaO_2$ [$(M+Na)^+$]: 259.16685, measured: 259.16651.



Scheme 5.4. Synthesis of a cyclohexyl-tagged acyclic methyl ether oCM substrate.

Methyl ester 5.23

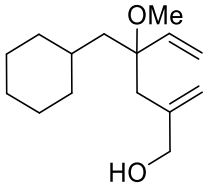


Lactone **5.19a** (0.5622 g, 2.552 mmol) was stirred for 24 h in 14 mL of 1:1 THF / 1 M NaOH, then the THF removed by rotary evaporation. The concentrate was diluted with 10 mL 1 M HCl and extracted with 3x25 mL EtOAc. The combined organic layers were washed sequentially with 5 mL each sat. aq. $NaHCO_3$ and brine, then dried over anhydrous Na_2SO_4, filtered, and concentrated. This afforded 0.5980 g or 98% yield of the carboxylic acid alcohol as a clear gum. This was used without further purification. **HRMS** (ESI) *m/z* calcd for $C_{14}H_{21}O_3$ [$(M–H)^–$]: 237.14962, measured: 237.14947.

To a solution of the carboxylic acid (0.2723 g, 1.143 mmol, 1 equiv) in 12 mL dry THF, cooled under argon over an ice bath, was added nearly oil-free KH (0.2322 g, 5.79 mmol, 5 equiv), then the reaction was stirred 5 minutes before addition of MeI (0.71 mL, 11.4 mmol, 10 equiv). The reaction was warmed in the bath to room temperature and stirred for 18 h. At this time, 5 mL sat.

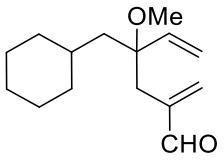
aq. NH_4Cl was added and the THF removed by rotary evaporation, 5 mL 1 N HCl was added, and the aqueous was extracted with 3x20 mL EtOAc. The combined organic layers were washed sequentially with 10 mL each water and brine, then dried over anhydrous Na_2SO_4, filtered, and concentrated. Silica gel flash chromatography with 1% AcOH in 10-20% EtOAc / hexanes afforded 0.1643 g or 54% yield of methyl ester **5.23**, which was used without further purification.

Alcohol 5.24



To a solution of ester **5.23** (0.1369 g, 0.5139 mmol, 1 equiv) in 5.1 mL dry PhMe at –95 °C (Et_2O / dry ice) was added DiBAL-H (25% in PhMe, 0.363 mL, 1.05 equiv) dropwise via syringe. The reaction was stirred 40 mins, then Fieser's workup was conducted and the resulting suspension filtered on celite. Silica gel flash chromatography with EtOAc / hexanes (R_f 0.32, 20% EtOAc / hexanes) afforded 39.7 mg or 32% yield of alcohol **5.24** as a clear colourless liquid. **IR** ν_{max} (neat liquid, cm^{-1}): 3375 (broad), 3083, 2920, 2849, 1766, 1644, 1448, 1412, 1201, 1059 (broad). **^{1}H NMR** (500 MHz, $CDCl_3$) δ 5.77 (dd, *J* = 17.7, 11.2 Hz, 1H), 5.20 (dd, *J* = 11.1, 1.1 Hz, 1H), 5.14 (dd, *J* = 17.7, 1.0 Hz, 1H), 5.12 – 5.08 (m, 1H), 4.85 (s, 1H), 4.08 – 4.00 (m, 2H), 3.41 (bs, 1H), 3.17 (s, 3H), 2.59 (d, *J* = 14.3 Hz, 1H), 2.27 (d, *J* = 14.3 Hz, 1H), 1.82 – 1.72 (m, 2H), 1.69 – 1.58 (m, 3H), 1.58 – 1.42 (m, 3H), 1.29 – 1.18 (m, 2H), 1.12 (dddd, *J* = 16.1, 12.6, 8.0, 3.2 Hz, 1H), 1.02 – 0.91 (m, 2H). **^{13}C NMR** (126 MHz, $CDCl_3$) δ 145.17, 141.40, 116.19, 115.32, 80.09, 67.21, 50.22, 42.43, 42.27, 35.46, 34.94, 32.96, 26.65, 26.62, 26.44. **HRMS** (ESI) *m/z* calcd for $C_{15}H_{26}NaO_2$ [$(M+Na)^+$]: 261.1825, measured: 261.1818.

Aldehyde 5.25

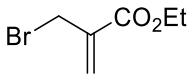


A solution of alcohol **5.24** (33.7 mg, 0.141 mmol, 1 equiv) and pyridinium chlorochromate (PCC; 46.2 mg, 0.214 mmol, 1.5 equiv) in 2 mL dry DCM was stirred 24 h until complete by TLC. AN

additional spatula tip of PCC was added about halfway through this period. The dark solution was chromatographed directly with 10-20% Et_2O / pentane (R_f 0.45, 20% EtOAc / hexanes) afforded 24.3 mg or 73% yield of aldehyde **5.25** as a clear colourless oil. **IR** ν_{max} (neat liquid, cm^{-1}): 2920, 2850, 2695, 1690, 1627, 1448, 1407, 1344, 1081. **^{1}H NMR** (400 MHz, $CDCl_3$) δ 9.45 (s, 1H), 6.48 (d, *J* = 1.1 Hz, 1H), 6.13 (s, 1H), 5.66 (dd, *J* = 17.1, 11.5 Hz, 1H), 5.17 – 5.07 (m, 2H), 3.16 (s, 3H), 2.60 (d, *J* = 14.5 Hz, 1H), 2.50 (dd, *J* = 15.1, 1.0 Hz, 1H), 1.81 – 1.47 (m, 6H), 1.46 – 1.33 (m, 2H), 1.31 – 1.03 (m, 3H), 0.99 – 0.79 (m, 2H). **^{13}C NMR** (101 MHz, $CDCl_3$) δ 195.00, 145.71, 141.71, 137.71, 114.91, 79.61, 49.89, 43.37, 35.15, 35.00, 33.04, 31.70, 26.63, 26.55, 26.48. **HRMS** (ESI) *m/z* calcd for $C_{15}H_{24}NaO_2$ [$(M+Na)^+$]: 259.1669, measured: 259.1665.

Note: This substrate displayed similarly uncooperative reactivity in the oCM reaction as the Bn-tagged acyclic substrate equivalent.

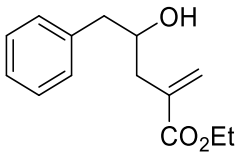
Allyl bromide 4.91



This compound was prepared as described by Hediger, and the characterization data are in agreement with that reported.[57] **^{1}H NMR** (500 MHz, $CDCl_3$) δ 6.33 (d, *J* = 0.7 Hz, 1H), 5.94 (d, *J* = 0.8 Hz, 1H), 4.27 (q, *J* = 7.1 Hz, 2H), 4.18 (d, *J* = 0.9 Hz, 2H), 1.33 (t, *J* = 7.1 Hz, 2H). **^{13}C NMR** (126 MHz, $CDCl_3$) δ 164.99, 137.73, 129.05, 61.45, 29.52, 14.29.

Note: This bromide is a severe lachrymator.

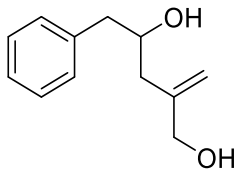
Ester 4.92



To a well-stirred mixture of allyl bromide **4.91** (6.7674 g, 35.06 mmol, 1 equiv) and phenylacetaldehyde (4.31 mL, 38.56 mmol, 1.1 equiv) in 140 mL THF was added 35 mL sat. aq. NH_4Cl and Zn dust (2.7575 g, 42.18 mmol, 1.2 equiv), then the suspension stirred 1 h at room temperature. The reaction was then filtered on a celite pad, which was rinsed with THF, and concentrated *in vacuo*. After adding 15 mL water and 10 mL 0.1 N HCl, the aqueous solution was

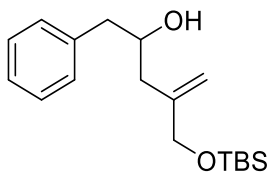
extracted with 3x50 mL EtOAc. The combined organic layers were washed sequentially with 10 mL each 5% aq. $NaHCO_3$, water, and brine, then dried over anhydrous Na_2SO_4, filtered, and concentrated. Silica gel flash chromatography with 15-20% EtOAc / hexanes (R_f 0.21, 25% EtOAc / hexanes) afforded 7.9637 g or 97% yield of alcohol **4.92** as a viscous yellow oil. The characterization data are in agreement with the literature.[61] **IR** ν_{max} (neat liquid, cm^{-1}): 3418 (broad), 3062, 3027, 2982, 2926, 1708, 1628, 1604, 1260, 1180, 1137, 1079, 1026. **^{1}H NMR** (500 MHz, $CDCl_3$) δ 7.35 – 7.27 (m, 2H), 7.26 – 7.20 (m, 3H), 6.26 (d, *J* = 1.5 Hz, 1H), 5.65 (d, *J* = 1.1 Hz, 1H), 4.21 (qd, *J* = 7.1, 2.2 Hz, 2H), 4.02 (qd, *J* = 8.6, 3.7 Hz, 1H), 2.83 (dd, *J* = 13.7, 5.1 Hz, 1H), 2.76 (dd, *J* = 13.7, 7.8 Hz, 1H), 2.63 (ddd, *J* = 14.1, 3.6, 0.9 Hz, 1H), 2.41 (dd, *J* = 14.1, 8.5 Hz, 1H), 2.17 (d, *J* = 3.8 Hz, 1H), 1.30 (t, *J* = 7.1 Hz, 3H). **^{13}C NMR** (126 MHz, $CDCl_3$) δ 167.77, 138.47, 137.78, 129.57, 128.66, 127.79, 126.62, 71.62, 61.14, 43.87, 39.82, 14.31.

Diol 4.105



To a solution of ester **4.92** (1.4285 g, 6.097 mmol, 1 equiv) in 50 mL dry PhMe at –78 °C was added DiBAL-H (25% in PhMe, 13.5 mL, 3.29 equiv) carefully dropwise, then the reaction was allowed to warm to room temperature overnight. After 18 h, Fieser's workup was conducted, and the resulting suspension filtered on celite. Silica gel flash chromatography with 25-50% EtOAc / hexanes (R_f 0.19, 50% EtOAc / hexanes) afforded 1.0318 g or 88% yield of diol **4.105** as a colourless liquid. The characterization data are in agreement with that from the preparation of this compound from keto-ester **5.10**.

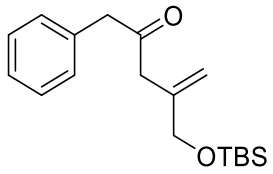
Silyl ether 4.93



To diol **4.105** (1.0199 g, 5.305 mmol, 1 equiv) and imidazole (0.5441 g, 7.992 mmol, 1.51 equiv) in 30 mL THF was added solid TBSCl (0.8065 g, 5.351 mmol, 1.01 equiv) in portions, and the

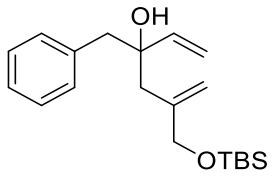
resulting suspension was stirred at room temperature 24 h. The reaction was poured into 40 mL water and extracted with 3x40 mL EtOAc, then the combined organic layers were washed with 20 mL brine, dried over anhydrous Na_2SO_4, filtered, and concentrated. Silica gel flash chromatography with 10% EtOAc / hexanes (R_f 0.69, 50% EtOAc / hexanes) afforded 1.6258 g or quantitative yield of alcohol **4.93** as a pale yellow liquid. **IR** ν_{max} (thin film, cm^{-1}): 3446 (broad), 3088, 3064, 3028, 2952, 2928, 2856, 1725, 1651, 1603, 1496, 1471, 1454, 1389, 1361, 1253, 1149, 1079, 1006. **^{1}H NMR** (500 MHz, $CDCl_3$) δ 7.34 – 7.27 (m, 2H), 7.23 (d, *J* = 7.2 Hz, 3H), 5.14 (d, *J* = 1.5 Hz, 1H), 4.94 (s, 1H), 4.10 (s, 2H), 3.97 (dtt, *J* = 9.1, 6.6, 3.3 Hz, 1H), 2.82 (dd, *J* = 13.6, 7.1 Hz, 1H), 2.77 (dd, *J* = 13.6, 5.8 Hz, 1H), 2.61 (d, *J* = 2.9 Hz, 1H), 2.35 (dd, *J* = 14.1, 3.0 Hz, 1H), 2.15 (dd, *J* = 14.1, 9.0 Hz, 1H), 0.91 (s, 9H), 0.07 (s, 6H). **^{13}C NMR** (126 MHz, $CDCl_3$) δ 145.59, 138.82, 129.60, 128.58, 126.48, 113.60, 71.36, 66.74, 43.86, 41.30, 26.04, 18.50, -5.25, -5.26. **HRMS** (ESI) *m/z* calcd for $C_{18}H_{30}O_2SiNa$ [$(M+Na)^+$]: 329.1907, measured: 329.1913.

Ketone 4.94



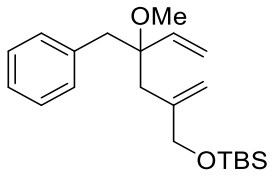
A suspension of secondary alcohol **4.93** (4.0792 g, 13.31 mmol, 1 equiv) and IBX (5.5975 g, 19.99 mmol, 1.5 equiv) in 130 mL EtOAc was refluxed at 90 °C for 24 h, then cooled to room temperature and filtered. Silica gel flash chromatography with 5-10% EtOAc / hexanes (R_f 0.29, 8% EtOAc / hexanes) afforded 3.16 g or 78% yield of ketone **4.94** as a pale yellow liquid. **IR** ν_{max} (thin film, cm^{-1}): 3067, 3031, 2954, 2929, 2886, 2856, 1715, 1496, 1471, 1462, 1455, 1408, 1390, 1361, 1253, 1080. **^{1}H NMR** (500 MHz, $CDCl_3$) δ 7.33 (t, *J* = 7.3 Hz, 2H), 7.26 (t, *J* = 7.4 Hz, 1H), 7.20 (d, *J* = 7.0 Hz, 2H), 5.23 (d, *J* = 1.5 Hz, 1H), 4.94 – 4.90 (m, 1H), 4.07 (s, 2H), 3.75 (s, 2H), 3.18 (s, 2H), 0.90 (s, 9H), 0.05 (s, 6H). **^{13}C NMR** (126 MHz, $CDCl_3$) δ 205.89, 142.19, 134.29, 129.65, 128.85, 127.17, 113.82, 65.84, 49.40, 46.48, 26.04, 18.50, -5.30. **HRMS** (ESI) *m/z* calcd for $C_{18}H_{29}O_2Si$ [$(M+H)^+$]: 305.19313, measured: 305.19311.

Allyl alcohol 4.95a



A solution of ketone **4.94** (2.00 mL, 1.90 g, 6.26 mmol, 1 equiv) in 3.0 mL dry THF was added dropwise by cannula to a solution of vinylmagnesium bromide (12.5 mL, 1.0 M in THF, 2.0 equiv) in 25 mL additional dry THF, cooled over an ice bath. The reaction was warmed in the bath to room temperature and stirred for 7 h total, then cooled over ice again before 10 mL sat. aq. NH_4Cl and 10 mL water were added. The reaction was then concentrated *in vacuo* and extracted with 3x65 mL EtOAc. The combined organic layers were washed sequentially with 10 mL each water and brine, then dried over anhydrous Na_2SO_4, filtered, and concentrated. Silica gel flash chromatography with 5-10% EtOAc / hexanes (R_f 0.39, 8% EtOAc / hexanes) afforded 1.74 g or 84% yield of alcohol **4.95a** as a clear colourless liquid. **IR** ν_{max} (neat liquid, cm^{-1}): 3417 (broad), 3086, 3063, 3028, 2952, 2928, 2885, 2856, 1725, 1644, 1604, 1495, 1471, 1463, 1407, 1253, 1100, 1083, 1061, 1004. **^{1}H NMR** (500 MHz, $CDCl_3$) δ 7.29 – 7.24 (m, 2H), 7.24 – 7.19 (m, 3H), 5.84 (dd, *J* = 17.2, 10.7 Hz, 1H), 5.17 (dd, *J* = 17.2, 1.6 Hz, 1H), 5.14 (q, *J* = 1.5 Hz, 1H), 5.05 (dd, *J* = 10.7, 1.6 Hz, 1H), 4.90 – 4.85 (m, 1H), 4.13 (d, *J* = 13.2 Hz, 1H), 4.06 (d, *J* = 13.2 Hz, 1H), 3.23 (s, 1H), 2.84 (s, 2H), 2.36 (s, 2H), 0.90 (s, 9H), 0.06 (s, 3H), 0.05 (s, 3H). **^{13}C NMR** (126 MHz, $CDCl_3$) δ 144.30, 143.73, 137.33, 131.02, 127.98, 126.47, 115.40, 113.11, 74.54, 67.47, 48.41, 45.08, 26.07, 18.52, -5.25. **HRMS** (ESI) *m/z* calcd for $C_{20}H_{32}NaO_2Si$ [$(M+Na)^+$]: 355.20638, measured: 355.20633.

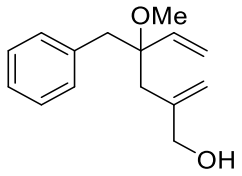
Methyl ether 4.95a′



General procedure **D** was followed using tertiary alcohol **4.95a** (0.9303 g, 2.797 mmol, 1 equiv), taking 5.5 h. To quench, 5 mL sat. aq. NH_4Cl and 20 mL water were added, THF removed *in vacuo*, and the aqueous layer extracted with 3x25 mL EtOAc. The combined organic layers were

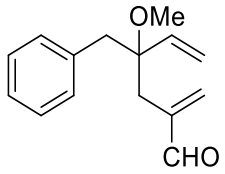
washed with 5 mL brine then dried over anhydrous Na_2SO_4, filtered, and concentrated. Silica gel flash chromatography with 1-10% EtOAc / hexanes (R_f 0.60, 20% Et_2O / hexanes) afforded 0.9262 g or 96% yield of ether **4.95a′** as a pale yellow oil. **IR** ν_{max} (thin film, cm^{-1}): 3087, 3064, 3029, 2952, 2929, 2856, 1709, 1643, 1603, 1496, 1455, 1413, 1253, 1080. **^{1}H NMR** (500 MHz, $CDCl_3$) δ 7.29 – 7.22 (m, 2H), 7.23 – 7.17 (m, 3H), 5.71 (dd, *J* = 17.7, 11.1 Hz, 1H), 5.25 (d, *J* = 1.9 Hz, 1H), 5.21 (dd, *J* = 11.1, 1.1 Hz, 1H), 5.13 (dd, *J* = 17.7, 1.1 Hz, 1H), 5.01 (s, 1H), 4.13 – 4.02 (m, 2H), 3.25 (s, 3H), 2.96 (d, *J* = 13.9 Hz, 1H), 2.89 (d, *J* = 13.9 Hz, 1H), 2.31 (d, *J* = 15.1 Hz, 1H), 2.21 (d, *J* = 15.1 Hz, 1H), 0.91 (s, 9H), 0.06 (s, 3H), 0.05 (s, 3H). **^{13}C NMR** (126 MHz, $CDCl_3$) δ 144.56, 141.63, 137.59, 130.91, 127.90, 126.25, 115.53, 112.62, 79.54, 66.79, 50.23, 42.26, 38.08, 26.11, 18.57, -5.18, -5.20. **HRMS** (ESI) *m/z* calcd for $C_{21}H_{34}NaO_2Si$ [$(M+Na)^+$]: 369.22203, measured: 369.22211.

Methyl ether alcohol 4.96a



To TBS ether **4.95a′** (0.9262 g, 2.672 mmol, 1 equiv) in 27 mL THF was added TBAF (1.0 M in THF, 4.0 mL, 1.5 equiv). After 2.5 h, 10 mL each sat. aq. NH_4Cl and H_2O were added along with 50 mL EtOAc, the layers separated, and the aqueous layer further extracted with 2x40 mL EtOAc. The combined organic layers were washed with 20 mL brine, then dried over anhydrous Na_2SO_4, filtered, and concentrated. Silica gel flash chromatography with 30% EtOAc / hexanes (R_f 0.25, 25% EtOAc / hexanes) afforded 0.5997 g or 97% yield of alcohol **4.96a** as a pale yellow liquid. **IR** ν_{max} (neat liquid, cm^{-1}): 3361 (broad), 3085, 3063, 3028, 2938, 2827, 1643, 1603, 1495, 1453, 1414, 1157, 1056, 1031. **^{1}H NMR** (500 MHz, $CDCl_3$) δ 7.31 – 7.17 (m, 5H), 5.78 (dd, *J* = 17.8, 11.2 Hz, 1H), 5.29 (dd, *J* = 11.2, 0.9 Hz, 1H), 5.21 (dd, *J* = 17.8, 0.8 Hz, 1H), 5.14 (d, *J* = 1.6 Hz, 1H), 4.89 (s, 1H), 4.06 (dd, *J* = 13.0, 6.0 Hz, 1H), 4.00 (dd, *J* = 13.0, 6.8 Hz, 1H), 3.32 (s, 3H), 3.17 (t, *J* = 6.6 Hz, 1H), 3.04 (d, *J* = 14.1 Hz, 1H), 2.91 (d, *J* = 14.1 Hz, 1H), 2.39 (d, *J* = 14.5 Hz, 1H), 2.32 (d, *J* = 14.6 Hz, 1H). **^{13}C NMR** (126 MHz, $CDCl_3$) δ 144.90, 140.43, 137.05, 130.87, 128.10, 126.50, 116.47, 116.23, 79.77, 67.28, 50.63, 41.79, 41.32. **HRMS** (ESI) *m/z* calcd for $C_{15}H_{20}NaO_2$ [$(M+Na)^+$]: 255.13555, measured: 255.13562.

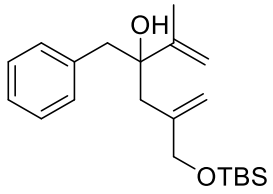
Methyl ether enal 4.97a



General Procedure **C** was followed using alcohol **4.96a** (0.5966 g, 2.568 mmol, 1 equiv) and IBX (1.4409 g, 5.146 mmol, 2.0 equiv), and the reaction complete in 1.5 h as determined by ^{1}H NMR spectroscopy. The aqueous filtrate was extracted with 3x100 mL Et_2O, then the combined organic layers were washed with 30 mL brine, dried over anhydrous $MgSO_4$, filtered, and concentrated. Silica gel flash chromatography with 15% Et_2O / hexanes (R_f 0.46, 25% EtOAc / hexanes) afforded 0.5130 g or 87% yield of enal **4.97a** as a clear colourless liquid. **IR** ν_{max} (neat liquid, cm^{-1}): 3086, 3063, 3028, 2936, 2826, 2699, 1687, 1626, 1603, 1496, 1454, 1414, 1345, 1078. **^{1}H NMR** (500 MHz, $CDCl_3$) δ 9.48 (s, 1H), 7.29 – 7.14 (m, 5H), 6.55 (d, *J* = 1.1 Hz, 1H), 6.18 (s, 1H), 5.62 (dd, *J* = 17.7, 11.1 Hz, 1H), 5.18 (dd, *J* = 11.1, 1.1 Hz, 1H), 5.11 (dd, *J* = 17.7, 1.1 Hz, 1H), 3.27 (s, 3H), 2.94 – 2.85 (m, 2H), 2.57 (s, 2H). **^{13}C NMR** (126 MHz, $CDCl_3$) δ 194.91, 145.64, 140.65, 137.93, 137.06, 130.82, 128.01, 126.44, 115.99, 79.49, 50.34, 42.63, 31.11. **HRMS** (ESI) *m/z* calcd for $C_{15}H_{18}NaO_2$ [$(M+Na)^+$]: 253.11990, measured: 253.12001.

Note: This compound was found to be totally stable in the freezer for months, and no rearrangement was detected upon handling, mild heating, or on standing at room temperature.

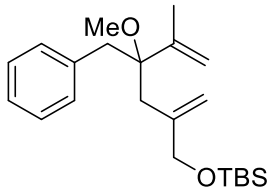
Isopropenyl allyl alcohol 4.95b



A solution of ketone **4.94** (0.7122 g, 2.339 mmol, 1 equiv) in 10 mL dry THF was added to 12.0 mL isopropenyl magnesium bromide (0.5 M in THF, 6.0 mmol, 2.6 equiv), dropwise via cannula over an ice bath. The reaction was allowed to warm to room temperature in the bath. After 20 h, the reaction was cooled again over ice, and 5 mL each sat. aq. NH_4Cl and water were added, then the layers were separated. The aqueous layer was further extracted with 2x10 mL EtOAc, then the

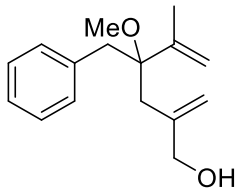
organic layers were washed separately with 5 mL brine, combined over anhydrous Na_2SO_4, filtered, and concentrated. Silica gel flash chromatography with 5-10% EtOAc / hexanes (R_f 0.64, 20% EtOAc / hexanes) afforded 0.3390 g or 42% yield of alcohol **4.95b** as a pale yellow oil, along with 0.2404 g or 34% yield of recovered ketone **4.94**. **IR** ν_{max} (thin film, cm^{-1}): 3424 (broad), 3064, 3030, 2953, 2929, 2886, 2857, 1720, 1643, 1604, 1253, 1082, 1005. **^{1}H NMR** (500 MHz, $CDCl_3$) δ 7.30 – 7.17 (m, 5H), 5.13 (q, *J* = 1.6 Hz, 1H), 4.94 – 4.90 (m, 1H), 4.89 (s, 1H), 4.86 – 4.81 (m, 1H), 4.15 (d, *J* = 13.5 Hz, 1H), 4.08 (d, *J* = 13.5 Hz, 1H), 3.06 (s, 1H), 2.91 (d, *J* = 13.6 Hz, 1H), 2.86 (d, *J* = 13.6 Hz, 1H), 2.54 (d, *J* = 14.2 Hz, 1H), 2.34 (d, *J* = 14.2 Hz, 1H), 1.85 – 1.80 (m, 3H), 0.88 (s, 9H), 0.04 (s, 3H), 0.03 (s, 3H). **^{13}C NMR** (126 MHz, $CDCl_3$) δ 148.30, 144.83, 137.39, 130.81, 127.94, 126.45, 114.35, 112.16, 77.10, 67.14, 46.29, 43.47, 26.06, 20.33, 18.49, -5.25. **HRMS** (ESI) *m/z* calcd for $C_{21}H_{34}NaO_2Si$ [$(M+Na)^+$]: 369.22203, measured: 369.22205.

Isopropenyl methyl ether 4.95b′



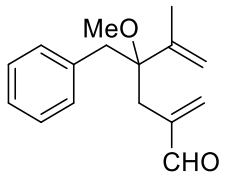
General procedure **D** was followed using tertiary alcohol **4.95b** (0.3347 g, 0.9657 mmol, 1 equiv), taking 3 h. To quench, 5 mL each sat. aq. NH_4Cl and water were added, then the layers separated. The aqueous layer was further extracted with 2x15 mL EtOAc, then the organic layers were washed separately with 5 mL brine, combined over anhydrous Na_2SO_4, filtered, and concentrated. Silica gel flash chromatography with 0-10% EtOAc / hexanes (R_f 0.70, 20% EtOAc / hexanes) afforded 0.3305 g or 95% yield of ether **4.95b′** as a pale yellow oil. **IR** ν_{max} (neat liquid, cm^{-1}): 3088, 3062, 3028, 2952, 2929, 2887, 2856, 2826, 1642, 1605, 1471, 1461, 1252, 1079. **^{1}H NMR** (500 MHz, $CDCl_3$) δ 7.26 – 7.15 (m, 5H), 5.23 (s, 1H), 5.16 (s, 1H), 5.07 – 5.02 (m, 1H), 4.86 (s, 1H), 3.98 (s, 2H), 3.21 (s, 3H), 3.06 (d, *J* = 14.3 Hz, 1H), 2.98 (d, *J* = 14.3 Hz, 1H), 2.22 (s, 2H), 1.79 – 1.75 (m, 3H), 0.91 (s, 9H), 0.05 (s, 6H). **^{13}C NMR** (126 MHz, $CDCl_3$) δ 146.21, 144.19, 137.84, 130.36, 127.90, 126.25, 114.98, 111.59, 82.11, 66.93, 49.66, 39.26, 34.99, 26.10, 19.61, 18.56, -5.20. **HRMS** (ESI) *m/z* calcd for $C_{22}H_{36}NaO_2Si$ [$(M+Na)^+$]: 383.23768, measured: 383.23735.

Isopropenyl methyl ether alcohol 4.96b



To TBS ether **4.95b′** (0.1555 g, 0.4312 mmol, 1 equiv) in 4 mL THF was added solid TBAF (0.1475 g, 0.5641 mmol, 1.3 equiv). After 2 h, 1 mL each sat. aq. NH_4Cl and H_2O were added, the THF was removed by rotary evaporation, 1 mL 1 N HCl added, and the aqueous mixture extracted with 3x20 mL EtOAc. The combined organic layers were washed sequentially with 5 mL each water and brine, then dried over anhydrous Na_2SO_4, filtered, and concentrated. Silica gel flash chromatography with 25% EtOAc / hexanes (R_f 0.25, 25% EtOAc / hexanes) afforded 98.6 mg or 93% yield of alcohol **4.96b** as a clear colourless gum. **IR** ν_{max} (thin film, cm^{-1}): 3375, 3087, 3062, 3029, 2928, 2826, 1641, 1604, 1496, 1453, 1373, 1203, 1072, 1031. **^{1}H NMR** (500 MHz, $CDCl_3$) δ 7.26 – 7.17 (m, 5H), 5.17 (s, 1H), 5.11 – 5.07 (m, 1H), 5.02 (s, 1H), 4.90 (s, 1H), 4.06 – 3.95 (m, 2H), 3.27 (s, 3H), 3.06 (d, *J* = 14.6 Hz, 1H), 3.01 (d, *J* = 14.6 Hz, 1H), 2.39 (s, 3H), 1.81 – 1.77 (m, 3H). **^{13}C NMR** (126 MHz, $CDCl_3$) δ 145.48, 144.85, 137.44, 130.36, 128.01, 126.40, 115.33, 115.20, 82.59, 67.24, 50.05, 39.63, 37.35, 19.86. **HRMS** (ESI) *m/z* calcd for $C_{16}H_{22}NaO_2$ $[(M+Na)^+]$: 269.15120, measured: 269.15117.

Isopropenyl methyl ether enal 4.97b

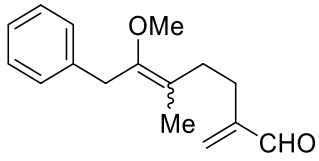


To a solution of alcohol **4.96b** (88.2 mg, 0.358 mmol, 1 equiv) in 1.8 mL each DCM and pyridine was added DMP (0.3089 g, 0.7283 mmol, 2.0 equiv) and the reaction was followed by TLC. After 2 h, the reaction was filtered on celite using minimal additional DCM, then the filtrate was concentrated. Silica gel flash chromatography with 20% Et_2O / pentane (R_f 0.46, 20% EtOAc / hexanes) afforded 63.1 mg or 72% yield of aldehyde **4.97b** as a clear colourless oil. **IR** ν_{max} (thin film, cm^{-1}): 3088, 3061, 3029, 2926, 2853, 2827, 2700, 1692, 1640, 1625, 1497, 1453, 1374, 1351, 1084. **^{1}H NMR** (500 MHz, $CDCl_3$) δ 9.45 (s, 1H), 7.26 – 7.15 (m, 3H), 7.14 – 7.08 (m, 2H), 6.68

(d, J = 1.2 Hz, 1H), 6.18 – 6.14 (m, 1H), 5.01 – 4.96 (m, 1H), 4.84 – 4.80 (m, 1H), 3.23 (s, 3H), 2.99 (d, J = 14.5 Hz, 1H), 2.93 (d, J = 14.5 Hz, 1H), 2.61 (d, J = 16.8 Hz, 1H), 2.54 (d, J = 16.8 Hz, 1H), 1.76 – 1.69 (m, 3H). **^{13}C NMR** (126 MHz, $CDCl_3$) δ 195.03, 145.74, 145.25, 137.34, 137.13, 130.18, 128.00, 126.45, 115.21, 82.15, 49.85, 39.90, 28.95, 19.78. **HRMS** (ESI) *m/z* calcd for $C_{16}H_{20}NaO_2$ [$(M+Na)^+$]: 267.13555, measured: 267.13567.

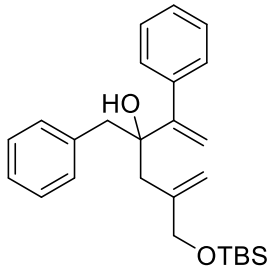
Note: The undesired simple oxy-Cope rearrangement of this substrate is extremely facile. The use of NEt_3-neutralized silica gel prevented rearrangement during chromatography, and heat was strictly avoided when removing solvents. However, even purified isopropenyl enal **4.97b** was found to rearrange at room temperature, both on standing as a neat substance and in $CDCl_3$ solution, producing inseparable mixtures of oxy-Cope products **4.97b′** and starting material. As such, it was desirable to initiate the catalytic oCM reaction as soon as possible.

Enol ether 4.97b′, *mixture of isomers*



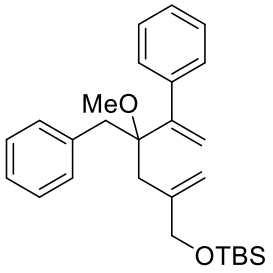
A $CDCl_3$ solution of isopropenyl methyl ether enal **4.97b** fully rearranged (95% conversion) in 6 d to produce methyl enol ether **4.97b′** as a 5:3 mixture of isomers, inseparable from each other and the starting material. **IR** ν_{max} (thin film, cm^{-1}): 3084, 3062, 3027, 2928, 2855, 2828, 2699, 1687, 1628, 1603, 1494, 1453, 1256, 1215, 1137, 1092. *Signals arising from the major and minor isomers are arbitrarily assigned based on integral magnitude*. **^{1}H NMR** (500 MHz, $CDCl_3$) δ 9.53 (s, 1H′), 9.49 (s, 1H″), 7.31 – 7.25 (m, 2H′, 2H″), 7.23 – 7.16 (m, 3H′, 3H″), 6.28 – 6.24 (m, 1H′), 6.23 – 6.18 (m, 1H″), 5.96 (s, 1H′), 5.95 (s, 1H″), 3.55 (s, 2H′), 3.53 (s, 2H″), 3.41 (s, 3H″), 3.40 (s, 3H′), 2.41 – 2.27 (m, 3H′, 3H″), 2.20 (dd, J = 9.3, 6.4 Hz, 1H′, 1H″), 1.74 (s, 3H″), 1.70 (s, 3H′). **^{13}C NMR** (126 MHz, $CDCl_3$) δ 194.88, 194.66, 150.10, 149.84, 149.33, 148.85, 139.26, 139.23, 134.42, 134.09, 128.55, 128.53, 128.46, 128.32, 126.21, 118.26, 117.70, 56.99, 56.96, 33.20, 31.70, 29.07, 27.09, 26.29, 16.74, 14.88. **HRMS** (ESI) *m/z* calcd for $C_{16}H_{20}NaO_2$ [$(M+Na)^+$]: 267.13555, measured: 267.13552, *m/z* calcd for $C_{16}H_{21}O_2$ [$(M+H)^+$]: 245.15361, measured: 245.15341.

Styrenyl alcohol 4.95c



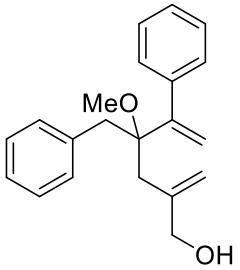
To a solution of freshly distilled α-bromostyrene[35] (0.7519 g, 4.11 mmol, 2.51 equiv) in 18 mL dry THF at –78 °C was added a solution of ^{t}BuLi (1.7 M in pentane, 2.36 mL, 4.01 mmol, 2.45 equiv) dropwise over 10 mins and the resulting mixture then stirred 60 mins. A solution of ketone **4.94** (0.4982 g, 1.636 mmol, 1 equiv) in 13.5 mL THF at –42 °C was then added dropwise by cannula over 30 mins, then the reaction allowed to warm to room temperature in the bath. After 19 h the reaction was cooled over ice, 10 mL each sat. aq. NH_4Cl and H_2O were added, the layers were separated, and the aqueous layer further extracted with 2x30 mL Et_2O. The organic layers were washed separately with 10 mL brine, dried over anhydrous $MgSO_4$, filtered, and concentrated. A 1:1 ratio of ketone **4.94** and desired product **4.95c** were observed in the crude mixture by ^{1}H NMR spectroscopy. Silica gel flash chromatography with 30-70% DCM / hexanes (R_f 0.52, 10% EtOAc / hexanes) afforded 0.3313 g or 50% yield of alcohol **4.95c** as a yellow liquid. **IR** ν_{max} (thin film, cm^{-1}): 3408 (broad), 3082, 3058, 3030, 2953, 2928, 2897, 2856, 1494, 1471, 1462, 1454, 1389, 1254, 1110, 1089. **^{1}H NMR** (500 MHz, $CDCl_3$) δ 7.29 – 7.15 (m, 10H), 5.39 (d, *J* = 1.4 Hz, 1H), 5.17 (d, *J* = 1.5 Hz, 1H), 5.14 (d, *J* = 1.4 Hz, 1H), 4.91 (s, 1H), 4.17 (d, *J* = 13.2 Hz, 1H), 4.08 (d, *J* = 13.2 Hz, 1H), 3.34 (s, 1H), 3.04 (d, *J* = 13.7 Hz, 1H), 2.98 (d, *J* = 13.7 Hz, 1H), 2.65 (d, *J* = 14.4 Hz, 1H), 2.46 (d, *J* = 14.3 Hz, 1H), 0.86 (s, 9H), 0.02 (s, 3H), 0.01 (s, 3H). **^{13}C NMR** (126 MHz, $CDCl_3$) δ 154.56, 144.53, 141.79, 137.46, 131.30, 128.85, 127.93, 127.85, 127.05, 126.44, 116.38, 115.45, 76.93, 67.64, 47.81, 44.72, 26.04, 18.46, -5.26, -5.28. **HRMS** (ESI) *m/z* calcd for $C_{26}H_{36}NaO_2Si$ [$(M+Na)^+$]: 431.23768, measured: 431.23816.

Styrenyl methyl ether 4.95c′



General procedure **D** was followed using tertiary alcohol **4.95c** (0.3233 g, 0.7911 mmol, 1 equiv), taking 3 h. To quench, 2 mL each sat. aq. NH_4Cl and water were added, and the mixture extracted with 3x10 mL EtOAc. The combined organic layers were washed with 5 mL brine, dried over anhydrous Na_2SO_4, filtered, and concentrated. Silica gel flash chromatography with 2% EtOAc / hexanes (R_f 0.50, 10% EtOAc / hexanes) afforded 0.3176 g or 95% yield of ether **4.95c′** as a pale yellow liquid. **IR** ν_{max} (thin film, cm^{-1}): 3085, 3062, 3029, 2952, 2928, 2896, 2855, 2825, 1721, 1650, 1572, 1493, 1471, 1461, 1252, 1075. **^{1}H NMR** (500 MHz, $CDCl_3$) δ 7.41 – 7.36 (m, 2H), 7.31 – 7.25 (m, 3H), 7.25 – 7.15 (m, 5H), 5.42 (d, *J* = 0.8 Hz, 1H), 5.31 (d, *J* = 0.8 Hz, 1H), 5.28 – 5.23 (m, 1H), 5.18 – 5.13 (m, 1H), 3.84 – 3.80 (m, 2H), 3.34 (s, 3H), 3.20 (d, *J* = 14.3 Hz, 1H), 3.08 (d, *J* = 14.3 Hz, 1H), 2.23 (d, *J* = 16.6 Hz, 1H), 2.18 (d, *J* = 16.6 Hz, 1H), 0.88 (s, 9H), 0.01 (s, 3H), -0.00 (s, 3H). **^{13}C NMR** (201 MHz, $CDCl_3$) δ 149.70, 144.06, 141.66, 137.83, 130.62, 128.71, 128.01, 127.90, 127.27, 126.24, 119.07, 111.44, 82.08, 67.00, 49.60, 39.64, 36.03, 26.07, 18.52, -5.24. **HRMS** (ESI) *m/z* calcd for $C_{27}H_{38}NaO_2Si$ $[(M+Na)^+]$: 445.25333, measured: 445.25320.

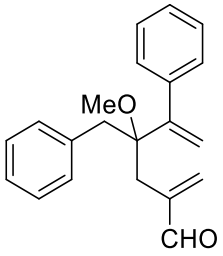
Styrenyl methyl ether alcohol 4.96c



To TBS ether **4.95c′** (0.3106 g, 0.7348 mmol, 1 equiv) in 7 mL THF was added TBAF (1.0 M in THF, 1.1 mL, 1.5 equiv). After 3 h, 5 mL each sat. aq. NH_4Cl and H_2O along with 15 mL EtOAc were added, the layers were separated, and the aqueous layer further extracted with 2x10 mL

EtOAc. The combined organic layers were washed with 10 mL brine, dried over anhydrous Na_2SO_4, filtered, and concentrated. Silica gel flash chromatography with 20-40% EtOAc / hexanes (R_f 0.42, 40% EtOAc / hexanes) afforded 0.2207 g or 97% yield of alcohol **4.96c** as a pale yellow oil. **IR** ν_{max} (thin film, cm^{-1}): 3375 (broad), 3086, 3057, 3029, 2936, 2825, 1648, 1620, 1601, 1572, 1492, 1453, 1442, 1230, 1209, 1186, 1059, 1029, 908. **^{1}H NMR** (500 MHz, $CDCl_3$) δ 7.38 (dd, *J* = 8.0, 1.6 Hz, 2H), 7.35 – 7.26 (m, 3H), 7.27 – 7.16 (m, 5H), 5.45 (d, *J* = 0.7 Hz, 1H), 5.32 (d, *J* = 0.7 Hz, 1H), 5.17 (s, 1H), 5.00 (s, 1H), 3.95 – 3.84 (m, 2H), 3.40 (s, 3H), 3.19 (d, *J* = 14.7 Hz, 1H), 3.07 (d, *J* = 14.7 Hz, 1H), 2.39 (s, 2H), 2.21 (t, *J* = 6.4 Hz, 1H). **^{13}C NMR** (126 MHz, $CDCl_3$) δ 148.91, 144.68, 141.56, 137.47, 130.58, 128.63, 128.13, 128.00, 127.42, 126.39, 119.44, 114.98, 82.59, 67.40, 49.94, 40.01, 38.27. **HRMS** (ESI) *m/z* calcd for $C_{21}H_{24}NaO_2$ [$(M+Na)^+$]: 331.16685, measured: 331.16683.

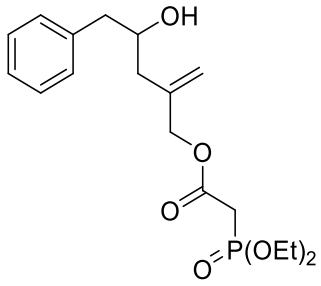
Styrenyl methyl ether enal 4.97c



To a solution of alcohol **4.96c** (0.1386 g, 0.4494 mmol, 1 equiv) in 2.2 mL each DCM and pyridine was added DMP (0.3843 g, 0.9461 mmol, 2.0 equiv) and the reaction was followed by TLC. After 1.5 h, the reaction was filtered on celite using minimal additional DCM, then the filtrate was concentrated. Silica gel flash chromatography with 30% Et_2O / pentane (R_f 0.53, 25% EtOAc / hexanes) afforded 77.3 mg or 56% yield of aldehyde **4.97c** as a pale yellow oil. **IR** ν_{max} (thin film, cm^{-1}): 3084, 3061, 3031, 2922, 2851, 2699, 1765, 1692, 1625, 1602, 1494, 1449, 1275, 1158, 1077. **^{1}H NMR** (400 MHz, $CDCl_3$) δ 9.39 (s, 1H), 7.37 – 7.26 (m, 5H), 7.24 – 7.16 (m, 3H), 7.09 (dd, *J* = 7.7, 1.7 Hz, 2H), 6.72 (d, *J* = 1.1 Hz, 1H), 6.21 – 6.16 (m, 1H), 5.35 (d, *J* = 1.0 Hz, 1H), 5.24 (d, *J* = 1.0 Hz, 1H), 3.33 (s, 3H), 3.07 (d, *J* = 14.5 Hz, 1H), 2.99 (d, *J* = 14.5 Hz, 1H), 2.66 (d, *J* = 16.8 Hz, 1H), 2.59 (d, *J* = 16.6 Hz, 1H). **^{13}C NMR** (126 MHz, $CDCl_3$) δ 194.84, 149.30, 145.89, 141.43, 137.35, 137.09, 130.53, 128.67, 128.09, 128.02, 127.41, 126.48, 119.33, 82.14, 49.86, 40.76, 30.32. **HRMS** (ESI) *m/z* calcd for $C_{21}H_{22}NaO_2$ [$(M+Na)^+$]: 329.15120, measured: 329.15097.

Note: All of the same comments for isopropenyl substrate **4.97b** apply here.

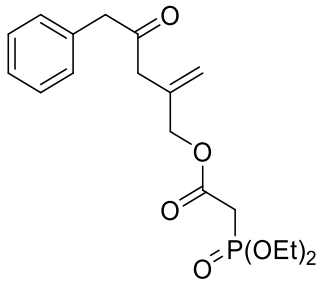
Phosphonate ester alcohol 5.15



To a solution of diol **4.105** (1.2388 g, 6.443 mmol, 1 equiv) in 64 mL dry DCM were added 4-dimethylaminopyridine (52.5 mg, 0.430 mmol, 0.07 equiv), *N,N′*-Dicyclohexylcarbodiimide (1.4676 g, 7.113 mmol, 1.1 equiv), a solution of diethylphosphonoacetic acid (1.3295 g, 6.778 mmol, 1.05 equiv) in 10 mL dry DCM, and NEt_3 (1.8 mL, 13 mmol, 2.0 equiv). The reaction was sealed and stirred 24 h under argon, then filtered on celite and concentrated to afford a 2:1 mixture of product and diol as observed by ^{1}H NMR. Silica gel flash chromatography with 0-5% MeCN / EtOAc (R_f 0.36, 10% MeCN / EtOAc) afforded 0.4015 g of pure and 0.7787 g of slightly less pure phosphonate **5.15** for a combined 49% yield as pale yellow oils. A 0.3605 g portion or 29 % yield of diol **4.105** was also recovered. **IR** ν_{max} (thin film, cm^{-1}): 3403, 3087, 3063, 3028, 2983, 2933, 1735, 1651, 1603, 1496, 1478, 1454, 1443, 1394, 1369, 1253, 1163, 1115, 1048, 1018, 969. **^{1}H NMR** (500 MHz, $CDCl_3$) δ 7.34 – 7.27 (m, 2H), 7.26 – 7.20 (m, 3H), 5.21 (d, *J* = 1.5 Hz, 1H), 5.08 (s, 1H), 4.68 (d, *J* = 13.1 Hz, 1H), 4.63 (d, *J* = 13.2 Hz, 1H), 4.21 – 4.10 (m, 4H), 4.04 – 3.97 (m, 1H), 2.98 (d, *J* = 21.6 Hz, 2H), 2.83 – 2.74 (m, 2H), 2.42 (d, *J* = 3.9 Hz, 1H), 2.36 (dd, *J* = 14.4, 4.0 Hz, 1H), 2.25 (dd, *J* = 14.4, 8.7 Hz, 1H), 1.34 (t, *J* = 7.1 Hz, 3H), 1.33 (t, *J* = 7.1 Hz, 3H). **^{13}C NMR** (126 MHz, $CDCl_3$) δ 165.60 (d, *J* = 6.1 Hz), 140.82, 138.66, 129.57, 128.64, 126.58, 116.20, 70.90, 68.09, 62.97 (d, *J* = 6.3 Hz), 62.94 (d, *J* = 6.4 Hz), 43.87, 41.30, 34.57 (d, *J* = 133.9 Hz), 16.50, 16.46. **HRMS** (ESI) *m/z* calcd for $C_{18}H_{27}NaO_6P$ [$(M+Na)^+$]: 393.1437, measured: 393.1449.

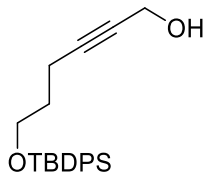
Note: The diethylphosphonoacetic acid was readily obtained by saponification of triethyl phosphonoacetate.

Phosphonate ester ketone 4.106



To a solution of alcohol **5.15** (0.3954 g, 1.068 mmol, 1 equiv) in 3.0 mL dry DMSO was added IBX (0.4453 g, 1.590 mmol, 1.5 equiv), and the reaction complete in 10 h as determined by ^{1}H NMR. The aqueous filtrate was extracted with 3x20 mL EtOAc, then the combined organic layers were washed sequentially with 10 mL each water and brine, dried over anhydrous Na_2SO_4, filtered, and concentrated. Silica gel flash chromatography with 0-15% MeCN / EtOAc (R_f 0.45, 10% MeCN / EtOAc) afforded 0.3439 g or 87% yield of alcohol **4.106** as a pale yellow liquid. **IR** ν_{max} (neat liquid, cm^{-1}): 2984, 2932, 2910, 1735, 1654, 1497, 1454, 1394, 1368, 1257, 1163, 1113, 1048, 1018, 965. **^{1}H NMR** (500 MHz, $CDCl_3$) δ 7.33 (t, *J* = 7.3 Hz, 2H), 7.30 – 7.25 (m, 1H), 7.21 (d, *J* = 7.1 Hz, 2H), 5.29 (s, 1H), 5.03 (s, 1H), 4.61 (s, 2H), 4.21 – 4.09 (m, 4H), 3.75 (s, 2H), 3.27 (s, 2H), 2.93 (d, *J* = 21.5 Hz, 2H), 1.33 (t, *J* = 7.1 Hz, 6H). **^{13}C NMR (**126 MHz, $CDCl_3$) δ 205.28, 165.48 (d, *J* = 6.2 Hz), 137.03, 134.02, 129.64, 128.92, 127.30, 118.03, 67.54, 62.87 (d, *J* = 6.2 Hz), 49.70, 46.46, 34.37 (d, *J* = 134.1 Hz), 16.51, 16.46. **HRMS** (ESI) *m/z* calcd for $C_{18}H_{25}NaO_6P$ $[(M+Na)^+]$: 391.1281, measured: 391.1277.

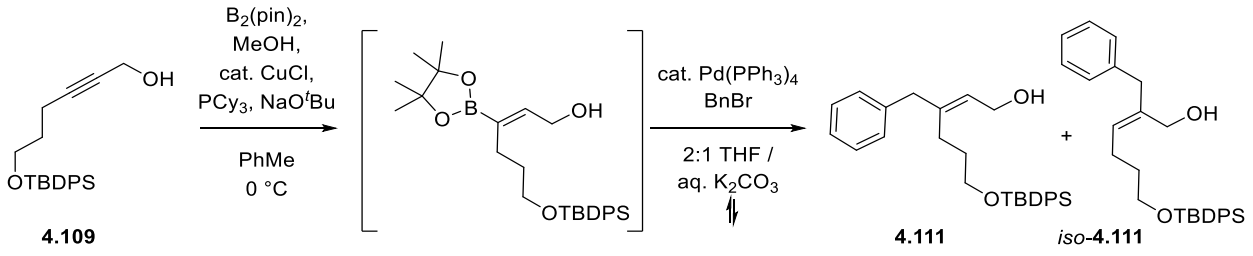
Propargyl alcohol 4.109



To a solution of commercially available 4-pentynol (5.0821 g, 0.060415 mol, 1 equiv) and imidazole (10.2602 g, 0.1507 mol, 2.5 equiv) in 10 mL dry DMF was added TBDPSCl (17.28 mL, 0.06645 mol, 1.1 equiv) dropwise over an ice bath. After 30 mins, the bath was removed and the reaction stirred 1.5 h longer. The suspension was filtered on celite with minimal Et_2O into 200 mL water and extracted with 3x60 mL Et_2O. The combined organic layers were washed with 50 mL

brine, dried over anhydrous $MgSO_4$, filtered, and concentrated without heat. The residue was taken up in 100 mL Et_2O, separated from a small volume of milky white suspension which formed, then washed sequentially with 25 mL each water and brine, dried over anhydrous $MgSO_4$, filtered, and concentrated without heat again to give the TBDPS ether as a pale yellow liquid. The spectroscopic data are agreement with the literature,[62] and this was used without further purification. **^{1}H NMR** (400 MHz, $CDCl_3$) δ 7.70 – 7.63 (m, 4H), 7.45 – 7.33 (m, 6H), 3.74 (t, *J* = 6.0 Hz, 2H), 2.35 (td, *J* = 7.2, 2.7 Hz, 2H), 1.91 (t, *J* = 2.6 Hz, 1H), 1.78 (p, *J* = 6.6 Hz, 2H), 1.05 (s, 9H).

To a solution of the TBDPS ether alkyne and 600 mL dry THF in a 3-neck flask cooled at –78 °C was added *n*-BuLi (2.5 M in hexane, 36 mL, 1.5 equiv) fast dropwise. After stirring 30 mins, formaldehyde powder (9.0 g, 0.30 mol, 5.0 equiv) was added in one portion through one neck under good argon flow. The suspension was stirred for 10 h, then the bath was removed and the mixture allowed to passively warm for 4 h at which time TLC indicated completion. The mixture was cooled over an ice bath, then 20 mL each sat. aq. NH_4Cl and water were added. and the suspension filtered on celite using minimal EtOAc. The layers were separated, the aqueous was extracted further with 2x50 mL EtOAc, then the organic layers were washed separately with 50 mL brine. The combined organic layers were dried over anhydrous Na_2SO_4, filtered, and concentrated. Silica gel flash chromatography with 10-20% EtOAc / hexanes (R_f 0.43, 30% EtOAc / hexanes) afforded 17.5409 g or 82% yield of alcohol **4.109** over two steps, as a pale yellow liquid, and with spectroscopic data in agreement with the literature.[62] **^{1}H NMR** (400 MHz, $CDCl_3$) δ 7.71 – 7.63 (m, 4H), 7.47 – 7.34 (m, 6H), 4.20 (dt, *J* = 6.0, 2.1 Hz, 2H), 3.74 (t, *J* = 6.0 Hz, 2H), 2.37 (tt, *J* = 7.0, 2.1 Hz, 2H), 1.76 (p, *J* = 6.6 Hz, 2H), 1.44 – 1.35 (m, 1H), 1.05 (s, 9H).



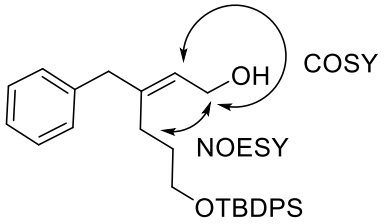
Based on an established procedure,[63] propargyl alcohol **4.109** (6.1983 g, 17.581 mmol, 1 equiv) was added as a solution in 48 mL dry PhMe to an argon-flushed solid mixture of CuCl (0.1733 g, 1.750 mmol, 0.10 equiv), $B_2(pin)_2$ (4.934 g, 19.42 mmol, 1.10 equiv), NaO^{t}Bu (0.2522 g, 2.624 mmol, 0.15 equiv), and PCy_3 (0.5929 g, 2.114 mmol, 0.12 equiv). The resulting suspension was

cooled over an ice bath and MeOH (1.42 mL, 35.1 mmol, 2.00 equiv) was added slowly dropwise, then the dark green solution stirred 2 h and followed by ^{1}H NMR spectroscopy while being allowed to warm in the bath. Following this, 10 mL of MeOH was added and briefly stirred, then the mixture filtered on celite and concentrated. Rapid silica gel flash chromatography with 30% EtOAc / hexanes (R_f 0.37, 30% EtOAc / hexanes) afforded a colourless mixture of regioisomeric vinylic pinacolboronic esters.

A solution of $Pd(OAc)_2$ (0.1963 g, 0.8743 mmol, 0.05 equiv) and PPh_3 (1.1615 g, 4.428 mmol, 0.25 equiv) was stirred for 1 h until bright yellow, then concentrated to a thick yellow residue. The boronic ester was added in 120 mL THF, then 60 mL of a ¼ aqueous dilution of sat. aq. K_2CO_3 was added, followed by BnBr (2.09 mL, 17.8 mmol, 1.00 equiv). The biphasic solution was refluxed at 95-100 °C for 13 h, then cooled to room temperature and the layers separated. The aqueous was further extracted with 2x100 mL EtOAc, then the organic layers separately washed sequentially with 20 mL water and 10 mL of brine. The combined organic layers were dried over anhydrous Na_2SO_4, filtered, and concentrated to give a 4:1 ratio of regioisomers in favour of **4.111**. Silica gel flash chromatography with 20% EtOAc / hexanes (R_f 0.44, 33% EtOAc / hexanes) gave partial separation of the regioisomers. Subsequent chromatography of the mixture of isomers, separately from the pure isomers, with 7-10% acetone / hexanes removed strongly coloured impurities and afforded 5.1136 g or 65% yield of alcohol **4.111** along with 1.0616 g or 14% yield of undesired regioisomer *iso*-**4.111**, both yellow oils.

Notes: It was found critical to control the exotherm with cooling when adding methanol to maintain regioselectivity.

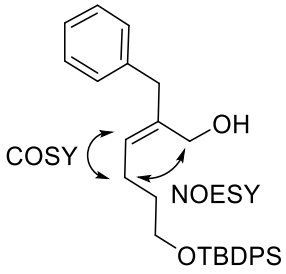
Allyl alcohol 4.111



IR ν_{max} (thin film, cm^{-1}): 3363 (broad), 3070, 3049, 3027, 2998, 2930, 2893, 2857, 1602, 1589, 1493, 1471, 1453, 1427, 1389, 1107, 1029. **^{1}H NMR** (500 MHz, $CDCl_3$) δ 7.70 – 7.61 (m, 4H), 7.47 – 7.40 (m, 2H), 7.40 – 7.35 (m, 4H), 7.31 – 7.23 (m, 2H), 7.23 – 7.17 (m, 1H), 7.20 – 7.10

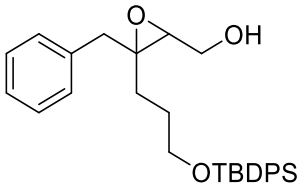
(m, 2H), 5.49 (t, J = 7.0 Hz, 1H), 4.20 – 4.13 (m, 2H), 3.63 (t, J = 6.1 Hz, 2H), 3.31 (s, 2H), 2.17 – 2.10 (m, 2H), 1.61 – 1.52 (m, 2H), 1.45 (t, J = 5.6 Hz, 1H), 1.05 (s, 9H). **^{13}C NMR** (126 MHz, $CDCl_3$) δ 142.83, 139.58, 135.72, 133.94, 129.78, 129.21, 128.46, 127.79, 126.46, 126.31, 63.38, 59.16, 43.46, 31.35, 27.01, 26.17, 19.31. **HRMS** (ESI) *m/z* calcd for $C_{29}H_{36}NaO_2Si$ [$(M+Na)^+$]: 467.23768, measured: 467.23934.

Allyl alcohol isomer *iso*-4.111



IR ν_{max} (thin film, cm^{-1}): 3069, 3049, 3028, 2997, 2954, 2930, 2890, 2856, 1495, 1471, 1455, 1427, 1389, 1361, 1252, 1173, 1109. **^{1}H NMR** (500 MHz, $CDCl_3$) δ 7.69 – 7.63 (m, 4H), 7.45 – 7.40 (m, 2H), 7.40 – 7.35 (m, 4H), 7.30 – 7.26 (m, 2H), 7.23 – 7.16 (m, 3H), 5.35 (t, J = 7.6 Hz, 1H), 4.07 (d, J = 6.0 Hz, 2H), 3.68 (t, J = 6.1 Hz, 2H), 3.45 (s, 2H), 2.23 (q, J = 7.4 Hz, 2H), 1.59 (p, J = 6.5 Hz, 2H), 1.38 (t, J = 6.0 Hz, 1H), 1.06 (s, 9H). **^{13}C NMR** (126 MHz, $CDCl_3$) δ 140.13, 138.83, 135.73, 134.01, 129.88, 129.77, 129.09, 128.54, 127.79, 126.26, 63.10, 59.84, 41.95, 32.57, 27.03, 23.93, 19.35. **HRMS** (ESI) *m/z* calcd for $C_{29}H_{36}NaO_2Si$ [$(M+Na)^+$]: 467.2377, measured: 467.2380.

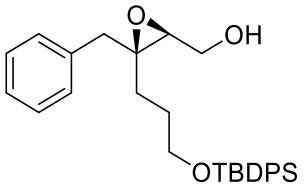
Epoxy alcohol 4.112 (racemate)



To a suspension of olefin **4.111** (25.7 mg, 0.0578 mmol, 1 equiv) and $NaHCO_3$ (14.4 mg, 0.171 mmol, 3.0 equiv) in 1.5 mL DCM was added *m*CPBA (17.0 mg, 0.0985 mmol, 1.7 equiv). After stirring 7 h, the reaction was filtered on celite, diluted with 10 mL Et_2O, then washed sequentially with 5 mL each of 1:1 sat. aq. Na_2CO_3 / 5% $Na_2S_2O_5$ and brine. The organic layer was dried over anhydrous $MgSO_4$, filtered, and concentrated. Silica gel flash chromatography with 30% EtOAc /

hexanes (R_f 0.27, 30% EtOAc / hexanes) afforded 16.1 mg or 60% yield of racemic epoxide **4.112** as a pale yellow oil. The racemate was analyzed by chiral HPLC for comparison with enantioenriched epoxide **4.112*** (*vide infra*). **IR** ν_{max} (thin film, cm^{-1}): 3431 (broad), 3070, 3028, 2956, 2930, 2893, 2857, 1603, 1589, 1427, 1107, 1091, 1030. **^{1}H NMR** (500 MHz, $CDCl_3$) δ 7.67 – 7.61 (m, 4H), 7.47 – 7.34 (m, 6H), 7.31 – 7.17 (m, 5H), 3.80 (d, *J* = 11.6 Hz, 1H), 3.69 (dq, *J* = 10.5, 6.3 Hz, 2H), 3.61 (dt, *J* = 10.5, 6.0 Hz, 1H), 2.98 (dd, *J* = 6.3, 5.0 Hz, 1H), 2.86 (s, 2H), 1.83 (bs, 1H), 1.73 – 1.51 (m, 4H), 1.04 (s, 9H). **^{13}C NMR** (126 MHz, $CDCl_3$) δ 136.64, 135.72, 135.69, 133.81, 129.82, 129.81, 128.53, 127.83, 127.81, 126.81, 64.18, 63.59, 62.32, 61.22, 41.37, 28.62, 26.99, 26.89, 19.29. **HRMS** (ESI) *m/z* calcd for $C_{29}H_{36}NaO_3Si$ [$(M+Na)^+$]: 483.2326, measured: 483.2321.

Epoxy alcohol 4.112* (enantioenriched)

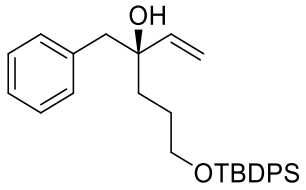


Catalytic asymmetric epoxidation was conducted on olefin **4.111** as follows, according to Sharpless's procedure.[64] To a suspension of 2.0 g of powdered activated 4Å molecular sieves (MS) in 50 mL dry DCM at –30 °C was added a solution of L-diisopropyl tartrate (0.2777 g, 1.19 mmol, 0.18 equiv) in 5 mL dry DCM, followed dropwise by neat $Ti(O^iPr)_4$ (0.288 mL, 0.973 mmol, 0.15 equiv), then finally dropwise ^{t}BuOOH (5.5 M in decane, 1.77 mL, 1.5 equiv), which had been treated with ca. 200 mg MS in a dry vial. The mixture was aged at –30 °C for 60 mins before adding olefin **4.111** (2.8808 g, 6.478 mmol, 1 equiv) as a solution, which had been treated with 0.8 g MS for over an hour, in 10 mL dry DCM dropwise by cannula. The reaction was stirred at –32 °C and followed by ^{1}H NMR spectroscopy for 20 h, then the bath was removed, 15 mL water was added, and the reaction allowed to warm to room temperature for 30 mins. To saponify the tartrate ester, 1.0 mL 50% NaOH was added and the reaction stirred 1 h, then filtered on celite and rinsed with 50 mL DCM. The layers were separated, the aqueous was diluted with 10 mL water, and extracted with 2x20 mL DCM. The combined organic layers were washed sequentially with 10 mL each water and brine, dried over anhydrous Na_2SO_4, filtered, and concentrated. Silica gel flash chromatography with 30% EtOAc / hexanes (R_f 0.31, 30% EtOAc / hexanes) afforded 2.9298

g or 98% yield of epoxide **4.112*** as a pale yellow oil. The characterization data match that of the racemic compound. Analysis by chiral HPLC indicated an *e.e.* of 72%.

Note: The assumed absolute epoxide stereochemistry is based on the model for S.A.E. and was not independently confirmed through other means since the precise enantiomer obtained is inconsequential.

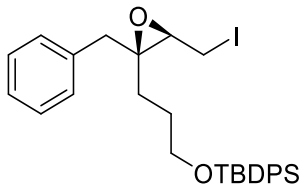
Allyl alcohol 4.113a



Following a known procedure,[65a] to a dry solution of epoxy alcohol **4.112*** (1.8102 g, 3.929 mmol, 1 equiv) in 8.8 mL of 5:3 MTBE / MeCN over an ice bath were added triphenylphosphine (3.0880 g, 11.773 mmol, 3.0 equiv), pyridine (1.20 mL, 14.9 mmol, 3.8 equiv), then solid iodine (1.9937 g, 7.855 mmol, 2.0 equiv). The yellow suspension was stirred for 3 h in the ice bath, then water (71 µL, 3.9 mmol, 1.0 equiv) was added and the suspension heated at 40 °C for 12 h before additional water (25 µL, 1.4 mmol, 0.35 equiv) was added, based on reaction progress observed by ^{1}H NMR spectroscopy. Heating was continued for a further 2.5 h, then the reaction was cooled to room temperature, 10 mL each of ½ sat. aq. $Na_2S_2O_3$ and sat. aq. $NaHCO_3$ were added, and the mixture was extracted with 3x20 mL EtOAc. The combined organic layers were washed with 10 mL brine, dried over anhydrous $MgSO_4$, filtered, and concentrated. Silica gel flash chromatography with 5-15% EtOAc / hexanes (R_f 0.50, 20% EtOAc / hexanes) afforded 1.0320 g or 59% yield of alcohol **4.113a** as a clear colourless liquid, along with 97.6 mg or 4% yield of iodide **4.114** as a pale yellow oil. **IR** ν_{max} (thin film, cm^{-1}): 3569, 3432 (broad), 3070, 3029, 2951, 2930, 2896, 2857, 1603, 1589, 1427, 1108, 1091. **^{1}H NMR** (500 MHz, $CDCl_3$) δ 7.69 – 7.63 (m, 4H), 7.46 – 7.41 (m, 2H), 7.41 – 7.34 (m, 4H), 7.32 – 7.19 (m, 5H), 5.86 (dd, *J* = 17.3, 10.8 Hz, 1H), 5.15 (dd, *J* = 17.3, 1.3 Hz, 1H), 5.11 (dd, *J* = 10.8, 1.3 Hz, 1H), 3.68 – 3.61 (m, 2H), 2.87 (d, *J* = 13.2 Hz, 1H), 2.82 (d, *J* = 13.3 Hz, 1H), 2.01 (s, 1H), 1.70 – 1.61 (m, 4H), 1.05 (s, 9H). **^{13}C NMR** (126 MHz, $CDCl_3$) δ 143.59, 136.94, 135.73, 133.89, 130.90, 129.72, 128.16, 127.77, 126.63, 113.29, 75.25, 64.47, 48.13, 36.78, 26.99, 26.80, 19.32. **HRMS** (ESI) *m/z* calcd for $C_{29}H_{36}NaO_2Si$ [$(M+Na)^+$]: 467.2377, measured: 467.2395.

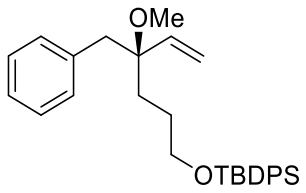
Note: Iodide **4.114** was isolable, but all attempts to elimination this epoxide under standard nucleophilic or reducing conditions were met with poor success.

Epoxy iodide 4.114



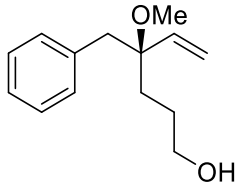
Iodide **4.114** was isolated as a byproduct from the direct conversion of epoxy alcohol **4.112*** to allylic tertiary alcohol **4.113a**. It was also directly prepared and isolated as follows, based on previous reports.[65] To epoxy alcohol **4.112*** (2.9149 g, 6.327 mmol, 1 equiv) in 63 mL dry PhMe over an ice bath was added triphenylphosphine (3.6520 g, 13.924 mmol, 2.2 equiv), imidazole (0.9434 g, 13.857 mmol, 2.2 equiv), then iodine (3.2084 g, 12.641 mmol, 2.0 equiv). The fine brown suspension was warmed over 2 h in the ice bath, by which time the suspension had settled despite stirring, leaving a clear colourless solution above, and conversion was complete according to TLC. The reaction was brought to room temperature, then 20 mL each water and EtOAc were added, followed by 50 mL 5% $Na_2S_2O_5$, then the layers were separated and the aqueous extracted 2x60 mL further with EtOAc. The combined organic layers were washed sequentially with 20 mL each water and brine, dried over anhydrous Na_2SO_4, filtered, and concentrated. Silica gel flash chromatography with 2-10% EtOAc / hexanes afforded 2.5533 g or 71% yield of iodide **4.114** (R_f 0.64, 80% DCM / hexanes) as a pale yellow oil, along with 0.5814 g or 21% yield of alcohol **4.113a** (R_f 0.42, 80% DCM / hexanes) as a clear colourless liquid. **IR** ν_{max} (thin film, cm^{-1}): 3069, 3029, 2998, 2955, 2930, 2857, 1720, 1701, 1607, 1589, 1511, 1455, 1427, 1389, 1361, 1293, 1185, 1110, 1032. **^{1}H NMR** (500 MHz, $CDCl_3$) δ 7.67 – 7.60 (m, 4H), 7.46 – 7.34 (m, 6H), 7.31 – 7.19 (m, 5H), 3.71 – 3.56 (m, 2H), 3.29 (dd, J = 10.0, 6.1 Hz, 1H), 3.14 (dd, J = 7.8, 6.1 Hz, 1H), 3.04 (dd, J = 10.0, 7.9 Hz, 1H), 2.91 (d, J = 14.5 Hz, 1H), 2.81 (d, J = 14.5 Hz, 1H), 1.74 (ddt, J = 16.8, 11.6, 5.9 Hz, 2H), 1.64 – 1.49 (m, 2H), 1.03 (s, 9H). **^{13}C NMR** (126 MHz, $CDCl_3$) δ 136.33, 135.72, 135.71, 133.90, 129.84, 129.78, 128.54, 127.81, 126.89, 67.22, 63.62, 62.65, 41.44, 28.59, 27.01, 26.21, 19.32, 1.97. **HRMS** (ESI) *m/z* calcd for $C_{29}H_{35}INaO_2Si$ [$(M+Na)^+$]: 593.1343, measured: 593.1313.

Methyl ether 4.113a′



General procedure **D** was followed using tertiary alcohol **4.113a** (0.5814 g, 1.307 mmol, 1 equiv), taking 2 h. To quench, 5 mL each sat. aq. NH_4Cl and water were added, and the mixture extracted with 3x15 mL EtOAc. The combined organic layers were washed with 5 mL brine, dried over anhydrous Na_2SO_4, filtered, and concentrated. Silica gel flash chromatography with 7% Et_2O / hexanes (R_f 0.52, 10% EtOAc / hexanes) afforded 0.5557 g or 93% yield of ether **4.113a′** as a clear colourless oil. **IR** ν_{max} (thin film, cm^{-1}): 3070, 3051, 3028, 2998, 2931, 2893, 2857, 2824, 1603, 1589, 1427, 1106, 1085, 1067. **^{1}H NMR** (500 MHz, $CDCl_3$) δ 7.70 (dd, *J* = 7.8, 1.3 Hz, 4H), 7.49 – 7.37 (m, 6H), 7.29 – 7.17 (m, 5H), 5.70 (dd, *J* = 17.7, 11.1 Hz, 1H), 5.23 (dd, *J* = 11.1, 1.3 Hz, 1H), 5.08 (dd, *J* = 17.7, 1.3 Hz, 1H), 3.69 (t, *J* = 6.1 Hz, 2H), 3.25 (s, 3H), 2.92 (d, *J* = 13.7 Hz, 1H), 2.85 (d, *J* = 13.7 Hz, 1H), 1.77 – 1.54 (m, 4H), 1.08 (s, 9H). **^{13}C NMR** (126 MHz, $CDCl_3$) δ 141.71, 137.48, 135.72, 134.12, 134.11, 130.71, 129.68, 127.92, 127.74, 126.24, 115.79, 79.68, 64.26, 49.93, 42.47, 29.95, 27.00, 26.48, 19.34. **HRMS** (ESI) *m/z* calcd for $C_{30}H_{38}NaO_2Si$ $[(M+Na)^+]$: 481.2533, measured: 481.2535.

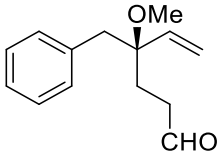
Alcohol 4.116a



To TBDPS ether **4.113a′** (0.5521 g, 1.204 mmol, 1 equiv) in 12 mL THF was added TBAF (1.0 M in THF, 1.5 mL, 1.2 equiv). After 1 h, 2 mL each sat. aq. NH_4Cl and H_2O were added, THF removed *in vacuo*, and the aqueous concentrate was extracted with 3x15 mL EtOAc. The combined organic layers were washed with 5 mL brine then dried over anhydrous Na_2SO_4, filtered, and concentrated. Silica gel flash chromatography with 20-40% EtOAc / hexanes (R_f 0.14, 25% EtOAc / hexanes) afforded 0.2600 g or 98% yield of alcohol **4.116a** as a clear colourless oil. **IR** ν_{max} (thin film, cm^{-1}): 3372 (very broad), 3085, 3062, 3028, 2943, 2873, 2826, 1640, 1603, 1496, 1453, 1414,

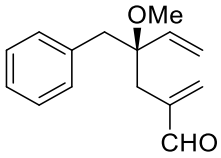
1058, 1004, 923. **^{1}H NMR** (500 MHz, $CDCl_3$) δ 7.30 – 7.24 (m, 2H), 7.24 – 7.19 (m, 3H), 5.73 (dd, *J* = 17.7, 11.1 Hz, 1H), 5.25 (dd, *J* = 11.1, 1.1 Hz, 1H), 5.12 (dd, *J* = 17.7, 1.1 Hz, 1H), 3.62 (t, *J* = 6.1 Hz, 2H), 3.27 (s, 3H), 2.94 (d, *J* = 13.8 Hz, 1H), 2.88 (d, *J* = 13.8 Hz, 1H), 1.79 (bs, 1H), 1.75 – 1.56 (m, 4H). **^{13}C NMR** (126 MHz, $CDCl_3$) δ 141.29, 137.33, 130.69, 128.00, 126.35, 116.01, 79.71, 63.31, 50.09, 42.09, 30.90, 26.70. **HRMS** (ESI) *m/z* calcd for $C_{14}H_{20}NaO_2$ $[(M+Na)^+]$: 243.1356, measured: 243.1354.

Aldehyde 4.117a



To a solution of alcohol **4.116a** (0.4422 g, 2.007 mmol, 1 equiv) in 20 mL DCM was added IBX (1.1267 g, 4.024 mmol, 2 equiv) and the resulting suspension heated at reflux for 22 h, at which time TLC indicated complete conversion. The suspension was filtered through cotton and concentrated. Silica gel flash chromatography with 5-20% EtOAc / hexanes (R_f 0.38, 20% EtOAc / hexanes) afforded 0.4059 g or 93% yield of aldehyde **4.117a** as a clear colourless liquid. **IR** ν_{max} (thin film, cm^{-1}): 3085, 3062, 3029, 2827, 2722, 1721, 1641, 1603, 1496, 1454, 1413, 1390, 1064. **^{1}H NMR** (500 MHz, $CDCl_3$) δ 9.75 (s, 1H), 7.29 – 7.24 (m, 2H), 7.23 – 7.17 (m, 3H), 5.68 (dd, *J* = 17.7, 11.1 Hz, 1H), 5.25 (d, *J* = 11.1 Hz, 1H), 5.14 (d, *J* = 17.7 Hz, 1H), 3.24 (s, 3H), 2.89 (s, 2H), 2.58 – 2.44 (m, 2H), 1.88 (dt, *J* = 9.0, 6.2 Hz, 2H). **^{13}C NMR** (126 MHz, $CDCl_3$) δ 202.33, 140.55, 136.91, 130.62, 128.13, 126.53, 116.38, 79.07, 50.08, 42.33, 38.37, 26.79. **HRMS** (ESI) *m/z* calcd for $C_{14}H_{18}NaO_2$ $[(M+Na)^+]$: 241.1199, measured: 241.1188.

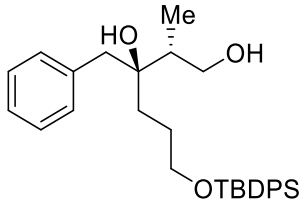
Methyl ether enal 4.97a* (enantio-enriched)



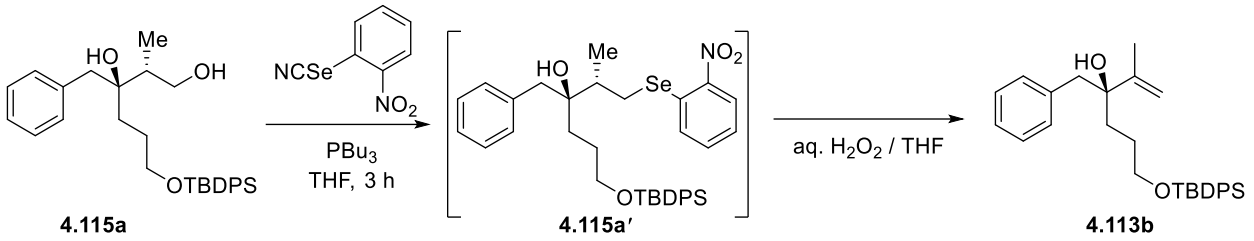
To a solution of aldehyde **4.117a** (0.1394 g, 0.6386 mmol, 1 equiv) in 6.4 mL dry DCM was added *p*-methoxybenzoic acid (10.1 mg, 0.0664 mmol, 0.1 equiv), aq. formaldehyde (37 wt.%, 48 μL, 0.64 mmol, 1.0 equiv), and finally pyrrolidine (5.0 μL, 0.006 mmol, 0.09 equiv). The

solution was immersed in a 45 °C oil bath[46] under a condenser for 2 h, then cooled. Silica gel flash chromatography of the reaction mixture directly with 5-10% EtOAc / hexanes (R_f 0.45, 20% EtOAc / hexanes) afforded 0.1248 g or 85% yield of enantioenriched enal **4.97a*** as a clear colourless liquid. The characterization data match that of the racemic compound. HPLC analysis indicated an *e.e.* of 73% for this batch, which indicated no erosion in the course of synthesis from epoxide **4.112*** of 72% *e.e.*

Diol 4.115a

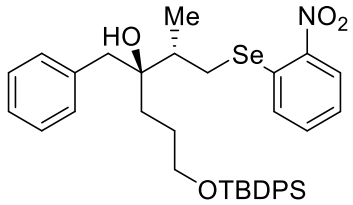


Epoxide **4.112*** (1.6085 g, 3.492 mmol, 1 equiv) in 35 mL dry THF was added to CuI•P(OEt)$_3$ (0.1266 g, 0.3550 mmol, 0.10 equiv), prepared as reported.[66] The solution was cooled to –78 °C and MeMgBr (3.0 M Et_2O, 5.82 mL, 5 equiv) was added dropwise over 10 mins, then the reaction was transferred to a –42 °C bath for 3 h and allowed to warm in that bath overnight. After 23 h total, the reaction was cooled over an ice bath, then 15 mL each sat. aq. NH_4Cl, H_2O, and EtOAc were added sequentially. The layers were separated, then the aqueous layer extracted further with 2x100 mL EtOAc. The combined organic layers were washed with 40 mL brine then dried over anhydrous Na_2SO_4, filtered, and concentrated. Silica gel flash chromatography with 30-40% EtOAc / hexanes (R_f 0.50, 15% EtOAc / DCM) afforded 1.5792 g or 95% yield of diol **4.115a** as a pale yellow gum. **IR** ν_{max} (thin film, cm^{-1}): 3336 (broad), 3070, 3029, 2953, 2930, 2893, 2857, 1389, 1361, 1259, 1106, 1092. **^{1}H NMR** (500 MHz, $CDCl_3$) δ 7.70 – 7.63 (m, 4H), 7.46 – 7.36 (m, 6H), 7.30 – 7.21 (m, 5H), 3.79 – 3.72 (m, 2H), 3.67 (t, *J* = 6.1 Hz, 2H), 3.01 (t, *J* = 5.2 Hz, 1H), 2.88 (d, *J* = 13.9 Hz, 1H), 2.86 (d, *J* = 13.9 Hz, 1H), 2.84 (s, 1H), 1.87 – 1.71 (m, 2H), 1.72 – 1.60 (m, 1H), 1.56 (t, *J* = 7.8 Hz, 2H), 1.06 (s, 9H), 0.96 (d, *J* = 7.1 Hz, 3H). **^{13}C NMR (**126 MHz, $CDCl_3$) δ 137.39, 135.73, 133.76, 133.74, 130.71, 129.84, 129.82, 128.42, 127.83, 126.61, 77.62, 65.88, 64.70, 43.55, 40.30, 32.36, 27.01, 26.86, 19.33, 12.78. **HRMS** (ESI) *m/z* calcd for $C_{30}H_{40}NaO_3Si$ [(M+Na)$^+$]: 499.2639, measured: 499.2655.



Elimination of primary alcohol **4.115a** was accomplished using Greico's method.[67] An argon-purged mixture of neat alcohol **4.115a** (1.5030 g, 3153 mmol, 1 equiv) and 2-nitrophenyl selenocyanate (1.6817 g, 7.406 mmol, 2.35 equiv), prepared as described by Sharpless,[68] was dissolved in 12.6 mL dry THF and P(*n*-Bu)$_3$ (1.85 mL, 7.41 mmol, 2.35 equiv) was added as a gentle stream. After stirring for 3 h, 10 mL each sat. aq. NH_4Cl and water were added, then the suspension was filtered through a cotton plug and extracted with 3x25 mL Et_2O. The organic layers were washed separately with 5 mL brine then dried over anhydrous $MgSO_4$, filtered, and concentrated. To a solution of this crude residue in 8 mL THF, cooled over an ice bath, was added 1.5 mL of 30% aq. H_2O_2, and the reaction allowed to warm to room temperature in the bath. After 10 h, 10 mL each sat. aq. $Na_2S_2O_3$ and water were added. The resulting suspension was filtered through a cotton plug, then through a celite pad, and finally extracted with 3x50 mL EtOAc. The combined organic layers were washed with 10 mL brine then dried over anhydrous $MgSO_4$, filtered, and concentrated. Silica gel flash chromatography with 5-10% EtOAc / hexanes (R_f 0.46, 10% EtOAc / hexanes) afforded 1.1411 g or 79% yield of allyl alcohol **4.113b** as a yellow liquid.

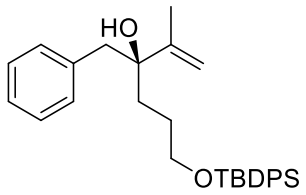
Alkyl selenenide 4.115a′



An analytical sample of the alkyl selenenide **4.115a′** was obtained by silica gel flash chromatography with 10% EtOAc / hexanes (R_f 0.54, 30% EtOAc / hexanes), then chromatography with 50% DCM / hexanes. **IR** ν_{max} (thin film, cm^{-1}): 3070, 3030, 2957, 2931, 2896, 2858, 2358, 2251, 1590, 1566, 1511, 1471, 1453, 1428, 1381, 1361, 1331, 1303, 1253, 1190, 1109, 1037, 998, 938, 906. **^{1}H NMR** (500 MHz, $CDCl_3$) δ 8.26 (dd, *J* = 8.3, 1.4 Hz, 1H), 7.72 – 7.64 (m, 4H), 7.62 – 7.57 (m, 1H), 7.47 – 7.36 (m, 7H), 7.32 – 7.20 (m, 6H), 3.70 (t, *J* = 5.5 Hz,

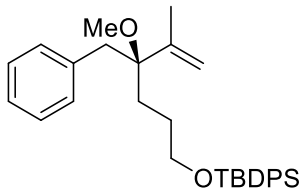
2H), 3.49 – 3.42 (m, 1H), 2.88 (d, *J* = 2.0 Hz, 2H), 2.57 (t, *J* = 11.0 Hz, 1H), 2.09 (s, 1H), 1.96 (dtt, *J* = 13.5, 6.7, 3.4 Hz, 1H), 1.80 – 1.56 (m, 4H), 1.20 (d, *J* = 6.8 Hz, 3H), 1.07 (s, 9H). **^{13}C NMR** (126 MHz, $CDCl_3$) δ 146.92, 136.96, 135.72, 135.70, 134.34, 133.67, 133.64, 133.57, 130.67, 129.84, 129.59, 128.49, 127.84, 127.83, 126.74, 126.43, 125.22, 76.07, 64.54, 42.82, 39.59, 32.37, 29.39, 27.00, 26.55, 19.31, 15.71. **HRMS** (ESI) *m/z* calcd for $C_{36}H_{43}NNaO_4SeSi$ [$(M+Na)^+$]: 684.2019ff, measured: 684.2010.

Isopropenyl alcohol 4.113b



IR ν_{max} (thin film, cm^{-1}): 3409 (broad), 3070, 3028, 2953, 2930, 2894, 2857, 1427, 1107, 1088. **^{1}H NMR** (500 MHz, $CDCl_3$) δ 7.69 – 7.61 (m, 4H), 7.46 – 7.35 (m, 6H), 7.31 – 7.18 (m, 5H), 4.91 – 4.85 (m, 1H), 4.87 (s, 1H), 3.63 (dp, *J* = 15.4, 5.4, 5.0 Hz, 2H), 2.94 (d, *J* = 13.4 Hz, 1H), 2.83 (d, *J* = 13.5 Hz, 1H), 1.89 (s, 1H), 1.89 – 1.81 (m, 1H), 1.82 (s, 3H), 1.65 – 1.45 (m, 3H), 1.04 (s, 9H). **^{13}C NMR** (126 MHz, $CDCl_3$) δ 148.03, 136.99, 135.73, 133.95, 133.92, 130.74, 129.70, 128.16, 127.76, 126.65, 112.00, 77.51, 64.33, 46.38, 35.27, 26.99, 26.64, 20.13, 19.32. **HRMS** (ESI) *m/z* calcd for $C_{30}H_{38}NaO_2Si$ [$(M+Na)^+$]: 481.25333, measured: 481.25337.

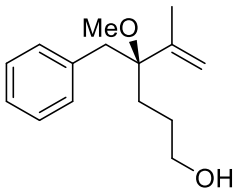
Isopropenyl methyl ether 4.113b′



General procedure **D** was followed using tertiary alcohol **4.113b** (0.3458 g, 0.7538 mmol, 1 equiv), taking 22 h. To quench, 5 mL each sat. aq. NH_4Cl and water were added, and the layers were separated. The aqueous was extracted with 2x10 mL EtOAc further, then the organic layers were separately washed with 5 mL brine, combined, dried over anhydrous Na_2SO_4, filtered, and concentrated. Silica gel flash chromatography with 0-10% EtOAc / hexanes (R_f 0.66, 25% EtOAc / hexanes) afforded 0.3438 g or 96% yield of ether **4.113b′** as a pale yellow oil. **IR** ν_{max} (thin film,

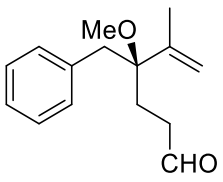
cm^{-1}): 3069, 3029, 2952, 2932, 2894, 2824, 1496, 1472, 1462, 1451, 1428, 1389, 1111, 1091. **^{1}H NMR** (500 MHz, $CDCl_3$) δ 7.66 (d, *J* = 7.8 Hz, 4H), 7.45 – 7.34 (m, 6H), 7.24 – 7.10 (m, 5H), 5.02 (s, 1H), 4.77 (s, 1H), 3.63 (t, *J* = 6.0 Hz, 2H), 3.15 (s, 3H), 2.91 (d, *J* = 14.1 Hz, 1H), 2.84 (d, *J* = 14.1 Hz, 1H), 1.74 (s, 3H), 1.66 – 1.57 (m, 2H), 1.54 (s, 2H), 1.03 (s, 9H). **^{13}C NMR** (126 MHz, $CDCl_3$) δ 146.12, 137.74, 135.73, 134.11, 130.19, 129.69, 128.00, 127.75, 126.24, 115.13, 82.10, 64.24, 49.71, 39.06, 28.58, 27.00, 26.80, 19.33, 19.30. **HRMS** (ESI) *m/z* calcd for $C_{31}H_{40}NaO_2Si$ [$(M+Na)^+$]: 495.26898, measured: 495.26868.

Isopropenyl methyl ether alcohol 4.116b



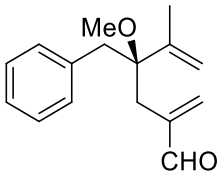
To TBDPS ether **4.113b′** (0.3393 g, 0.7177 mmol, 1 equiv) in 7 mL THF was added TBAF (1.0 M in THF, 0.90 mL, 1.3 equiv). After 4.5 h, 1 mL sat. aq. NH_4Cl and 5 mL H_2O were added, the THF was removed *in vacuo*, and the aqueous concentrate was extracted with 3x15 mL EtOAc. The combined organic layers were washed with 5 mL brine then dried over anhydrous Na_2SO_4, filtered, and concentrated. Silica gel flash chromatography with 10-50% EtOAc / hexanes (R_f 0.18, 25% EtOAc / hexanes) afforded 0.1597 g or 95% yield of alcohol **4.116b** as a clear colourless oil. **IR** ν_{max} (thin film, cm^{-1}): 3390 (broad), 3087, 3062, 3028, 2947, 2877, 2825, 1641, 1604, 1496, 1451, 1057, 903. **^{1}H NMR** (500 MHz, $CDCl_3$) δ 7.27 – 7.15 (m, 5H), 5.08 – 5.03 (m, 1H), 4.83 (s, 1H), 3.61 (q, *J* = 6.0 Hz, 2H), 3.19 (s, 3H), 2.94 (d, *J* = 14.3 Hz, 1H), 2.89 (d, *J* = 14.3 Hz, 1H), 1.79 – 1.74 (m, 3H), 1.67 – 1.57 (m, 2H), 1.59 – 1.50 (m, 2H), 1.35 (t, *J* = 5.2 Hz, 1H). **^{13}C NMR** (126 MHz, $CDCl_3$) δ 145.89, 137.64, 130.19, 128.06, 126.37, 115.32, 82.08, 63.36, 49.78, 38.93, 28.69, 26.98, 19.33. **HRMS** (ESI) *m/z* calcd for $C_{15}H_{22}NaO_2$ [$(M+Na)^+$]: 257.15120, measured: 257.15118.

Isopropenyl methyl ether aldehyde 4.117b



A batch of compound **4.113b** (1.1366 g, 2.478 mmol) was methylated and deprotected as described above, then the alcohol **4.116b** was combined with IBX (1.3958 g, 4.985 mmol, 2 equiv) in 25 mL DCM and refluxed for 8 h. The reaction was cooled and allowed to precipitate overnight in the freezer, then filtered on celite with an additional 10 mL DCM and concentrated. Silica gel flash chromatography with 10-15% EtOAc / hexanes (R_f 0.17, 10% EtOAc / hexanes) afforded 0.4195 g or 73% yield of aldehyde **4.117b** over three steps as a pale yellow liquid. **IR** ν_{max} (thin film, cm^{-1}): 3088, 3062, 3029, 2944, 2826, 2723, 1722, 1641, 1604, 1497, 1452, 1412, 1390, 1375, 1191, 1082, 1032. **^{1}H NMR** (500 MHz, $CDCl_3$) δ 9.78 (t, *J* = 1.4 Hz, 1H), 7.30 – 7.14 (m, 5H), 5.10 – 5.05 (m, 1H), 4.88 (s, 1H), 3.18 (s, 3H), 2.94 (d, *J* = 14.5 Hz, 1H), 2.87 (d, *J* = 14.5 Hz, 1H), 2.50 (td, *J* = 8.0, 1.4 Hz, 2H), 1.92 (dt, *J* = 15.3, 7.7 Hz, 1H), 1.84 (dt, *J* = 14.7, 7.8 Hz, 1H), 1.79 – 1.74 (m, 3H). **^{13}C NMR** (126 MHz, $CDCl_3$) δ 202.05, 145.24, 137.12, 130.03, 128.17, 126.55, 115.67, 81.60, 49.80, 39.41, 38.61, 24.43, 19.44. **HRMS** (ESI) *m/z* calcd for $C_{15}H_{20}NaO_2$ $[(M+Na)^+]$: 255.13555, measured: 255.13543.

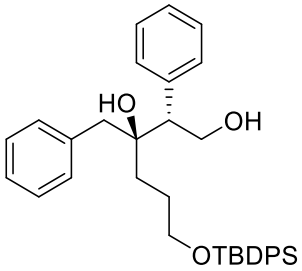
Isopropenyl methyl ether enal 4.97b* (enantio-enriched)



To a solution of aldehyde **4.117b** (0.1996 g, 0.8592 mmol, 1 equiv) in 8.5 mL dry DCM was added a solution of pyrrolidine (0.1 M in DCM, 859 µL, 0.1 equiv), aq. formaldehyde (37 wt.%, 65 µL, 0.64 mmol, 1.0 equiv), and finally *p*-methoxybenzoic acid (13.0 mg, 0.0854 mmol, 0.1 equiv).[46] The solution was immersed in a 42 °C oil bath for 3.5 h, then solvent was removed *in vacuo*. Silica gel flash chromatography with 10% EtOAc / hexanes (R_f 0.51, 25% EtOAc / hexanes) afforded 0.1384 g or 66% yield of an inseparable 8:2 mixture of desired enal **4.97b*** and the corresponding enol ethers as a clear colourless liquid. The characterization data of the enal match that of the racemic compound.

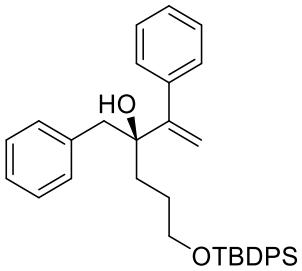
Notes: The comments for racemic isopropenyl substrate **4.97b** regarding handling apply here.

Diol 4.115b



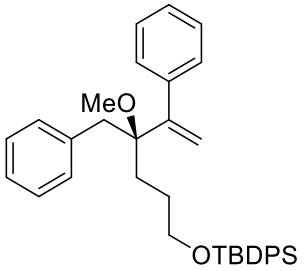
PhMgBr was added to epoxide **4.112*** (1.0252 g, 2.225 mmol, 1 equiv), as done for diol **4.115a**, except the reaction was allowed to warm from –78 °C overnight directly. After 21 h, the reaction was cooled over an ice bath, then 15 mL each sat. aq. NH_4Cl, H_2O, and EtOAc were added sequentially. The layers were separated, then the aqueous layer extracted further with 2x50 mL EtOAc. The combined organic layers were washed with 30 mL brine then dried over anhydrous Na_2SO_4, filtered, and concentrated. Silica gel flash chromatography with 30% EtOAc / hexanes (R_f 0.53, 10% EtOAc / DCM) afforded 1.1027 g or 92% yield of diol **4.115b** as a pale green gum. **IR** ν_{max} (thin film, cm^{-1}): 3391 (broad), 3070, 3031, 2931, 2858, 1602, 1589, 1494, 1472, 1454, 1427, 1389, 1361, 1108, 1091, 906. **^{1}H NMR** (500 MHz, $CDCl_3$) δ 7.63 – 7.58 (m, 4H), 7.45 – 7.40 (m, 2H), 7.40 – 7.34 (m, 6H), 7.33 – 7.22 (m, 8H), 4.25 (ddd, *J* = 11.1, 6.8, 4.2 Hz, 1H), 4.17 (ddd, *J* = 11.2, 7.5, 5.0 Hz, 1H), 3.54 – 3.41 (m, 2H), 3.02 (d, *J* = 13.8 Hz, 1H), 2.96 (dd, *J* = 6.6, 5.2 Hz, 1H), 2.89 (d, *J* = 13.8 Hz, 1H), 2.62 (s, 1H), 2.34 (dd, *J* = 7.5, 4.2 Hz, 1H), 1.73 (ddt, *J* = 16.2, 12.8, 6.2 Hz, 1H), 1.69 – 1.58 (m, 1H), 1.39 (ddd, *J* = 9.7, 7.6, 5.9 Hz, 2H), 1.01 (s, 9H). **^{13}C NMR** (126 MHz, $CDCl_3$) δ 139.74, 137.28, 135.69, 133.71, 133.69, 130.75, 130.13, 129.76, 128.53, 128.46, 127.78, 127.14, 126.67, 77.11, 64.40, 64.36, 54.25, 43.51, 34.09, 26.96, 26.87, 19.26. **HRMS** (ESI) *m/z* calcd for $C_{35}H_{42}NaO_3Si$ [$(M+Na)^+$]: 561.2795, measured: 561.2802.

Styrenyl alcohol 4.113c



Elimination of primary alcohol **4.115b** (1.0711 g, 1.988 mmol) was accomplished as described for **4.115a** (*vide supra*), except that final extraction of the olefin was performed with Et_2O rather than EtOAc. Silica gel flash chromatography with 5-10% EtOAc / hexanes (R_f 0.34, 10% EtOAc / hexanes) afforded 0.8096 g or 78% yield of tertiary alcohol **4.113c** as a yellow oil. **IR** ν_{max} (thin film, cm^{-1}): 3404 (broad), 3070, 3030, 2931, 2858, 1493, 1472, 1453, 1427, 1389, 1109, 1088, 906. **^{1}H NMR** (500 MHz, $CDCl_3$) δ 7.69 – 7.59 (m, 4H), 7.47 – 7.39 (m, 2H), 7.41 – 7.33 (m, 4H), 7.32 – 7.20 (m, 10H), 5.42 (d, *J* = 1.6 Hz, 1H), 5.16 (d, *J* = 1.5 Hz, 1H), 3.63 (t, *J* = 6.0 Hz, 2H), 3.03 (d, *J* = 13.5 Hz, 1H), 2.89 (d, *J* = 13.5 Hz, 1H), 2.14 (s, 1H), 2.02 – 1.92 (m, 1H), 1.78 – 1.69 (m, 2H), 1.66 – 1.57 (m, 1H), 1.04 (s, 9H). **^{13}C NMR** (126 MHz, $CDCl_3$) δ 154.25, 141.74, 137.10, 135.74, 135.74, 133.84, 133.81, 131.18, 129.73, 129.71, 128.73, 128.16, 128.05, 127.78, 127.19, 126.63, 116.05, 77.32, 64.37, 47.47, 36.02, 26.99, 26.97, 19.31. **HRMS** (ESI) *m/z* calcd for $C_{35}H_{40}NaO_2Si$ [$(M+Na)^+$]: 543.26898, measured: 543.26933.

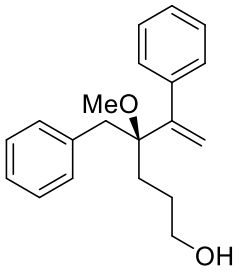
Styrenyl methyl ether 4.113c′



General procedure **D** was followed using tertiary alcohol **4.113c** (0.7873 g, 1.512 mmol, 1 equiv), taking 15 h. To quench, 10 mL each sat. aq. NH_4Cl and water were added, along with 20 mL 0.1 N HCl, then this mixture was extracted with 3x30 mL EtOAc. The organic layers were separately washed with 10 mL brine, combined, dried over anhydrous Na_2SO_4, filtered, and concentrated. Silica gel flash chromatography with 5% EtOAc / hexanes (R_f 0.51, 10% EtOAc / hexanes) afforded 0.8080 g or quantitative yield of ether **4.113c′** as a pale yellow oil. **IR** ν_{max} (thin film, cm^{-1}): 3069, 3052, 3029, 2998, 2952, 2930, 2895, 2856, 2824, 1620, 1601, 1589, 1572, 1492, 1471, 1461, 1427, 1388, 1107, 1088. **^{1}H NMR** (500 MHz, $CDCl_3$) δ 7.63 – 7.57 (m, 4H), 7.44 – 7.37 (m, 2H), 7.38 – 7.32 (m, 6H), 7.31 – 7.25 (m, 3H), 7.24 – 7.12 (m, 5H), 5.43 – 5.39 (m, 1H), 5.30 – 5.26 (m, 1H), 3.52 (t, *J* = 5.7 Hz, 2H), 3.29 (s, 3H), 3.09 (d, *J* = 14.3 Hz, 1H), 2.92 (d, *J* = 14.3 Hz, 1H), 1.69 – 1.57 (m, 4H), 0.99 (s, 9H). **^{13}C NMR** (126 MHz, $CDCl_3$) δ 149.75, 141.65, 137.68, 135.71, 134.09, 130.47, 129.65, 128.63, 128.05, 127.72, 127.27, 126.28, 119.04, 82.20, 64.17,

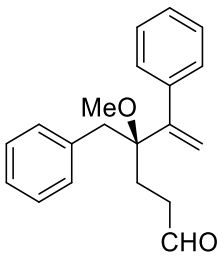
49.72, 39.99, 29.77, 26.98, 26.75, 19.30. **HRMS** (ESI) *m/z* calcd for $C_{36}H_{42}NaO_2Si$ [$(M+Na)^+$]: 557.28463, measured: 557.28537.

Styrenyl methyl ether alcohol 4.116c



To TBDPS ether **4.113c′** (0.8080 g, 1.512 mmol, 1 equiv) in 15 mL THF was added TBAF (1.0 M in THF, 2.0 mL, 1.3 equiv). After 2 h, 5 mL each sat. aq. NH_4Cl and H_2O were added, the layers separated, and the aqueous layer further extracted with 2x10 mL EtOAc. The organic layers were washed separately with 5 mL brine, then combined, dried over anhydrous Na_2SO_4, filtered, and concentrated. Silica gel flash chromatography with 20-50% EtOAc / hexanes (R_f 0.22, 30% EtOAc / hexanes) afforded 0.4247 g or 95% yield of alcohol **4.116c** as a pale yellow oil. **IR** ν_{max} (thin film, cm^{-1}): 3390 (broad), 3085, 3056, 3030, 2950, 2876, 2825, 1601, 1493, 1453, 1060. **^{1}H NMR** (500 MHz, $CDCl_3$) δ 7.44 – 7.36 (m, 2H), 7.33 – 7.22 (m, 5H), 7.23 – 7.18 (m, 3H), 5.46 (d, *J* = 0.9 Hz, 1H), 5.34 (d, *J* = 0.9 Hz, 1H), 3.45 (bs, 2H), 3.34 (s, 3H), 3.16 (d, *J* = 14.5 Hz, 1H), 2.93 (d, *J* = 14.5 Hz, 1H), 1.69 – 1.51 (m, 4H), 1.19 (bs, 1H). **^{13}C NMR** (126 MHz, $CDCl_3$) δ 149.50, 141.51, 137.61, 130.39, 128.60, 128.14, 128.13, 127.40, 126.41, 119.27, 82.14, 63.18, 49.86, 39.35, 29.90, 26.95. **HRMS** (ESI) *m/z* calcd for $C_{20}H_{24}NaO_2$ [$(M+Na)^+$]: 319.16685, measured: 319.16705.

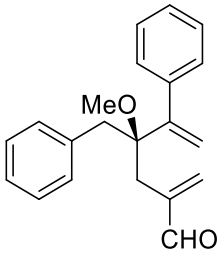
Styrenyl methyl ether aldehyde 4.117c



General Procedure **C** was followed using alcohol **4.116c** (0.4115 g, 1.388 mmol, 1 equiv) and IBX (0.5845 g, 2.087 mmol, 1.5 equiv), taking 21 h, with additional IBX (0.4448 g, 1.588 mmol, 1.1

equiv) added after 6 h. The aqueous filtrate was extracted with 3x45 mL EtOAc, then the combined organic layers were washed with 20 mL brine, dried over anhydrous Na_2SO_4, filtered, and concentrated. Silica gel flash chromatography with 10-20% EtOAc / hexanes (R_f 0.34, 20% EtOAc / hexanes) afforded 0.2208 g or 54% yield of aldehyde **4.117c** as a yellow oil, which crystallized on standing for some weeks at –20 °C. **IR** ν_{max} (thin film, cm^{-1}): 3084, 3058, 3028, 2936, 2902, 2855, 2825, 2723, 1722, 1601, 1493, 1108, 1087. **^{1}H NMR** (500 MHz, $CDCl_3$) δ 9.64 (t, *J* = 1.5 Hz, 1H), 7.39 – 7.33 (m, 2H), 7.35 – 7.27 (m, 3H), 7.28 – 7.14 (m, 5H), 5.46 (d, *J* = 0.8 Hz, 1H), 5.34 (d, *J* = 0.8 Hz, 1H), 3.31 (s, 3H), 3.06 (d, *J* = 14.7 Hz, 1H), 2.94 (d, *J* = 14.7 Hz, 1H), 2.57 – 2.41 (m, 2H), 1.98 (ddd, *J* = 15.3, 9.9, 5.6 Hz, 1H), 1.92 – 1.83 (m, 1H). **^{13}C NMR** (126 MHz, $CDCl_3$) δ 201.98, 149.10, 141.18, 137.11, 130.27, 128.54, 128.25, 127.56, 126.59, 119.52, 81.70, 49.92, 40.09, 38.60, 25.73. **HRMS** (ESI) *m/z* calcd for $C_{20}H_{22}NaO_2$ [$(M+Na)^+$]: 317.15120, measured: 317.15125.

Styrenyl methyl ether enal 4.97c* (enantio-enriched)



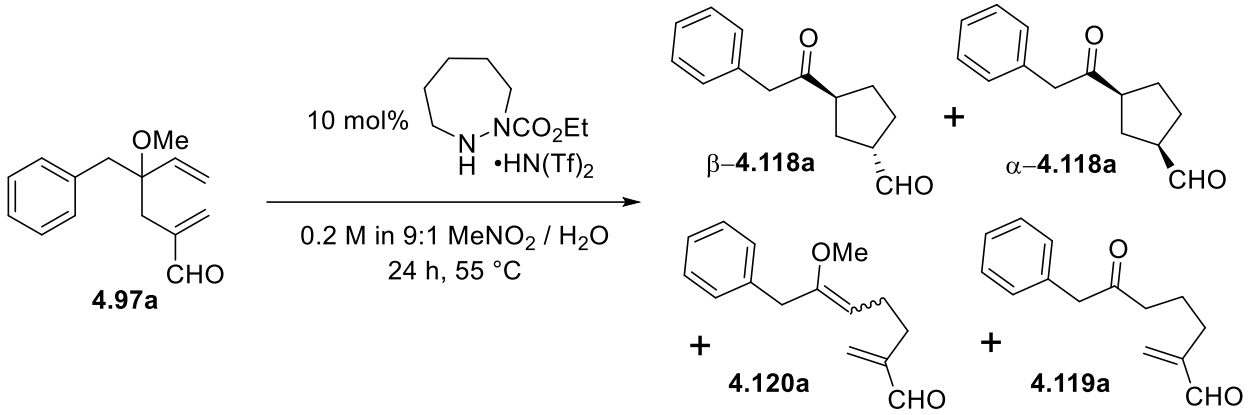
To a solution of aldehyde **4.117c** (93.4 mg, 0.317 mmol, 1 equiv) in 3 mL dry DCM was added a small drop of pyrrolidine, aq. formaldehyde (37 wt.%, 23.6 μL, 0.64 mmol, 1.0 equiv), and finally *p*-methoxybenzoic acid (5.1 mg, 0.0335 mmol, 0.1 equiv).[46] The solution was immersed in a 48 °C oil bath for 1 h, then cooled and chromatographed directly. Silica gel flash chromatography with DCM (R_f 0.48) afforded 76.9 mg or 79% yield of an inseparable 8:2 mixture of desired enal **4.97c*** and corresponding enol ethers as a clear colourless liquid. The characterization data of the enal match that of the racemic compound.

Note: All comments for racemic isopropenyl substrate **4.97b** apply here.

General Procedure F for esterification of oCM oxidation products:

The oxidized residue of the cyclopentane carboxaldehydes, containing the corresponding carboxylic acid, was taken up in 2-5 mL of dry DCM and 100-250 μL of oxalyl chloride, depending

on scale, was added over an ice bath. The reaction was stirred 30 mins over an ice bath, then 0.5 mL dry MeOH was carefully added and the reaction continued a further 30 mins. The reaction solvent and dimethyl oxalate were removed *in vacuo* without the aid of heat, and the yellow residue obtained was chromatographed directly.



General procedure **E** was followed using enantioenriched aldehyde **4.97a*** (92.1 mg, 0.400 mmol) except that the reaction was heated at 59 °C for 20 h. A 62% yield of keto-aldehyde **4.118a**, as determined by ^{1}H NMR analysis, was observed as a 1:1 mixture of epimers, along with a 7% NMR yield of oxy-Cope product ketone **4.119a**. Silica gel flash chromatography with 40% Et_2O / pentane afforded 15.7 mg of aldehyde *trans*-**4.118a** (R_f 0.22, 20% EtOAc / hexanes), 15.2 mg of aldehyde *cis*-**4.118a** (R_f 0.18, 20% EtOAc / hexanes), and 29.5 mg of a mixture of the two isomers along with ketone **4.119a**, all as yellow oils in 70% total yield. By analysis of the NMR ratio, the isolated yield of ketone **4.119a** matches the NMR yield and is approximately 7%. An analytically pure sample of oxy-Cope enal **4.119a** was obtained by further chromatography. The pure samples of each epimer were concentrated in flasks to maximize surface area and left exposed to air to allow oxidation to the corresponding carboxylic acids **4.121a**, taking 3-7 days depending on quantity. These were then separately esterified by a modification of General Procedure **F** to avoid isomerization, where 6.0 μL of $(COCl)_2$ was added to a solution of 5.0 mg carboxylic acid and 10.0 μL pyridine in 1 mL dry PhMe at 0 °C. When finished, the reaction was poured into 5 mL 0.1 N HCl and extracted with 3x8 mL EtOAc. The combined organic layers were washed with 2 mL brine, then dried over anhydrous Na_2SO_4, filtered, and concentrated. Silica gel flash chromatography with 10-20% EtOAc / hexanes (R_f 0.40, 30% EtOAc / hexanes) afforded 2.6 mg of the corresponding methyl esters **4.122a**, both clear colourless oils, for HPLC analysis.

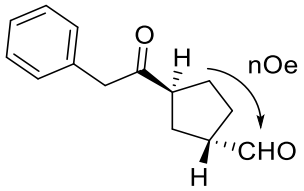
Note 1: The racemic material produced the same NMR yield of oCM products (60%) and ketone **4.119a** (7%) with 100 mg of substrate at 55 °C for 24 h. The racemic material was esterified according to General Procedure **F**, where inconsequential isomerization was observed, uniquely for these disubstituted cyclopentanes.

Note 2: The reaction was extremely slow at room temperature using either set of optimized catalytic conditions.

Note 3: A control reaction using the same conditions without catalyst or acid produced 39% conversion in 24 h to a mixture of oxy-Cope products consisting of the intermediate enol ethers and ketone **4.119a** in a 25:7:7 ratio (NMR). The reaction took 8 d to achieve full conversion and a 64% NMR yield of ketone **4.119a**. No oCM product was observed in the reaction. A 35% NMR yield of oxy-Cope/aldol isomers **5.26** was also observed.

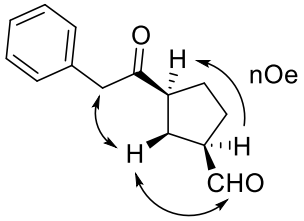
Note 4: No oCM product was obtained using 10 mol% of N-Me hydrazide **5.27** as its $HN(Tf)_2$ salt.

Aldehyde *trans*-4.118a



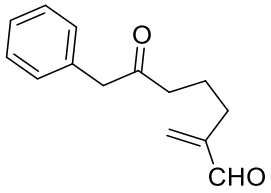
IR ν_{max} (thin film, cm^{-1}): 3084, 3063, 3029, 2922, 2853, 2717, 1712, 1495, 1454, 1361, 1311. **^{1}H NMR** (500 MHz, $CDCl_3$) δ 9.63 (d, *J* = 1.6 Hz, 1H), 7.36 – 7.30 (m, 2H), 7.30 – 7.23 (m, 1H), 7.22 – 7.16 (m, 2H), 3.74 (s, 2H), 3.04 (p, *J* = 7.6 Hz, 1H), 2.96 – 2.86 (m, 1H), 2.10 – 1.98 (m, 2H), 1.96 – 1.76 (m, 4H). **^{13}C NMR** (126 MHz, $CDCl_3$) δ 209.47, 202.90, 134.08, 129.58, 128.88, 127.22, 51.35, 49.78, 49.43, 29.11, 28.45, 26.22. **HRMS** (ESI) *m/z* calcd for $C_{14}H_{16}NaO_2$ $[(M+Na)^+]$: 239.10382, measured: 239.10417.

Aldehyde *cis*-4.118a



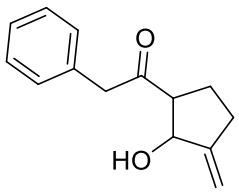
IR ν_{max} (thin film, cm^{-1}): 3061, 3029, 2955, 2921, 2870, 2852, 2826, 2724, 1712, 1603, 1584, 1495, 1453, 1360, 1309, 1262, 1206, 1187, 1155, 1088, 1072, 1030. **^{1}H NMR** (500 MHz, $CDCl_3$) δ 9.60 (d, *J* = 2.4 Hz, 1H), 7.33 (t, *J* = 7.3 Hz, 2H), 7.30 – 7.23 (m, 1H), 7.20 (d, *J* = 7.2 Hz, 2H), 3.75 (s, 2H), 3.13 – 3.03 (m, 1H), 2.79 – 2.69 (m, 1H), 2.14 (dt, *J* = 13.4, 7.9 Hz, 1H), 2.01 – 1.92 (m, 2H), 1.90 – 1.78 (m, 3H). **^{13}C NMR** (126 MHz, $CDCl_3$) δ 209.31, 203.12, 134.13, 129.60, 128.89, 127.22, 51.56, 50.41, 49.31, 29.17, 29.10, 26.36. **HRMS** (ESI) *m/z* calcd for $C_{14}H_{16}NaO_2$ $[(M+Na)^+]$: 239.10425, measured: 239.10417.

Keto-enal 4.119a



IR ν_{max} (thin film, cm^{-1}): 3061, 3030, 2923, 2850, 2708, 1714, 1603, 1496, 1454, 1408, 1363, 1311, 1208, 1182, 1094, 1077, 1031. **^{1}H NMR** (400 MHz, $CDCl_3$) δ 9.50 (s, 1H), 7.36 – 7.30 (m, 2H), 7.29 – 7.23 (m, 1H), 7.23 – 7.16 (m, 2H), 6.19 (q, *J* = 1.3 Hz, 1H), 5.97 (d, *J* = 0.7 Hz, 1H), 3.68 (s, 2H), 2.47 (t, *J* = 7.2 Hz, 2H), 2.19 (t, *J* = 7.6 Hz, 2H), 1.71 (p, *J* = 7.4 Hz, 2H). **^{13}C NMR** (101 MHz, $CDCl_3$) δ 207.95, 194.67, 149.64, 134.60, 134.34, 129.54, 128.91, 127.21, 50.37, 41.27, 27.15, 21.83. **HRMS** (ESI) *m/z* calcd for $C_{14}H_{16}NaO_2$ $[(M+Na)^+]$: 239.1043, measured: 239.1036.

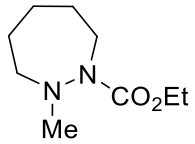
Aldol product 5.26, *mixture of isomers*



This compound was isolated from control experiments (see *Note 3* above) by silica gel flash chromatography with 20% EtOAc / hexanes, then again with 5% Et_2O / DCM to afford a mixture of this and oxy-Cope product **4.119a**. This mixture was allowed to age exposed to air, since selective decomposition of the aldehyde was both expected and observed, at which time chromatography was repeated to obtain an analytical sample of pure compound **5.26** as a mixture

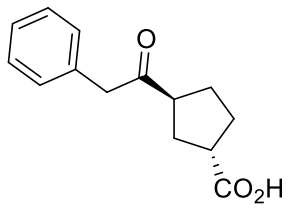
of isomers. **IR** ν_{max} (thin film, cm^{-1}): 3435 (broad), 3099, 3077, 3029, 2953, 2927, 2876, 1708, 1603, 1496, 1454, 1436, 1405, 1362, 1312, 1259, 1206, 1185, 1145, 1095, 1031, 970. **^{1}H NMR** (500 MHz, $CDCl_3$) δ 7.36 – 7.31 (m, 3.59H), 7.29 – 7.27 (m, 1.84H), 7.23 – 7.20 (m, 3.46H), 5.21 (s, 1H), 5.11 (q, *J* = 2.4 Hz, 0.64H), 5.04 (d, *J* = 2.0 Hz, 1.00H), 5.00 (q, *J* = 2.3 Hz, 0.64H), 4.59 (t, *J* = 4.8 Hz, 1.50H), 3.82 (s, 1.26H), 3.81 (s, 1.99H), 3.04 (ddd, *J* = 9.5, 7.4, 5.4 Hz, 1.03H), 2.88 (ddd, *J* = 11.0, 8.7, 7.6 Hz, 0.74H), 2.61 – 2.52 (m, 1.97H), 2.43 (s, 1.34H), 2.28 (dtt, *J* = 16.9, 8.5, 2.4 Hz, 1.18H), 2.11 (dq, *J* = 12.8, 9.1 Hz, 1.31H), 1.96 – 1.85 (m, 2.86H), 1.72 (ddt, *J* = 12.9, 11.0, 9.4 Hz, 1.15H). **^{13}C NMR** (126 MHz, $CDCl_3$) δ 209.99, 209.67, 152.76, 151.93, 133.93, 133.80, 129.73, 129.69, 128.89, 128.89, 127.26, 127.25, 110.02, 107.53, 76.51, 75.74, 58.48, 55.27, 50.12, 50.04, 29.28, 28.75, 25.28, 24.58. **HRMS** (ESI) *m/z* calcd for $C_{14}H_{16}NaO_2$ $[(M+Na)^+]$: 239.1043, measured: 239.1035.

_N_-Me hydrazide 5.27



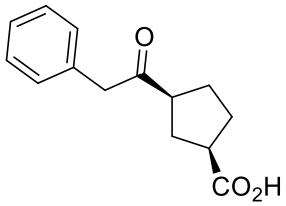
Prepared as previously described by our group.[69] **IR** ν_{max} (neat liquid, cm^{-1}): 2978, 2930, 2852, 2800, 1698, 1447, 1398, 1378, 1346, 1275, 1241, 1221, 1189, 1170, 1129, 1108, 1054, 1033, 1018, 994. *Poor ^{1}H NMR signal definition is due to rotational isomerism, which also gives rise to double the expected ^{13}C signals.* **^{1}H NMR** (500 MHz, methanol-*d*$_4$) δ 4.23 – 4.09 (m, 2H), 3.83 (bs, 1H), 3.22 (bs, 1H), 3.00 (bs, 1H), 2.62 – 2.58 (m, 3H), 1.96 – 1.41 (m, 6H), 1.34 – 1.21 (m, 4H). **^{13}C NMR** (126 MHz, methanol-*d*$_4$) δ 158.78, 157.94, 62.61, 62.40, 57.16, 56.76, 46.64, 46.59, 43.12, 42.71, 29.57, 28.77, 27.90, 27.85, 27.42, 27.30, 15.07, 15.02. **HRMS** (ESI) *m/z* calcd for $C_9H_{19}N_2O_2$ $[(M+H)^+]$: 187.14410, measured: 187.14355.

Carboxylic acid *trans*-4.121a



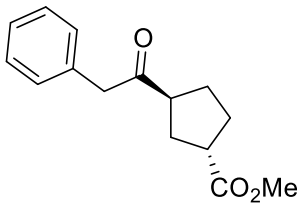
IR ν_{max} (thin film, cm^{-1}): 3600-2400 (very broad), 3096, 3065, 3029, 2926, 2874, 2855, 1703, 1603, 1496, 1453, 1410, 1360, 1310, 1189, 1102, 1050. **^{1}H NMR** (500 MHz, DMSO-d_6) δ 12.10 (s, 1H), 7.30 (t, J = 7.3 Hz, 2H), 7.23 (t, J = 7.4 Hz, 1H), 7.21 – 7.15 (m, 2H), 3.82 (s, 2H), 3.13 (p, J = 7.7 Hz, 1H), 2.70 (p, J = 7.3 Hz, 1H), 1.99 – 1.83 (m, 4H), 1.75 – 1.63 (m, 2H). **^{13}C NMR** (126 MHz, DMSO-d_6) δ 209.32, 176.51, 134.87, 129.65, 128.22, 126.44, 49.66, 47.73, 42.92, 31.17, 29.45, 28.43. **HRMS** (ESI) *m/z* calcd for $C_{14}H_{15}O_3$ [$(M–H)^–$]: 231.10267, measured: 231.10232.

Carboxylic acid *cis*-4.121a



IR ν_{max} (thin film, cm^{-1}): 3600-2400 (very broad), 3081, 3060, 3029, 2924, 2873, 1703, 1603, 1496, 1453, 1408, 1361, 1309, 1289, 1208, 1188, 1100, 1074. **^{1}H NMR** (500 MHz, DMSO-d_6) δ 12.08 (s, 1H), 7.30 (t, J = 7.4 Hz, 2H), 7.23 (t, J = 7.4 Hz, 1H), 7.18 (d, J = 7.0 Hz, 2H), 3.81 (s, 2H), 3.06 (p, J = 7.9 Hz, 1H), 2.71 (p, J = 7.9 Hz, 1H), 2.05 (dt, J = 12.9, 8.0 Hz, 1H), 1.89 – 1.66 (m, 5H). **^{13}C NMR** (126 MHz, DMSO-d_6) δ 208.97, 176.30, 134.89, 129.64, 128.23, 126.44, 50.24, 47.76, 43.33, 31.83, 28.86, 27.74. **HRMS** (ESI) *m/z* calcd for $C_{14}H_{15}O_3$ [$(M–H)^–$]: 231.10267, measured: 231.10228.

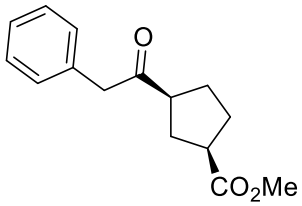
Carboxylic ester *trans*-4.122a



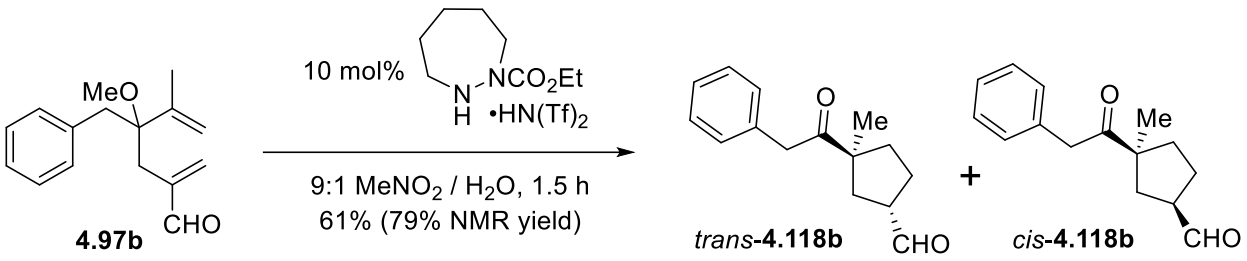
IR ν_{max} (thin film, cm^{-1}): 3031, 2951, 2923, 2853, 1732, 1715, 1602, 1496, 1454, 1436, 1360, 1309, 1266, 1201, 1171, 1100, 1052, 1030. **^{1}H NMR** (500 MHz, $CDCl_3$) δ 7.34 (t, J = 7.3 Hz, 2H), 7.30 – 7.24 (m, 1H), 7.23 – 7.18 (m, 2H), 3.75 (s, 2H), 3.67 (s, 3H), 3.18 (p, J = 7.8 Hz, 1H), 2.89 (p, J = 7.7 Hz, 1H), 2.11 (ddd, J = 13.2, 8.7, 6.7 Hz, 1H), 2.07 – 1.91 (m, 3H), 1.87 – 1.72 (m, 2H). **^{13}C NMR** (126 MHz, $CDCl_3$) δ 209.74, 176.46, 134.20, 129.61, 128.84, 127.15, 51.91, 49.95,

49.40, 43.44, 31.97, 30.19, 29.36. **HRMS** (ESI) *m/z* calcd for $C_{15}H_{18}NaO_3$ [$(M+Na)^+$]: 269.1148, measured: 269.1148.

Carboxylic ester *cis*-4.122a



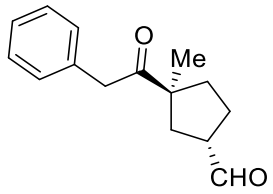
IR ν_{max} (thin film, cm^{-1}): 3030, 2953, 2923, 2852, 1732, 1714, 1602, 1496, 1454, 1436, 1362, 1308, 1269, 1201, 1169, 1097, 1031. **^{1}H NMR** (500 MHz, $CDCl_3$) δ 7.32 (t, *J* = 7.4 Hz, 2H), 7.29 – 7.23 (m, 1H), 7.20 (d, *J* = 7.2 Hz, 2H), 3.75 (s, 2H), 3.67 (s, 3H), 3.00 (p, *J* = 8.5 Hz, 1H), 2.83 – 2.72 (m, 1H), 2.14 – 2.04 (m, 2H), 1.98 – 1.87 (m, 3H), 1.84 – 1.76 (m, 1H). **^{13}C NMR** (126 MHz, $CDCl_3$) δ 209.05, 175.72, 134.32, 129.62, 128.84, 127.13, 51.93, 50.57, 49.12, 44.13, 32.68, 29.32, 28.37. **HRMS** (ESI) *m/z* calcd for $C_{15}H_{18}NaO_3$ [$(M+Na)^+$]: 269.1148, measured: 269.1150.



General Procedure **E** was followed using aldehyde **4.97b** (62.7 mg, 0.257 mmol) and the reaction was complete in 90 mins in 80% yield as determined by ^{1}H NMR analysis, with the product formed as a 1:1 mixture of epimers. It should be noted that extraction was performed with 3x5 mL Et_2O rather than EtOAc, and this was dried over anhydrous $MgSO_4$. Silica gel flash chromatography with 10-15% EtOAc / pet. ether afforded pure sample of each epimer of **4.118b**, along with a mixture of the epimers (R_f 0.39 and 0.33, 25% EtOAc / hexanes). Since some aldehyde oxidation had already occurred upon sample recovery, these clear colourless oily residues were left exposed to air for 2 d, at which time oxidation of the aldehydes to the corresponding carboxylic acids had occurred and they became more opaque gums. This provided 12.8 mg of *trans*-**4.121b**, 15.1 mg of *cis*-**4.121b**, and 10.7 mg of a mixture of epimers in 61% combined yield from the catalytic substrate. The acids were converted to the corresponding methyl esters according to General

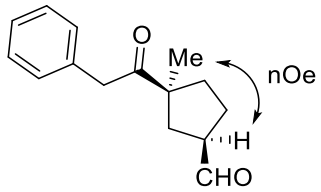
Procedure **F**, then purified by silica gel flash chromatography with 15-20% EtOAc / hexanes (R_f 0.33 and 0.28, 20% EtOAc / hexanes) in 35-72% yield of esters **4.122b** as clear-colourless films. Comparison of both ester epimers obtained in each case from racemic and enantioenriched substrate by chiral HPLC analysis demonstrated a essentially no *e.e.* in any samples.

Keto-aldehyde *trans*-4.118b



IR ν_{max} (thin film, cm^{-1}): 3086, 3061, 3029, 2962, 2872, 2710, 1707, 1496, 1455, 1180, 1001. **^{1}H NMR** (500 MHz, $CDCl_3$) δ 9.67 (d, *J* = 1.7 Hz, 1H), 7.32 (t, *J* = 7.3 Hz, 2H), 7.24 (d, *J* = 7.3 Hz, 1H), 7.19 (d, *J* = 7.3 Hz, 2H), 3.81 (s, 2H), 2.90 – 2.80 (m, 1H), 2.43 (dd, *J* = 13.5, 9.4 Hz, 1H), 2.18 (dt, *J* = 13.1, 7.0 Hz, 1H), 2.01 – 1.92 (m, 1H), 1.87 – 1.79 (m, 1H), 1.73 (dd, *J* = 13.6, 7.6 Hz, 1H), 1.57 – 1.51 (m, 1H), 1.34 (s, 3H). **^{13}C NMR** (126 MHz, $CDCl_3$) δ 210.91, 202.94, 134.71, 129.56, 128.68, 127.00, 56.63, 51.19, 44.11, 36.16, 35.52, 25.43, 24.18. **HRMS** (ESI) *m/z* calcd for $C_{15}H_{18}NaO_2$ [$(M+Na)^+$]: 253.1193, measured: 253.1199.

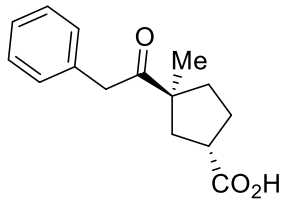
Keto-aldehyde *cis*-4.118b



The data reported here exclude signals arising from the rapidly formed and separately characterized carboxylic acid (vide infra). **IR** ν_{max} (thin film, cm^{-1}): 3087, 3064, 3030, 2930, 2873, 2813, 2723, 1719, 1709, 1604, 1497, 1455, 1328, 1313, 1075, 1031. **^{1}H NMR** (400 MHz, $CDCl_3$) δ 9.60 (d, *J* = 2.1 Hz, 1H), 7.34 – 7.28 (m, 2H), 7.26 – 7.21 (m, 1H), 7.21 – 7.15 (m, 2H), 3.82 (s, 2H), 2.89 (ttd, *J* = 9.0, 7.1, 2.0 Hz, 1H), 2.49 (dd, *J* = 13.5, 7.0 Hz, 1H), 2.14 (ddd, *J* = 13.2, 8.4, 6.1 Hz, 1H), 2.00 – 1.89 (m, 2H), 1.69 (dd, *J* = 13.5, 9.1 Hz, 1H), 1.59 (dt, *J* = 13.1, 7.5 Hz, 1H), 1.34 (s, 3H). **^{13}C NMR** (101 MHz, $CDCl_3$) δ 210.99, 203.13, 134.66, 129.62, 128.64, 126.95,

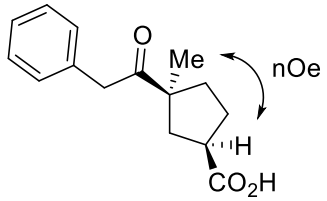
56.42, 50.74, 44.32, 36.11, 36.00, 25.40, 24.31. **HRMS** (ESI) *m/z* calcd for $C_{15}H_{18}NaO_2$ [$(M+Na)^+$]: 253.1199, measured: 253.1199.

Keto-carboxylic acid *trans*-4.121b



IR ν_{max} (thin film, cm^{-1}): 3300-2500 (very broad), 3030, 2965, 2874, 1701 (broad), 1496, 1454, 1416, 1312, 1236, 1181, 1032. **^{1}H NMR** (500 MHz, $CDCl_3$) δ 12.67-8.85 (bs, 1H), 7.35 – 7.28 (m, 2H), 7.28 – 7.22 (m, 1H), 7.21 – 7.16 (m, 2H), 3.80 (s, 2H), 2.93 – 2.78 (m, 1H), 2.56 (dd, *J* = 13.4, 8.9 Hz, 1H), 2.16 (dt, *J* = 13.3, 7.3 Hz, 1H), 1.97 (ddp, *J* = 20.1, 13.3, 6.7, 5.7 Hz, 2H), 1.73 (dd, *J* = 13.4, 8.4 Hz, 1H), 1.66 (dt, *J* = 13.8, 7.1 Hz, 1H), 1.38 (s, 3H). **^{13}C NMR** (126 MHz, $CDCl_3$) δ 210.97, 181.17 (broad), 134.74, 129.56, 128.66, 126.97, 56.61, 44.08, 43.19 (broad), 39.00, 36.35, 28.97, 24.50. **HRMS** (ESI) *m/z* calcd for $C_{15}H_{18}NaO_3$ [$(M+Na)^+$]: 269.1148, measured: 269.1149.

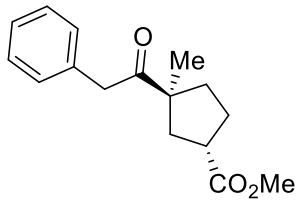
Keto-carboxylic acid *cis*-4.121b



IR ν_{max} (thin film, cm^{-1}): 3500-2500 (very broad), 3029, 2965, 2874, 1699, 1496, 1454, 1414, 1310, 1237, 1180, 1032. **^{1}H NMR** (400 MHz, $CDCl_3$) δ 7.31 (t, *J* = 7.2 Hz, 2H), 7.26 – 7.14 (m, 3H), 3.83 (s, 2H), 3.00 (p, *J* = 8.3 Hz, 1H), 2.45 (dd, *J* = 13.4, 8.4 Hz, 1H), 2.27 (ddd, *J* = 13.2, 8.7, 6.0 Hz, 1H), 2.09 (td, *J* = 13.7, 8.0 Hz, 1H), 2.01 – 1.90 (m, 1H), 1.85 (dd, *J* = 13.4, 8.5 Hz, 1H), 1.54 (dt, *J* = 12.7, 7.4 Hz, 1H), 1.30 (s, 3H). **^{1}H NMR** (500 MHz, DMSO-d_6) δ 12.09 (s, 1H), 7.28 (t, *J* = 7.3 Hz, 2H), 7.21 (t, *J* = 7.4 Hz, 1H), 7.16 (d, *J* = 6.8 Hz, 2H), 3.89 (s, 2H), 2.89 (p, *J* = 8.5 Hz, 1H), 2.22 (dd, *J* = 13.1, 8.8 Hz, 1H), 2.10 (ddd, *J* = 12.8, 8.7, 6.2 Hz, 1H), 1.99 – 1.91 (m, 1H), 1.79 – 1.70 (m, 2H), 1.47 (dt, *J* = 12.1, 7.4 Hz, 1H), 1.23 (s, 3H). **^{13}C NMR** (126 MHz,

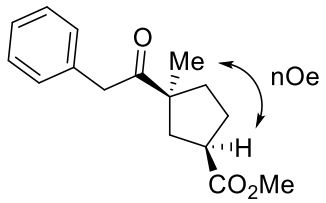
$CDCl_3$) δ 211.02, 181.03, 134.76, 129.66, 128.61, 126.91, 56.32, 44.34, 42.93, 39.21, 35.93, 28.90, 24.51. **HRMS** (ESI) *m/z* calcd for $C_{15}H_{18}NaO_3$ [$(M+Na)^+$]: 269.1148, measured: 269.1139.

Keto-carboxylic ester *trans*-4.122b

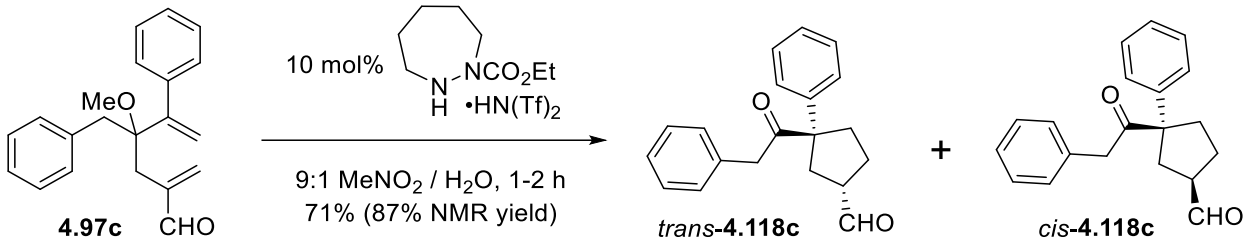


IR ν_{max} (thin film, cm^{-1}): 3088, 3064, 3029, 2955, 2874, 1730, 1706, 1603, 1496, 1454, 1436, 1197, 1171, 1002. **^{1}H NMR** (500 MHz, $CDCl_3$) δ 7.31 (t, *J* = 7.4 Hz, 2H), 7.26 – 7.22 (m, 1H), 7.19 (d, *J* = 7.2 Hz, 2H), 3.80 (s, 2H), 3.67 (s, 3H), 2.81 (p, *J* = 8.6 Hz, 1H), 2.52 (dd, *J* = 13.4, 8.8 Hz, 1H), 2.15 (dt, *J* = 13.4, 7.5 Hz, 1H), 2.00 – 1.84 (m, 2H), 1.70 (dd, *J* = 13.4, 8.7 Hz, 1H), 1.64 (ddd, *J* = 13.9, 8.1, 6.2 Hz, 1H), 1.37 (s, 3H). **^{13}C NMR** (126 MHz, $CDCl_3$) δ 211.03, 176.49, 134.83, 129.58, 128.64, 126.93, 56.53, 51.93, 44.06, 43.36, 39.22, 36.29, 29.07, 24.57. **HRMS** (ESI) *m/z* calcd for $C_{16}H_{20}NaO_3$ [$(M+Na)^+$]: 283.1305, measured: 283.1300.

Keto-carboxylic ester *cis*-4.122b

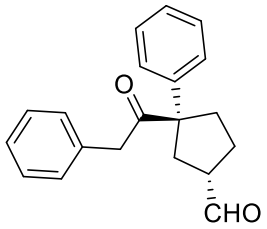


IR ν_{max} (thin film, cm^{-1}): 3064, 3030, 2955, 2874, 1729, 1706, 1603, 1496, 1453, 1435, 1374, 1309, 1269, 1200, 1171, 1076, 1031. **^{1}H NMR** (500 MHz, $CDCl_3$) δ 7.31 (t, *J* = 7.5 Hz, 2H), 7.24 (t, *J* = 7.4 Hz, 1H), 7.20 (d, *J* = 7.3 Hz, 2H), 3.83 (s, 2H), 3.67 (s, 3H), 2.96 (p, *J* = 8.4 Hz, 1H), 2.40 (dd, *J* = 13.3, 8.8 Hz, 1H), 2.27 (ddd, *J* = 13.2, 8.9, 6.1 Hz, 1H), 2.05 (td, *J* = 13.9, 8.1 Hz, 1H), 1.99 – 1.88 (m, 1H), 1.83 (dd, *J* = 13.3, 8.2 Hz, 1H), 1.52 (dt, *J* = 14.3, 7.4 Hz, 1H), 1.28 (s, 3H). **^{13}C NMR** (126 MHz, $CDCl_3$) δ 210.80, 176.09, 134.91, 129.67, 128.58, 126.85, 56.19, 51.98, 44.33, 43.05, 39.47, 35.70, 28.96, 24.62. **HRMS** (ESI) *m/z* calcd for $C_{16}H_{20}NaO_3$ [$(M+Na)^+$]: 283.1305, measured: 283.1300.



General Procedure **E** was followed using aldehyde **4.97c** (75.3 mg, 0.246 mmol) and the reaction was complete in 2 h in 87% yield as determined by ^{1}H NMR analysis, with the product formed as a 1:1 mixture of epimers. It should be noted that extraction was performed with 3x5 mL Et_2O rather than EtOAc, and this was dried over anhydrous $MgSO_4$. Silica gel flash chromatography with 10-15% EtOAc / pet. ether afforded 53.5 mg or 71% yield of a 1:1 mixture of epimers of **4.118c** (R_f 0.39, 25% EtOAc / hexanes). The bulk clear colourless oily residue was left exposed to air for 5 d, at which time oxidation of the aldehyde epimers to the corresponding carboxylic acid epimers **4.121c** had occurred and they became more opaque gums. The acid epimers were treated according to General Procedure **F**, then purified by silica gel flash chromatography with 10-20% EtOAc / hexanes (R_f 0.31 and 0.28, 20% EtOAc / hexanes), and afforded samples of each epimer of ester **4.122c** as clear colourless films. Comparison of both ester epimers obtained in each case from racemic and enantioenriched substrate by chiral HPLC analysis demonstrated essentially no *e.e.* in any samples.

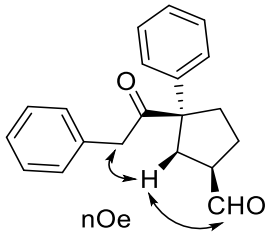
Keto-aldehyde *trans*-4.118c



IR ν_{max} (thin film, cm^{-1}): 3484 (broad, CO_2H content), 3085, 3061, 3029, 2925, 2855, 2716, 1731, 1711, 1601, 1495, 1454, 1330, 1311, 1110, 1081, 1053, 1031, 1001. **^{1}H NMR** (500 MHz, $CDCl_3$) δ 9.62 (d, *J* = 1.5 Hz, 1H), 7.40 – 7.34 (m, 2H), 7.33 – 7.27 (m, 3H), 7.25 – 7.14 (m, 3H), 6.89 (dd, *J* = 7.9, 1.5 Hz, 2H), 3.56 (d, *J* = 15.7 Hz, 1H), 3.52 (d, *J* = 15.7 Hz, 1H), 2.98 – 2.86 (m, 2H), 2.64 – 2.54 (m, 1H), 2.16 – 1.99 (m, 3H), 1.89 – 1.76 (m, 1H). **^{13}C NMR** (126 MHz, $CDCl_3$) δ 207.90, 202.52, 141.11, 134.79, 129.34, 129.14, 128.48, 127.73, 127.29, 126.84, 65.89, 49.87,

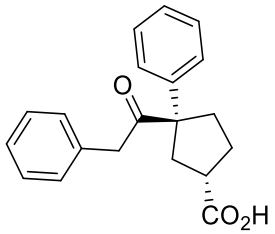
43.92, 34.39, 33.46, 24.37. **HRMS** (ESI) *m/z* calcd for $C_{20}H_{20}NaO_2$ [$(M+Na)^+$]: 315.1356, measured: 315.1353.

Keto-aldehyde *cis*-4.118c



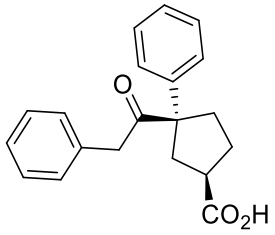
IR ν_{max} (thin film, cm^{-1}): 3424 (broad, CO_2H content), 2982, 2931, 1737 (broad), 1653, 1603, 1496, 1454, 1394, 1369, 1265, 1163, 1115, 1051, 1025, 975. **^{1}H NMR** (400 MHz, $CDCl_3$) δ 9.67 (d, *J* = 1.7 Hz, 1H), 7.43 – 7.33 (m, 2H), 7.36 – 7.26 (m, 3H), 7.24 – 7.13 (m, 3H), 6.85 (dd, *J* = 7.6, 1.7 Hz, 2H), 3.53 (s, 2H), 2.96 (ddd, *J* = 13.3, 5.5, 1.2 Hz, 1H), 2.92 – 2.79 (m, 1H), 2.52 (ddd, *J* = 11.9, 7.1, 4.1 Hz, 1H), 2.24 – 2.12 (m, 2H), 2.09 – 1.95 (m, 1H), 1.98 – 1.84 (m, 1H). **^{13}C NMR** (101 MHz, $CDCl_3$) δ 208.05, 203.30, 141.25, 134.67, 129.43, 129.18, 128.39, 127.69, 127.19, 126.77, 65.41, 49.84, 44.30, 34.89, 34.00, 24.45. **HRMS** (ESI) *m/z* calcd for $C_{20}H_{20}NaO_2$ [$(M+Na)^+$]: 315.1356, measured: 315.1345.

Keto-carboxylic acid *trans*-4.121c



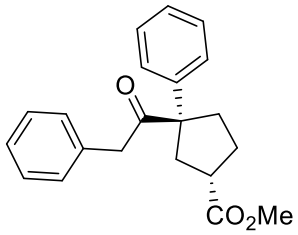
IR ν_{max} (thin film, cm^{-1}): 3550-2450 (very broad), 3061, 3028, 2951, 2877, 1731, 1707, 1600, 1583, 1495, 1447, 1366, 1314, 1267, 1203, 1173, 1083, 1055, 1031. **^{1}H NMR** (500 MHz, DMSO-d_6) δ 12.17 (bs, 1H), 7.43 – 7.37 (m, 2H), 7.38 – 7.29 (m, 3H), 7.21 – 7.11 (m, 3H), 6.84 – 6.77 (m, 2H), 3.66 (d, *J* = 16.2 Hz, 1H), 3.61 (d, *J* = 16.2 Hz, 1H), 2.94 (dd, *J* = 12.6, 8.0 Hz, 1H), 2.77 – 2.68 (m, 1H), 2.67 – 2.60 (m, 1H), 2.02 – 1.93 (m, 2H), 1.92 – 1.83 (m, 1H), 1.83 – 1.71 (m, 1H). **^{13}C NMR** (126 MHz, DMSO-d_6) δ 207.55, 176.52, 141.48, 135.31, 129.25, 128.75, 127.97, 127.21, 127.16, 126.22, 65.35, 42.78, 41.49, 37.23, 33.12, 27.35. **HRMS** (ESI) *m/z* calcd for $C_{20}H_{19}O_3$ [$(M–H)^–$]: 307.13397, measured: 307.13363.

Keto-carboxylic acid *cis*-4.121c



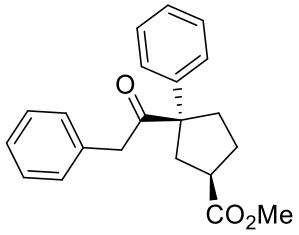
IR ν_{max} (thin film, cm^{-1}): 3580-2290 (very broad), 3062, 3029, 2923, 2853, 1709 (broad), 1637, 1599, 1582, 1505, 1495, 1481, 1448, 1373, 1356, 1304, 1285, 1260, 1203, 1176, 1157, 1084, 1029. **^{1}H NMR** (400 MHz, DMSO-d_6) δ 12.17 (bs, 1H), 7.44 – 7.29 (m, 5H), 7.21 – 7.09 (m, 3H), 6.83 – 6.75 (m, 2H), 3.64 (d, J = 16.4 Hz, 1H), 3.59 (d, J = 16.5 Hz, 1H), 2.82 (p, J = 8.3 Hz, 1H), 2.69 (dd, J = 13.3, 7.2 Hz, 1H), 2.56 – 2.46 (m, 1H, *observed by HSQC*), 2.32 (dd, J = 13.1, 9.5 Hz, 1H), 2.04 (dt, J = 12.7, 7.8 Hz, 1H), 1.97 – 1.84 (m, 1H), 1.82 – 1.69 (m, 1H). **^{13}C NMR** (101 MHz, DMSO-d_6) δ 207.24, 176.45, 141.42, 135.29, 129.34, 128.82, 127.91, 127.16, 127.03, 126.18, 64.90, 43.52, 41.52, 36.74, 33.73, 27.32. **HRMS** (ESI) *m/z* calcd for $C_{20}H_{19}O_3$ [$(M–H)^–$]: 307.13397, measured: 307.13362.

Keto-carboxylic ester *trans*-4.122c



IR ν_{max} (thin film, cm^{-1}): 3087, 3060, 3028, 2951, 2878, 1730, 1709, 1600, 1583, 1495, 1447, 1436, 1364, 1315, 1267, 1202, 1171, 1082, 1057, 1032, 1001. **^{1}H NMR** (500 MHz, $CDCl_3$) δ 7.39 – 7.33 (m, 2H), 7.33 – 7.27 (m, 3H), 7.23 – 7.14 (m, 3H), 6.91 – 6.85 (m, 2H), 3.65 (s, 3H), 3.55 (d, J = 15.7 Hz, 1H), 3.51 (d, J = 15.7 Hz, 1H), 3.00 – 2.86 (m, 2H), 2.61 (dddd, J = 12.9, 7.5, 3.7, 1.7 Hz, 1H), 2.18 – 2.10 (m, 2H), 2.02 (dddd, J = 12.9, 9.2, 5.8, 3.8 Hz, 1H), 1.89 (dtd, J = 13.2, 9.5, 7.7 Hz, 1H). **^{13}C NMR** (126 MHz, $CDCl_3$) δ 207.98, 176.44, 141.50, 134.90, 129.37, 129.04, 128.43, 127.55, 127.31, 126.77, 65.95, 51.97, 43.84, 42.02, 37.97, 33.64, 27.80. **HRMS** (ESI) *m/z* calcd for $C_{21}H_{22}NaO_3$ [$(M+Na)^+$]: 345.14612, measured: 345.14638.

Keto-carboxylic ester *cis*-4.122c



IR ν_{max} (thin film, cm^{-1}): 3063, 3030, 2954, 2926, 2852, 1728, 1712, 1601, 1495, 1453, 1437, 1365, 1305, 1260, 1206, 1174, 1093, 1076, 1031, 1018. **^{1}H NMR** (500 MHz, $CDCl_3$) δ 7.39 – 7.34 (m, 2H), 7.33 – 7.28 (m, 3H), 7.21 – 7.13 (m, 3H), 6.88 – 6.83 (m, 2H), 3.68 (s, 3H), 3.56 (s, 1H), 3.56 (s, 1H), 2.91 (tt, *J* = 8.9, 7.8 Hz, 1H), 2.79 (dd, *J* = 13.4, 7.7 Hz, 1H), 2.56 (ddd, *J* = 12.8, 8.2, 5.2 Hz, 1H), 2.41 (dd, *J* = 13.4, 9.0 Hz, 1H), 2.17 – 1.92 (m, 3H). **^{13}C NMR** (126 MHz, $CDCl_3$) δ 207.45, 176.01, 141.44, 134.89, 129.52, 129.13, 128.33, 127.52, 127.11, 126.66, 65.40, 52.04, 44.62, 42.17, 37.61, 34.19, 27.80. **HRMS** (ESI) *m/z* calcd for $C_{21}H_{22}NaO_3$ [$(M+Na)^+$]: 345.14612, measured: 345.14619.

5.4 *Biological Assay Methods*

Histone Deacetylase (HDAC) fluorogenic inhibition assay

The assay for inhibition against HDAC1 was adapted from previous reports.[70,71] All HDAC inhibition assays were performed using black medium binding Fluorotrac 200 96-well plates from Greiner Bio-One. Fluorescence measurements were recorded with a Molecular Devices SpectraMax i3x plate reader using 10 scans per well with respective excitation and emission wavelengths of 360 and 460 nm (15 nm bandwidth). Assay buffer consisting of 50 mM Tris base, 137 mM NaCl, 2.7 mM KCl, 1 mM $MgCl_2$, and 1.7 vol% DMSO was brought to pH 8.0 before adding bovine serum albumin (0.5 mg/mL). The buffer was passed through a 40 μM filter by syringe and refrigerated. Human recombinant HDAC1, purchased from the Cayman Chemical Company (> 90% pure as estimated by the supplier using SDS-PAGE), was divided into 2.5 μg aliquots and stored at –80 °C. Each aliquot was thawed on ice and diluted with assay buffer to provide a stock solution of 0.5 ng/μL the day of use. HDAC substrate Ac-Leu-Gly-Lys(Ac)-AMC,[13] synthesized by Adam Elmehriki and Anthony Palermo, was dissolved in DMSO to 8.000 mM then diluted to 7.50 μM with assay buffer. Trypsin from porcine pancreas (25 g/L in 0.9% NaCl from Sigma Aldrich) was diluted to 0.4 mg/mL with assay buffer immediately before use.

Dilution series of inhibitor candidates were prepared at 10-12 concentrations from 0.0100 M DMSO stock solutions with assay buffer. Due to poor activity otherwise, the dilution series for RB-321 was pre-incubated with an appropriate quantity of HDAC overnight (18 h) at 4 °C before use.

Plates were typically set up pairwise with triplicate measurements of 5 inhibitors at 12 concentrations each, along with 6 wells of each control. Negative controls received 25 μL of assay buffer and positive controls received 10 μL of buffer and 15 μL of HDAC enzyme solution (7.5 ng per well). Other wells received 10 μL of inhibitor solution and 15 μL of HDAC enzyme solution. The assays were initiated by addition of 25 μL of substrate (final concentration of 3.75 μM) to all wells. The plate was gently tapped and incubated at 22 °C for 30 mins, at which time 50 μL of trypsin solution was added to all wells and incubation was continued for a further 30 mins. Endpoint fluorescence measurements were then recorded and IC_{50} values were calculated by nonlinear regression using a sigmoidal 4PL analysis with GraphPad Prism 8.2.

The same procedure was followed for HDAC2, also purchased from the Cayman Chemical Company, except that 5 ng of enzyme were added to each well and the substrate concentration was 3.00 μM. Using this assay, we obtained an IC_{50} value of 19 nM for SAHA against HDAC2.

Antiandrogen BRET inhibition assay cell lines, **plasmids**, **and reagents**

Cell lines were purchased from the American Type Culture Collection (ATCC) and maintained in a humidified 37 °C, 5% CO_2 incubator. HEK293T cells were maintained in Dulbecco's modified Eagle's Media (DMEM, Wisent) supplemented with 10% Fetal Bovine Serum (FBS, Sigma) and 100 UI/mL penicillin-streptomycin (Wisent). The transfection reagent linear polyethylenimine (PEI) was ordered from Polysciences, Inc. Vectors for Protein Complementation Assay – Bioluminescence Resonance Energy Transfer (PCA-BRET) assays were generated by David Cotnoir-White at IRIC. The pcDNA3.1-AR-F1RLucII and pcDNA3.1-AR-F2RLucII vectors were obtained by splitting RlucII in two fragments (F1 and F2) and cloning them to the C-terminus of human androgen receptor AR. The pTopaz-N1-RNF14peptide was obtained by fusing two copies of YFP (Topaz) at the N- and C-termini of a tandem FXXLF motif from aa 450-461 of human RNF14 and of the glucocorticoid receptor nuclear localization signal (NLS peptide: DRAHSTPPKNKRNVRDPKDRAHSTPPKNKRNVRDPK).

Antiandrogen BRET inhibition assay cell transfection

Before each experiment, cells were switched for 48 h in DMEM without phenol red, supplemented with 10% charcoal-dextran-stripted FBS, 4 mM L-glutamine and 100 UI/mL penicillin/streptomycin. Cells were seeded at 10 million of cells per 15 cm^2 plates and co-transfected with equal amounts of pcDNA3.1-AR-F1RLucII and F2RlucII expression vectors to reconstitute full length RlucII (1.2 µg of each) either alone (for background evaluation) or together with 9.6 µg of pTopaz-N1-RNF14peptide in 1 mL of PBS (12 µg of DNA total per 10 million of cells). Transient transfections were performed using PEI (3 µg of linear PEI for each µg of DNA diluted in PBS) that was mixed with DNA (1V/V, 2 mL total) and left for 13 min at room temperature. The PEI:DNA mixture was added to attached cells and left for 48 h. Cells were harvested in Hank's Balanced Salt Solution (HBSS) supplemented with 4.5 g/L dextrose, seeded in a 96-well white plate (Costar, Corning) and immediately co-treated with 2 nM DHT and different doses of tested compounds in triplicates for 1 h before BRET assays.

Antiandrogen BRET inhibition assay

Coelenterazine H (Coel-h, Nanolight Technology) was added to each well to a final concentration of 10 µM and incubated for 5 min at room temperature protected from light. Readings were then collected using a MITHRAS LB940 (Berthold Technology) multidetector plate reader, allowing the sequential integration of the signals detected in the 485/20 nm and 530/25 nm windows, for luciferase and YFP light emissions, respectively. The BRET signal was determined by calculating the ratio of the light intensity emitted by the YFP fusion over the light intensity emitted by the Luc fusion. The values were corrected by subtracting the background BRET signal detected when the Luc fusion construct was expressed alone. IC_{50} values were calculated with GraphPad from 3 independent experiments.

Cell viability assay

LNCaP prostate cancer epithelial cells (ATCC) were maintained in RPMI supplemented with 10% FBS. PC3 prostate cancer epithelial cells (ATCC) were maintained in DMEM/F12 supplemented with 10% FBS. BPH-1 non-tumorigenic prostate epithelial cells[72] and BHPrS benign prostate stromal cells[73] were maintained in DMEM supplemented with 10% FBS. All cells were used between passage 5 and 10 and were cultured without the use of antibiotics.

For hybrid compound treatment, 2500 LNCaP cells and 750 PC3, BPH-1 and BHPrS cells were seeded per well in a volume of 50 µl in half-area, clear bottom, white 96-well plates (Corning) and left for 24 hours. 50 µl of medium supplemented with compounds or DMSO as a vehicle control (0.001%) was added and cells were cultured for 5 days or 72 hours. Cell viability was measured using CellTiter-Glo® (Promega) according to manufacturer's guidelines.

5.5 *References for Chapter 5*

1. Suzuki, T.; Ando, T.; Tsuchiya, K.; Fukazawa, N.; Saito, A.; Mariko, Y.; Yamashita, T.; Nakanishi, O. *J. Med. Chem.* **1999**, *42,* 3001.
2. Jung, M. E.; Sawyers, C. L.; Ouk, S.; Tran, C.; Wongvipat, J. US 8445507 B2, May 21, 2013.
3. Jung, M. E.; Ouk, S.; Yoo, D.; Sawyers, C. L.; Chen, C.; Tran, C.; Wongvipat, J. *J. Med. Chem.* **2010**, *53,* 2779.
4. Teutsch, G.; Goubet, F.; Battmann, T.; Bonfils, A.; Bouchoux, F.; Cerede, E.; Gofflo, D.; Gaillard-Kelly, M.; Philbert, D. *J. Steroid Biochem. Molec. Biol.* **1994**, *48,* 111.
5. Tachibana, K.; Imaoka, I.; Shiraishi, T.; Yoshino, H.; Nakamura, M.; Ohta, M.; Kawata, H.; Taniguchi, K.; Ishikura, N.; Tsunenari, T.; Saito, H.; Nagamuta, M.; Nakagawa, T.; Takanashi, K.; Onuma, E.; Sato, H. *Chem. Pharm. Bull.* **2008**, *56,* 1555.
6. Chong, M. J.; Heuft, M. A.; Rabbat, P. *J. Org. Chem.* **2000**, *65,* 5837.
7. Demmer, O.; Frank, A. O.; Hagn, F.; Schottelius, M.; Marinelli, L.; Cosconati, S.; Brack-Werner, R.; Kremb, S.; Wester, H.; Kessler, H. *Angew. Chem. Int. Ed.* **2012**, *51,* 8110.
8. Doyle, C. M.Sc. Dissertation, McGill University, Montréal, QC, 2014.
9. Barrett, R. R. G.; Nash, C.; Diennet, M.; Cotnoir-White, D.; Doyle, C.; Mader, S.; Thomson, A. A.; Gleason, J. L. *Bioorg. Med. Chem. Lett.* **2022**, *55,* 128441.
10. López-Cara, L. C.; Carrión, M. D.; Entrena, A.; Gallo, M. A.; Espinosa, A.; López, A.; Escames, G.; Acuña-Castroviejo, D.; Camacho, M. E. *Eur. J. Med. Chem.* **2012**, *50,* 129.
11. Chen, L.; Ju, L.; Bustin, K. A.; Hoover, J. M. *Chem. Commun.* **2015**, *51,* 15059.
12. Cui, L.-Q.; Dong, Z.-L.; Liu, K.; Zhang, C. *Org. Lett.* **2011**, *13,* 6488.
13. Bell, M. G.; Doti, R. A.; Genin, M. J.; Lander, P. A.; Ma, T.; Manninen, P. R.; Ochoada, J. M.; Qu, F.; Stelzer, L. S.; Stites, R. E.; Warshawsky, A. M. WO 2007/140183 A1, December 6, 2007.
14. Narayanan, R.; Miller, D. D.; Ponnusamy, T.; Hwang, D.-J.; He, Yali. WO 2019/222556 A1, November 21, 2019.
15. Stolfa, D. A.; Stefanachi, A.; Gajer, J. M.; Nebbioso, A.; Altucci, L.; Cellamare, S.; Jung, M.; Carotti, A. *ChemMedChem* **2012**, *7*, 1256.
16. Chang, F. C.; Wood, N. F. *Tetrahedron Lett.* **1964**, 2969.
17. Zhou, A.; Li, B.; Ruan, L.; Wang, Y.; Duan, G.; Li, J. *Chin. Chem. Lett.* **2017**, *28*, 426.

18. Rosati, R.; Chen, B.; Patki, M.; McFall, T.; Ou, S.; Heath, E.; Ratnam, M.; Qin, Z. *Mol. Pharmacol.* **2016***, 90*, 225.
19. Jadhavar, P. S.; Ramachandran, S. A.; Riquelme, E.; Gupta, A.; Quinn, K. P.; Shivakumar, D.; Ray, S.; Zende, D.; Nayak, A. K.; Miglani, S. K.; Sathe, B. D.; Raja, M., Farias, O.; Alfaro, I., Belmar, S.; Guerrero, J.; Bernales, S.; Chakravarty, S.; Hung, D. T.; Lindquist, J. N.; Rai, R. *Bioorg. Med. Chem. Lett.* **2016**, *26,* 5222.
20. Hughes, J. M. E.; Scarlata, D. A.; Chen, A. C.-Y.; Burch, J. D.; Gleason, J. L. *Org. Lett.* **2019**, *21,* 6800.
21. Makarov, I. S.; Brocklehurst, C. E.; Karaghiosoff, K.; Koch, G.; Knochel, P. *Angew. Chem. Int. Ed.* **2017**, *56,* 12774.
22. Applequist, D. E.; Renken, T. L.; Wheeler, J. W. *J. Org. Chem.* **1982**, *47,* 4985.
23. Carlsen, H. J.; Katsuki, T.; Martin, V. S.; Sharpless, K. B. *J. Org. Chem.* **1981**, *46,* 3936.
24. Goh, Y. L.; Cui, Y. T.; Pendharkar, V.; Adsool, V. A. *ACS Med. Chem. Lett.* **2017**, *8,* 516.
25. (a) Shi, G.; Shao, C.; Pan, S.; Yu, J.; Zhang, Y. *Org. Lett.* **2015**, *17,* 38. (b) Yang, B.; Yu, D.; Xu, X.-H.; Qing, F.-L. *ACS Catal.* **2018**, *8,* 2839.
26. (a) Mistico, L.; Querolle, O.; Meerpoel, L.; Angibaud, P.; Durandetti, M.; Maddaluno, J. *Chem. Eur. J.* **2016**, *22,* 9687. (b) Ahmed, B. M.; Mezei, G. *RSC Adv.* **2015**, *5,* 24081.
27. McLaughlin, M.; Marcantonio, K.; Chen, C.; Davies, I. W. *J. Org. Chem.* **2008**, *73,* 4309.
28. Coffey, S. *Rec. Trav. Chim.* **1923,** *42,* 387.
29. Newman, M. S.; VanderWerf, C. A. *J. Am. Chem. Soc.* **1945,** *67,* 233.
30. Parent, J.-F.; Bertrand, X.; Deslongchamps, G.; Deslongchamps, P. *J. Org. Chem.* **2020,** *85,* 758.
31. Sworin, M.; Lin, K-C. *J. Org. Chem.* **1987,** *52,* 5640.
32. Sworin, M.; Lin, K-C. *J. Am. Chem. Soc.* **1989,** *111,* 1815.
33. Zulfiqar, F.; Malik, A. *Z. Naturforsch* **2001,** *56b,* 1227.
34. Cyclopentenyl bromide and 4-OMe-Ph-α-bromostyrene were prepared on multi-gram scale using triphenyl phosphite dibromide, essentially as described in "General Method A" of the following reference. Alazet, S.; Preindl, J.; Simonet-Davin, R.; Nicolai, S.; Nanchen, A.; Meyer, T.; Waser, J. *J. Org. Chem.* **2018,** *83,* 12334.
35. Silveira, P. B.; Monteiro, A. L. *J. Mol. Catal. A Chem.* **2006,** *247,* 6.
36. Warrington, J. M.; Barriault, L. *Org. Lett.* **2005,** *7,* 4589.

37. (a) Baldwin, J. E.; Hoefle, G. A.; Lever, O. W. *J. Am. Chem. Soc.* **1974**, *96,* 7125. (b) Jacobsen, E. J.; Levin, J.; Overman, L. E. *J. Am. Chem. Soc.* **1988**, *110,* 4329.
38. Smith, M. B. *Synth. Commun.* **1986**, *16,* 85.
39. Curini, M.; Epifano, F.; Marcotullio, M. C.; Rosati, O.; Guo, M.; Guan, Y.; Wenkert, E. *Helv. Chim. Acta.* **2005**, *88,* 330.
40. Asselin, A. A.; Humber, L. G.; Dobson, T. A.; Komlossy, J. *J. Med. Chem.* **1976**, *19,* 787.
41. (a) Roscini, C.; Cubbage, K. L.; Berry, M.; Orr-Ewing, A. J.; Booker-Milburn, K. I. *Angew. Chem. Int. Ed.* **2009**, *48,* 8716. (b) Viveros-Ceballos, J. L.; Martínez-Toto, E. I.; Eustaquio-Armenta, C.; Cativiela, C.; Ordóñez, M. *Eur. J. Org. Chem.* **2017**, 6781. (c) Chen, L.; Li, L.; Sampson, N. S. *J. Org. Chem.* **2018**, *83,* 2892. (d) Yasuda, M.; Oh-hata, T.; Shibata, I.; Baba, A.; Matsuda, H. *J. Chem. Soc. Perkin Trans. 1* **1993**, 859.
42. Overman, L. E.; Wolfe, J. P. *J. Org. Chem.* **2002**, *67,* 6421.
43. Jackson, J. A.; Hammond, G. B.; Wiemer, D. F. *J. Org. Chem.* **1989**, *54,* 4750.
44. Abu Deiab, G. I.; Croatt, M. P. *Bioorg. Med. Chem.* **2019,** *27,* 338.
45. Molander, G. A.; Harris, C. R. *J. Org. Chem.* **1998,** *63,* 812.
46. (a) Erkkilä, A.; Pihko, P. *J. Org. Chem.* **2006,** *71,* 2538. (b) Erkkilä, A.; Pihko, P. M. *Eur. J. Org. Chem.* **2007,** 4205.
47. (a) Holloway, C. A.; Muratore, M. E.; Storer, R. I.; Dixon, D. J. *Org. Lett.* **2010,** *12,* 4720. (b) Li, Z.; Lam, S. M.; Ip, I.; Wong, W.; Chiu, P. *Org. Lett.* **2017,** *19,* 4464.
48. House, H. O.; Yau, C.-C.; VanDerveer, D. *J. Org. Chem.* **1979,** *44,* 3031.
49. Marshall, J. A.; Huffman, W. F. *J. Am. Chem. Soc.* **1970,** *92,* 6358.
50. McNulty, J.; Nair, J. J.; Cheekoori, S.; Larichev, V.; Capretta, A.; Robertson, A. J. *Chem. Eur. J.* **2006**, *12,* 9314.
51. Zhang, J.; Li, Y.; Zhang, F.; Hu, C.; Chen, Y. *Angew. Chem. Int. Ed.* **2016**, *55,* 1872.
52. Holz, J.; Schäffner, B.; Zayas, O.; Spannenberg, A.; Börner, A. *Adv. Synth. Catal.* **2008**, *350,* 2533.
53. Brass, S.; Chan, N.-S.; Gerlach, C.; Luksch, T.; Böttcher, J.; Diederich, W. E. *J. Organomet. Chem.* **2006**, *691,* 5406.
54. Hrizi, A.; Thiery, E.; Romdhani-Younes, M.; Jacquemin, J.; Thibonnet, J. *Eur. J. Org. Chem.* **2021**, 3798.
55. Omura, K.; Swern, D. *Tetrahedron* **1978**, *34,* 1651.

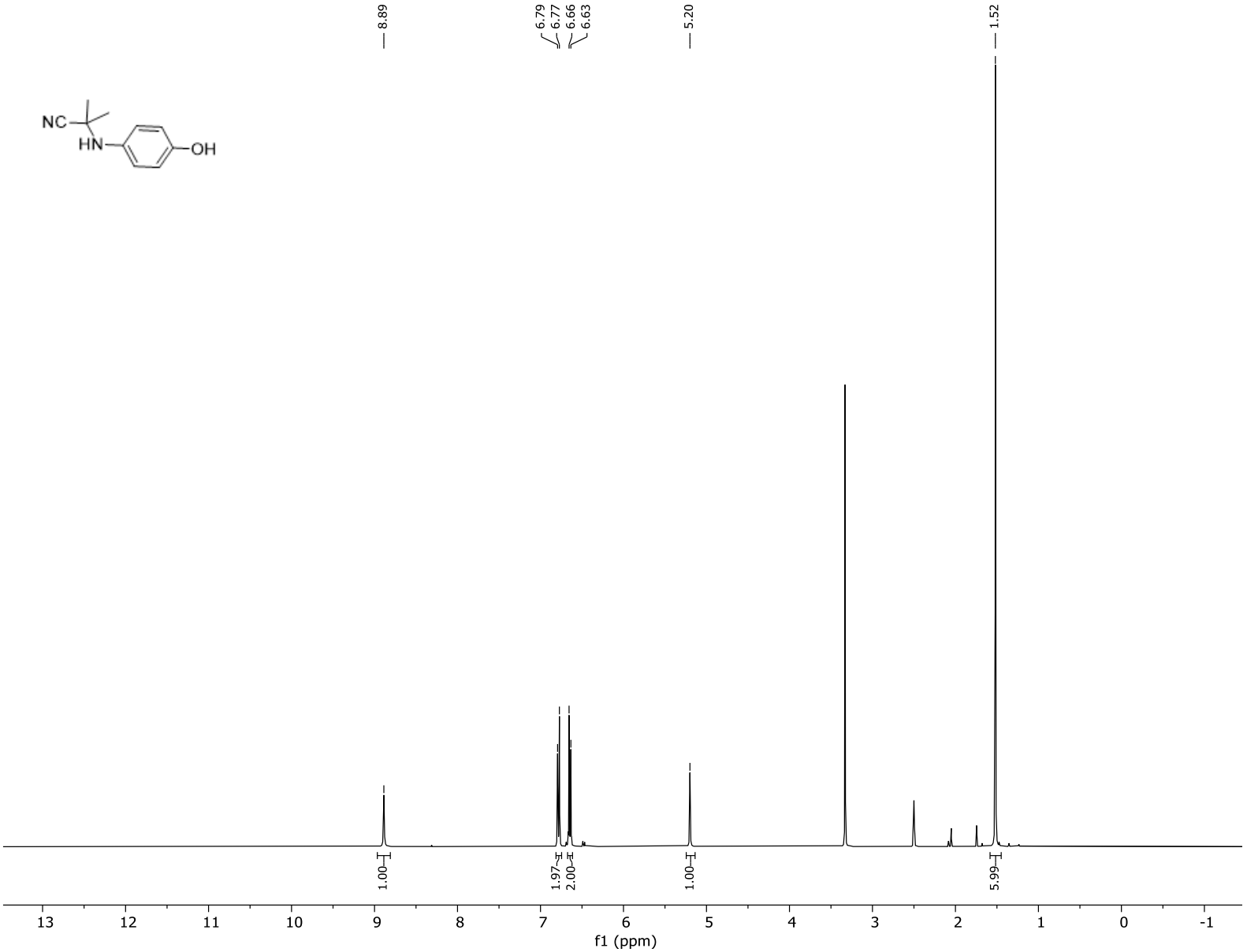
56. Righi, G.; Rumboldt, G. *J. Org. Chem.* **1996**, *61,* 3557.
57. Hediger, M. E. *Bioorg. Med. Chem.* **2004**, *12,* 4995.
58. Kyne, R. E.; Ryan, M. C.; Kliman, L. T.; Morken, J. P. *Org. Lett.* **2010**, *12,* 3796.
59. Imagawa, H.; Asai, Y.; Takano, H.; Hamagaki, H.; Nishizawa, M. *Org. Lett.* **2006**, *8,* 447.
60. Valente, C.; Organ, M. G. *Chem. Eur. J.* **2008**, *14,* 8239.
61. Zhang, J.; Li, Y.; Xu, R.; Chen, Y. *Angew. Chem. Int. Ed.* **2017,** *56,* 12619.
62. (a) Nacro, K.; Baltas, M.; Gorrichon, L. *Tetrahedron* **1999,** *55,* 14013. (b) Clausen, D. J.; Wan, S.; Floreancig, P. E. *Angew. Chem. Int. Ed.* **2011,** *50,* 5178.
63. Moure, A. L.; Arrayas, R. G.; Cardenas, D. J., Alonso, I.; Carretero, J. C. *J. Am. Chem. Soc.* **2012,** *134,* 7219.
64. Gao, Y.; Hanson, R. M.; Klunder, J. M.; Ko, S. Y.; Masamune, H.; Sharpless, K. B. *J. Am. Chem. Soc.* **1987,** *109,* 5765.
65. (a) Zhang, F.; Zeng, J.; Gao, M.; Wang, L.; Chen, G-Q.; Lu, Y.; Zhang, X. *Nat. Chem.* **2021,** *13,* 692. (b) Dorta, R. L.; Rodriguez, M. S.; Salazar, J. A.; Suarez, E. *Tetrahedron Lett.* **1997,** *38,* 4675.
66. (a) Langille, N. F.; Jamison, T. F. *Org. Lett.* **2006,** *8*, 3761. (b) Nishizawa, Y. *Bull. Chem. Soc. Jpn.* **1961,** *34,* 1170.
67. Greico, P. A.; Gilman, S.; Nishizawa, M. *J. Org. Chem.* **1976,** *41,* 1485.
68. Sharpless, K. B.; Young, M. W. *J. Org. Chem.* **1975,** *40,* 947.
69. Kaldre, D. Ph.D. Thesis, McGill University, Montreal, Canada, 2015.
70. Bradner, J. E.; West, N.; Grachan, M. L.; Greenberg, E. F.; Haggarty, S. J.; Warnow, T.; Mazitschek, R. *Nat. Chem. Bio.* **2010**, *6,* 238.
71. Villadsen, J. S.; Stephansen, H. M.; Maolanon, A. R.; Harris, P.; Olsen, C. A. *J. Med. Chem.* **2013**, *56,* 6512.
72. Hayward, S. W.; Dahiya, R.; Cunha, G. R.; Bartek, J.; Deshpande, N.; Narayan, P. *In Vitro Cell. Dev. Biol.-Animal* **1995**, *31,* 14.
73. Franco, O. E.; Jiang, M.; Strand, D. W.; Peacock, J.; Fernandez, S.; Jackson, R. S.; Revelo, M. P.; Bhowmick, N. A.; Hayward, S. W. *Cancer Res.* **2011**, *71*, 1272.

Chapter 6. Appendix.

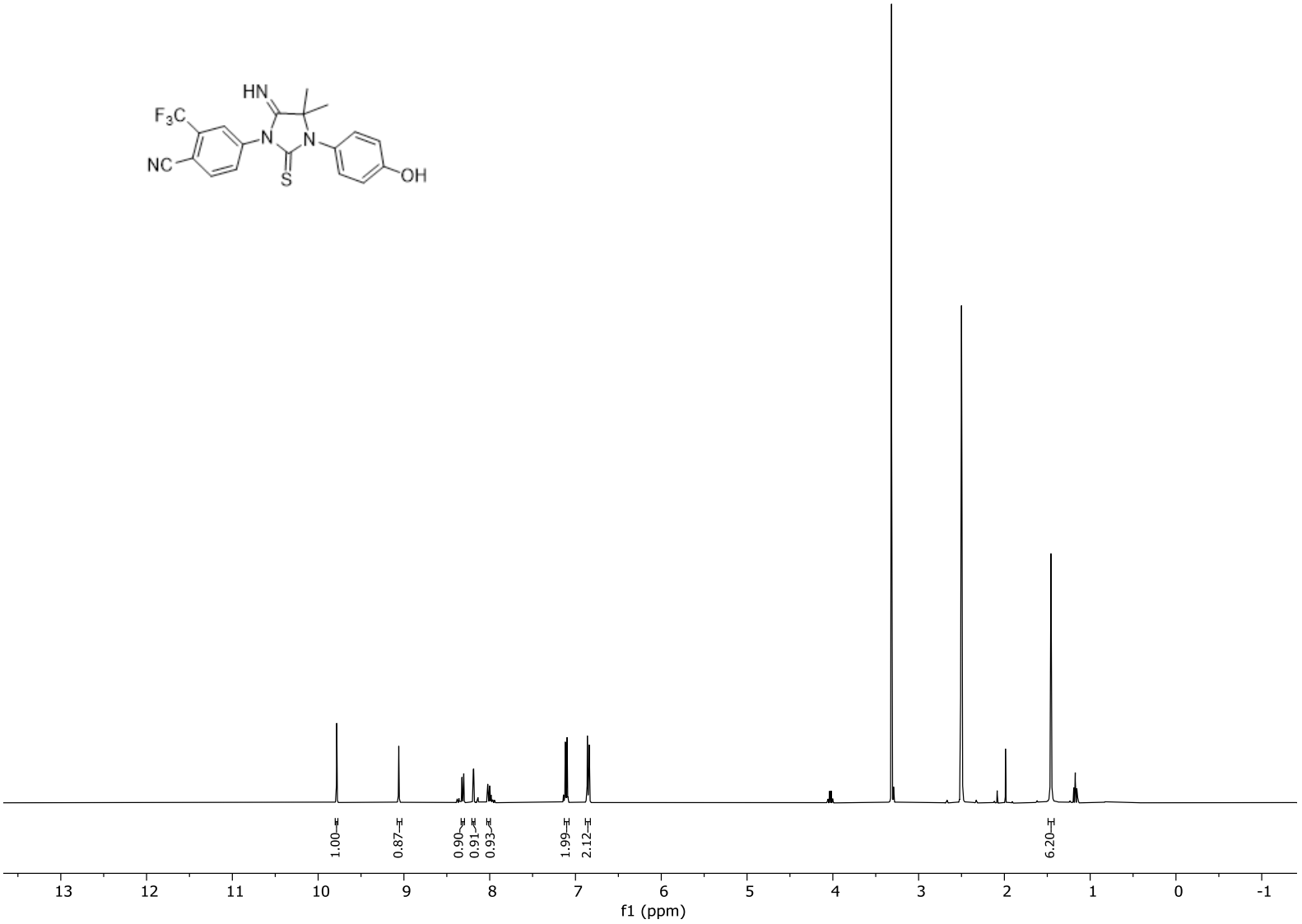
Unpublished NMR spectra for Part I and Part II.

LC-MS traces for hybrids in Chapter **2**.

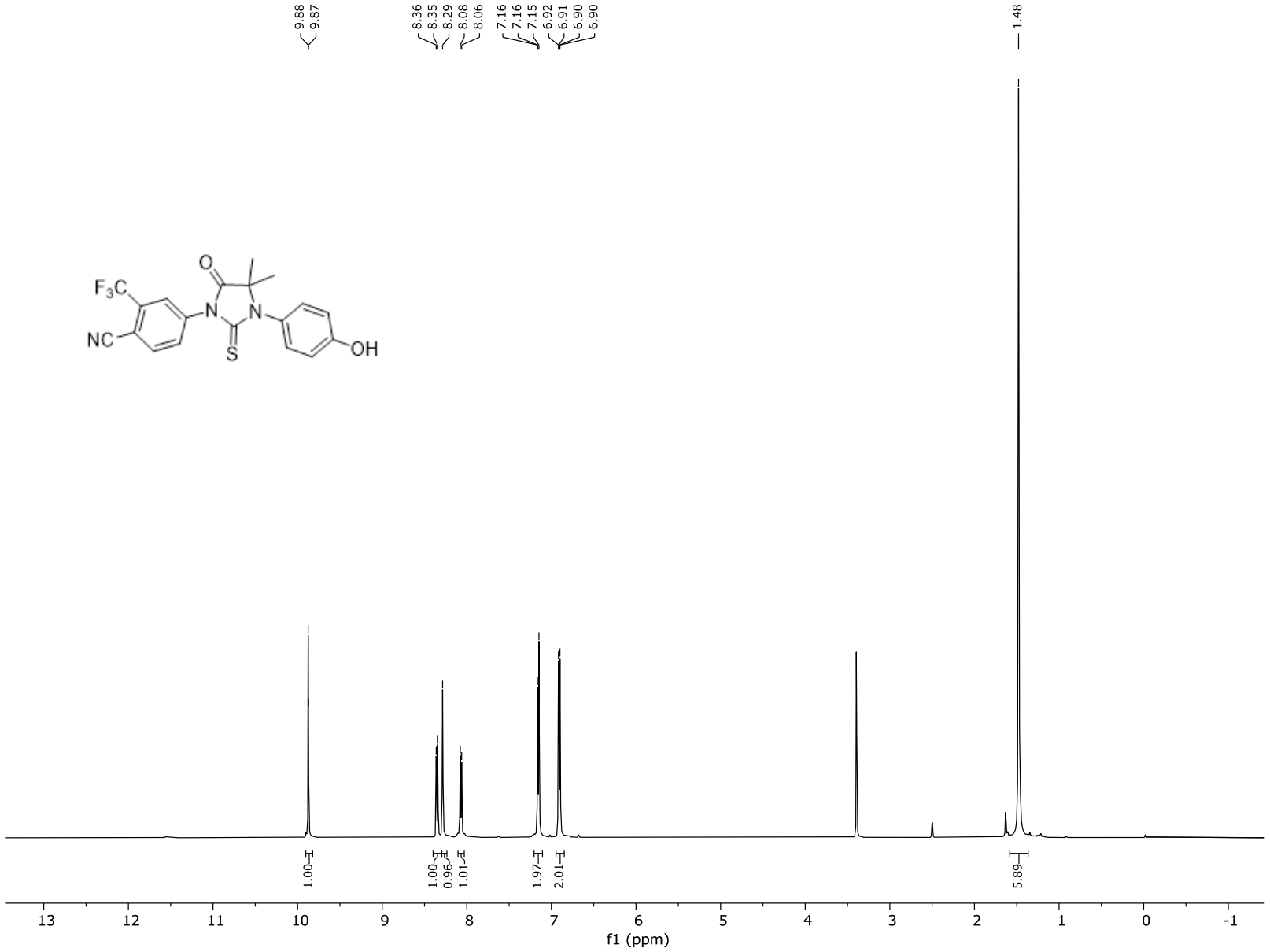
2.15 ^{1}H NMR (400 MHz, DMSO-d_6)



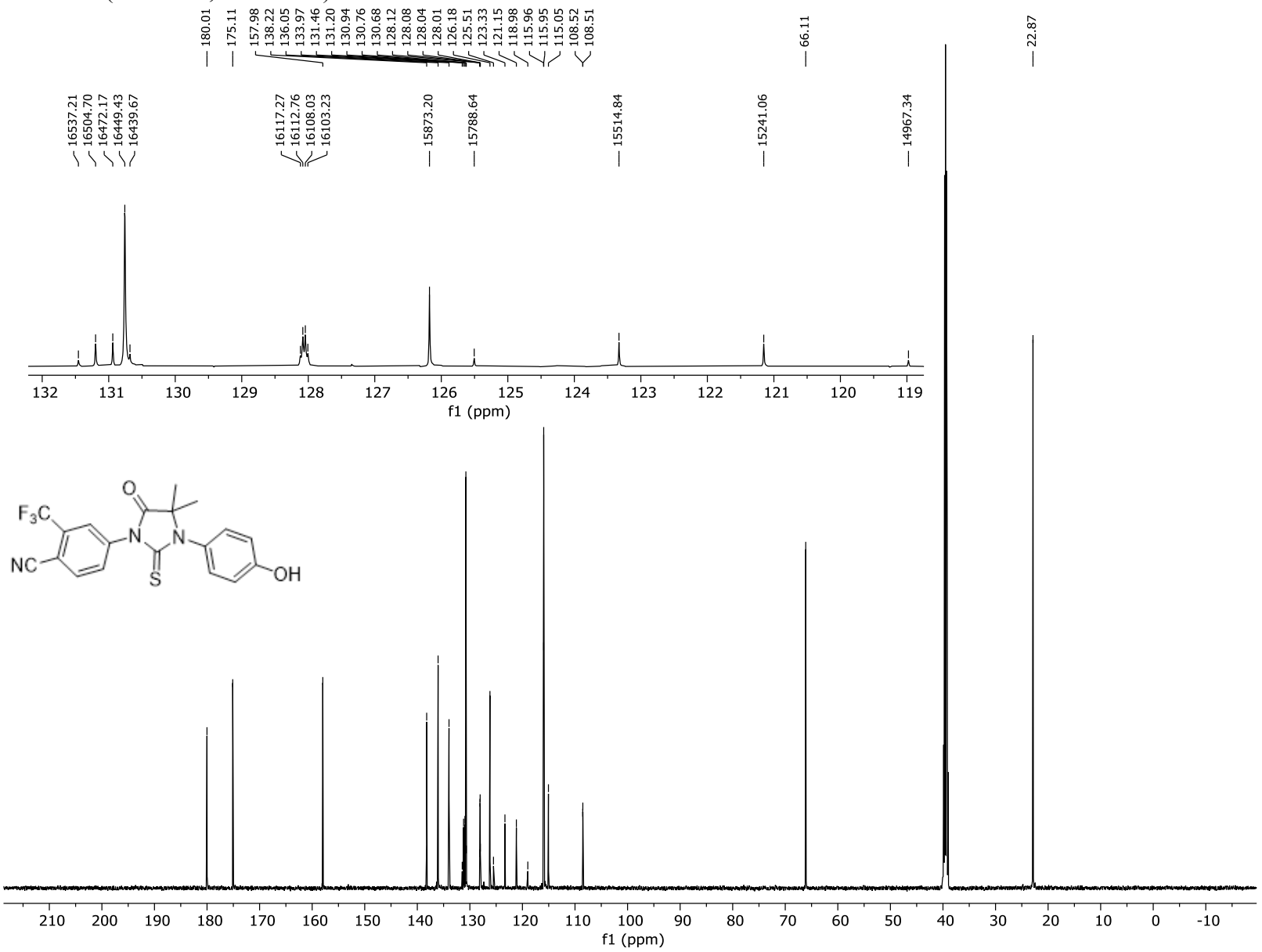
2.16a ^{1}H NMR (400 MHz, DMSO-d_6)



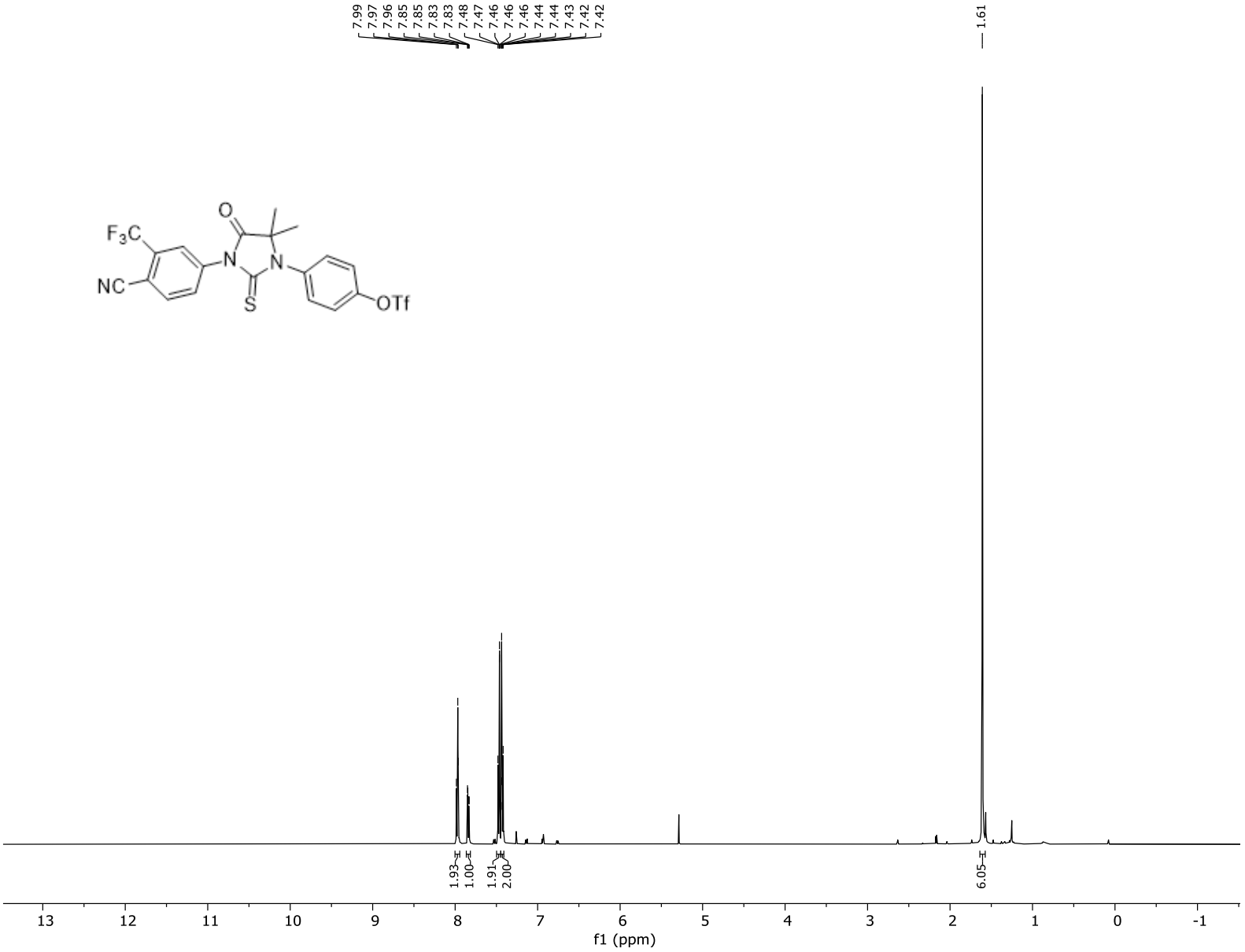
2.16 ^{1}H NMR (500 MHz, DMSO-d_6)



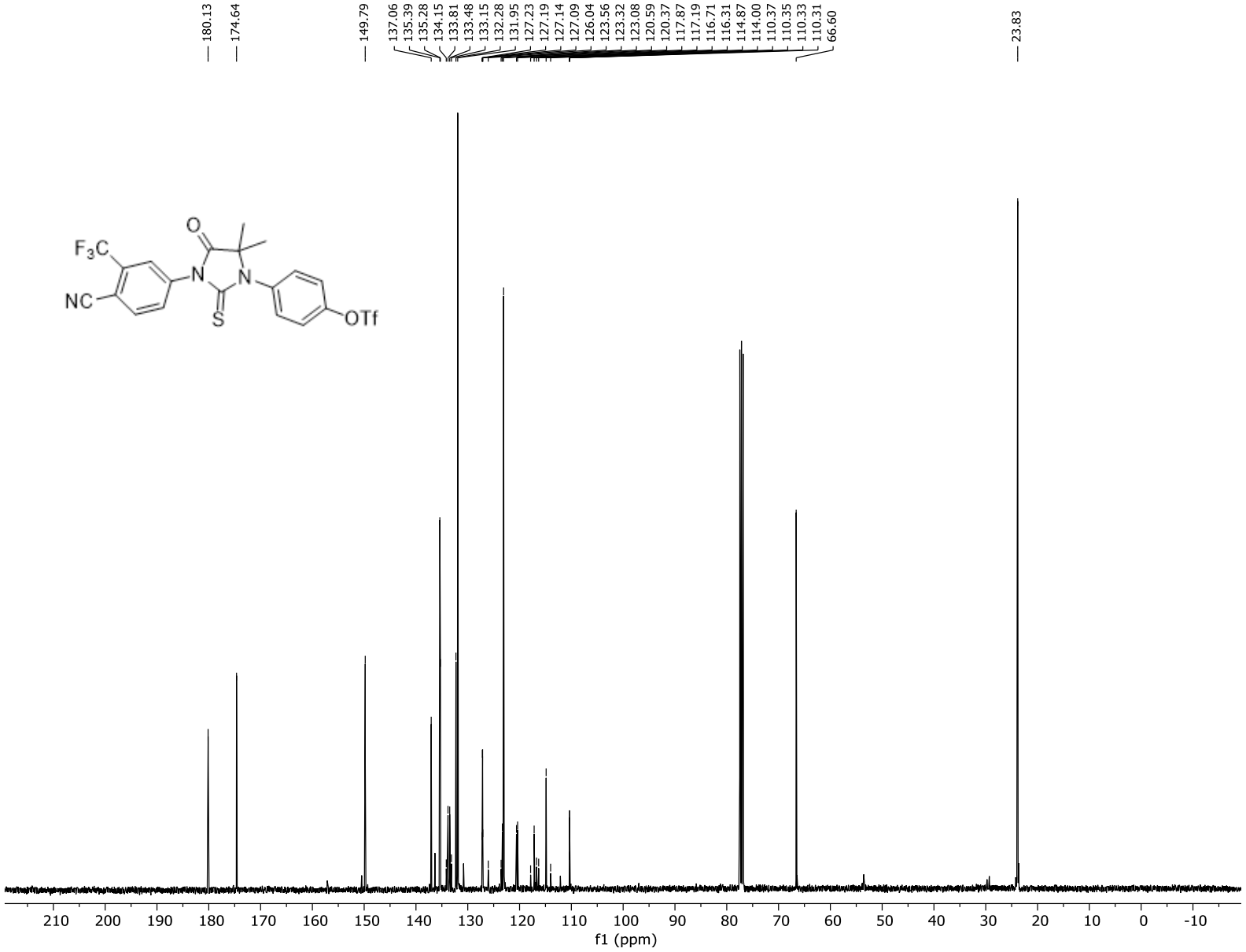
2.16 ^{13}C NMR (126 MHz, DMSO-d_6)



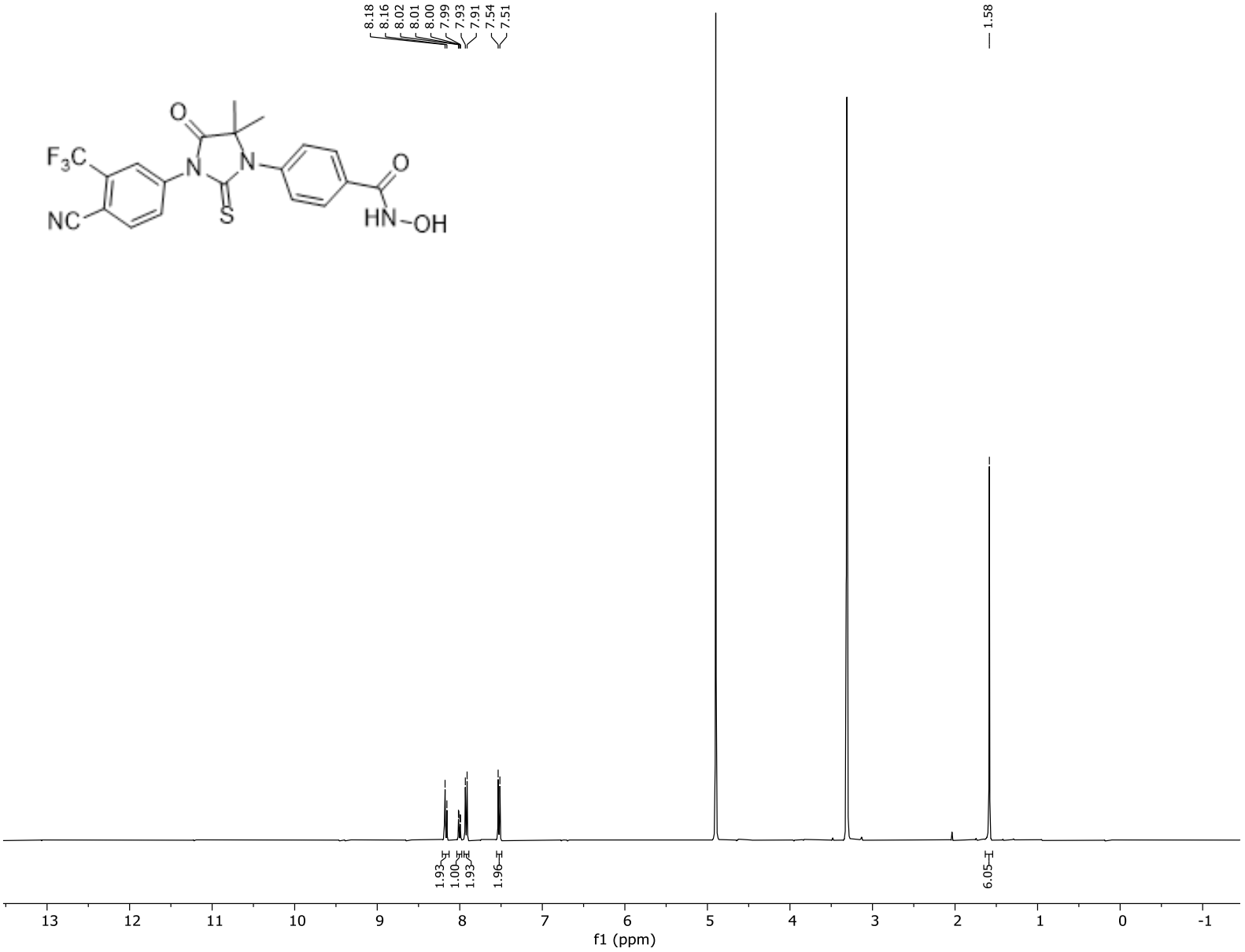
2.17 ^{1}H NMR (500 MHz, $CDCl_3$)



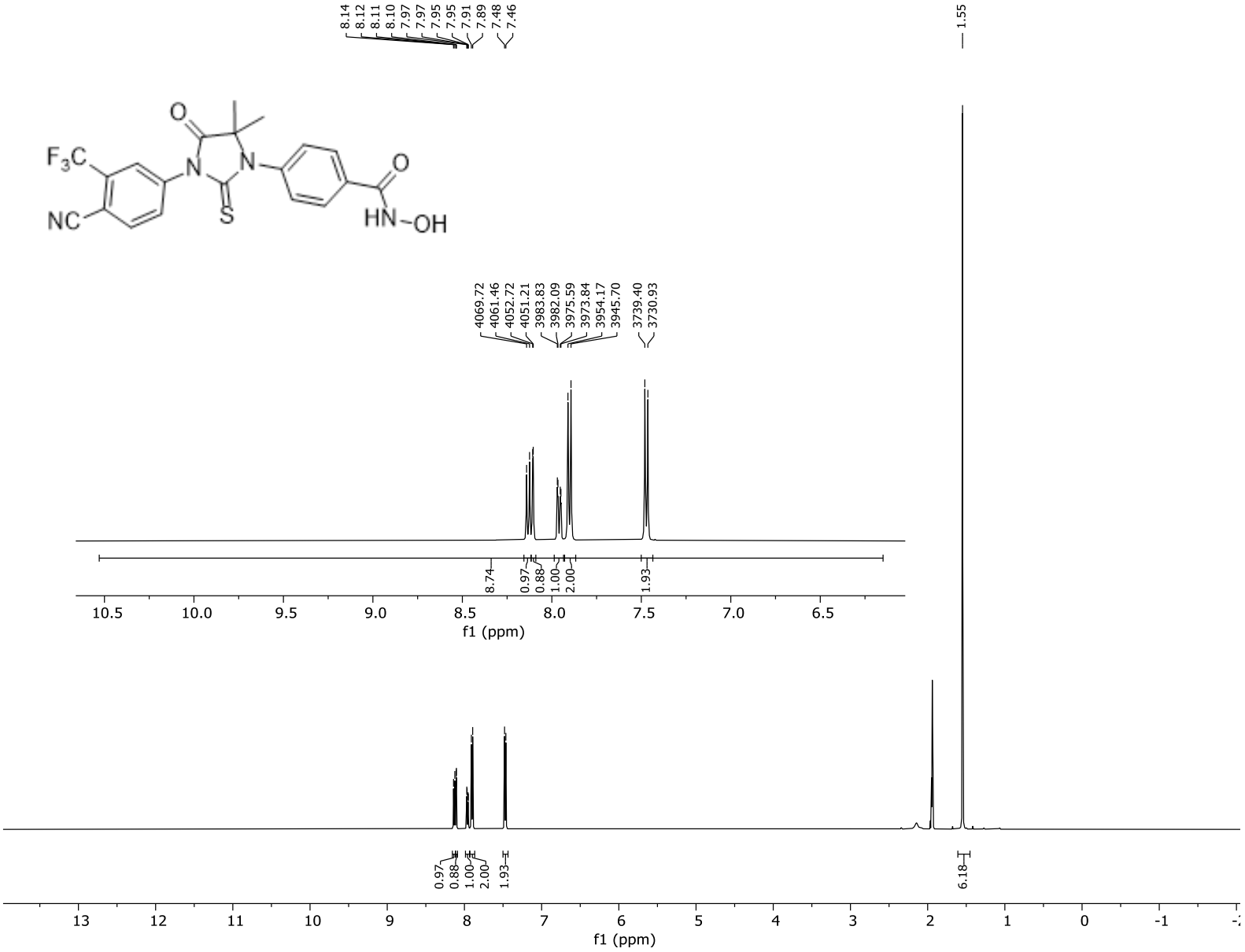
2.17 ^{13}C NMR (101 MHz, $CDCl_3$)



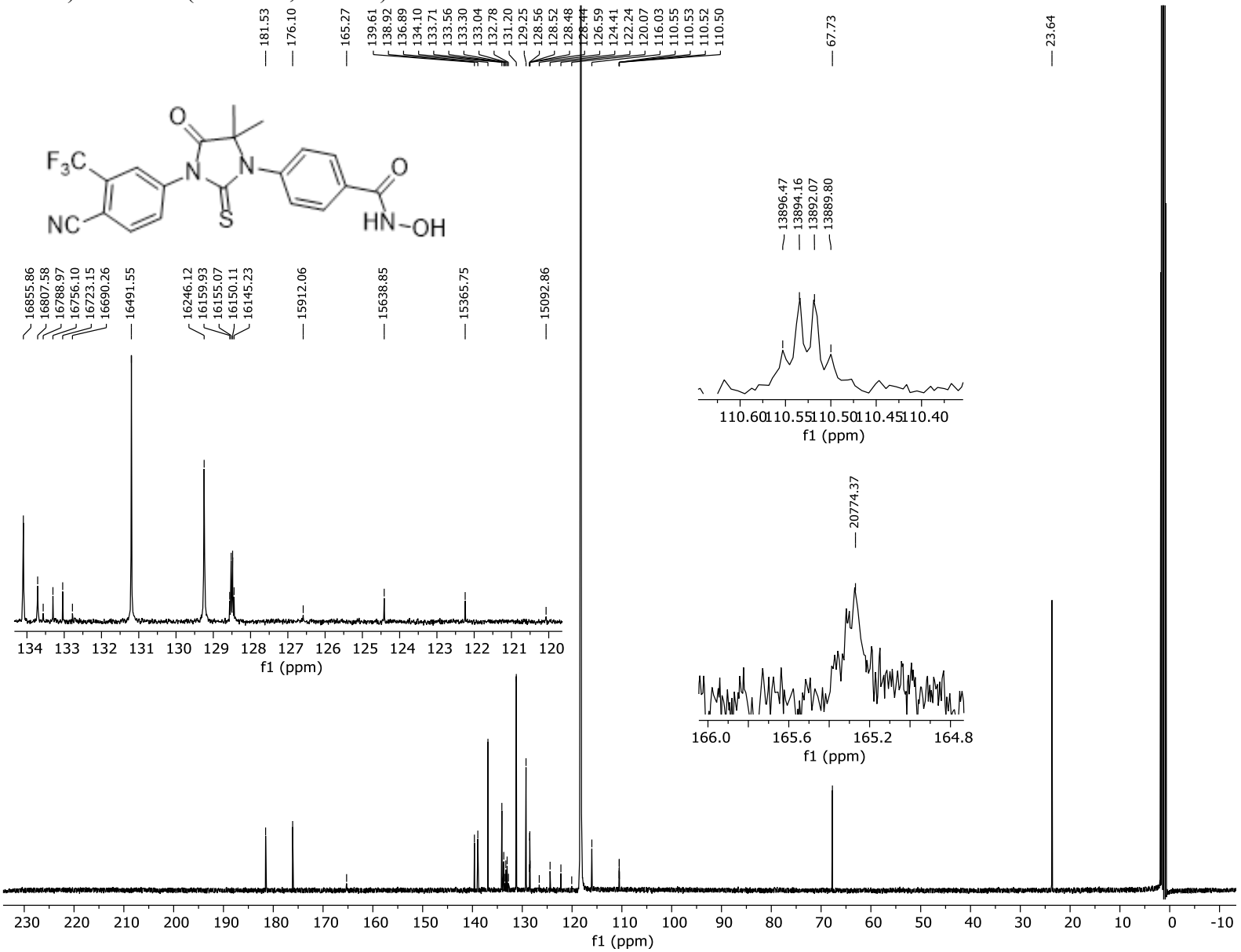
2.4 (RB-318) ^{1}H NMR (400 MHz, CD_3OD)



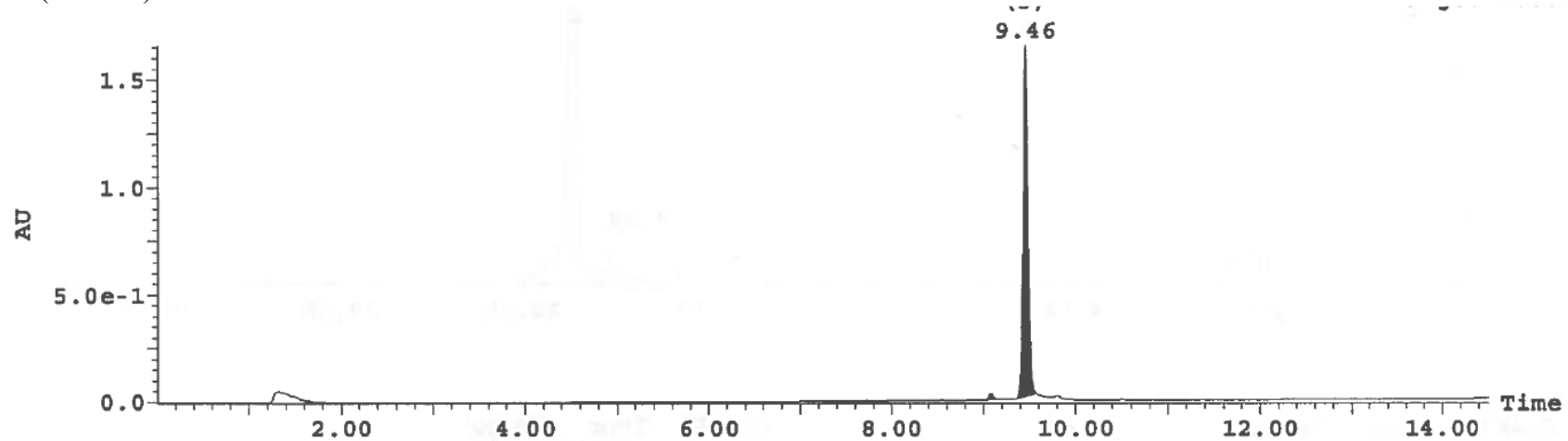
2.4 (RB-318) ^{1}H NMR (500 MHz, CD_3CN)



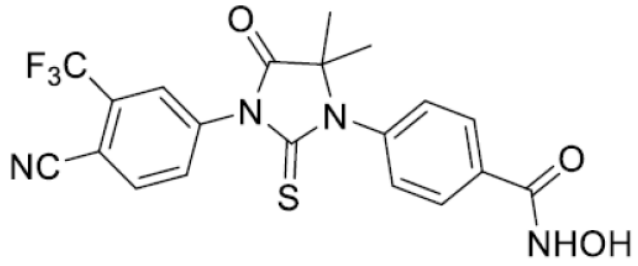
2.4 (RB-318) ^{13}C NMR (126 MHz, CD_3CN)



2.4 (RB-318) LC-MS UV trace

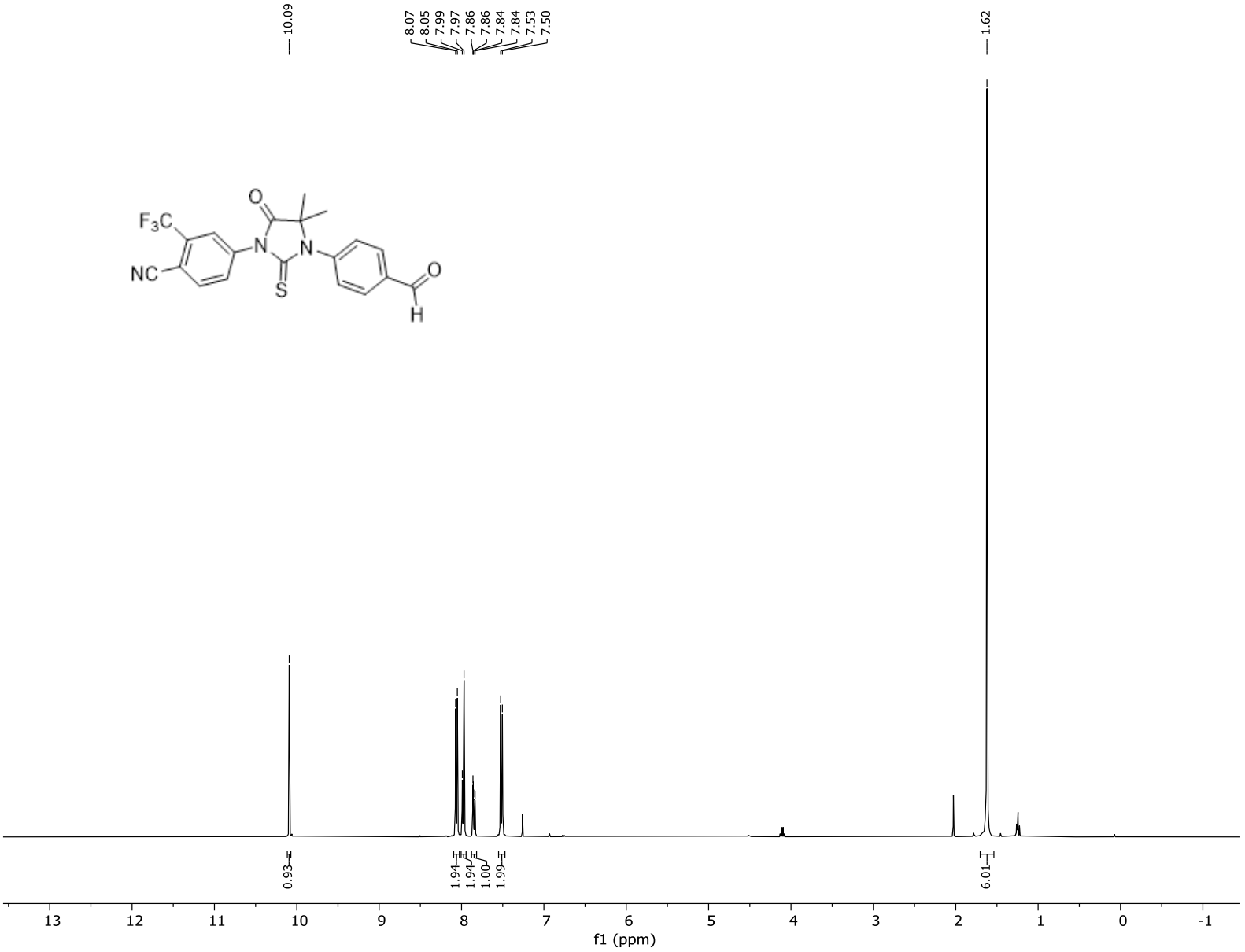


Peak Number	Time	AreaAbs	Area %Total	Height	Mass Found
2	9.09	1950	1.85	27594	
3	9.46	103380	98.15	1634127	

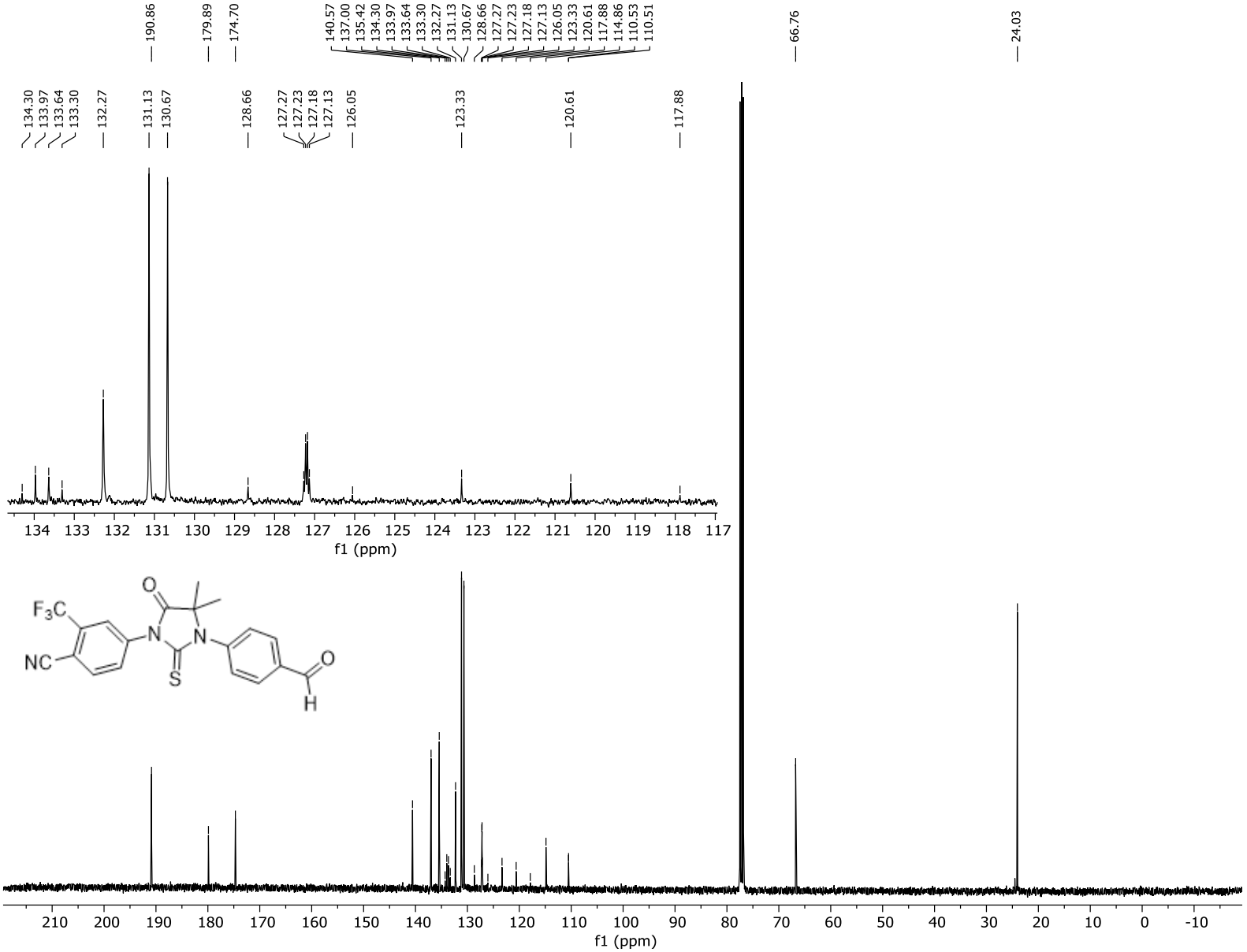


RB-318

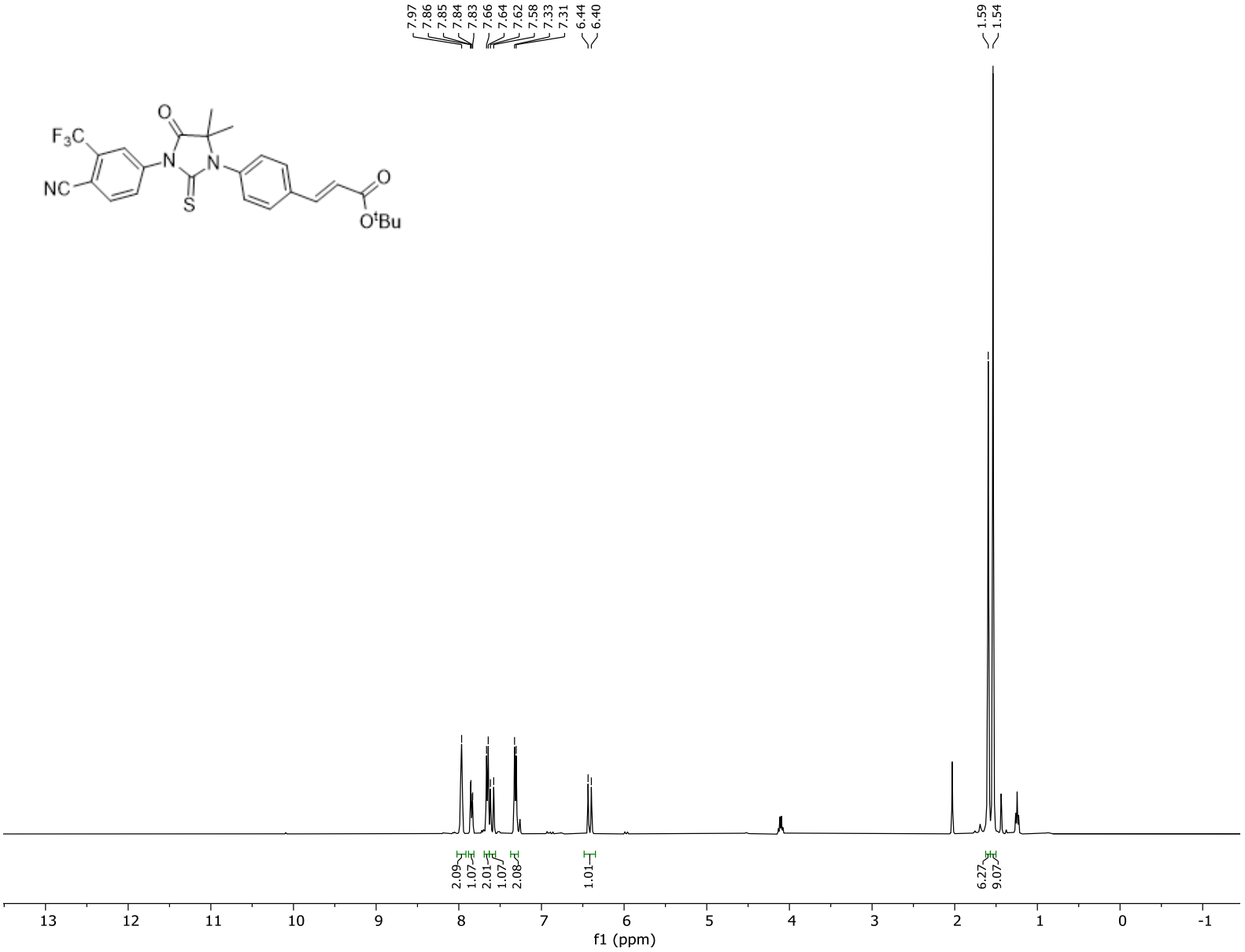
2.19 ^{1}H NMR (400 MHz, $CDCl_3$)



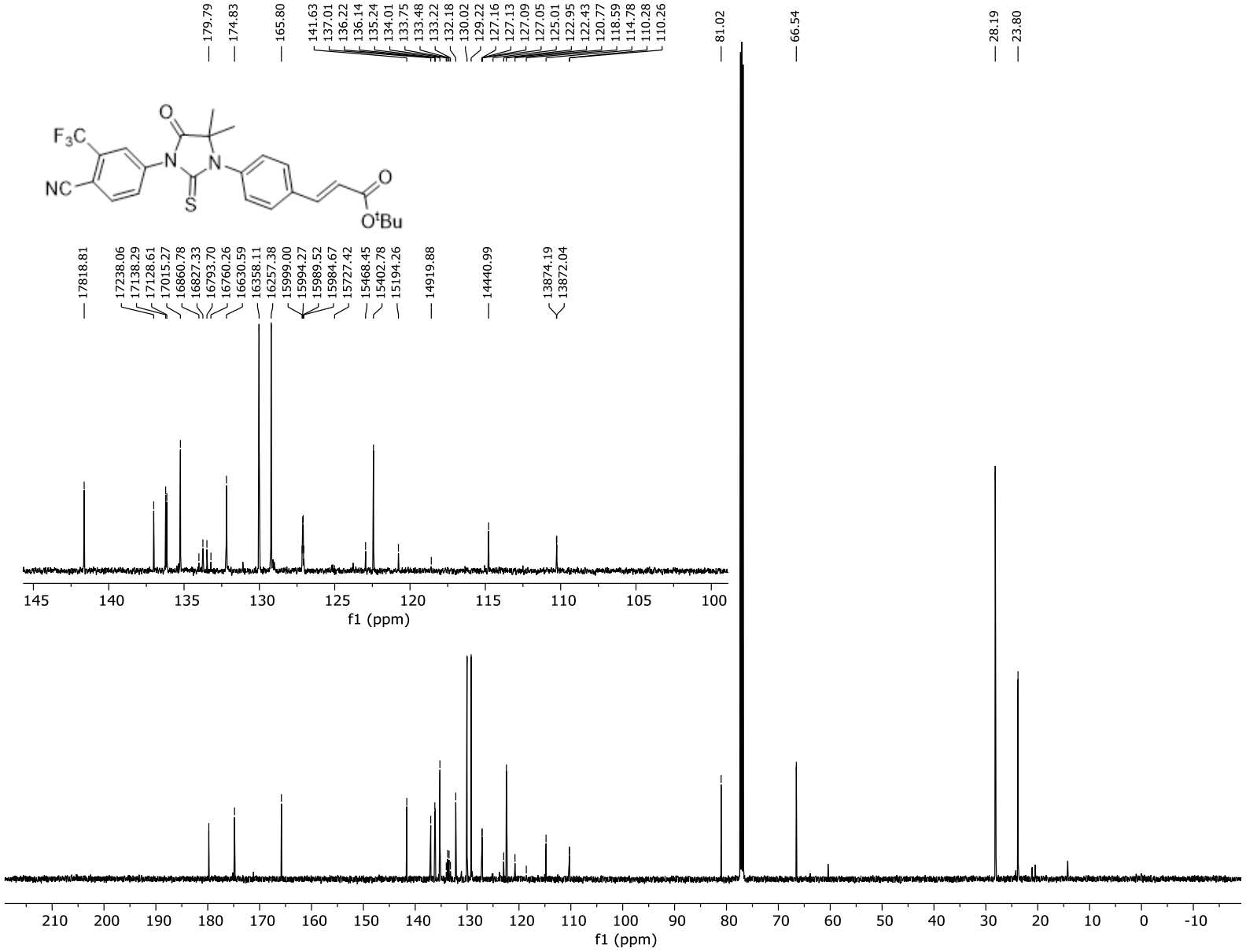
2.19 ^{13}C NMR (101 MHz, $CDCl_3$)



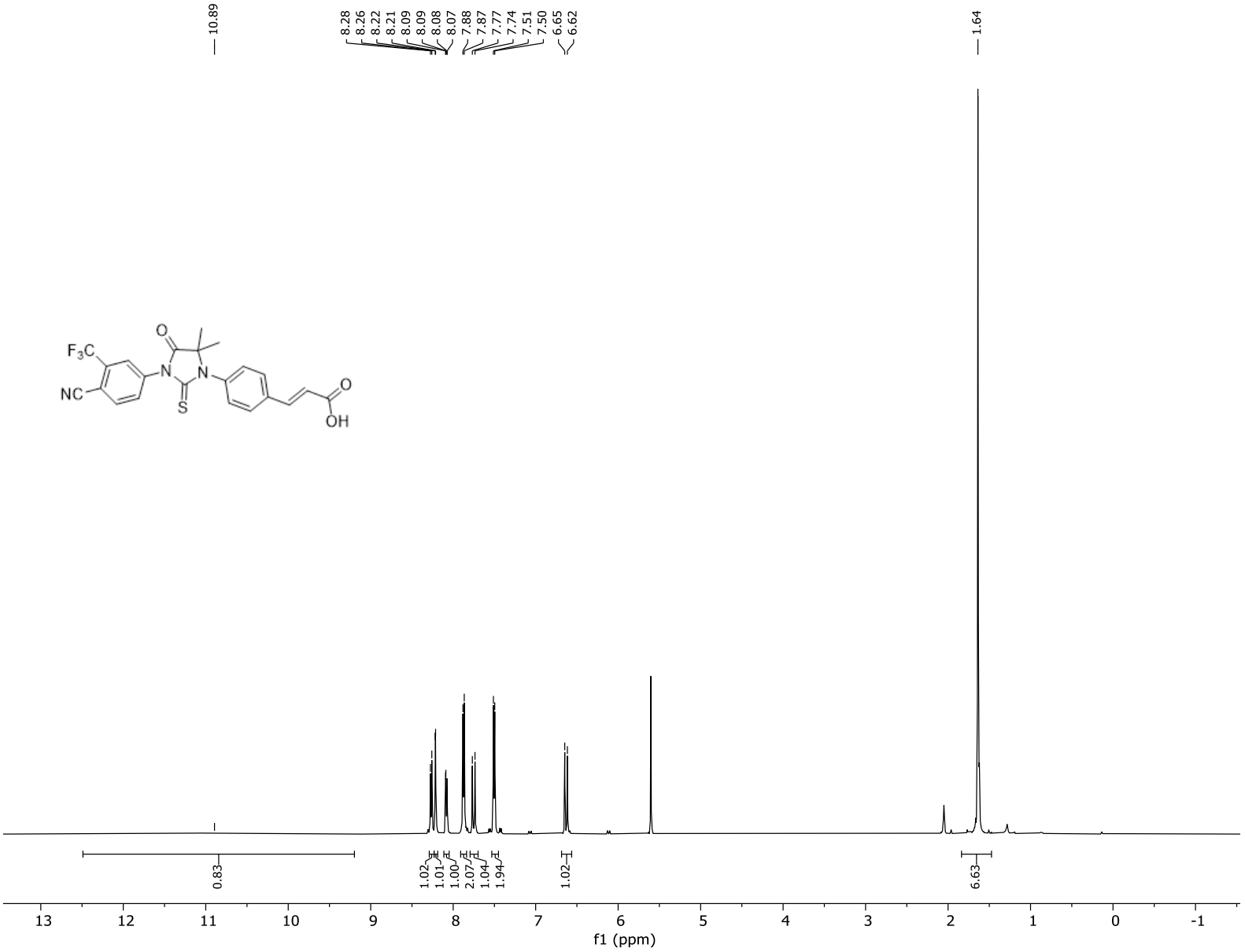
2.20 ^{1}H NMR (400 MHz, $CDCl_3$)



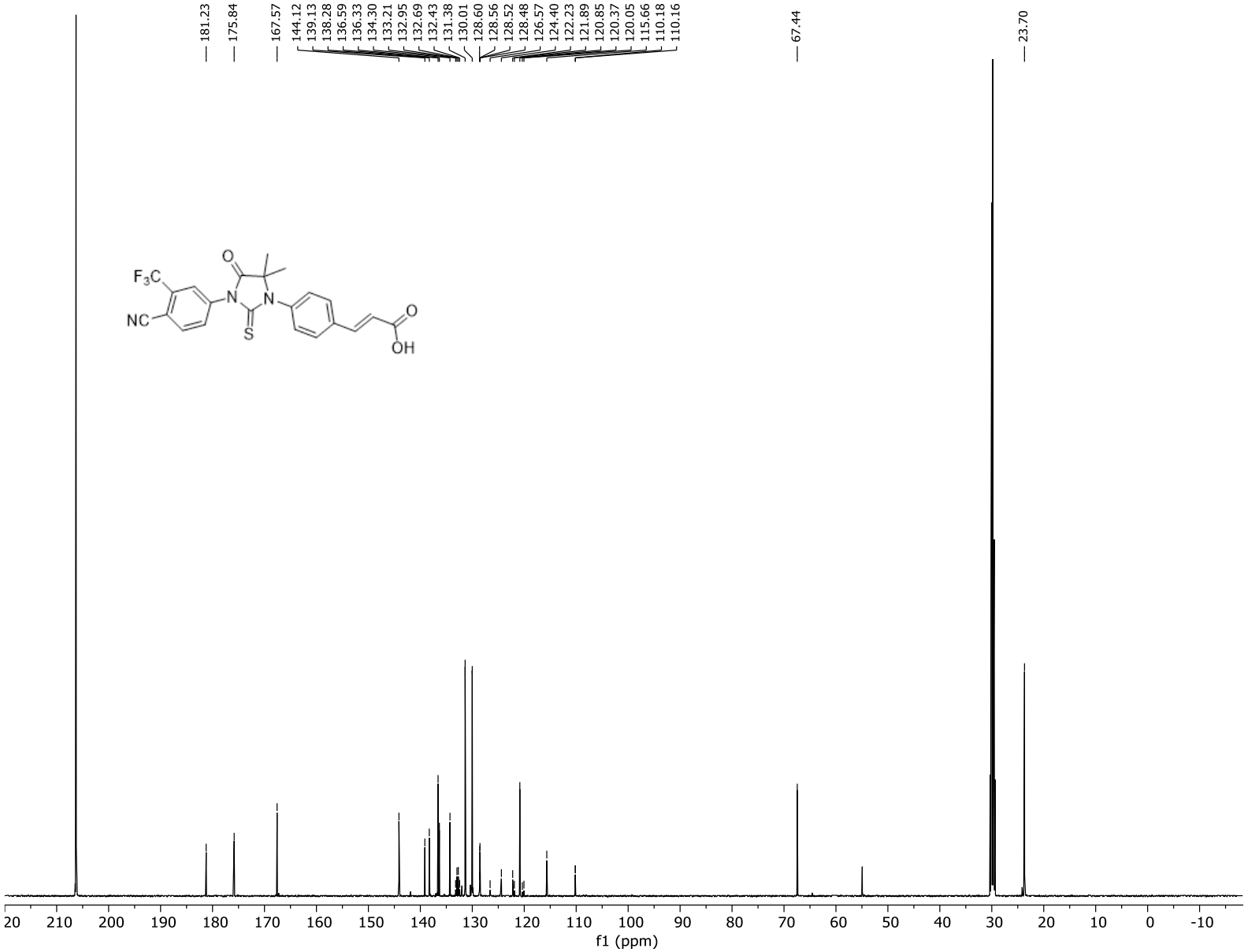
2.20 ^{13}C NMR (126 MHz, $CDCl_3$)



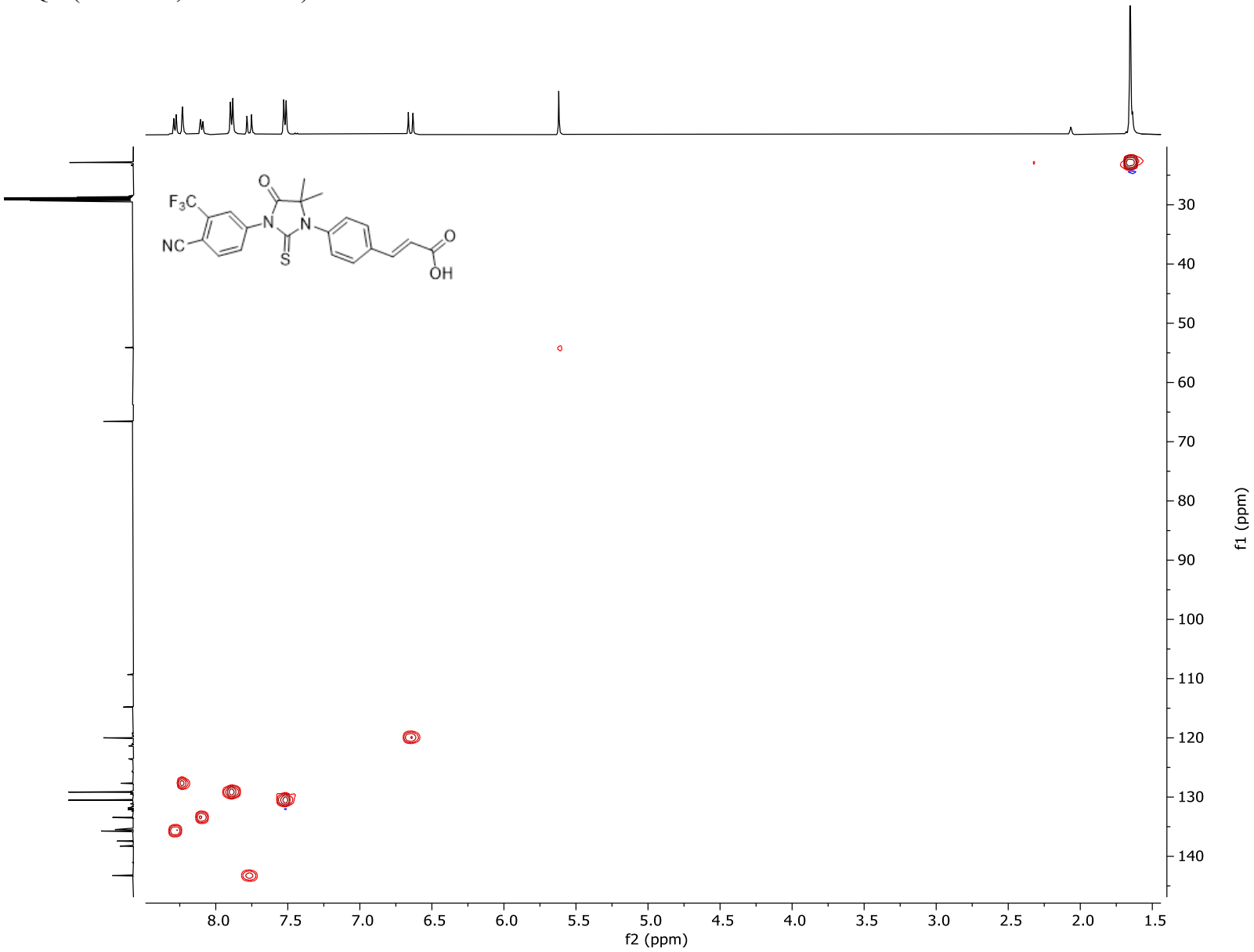
2.21 ^{1}H NMR (500 MHz, Acetone-d_6)



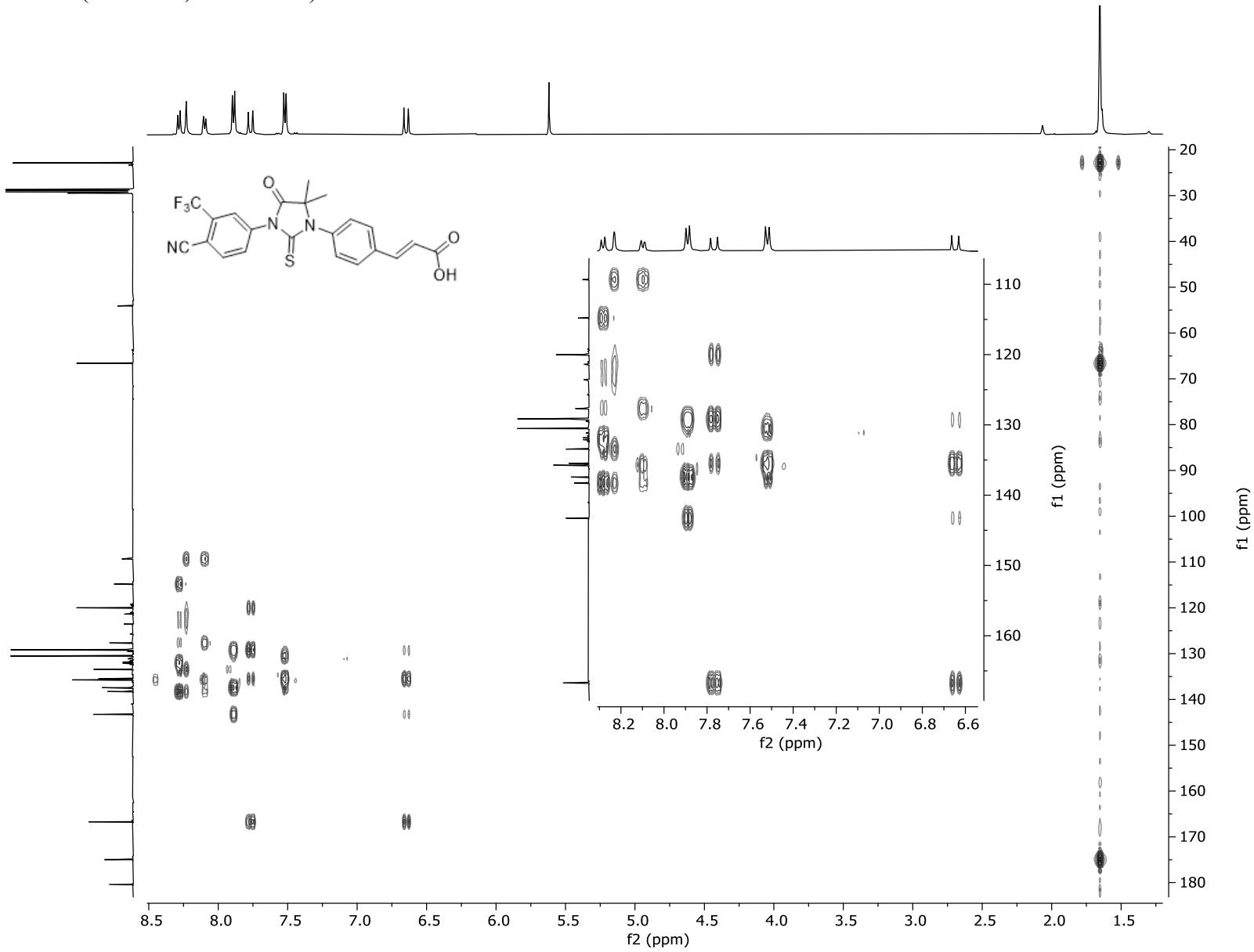
2.21 ^{13}C NMR (126 MHz, Acetone-d_6)



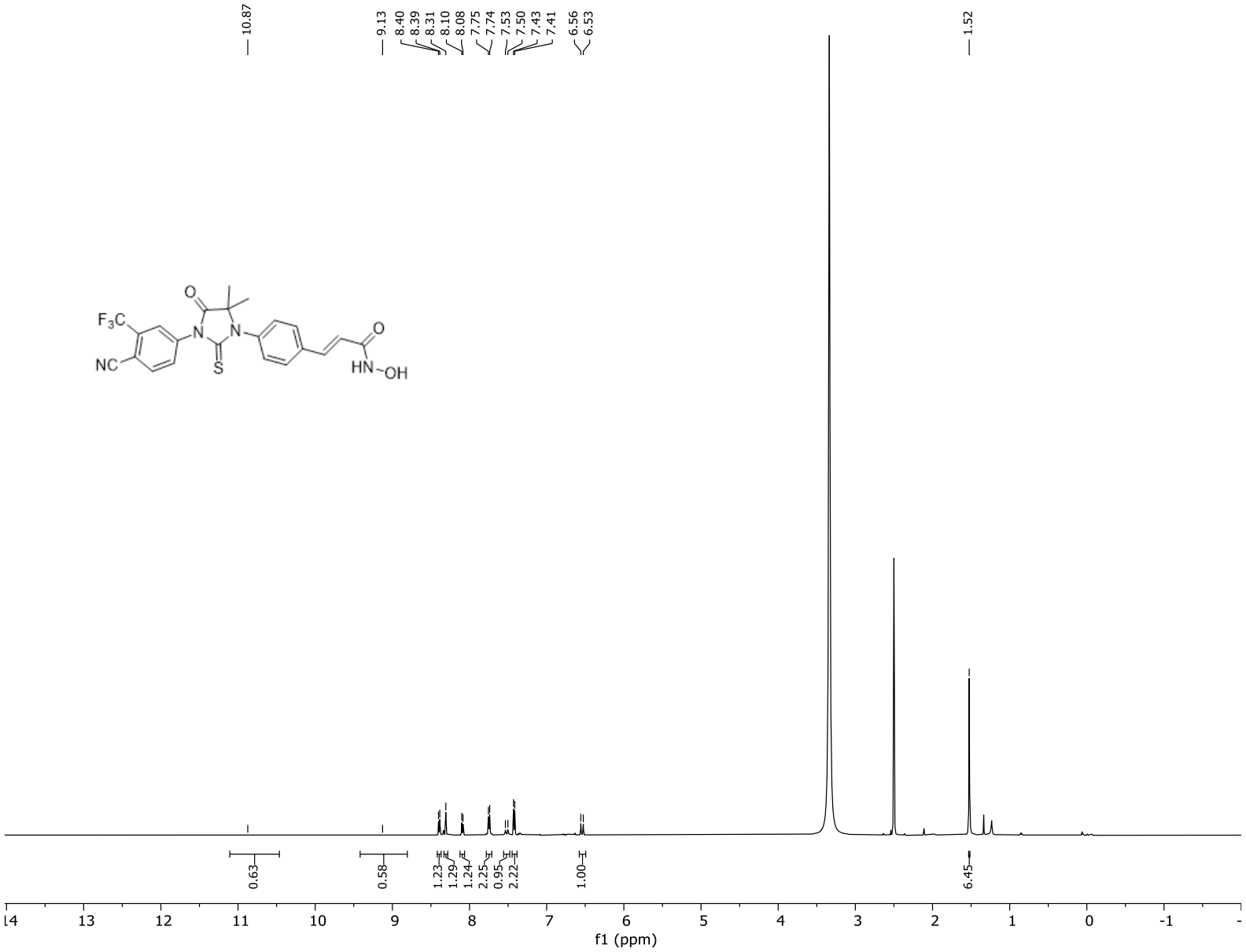
2.21 HSQC (500 MHz, Acetone-d_6)



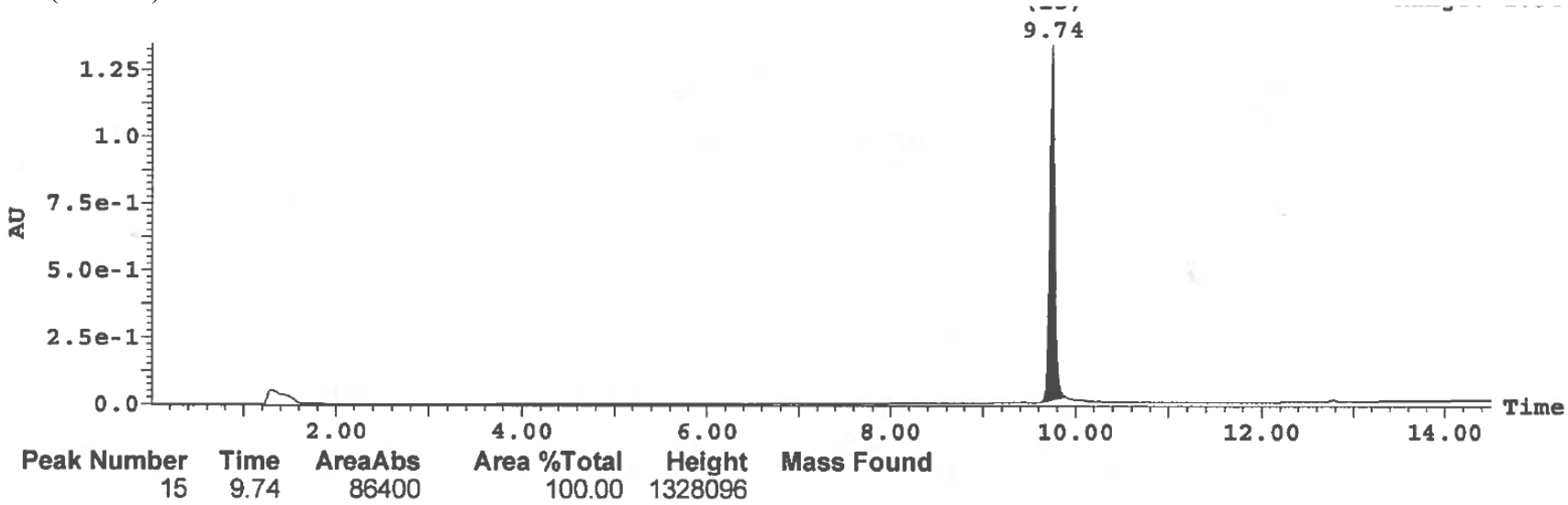
2.21 HMBC (500 MHz, Acetone-d_6)



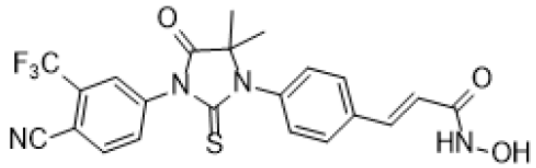
2.5 (RB-331) ^{1}H NMR (500 MHz, DMSO-d_6)



2.5 (RB-331) LC-MS UV trace

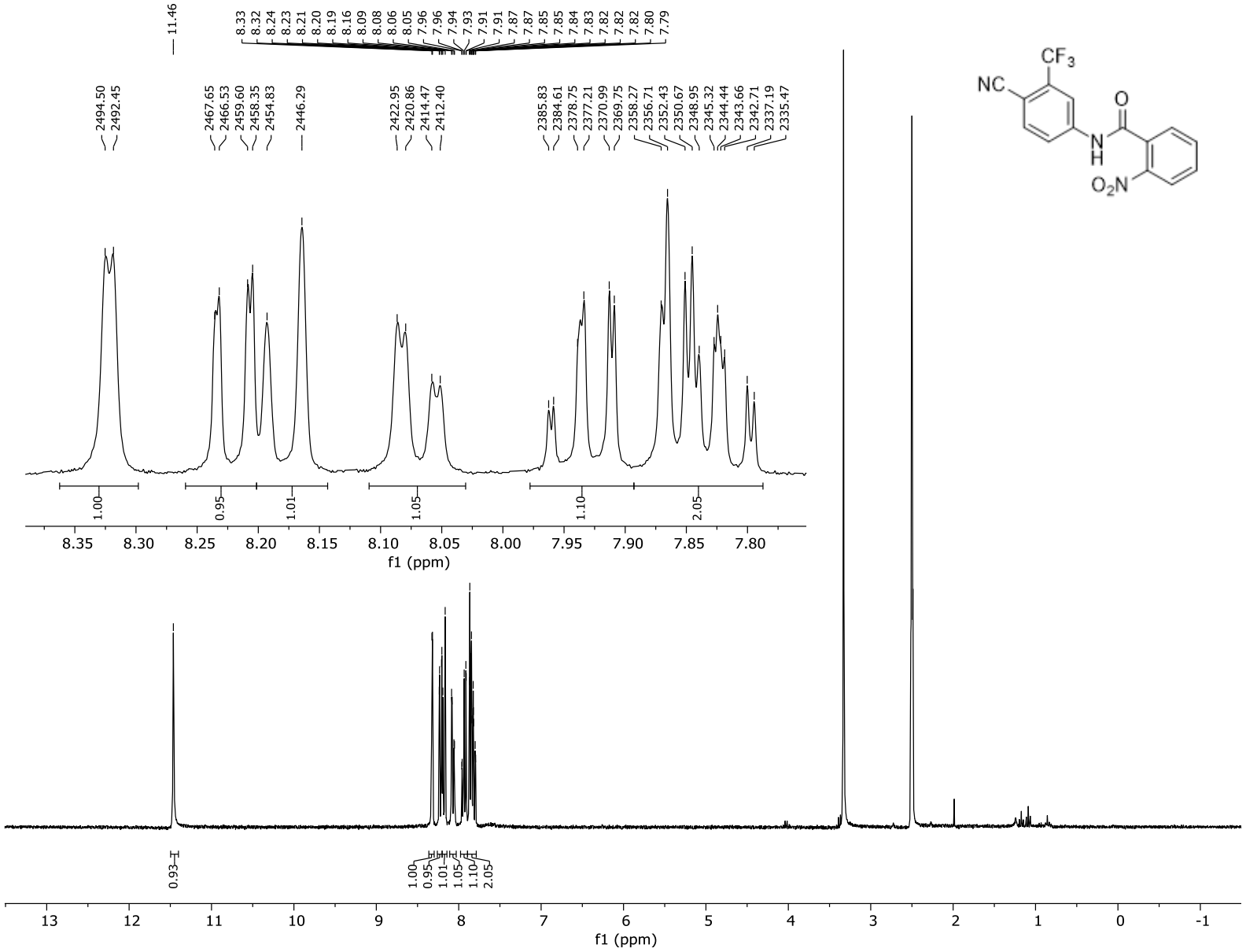


Peak Number	Time	AreaAbs	Area %Total	Height	Mass Found
15	9.74	86400	100.00	1328096	

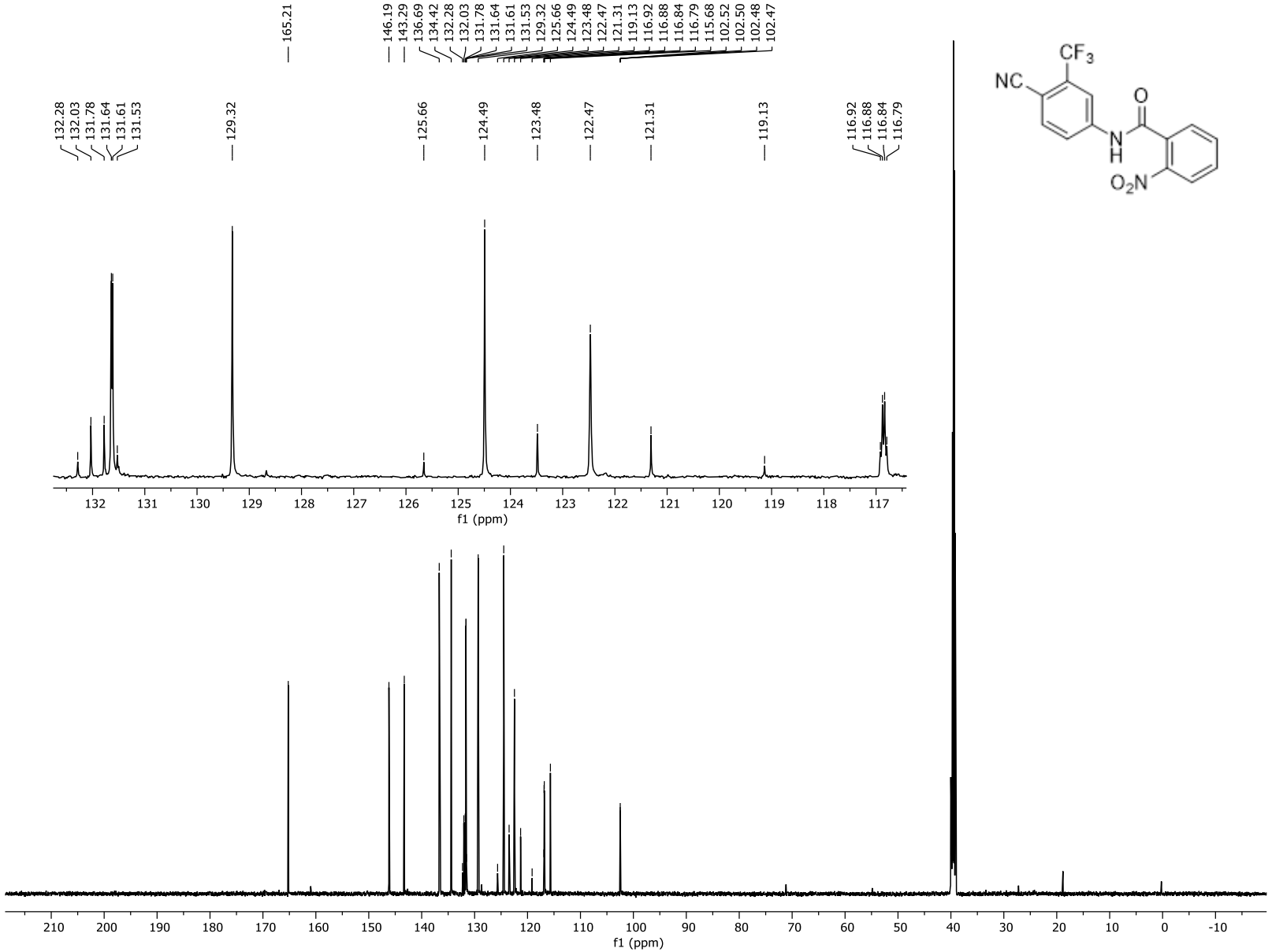


RB-331

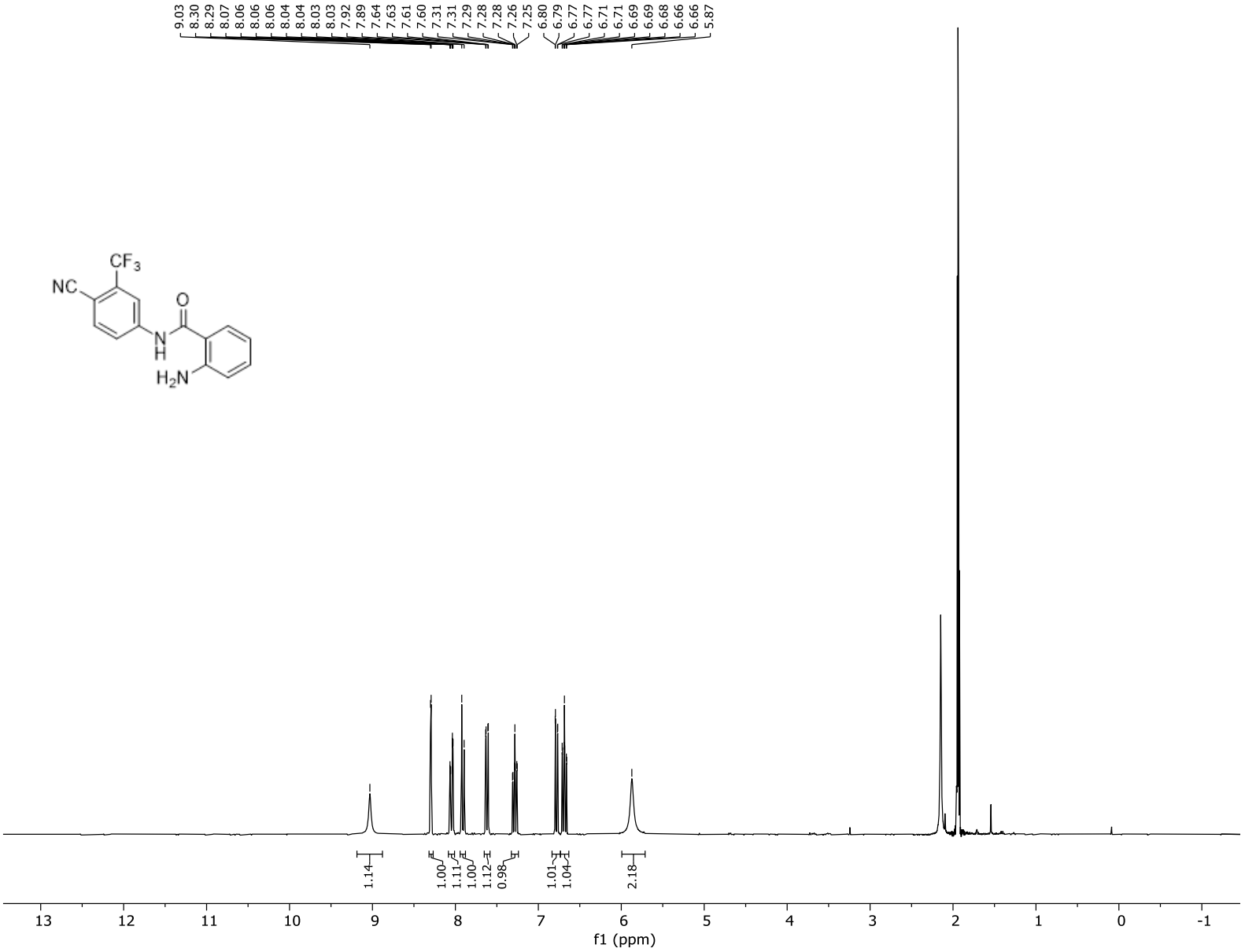
2.28a ^{1}H NMR (300 MHz, DMSO-d_6)



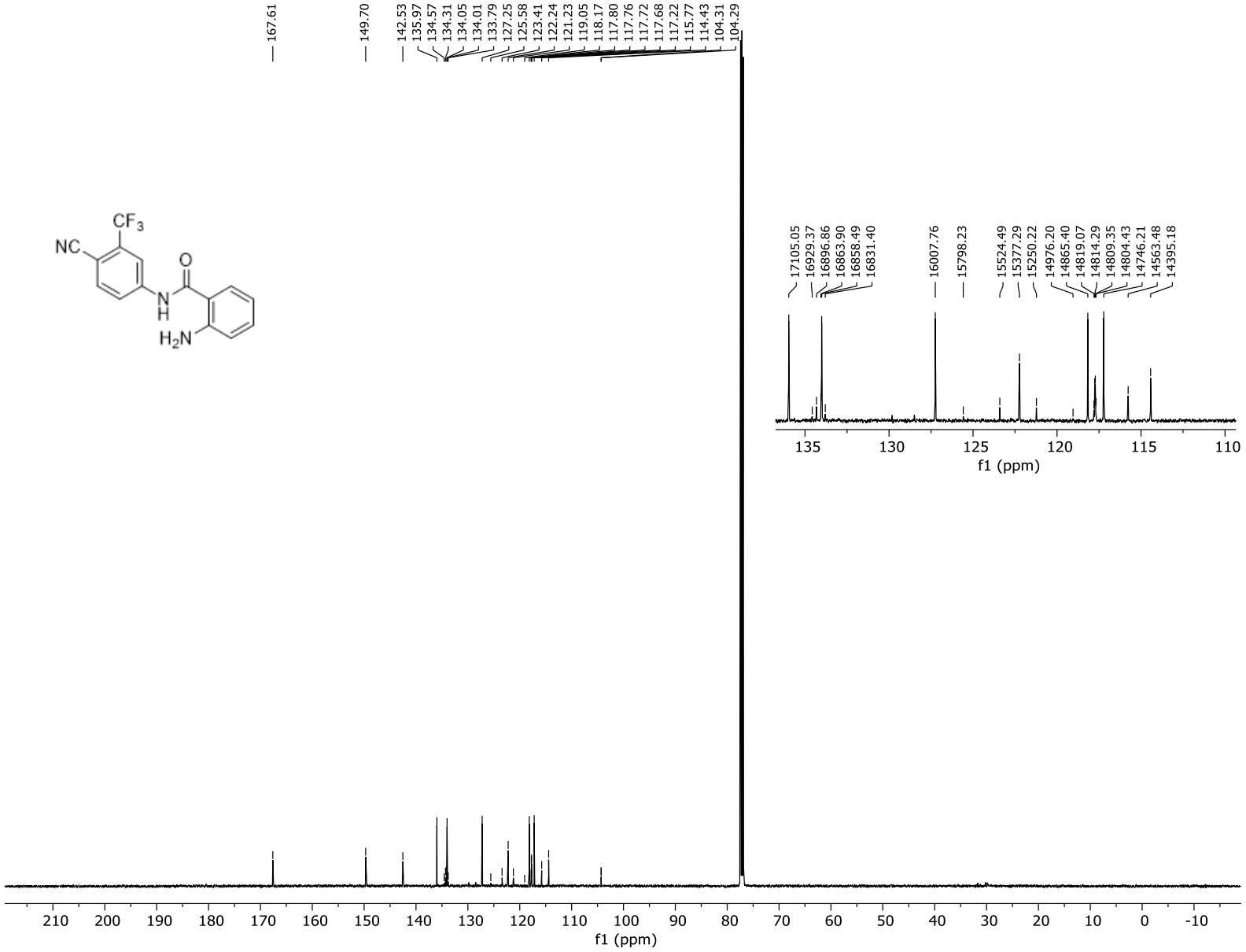
2.28a ^{13}C NMR (126 MHz, DMSO-d_6)



2.7a (RB-15) ^{1}H NMR (300 MHz, CD_3CN)



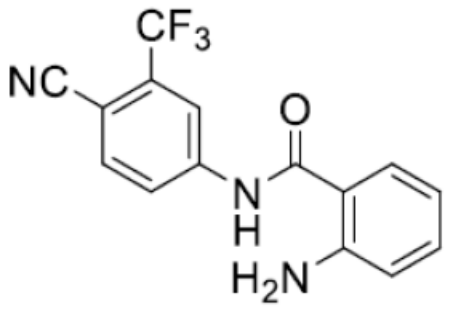
2.7a (RB-15) ^{13}C NMR (126 MHz, $CDCl_3$)



2.7a (RB-15) LC-MS UV trace

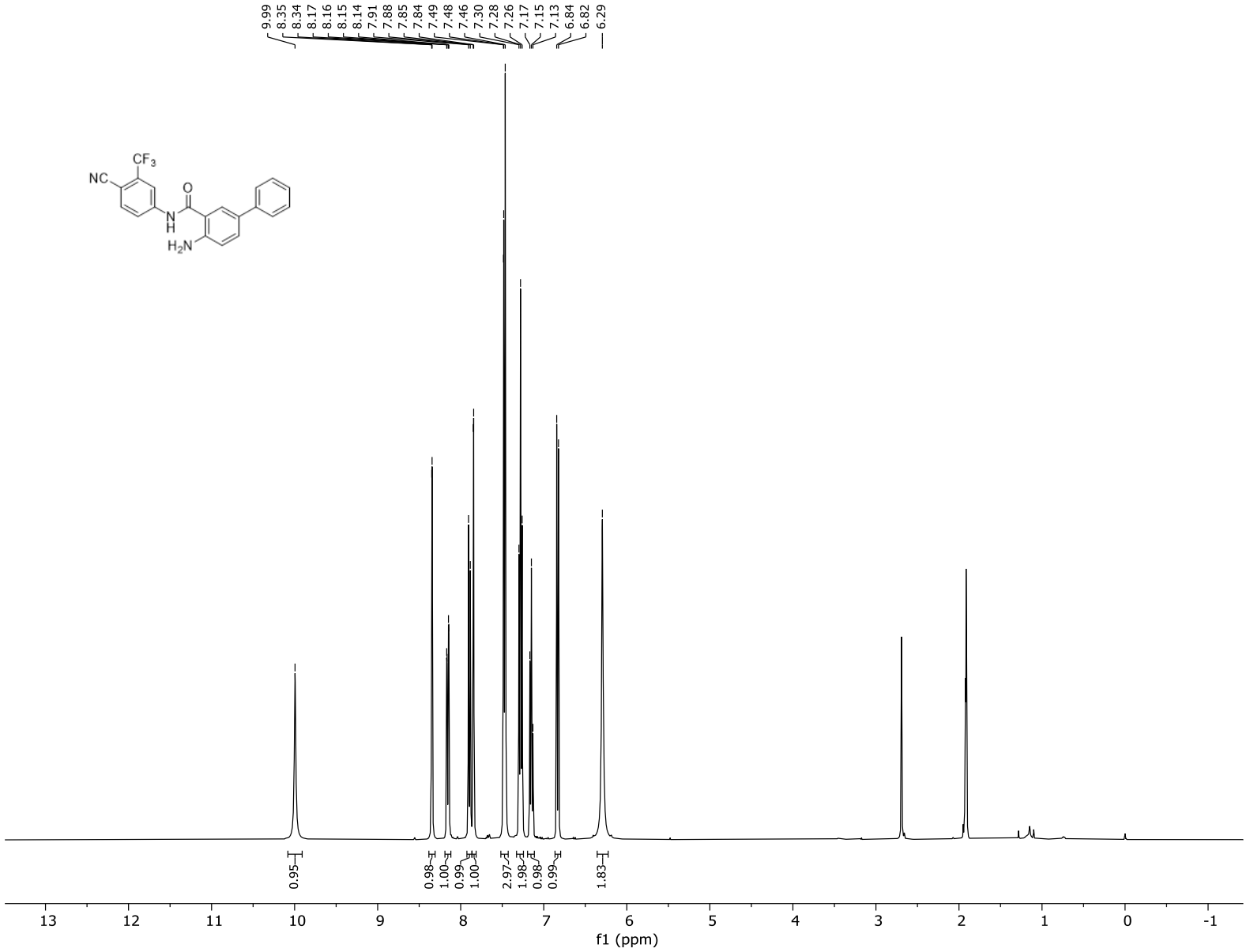


Peak Number	Time	AreaAbs	Area %Total	Height	Mass Found
3	10.39	2412	4.44	35598	
4	10.96	51870	95.56	748728	

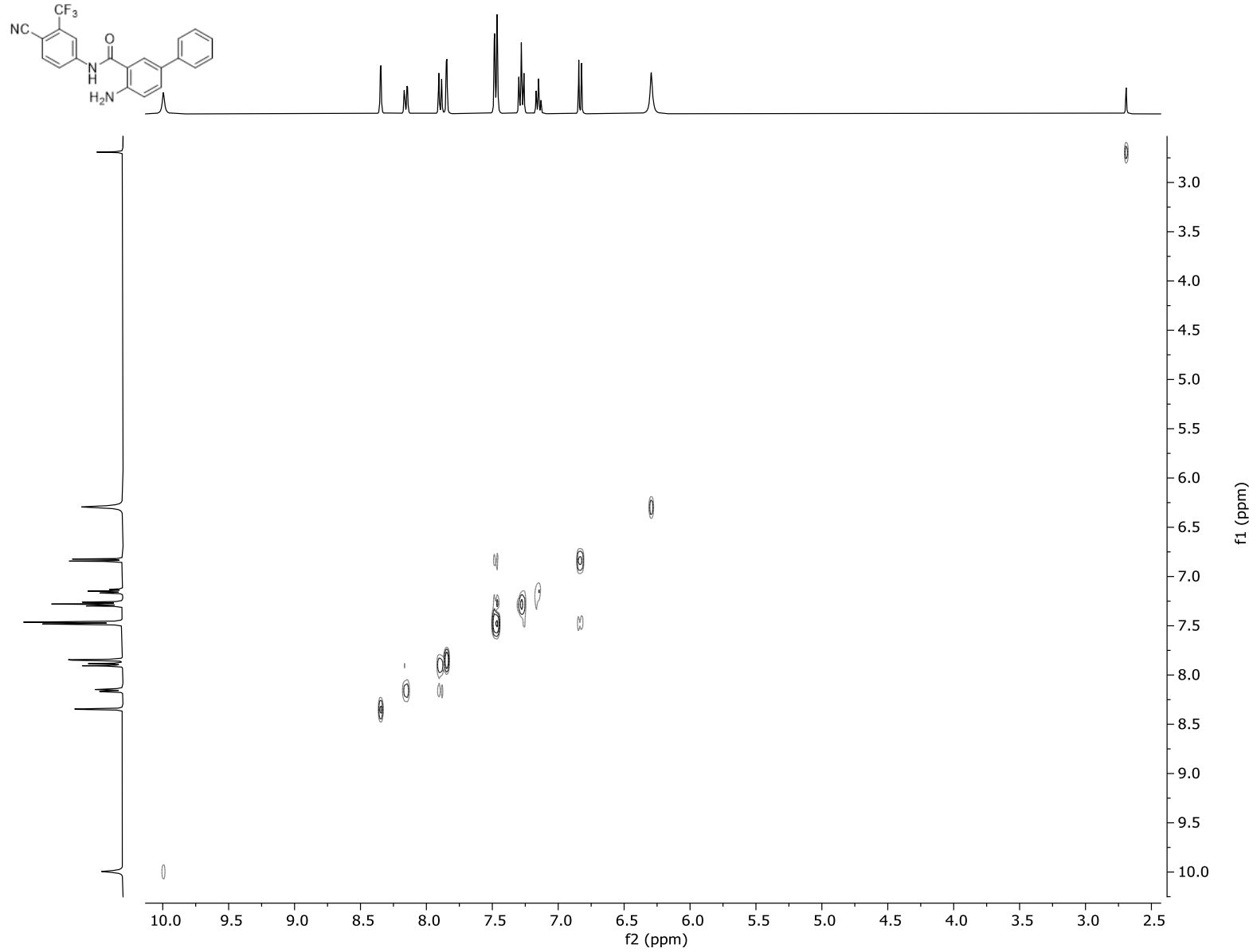


RB-15

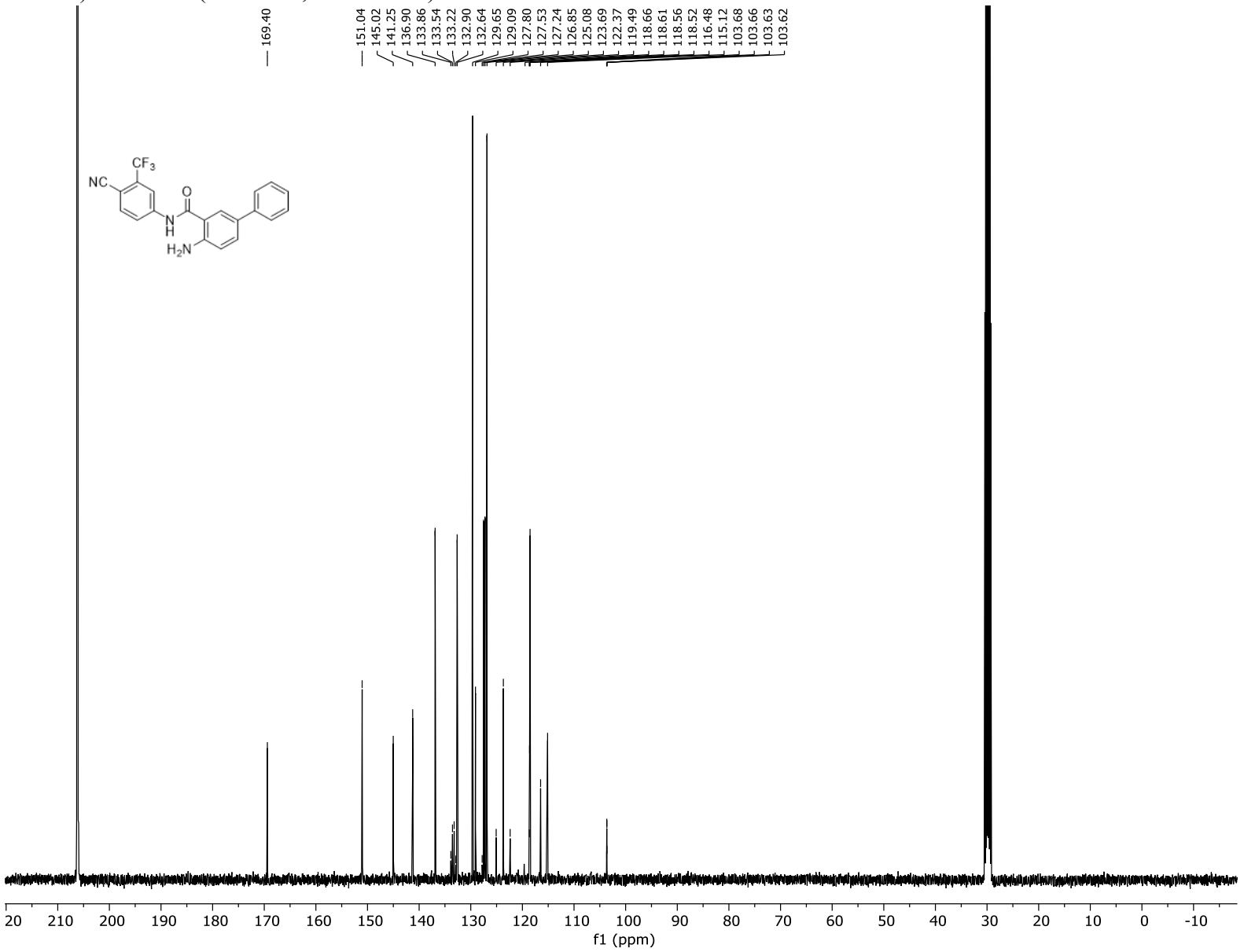
2.7b (RB-265) ^{1}H NMR (400 MHz, Acetone-d_6)



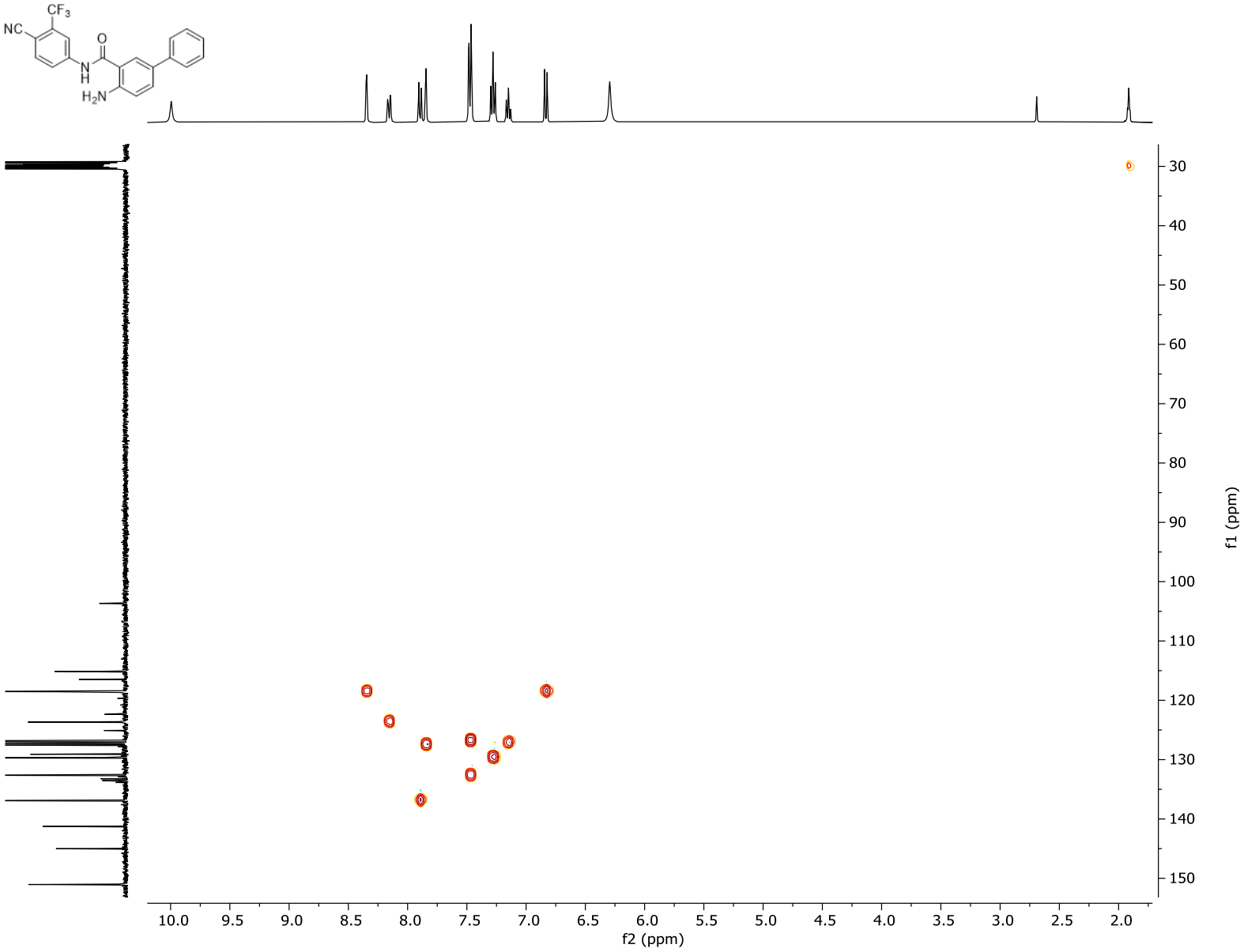
2.7b (RB-265) COSY (400 MHz, Acetone-d_6)



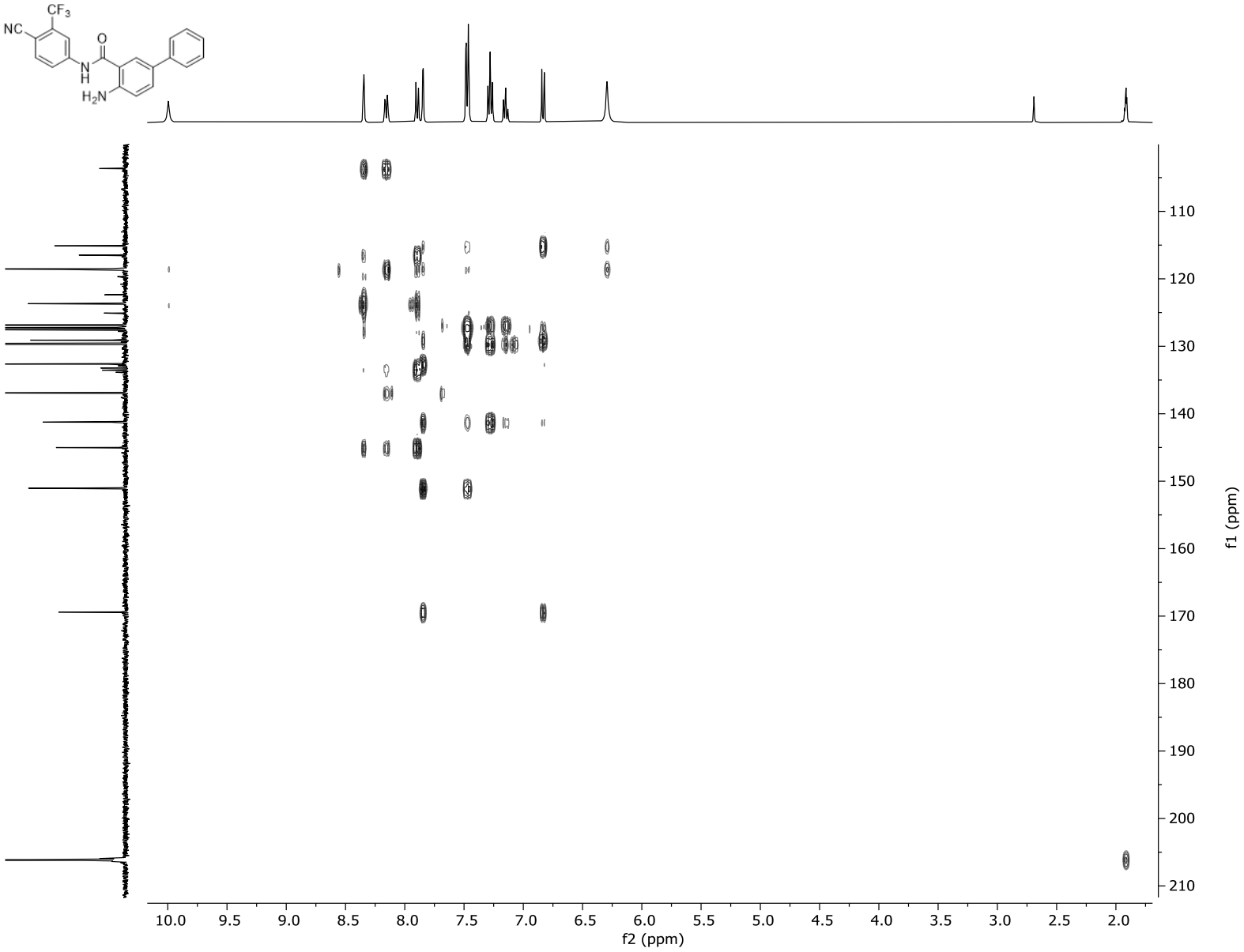
2.7b (RB-265) ^{13}C NMR (101 MHz, Acetone-d_6)



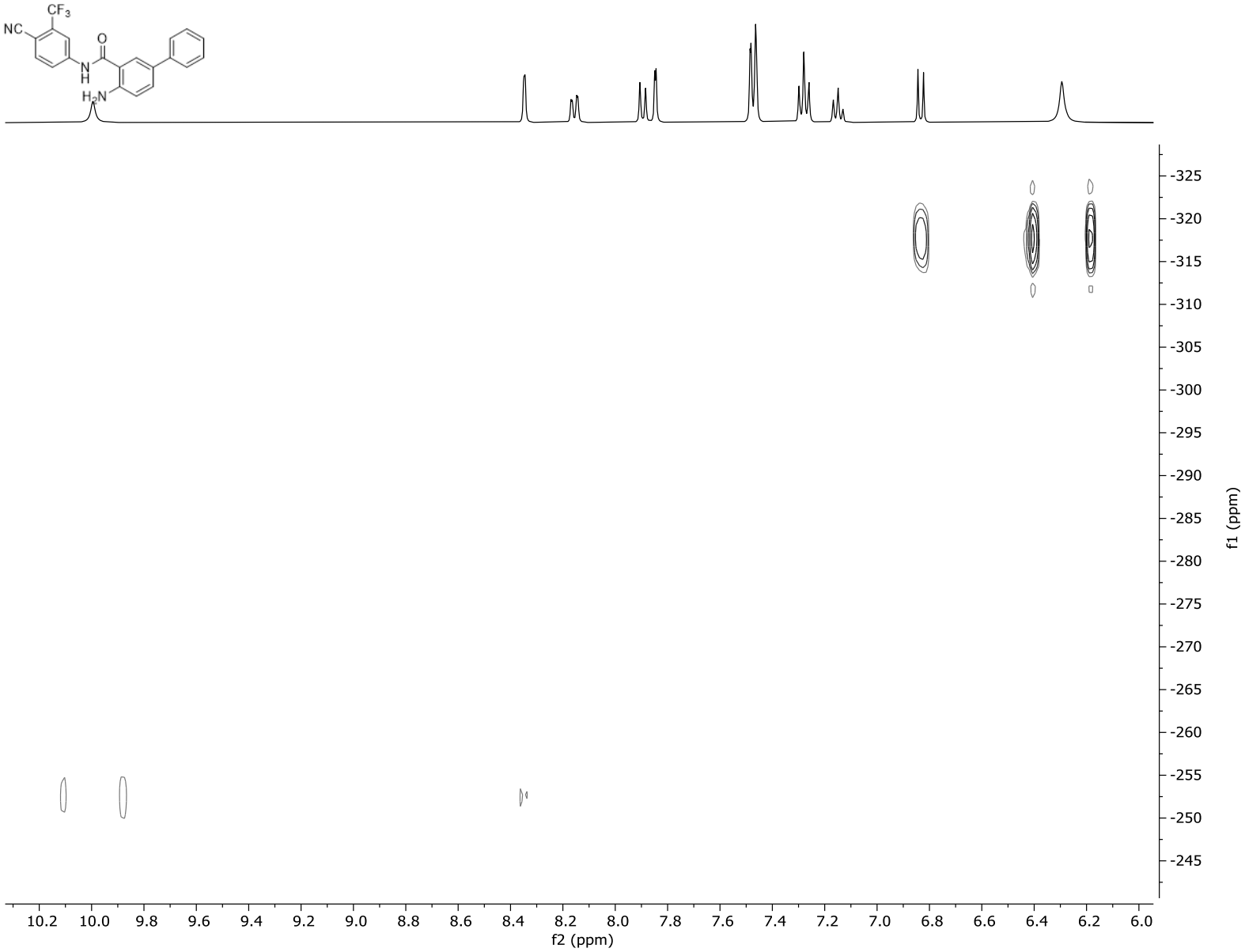
2.7b (RB-265) HSQC (400 MHz, Acetone-d_6)



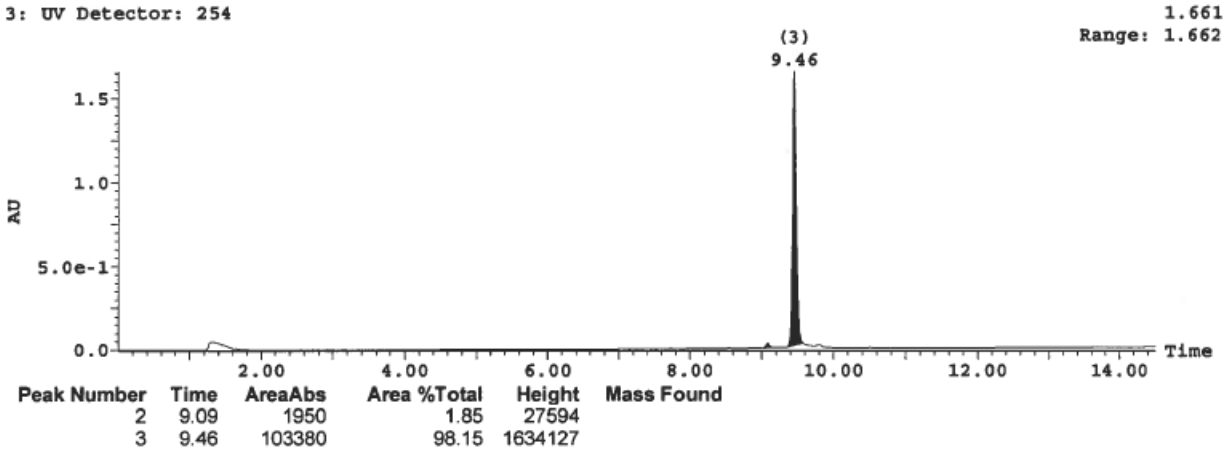
2.7b (RB-265) HMBC (400 MHz, Acetone-d_6)



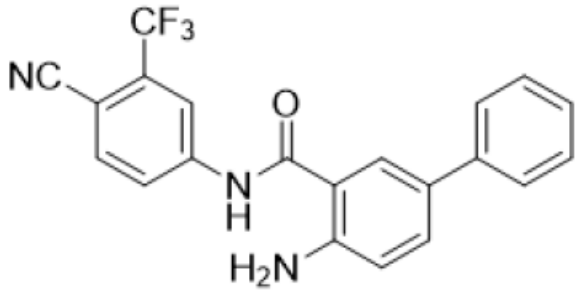
2.7b (RB-265) ^{1}H-^{15}N HMBC (400 MHz, Acetone-d_6)



2.7b (RB-265) LC-MS UV trace

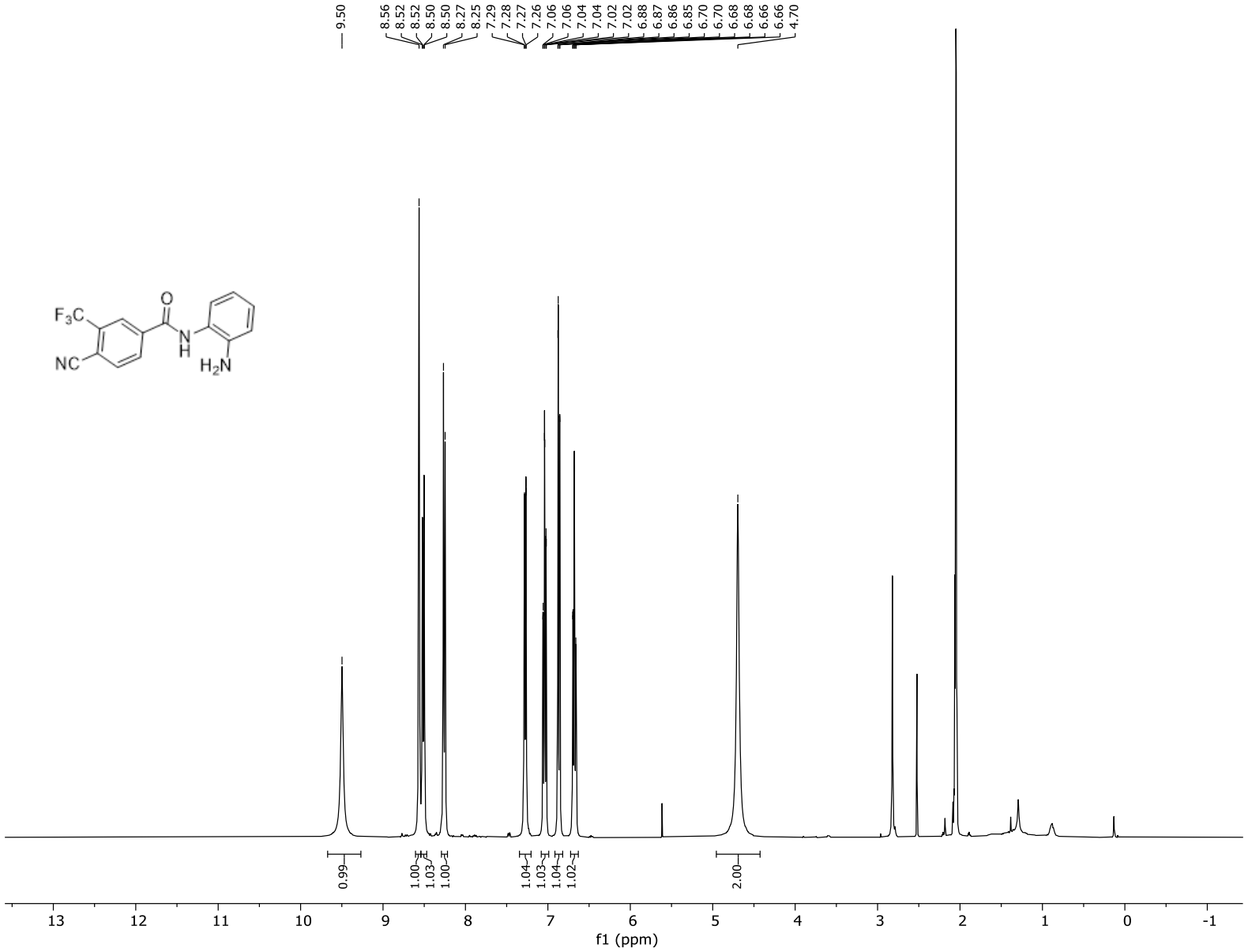


Peak Number	Time	AreaAbs	Area %Total	Height	Mass Found
2	9.09	1950	1.85	27594	
3	9.46	103380	98.15	1634127	

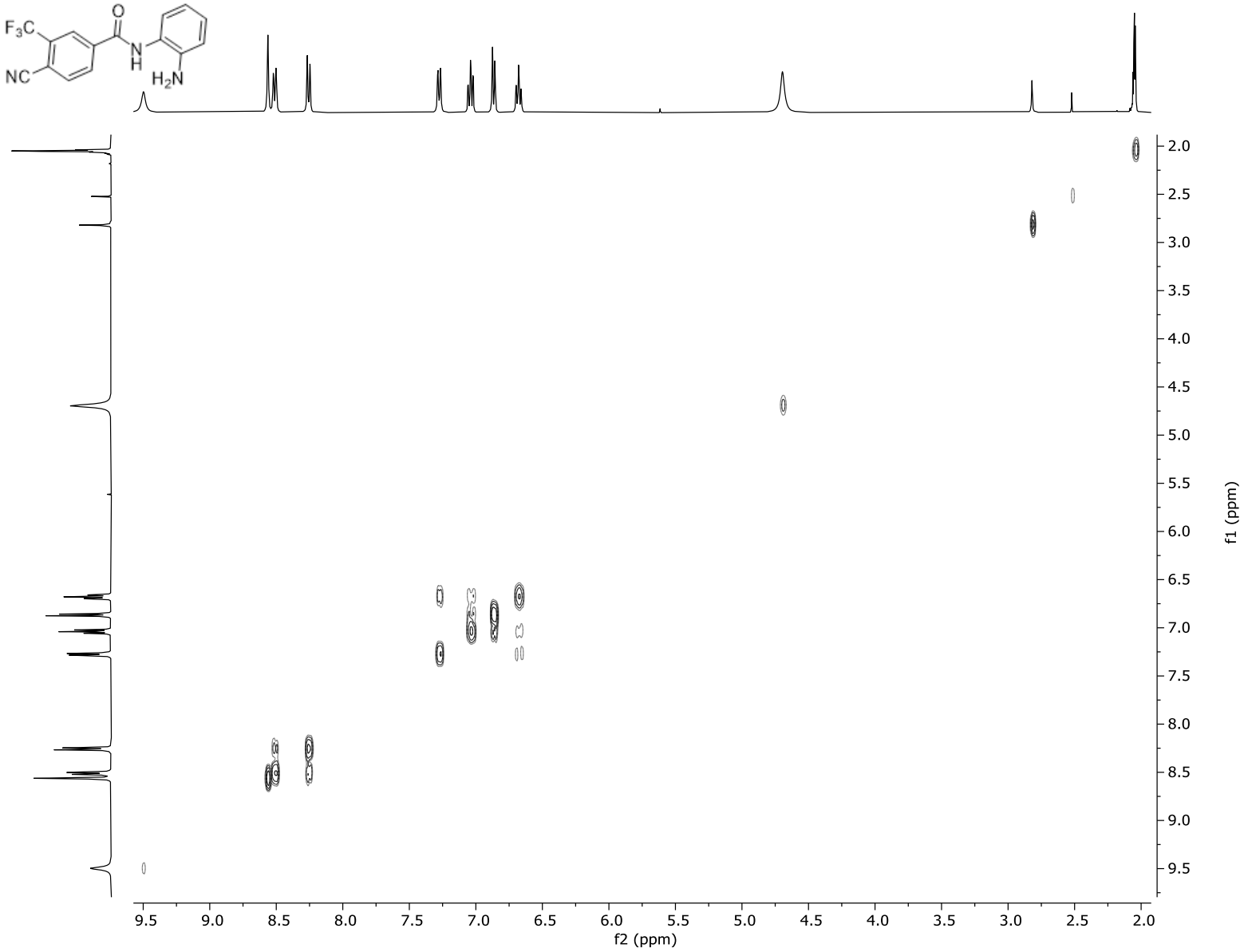


RB-265

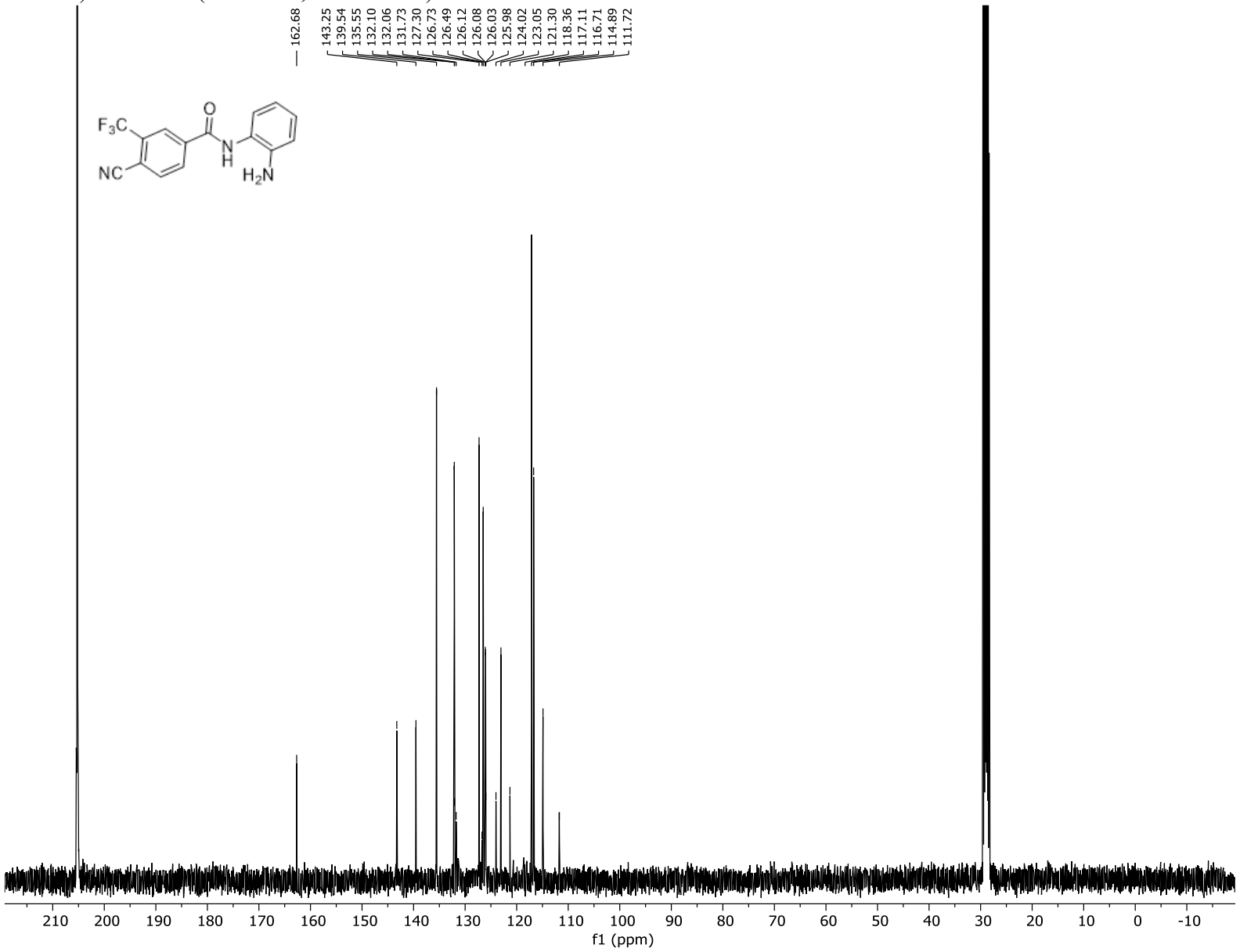
2.8a (RB-136) ^{1}H NMR (400 MHz, Acetone-d_6)



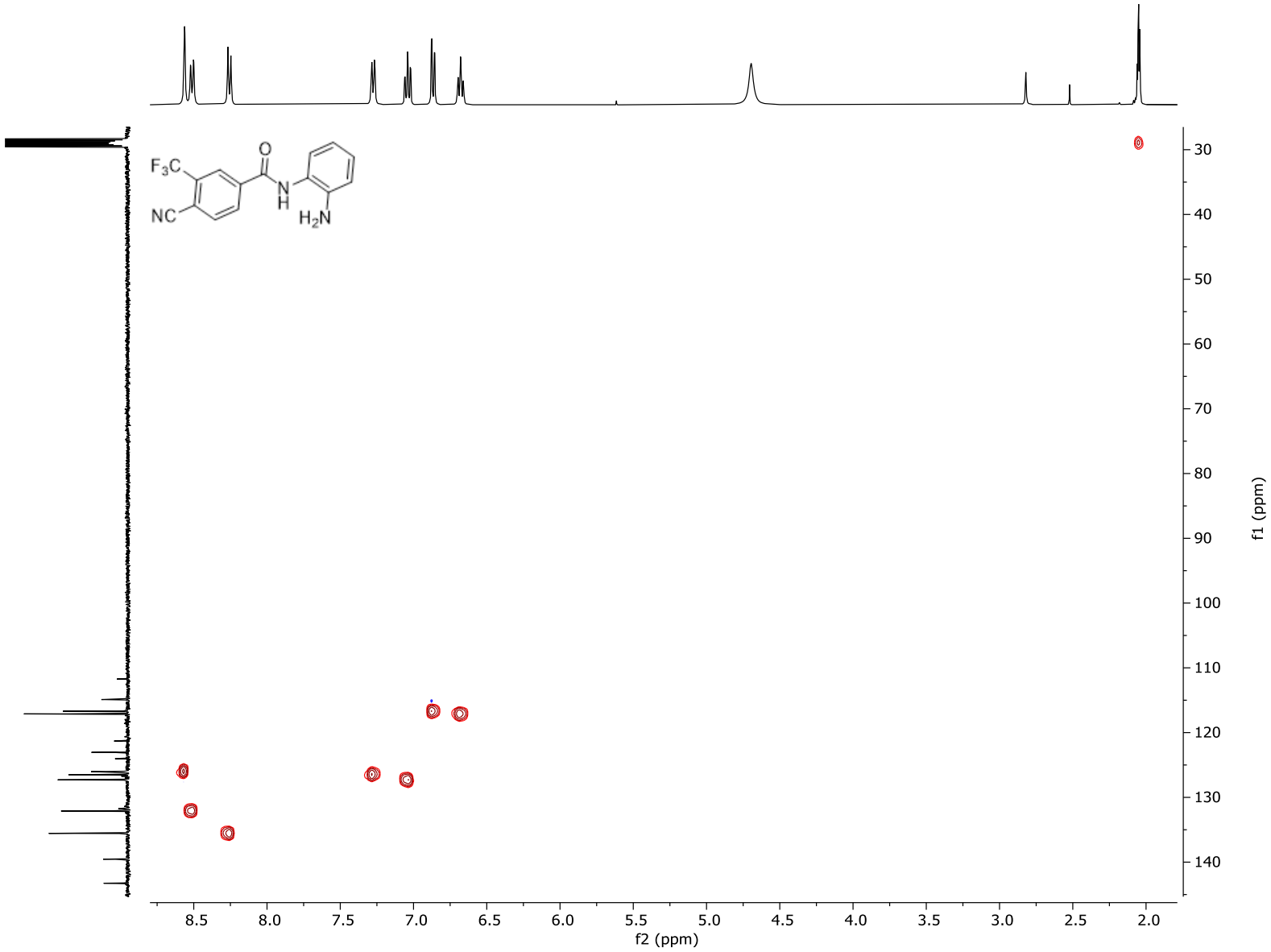
2.8a (RB-136) COSY (400 MHz, Acetone-d_6)



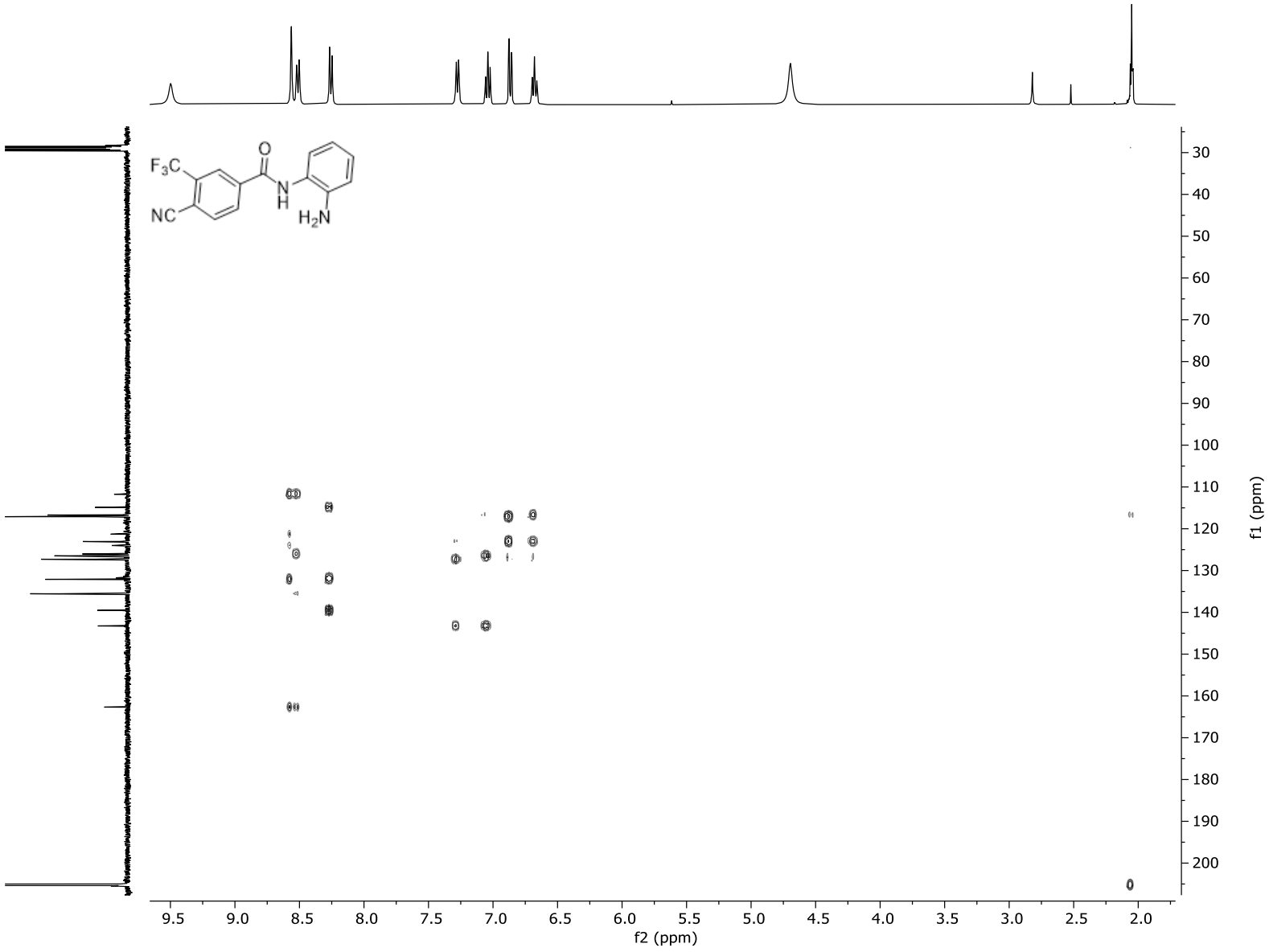
2.8a (RB-136) ^{13}C NMR (101 MHz, Acetone-d_6)



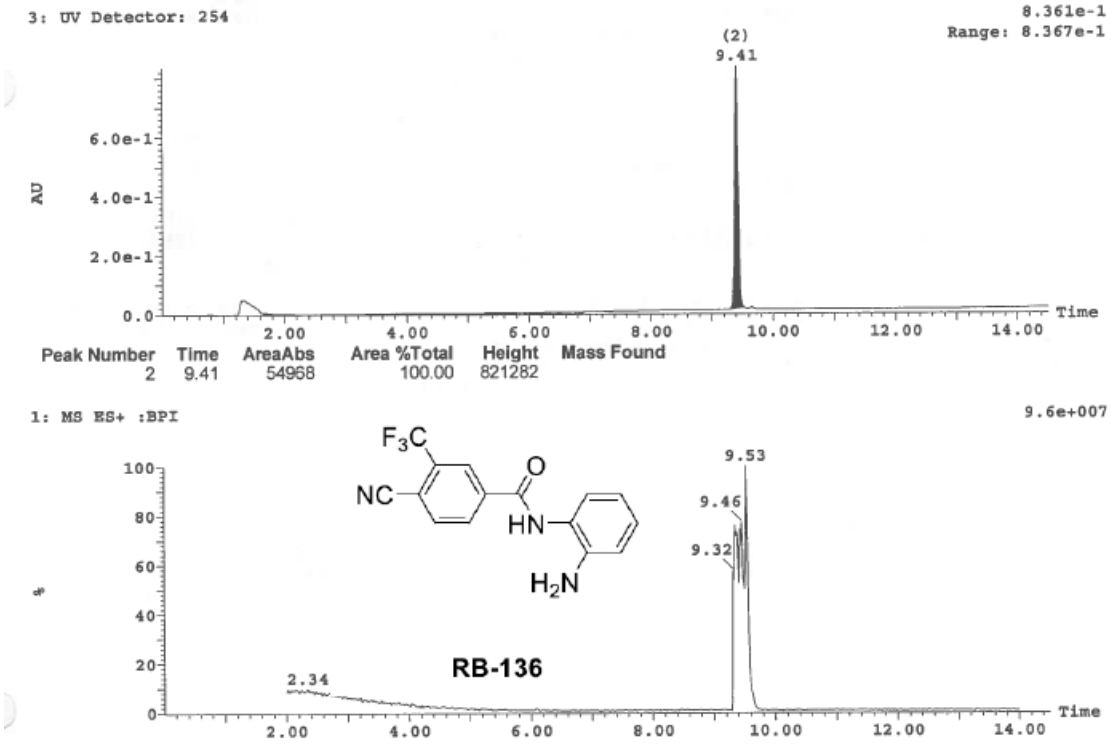
2.8a (RB-136) HSQC (400 MHz, Acetone-d_6)



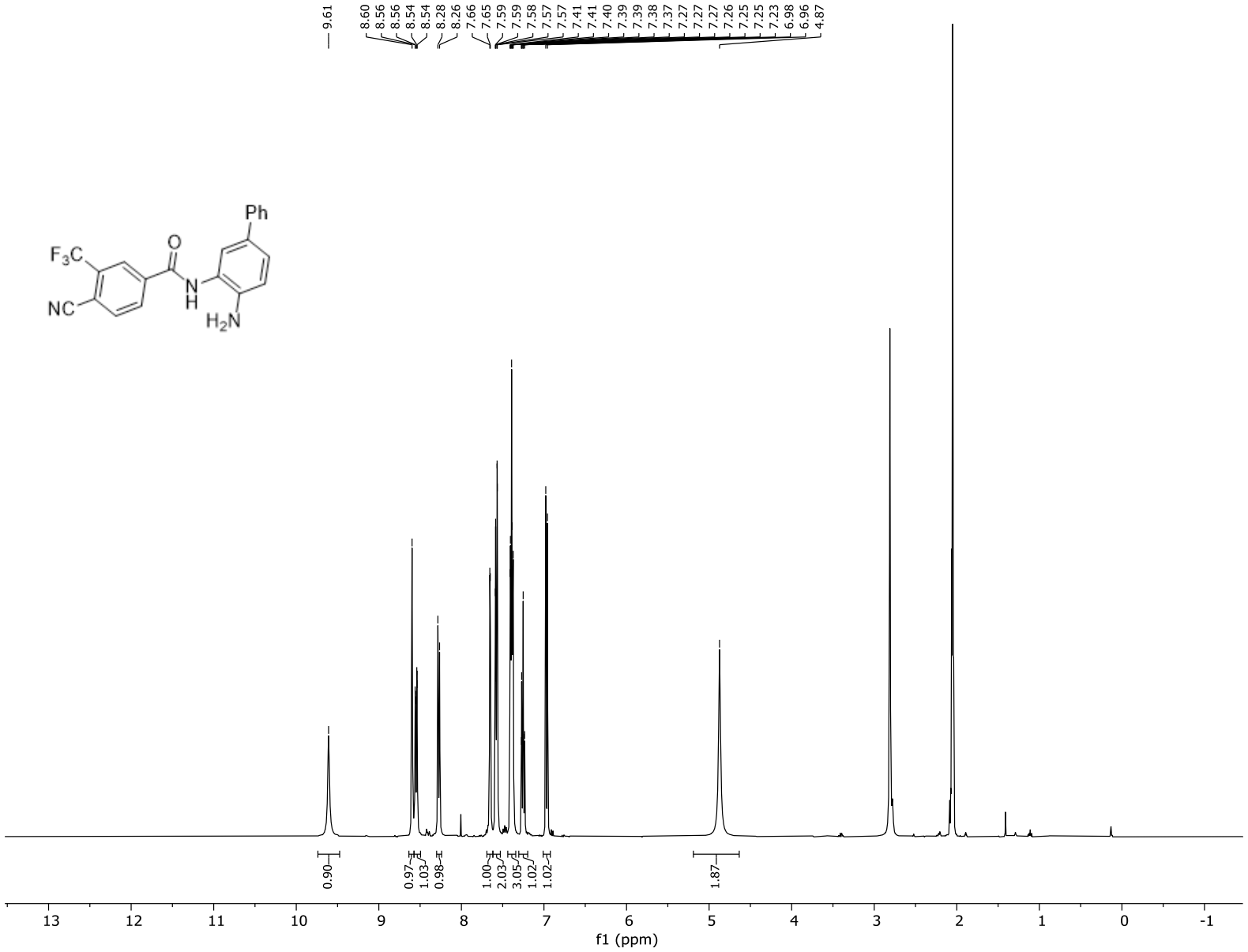
2.8a (RB-136) HSQC (400 MHz, Acetone-d_6)



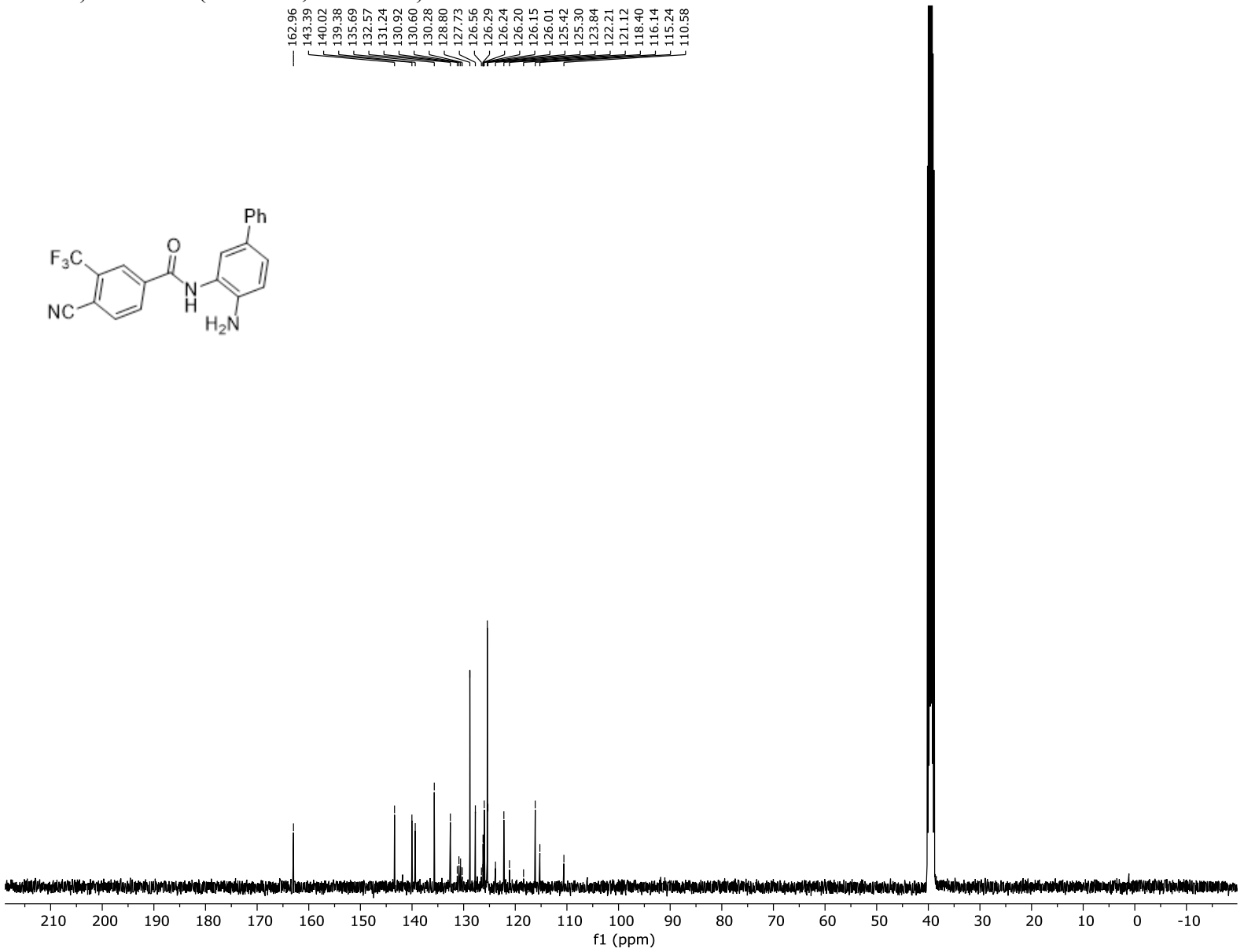
2.8a (RB-136) LC-MS UV trace



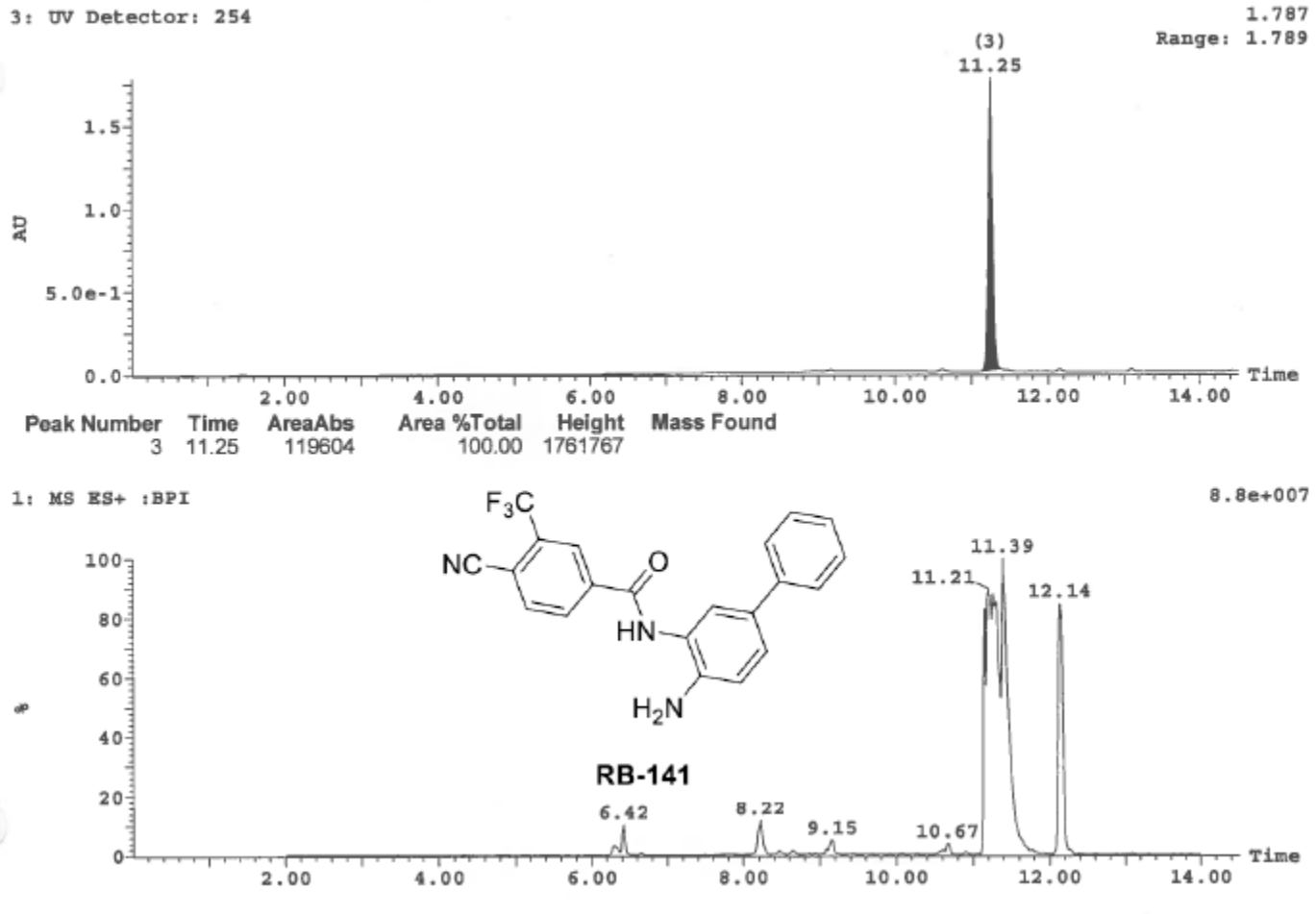
2.8b (RB-141) ^{1}H NMR (400 MHz, Acetone-d_6)



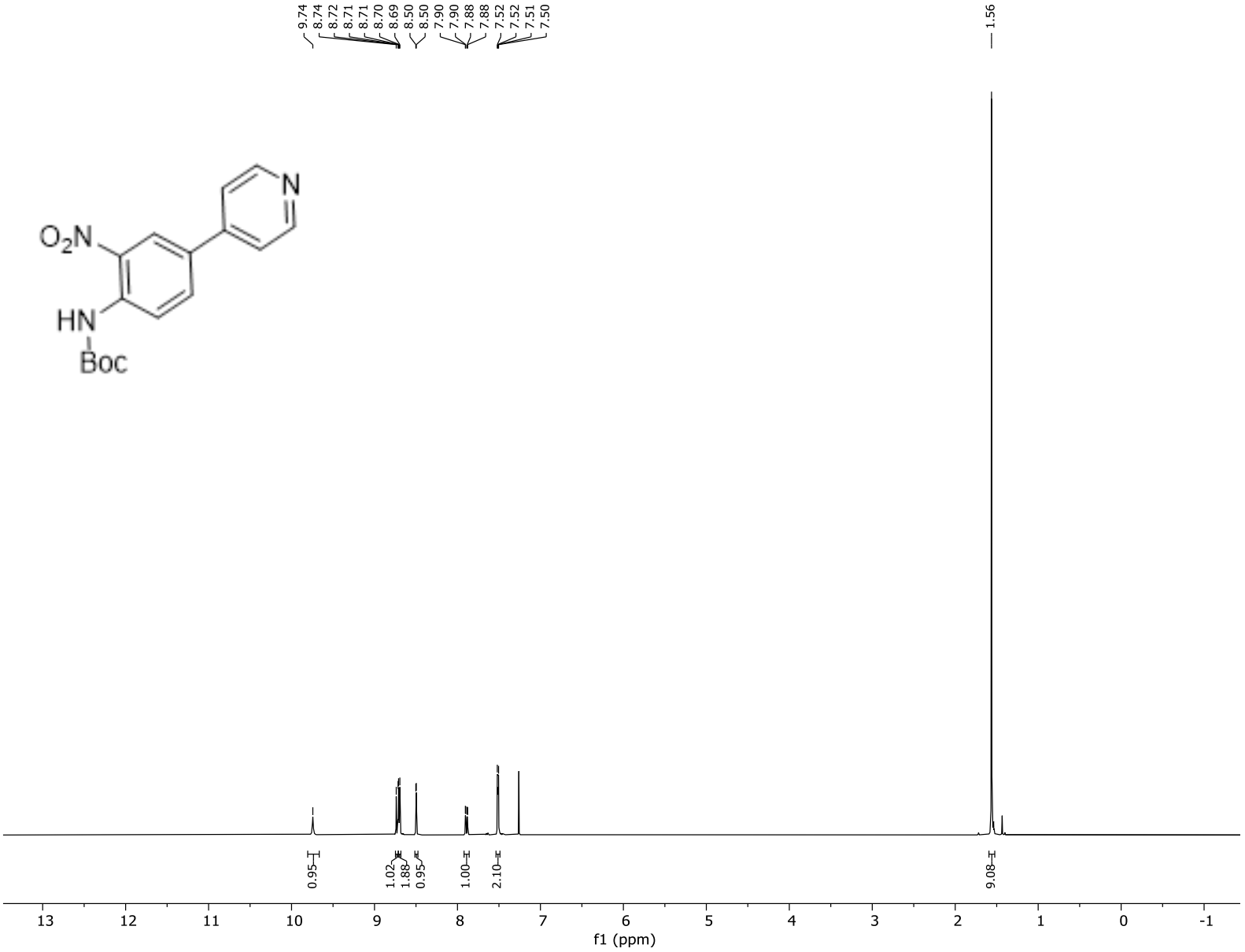
2.8b (RB-141) ^{13}C NMR (101 MHz, DMSO-d_6)



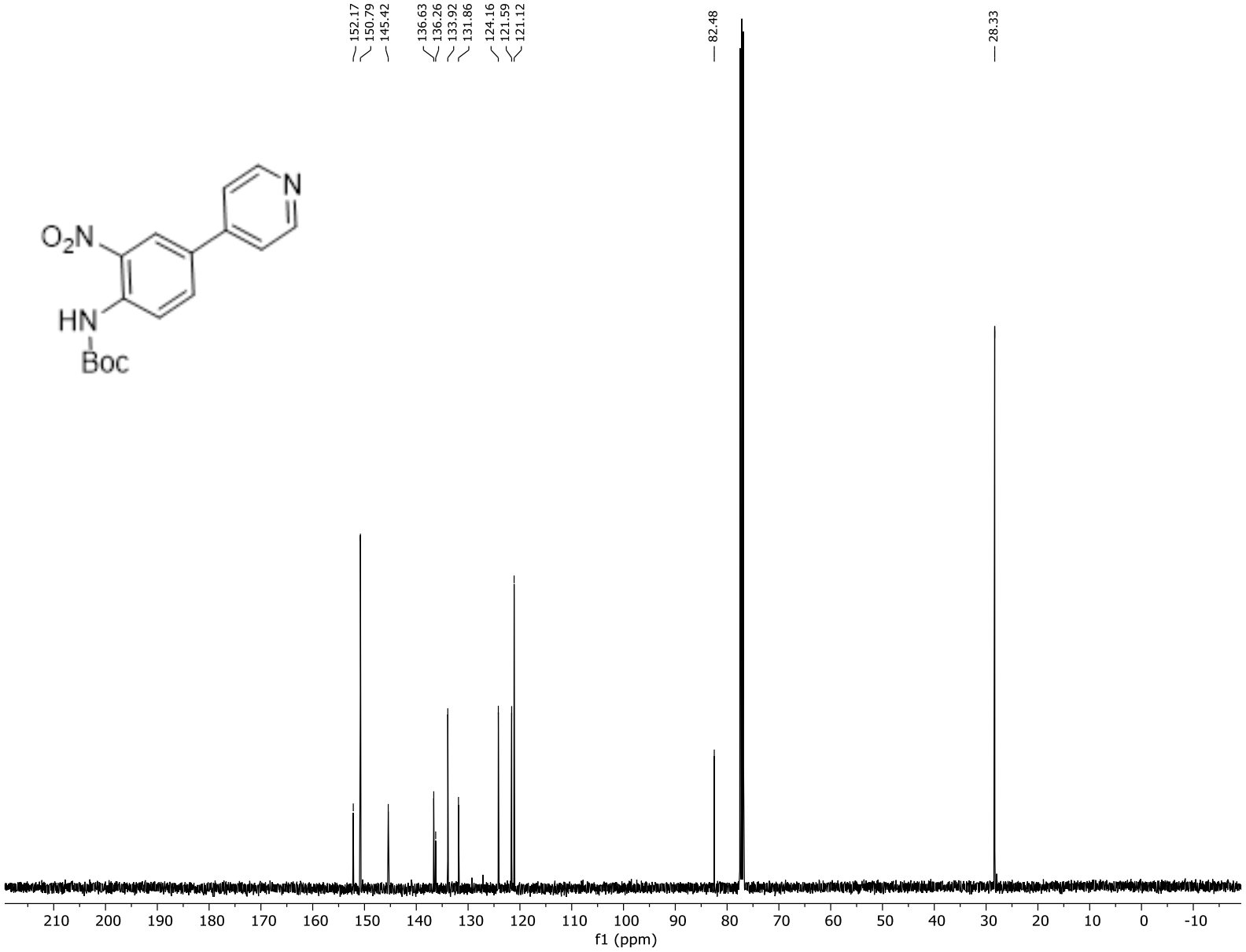
2.8b (RB-141) LC-MS UV trace



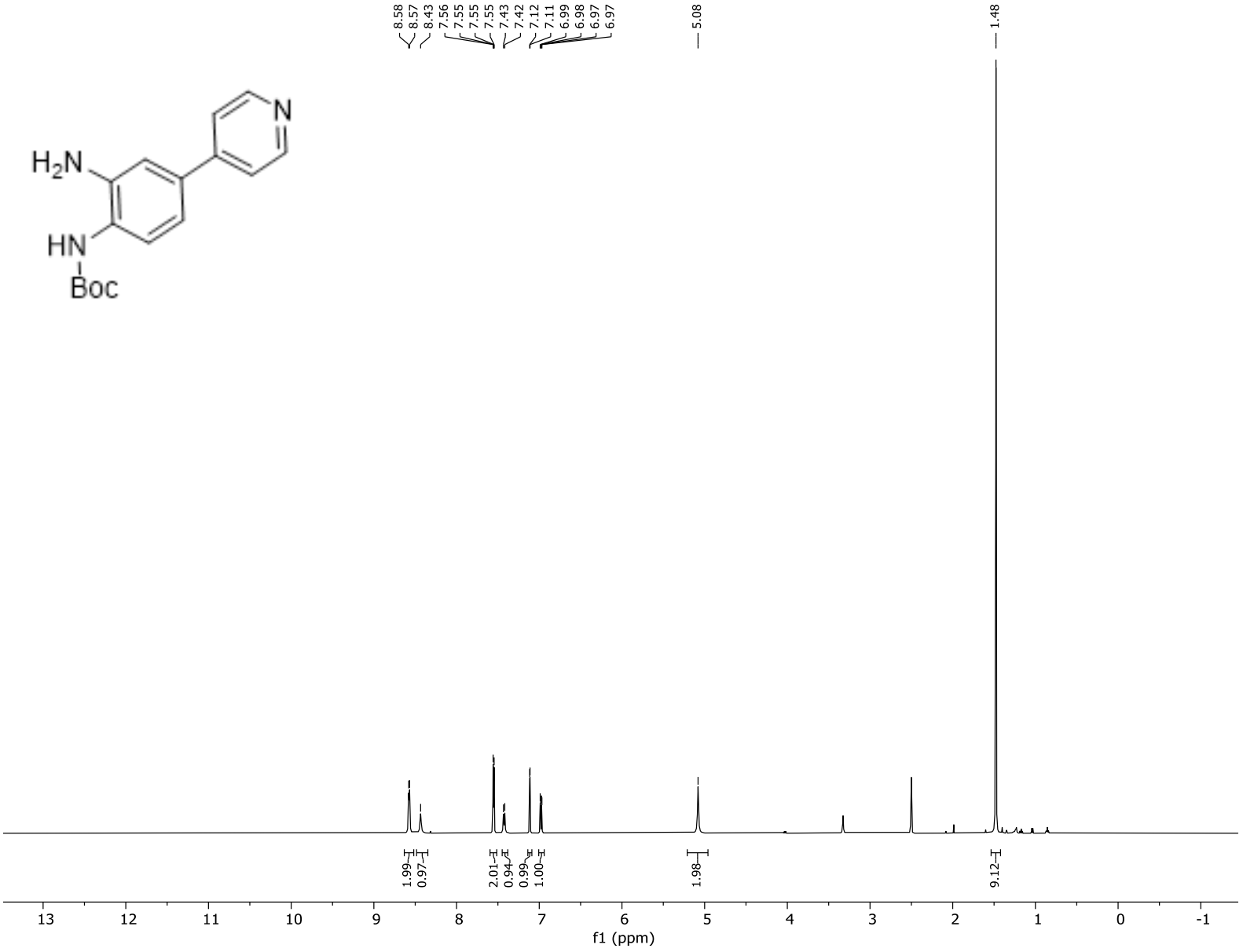
5.2 ^{1}H NMR (400 MHz, DMSO-d_6)



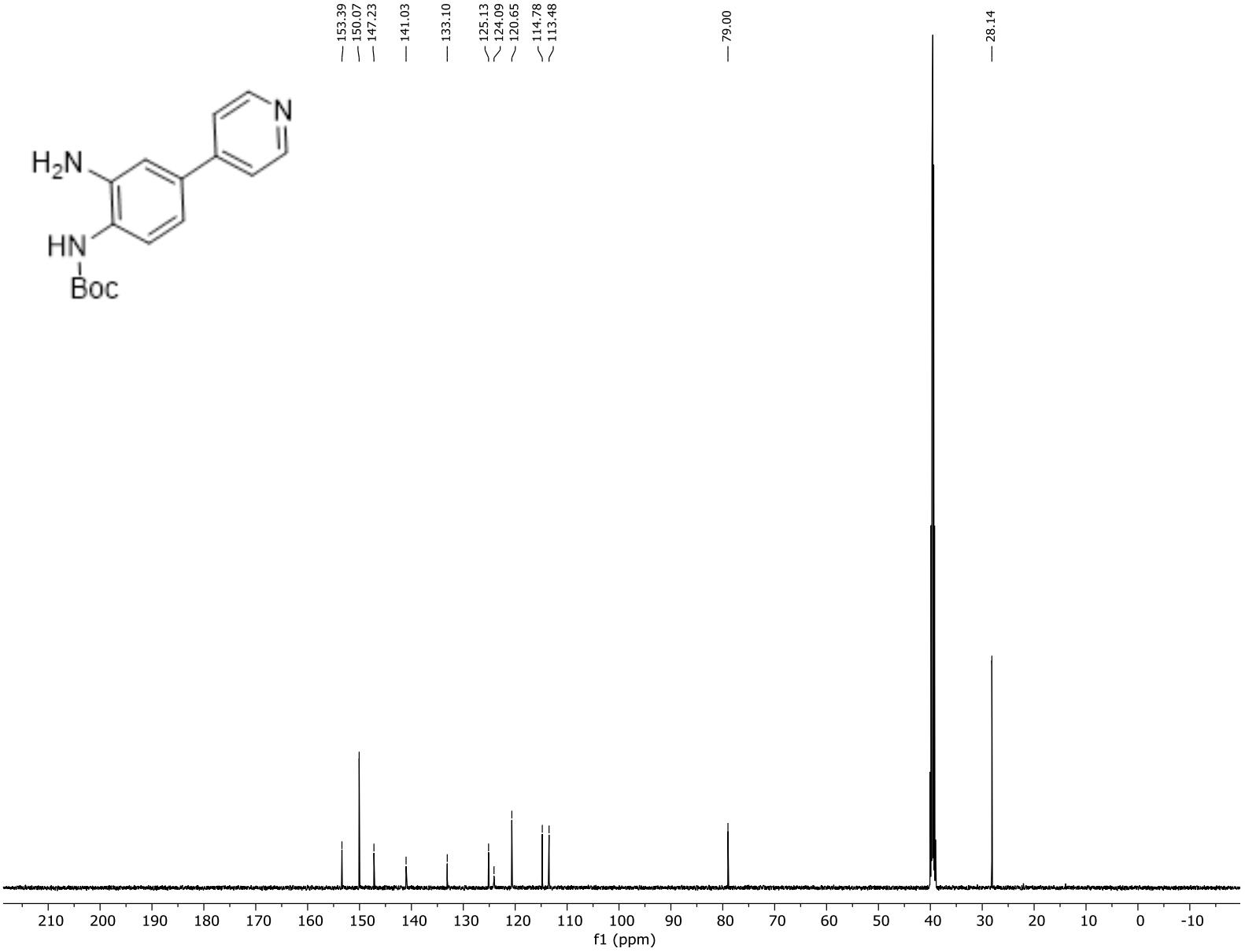
5.2 ^{13}C NMR (101 MHz, DMSO-d_6)



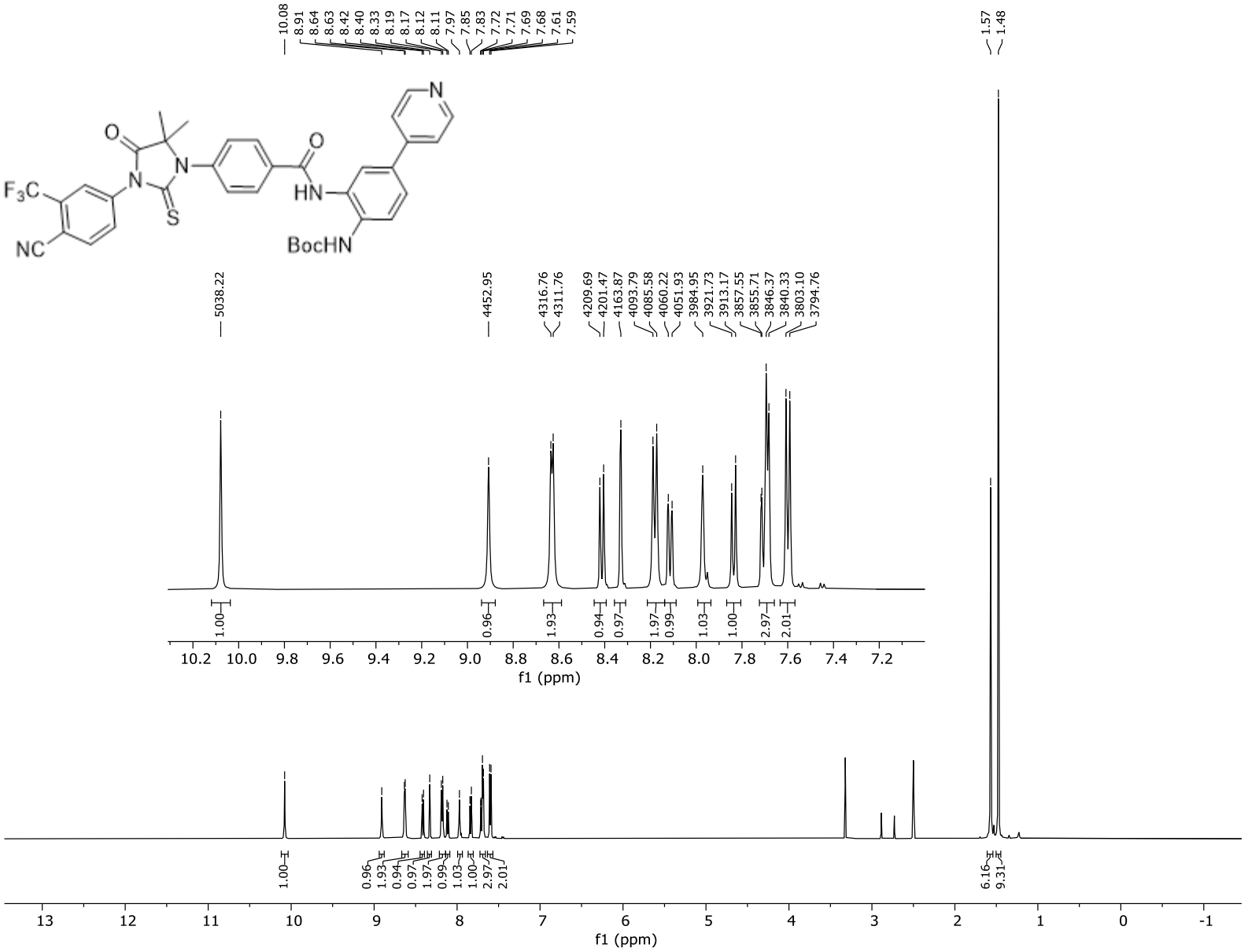
2.22d ^{1}H NMR (500 MHz, DMSO-d_6)



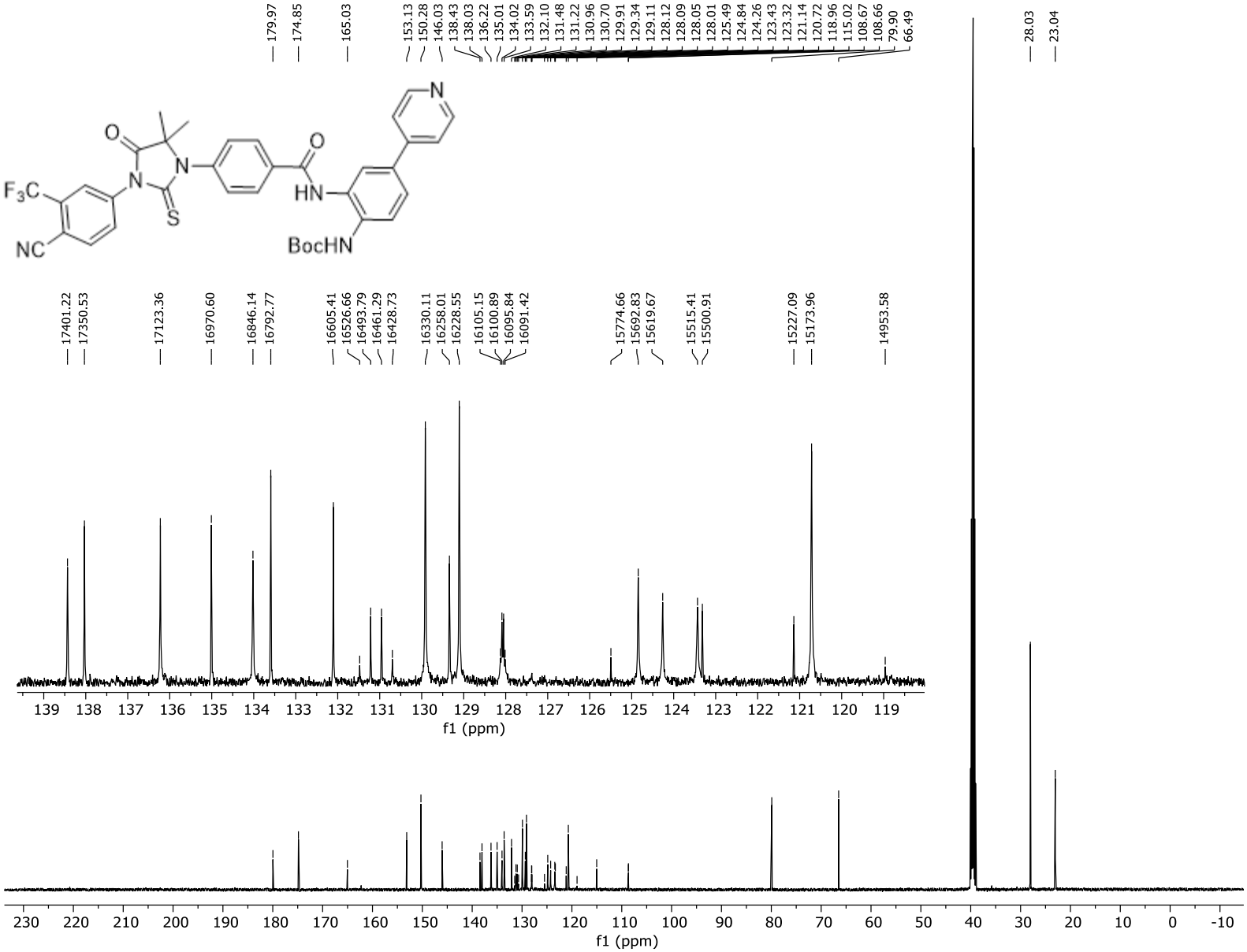
2.22d ^{13}C NMR (126 MHz, DMSO-d_6)



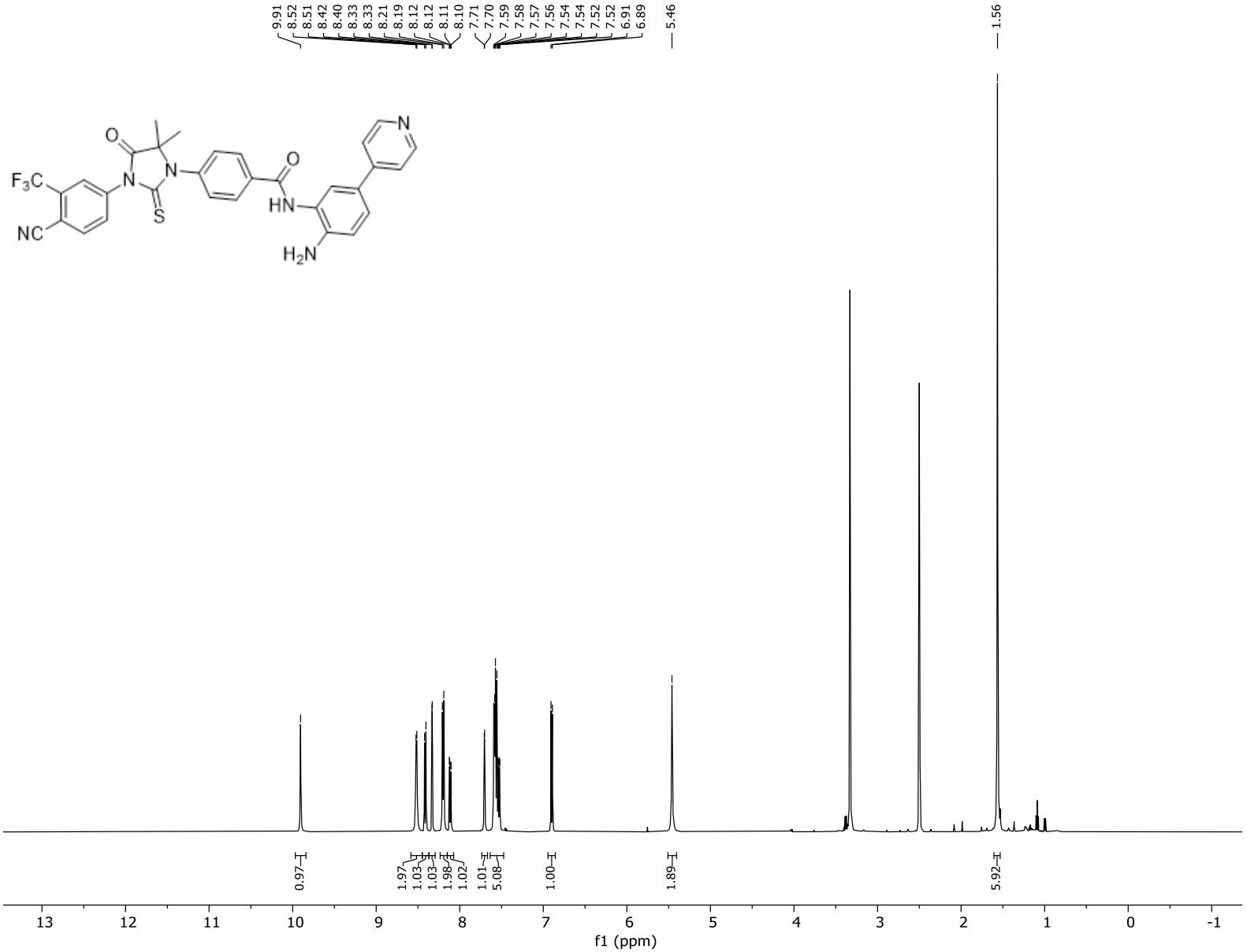
5.3 ^{1}H NMR (500 MHz, DMSO-d_6)



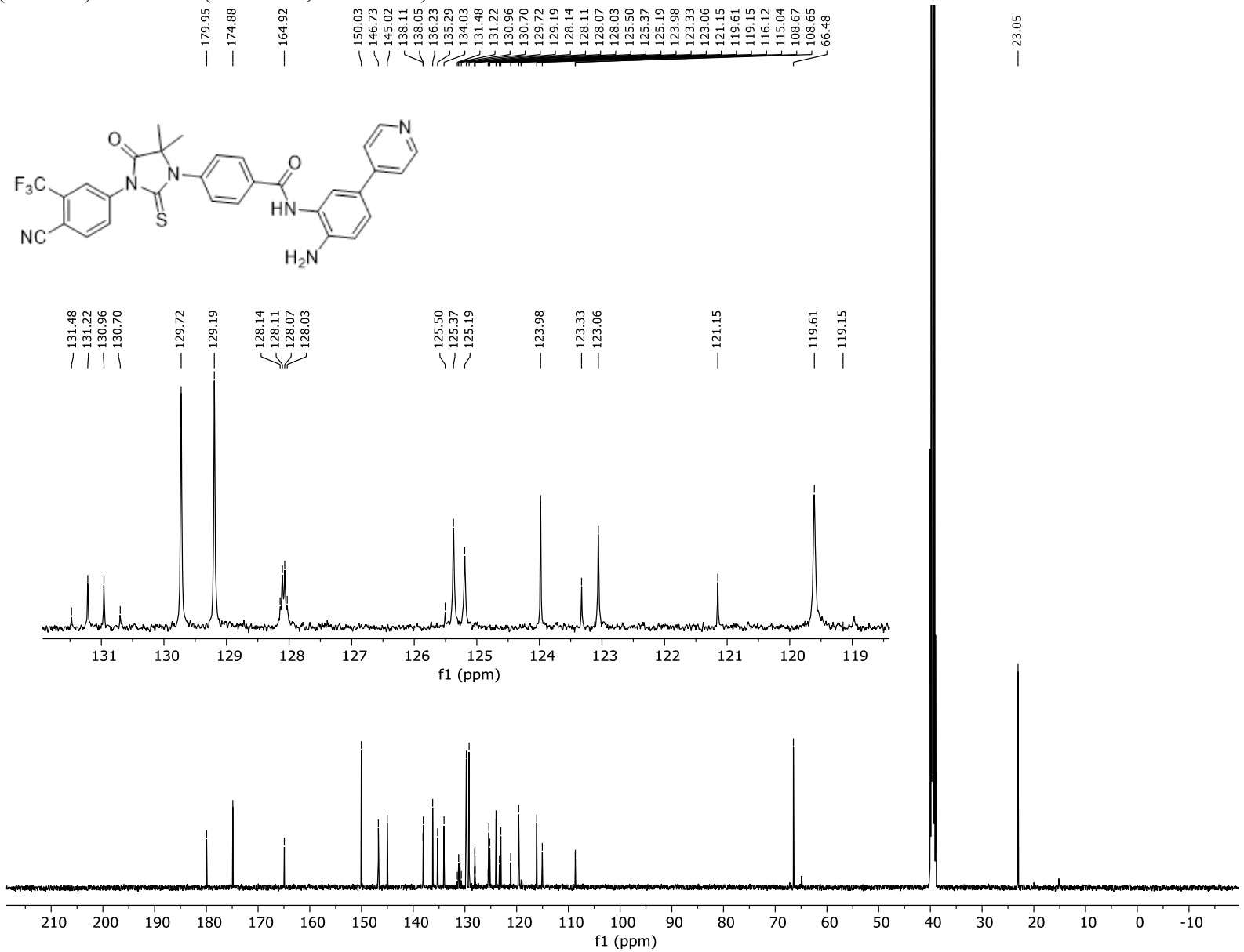
5.3 ^{13}C NMR (126 MHz, DMSO-d_6)



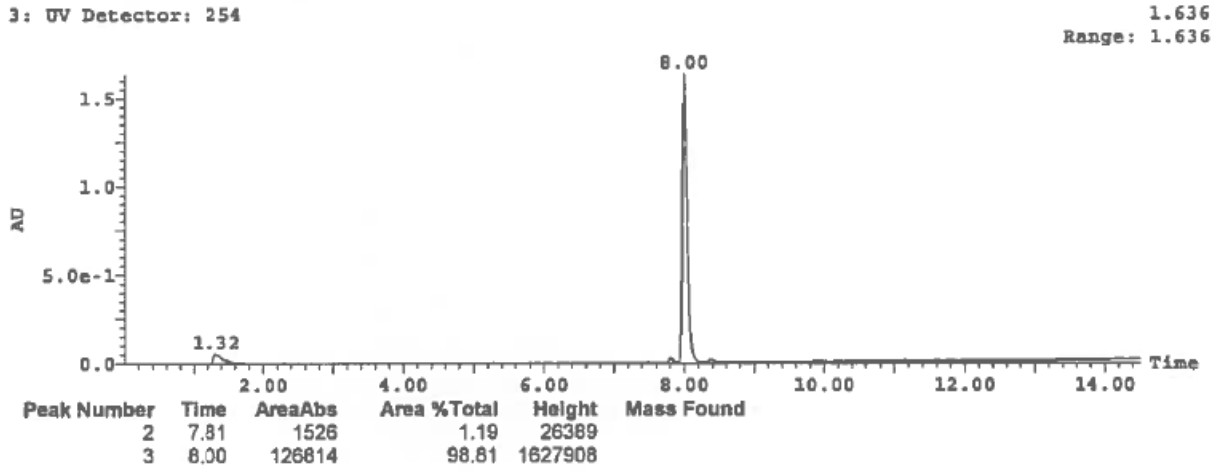
2.6d (RB-416) ^{1}H NMR (500 MHz, DMSO-d_6)



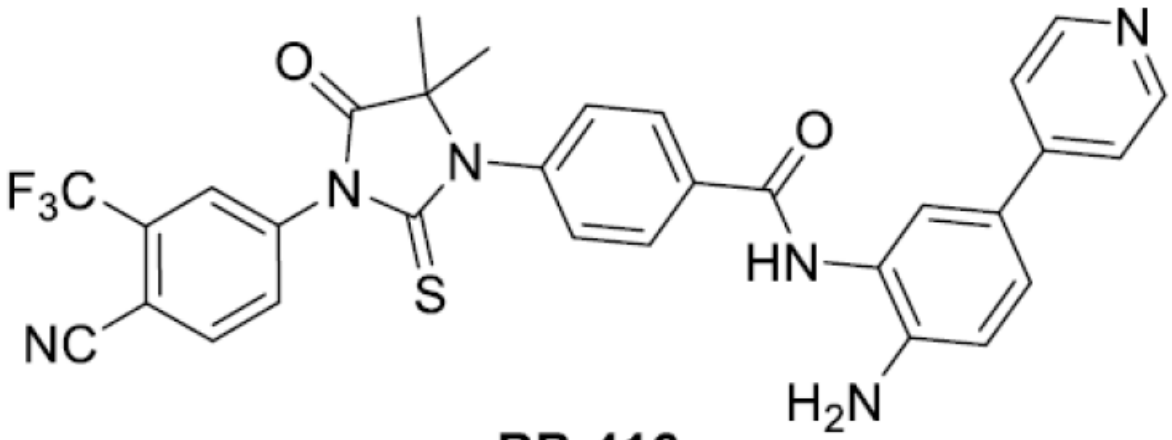
2.6d (RB-416) ^{13}C NMR (126 MHz, DMSO-d_6)



2.6d (RB-416) LC-MS UV trace

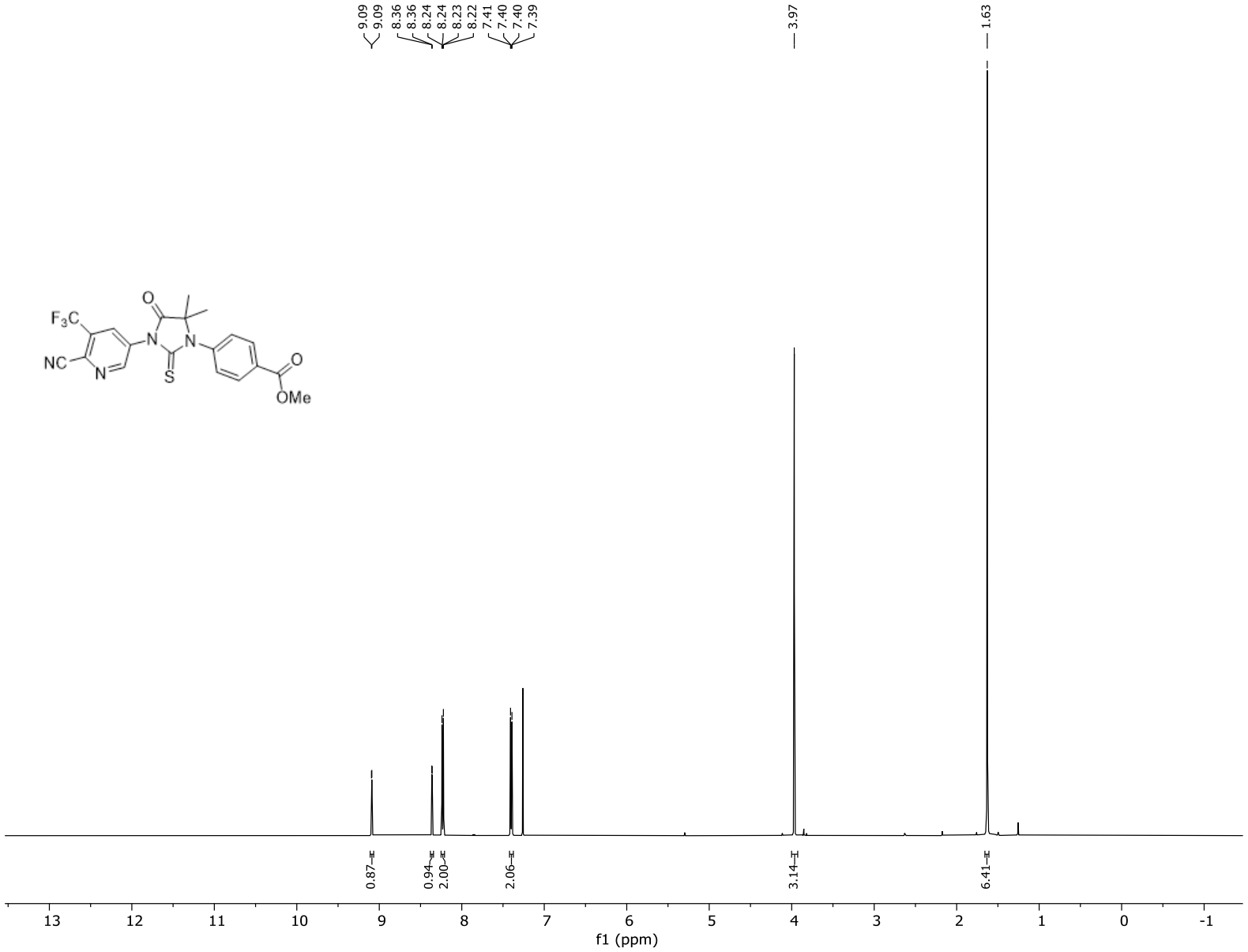


Peak Number	Time	AreaAbs	Area %Total	Height	Mass Found
2	7.81	1526	1.19	26389	
3	8.00	126814	98.81	1627908	

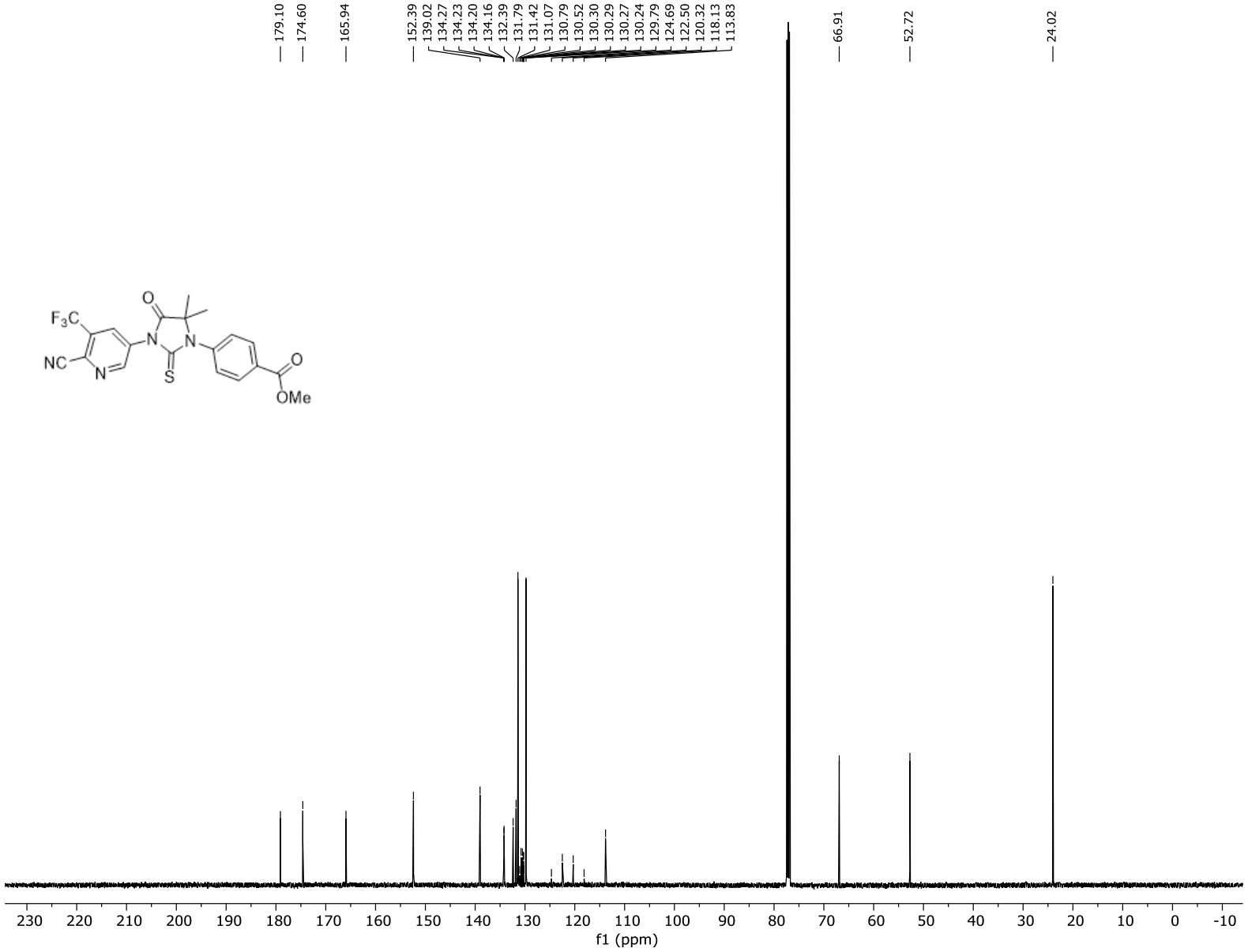


RB-416

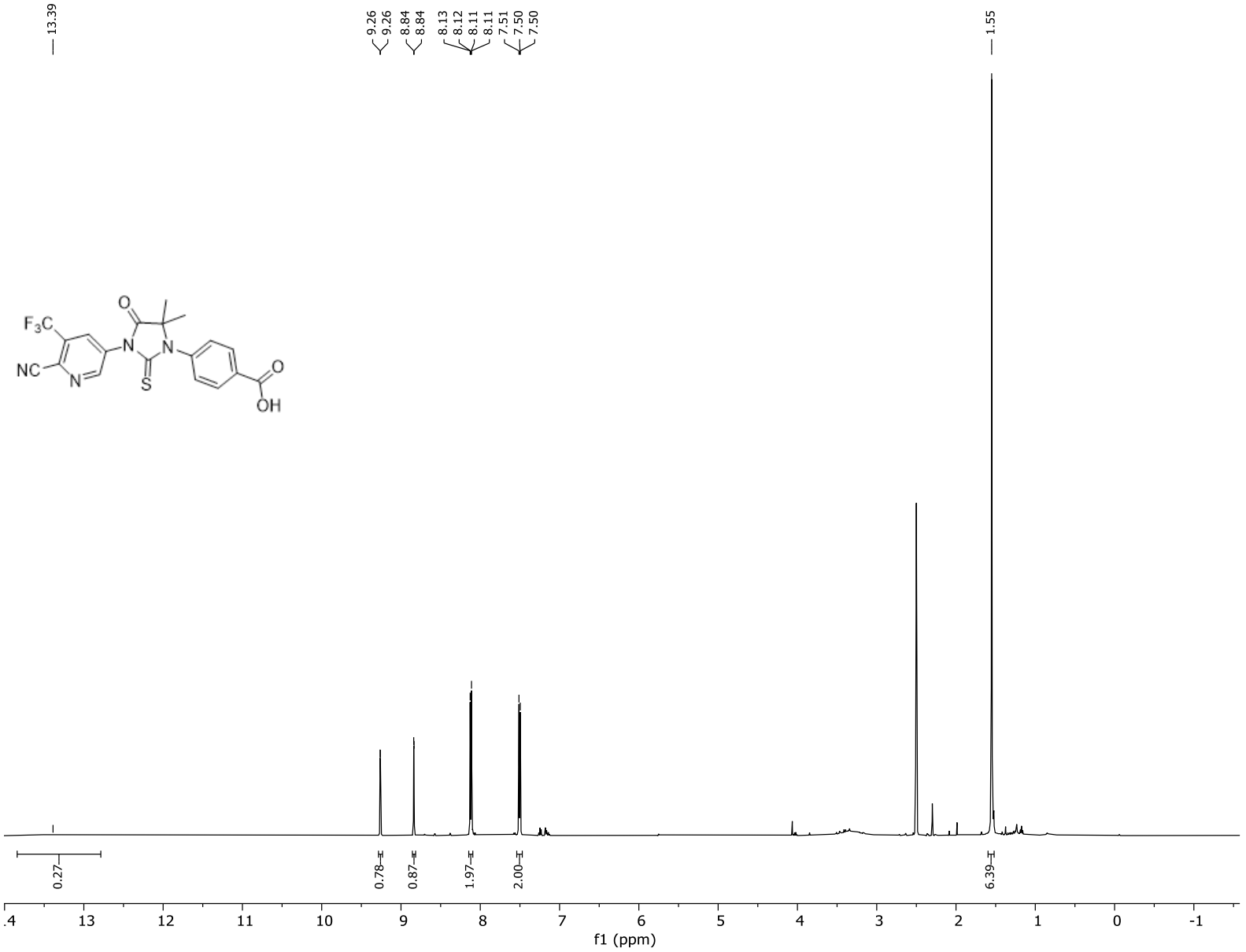
2.45c ^{1}H NMR (500 MHz, $CDCl_3$)



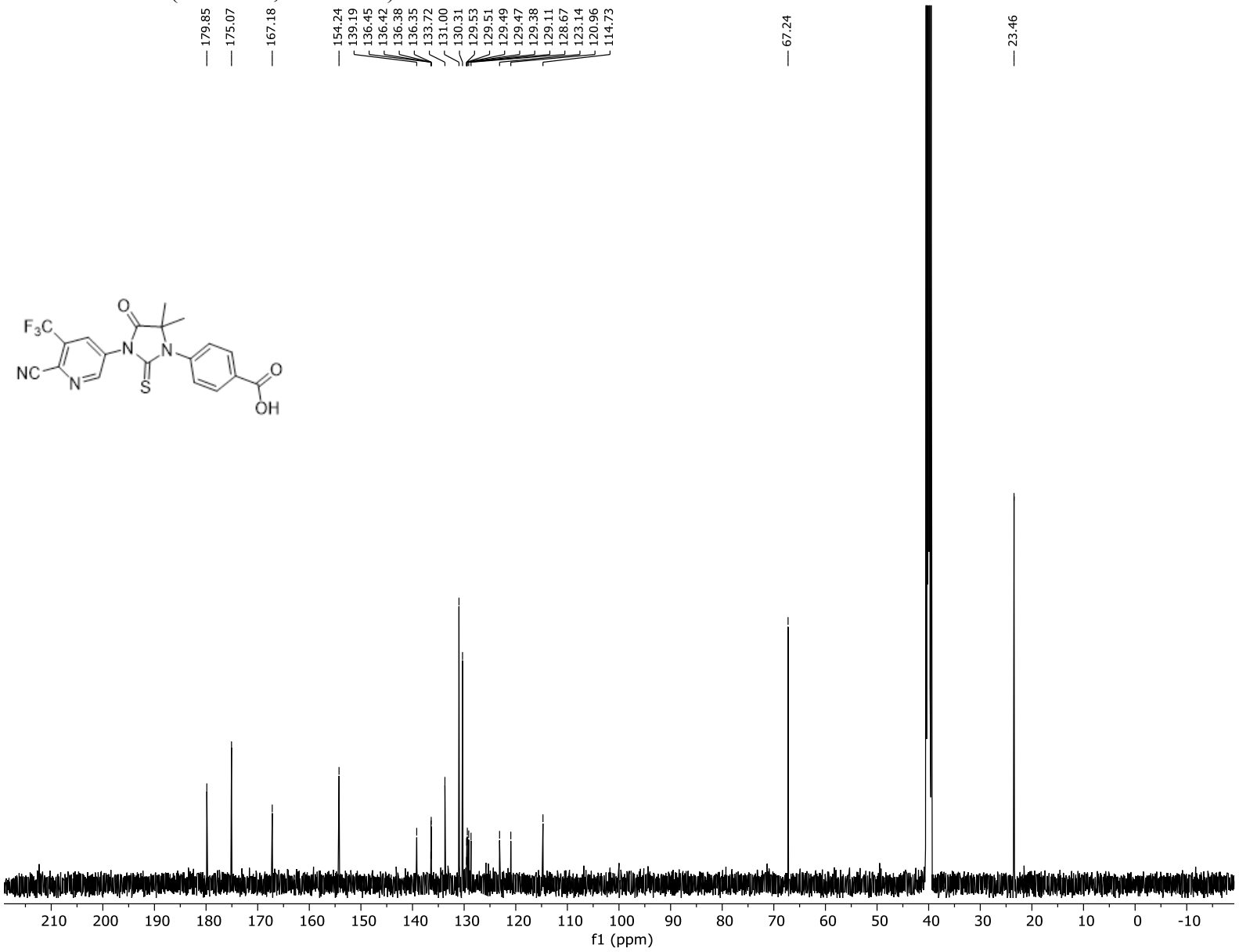
2.45c ^{13}C NMR (126 MHz, $CDCl_3$)



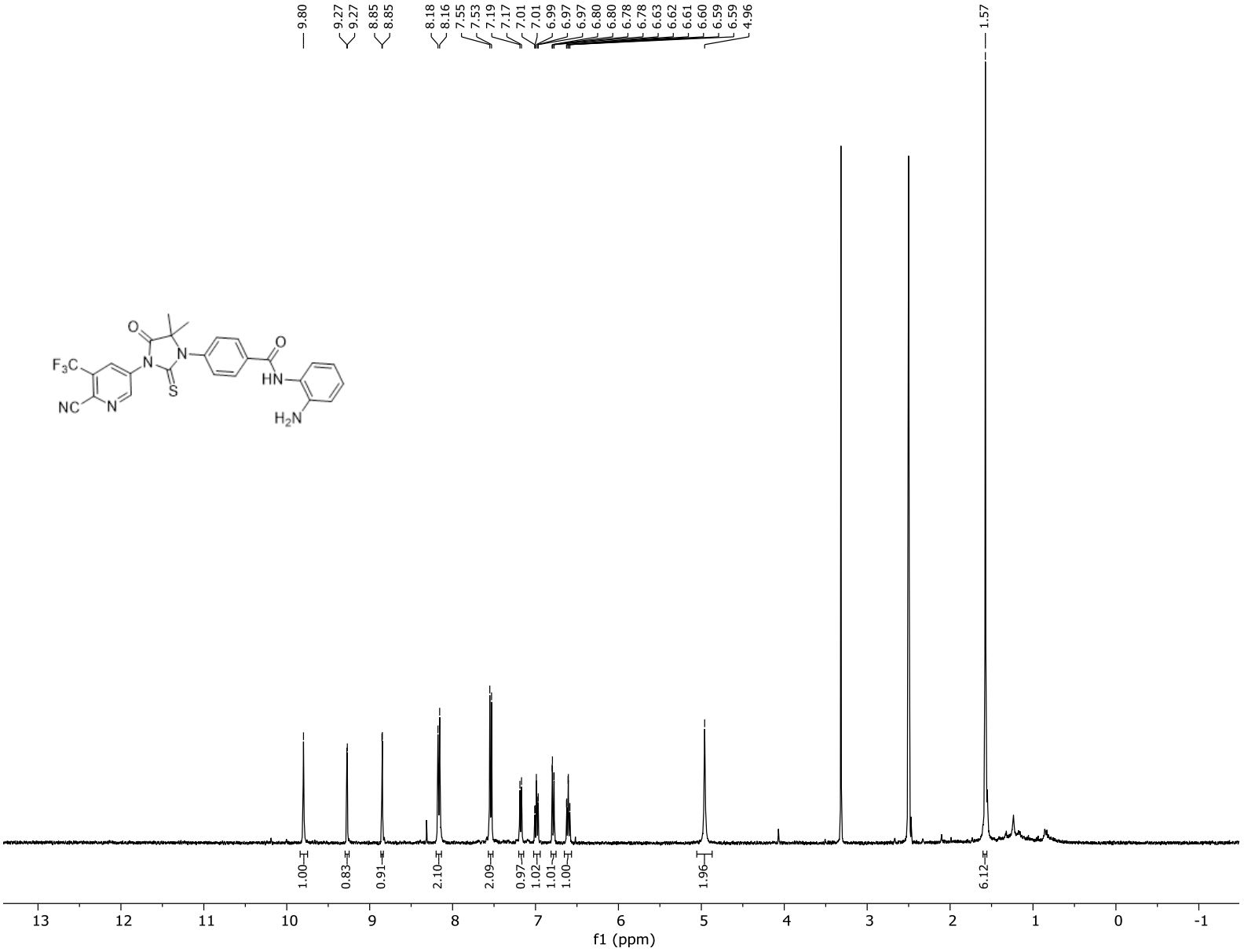
2.48a ^{1}H NMR (500 MHz, DMSO-d_6)



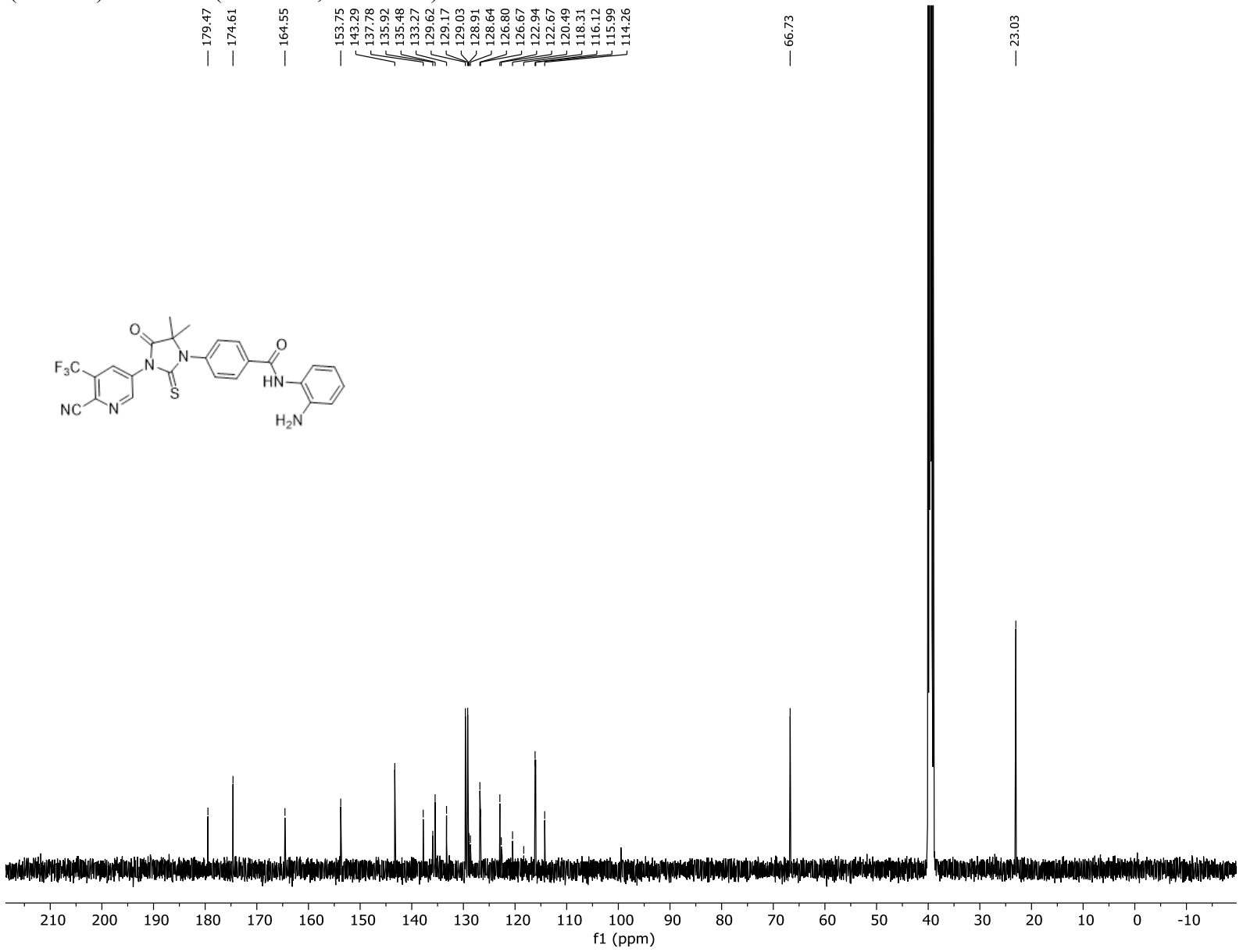
2.48a ^{13}C NMR (126 MHz, DMSO-d_6)



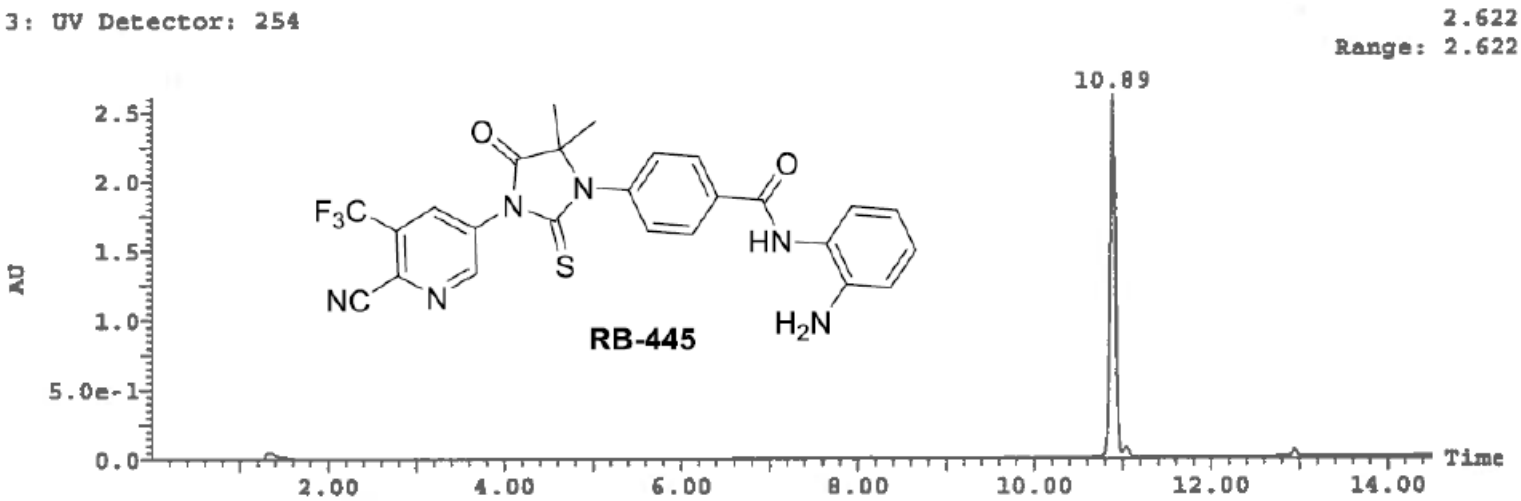
2.35a (RB-445) ^{1}H NMR (400 MHz, DMSO-d_6)



2.35a (RB-445) ^{13}C NMR (126 MHz, DMSO-d_6)

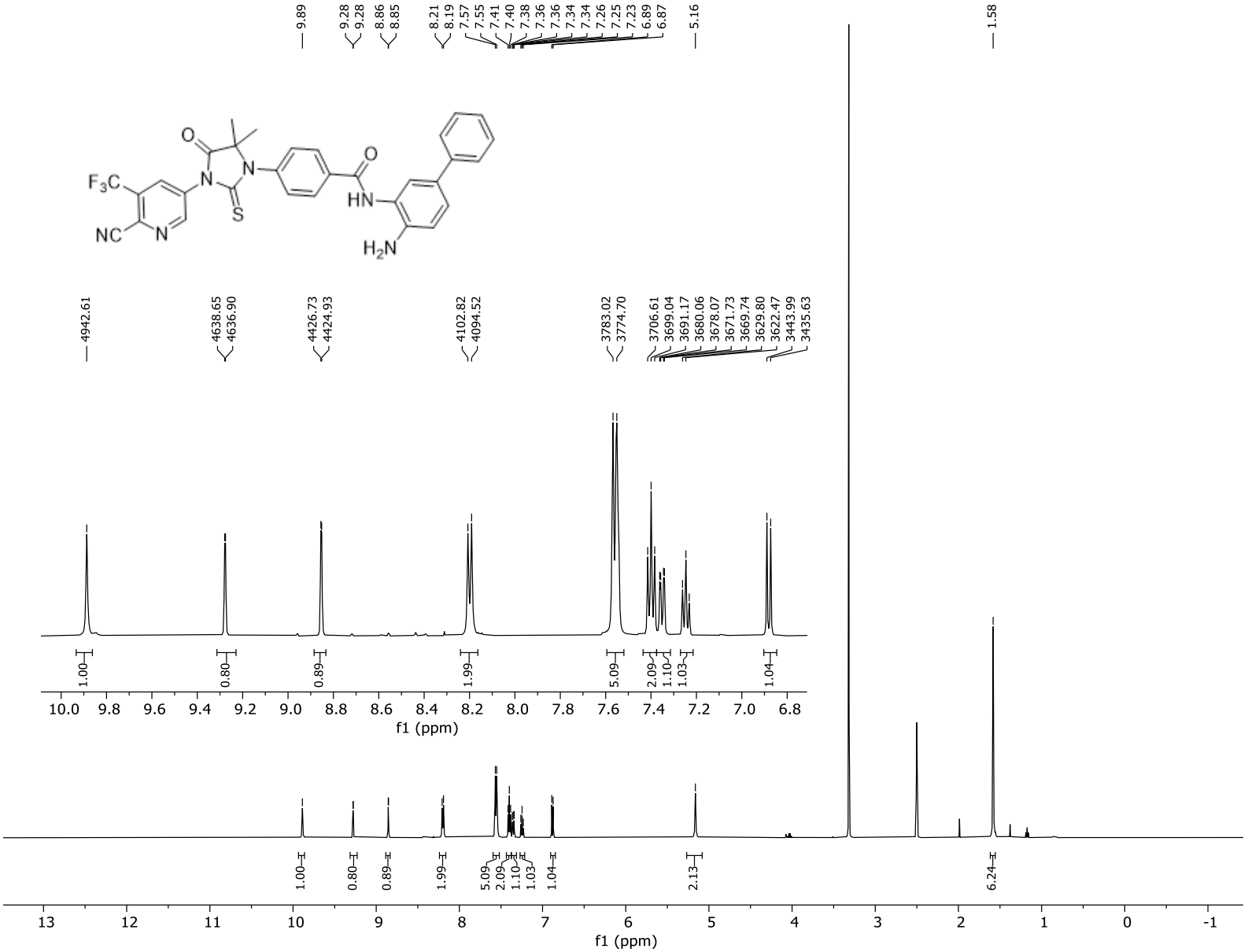


2.35a (RB-445) LC-MS UV trace

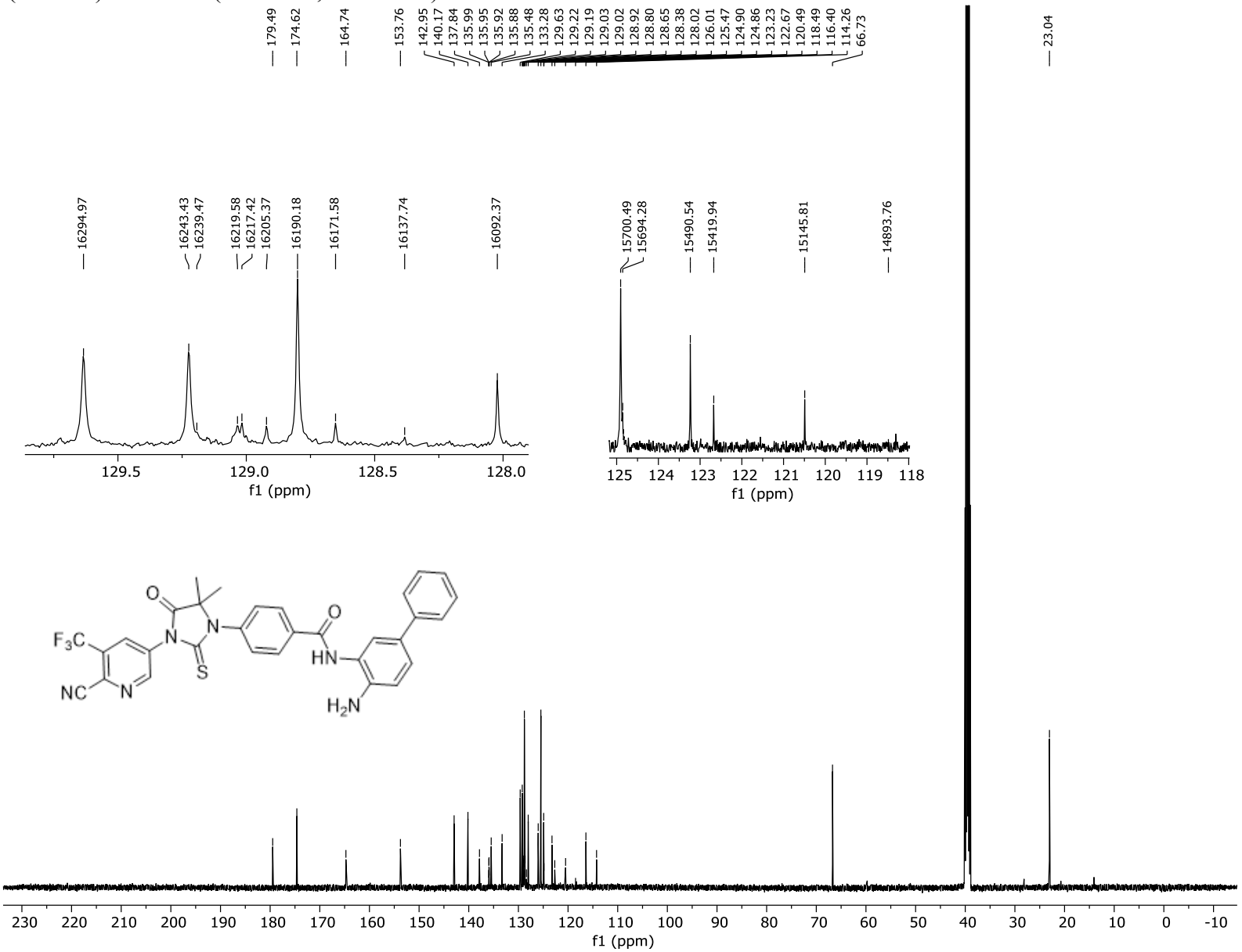


Peak Number	Time	AreaAbs	Area %Total	Height	Mass Found
1	10.89	181074	95.27	2607833	
2	11.04	5426	2.85	73575	
3	12.94	3565	1.88	59534	

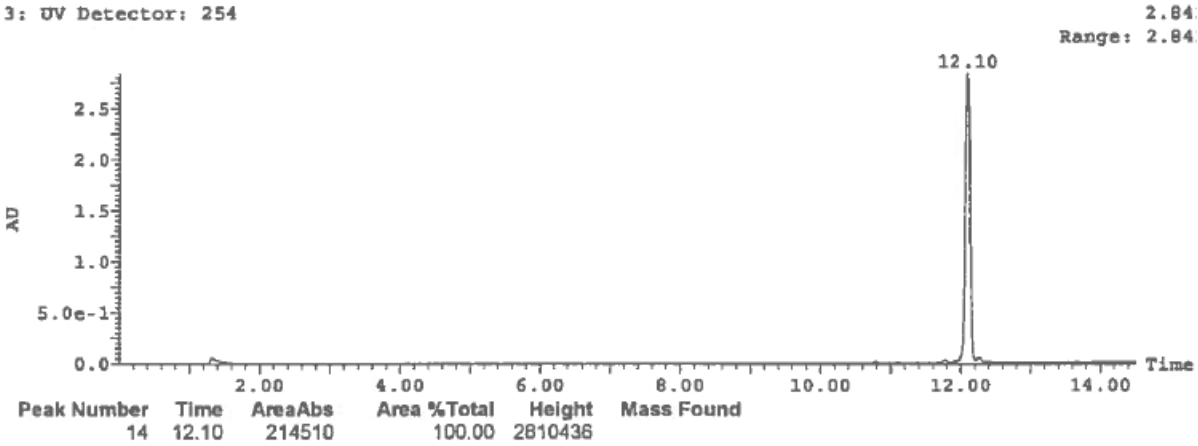
2.35b (RB-446) ^{1}H NMR (500 MHz, DMSO-d_6)



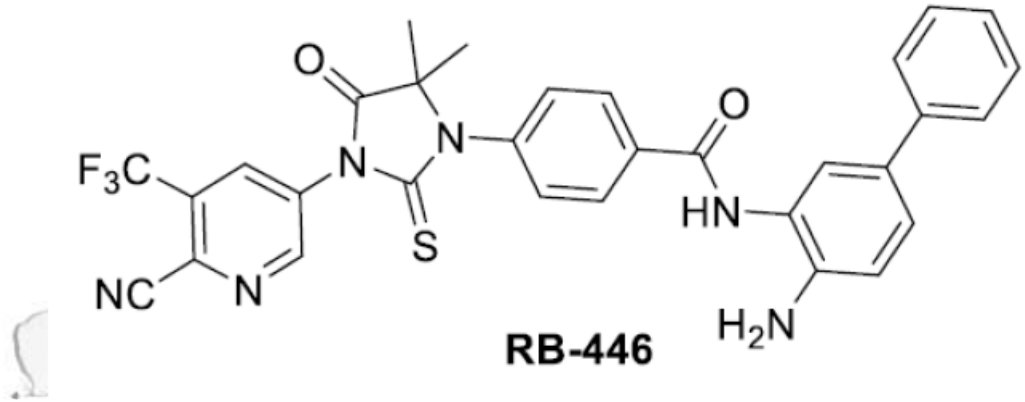
2.35b (RB-446) ^{13}C NMR (126 MHz, DMSO-d_6)



2.35b (RB-446) LC-MS UV trace

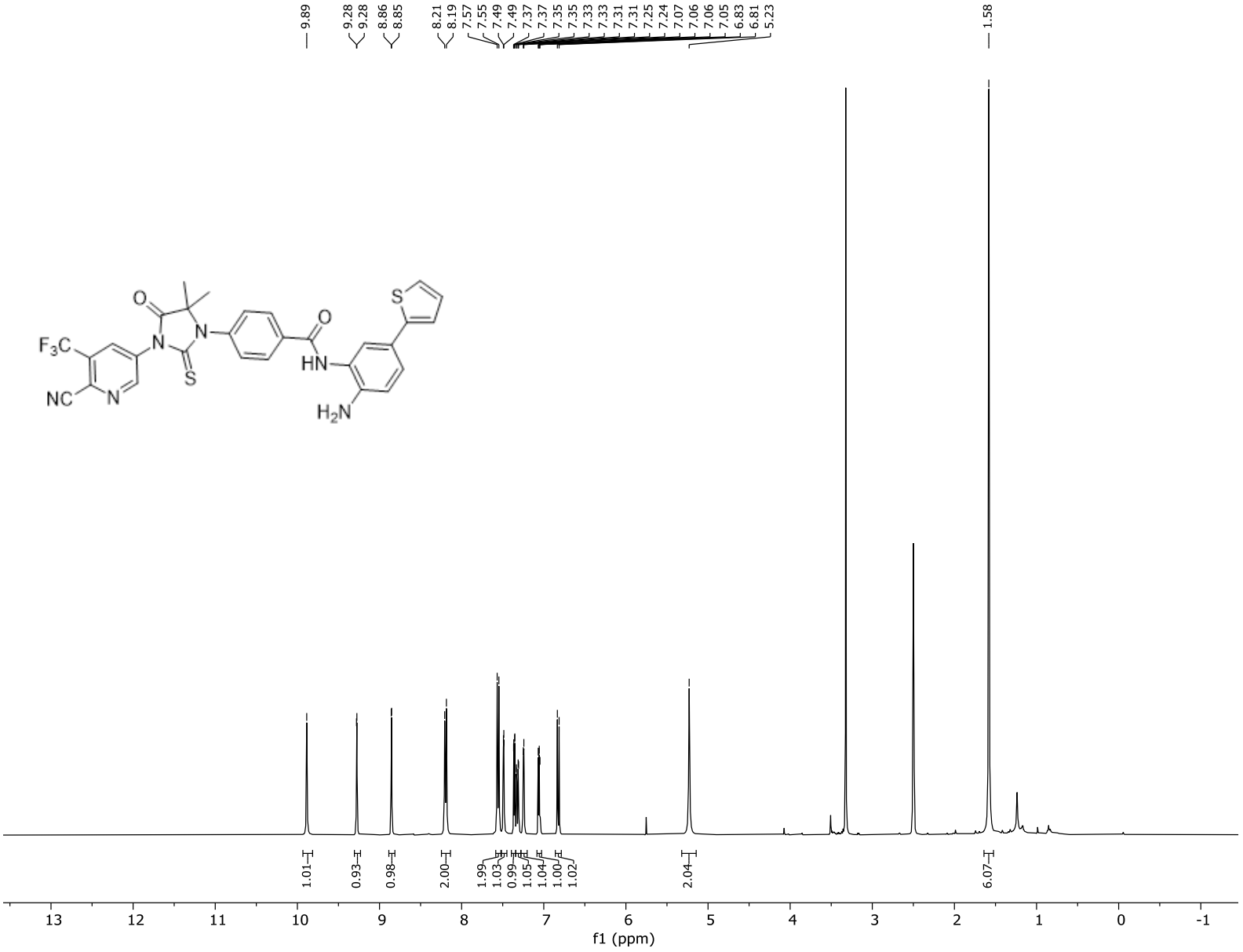


Peak Number	Time	AreaAbs	Area %Total	Height	Mass Found
14	12.10	214510	100.00	2810436	

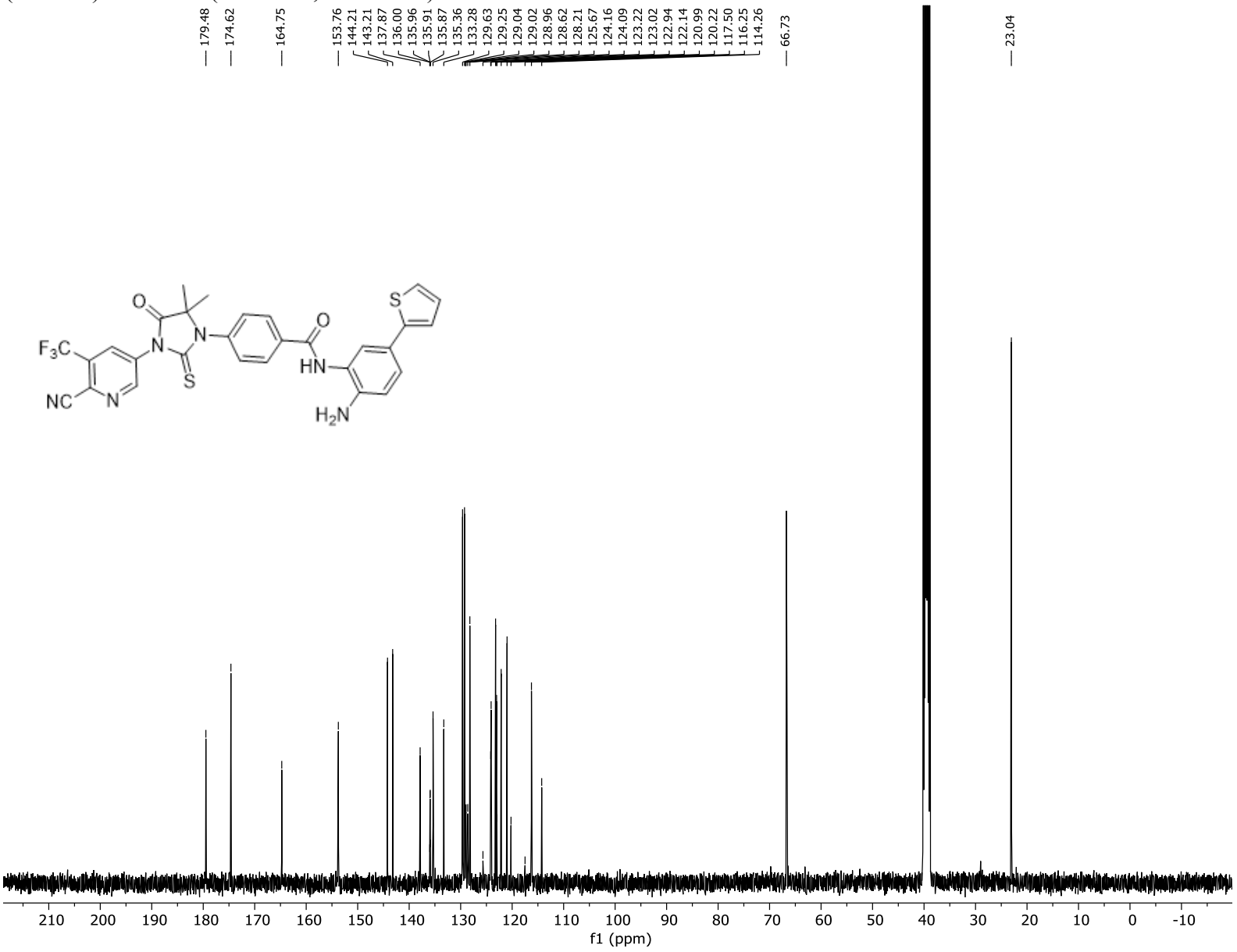


RB-446

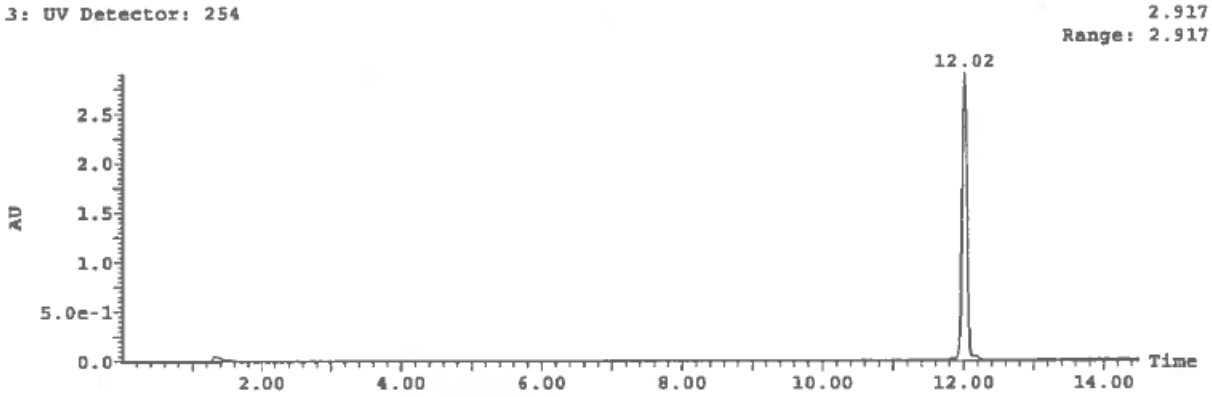
2.35c (RB-447) ^{1}H NMR (400 MHz, DMSO-d_6)



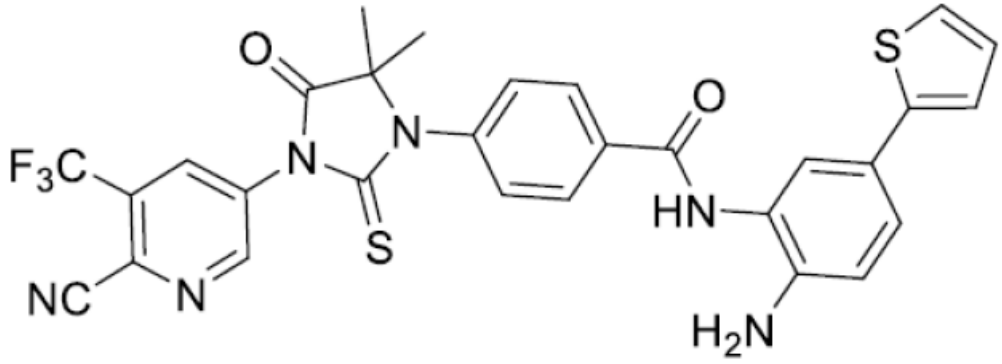
2.35c (RB-447) ^{13}C NMR (101 MHz, DMSO-d_6)



2.35c (RB-447) LC-MS UV trace

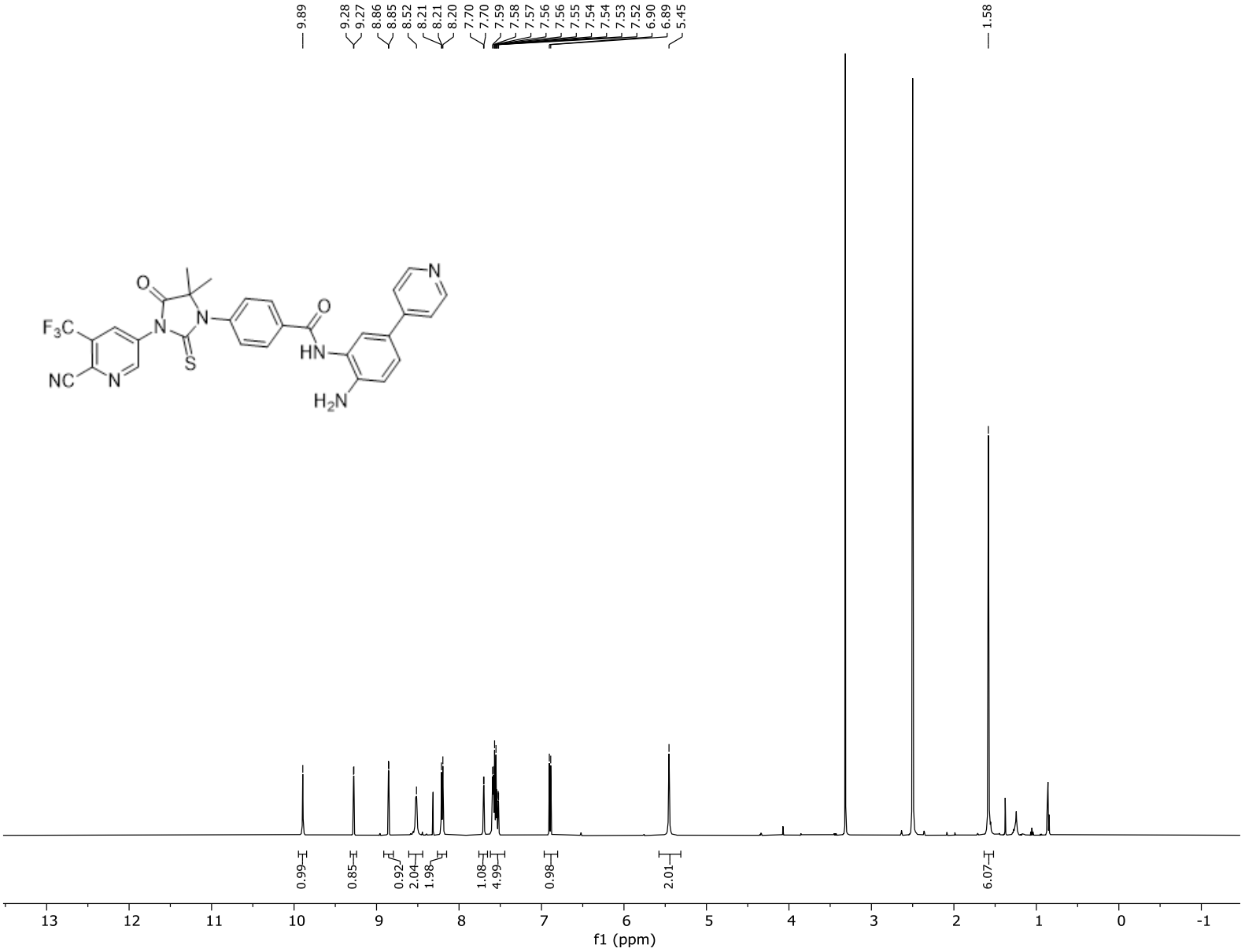


Peak Number	Time	AreaAbs	Area %Total	Height	Mass Found
2	12.02	237581	98.67	2897988	
3	12.19	3198	1.33	44029	

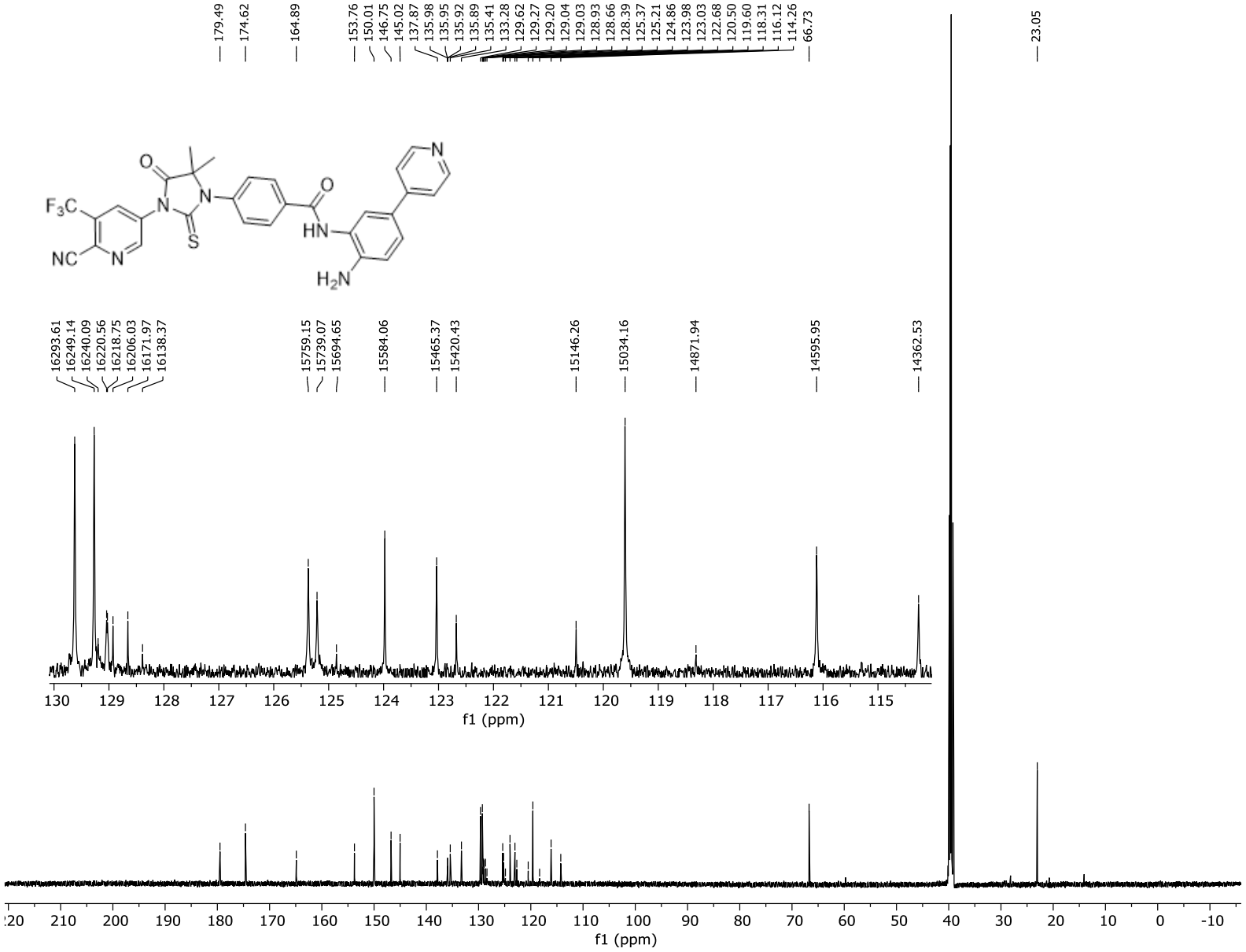


RB-447

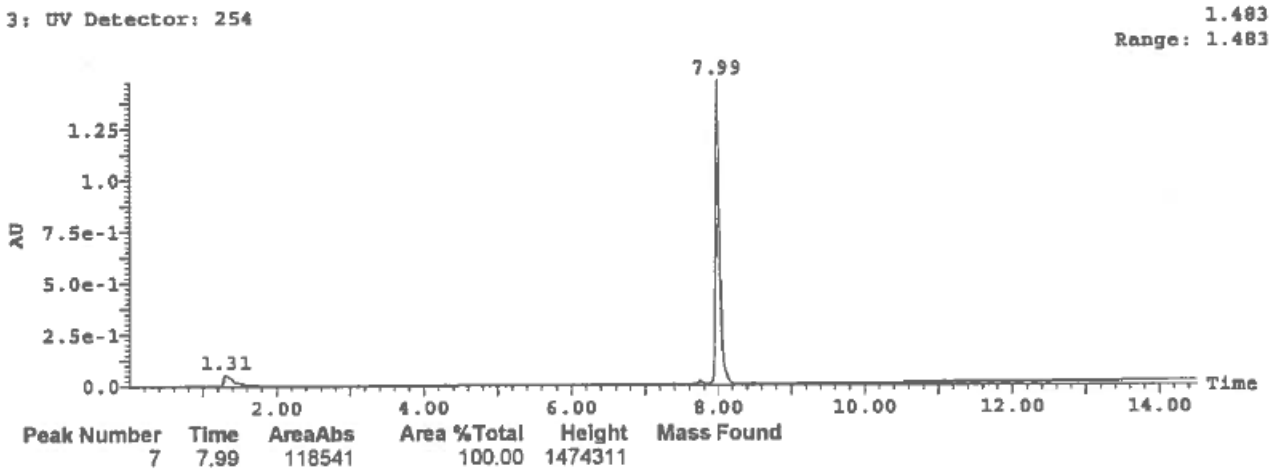
2.35d (RB-448) ^{1}H NMR (500 MHz, DMSO-d_6)

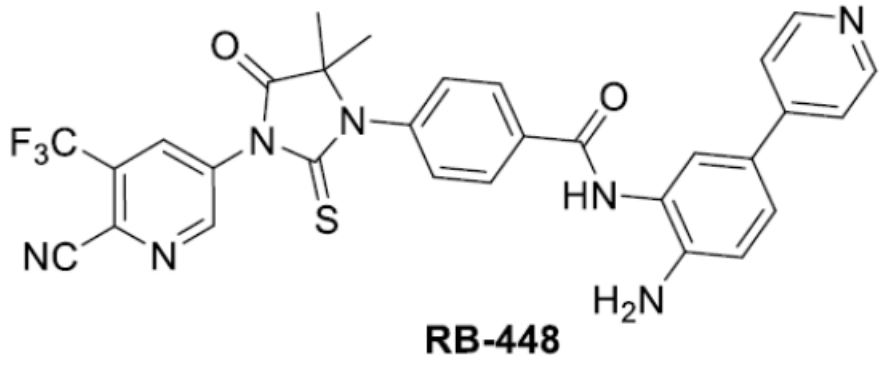


2.35d (RB-448) ^{13}C NMR (126 MHz, DMSO-d_6)



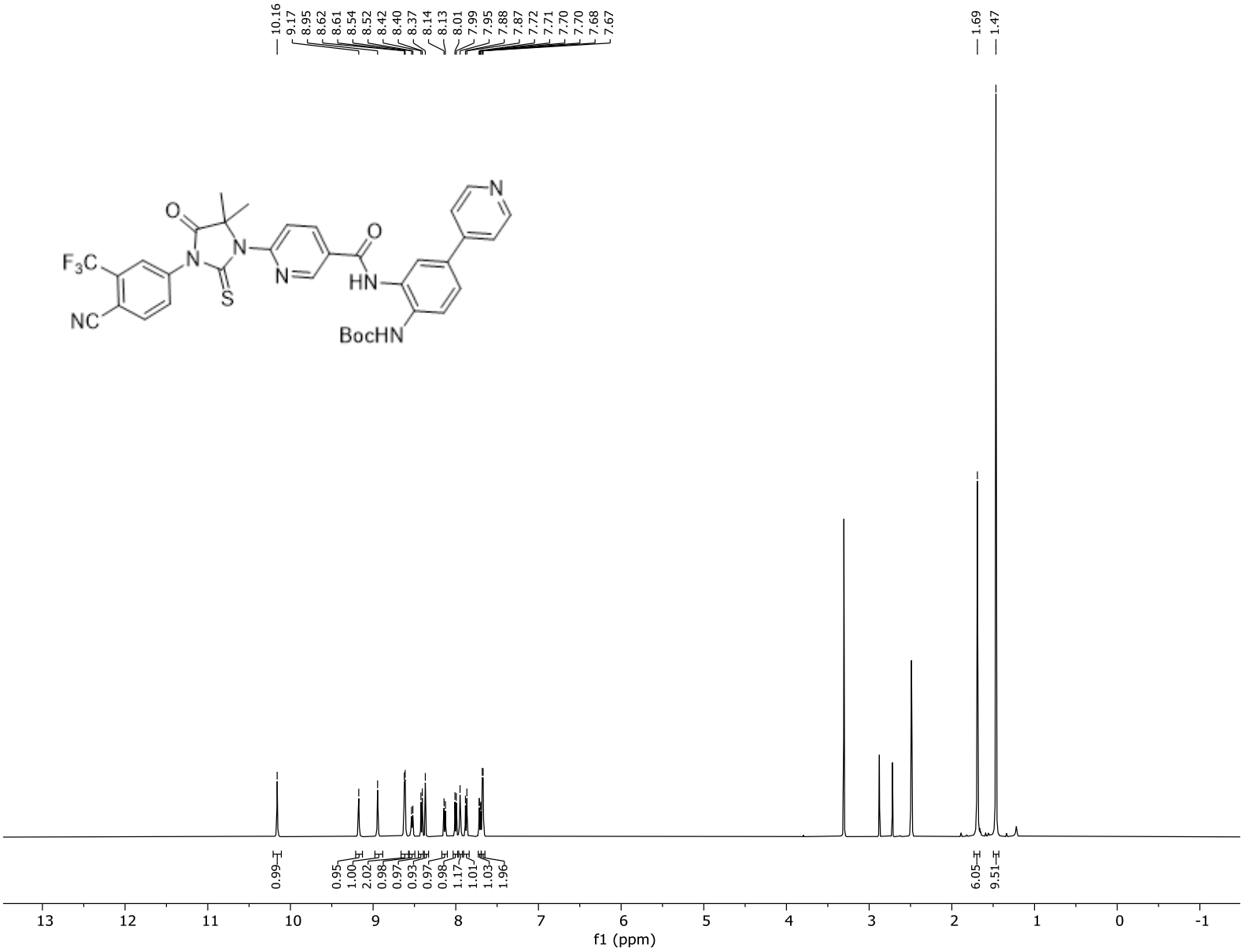
2.35d (RB-448) LC-MS UV trace



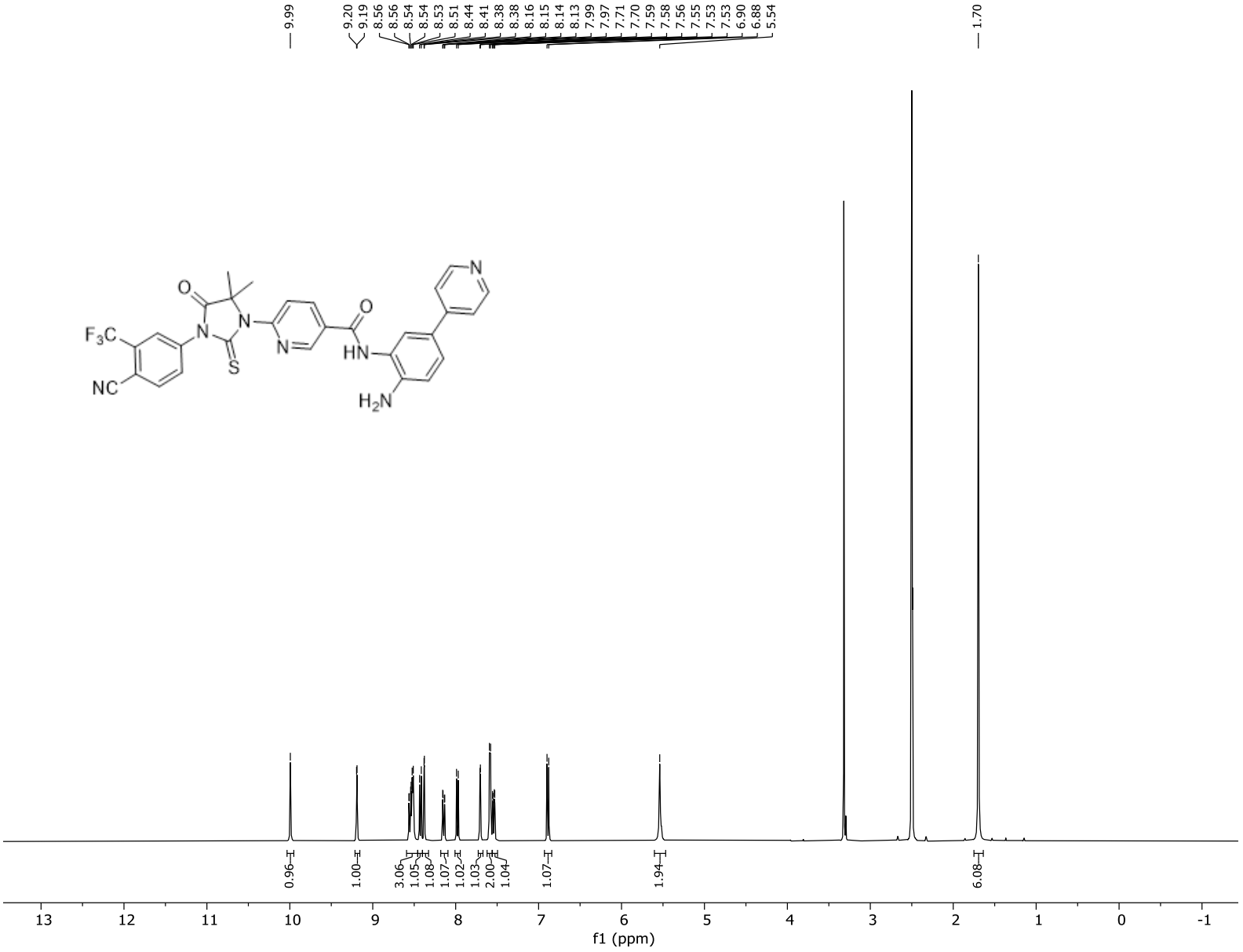


RB-448

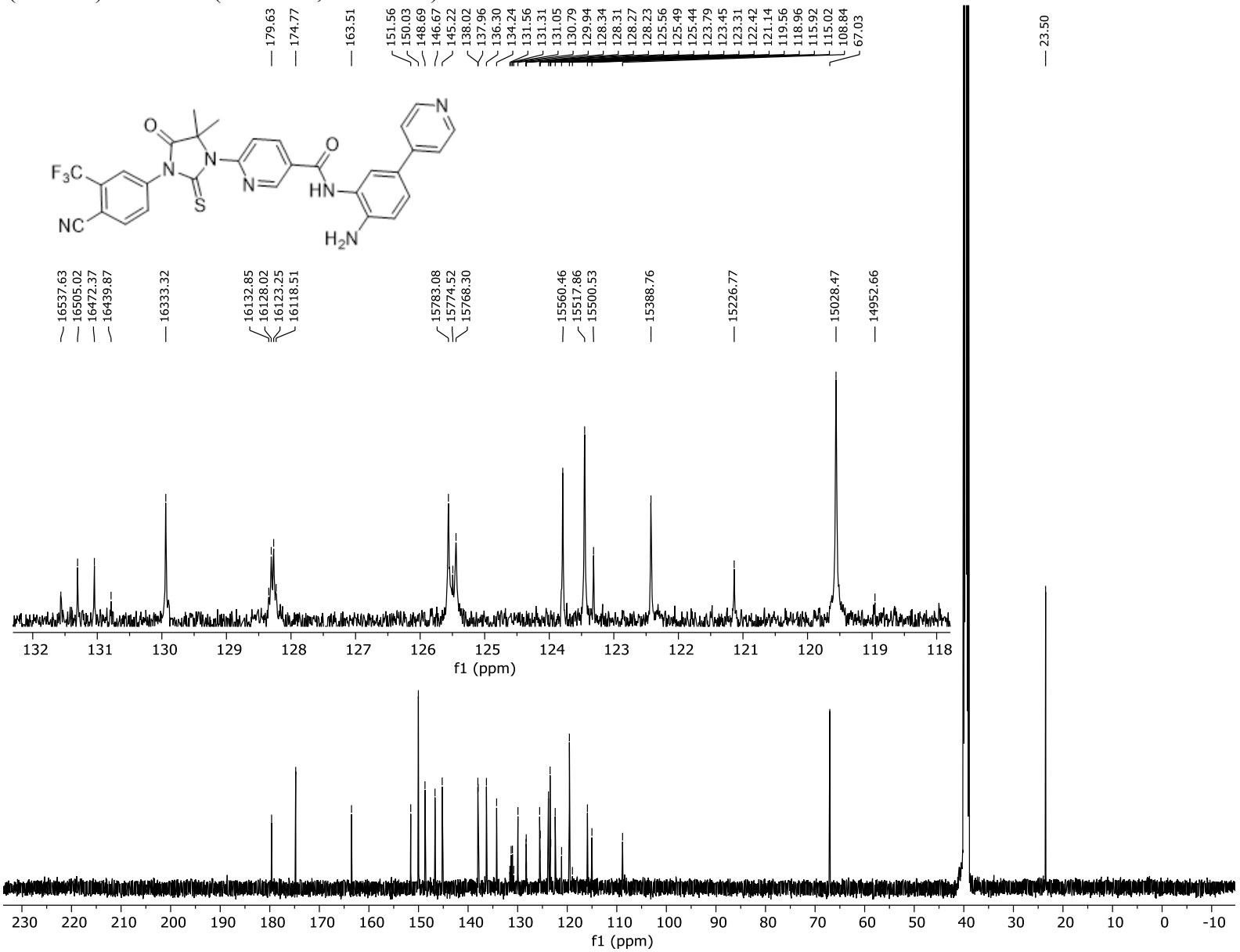
5.4 ^{1}H NMR (500 MHz, DMSO-d_6)



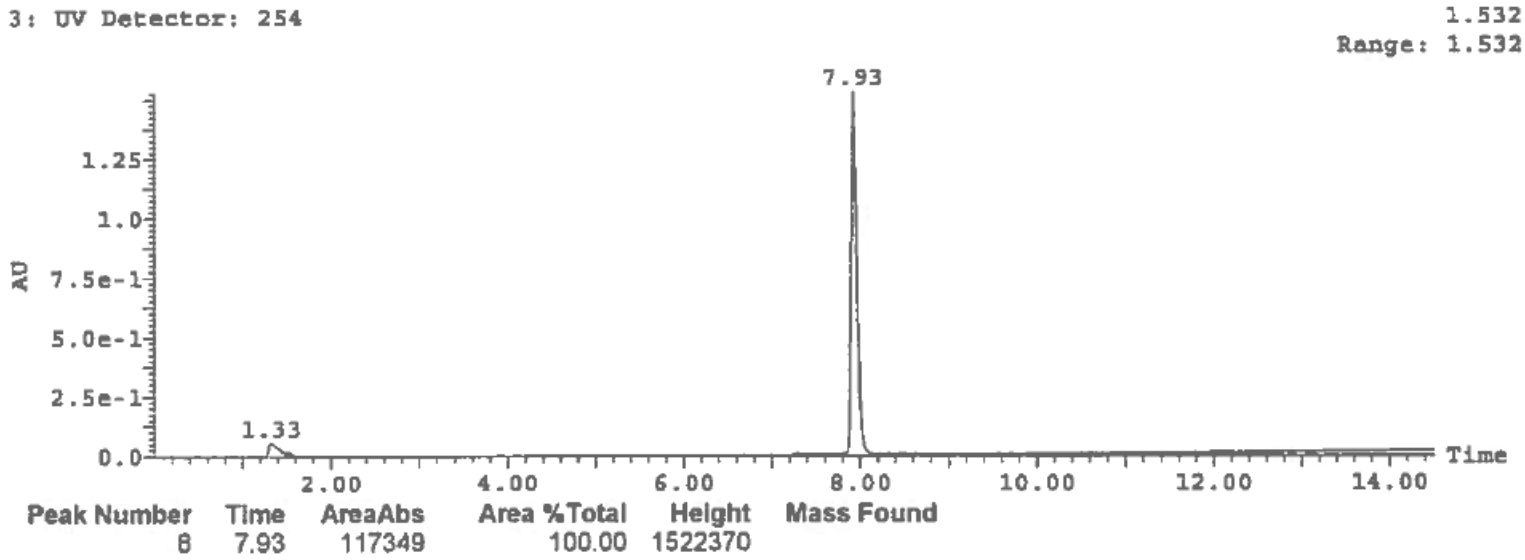
2.36d (RB-440) ^{1}H NMR (400 MHz, DMSO-d_6)

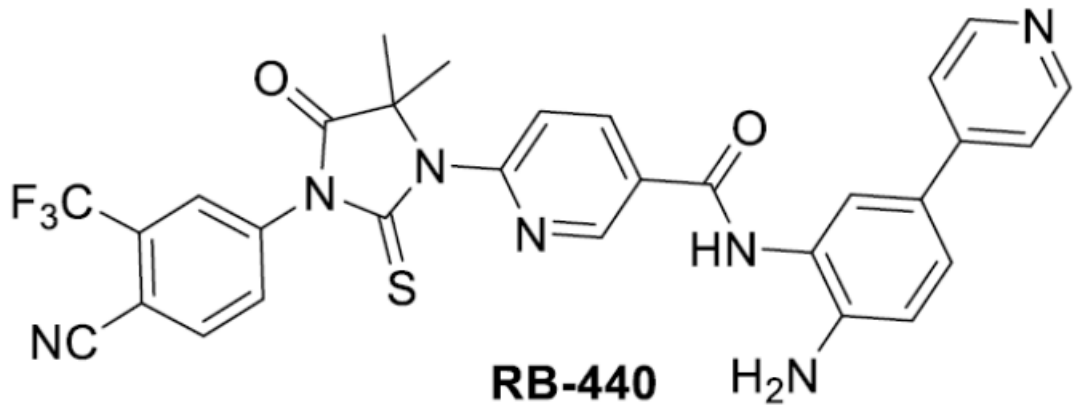


2.36d (RB-440) ^{13}C NMR (126 MHz, DMSO-d_6)



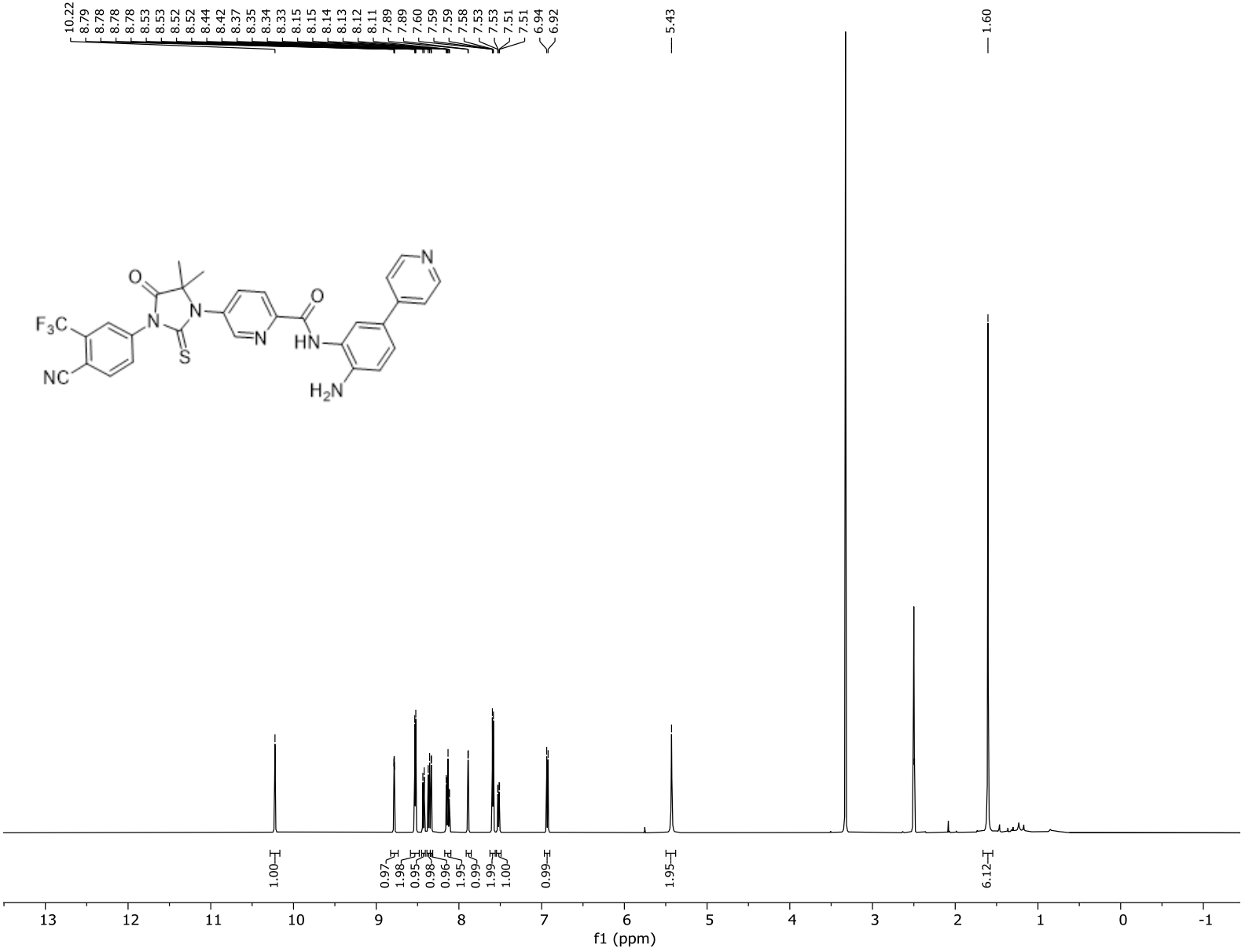
2.36d (RB-440) LC-MS UV trace



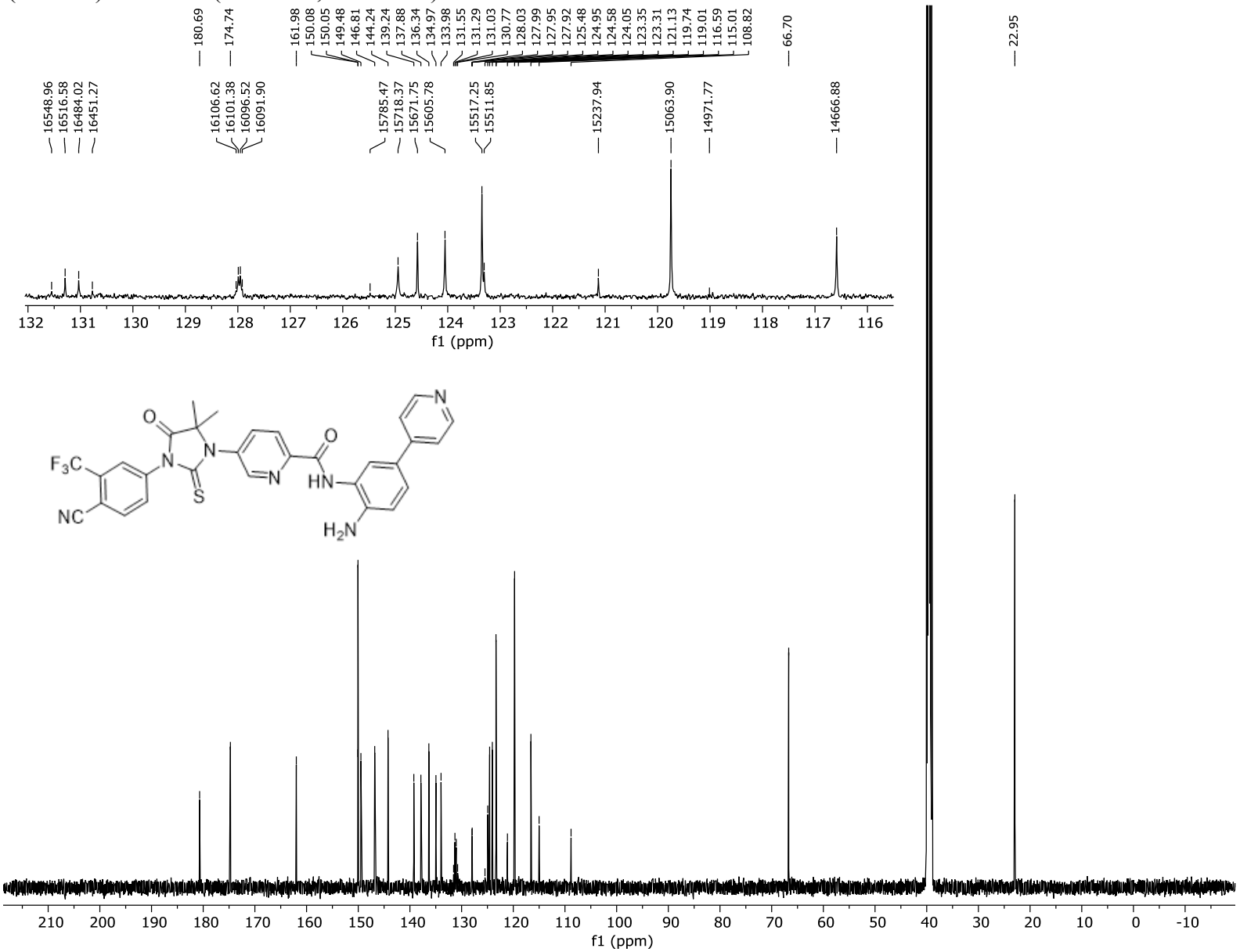


RB-440

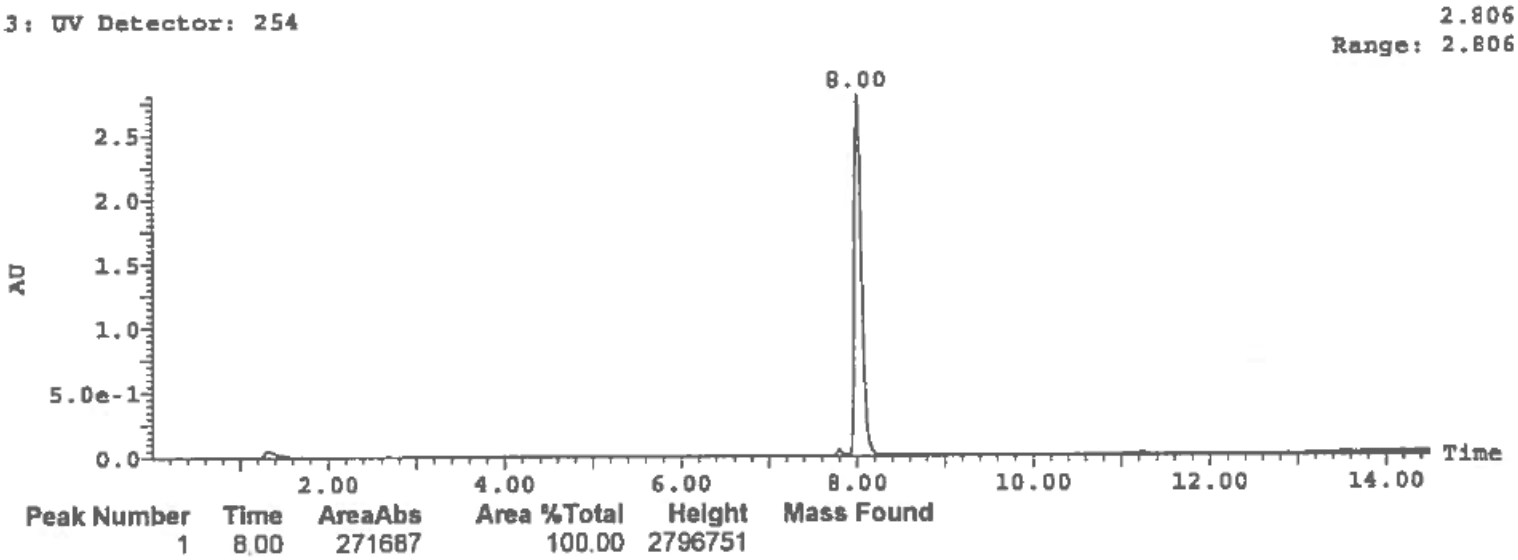
2.37d (RB-439) ^{1}H NMR (500 MHz, DMSO-d_6)

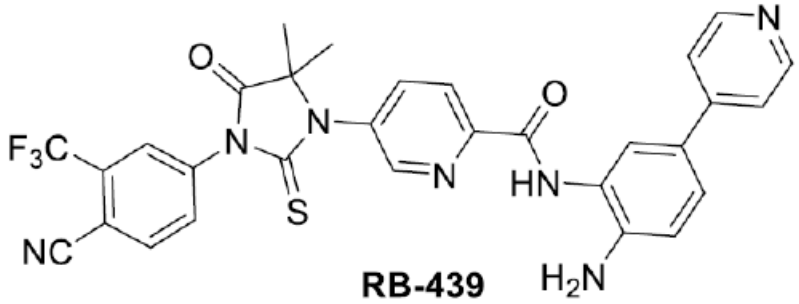


2.37d (RB-439) ^{13}C NMR (126 MHz, DMSO-d_6)



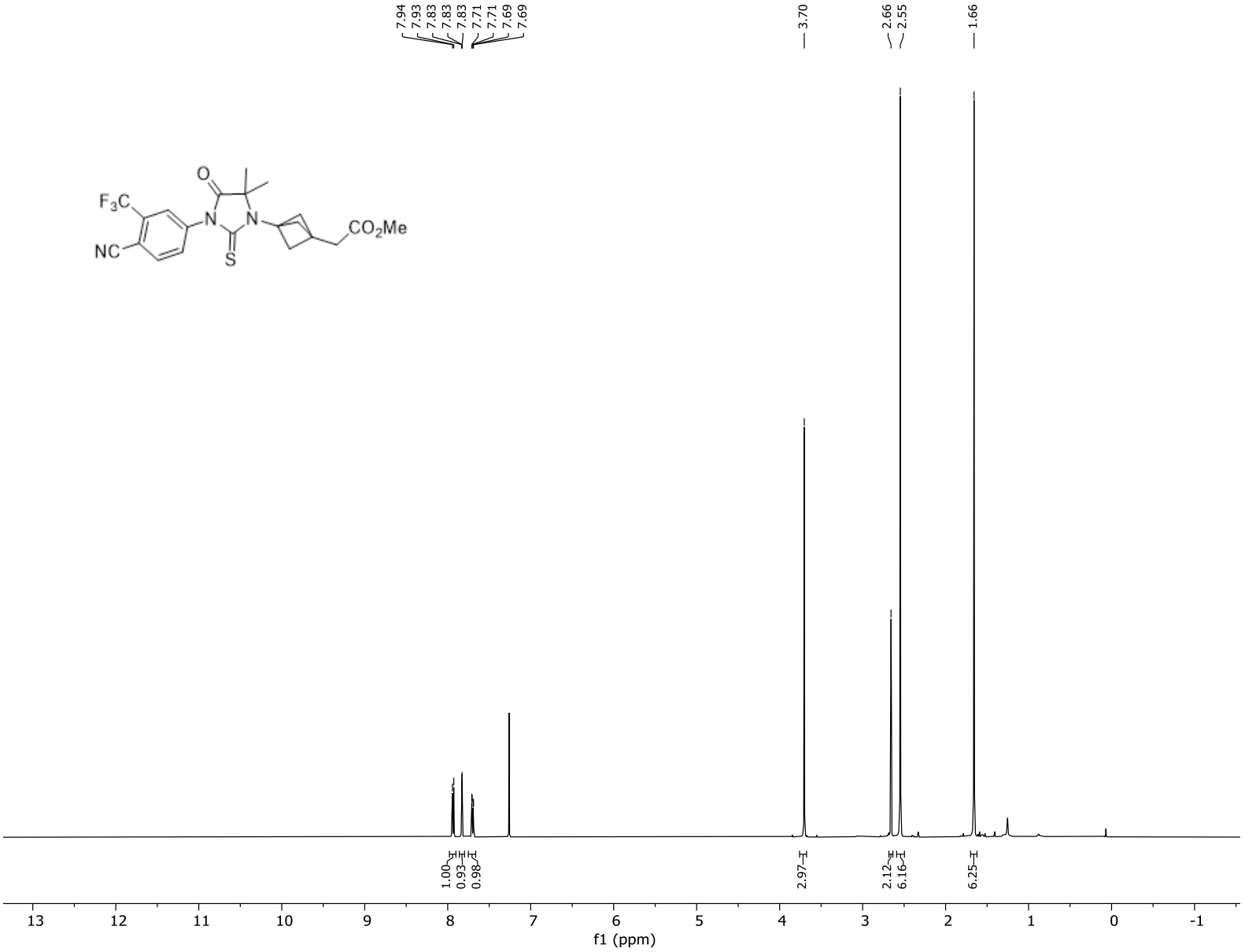
2.37d (RB-439) LC-MS UV trace



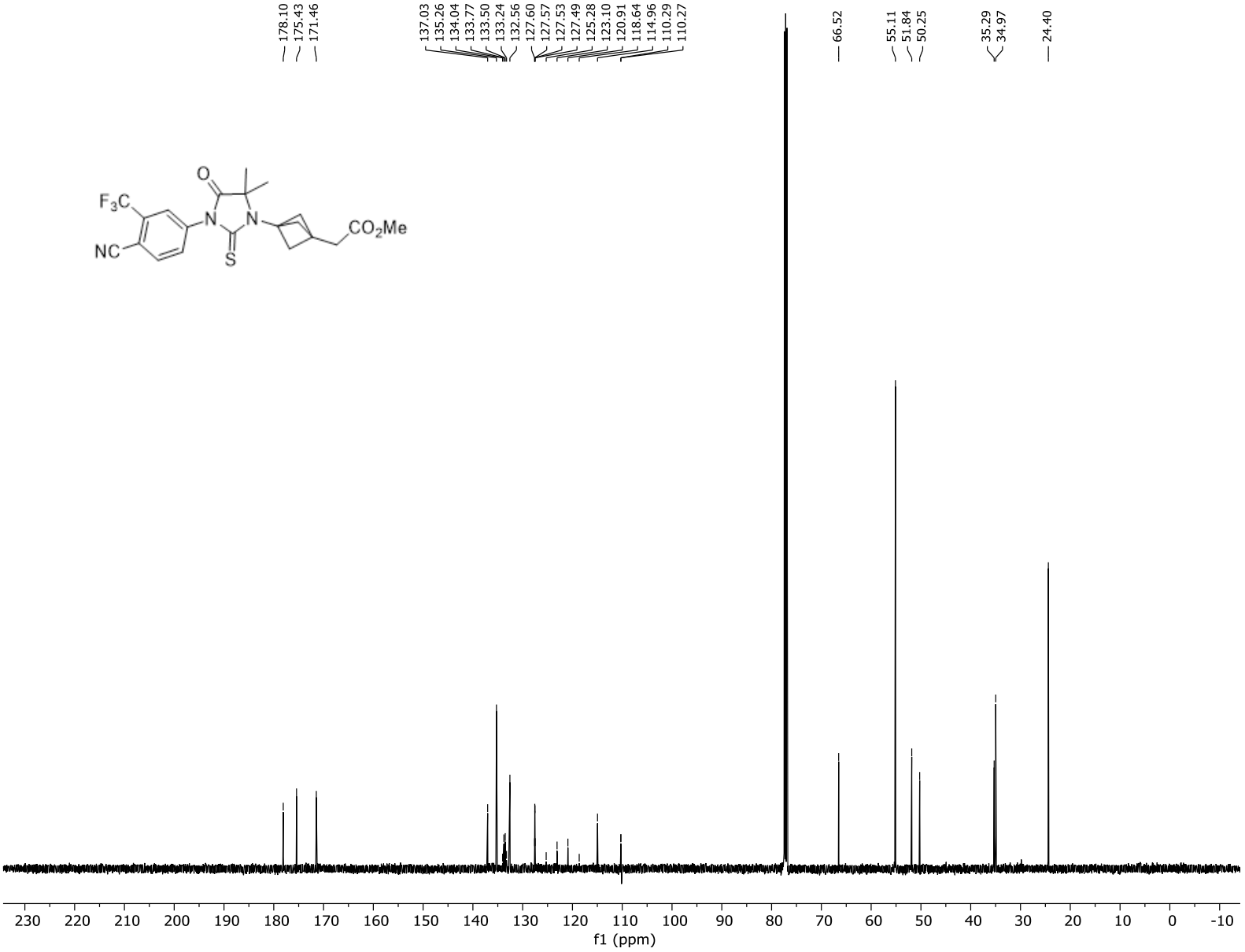


RB-439

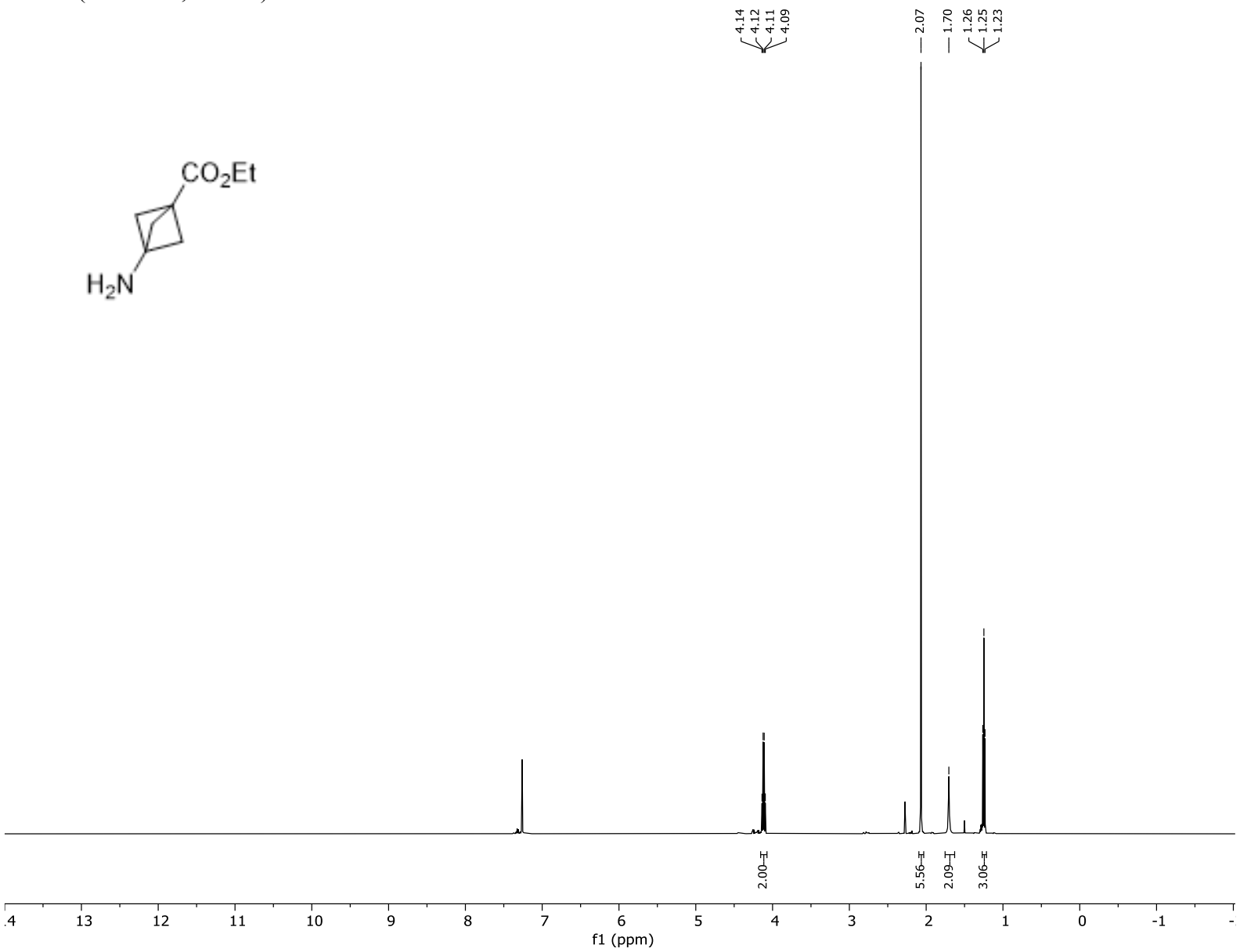
2.53a ^{1}H NMR (500 MHz, $CDCl_3$)



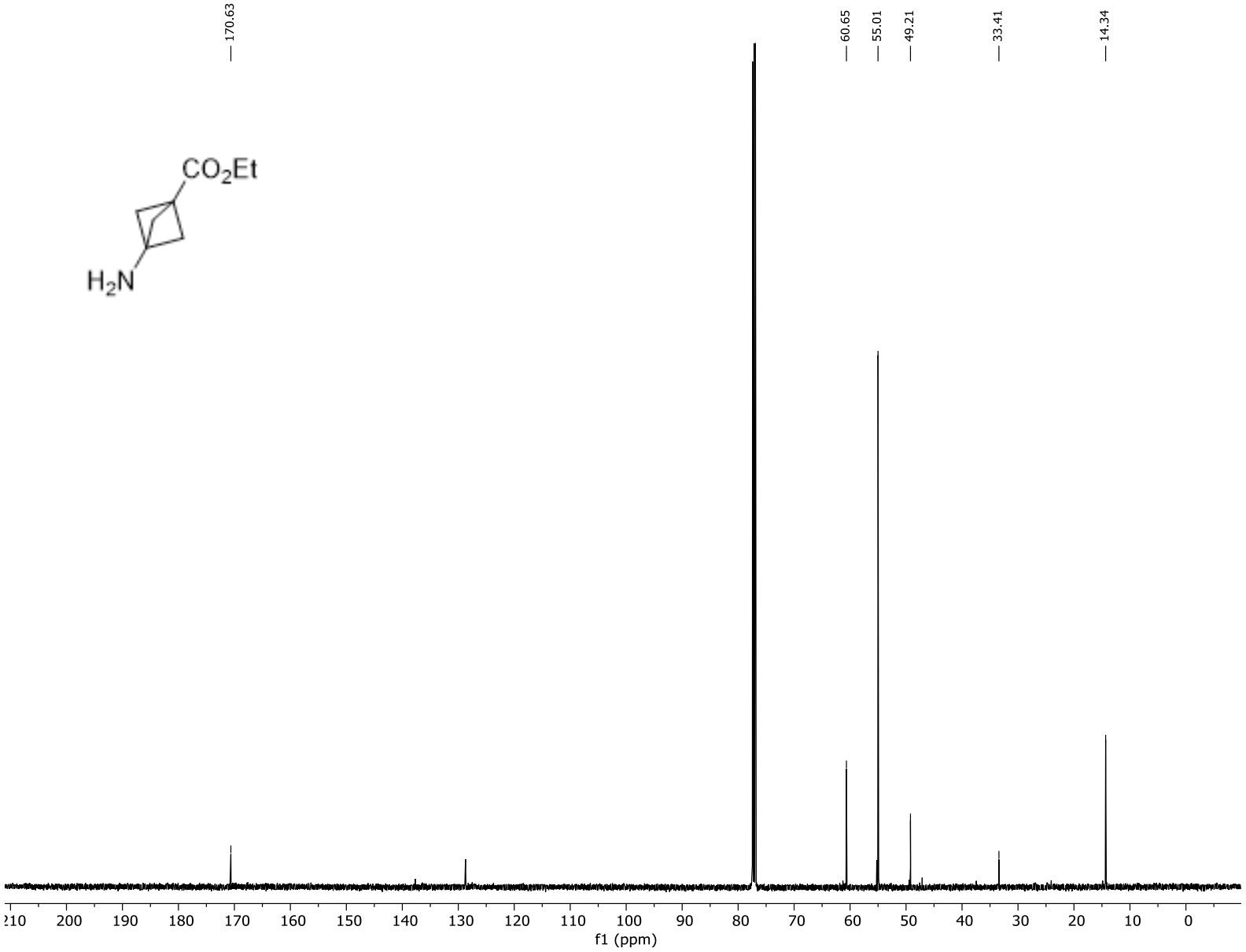
2.53a ^{13}C NMR (126 MHz, $CDCl_3$)



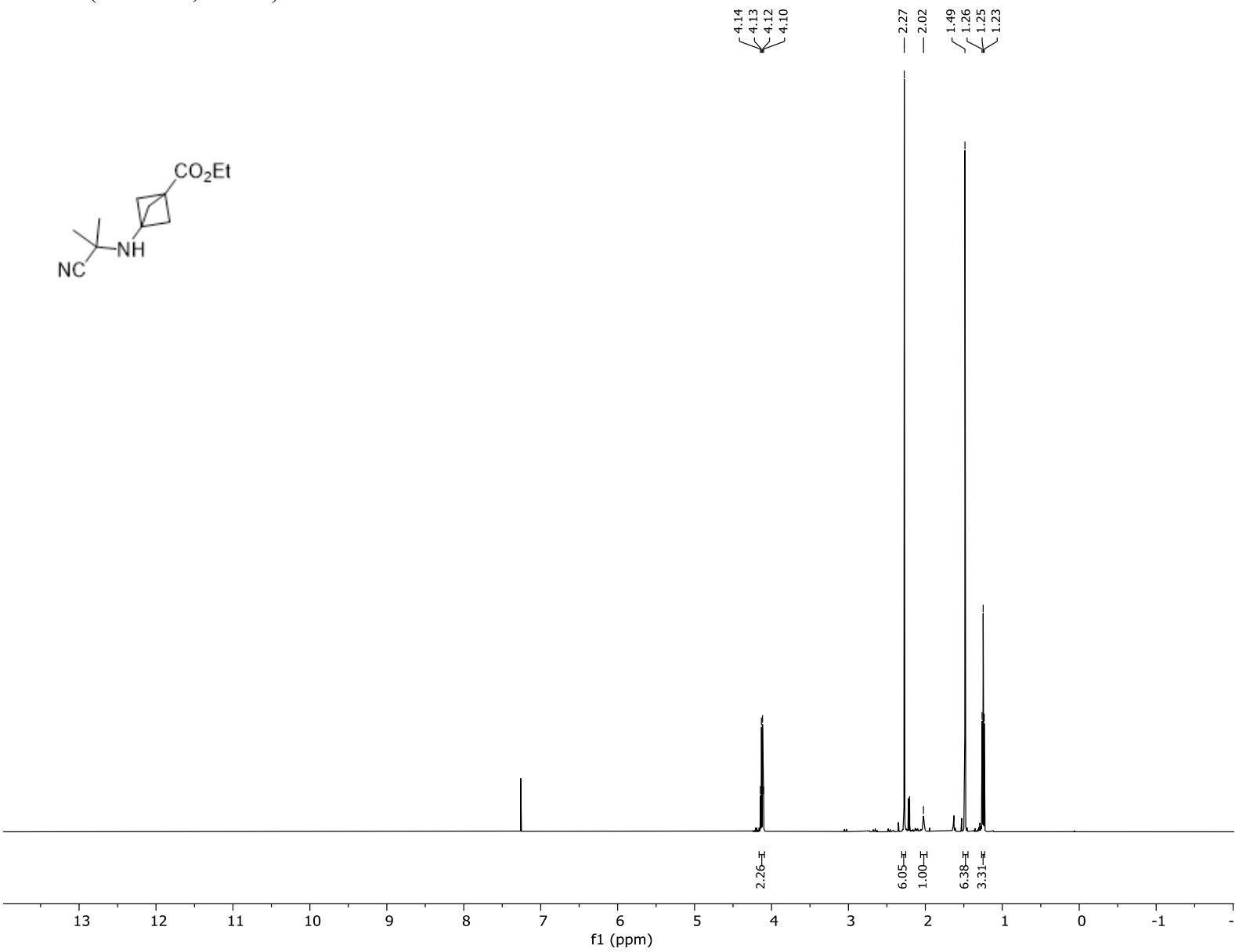
5.5 ^{1}H NMR (500 MHz, $CDCl_3$)



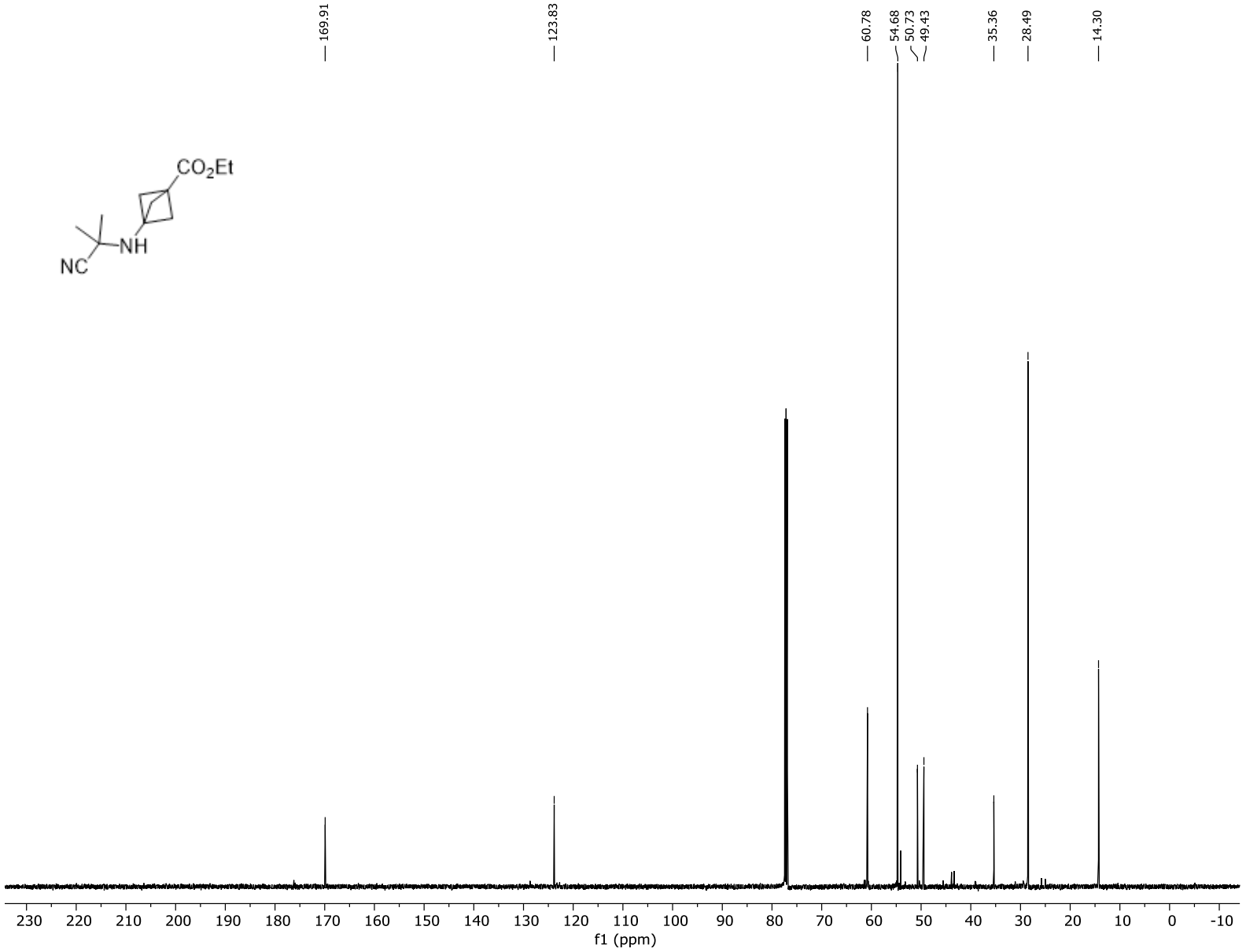
5.5 ^{13}C NMR (126 MHz, $CDCl_3$)



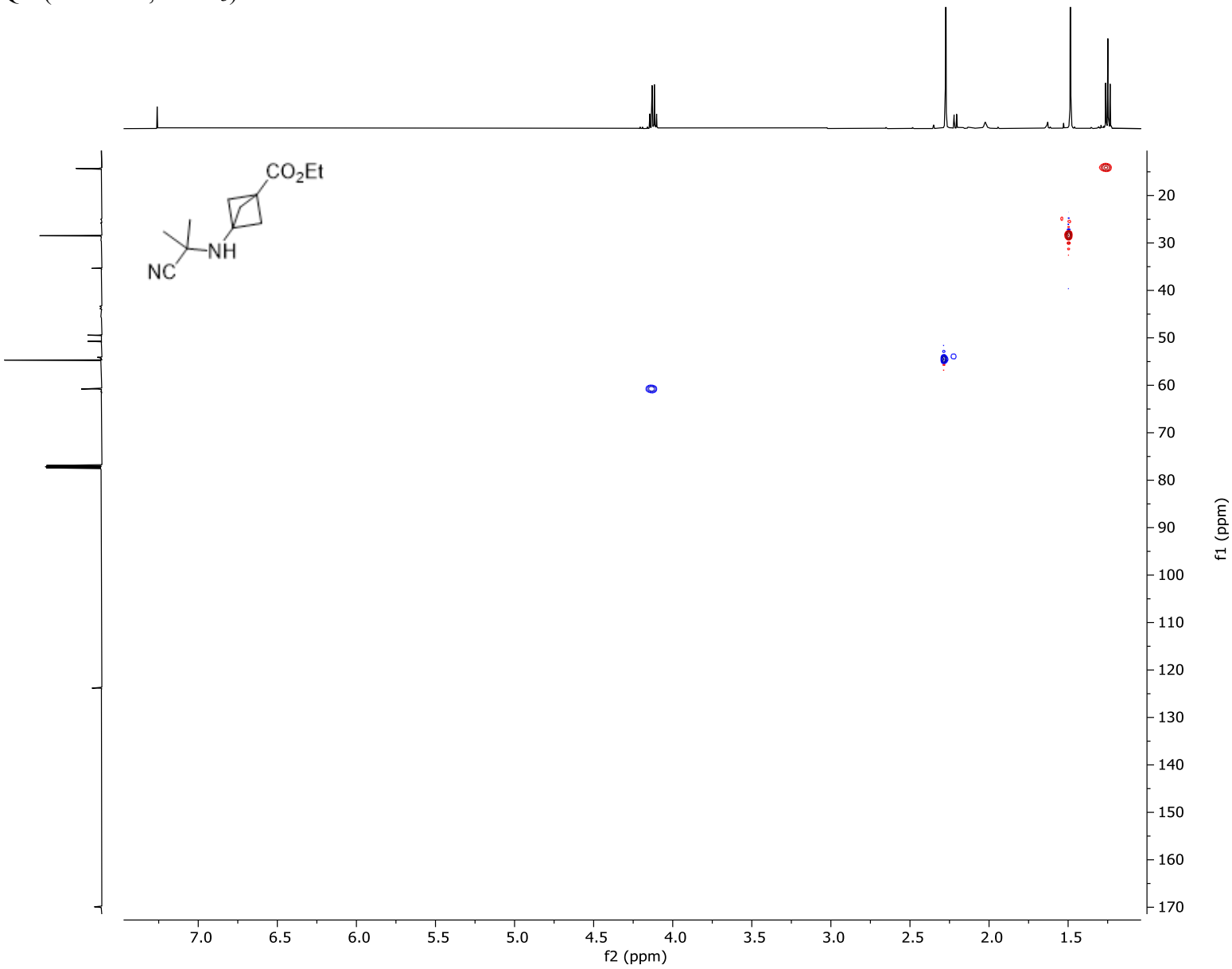
2.56 ^{1}H NMR (500 MHz, $CDCl_3$)



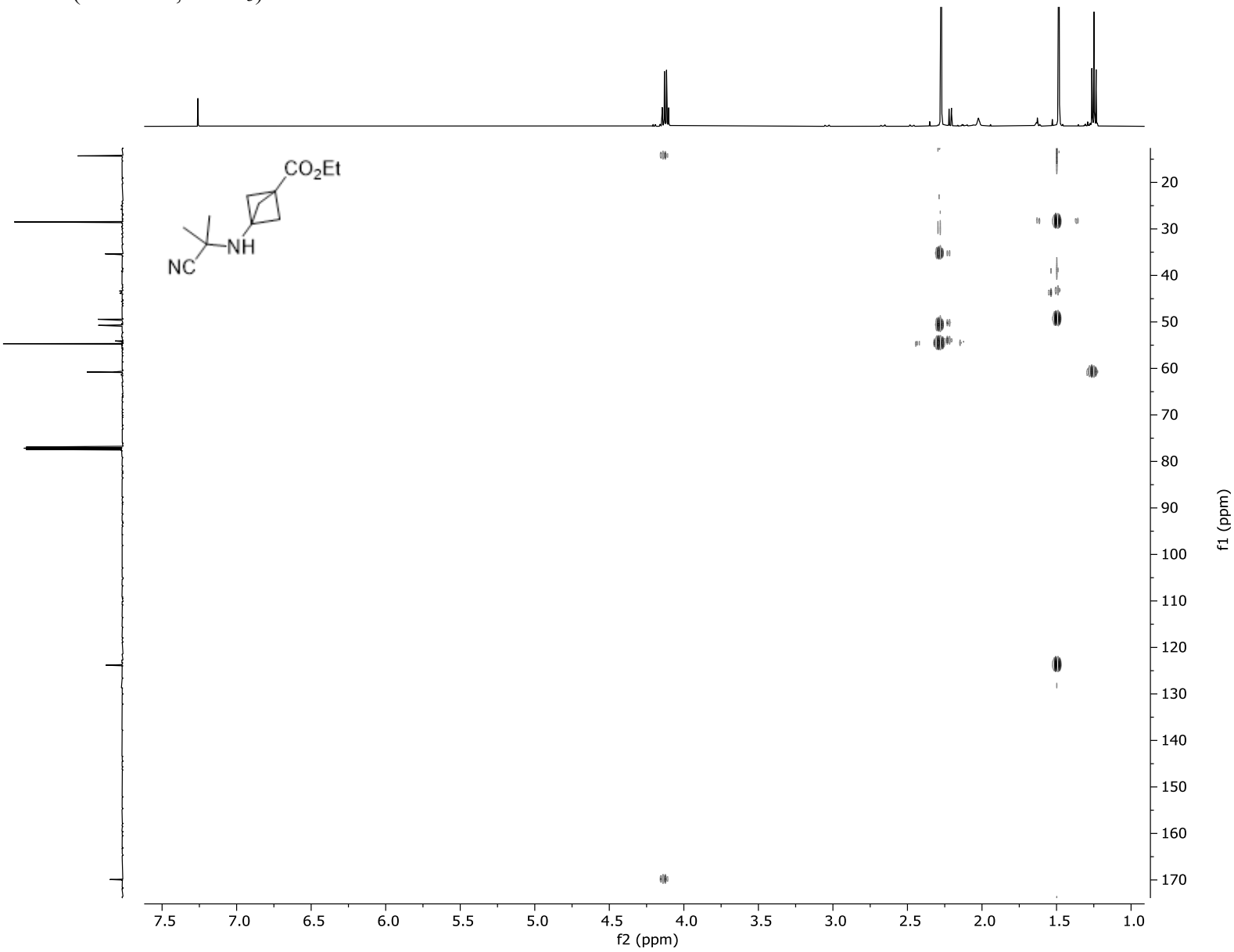
2.56 ^{13}C NMR (126 MHz, $CDCl_3$)



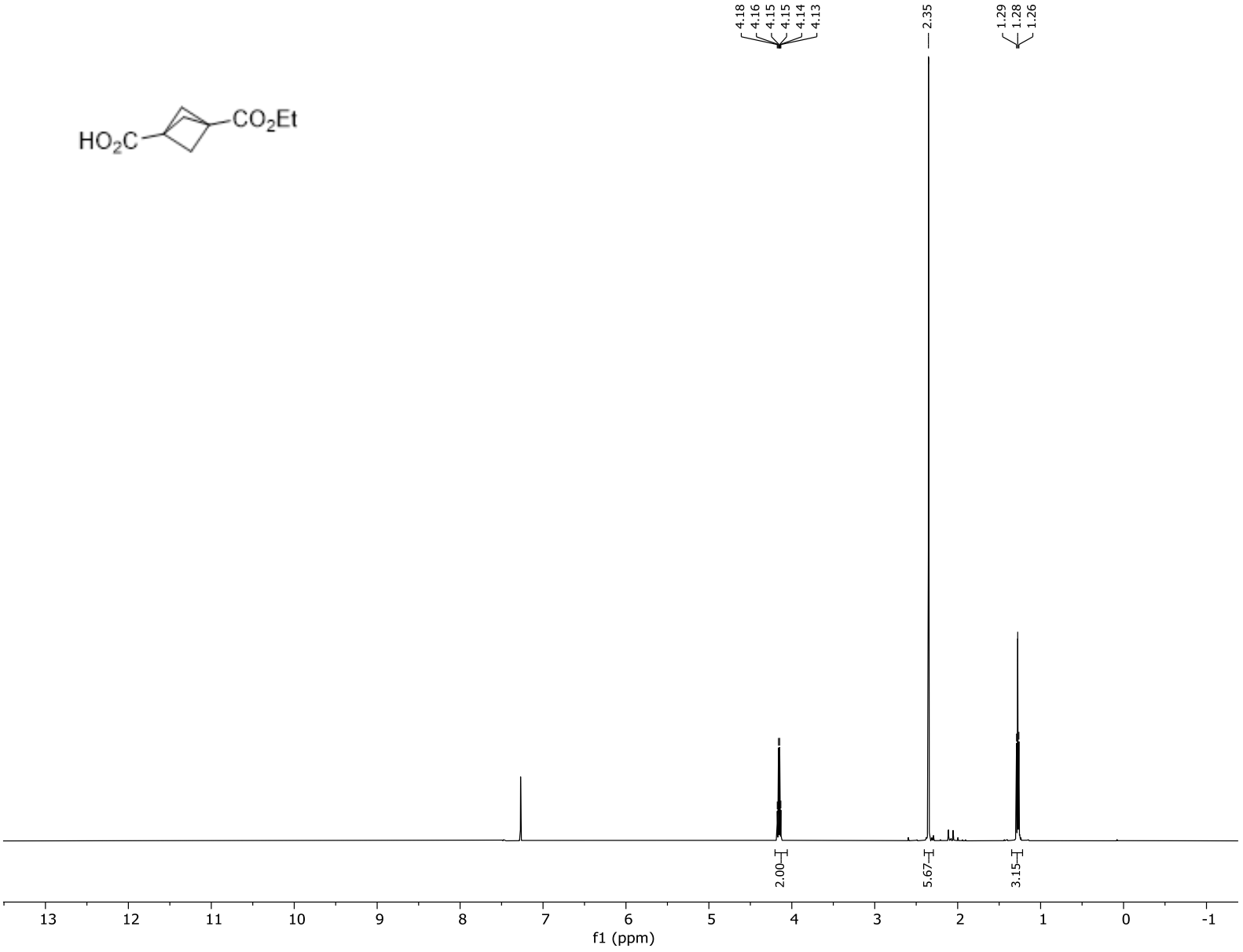
2.56 HSQC (500 MHz, $CDCl_3$)



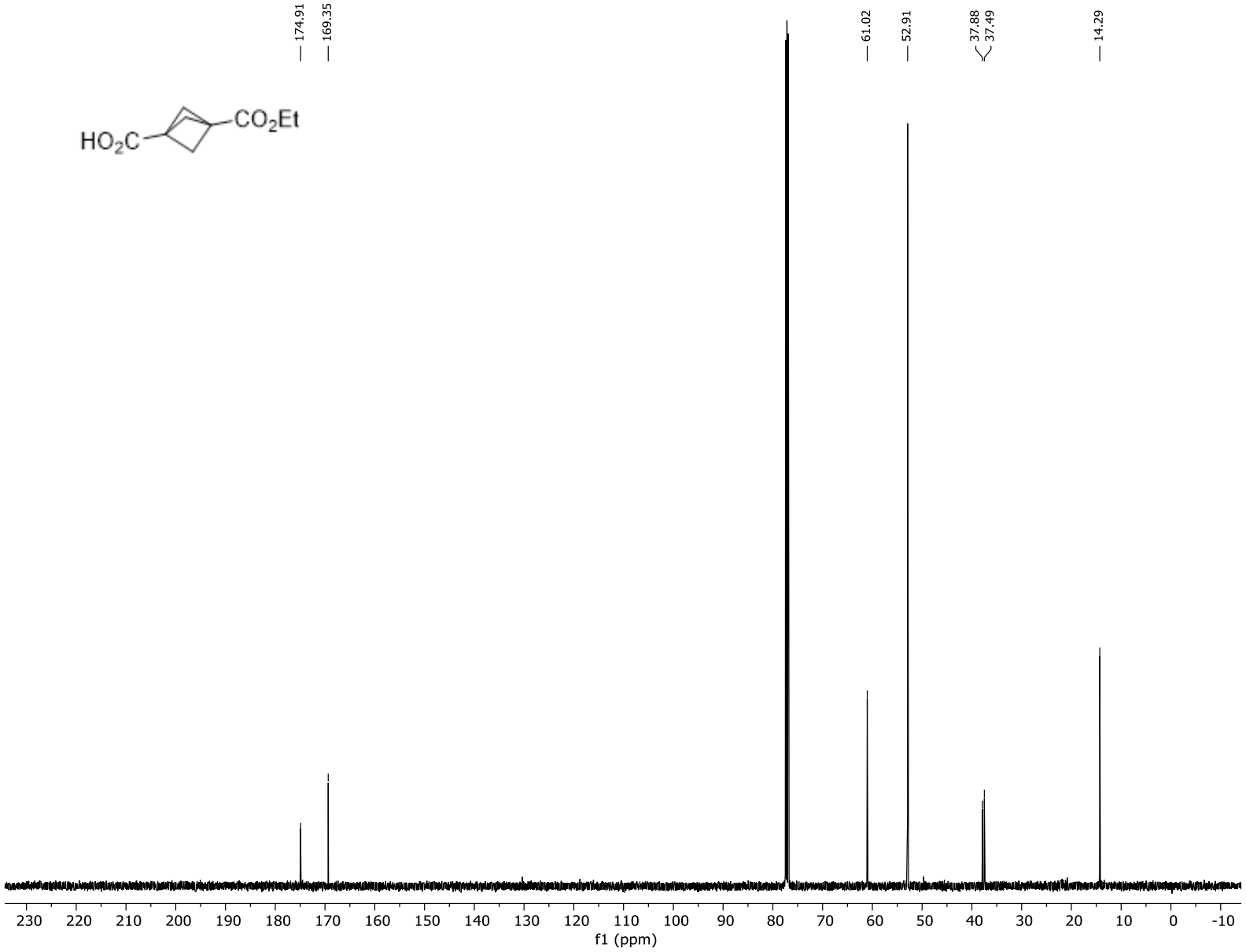
2.56 HMBC (500 MHz, $CDCl_3$)



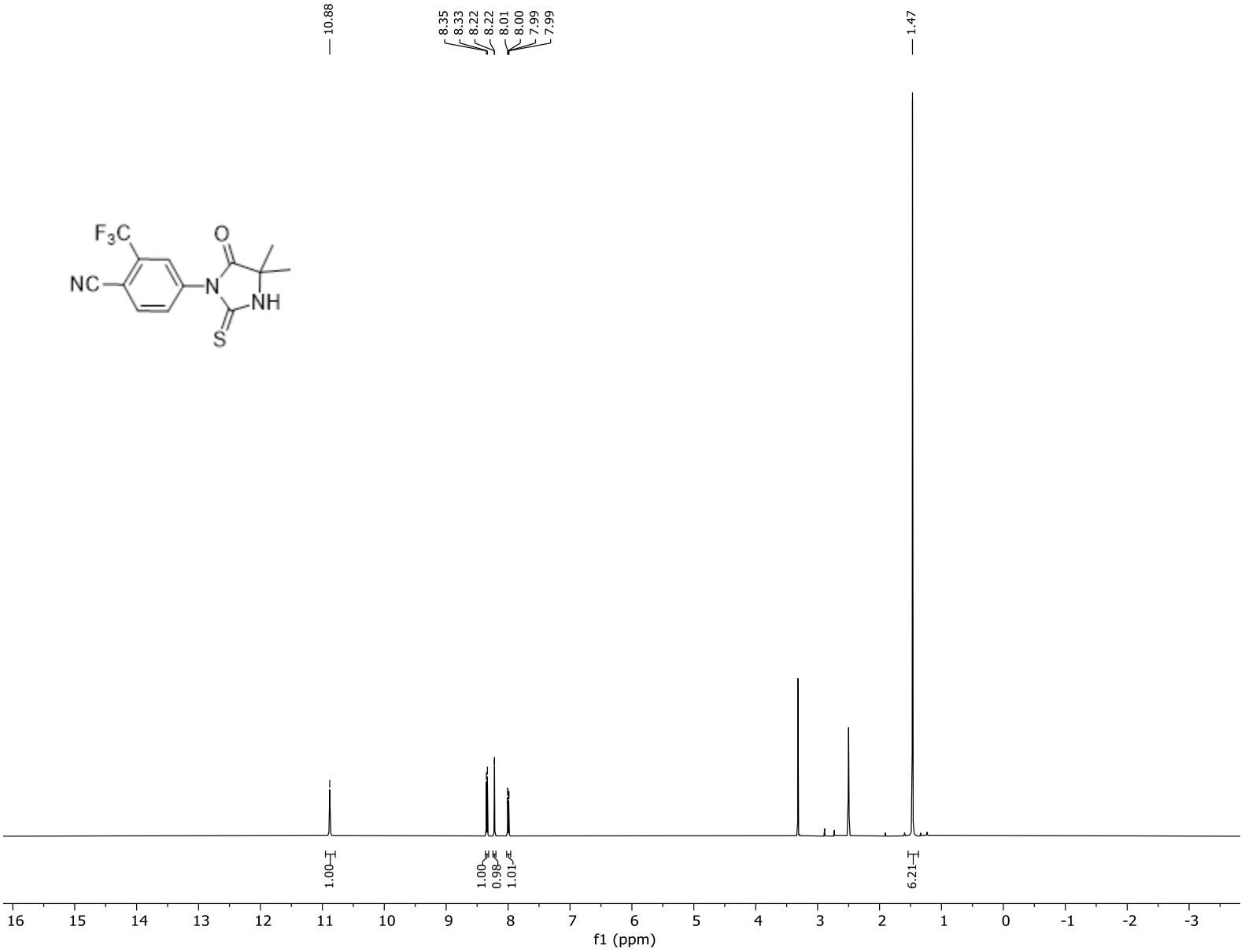
2.59 ^{1}H NMR (500 MHz, $CDCl_3$)



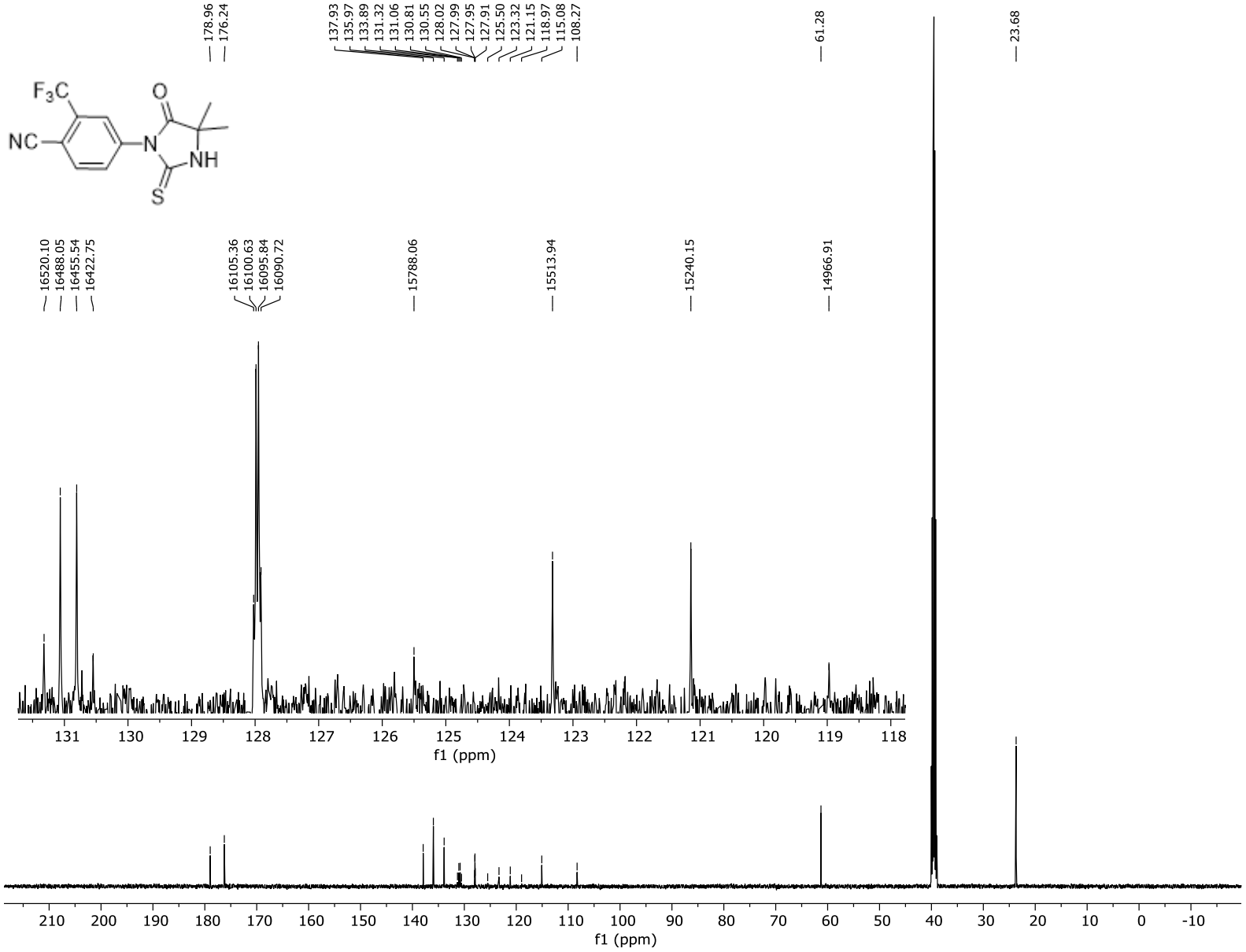
2.59 ^{13}C NMR (126 MHz, $CDCl_3$)



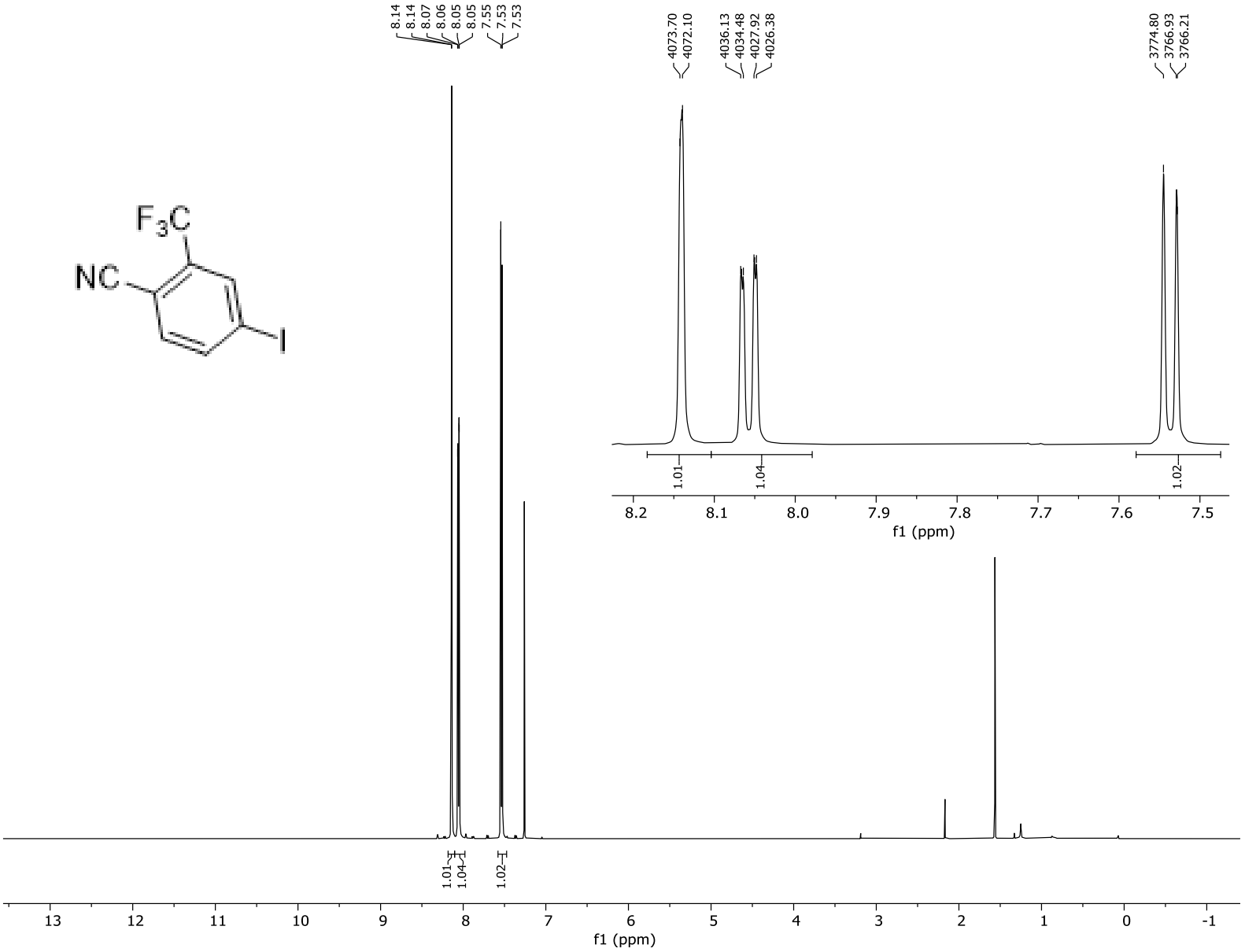
2.61 ^{1}H NMR (500 MHz, DMSO-d_6)



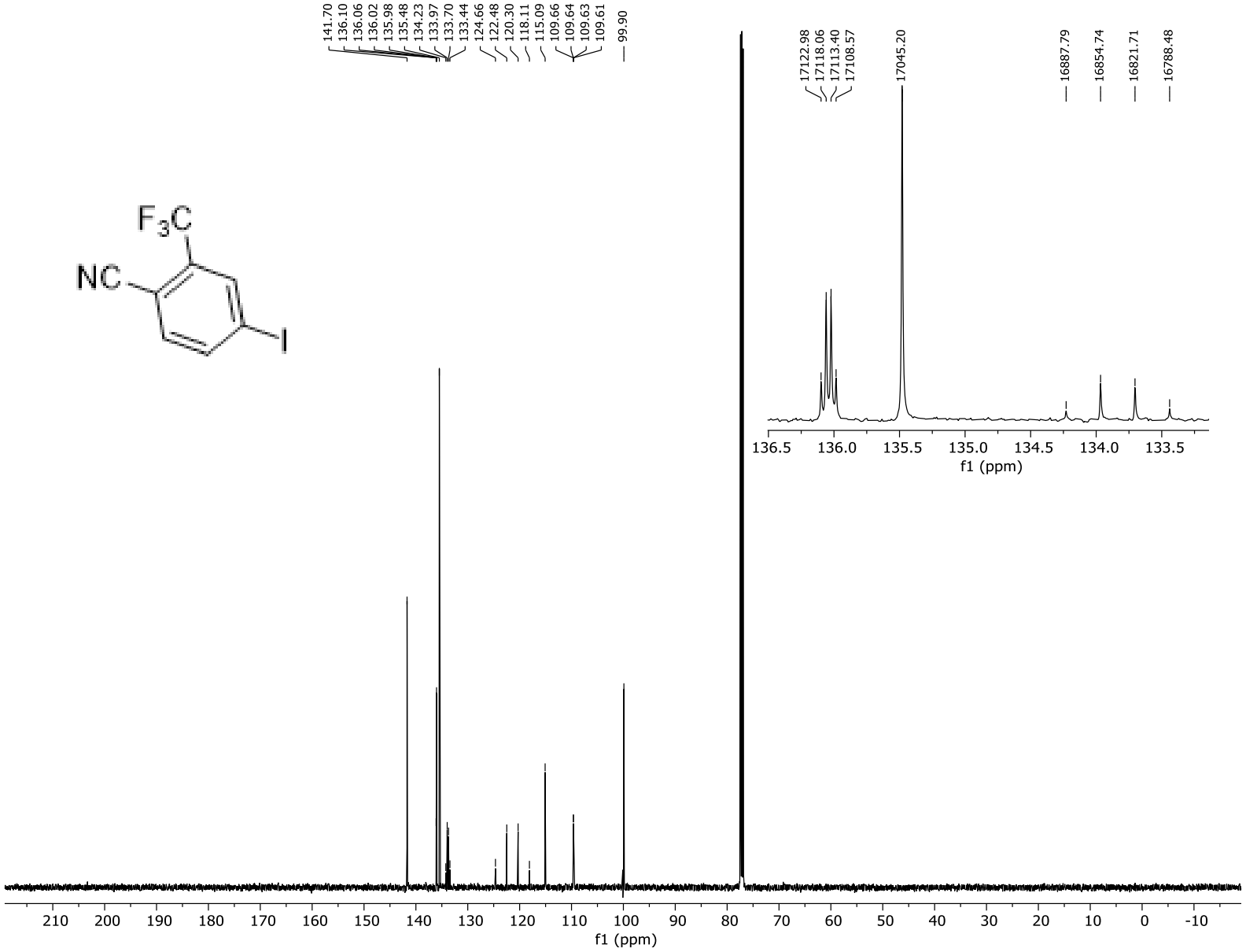
2.61 ^{13}C NMR (126 MHz, DMSO-d_6)



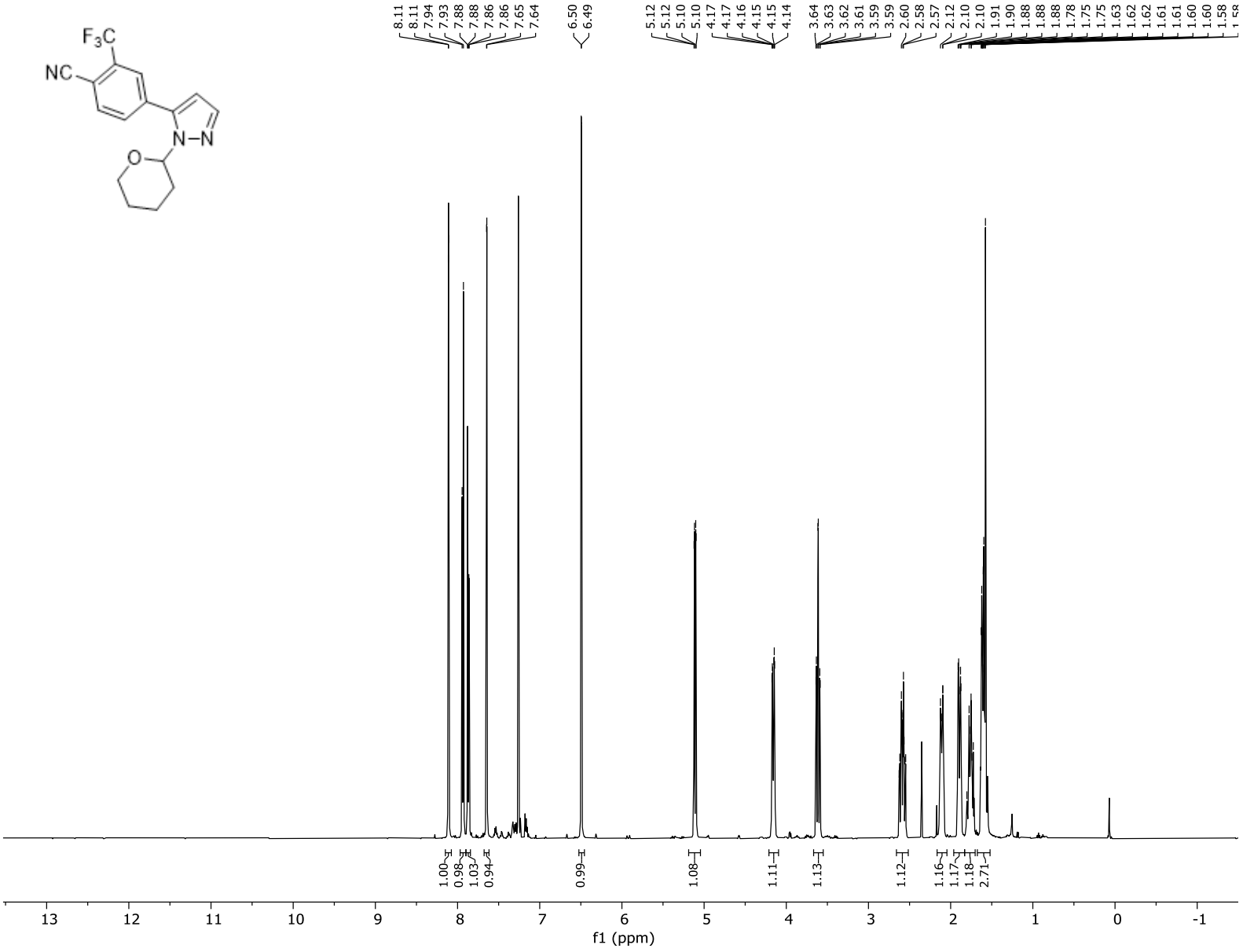
2.65 ^{1}H NMR (500 MHz, $CDCl_3$)



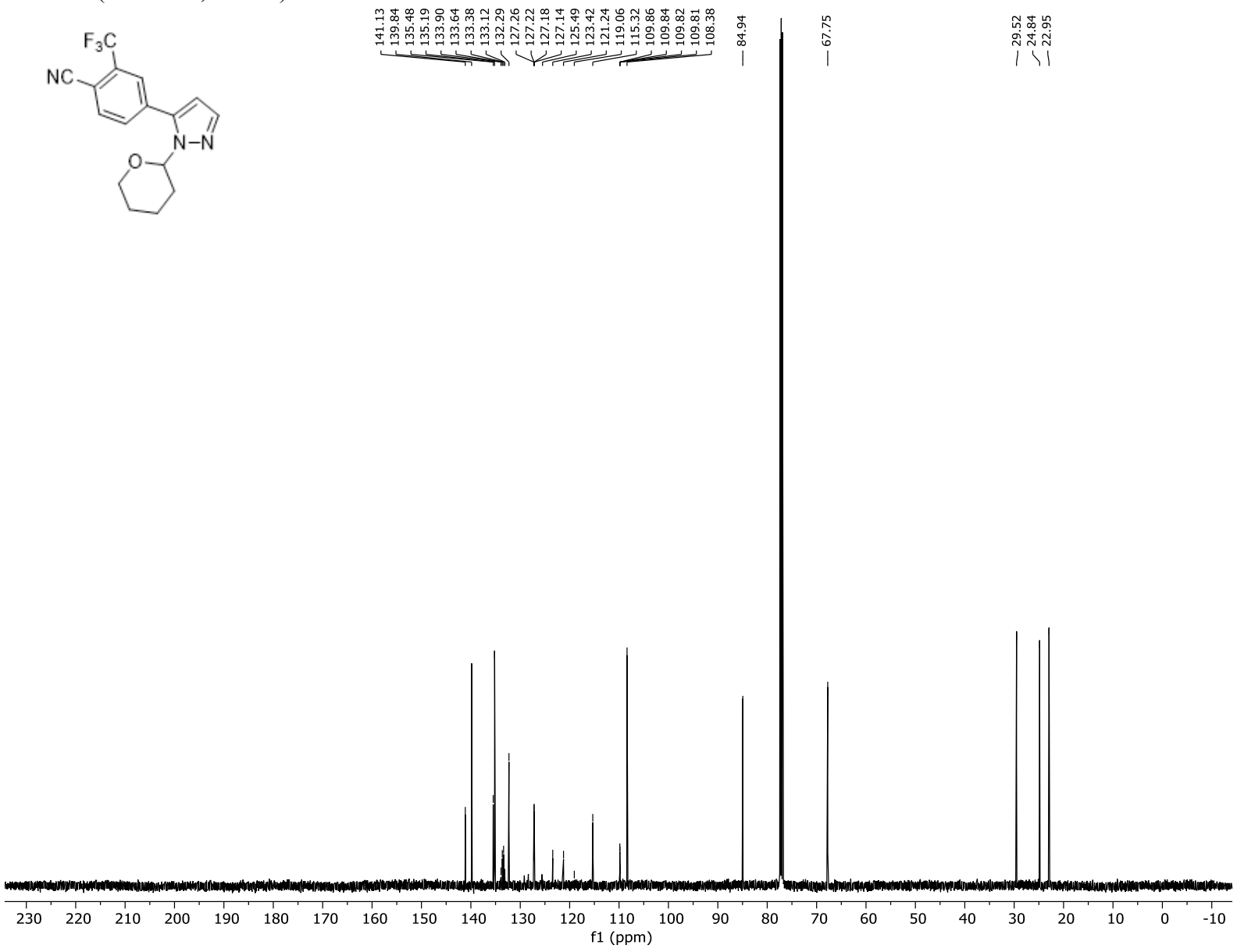
2.65 ^{13}C NMR (126 MHz, $CDCl_3$)



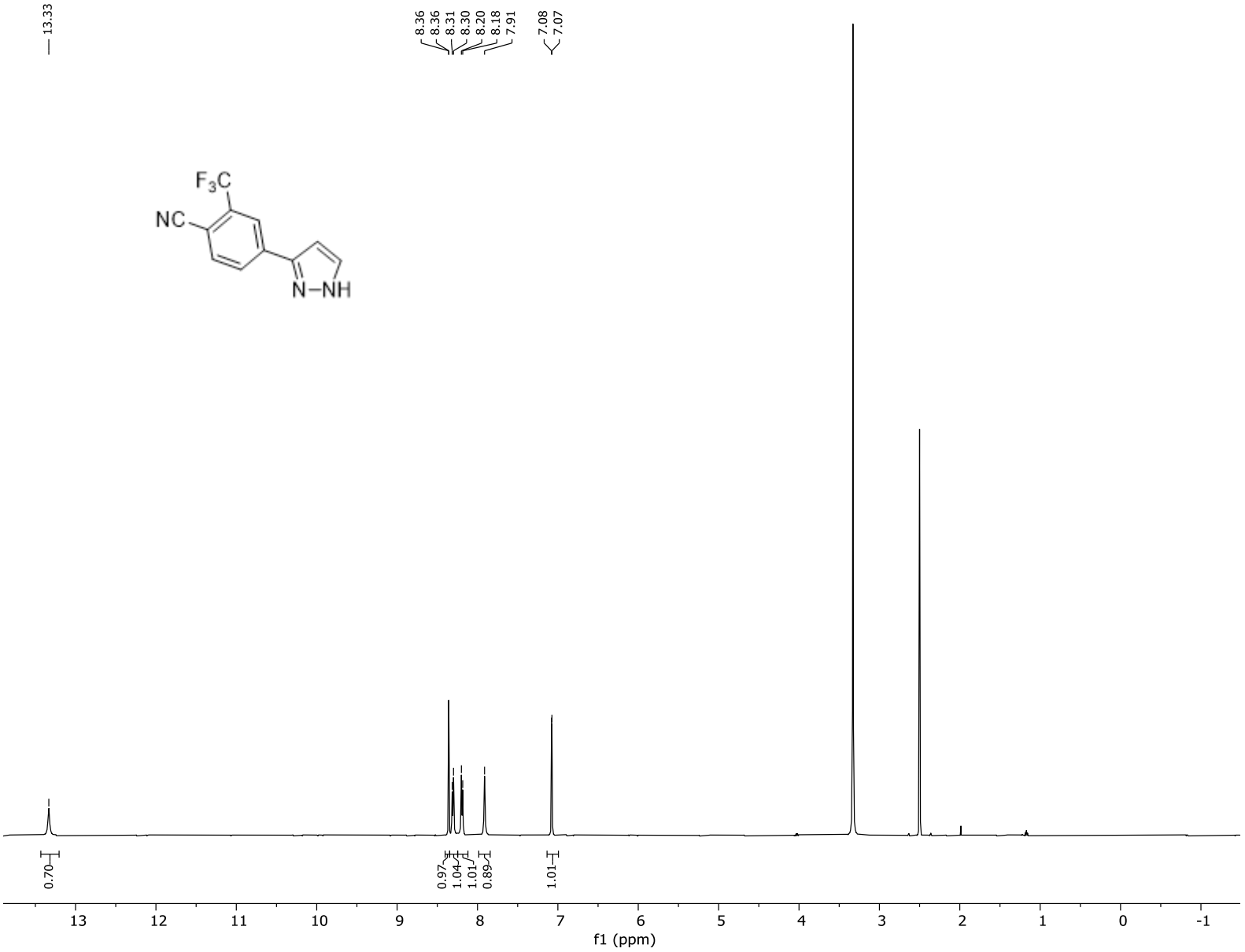
2.66 ^{1}H NMR (500 MHz, $CDCl_3$)



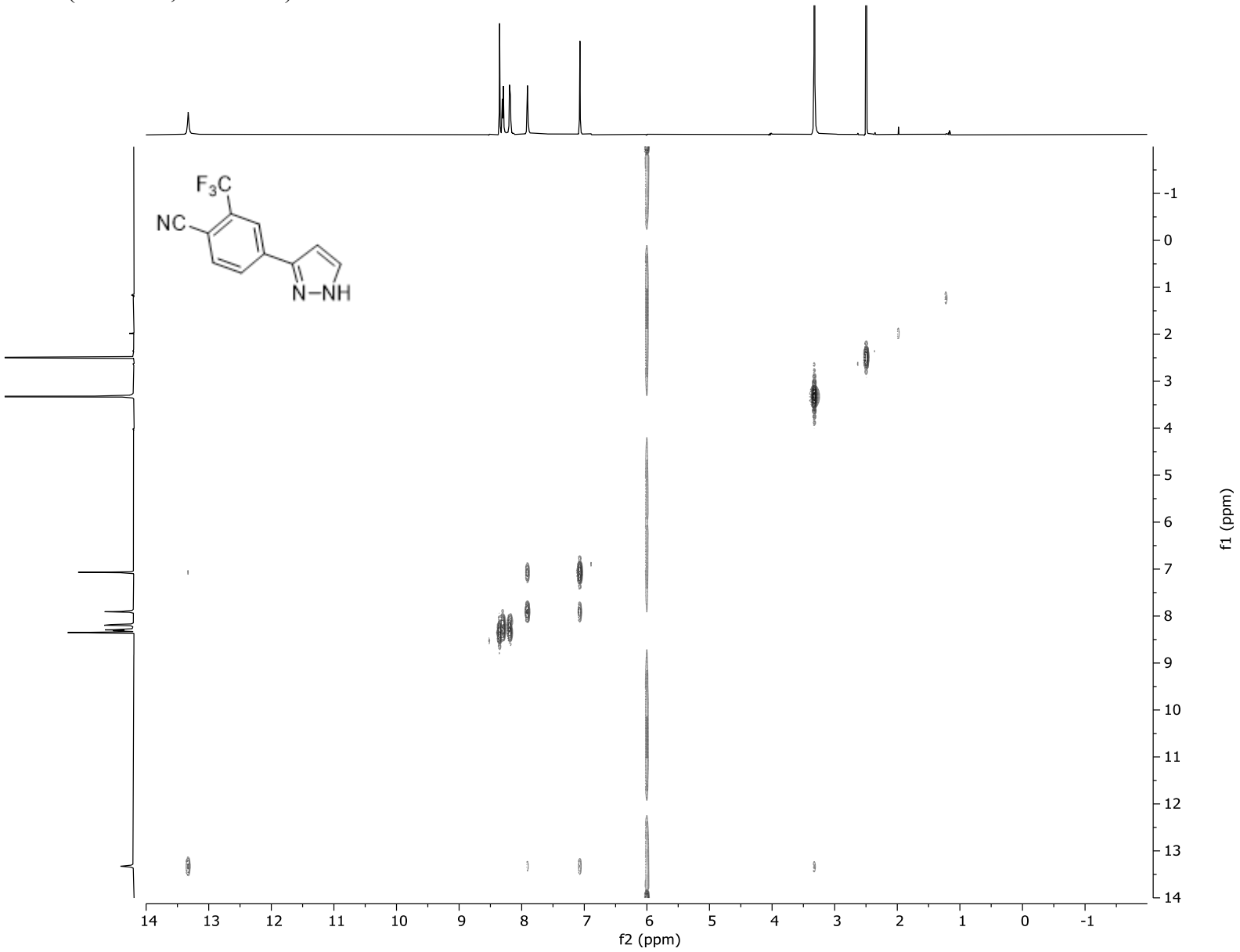
2.66 ^{13}C NMR (126 MHz, $CDCl_3$)



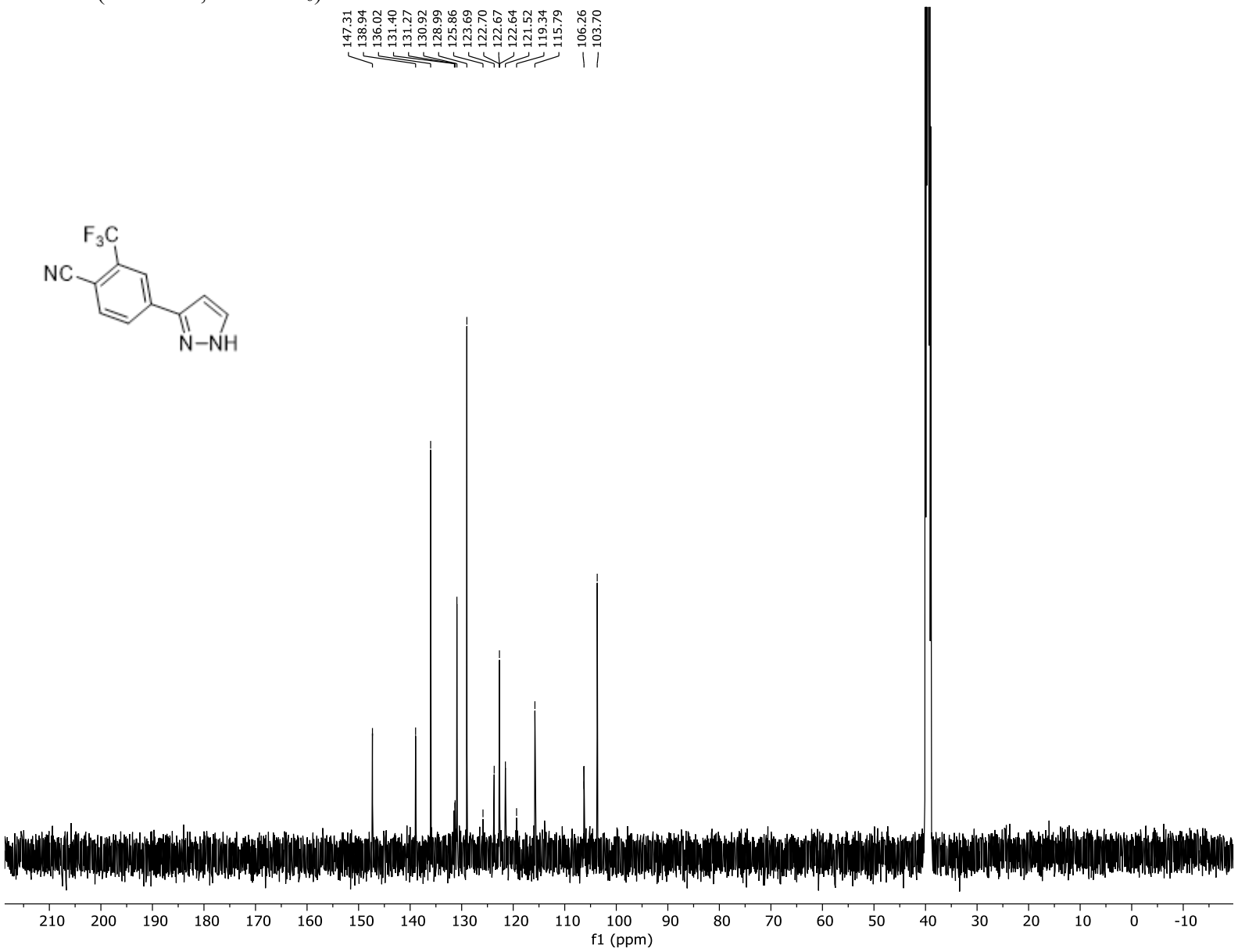
2.67 ^{1}H NMR (500 MHz, DMSO-d_6)



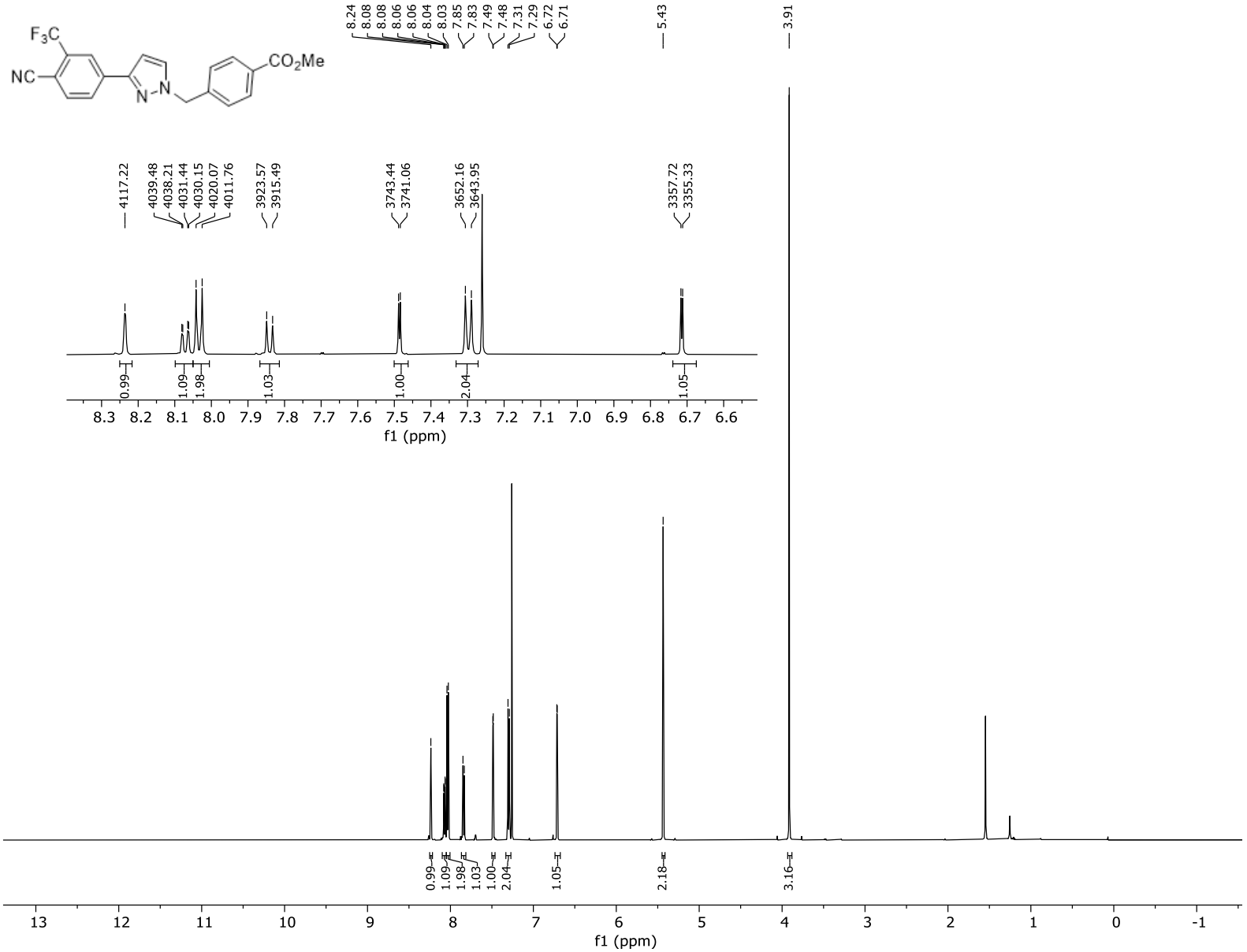
2.67 COSY (500 MHz, DMSO-d_6)



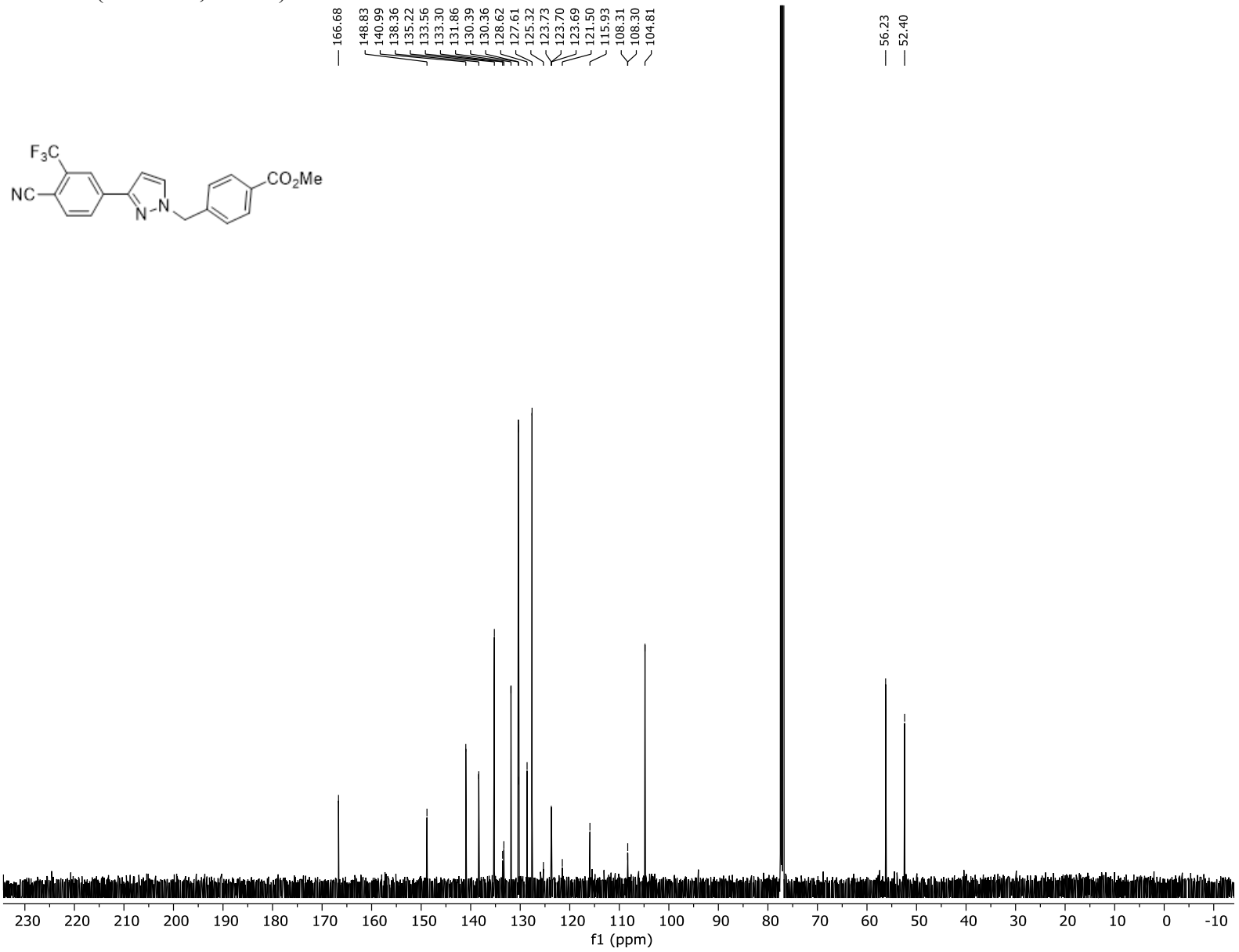
2.67 ^{13}C NMR (126 MHz, DMSO-d_6)



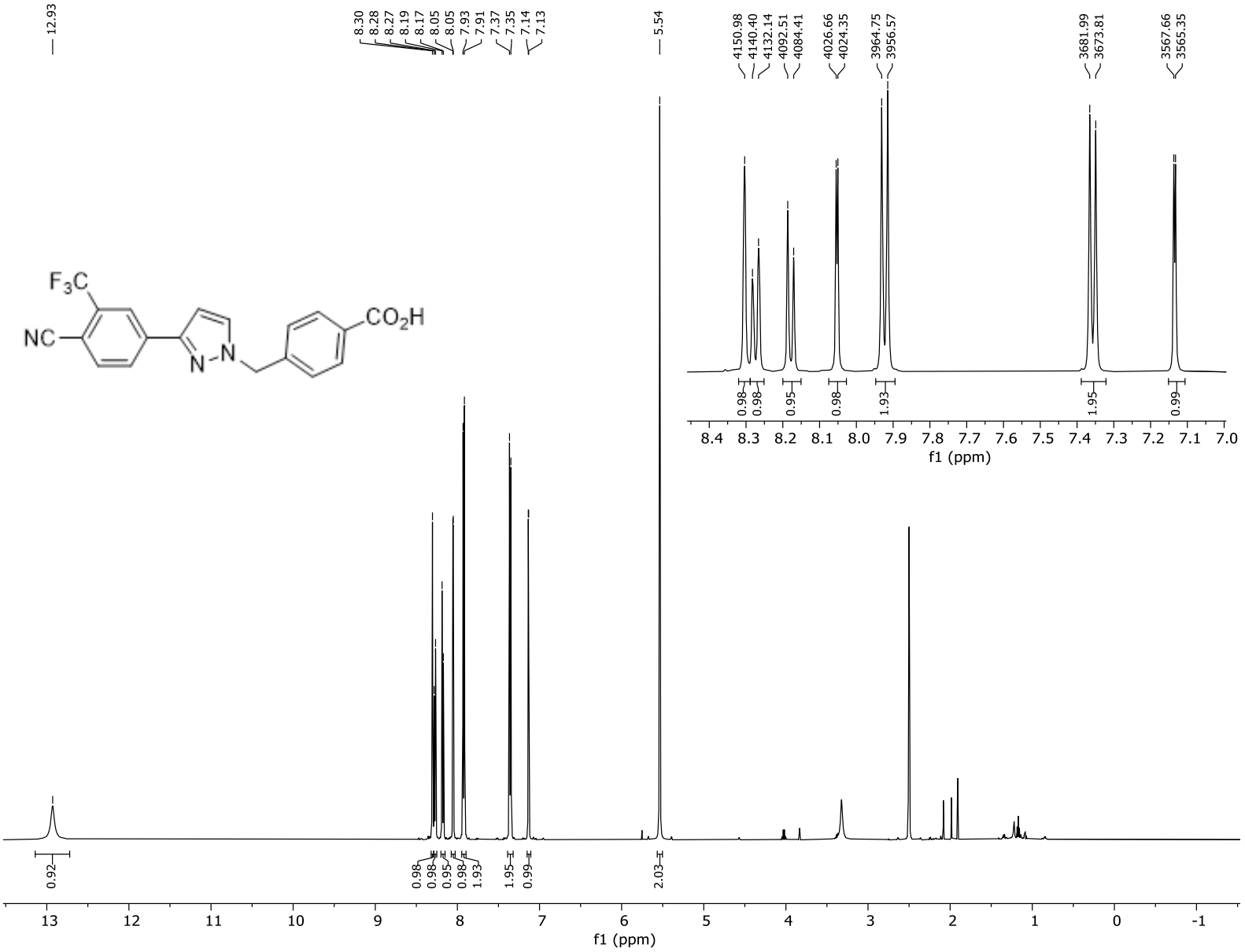
2.68 ^{1}H NMR (500 MHz, $CDCl_3$)



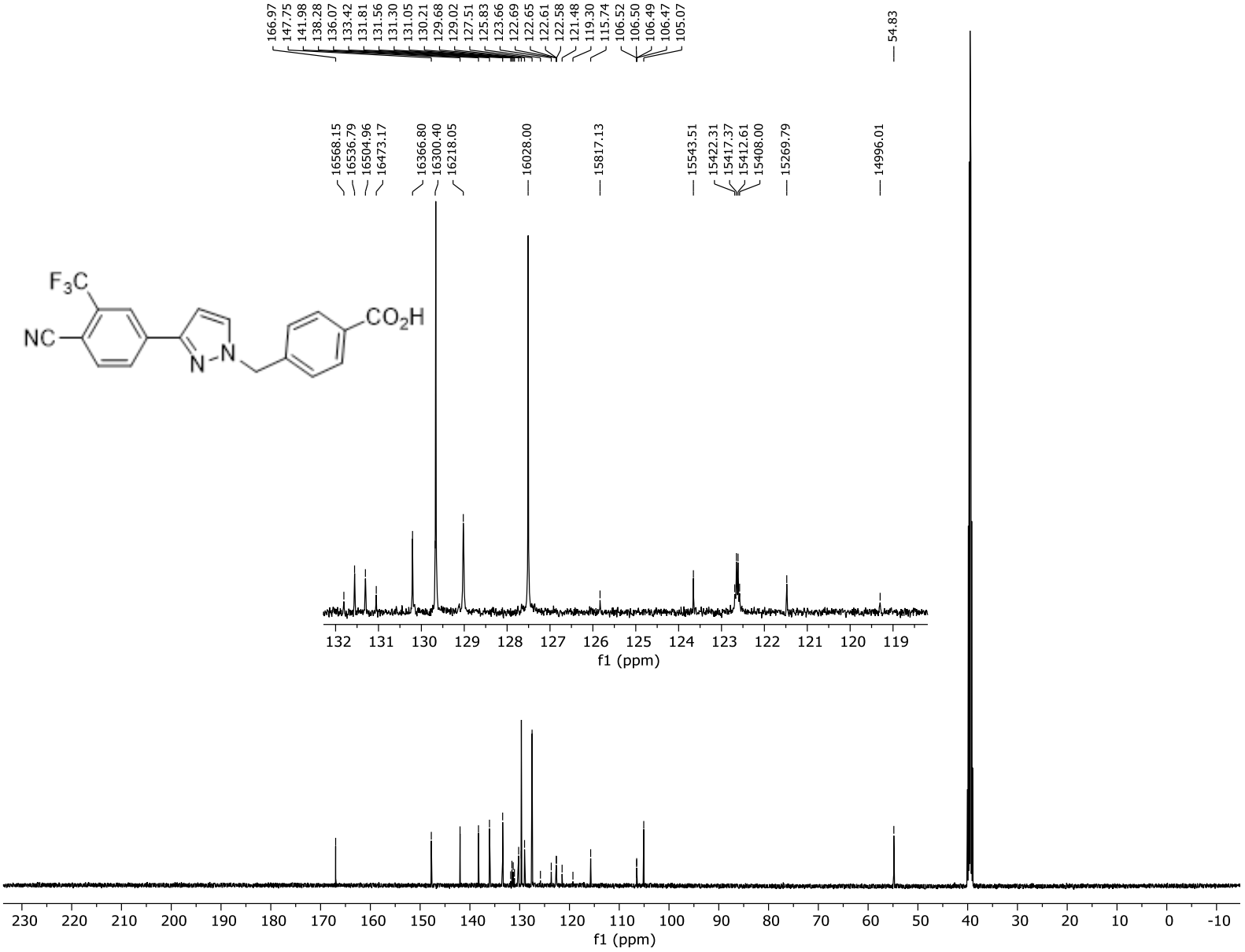
2.68 ^{13}C NMR (126 MHz, $CDCl_3$)



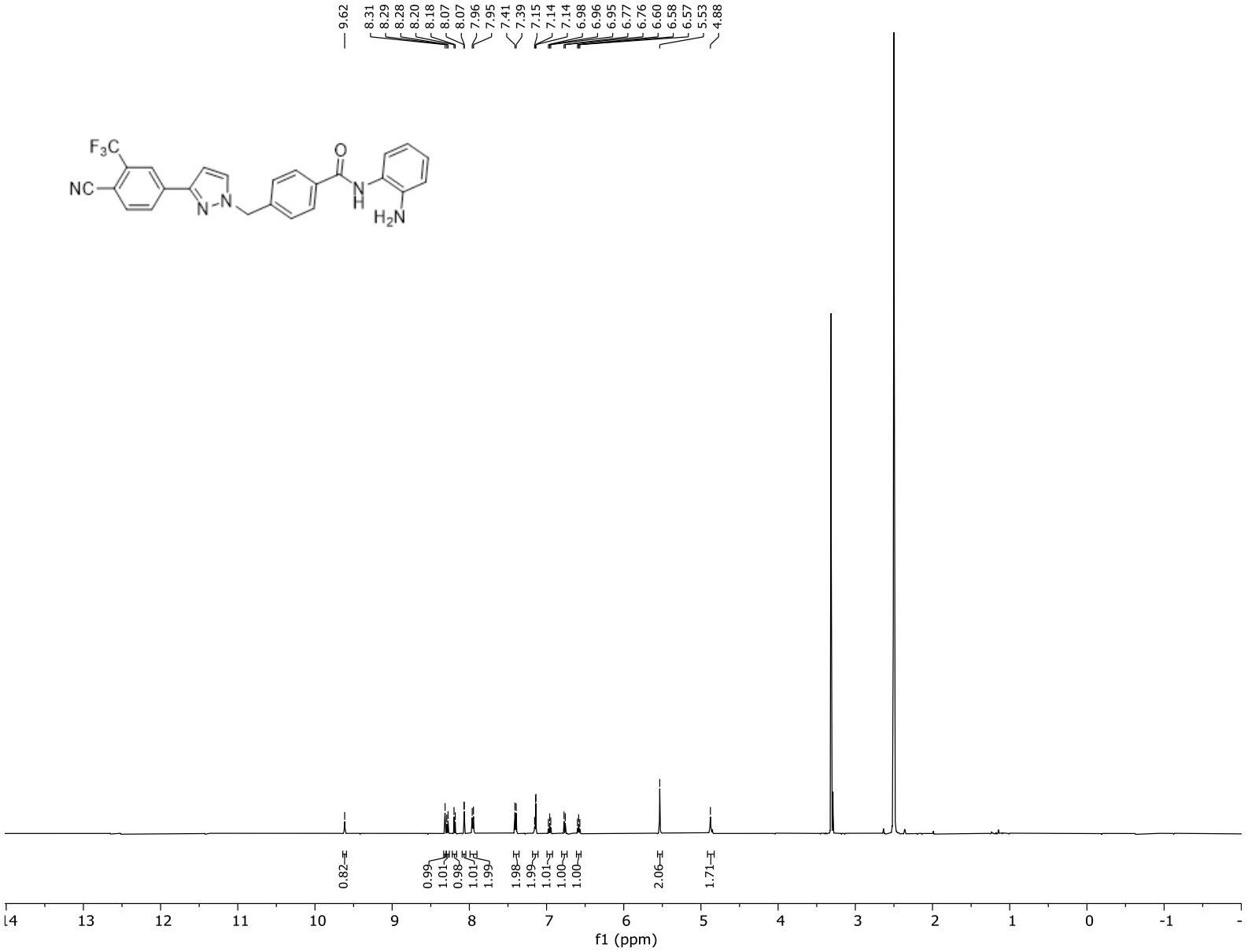
2.69 ^{1}H NMR (500 MHz, DMSO-d_6)



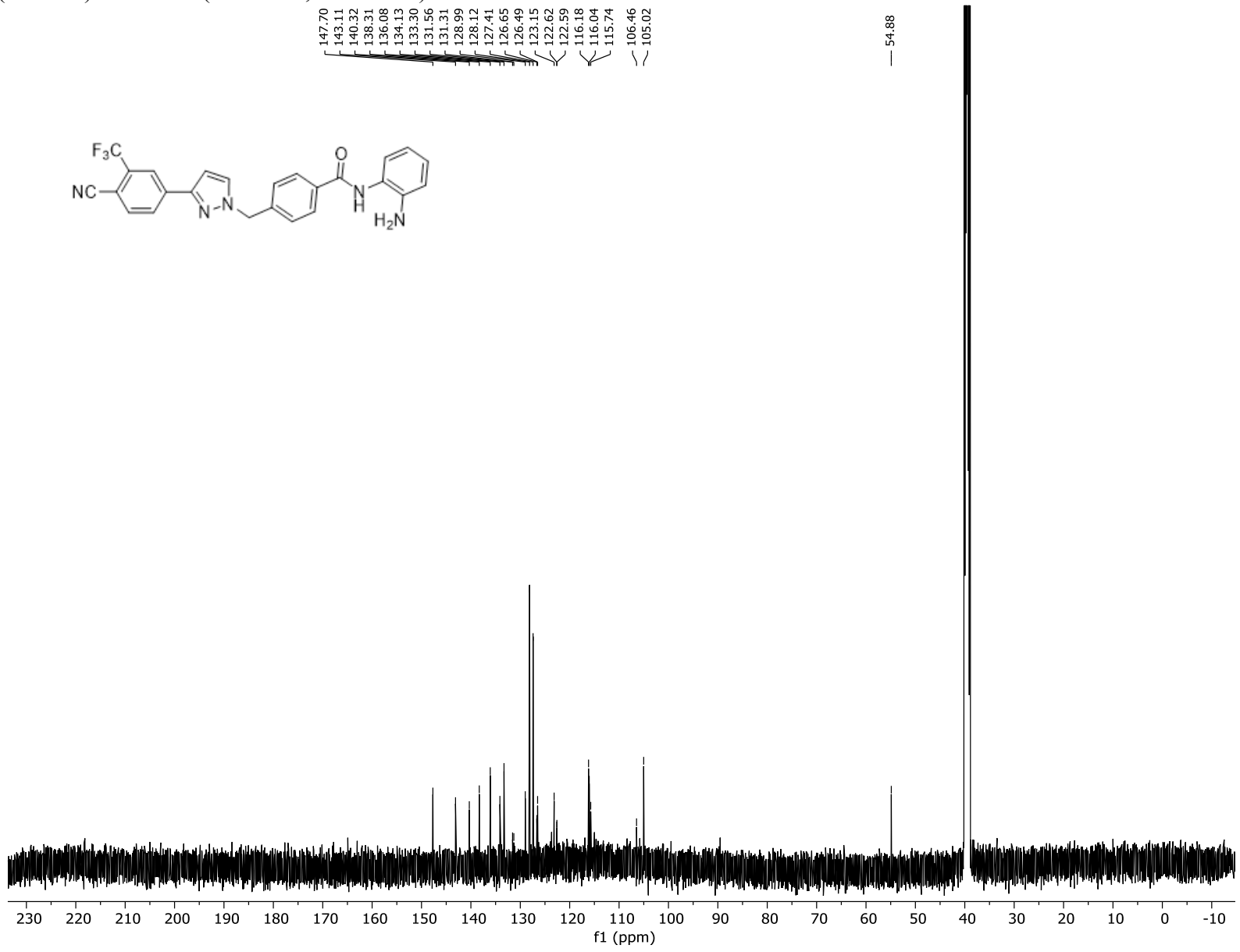
2.69 ^{13}C NMR (126 MHz, DMSO-d_6)



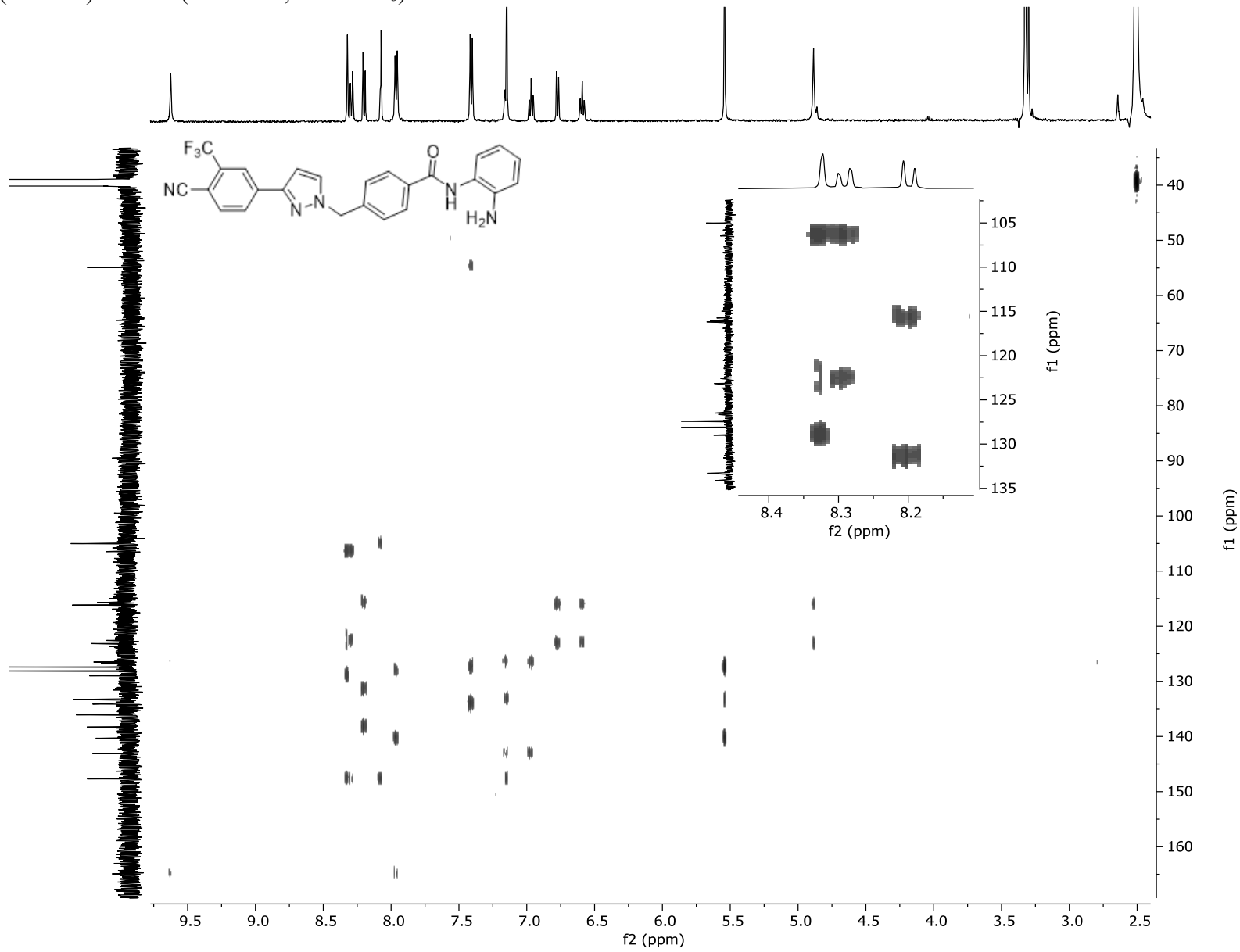
2.42 (RB-461) ^{1}H NMR (500 MHz, DMSO-d_6)



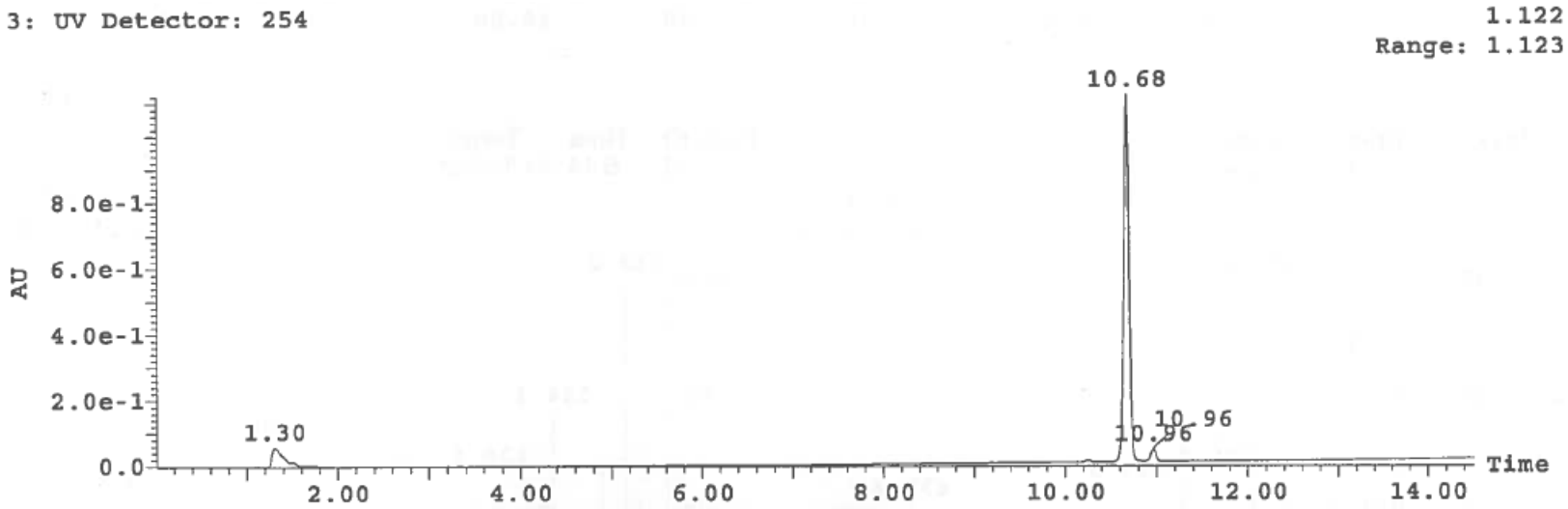
2.42 (RB-461) ^{13}C NMR (126 MHz, DMSO-d_6)



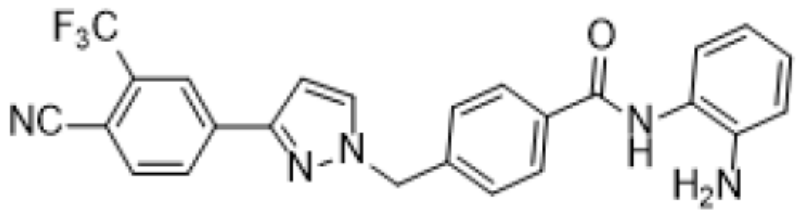
2.42 (RB-461) HMBC (500 MHz, DMSO-d_6)



2.42 (RB-461) LC-MS UV trace

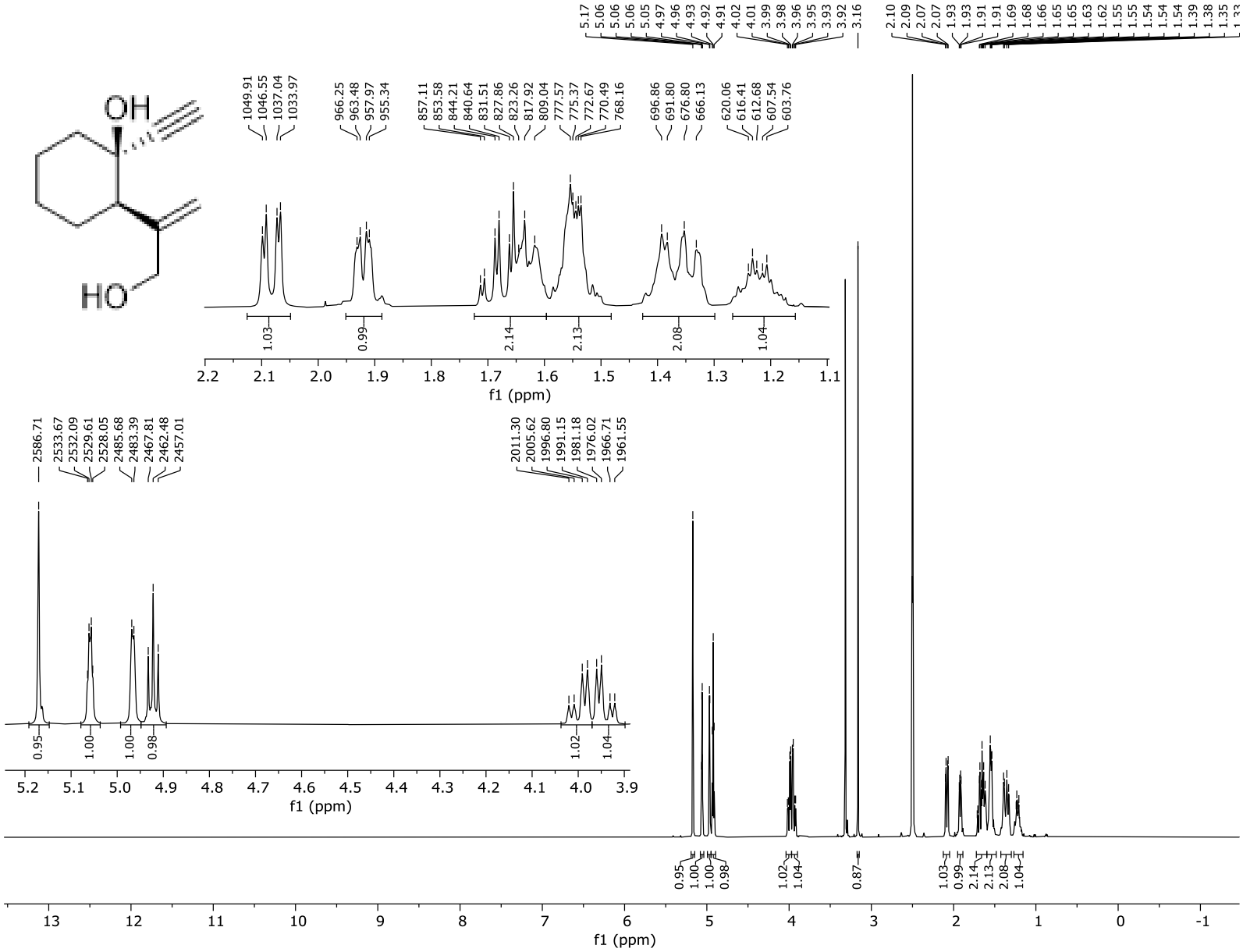


Peak Number	Time	AreaAbs	Area %Total	Height	Mass Found
15	10.68	72901	96.82	1109194	
16	10.96	2398	3.18	37041	

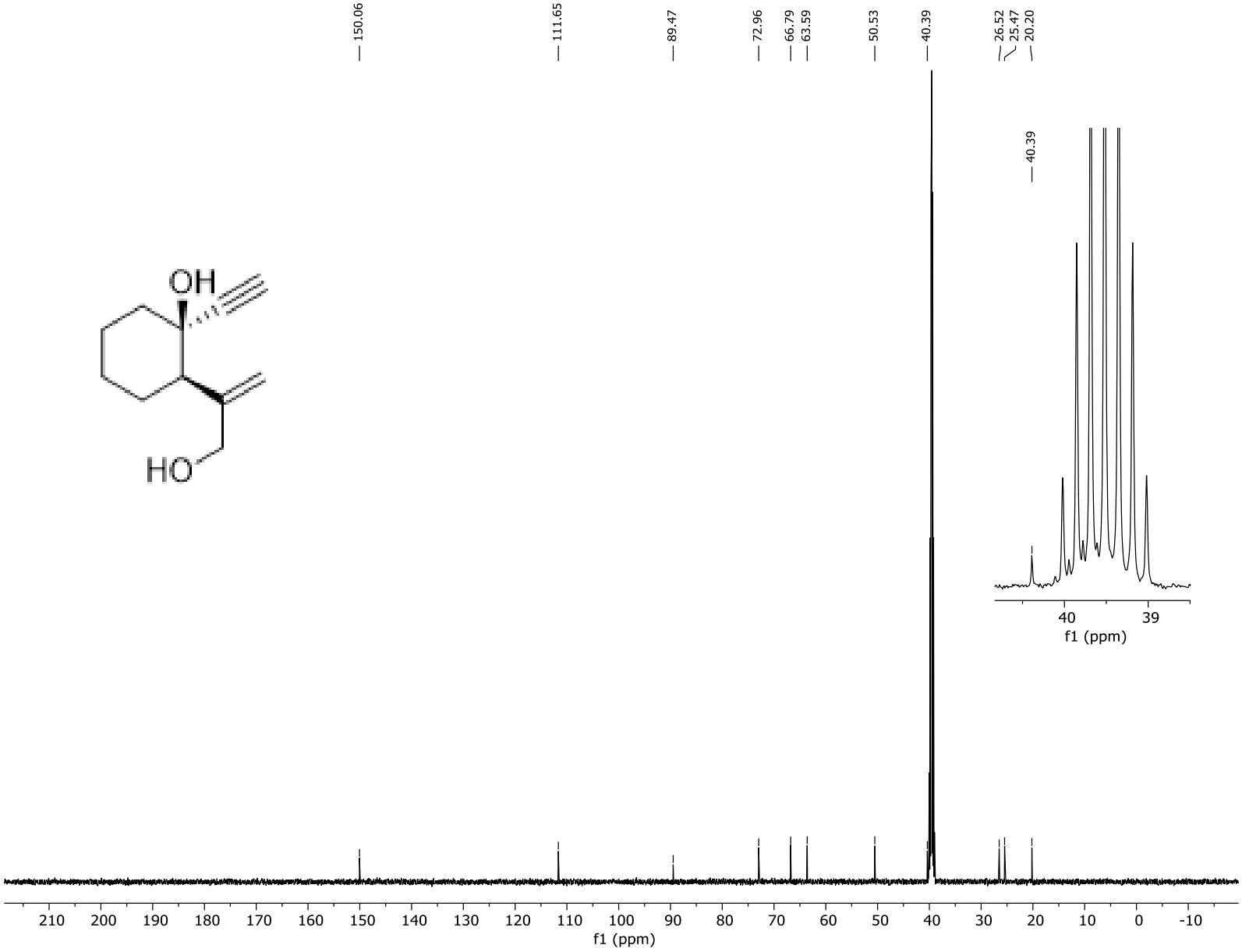


RB-461

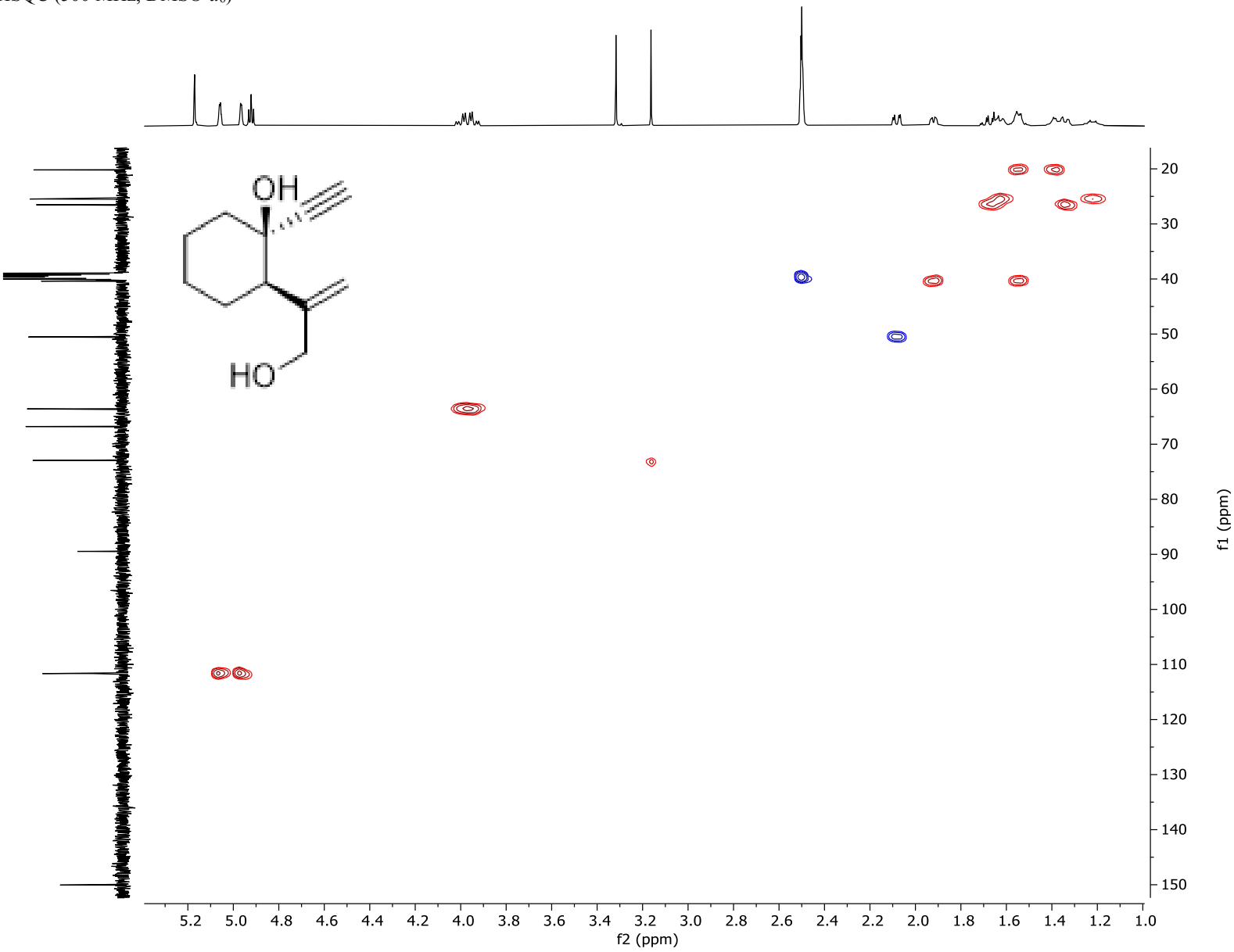
4.24e′ ^{1}H NMR (500 MHz, DMSO-d_6)



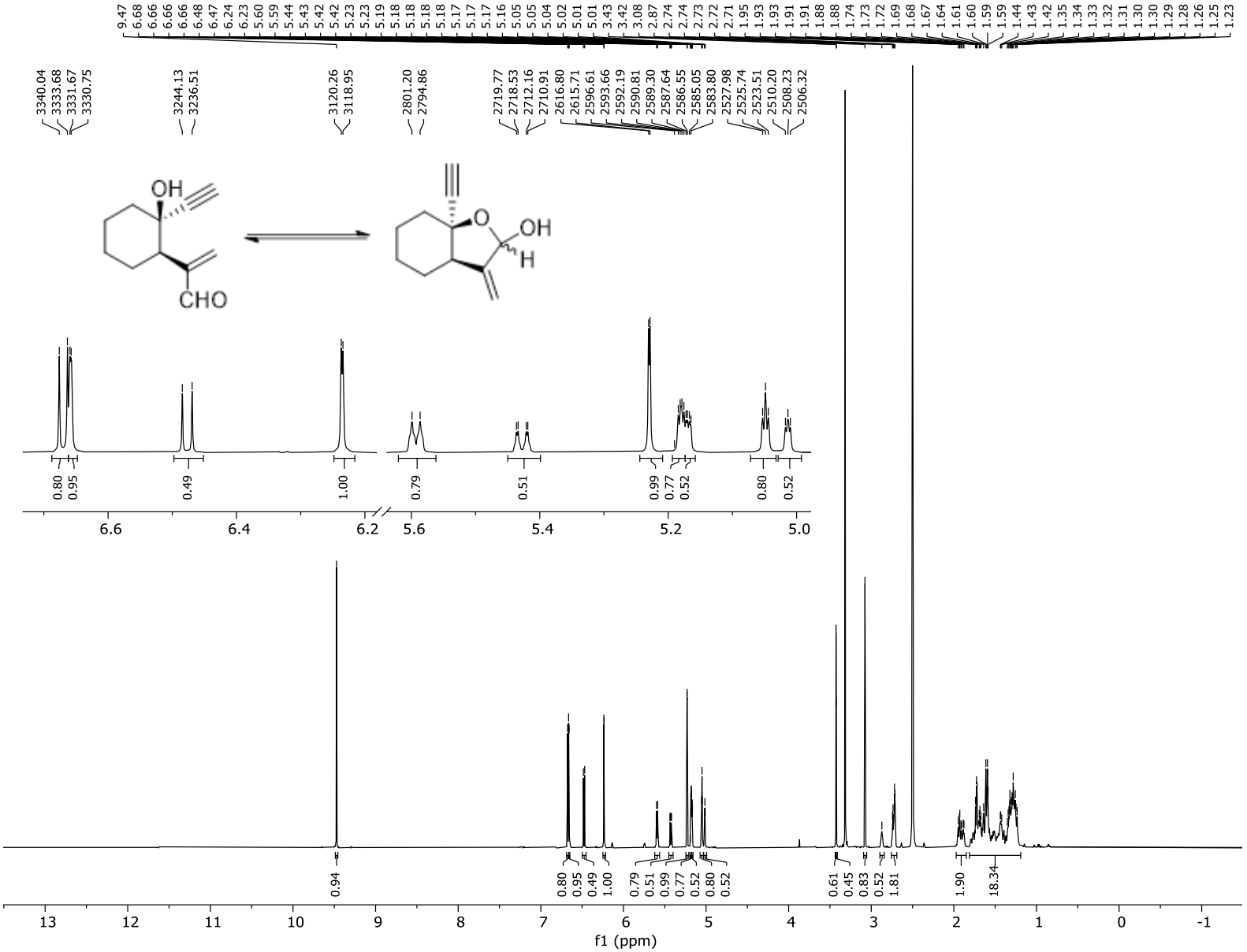
4.24e′ ^{13}C NMR (126 MHz, DMSO-d_6)



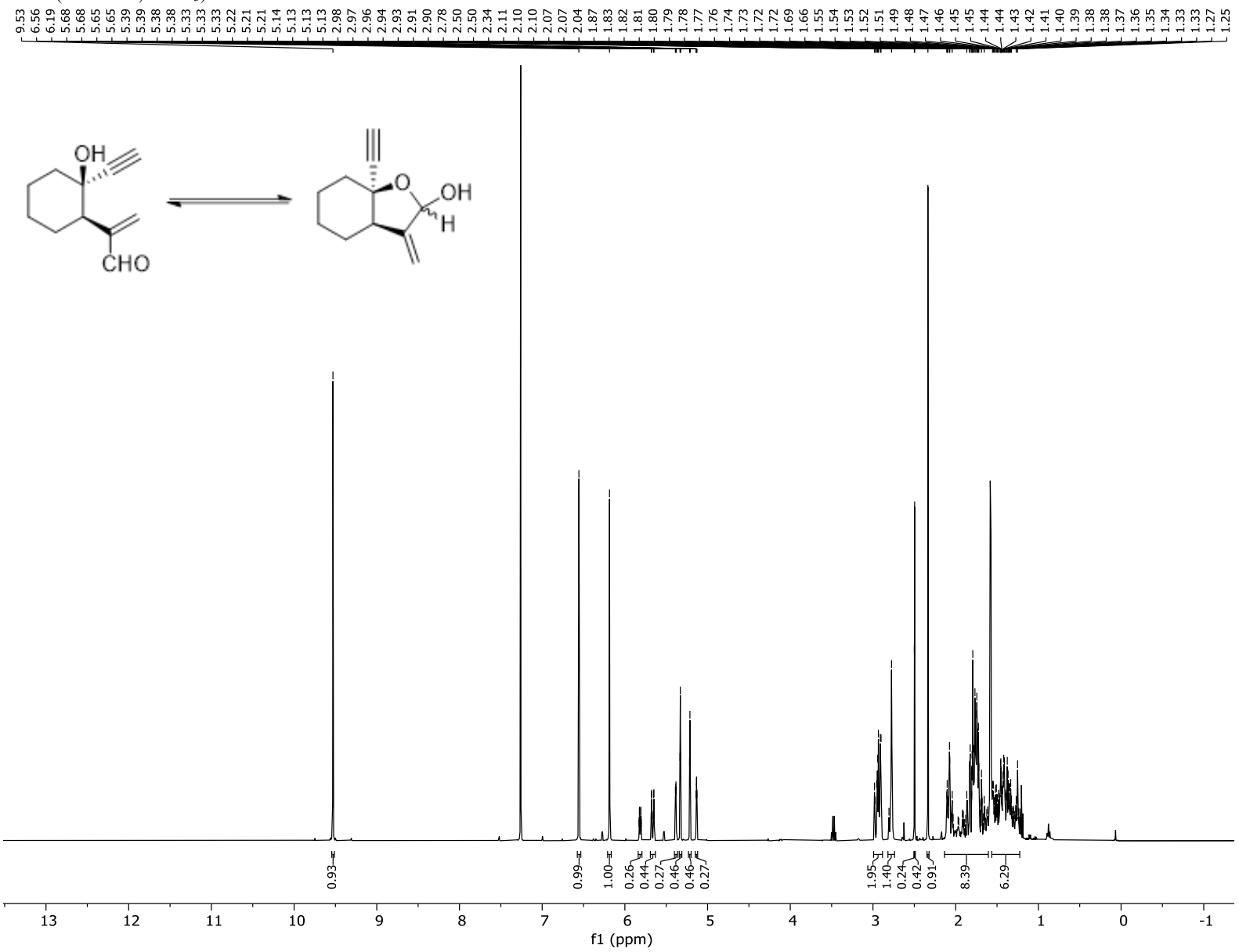
4.24e′ HSQC (500 MHz, DMSO-d_6)



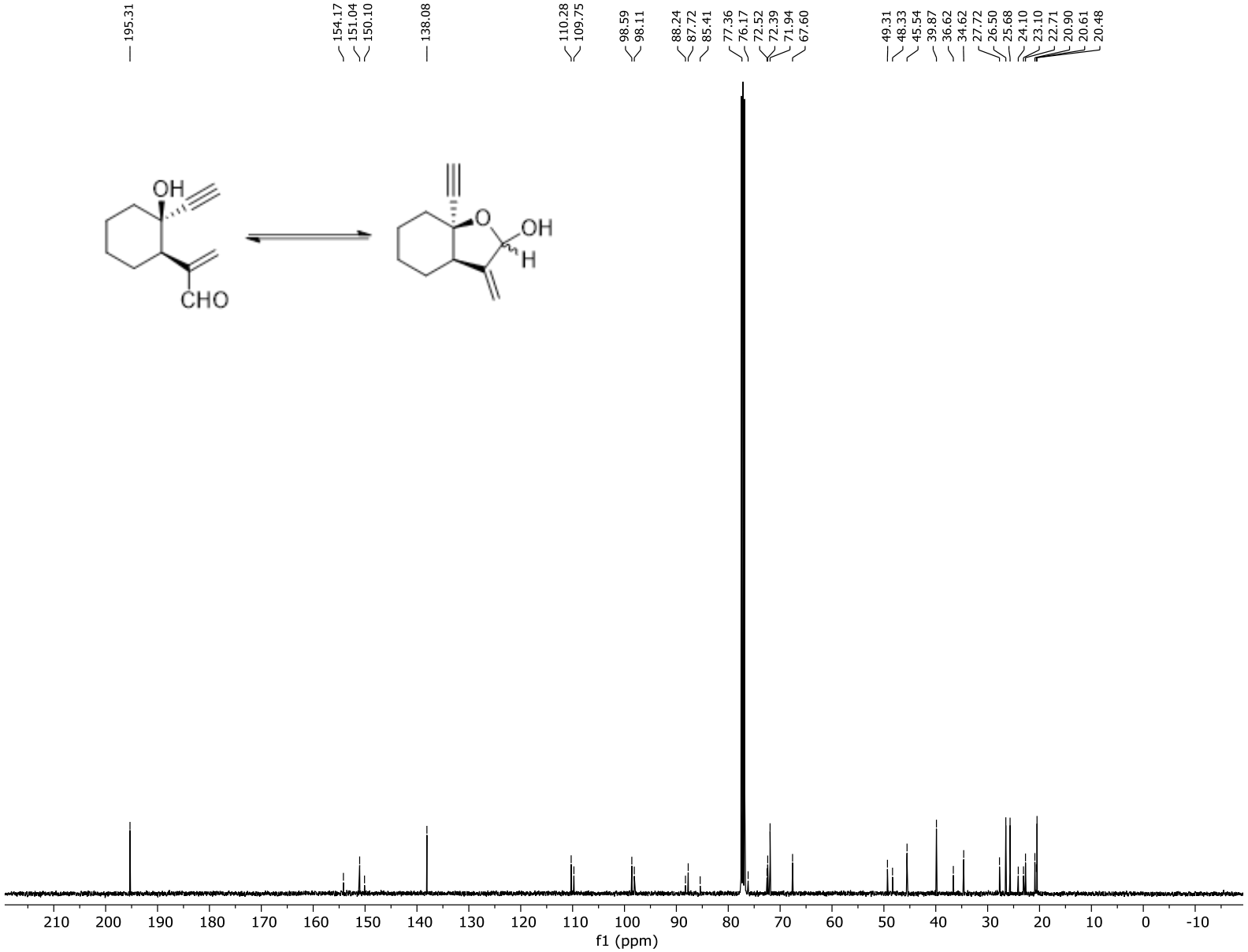
4.30 ^{1}H NMR (500 MHz, DMSO-d_6)



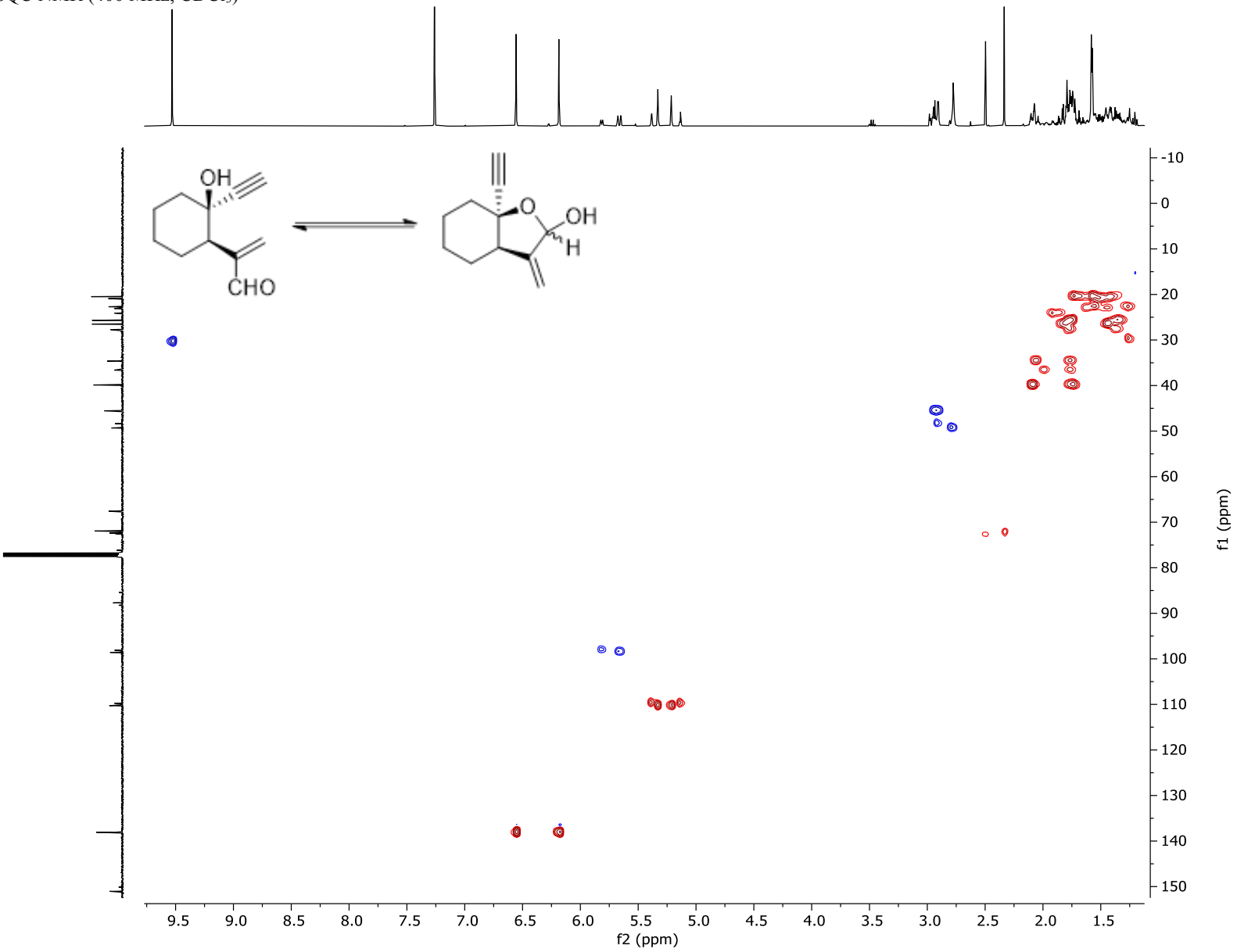
4.30 ^{1}H NMR (400 MHz, $CDCl_3$)



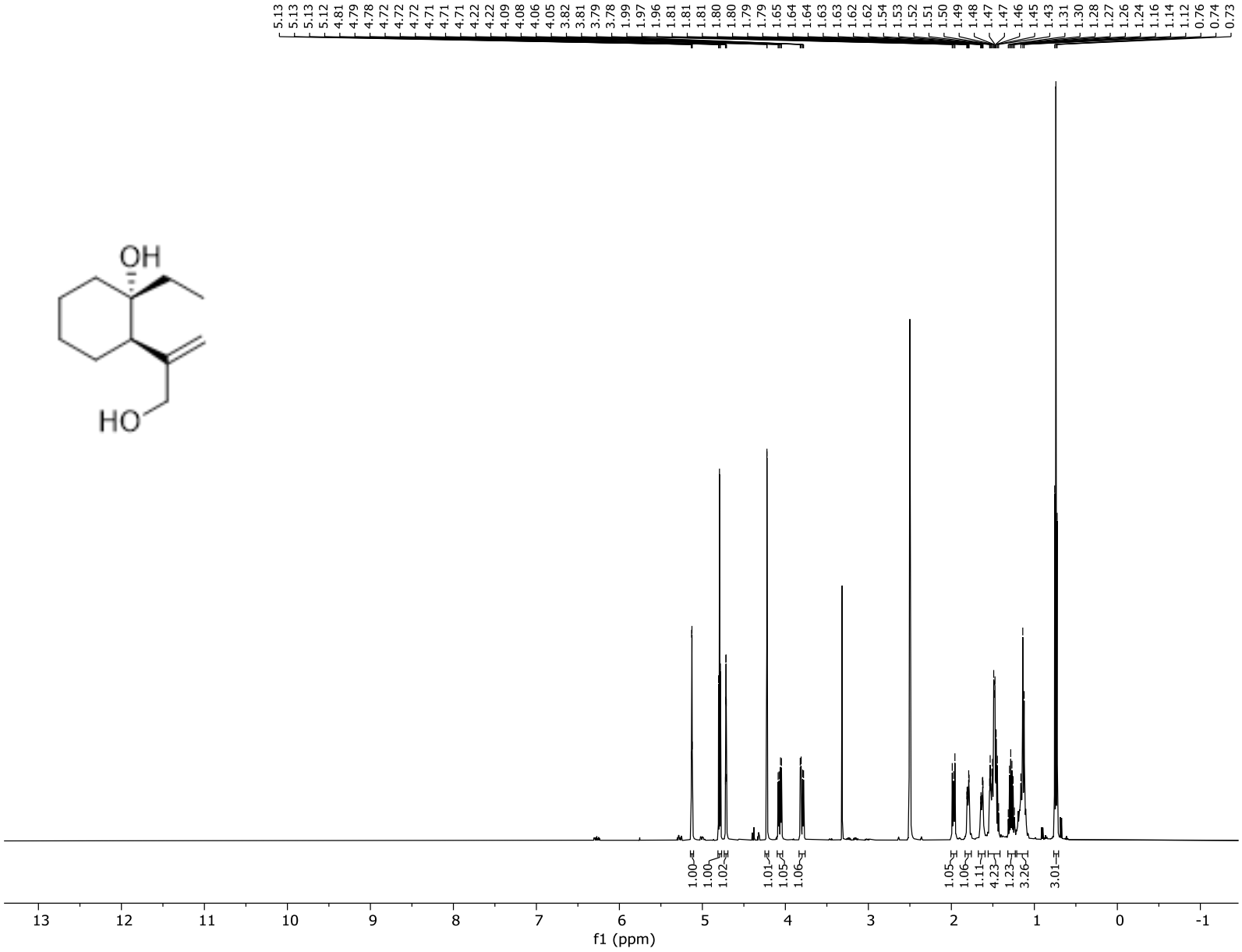
4.30 ^{13}C NMR (101 MHz, $CDCl_3$)



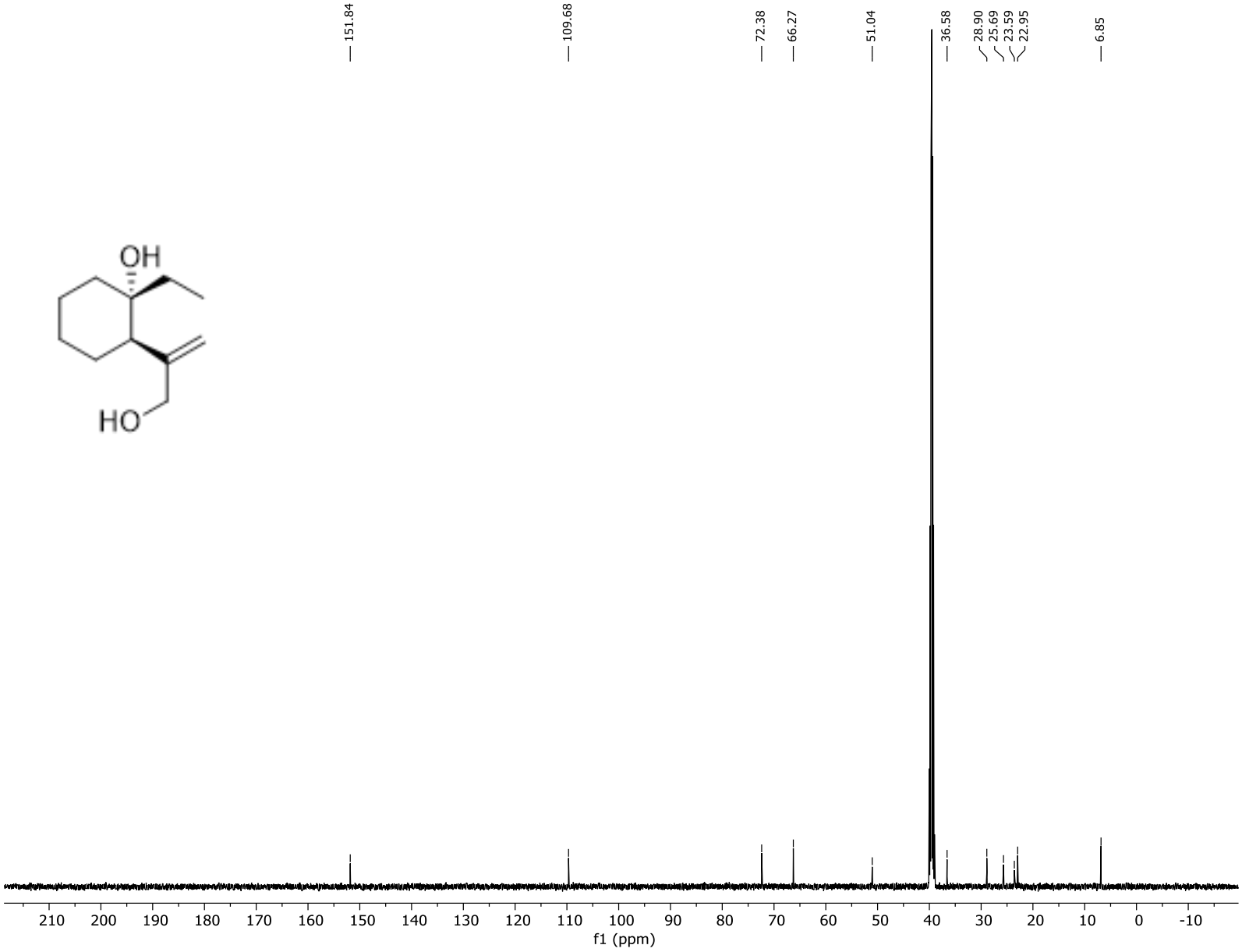
4.30 HSQC NMR (400 MHz, $CDCl_3$)



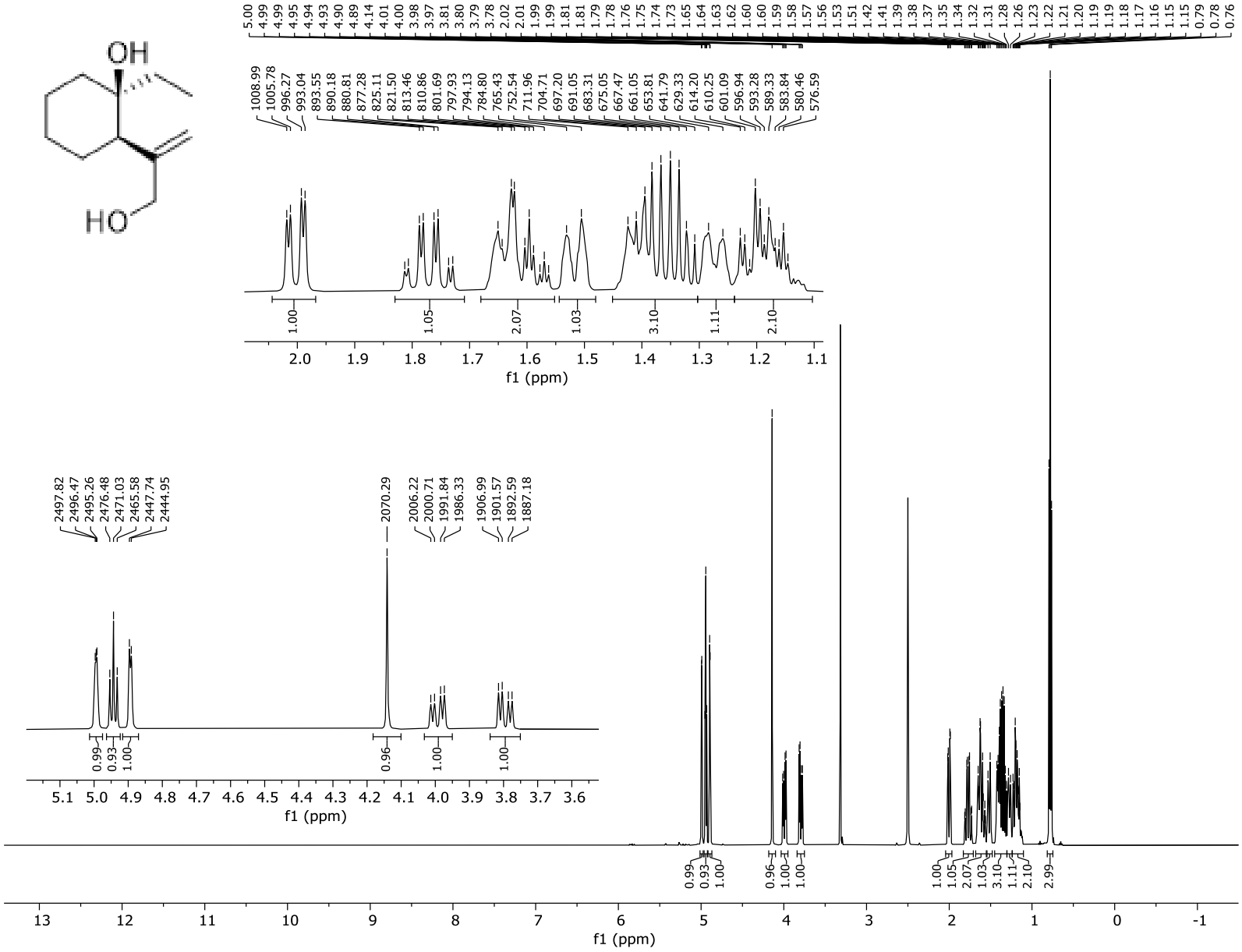
epi-**4.22′** ^{1}H NMR (500 MHz, DMSO-d_6)



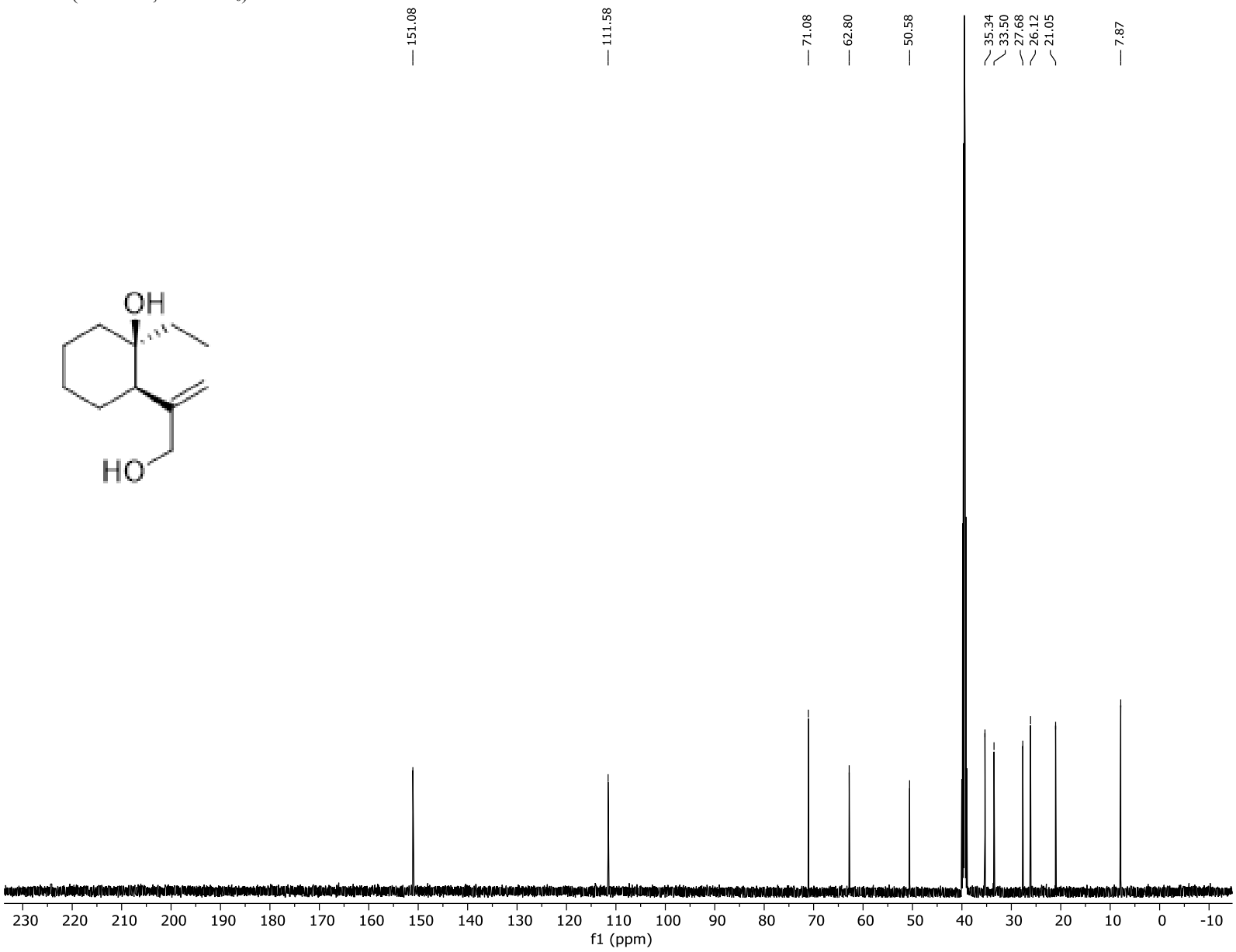
epi-**4.22′** ^{13}C NMR (126 MHz, DMSO-d_6)



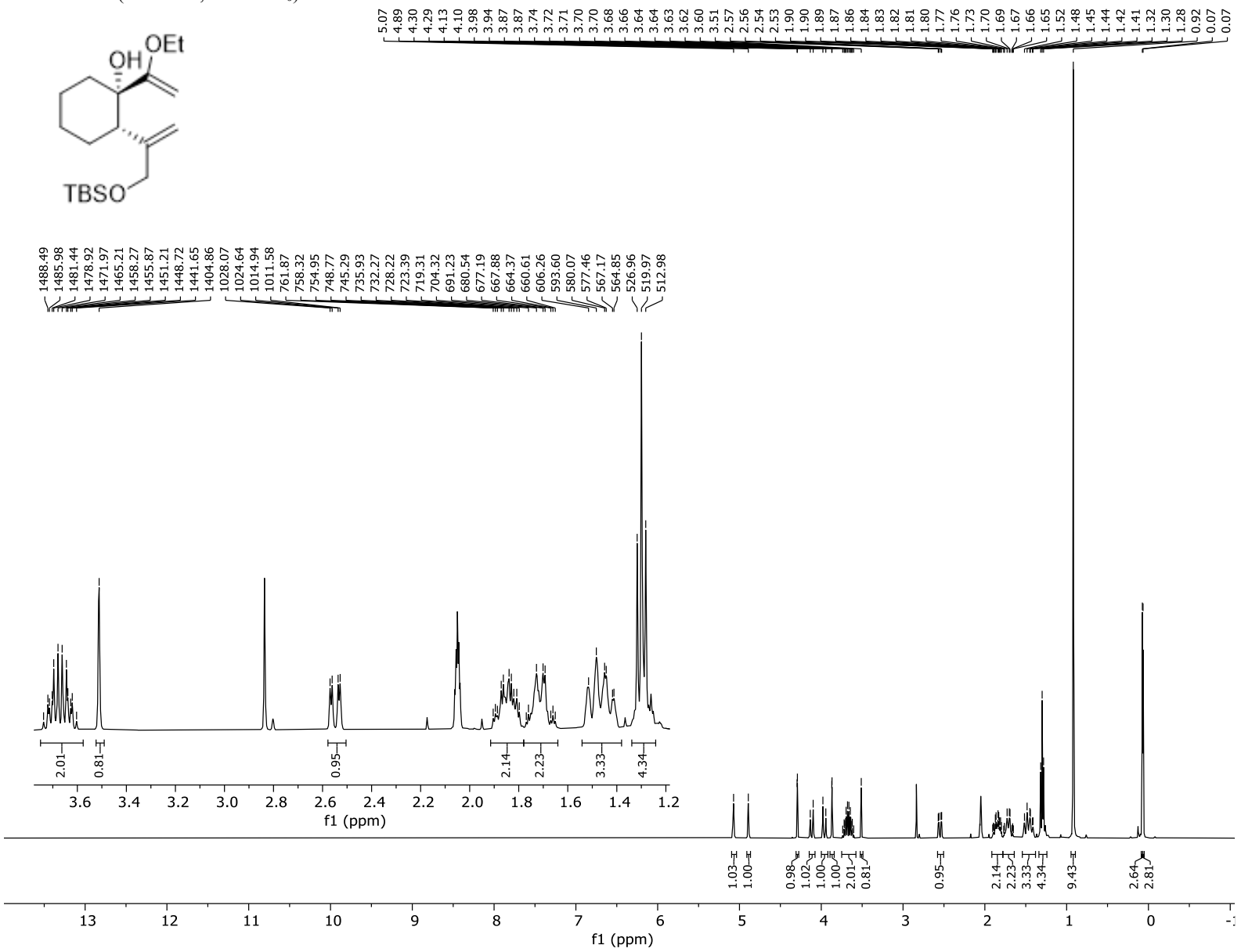
4.22′ ^{1}H NMR (500 MHz, DMSO-d_6)



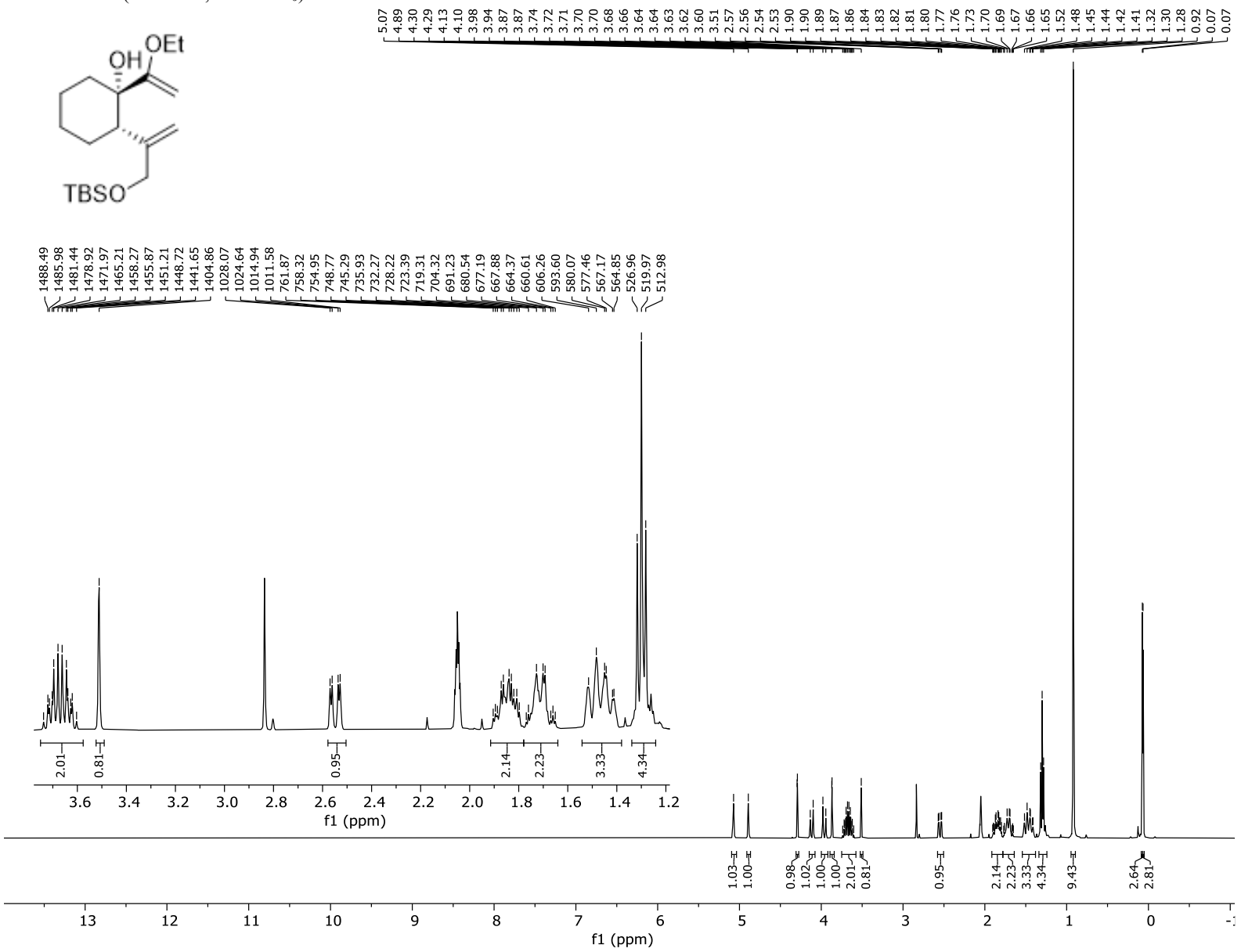
4.22′ ^{13}C NMR (126 MHz, DMSO-d_6)



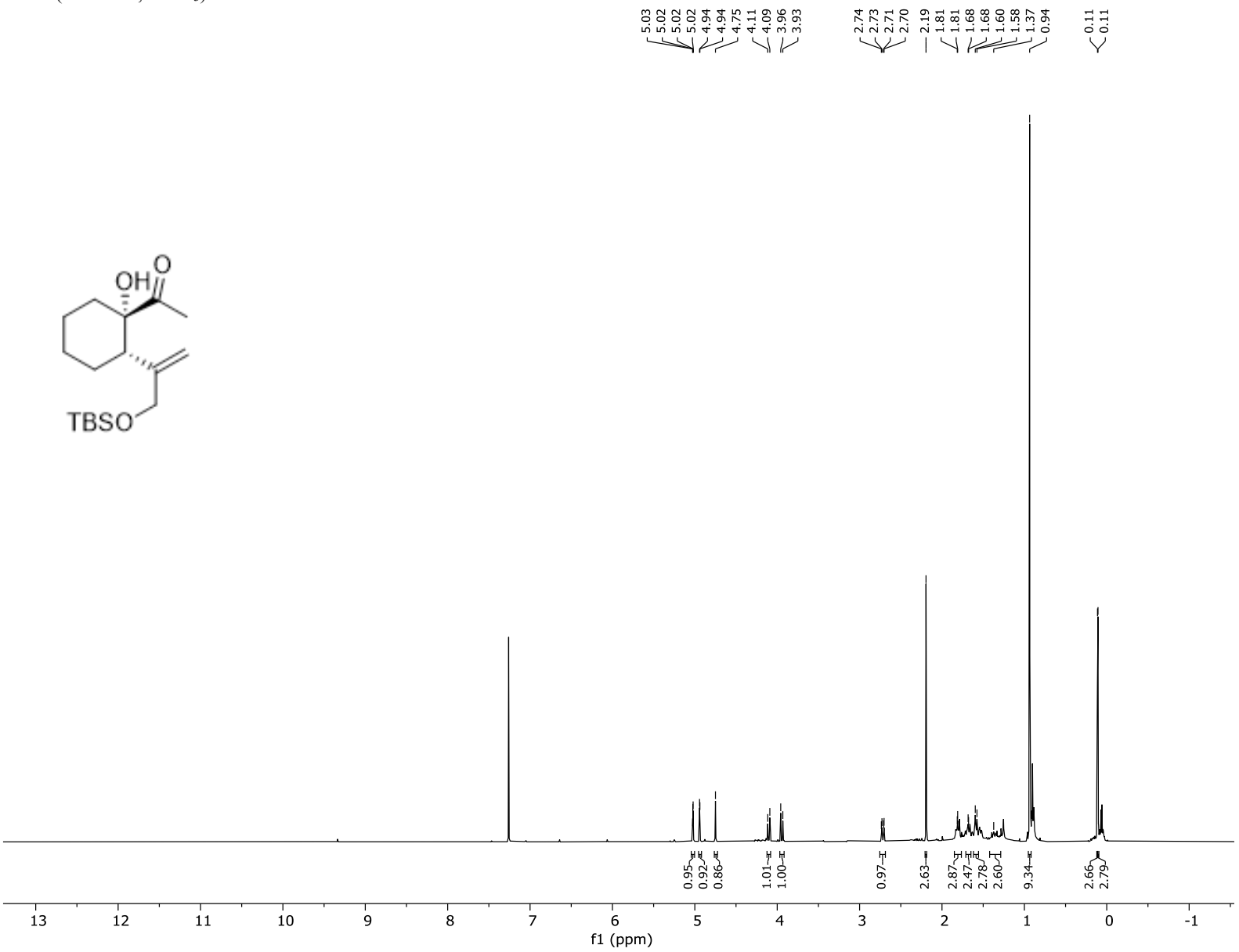
4.31 ^{1}H NMR (400 MHz, acetone-d_6)



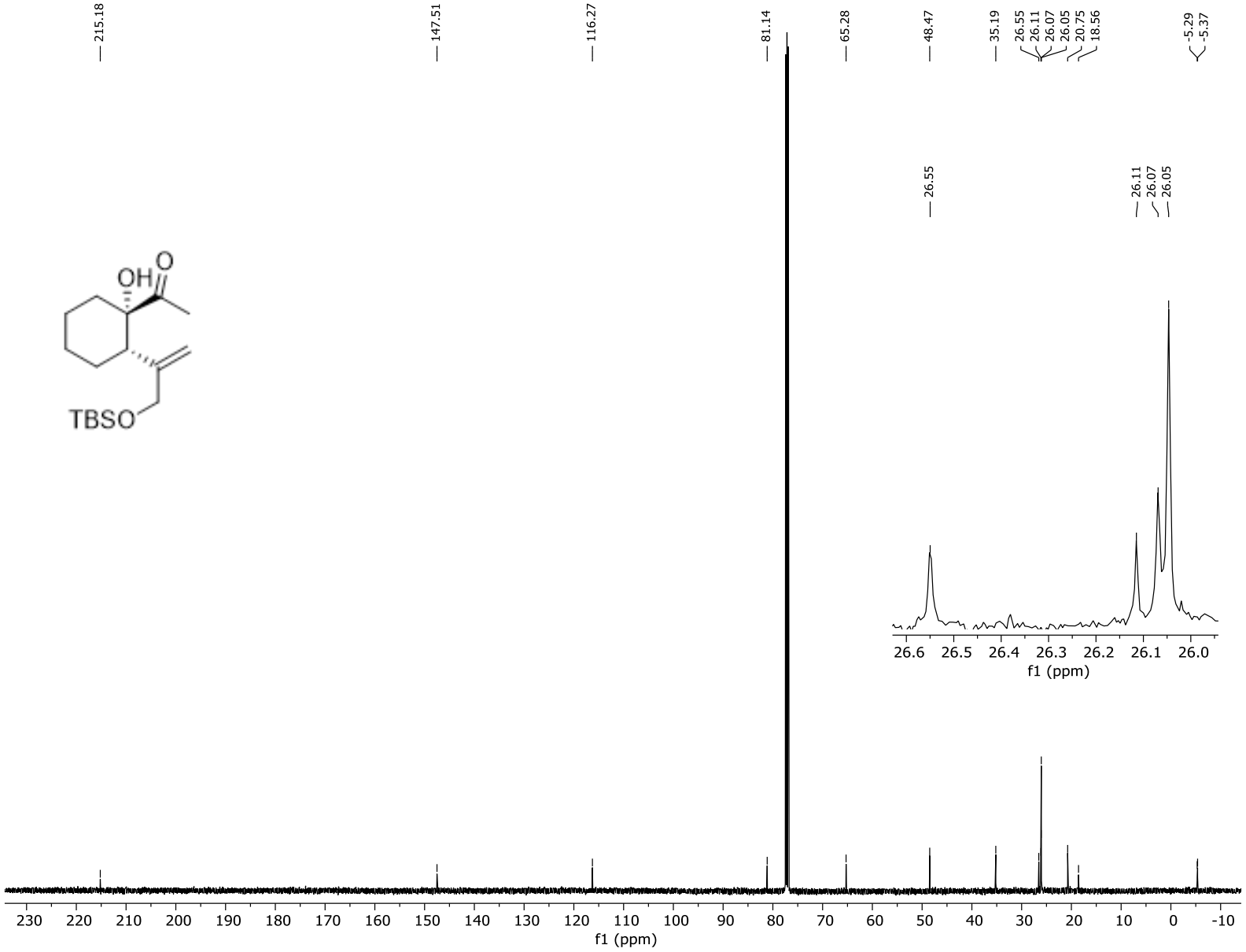
4.31 ^{13}C NMR (101 MHz, acetone-d_6)



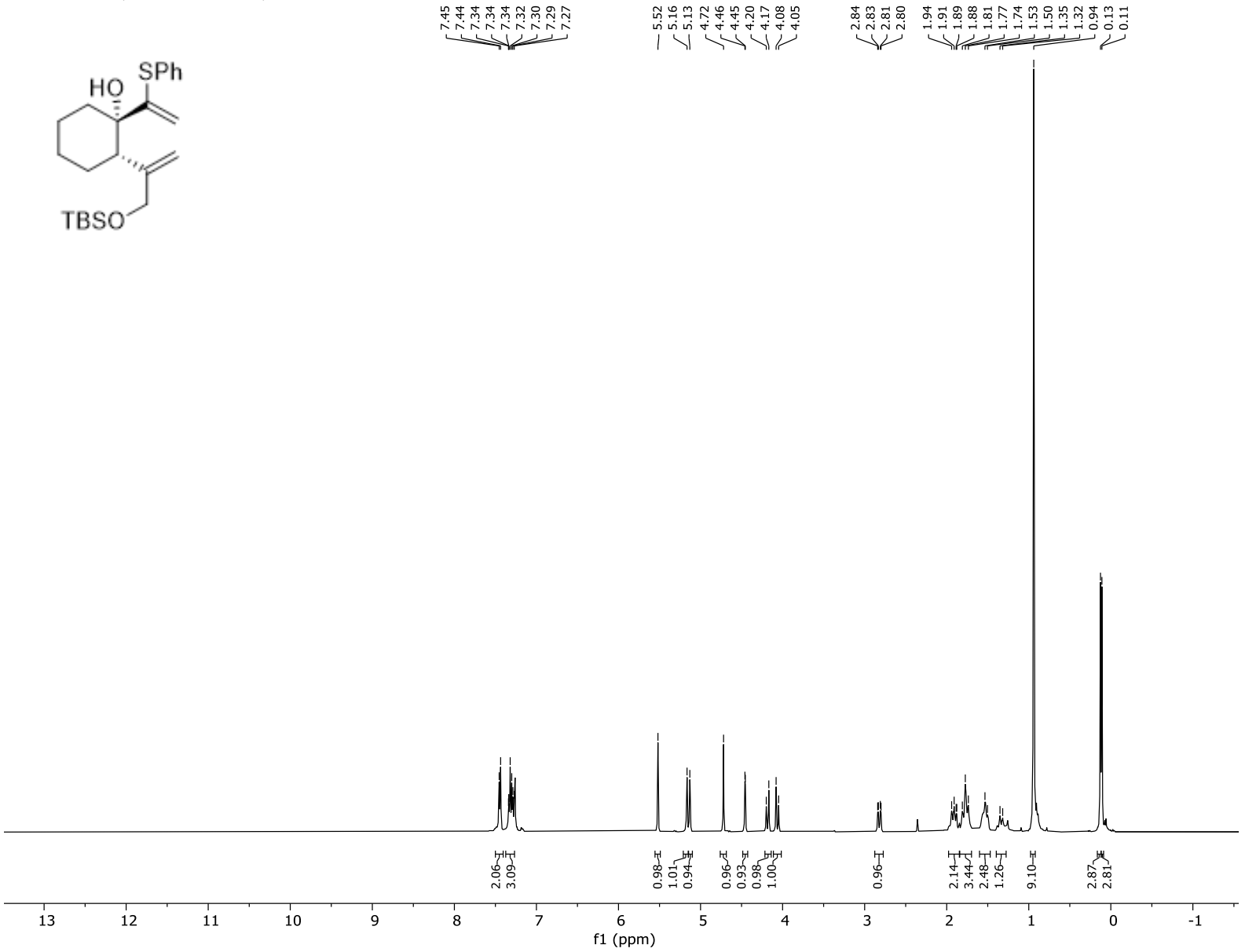
4.32 ^{1}H NMR (500 MHz, $CDCl_3$)



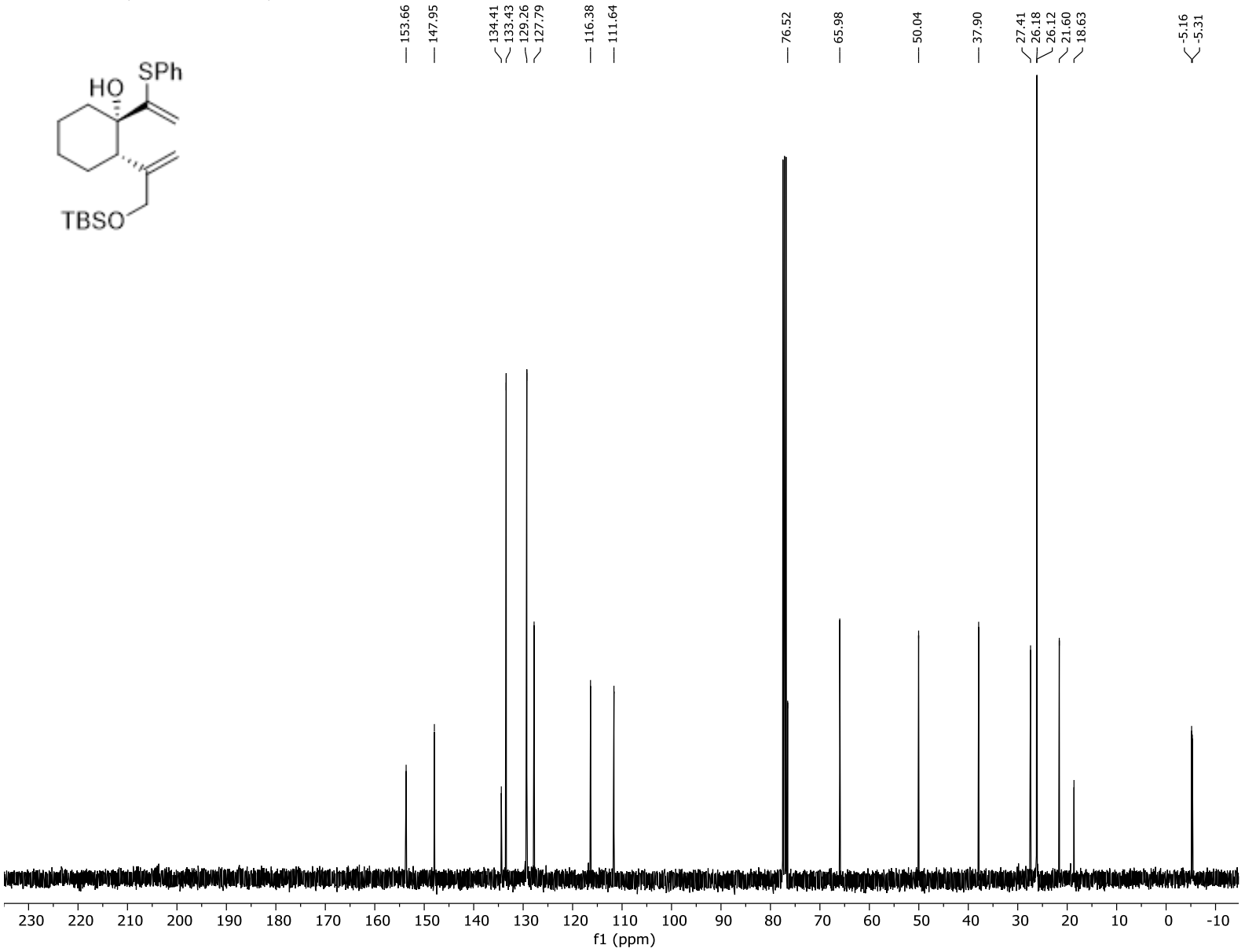
4.32 ^{13}C NMR (126 MHz, $CDCl_3$)



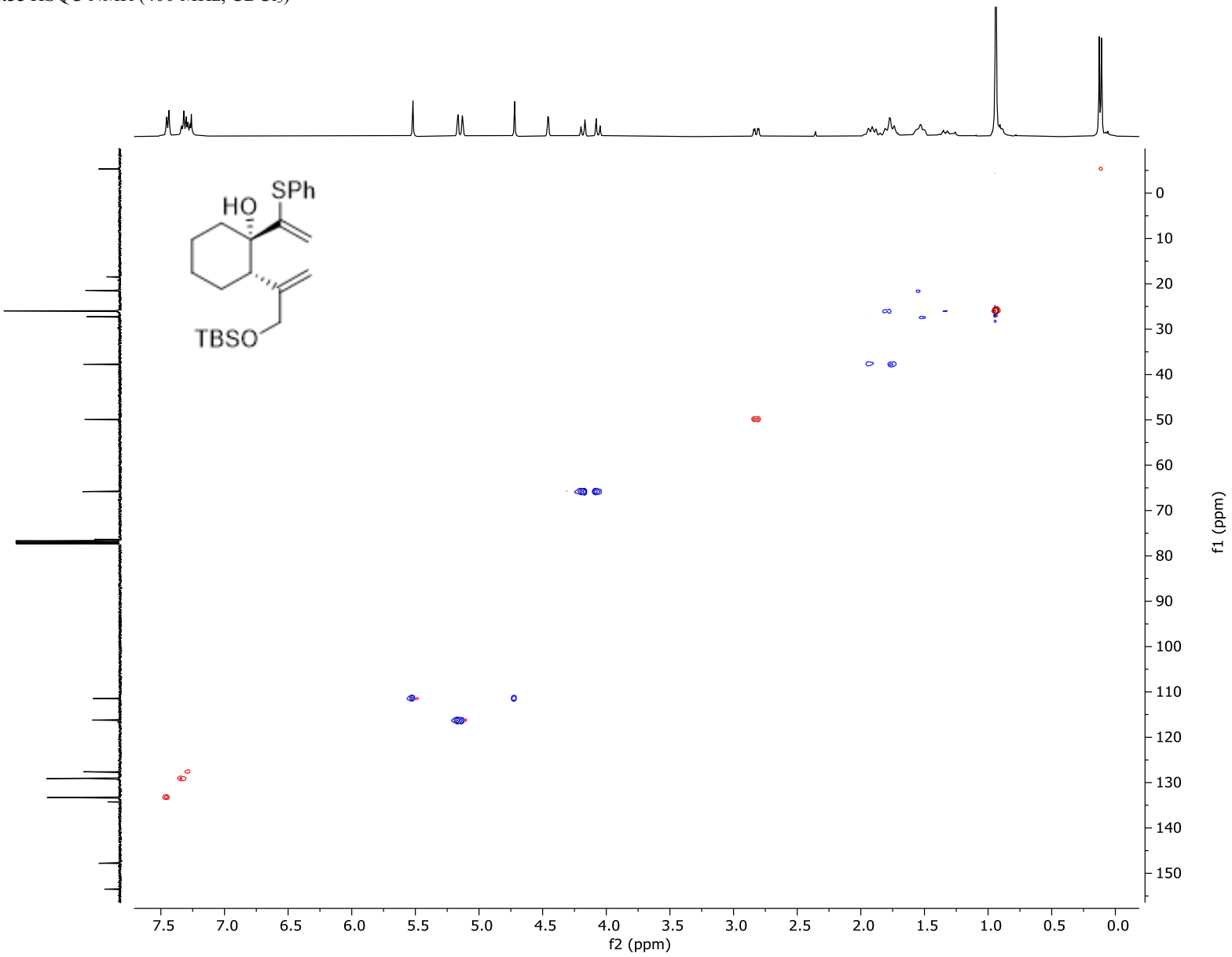
4.33 ^{1}H NMR (400 MHz, $CDCl_3$)



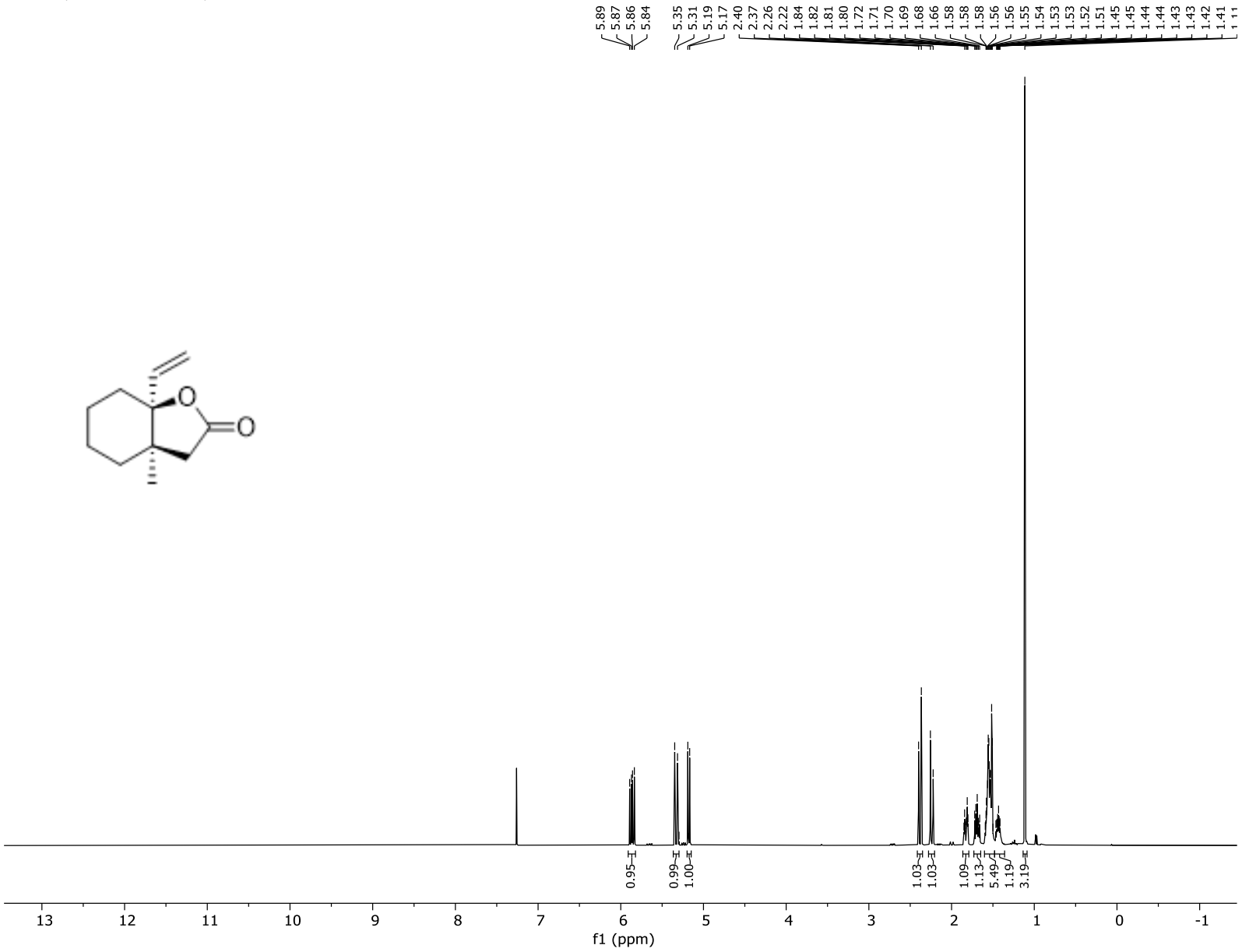
4.33 ^{13}C NMR (101 MHz, $CDCl_3$)



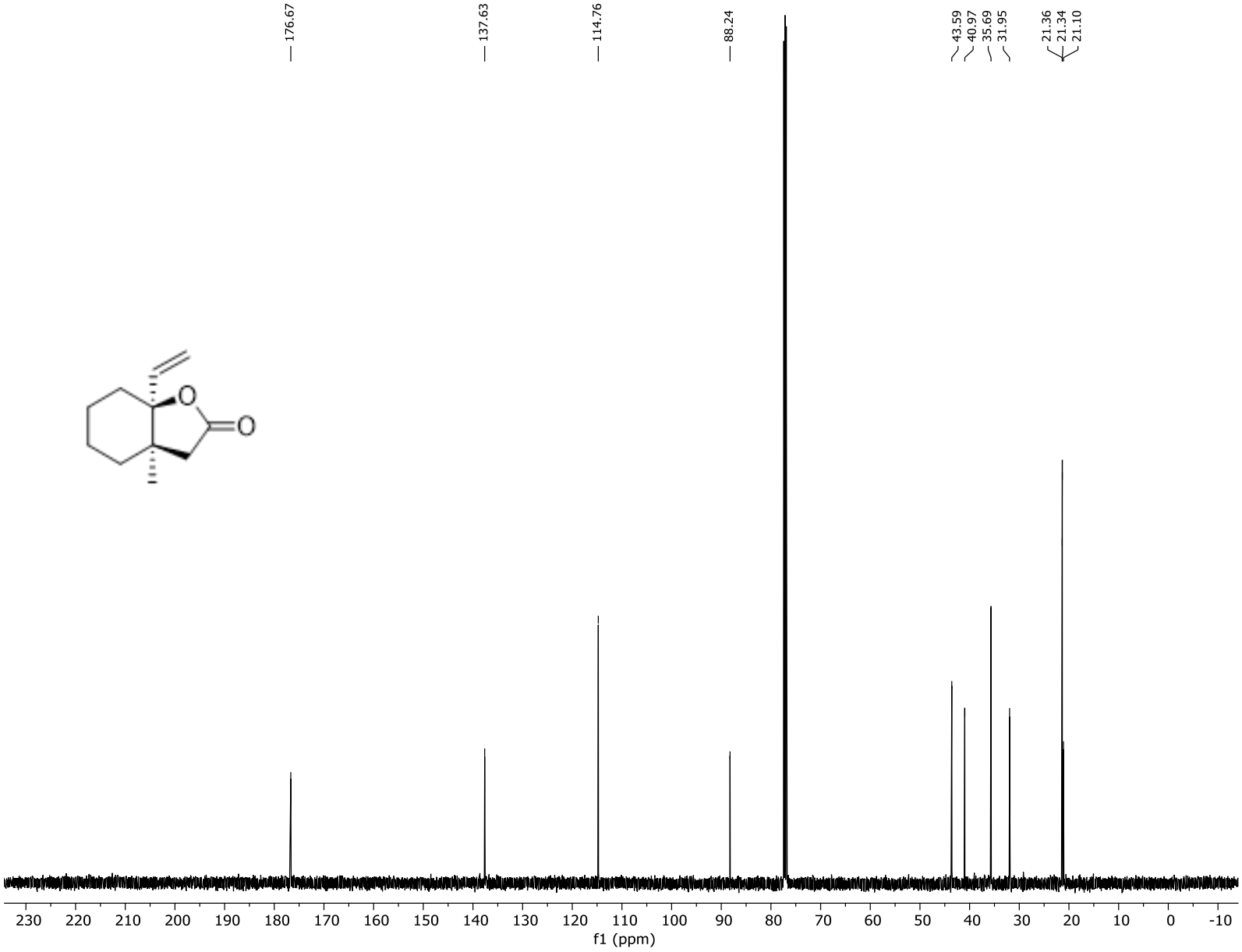
4.33 HSQC NMR (400 MHz, $CDCl_3$)



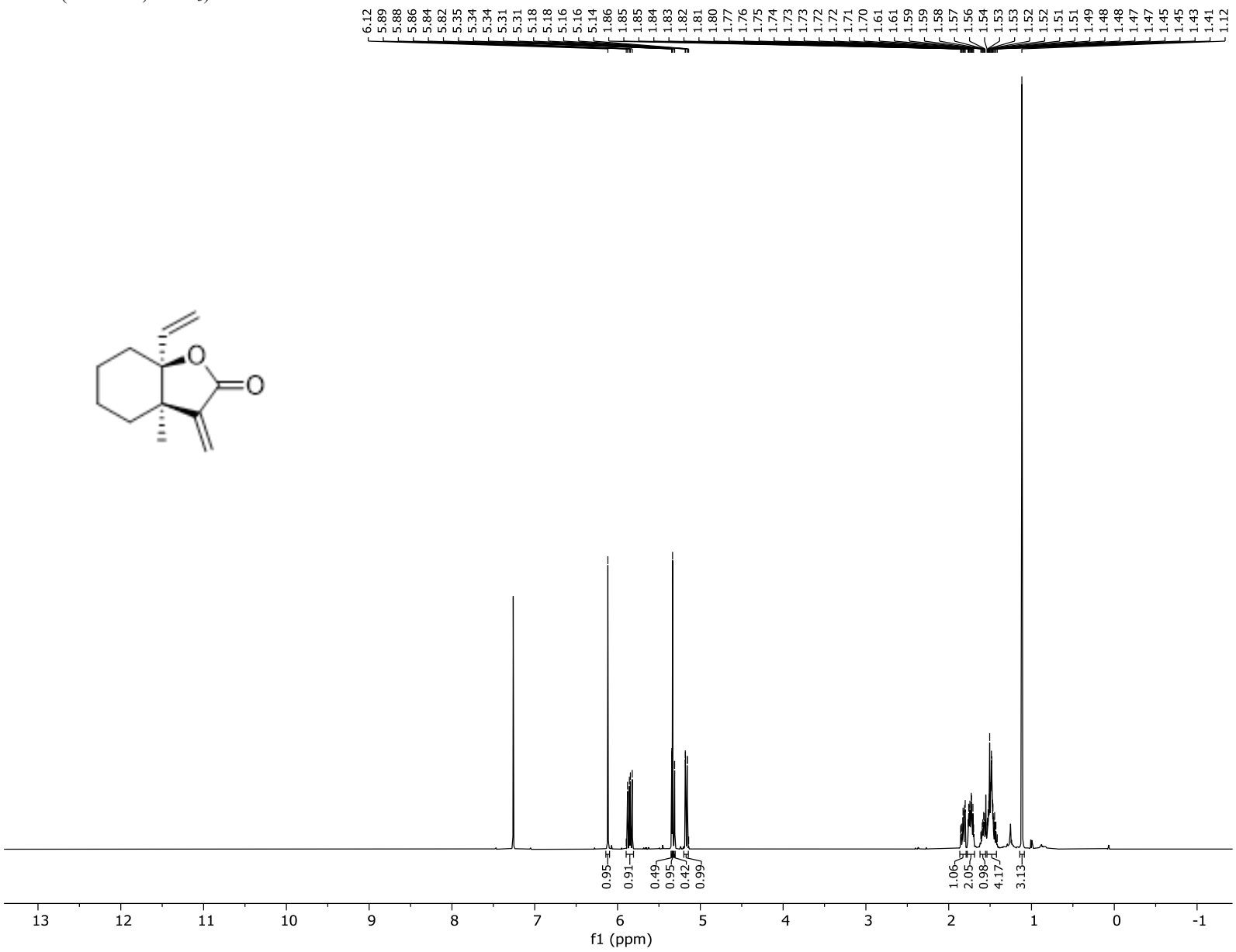
4.37 ^{1}H NMR (500 MHz, $CDCl_3$)



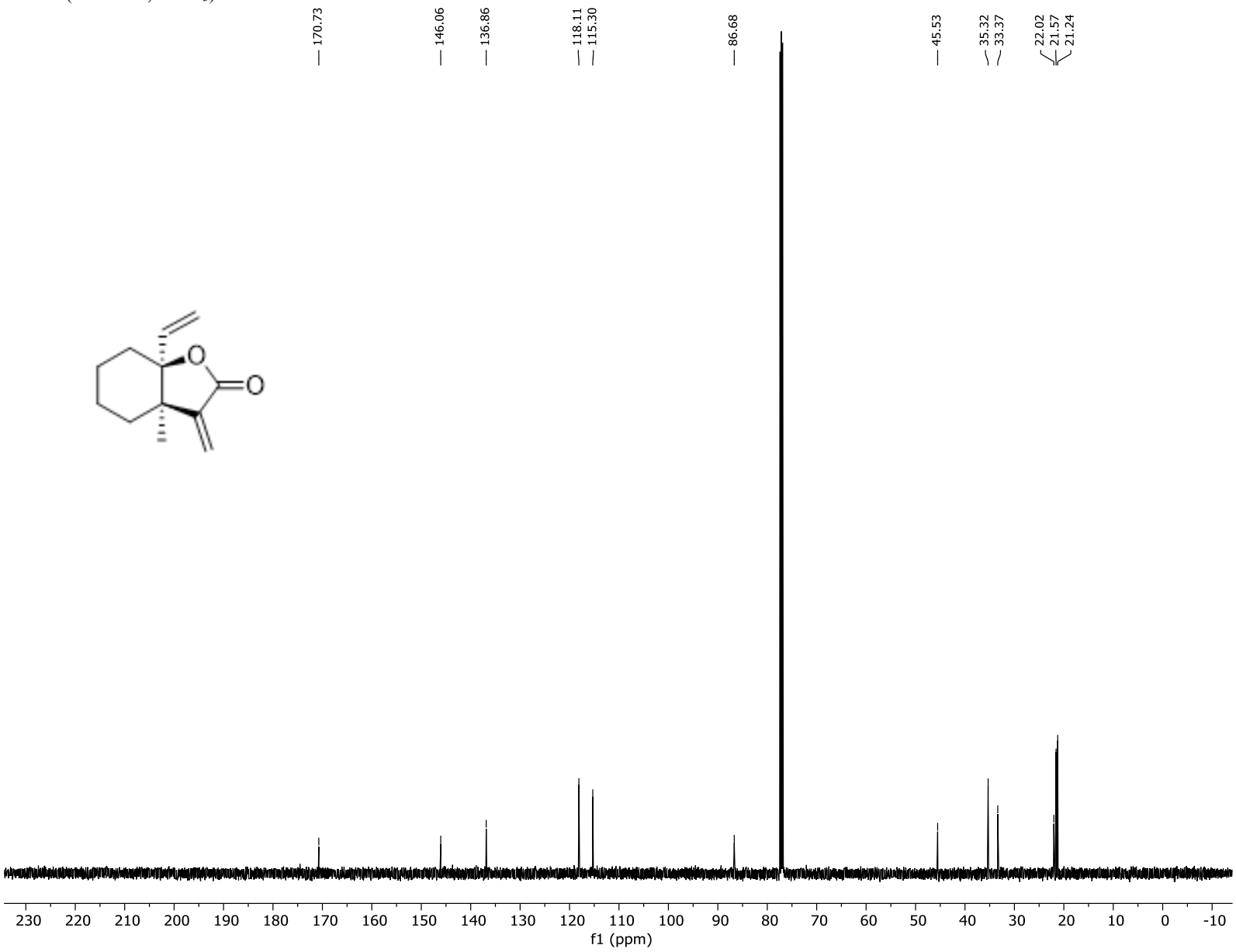
4.37 ^{13}C NMR (126 MHz, $CDCl_3$)



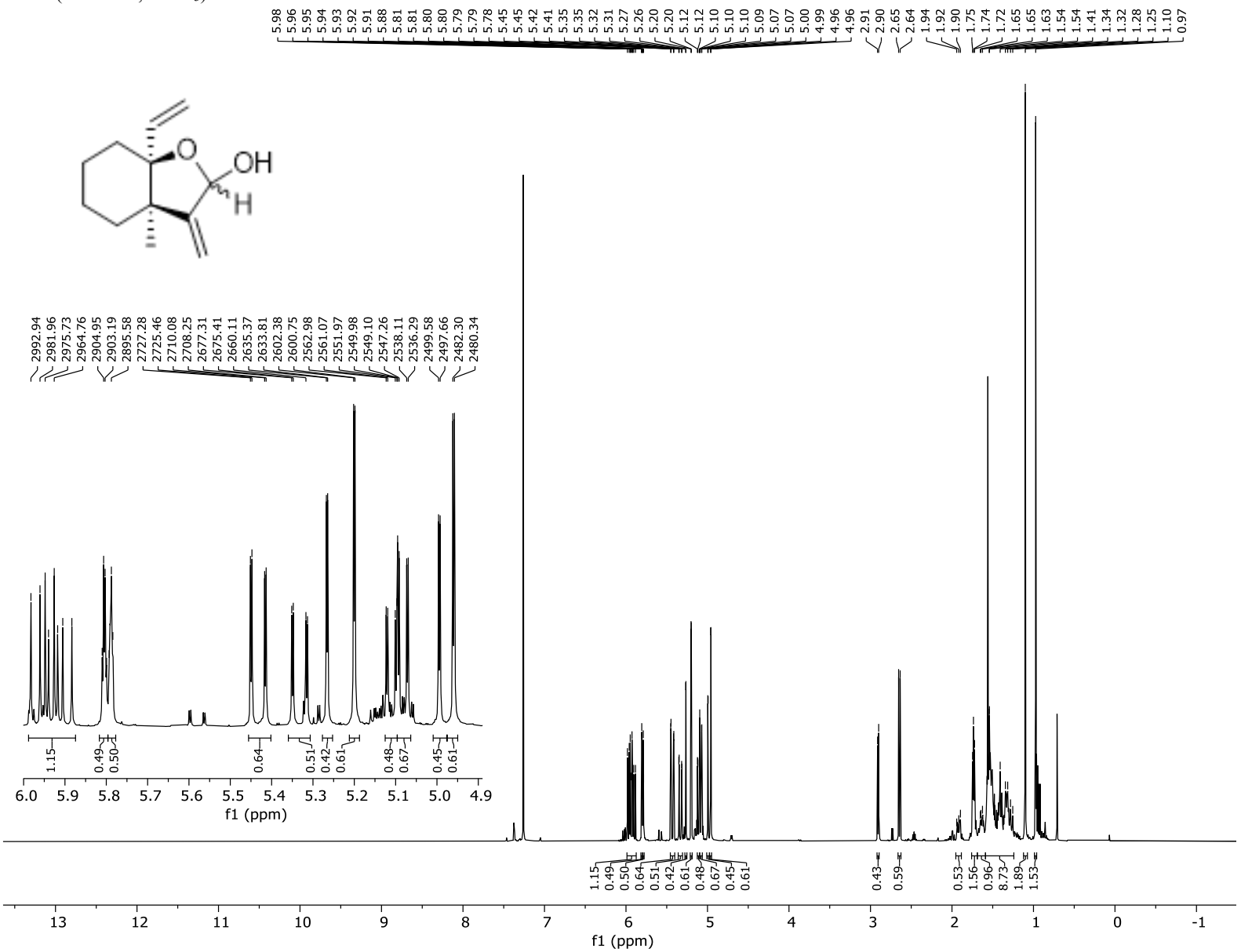
4.38 ^{1}H NMR (500 MHz, $CDCl_3$)



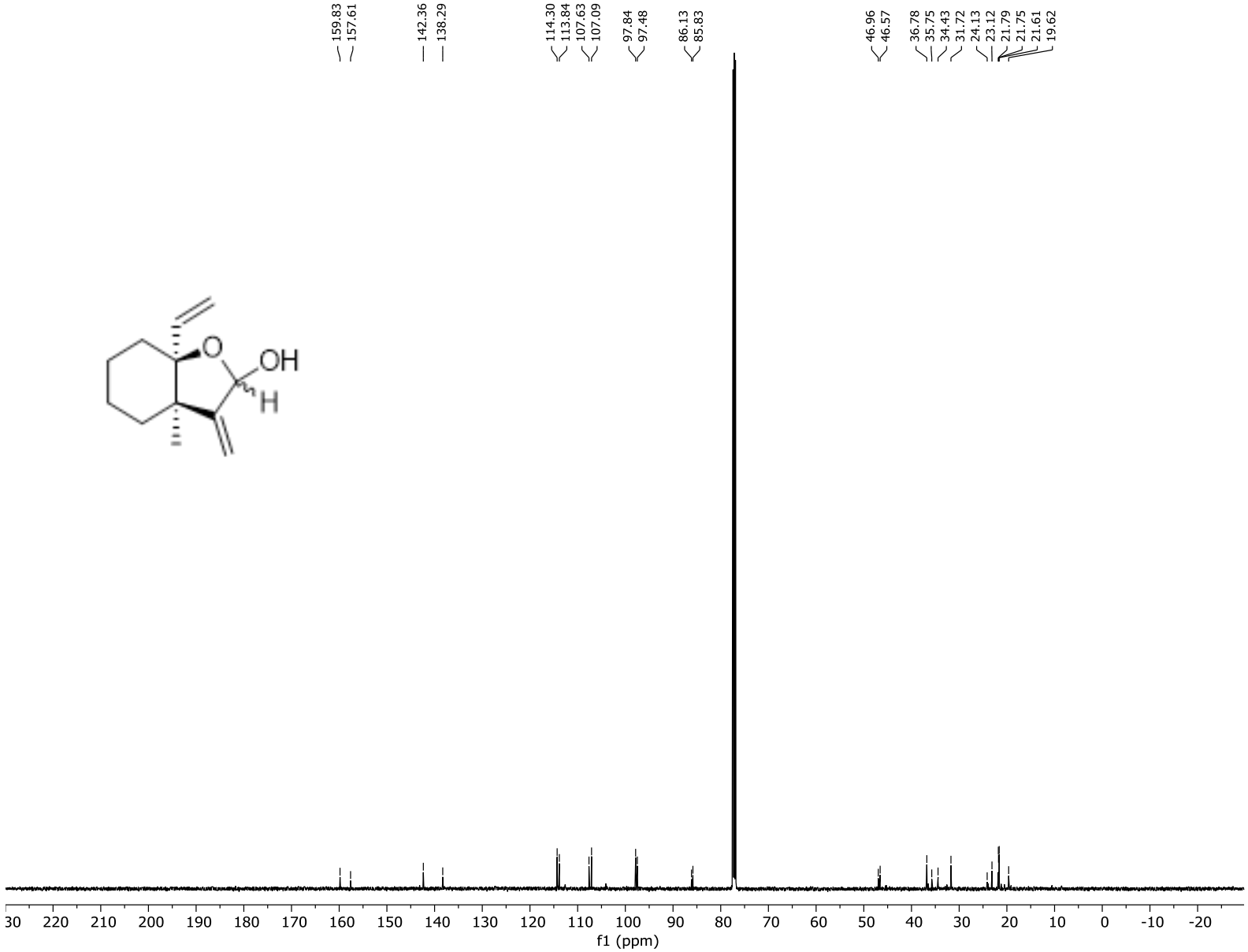
4.38 ^{13}C NMR (126 MHz, $CDCl_3$)



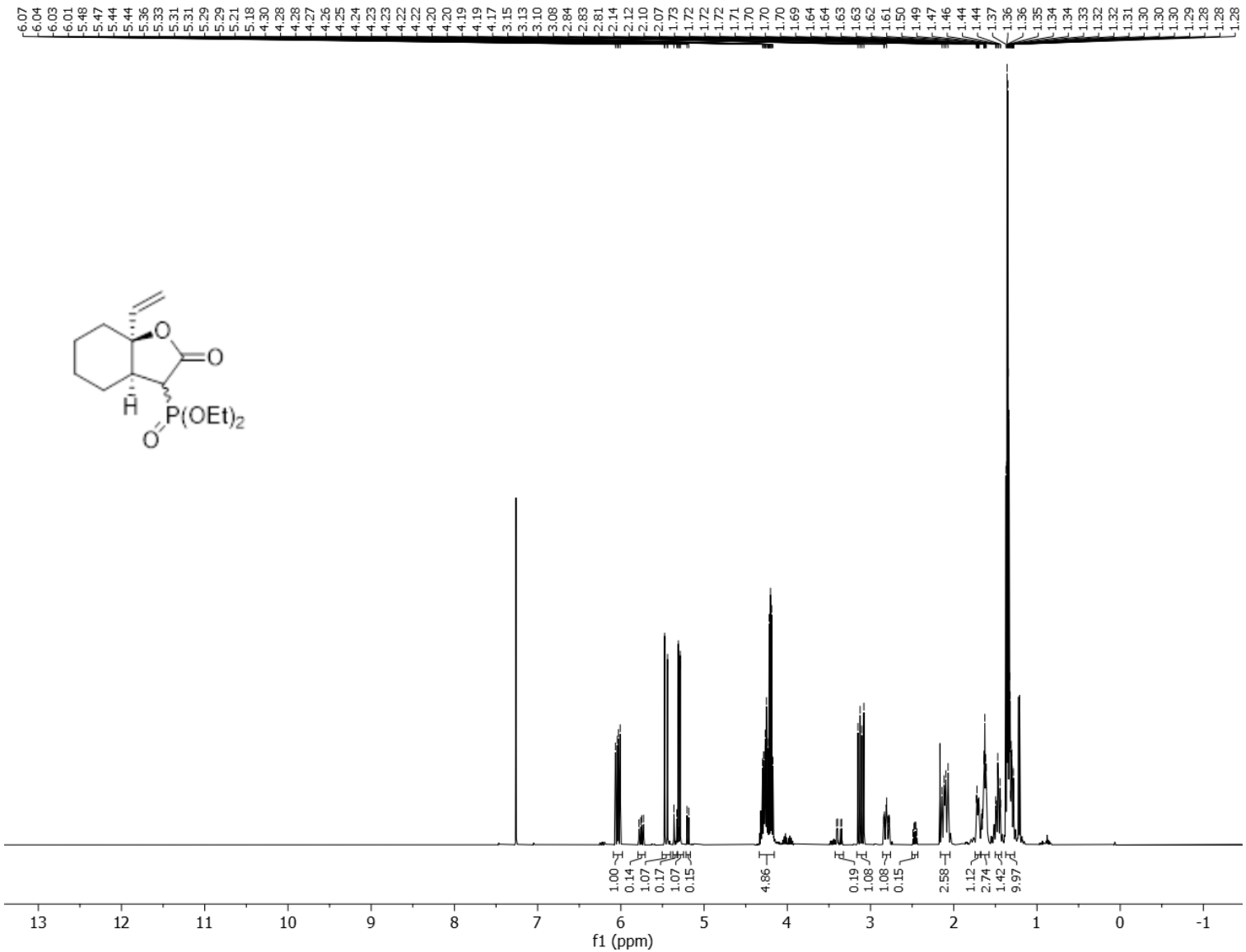
4.39 ^{1}H NMR (500 MHz, $CDCl_3$)



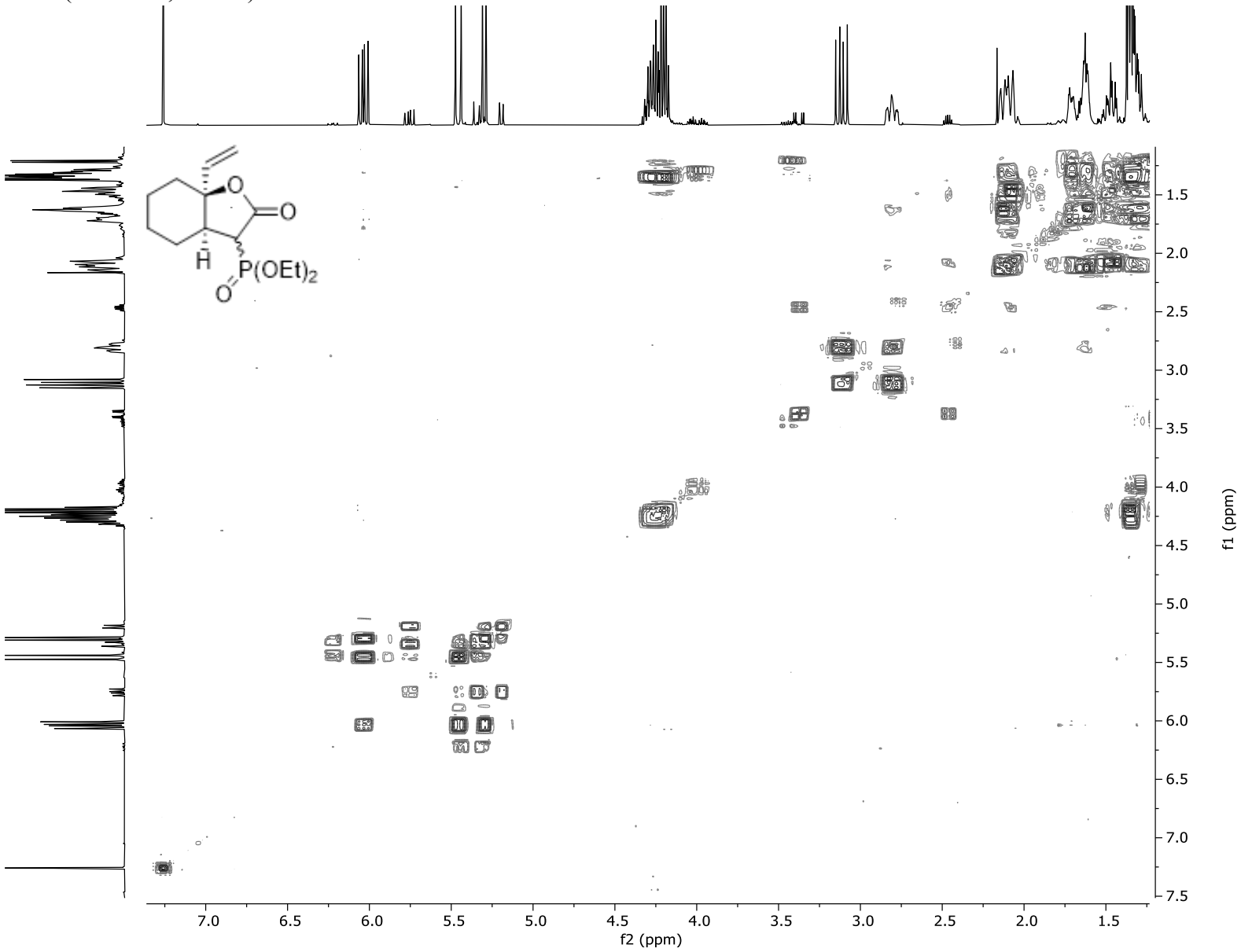
4.39 ^{13}C NMR (126 MHz, $CDCl_3$)



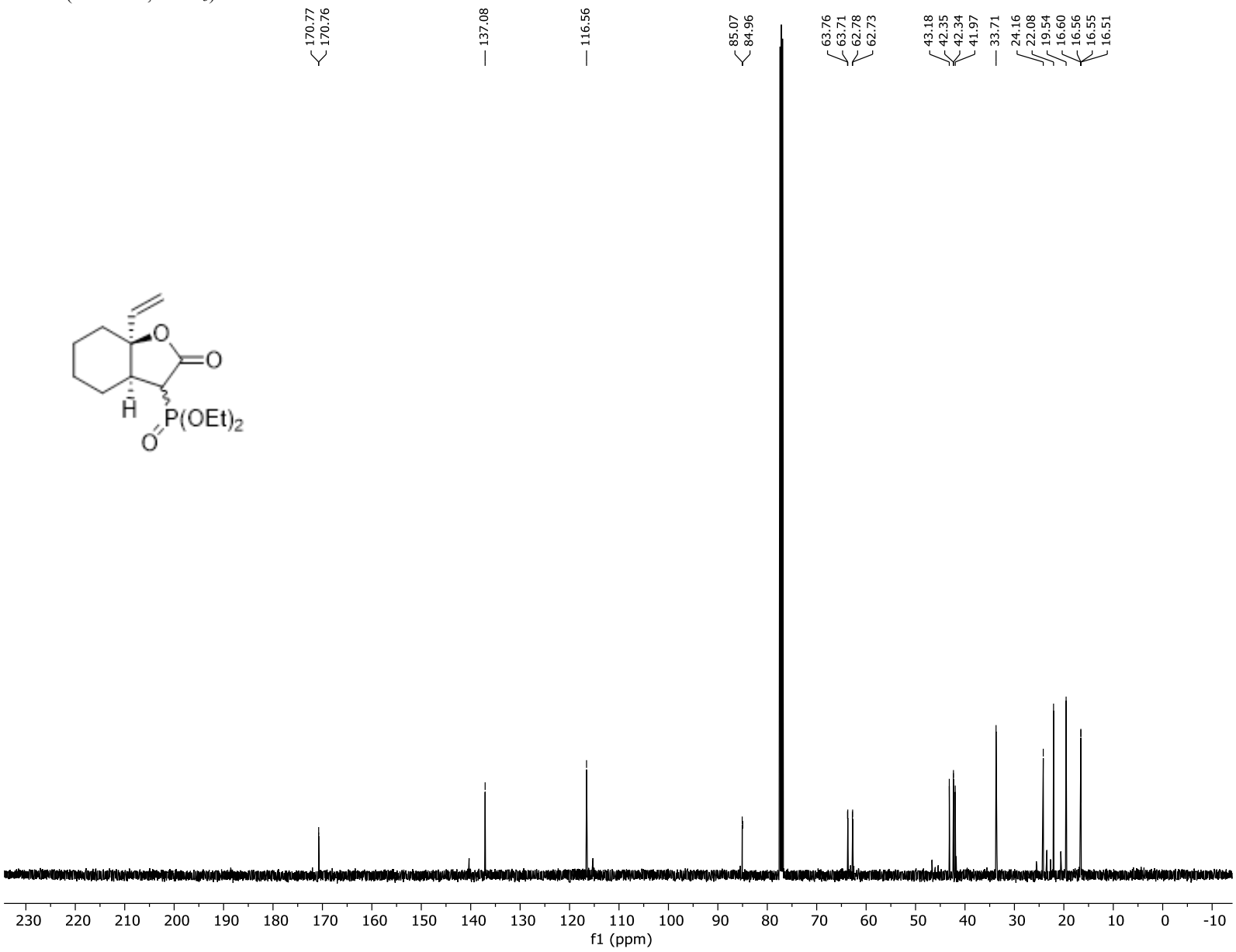
4.43 ^{1}H NMR (500 MHz, $CDCl_3$)



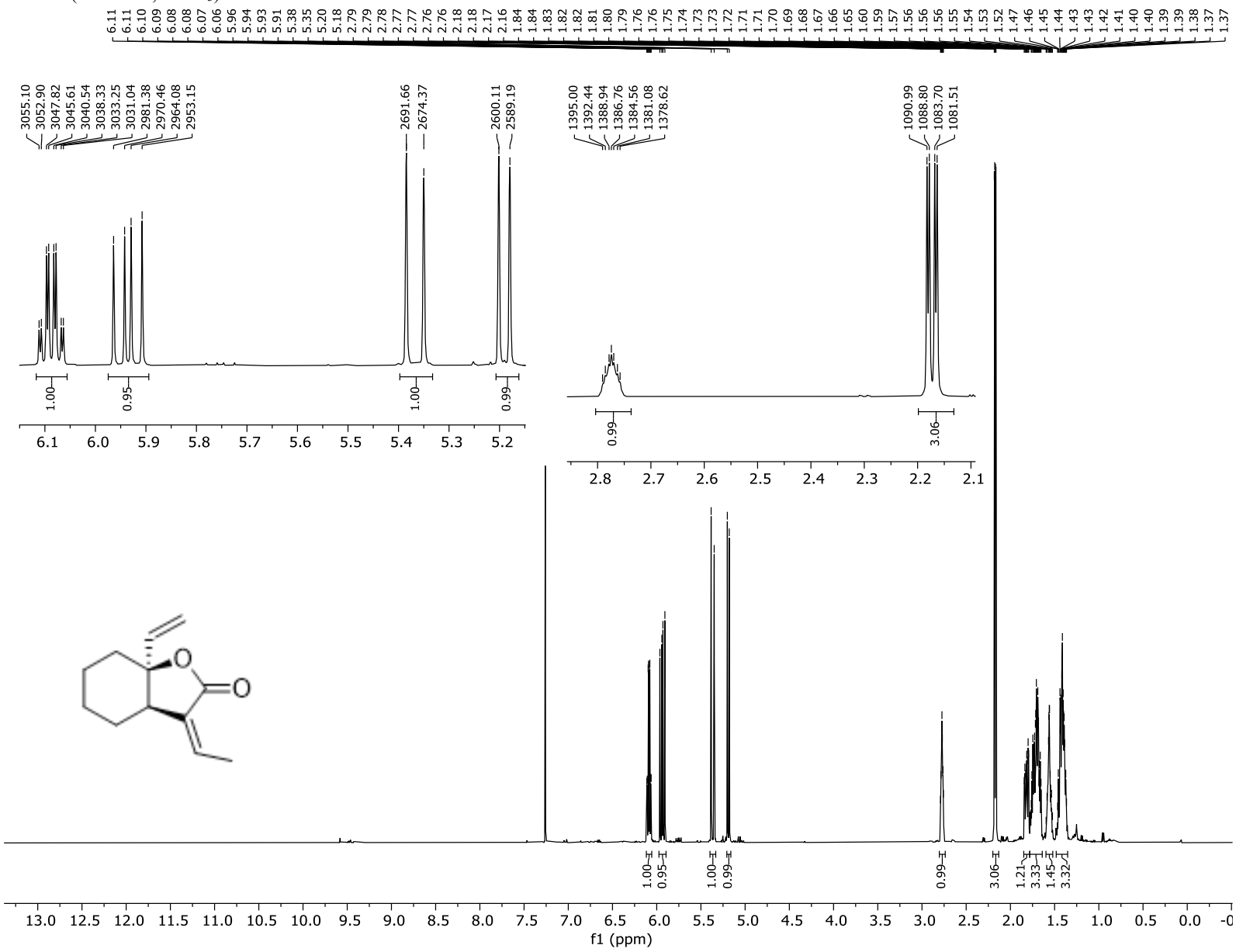
4.43 COSY (500 MHz, $CDCl_3$)



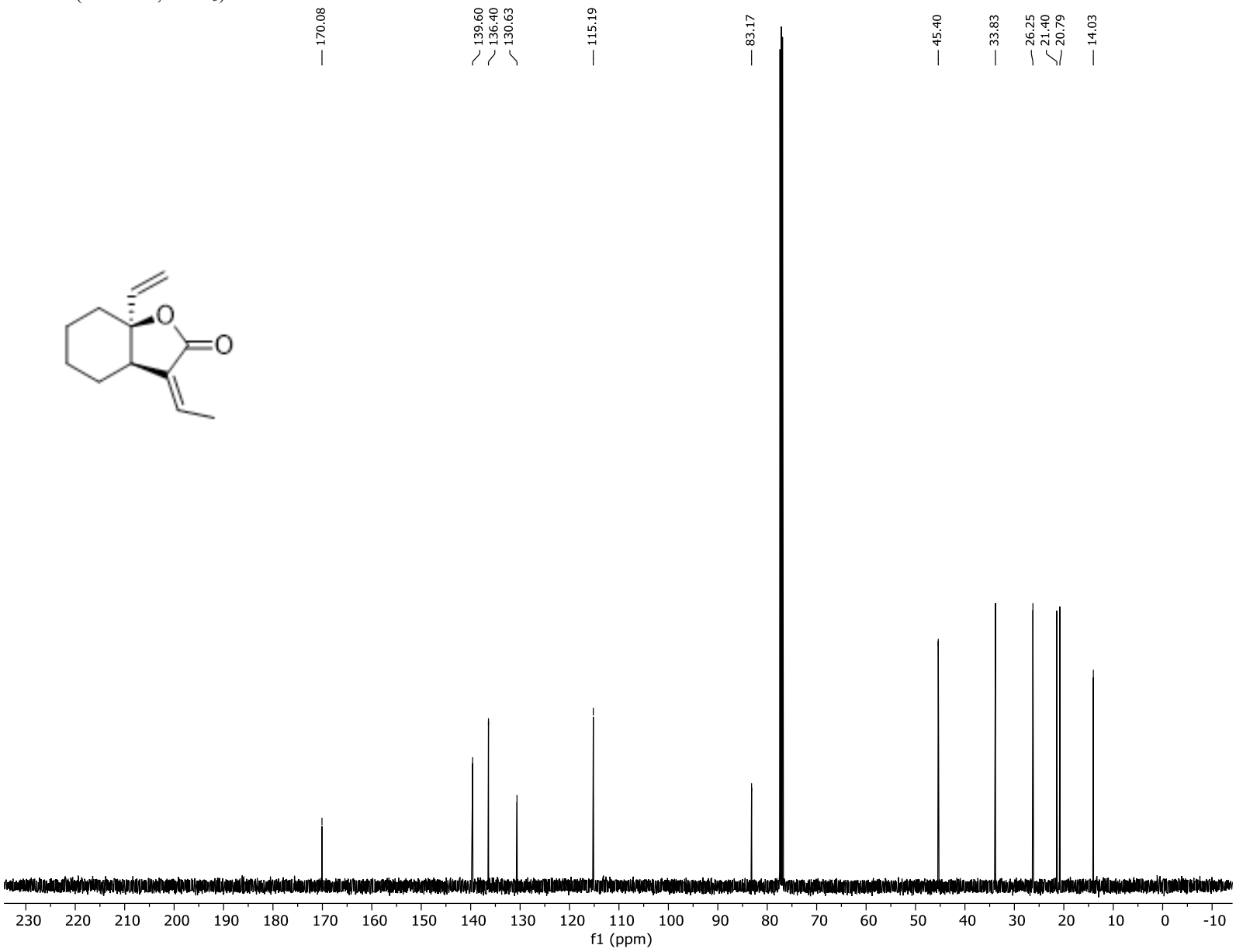
4.43 ^{13}C NMR (126 MHz, $CDCl_3$)



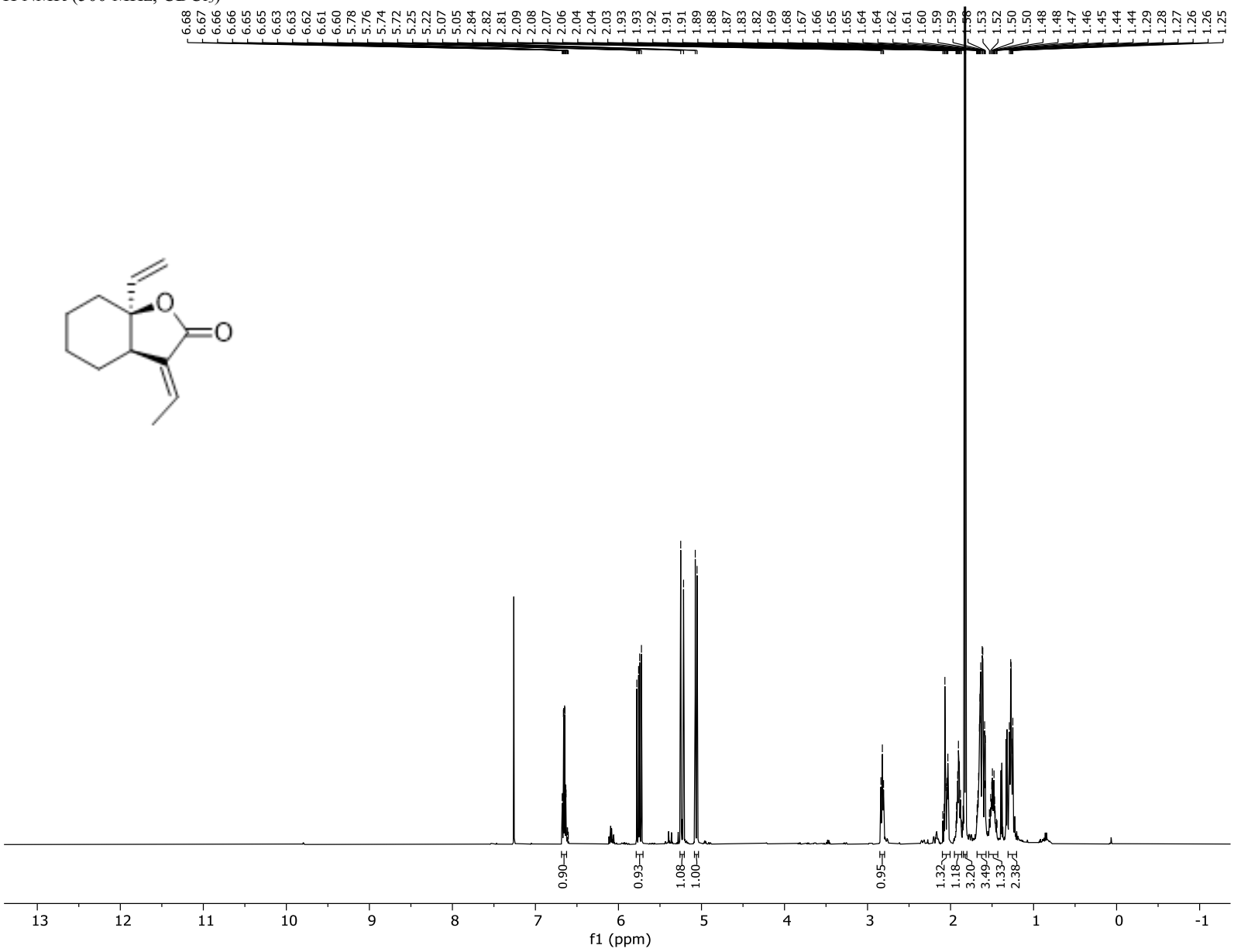
4.44a ^{1}H NMR (500 MHz, $CDCl_3$)



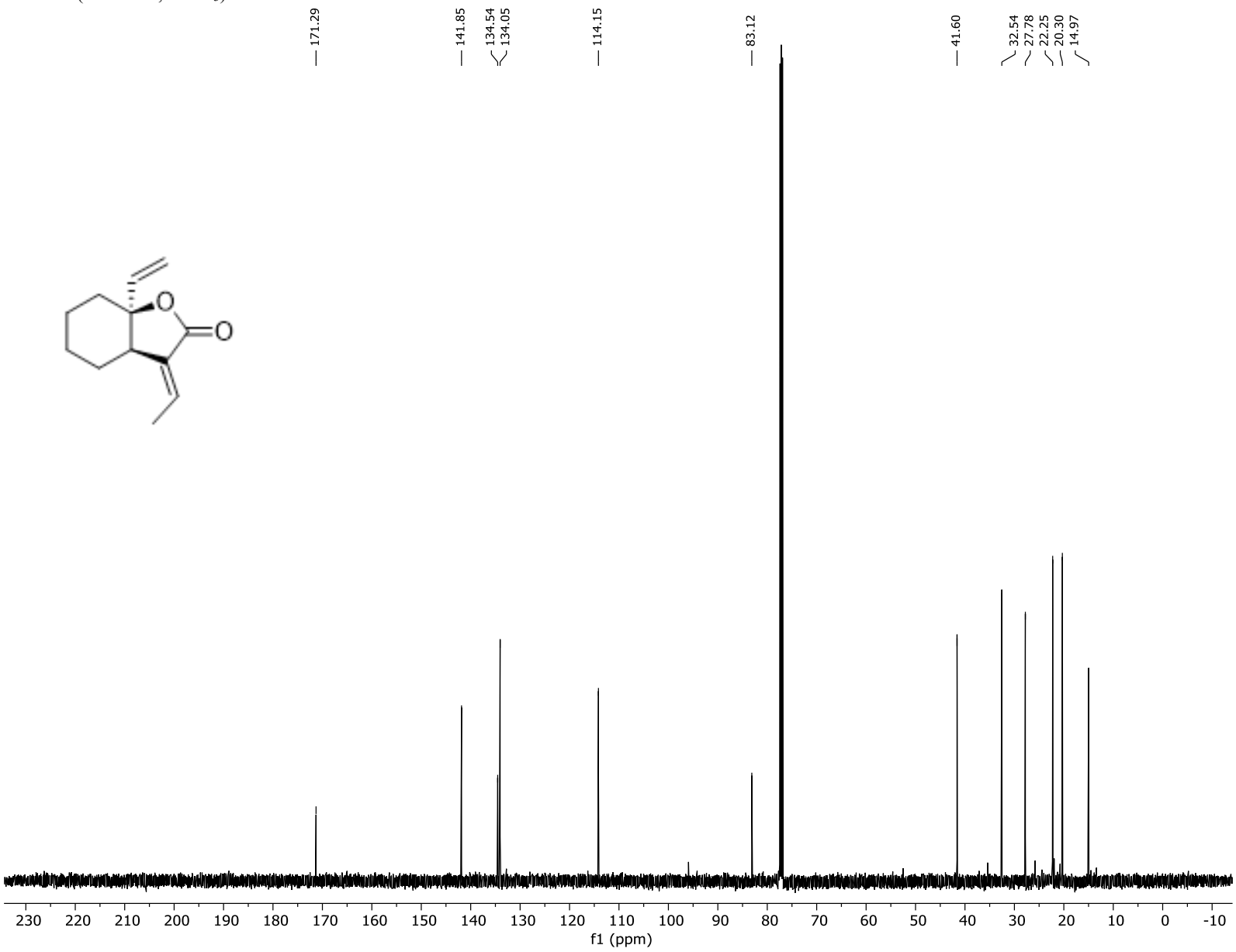
4.44a ^{13}C NMR (126 MHz, $CDCl_3$)



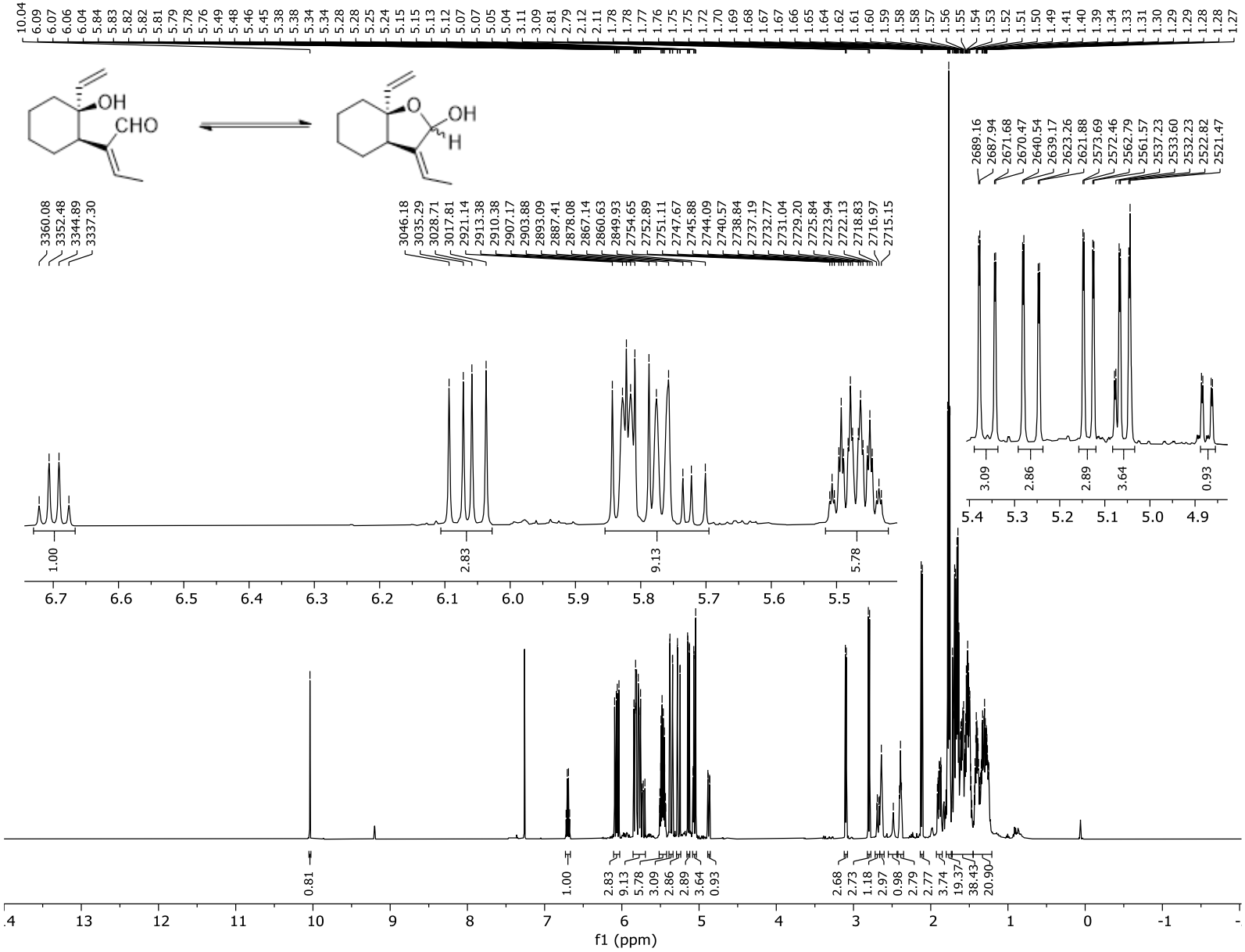
4.44b ^{1}H NMR (500 MHz, $CDCl_3$)



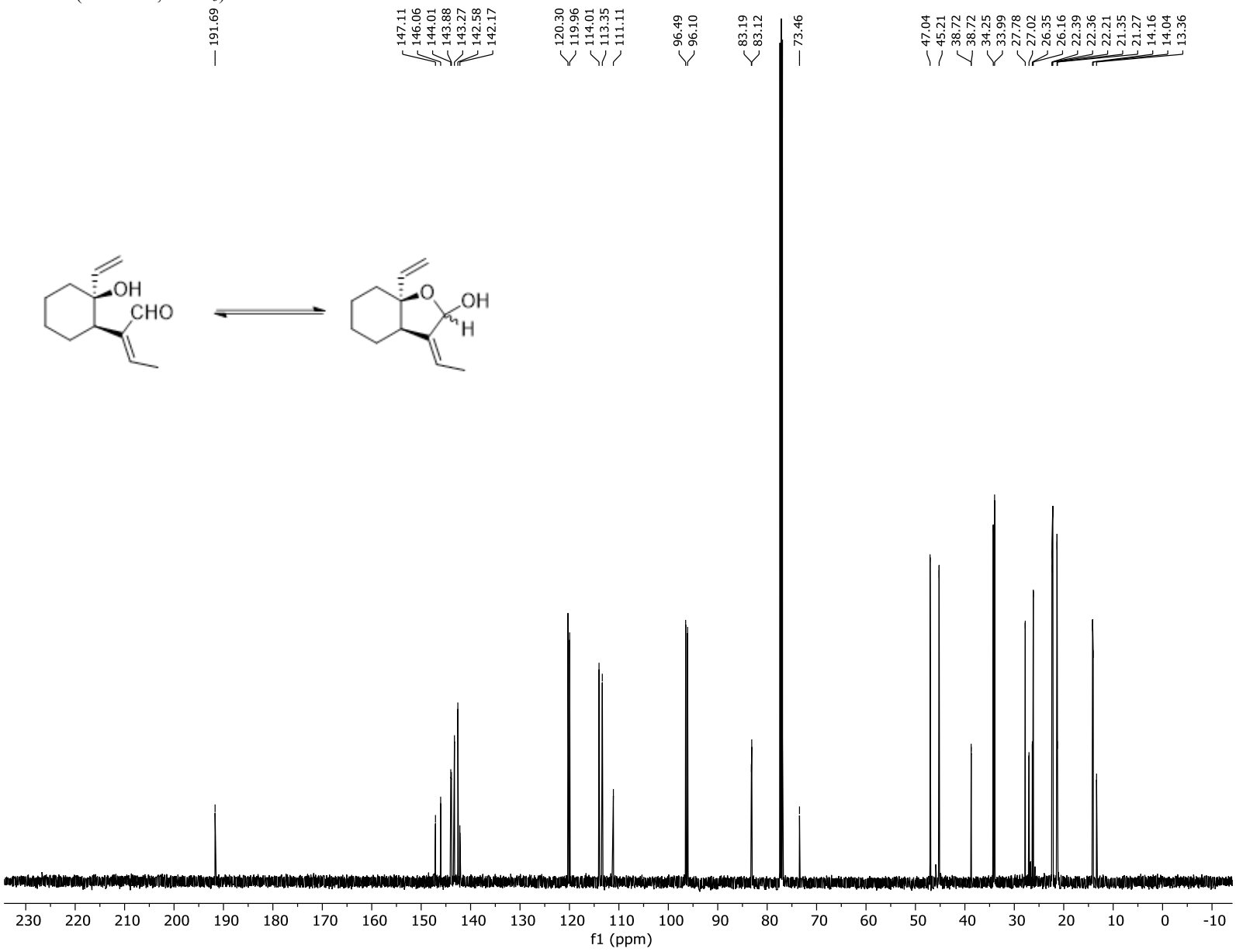
4.44b ^{13}C NMR (126 MHz, $CDCl_3$)



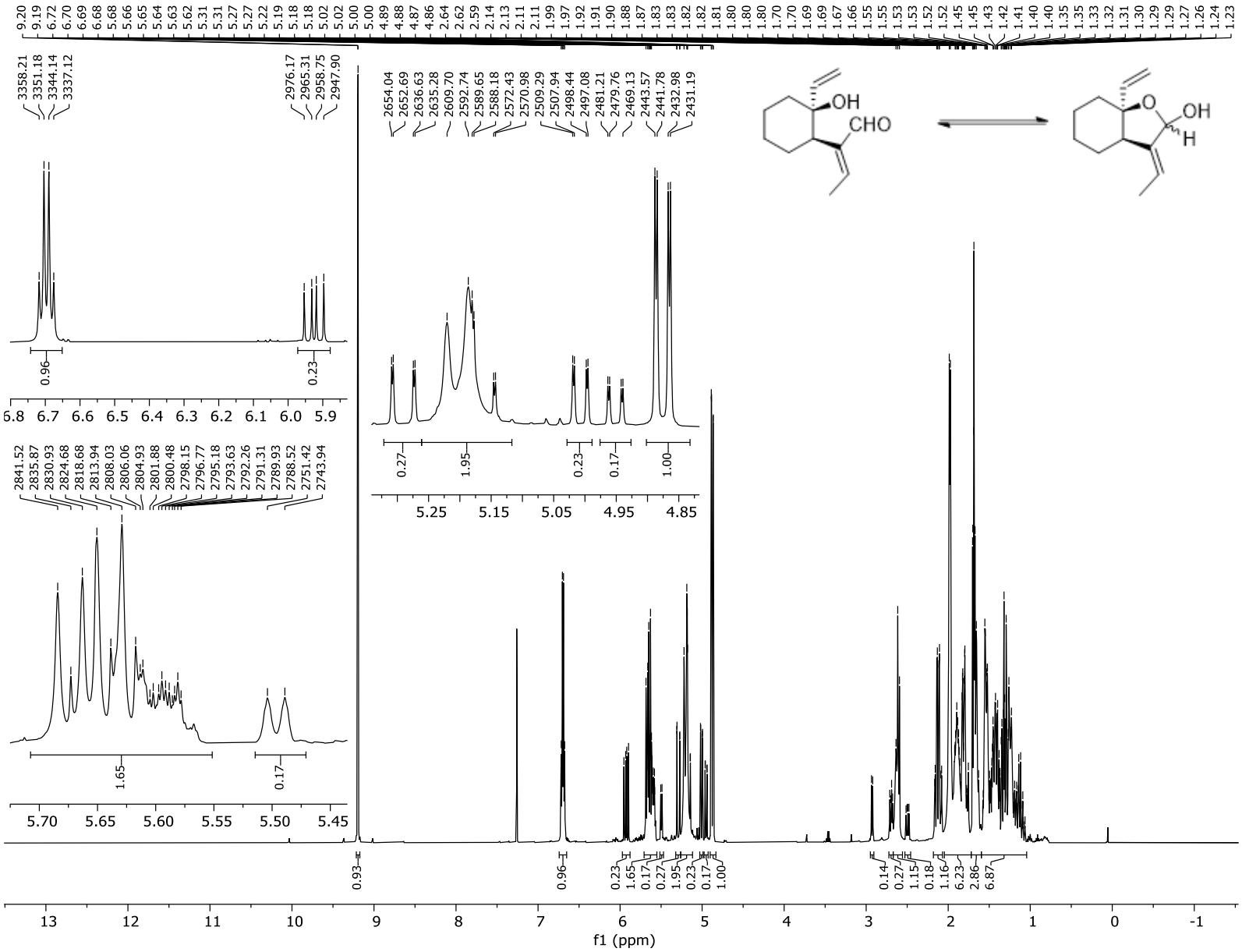
4.45a ^{1}H NMR (500 MHz, $CDCl_3$)



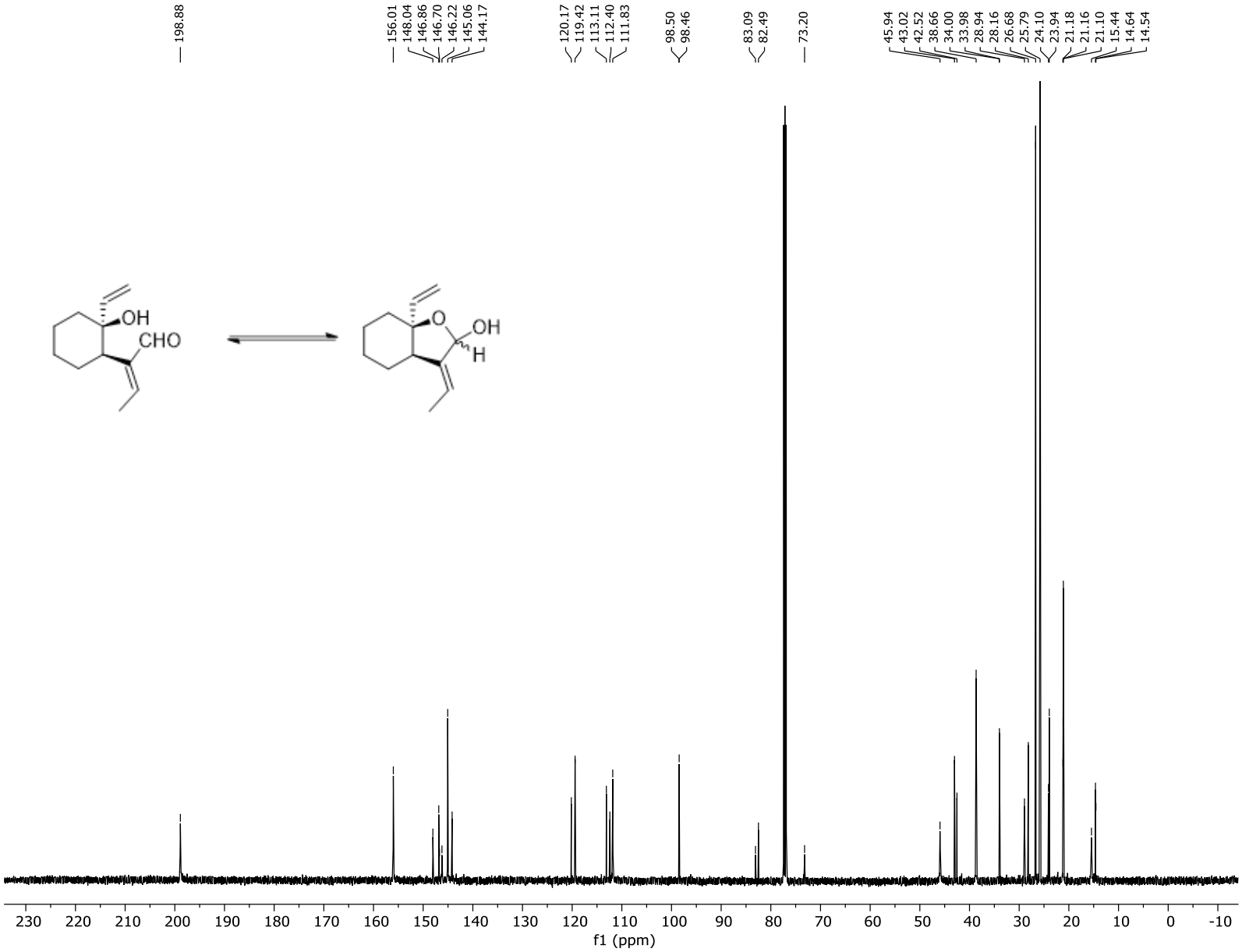
4.45a ^{13}C NMR (126 MHz, $CDCl_3$)



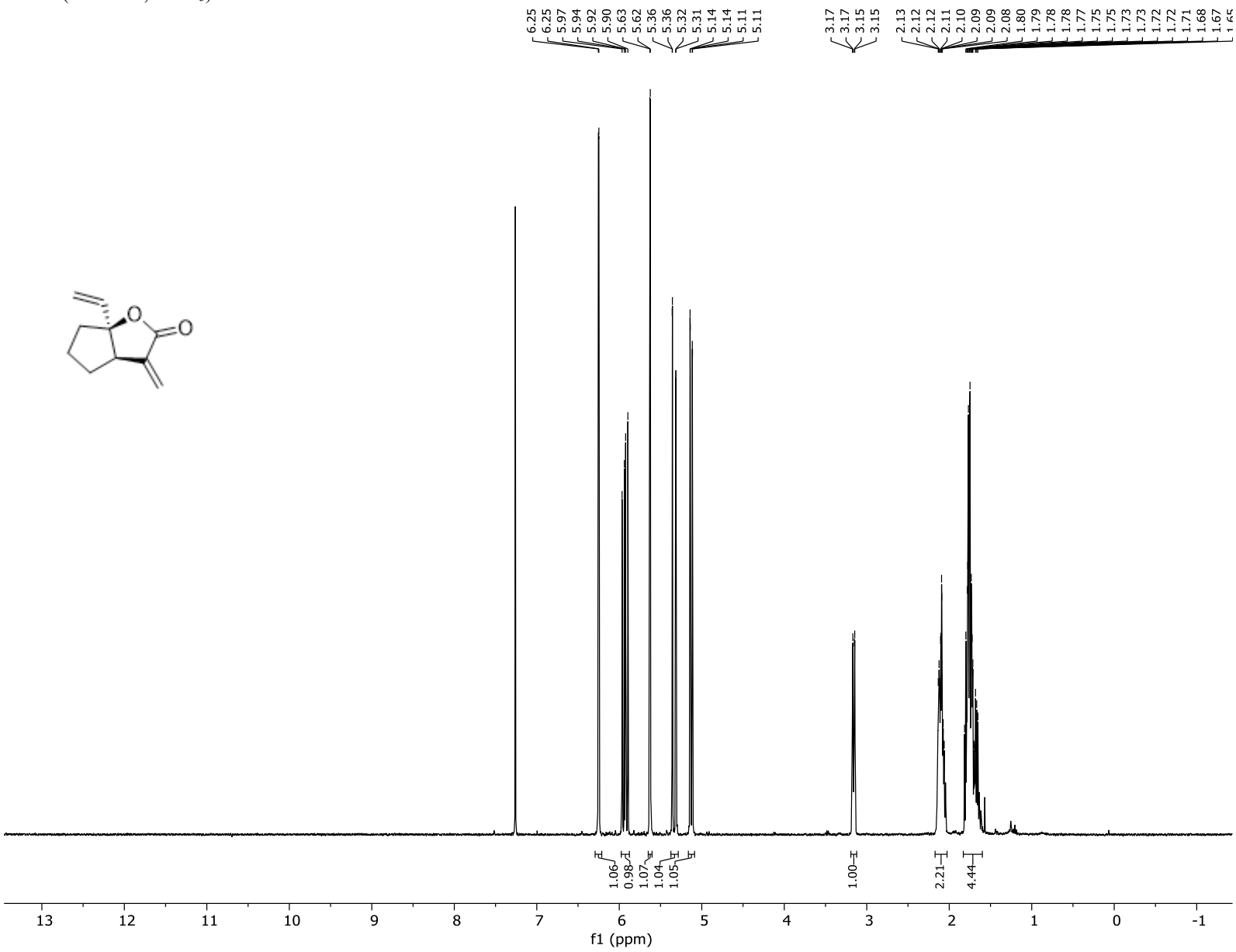
4.45b ^{1}H NMR (500 MHz, $CDCl_3$)



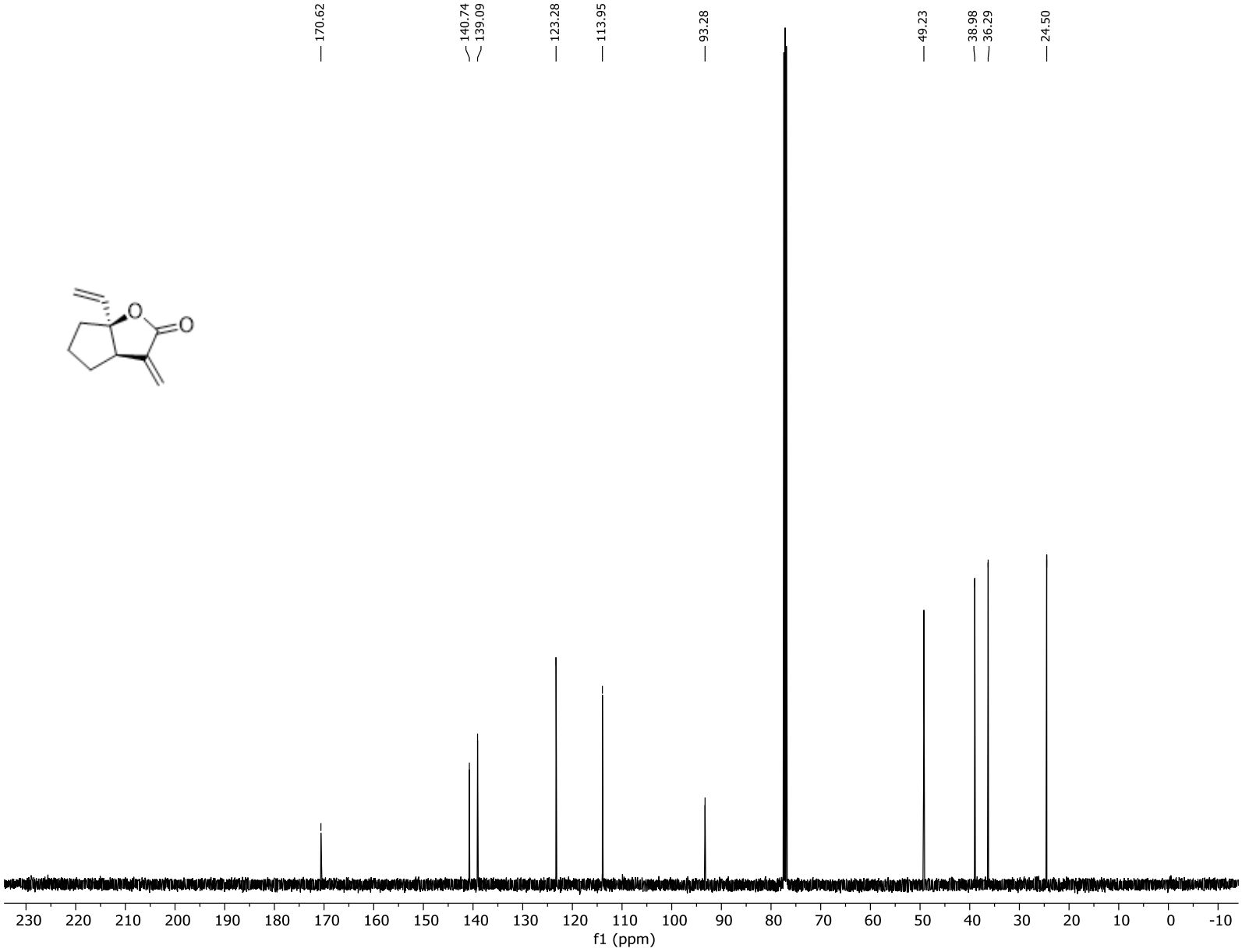
4.45b ^{13}C NMR (126 MHz, $CDCl_3$)



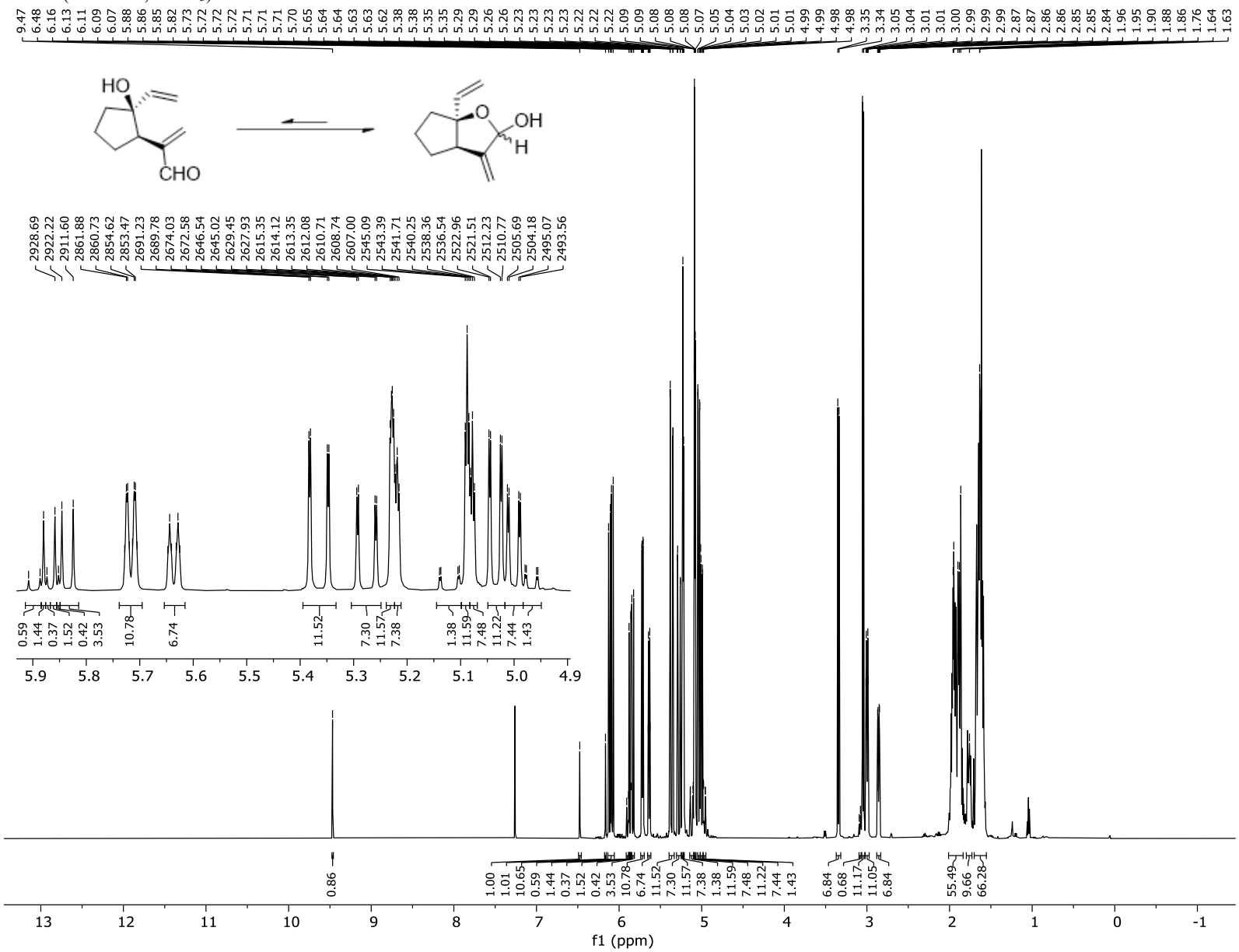
4.53 ^{1}H NMR (400 MHz, $CDCl_3$)



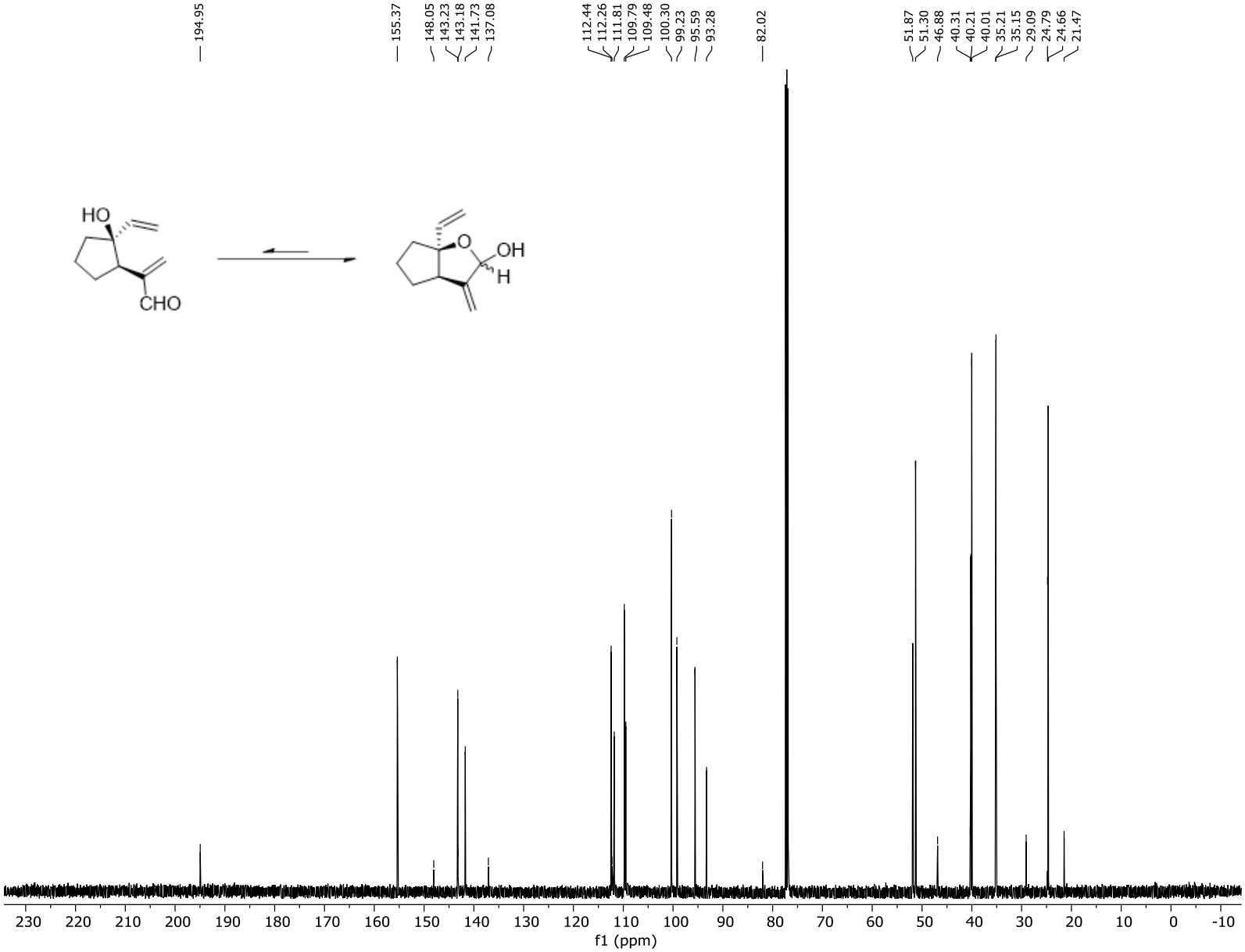
4.53 ^{13}C NMR (126 MHz, $CDCl_3$)



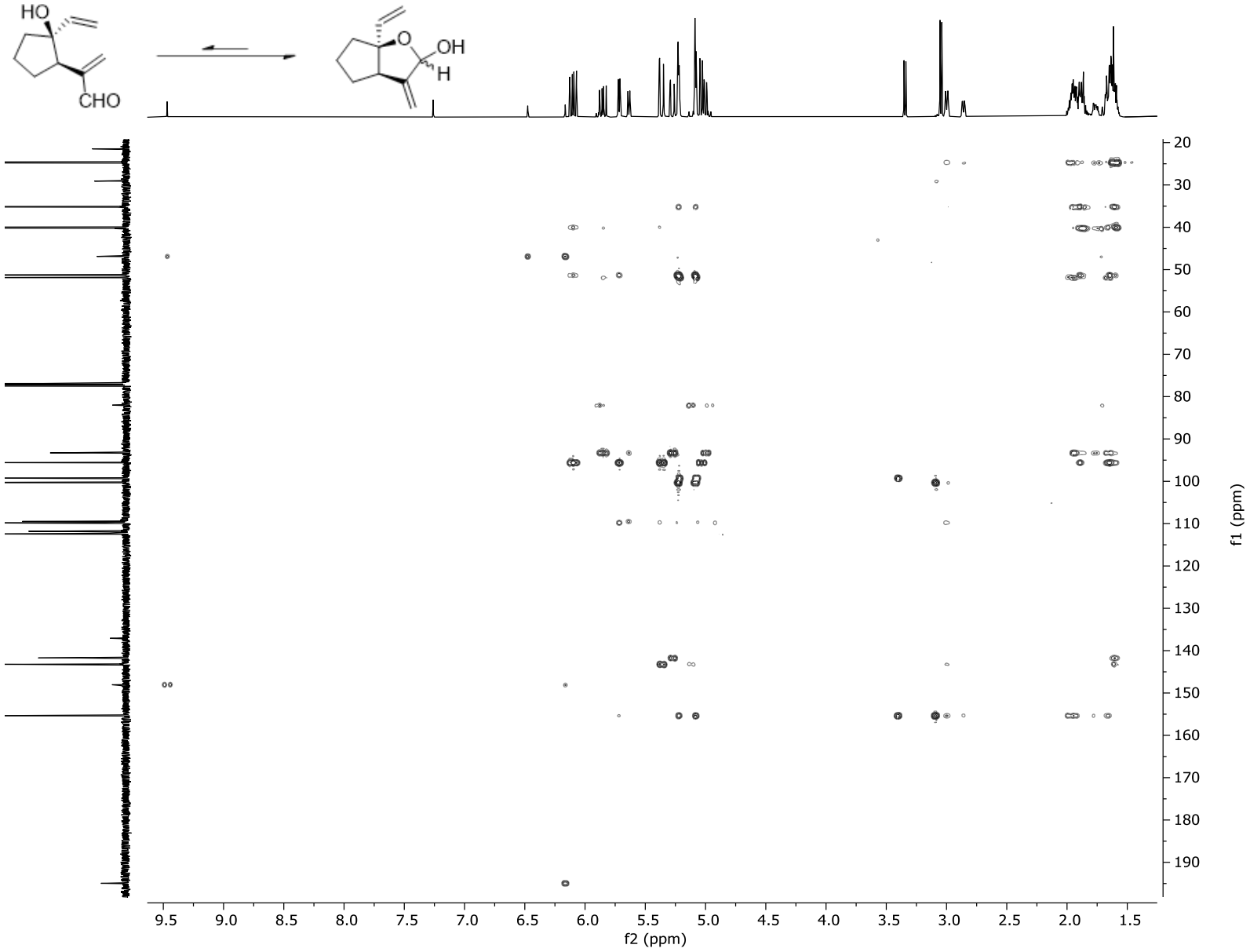
4.50 ^{1}H NMR (500 MHz, $CDCl_3$)



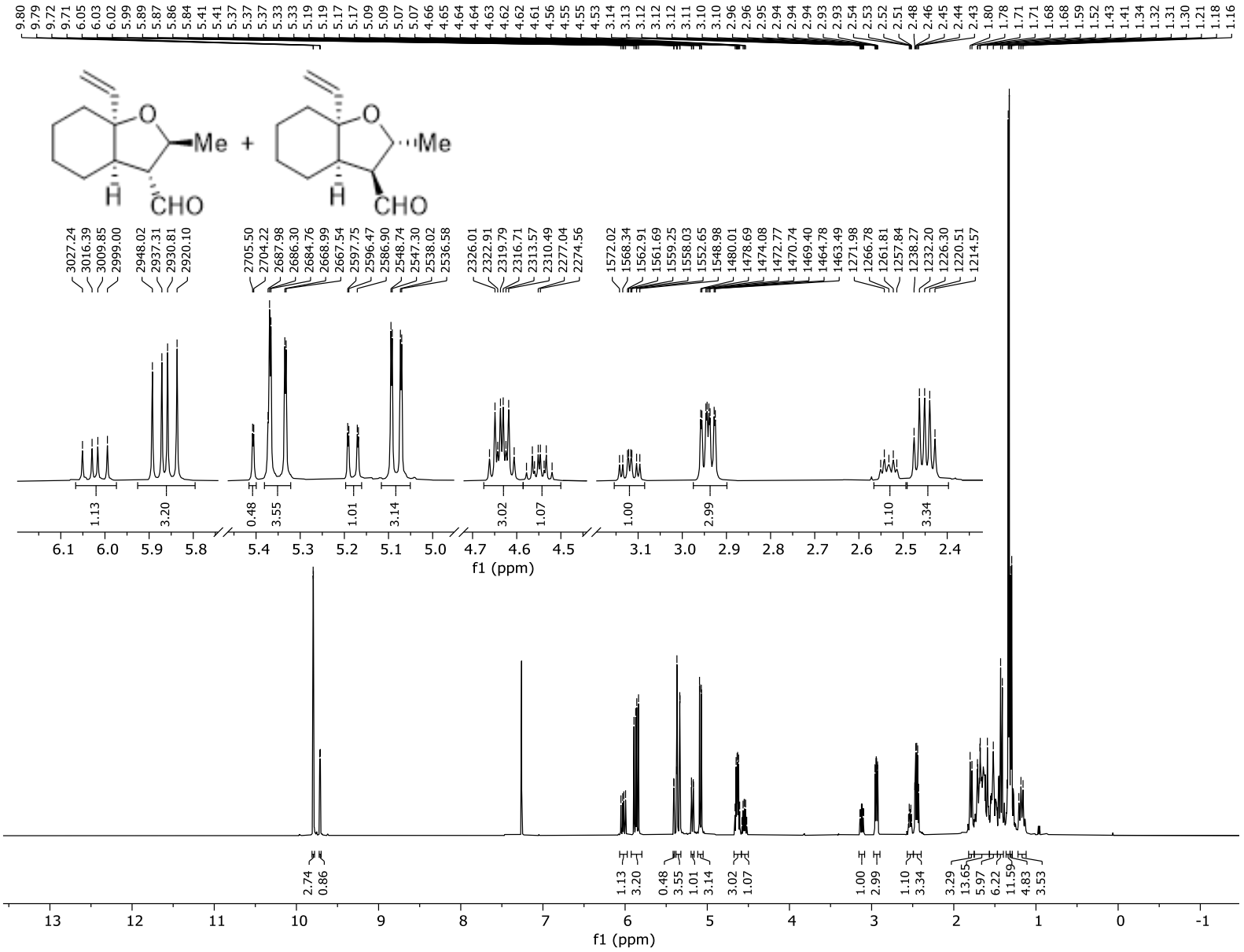
4.50 ^{13}C NMR (126 MHz, $CDCl_3$)



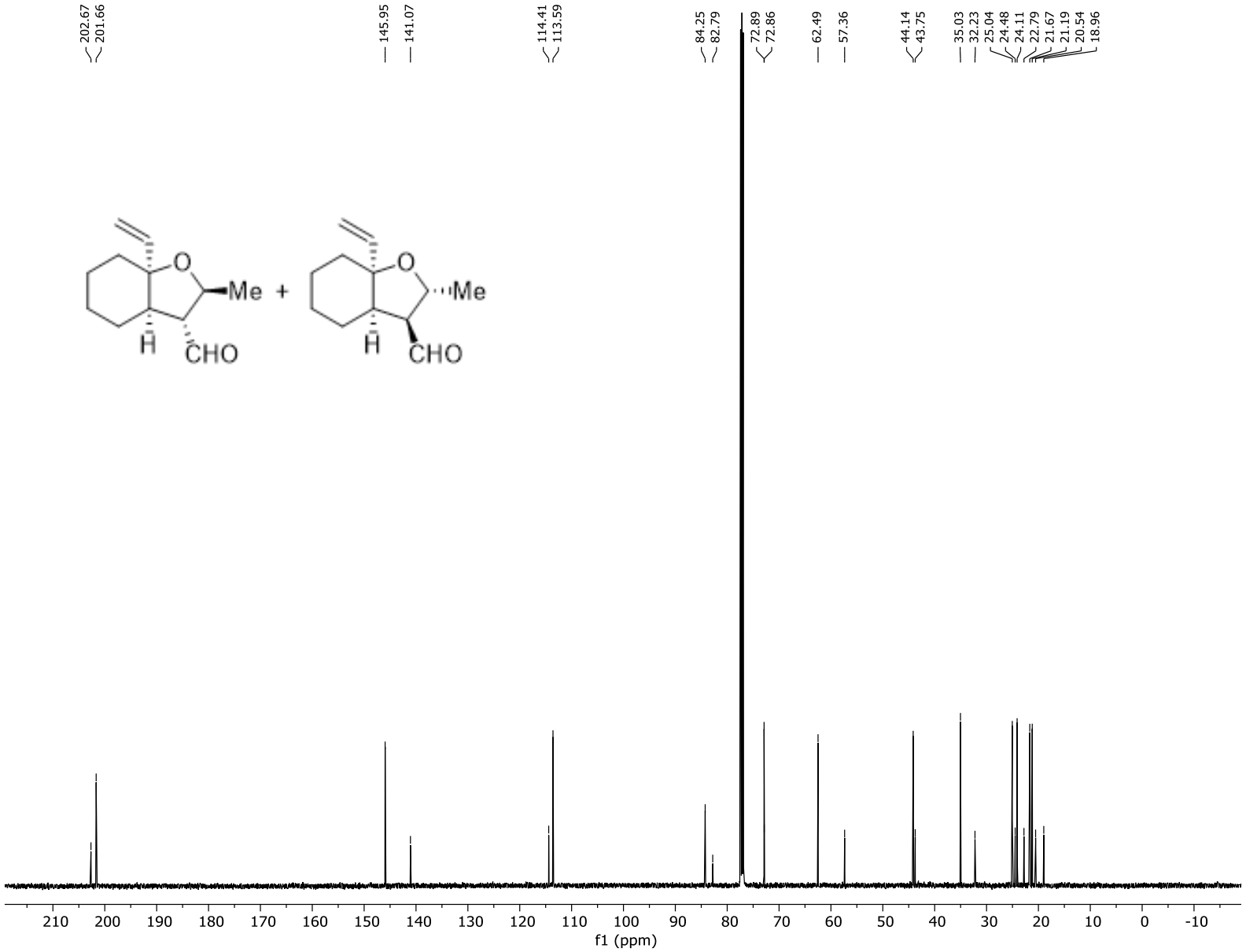
4.50 HMBC (500 MHz, $CDCl_3$)



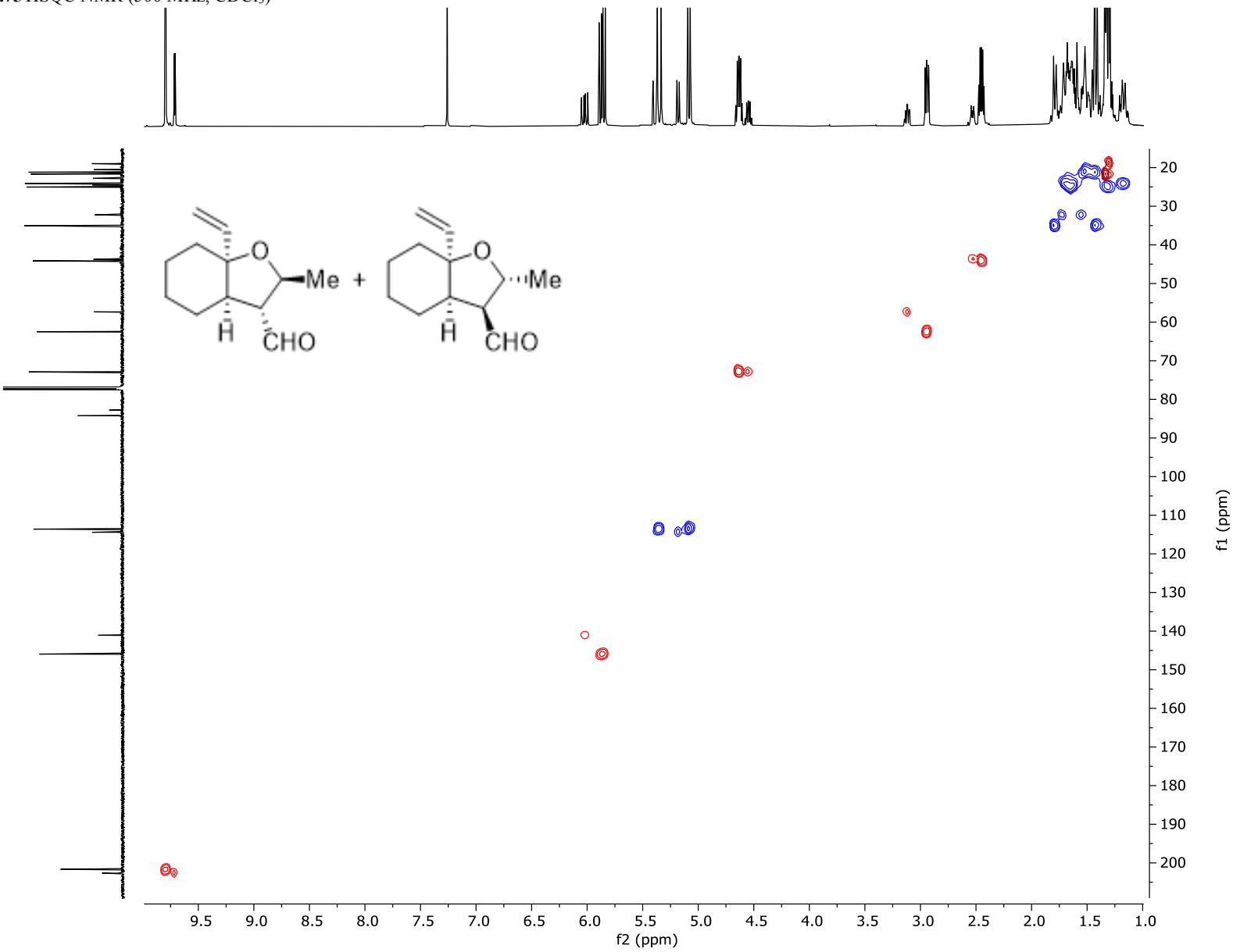
4.74 / **4.75** ^{1}H NMR (500 MHz, $CDCl_3$)



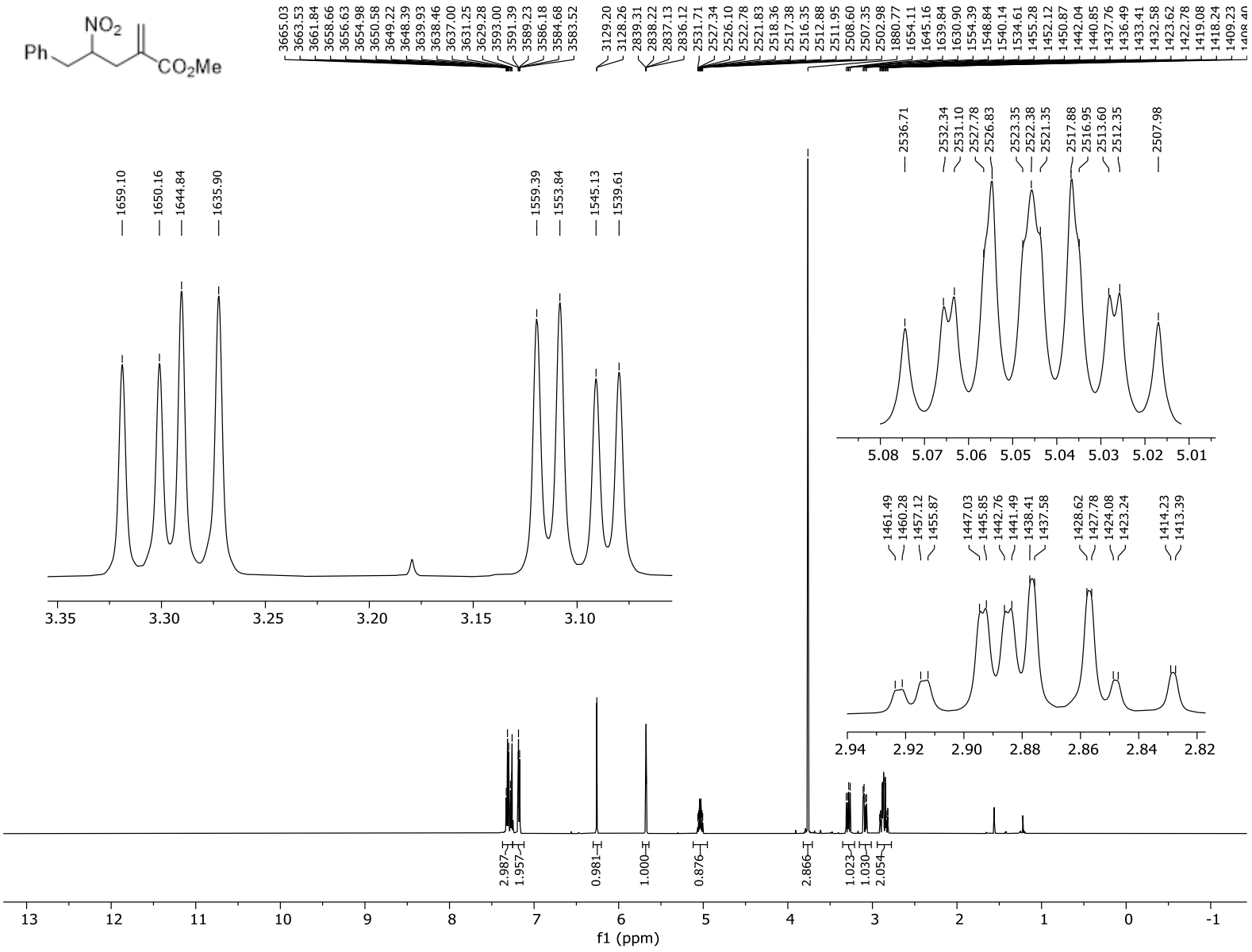
4.74 / **4.75** ^{13}C NMR (126 MHz, $CDCl_3$



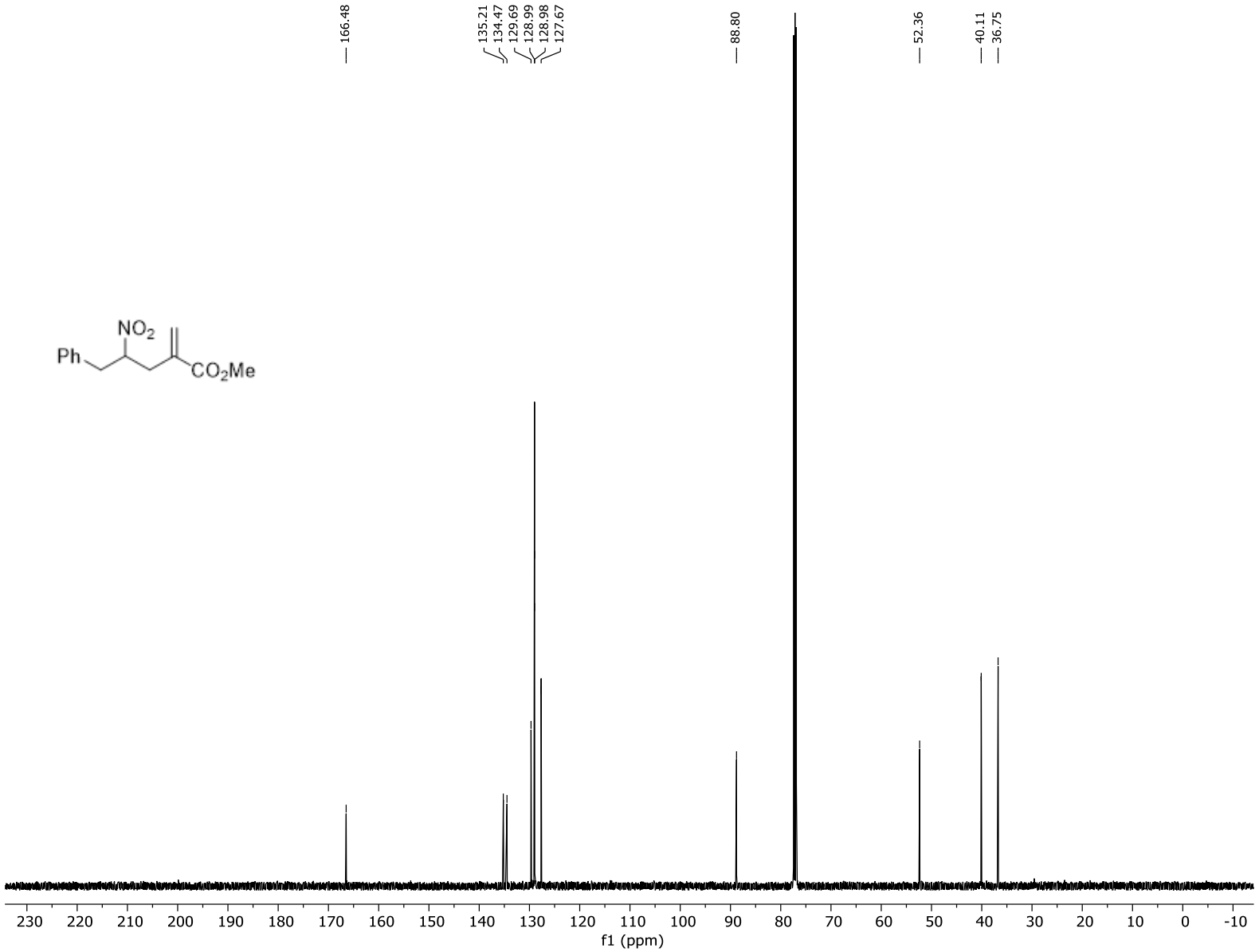
4.74 / **4.75** HSQC NMR (500 MHz, $CDCl_3$)



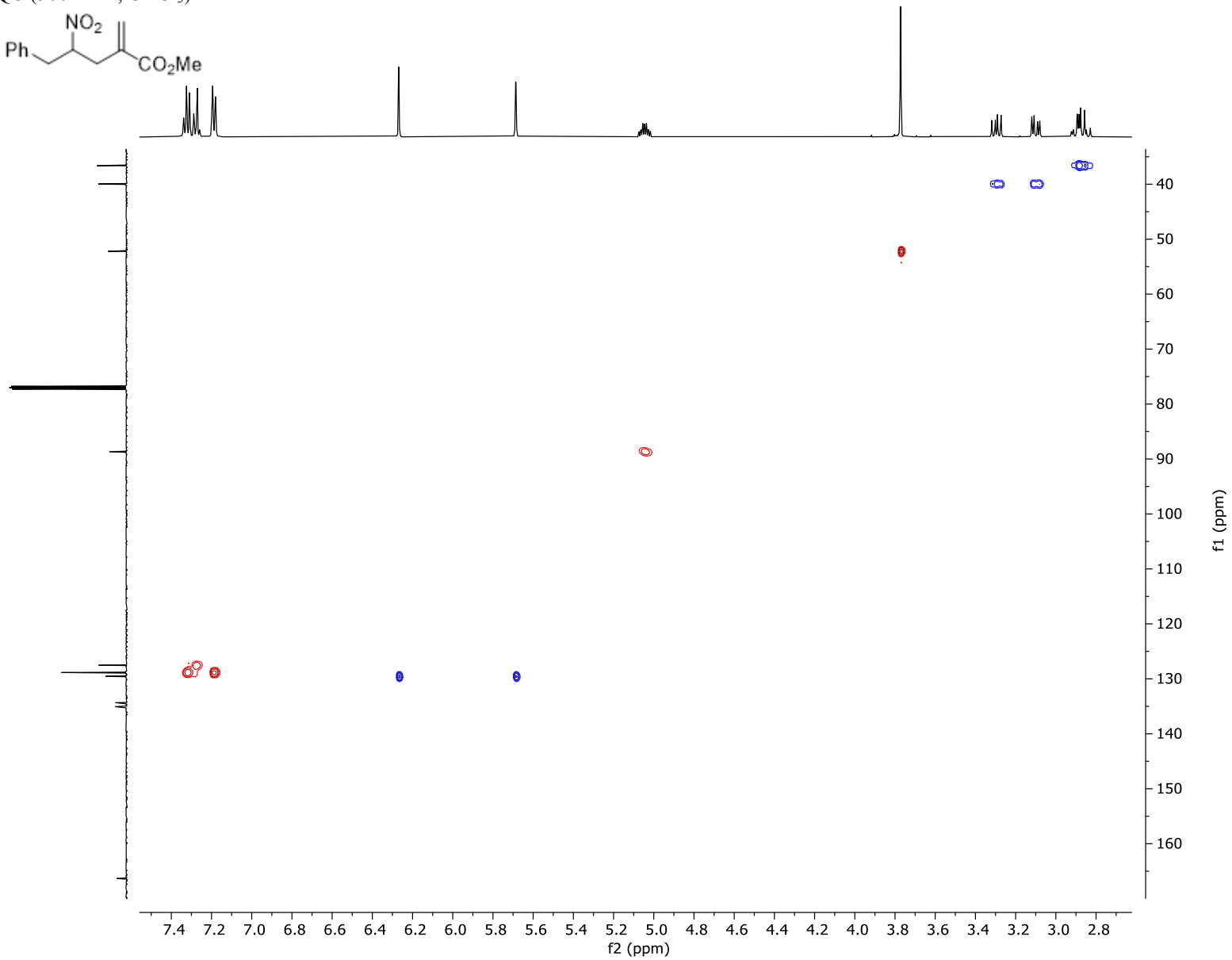
4.83 ^{1}H NMR (500 MHz, $CDCl_3$)



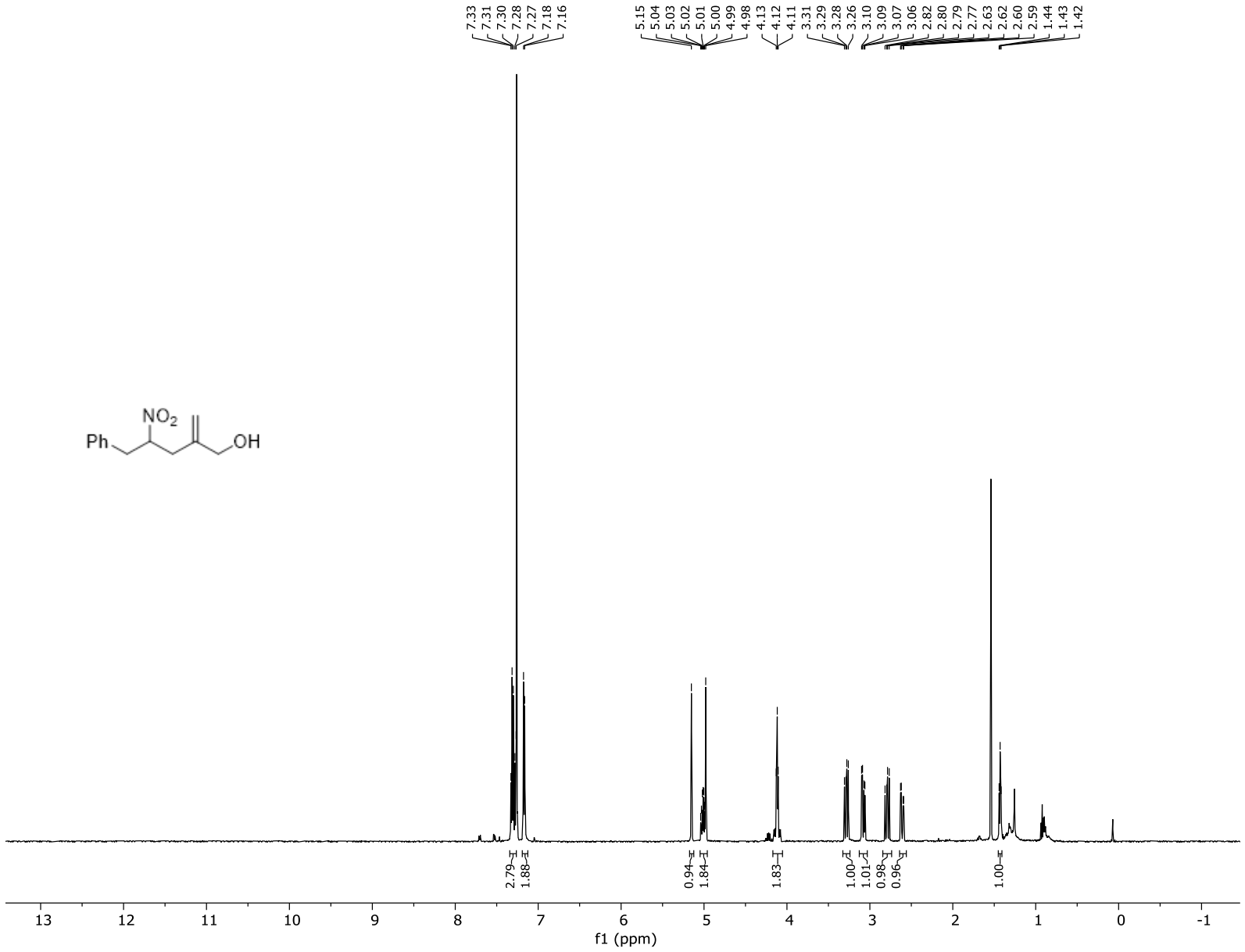
4.83 ^{13}C NMR (126 MHz, $CDCl_3$)



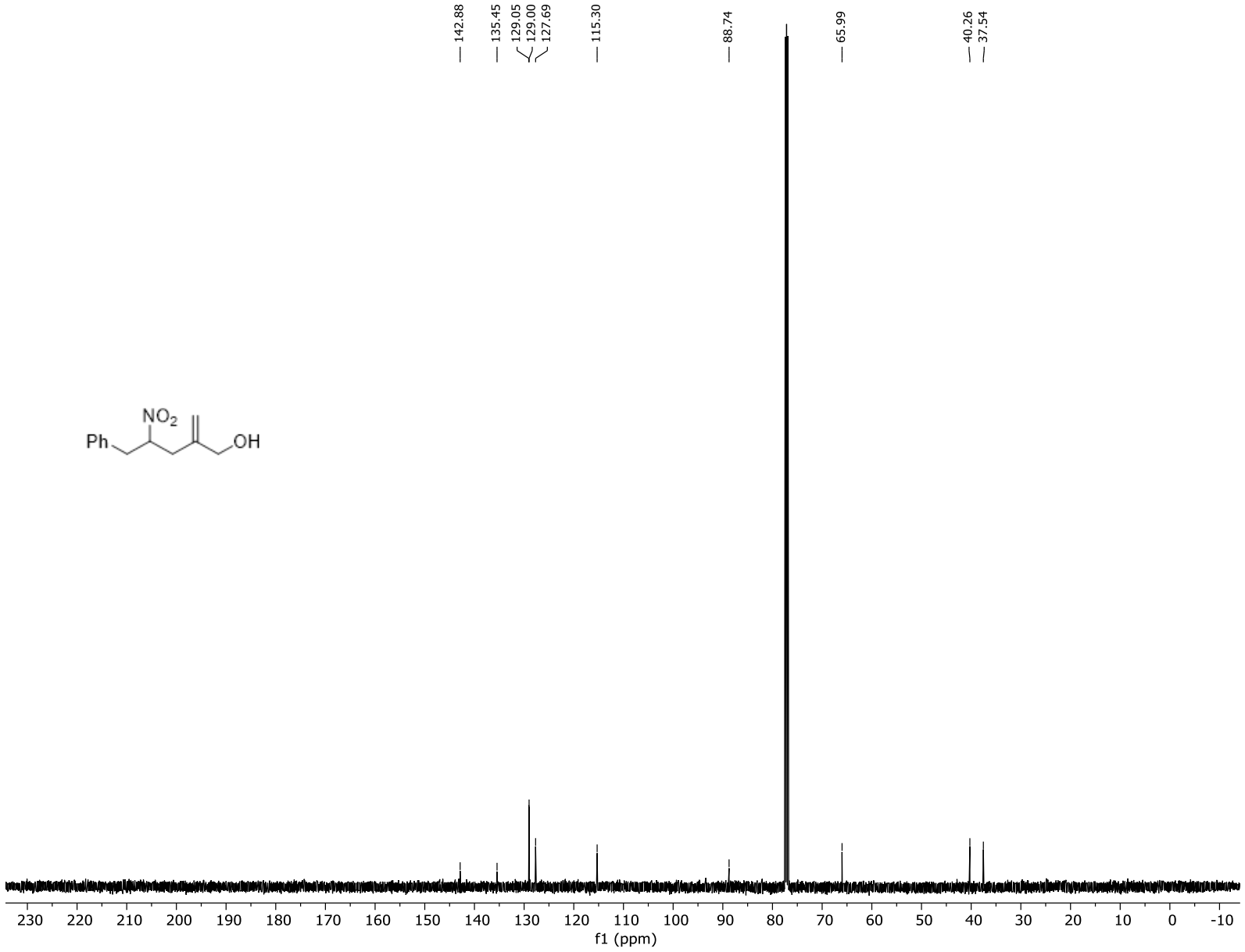
4.83 HSQC (500 MHz, $CDCl_3$)



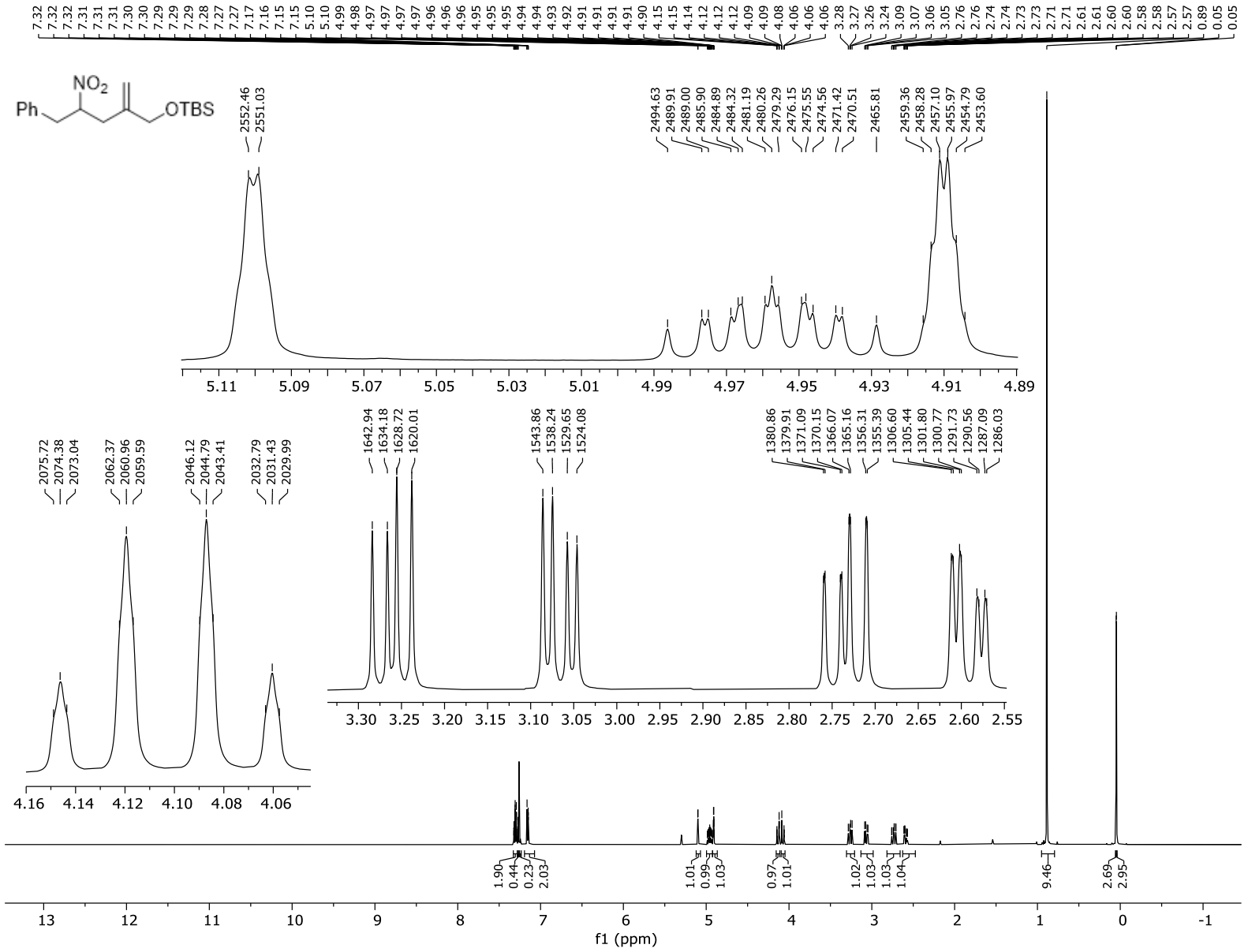
4.84 ^{1}H NMR (500 MHz, $CDCl_3$)



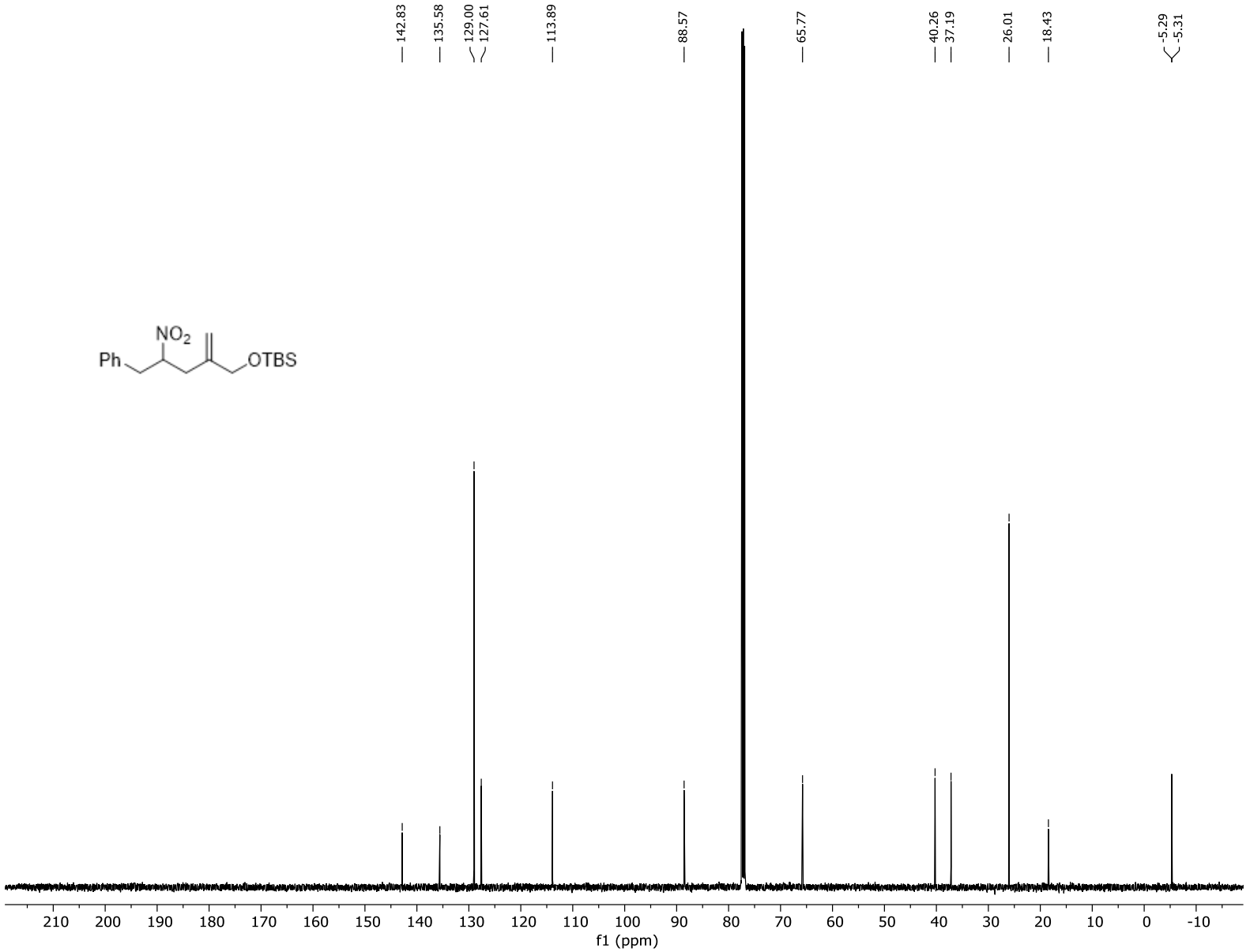
4.84 ^{13}C NMR (126 MHz, $CDCl_3$)



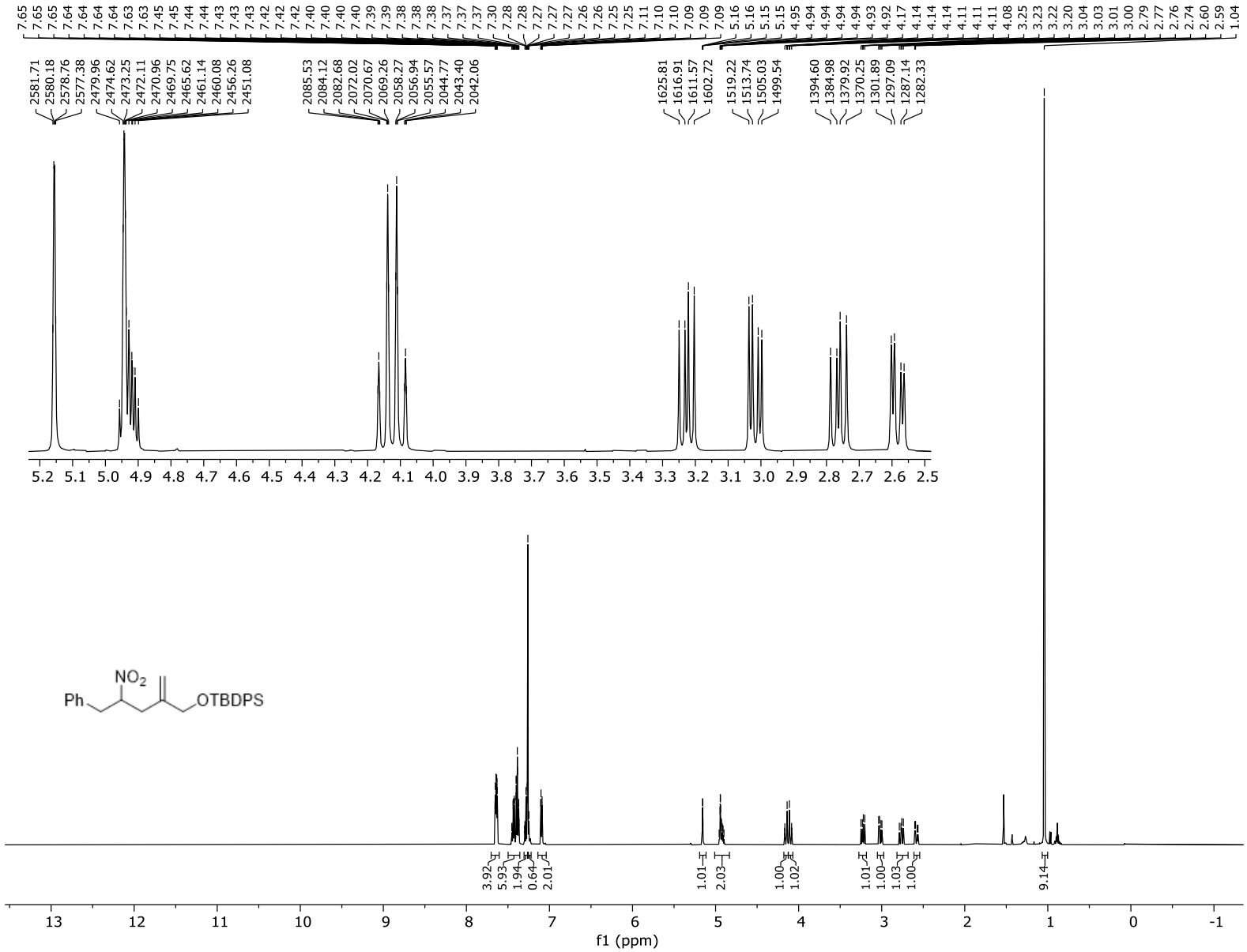
4.86 ^{1}H NMR (500 MHz, $CDCl_3$)



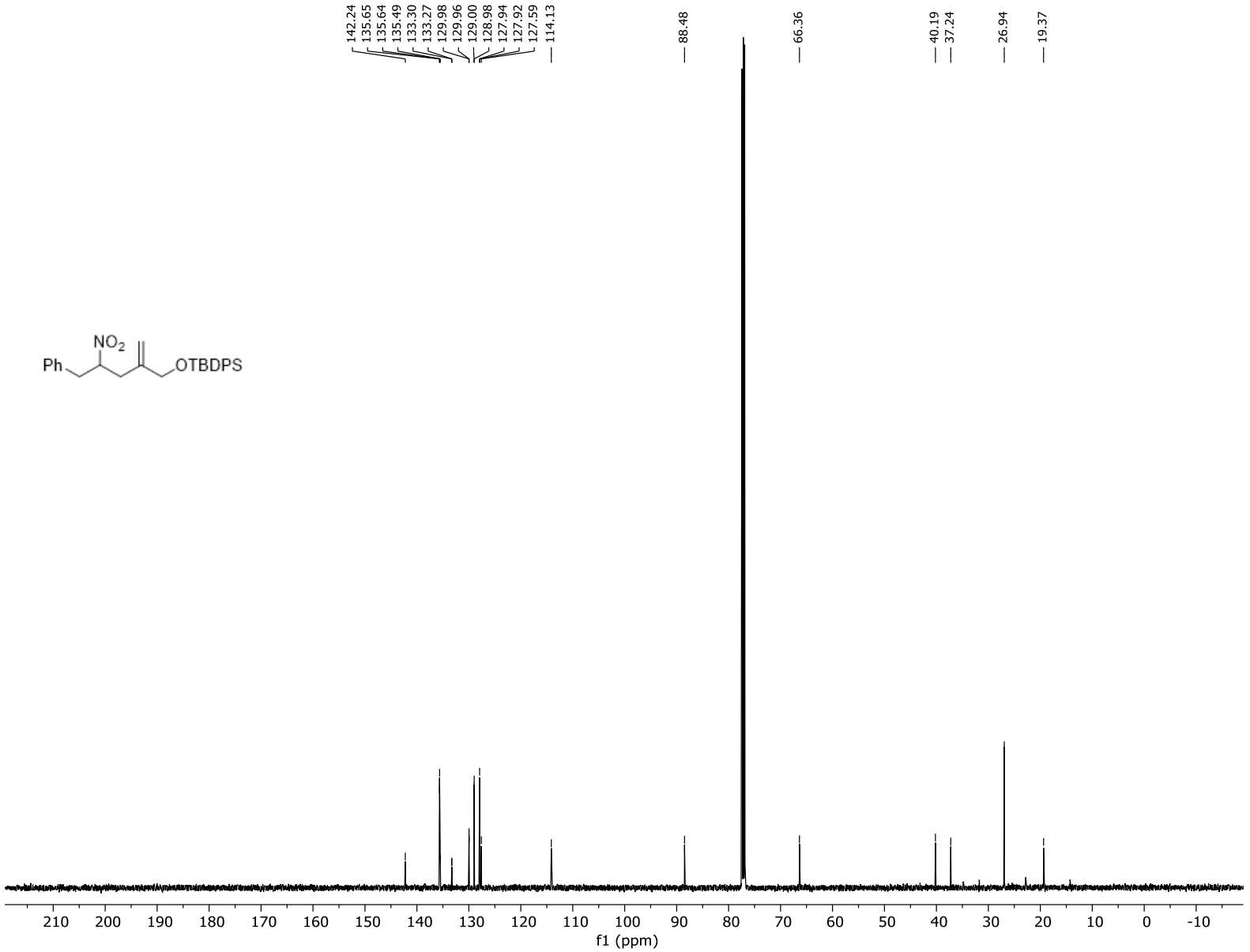
4.86 ^{13}C NMR (126 MHz, $CDCl_3$)



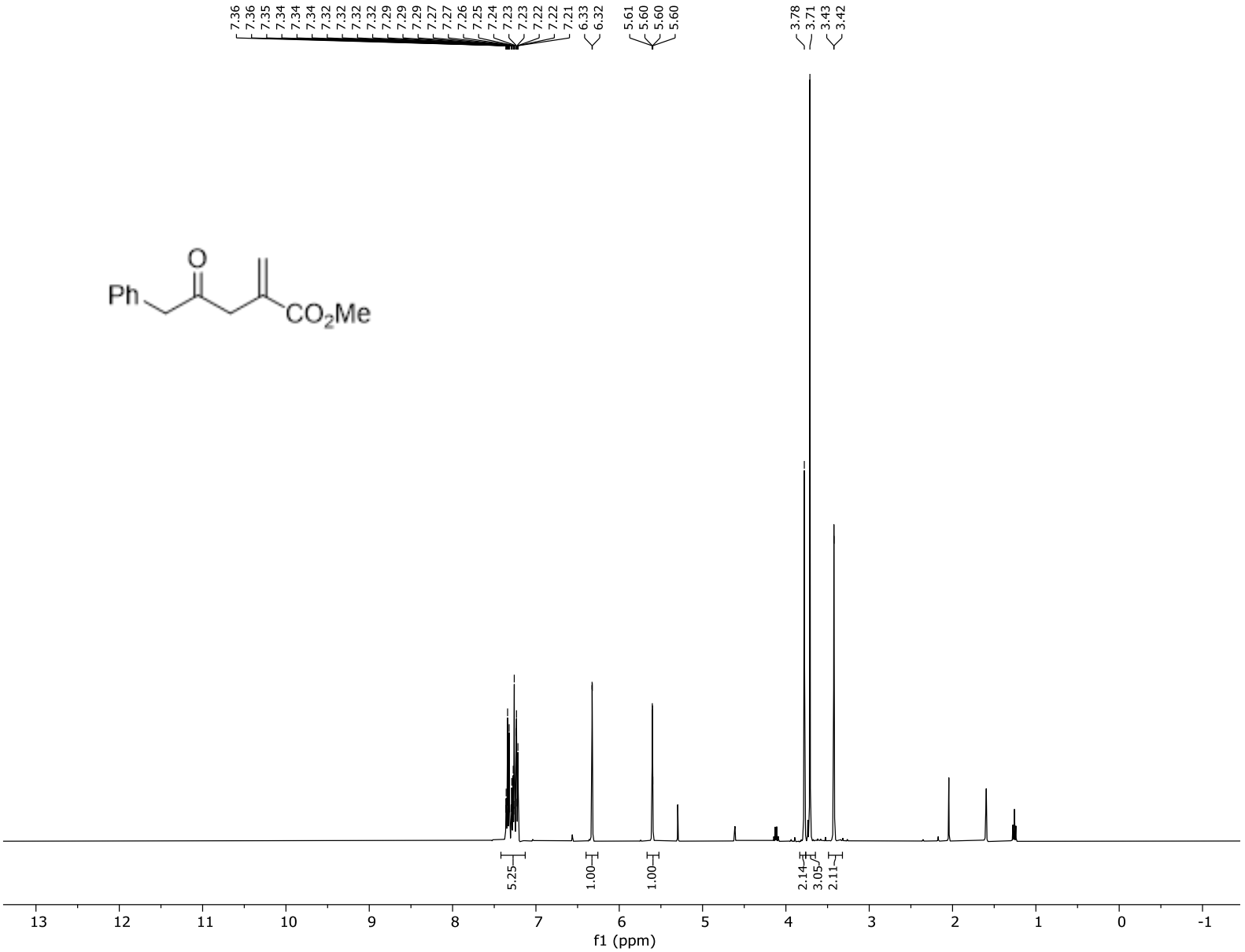
4.88 ^{1}H NMR (500 MHz, $CDCl_3$)



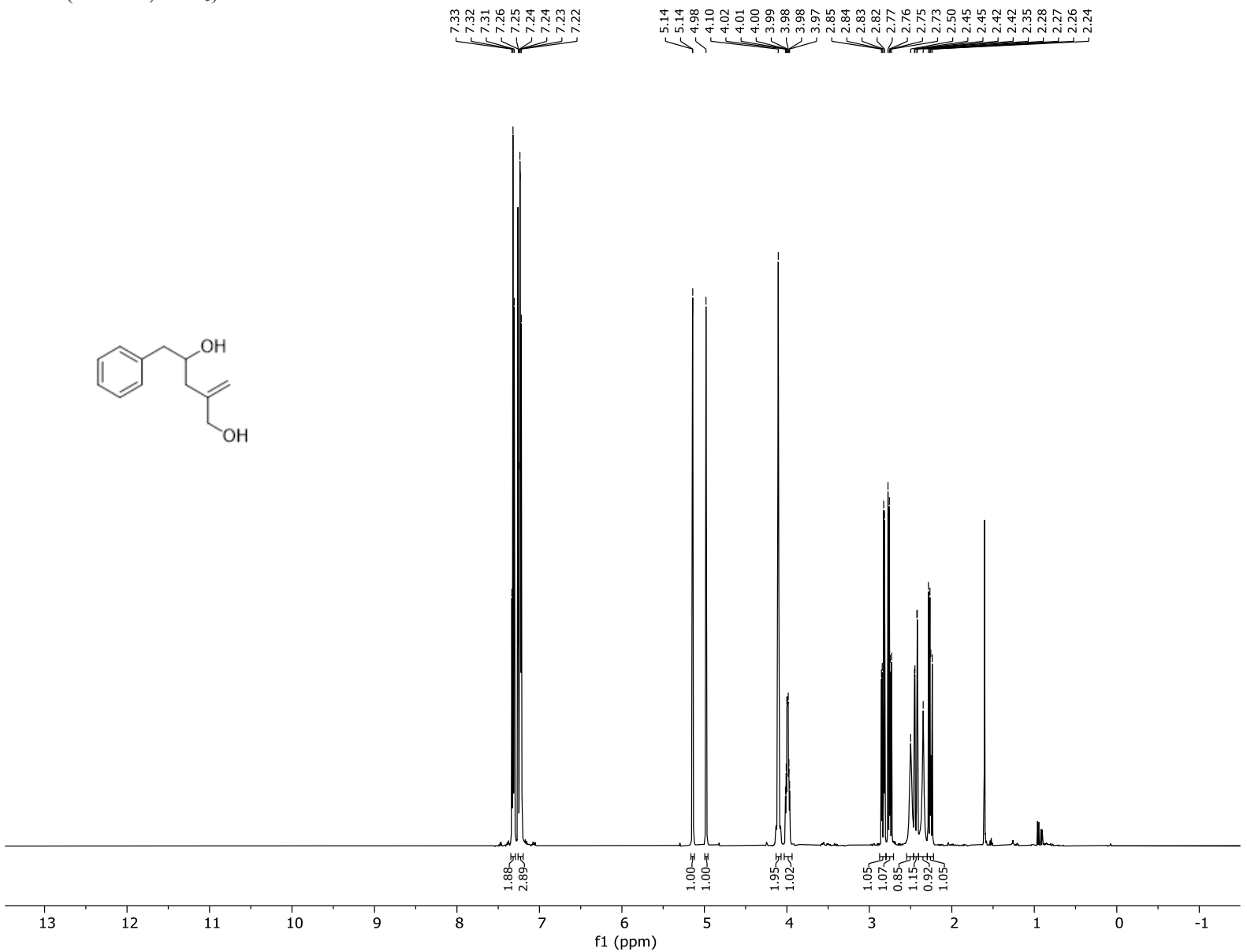
4.88 ^{13}C NMR (126 MHz, $CDCl_3$)



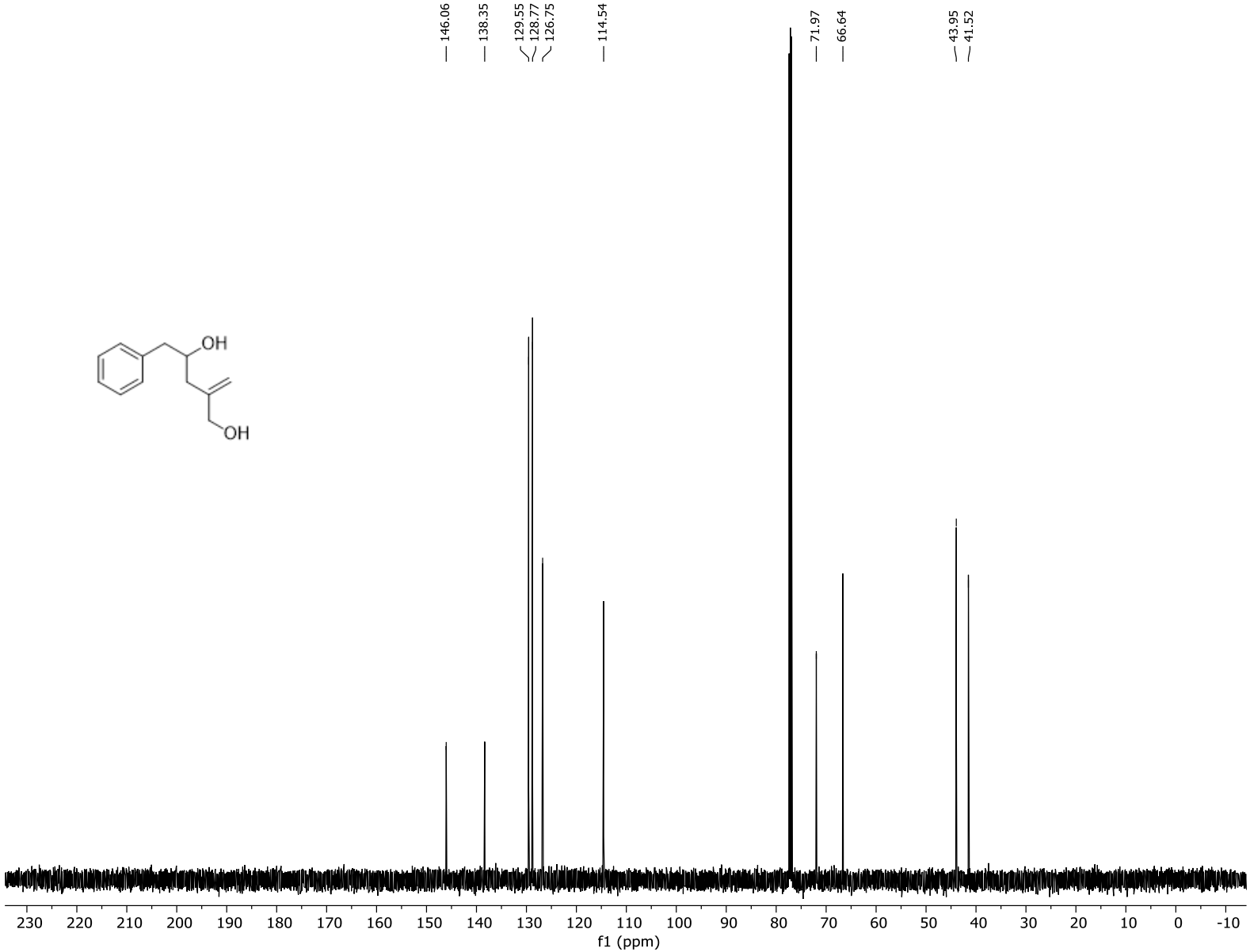
5.10 ^{1}H NMR (400 MHz, $CDCl_3$)



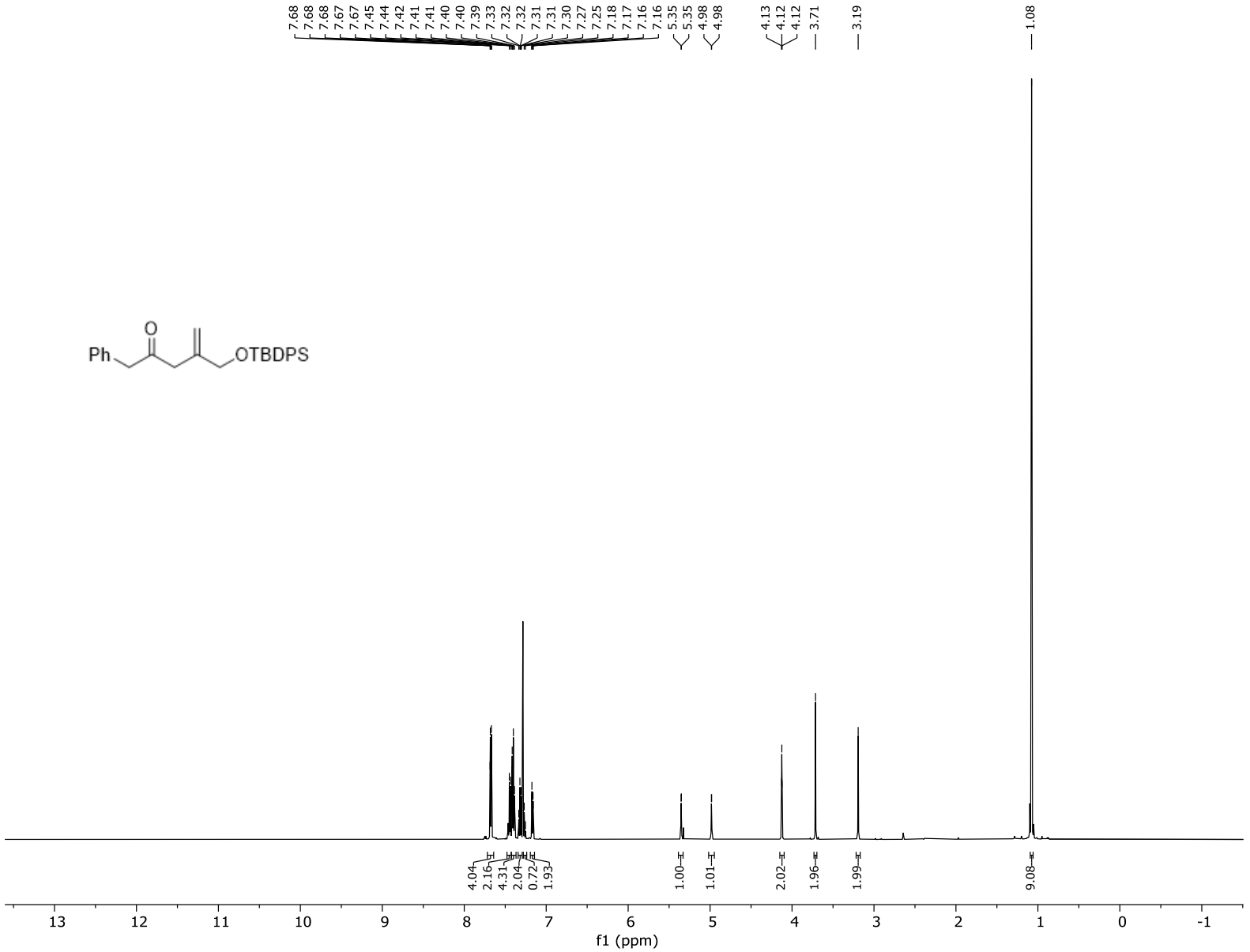
4.105 ^{1}H NMR (500 MHz, $CDCl_3$)



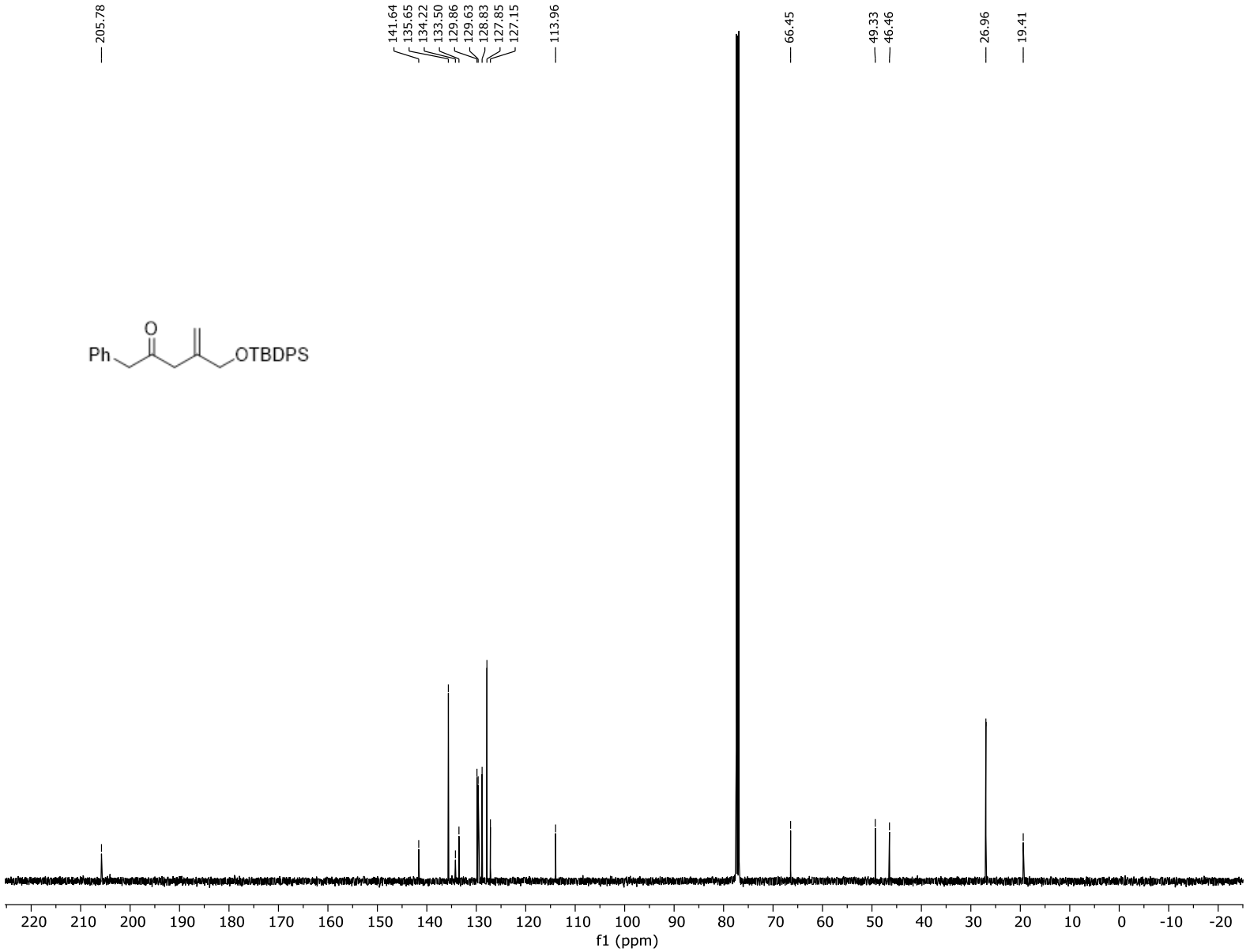
4.105 ^{13}C NMR (126 MHz, $CDCl_3$)



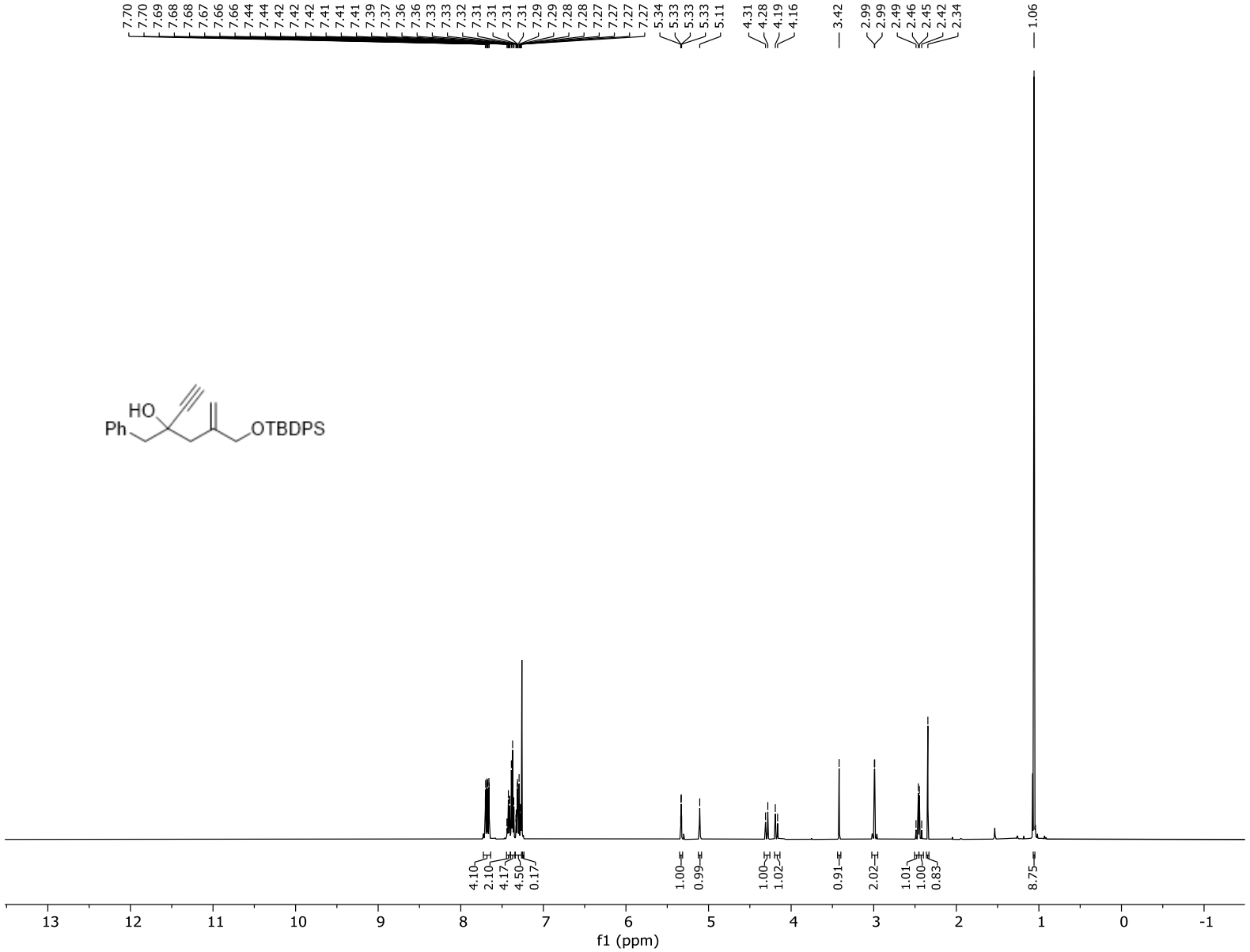
4.89 ^{1}H NMR (500 MHz, $CDCl_3$)



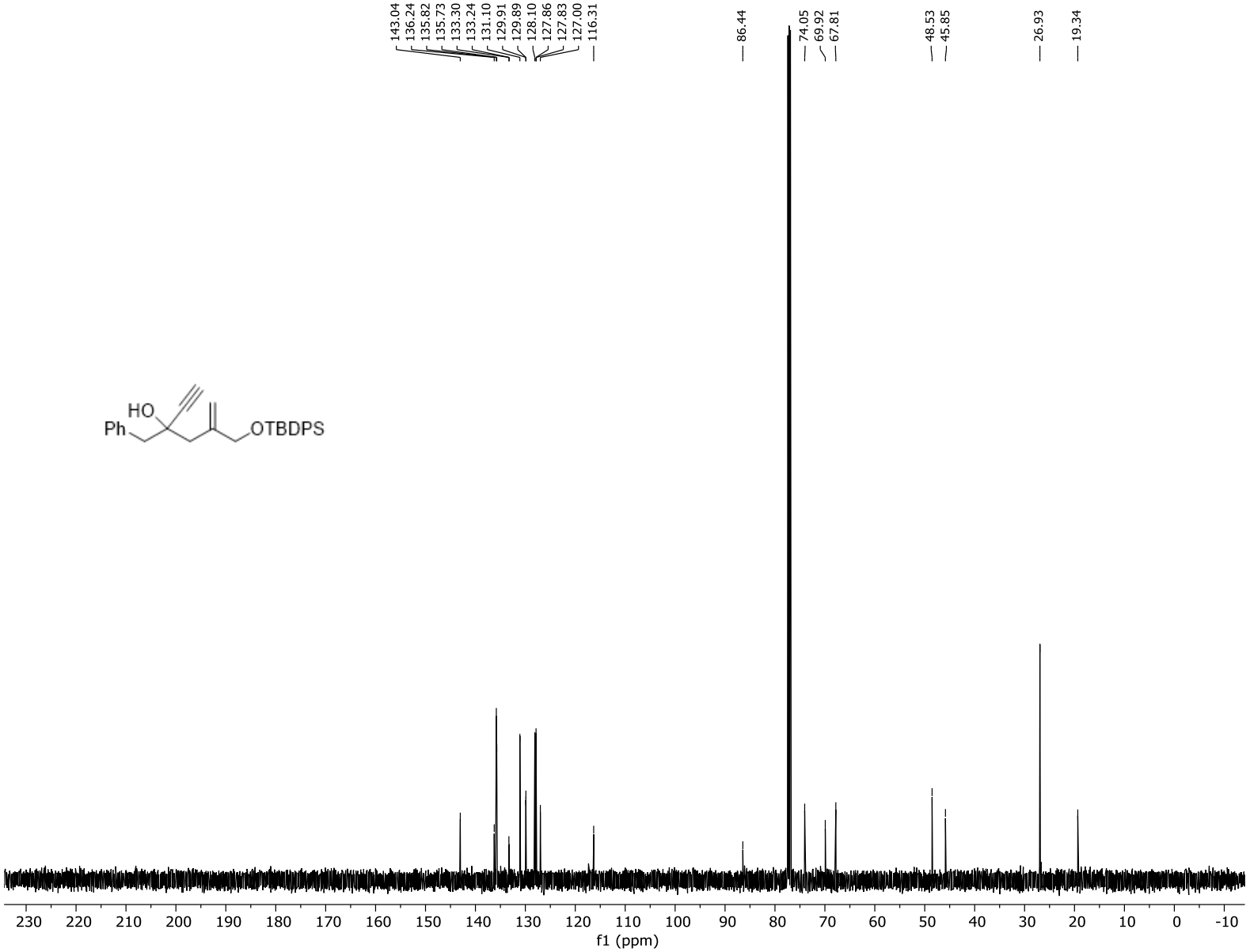
4.89 ^{13}C NMR (126 MHz, $CDCl_3$)



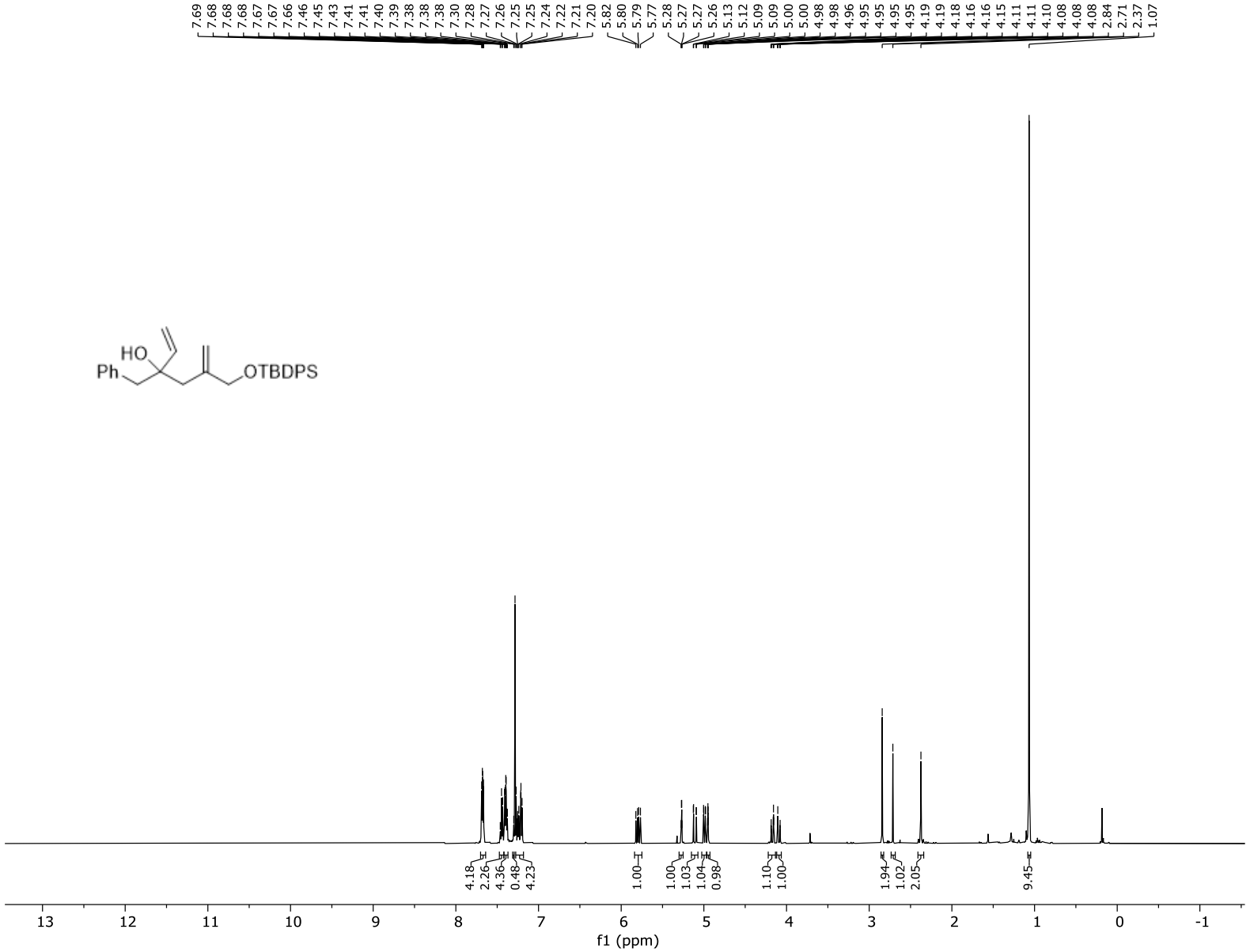
4.90 ^{1}H NMR (500 MHz, $CDCl_3$)



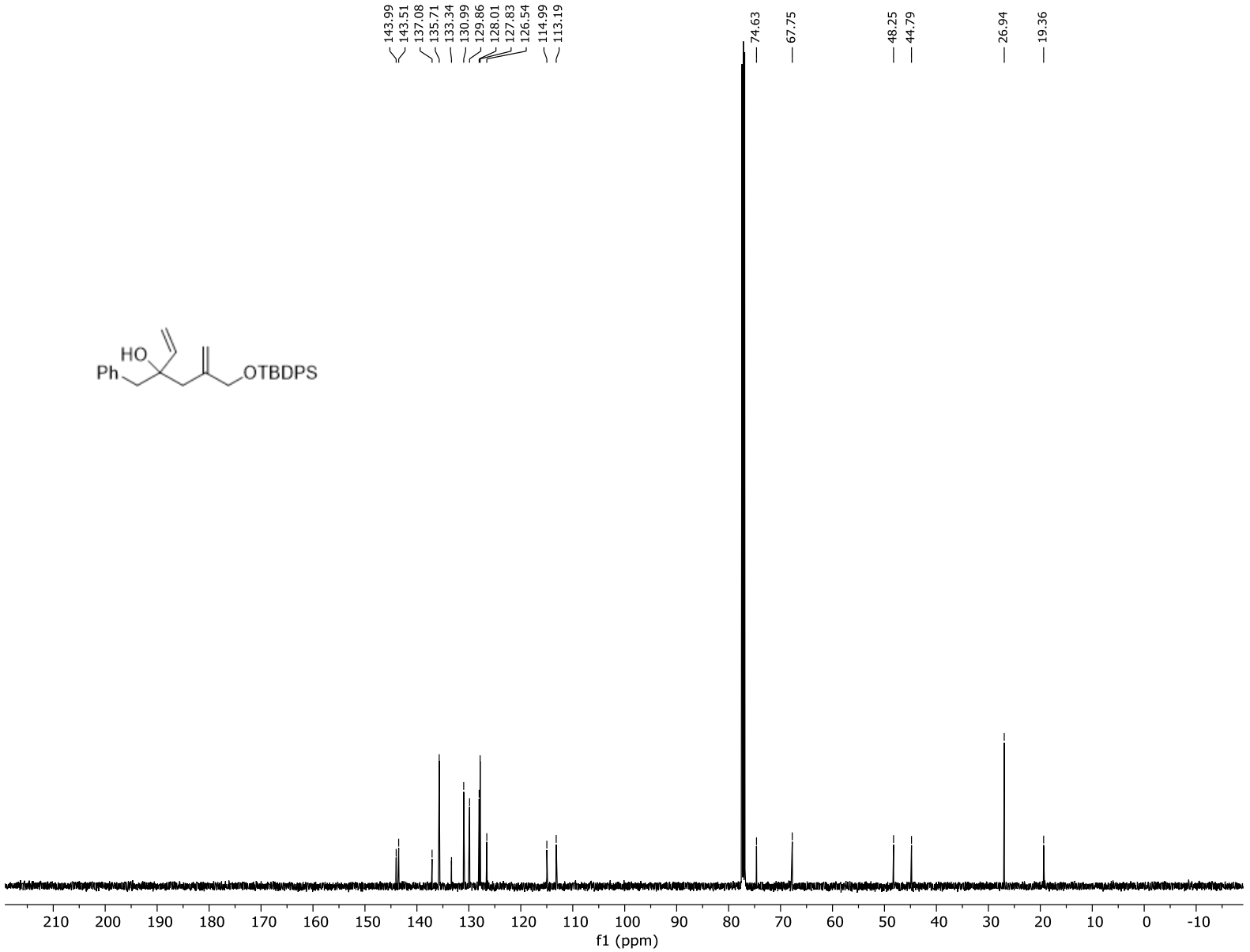
4.90 ^{13}C NMR (126 MHz, $CDCl_3$)



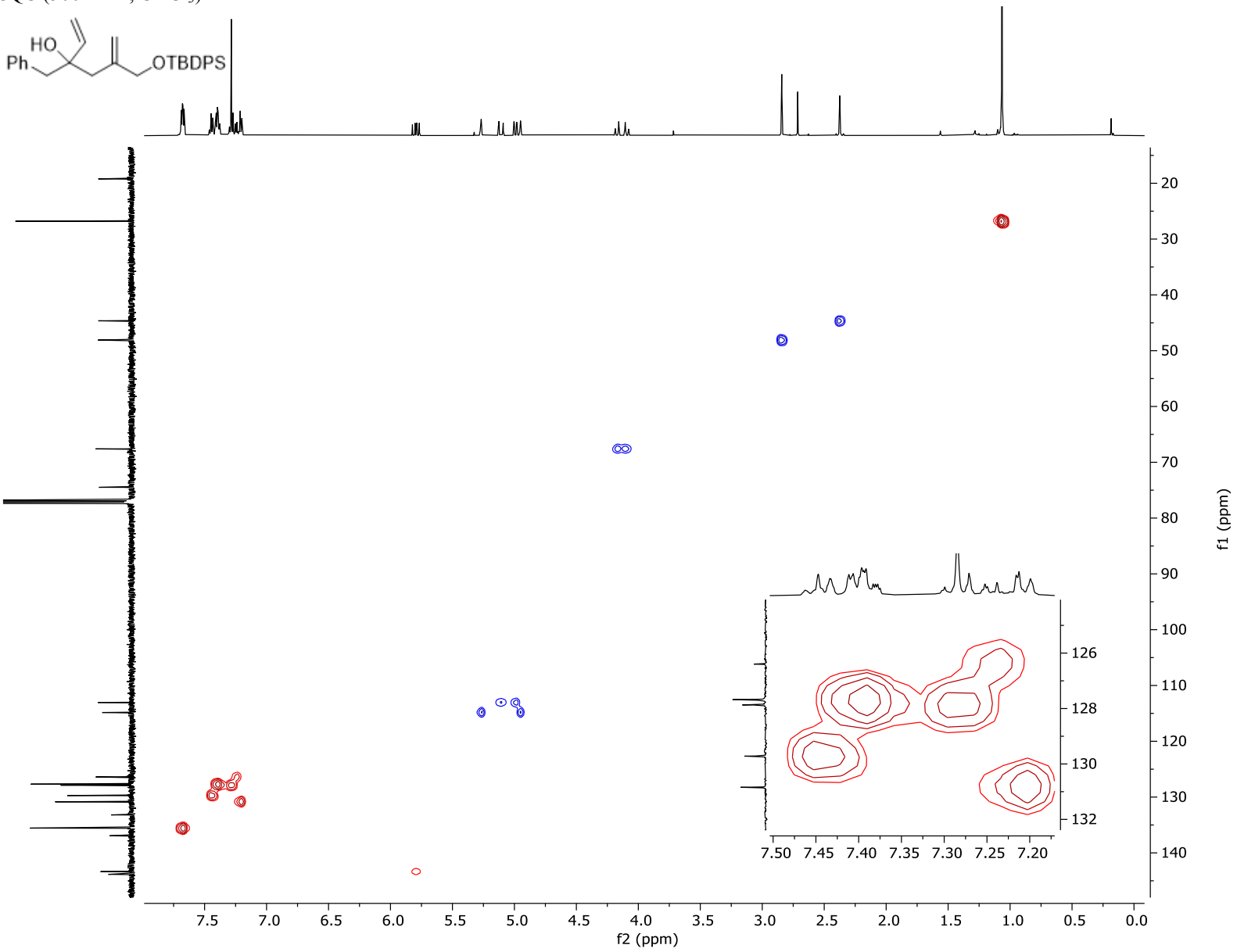
5.12 ^{1}H NMR (500 MHz, $CDCl_3$)



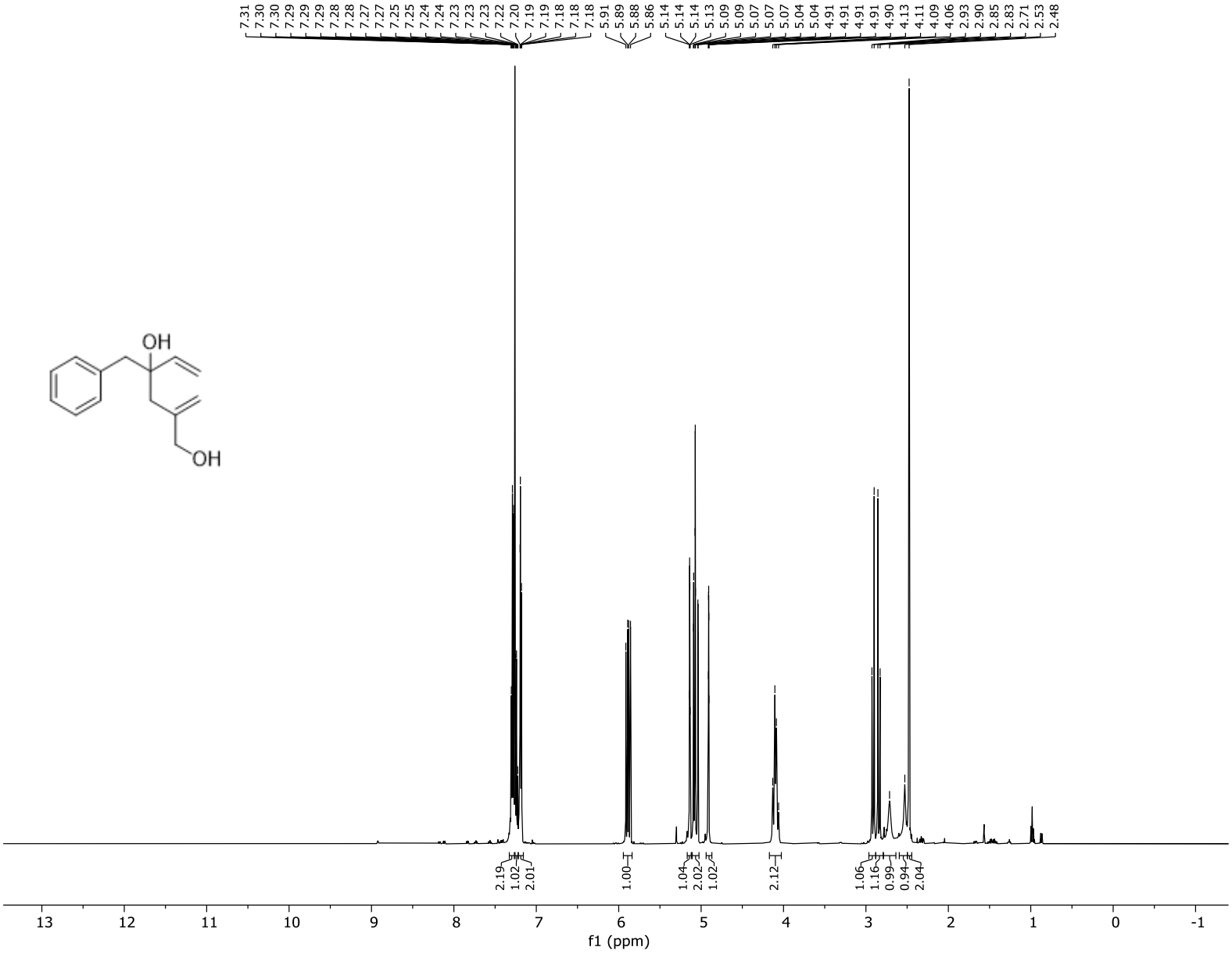
5.12 ^{13}C NMR (126 MHz, $CDCl_3$)



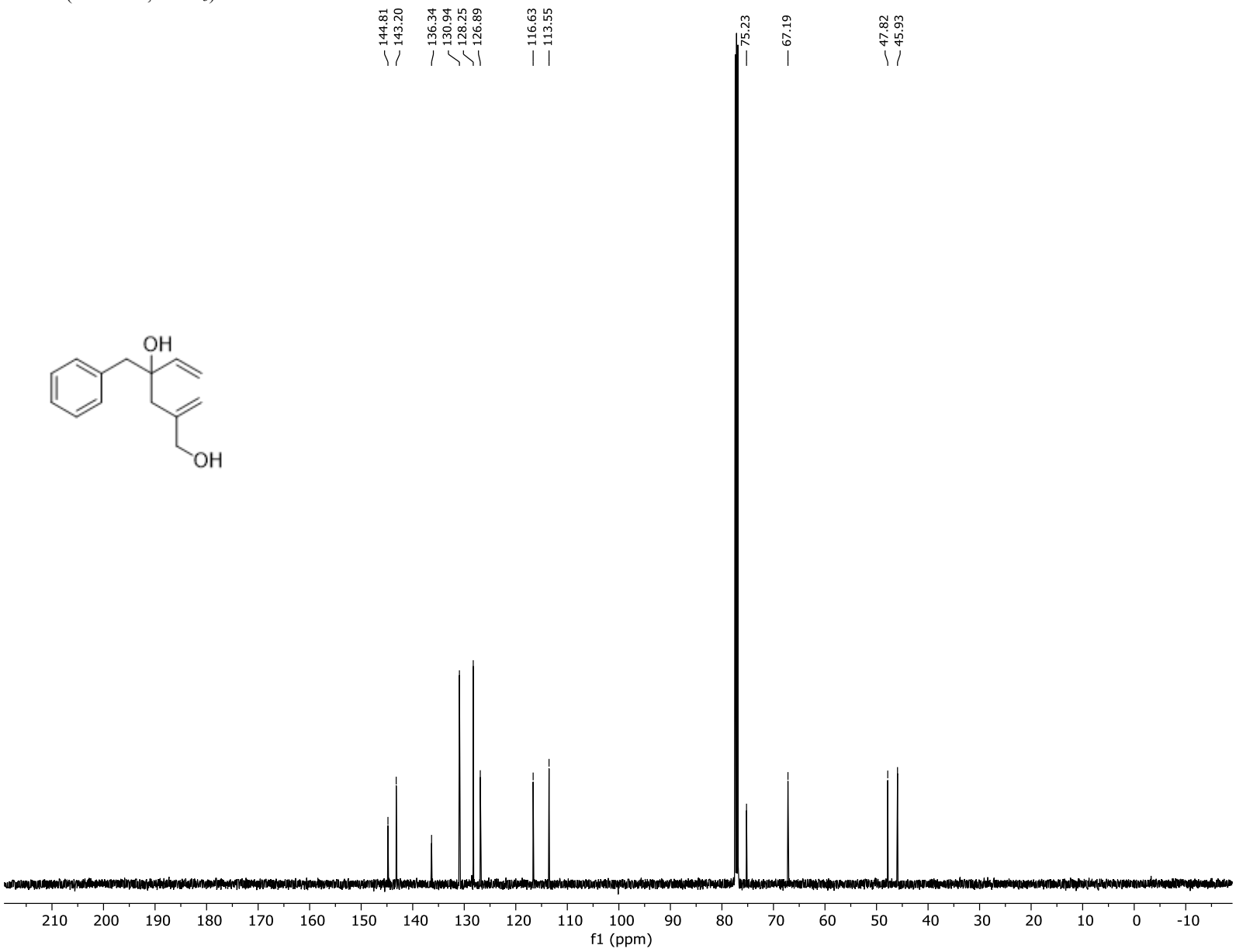
5.12 HSQC (500 MHz, $CDCl_3$)



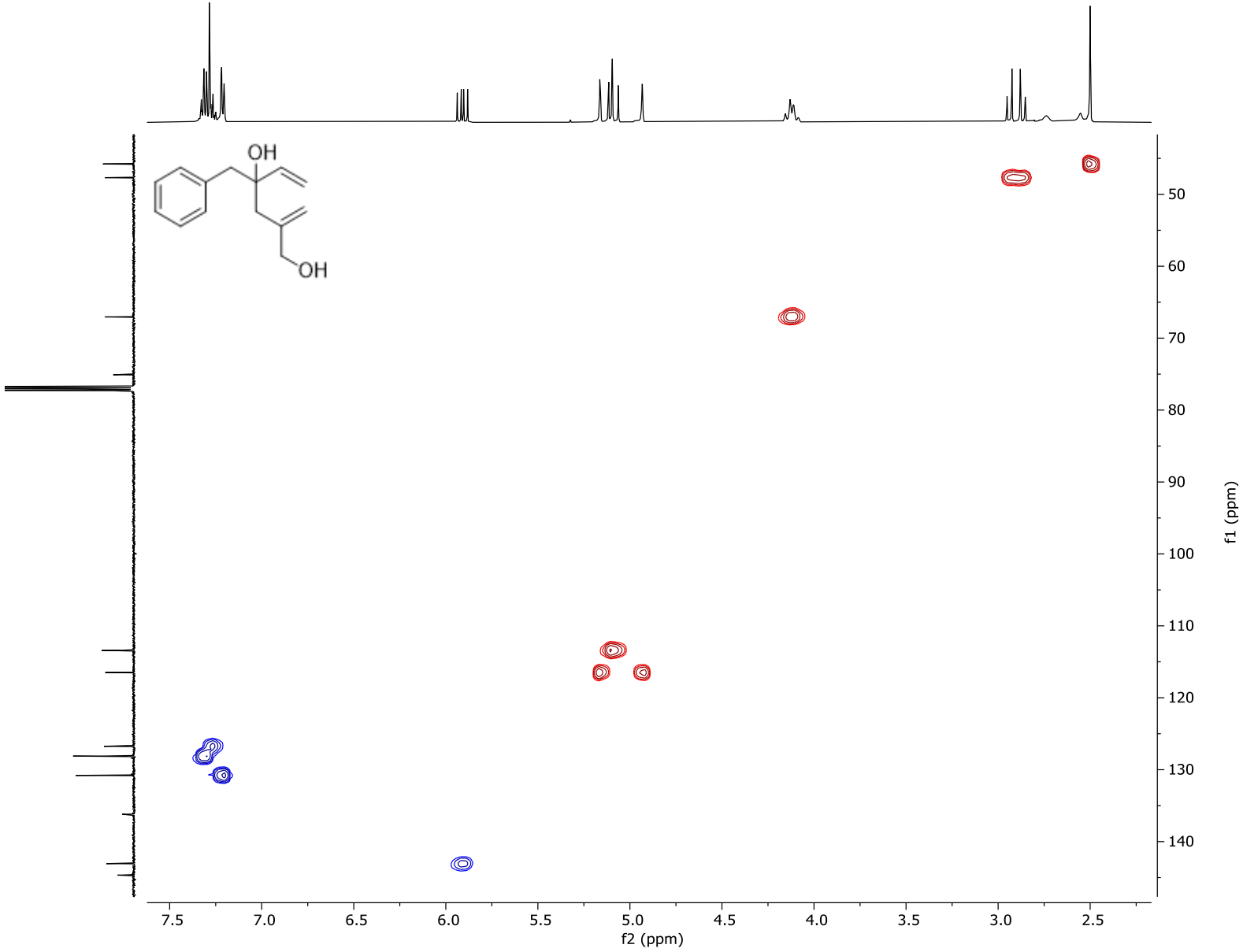
5.13 ^{1}H NMR (500 MHz, $CDCl_3$)



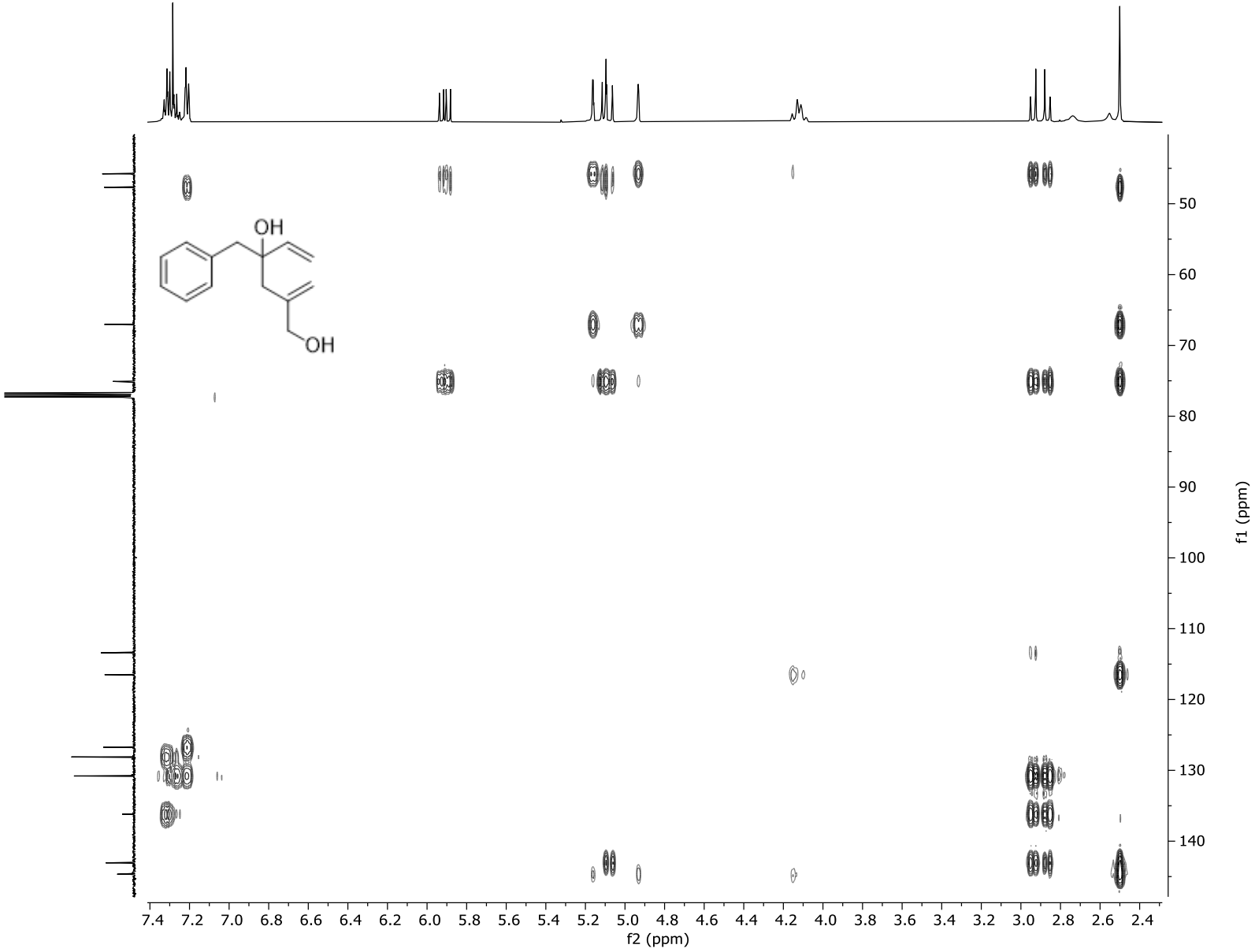
5.13 ^{13}C NMR (126 MHz, $CDCl_3$)



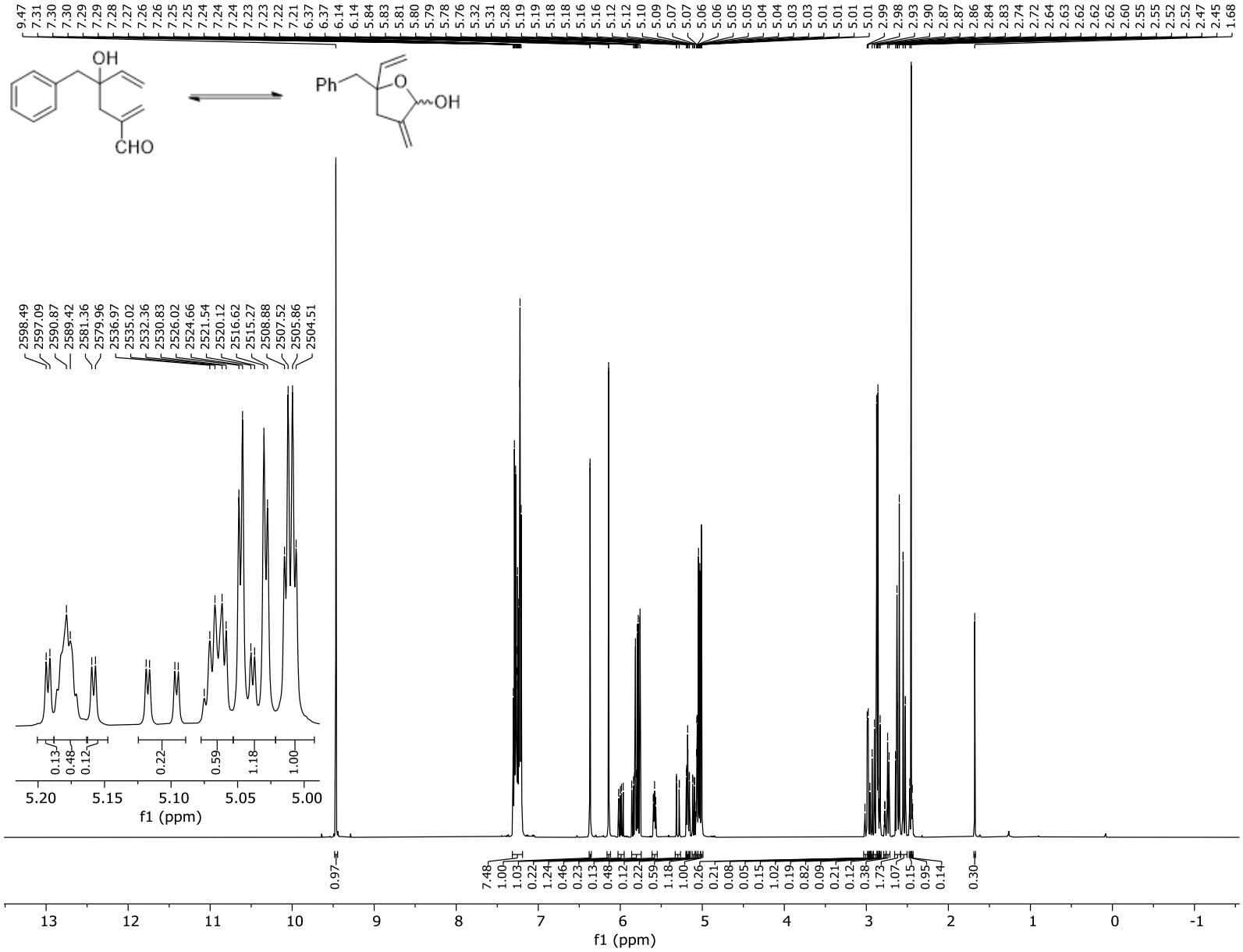
5.13 HSQC (500 MHz, $CDCl_3$)



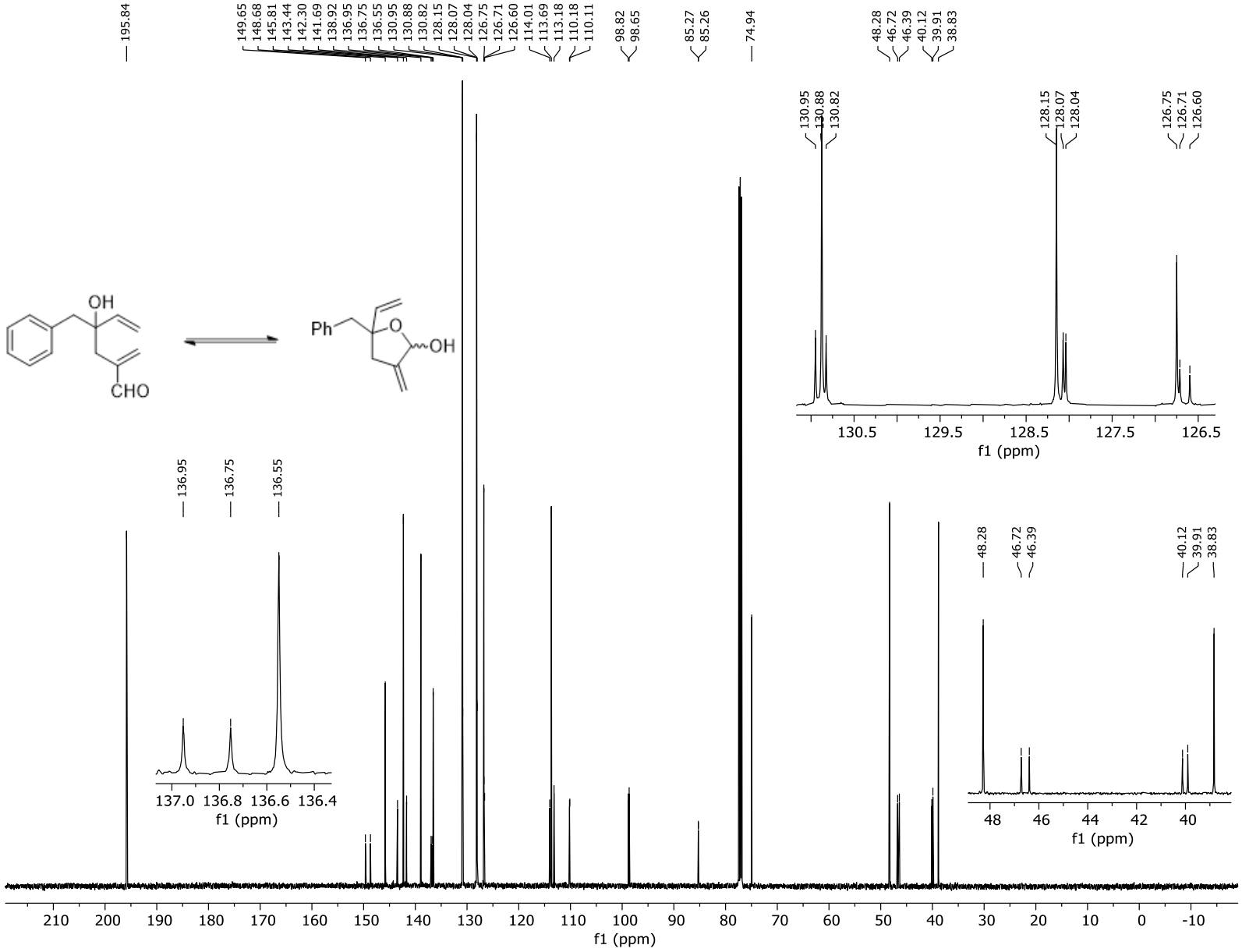
5.13 HMBC (500 MHz, $CDCl_3$)



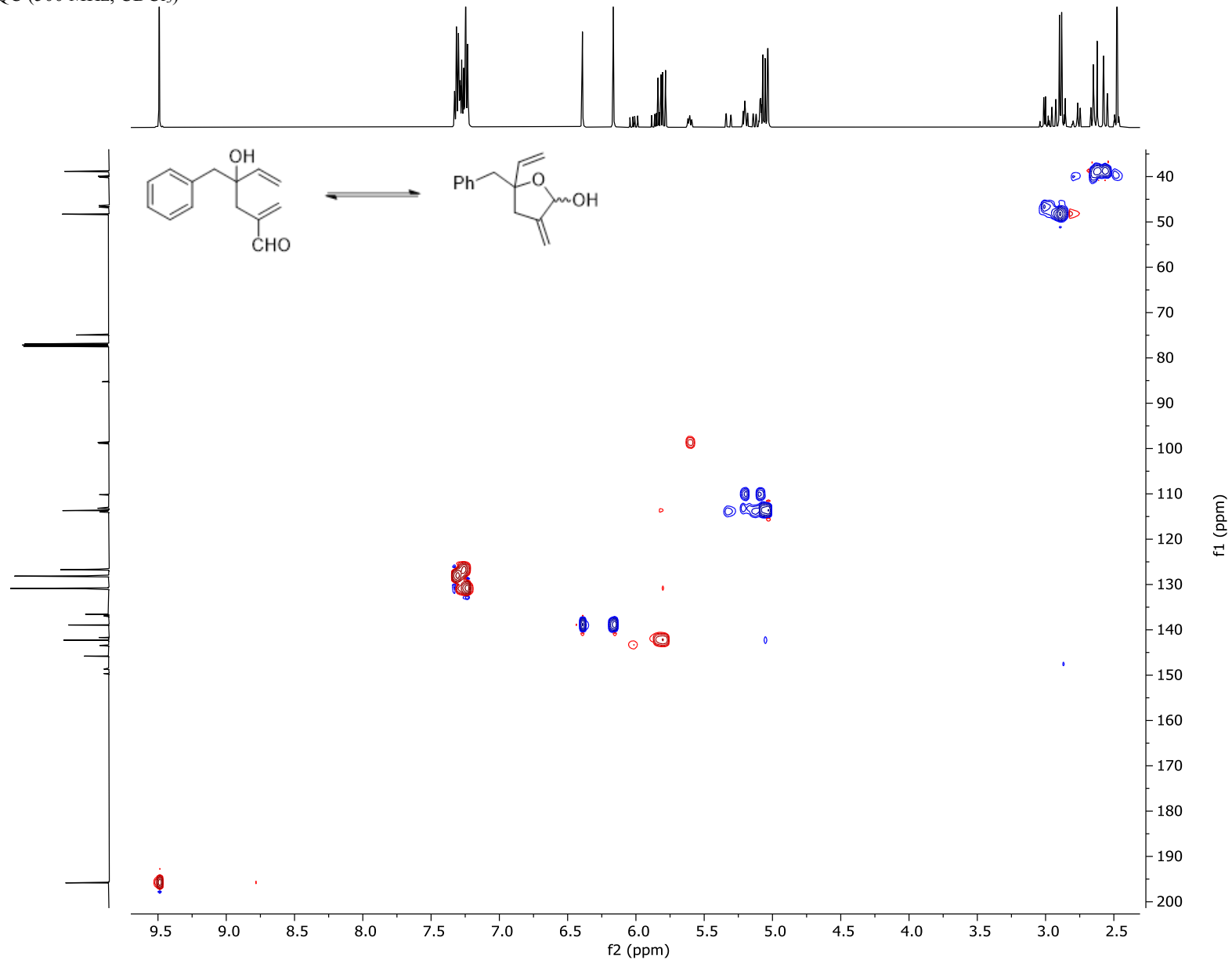
4.80 ^{1}H NMR (500 MHz, $CDCl_3$)



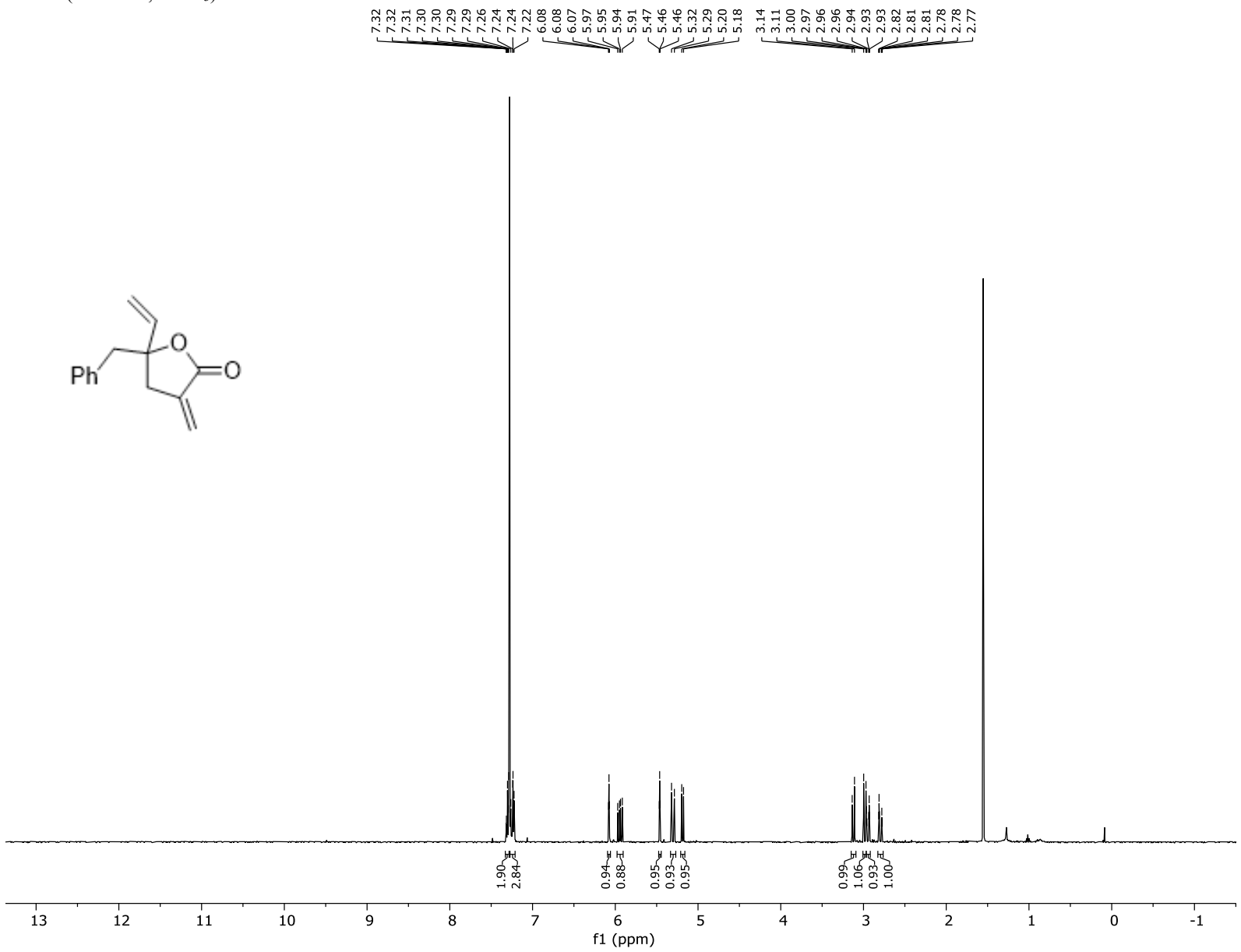
4.80 ^{13}C NMR (126 MHz, $CDCl_3$)



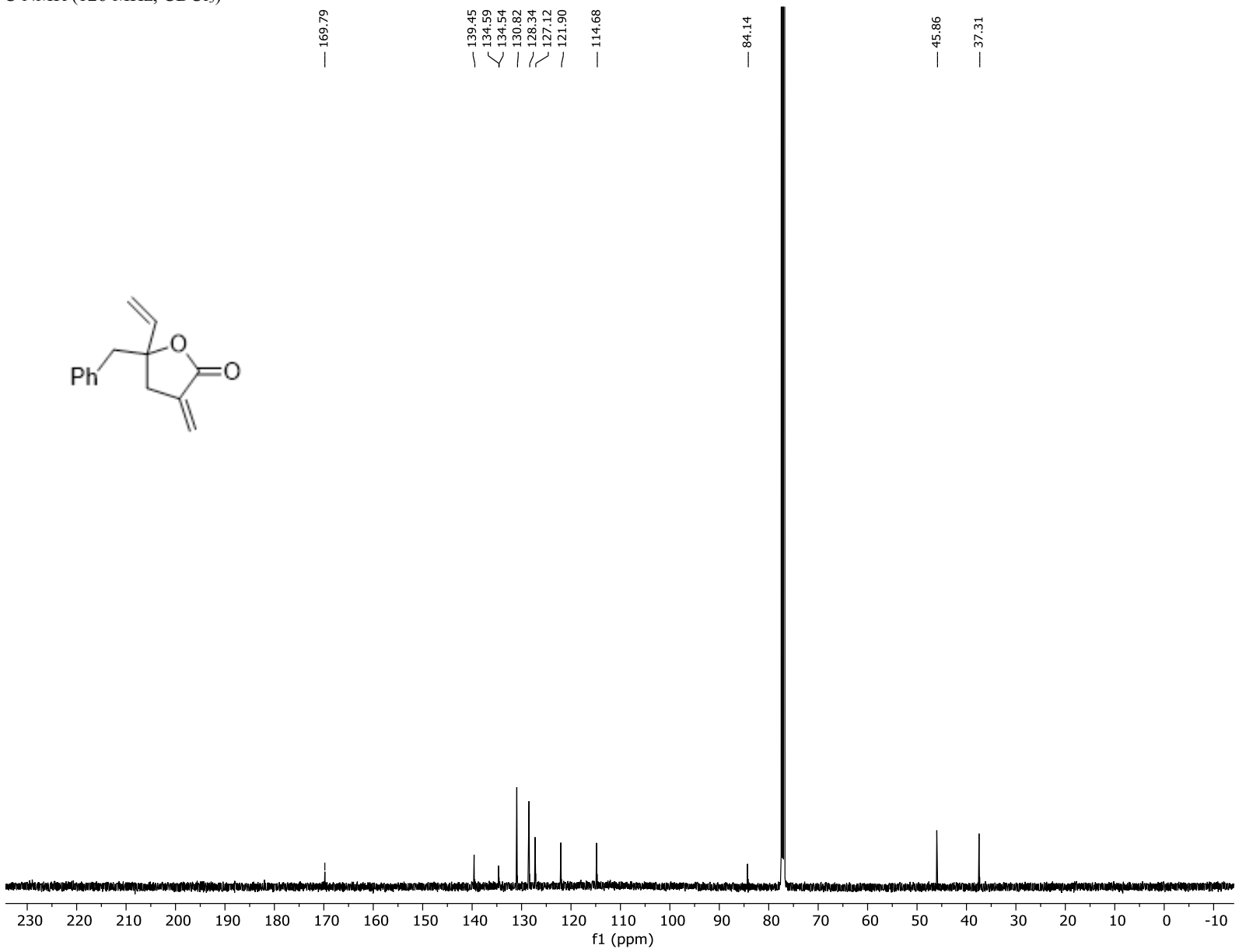
4.80 HSQC (500 MHz, $CDCl_3$)



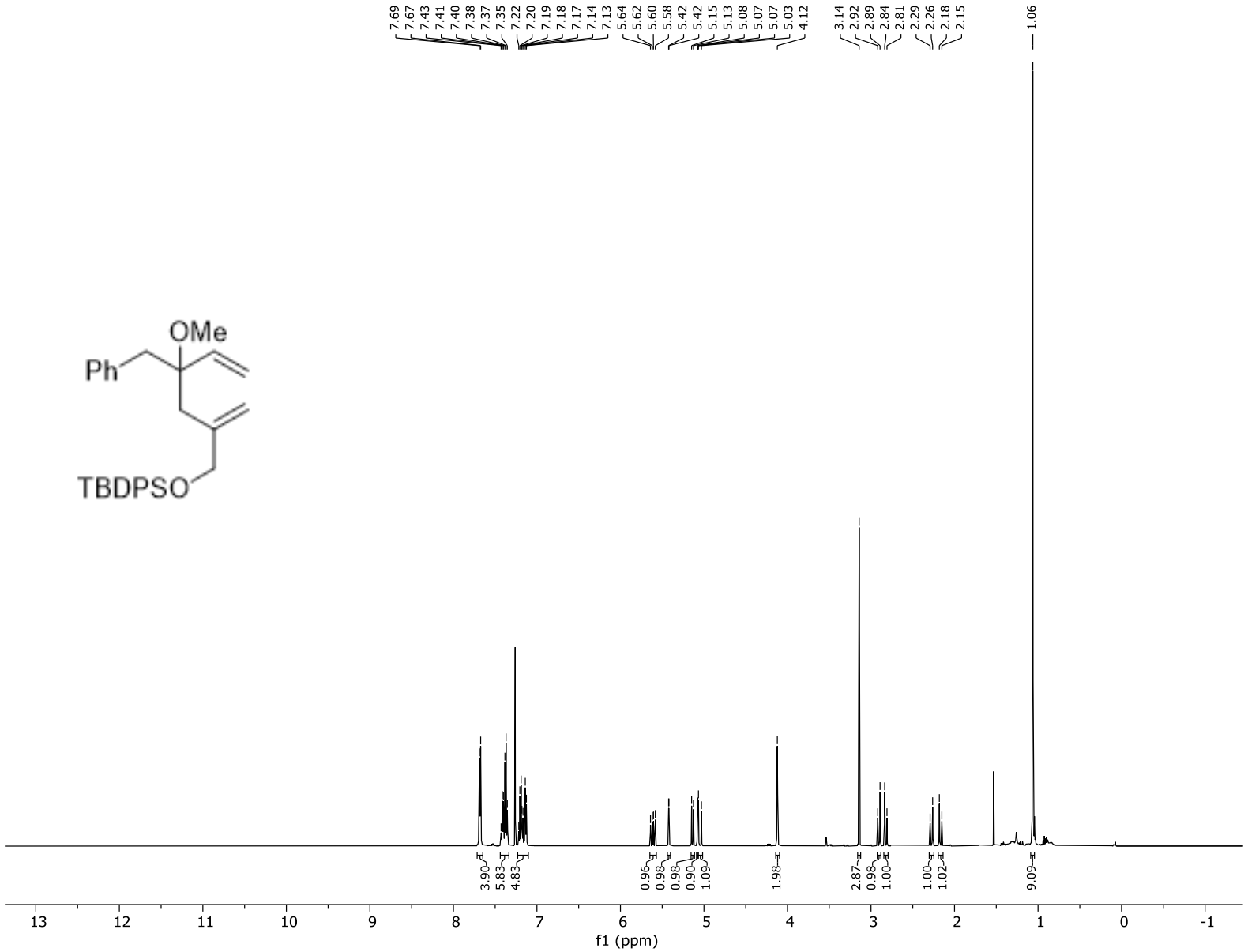
4.80′ ^{1}H NMR (500 MHz, $CDCl_3$)



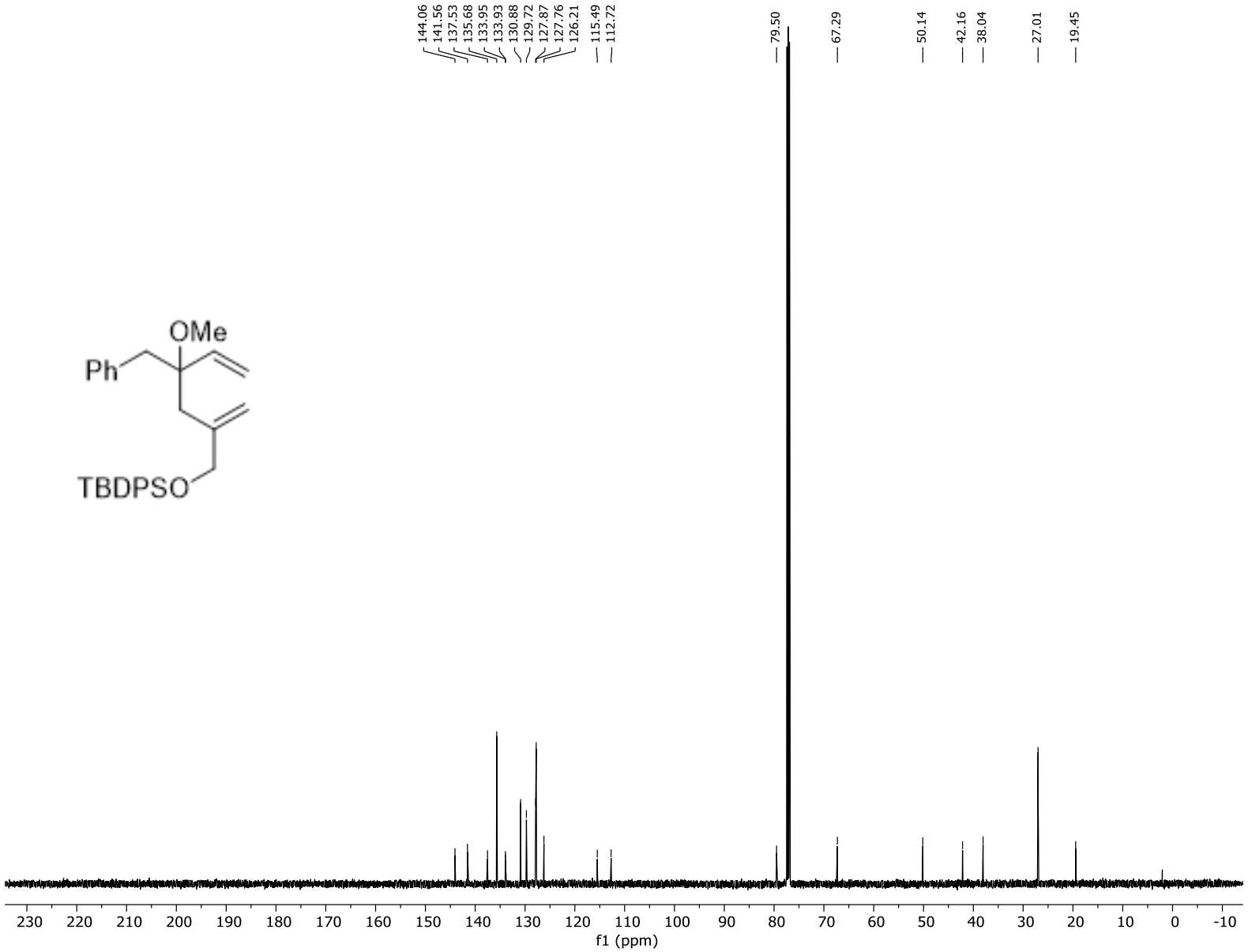
4.80′ ^{13}C NMR (126 MHz, $CDCl_3$)



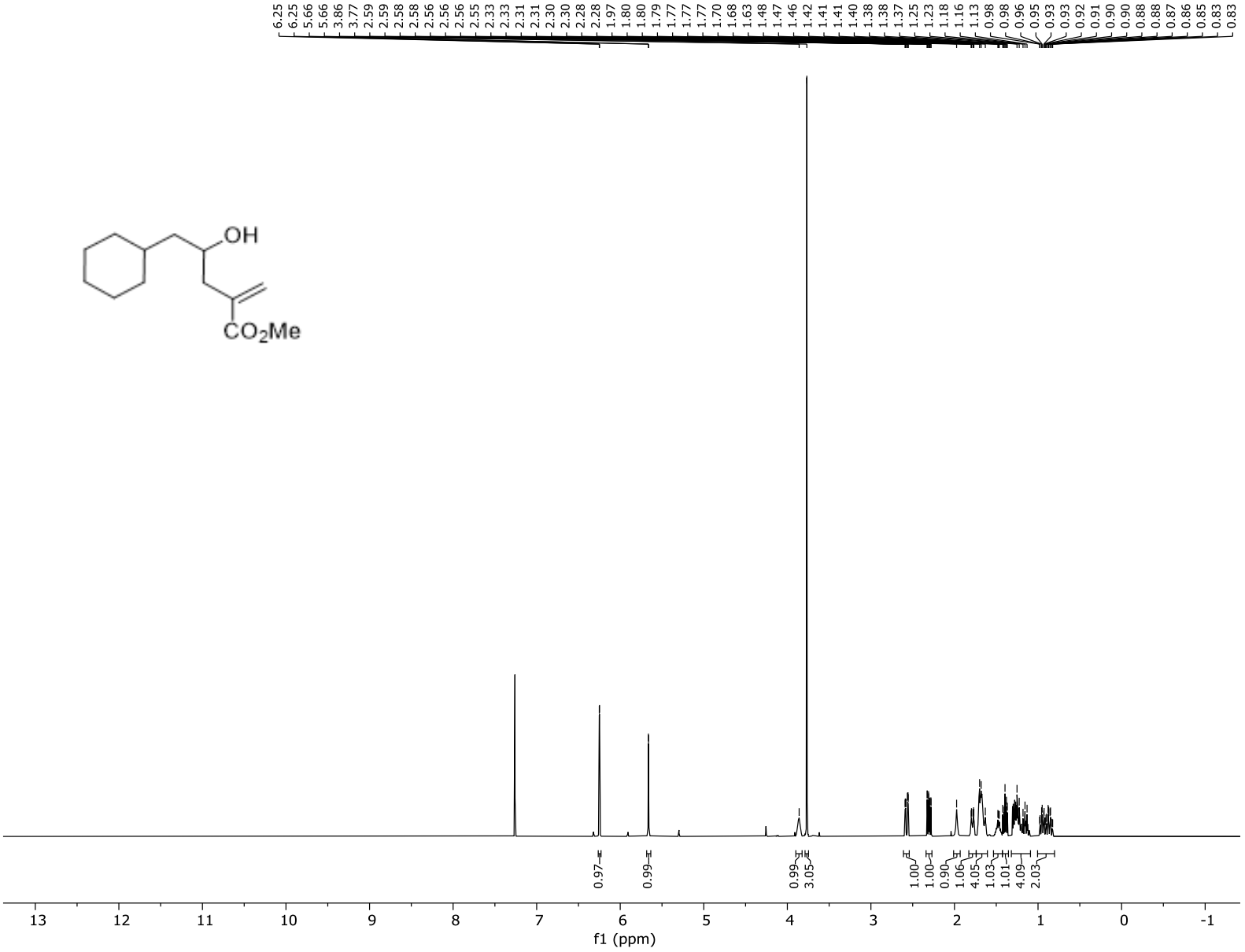
5.14 ^{1}H NMR (500 MHz, $CDCl_3$)



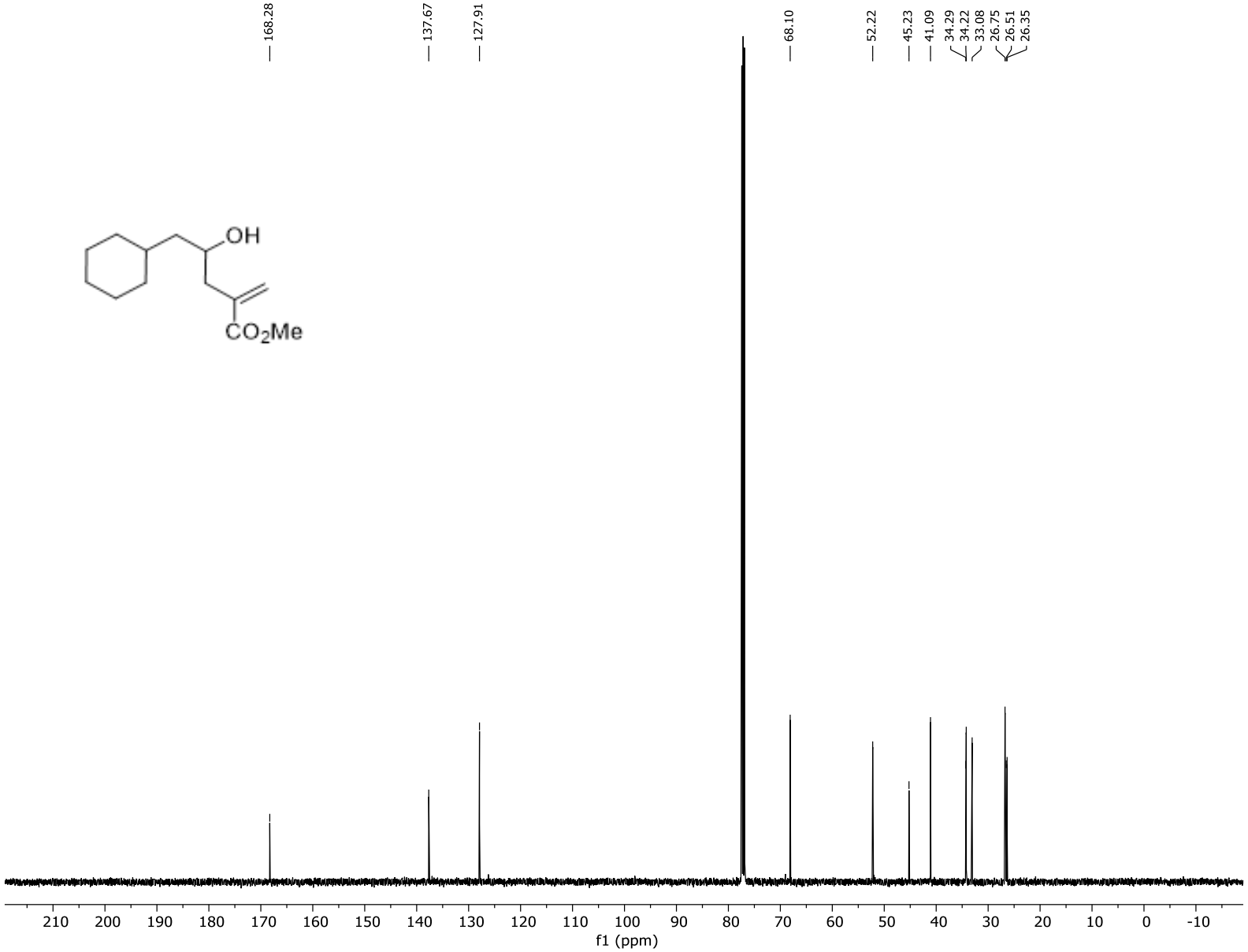
5.14 ^{13}C NMR (126 MHz, $CDCl_3$)



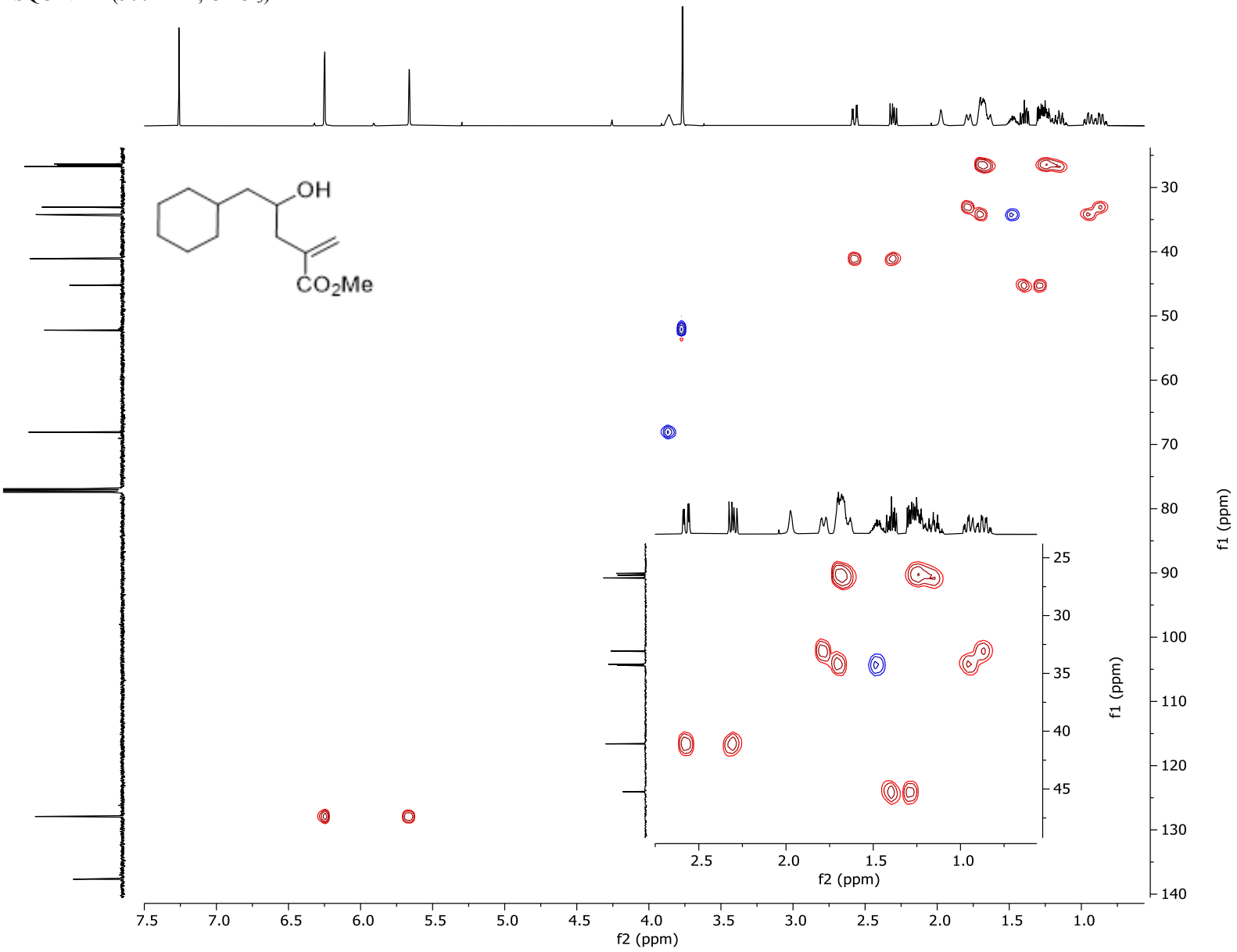
5.17a′ ^{1}H NMR (500 MHz, $CDCl_3$)



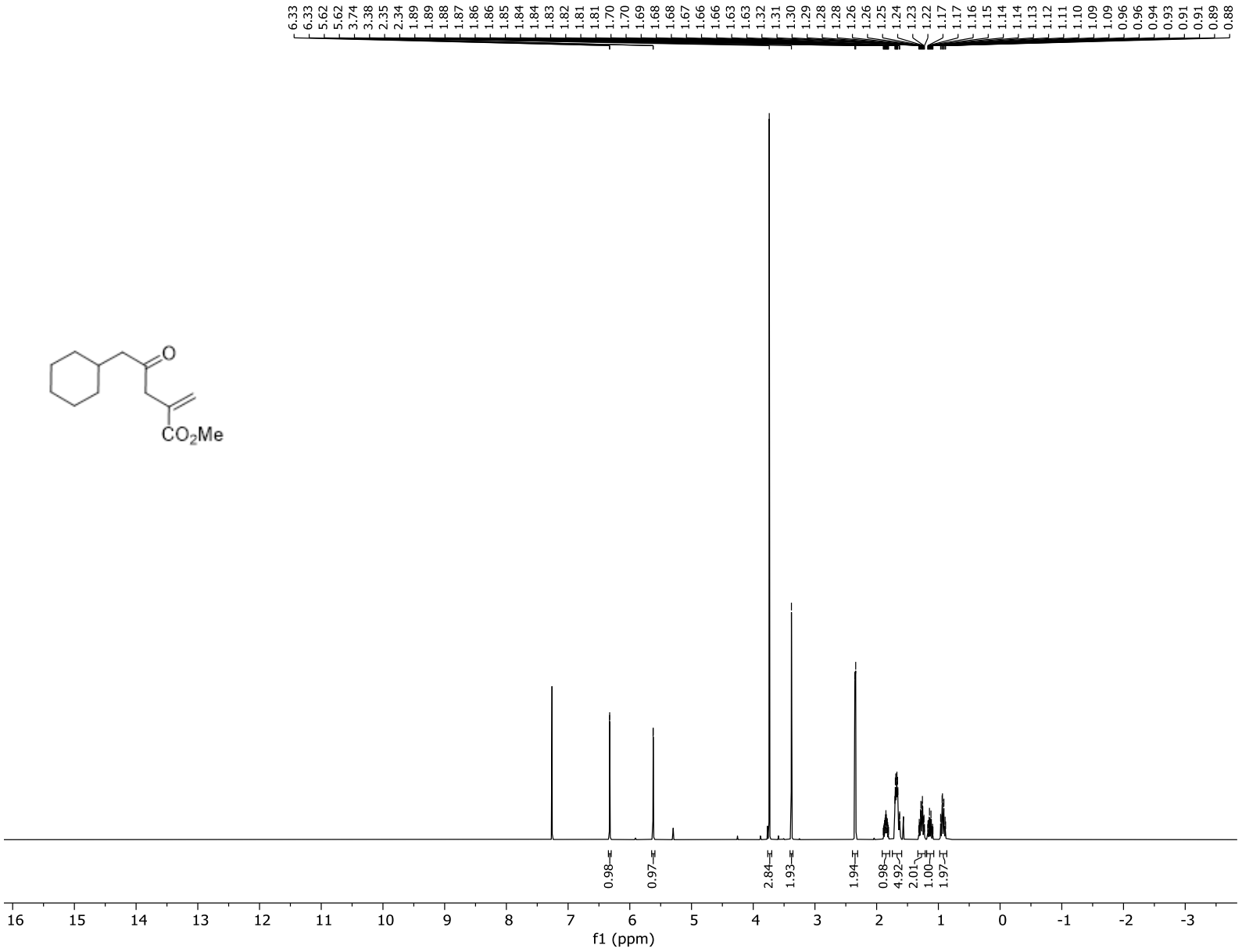
5.17a′ ^{13}C NMR (126 MHz, $CDCl_3$)



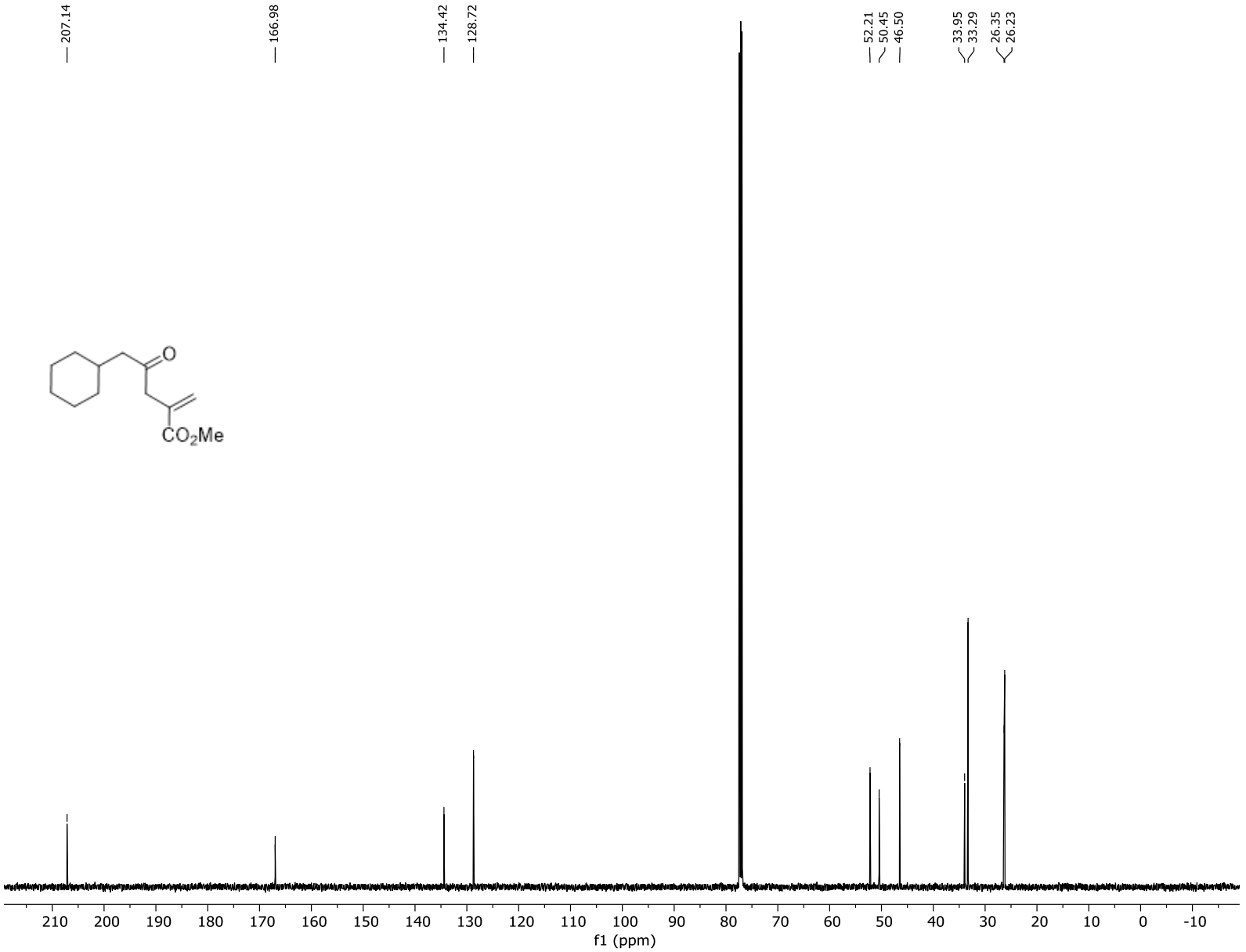
5.17a′ HSQC NMR (500 MHz, $CDCl_3$)



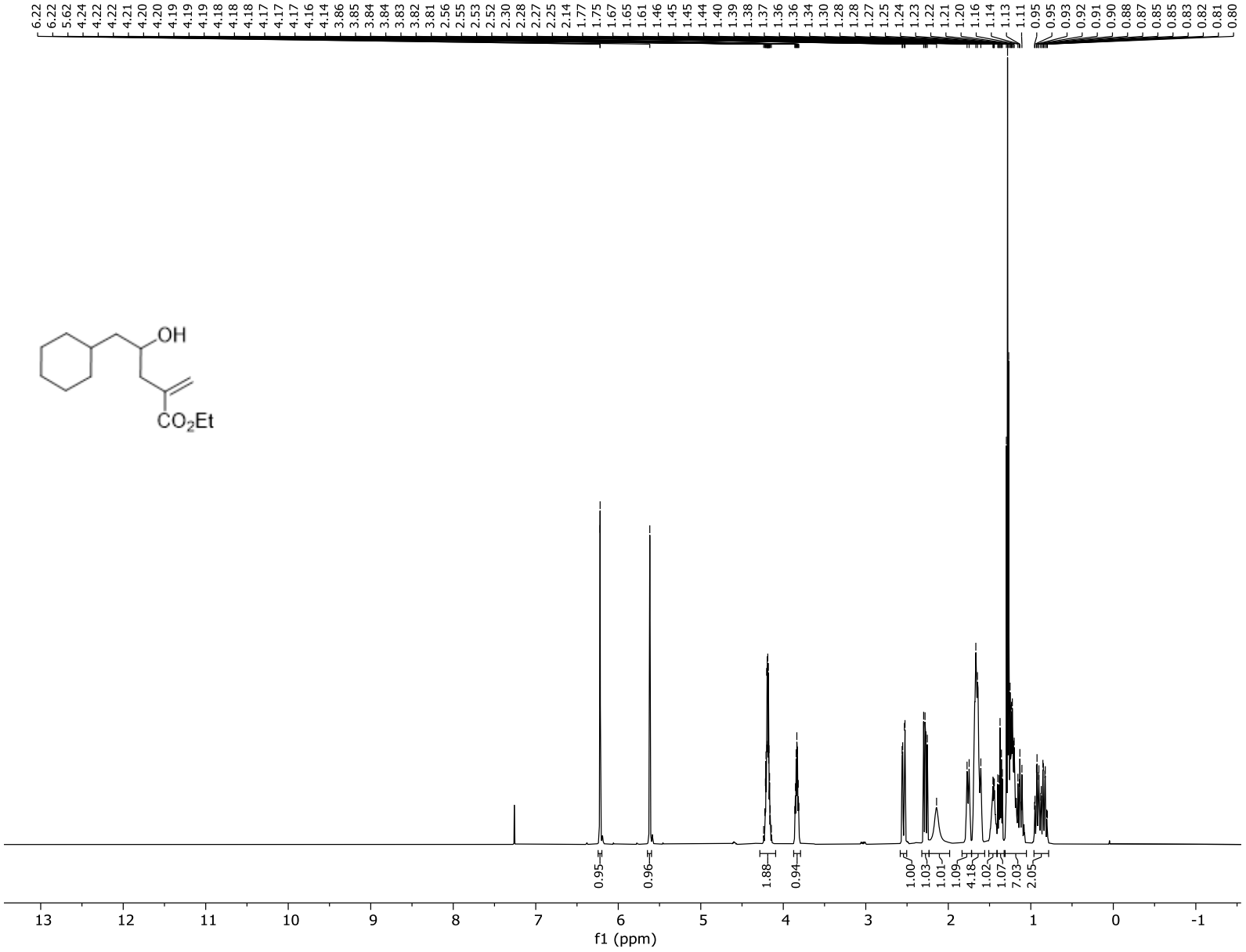
5.17a ^{1}H NMR (500 MHz, $CDCl_3$)



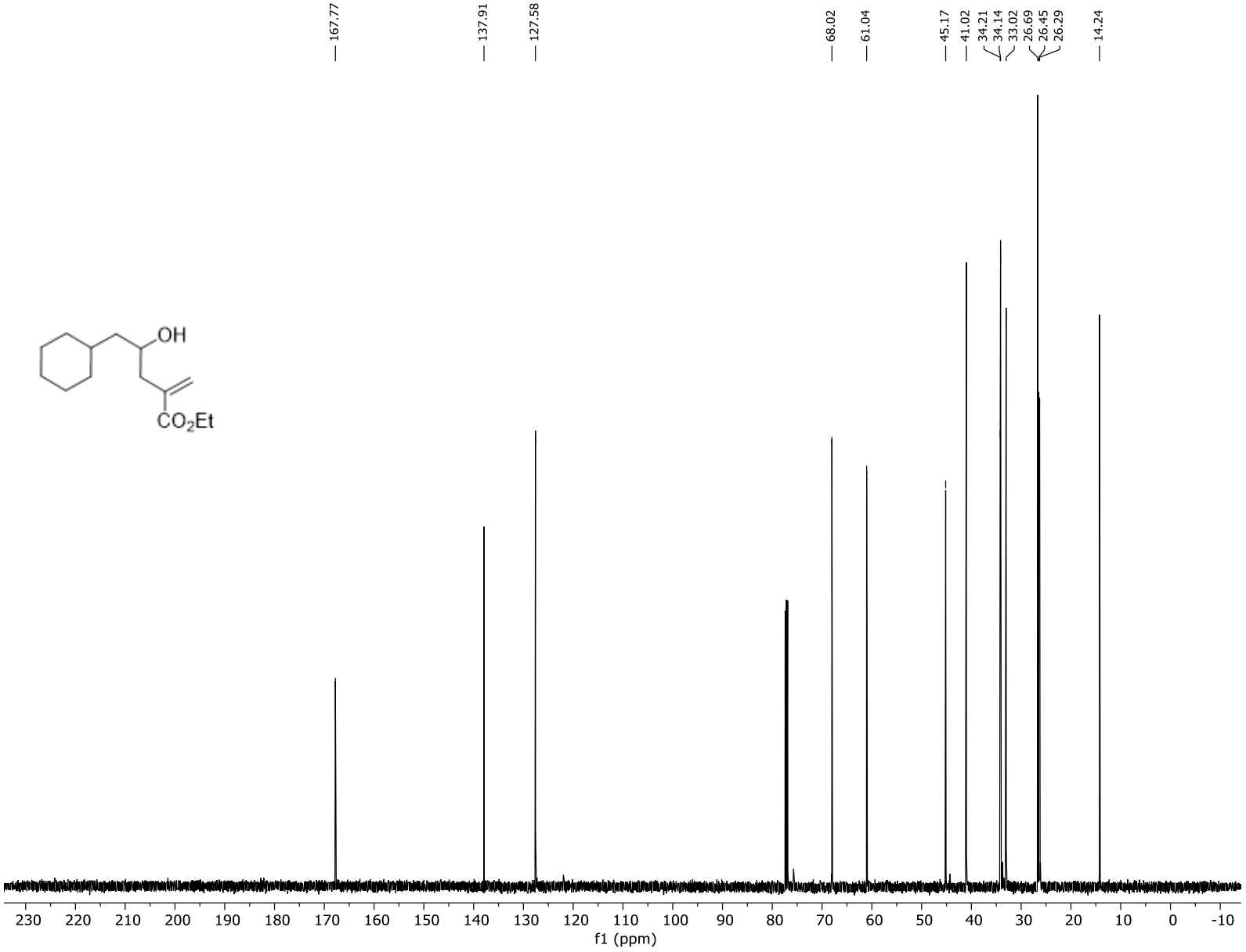
5.17a ^{13}C NMR (126 MHz, $CDCl_3$)



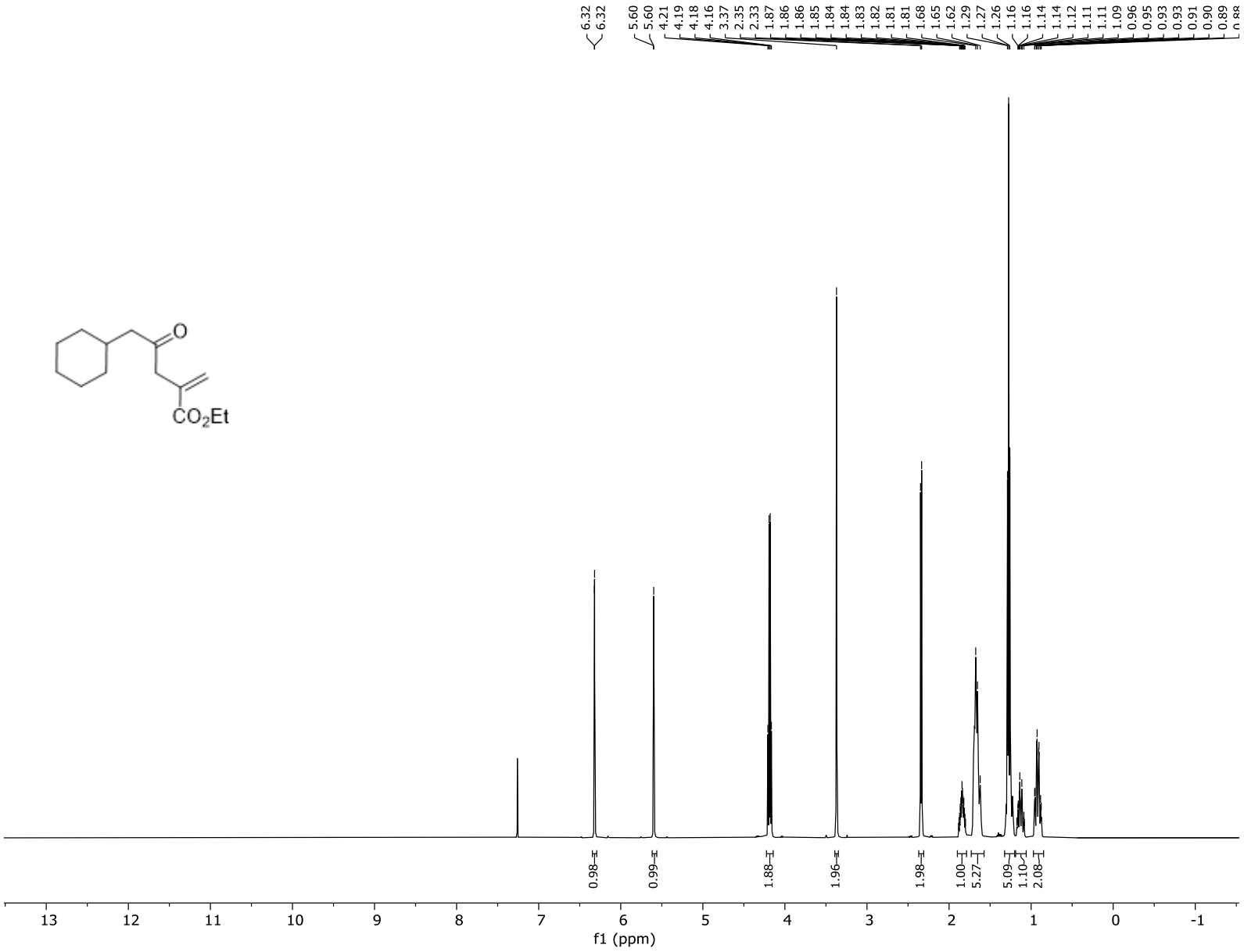
5.17b′ ^{1}H NMR (500 MHz, $CDCl_3$)



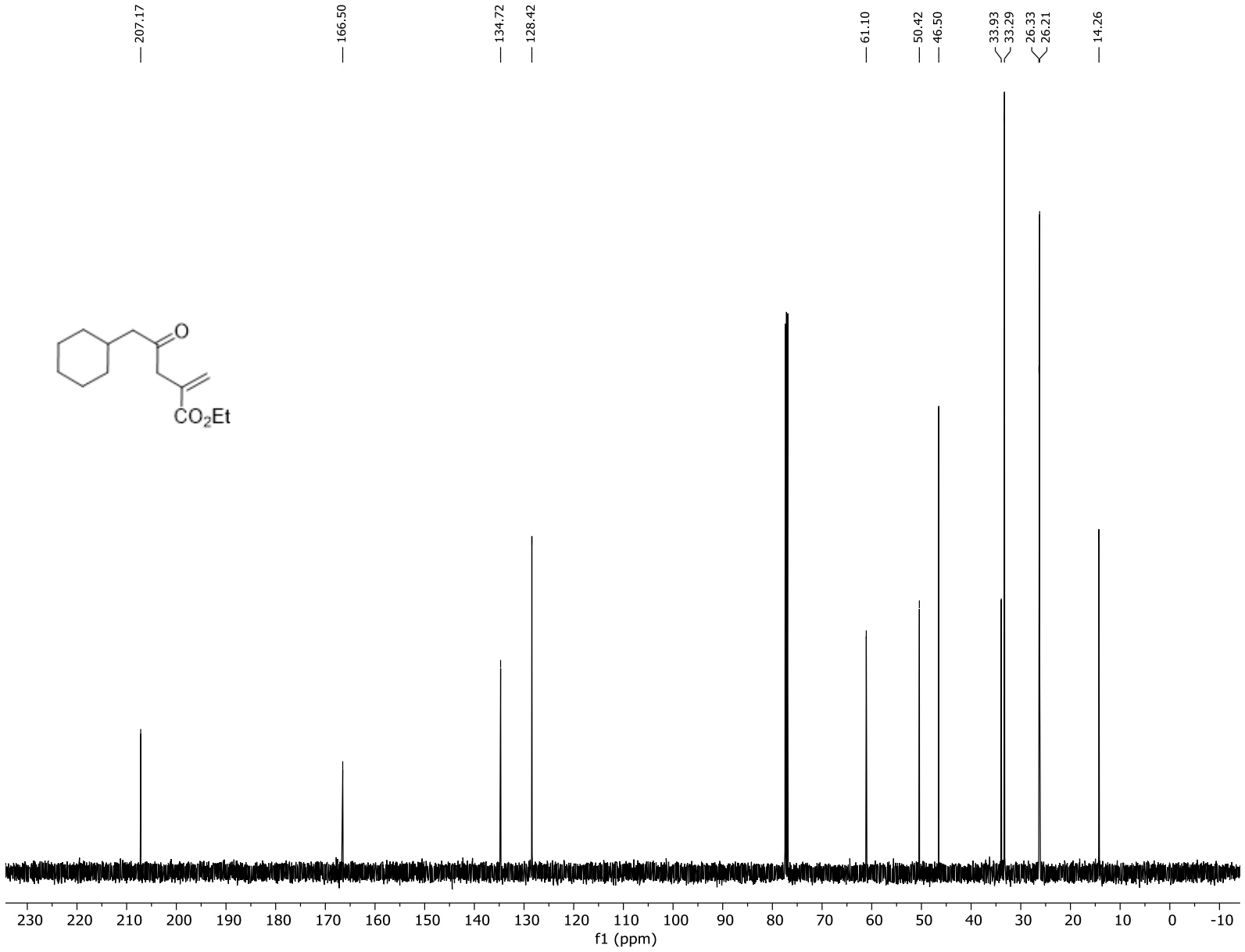
5.17b′ ^{13}C NMR (126 MHz, $CDCl_3$)



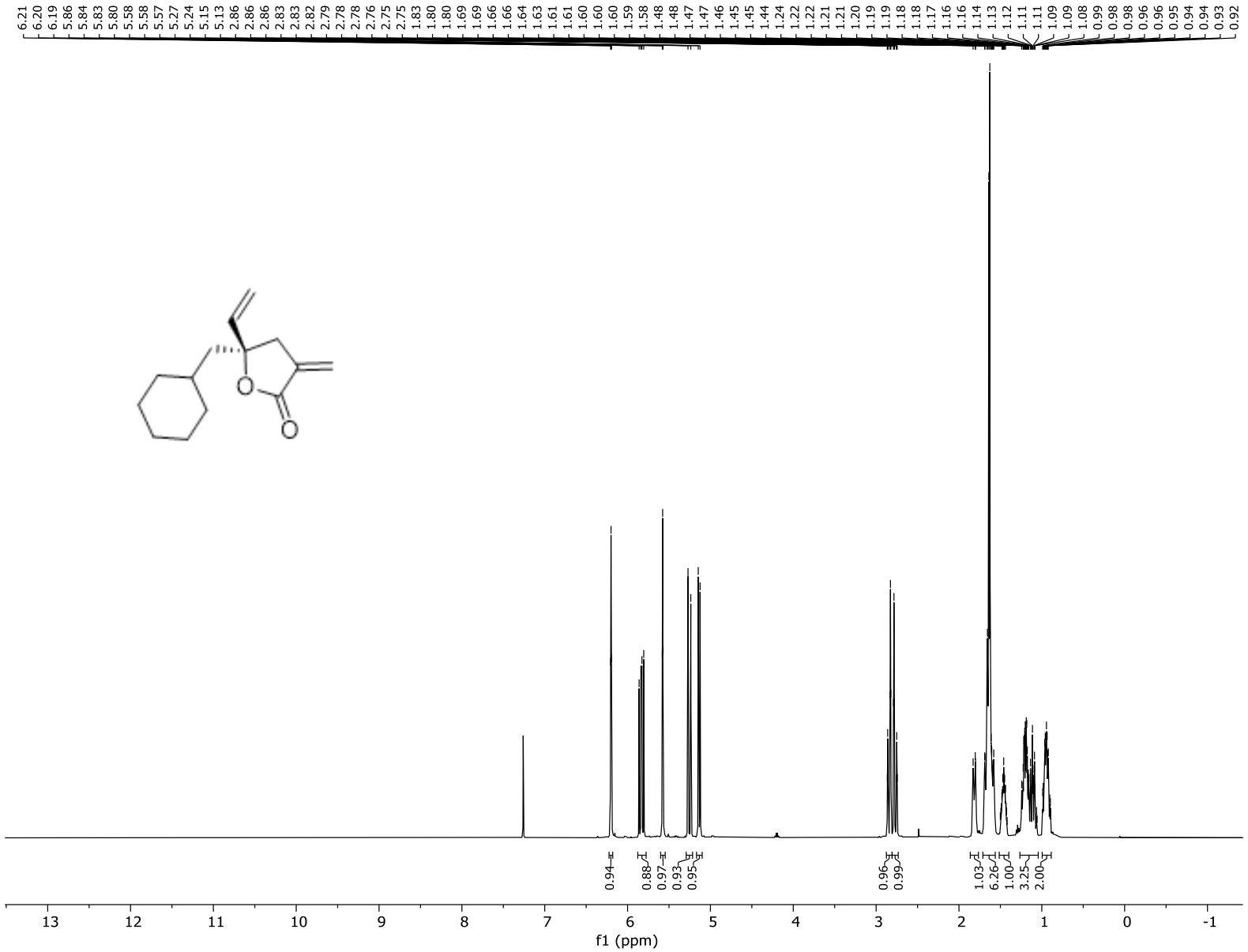
5.17b ^{1}H NMR (500 MHz, $CDCl_3$)



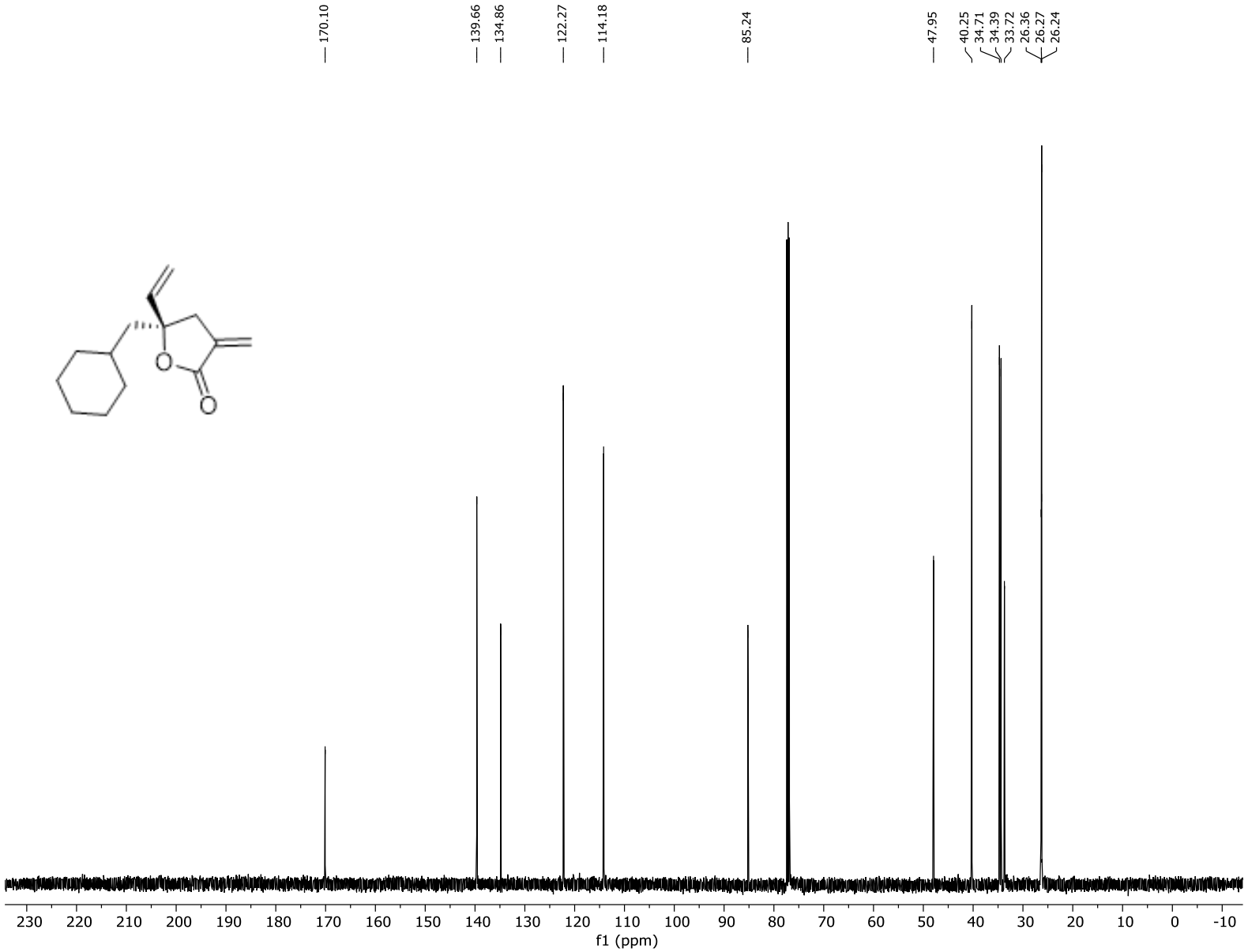
5.17b ^{13}C NMR (126 MHz, $CDCl_3$)



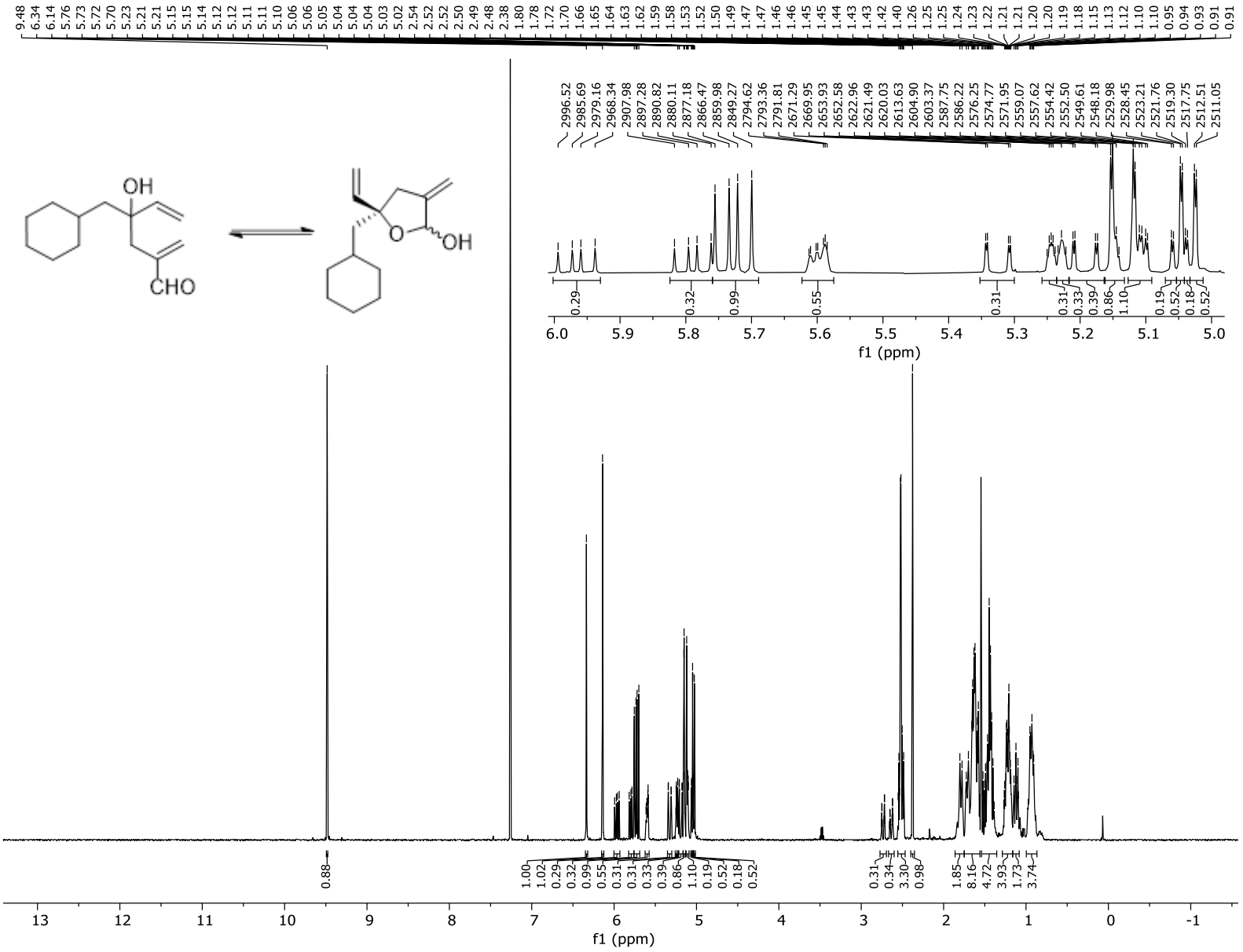
5.19a ^{1}H NMR (500 MHz, $CDCl_3$)



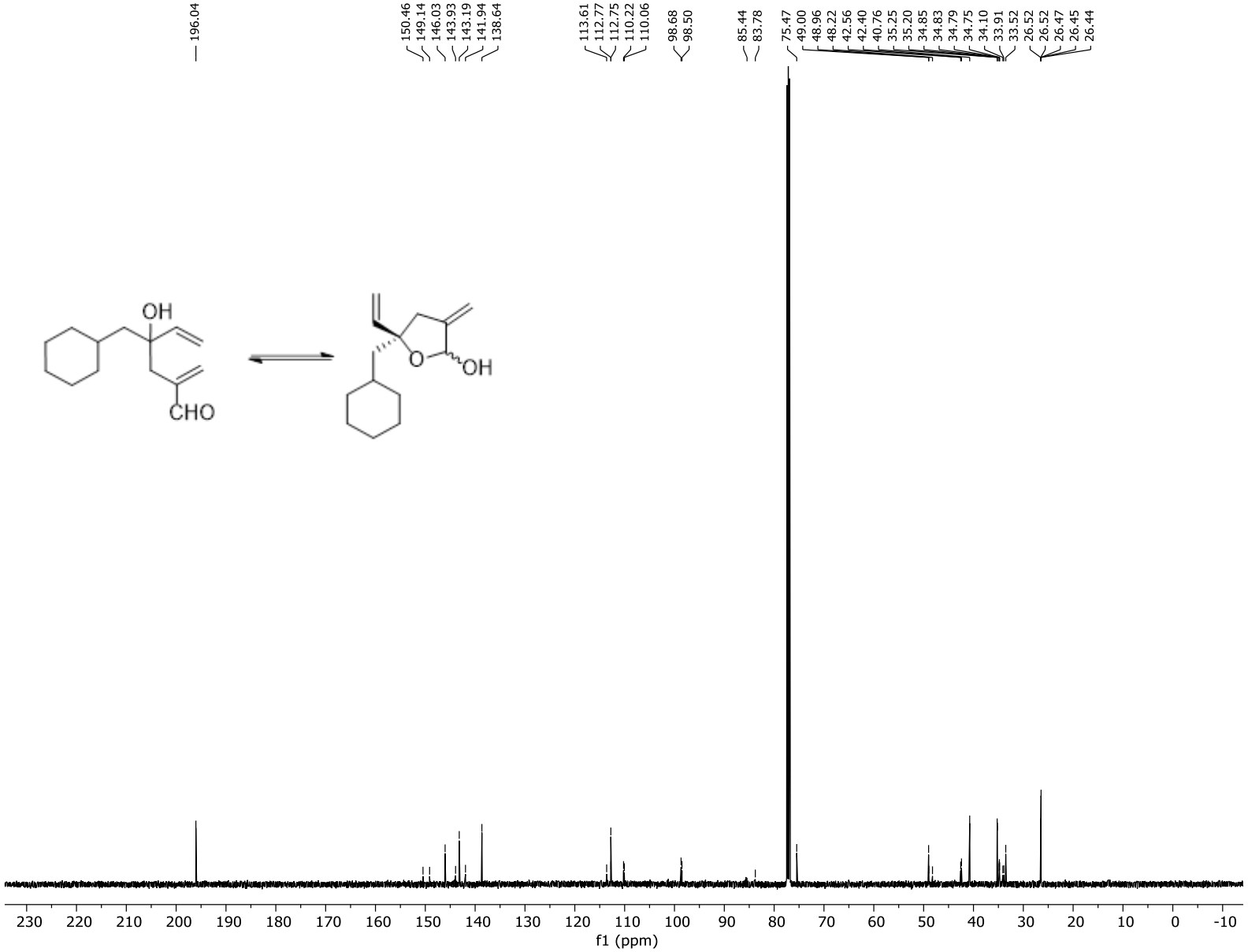
5.19a ^{13}C NMR (126 MHz, $CDCl_3$)



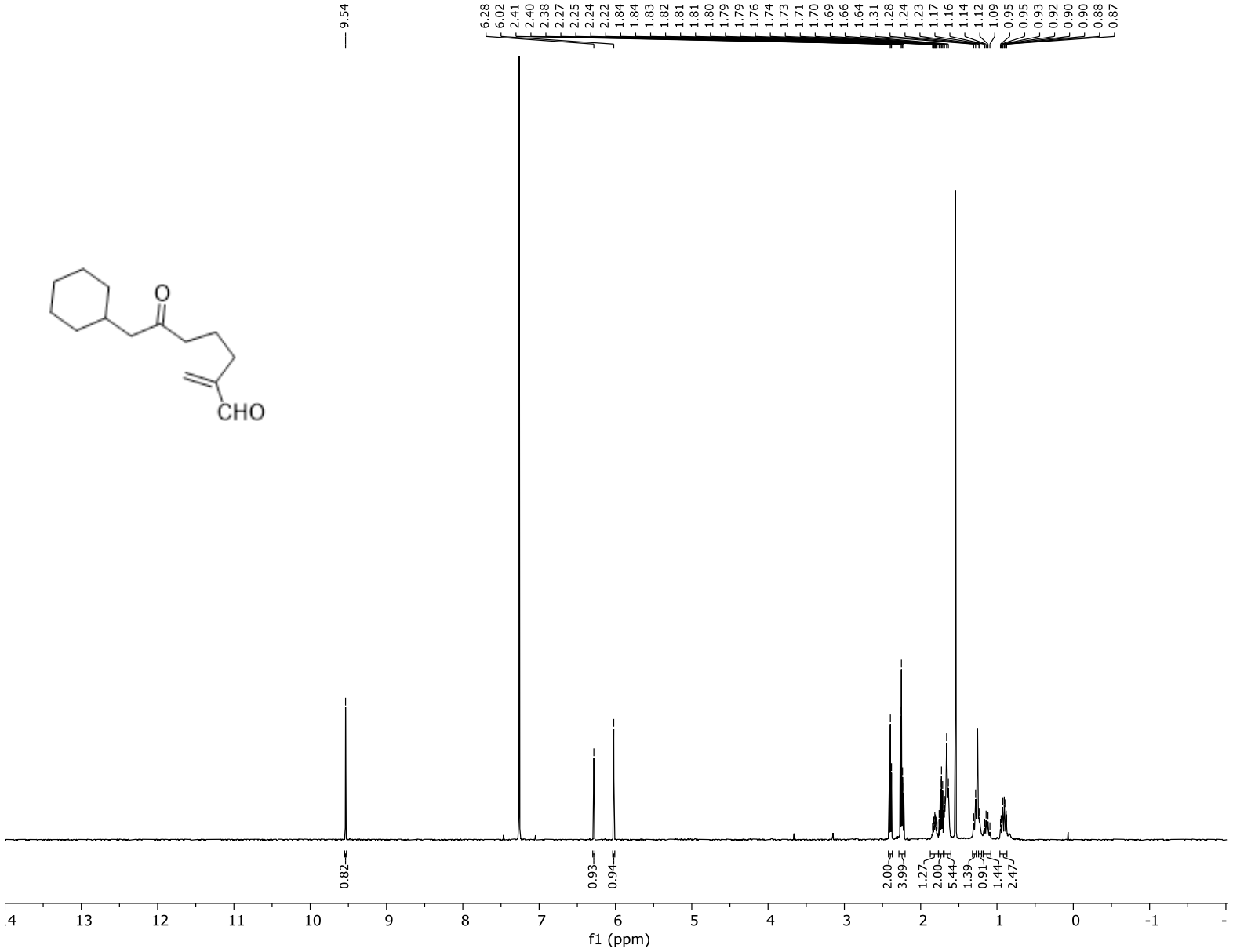
5.20 ^{1}H NMR (500 MHz, $CDCl_3$)



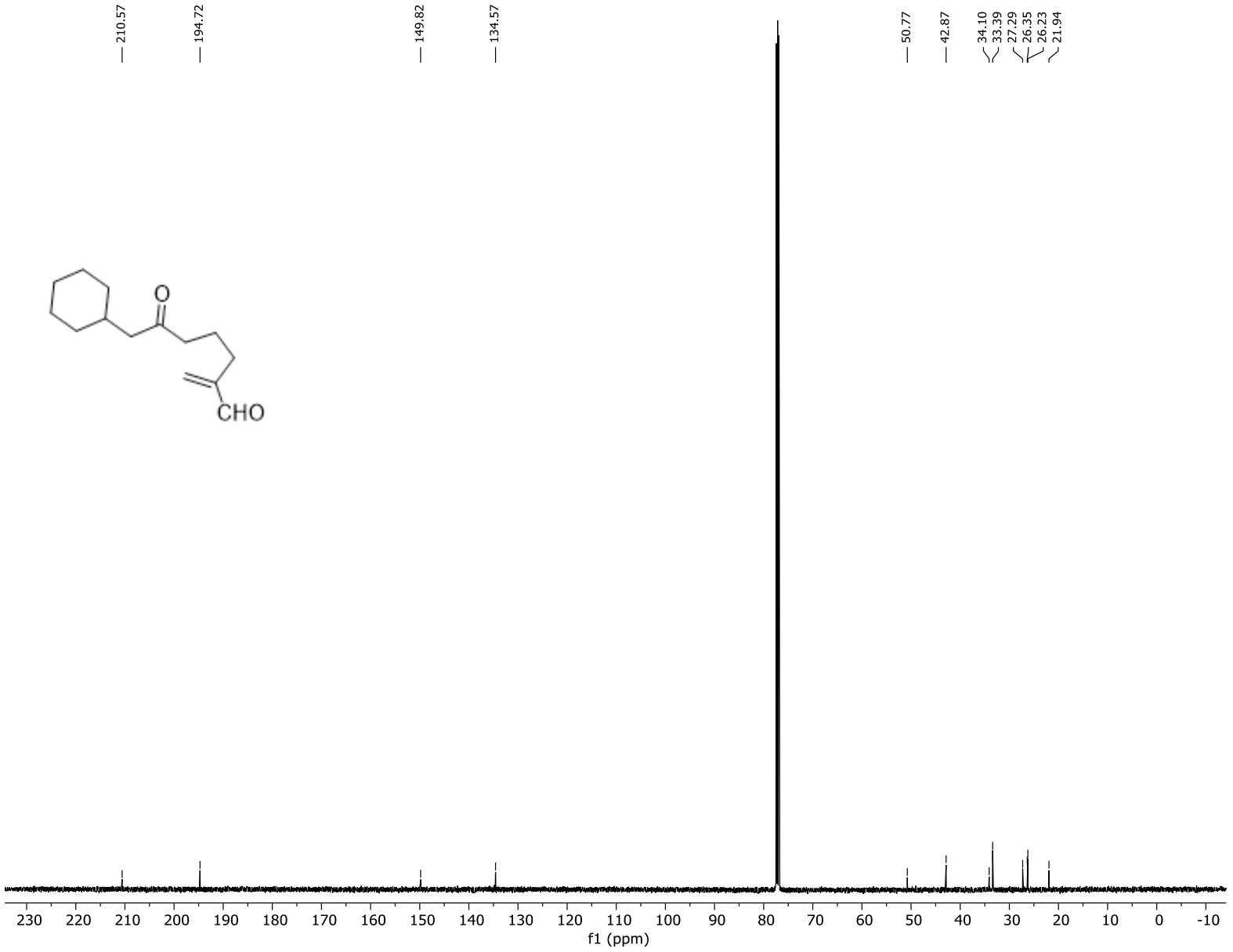
5.20 ^{13}C NMR (126 MHz, $CDCl_3$)



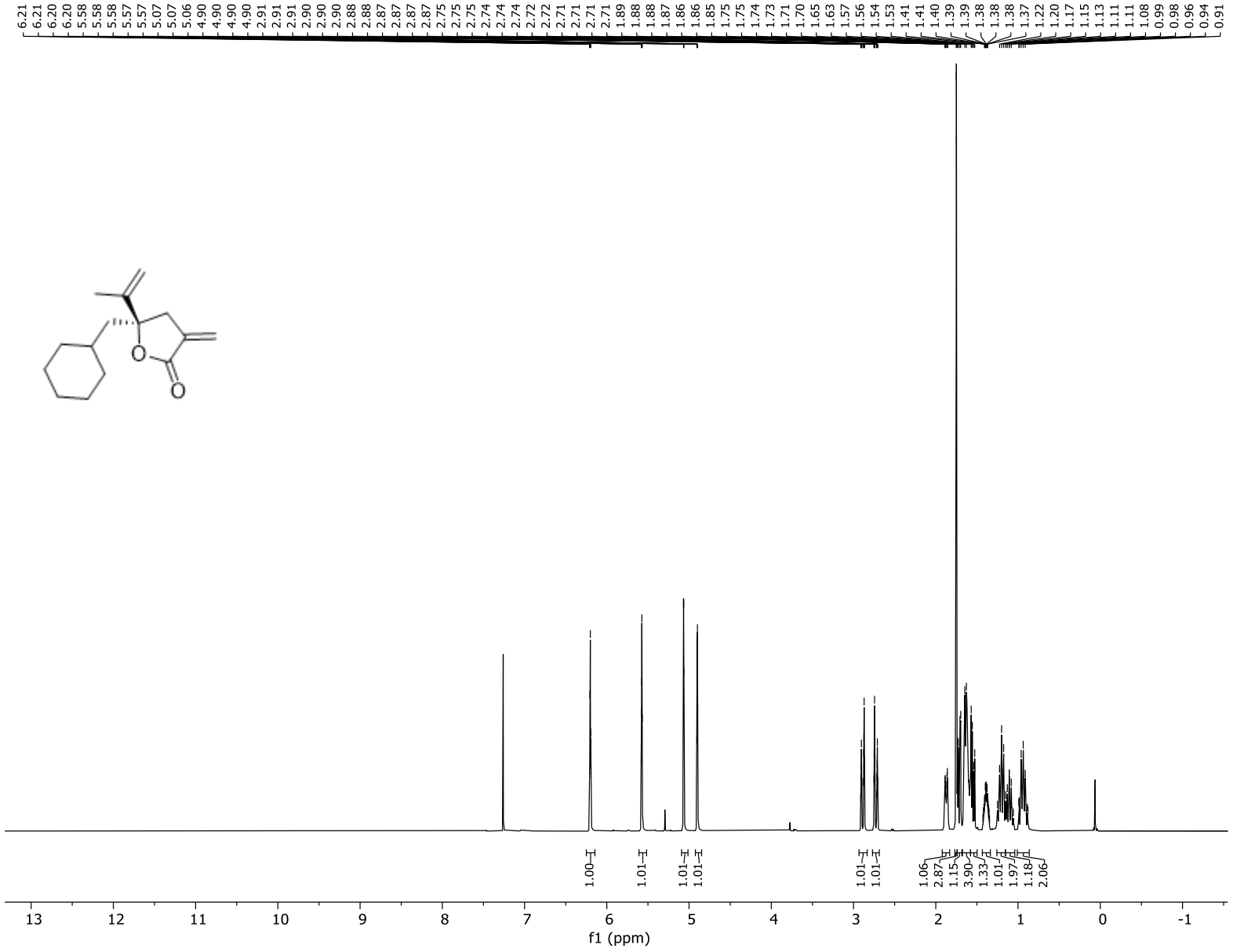
5.21 ^{1}H NMR (500 MHz, $CDCl_3$)



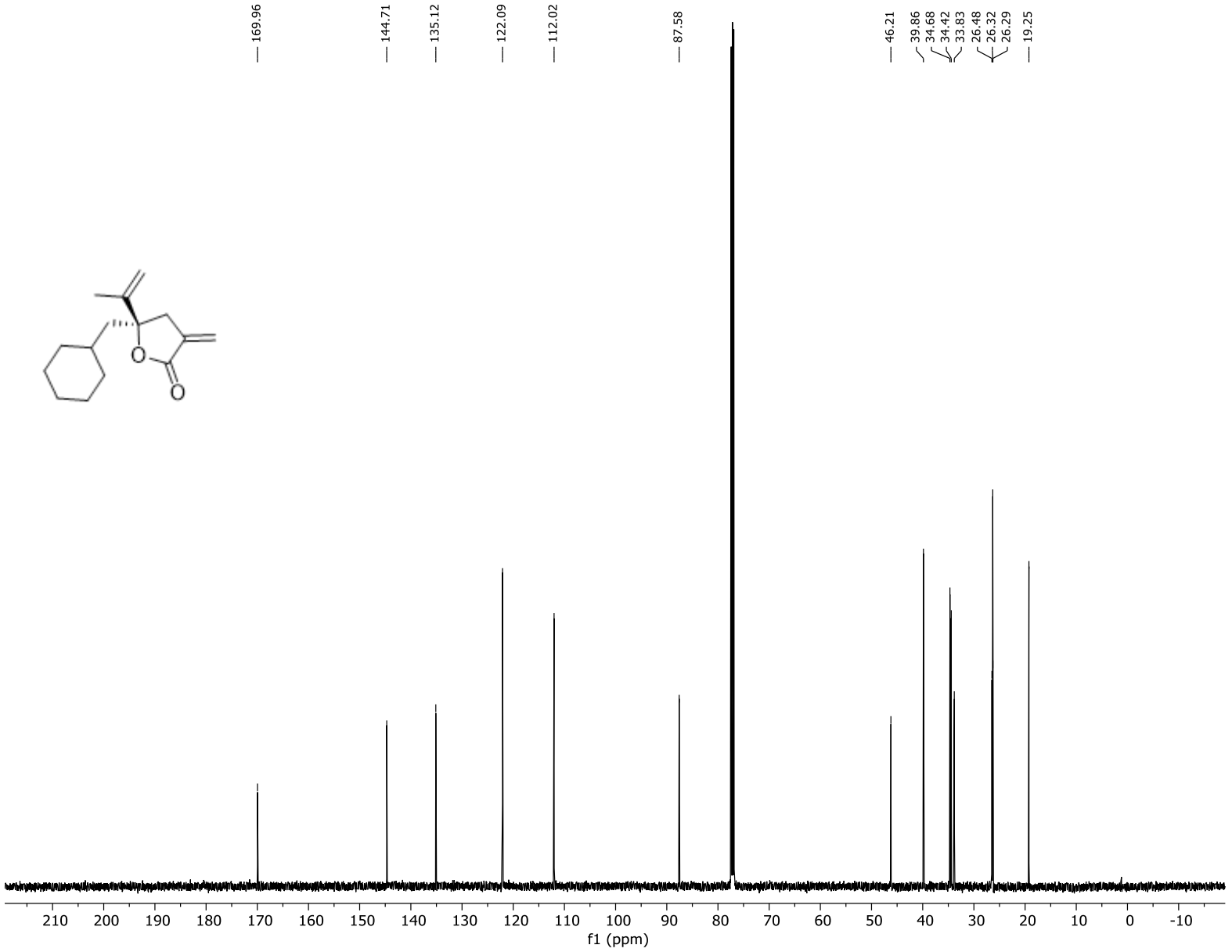
5.21 ^{13}C NMR (126 MHz, $CDCl_3$)



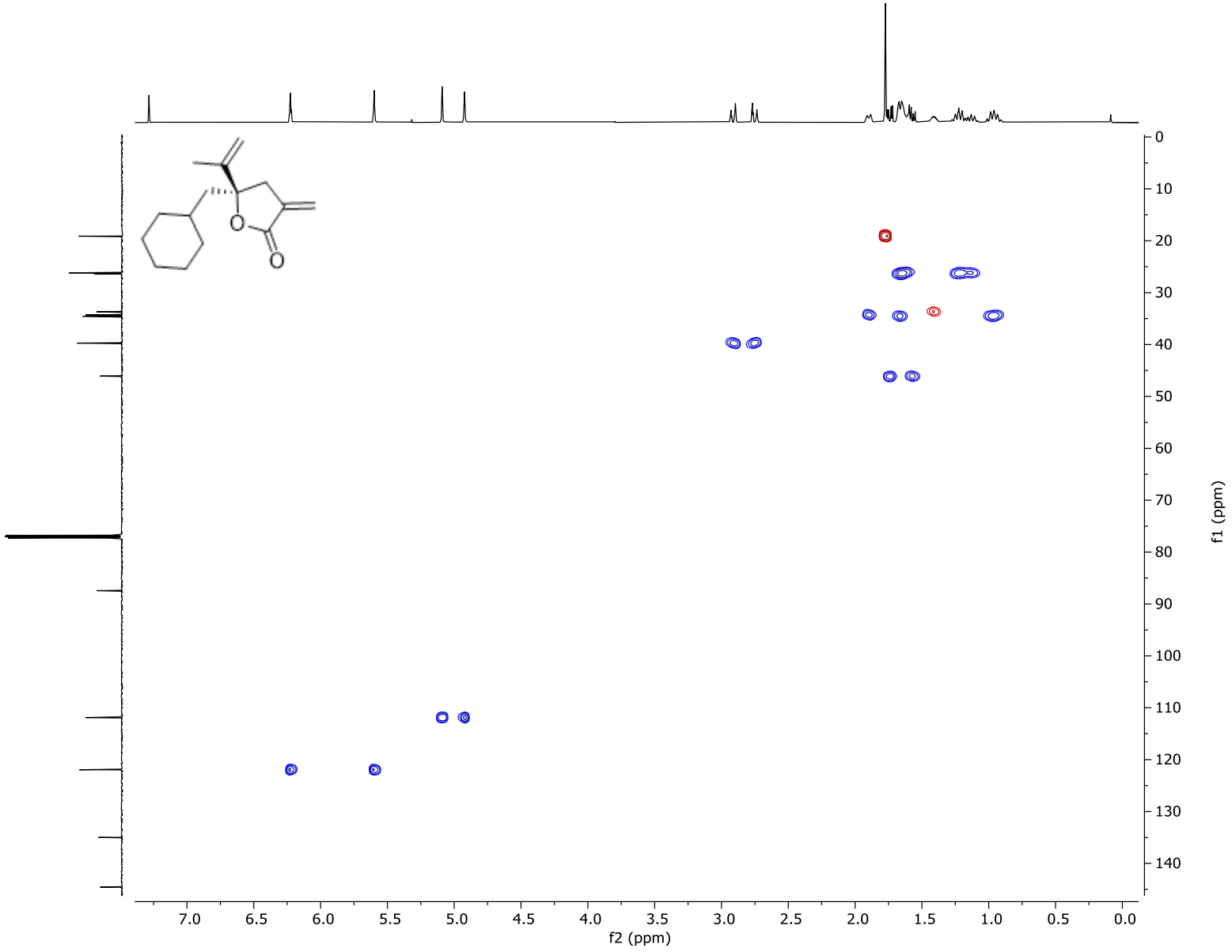
5.19b ^{1}H NMR (500 MHz, $CDCl_3$)



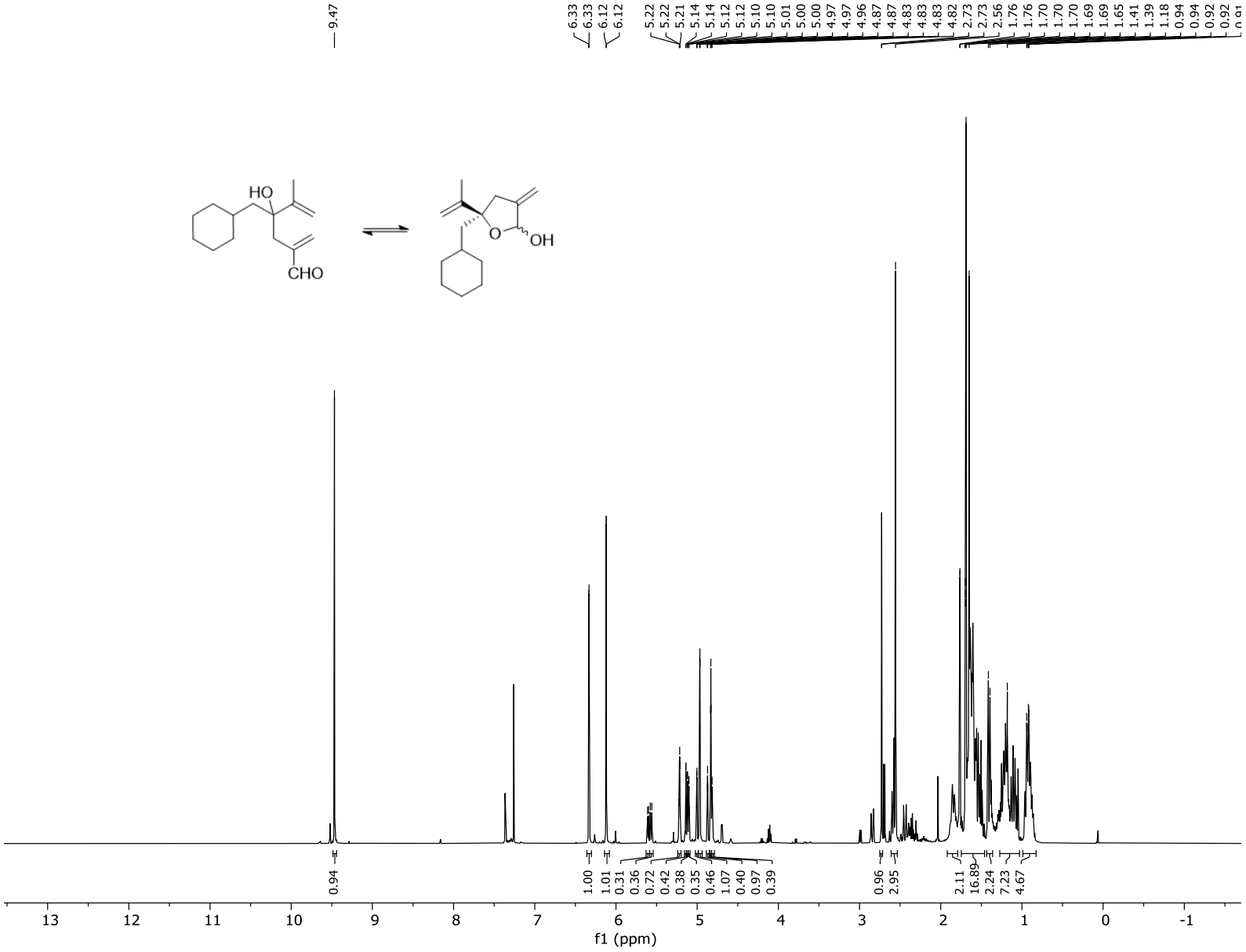
5.19b ^{13}C NMR (126 MHz, $CDCl_3$)



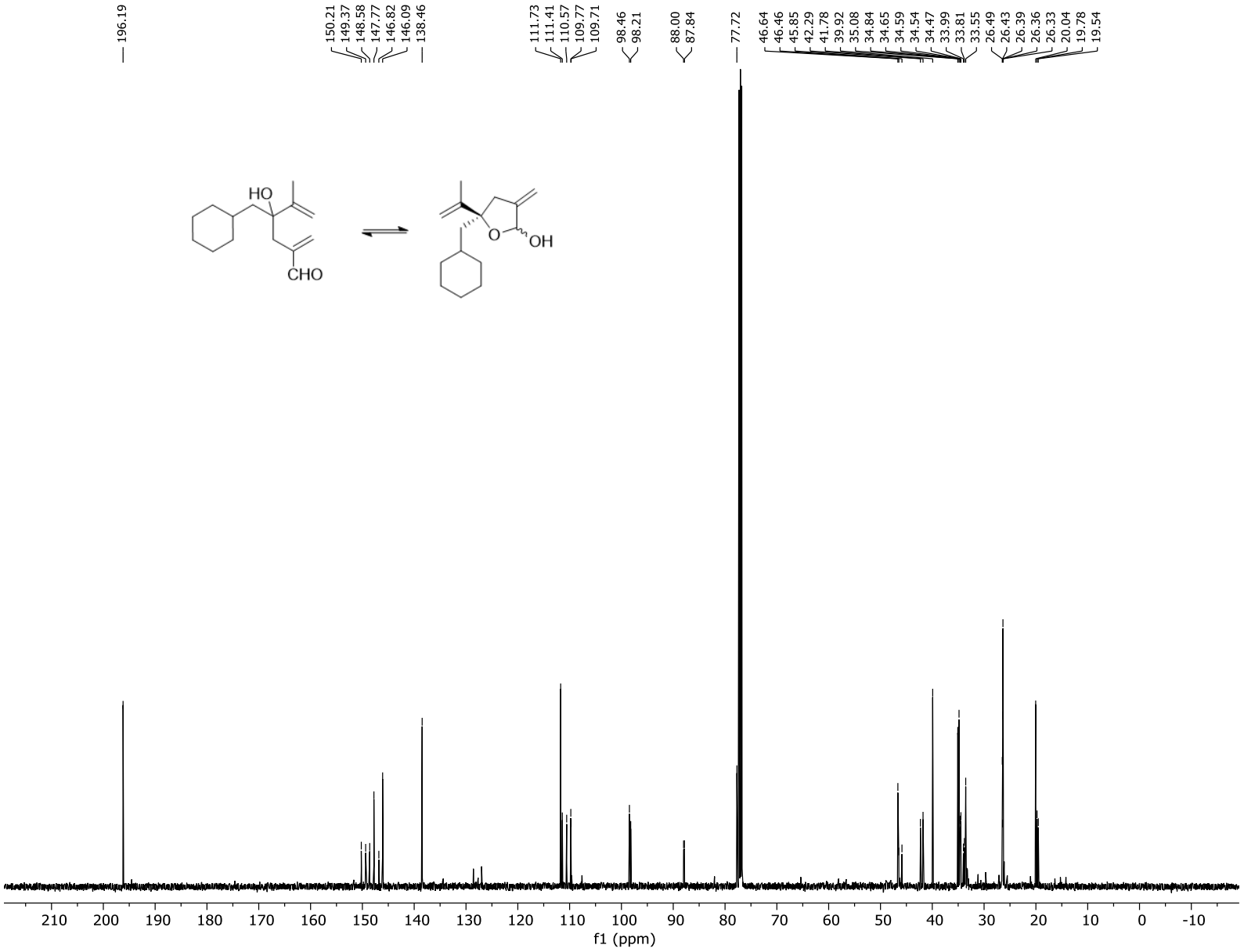
5.19b HSQC (500 MHz, $CDCl_3$)



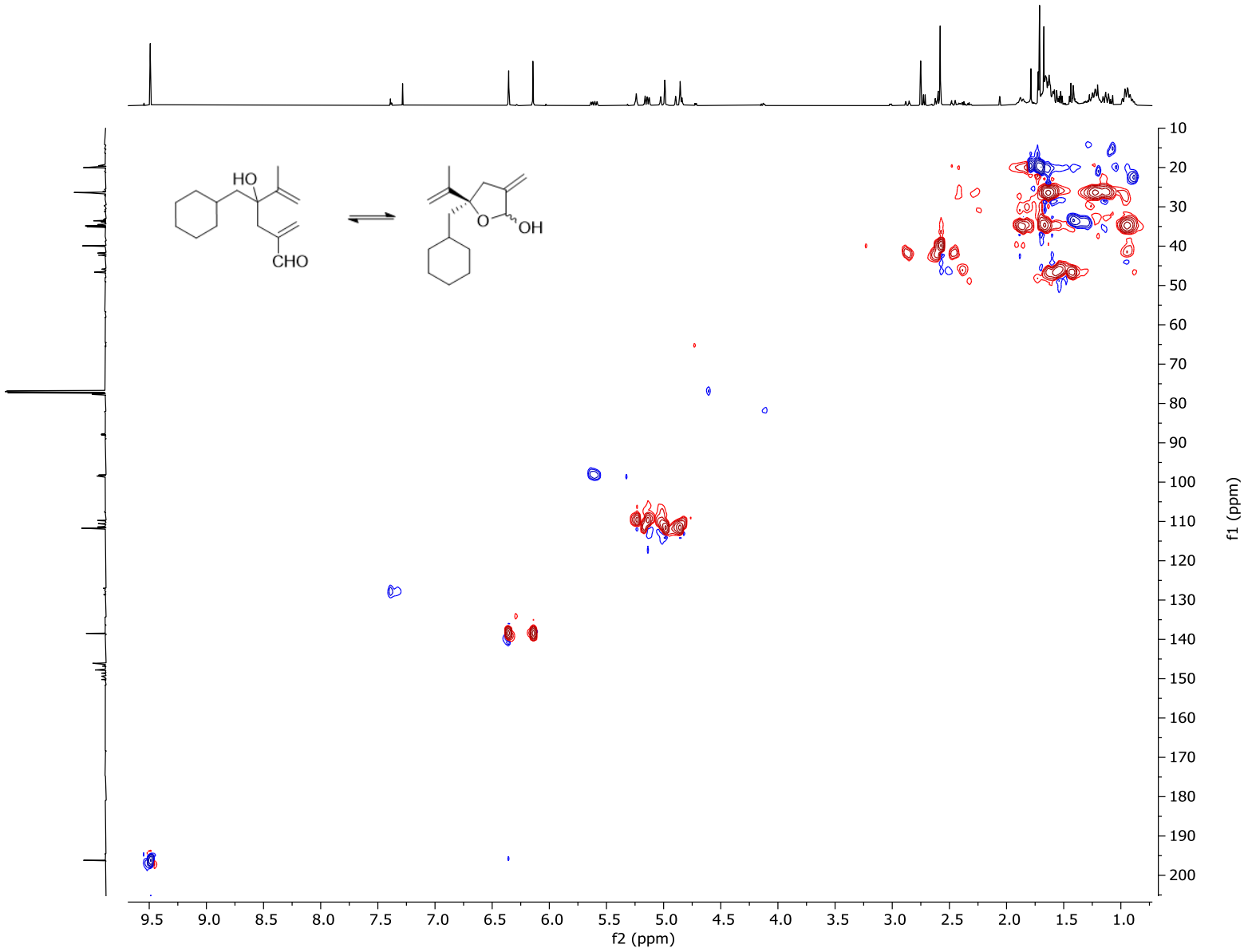
5.20b ^{1}H NMR (500 MHz, $CDCl_3$)



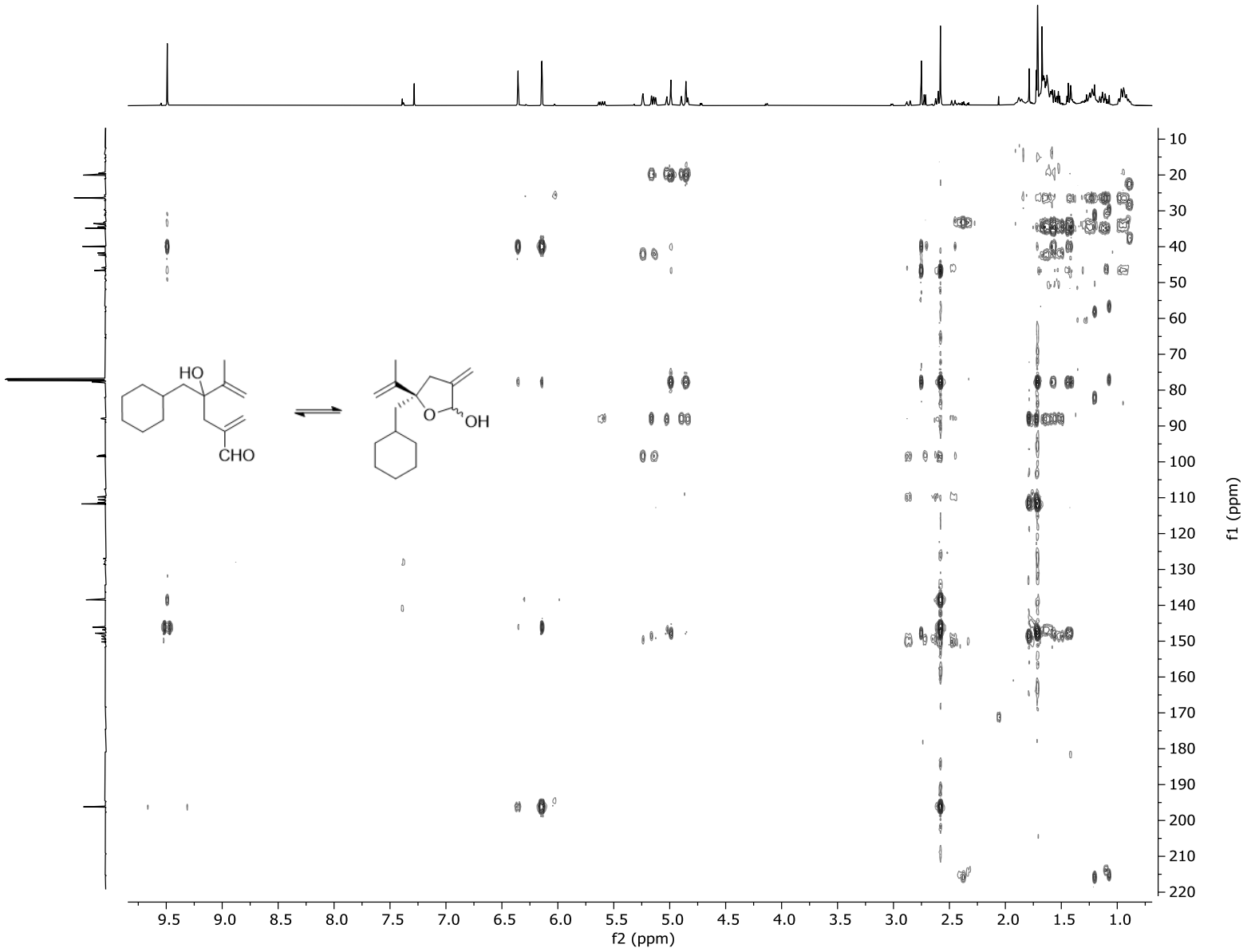
5.20b ^{13}C NMR (126 MHz, $CDCl_3$)



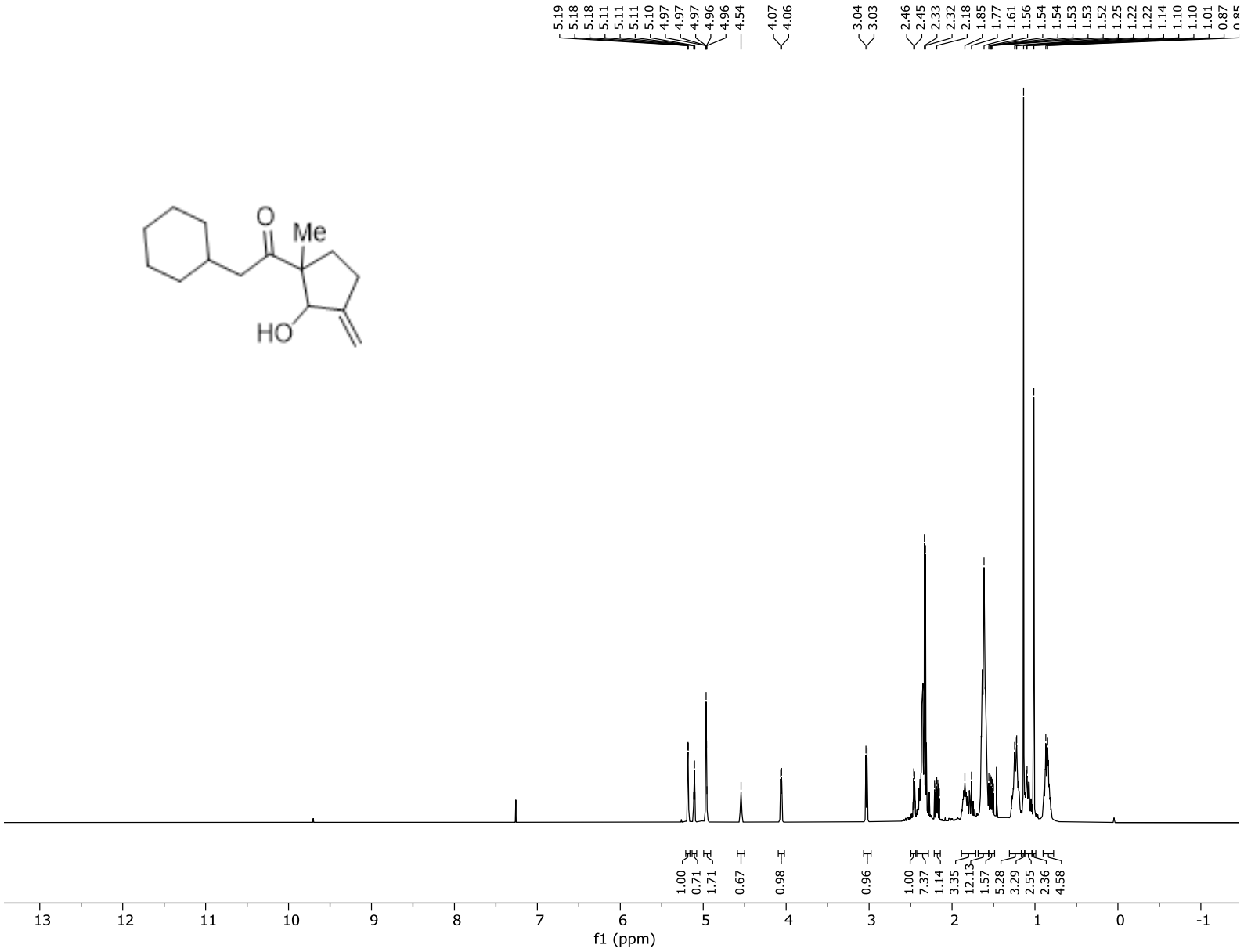
5.20b HSQC (500 MHz, $CDCl_3$)



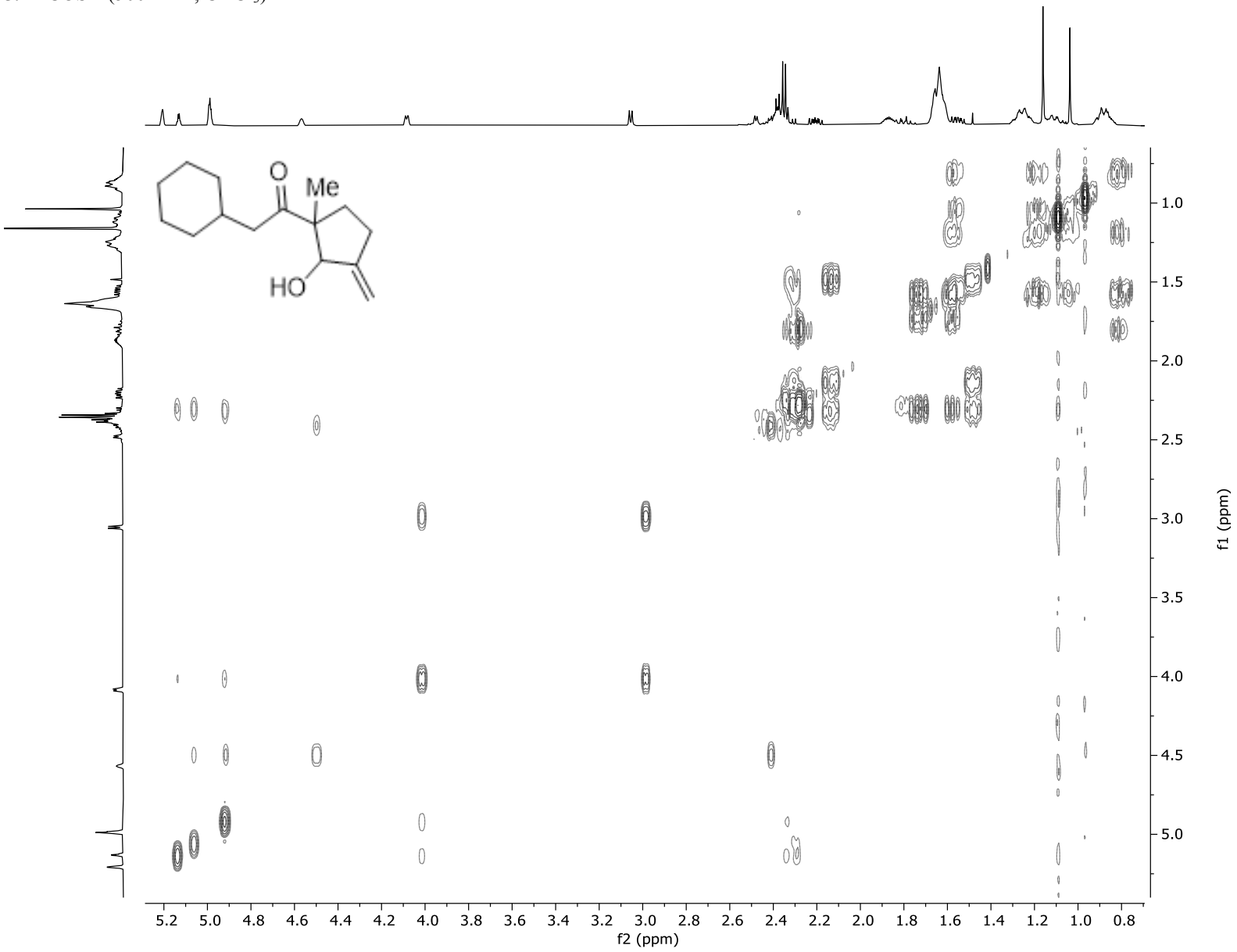
5.20b HMBC (500 MHz, $CDCl_3$)



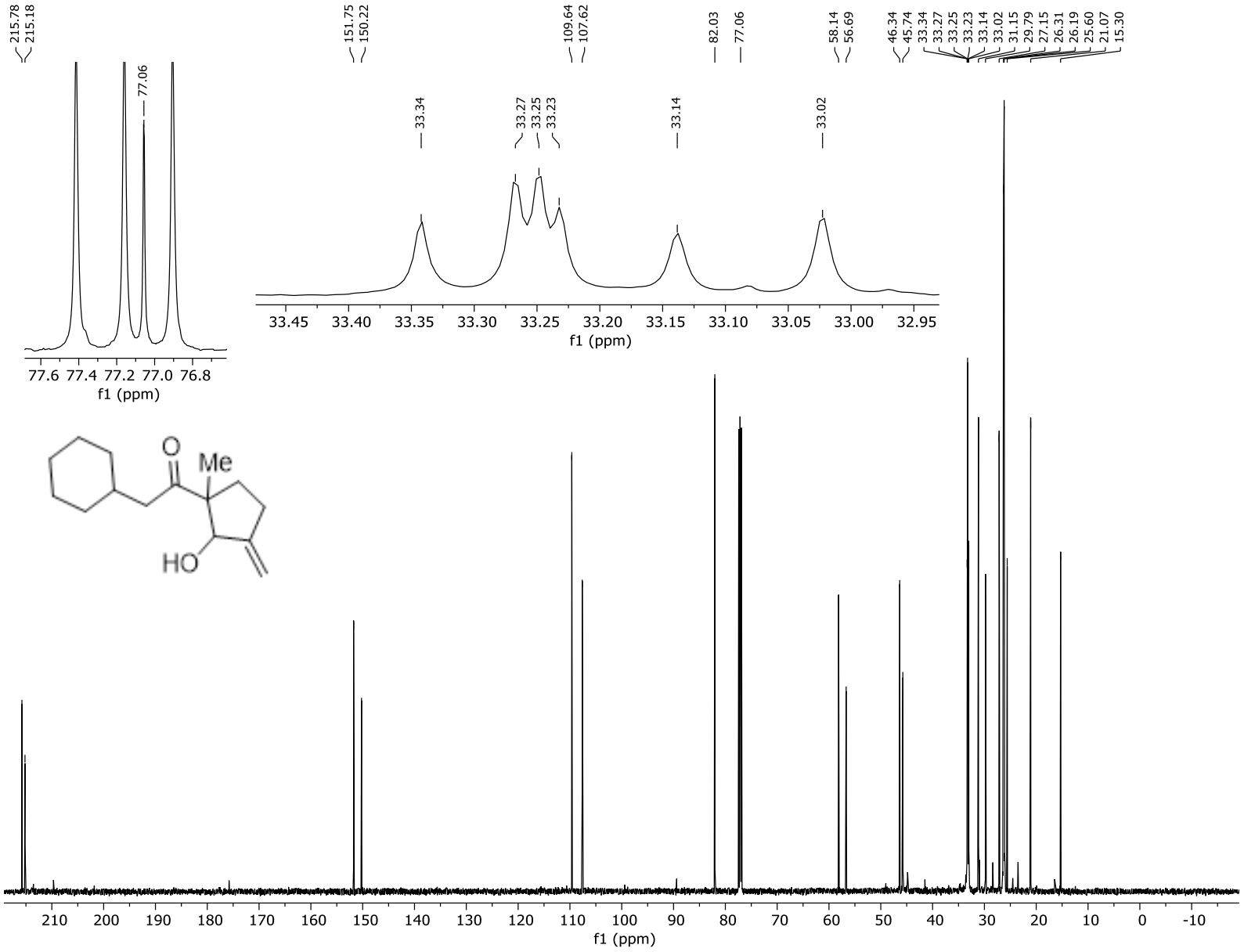
5.22 ^{1}H NMR (500 MHz, $CDCl_3$)



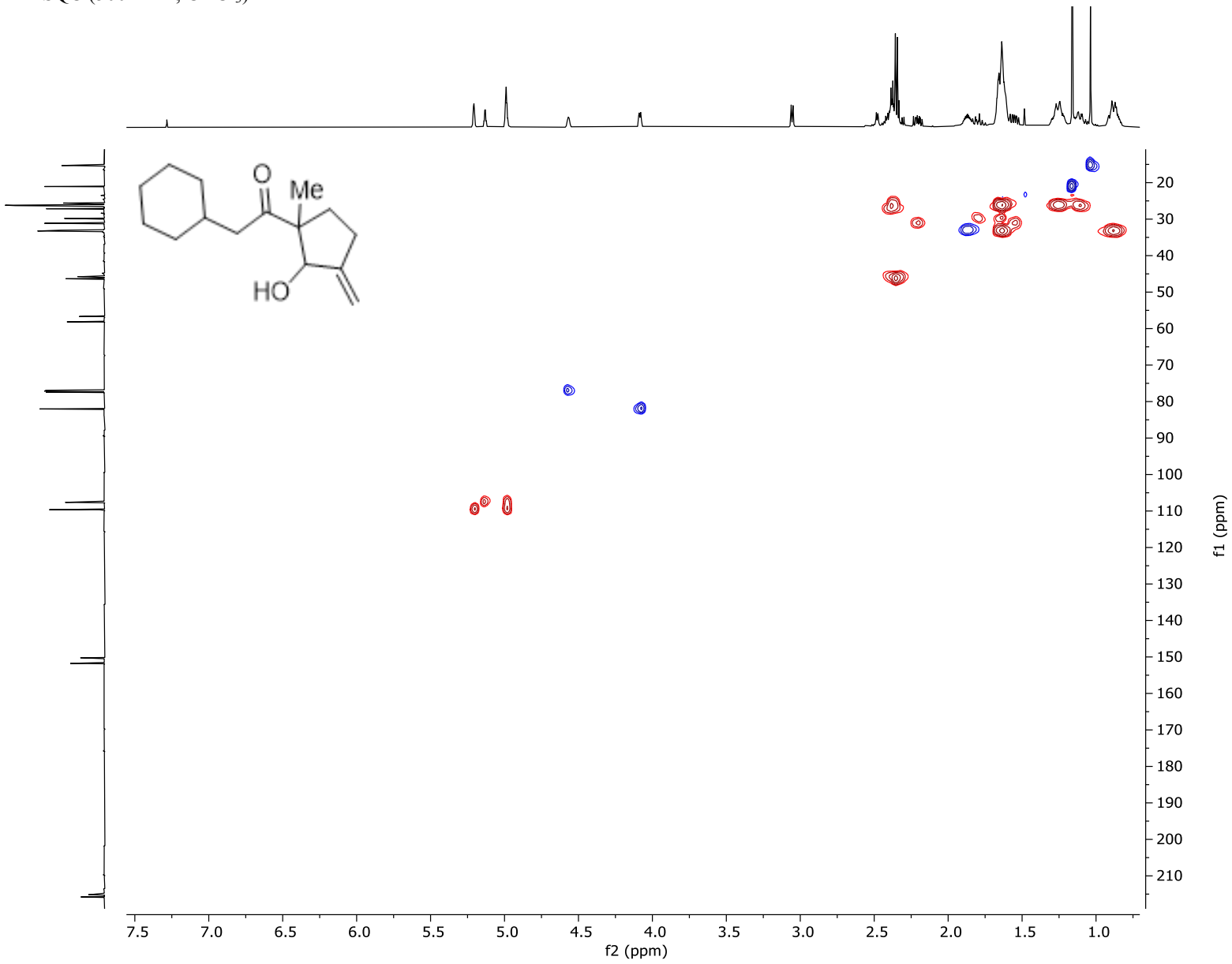
5.22 COSY (500 MHz, $CDCl_3$)



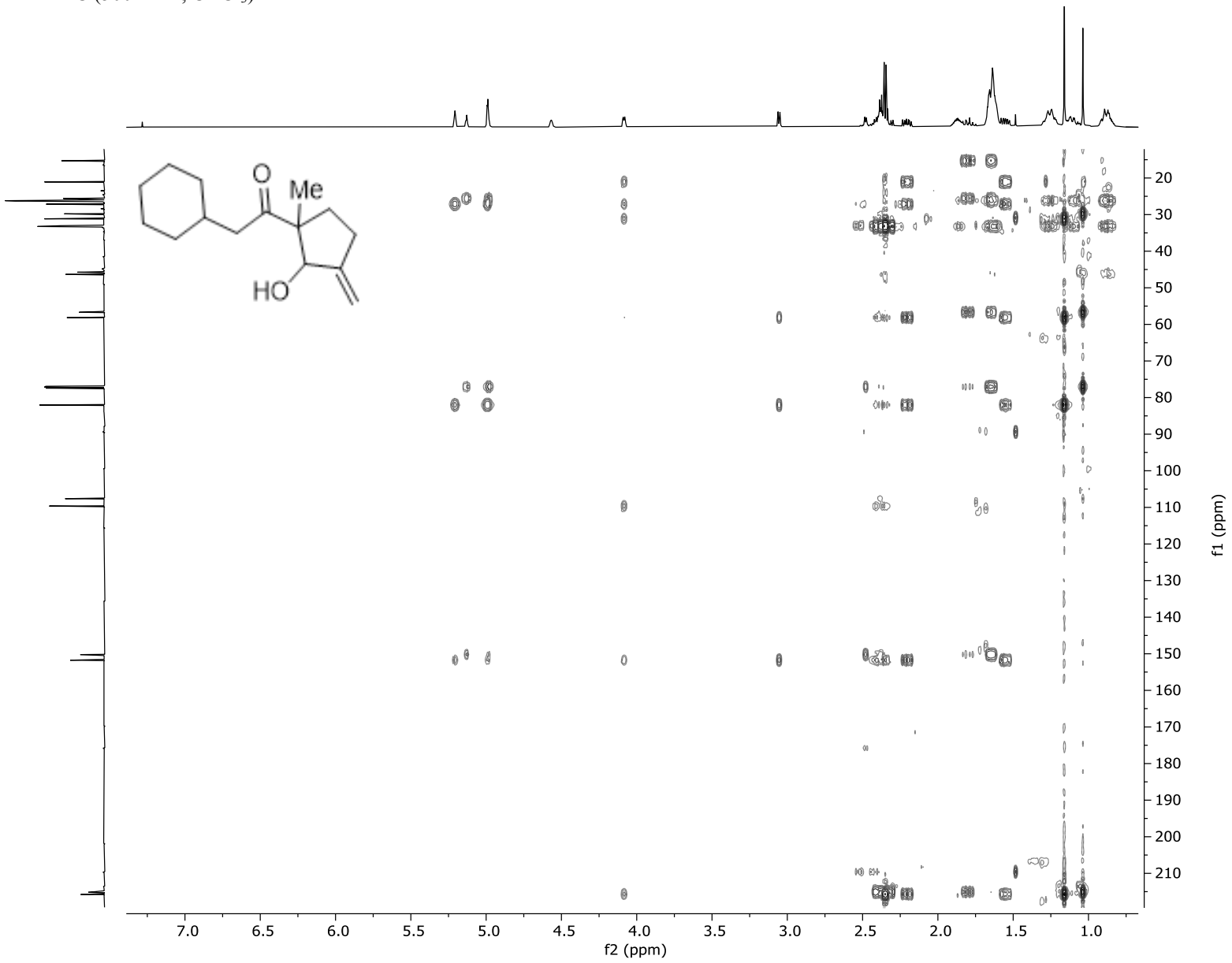
5.22 ^{13}C NMR (126 MHz, $CDCl_3$)



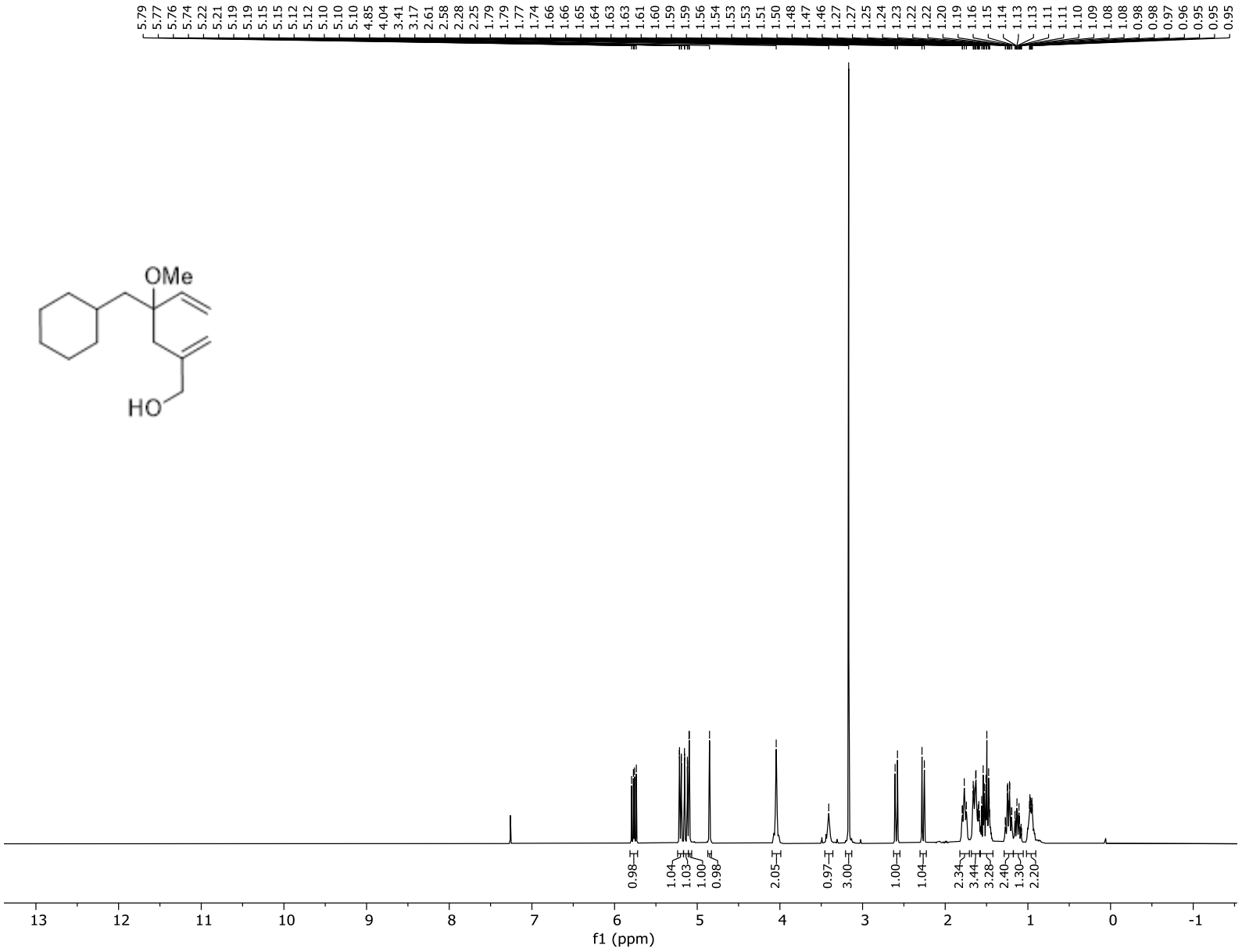
5.22 HSQC (500 MHz, $CDCl_3$)



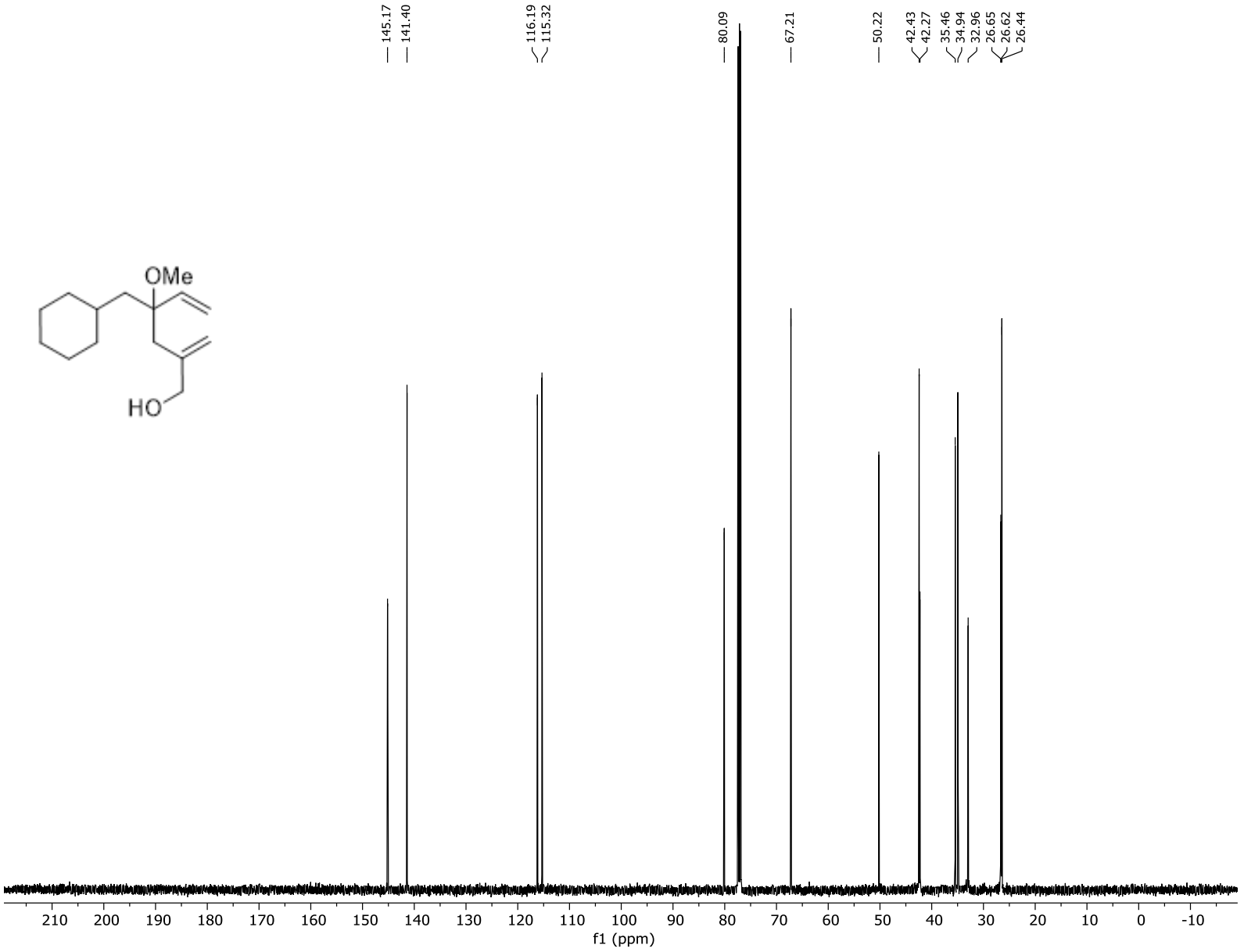
5.22 HMBC (500 MHz, $CDCl_3$)



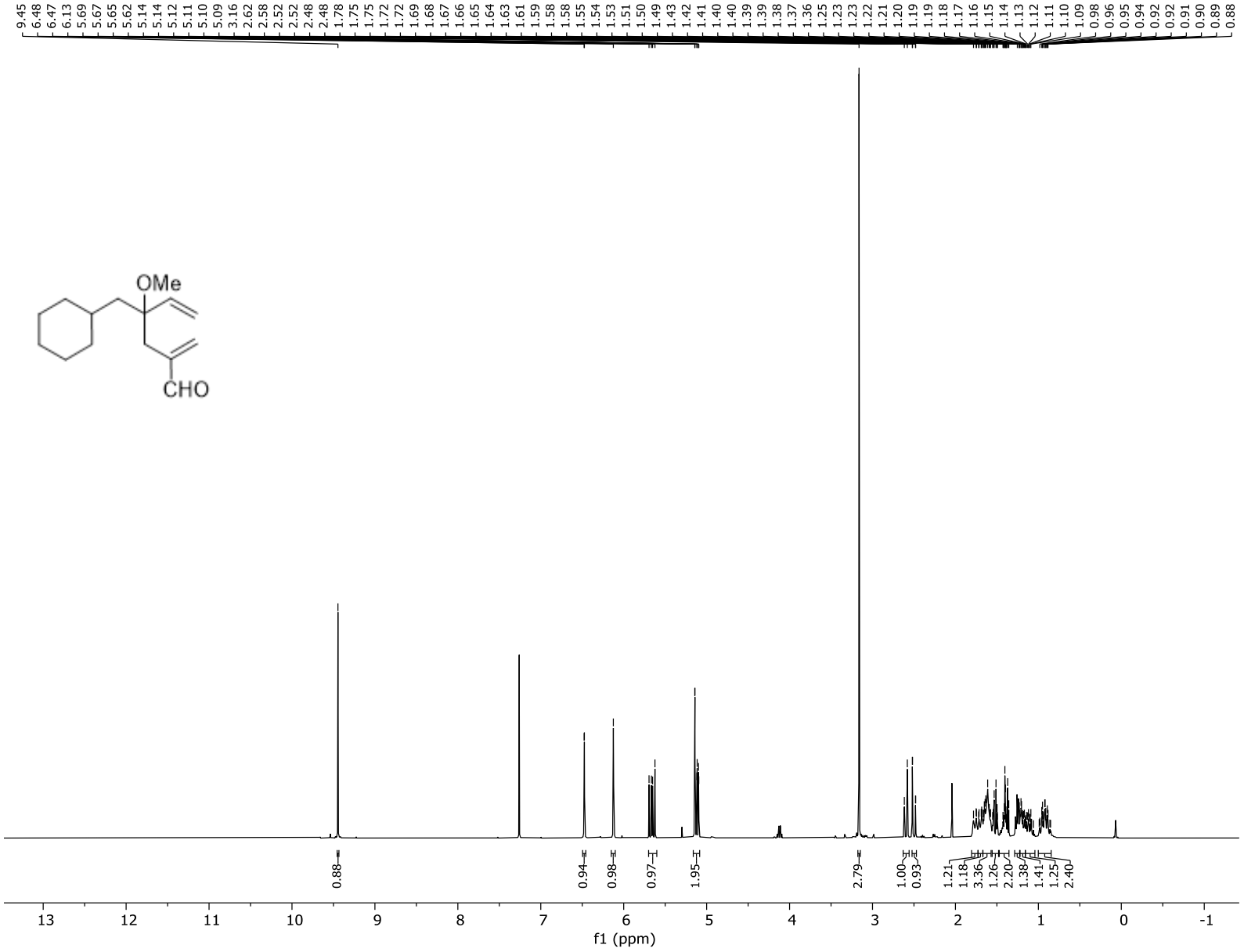
5.24 ^{1}H NMR (500 MHz, $CDCl_3$)



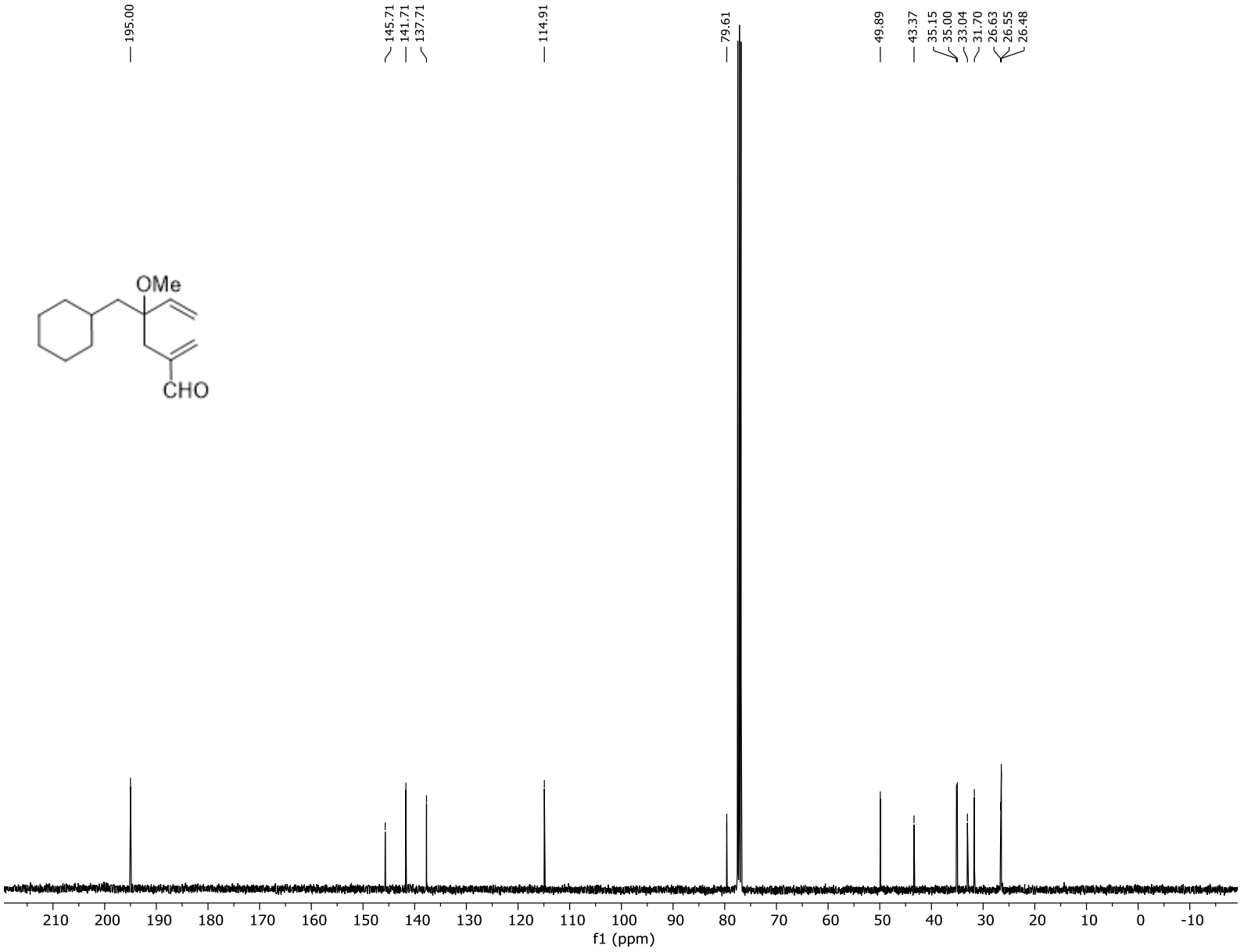
5.24 ^{13}C NMR (126 MHz, $CDCl_3$)



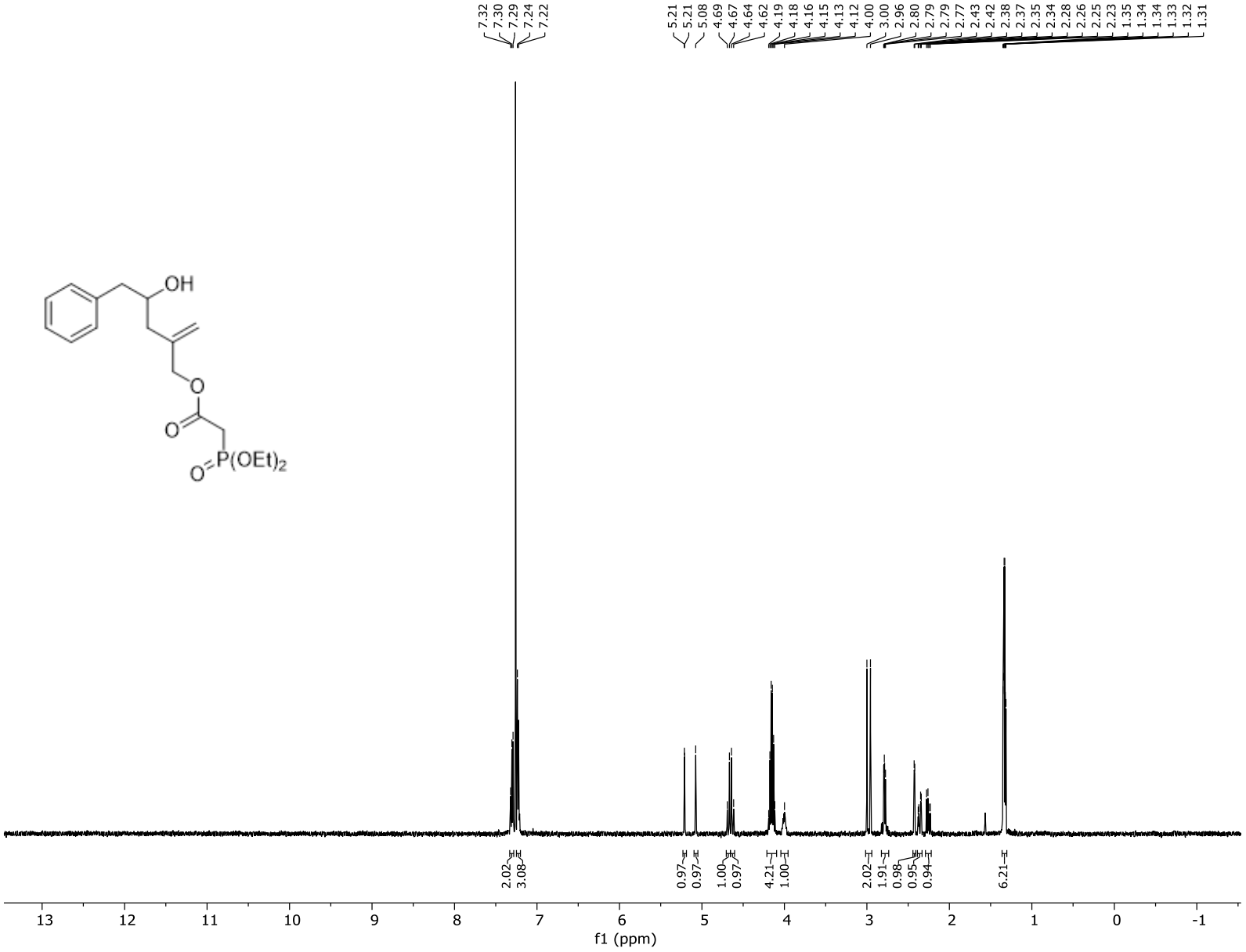
5.25 ^{1}H NMR (400 MHz, $CDCl_3$)



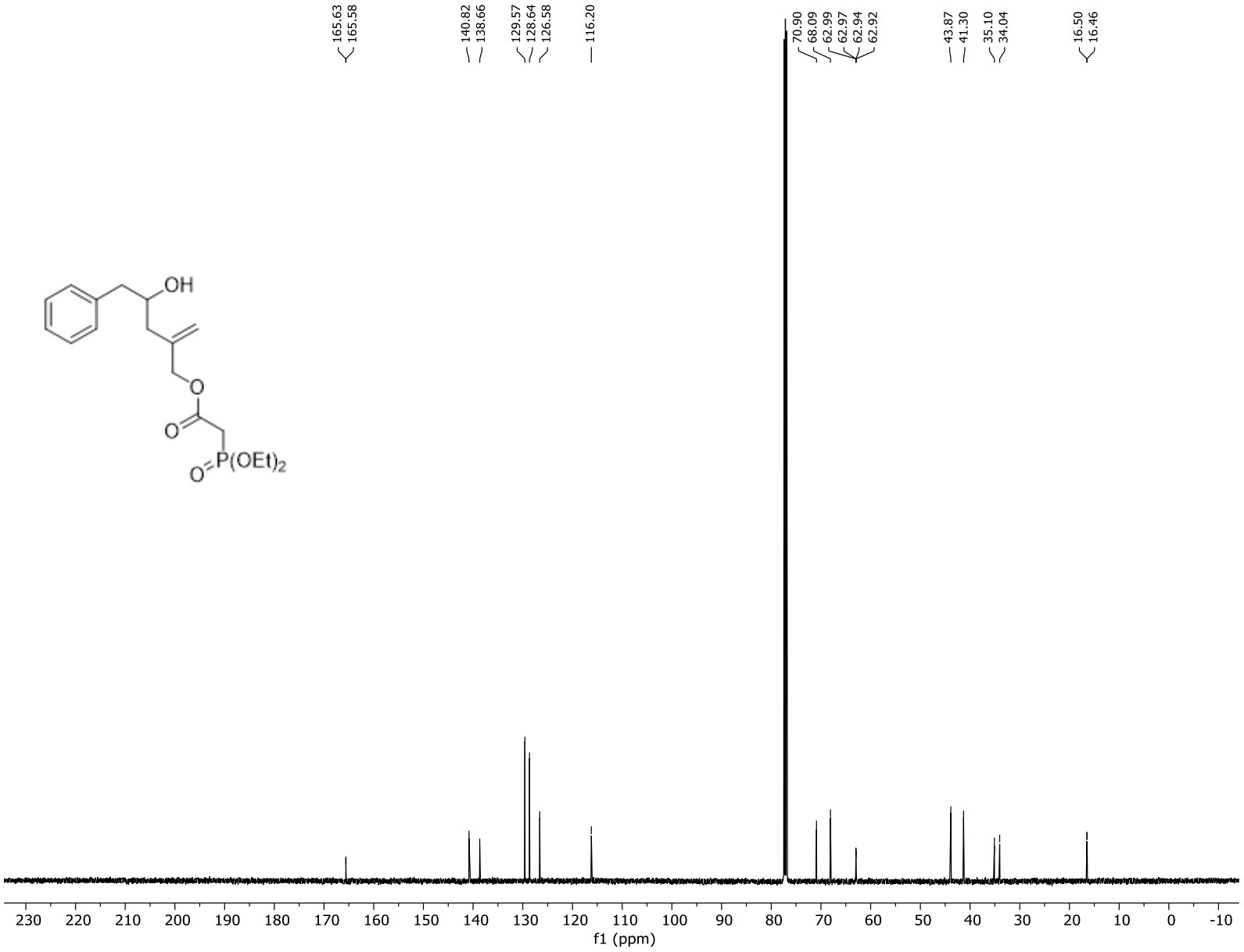
5.25 ^{13}C NMR (101 MHz, $CDCl_3$)



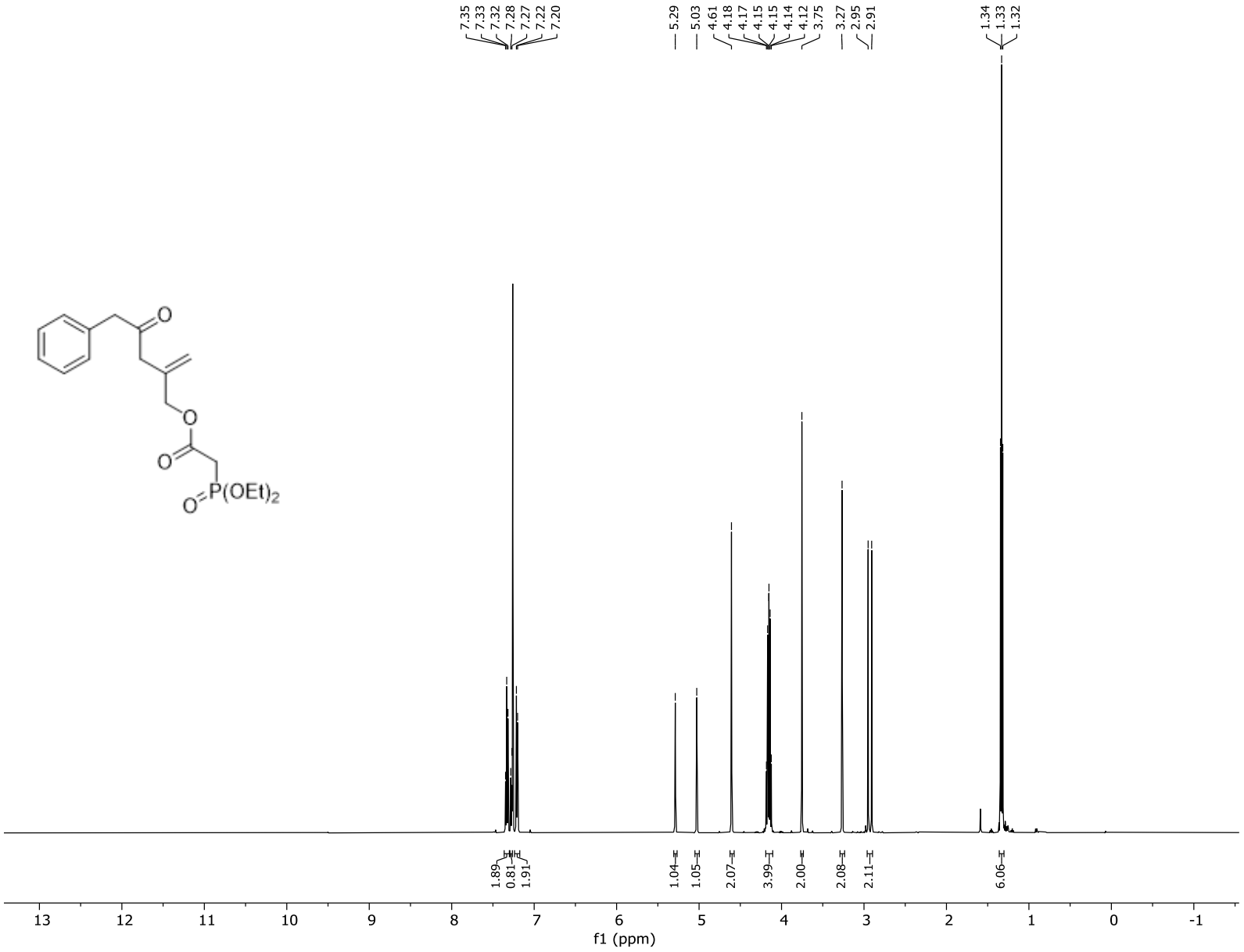
5.15 ^{1}H NMR (500 MHz, $CDCl_3$)



5.15 ^{13}C NMR (126 MHz, $CDCl_3$)



4.106 ^{1}H NMR (500 MHz, $CDCl_3$)



4.106 ^{13}C NMR (126 MHz, $CDCl_3$)

